GEOLOGICAL SURVEY OF CANADA
COMMISSION GÉOLOGIQUE DU CANADA

PAPER 79-1A

This document was produced
by scanning the original publication.

Ce document est le produit d'une
numérisation par balayage
de la publication originale.

CURRENT RESEARCH
PART A

Energy, Mines and Resources Canada
Énergie, Mines et Ressources Canada

1979

Notice to Librarians and Indexers

The Geological Survey's thrice-yearly "Current Research" series contains many reports comparable in scope and subject matter to those appearing in scientific journals and other serials. All contributions to the Scientific and Technical Report section of "Current Research" include an abstract and bibliographic citation. It is hoped that these will assist you in cataloguing and indexing these reports and that this will result in a still wider dissemination of the results of the Geological Survey's research activities.

Technical editing and compilation
R.G. Blackadar
P.J. Griffin
H. Dumych
E.R.W. Neale

Production editing and layout
Leona R. Mahoney
Lorna A. Firth
Michael J. Kiel

Typed and checked by
Debby Busby
Janet Gilliland
Suzanne Lalonde
Janet Legere
Sharon Parnham



GEOLOGICAL SURVEY
PAPER 79-1A

CURRENT RESEARCH
PART A



1979

© Minister of Supply and Services Canada 1979

available by mail from

Printing and Publishing
Supply and Services Canada,
Hull, Québec, Canada K1A 0S9,

and

The Geological Survey of Canada
601 Booth St., Ottawa, K1A 0E8

or

Through your bookseller.

Catalogue No.	M-44-79-1A	Price: Canada:	$5.00
ISBN -	0-660-10121-1	Other Countries:	$6.00

Price subject to change without notice

The Geological Survey of Canada

D.J. McLAREN, Director General

J.O. WHEELER, Deputy Director General

E. HALL, Scientific Executive Officer

M.J. KEEN, Director, Atlantic Geoscience Centre, Dartmouth, Nova Scotia

J.A. MAXWELL, Director, Central Laboratories and Administrative Services Division

PETER HARKER, Director, Geological Information Division

D.F. STOTT, Director, Institute of Sedimentary and Petroleum Geology, Calgary, Alberta

J.E. REESOR, Director, Regional and Economic Geology Division

A.G. DARNLEY, Director, Resource Geophysics and Geochemistry Division

J.S. SCOTT, Director, Terrain Sciences Division

ERRATUM

Current Research, Part C

Geological Survey of Canada Paper 78-1C

p. 99, left col., para. 4, line 18 should read:

Within the bottom 400 m the concentration of suspended particulate matter (SPM) increases slightly to a uniform 10 .....

p. 100 References, add:

Baker, E.T. and Feelg, R.A.
1978: Chemistry of oceanic particulate matter and sediments: implications for bottom sediment resuspensions; Science, v. 200, p. 533.

I : SCIENTIFIC AND TECHNICAL REPORTS

Page

ECONOMIC GEOLOGY

Metallic Mineral Deposits

E.M. CAMERON: Investigation of base metal mineralization in Proterozoic metasediments, Melville Peninsula, District of Franklin 187

K.M. DAWSON: Regional metallogeny of the northern Cordillera: Recent stratiform base metal discoveries in Yukon Territory and District of Mackenzie 375

L.A. DICK: Tungsten and base metal skarns in the Northern Cordillera 259

W.N. PEARSON: Copper metallogeny, north shore region of Lake Huron, Ontario..... 289

W.D. SINCLAIR: Copper-molybdenum occurrences of the Matachewan area, Ontario 253

Uranium

D.R. BOYLE: The dispersion of uranium in the vicinity of Miocene 'basal type' uranium occurrences in the Lassie Lake area, south-central British Columbia..... 349

I.R. JONASSON and H.E. DUNSMORE: Low grade uranium mineralization in carbonate rocks from some salt domes in the Queen Elizabeth Islands, District of Franklin..... 61

Y.T. MAURICE: A preliminary assessment of the uranium potential of southern Melville Peninsula, District of Franklin 281

A.R. MILLER: Uranium geology in the central Baker Lake Basin, District of Keewatin..... 57

V. RUZICKA: Uranium and thorium in Canada, 1978..... 139

GEOCHEMISTRY

W.B. COKER and L.G. CLOSS: Detailed geochemical studies, southeastern Ontario 247

R.G. GARRETT: Sampling considerations for regional geochemical surveys 197

W.D. GOODFELLOW: Geochemistry of copper, lead, and zinc mineralization in Proterozoic rocks near Gillespie Lake, Yukon..... 333

G.E.M. HALL: A study of the stability of uranium in waters collected from various geological environments in Canada 361

J. LEE: A scheme for the separation and characterization of possible metal-organic species in natural waters – some preliminary data..... 121

B.W. SMEE: A theoretical estimation of ion mobilities through glaciolacustrine sediments: Diffusion down a concentration gradient..... 367

GEOPHYSICS

J.G. CONAWAY: Problems in gamma-ray logging: The effect of dipping beds on the accuracy of ore grade determinations 41

MARINE GEOSCIENCE

C.E. KEEN, A. FRICKER, M.J. KEEN, and L. BLINN: A study of the Reykjanes Ridge by surface waves using an earthquake-pair technique 273

MINERALOGY

A.P. SABINA: Minerals of the Francon Quarry (Montreal Island): A progress report ... 115

PALEONTOLOGY

G.S. NOWLAN: Fused clusters of the conodont genus **Belodina** Ethington from the Thumb Mountain Formation (Ordovician), Ellesmere Island, District of Franklin 213

T.T. UYENO and U. MAYR: Lithofacies interpretation and conodont biostratigraphy of the Blue Fiord Formation in the subsurface of Cameron and Vanier islands, Canadian Arctic Archipelago 233

PETROLOGY

E. DIMROTH, P. COUSINEAU, M. LEDUC, Y. SANSCHAGRIN, and G. PROVOST: Flow mechanisms of Archean subaqueous basalt and rhyolite flows..... 207

E. FROESE and L.S. JEN: A reaction grid for biotite-bearing mafic granulites 83

J. GITTINS and K.L. CURRIE: Petrologic studies of sapphirine-bearing granulites around Wilson Lake, Labrador 77

P.A. NIELSEN: Fe-Mg cation exchange thermobarometry of polymetamorphic rocks from the Precambrian Shield of northeastern Alberta 133

R.H. SUTCLIFFE and J.J. FAWCETT: Petrological and geochronological studies on the Rainy Lake Granitoid Complex, northwestern Ontario: A progress report 377

QUATERNARY GEOLOGY

Engineering and Environmental Geology Studies

J.J. CLAGUE: The Denali Fault System in southwest Yukon Territory — A geologic hazard? 169

J.R. MACKAY: An equilibrium model for hummocks (nonsorted circles), Garry Island, Northwest Territories 165

Inventory Mapping and Stratigraphic Studies

L.E. JACKSON, JR.: New evidence for the existence of an ice free corridor in the Rocky Mountain Foothills near Calgary, Alberta, during Late Wisconsinan time 107

Paleoecology and Geochronology

W. BLAKE, JR. and J.V. MATTHEWS, JR.: New data on an interglacial peat deposit near Makinson Inlet, Ellesmere Island, District of Franklin 157

Sedimentology and Geomorphology

L. DYKE: Bedrock heave in the central Canadian Arctic 241

REGIONAL GEOLOGY

Appalachian Region

K.L. CURRIE, G.E. PAJARI, JR., and R.K. PICKERILL: Tectono-stratigraphic problems in the Carmanville area, northeastern Newfoundland 71

R.K. HERD and G.R. DUNNING: Geology of Puddle Pond map area, southwestern Newfoundland 305

D. KNAPP, D. KENNEDY, and Y. MARTINEAU: Stratigraphy, structure, and regional correlation of rocks at Grand Lake, western Newfoundland 317

N. RAST and G.G. LUTES: The metamorphic aureole of the Pokiok-Skiff Lake Granite, southern New Brunswick 267

S. SCHILLEREFF and H. WILLIAMS: Geology of Stephenville map area, Newfoundland 327

Cordilleran Region

R.L. BROWN and J.F. PSUTKA: Stratigraphy of the east flank of Frenchman Cap dome, Shuswap Complex, British Columbia 35

R.B. CAMPBELL and C.J. DODDS: Operation Saint Elias, British Columbia..... 17

M.P. CECILE and B.S. NORFORD: Basin to platform transition, Lower Paleozoic strata of Ware and Trutch map areas, northeastern British Columbia 219

S.P. GORDEY: Stratigraphy of southeastern Selwyn Basin in the Summit Lake area, Yukon Territory and Northwest Territories..... 13

P.S.W. GRAHAM and D.G.F. LONG: The Tranquille beds of the Kamloops Group: a Tertiary (middle Eocene) coal-bearing sequence in the vicinity of Kamloops Lake, British Columbia 357

P.B. READ: Relationship between the Shuswap Metamorphic Complex and Kootenay Arc, Vernon east-half, southern British Columbia 37

P.B. READ and R.L. BROWN: Inverted stratigraphy and structures, Downie Creek, southern British Columbia 33

G.C. TAYLOR, M.P. CECILE, C.W. JEFFERSON, and B.S. NORFORD: Stratigraphy of Ware (east half) map area, northeastern British Columbia 227

D.J. TEMPELMAN-KLUIT: Five occurrences of transported synorogenic clastic rocks in Yukon Territory 1

L. THORSTAD: The Lower Mesozoic King Salmon Assemblage – Cry Lake map area, British Columbia 21

H.W. TIPPER: Jurassic stratigraphy of the Whitesail Lake map area, British Columbia . 31

G.J. WOODSWORTH: Geology of Whitesail Lake map area, British Columbia 25

Precambrian Shield

F.H.A. CAMPBELL and M.P. CECILE: The northeastern margin of the Aphebian Kilohigok Basin, Melville Sound, Victoria Island, District of Franklin 91

K.D. CARD: Regional geological synthesis, central Superior Province 87

T. FRISCH: Reconnaissance studies of the Precambrian crystalline basement on Devon Island, District of Franklin 113

J.R. HENDERSON, D. SHAW, M. MAZURSKI, M. HENDERSON, R. GREEN, and D. BRISBIN: Geology of part of Foxe Fold Belt, central Baffin Island, District of Franklin..... 95

T.R. IANNELLI: Stratigraphy and depositional history of some Upper Proterozoic sedimentary rocks on northwestern Baffin Island, District of Franklin 45

A.N. LeCHEMINANT, M.B. LAMBERT, A.R. MILLER, and G.W. BOOTH: Geological studies: Tebesjuak Lake map area, District of Keewatin 179

J.C. McGLYNN: Geology of the Precambrian rocks of the Rivière Grandin and in part of the Marian River map areas, District of Mackenzie 127

C.R. TIPPETT: Basement-supracrustal rock relationships on the southern margin of the Foxe Fold Belt, central Baffin Island, District of Franklin 101

M. SCHAU and K.E. ASHTON: Granulites and plutonic complexes northeast of Baker Lake, District of Keewatin 311

II : SCIENTIFIC AND TECHNICAL NOTES

J.B. HENDERSON: Healey Lake map area, District of Mackenzie 400

R.T. BELL and L.D. JONES: Geology of some uranium occurrences in Western Canada 397

J.R. MACKAY, J. OSTRICK, C.P. LEWIS, and D.K. MACKAY: Frost heave at ground temperatures below 0°C, Inuvik, Northwest Territories 403

L. NADEAU and M. SCHAU: Surficial geology near the mouth of the Quoich River, District of Keewatin 389

R.G. ANDERSON: Distribution and emplacement history of plutons within the Hotailuh Batholith in the Cry Lake and Spatsizi map areas, north-central British Columbia 393

B.S. NORFORD: Lower Devonian graptolites in the Road River Formation, northern British Columbia 383

R.W. KLASSEN: Thermokarst terrain near Whitehorse, Yukon Territory 385

S. CREANEY: Organic material in the Tranquille beds of the (Tertiary) Kamloops Volcanic Group near Afton Mine, Kamloops, British Columbia 381

J. LEROUX and J.L. LUTERNAUER: Evaluation of the morpho-sedimentologic character of the Nanaimo River Delta tidal flats using selected remote sensing and photogrammetric techniques – preliminary report 401

A.G. PLANT and A.C. ROBERTS: New data on unnamed $CaZrSi_2O_7$ from Kipawa, Quebec 391

H.W. TIPPER and B.E.B. CAMERON: Jurassic biostratigraphy of Skidegate Inlet, Queen Charlotte Islands 396

Note to Contributors 406

Author Index 407

INTRODUCTION

For many years of Geological Survey of Canada has been concerned with providing the scientific and technical information needed to support national growth related to resource development and land use. Systematic programs have been developed to provide the information needed by governments and the private sector. In this the Survey follows the long standing objectives of the departments of which it has been a part – Mines, then Mines and Resources, Mines and Technical Surveys and latterly Energy, Mines and Resources. In the late 1960's it became clear that the Federal Government had to play a more active role in developing and implementing policies for the exploitation and use of nonrenewable resources. The action of the OPEC nations in late 1973 reinforced this. It became clear that more accurate and more detailed geological and economic information was needed on all forms of energy resources. This requirement resulted in significant changes in the Survey's programs and in redeployment of staff. Greater emphasis was given to specific studies and there was a corresponding reduction of the effort devoted to the systematic development of basic landmass information. Many of the projects reported on in the following pages are designed to solve specific problems but every effort is being made by the management of the Survey to keep the data base replenished. This is becoming increasingly difficult during a time of fiscal restraint and static if not decreasing staff allocations.

Canada has followed a path of economic development which depends markedly on the use of land and resources. It appears that this will continue to be a dominant feature of our economy in the foreseeable future. As a result the Department of Energy, Mines and Resources will continue to play an important role. Fuel and non-fuel minerals currently account for 30 per cent of Canada's export earnings. As is appears probable that this level will be continued, the distribution of resource projects will have a significant influence on regional development. Resource development is not always without its disadvantages; the lessons of the uncontrolled past must be accepted and environmental impact taken into consideration. Few developments can occur without altering the environment but an acceptable balance can commonly be reached.

During 1978-79 the programs of the Department of Energy, Mines and Resources in the field of Earth Sciences call for (1) increased effort devoted to physical environment studies especially those related to major energy development; (2) continuing geological studies concerned with improving understanding of our resource base; and (3) assessments of the options available for nuclear waste disposal. The second objective covers a large part of the Survey's activities. It includes regional bedrock reconnaissance mapping, shared-cost federal-provincial surveys comprising national geochemical and airborne radiometric and magnetic surveys and the National Aeromagnetic Program. The larger part of this work is being carried out north of latitude 60° where the present level of information is the lowest in Canada. This area, relatively unknown as it is a present, is likely to be the site of much development in the next few decades. If there is to be orderly development of frontier energy and mineral resources the information gap must be narrowed.

Many of the reports that comprise the annual, three-part, Current Research series present the first results of such studies. Further results are released as geological, geophysical and geochemical maps, papers, and in some cases as syntheses in final reports. The information collected by the Geological Survey is of demonstrable value to industry as an aid to the discovery and development of mineral and energy resources. The industry has stated repeatedly that the relatively high level of information provided by government agencies makes Canada attractive for resource exploration. The pressure for the speedy release of information is a measure of the need. "Current Research" reports are one response to this demand. The release of manuscript compilation maps and reports through the Open File system is another. In the remainder of this Introduction some of the results of the 1978 program are highlighted.

Reports 42 and 56 present results of studies of the metallogeny of the northern Cordillera undertaken with a view to integrating existing mineral commodity and regional geological work. The idea is to examine large scale geological controls in relation to the distribution of known mineral deposits and to pinpoint areas where more detailed geological mapping should be done in the future. The work is of course primarily designed to aid in assessing the mineral potential of this promising area. Report 42 presents the results of a study of 33 skarn deposits and a subdivision of these into four main groups of which only the W-Cu group is economically significant. Report 56 describes the metallogeny of three significant stratiform base metal occurrences discovered recently in Lower Paleozoic sedimentary rocks in Yukon and adjacent Northwest Territories. Reports 41 and 46 are progress reports on a major study of the geology of copper and molybdenum resources of Canada. This study is designed to assist in estimating Canada's resources of these commodities, to provide guides to their discovery, and to provide advice to government on which mineral policy can be based. The similarity of the Cu-Mo occurrences at Matachewan, Ontario to those of the Cordillera are outlined in report 41. Report 46 describes a variety of copper occurrences found on the north shore of Lake Huron.

Uranium continues to play a major role in our energy strategy and reports 12, 13, 27, 45, and 52 present results from a variety of studies on uranium deposits carried out in widely separated areas.

A variety of geochemical studies were carried out during the 1978 field season. Most of these were concerned with the search for and appraisal of mineral resources. Such studies obviously interface with those concerned with Economic Geology described above. Report 51 supplements the study of the metallogeny of the northern Cordillera mentioned above. The measurement of uranium in water samples is useful in indicating possible mineral occurrences. Report 54 present the results of a study on the stability of uranium in such waters and the conclusion is drawn that uranium is stable and that such tests are valid.

Paleontology is one of the most important tools for dating rocks, for correlating them and for understanding the conditions under which they were deposited. This information is of great importance in evaluating our hydrocarbon resources. For example report 38 describes the most recent results of a study of the conodont biostratigraphy of the Siluro-Devonian rocks of the Canadian Arctic Islands. Conodonts are small plate-like structures whose biological function is not understood but which have proven useful in correlation. This study, initiated in 1968, is designed to set up a biostratigraphic framework based on conodonts and to relate this to others based on other fossils. The final result will be a correlation tool useful in areas that lack other fossil assemblages.

Studies in petrology are carried out to provide a better understanding of the processes of formation of igneous and metamorphic rocks. Such knoledge is fundamental to broadening our understanding of the geology of Canada and thus to more immediate concerns such as mineral resource evaluation. Reports 15, 16, 26, 34, and 57 contribute to this objective. For example report 15 presents results of an ongoing study of the alkaline rocks of Canada. Alkaline rocks have been somewhat ignored in the search for minerals deposits but molybdenum, zirconium, copper and apatite are currently being recovered from alkaline rocks and they are a major source of niobium, rare earths, nepheline, barite, vermiculite, corundum and diamond.

Regional geology studies form a principal input into the data base which must continue to be expanded if more sophisticated resource estimates are to be made. The balance of this introduction highlights some of these activities.

The Cordilleran region is one of complex geology and considerable mineral potential and during 1978 studies continued in various parts of the area including the following. Detailed studies of the Shuswap Metamorphic Complex (report 8) were continued west of Downie Creek, B.C. as part of an ongoing study of the Selkirk and Shuswap terranes. Besides its classical geological aspect the study has engineering geology implications in view of the projected Revelstoke reservoir. Reports 36 and 37 present preliminary results of studies of an area in northeastern British Columbia underlain by rocks which range in age from Helikian to Cretaceous. These studies are part of a project initiated in 1963 and designed to establish the stratigraphic framework of the northern Rocky Mountains. A study of possible coal-bearing beds in the Kamloops Group (report 53) indicates that there is little chance that economic coal seams are present due to the conditions under which the beds were deposited.

The Precambrian Shield continues to be the site of considerable field activity by geologists of the Survey. Reports 19 and 20 present results of studies of the geology of the Foxe Fold Belt, Baffin Island. This project, started in 1974 is nearing completion. It is designed to establish the stratigraphy, structure, and metamorphic history of the Aphebian sedimentary, volcanic and plutonic rocks of the Piling Group to elucidate their relationships to the rocks of the Mary River Group some of which contain significant iron deposits. Systematic 1:250 000 scale mapping continued in several areas of the Shield. Report 25 gives preliminary results for areas 85 N and 86 D. Report 31 presents results of detailed mapping in 65 O where 1:250 000 mapping is planned for 1979. Mapping at the same scale was carried out on eastern Devon Island (report 22).

Reports 43, 49 and 50 contain preliminary results of investigations carried out in the Appalachian Region by university staff members under contract to the Geological Survey. Other reports in this volume of Current Research are also theresult of contract work. This approach allows the Survey to undertake activities that might not otherwise be possible during a period of restraint.

December 1, 1978

R.G. Blackadar
Chief, Scientific Editor

Separates

A limited number of separates of the papers that appear in this volume are available by direct request to the individual authors. The addresses of the Geological Survey of Canada offices follow:

601 Booth Street,
OTTAWA, Ontario
K1A 0E8

Institute of Sedimentary and Petroleum Geology,
3303-33rd Street N.W.,
CALGARY, Alberta
T2L 2A7

British Columbia Office,
100 West Pender Street,
VANCOUVER, B.C.
V6B 1R8

Atlantic Geoscience Centre,
Bedford Institute of Oceanography,
P.O. Box 1006,
DARTMOUTH, N.S.
B2Y 4A2

When no location accompanies an author's name in the title of a paper, the Ottawa address should be used.

1. # FIVE OCCURRENCES OF TRANSPORTED SYNOROGENIC CLASTIC ROCKS IN YUKON TERRITORY

Project 730037

D.J. Tempelman-Kluit
Regional and Economic Geology Division, Vancouver

Tempelman-Kluit, D.J., Five occurrences of transported synorogenic clastic rocks in Yukon Territory; in Current Research, Part A, Geol. Surv. Can., Paper 79-1A, p. 1-12, 1979.

Abstract

Sheared immature clastic rocks are structurally interleaved with cataclastic rocks that occur as an extensive allochthon (Yukon Cataclastic Complex) in western Omineca Crystalline Belt. This clastic assemblage, not previously recognized as one unit because of its heterogeneity, probably represents fanglomerate and turbidite deposits. It contains clasts of mylonite, volcanic rocks, limestone, quartz, feldspar, chert and granitic rocks derived from the allochthonous cataclastic complex and not the autochthon below. At one locality two separate tectonic slices of these rocks, each of different facies, contain Upper Triassic conodonts which probably date the entire assemblage. Near Dawson City a clastic unit, hitherto regarded as late Precambrian, contains mylonite debris like that of the Triassic synorogenic suite. The synorogenic rocks record the cataclasis attendant upon collision along Teslin Suture in the Late Triassic (?and Early Jurassic?). Their final emplacement above autochthonous strata occurred in the Early Cretaceous.

Introduction

In Quiet Lake and Finlayson Lake map-areas (105 F, G) three slices of allochthonous transported cataclastic rocks, a siliceous mylonite, a dismembered ophiolite and a sheared suite of granitic rocks, are thrust northeastward over autochthonous Paleozoic and early Mesozoic miogeoclinal strata (see Fig. 1.1) (Tempelman-Kluit, 1977a, 1977b). Locally within the transported cataclastic rocks and at their tectonic base are clastic rocks with debris from the allochthonous assemblages. Five localities (Fig. 1.1), where reconnaissance mapping suggested possible occurrences of these clastics, are described and their tectonic significance is summarized.

Locality 1

Localities 1 and 2 are two of eight klippen near McNeil Lake in southwestern Finlayson Lake map-area (Fig. 1.2). At locality 1 (Fig. 1.3 and 1.4) muscovite quartz blastomylonite, the siliceous mylonite, is preserved as a subhorizontal sheet about 5 km long and as much as 500 m thick above late Paleozoic and Early Mesozoic strata. It is a penetratively deformed and recrystallized cataclasite (Plate 1.1) which may be the tectonized Nasina quartzite, a sandstone deposited near the southwest margin of North America in the early Paleozoic. Its cataclastic fabric is planar and dips gently southwest. In places this fabric is folded and transposed on a newer crenulation foliation that dips southwest at moderate angles.

On the northern side of the klippe a wedge of sheared, immature sandstone, about 200 m at its thickest, lies below the siliceous mylonite and above a discontinuous slice of sheared and serpentinized gabbro and basalt considered a tectonic "fish" of the Anvil Allochthon. This sandstone contains granules to fine-sand sized angular to subrounded grains of siliceous mylonite (70 per cent) and smaller subrounded grains of quartz (10 per cent), chert (5 per cent), feldspar (5 per cent) and fine grained porphyritic andesite and basalt (10 per cent) (Plate 1.2). Shaly and silty layers within the sequence contain angular grains of the same materials with up to 20 per cent detrital muscovite. The sandstone locally shows layering by shape alignment of the tabular grains, but bedding is rare. The unit appears massive or very thick-bedded and the general orientation of bedding is unknown.

The sandstone is strongly sheared and in places approaches mylonite. The strain is concentrated in discontinuous, subhorizontal, lenticular zones tens of metres thick and hundreds of metres long which separate weakly strained or unsheared rocks. The sandstone is particularly sheared near its upper and lower contacts (Fig. 1.4). In the shear zones the rocks are dismembered through movement on irregular, sinuous, branching surfaces of varied spacing and displacement (Fig. 1.6) which separate lenses of less deformed sandstone. In places the sandstone is so strongly sheared that it approaches mylonite and distinction between sandstone and tectonite is difficult.

The youngest rocks preserved beneath the klippe are thin bedded calcareous siltstone with interbedded silty limestone of Upper Triassic age. These rocks are neither metamorphosed nor sheared and conodonts as well as fine detail of sedimentary structures are preserved in them immediately beneath the transported rocks (Fig. 1.5).

Locality 2

Synorogenic clastics at locality 2 (Fig. 1.7 and 1.8) are immature greywacke as at locality 1, but they contain a preponderance of porphyritic andesite and basalt granules and grains (80 per cent) with comparatively few fragments of siliceous mylonite and quartz (20 per cent) (Plate 1.3). Shaly and silty rocks are more voluminous than sandstone and the finer grained rocks contain less detrital muscovite than those at the first locality. The rocks are dark, massive and strongly factured and weather recessively. On some weathered surfaces graded bedding and small scale crossbeds can be seen. As at the first locality, the sandstone is strongly sheared in discrete zones and approaches mylonite (Plate 1.4). Toward its upper contact the sandstone is progressively more sheared and, in places, the transition to the overlying mylonite is structurally gradational. Distinction between mylonite and sandstone is arbitrary and it is uncertain how much of the mylonite is simply cataclastized sandstone. In contrast, the contact between the sandstone and autochthonous rocks below shows an abrupt change in the degree of shearing. The underlying Devono-Mississippian black slate is not sheared whereas the overthrust sandstone generally has a protoclastic fabric.

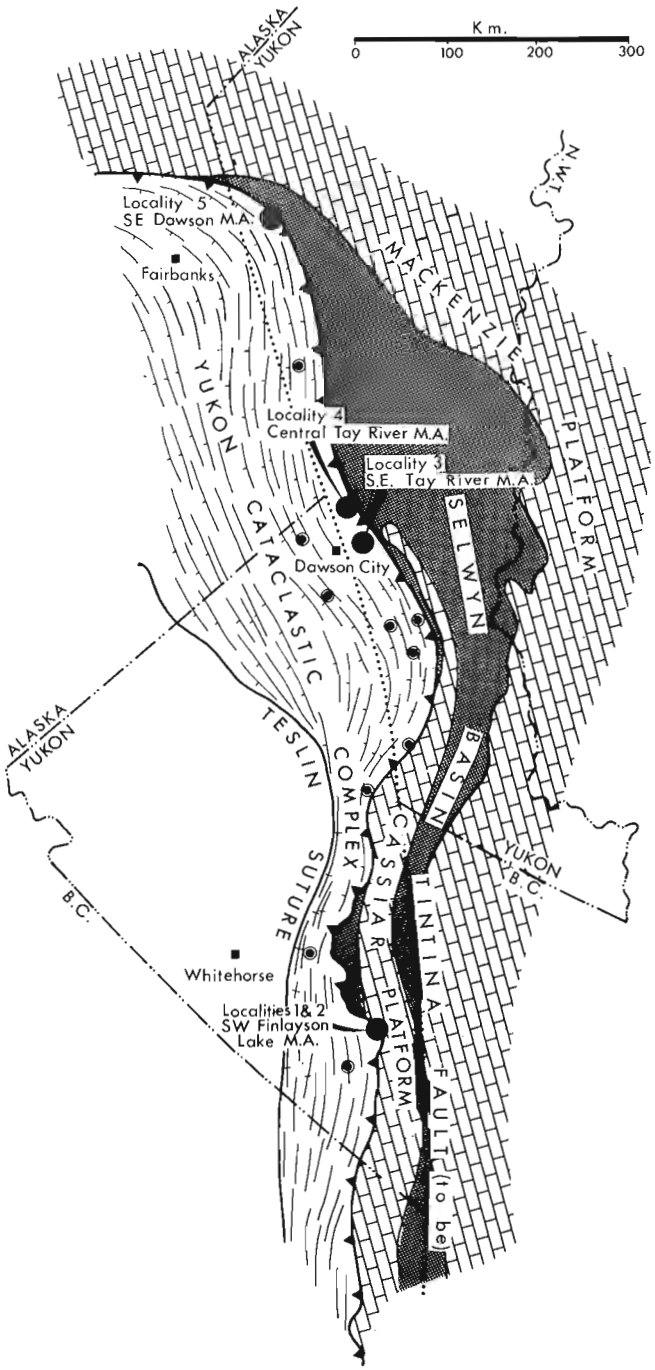


Figure 1.1. *Reconstruction of part of the northern Cordillera showing occurrences of synorogenic clastic rocks within or beneath transported cataclastic rocks. The sketch does not distinguish the three assemblages that make up the allochthonous Yukon Cataclastic Complex, but some of the Early Paleozoic depositional elements in the autochthon are shown for reference (Mackenzie Platform, Selwyn Basin, Cassiar Platform). Occurrences are shown by circled dots and the numbered localities (large dots) are described in this report. This reconstruction is made by restoring the 450 km of right lateral displacement on the Tintina and northern Rocky Mountain faults that took place in the mid-Cretaceous.*

Locality 3

Locality 3 on the north Canol road near the mouth of Tenas Creek exposes an unusually chert-rich variety of the synorogenic clastics (Plate 1.5). Exposure does not show the field relations and young faults are presumed to separate the conglomerate from surrounding exposures of Anvil and Nisutlin allochthonous rocks. The rocks contain grey and black chert (70 per cent) and quartz (10 per cent) grains, granules and pebbles with numerous phyllonite fragments (20 per cent), some detrital muscovite, and minor intermediate volcanic grains. Chert pebbles contain radiolarians that are partly recrystallized. Phyllonite grains appear to show all gradations to chert and are assumed to be the cataclastic product of chert. Texturally the rock is as immature as at the other localities examined and has suffered similar postdepositional shearing. At locality 3 the clastics resemble the "Black Clastic", a Devono-Mississippian chert conglomerate, and part of the synorogenic suite may previously have been mapped as the "Black Clastic".

Locality 4

The coarsest grained variety of the synorogenic assemblage, dominantly cobble conglomerate, is found at locality 4 on the south flank of Rose Mountain and near Faro.

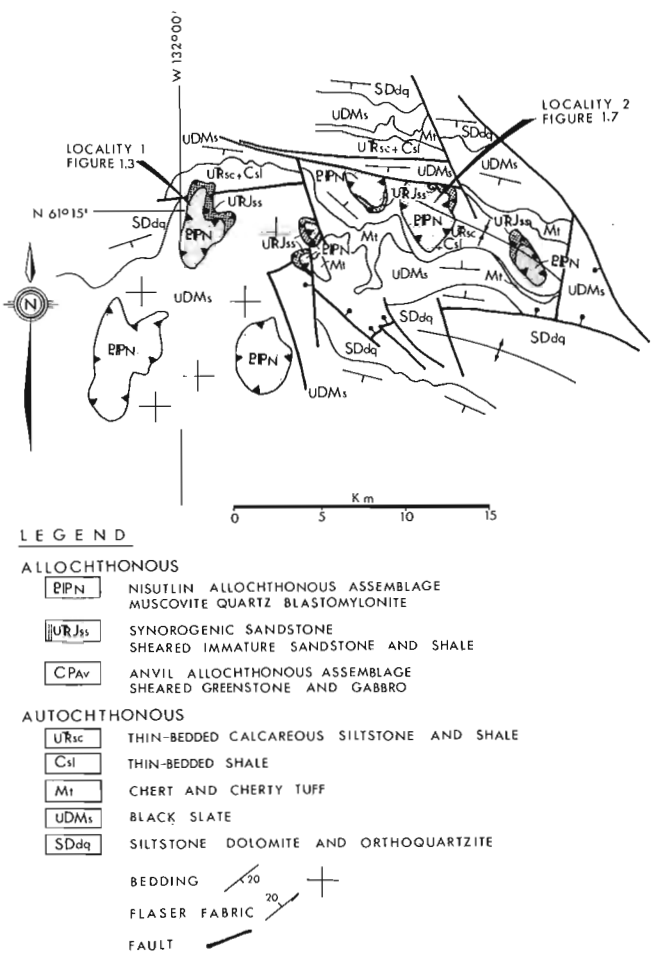


Figure 1.2. *Map of the eight McNeil klippen to show their relative location and setting of localities 1 and 2 (Fig. 1.3 and 1.7).*

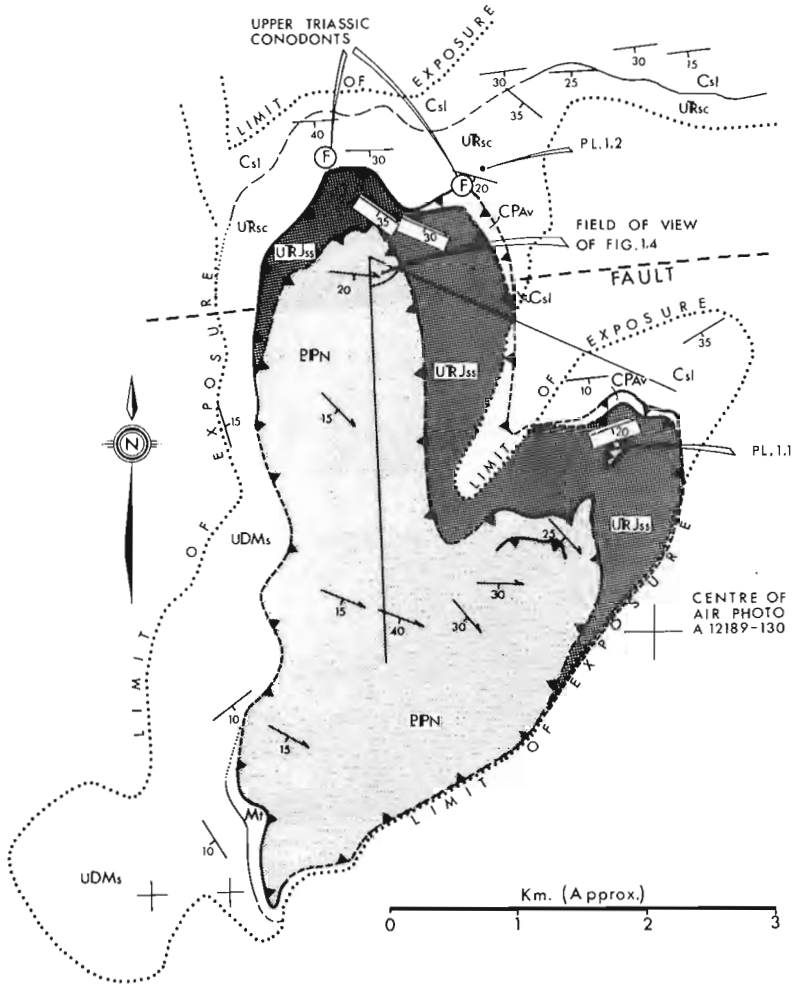


Figure 1.3. Sketch map of one of the McNeil klippen at locality 1. Sheared synorogenic sandstone with debris derived from the overthrust allochthonous rocks lies above undeformed autochthonous Late Paleozoic and Early Mesozoic strata. Airphoto A12189-130 is the base for the sketch. The legend is as for Figure 1.2.

The rocks are well indurated, massive, brown-weathering conglomerate and sandstone (Plate 1.6A) with subrounded cobbles to sand-sized grains of siliceous mylonite and blastomylonite (40 per cent), phyllonite (15 per cent), chert (10 per cent), greenstone (15 per cent), sheared granitic rocks (10 per cent), limestone (5 per cent) and clasts of the sandstone (5 per cent). Sand-sized grains are much more angular than the larger granules pebbles and cobbles. Mylonite clasts resemble the siliceous mylonite found, for example, in the McNeil klippen (Plate 1.6B and 1.6C). Phyllonite and chert clasts are like those of locality 3. The sandstone clasts are finer grained varieties of the conglomerate (Plate 1.6D and 1.6E). Most granitic pebbles are weakly sheared biotite quartz monzonite with large, zoned, subhedral perthite and albite phenocrysts in a finer, quartzofeldspathic groundmass that locally preserves vermiform and cuneiform intergrowths but which is generally sheared and comminuted around the feldspar (Plate 1.6F and 1.6G). Sheared hornblende granodiorite pebbles also occur. The limestone cobbles, commonly the largest fragments in the conglomerate, attain a diameter of a metre and include several varieties. Some are limestone mylonite, but most are not sheared. Of those that are not cataclastic most are probably Upper Triassic; conodonts of that age are found commonly. One boulder has Lower Paleozoic conodont fragments and another Upper Paleozoic fusulinids.

Relations of the conglomerate are well exposed in a small tributary of Pelly River 3 km west-southwest of the peak of Rose Mountain. Here the conglomerate is variably sheared and tectonically interleaved with its finer grained equivalents, which are similarly sheared. Different depositional facies of the synorogenic sequence are therefore juxtaposed tectonically (Fig. 1.9).

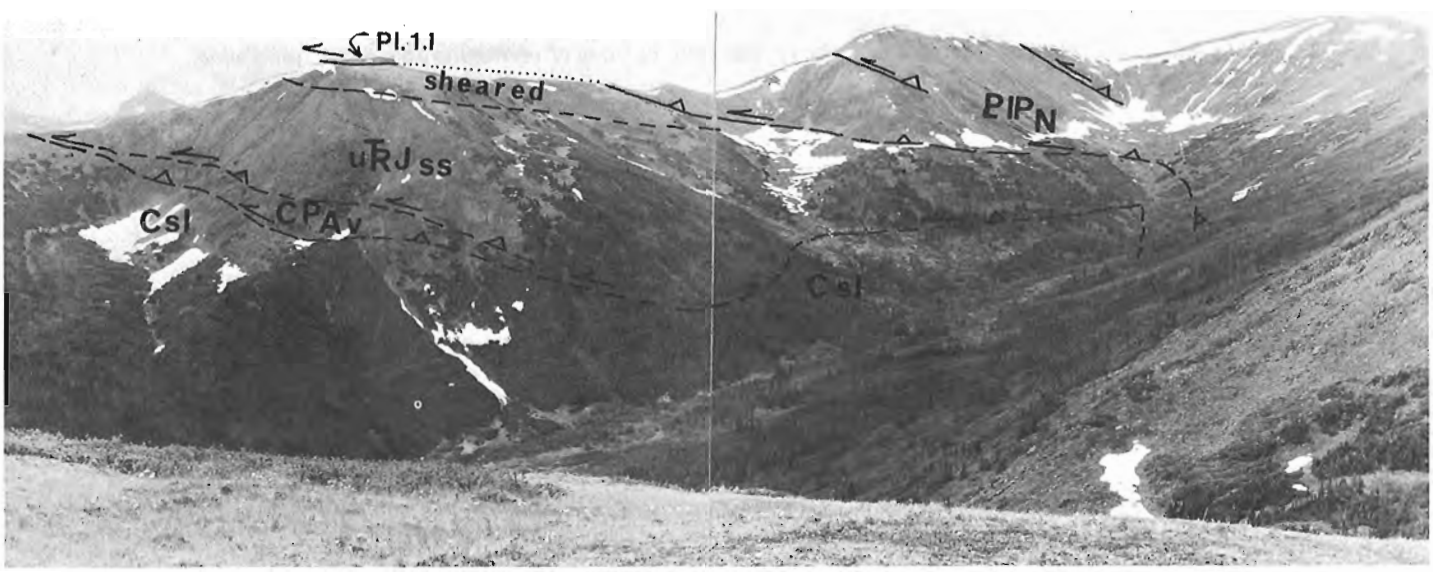
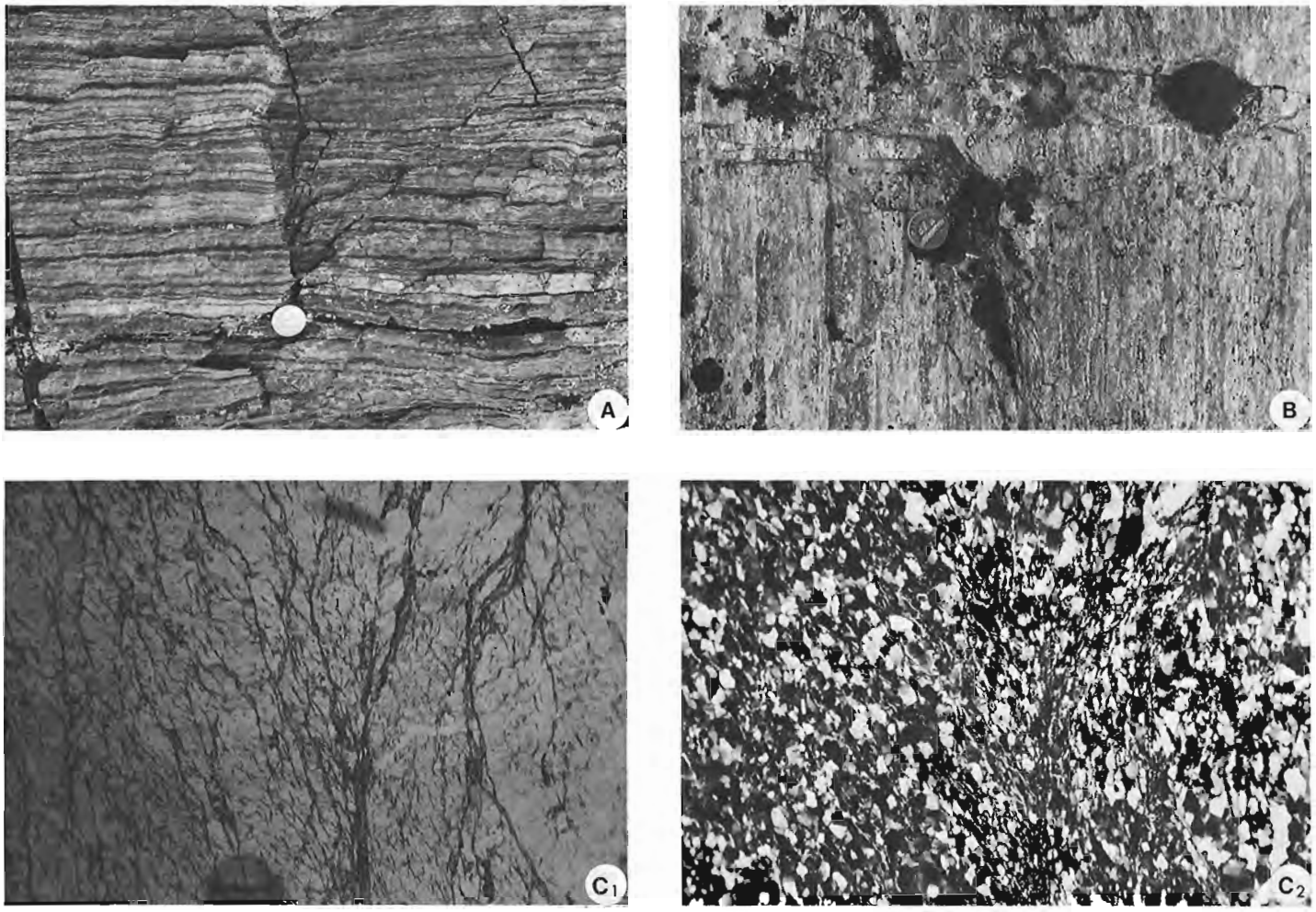


Figure 1.4. View of the eastern ridge at locality 1 (Fig. 1.3). Structural sequence from the base up (left to right) is Csl – undeformed Carboniferous slate (autochthon); CPAv – strongly sheared basalt and gabbro (lowest allochthonous wedge); uTJss – sheared synorogenic sandstone with a strongly sheared zone about 40 m thick at the top; PPN – siliceous mylonite.



A is a view perpendicular to the flaser fabric.

B shows the well developed rodding or lineation on many of the flaser surfaces.

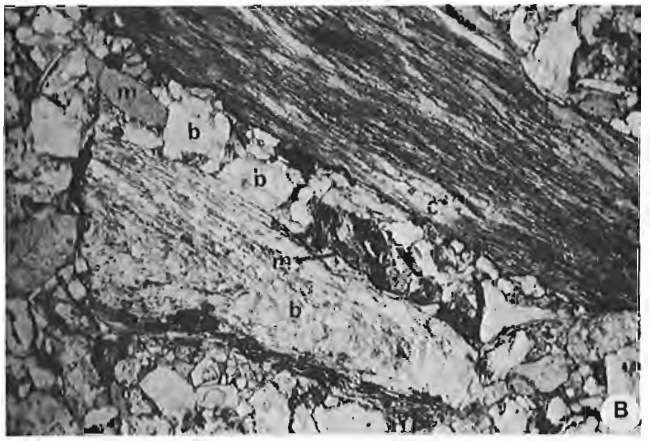
C is a pair of photomicrographs of the same rock in plane polarized light and with crossed nicols.

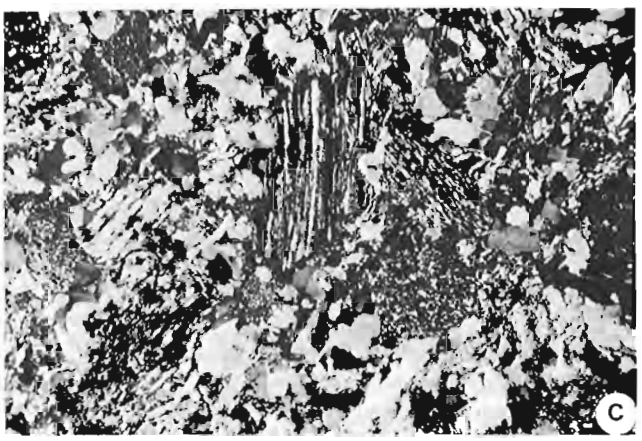
Plate 1.1. *Siliceous mylonite at locality 1. The field of view of photomicrographs is 2 mm wide.*

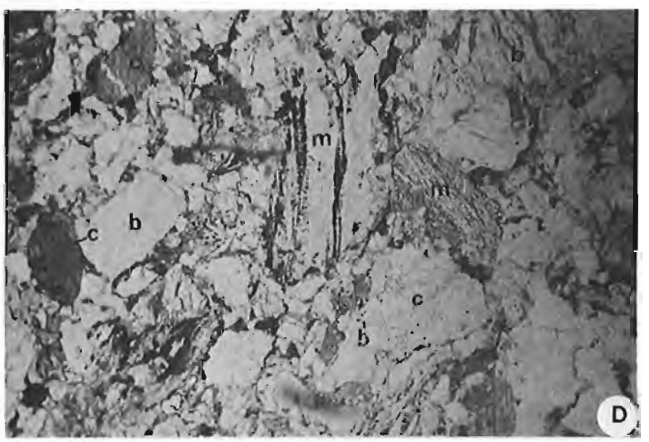
Plate 1.2 *(opposite)*

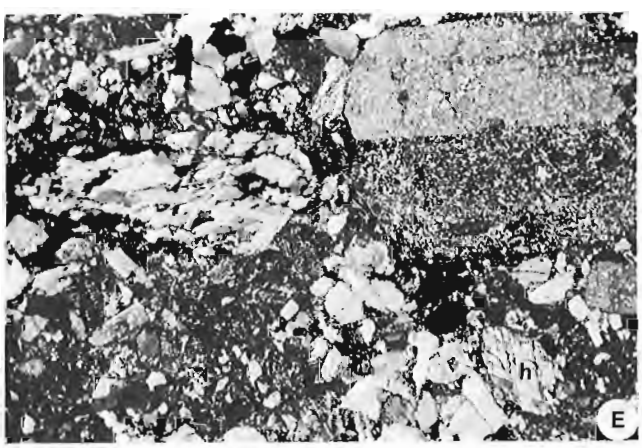
Pairs of photomicrographs of synorogenic sandstone from locality 1 in plane polarized light and under crossed nicols. Note the tabular grain shape, textural immaturity and grain size variation. Most grains are mylonite (m), blastomylonite (b), quartz (q), feldspar (f), hornblende (h) or sheared chert? (c) but fragments of andesite (v) are present. Note particularly that the cataclastic fabric of the grains has different orientation from grain to grain. In some grains the flaser fabric is folded. All degrees of blastesis are represented by the detritus. The field of view is 2 mm wide.

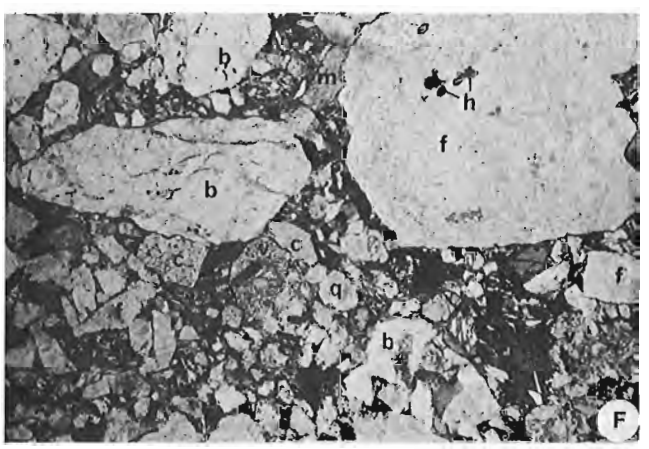

A

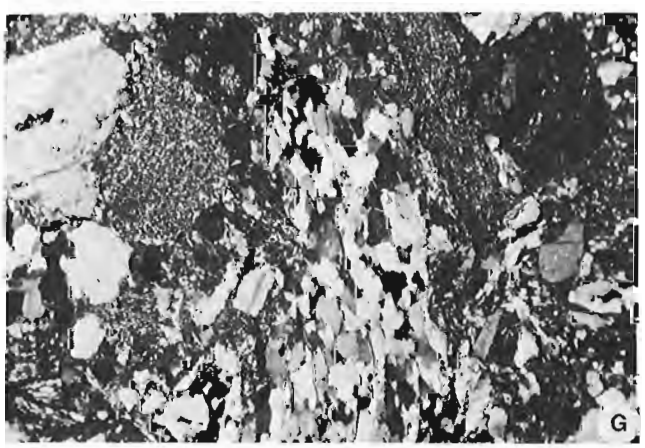

m
b
b
m
b
B

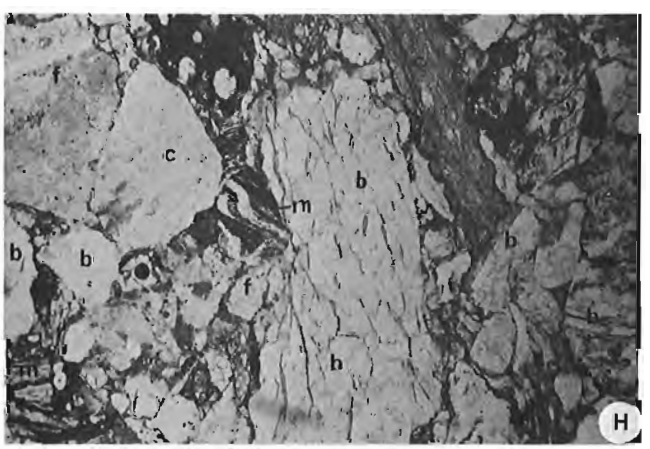

C


m
m
c
b
c
b
D


h
E


b
m
h
f
b
c
q
b
f
F


G


c
b
m
b
b
b
f
b
H

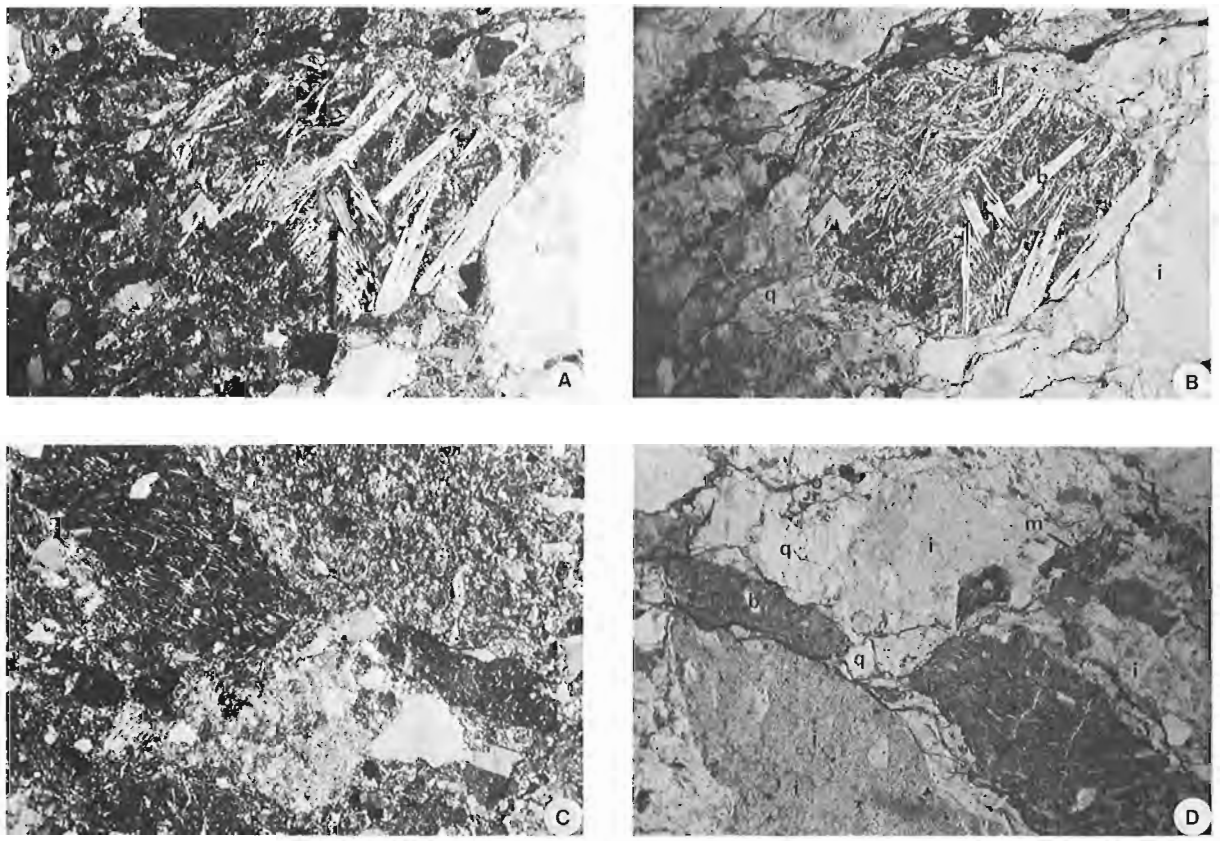


Plate 1.3. *Photomicrographs of sandstone from locality 2. In contrast to sandstone from locality 1 this rock contains a preponderance of intermediate (i) to basic (b) volcanic fragments with relatively little mylonite (m) and quartz (q). Note the absence of shearing in the volcanic clasts. Although many of the clasts are fresh like those in the photos others are strongly saussuritized. The field of view is 2 mm wide.*

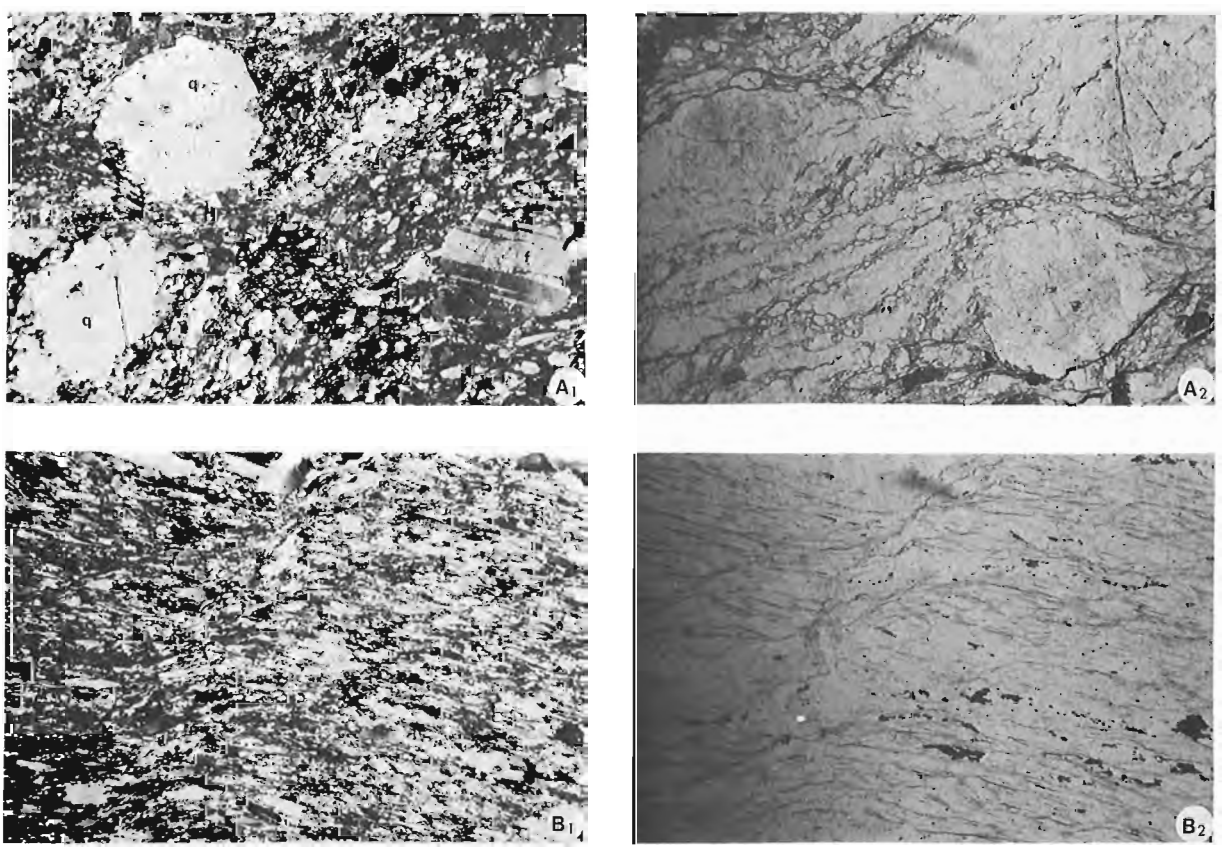


Plate 1.4. *Photomicrographs of protoclastic and more highly sheared sandstone from locality 2. Note the augen in A which represent weakly granulated originally detrital grains surrounded by a more tectonized finer grained groundmass. Where extreme shearing has occurred (B) the rock is indistinguishable from the siliceous mylonite (compare with Plate 1.1C). The field of view is 2 mm wide.*



Figure 1.5. *Thin bedded calcareous siltstone and silty limestone (uTsc), the youngest autochthonous strata exposed at locality 1. The outcrop is about 20 m below the lowest allochthonous cataclastic rocks (CPAv). Note particularly the lack of deformation as illustrated by the preservation of the horizontal worm burrows and flame structure left and right of the coin and the fine lamination and crosslamination. Contrast this with the photographs of the sheared sandstone (Fig. 1.6).*

Direct evidence for the age of the clastic assemblage is available in two of the tectonic slices at locality 4. Upper Triassic conodonts were found in two facies of the clastic rocks. In the tectonically higher one they are in limy sandstone that is interbedded with conglomerate; in the lower slice the conodonts were found in impure shaly limestone which also contains phyllonite chips (Plate 1.7). Neither conodont collection contains mixed faunas or other features that might suggest the fossils are detrital and derived from older rocks. The collections date the synorogenic clastics at locality 4.

Locality 5

About 5 km northeast of Dawson City shale, sandstone, gritty conglomerate and minor limestone are thrust as a tectonically imbricated stack above Upper Jurassic black slate which is in turn thrust over a thick Lower Cretaceous siltstone (Fig. 1.10). The overthrust shale is maroon and olive green and contains much detrital muscovite. The gritty rocks contain mostly subrounded quartz (70 per cent), blastomylonite (15 per cent) and feldspar (15 per cent) granules and grains (Plate 1.8). The rocks are less sheared internally than at other localities. The tectonically imbricated stack has been regarded as part of the Late Precambrian "Grit Unit" (Green, 1972; Tempelman-Kluit, 1970) but the cataclastic fragments and muscovite are not compatible with that correlation and these gritty rocks are more likely equivalents of the synorogenic suite described above. This implies that the 120 km wide, 300 km long stretch (broadly between Dawson and Ross River on the northeast side of Tintina Fault) mapped as "Grit Unit" is possibly in part or altogether the Mesozoic synorogenic sequence and that these rocks were tectonically emplaced during the Laramide orogeny.

Synthesis

Strata at the five localities are thought to be part of the same synorogenic clastic assemblage. They are an immature, heterogeneous assemblage of conglomerate, sandstone and shale that differs from place to place, in composition, in grain size, and in grain roundness. Some or all of the common clast-types are found at each locality. These include mylonite, blastomylonite, quartz, muscovite, chert, phyllonite, unsheared intermediate volcanics, protoclastic quartz monzonite and granodiorite and limestone.



Figure 1.6.

Sheared synorogenic sandstone immediately beneath overthrust siliceous cataclasite (see Fig. 1.3 for location). This rock is dismembered by movement on numerous discrete, sinuous, irregular branching surfaces that separate blocks or lenses of varied shape and dimensions that are much less strained.

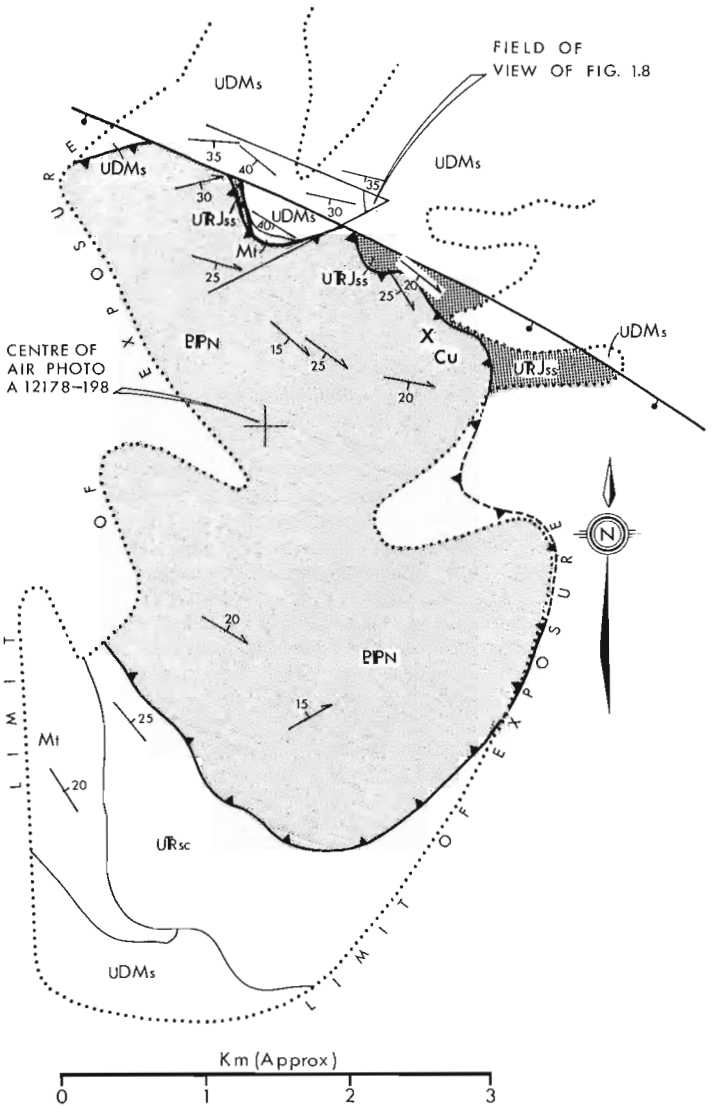


Figure 1.7. Sketch map of locality 2. Sheared synorogenic sandstone lies beneath siliceous mylonite and is faulted against the autochthonous Upper Paleozoic strata to the north on a steep normal? fault along most of its length. The legend is the same as for Figure 1.2.

Most clasts are derived from the allochthonous rocks northeast of Teslin Suture and the sedimentary and volcanic rocks southwest of the suture. Mylonite, muscovite, and part of the quartz are abundant in the siliceous cataclastic rocks that were thrust over autochthonous miogeoclinal strata. Chert may originate from the dismembered ophiolite slice and feldspar, some quartz and the granitic pebbles from the transported suite of sheared plutonic rocks. The limestone clasts probably derive mainly from the Lewes River Group along Teslin Suture because many contain Upper Triassic conodonts as does that limestone. Some limestone clasts derive from the siliceous allochthon, which contains sheared limestone and some Late Paleozoic carbonate. The source of the intermediate volcanics may be the Lewes River – Laberge groups which include basalt and whose clastic rocks contain volcanic debris like that found in the synorogenic rocks. The origin of the Lower Paleozoic limestone clast at locality 4 is not known. None of the clast-types originates from the overridden autochthonous Paleozoic or Mesozoic miogeoclinal strata.

The clastics are probably at least in part Upper Triassic. Two distinct facies exposed in separate tectonic slices contain late Triassic conodonts at locality 4 and the clastic rocks elsewhere are presumed to be of like age. Even if the conodonts at locality 4 are detrital, and the absence of mixed fossil populations suggests otherwise, the clastic rocks must be late Triassic or younger. Parts of the sequence with abundant volcanic and granitic debris resemble beds of the Lewes River – Laberge groups, the Upper Triassic and Lower Jurassic turbidite of the Intermontane Belt southwest of Teslin Suture (Fig. 1.1). However cataclastic detritus is unknown in the Lewes River and Laberge sediments.

Depositional features of the sandstone were rarely seen and although many characteristics associated with turbidite sequences are absent or obscured by shearing, the assemblage was probably laid down as fanglomerate and turbidite deposits.

Structural relations of the synorogenic clastics differ. At each locality where relationships are seen the sandstone is tectonically emplaced and is imbricated and much more sheared than the autochthonous rocks below. In places the shearing was so penetrative that the sandstone is mylonite indistinguishable from the superjacent allochthonous cataclastic rocks. How much mylonite results from cataclasis of sandstone and how much is the parent that supplied mylonite detritus to the sandstone is therefore unknown. (The chicken and the egg.)



Figure 1.8.

View of synorogenic greywacke (uTJss), autochthonous Devono-Mississippian black slate (uDMs) and allochthonous siliceous mylonite (PPN). Note the strongly sheared zone in the lower part of the sandstone slice. The location of this view is shown in Figure 1.7.

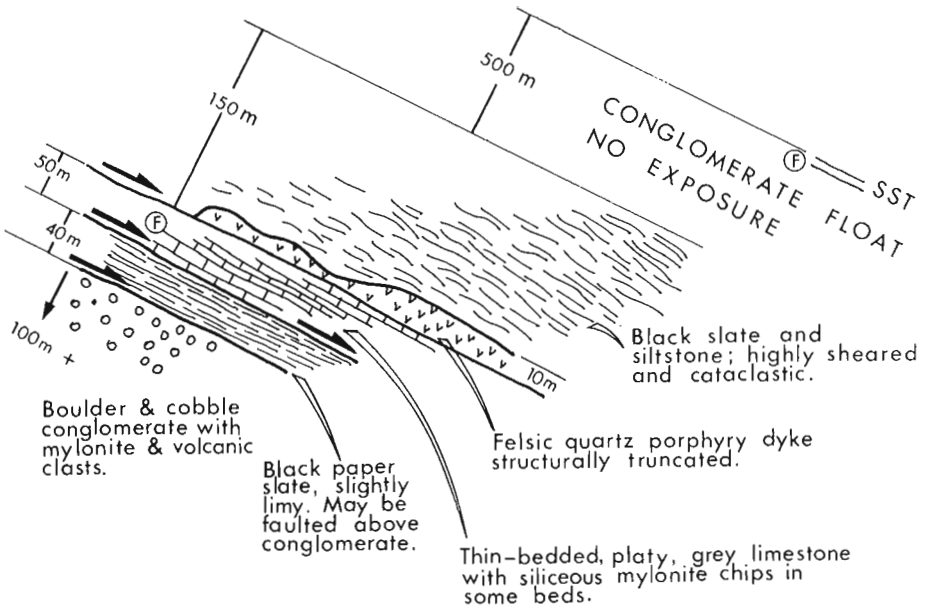


Figure 1.9.

Sketch of relations exposed in small tributary of Pelly River 3 km west-southwest of the peak of Rose Mountain. Different facies of the synorogenic sequence are tectonically juxtaposed on gently northeast dipping faults. The tectonic wedges contain similar detritus in varied proportions and exhibit varied texture and degree of post-depositional shear. Upper Triassic conodonts were found in both a limy sandstone (top) with mylonite grains and much detrital muscovite and a structurally lower limestone with mylonite and phyllonite grains (Plate 1.7).

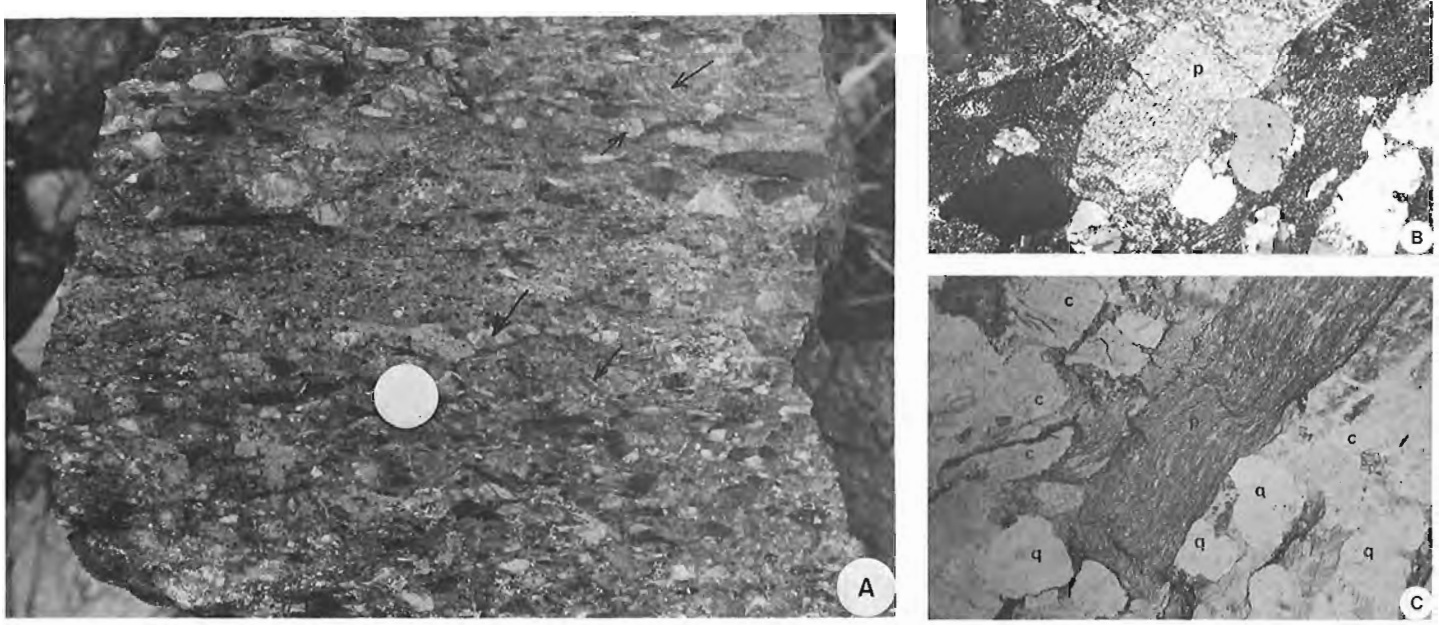
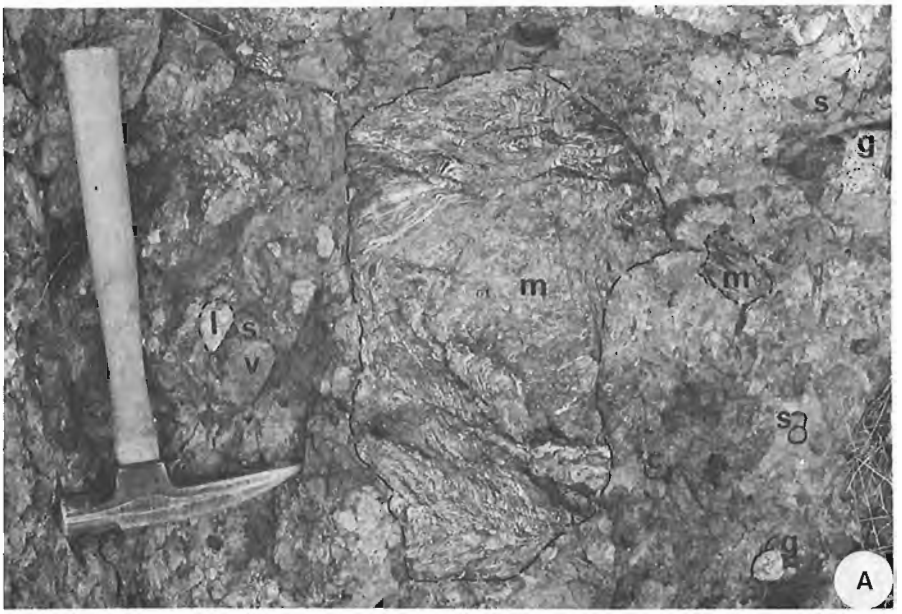


Plate 1.5. *Conglomerate from locality 3. This rock contains chert, quartz and phyllonite grains with some detrital muscovite. It is texturally immature and has been post-depositionally sheared. Note the flattened grains and closely spaced quartz filled fractures sloping across the flattening fabric (arrows). The pair of photomicrographs (crossed nicols and plane polarized light) shows one end of a tabular phyllonite fragment (p) surrounded by chert (c) and quartz (q) grains. The field of view is 2 mm wide.*

Plate 1.6

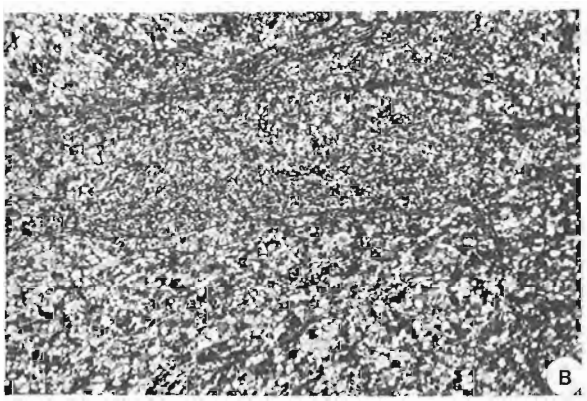


A. Conglomerate from locality 4 near Faro. Note the range in clast size and the variety in clast lithology; mylonite-m; granitic-g; sandstone-s; limestone-l; greenstone-v. The large mylonite fragment is slab shaped and its flaser fabric is folded and transposed by a newer crenulation foliation.

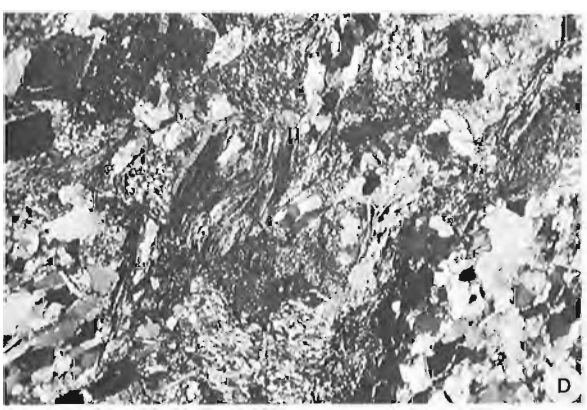
B-C. Photomicrographs of part of a mylonite-blastomylonite clast from the conglomerate in A. Note that this rock closely resembles the mylonite of Nisutlin Allochthon (Plate 1.1C). The field of view of the photomicrographs is 2 mm wide.

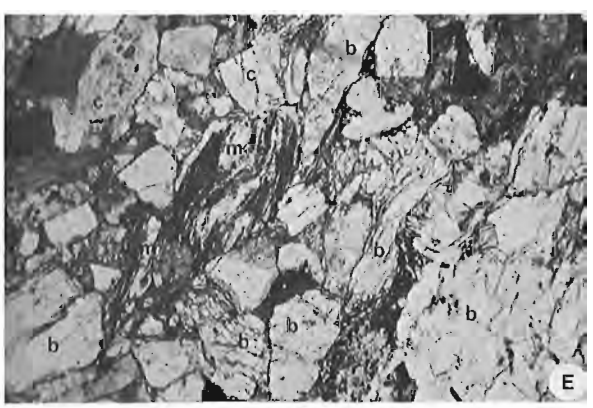
D-E. Photomicrographs of part of a sandstone fragment from the conglomerate in A. Note that the mylonite (m) and blastomylonite (b) grains have fabric at different orientations indicating the fabric is predepositional.

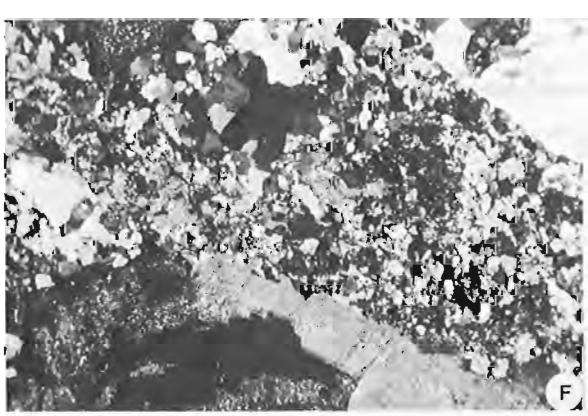
F-G. Photomicrographs of part of a biotite quartz monzonite cobble from the conglomerate in A. Note the large zoned K-spar (partly sericitized) rimmed by the fine grained, quartzofeldspathic groundmass which exhibits weak protoclastic fabric.

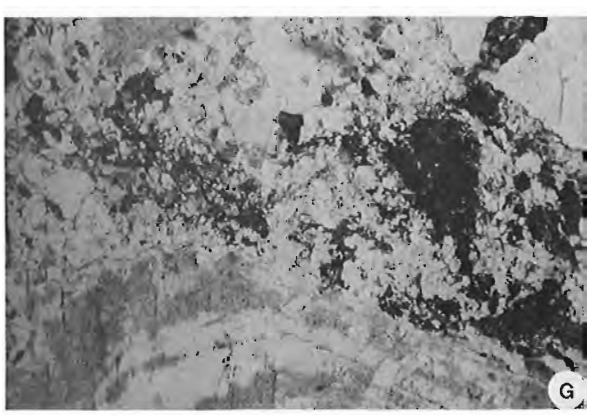




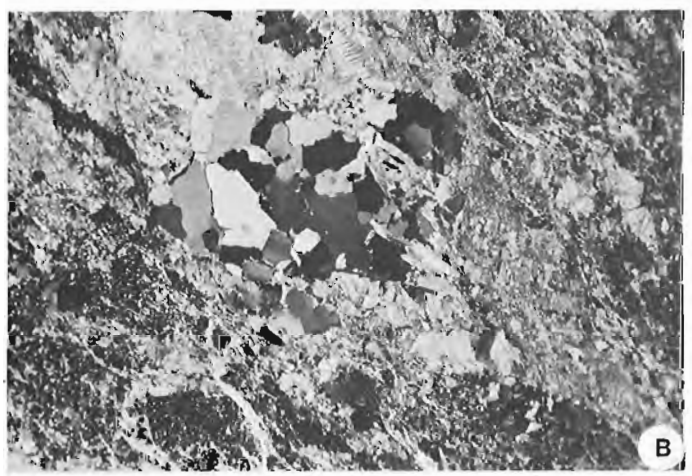












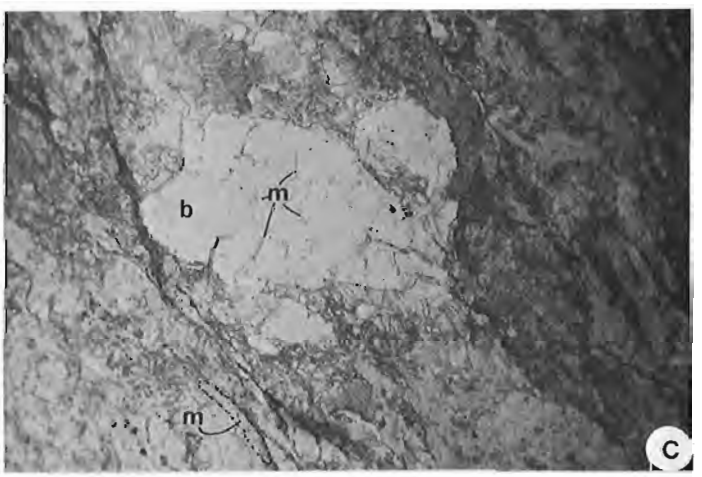


Plate 1.7

A. Bedding surface of thin bedded, dark grey limestone with phyllonite and mylonite chips which is structurally interleaved with coarser grained facies of the synorogenic sequence (see Fig. 1.9).

B-C. Photomicrographs of a blastomylonite chip (b) and muscovite flakes (m) in sparry calcite (c) from the limestone shown in A. Calcite partly replaces the cataclastic fragment. The field of view is 2 mm wide.

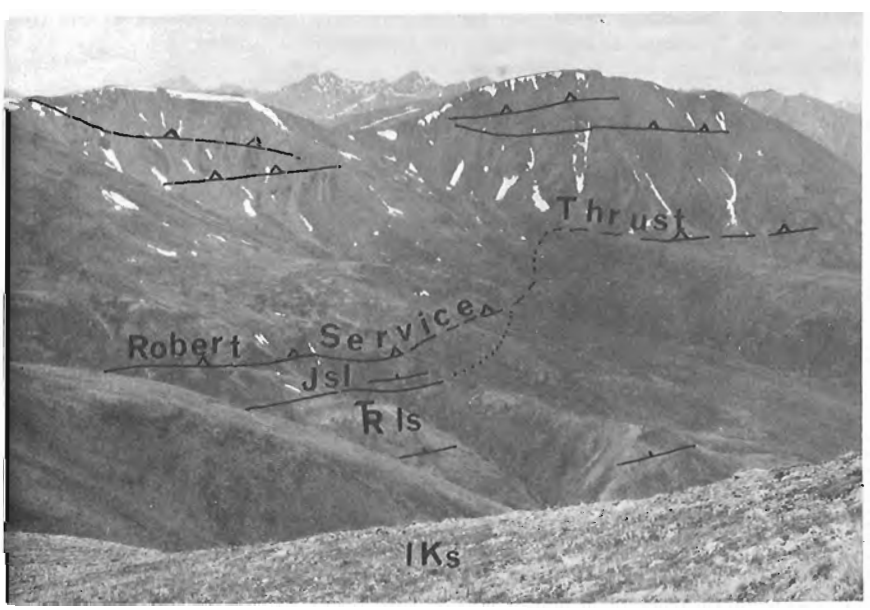


Figure 1.10.

View of the Robert Service Thrust 5 km east of Mile 38 on Dempster highway (locality 5). Gritty and shaly rocks form an imbricated tectonic stack above the thrust. They contain much detrital mylonite and muscovite and are therefore probably part of the synorogenic suite instead of the Late Proterozoic "Grit Unit" as has been thought. Note that the autochthonous rocks below the imbricated tectonic stack are themselves repeated and that this involves strata as young as Early Cretaceous.

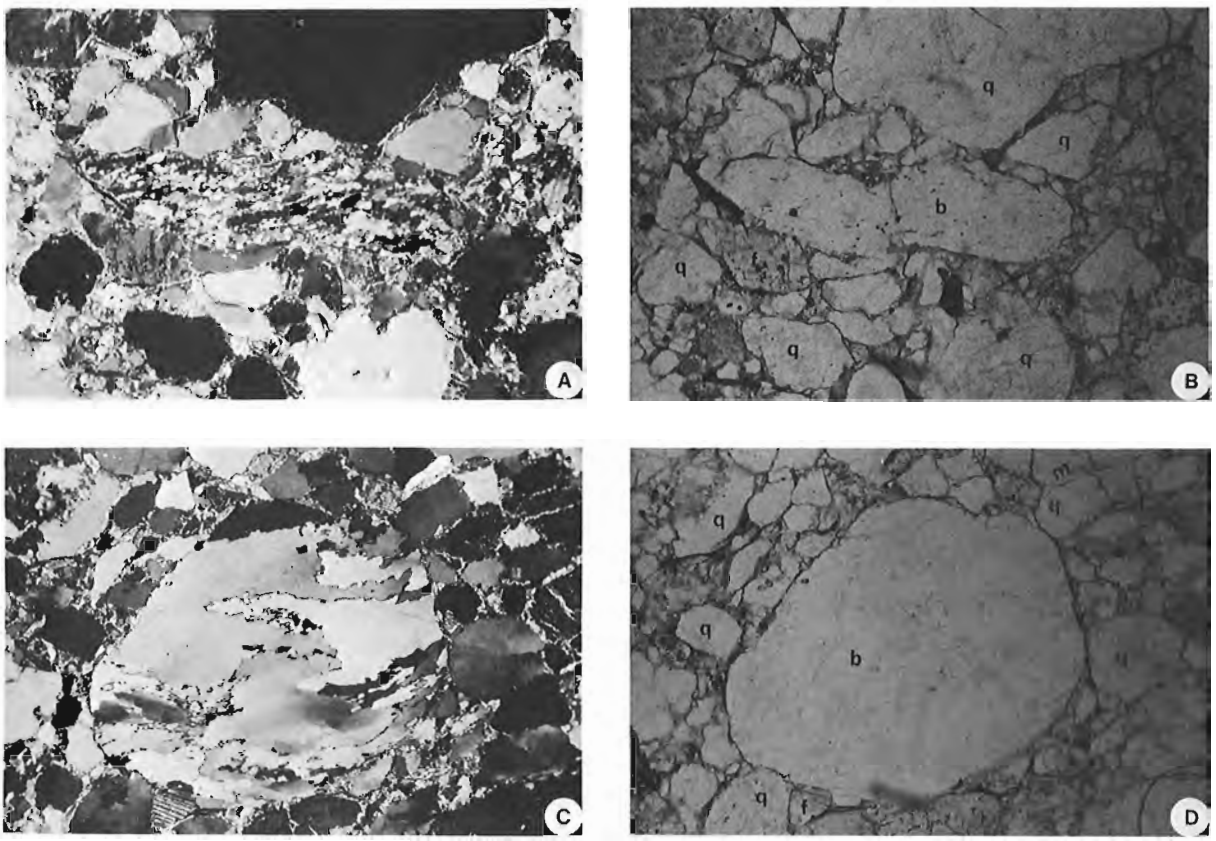


Plate 1.8. *Photomicrographs (crossed nicols and plane polarized light) of two blastomylonite grains (b), muscovite flakes (m) and albite (f) in gritty sandstone above the Robert Service Thrust (locality 5). Compared to the sandstone at other localities this rock contains more quartz and large grains are better rounded illustrating another variable in the heterogeneity of the synorogenic suite. The field of view is 2 mm wide.*

In southern localities (1 and 2) the youngest autochthonous strata below the synorogenic sandstone are Upper Triassic, but in the north (locality 5) Lower Cretaceous rocks are overridden. In both areas mid-Cretaceous plutonic rocks postdate thrusting. These relations probably reflect two discrete tectonic events. The first in the Upper Triassic (? and Lower Jurassic?) involved shearing along Teslin Suture zone. This formed the mylonite from which debris was incorporated in the Upper Triassic synorogenic clastics. Later, but possibly continuous with the first event, the clastics were sheared and imbricated by continued movement that may have involved northeastward thrusting as well as shearing along Teslin Suture. The second event in the Early Cretaceous entailed northeast thrusting of the cataclastic rocks and their derived detrital and sheared detrital products. The cataclastic rocks were thrust as an already imbricated stack over the North American miogeoclinal margin during imbrication of the autochthonous rocks.

Exploration Implications

In view of the probable Upper Triassic age of the synorogenic rocks they may contain concentrations of copper as do time equivalent strata of the Lewes River – Laberge groups. Minor, fine grained chalcopyrite disseminated in two small specimens of float of the sheared sandstone or mylonite were found in talus at locality 2 (see Fig. 1.7). The occurrence may be insignificant, but the source of the float and its extent were not determined.

References

Green, L.H.
1972: Geology of Nash Creek, Larsen Creek and Dawson map-areas, Yukon Territory; Geological Survey of Canada, Memoir 364.

Tempelman-Kluit, D.J.
1970: Stratigraphy and structure of the "Keno Hill Quartzite" in Tombstone River – Upper Klondike River map-areas, Yukon Territory; Geological Survey of Canada, Bulletin 180.

1977a: Stratigraphic and structural relations between the Selwyn Basin Pelly Cassiar Platform and Yukon Crystalline Terrane in the Pelly Mountains, Yukon; in Report of Activities, Part A, Geological Survey of Canada, Paper 77-1A, p. 223-227.

1977b: Quiet Lake (105F) and Finlayson Lake (105G) map-areas, Yukon; Geological Survey of Canada, Open File 486.

2. STRATIGRAPHY OF SOUTHEASTERN SELWYN BASIN IN THE SUMMIT LAKE AREA, YUKON TERRITORY AND NORTHWEST TERRITORIES

Project 730069

S.P. Gordey
Regional and Economic Geology Division, Vancouver

Gordey, S.P., Stratigraphy of southeastern Selwyn Basin in the Summit Lake area, Yukon Territory and Northwest Territories; in Current Research, Part A, Geol. Surv. Can., Paper 79-1A, p. 13-16, 1979.

Abstract

Detailed examination of stratigraphy in the Summit Lake area has revealed: (1) coarse clastics of the late Proterozoic 'Grit Unit' are a turbidite sequence with local southeasterly paleoflow; (2) intermediate volcanic tuff, dolomite, and quartz arenite near Howard's Pass are of Cambro-Ordovician age; (3) the orange mudstone member of the Road River Formation is equivalent to graptolitic shale and siltstone which overlap platform carbonates in Mackenzie Mountains; it is overlain unconformably by Middle Devonian black shale and chert; (4) Middle Devonian chert is markedly similar to and as thick as Ordovician – Silurian (Road River) chert; (5) paleoflow of turbiditic Devono-Mississippian chert-pebble conglomerate and chert sandstone was easterly and southeasterly in the Howard's Pass area; and (6) sub-Rabbitkettle uplift involved gentle folding and local faulting.

Introduction

The stratigraphy and structure of the Summit Lake area in Nahanni map area (105 I) has been outlined previously (Gordey, 1978). This report presents additional information and modifications of the stratigraphy, and a stratigraphic cross-section from Mackenzie Mountains southwesterly into Selwyn Basin (Fig. 2.1).

Proterozoic to Lower Cambrian

Coarse quartzofeldspathic clastics of the late Proterozoic 'Grit Unit' are at least 3000 m thick. They show features typical of turbidites including graded bedding, bouma sequences, sole marks, and monotonous sequences of alternating sandstone and shale (Fig. 2.2). Fine- to medium-grained sandstone is thin to medium bedded and has shale interbeds. Coarse sandstone and minor granule or fine quartz-pebble conglomerate comprise thick (up to 110 m) medium to thick bedded units devoid of shale. Shale clasts up to 0.3 m are common in coarse grained beds (Fig. 2.3). Thin bedded, black, finely crystalline limestone occurs as a member 40 m thick low in the section. The top 800(?) m of the coarse clastics are highly calcareous, and differential weathering and different colours of calcareous (orange-brown) and siliceous (grey) cemented sandstone outline irregular concretionary patches along and locally across bedding. The coarse clastics are capped by massive, white weathering, grey to black, finely crystalline, locally sandy limestone (0-15 m). Thin to thick beds of orange weathering sandy limestone are common within coarse and fine clastics just below this stratigraphic level.

Maroon, green, purple and brown weathering shale with members of fine grained, thin to medium bedded sandstone forms the upper part of the 'Grit Unit'. The sandstone is commonly massive or, less commonly, parallel laminated or ripple cross-laminated. Local graded bedding, sole marks, and the regular alternation of sandstone with shale suggest they are turbidites. The maroon and green shales are, in part, correlative with the Backbone Ranges Formation of Mackenzie Mountains.

Coarse clastics of the lower 'Grit Unit' are interpreted as a turbidite sequence which, as indicated by the calcareous content and common limestone in the upper part may have 'shallowed' upwards. Paleocurrent data are meagre, and the southeasterly paleoflow may not be regionally representative or indicative of source direction. The rapid change from coarse clastics to fine clastics of the upper 'Grit Unit' indicates a relative rise of sea level or lowering of source area relief or both.

Lower Cambrian

Lower Cambrian strata, comprising 665 m of buff weathering noncalcareous shale and siltstone overlain by 385 m of blue-grey mudstone, are correlative with the Sekwi Formation in Mackenzie Mountains. Limestone conglomerate immediately above 'Grit Unit' shale contains archeocyathids, and was likely deposited as debris flows, basin or slope deposits derived from the Sekwi carbonate shelf.

Cambro-Ordovician

Silty argillaceous limestone of the Rabbitkettle Formation thickens northeasterly to include minor intermediate volcanic tuff, dolomite, and quartz arenite previously included in the Sekwi Formation (Gordey, 1978) but on the basis of new fossil evidence is now known to be Cambro-Ordovician. The tuff forms local thick members (0-185 m) at several horizons within the Rabbitkettle. The quartz arenite and dolomite are correlative with a similar sequence at the base of the Broken Skull Formation in Mackenzie Mountains (Fig. 2.1).

The Rabbitkettle rests unconformably on rocks as old as the upper 'Grit Unit'. Pre-Rabbitkettle gentle folding and local faulting has produced in places, angular unconformable relations and rapid changes in stratigraphic level of underlying units.

Ordovician and Silurian

The Road River Formation undergoes a marked change in facies and thickness from black graptolitic shale and minor chert and limestone near Howard's Pass to thick bedded black chert southwest of Summit Lake. Thick bedded dolomites in Mackenzie Mountains are correlative strata defining the eastern margin of Selwyn Basin. Orange weathering wispy laminated pyritic mudstone (Fig. 2.4), a good marker in the Summit Lake area, thickens to the southwest beneath the sub-Middle(?) Devonian unconformity. It is correlative with graptolitic siltstone and shale which overlaps the carbonate platform to the northeast (Fig. 2.1, section c).

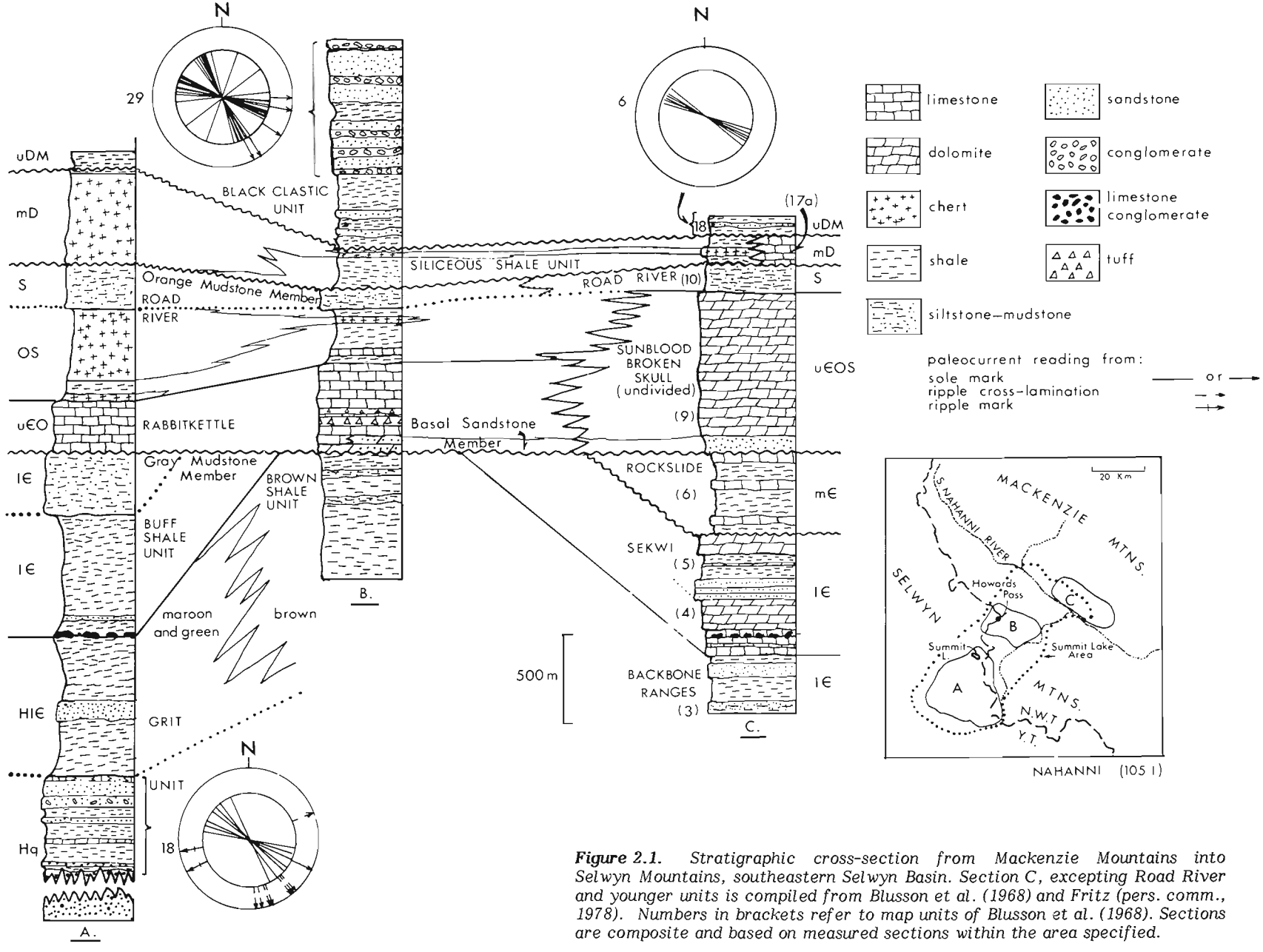


Figure 2.1. *Stratigraphic cross-section from Mackenzie Mountains into Selwyn Mountains, southeastern Selwyn Basin. Section C, excepting Road River and younger units is compiled from Blusson et al. (1968) and Fritz (pers. comm., 1978). Numbers in brackets refer to map units of Blusson et al. (1968). Sections are composite and based on measured sections within the area specified.*



Figure 2.2. *Turbiditic sandstone and conglomerate of the lower 'Grit Unit'. Medium bedded medium- to coarse-grained sandstone is flanked to the left by a dark rib of cobble conglomerate and massive amalgamated coarse grained sandstone.*



Figure 2.3. *Large shale clasts within massive quartzo-feldspathic granule conglomerate of the lower 'Grit Unit'.*



Figure 2.4. Characteristic wispy lamination in the orange mudstone member of the Road River Formation (match head for scale). The member is a marker in the Summit Lake area.

Devonian and Mississippian

Middle Devonian black siliceous shale and chert overlie the Road River Formation unconformably and are correlative with bioclastic grey weathering crinoidal limestone of lower Middle Devonian age (Fig. 2.1) in Mackenzie Mountains. To the southwest this siliceous shale unit changes facies to thin to thick bedded black chert markedly similar to and as thick as the Road River Formation chert (Fig. 2.1).

The 'Black Clastic Unit' unconformably overlies Middle Devonian strata and consists of brown weathering, noncalcareous turbiditic quartz-chert sandstone, chert-pebble conglomerate, and shale. Characteristics typical of turbidites include graded bedding, rare bouma sequences, sole marks, and alternating sandstone-shale sequences. Coarse sandstone and conglomerate occur in thick bedded units up to 290 m thick devoid of shale, whereas fine grained sandstone is thinner bedded and has shale interbeds. Sole marks in the upper 'Black Clastic Unit' indicate easterly and southeasterly paleoflow in the Howard's Pass area. Composition of detritus indicates Road River (Tempelman-Kluit and Blusson, 1977) and Middle Devonian chert as well as the 'Grit Unit' rocks (Gordey, 1978) were possible sources. Regionally, deposition may have been on one or a number of submarine fans whose distribution and paleobathymetry may have been complex and influenced by contemporaneous faulting (Gordey, 1978).

Acknowledgments

The writer is grateful for the logistical assistance of Union Carbide Exploration Corp. and Placer Development Ltd.

References

Blusson, S.L., Green, L.H., and Roddick, J.A.
1968: Nahanni map-area, District of Mackenzie and Yukon Territory; Geological Survey of Canada, Map 8-1967.

Gordey, S.P.
1978: Stratigraphy and Structure of the Summit Lake area, Yukon and Northwest Territories; in Current Research, Part A, Geological Survey of Canada, Paper 78-1A, p. 43-48.

Tempelman-Kluit, D.J. and Blusson, S.L.
1977: Pelly-Cassiar Platform and Selwyn Basin: neither without the other; Geological Association of Canada, Annual Meeting (Cordilleran Section), Program with Abstracts, v. 2, p. 52.

3. OPERATION SAINT ELIAS, BRITISH COLUMBIA

Project 730035

R.B. Campbell and C.J. Dodds
Regional and Economic Geology Division, Vancouver

Campbell, R.B. and Dodds, C.J., Operation Saint Elias, British Columbia; in Current Research, Part A, Geol. Surv. Can., Paper 79-1A, p. 17-20, 1979.

Abstract

The five geological terranes, bounded by faults, noted in the Saint Elias Mountains in Yukon Territory, continue southward into British Columbia and four of them extend into southeastern Alaska. From southwest to northeast these terranes are: 1. Cretaceous (?) greywacke and argillite (Valdez Group ?) bounded on the northeast by the "Border Ranges Fault"; 2. Permian (?) greenschist, argillite, limestone, conglomerate and chert bounded on the east by the Art Lewis Fault; 3. Paleozoic limestone, argillite, greywacke and volcanics (Kaskawulsh Group) bounded on the east partly by the Duke River Fault and partly by the Denali Fault System; 4. A second belt of Permian rocks (Skolai Group) between the Duke River Fault and Denali Fault System; and 5. Jurassic and Cretaceous greywacke, argillite and greenstone (Dezadeash Group) and metamorphic equivalents in the Coast Plutonic Complex east of the Denali Fault System. The Dezadeash Group is inferred to rest on Permian (Skolai Group) and related Triassic rocks which are thus east of the Denali Fault System.

The Denali Fault System cuts rocks perhaps as young as Pliocene but clear evidence of Pleistocene or recent movement on this or other faults was not observed.

Introduction

Previous field work on Operation Saint Elias (1974 to 1977) was restricted almost entirely to the Saint Elias Mountains in Yukon Territory (Campbell and Dodds, 1975; 1978; Read and Monger, 1975; 1976; Eisbacher, 1975; 1976; Eisbacher and Hopkins, 1977; Souther and Stanciu, 1975). Field work in 1978 extended the study to the Saint Elias Mountains in British Columbia (Tatshenshini, 114 P and Yakutat, 114 O map areas). Earlier work in the region by Watson (1948) provided valuable information to the writers.

D.A. Brew, E.M. MacKevett, Jr. and George Plafker of the United States Geological Survey, who have all studied adjacent areas of Alaska, gave freely of their data and ideas during visits in the field. Their contributions have been of immense benefit to the writers, particularly with respect to the delineation of the major fault-bounded terranes of the region. The interpretations given here, however, are the sole responsibility of the writers.

The principal objectives of the authors, as in 1977, were to map the more distant, rugged and inaccessible parts of the mountains based on helicopter fly-by and landing-site observations whereas more detailed work focused on the geology of the relatively accessible and less rugged part of the region in the northeastern quadrant of the Tatshenshini map-area, particularly on the Paleozoic rocks west of the Denali Fault System (Fig. 3.1).

Geological Terranes of the Saint Elias Mountains

The five geological terranes of the Saint Elias Mountains in Yukon Territory (Campbell and Dodds, 1978) extend southward into British Columbia where, as to the north, they are separated by major faults (Fig. 3.1).

1. Southwest of the "Border Ranges Fault" in the southwestern part of the area Cretaceous (?) greywacke and argillite is metamorphosed, deformed, and intruded by Tertiary plutons.
2. Immediately to the northeast of the "Border Ranges Fault" is a narrow and probably discontinuous belt of Permian (?) greenstone, limestone, argillite, conglomerate and possibly chert that is intruded by medium to coarse grained hornblende diorite. This terrane is bounded on the northeast by the Art Lewis Fault, a name proposed by George Plafker (pers. comm., 1976).
3. An extensive area of Paleozoic sedimentary and volcanic rocks informally named the Kaskawulsh Group is bounded on the southwest by the Art Lewis Fault and on the northeast partly by the Duke River Fault and partly by the Denali Fault System. The rocks are extensively intruded by plutons that range from late Paleozoic to Tertiary in age.
4. Between Duke River Fault and the Denali Fault System is a second terrane of Permian and possibly some Triassic volcanic and sedimentary rocks cut by Cretaceous plutons.
5. Northeast of the Denali Fault System in the Saint Elias and Coast Mountains are Jura-Cretaceous greywacke, argillite and greenstone. To the southeast and east these rocks grade into or interfinger with schist, gneiss and amphibolite with some marble. They are intruded by extensive Early Tertiary (?) plutons of the Coast Plutonic Complex.

   Tertiary volcanic and sedimentary rocks locally rest unconformably on strata of the three northeasterly terranes.

Southwest of the "Border Ranges Fault" (Terrane 1)

The fault bounding the Cretaceous (?) metagreywacke and argillite (Valdez Group?) on the northeast cannot unequivocally be traced into the Border Ranges Fault near Mount Logan (Campbell and Dodds, 1978) because of complexities near Mount Vancouver and Mount Seattle which remain to be resolved. The use of the name in quotes is meant to express a degree of uncertainty. Also somewhat uncertain is the age of the sedimentary rocks within the terrane. No fossils were found but the strata are similar in terms of lithology, metamorphism, nature of related plutons, and structural position to the Valdez Group near and west of Mount Logan (Campbell and Dodds, 1978; MacKevett and Plafker, 1974).

The rocks southwest of the "Border Ranges Fault" (terrane 1) are coextensive with similar rocks to the south in Glacier Bay National Monument, Alaska, where Brew et al. (1977) provisionally assigned them a Precambrian or Early Paleozoic age. This age is now deemed unlikely and the rocks are thought to be equivalent to the Cretaceous Valdez Group (D.A. Brew, pers. comm., 1978). The western boundary of the Tarr Inlet suture zone (Brew and Morrell, 1978) in the Glacier

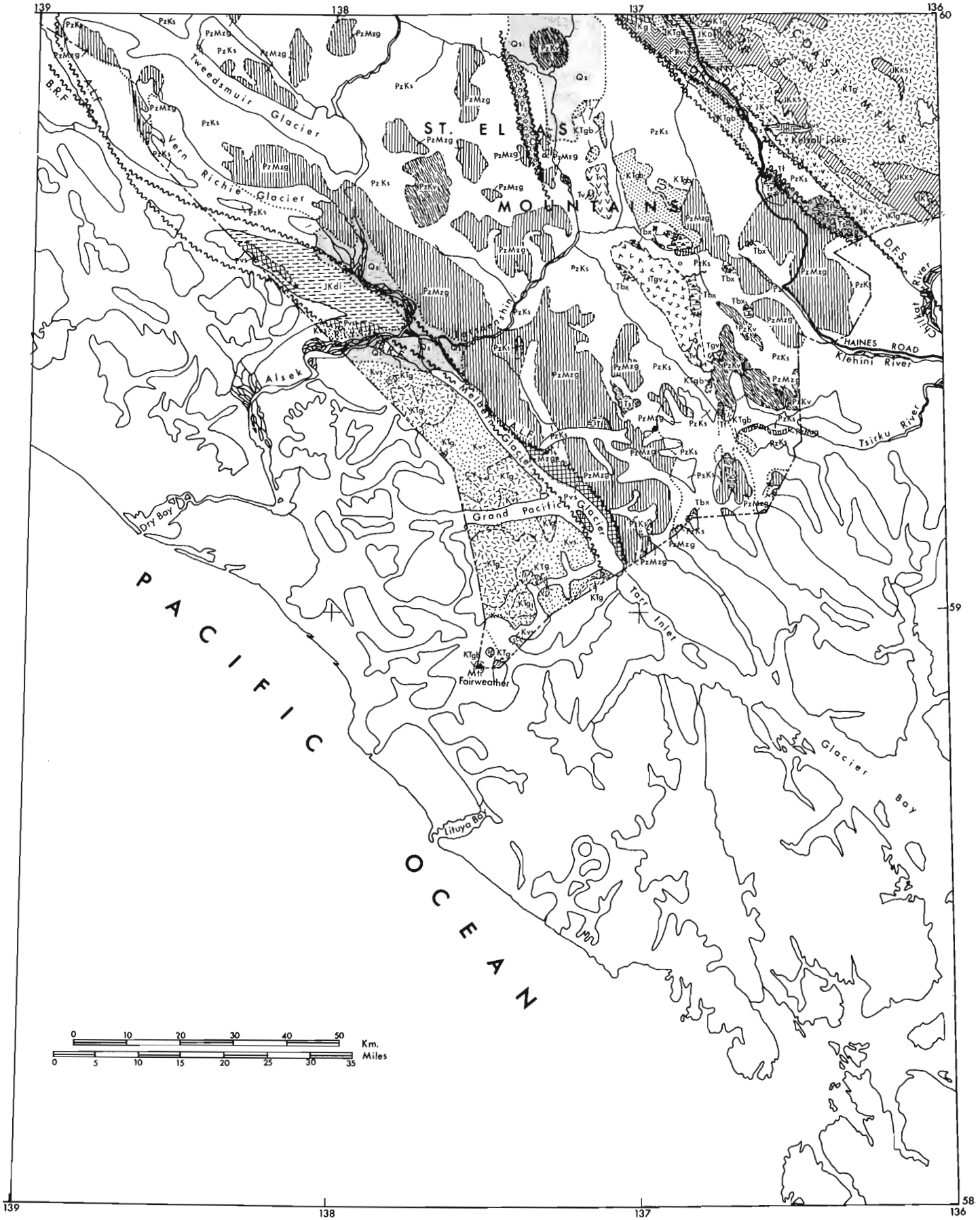
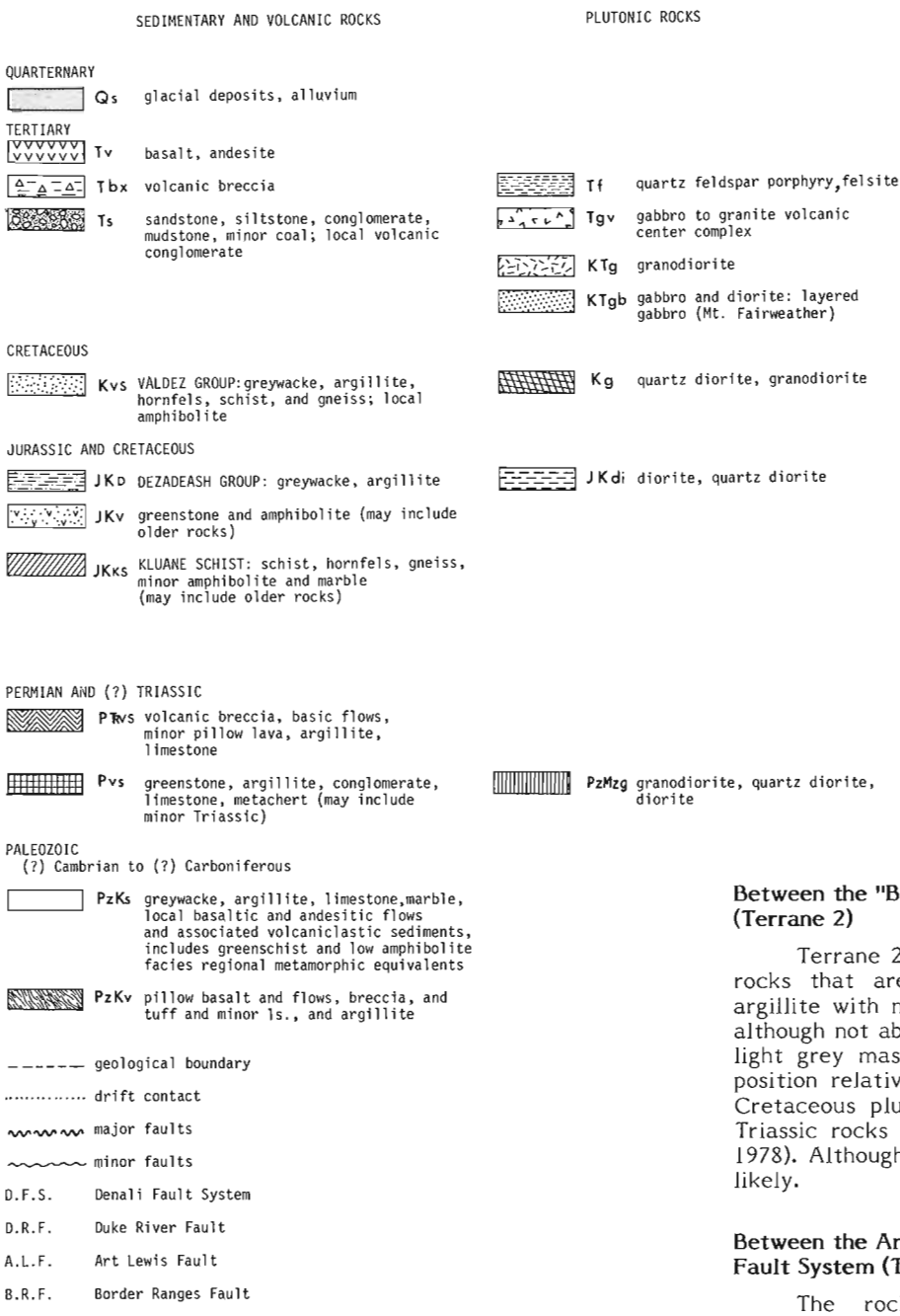

139
138
137
136
60
59
58
ST. ELIAS MOUNTAINS
COAST MTNS.
PACIFIC OCEAN
Tweedsmuir Glacier
Vern Richie Glacier
Alsek
Melbern Glacier
Grand Pacific Glacier
Dry Bay
Lituya Bay
Mt. Fairweather
Taylor Inlet
Glacier Bay
Kelsall Lake
Klehini River
Chilkat River
HAINES ROAD
Tsirku River
B.R.F.
D.F.S.
0 10 20 30 40 50 Km.
0 5 10 15 20 25 30 35 Miles

Figure 3.1

Legend for Figure 3.1



Bay area would correspond to the southern extension of the "Border Ranges Fault" and the rocks within the suture zone (considered to be Permian, Brew and Morrell, 1978) are the equivalent of terrane 2 in this report and thus are bounded by the "Border Ranges" and Art Lewis Faults in the area discussed herein.

If the above inferences as to the age and correlation of the rocks of terrane 1 and to the continuity of the Border Ranges Fault are correct then the Border Ranges Fault forms an arc, convex northward, on the inboard side of the Valdez Group for about 2000 km. Similarly, it apparently forms the oceanward boundary of a Permo-Triassic terrane (terrane 2).

Between the "Border Ranges" and Art Lewis Faults (Terrane 2)

Terrane 2 consists of a narrow belt of highly deformed rocks that are dominantly metavolcanic greenschist and argillite with metachert and local conglomerate. Limestone, although not abundant, is widespread and locally forms thick, light grey masses. These rocks occupy a similar structural position relative to adjoining terranes and are cut by Jura-Cretaceous plutons (about 150 Ma old) as are the Permo-Triassic rocks north of Mount Logan (Campbell and Dodds, 1978). Although proof is lacking a Permo-Triassic age seems likely.

Between the Art Lewis and Duke River Fault-Denali Fault System (Terrane 3)

The rocks of terrane 3, informally called the Kaskawulsh Group, extend southward from Yukon where they have been previously described (Campbell and Dodds, 1975; 1978; Read and Monger, 1976). Evidence from the British Columbia part of the mountains suggests that the sequence may contain thick Ordovician and/or Silurian carbonate and greywacke with local thick accumulations of pillow lava and breccia (Fig. 3.1). The latter may be Cambrian and/or Ordovician in age. In addition, the group includes Devonian and possibly younger carbonate and clastic rocks. The sequence is intruded by a variety of plutons that range in age from late Paleozoic to Tertiary. Most cannot be differentiated until isotopic dating studies are complete. An interesting plutonic assemblage of probable Tertiary age lies east of Tkope River. This body consists of several phases ranging from microgabbro to granite that apparently formed the intrusive core of a volcanic complex. The volcanic edifice must have consisted of a vast volcano or series of volcanoes

of which only small areas of flows and breccia remain. The breccia, intruded by some of the granitic phases, rests unconformably on older plutonic and Kaskawulsh Group rocks. Spatially separate gabbroic and dioritic plutons and dykes may be related to the volcanic episode. The volcanism seems to have been mainly andesitic and silicic rather than basaltic.

Between the Duke River Fault and Denali Fault System (Terrane 4)

Permian and Triassic rocks of terrane 4 have been previously described by Read and Monger (1976). These rocks, intruded by Cretaceous plutons, extend from the Yukon southerly into British Columbia and apparently terminate where the Denali Fault System intersects the Duke River Fault.

East of the Denali Fault System (Terrane 5)

Greywacke and argillite of the Upper Jurassic and Lower Cretaceous Dezadeash Group extend from the north (Eisbacher, 1975; 1976) into British Columbia where they apparently interfinger with a sequence of greenschist and amphibolite and become metamorphosed into hornfels, schist and gneiss. From regional considerations the Dezadeash Group is believed to rest on a basement of Permian and Triassic strata correlative with the Skolai Group, Nikolai Greenstone and related Triassic rocks found to the northwest in the Saint Elias Mountains and beyond (Read and Monger, 1976; Richter, 1976). Some of the amphibolite and local marble layers may represent the metamorphosed equivalent of these rocks. Terrane 5 is within the northern part of the Coast Plutonic Complex and exhibits extensive areas of granitic plutonic rocks of which all or most are believed to be early Tertiary in age.

Tertiary Volcanic and Sedimentary Rocks

Thick sections of Tertiary sedimentary rocks, possibly Eocene or Oligocene to Miocene in age, occupy a graben between Tatshenshini and Alsek rivers and a faulted syncline, cut by the Denali Fault System, south of Kelsall Lake. In the latter area the sediments are associated with sills and dykes and possible flows of quartz-feldspar porphyry. Felsite dykes are common throughout the region east of Alsek River and two felsite intrusives in the south central part of the region may be related to the volcanic centre complex east of Tkope River discussed in the section on terrane 3.

North of Kelsall Lake small patches of basaltic flows and cinder deposits cap several ridges and hills. These may be Pliocene or Pleistocene in age.

Fault Movements

No evidence of postglacial fault movements was noted anywhere within the map area but this might be easily overlooked in the western, ice-laden part of the mountains which are near the active Fairweather and related faults in Alaska. Although rocks as young as Miocene and possibly Pliocene are cut by the Denali Fault System, glacial and recent deposits are apparently undisturbed.

References

Brew, D.A., Loney, R.A., Kistler, R.W., Czamanske, G.K., Gromme, C.S., and Tatsumoto, M.
1977: Probable Precambrian or lower Paleozoic rocks in the Fairweather Range, Glacier Bay National Monument, Alaska; in Blean, K.M. ed., The U.S. Geological Survey in Alaska: Accomplishments during 1976; U.S. Geological Survey Circular 751-B, p. 91-93.

Brew, D.A. and Morrell, R.P.
1978: Tarr Inlet Suture Zone, Glacier Bay National Monument, Alaska; in Johnson, K.M., ed., The United States Geological Survey in Alaska; Accomplishments during 1977; U.S. Geological Survey Circular, in press.

Brew, D.A., Johnson, B.R., Ford, A.B., and Morrell, R.P.
1978: Intrusive rocks of the Fairweather Range, Glacier Bay National Monument, Alaska; in Johnson, K.M., ed., The United States Geological Survey of Alaska; accomplishments during 1977; U.S. Geological Survey Circular, in press.

Campbell, R.B. and Dodds, C.J.
1975: Operation Saint Elias, Yukon Territory; in Report of Activites, Part A, Geological Survey of Canada, Paper 75-1A, p. 51-53.

1978: Operation Saint Elias, Yukon Territory; in Current Research, Part A, Geological Survey of Canada, Paper 78-1A, p. 35-41.

Eisbacher, G.H.
1975: Operation Saint Elias, Yukon Territory: Dezadeash Group and Amphitheatre Formation; in Report of Activities, Part A, Geological Survey of Canada, Paper 75-1A, p. 61-62.

1976: Sedimentology of the Dezadeash flysch and its implication for strike-slip faulting along the Denali Fault, Yukon Territory and Alaska; Canadian Journal of Earth Sciences, v. 13, p. 1495-1513.

Eisbacher, G.H. and Hopkins, S.L.
1977: Mid-Cenozoic paleogeomorphology and tectonic setting of the St. Elias Mountains, Yukon Territory; in Report of Activities, Part B, Geological Survey of Canada, Paper 77-1B, p. 319-335.

MacKevett, E.M., Jr. and Plafker, George
1974: The Border Ranges Fault in south-central Alaska; U.S. Geological Survey Journal of Research, v. 2, p. 323-329.

Read, P.B. and Monger, J.W.H.
1975: Operation Saint Elias, Yukon Territory: The Mush Lake Group and Permo-Triassic rocks in Kluane Ranges; in Report of Activities, Part A, Geological Survey of Canada, Paper 75-1A, p. 55-59.

1976: Pre-Cenozoic volcanic assemblages of the Kluane and Alsek Ranges, southwestern Yukon Territory; unedited report to accompany Geological Survey of Canada, Open File 381.

Richter, D.H.
1976: Geologic map of the Nabesna Quadrangle, Alaska; U.S. Geological Survey Map 1-932.

Souther, J.G. and Stanciu, C.
1975: Operation Saint Elias, Yukon Territory: Tertiary volcanic rocks; in Report of Activities, Part A, Geological Survey of Canada, Paper 75-1A, p. 63-70.

Watson, K. de P.
1948: The Squaw Creek-Rainy Hollow area, northern British Columbia; British Columbia Department of Mines, Bulletin 25.

4. THE LOWER MESOZOIC KING SALMON ASSEMBLAGE – CRY LAKE MAP AREA BRITISH COLUMBIA

Project 770016

L. Thorstad
Regional and Economic Geology Division, Vancouver

Thorstad, L., The Lower Mesozoic King Salmon Assemblage – Cry Lake map area British Columbia; in Current Research, Part A, Geol. Surv. Can., Paper 79-1A, p. 21-24, 1979.

Abstract

The lower Mesozoic King Salmon Assemblage forms a discrete structural belt that spans the width of the Cry Lake map area. The rocks lie within a thrust sheet, floored by the King Salmon Thrust Fault, and are bounded to the north by the Nahlin Fault. A lower division, the upper Triassic Kutcho 'Formation'; a volcano-sedimentary sequence, hosts an important economic mineral deposit. Uppermost Triassic limestone, correlated with the Sinwa Formation caps the lower division. An upper unit, a lower Jurassic greywacke-phyllite sequence, the Inklin Formation, overlies, and is gradational with the Kutcho and Sinwa strata. Isoclinal folds with a well developed, axial planar cleavage typify the rocks.

Chemical analyses suggest rocks of the Kutcho volcano-sedimentary sequence are generally calcalkaline.

Introduction

The purpose of this report is to present a summary of preliminary chemical data on Mesozoic rocks collected in the 1977 field season, and to elaborate on specific Mesozoic rocks of the Cry Lake map area (see Monger and Thorstad, 1978).

Geological mapping in the Cry Lake map area (104I), north-central British Columbia was continued during the 1978 field season. The focus of mapping was the southern part of the Hinterland Belt, (see Monger and Thorstad, 1978) which forms a discrete structural unit, the King Salmon Thrust plate, bounded to the south by the King Salmon Fault and to the north by the Nahlin Fault. Rocks within the King Salmon plate include the Upper Triassic Kutcho 'Formation', a volcano-sedimentary sequence, the Upper Triassic Sinwa Formation and Lower Jurassic Inklin Formation, a greywacke-phyllite sequence. Rocks strongly resembling the Kutcho 'Formation' occur north of the Kutcho fault, a major dextral strike slip fault. The Kutcho 'Formation' hosts an important, potentially economic, massive sulphide deposit. Mesozoic rocks are believed to have formed in an island arc environment.

The Nahlin fault juxtaposes Permo-Triassic Cache Creek Group against the lower Mesozoic rocks. To the south the King Salmon Assemblage is thrust on Lower to Middle Jurassic volcanic and sedimentary rocks.

Stratigraphy

The base of the King Salmon Assemblage is not exposed and therefore a complete stratigraphic section of the lowest division, the upper Triassic Kutcho 'Formation' is not known. North of the Kutcho fault, 'Kutcho-like' rocks are in contact with and overlie mid-Paleozoic slope and platformal rocks. A covered interval obscures the nature of this contact.

The Kutcho 'Formation' consists of intermediate to dacitic breccia and tuff, commonly epidotized, overlain by dacitic to rhyolitic tuffs and flows with minor chlorite schist. A massive sulphide lens overlies these rocks, and is in turn overlain by sericite schist and rhyolite flows with minor basalt porphyry lenses. A tuff-argillite and upper conglomerate sequence that have gradational contacts and are, in part, facies equivalents cap the volcanic rocks. The predominant lithologies (dacitic and rhyolitic equivalents) are quartz-eye, feldspar sericite schist and quartz-eye sericite schist. Dolomite is commonly associated with the ore (D. Bridge, pers. comm., 1978). A basic to intermediate lens occurs within the area of the deposit, above the ore horizon, and may be a metamorphic equivalent of the upper Triassic volcanics that outcrop to the south and northeast in the Cry Lake map area. Total apparent thickness is approximately 3300 m.

The middle division of the King Salmon Assemblage, correlated with the Sinwa Formation, has gradational contacts with the upper conglomerate of the Kutcho 'Formation'. The carbonate is coarsely to finely crystalline, due to metamorphism and dolomitization, respectively. Fossils are sparse (Monger and Thorstad, 1978). Total thickness ranges from 0 to 150 m.

Greywacke, phyllite and some conglomerate of the Inklin Formation overlies the Sinwa Formation. It is commonly conglomeratic near the base and, in one location, where Sinwa is absent, a gradational contact of lower Inklin with conglomerate of upper Kutcho is found. Total thickness in the map area is not known but must exceed 500 m.

Age

The King Salmon Assemblage is considered to be of early Mesozoic age. Rocks of the Kutcho 'Formation' have yielded no fossils but a gradational contact of upper conglomerate with upper Triassic limestone and with lower Jurassic greywacke, phyllite and conglomerate suggests late Triassic age. The conglomerate does not appear to reflect a major unconformity.

The Sinwa Formation contains fossils of definitely post Paleozoic, probably late Triassic age (Monger, 1977; H.W. Tipper, pers. comm., 1977). Conodonts have now been obtained from the carbonates, but identification has not been made to date.

No fossils have been obtained from the Inklin Formation but the rocks are correlated with the lower Jurassic Laberge Group on the basis of lithology (Monger and Thorstad, 1978).

Structure

The King Salmon Assemblage occurs almost exclusively in a structural belt bounded by the Nahlin and King Salmon faults to the north and south, respectively. The Nahlin Fault juxtaposes chert, argillite, greenstone and ultramafics of the Cache Creek Group against the King Salmon Assemblage. The King Salmon Fault juxtaposes deformed Mesozoic King Salmon Assemblage against less deformed Mesozoic volcanic and sedimentary rocks.

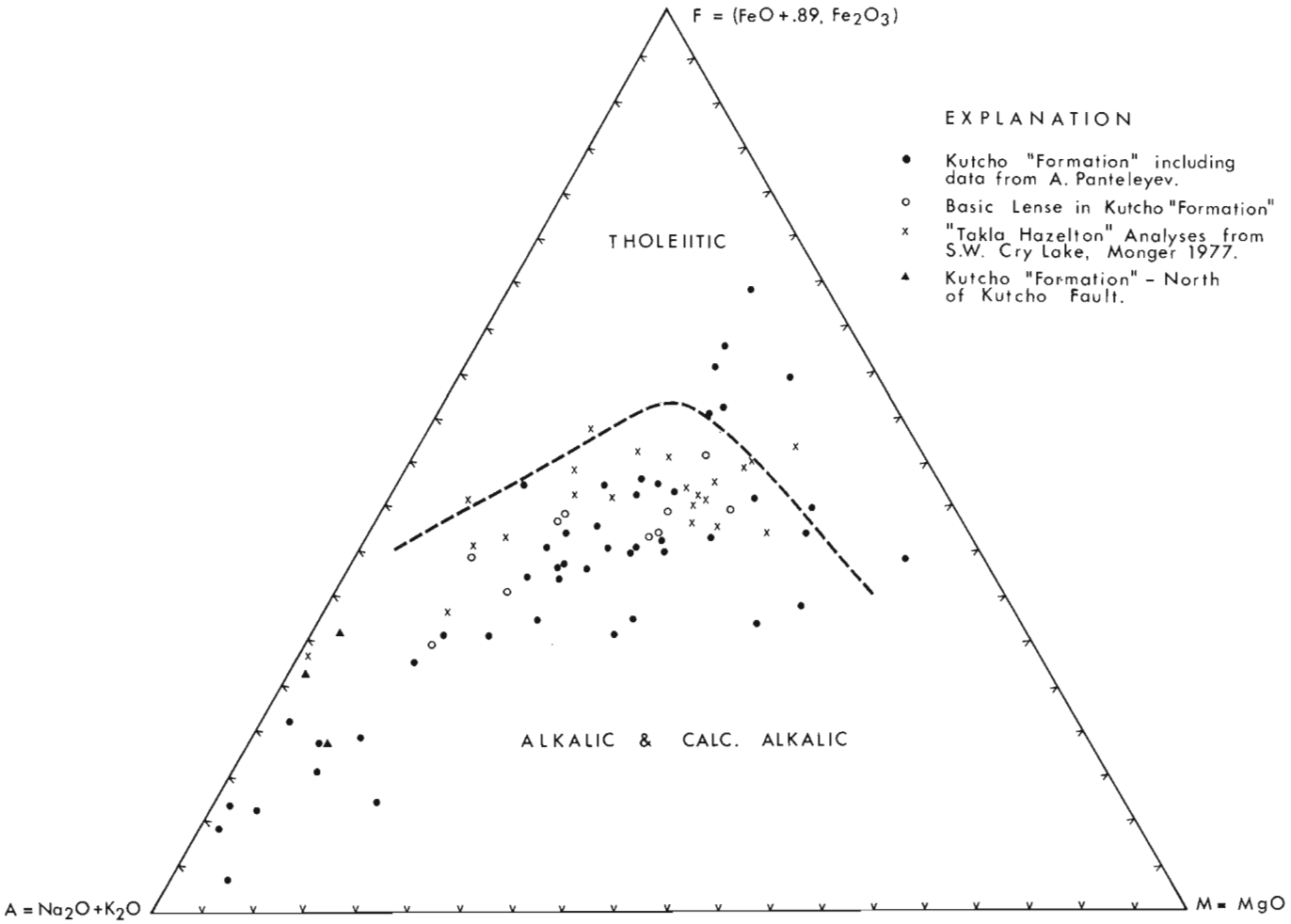


Figure 4.1. *AFM diagram for lower Mesozoic rocks of Cry Lake map area (after Irvine and Baragar, 1971).*

Rocks within the King Salmon Assemblage are typified by southwesterly overturned, isoclinal folds that have westerly plunges. A penetrative, axial planar foliation with generally steep northeasterly dips is well developed. Deformation appears to be less intense away from the leading edge of the thrust, suggesting that it is contemporaneous with thrusting.

At the leading edge of the King Salmon Fault imbrications with rocks of the Cache Creek Group (primarily serpentinites) occur. Imbrication of thrust sheets points to contemporaneity of thrusting of both the Permo-Triassic Cache Creek Group and the lower Mesozoic King Salmon Assemblage. An earlier deformational event is believed to have affected the Cache Creek Group (Monger, 1969).

Metamorphism

Characteristic mineral assemblages albite-epidote-quartz with abundant chlorite and sericite suggest rocks of the King Salmon Assemblage are metamorphosed to lower greenschist facies (Weber, 1977).

Economic Importance

The upper Triassic Kutcho 'Formation' hosts a stratabound, in part stratiform, deposit of volcanic origin. Copper, iron and zinc are the major commodities. The deposit shows many affinities to Kuroko-type deposits of Japan and to Archean massive sulphide deposits of Canada. Definition of chemical and lithological characteristics of rocks of the Kutcho 'Formation' may prove useful for further exploration throughout the Cordillera.

Chemical Analyses

Analyses obtained from rocks collected during the 1977 field season are plotted on AFM and 'Alkalis versus Silica' diagrams (see Fig. 4.1, 4.2). The diagrams provide a rapid means of examination and classification of the rocks. Tables of chemical analyses are not included. Analyses are by Analytical Chemistry Section, Geological Survey of Canada.

Analyses of rocks of the Kutcho 'Formation' range from tholeiitic basalt to andesite to calcalkaline andesite to rhyolite. Rock names are derived from Irvine and Baragar, 1971. Analyses were recalculated to 100 per cent, water free; and Fe_2O_3 was corrected for by per cent Fe_2O_3 = per cent TiO_2 + 1.5. Excess Fe_2O_3 was recalculated as FeO (Irvine and Baragar, 1971).

Rocks are generally metamorphosed to greenschist facies and, as a result, questions arise as to the validity of the AFM and 'Alkalis versus Silica' plots. In greenschist metamorphism CaO, Al_2O_3, Na_2O, and K_2O may be very mobile, whereas MgO, FeO and SiO_2 are less affected (Pearce and Cann, 1973). Weathering also promotes mobilization of several elements, i.e. K_2O, CaO, MgO, Na_2O and to a lesser extent SiO_2 (Pearce and Cann, 1973). Despite the potential great mobility of elements many Archean rocks have been examined, assuming little overall change in bulk composition. (Gelinas et al., 1977; Wilson et al., 1965).

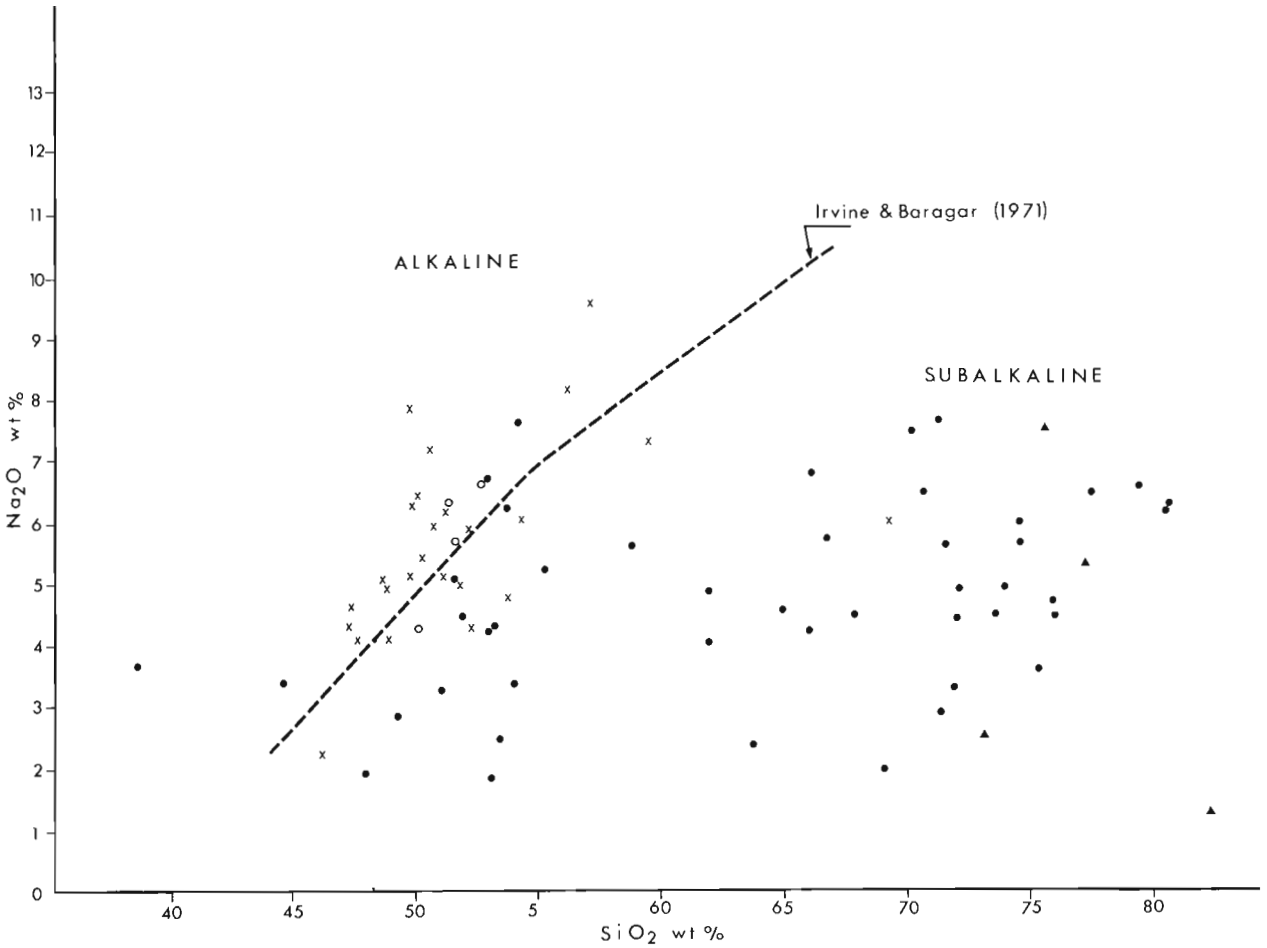


Figure 4.2. *Alkalis vs. silica diagram for lower mesozoic rocks (after Irvine and Baragar, 1971). See AFM Diagram Fig. 4.1 for explanation.*

AFM and 'Alkalis versus Silica' diagrams may still provide useful information, despite alteration. Analyses from J. Monger, of rocks collected during the 1977 field season, of 'Takla-Hazelton' rocks in the Cry Lake map area are presented for comparative purposes.

Rocks of the Kutcho 'Formation' plot almost exclusively in the alkaline and subalkaline fields of the AFM diagram (see Fig. 4.1). A small number of samples plot in the tholeiitic field but are generally close to the tholeiitic-subalkaline boundary. Plots compare favourably with analyses of 'Takla-Hazelton' rocks of Monger showing marked similarities in composition.

Analyses of Kutcho rocks plot mainly in the subalkaline field in the 'Alakalis versus Silica' diagram (see Fig. 4.2). The basic to intermediate lens near the deposit plots near or in the alkaline field as do analyses of the 'Takla-Hazelton' rocks of Monger. This may lend credence to the suggestion that the lens may be Takla volcanics interfingered with rocks of the Kutcho 'Formation'.

Plots of chemical analyses shows rocks of the Kutcho 'Formation' to be largely calcalkaline with very minor amounts of tholeiitic and alkalic components.

Summary

Lithology and chemistry suggest that rocks of the Kutcho 'Formation' are probably of Mesozoic island arc origin. The rocks outcrop in a structural belt spanning the Cry Lake map area. It is very likely that 'Kutcho-like' rocks may occur in the adjacent Dease Lake map area (H. Gabrielse, J.W.H. Monger, pers. comm., 1978).

References

Gelinas, L., Brooks, C., Perault, G., Carignan, J., Trudel, P., and Grasso, F.
1977: Chemo-Stratigraphic Divisions Within the Abitibi Volcanic Belt, Rouyn-Noranda District, Quebec in Volcanic Regimes in Canada; Geological Association of Canada Special Paper 16, edited by Baragar, W.R.A., Coleman, L.C., and Hall, J.M.

Irvine, T.N. and Baragar, W.R.A.
1971: A Guide to the Chemical Classification of the Common Volcanic Rocks; Canadian Journal of Earth Sciences, v. 8, p. 523-548.

Monger, J.W.H.
1969: Stratigraphy and structure of upper Paleozoic Rocks northeast Dease Lake map area, British Columbia; Geological Survey of Canada, Paper 68-48.

1977: The Triassic Takla Group in McConnell Creek Map Area, North-Central British Columbia; Geological Survey of Canada, Paper 76-29, 45 p.

Monger, J.W.H. and Thorstad, L.E.
1978: Lower Mesozoic Stratigraphy, Cry Lake (104I) and Spatsizi (104J) map areas; in Current Research, Part A, Geological Survey of Canada, Paper 78-1A, p. 21-24.

Pearce, J.A. and Cann, J.R.
1973: Tectonic Setting of basic volcanic rocks determined using trace element analysis; Earth and Planetary Science Letters, v. 19, p. 290.

Weber, M.
1977: The Geology and Mineralogy of the Cu, Zn, Fe Massive Sulphide Deposit at Kutcho Creek, British Columbia; unpublished B.Sc. thesis.

Wilson, H.D.B., Andrews, P., Moxham, R.L., and Ramlal, K.
1965: Archean Volcanism in the Canadian Shield; Canadian Journal of Earth Sciences, v. 2, p. 161-175.

5.

GEOLOGY OF WHITESAIL LAKE MAP AREA, BRITISH COLUMBIA

Project 770020

G.J. Woodsworth
Regional and Economic Geology Division, Vancouver

Woodsworth, G.J., Geology of Whitesail Lake map area, British Columbia; in Current Research, Part A, Geol. Surv. Can., Paper 79-1A, p. 25-29, 1979.

Abstract

The Intermontane Belt is underlain mainly by the largely volcanic Lower Jurassic Hazelton Group, the sedimentary Middle Jurassic Ashman Formation, the sedimentary Lower Cretaceous Skeena Group, and Upper Cretaceous to Miocene(?) nonmarine volcanics. Block faults dominate the structure. The Coast Plutonic Complex is underlain by isoclinally folded Central Gneiss Complex, Gamsby group, and plutonic rock. The Gamsby group grades by increasing metamorphism into Central Gneiss Complex. Between the Coast Plutonic Complex and the Intermontane Belt is a zone characterized by intense faulting, numerous dyke swarms, Lower Permian limestone and Lower Cretaceous(?) volcanics that may represent the northwest extension of one strand of the Yalakom Fault.

Introduction

Remapping of Whitesail Lake (93E) map area, begun in 1977 (Woodsworth, 1978), continued in 1978. The area was originally mapped by Duffell (1959); parts of the area have been mapped in more detail by Stuart (1960), Read (unpubl. rep., 1963), and MacIntyre (1976). Emphasis in the present study is on the structural and stratigraphic relations between the Coast Plutonic Complex and the flanking Intermontane Belt and on revision of the Mesozoic stratigraphy in the Intermontane Belt. Excellent field assistance was given by B. Douglas, L. Erdman, C. Evenchick, R. Helgason, B. Hayden, P. van der Heyden, M.L. Hill, P. Holbek, R. Rodman, R. Yamamoto, by cooks J. Wheeler and B. Souther, and by pilot B. McLaughlin of Quasar Aviation. T.A. Richards spent five weeks on the project; H.W. Tipper (see this publication, report 6) studied the Jurassic biostratigraphy of the area. J.W.H. Monger examined several areas of Paleozoic and Triassic strata. The following notes are a supplement to a map of Whitesail Lake map area to be released later in 1979.



Figure 5.1. *Cliffs of Gamsby group, about 700 m high, between Tsaytis and Gamsby rivers. The lower part of the cliffs are nondescript volcaniclastics characteristic of the Gamsby group; the upper part is the thin bedded marble and skarn member that serves as a useful marker horizon in the group. The white rock about halfway up the cliff on the left is also marble.*

The map area is underlain by the Coast Plutonic Complex on the west, the Intermontane Belt on the east, and by a narrow, intensely faulted transition zone.

Stratigraphy

Central Gneiss Complex

The Central Gneiss, the dominant unit in the southwest part of the map area, consists largely of banded amphibolite, gneisses, agmatite, plutonic rock, and minor schist, skarn, and marble. Bodies of plutonic rock form an important part of the Central Gneiss Complex and only the larger and more homogeneous bodies are mapped separately. The Central Gneiss Complex was, at least in part, derived by increasing migmatization of the Gamsby group.

Gamsby group

The Gamsby group (Woodsworth, 1978) underlies much of a belt extending southwest from Nanika Lake to near the south boundary of the map area. The unit consists largely of felsic and mafic tuff, commonly laminated, with lesser volcanogenic sandstone and one or more limestone and skarn members up to 200 m thick (Fig. 5.1). The Gamsby group has been metamorphosed to greenschist facies and the transition from Gamsby group to Central Gneiss Complex is arbitrarily placed at the first appearance of a significant amount of granitoid material. No diagnostic fossils have been found in the Gamsby group but a Paleozoic age appears probable.

Paleozoic(?) strata northwest of Atna River

Quartz-biotite schist and schistose metagreywacke containing andalusite and staurolite underlie the extreme northwest corner of the map area. These strata have been isoclinally folded about northeast-trending axes and are faulted against the Telkwa Formation to the east.



Figure 5.2. *Polymict conglomerate about 9 km southeast of Sandifer Lake. Clasts are mainly red and green volcanics, tuffs, and breccias with some limestone clasts. This conglomerate may form the base of the Telkwa Formation in the map area.*



Figure 5.3. *Well sorted and winnowed conglomerate (Lower Cretaceous(?)) at head of Tsaytis River. Most clasts are a great variety of volcanics and high-level porphyries with lesser tuff, breccia, and altered granitic material. The conglomerate fines downward into sands and siltstone.*

Permian and Triassic strata southeast of Sandifer Lake

About 9 km southeast of Sandifer Lake is a small complex area of rocks ranging in age from Permian to Jurassic. Four units, separated from one another by faults or intrusions, are present (J.W.H. Monger, pers. comm.). From oldest to youngest they are:

1. Massive to thin bedded limestone with chert nodules containing Early Permian fusulinids (C.A. Ross, pers. comm., 1978). This limestone is correlative with lithologically similar limestone described by Monger (1977) from the Terrace area.
2. About 100 m of thin bedded black shale and calcareous siltstone containing Middle or Upper Triassic fossils.
3. About 80 m of Upper Triassic strata consisting of boulder conglomerate with abundant limestone clasts that grades upwards into shales and limestone.
4. A red polymict conglomerate (Fig. 5.2) with some limestone clasts that is similar to the basal conglomerate of the Telkwa Formation in the Terrace area. This conglomerate appears to grade up into volcanic rocks typical of the Telkwa Formation.

Triassic(?) rocks near Smaby Peak

Thin bedded tuff, breccia, feldspar porphyry and minor limestone occur in several areas southwest of Lindquist Lake. No diagnostic fossils have been found in these rocks but an Upper Triassic age is suggested on the basis of lithologic similarities with Upper Triassic rocks in the Mount Waddington map area (Tipper, 1969), about 250 km to the southeast.

Hazelton Group: Telkwa and Smithers formations

Red, maroon, and green rhyolite basalt breccia, tuff and minor sediments and flows of the Telkwa Formation underlie large areas of the eastern part of the map area. The age of the Telkwa Formation is assumed to be largely Early Jurassic (Tipper and Richards, 1976) but lithologically similar red volcanics on Whitesail Range are Bajocian in age (Tipper, this publication, report 6). The base of the Telkwa Formation may be exposed southeast of Sandifer Lake, where a red polymict conglomerate grades up into typical Telkwa volcanics.

Grey to green volcanic sandstone, volcanic breccia and tuff, pebble conglomerate and rare limestone of the Smithers Formation overlie the Telkwa Formation. The Smithers Formation is probably mostly Middle Jurassic in age, but Lower Jurassic strata are present west of Michel Lake.

Bowser Lake Group: Ashman Formation

Thin bedded shale, siltstone, and limy sandstone of the upper Bajocian to Callovian Ashman Formation outcrop in several areas from Sibola Range southeast to near the south margin of the map area. The unit appears to overlie the Smithers Formation; the top of the unit is not exposed.



Figure 5.4. *Looking southeast from Swing Peak to typical strata of the Kasalka Group. Rocks are dominantly flow-banded rhyolite, feldspar porphyry, and lahar. Strata are slightly tilted and faulted but otherwise undeformed.*

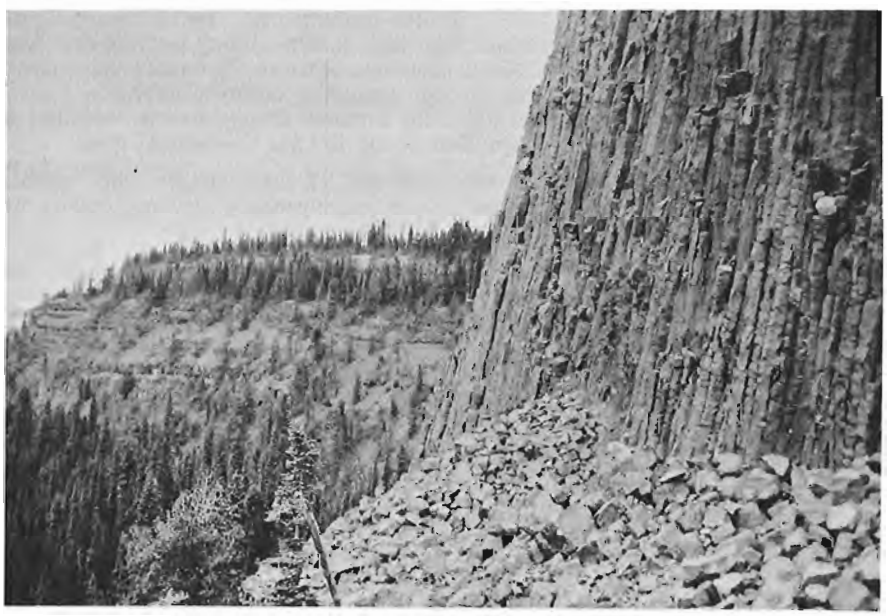


Figure 5.5. *In the background are flat lying, undeformed flows of the plateau basalts. These flows form a conspicuous escarpment east of St. Thomas River. The plateau basalts are cut by a plug of columnar-jointed basalt (foreground) that extends about 20 m above the plateau formed by the plateau basalts.*

Lower Cretaceous(?) volcanic rocks

Extensive areas just east of the Coast Plutonic Complex, particularly near Salient Peak and Mount Tsaydaychuz, are underlain by thick bedded, brownish weathering andesite to rhyolite flows and pyroclastics. These volcanics are distinguished in the field from the Telkwa Formation by their relatively fresh mafic minerals, by their steep, cliff-forming nature and by the drab colour of their talus slopes (as distinct from the maroon talus common in the Telkwa volcanics). No fossils have been found in these rocks, but they are lithologically indistinguishable from Hauterivian volcanics in the Mount Waddington (Tipper, 1969) and Bella Coola (Baer, 1973) map areas.

Similar volcanics with interbedded sediments, including a well sorted granitic-cobble conglomerate (Fig. 5.3) outcrop near the head of Tsaytis River.

Skeena Group

Micaceous sandstone, shale, and conglomerate of the Lower Cretaceous Skeena Group outcrop in the western part of the Intermontane Belt. Paleocurrent data indicate a west to southwest paleoslope. The base of the Skeena Group is not exposed in the map area; the unit is unconformably overlain by the Kasalka Group.

Kasalka Group

The Kasalka Group was defined by MacIntyre (1976) as a sequence of Upper Cretaceous nonmarine volcanics and sediments in the vicinity of Tahtsa Lake. The term is used here for all presumed Upper Cretaceous volcanics in the map area that are lithologically similar to rocks in the type area.

The Kasalka Group overlies the Skeena Group with distinct angular unconformity. The base of the Kasalka Group is marked by a distinctive red conglomerate containing volcanic and sandstone clasts in a hematitic matrix. This conglomerate is normally less than 50 m thick, but northwest of Seel Lake what is probably the same conglomerate is about 200 m thick. There the conglomerate contains abundant boulders of Tahtsa complex, representing the first direct evidence, in the map area, of exposure of part of the Coast Plutonic Complex.

The conglomerate is overlain by a thick succession of andesite to rhyolite flows, pyroclastics, and lahar (Fig. 5.4).

Ootsa Lake and Endako groups

Nonmarine volcanics of the Ootsa Lake Group, dominantly rhyolite and dacite flows and pyroclastics with minor basalt and sediments, underlie a large part of the eastern half of the map area. Except for the Whitesail Range, most outcrops of the Ootsa Lake Group are in topographically low areas. Tectonic and age relations between the Ootsa Lake and Kasalka groups are unknown.

Basalt, andesite, and minor gabbro of the early Tertiary Endako Group are found east of Whitesail Reach and Eutsuk Lake, and probably underlie a large part of Mosquito Hills.

Plateau basalts

Flat lying undeformed basalt flows form a conspicuous plateau about 1700 m in elevation west of Wells Gray Peak (Fig. 5.5). The lack of deformation suggests correlation with the Miocene-Pliocene plateau basalts in map areas to the east.



Figure 5.6. *Well layered diorite of the Black Dome complex, about 1 km southeast of Black Dome. The layering is defined by variations in the amount of hornblende and pyroxene, in grain size, and in texture. Much of the feldspar has a distinct purplish hue.*

Small necks of columnar jointed basalt are common in the low country east of Eutsuk Lake and may be feeders to the plateau basalts.

Plutonic Rocks

Plutons in the Intermontane Belt are high-level stocks forcibly emplaced into the surrounding strata. Most of the plutons fall into one of four categories:

1. Pink granite, monzonite and syenite of the Lower Jurassic Topley Intrusions. These are probably deep-seated equivalents of the Hazelton Group (Tipper and Richards, 1976) and are highly faulted and altered.
2. Small microdiorite, gabbro, and diabase plugs that may be feeders for the Kalsalka Group.
3. Granodiorite, quartz diorite, monzodiorite and monzonite stocks of the Upper Cretaceous Bulkley Intrusions.
4. Granite, quartz monzonite and their porphyritic equivalents of the Lower Tertiary (mainly Eocene) Nanika Intrusions. Included in this category are numerous small felsite and quartz-feldspar porphyry stocks that may be correlatives of the Ootsa Lake Group.

Plutonic rocks in the Coast Plutonic Complex show a great variety of composition, structure, and probably age that defies adequate summation in a paragraph. Much of the granodiorite, quartz diorite, and quartz monzonite in the southwestern part of the map area is intimately related to the Central Gneiss Complex. Contacts between Central Gneiss Complex and plutons are in many places arbitrary, because many plutons grade into the gneiss in some places but in others, contacts are highly discordant.

Several dioritic complexes, notably the Tahtsa complex (Woodsworth, 1978) and Black Dome complex, occur near the east margin of the Coast Plutonic Complex. The Black Dome complex consists of heterogeneous, massive to well layered diorite (Fig. 5.6), greenstone, and numerous mafic dykes. The relationships among the various lithologies are poorly understood, and the entire complex has been metamorphosed to greenschist facies, possibly in conjunction with metamorphism of the Gamsby group.

Several post-tectonic plutons cut the Coast Plutonic Complex. These include the large miarolitic granite stock in the Gamsby River valley that gives an Eocene K-Ar age, and the Horetzky Dyke, a 74 Ma old diorite and quartz diorite body that cuts Central Gneiss Complex, Gamsby group, and Tahtsa complex.

Structure

Faults dominate the structure in the Intermontane Belt. The major mountain massifs may represent uplift blocks, some of which are cored by plutons of the Bulkley and Nanika intrusions. Block faults affect all rocks except the Miocene-Pliocene(?) plateau basalts. Block faulting may have begun in the mid-Cretaceous, because the basal conglomerate of the Kasalka Group, deposited unconformably on faulted Skeena Group, indicates a major change in the tectonics of the Intermontane Belt in mid to Late Cretaceous time.

Northwesterly-directed thrust faults on Sibola, Whitesail and Chickamin ranges predate at least some of the block faulting.

The structure of the Coast Plutonic Complex in the map area is dominated by at least one period of isoclinal folding. Minor fold axes, with many exceptions, plunge gently to moderately northwest to northeast and southwest to southeast. In the Central Gneiss Complex much of the granitoid material predates or is synchronous with the isoclinal folding, but the structure is complicated by at least one later period of folding (perhaps related to uplift of the Coast Plutonic Complex) and by the emplacement of post-tectonic plutons.

The structure of the Gamsby group is approximately a southwest-dipping homocline, but there is some evidence for isoclinal folding about southwest-plunging fold axes.

The transition between Coast Plutonic Complex and Intermontane Belt is marked by a zone up to 10 km wide characterized by intense faulting, numerous diabase dyke swarms, and the juxtaposition of greatly differing rock units. Several map units, particularly the Lower Permian and Upper Triassic carbonates and the Lower Cretaceous(?) volcanics, are restricted to this belt. The zone may in part represent one strand of the Yalakom Fault, but whether the movement in Whitesail Lake map area is transcurrent is not known.

References

Baer, A.J.
1973: Bella Coola-Laredo Sound map areas, British Columbia; Geological Survey of Canada, Memoir 372, 122 p.

Duffell, S.
1959: Whitesail Lake map-area, British Columbia; Geological Survey of Canada, Memoir 299, 119 p.

MacIntyre, D.G.
1976: Evolution of Upper Cretaceous volcanic and plutonic centers and associated porphyry copper occurrences, Tahtsa Lake area, British Columbia; unpublished Ph.D. dissertation, University of Western Ontario, 149 p.

Monger, J.W.H.
1977: Upper Paleozoic rocks of northwestern British Columbia; in Report of Activities, Part A, Geological Survey of Canada, Paper 77-1A, p. 255-262.

Stuart, R.A.
1960: Geology of the Kemano-Tahtsa area; British Columbia Department of Mines and Petroleum Resources, Bulletin 42, 52 p.

Tipper, H.W.
1969: Mesozoic and Cenozoic geology of the northeastern part of Mount Waddington map-area (92N), Coast District, British Columbia; Geological Survey of Canada, Paper 68-33, 103 p.

Tipper, H.W. and Richards, T.A.
1976: Jurassic stratigraphy and history of north-central British Columbia; Geological Survey of Canada, Bulletin 270, 73 p.

Woodsworth, G.J.
1978: Eastern margin of the Coast Plutonic Complex in Whitesail Lake map-area, British Columbia; in Current Research, Part A, Geological Survey of Canada, Paper 78-1A, p. 71-75.

6. JURASSIC STRATIGRAPHY OF THE WHITESAIL LAKE MAP AREA, BRITISH COLUMBIA

Project 750035

H.W. Tipper
Regional and Economic Geology Division, Vancouver

Tipper, H.W., Jurassic stratigraphy of the Whitesail Lake map area, British Columbia; in Current Research, Part A, Geol. Surv. Can., Paper 79-1A, p. 31-32, 1979.

Abstract

In the Whitesail Lake map area, several Lower and Middle Jurassic volcanic and sedimentary formations correlative with and lithologically similar or identical to formations of the Hazelton and Bowser Lake groups have been recognized. They are a southerly extension of rocks exposed in the Smithers map area. These strata characterize the Nechako Basin south of the Skeena Arch and are the oldest strata in much of the area east of the Coast Mountains.

In conjunction with the remapping of Whitesail Lake map area (see G.S. Woodsworth, this publication, report 5) the Jurassic rocks of the area were studied with a view to relating them to the stratigraphic and tectonic model proposed for the Jurassic immediately to the north (Tipper and Richards, 1976).

The Hazelton Group

In the areas to the north of Whitesail Lake map area, the Telkwa Formation is volumetrically and areally the most prominent formation of the Hazelton Group. Typically it is composed of reddish, maroon, purple, grey and green pyroclastic and flow rocks of marine and nonmarine origin of Sinemurian to (?) Early Pliensbachian age. The rocks of the Telkwa Formation in Whitesail Lake map area appear to be a direct southerly extension of those exposed in the Smithers area where similarly it is nonmarine in the west part and marine in the east. In Whitesail Lake, however, the age is not defined. The rocks underlie a wide area east of the Coast Mountains and are, for the most part, nonmarine. Only in the Quanchus Mountains in the east half of the map area were Lower Jurassic marine fossils found. These beds resemble the Smithers Formation.

Overlying the Telkwa Formation is a unit that is unlike any of the formations of the Hazelton Group in the areas to the north. It appears to represent an eruptive centre in which cream coloured, reddish and dark grey rhyolitic flows and pyroclastic rocks predominate. In part the unit is marine with, in some beds, abundant ammonites and pelecypods. Minor siltstone and rare sandstone is interbedded with the rhyolitic tuffs in thin, well laminated beds. The age is Middle Jurassic (Lower Bajocian) but may extend down into the Early Jurassic (Toarcian). Thick beds of red tuff and breccia overlie the cream-coloured rhyolite near the top of the unit. The reddish pyroclastics are difficult to distinguish from the Telkwa Formation and, hence, in places the unit may be mapped as Telkwa Formation. It does, however, have a more consistently red or maroon colour and is more regularly bedded than the Telkwa Formation. In these respects the rocks resemble the Red Tuff Member of the Nilkitkwa Formation in the Smithers and Hazelton map areas to the north. They are approximately the same age. They are also similar in lithology and age, in whole or in part, to the 'Toodoggone Volcanics' of the Spatsizi and Cry Lake map areas of northern British Columbia (Gabrielse, 1978). In the Quanchus Mountains, eastern part of the Whitesail map area, a correlative and lithologically similar unit has conglomerate at its base and appears to rest with erosional unconformity on the Telkwa Formation.

The Smithers Formation is widespread in the map area. It is composed of well bedded marine tuff, volcanic breccia, siltstone and minor grit, conglomerate and flows. The volcanics are largely andesitic and the coarse clastic strata contains abundant feldspar fragments. It is characteristically well bedded or coarsely laminated, poorly sorted, resistant, and breaks along blocky, closely spaced joints. Fossils, particularly pelecypods, are common but belemnites and ammonites are present at many localities. In the northern part of the map area early Middle Bajocian and late Middle Bajocian fauna were collected but the base was not exposed. However, on Chikamin Mountain, in the central part of the area, strata with a late Middle Bajocian fauna rest directly on Telkwa Formation. The Lower Bajocian – Toarcian rhyolitic strata and the early Middle Bajocian beds are missing. On Chikamin Mountain conglomerate and conglomeratic beds occur at the base of the Smithers Formation and together with the probable absence of beds present elsewhere, suggests an erosional interval in Middle Bajocian time. The shelly fauna and the coarseness of the clastic material indicates probable shallow sea with many nearby volcanic sources of material.

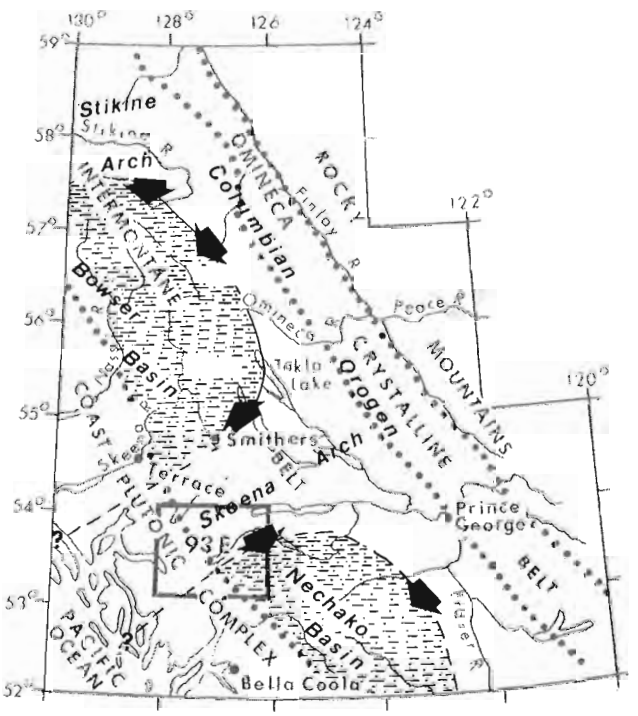


Figure 6.1. *Middle and Upper Jurassic basins.*

Bowser Lake Group

Only one formation of this group, the Ashman Formation, is recognized in the Whitesail map area. In the type area it is characteristically dark grey to black shale, feldspathic to quartzose sandstone, greywacke, chert-pebble conglomerate, and greywacke conglomerate. This description is applicable to the formation in the Whitesail Lake map area as well. In the type area tuffaceous laminae and thin beds are present as in the Whitesail Lake area, particularly near the Coast Mountains, suggesting that the source may have lain to the west. Coarseness of the sediments along the northern part of the area becoming shaly to the south suggests that the basin of deposition had one shoreline oriented east-west with detritus supplied from the north. Although exposure is sparse, there are sufficient occurrences to indicate that the basin extended from the north part of the map area to the southern boundary and from the Coast Mountains easterly, possibly into the map area to the east. Marine fossils, mainly ammonites and belemnites indicate an age of Late Bajocian to Early Callovian. Only in the area of the basin margin, in the north, are fossils abundant or are pelecypods common.

The configurations of the Jurassic basins in the Whitesail Lake area are difficult to determine. The western margin is fault bounded, the eastern margin is covered with younger rocks, and the central part is intruded, covered, and highly faulted. The Lower Jurassic Telkwa Formation apparently was deposited in the western part under subaerial conditions and graded easterly into a marine basin that extended easterly beyond the area into the Nechako River map area. The formation is an extension of the Sinemurian volcanics of the Smithers area to the north and extends into the Bella Coola and Anahim Lake areas to the south and southeast where it is obscured by Tertiary cover. In the Smithers area the Skeena Arch (Fig. 6.1) came into existence late in Early Jurassic time. It was a linear uplifted terrane oriented northeasterly and lying just north of the Whitesail Lake area. It divided the Hazelton Trough into two basins – the Bowser Basin to the north and the Nechako Basin to the south. The Skeena Arch was a source of detritus for these basins. In the Smithers area it was clearly demonstrated that several shoreline facies were developed on the north side of the Arch but the nature of the south side was in doubt. Certainly the Arch separates two areas underlain by Smithers Formation but little has been documented about direction of transport nor can shoreline facies be recognized. However the sediments of the Ashman Formation clearly show that a shoreline facies existed on the south side of the Skeena Arch, that sediment transport was from the north into the Nechako Basin and that the basin extended far to the south beyond the Whitesail Lake area in Early Callovian time. Nothing is known about the Nechako Basin in Jurassic time after Early Callovian.

References

Gabrielse, H.
1978: Operation Dease; in Current Research, Part A, Geological Survey of Canada, Paper 78-1A, p. 1-4.

Tipper, H.W. and Richards, T.A.
1976: Jurassic stratigraphy and history of north-central British Columbia; Geological Survey of Canada, Bulletin 270.

7. INVERTED STRATIGRAPHY AND STRUCTURES, DOWNIE CREEK, SOUTHERN BRITISH COLUMBIA

E.M.R. Research Agreement No. 170-4-78

Peter B. Read[1] and Richard L. Brown[2]
Regional and Economic Geology Division

Read, Peter B. and Brown, Richard L., Inverted stratigraphy and structures, Downie Creek, southern British Columbia; in Current Research, Part A, Geol. Surv. Can., Paper 79-1A, p. 33-34, 1979.

Abstract

Near the head of Downie Creek, two phases of intense deformation affect the map pattern of rock units. East of Downie Creek, sedimentary structures in the Hamill Group indicate that polyphase deformation produced antiformal anticlines and synformal synclines and left rocks in normal stratigraphic order. West of Downie Creek, second phase folding developed synformal anticlines and antiformal synclines. The inverted stratigraphy is widespread and probably results from second phase folding of an inverted limb of a first phase fold.

Introduction

Five weeks were devoted to detailed mapping of a 20 km long area straddling the head of Downie Creek from Mount Anstey in the east (82N W/2) to Carnes Peak in the west (82M E/2) (Fig. 7.1). North of this area, a detailed structural analysis by Lane (1977) required an early structure (first generation) to invert the stratigraphy. The purpose of the present investigation was to: (a) study structures involving the Hamill, Badshot and Lardeau units where fossils establish the prominent limestone as the Badshot Formation and sedimentary structures in the Hamill Group give the facing of the stratigraphy; (b) use the stratigraphy and facing to determine if the rocks have been inverted; and (c) initiate mapping to separate areas of inverted from normal stratigraphy.

Structure

Metamorphic rocks of the Selkirk Mountains exhibit polyphase deformation. Within the map area, the first two phases of folding affect the map pattern of rock units. Six new fossil localities establish the widespread marble mapped by Wheeler (1963, 1965) as the Badshot Formation. East of Downie Creek near Mount Anstey, sedimentary structures in impure quartzite of the Hamill Group yield numerous facing directions. These indicate that polyphase deformation produced antiformal anticlines and synformal synclines, but left the highly deformed rocks in normal stratigraphic order (Fig. 7.2). The isoclinal first phase folds and tight second phase folds have subparallel, northeasterly dipping axial planes. Southeasterly trending and gently plunging first phase folds are oblique to the northeasterly plunging and reclined second phase folds. Faults, which strike more northerly than the trends of the folds, cause omission or repetition of fold limbs.

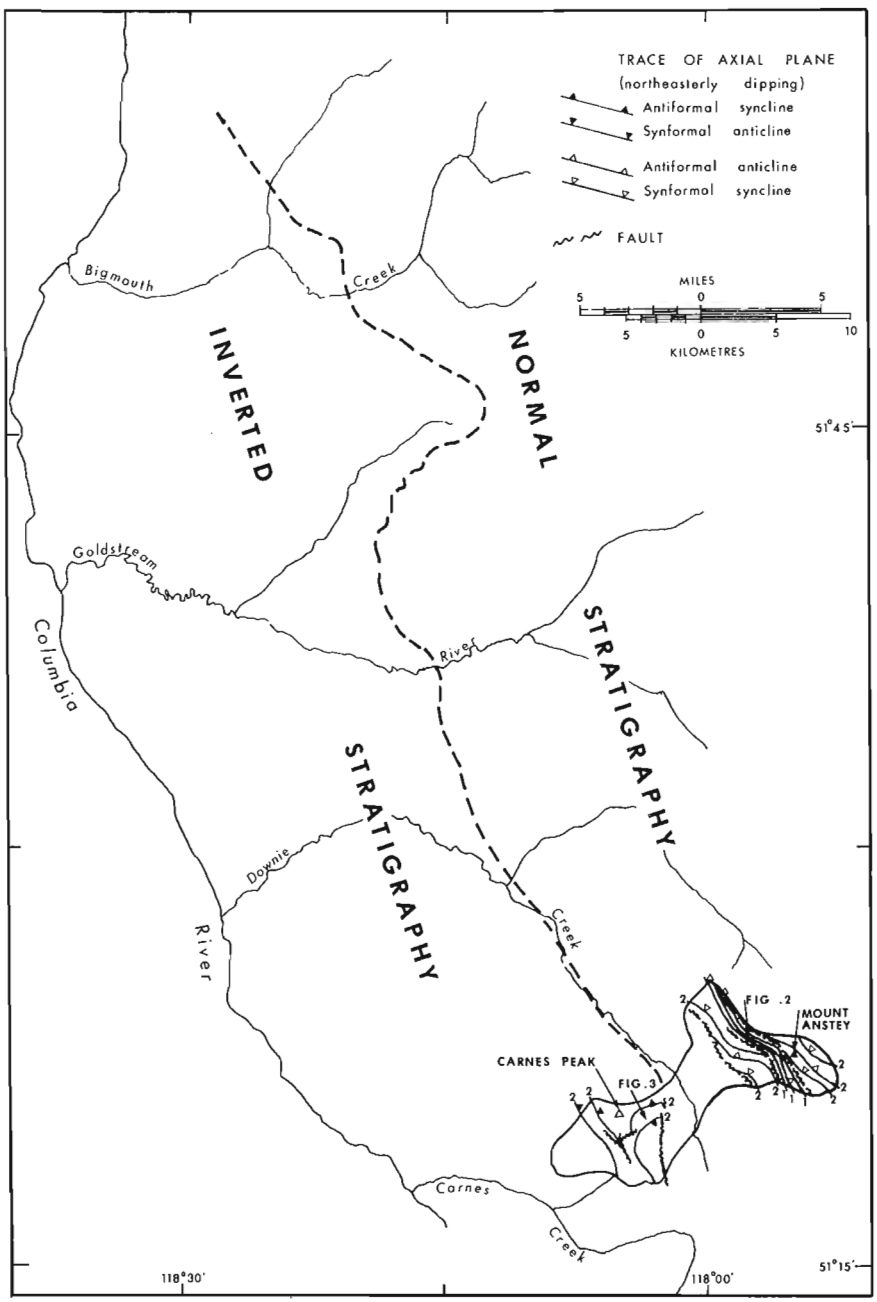


Figure 7.1.

Location map showing outlined map area, distribution of first and second generation folds, and regional distribution of normal and inverted stratigraphy in the northern Selkirk Mountains.

[1]Geotex Consultants Limited, 1103 – 100 W. Pender St., Vancouver, B.C.
[2]Department of Geology, Carleton University, Ottawa, Ont.

West of Downie Creek, near Carnes Peak, second phase folding intensifies and largely obliterates mesoscopic evidence of the earlier deformation. Folding of the upper part of the Hamill Group, Badshot Formation and lower part of the Lardeau Group produced synformal anticlines and antiformal synclines, and left the intensely deformed rocks in an inverted stratigraphic order (Fig. 7.3). Both phases of folding have northeasterly dipping axial planes and plunge gently southeasterly or northwesterly. Locally the folds become reclined.

Discussion

Within the Selkirk Mountains to the north of the map area, several workers have presented evidence for mesoscopic first phase folds (Franzen, 1974; Van der Leeden, 1976; Brown and Tippett, 1978), and in the western part of this region second phase folds apparently deformed previously inverted strata (Van der Leeden, 1976; Lane, 1977). Brown and Tippett (1978) proposed that the inverted limb of at least one macroscopic first phase nappe underlies this western region.

West of Downie Creek, inverted folds could develop from first phase folds inverted by second phase folding, or by second phase folds developed on the inverted limb of an early fold. Because mesoscopic second phase folds are apparently parasitic to the inverted folds, macroscopic second phase folds probably developed on the inverted limb of a first phase fold. These new results confirm the existence of macroscopic first phase folds and increase their extent on the western flank of the northern Selkirks.



Figure 7.2. *A view northward from Mount Anstey showing first generation folds outlined by light grey limestone of the Badshot Formation surrounded by darker rocks of the Hamill Group.*

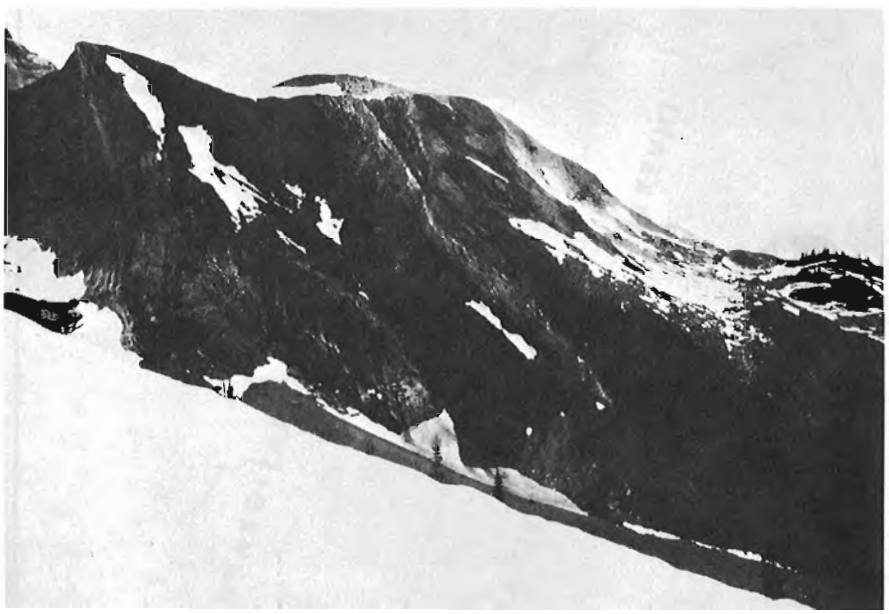


Figure 7.3. *East of Carnes Peak, a view looking northwestward of light grey Badshot limestone forming a second generation synformal anticline surrounded by dark grey phyllite of the Lardeau Group.*

References

Brown, R.L. and Tippett, C.R.
1978: The Selkirk fan structure of the southeastern Canadian Cordillera; Geological Society of America Bulletin, v. 89, p. 548-558.

Franzen, J.P.
1974: Structural analysis in the Selkirk fan axis near Argonaut Mountain, southeastern British Columbia; unpublished M.Sc. thesis, Department of Geology, Carleton University, Ottawa, 55 p.

Lane, L.S.
1977: Structure and stratigraphy, Goldstream River-Downie Creek area, Selkirk Mountains, British Columbia; unpublished M.Sc. thesis, Department of Geology, Carleton University, Ottawa, 140 p.

Van der Leeden, J.
1976: Stratigraphy, structure and metamorphism in the northern Selkirk Mountains southwest of Argonaut Mountain, southeastern British Columbia; unpublished M.Sc. thesis, Department of Geology, Carleton University, Ottawa, 105 p.

Wheeler, J.O.
1963: Rogers Pass map-area, British Columbia and Alberta; Geological Survey of Canada, Paper 62-32.

1965: Big Bend map-area, British Columbia; Geological Survey of Canada, Paper 64-32.

8.

STRATIGRAPHY OF THE EAST FLANK OF FRENCHMAN CAP DOME, SHUSWAP COMPLEX, BRITISH COLUMBIA

E.M.R. Research Agreement 2239-4-170/78

Richard L. Brown[1] and John F. Psutka[1]
Regional and Economic Geology Division

Brown, Richard L. and Psutka, John F., Stratigraphy of the east flank of Frenchman Cap Dome, Shuswap Complex, British Columbia; in Current Research, Part A, Geol. Surv. Can., Paper 79-1A, p. 35-36, 1979.

Abstract

A stratigraphic succession that attains a thickness of 4 km, rests conformably upon gneissic rocks of Frenchman Cap dome. Nine map units are recognized including the core of K-feldspar augen gneiss and overlying paragneisses; units 3 to 9 consist of quartzite, calc-silicate, marble, and pelitic rocks. Unit 9 is the highest stratigraphic level in the succession but its contact relationships with unit 8 are unclear. Unit 9 is tentatively correlated with Proterozoic (Windermere) rocks of the Kaza Group. Direct correlation eastward with strata in the Selkirk Mountains is not possible due to disruption by a major fault zone along the valley of the Columbia River.

Introduction

West of Downie Creek, a part of the northeast flank of Frenchman Cap gneiss dome has been mapped on a scale of 1:25 000 (Psutka, 1978). This work demonstrated that about 4 km of right way up strata lie conformably upon gneissic rocks that are exposed in the core of the dome. We have extended the mapping on a scale of 1:50 000 to include the entire eastern flank of the dome, and have delineated nine map units (Fig. 8.1).

Stratigraphy

The thickness of the lowest stratigraphic unit, a coarse grained K-feldspar augen gneiss is unknown; it is overlain with gradational contact by a variable thickness (100-800 m) of mixed paragneisses that range in composition from semipelitic to psammitic and frequently include thin discontinuous layers of amphibolite. These gneissic rocks are overlain by map units 3 to 9 consisting of quartzite, calc-silicate, marble, and pelitic rocks (Fig. 8.1).

West of Downie Creek the structure is simple and units 1 to 7 lie in normal stratigraphic order. Well preserved graded bedding in units 3 and 5 confirm that the succession is right way up. Unit 5 is dominantly pelitic, ranges in thickness from 400 to 800 m, and has been traced southward along the eastern flank of the dome to the area west of La Forme Creek (Fig. 8.1). In this area, between Columbia River and Jordan River, the structure is more complex; phase 3 folds are antiformal synclines and synformal anticlines that have been superimposed on the inverted limb of a south facing phase 2 nappe (Fig. 8.1). Despite the structural complexity of this southern region we are confident that stratigraphic units observed in the northern ground can be correlated with the southern strata. Unit 8 is a distinctive red and green banded calc-silicate that overlies the quartzite of unit 7 in the Jordan River area.

The highest unit in the succession, unit 9, is semipelitic to pelitic with large boudins of amphibolite and extensive lenses of concordant and discordant pegmatite. In the southern part of the area this unit rests on unit 8. However, north of La Forme Creek the same lithology rests on unit 5 and north of Downie Creek upon unit 7. Contact relationships in the Columbia River valley are obscured by the Columbia River fault zone, but south of Ruddock Creek unit 9 is also in contact with quartzites that are tentatively ascribed to unit 7. More work is required, but there appears to be a discordant relationship between unit 9 and underlying strata. The nature of this discordance is significant since amphibolite bearing pelitic rocks identical to unit 9 extend northward into the Canoe River area where they have been included by Campbell (1968) with Proterozoic rocks of the Kaza Group. At present it is not possible to clearly ascertain the age of units 1 to 8, but if the contact between units 8 and 9 is not a major structural break the underlying strata must be older than the Proterozoic rocks of the Kaza Group.

Columbia River Fault Zone

Stratigraphic units on the east flank of Frenchman Cap dome have been metamorphosed to upper amphibolite grade while east of the Columbia River Proterozoic and Lower Paleozoic strata have attained only greenschist grade. These two terranes are juxtaposed in the valley floor of the Columbia River (Wheeler, 1965). Strata adjacent to this boundary display cataclastic fabrics in a zone approximately 1 km thick that extends at least as far as Revelstoke in the south and Ruddock Creek in the north. Cataclastic foliation has an average dip of 20° to the northeast. This fabric appears to have developed by postmetamorphic reactivation of synmetamorphic foliation which parallels axial surfaces of westward verging phase two folds (Psutka, 1978; Brown and Tippett, 1978). Most recent movements have brecciated the cataclastic rocks and developed extensive zones of clay gouge. Slickensides and fiber growth in the brecciated and gouged material indicate a predominance of down dip to oblique normal displacement.

Stratigraphic units of Frenchman Cap terrane that extend into the Columbia River valley are truncated by the fault zone (Fig. 8.1). In the south between Revelstoke and La Forme Creek they are faulted against hanging wall rocks of the igneous complex of the Clachnacudainn salient. North of La Forme Creek, Lower Paleozoic rocks of the Selkirk terrane form the hanging wall.

More work is required to unravel the early history of this cataclastic belt, but it is clear that most recent faulting has moved Selkirk terrane northeastward down slope off the eastern flank of the Monashee (Shuswap) terrane. The northern limit of the fault is yet to be established; it appears to continue southward beyond Revelstoke in the Columbia River valley according to mapping by Read (pers. comm.).

Summary

A stratigraphic succession that attains a thickness of 4 km, rests conformably upon gneissic rocks of Frenchman Cap dome. The age of these rocks remains obscure since the observed contact with overlying Proterozoic strata appears to be tectonic. In the Columbia River valley the succession is truncated by the Columbia River fault zone, and elsewhere overlying Kaza Group may rest with tectonic contact upon the succession.

[1]Department of Geology, Carleton University, Ottawa, Ontario. K1S 2X9.

Acknowledgments

This investigation is part of a continuing study of the Selkirk and Shuswap terranes. Since 1972 the program has been funded primarily by grants from Energy, Mines and Resources (research agreements) and National Research Council (operating grant A2693). During the summers of 1977 and 1978 this work was also supported by the British Columbia Hydro and Power Authority as part of a geological investigation of the Revelstoke reservoir.

References

Brown, R.L. and Tippett, C.R.
1978: The Selkirk fan structure of the southeastern Canadian Cordillera; Geological Society of America Bulletin, v. 89, p. 548-558.

Campbell, R.B.
1968: Canoe River, B.C.; Geological Survey of Canada, Map 15-1967.

Psutka, F.J.
1978: Structural setting of the Downie Slide, northeast flank of Frenchman Cap gneiss dome, Shuswap complex, southeastern British Columbia; unpublished M.Sc. thesis, Carleton University, Ottawa, Ontario, 70 p.

Wheeler, J.O.
1965: Big Bend map-area, British Columbia; Geological Survey of Canada, Paper 64-32, 37 p.

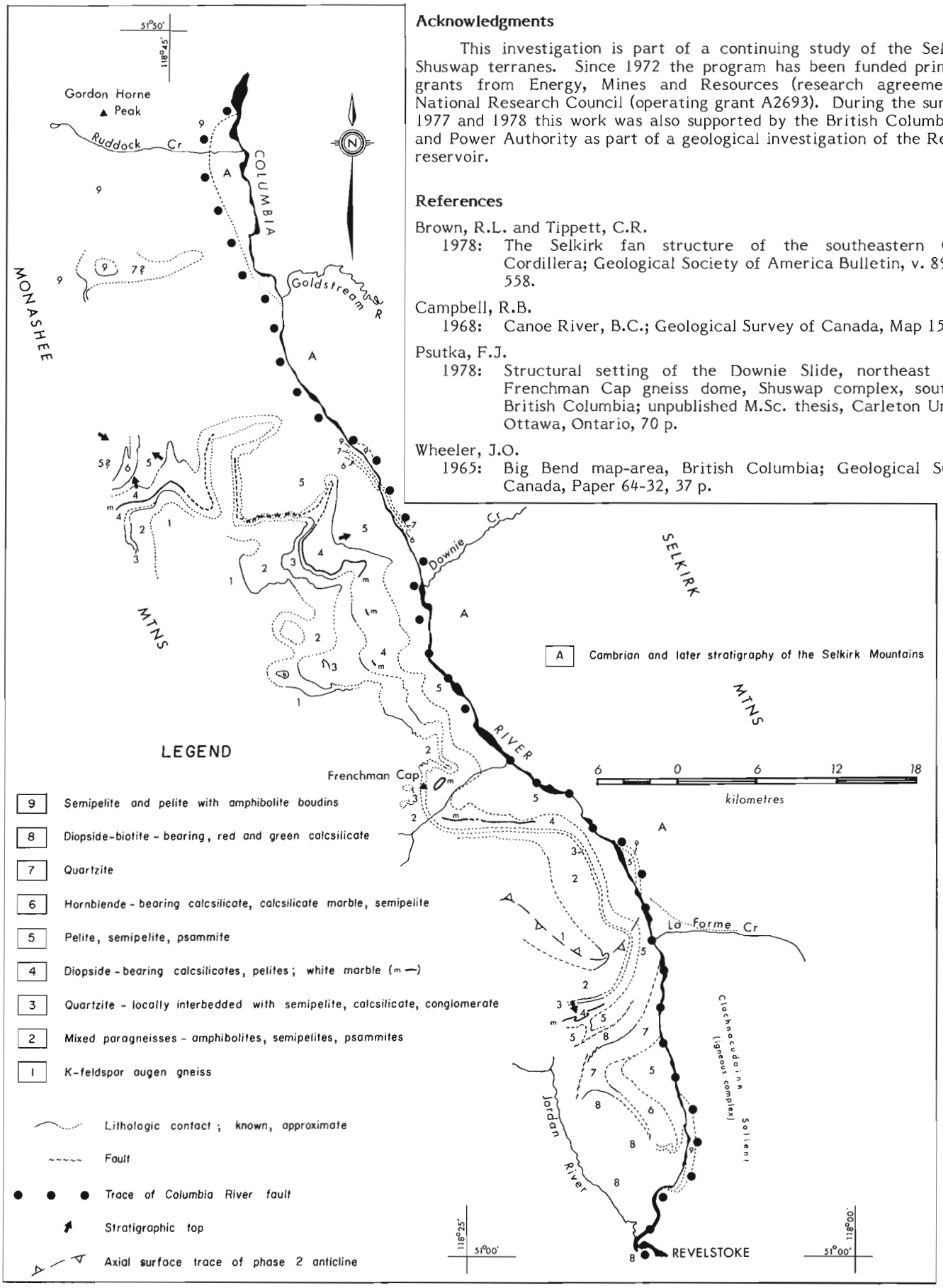


Figure 8.1. *Stratigraphy of the east flank of Frenchman Cap dome, Shuswap Complex.*

9. RELATIONSHIP BETWEEN THE SHUSWAP METAMORPHIC COMPLEX AND KOOTENAY ARC, VERNON EAST-HALF, SOUTHERN BRITISH COLUMBIA

DSS Contract No. OSQ78-00038

Peter B. Read[1]
Regional and Economic Geology Division

Read, Peter B., Relationship between the Shuswap Metamorphic Complex and Kootenay Arc, Vernon east-half, southern British Columbia; in Current Research, Part A, Geological Survey of Canada, Paper 79-1A, p. 37-40, 1979.

Abstract

Two major faults delimit three tectonic elements which in part underlie the map area. From west to east, the Columbia River fault zone separates the Shuswap Metamorphic Complex to the west from the Kootenay Arc and Clachnacudainn Salient to the east. East of Revelstoke, Standfast Creek slide sets the Clachnacudainn Salient against the Kootenay Arc. In the Shuswap Metamorphic Complex, over 7000 m of stratified amphibolite facies rocks form Thor-Odin, Pinnacle Peaks and the southern flank of Frenchman Cap gneiss domes. Within the dominant biotite-quartz-feldspar gneiss with local sillimanite-garnet ± muscovite-bearing layers and calc-silicate gneiss are four distinctive horizons of quartzite and an uppermost marble horizon. Gneiss and schist of Frenchman Cap and Thor-Odin domes host the lowest three quartzite layers, and to the south in Pinnacle Peaks dome they contain the uppermost quartzite and marble units. Low grade metamorphic rocks of the Slocan and Rossland groups form two known and several inferred klippen which lie on sillimanite-bearing rocks of the complex. In the southern part of Clachnacudainn Salient, mica schist, local quartzite and an amphibolite of the Lardeau Group are host to Devonian and younger plutonic rocks. In the polydeformed Shuswap Metamorphic Complex, two phases of tight to isoclinal folding affect the distribution of map units. The quartzite and marble horizons outline folds which seem to have orientations spatially related to their positions on the gneiss domes. Within the map area, Standfast Creek slide is a premetamorphic fault which dips gently eastward. The Columbia River fault zone is a postmetamorphic fault zone which dips gently eastward and truncates Standfast Creek slide north and south of Revelstoke to create the tectonic slice called Clachnacudainn Salient. Movement on the Columbia River fault zone is probably normal and exceeds 15 km dip-slip.

Introduction

Two months were devoted to examining the stratified metamorphic rocks enveloping the Core Zone of Thor-Odin gneiss dome (Fig. 9.1) in Vernon (east half) (eastern part of 82L E/2) map area. Mapping along the Columbia River valley, between Thor-Odin and Pinnacle Peaks gneiss domes, and in the vicinity of the Trans-Canada Highway supplements the earlier published work of Reesor (1970 and 1973), Reesor and Froese (1968 and 1969) and Reesor and Moore (1971) and unpublished data of Craig (1966), Duncan (in prep.), Hill (1975), Mutti (in prep.) and Thompson (1972).

Two major faults delimit three tectonic elements which in part underlie the map area. From west to east, the Columbia River fault zone separates the Shuswap Metamorphic Complex to the west from the Kootenay Arc and Clachnacudainn Salient to the east. East of Revelstoke, Standfast Creek slide sets Clachnacudainn Salient against Kootenay Arc. To emphasize the importance of the Columbia River fault zone, a description of the stratigraphy of the Shuswap Metamorphic Complex precedes that of the Kootenay Arc and Clachnacudainn Salient combined. As the boundary selected for the Shuswap Metamorphic Complex in this report differs slightly in position from the sillimanite isograd chosen as the boundary by some workers (Reesor, 1970, p. 73), the criteria controlling the placement of the boundary are given. The Shuswap Metamorphic Complex exposed in the Omineca Crystalline Belt in southeastern British Columbia is a terrane of moderate to high grade regional metamorphic rocks of uncertain stratigraphic correlation.

Stratigraphy

Shuswap Metamorphic Complex

Over 7000 m of stratified, amphibolite facies rocks form Thor-Odin, Pinnacle Peaks and the southern flank of Frenchman Cap gneiss domes. The rocks are predominantly metasedimentary, lie mainly in the sillimanite zone, and locally contain abundant quartz-feldspar pegmatites and leucogranitic sills and dykes. Although stratigraphic facing is uncertain, the direction chosen in this report yields an upright sequence for successions exposed in the three gneiss domes and coincides with primary facing directions found in the basal quartzite on the southern and western sides of Frenchman Cap gneiss dome (Fyles, 1970; McMillian, 1973). The succession is described briefly in the assumed ascending order.

Within the dominant biotite-quartz-feldspar gneiss with local sillimanite-garnet ± muscovite-bearing layers and calc-silicate gneiss are distinctive horizons of quartzite and marble (Fig. 9.2). Near Clanwilliam, the lowest muscovite-bearing quartzite (Q1) grades down through micaceous and feldspathic meta-grit into leucocratic biotite-quartz-feldspar paragneiss and orthogneiss. Above overlying biotite ± muscovite schist, biotite-hornblende schist and biotite-diopside bearing calc-silicate gneiss is a second quartz (Q2) which extends from north of the map area to the south side of Thor-Odin gneiss dome where it apparently forms the base of the Mantling Zone of Reesor and Moore (1971). Muscovite-quartzite (Q2) is a few hundred metres thick and southwest of Revelstoke contains a medial package of schist, marble and calc-silicate gneiss. A stratigraphically higher(?) quartzite (Q3) outcrops at the west end of Victor Lake above a sequence of interbedded mica schist and diopside-bearing calc-silicate gneiss. The complete sequence of gneiss, schist and quartzite forms the southern flank of Frenchman Cap gneiss dome and comprises the Mantling and much of the Fringing zones of Thor-Odin gneiss dome.

[1]Geotex Consultants Limited, 1103 – 100 W. Pender St., Vancouver, B.C.

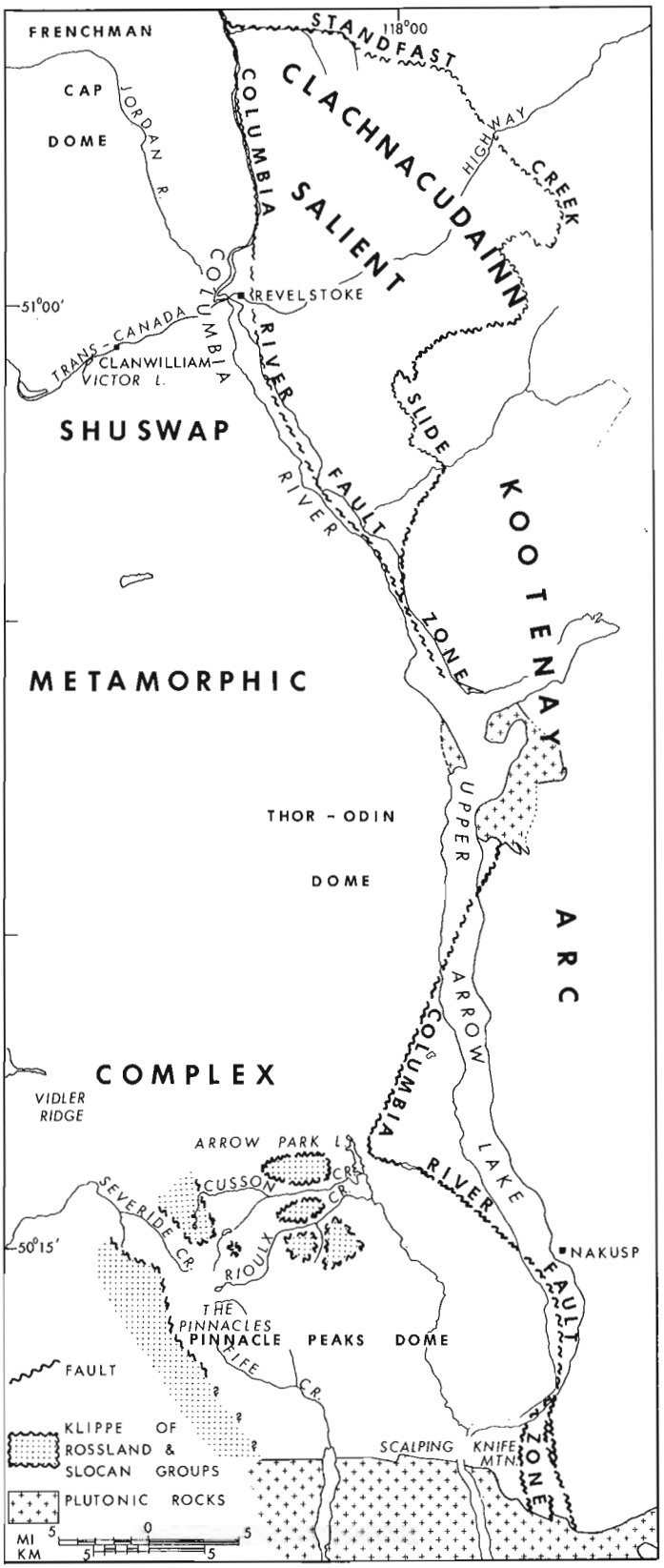


Figure 9.1. Location map showing major faults, tectonic elements and locations of gneiss domes on the eastern side of the Shuswap Metamorphic Complex, southern British Columbia.

A white, calcite- and diopside-bearing quartzite (Q4) links the underlying sequence exposed in Thor-Odin and Frenchman Cap gneiss domes to the overlying stratigraphy involved in Pinnacle Peaks dome. It outcrops over a distance of 30 km from The Pinnacles eastward to Scalping Knife Mountain. Probably the same quartzite exposed in the Fringing Zone of Thor-Odin gneiss dome on Vidler Ridge was included incorrectly with the Supracrustal Zone 5 km northeast of Arrow Park Lake (Reesor and Moore, 1971) and within the Milford Group east of Upper Arrow Lake north and south of Nakusp (unit uMMq of Read and Wheeler, 1976). Overlying the quartzite is a 2000 m thick succession of biotite-quartz-feldspar paragneiss, quartz-rich mica schist, calc-silicate gneiss and minor amphibolite. A white to light grey, layered marble (M) about 100 m thick is the highest marker horizon of the stratified metamorphic rocks. It extends over 30 km westward from the west shore of Upper Arrow Lake opposite Nakusp to west of Severide Creek. Up to 500 m of quartz-rich mica schist and an uppermost aluminosilicate- or staurolite-bearing schist top the marble. Rocks from the calcite-bearing quartzite to the aluminosilicate schist underlie Pinnacle Peaks dome.

Kootenay Arc and Clachnacudainn Salient

East, west and southwest of Arrow Park Lake, a well bedded sequence of grey phyllite and siltstone, and tuff, breccia and flows caps ridges. The metamorphic grade of these rocks increases southwestwards across Arrow Park Lake from chlorite zone to garnet zone. South of Rioulx Creek and west of Cusson Creek, similar rocks are in the staurolite zone. Southwest of Fife and Severide creeks, grey phyllite, siltstone and calcareous siltstone underlie flows and pyroclastic rocks which are mainly in the chlorite zone. Although the well preserved sedimentary and overlying volcanic rocks of these areas are unfossiliferous, they lithologically resemble sedimentary rocks of the Slocan Group and volcanic rocks of the Rossland Group exposed in the Kootenay Arc.

In the map area, the southern part of the Clachnacudainn Salient consists of biotite-muscovite schist, local micaceous quartzite and a calcite- and biotite-bearing amphibolite (A on Fig. 9.2). The 50 to 75 m thick amphibolite is lithologically similar to the Jowett Formation, and the schist and micaceous quartzite resemble the Index and Broadview formations of the Lardeau Group as exposed east of Standfast Creek slide in the Kootenay Arc.

Structure

Shuswap Metamorphic Complex

In the polydeformed Shuswap Metamorphic Complex, two phases of tight to isoclinal folding significantly affect the distribution of map units. Because the orientation of folds seems spatially related to their positions on the gneiss domes, at present no phase of deformation can be traced or correlated the length of the map area. The parts of each gneiss dome within the map area will be treated separately proceeding from north to south.

Southern Flank of Frenchman Cap gneiss dome in Jordan River area, Fyles (1970) described three phases of deformation which continue southwards into the map area. Widespread, west-northwesterly trending folds with southwesterly dipping axial planes correspond to Fyles' phase 2 folds. Mesoscopic folds and lineations which trend northeasterly or southwesterly are probably parasitic to phase 1 folds described by Fyles and the Begbie fold defined by Reesor (pers. comm., 1978). A broad, southerly trending antiform, centred along Jordan River, continues as far south as the Trans-Canada Highway. The Columbia River fault zone truncates all structures on the east.

Thor-Odin gneiss dome Reesor (1970, p. 78) described three phases of folding consisting of: (a) a first phase composed of macroscopic isoclinal folds outlined by quartzite, (b) a second phase comprised of mesoscopic folds, compositional streaking or aligned sillimanite, and (c) a third phase consisting of open warps along northwesterly trending axes. According to Reesor and Moore (1971, Fig. 13), the trend of the first phase ranges from westerly on the southern flank of the dome through northwesterly in the core of the dome to northerly on the eastern flank. Reesor and Moore's second phase structures defined by a sillimanite lineation, are of similar orientation to Fyles' first phase on the southern side of Frenchman Cap gneiss dome. East of Thor-Odin gneiss dome, the Columbia River fault zone truncates all structures and sets them against those of the Kootenay Arc.

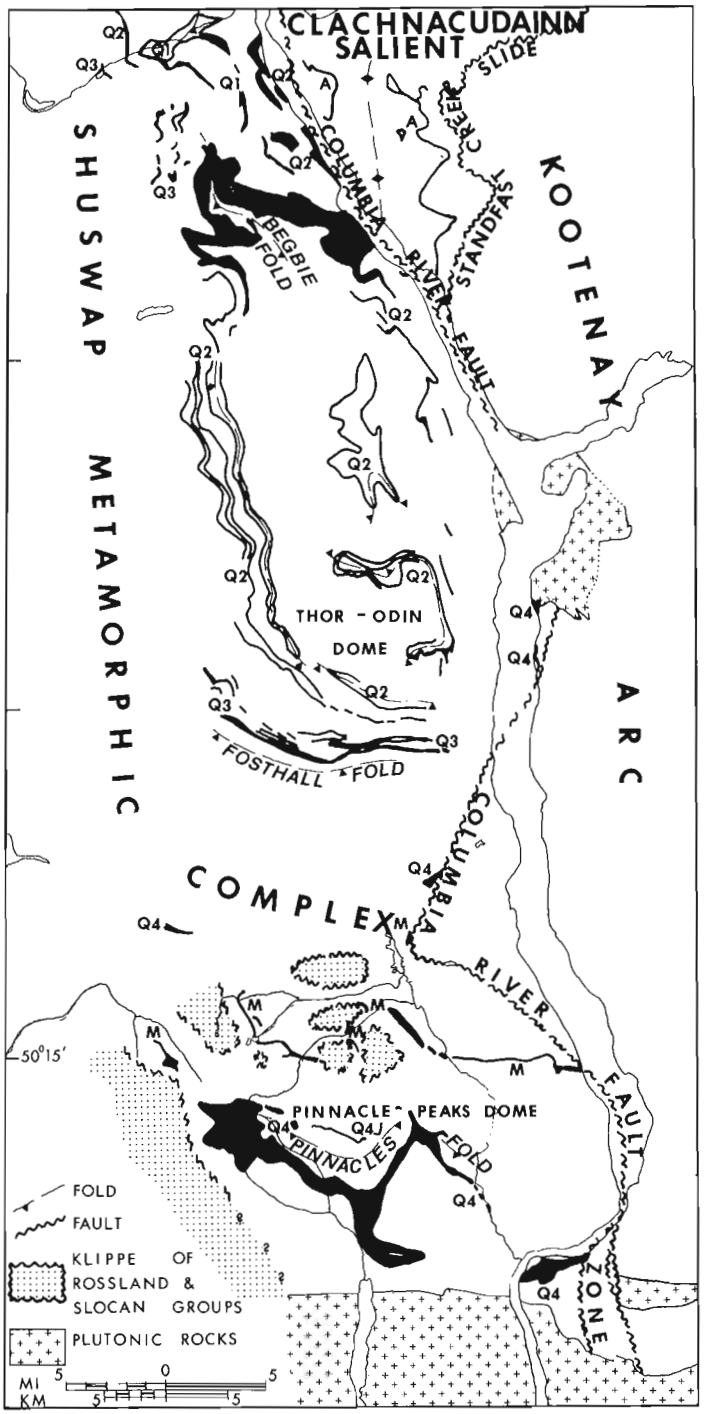


Figure 9.2. *Distribution of quartzite (Q1, Q2, Q3, and Q4) and marble (M) units on the southeastern side of the Shuswap Metamorphic Complex, amphibolite (A) in the Clachnacudainn Salient, and klippen of the Rossland and Slocan groups lying on the southern edge of the complex.*

Pinnacle Peaks dome Reesor and Froese (1969) outlined the westerly trending, northward closing Pinnacles fold as a major structure. North and west of Arrow Park Lake, mesoscopic fold axes, compositional streaking and sillimanite lineation parallel the Pinnacles fold developed farther south, and the Fosthall fold developed farther north. The absence of earlier structures in Pinnacle Peaks dome suggests that the Pinnacles fold is first phase even though the coaxial compositional streaking and sillimanite alignment are typical of second phase structures in Thor-Odin gneiss dome.

Clachnacudainn Salient

At the south end of Clachnacudainn Salient, lineation and mesoscopic fold axes plunge gently northwestward or southeastward. Attitudes of bedding and foliation and distributon of the amphibolite outline an upright, open antiform which plunges gently southward. The late antiform controls the plunge of earlier linear structures and it disappears southward against the Columbia River fault zone.

Standfast Creek slide and the Columbia River fault zone

Standfast Creek slide forms the northern, eastern and southern edges of the Clachnacudainn Salient. Within the map area, it is a premetamorphic fault which dips gently eastward. The salient contains rocks of the Lardeau Group, intrusions, and a gneiss of at least 400 Ma age (Wanless and Okulitch, 1976). The nearest gneiss of similar age is the Mount Fowler Batholith (Okulitch et al., 1975) enveloped by the Eagle Bay Formation which is lithologically similar to the Lardeau Group. This correlation implies that the salient could have been derived from as far as 50 km to the west.

The Columbia River fault zone forms the western edge of the Clachnacudainn Salient and southwards the western edge of the Kootenay Arc. It is a postmetamorphic fault, dips gently eastward, and truncates Standfast Creek slide north and south of Revelstoke to create the tectonic slice which is called the Clachnacudainn Salient. To the south, the fault zone forms the boundary between the Supracrustal and Fringing zones of Reesor and Moore (1971). East of Arrow Park Lake, it veers to the southeast and flattens in dip. The gentle dip results in a sinuous fault trace and north and south of Cusson Creek it cuts rocks of the Slocan and Rossland groups and leaves them as klippen lying on sillimanite-bearing rocks of the Shuswap Metamorphic Complex. Low grade metamorphic rocks similar in lithology to those of the Rossland and Slocan groups outcrop south of Rioulx Creek, west of Cusson Creek, and southwest of Fife and Severide creeks. The sudden downward increase in metamorphic grade near the lower contact of these rocks (Moore et al., in prep.), and the apparent discontinuity in orientation of folds in these rocks compared to that of folds in the sillimanite-bearing rocks (Reesor, 1970, p. 82-83; Reesor and Froese, 1969), are suggestive of, but do not necessitate the faulted basal contact inferred for several areas of rocks of the Slocan and Rossland groups (Fig. 9.2). Normal fault movement suggested by Read (1977) remains probable and the amount of displacement, which exceeds 15 km based on metamorphic considerations, could be much larger. If the allochthonous relationship between rocks of known correlation and those of uncertain correlation in the Shuswap Metamorphic Complex is widespread, then the complex in the map area could involve stratified rocks as old as the Belt-Purcell Supergroup.

References

Craig, D.B.
1966: Structure and petrology within Shuswap Metamorphic Complex, Revelstoke, British Columbia; unpublished Ph.D. thesis, Department of Geology, University of Wisconsin, 130 p.

Fyles, J.T.
1970: The Jordan River area, near Revelstoke, British Columbia; British Columbia Department of Mines and Petroleum Resources, Bulletin 57.

Hill, R.P.
1975: Structural and petrological studies in the Shuswap Metamorphic Complex near Revelstoke, British Columbia; unpublished M.Sc. thesis, Department of Geology, University of Calgary, 147 p.

McMillian, W.J.
1973: Petrology and structure of the west flank, Frenchman's Cap dome near Revelstoke, British Columbia; Geological Survey of Canada, Paper 71-29.

Moore, J.M., Reesor, J.E., and Froese, E.
Tectonic and metamorphic history of the gneiss domes in the Shuswap Complex of British Columbia. (in prep.)

Okulitch, A.V., Wanless, R.K., and Loveridge, W.D.
1975: Devonian plutonism in south-central British Columbia; Canadian Journal of Earth Sciences, v. 12, p. 1760-1769.

Read, P.B.
1977: Relationship of the Kootenay Arc to the Shuswap Metamorphic Complex, southern British Columbia; in Geological Association of Canada, Program with Abstracts, v. 2, p. 43.

Read, P.B. and Wheeler, J.O.
1976: Geology, Lardeau west-half, British Columbia; Geological Survey of Canada, Open File 432.

Reesor, J.E.
1970: Some aspects of structural evolution and regional setting in part of the Shuswap Metamorphic Complex; in Geological Association of Canada, Special Paper 6, p. 73-86.

1973: Blanket Mountain area, British Columbia; in Report of Activities, Part A, Geological Survey of Canada, Paper 73-1A, p. 38.

Reesor, J.E. and Froese, E.
1968: Petrology and structure, Pinnacle Peaks map-area, British Columbia; in Report of Activities, Part A, Geological Survey of Canada, Paper 68-1A, p. 111-112.

1969: Structural and Petrological study of Pinnacle Peaks gneiss dome, British Columbia; in Report of Activities, Part A, Geological Survey of Canada, Paper 69-1A, p. 139-140.

Reesor, J.E. and Moore, J.M.
1971: Petrology and structure of Thor-Odin gneiss dome, Shuswap Metamorphic Complex, British Columbia; Geological Survey of Canada, Bulletin 195.

Thompson, R.I.
1972: Geology of the Akolkolex River area near Revelstoke, British Columbia; unpublished Ph.D. thesis, Department of Geological Sciences, Queen's University, Kingston, Ont., 123 p.

Wanless, R.K. and Okulitch, A.V.
1976: Geochronological studies of the Shuswap Metamorphic Complex, southern British Columbia; Geological Association of Canada, Program with Abstracts, v. 1, p. 47.

10.

PROBLEMS IN GAMMA-RAY LOGGING: THE EFFECT OF DIPPING BEDS ON THE ACCURACY OF ORE GRADE DETERMINATIONS

Project 740085

John G. Conaway
Resource Geophysics and Geochemistry Division

Conaway, John G., Problems in gamma-ray logging: The effect of dipping beds on the accuracy of ore grade determinations; in Current Research, Part A, Geol. Surv. Can., Paper 79-1A, p. 41-44, 1979.

Abstract

When the grade-thickness product of a uranium ore zone is computed on the basis of a gamma-ray log, it is assumed that the borehole was drilled perpendicular to the plane of the ore zone. If this assumption is not valid the grade-thickness determination will indicate more uranium ore than is actually present. A simple geometrical treatment shows that for a relative dip angle of 0 to 20° (between the normal to the borehole and the plane of the ore zone) the error is small, about 6 per cent or less. For larger relative dip angles the error can be substantial, e.g. 100 per cent for a relative dip of 60°. If the relative dip can be determined from dipmeter logs or estimated from the geology, a simple linear correction factor can be applied to the apparent ore grade-thickness values to compensate for the error due to dipping beds.

Introduction

One of the fundamental assumptions involved in determining ore grade values from gamma-ray logs is that the borehole was drilled perpendicular to the plane of the ore zone. Clearly this assumption is not always valid. Thus, it is important to understand what sort of errors in computed ore grade values will occur if the borehole is not drilled perpendicular to the ore zone, and what steps can be taken to compensate for these errors. For simplicity the term dip angle will be used to describe the angle between the normal to the borehole axis and the plane of the ore zone, whether or not the borehole is vertical.

In practice, the problem of making accurate ore grade determinations in the presence of dipping beds is complex. A precise solution will require a study involving model holes with dipping ore zones, combined with tests in specially drilled sets of field boreholes, in order to investigate all of the second-order effects involved. Since this problem is of immediate economic interest to the uranium mining industry, a simple geometrical treatment is given here to provide correction factors for improving the accuracy of ore grade determinations in the presence of dipping beds. For the purposes of this treatment second-order effects such as density variations in the rock are ignored. In addition, the borehole and probe are assumed to be of negligible diameter compared with the volume of rock being sampled. In the case of the slim holes (48-60 mm diameter) most commonly used in Canada's hard-rock mining areas this latter assumption should be reasonable.

The Effect of Dipping Beds

When an anomaly is found on a gamma-ray log we would like to determine the grade G and thickness T of the ore zone (or other radioactive zone) which caused the anomaly. Since an ore zone is not necessarily of uniform grade throughout its thickness, it is conventional to compute the grade-thickness product GT over the zone (see Scott et al., 1961). This process is illustrated in Figure 10.1. The average gamma-ray intensity $\overline{C(z)}$ (counts/sec) over each depth interval Δz is multiplied by the system sensitivity K (%U_3O_8sec/count) and by the value of Δz(cm). This is repeated over the entire anomaly and summed to give the grade-thickness product of the anomaly:

$$GT = K \sum \Delta z \, \overline{C(z)} = KA \qquad (1)$$

where A is the area under the anomaly curve.

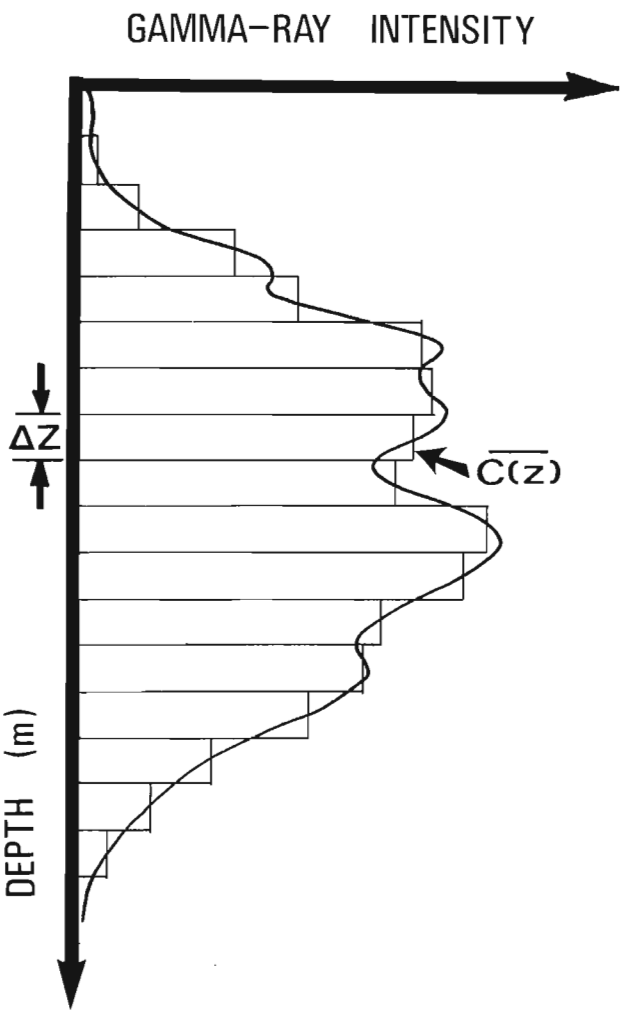


Figure 10.1. *Simulated gamma-ray log showing the procedure for computing the grade-thickness product for an ore zone (see text).*

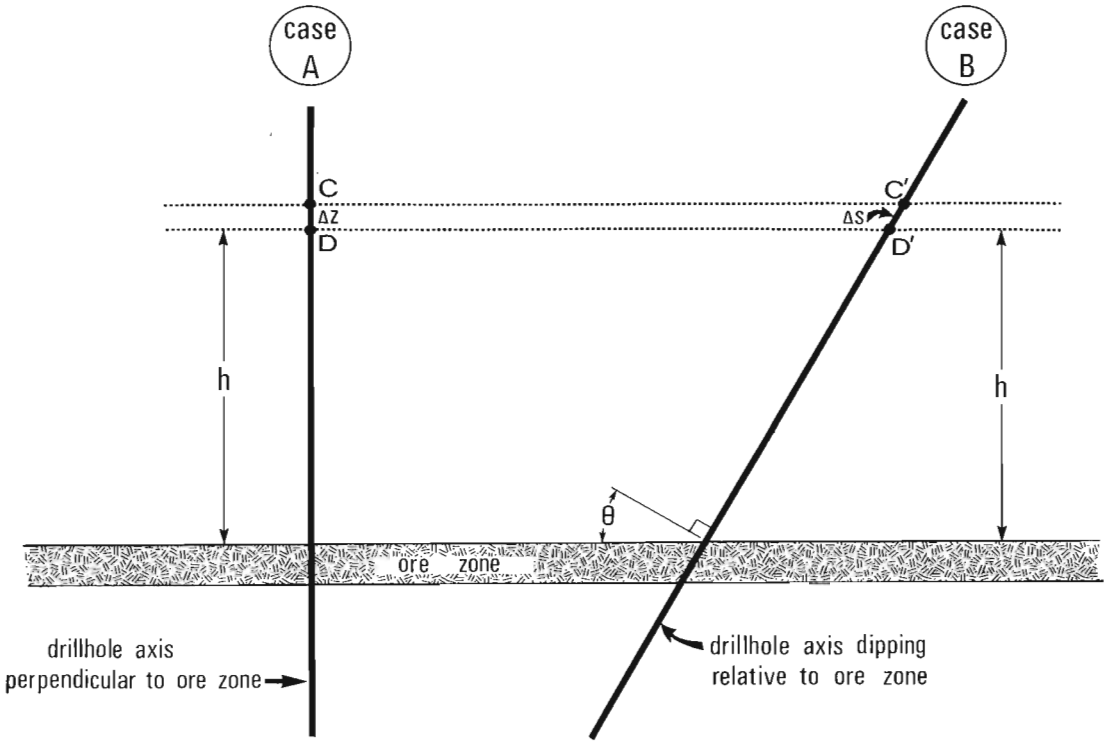


Figure 10.2. *Sketch of an ore zone with two boreholes passing through it. In case A the borehole was drilled perpendicular to the ore zone while in case B there is a relative dip θ between the normal to the borehole and the ore zone.*

Now consider two holes drilled through the same ore zone (Fig. 10.2). In case 'A' the borehole is perpendicular to the ore zone, and in case 'B' there is a relative dip θ between the normal to the borehole and the ore zone. In case 'A' the average gamma-ray intensity over the interval between points C and D is multiplied by their separation (Δz). This is repeated for all such sample intervals Δz to give the grade-thickness product for the ore zone. In case 'B', the average reading over the inverval C'D' will be essentially the same as for the interval CD in case A, since the perpendicular distance to the ore zone is the same. However the separation is now Δs where

$$\Delta s = \frac{\Delta z}{\cos\theta} \qquad (2)$$

and thus the apparent grade-thickness product GT_{app} in the dipping case is related to the true grade-thickness product GT by

$$GT_{app} = \frac{GT}{\cos\theta} \qquad (3)$$

This simple result is illustrated in Figure 10.3, where curve 1 shows the simulated gamma-ray anomaly due to a thin ore zone (see Conaway and Killeen, 1978) measured along a borehole perpendicular to the plane of the ore zone. Curve 2 shows the anomaly resulting from the same ore zone, measured along a borehole dipping relative to the ore zone. The area under curve 2 (the apparent grade-thickness product) is clearly different from the area under curve 1, or true grade-thickness product. The error $e(\%U_3O_8)$ between the apparent grade-thickness GT_{app} and the true grade-thickness GT is given by:

$$e = GT_{app} - GT = KA\left(\frac{1}{\cos\theta} - 1\right) \qquad (4)$$

and the percentage error E is given by:

$$E = 100\,\frac{e}{GT} = 100\left(\frac{1}{\cos\theta} - 1\right) \qquad (5)$$

Figure 10.4 shows the percentage error E resulting from various relative dip angles θ. Figure 10.5 shows the dimensionless correction factor δ needed to convert the apparent grade-thickness product GT_{app} for various dip angles θ into the true grade-thickness product according to the relation:

$$GT = \delta GT_{app} \qquad (6)$$

It is obvious from Equation (3) that δ is given by

$$\delta = \cos\theta \qquad (7)$$

The correction factor δ is useful in cases where the relative dip of the ore zone is known or can be estimated from geologic logs, dipmeter records, etc. Generally in mining applications an attempt is made to drill perpendicular to the dip of the ore zones, if the dip can be inferred on the basis of the geology or previous drilling in the region. In such cases, θ should be comparatively small; a relative dip of 20° gives an error of only about 6 per cent. If θ is known then the appropriate correction factor δ can be applied to compensate.

Effective Depth Interval

The concept of effective depth interval is useful in dealing with the problem of dipping ore zones. The effective depth interval, Δz_e, is related to the true depth interval Δs and relative dip θ by the expression:

$$\Delta z_e = \Delta s \cos\theta - \Delta s\,\delta \qquad (8)$$

The concept of effective depth is especially important when inverse filtering of the data is to be carried out (see Conaway and Killeen, 1978). Throughout the processing, the gamma

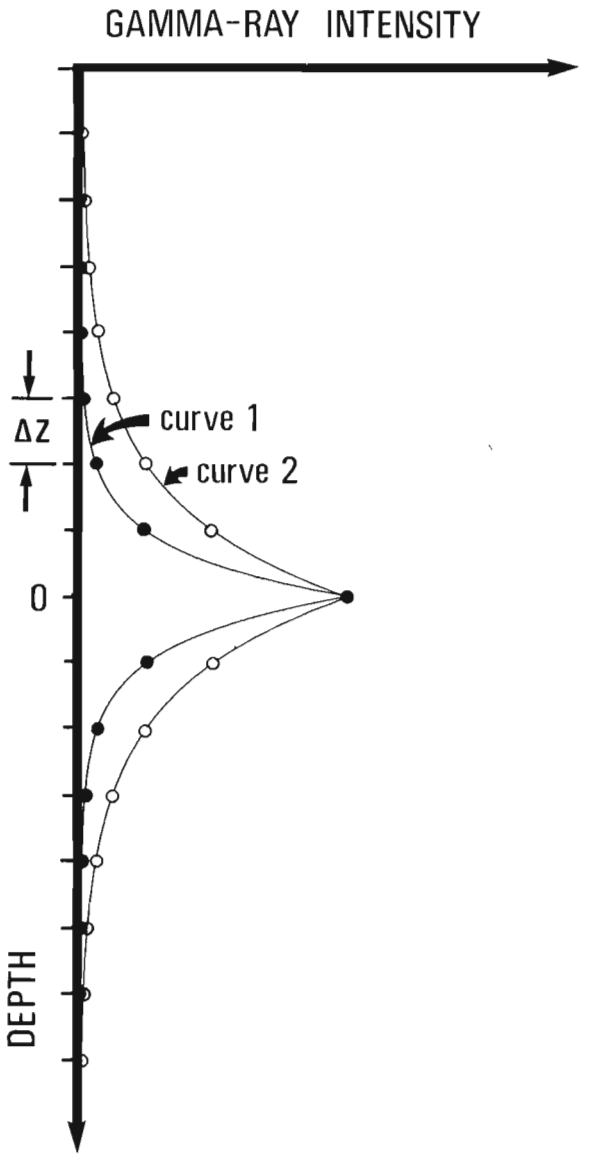


Figure 10.3. *Curve 1 shows the ideal gamma-ray log past a thin ore zone perpendicular to the borehole. Curve 2 shows the ideal log past a thin ore zone dipping relatives to the borehole.*

ray log is treated as if the sample interval were Δz_e rather than the true value Δs. Furthermore, the effective depth interval is used rather than the true depth interval in computing the inverse filter (Conaway and Killeen, 1978). Thus the inverse filter technique for determining the distribution of radioactive material from the gamma-ray log is extended to the case of dipping ore zones. If the inverse filter is computed on the basis of the true sample interval rather than the effective interval, the processed log will not only indicate incorrect magnitudes, but will be distorted in shape was well.

Conclusions

It is likely that the procedure for correcting ore grade-thickness determinations for errors due to dipping beds will be refined as experimental studies in model boreholes and field boreholes are pursued. In the meantime, the simple treatment of the dipping bed case given here should serve to illustrate the magnitude of errors which can be expected in

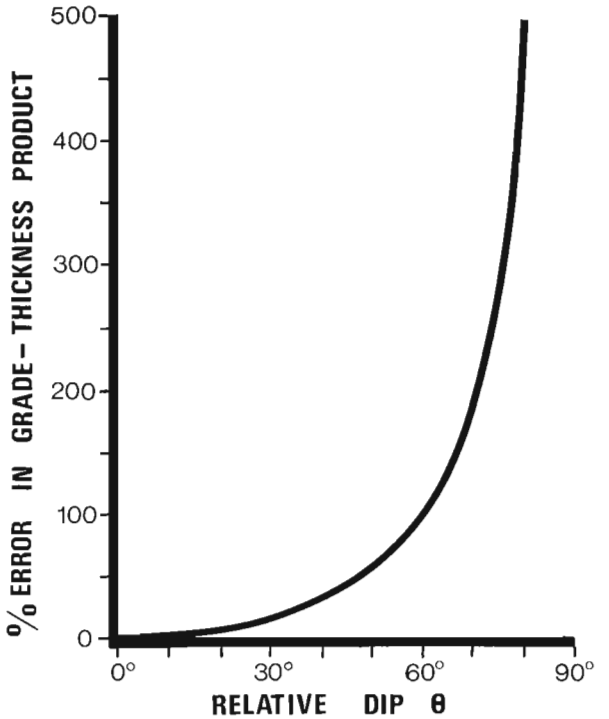


Figure 10.4. *Percentage error E in ore grade-thickness computations in the case of a dipping ore zone where it was assumed that the borehole was drilled perpendicular to the plane of the ore zone.*

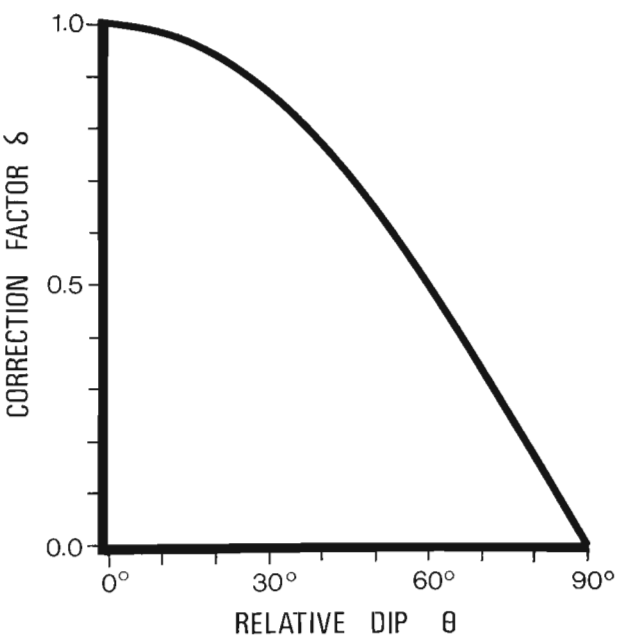


Figure 10.5. *Correction factor δ to compensate for the effect of a dipping ore zone on the grade-thickness calculations.*

practice, and demonstrate techniques for compensating for these errors. The result should be an improved estimate of the ore grade-thickness product.[1]

If the data are to be computer processed to determine the distribution of radioactive material along the borehole, the use of the effective depth interval in computing the inverse filter and processing the data will avoid the distortion which would result from using an incorrect inverse filter based on the true sampling interval.

Acknowledgment

The author is indebted to P.G. Killeen for helpful discussions regarding the mansucript.

References

Conaway, J.G. and Killeen, P.G.
1978: Quantitative uranium determinations from gamma-ray logs by application of digital time series analysis; Geophysics, v. 43, p. 1204-1221.

Scott, J.H., Dodd, P.H., Droullard, R.F., and Mudra, P.J.
1961: Quantitative interpretation of gamma-ray logs; Geophysics, v. 26, p. 182-191.

[1] Experimental results presented by Moore (1978) from two model boreholes with thin dipping ore zones indicate that the simple correction factor given by equation (6), and independently by Moore, provides surprisingly good results in practice. Moore has apparently not attempted to apply deconvolution techniques to his experimental data, so the accuracy of such techniques in the presence of dipping beds remains to be demonstrated experimentally. Moore's results were not available to the author until the present paper was in the galley proof stage.

Reference

Moore, D.C.
1978: Problems associated with calibration of radiation detectors for measurements in thin and dipping ore zones; paper presented at 48th annual meeting of the Society of Exploration Geophysicists, San Francisco, Oct. 29-Nov. 2.

11.

STRATIGRAPHY AND DEPOSITIONAL HISTORY OF SOME UPPER PROTEROZOIC SEDIMENTARY ROCKS ON NORTHWESTERN BAFFIN ISLAND, DISTRICT OF FRANKLIN

Contract 94843

Thomas R. Iannelli[1]
Regional and Economic Geology Division

Iannelli, Thomas, R., Stratigraphy and depositional history of some Upper Proterozoic sedimentary rocks on northwestern Baffin Island, District of Franklin; in Current Research, Part A, Geol. Surv. Can., Paper 79-1A, p. 45-56, 1979.

Abstract

Neohelikian strata outcropping on southwest Borden Peninsula and southeast into the Paquet Bay area (northwestern Baffin Island) include about 4500 m of shales, quartzarenites, subarkoses, stromatolitic dolostones and conglomerates. These beds were deposited in environments that ranged from fluvial braided stream, delta fan complex, to marine basin supratidal, intertidal and subtidal. Paleocurrent dispersal patterns indicate that the dominant depositional trends were from the east and southeast.

The pattern of sediment deposition was influenced by faulting, which occurred within northwest trending zones.

Introduction

Upper Proterozoic sedimentary rocks are well preserved in a fault bounded graben that extends across Borden Peninsula, southeast to the Paquet Bay area. During the 1978 field season nearly three months were spent studying preselected areas within NTS sheets 48A, 38B and 37G (Fig. 11.1) that contain strata of the Adams Sound, Fabricius Fiord, Arctic Bay and Society Cliffs formations. Foot and boat traverses were augmented by helicopter reconnaissance. Mapping was carried out at a scale of 1:50 000 and about 40 stratigraphic sections were measured.

The data collected will be incorporated into a doctoral thesis, at the University of Western Ontario. The work, which is sponsored by the Geological Survey of Canada under the supervision of G.D. Jackson, is part of a continuing study of the Neohelikian strata of the North Baffin Rift Zone that was begun in 1977 (Jackson et al., 1978). Carbonate rocks were classified according to Grabau (1904) whereas sandstones were classified according to Pettijohn (1975).

Regional Geology

A crystalline, Archean to Aphebian basement complex underlies most of the region. These rocks are chiefly irregularly banded, complexly folded, migmatites intruded by massive granite to granodiorite. Nebulitic to porphyroblastic gneiss and paragneiss are also present. Minor pegmatite veins are common.

Several thousand metres of Neohelikian sediments overlie the gneisses unconformably. The rock types include shale, siltstone, quartzarenite, subarkose, conglomerate and stromatolitic dolostone. The rocks are generally flat lying to gently dipping with highly folded beds common near major faults which separate them from the basement complex. The Neohelikian beds are overlain by Paleozoic strata in adjacent areas.

The Neohelikian rocks of Borden Peninsula were first defined and subdivided by Lemon and Blackadar (1963) and originally examined in the present study area by Blackadar (1970). Subsequent investigations include those by Geldsetzer (1973), Jackson et al. (1975, 1978) and Olson (1977).

Adams Sound Formation

The Adams Sound Formation outcrops extensively southwest of Magda Plateau. It is also found in Alfa River valley and along Tay Sound and Paquet Bay. It is characterized by thin- to thick-bedded and massive quartzarenite, with thin interbeds of subarkose and quartz pebble orthoconglomerate. These rocks are greyish purple, and locally have poorly defined, conglomerate-based, fining upward cycles.

This formation has a thickness of nearly 300 m west of Milne Inlet (Jackson et al., 1978) but is only 50 m thick east of the inlet (Fig. 11.2 — locality 6). The Adams Sound rests directly upon basement gneiss in the vicinity of, and east of

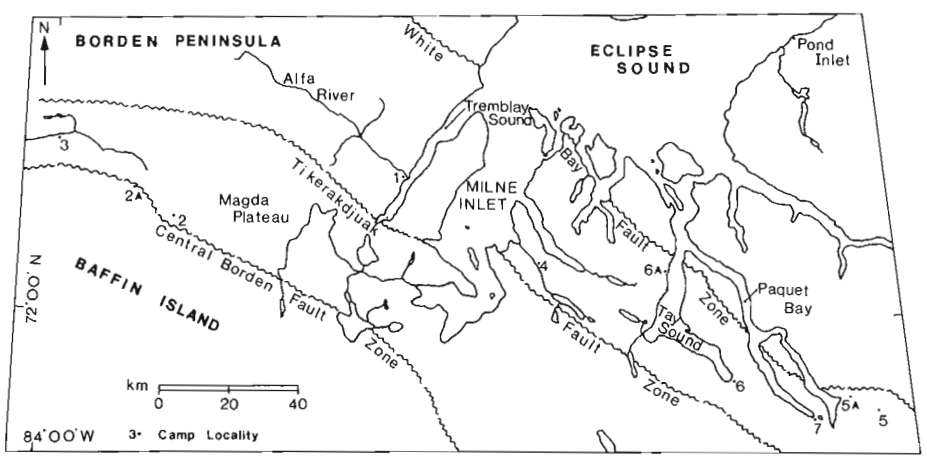


Figure 11.1. Location map.

[1]Department of Geology, University of Western Ontario, London, Ontario. N6A 5B7.

Table 11.1

Table of Formations

	West of Milne Inlet				East of Milne Inlet	
NEOHELIKIAN	Victor Bay Fm. (610 m)	VB: Shale, siltstone, dolostone				
		Conformable?				
	Society Cliffs Fm. (580 m)	SC_2: Stromatolitic and massive dolostone			SC_2:	Stromatolitic dolostone, minor siltstone, quartzarenite
		Unconformable				
	Fabricius Fiord Fm. (1500-2000 m)	FF_4:	FF_{4c}: Breccia-conglomerate FF_{4b}: Gritty, stromatolitic dolostone FF_{4a}: Subarkose, arkose	SC_1: Stromatolitic dolostone, minor quartzarenite, subarkose, shale	SC_1:	Redbed sequences, stromatolitic dolostone, minor quartzarenite
		FF_3:	Subarkose, conglomerate	Gradational to	Unconformable	
		FF_2: U-	Quartzarenite dominated, large coarsening up cycles	AB_4: Shale, minor stromatolitic dolostone	AB_4:	Quartzarenite, dolarenite, shale, stromatolitic dolostone
		M-	Shale dominated, large coarsening up cycles	Arctic Bay Fm. (610-770 m) AB_3: Shale	AB_3:	Shale, minor siltstone
		L-	Coarsening up cycles of shale, siltstone, quartzarenite	AB_2: Shale dominated, small coarsening up cycles	AB_2:	Quartzarenite dominated, small coarsening up cycles
		FF_1:	Subarkose, quartzarenite, minor shale, conglomerate	AB_1: Quartzarenite, siltstone, minor shale	AB_1:	Quartzarenite, siltstone, minor shale
				Gradational		
	Adams Sound Fm. (50-300 m)	AS_3: Quartzarenite, minor conglomerate AS_2: Quartzarenite AS_1: Quartzarenite			AS_5: Quartzarenite, conglomerate AS_4: Conglomerate	
		Nonconformity				
ARCHEAN-APHEBIAN	Amg	–	Granitic gneiss basement			

Milne Inlet. Adams Sound quartzarenite grades upward into both the Arctic Bay and Fabricius Fiord formations (Table 11.1).

The strata commonly contain medium sized, undulatory- to lunate-current ripple marks, planar- and trough-crossbeds and a few megaripples and bulbous load casts. Hematite staining and pyrite bedding plane coatings were seen in a few places.

The Adams Sound Formation is divisible into the AS_1, AS_2 and AS_3 members west of Milne Inlet (Jackson et al., 1978) and into the AS_4 and AS_5 members east of Milne Inlet.

AS_1 and AS_2 members

These members are present at locality 3 where they are poorly exposed. The AS_1 member grades upward into the overlying AS_2 member, and thin- to medium-bedded, greyish purple quartzarenite is characteristic of both units.

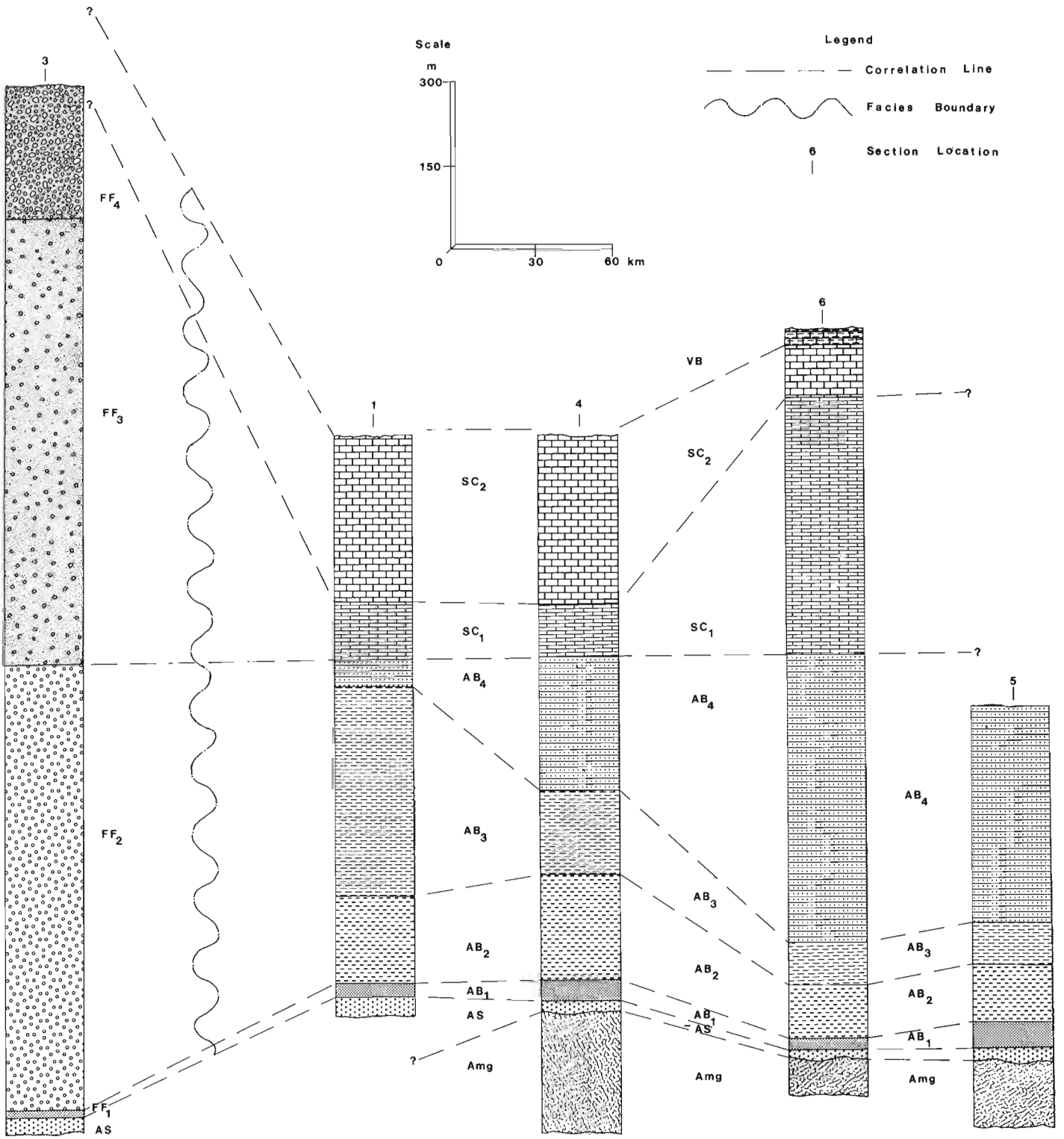


Figure 11.2. Representative stratigraphic sections from the study area. The formation abbreviations are listed in Table 11.1.

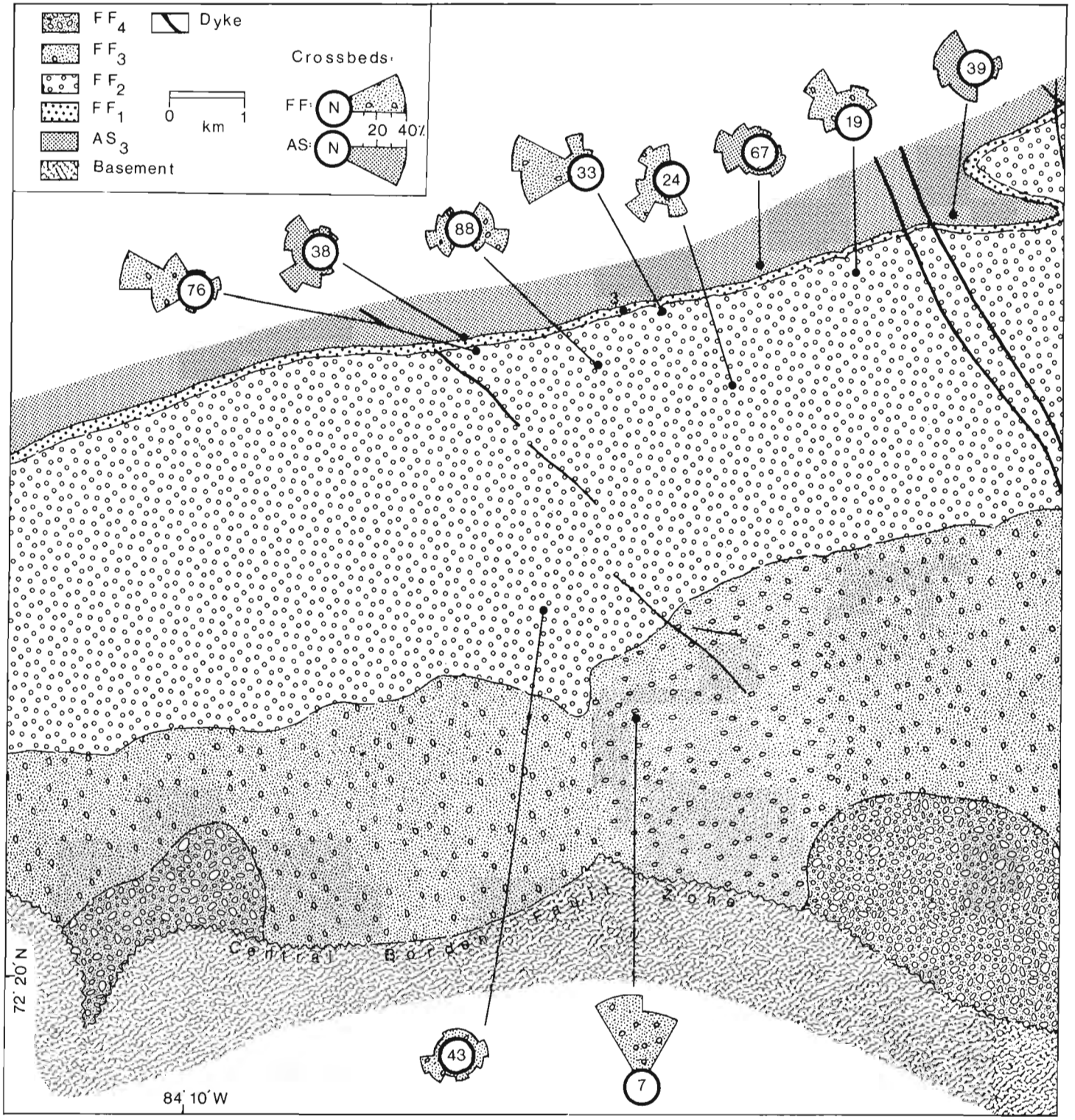


Figure 11.3. *General geology in the vicinity of locality 3. The map includes paleocurrent patterns of trough- and planar-crossbeds from the Fabricius Fiord and Adams Sound formations. The number of readings from each station is shown in the centre of the rose diagram.*

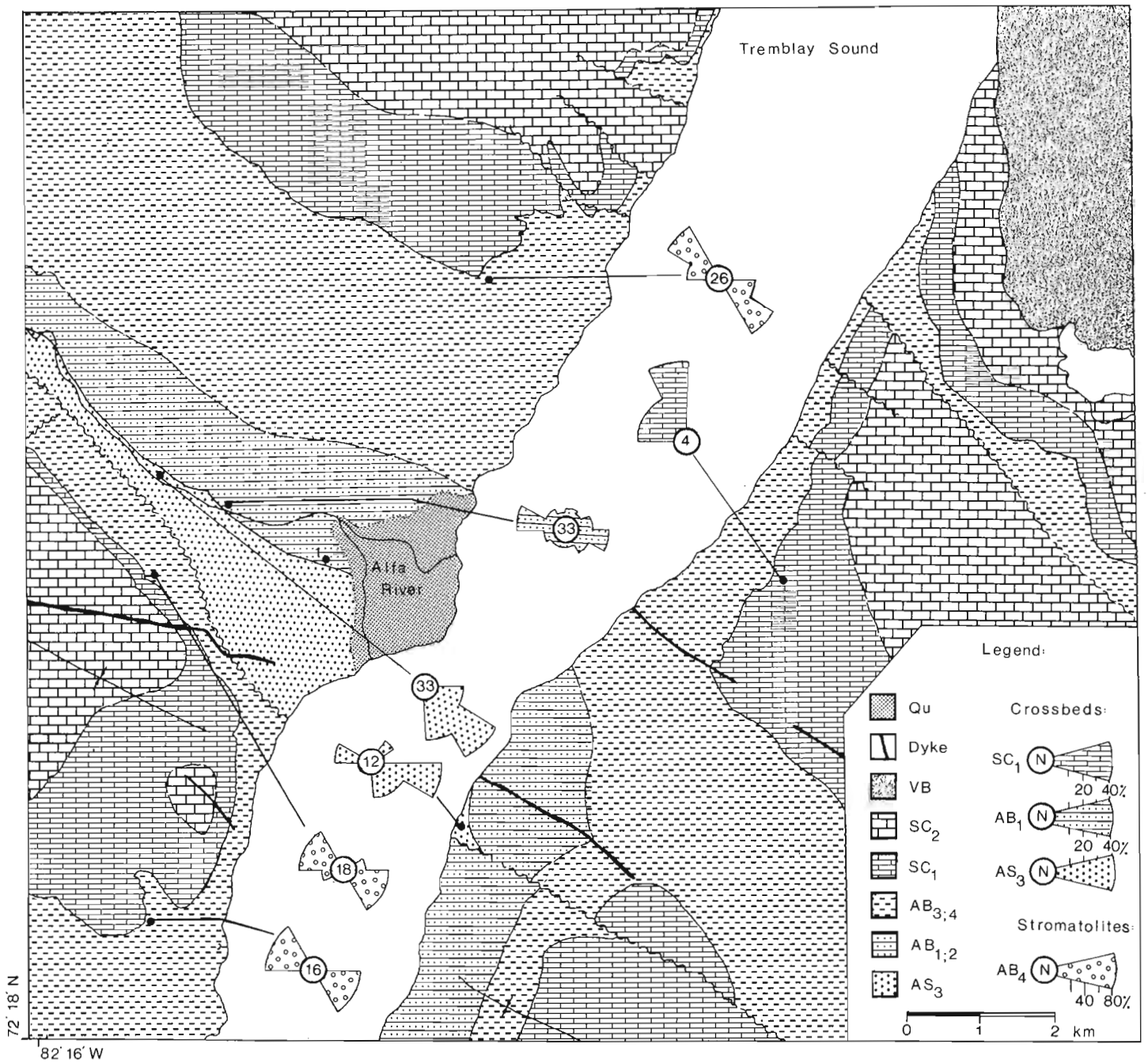


Figure 11.4. *General geology of the Tremblay Sound area, in the vicinity of locality 1. The map includes paleocurrent patterns of trough- and planar-crossbeds from the Adams Sound, Arctic Bay and Society Cliffs formations, and stromatolite elongation orientations from the Arctic Bay Formation. The number of readings from each station is shown in the centre of the rose diagram.*

AS_3 member

Mottled grey-white to pink-grey, medium bedded quartzarenite, and thin lenticular beds of quartz pebble orthoconglomerate are the predominant lithologies in this member. Incomplete measured sections range from 25 m thick at locality 1, to 64 m thick at locality 3.

Megaripples, with wavelengths of 1 to 2 m, heights of 0.3 to 0.6 m and consisting of large planar crossbeds occur in most sections. These have smaller undulatory current ripple marks superimposed on their upper surfaces. Ripple marked beds alternate with those having overturned planar crossbeds and with beds of structureless quartzarenite. Paleocurrent trends are mostly unimodal and less commonly bimodal, with depositional currents originating from the northwest (Fig. 11.4) and east to southeast (Fig. 11.3).

Localized occurrences of microfaulted quartzarenite and of wedge shaped clastic dykes indicate postdepositional disturbance. This is also implied at locality 1 where a sedimentary breccia channel 3 m wide, 2 m high and over 5 m long contains partially detached quartzarenite wall blocks and angular, ripple marked quartzarenite clasts set within a coarse grained quartzarenite matrix.

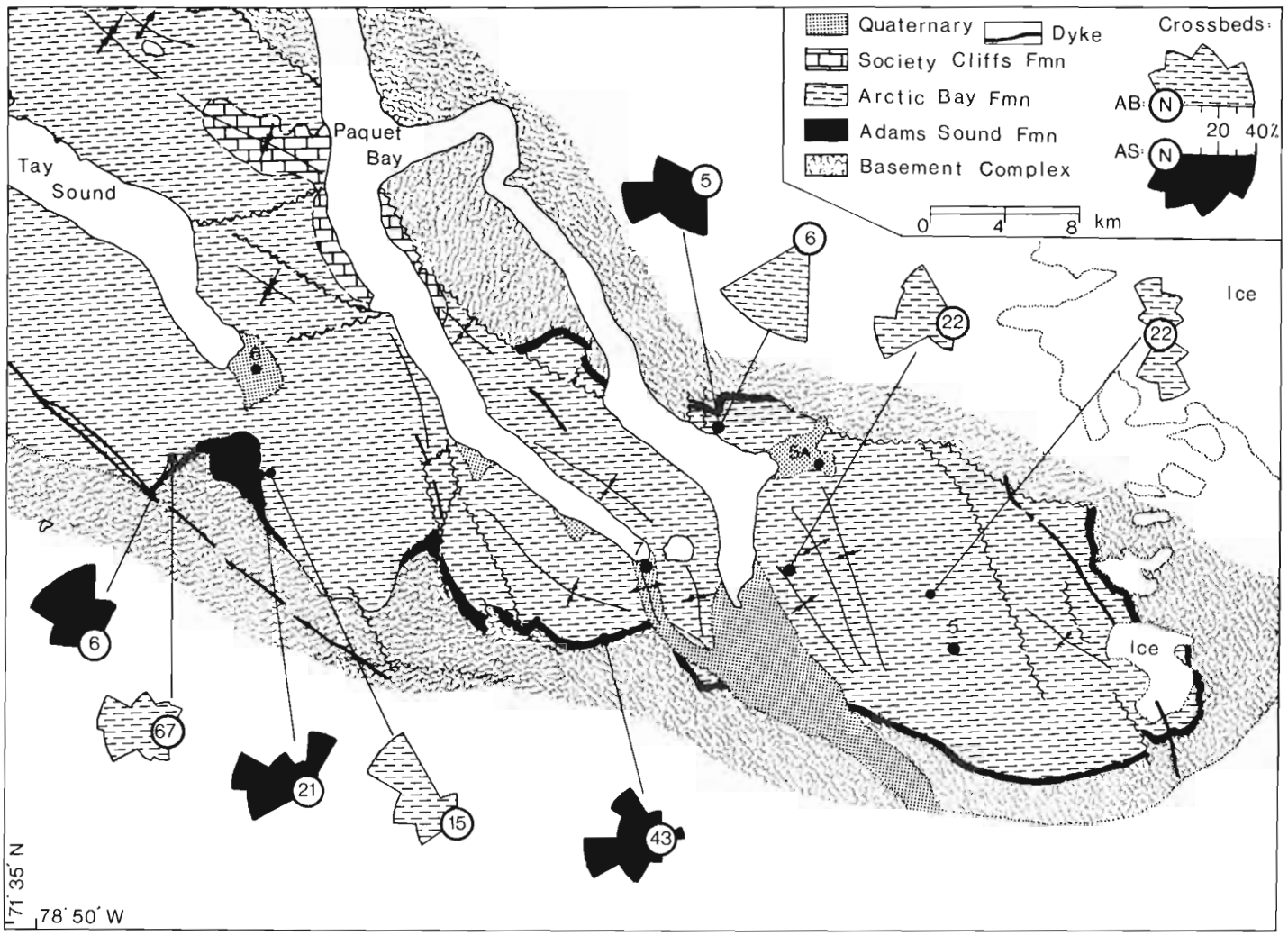


Figure 11.5. *General geology of the eastern map area, in the vicinity of localities 5 to 7. The map includes paleocurrent patterns of trough- and planar-crossbeds from the Adams Sound and Arctic Bay formations. The number of readings from each station is shown in the centre of the rose diagram.*

AS_4 member

Most of the AS_4 member is thick bedded to poorly bedded to massive, polymictic orthoconglomerate. Minor interbeds of purple-orange to grey subarkose, pebbly subarkose and quartzarenite also occur. Clasts within the conglomerate are chiefly quartz pebbles and cobbles, although quartzarenite, feldspar and gneiss clasts are found locally. The gneiss clasts increase in abundance downward toward the basal contact. AS_4 beds are found only east of Milne Inlet where the member ranges from 1 to 10 m thick.

The conglomerates unconformably overlie the basement complex at an undulatory contact whose relief is estimated to be 1 to 2 m. The beds are draped over the irregular basement surface, giving this member a pinch and swell character. Lower beds within the member appear to pinch out against the underlying gneisses. A regolith 3 m thick occurs at locality 5, immediately below the AS_4 contact.

Planar crossbeds in the conglomerates range up to 2.5 m thick, and contain current-aligned quartz pebbles along foreset and bottomset beds. Paleocurrent dispersal patterns from these crossbeds indicate sediment transport from the north and southeast (Fig. 11.5).

AS_5 member

This member includes medium bedded to massive quartzarenite which alternates with thin to thick beds of quartz pebble orthoconglomerate. At locality 7 these brown-grey to white rocks occur in conglomerate-based fining upward cycles. The member is present east of Milne Inlet where it is 18 to 28 m thick and is gradational with both the underlying AS_4 member and the overlying lower Arctic Bay strata.

Large scale planar crossbeds with graded foreset beds, crescent shaped current ripple marks with wavelengths of 0.3 to 1 m, and surface channels occasionally occur in these beds. The planar crossbeds have unimodal paleocurrent trends that indicate depositional currents from the southeast and south (Fig. 11.5).

Interpretation

On Borden Peninsula, west of the present day Milne Inlet, an extensive accumulation of fluvial quartzarenite (AS_1) gradually blanketed the basement terrane, in early Adams Sound time. Sedimentation progressed with little influence

from fault related tectonism. Deposition of mixed fluvial-intertidal sand bodies (AS_2, AS_3) followed as subsidence caused marine waters to encroach upon the earlier river systems.

Adams Sound sedimentation patterns east of the present day Milne Inlet, were probably influenced by periodic faulting and restriction within the narrow southeast arm of the Milne Inlet Trough of Jackson et al. (1975). Early Adams Sound deposition here was characterized by episodic shedding of clastic material, resulting in the formation of conglomerate-dominated proximal braided stream deposits (AS_4) and quartz-arenite-dominated distal braided stream cycles (lower AS_5). As tectonic activity subsided, or as source areas were worn down, these fluvial deposits were overlain by intertidal to subtidal sand bodies (upper AS_5; lower Arctic Bay strata) when transgressive marine water overwhelmed the trough.

Fabricius Fiord Formation

The Fabricius Fiord Formation outcrops in a belt 54 km long and 10 km wide, extending west from Magda Plateau (Fig. 11.1). It contains a thick lower unit of shale-siltstone-quartzarenite cycles and a thick upper unit of pebbly subarkose and conglomerate beds. Minor lithologies include stromatolitic dolostone, gritty dolostone, and granite clast breccia conglomerate. The formation ranges in thickness from 1500 m at locality 2A to 2000 m at locality 3 (Fig. 11.2).

The Fabricius Fiord was previously subdivided into three members (Jackson et al., 1978). Detailed examination in 1978 allowed subdivision into four intergradational members (Table 11.1). In addition, the FF_2 member has been expanded to include the lower two thirds of the FF_3 member of Jackson et al. (1978). The upper one third of the same FF_3 member is equivalent to the lower FF_3 member of the present study.

The contact with the underlying Adams Sound Formation is both conformable and gradational. The lower two members grade laterally northeast along strike into the Arctic Bay Formation (Fig. 11.6). Upper members are overlain at locality 2A by massive Society Cliffs dolostone and are laterally correlated with the lower member of the Society Cliffs Formation. The Fabricius Fiord strata are downfaulted against basement gneiss along the Central Borden Fault Zone (Fig. 11.3).

Siltstone and quartzarenite of the lower two members commonly contain small- to medium-sized, straight- and undulatory- to lunate-current ripple marks, trough- and planar-crossbeds, tubular to bulbous load structures and synaeresis cracks. The paleocurrent patterns, for the lower three members, indicate unimodal to bimodal trends with dominant clastic sources from the southeast and east (Fig. 11.3).

FF_1 member

This member contains a lower sequence predominantly of thin bedded quartzarenite and subarkose. Thin interbeds of pebbly subarkose, quartz- and feldspar-pebble orthoconglomerate, siltstone and shale are also present. The rocks are greyish green and 15 to 23 m thick.

The upper beds are more massive, brown to grey quartzarenite and contain graded crossbeds and structureless to load casted interbeds.

FF_2 member

The FF_2 member consists of clastic strata that were deposited in coarsening upward cycles which range from 9 to over 30 m thick and contain three subunits. The member ranges from 370 m thick, at locality 2, to 860 m thick at locality 3.

The lower subunit of each cycle contains planar thin- to thick-laminated, black to grey, shale and silty shale, with minor thinly bedded siltstone. This subunit is 3 to 15 m thick. It grades up into middle subunits of interlayered, thin- to medium-bedded, brownish grey quartzarenite, siltstone and shale. The quartzarenite and siltstone beds are undulatory to

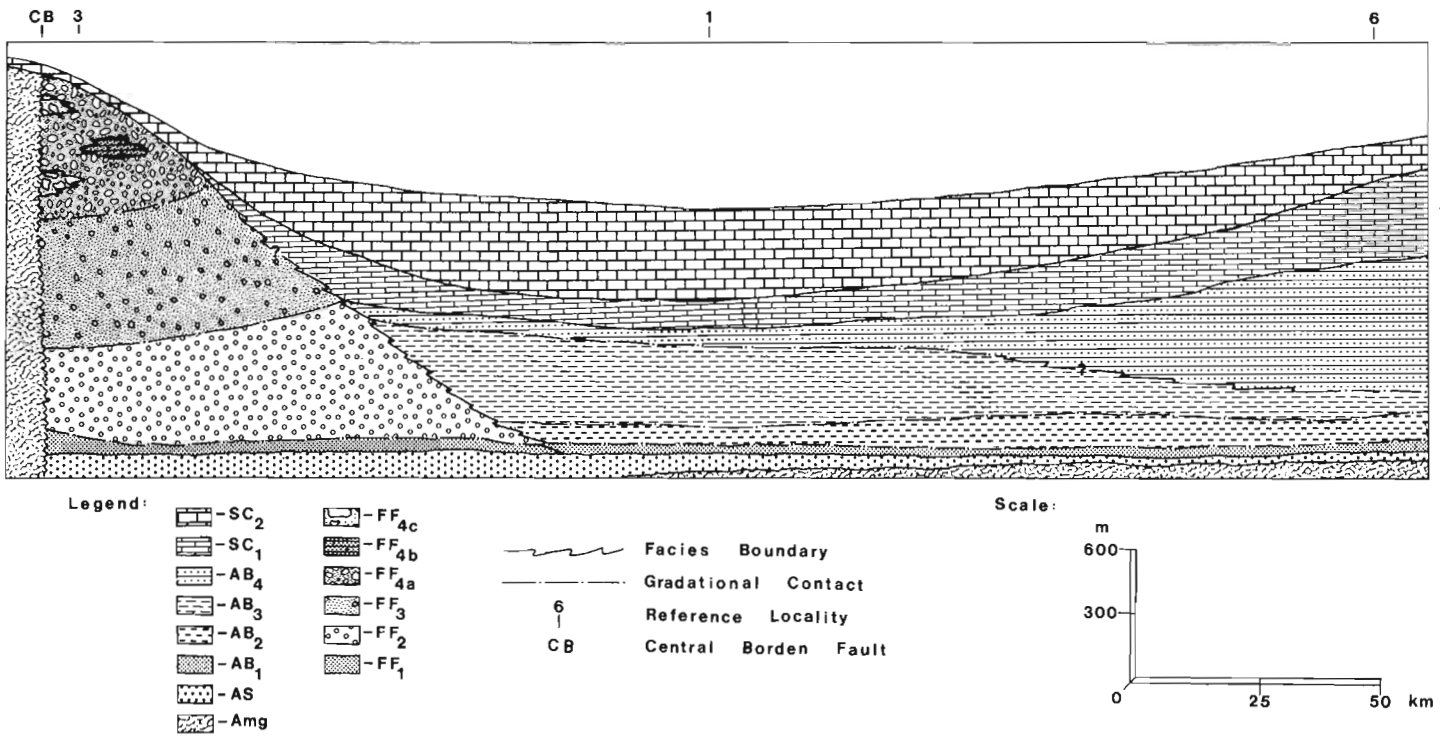


Figure 11.6. *Facies relationships between the Fabricius Fiord, Arctic Bay and Society Cliffs formations.*

lenticular and increase upwards in amount from 10 to 60 per cent. The interlayered subunit commonly is 1.5 to 6 m thick.

The upper subunits, of FF_2 cycles, consist of thin- to medium-bedded quartzarenite, with thin siltstone or shale partings. These rocks are brownish white to grey and vary considerably in thickness ranging from 0.5 to 15 m. In addition to the sedimentary structures noted above, the beds contain planar- and herringbone-crossbeds which are up to 0.3 m thick, straight-crested wave ripple marks with wavelengths of 0.3 to 1 m, and surface channels.

The FF_2 cycles change from lower member cycles that contain equal amounts of shale, siltstone and quartzarenite, through middle member shale-dominated cycles, into upper member quartzarenite dominated cycles. The FF_2 member may lend itself to further subdivision, based upon the proportion of shale, siltstone and quartzarenite, within the cycles.

FF_3 member

Medium- to thick-bedded and massive subarkose and pebbly subarkose alternating with thin beds of quartz-feldspar pebble conglomerate are the predominant lithologies of this member. The rocks range in colour from yellowish grey to brown and locally occur as conglomerate capped, vaguely defined coarsening upward cycles ranging in thickness from 15 to over 30 m.

The FF_3 member attains a maximum thickness of 840 m, at locality 3. The beds are generally devoid of sedimentary structures and contain only scattered large planar crossbeds. These structures are up to 1.5 m thick and show current aligned quartz pebbles along foreset and bottomset beds.

FF_4 member

Thick beds of subarkose, arkose, stromatolitic dolostone and breccia conglomerate constitute the uppermost FF_4 member of the Fabricius Fiord Formation. These beds are situated adjacent to the Central Borden Fault Zone and are 150 m thick at locality 2A and 245 m thick at locality 3. Three major laterally and vertically intergradational lithological associations can be defined from data collected at these localities.

FF_{4a} Association. This lithological association is predominantly medium- to thick-bedded subarkose and pebbly subarkose, with minor interlayers of arkose and pebbly arkose. These arkoses are present as wedges, which increase in thickness towards the fault zone. At a distance of about 1 km they average 5 to 10 cm thick and increase to upwards of 0.6 m at the fault contact. Fresh surfaces are mostly yellowish brown, grey, and reddish orange, whereas weathered surfaces are brownish grey to dark chocolate brown. The latter colour is probably due to the weathering of iron-rich carbonates in the matrix, and helps to distinguish FF_{4a} subarkoses from FF_3 subarkoses which are lighter coloured. Dark steel-grey coatings of hematite are found on some beds.

The only sedimentary structure observed in these beds, are scattered medium- to large-scale planar crossbeds. More than 65 per cent of FF_4 exposure area consists of FF_{4a} subarkose and arkose. The remainder of the member consists of scattered, lenticular zones of FF_{4b} lithological associations, and unstratified wedges of FF_{4c} lithological associations marginal to the fault zone (see Fig. 11.6). Both associations occur at various stratigraphic positions within FF_{4a} strata.

FF_{4b} Association. This carbonate-rich lithological association contains medium- to thick-bedded stromatolitic dolostone and more massive gritty dolostone. The grit component is chiefly quartz and feldspar sand- to pebble-sized clasts in amounts of 5 to 25 per cent. Fresh surfaces are light to medium grey; weathered surfaces are typically chocolate brown to light brown. The beds are sometimes coated by steel-grey hematite.

The stromatolites include planar, laterally linked low domal, and unbranching columnar forms. The low domal forms are 5 to 10 cm high; the columnar forms are up to 20 cm high and are found in situ and overturned. Breccia wedges and 'pipes' of angular, pebble size stromatolitic dolostone, and thin beds of dolostone-clast flat pebble conglomerate, occur locally as part of the association. These breccias and conglomerates contain a granular subarkose matrix.

The stromatolites found in these strata are distinct from those present within the upper Arctic Bay beds (AB_4 member), but similar to some of the forms that occur within the Society Cliffs dolostone. Further study may allow a more specific intrabasin correlation between the upper Fabricius Fiord and Society Cliffs formations.

FF_{4c} Association. Structureless, massive breccia conglomerate constitutes the third lithological association. It occurs as wedges, as much as 5 m thick, adjacent to the Central Borden Fault Zone usually no more than 0.5 km north of this contact. The breccia-conglomerate contains granule- to cobble-size, subrounded to subangular quartz and feldspar clasts, and pebble- to boulder-size subangular to angular granite and gneiss clasts. The clasts are supported in a dolostone matrix that makes up 10 to 40 per cent of the rock, and contains scattered small biotite flakes and sand-size quartz and feldspar grains. These rocks weather chocolate- to pink-brown and have pink-grey to brownish grey fresh surfaces.

A gradual increase in clast size occurs towards the fault contact. At locality 3, pebble size clasts dominate 0.5 km north from the contact. Adjacent to the contact the average has increased into the cobble- to boulder-size range.

Interpretation

To date the Fabricius Fiord Formation has been found only in restricted areas due north of the Central Borden Fault Zone. That periodic syndepositional faulting influenced the deposition of the Fabricius Fiord sediments is suggested by the paleocurrent dispersal patterns, the large amount of immature sediments and the increased abundance of arkose and breccia conglomerate wedges towards the fault margin. Most of the movement probably occurred along the Central Borden Fault Zone although movement along fault zones farther to the south cannot yet be ruled out as a major influence.

The lithologies and sedimentary structures, the overall coarsening upward trend, the cyclic nature of the beds, and their outcrop pattern suggest deposition within large delta fan complexes. They may be marine equivalents of alluvial fans, such as the Devonian Karlskaret fan in Norway (Larsen and Steel, 1978) and ancient analogs of recent continental margin submarine fans (Normark, 1978). The sequence of beds observed are similar to those produced by prograding delta fans (Pettijohn, 1975). If this interpretation is correct, then it appears that Neohelikian delta fan complexes in excess of 10 km in basinward extent and 2 to 3 km in height, dominated the southern margins of the Milne Inlet Trough throughout Fabricius Fiord depositional time (Fig. 11.3 and 11.7).

Faulting, beginning in FF_1 time, initiated delta fan deposition in the southern part of the trough. Early intertidal to subtidal deposited sands (FF_1) spread northeast over the basin gradually covering the largely fluvial Adams Sound quartzarenites. Deposition of the FF_2 member occurred as the prograding delta migrated over the basin tidal flats. Nearer to the fault zone, large amounts of coarse clastics accumulated as proximal and distal delta sheet sands (FF_3, FF_{4a}; Fig. 11.7). These were actively reworked by distributary channels. As the upper fan platform built up and extended seaward, shallow restricted interdistributary basins and embayments formed over its surface. These were the centres for carbonate deposition and formation of stromatolitic beds (FF_{4b}). Migration of distributary channels through these small basins brought carbonate deposition on the fan to a close. At the fault margin, tectonic pulses caused rapid shedding of breccia wedges onto the upper fan platform.

Arctic Bay Formation

The Arctic Bay Formation outcrops across the entire study area, being especially well exposed in sections along Alfa River, Tremblay Sound and at the mouth of Paquet Bay. West of Milne Inlet it is composed of micaceous black to grey shale and minor, greyish brown, interbedded siltstone, quartzarenite, dolosiltite and stromatolitic dolostone. East of Milne Inlet the shale content is significantly reduced, being replaced by increased amounts of white to greyish green quartzarenite-siltstone and orange- to rust-brown dolosiltite, dolarenite and stromatolitic dolostone. Thicknesses vary from 610 m at locality 1 to about 770 m at localities 6 and 7 (Fig. 11.2).

The contact with the overlying Society Cliffs Formation is conformable at locality 4. At localities 1 and 6A it is unconformable, being undulatory and erosional in nature. The Arctic Bay is normally underlain by the Adams Sound Formation. However, at localities 4 and 6 it nonconformably overlies the basement in areas where the Adams Sound has wedged out against the gneisses.

Sedimentary structures are common in the siltstone, quartzarenite and dolostone beds. These rocks contain small to medium sized, undulatory bifurcating- to lunate-current ripple marks, trough- and planar-crossbeds, cylindrical to subspherical load casts, synaeresis cracks and tool marks. The shale beds sometimes include cone-in-cone concretions, thin lenses and beds of pyrite and gypsum efflorescence.

The formation has been subdivided into four intergradational members (Table 11.1). In reference to the previous subdivision in Jackson et al. (1978), the AB_5 member was not identified in the study area. It is tentatively assumed that the AB_4 and AB_5 members of Jackson et al. (1978) are equivalent to the AB_4 member of this report. Also, the AB_4 is equivalent to Jackson's et al. (1975) AB-U member. The detailed mapping carried out in the Paquet Bay region in 1978 has shown that the AB_4 member covers a larger area than had been previously realized.

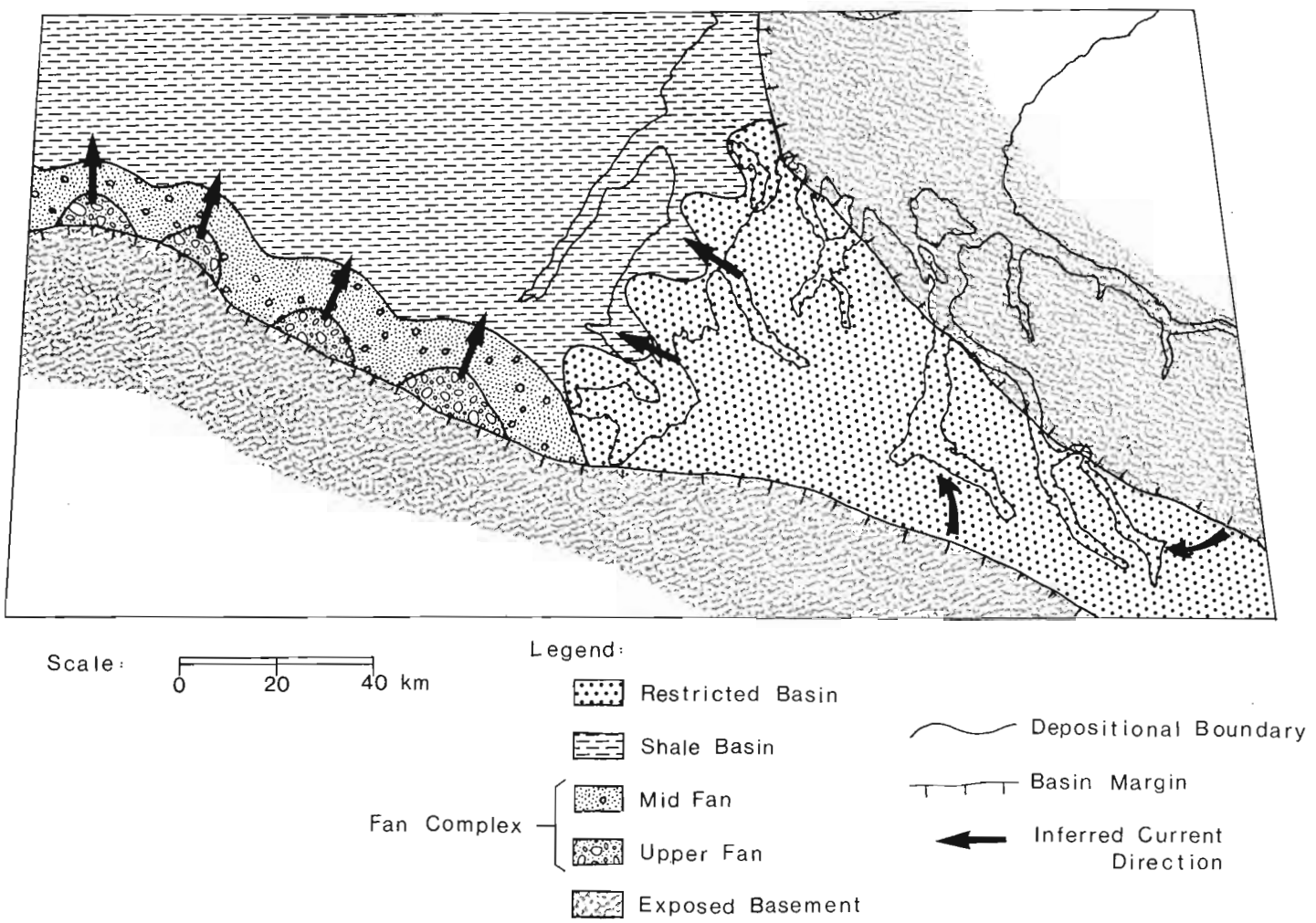


Figure 11.7. *Hypothetical reconstruction of depositional environments during the early history of the Milne Inlet Trough. The area is the same as that shown in Figure 11.1.*

AB_1 member

Thin- to medium-bedded quartzarenite and siltstone dominate the member. These beds also contain some thin shale interlayers and partings. The weathered surfaces range from rust-brown to greenish brown whereas the fresh surfaces are greyish green to white. This member is 17 m thick at locality 1, 45 m thick at locality 5 and 13 m thick at locality 7. In some sections, as at locality 1, the beds contain abundant planar- and trough-crossbeds and scattered megaripples. Paleocurrent patterns from the crossbeds show 180° opposed bimodal trends and indicate depositional currents from both the northwest and southeast (Fig. 11.4).

AB_2 member

This member consists of coarsening upward cycles which contain three subunits ranging in thickness from 9 to 15 m. These cycles are smaller and include larger proportions of shale than the similar FF_2 types.

The lowest subunit of these AB_2 cycles is chiefly thin- to thick-laminated, planar shale and scattered thin beds of silty shale and quartzarenite. These rocks have rust-brown to grey weathered surfaces and black to dark grey fresh surfaces. The beds are micaceous, range from 3 to 9 m thick, and are generally devoid of sedimentary structures.

The shale grades up into an interlayered middle subunit of thin- to medium-bedded shale, siltstone and quartzarenite. The siltstone-quartzarenite beds are undulatory to lenticular and increase in amount upwards from 15 to 50 per cent. These rocks have brownish grey weathered surfaces and grey to white fresh surfaces. This subunit is 1.5 to 6 m thick west of Milne Inlet and 1.5 to 4.5 m thick east of the inlet.

AB_2 cycles to the west of Milne Inlet are capped by thin bedded quartzarenite which contains shale and siltstone partings. The rocks are greyish brown to greyish white and range in thickness from 0.3 to 1.5 m thick at locality 1. East of Milne Inlet this upper subunit consists of thick bedded quartzarenite. Weathered rock surfaces are yellowish white to brownish green, whereas fresh surfaces are light grey to white. Beds range from 3 to 7.5 m thick and include medium- to large-sized trough-, planar- and herringbone-crossbeds, megaripples with wavelengths of 1 to 2 m, and surface channels. Paleocurrent patterns include unimodal to 180° opposed bimodal trends with the dominant depositional currents coming from the east and southeast (Fig. 11.5).

Cycles of the AB_2 member, west of Milne Inlet, pass upward into shale dominated forms. Those east of the inlet pass up into quartzarenite dominated forms. The member changes in thickness from 155 m at locality 1 to 60 m at localities 5 and 7.

AB_3 member

AB_3 beds consist chiefly of very thin- to thick-laminated, planar black shale and scattered thin silty shale, siltstone and dololutite interlayers. These interlayers are rare west of Milne Inlet, but increase in amount to the east. At locality 4, a 1 m thick bed of concretionary limestone occurs in the middle of the member. The beds have few sedimentary structures. This member averages 380 m thick at locality 1 but thins considerably east of Milne Inlet to a thickness of 92 m at locality 4 and 64 m at locality 7.

AB_4 member

West of Milne Inlet. In this area, the AB_4 member consists largely of thick laminated, planar black shale with carbonate interbeds ranging from 20 to 30 per cent by volume. These are chiefly thin bedded limestone, dolostone and stromatolitic dolostone and occur as beds 0.6 to 3.3 m thick, with orange-brown weathered surfaces and grey fresh surfaces. Small vugs lined by dolomite and smoky quartz occur in some beds. The entire member is 46 m thick.

The stromatolitic dolostone occurs as lenticular beds consisting of small mounds. The stromatolites change from planar forms near the mound base, through low domal, into diverse columnar forms. These columns divide, branch and expand upwards. They average 0.5 to 0.8 m high and are found both upright in the mounds and inclined in one direction. The mounds have ripple marked surfaces and wedges of stromatolite-clast breccia. Stromatolite mound elongation orientations show southeast to northwest trends (Fig. 11.4).

East of Milne Inlet. The AB_4 member constitutes the majority of the Arctic Bay Formation east of Milne Inlet. The beds occur in cyclic sequences that contain three subunits. The lower is black, thick laminated planar shale and silty shale and is 1.5 to 7.7 m thick. These shales grade up into interlayered thin bedded shale, siltstone, quartzarenite and doloarenite. The beds are undulatory and have orange-brown to greenish grey weathered surfaces, and greenish white to grey fresh surfaces. The middle subunit is 0.6 to 6 m thick. The upper beds of AB_4 cycles include calcareous siltstone to quartzarenite, dolosiltite, doloarenite, dololutite, dolostone, limestone and planar to columnar stromatolitic dolostone. These rocks have medium, undulatory to lenticular bedding, orange-brown to greenish brown weathered surfaces and brown-grey to greenish grey fresh surfaces. The subunit ranges from 3 to 15 m thick. In addition to the sedimentary structures noted before, these beds also contain molar tooth structures, scoured bases, scattered large, southeast-trending planar crossbeds and megaripples. Small pyrite and dolomite filled vugs are common in some beds.

Thicknesses for the entire member range from 370 m at locality 7 to about 615 m at locality 6.

Interpretation

Most of the Arctic Bay Formation accumulated in an extensive basin situated west of Milne Inlet where Arctic Bay sediments were deposited as the basinward, fine clastic equivalent of the outer portions of the Fabricius Fiord fan complexes (Fig. 11.6 and 11.7). The prograding fans deposited shallow subtidal proximal basin fringes of sand-silt mud (AB_1, AB_2 members) and deep subtidal, thick distal basin, blanket deposits of fine silt and mud (AB_3 member). Progressive filling of this basin resulted in a shallowing trend and eventually in carbonate deposition in thin stromatolitic mounds (AB_4 west). This shallowing trend continued into Society Cliffs depositional time.

In the Tay Sound-Paquet Bay region, the Milne Inlet Trough appears to have been more restricted and tectonically active. Northwest-southeast trending faulted margins may have confined deposition to a narrow basin (Fig. 11.7). The abundance of thick, coarse sand bodies hints at rapid deposition rates perhaps influenced by tectonic activity along the White Bay and Tikerakdjuak Fault Zones. The smaller eastern basin remained shallow throughout most of Arctic Bay time, with sediments accumulating in deltaic-intertidal (AB_1, AB_2 east), to intertidal-shallow subtidal (AB_3, AB_4 east) environments. This clastic- and carbonate-dominated small basin retained its relatively restricted and shallowing character into Society Cliffs depositional time.

Society Cliffs Formation

The carbonate-rich Society Cliffs Formation extends from Alfa River valley, eastwards into Pacquet Bay area. It is divisible, in the study area, into a lower SC_1 member of

brownish grey alternating subarkose, quartzarenite, shale and stromatolitic dolostone, and an upper SC_2 member of grey stromatolitic to massive dolostone. Interbedded red, green and grey shale, siltstone and quartzarenite appear cyclically throughout the SC_1 member east of Tay Sound. Minor lithologies include dolostone-clast flat pebble conglomerate and breccia, and black to grey, thinly bedded to nodular chert. To the west, in the Arctic Bay – Nanisivik region, the Society Cliffs has not yet been subdivided (Jackson et al., 1978), and is equivalent to both members of the present study.

The thickness of this formation averages 580 m at localities 1 and 6A. The overlying contact with the Victor Bay Formation is typically poorly exposed, but appears conformable. The beds commonly contain synaeresis and desiccation cracks, molar tooth and small teepee structures, medium to large symmetrical wave ripple marks, small load casts and scoured beds. Small vugs lined by calcite, dolomite and quartz crystals are found in the more massive dolostones. Some of the carbonate rocks emit a strong petroliferous odour.

SC_1 member

West of Tay Sound. This member contains cyclically arranged beds. Cycles in the lower part of the member have a lower subunit composed of pebbly subarkose, subarkose and quartzarenite beds, 1 to 2 m thick, as well as thinly bedded dolostone, dololutite and shale. These grade upward into upper subunits of medium- to thick-bedded, planar stromatolitic dolostone with flat pebble conglomerate and breccia. The rocks have brownish grey weathered surfaces, and light grey fresh surfaces. Lower subunits range in thickness from 3 to 12 m; upper subunits are 4.5 to 6 m thick. The subarkose and quartzarenite contain graded beds and medium to very large scale planar-crossbeds which are up to 1.2 m thick. Dispersal patterns from these crossbeds indicate current deposition from the south and southeast.

The upper part of this member consists of vague cycles of interlayered, thinly bedded dolostone and shale, which grade up into thick bedded stromatolitic dolostone. The stromatolites include both planar and laterally linked low domal forms, and are disrupted by beds of flat pebble conglomerate and breccia.

The member averages 105 m thick, and passes gradationally into the overlying SC_2 beds.

East of Tay Sound. The SC_1 member thickens eastwards, where it contains much more clastic material, including at least eight redbed sequences. These consist of alternating, thinly bedded, planar shale, argillaceous to sandy siltstone, minor argillaceous quartzarenite and dolostone. The rocks range from dark reddish purple and pink to dark green. The redbeds range in thickness from 10 to 30 m. Interspersed are sequences of thin bedded interlayered grey shale, dololutite and stromatolitic dolostone 2 to 18 m thick. There are also several 3 to 5 m-thick massive beds of yellowish brown, coarse grained to pebbly quartzarenite and sublitharenite and scattered thinly bedded, granite-bearing grit bands. The planar to domal stromatolitic dolostone includes some thin beds of chert and lenses of gypsum. The member averages 460 m in thickness.

SC_2 member

This member consists mainly of medium- to thick-bedded, stromatolitic dolostone and more massive, vuggy dolostone. The beds have light grey to medium grey weathered and fresh surfaces. To the west of Tay Sound the member is more than 305 m thick at locality 1 (Fig. 11.2). However, east of Tay Sound it thins to less than 185 m at locality 6A where thin interlayers of red siltstone and quartzarenite occur in the lower parts of the member. Stromatolites in the dolostone are of several forms including hemispherical to chevron-laminated domes ranging from 0.2 to over 1 m in height, planar and low domal forms, and short unbranching columnar forms 5 to 15 cm high.

Interpretation

The basin shallowing trend initiated during late Arctic Bay time continued into the early depositional history of the Society Cliffs Formation. West of present day Tremblay Sound, carbonate shelf deposition commenced with the formation of extensive algal mats within a shallow subtidal to intertidal environment. East of Tremblay Sound, the clastic deposition that had periodically disrupted earlier AB_4 sediments continued into Society Cliffs depositional time. These clastic influxes may have been tectonically induced, perhaps by faulting along the White Bay and Tikerakdjuak fault zones. Clastic deposition for most of the eastern Society Cliffs took place within supratidal and intertidal environments and to a lesser extent within fluvial influenced environments. These were replaced later on by carbonate deposition in shallow subtidal environments as the major basin waters spread into this semirestricted eastern arm.

Structural Notes

Major faults, such as the Central Borden Fault Zone, may have originated in late Aphebian time and been reactivated in the Neohelikian (Jackson et al., 1978). Faulting along or near the Central Borden Fault Zone during deposition of the Fabricius Fiord Formation influenced the nature of the sediments and the sites of maximum sediment accumulation. This in turn affected the sedimentation patterns of the Arctic Bay Formation to the north. Syndepositional faulting appears to be responsible for the increased clastic content of the Arctic Bay and Society Cliffs formations east of Milne Inlet. Most faults in the study area, however, appear to have formed after Neohelikian sedimentation and both before and after deposition of Paleozoic strata.

The formations are subhorizontal to gently dipping over most of the map area. Dips increase substantially towards the margins of the fault zones. In the Fabricius Fiord Formation dips of 20° to 30° are found in the downfaulted portions along the Central Borden Fault. In the Tay Sound-Paquet Bay region, steeply dipping beds were found at localities 5, 6A and 7. Here, along the Tikerakdjuak Fault zones, beds in the Adams Sound and Arctic Bay formations have dips of 20° to 30°. Northwards, at the margin of the White Bay Fault Zone, beds of the Adams Sound, Arctic Bay and Society Cliffs formations are more steeply dipping, in the range of 40° to 60°. In these areas some of the beds are tightly folded into moderately plunging anticlines and synclines. Elsewhere, between the major fault zones, the beds are gently folded into broad anticlines and synclines. Within the SC_1 member, at locality 7, a single 5 m unit of shale, siltstone and dolostone displays tight, plastically deformed recumbent folds. The overlying and underlying beds, however, are planar and not deformed.

Hadrynian, Franklin diabase dykes intrude the Neohelikian strata. Widths in excess of 60 m and lengths of over 40 km are common. These dykes trend northwest and emplacement was, at least in part, controlled by the pre-existing fault planes. In areas of intensive intrusion, the Neohelikian strata have been upwarped and folded along the dyke margins. The dykes are near vertical and form resistant ridges which commonly protect fringes of less resistant beds from erosion.

Acknowledgments

Excellent assistance in the field was provided by Reid Myles of the University of Western Ontario. The author is also indebted to the Polar Continental Shelf Project which supplied logistical support. G.D. Jackson, G.M. Young and K.E. Eade critically read the manuscript and contributed valuable geological discussions.

References

Blackadar, R.G.
1970: Precambrian geology, northwestern Baffin Island, District of Franklin; Geological Survey of Canada, Bulletin 191, 89 p.

Geldsetzer, H.
1973: The tectono-sedimentary development of an algal-dominated Helikian succession on northern Baffin Island, N.W.T.; in Symposium on Arctic Geology, Geological Association of Canada, Memoir 19, p. 99-126.

Grabeau, A.W.
1904: On the classification of sedimentary rocks; American Geological Journal, v. 33, p. 228-247.

Jackson, G.D., Davidson, A., and Morgan, W.C.
1975: Geology of the Pond Inlet map-area, Baffin Island, District of Franklin; Geological Survey of Canada, Paper 74-75, 33 p.

Jackson, G.D., Iannelli, T.R., Narbonne, G.M., and Wallace, P.J.
1978: Upper Proterozoic sedimentary and volcanic rocks of northwestern Baffin Island; Geological Survey of Canada, Paper 78-14, 15 p.

Larsen, V. and Steel, R.J.
1978: The sedimentary history of a debris-flow dominated, Devonian alluvial fan – a study of textural inversion; Sedimentology, v. 25, p. 37-60.

Lemon, R.R.H. and Blackadar, R.G.
1963: Admiralty Inlet area, Baffin Island, District of Franklin; Geological Survey of Canada, Memoir 328, 84 p.

Normark, W.R.
1978: Fan valleys, channels, and depositional lobes on modern submarine fans: characters for recognition of sandy turbidite environments; American Association of Petroleum Geology Bulletin, v. 62, p. 911-931.

Olson, R.A.
1977: Geology and genesis of zinc-lead deposits within a late Precambrian dolomite, northern Baffin Island, N.W.T.; University of British Columbia, unpublished Ph.D. thesis, 371 p.

Pettijohn, F.J.
1975: Sedimentary rocks, 3rd edition; Harper & Row Publishers, 628 p.

12. URANIUM GEOLOGY IN THE CENTRAL BAKER LAKE BASIN, DISTRICT OF KEEWATIN

Project 750010

A.R. Miller
Regional and Economic Geology Division

Miller, A.R., Uranium geology in the central Baker Lake Basin, District of Keewatin; in Current Research, Part A, Geol. Surv. Can., Paper 79-1A, p. 57-59, 1979.

Abstract

Epigenetic uranium occurrences within the Dubawnt Group rocks and underlying gneisses are associated with unconformity surfaces, fault-fracture zones and a contact aureole related to a fluorite-bearing granitic intrusion. Syngenetic mineralization is associated with uranium-thorium-bearing red bostonitic syenitic dykes and stocks.

Introduction

Field work during the 1978 field season involved mapping of selected areas in the Thirty Mile Lake map sheet (65 P/W1/2) and the Tebesjuak Lake map sheet 65 O/1 as part of a continuing project to study the uranium metallogeny in the Dubawnt Group rocks and underlying gneiss. The field work was conducted in conjunction with geological studies under the direction of A.N. LeCheminant.

This report discusses the geological setting of the various types of uranium mineralization within the Dubawnt Group rocks and underlying gneisses, and the mineralogy, petrography, and chemistry of selected rock types.

The reader is referred to LeCheminant and Leatherbarrow (in prep.) and LeCheminant et al. (1979) for the lithological and structural relationships in and between the Dubawnt Group rocks and the basement complex.

Uranium geology

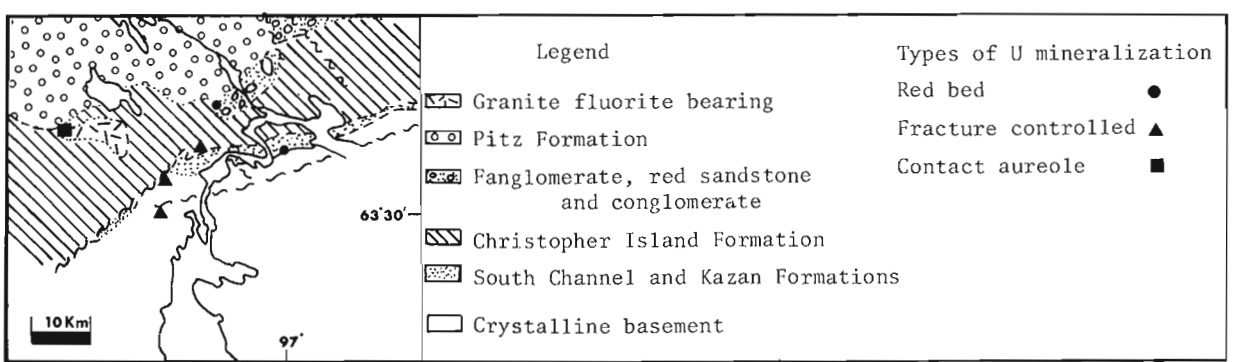
Four types of uranium associations were recognized in the Dubawnt Group rocks and underlying gneiss: 1) unconformity related occurrences in redbeds; 2) fracture controlled mineralization; 3) epigenetic mineralization within the thermal aureole of a fluorite-bearing granite; and 4) syngenetic uranium-thorium-bearing syenite.

The distribution of the first two associations exhibits a close spatial relationship to the Dubawnt unconformity or its faulted equivalent (Fig. 12.1). The distribution is similar to that of the uraniferous occurrences extending from Christopher Island, eastern end of Baker Lake southwestwards to the Thirty Mile Lake area (Miller, in prep.). The other two represent new associations within the Baker Lake Basin.

Unconformity related occurrence in redbeds

Epigenetic copper and uranium mineralization was examined along the contact of porphyritic feldspar-biotite trachyte lava of the Christopher Island Formation and the unconformably overlying red fanglomerate deposits. The red clastic sediments consist of red siltstone, sandstone, and conglomerate derived from the Christopher Island Formation. The principal cements are calcite and hematite.

Sparse mineralization is stratigraphically confined to the contact zone and is associated with extensive bleaching of the basal siltstone and sandstone. The reduction or removal of the hematite has resulted in an irregularly mottled rock with relict red hematite patches and cream to grey altered patches. The cream to grey altered patches crosscut bedding indicating a postdepositional alteration. Malachite and metatyuyamunite are present on fractures and within cream to grey altered sandstone laminae.



Location of Uranium occurrences

	Northing	Easting	Map
Unconformity related in red beds	7061090	586720	65P/11
	7053700	600070	65P/10
Fracture controlled	7043400	576850	65P/11
	7043590	576860	65P/11
	7049030	577680	65P/11
	7053900	585650	65P/11
	7053820	586540	65P/11
Contact aureole	7049030	577680	65P/11

Figure 12.1

Geological setting of uranium occurrences in a portion of 65 P west half. Geology from LeCheminant and Leatherbarrow, (in prep.).

Table 12.1

Analyses (in per cent) of uranium-thorium-bearing syenitic units

	Red bostonitic dykes			Chilled margin	Porphyritic stock	
SiO_2	60.2	63.0	62.0	63.8	62.9	64.1
TiO_2	1.09	0.91	0.93	0.85	0.63	0.50
Al_2O_3	16.7	17.7	17.3	16.4	17.3	16.4
Fe_2O_3	6.0	3.7	4.9	3.6	2.5	0.2
FeO	0.5	1.5	0.4	0.5	0.9	3.4
MnO	0.05	0.05	0.07	0.07	0.04	0.04
MgO	0.54	0.59	0.49	1.25	1.02	1.11
CaO	0.67	0.36	1.11	0.63	0.97	0.67
Na_2O	5.9	5.8	6.3	5.1	3.1	3.1
K_2O	5.01	5.82	5.02	5.12	8.64	7.80
P_2O_5	0.05	0.08	0.06	0.04	0.24	0.21
H_2O_T	0.7	0.8	0.8	1.4	1.2	1.1
CO_2	0.60	0.0	1.0	0.1	0.3	0.0
S	0.00	0.11	0.00	0.00	0.00	0.00
Total	98.01	100.42	100.38	98.86	99.74	98.63
U(ppm)*	115	134	38.9	130	28.2	20.3
Th(ppm)†	410	310	290	330	130	120

* Analyses by neutron activation
† Analyses by XRF

The presence of trace amounts of uranium and copper associated with continental clastic sediments indicates sufficient porosity and permeability for groundwater migration and the appropriate chemical environment for metal concentrations. Coarse volcaniclastic sediments interbedded with the subaerial lava and pyroclastic rocks of the Christopher Island Formation may also represent favourable horizons for mineralization.

A small pod of disseminated sulphide and uranium mineralization was examined in the South Channel conglomerate at the contact with felsic basement gneiss. The Dubawnt Group rocks in the area comprise a moderate to steeply dipping sequence of hematite cemented conglomerate and arkose intruded by numerous northwest-trending biotite lamprophyre dykes.

The unconformity plane dips north at attitudes of 40 to 75°. Local topographic undulations in the order of 5 to 10 m are present along the erosional trace of the unconformity plane. The form of the framework clasts of the conglomerate is generally subround to round. Locally the framework clasts at the unconformity are angular to subrounded and are cemented by brown weathering carbonate. The angularity of the clasts and their restriction to the unconformity plane may be interpreted as very immature locally derived detritus or a relict portion of a regolith developed from the basement gneiss.

The occurrence is situated at the inflection point in a local topographic depression. Pitchblende, pyrite, and chalcopyrite are disseminated through the chlorite- and calcite bearing arkosic matrix of an angular to subrounded granule to pebbly conglomerate. The underlying felsic gneiss contains minor hematite veinlets and traces of malachite but no alteration suggestive of hydrothermal or weathering processes.

Fracture-controlled occurrences

The distribution of Dubawnt Group rocks northwest of Forde Lake is controlled by northeast- and east-northeast-trending mylonitic zones. The mylonite zones are interpreted as a series of fault slices that involve basement gneiss, the basal clastic arkose-conglomerate sequence, and lava of the Christopher Island Formation (LeCheminant and Leatherbarrow, in prep.). Pitchblende with minor chalcopyrite and pyrite is associated with finely fractured, chloritized and hematitized granitoid gneiss.

Two uranium occurrences were examined in the basal portion of the Christopher Island Formation that overlie quartz-specularite veined South Channel conglomerate. Mineralization is situated on the northerly projection of the northeast-trending fault zone which defines the distribution of Dubawnt Group rocks northwest of Forde Lake. Small pods of uranium mineralization are confined to fractured porphyritic, mafic and felsic Christopher Island lava. The pods parallel north-trending fractures and contain quartz-calcite stringers, hematitic and an intense propylitic alteration.

Contact aureole related mineralization

The association of purple fluorite-pitchblende mineralization was recognized within thermally recrystallized Dubawnt supercrustal rocks adjacent to an epizonal fluorite-bearing granitic intrusion (Fig. 12.1).

In the mineralized area, porphyritic biotite and feldspar-biotite mafic lava and flow breccia of the Christopher Island Formation are overlain by porphyritic quartz-feldspar rhyolite lava of the Pitz Formation. These units are intruded by a subporphyritic alkali feldspar fluorite-bearing granite.

The Christopher Island lava in the contact aureole is recrystallized and metasomatized. The felted to trachytic groundmass is recrystallized to a very fine grained feldspathic mosaic. Recrystallization is accompanied by the development of garnet-tremolite-epidote aggregates within the host trachyte and veinlets of grossularite-diopside-quartz-microcline-epidote-purple fluorite-calcite. Fluorite is impregnated throughout the host trachyte. The associated metallic minerals include pitchblende with minor pyrite and chalcopyrite. Uranophane and masuyite coat fracture planes.

Fluorite is commonly disseminated throughout the overlying Pitz lava and is also concentrated along fractures. Elevated radiometric signatures were observed associated with purple fluorite veining.

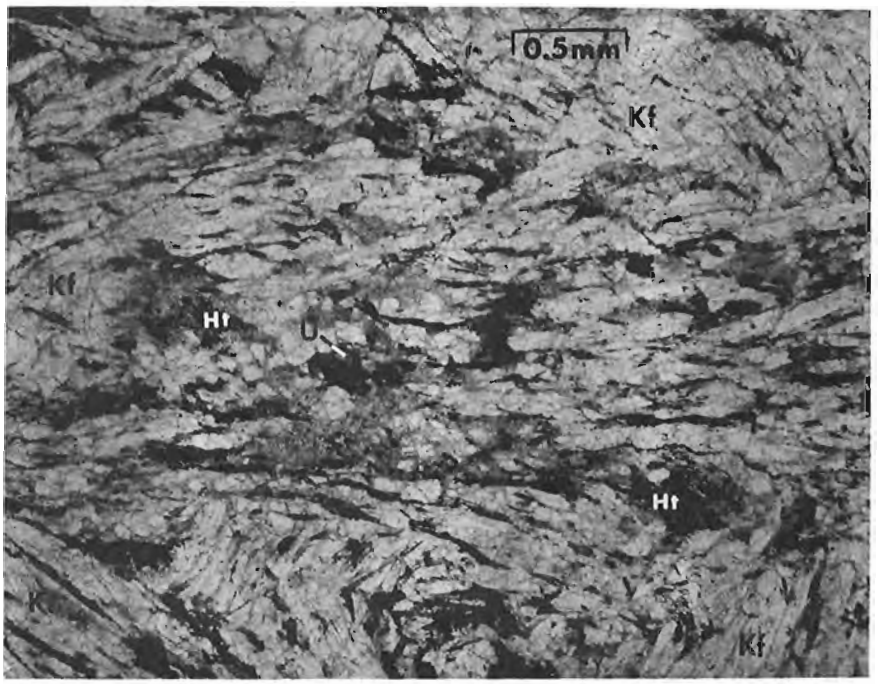


Figure 12.2. *Photomicrograph of bostonitic syenite with divergent clusters of alkali feldspar laths (Kf), opaque hematite (Ht) and metamict uranium-thorium phase (U). Transmitted light.*

The granitic intrusions that invade the Dubawnt supercrustal lava contain subporphyritic alkali feldspar phenocrysts, set in an assemblage of albite-quartz-biotite-hornblende-sphene-purple fluorite. Microlitic cavities of quartz-specularite are common.

This occurrence is characterized by the lack of hematitization, extensive fluoritization of the recrystallized host rock, garnet-fluorite-epidote veinlets and epizonal fluorite-rich granite. These features resemble fluorite-pitchblende mineralization associated with granitic intrusions in the Karlovy Vary massif, Czechoslovakia (Ruzicka, 1971).

Uranium-thorium alkaline syenite

In the Nutarawit Lake area (65 O/1) and Tulemalu Lake area (65 O/2) alkaline syenite stocks and dykes intrude the basement complex, the basal Dubawnt fluvial clastic sediments, and lower sedimentary and volcanic rocks of the Christopher Island Formation (Figs. 31.2, 31.3, LeCheminant et al., 1979). The syenitic units are present as dykes and irregular dyke-like bodies which trend northwest to north-northwest crosscutting the basement structural fabric and Dubawnt stratigraphy. The syenitic units vary from 20-80 m in width and are characterized by a pink to cherry red colour, very fine grained phaneritic aligned feldspar, and a high radiometric signature.

Microscopically, these units consist of very fine grained (0.4-1.5 mm), interlocking laths of alkali feldspar. The laths are present as divergent clusters. This textural relationship is termed bostonitic (Fig. 12.1). Minor biotite or its chloritized equivalent and subhedral microphenocrysts of apatite are interstitial to feldspar laths. Rutile and ubiquitous hematite are disseminated throughout the feldspathic groundmass.

A syenitic stock in the Kunwak River area intrudes Christopher Island volcanics and sediments and consists of a coarse porphyritic alkali feldspar core with a red very fine grained chilled margin. The chilled margin and related peripheral fine grained dyke swarm are identical petrographically and chemically to the bostonitic dykes in the Nutarawit Lake area (see Table 12.1).

The alkaline nature of the red bostonitic dykes and stocks is shown by the high total alkali content 10.22 to 11.74 weight per cent and K_2O/Na_2O ratios of 0.79 to 1.0 for dyke rocks and 2.52 and 2.79 for the porphyritic phase of the stock (Table 12.1). The mafic-poor character of these intrusive units is shown by low MgO contents, 0.49-1.25 weight per cent and the red hues are the result of high Fe^{+3}/Fe^{+2} ratios (Table 12.1). Uranium and thorium are present in sparsely disseminated, very fine grained (0.2 to 0.5 mm), hematite jacketed metamict and weakly birefringent phases (Fig. 12.1). Higher uranium and thorium contents are present in the red bostonitic dykes and chilled margin of the stock rather than the porphyritic central portion of the stock (Table 12.1). Energy dispersive spectra indicate the principal elements in the metamict phases are Th, Si, and Ce with minor Ca and Fe. The weakly birefringent phases contain Si and Zr as major elements and minor Ca, Fe, and traces of U and Th. X-ray diffraction patterns indicate cyrtolite for the latter phases. These data suggest that the uranium and thorium are present in syngenetic refractory minerals. Mineralogical studies on this type of mineralization are in progress.

References

LeCheminant, A.N., Lambert, M.B., Miller, A.R., and Booth, G.W.
1979: Geological studies: Tebesjuak Lake map area, District of Keewatin; in Current Research, Part A, Geological Survey of Canada, Paper 79-1A, Rep. 31.

Ruzicka, V.
1971: Geological comparison between East European and Canadian uranium deposits; Geological Survey of Canada, Paper 70-48.

13.

LOW GRADE URANIUM MINERALIZATION IN CARBONATE ROCKS FROM SOME SALT DOMES IN THE QUEEN ELIZABETH ISLANDS, DISTRICT OF FRANKLIN

Projects 740081 and 760014

I.R. Jonasson[1] and H.E. Dunsmore[2]

Jonasson, I.R. and Dunsmore, H.E., Low grade uranium mineralization in carbonate rocks from some salt domes in the Queen Elizabeth Islands, District of Franklin; in Current Research, Part A, Geol. Surv. Can., Paper 79-1A, p. 61-70, 1979.

Abstract

A reconnaissance survey was made of parts of the Queen Elizabeth Islands to determine suitable geological settings in which U mineralization might be located. The geological studies were integrated with, and supported by, detailed geochemical studies of stream sediments, waters and rocks.

Two main target types were selected: Paleozoic and Mesozoic continental sandstones on Melville and Ellef Ringnes islands, and Pennsylvanian anhydrite-halite diapirs intruding these sediments at the same locations.

Sandstone did not yield any U occurrences although its potential remains undiminished. However significant signs of radioactivity were encountered within the Dumbbells Dome, Ellef Ringnes Island. These led ultimately to the discovery of extensive, low grade U mineralization hosted by Pennsylvanian limestone breccias. Stream waters analyzed for uranium proved particularly useful in outlining favourable zones, especially when used in detailed studies. Sediments, leached by sulphate-bearing waters, were less effective. However all geochemical and radiochemical methods were found to be restricted by the nature of the generally wet and deeply weathered arctic terrain.

Introduction

The Queen Elizabeth Islands of the high arctic of Canada are underlain primarily by Phanerozoic sedimentary rocks, including thick sequences of continental sandstone and conglomerate. These settings, like similar rocks in Appalachia and the southwestern U.S.A., may host tabular and roll-type uranium ore deposits. The proximity of Shield rocks, including granite, to the east suggests that uranium could have been derived through prolonged weathering of the Precambrian basement rocks and concentrated at suitable settings within younger sedimentary strata.

Other exploration targets are the piercement diapirs of Pennsylvanian gypsum, anhydrite, halite, and various carbonate rocks which have intruded younger rocks, including Cretaceous sandstone and shale. Frequently, the diapirs themselves are intruded by basic igneous rocks in the form of diabase sills, dykes, and ring dykes. An association between marine evaporites and uranium mineralization has been observed in Atlantic Canada, with concentrations found in sandstone on the flanks of diapirs and in carbonate at the base of the evaporitic sequence. There are about 100 diapirs in the Queen Elizabeth Islands with most located on Axel Heiberg and the Ringnes islands. Some of these structures have been found to trap natural gas on their flanks.

It was decided to confine our initial field investigations to a brief survey of selected Mesozoic and Paleozoic rocks on Eastern Melville Island, including the Barrow Dome; and to Mesozoic rocks in the vicinity of the Dumbbells Dome, Ellef Ringnes Island. The results of these surveys are presented here.

Generalized Geology and Sample Locations

The simplified geology of Ellef Ringnes Island is presented in Figure 13.1 (after Stott, 1967) on which Dumbbells Dome is marked "D" and Isachsen Dome, which lies to the southwest but was not visited, is marked "I". Figure 13.2 is a simplified geological map of the Weatherall Bay area of eastern Melville Island (after Tozer and Thorsteinsson, 1964) showing sample locations resulting from foot traverses. Sample locations for Dumbbells Dome are shown on Figure 13.3. These samples were taken during traverses using a Honda ATC-90 autobike.

Analytical Methods

Uranium was analyzed in waters by fluorometry (Geological Survey of Canada, GSC) and in sediments by delayed neutron activation (Atomic Energy of Canada Ltd., AECL). All other analyses on waters were made by standard methods in use at GSC; sediment analyses were provided by Chemex Ltd., Vancouver. Rock analyses for U were made by AECL. Table 13.1 summarizes the analytical methods used.

Geochemical Studies – Melville Island

Waters

Results are presented in Table 13.3 for water samples collected from the Weatherall Bay area (78G-H) and from the Barrow Dome gypsum diapir (79B). Table 13.2a gives the location of the samples.

It is immediately apparent that our limited sampling program did not detect any high U levels in waters draining Paleozoic sandstone and conglomerate around Weatherall Bay. The pH values of all but one water (sample 7) were neutral or slightly alkaline, and this single sample was significant only for a small quantity of Zn (1.7 ppb). Salt contents, i.e., Na, K, Cl, F, Ca, $SO_4^=$, were found to be quite low. pH is probably controlled by small amounts of dissolved calcium carbonate, precipitates and cements of which are commonly observed in the area.

However, samples from two of the three streams which cut the Barrow Dome diapir contained small amounts of dissolved U and substantial quantities of Ca and $SO_4^=$ ions, as might be anticipated. We do not view these data as unusual, although similar levels found in similar terrain on Ellef Ringnes Island suggest that a closer look at Barrow Dome rocks would be in order.

[1] Resource Geophysics and Geochemistry Division
[2] Regional and Economic Geology Division

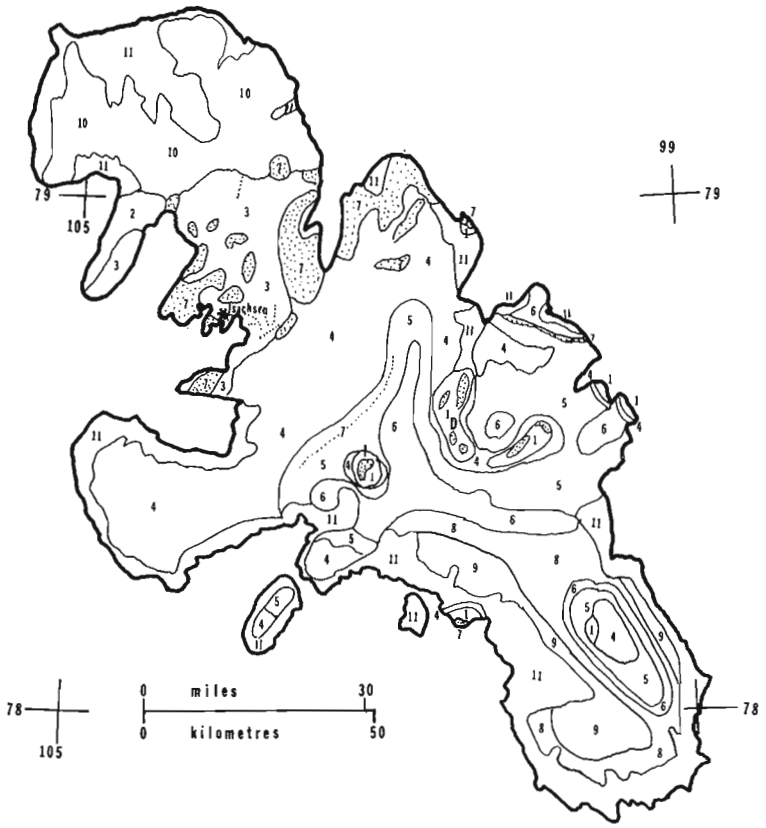


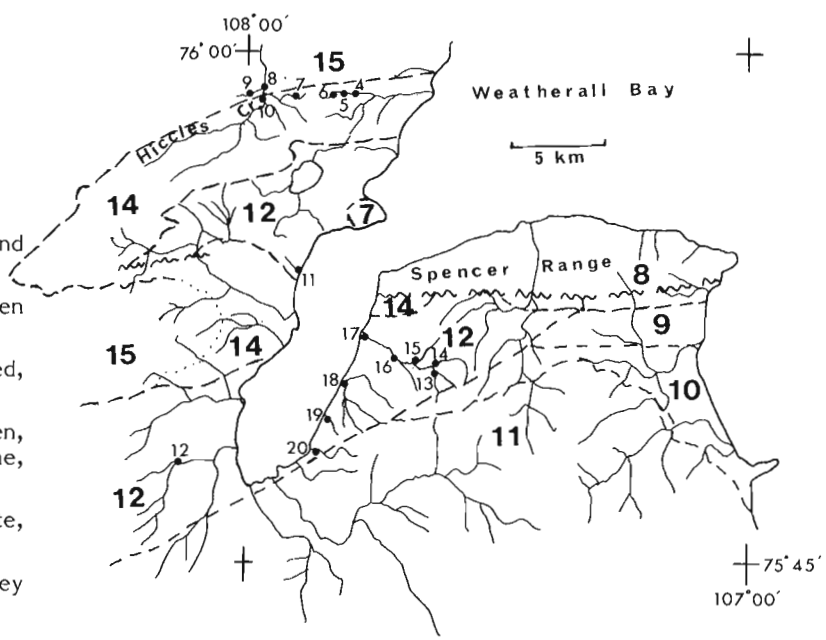
Figure 13.1. *Simplified geology of Ellef Ringnes Island (after Stott, 1967) (D = Dumbbells Dome, I = Isachsen Dome).*

LEGEND

(Figures 13.1 and 13.3)

11. PLEISTOCENE AND RECENT: alluvial and deltaic sand, marine beach deposits.
10. TERTIARY: Beaufort Formation; nonmarine sands and gravels, fossil wood.
9. UPPER CRETACEOUS and TERTIARY: Eureka Sound Formation; sandstone, siltstone, shale, sand, and lignite.
8. UPPER CRETACEOUS: Kanguk Formation; dark grey marine shale, siltstone.
7. LOWER and UPPER CRETACEOUS: diabase, gabbro sills, dykes.
6. LOWER and UPPER CRETACEOUS: Hassel Formation; sand and sandstone, shale, coal.
5. LOWER CRETACEOUS: Christopher Formation; grey to black shale, minor siltstone and limestone.
4. LOWER CRETACEOUS: Isachsen Formation; sandstone, sand, shale, coal.
3. UPPER JURASSIC and LOWER CRETACEOUS: Deer Bay Formation; dark grey and black marine shale.
2. JURASSIC: Savik Formation; grey marine shale. Borden Island Formation; white sandstone, siltstone. Jaeger Formation; green, glauconitic and ferruginous sandstone.
1. CARBONIFEROUS: gypsum, anhydrite; limestone, limestone breccia

- • geochemical sample
- x rock sample
- c carbonate



LEGEND

(Figure 13.2)

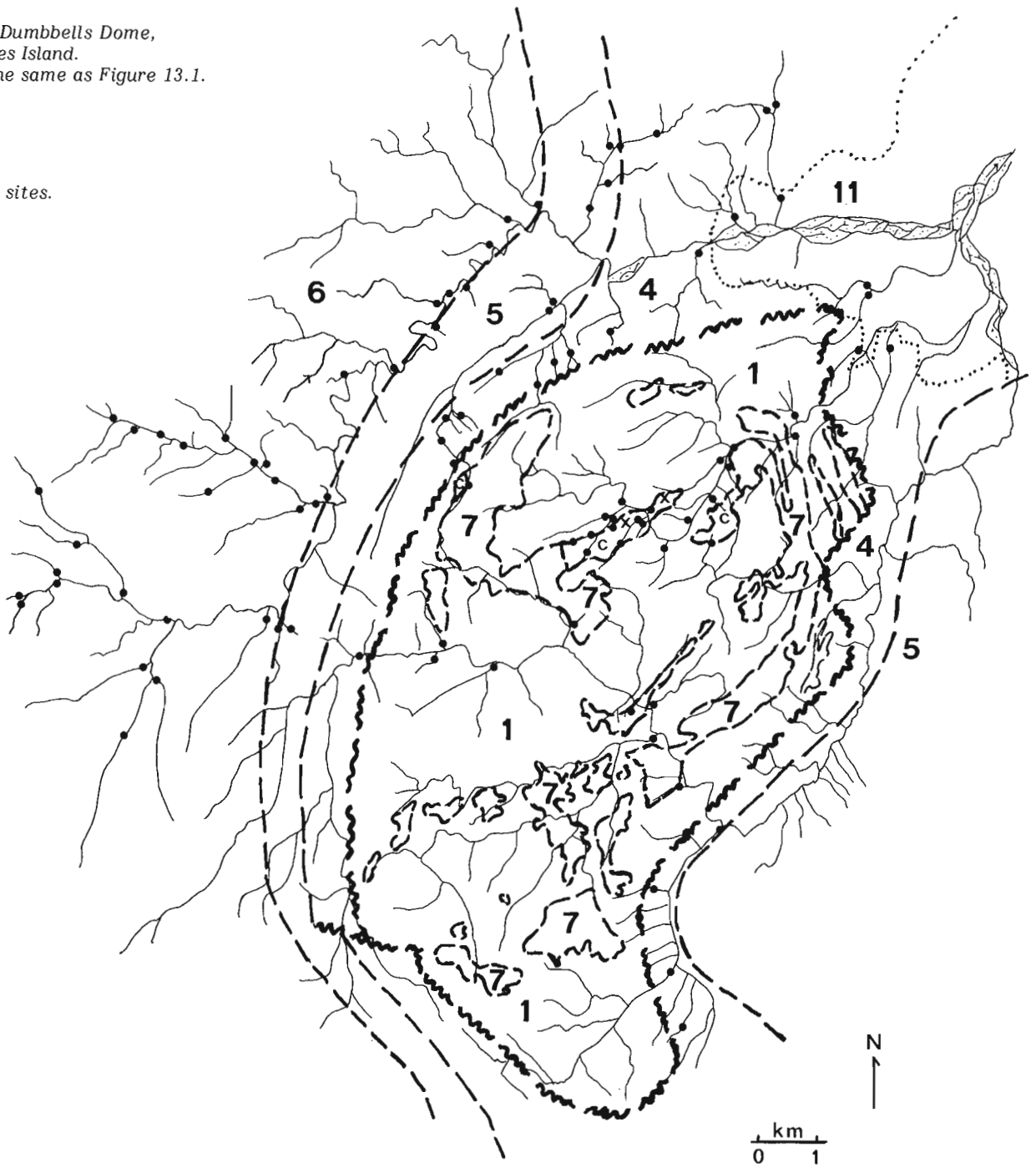
15. PERMIAN: Assistance Formation; green, grey and dusky red sandstone, grey limestone; marine.
14. LOWER PERMIAN: Sabine Bay Formation; green and grey calcareous sandstone, limestone.
12. PENNSYLVANIAN: Canyon Fiord Formation; red, brown, and orange sandstone, conglomerate.
11. UPPER DEVONIAN: Griper Bay Formation; green, grey, white carbonaceous sandstone, siltstone, shale, thin coal seams.
10. UPPER DEVONIAN: Hecla Bay Formation; white, yellow, red nonmarine sandstone.
9. MIDDLE DEVONIAN: Weatherall Formation; grey marine and nonmarine sandstone, shale, siltstone.
8. MIDDLE DEVONIAN: Blue Fiord Formation; grey limestone.
7. SILURIAN: grey dolomite.

Figure 13.2. *Geology and sample locations, Weatherall Bay area, Melville Island.*

Figure 13.3

Geology of Dumbbells Dome, Ellef Ringnes Island. Legend is the same as Figure 13.1.

• *Sample sites.*



Sediments

Results are presented in Table 13.4 for sediment samples collected in the same areas noted above. In contrast to water data (Table 13.3), some low level anomalies for U were found in streams draining the Griper and Sabine Bay formations. Small amounts of Zn and Ni accompany U. A realistic assessment of the significance of these values cannot be made in view of the limited data.

On the other hand, the conclusion that the Barrow Dome diapir is worth further investigation is substantiated by the presence of small amounts of U, Zn, Cu, and Ni in three stream sediments collected there. A little Mo is also present. Similar element groupings were observed in sediments collected from a uraniferous area in Dumbbells Dome (69F).

Geochemical Studies — Ellef Ringnes Island

Waters

Results are presented in Table 13.3 for water samples collected on and around the Dumbbells Dome diapir (69F). Table 13.2b gives the locations of the samples.

Table 13.1

Analytical methods

(a) Waters

Entity	Method	Detection Limit	Remarks
pH	pH meter		± 0.02
Cl^-	colorimetry	1.0 ppm	thiocyanate
Na	atomic absorption	100 ppb	direct aspiration
K	atomic absorption	100 ppb	direct aspiration
$SO^=_4$	colorimetry	10 ppm	barium titration
Ca	atomic absorption	100 ppb	direct aspiration
Mg	atomic absorption	100 ppb	direct aspiration
Zn	atomic absorption	1.0 ppb	APDC-MIBK extraction
Cu	atomic absorption	1.0 ppb	APDC-MIBK extraction
F^-	ion sensitive electorde	40 ppb	–
U	fluorometry	0.10 ppb	–

(b) Sediments and Rocks

U	neutron activation	0.1 ppm	
Zn	atomic absorption	1 ppm	conc HNO_3 - HCl
Cu	atomic absorption	1 ppm	conc HNO_3 - HCl
Pb	atomic absorption	2 ppm	conc HNO_3 - HCl
Ni	atomic absorption	1 ppm	conc HNO_3 - HCl
Co	atomic absorption	1 ppm	conc HNO_3 - HCl
Ag	atomic absorption	0.1 ppm	conc HNO_3 - HCl
Mn	atomic absorption	1 ppm	conc HNO_3 - HCl
Fe	atomic absorption	1 ppm	conc HNO_3 - HCl
Ba	atomic absorption	10 ppm	conc HNO_3 - HCl
Mo	atomic absorption	1 ppm	conc HNO_3 - HCl
W	colorimetry	2 ppm	fusion
Hg	atomic absorption	20 ppb	cold vapour

As in the case for the streams draining similar sandstone formations on Melville Island, streams outside the dome (units 4, 5, 6; Fig. 13.3) are generally low in U. There are some exceptions and these lie to the north of the dome (samples 46, 47) within the Isachsen Formation (Fig. 13.1) near its contact with overlying Christopher shale. Samples 54-62 from another group of streams draining Isachsen sandstone on the western limits of the dome and some gypsum masses also contain dissolved U up to 2.50 ppb with an average around 0.70 ppb. It is difficult to decide, on this evidence, whether the main source of U is sandstone, evaporite, or both. Elsewhere, in the Hassel sandstone, which like the Isachsen, is coaly in places, U levels are low at around 0.05 ppb. These values should be regarded as typical for waters draining these formations. Streams draining more erosion resistant Christopher shale are commonly dry.

Within the Dumbbells Dome complex significantly higher U levels were measured. Tributaries (samples 2-10) of a major arm of the East Dumbbells River, which bisects the Dome carried dissolved U in the range 0.05 – 3.05 ppb. Another fork to the north, draining the core of the Dome (samples 64-68; 83-97) comprising limestone breccias and gypsum, also carried similar quantities of dissolved U.

U anomalies in the study area fall into two categories. One is characterized by waters high in dissolved Ca, $SO_4^=$, Mg and F. Clearly, the chemistry is controlled by gypsum with Ca levels moderated by calcium carbonate. A few hand specimens of crystalline and massive gypsum were found to contain thin seams of fluorite and thus the presence of F in the waters is readily explained. These samples also carry a little U (site 66, Table 13.5).

The second group of U anomalies is characterized by waters containing appreciably more Na, K, and Cl, but less Ca and $SO_4^=$. F is present, as is Mg, in similar quantities in both groups.

Each category contains occasional high values of Zn; sample 24 reached 628 ppb Zn in an acid stream water draining coaly sandstone and coal seams of the Hassel Formation. Others (samples 38, 73) contain dissolved Zn around 40 ppb, and these too drain coaly sandstone (Fig. 13.3). Zn levels of 2.0-4.0 ppb were measured in certain stream waters within the salt dome. Low Cu values (1.0 – 4.0 ppb) were found rarely, usually in streams draining Hassel sandstone.

One small group of water samples (52-62) appears to receive contributions of U from both coaly sandstone (Isachsen Formation) and massive gypsum outcrop. The chemistry reflects this; the waters carry high levels of Cl, Na, K, $SO_4^=$, Ca, Mg, and F (Table 13.3b).

The pH of all water samples is generally close to 8.0; occasional low levels, as noted above, are around 4.4. We consider that the former are controlled by carbonate buffering, whereas the latter are effected by oxidizing pyrite or other iron sulphides within the coal seams. Moreover, it is likely that the small amounts of Cu and Zn owe their origins to iron sulphides in coal (Hassel and Isachsen) and in pyritic limestone breccias found within the Dome.

Sediments

Results of analyses of sediment samples collected at the same sites described above (69F) and in Table 13.2b are presented in Table 13.4.

Table 13.2

Stream sediment and water sample locations

a) Melville Island, District of Franklin

NTS	SAMPLE NUMBER	ZONE UTM	COORDINATES EAST	NORTH	BEDROCK TYPE	GEOLOGICAL FORMATION
78G	770012	12	5783008	414800	CGLM	CANYON FJORD FM
78H	770002	13	4555008	379500	SNDS	GRIPER FM
78H	770003	13	4564008	379900	SNDS	GRIPER FM
78H	770004	13	4246008	434600	SNDS	SABINE BAY FM
78H	770005	13	4242008	434500	SNDS	SABINE BAY FM
78H	770006	13	4237008	434500	SNDS	SABINE BAY FM
78H	770007	13	4214008	434200	SNDS	SABINE BAY FM
78H	770008	13	4196008	434700	SNDS	SABINE BAY FM
78H	770009	13	4193008	434500	SNDS	SABINE BAY FM
78H	770010	13	4195008	434300	SNDS	SABINE BAY FM
78H	770011	13	4212008	425100	SNDS	CANYON FJORD FM
78H	770013	13	4286008	418800	SNDS	CANYON FJORD FM
78H	770014	13	4278008	419200	CGLM	CANYON FJORD FM
78H	770015	13	4276008	419300	SNDS	CANYON FJORD FM
78H	770016	13	4264008	419600	CGLM	CANYON FJORD FM
78H	770017	13	4255008	420400	SNDS	CANYON FJORD FM
78H	770018	13	4237008	418700	SNDS	CANYON FJORD FM
78H	770019	13	4226008	416800	SNDS	CANYON FJORD FM
78H	770020	13	4216008	414900	SNDS	CANYON FJORD FM
79B	770014	12	5495008	505400	GPSM	BARROW DOME, OTTO FJORD FM
79B	770015	12	5497008	505900	GPSM	BARROW DOME, OTTO FJORD FM
79B	770016	12	5498008	506200	GPSM	BARROW DOME, OTTO FJORD FM

b) Ellef Ringnes Island

NTS	SAMPLE NUMBER	ZONE UTM	COORDINATES EAST	NORTH	BEDROCK TYPE	GEOLOGICAL FORMATION
69F	770002	14	4455008	724700	SNDS	ISACHSEN FM
69F	770003	14	4458008	725100	GPSM	DUMBELLSDOME, OTTO FJORD FM
69F	770004	14	4472008	725400	GPSM	DUMBELLSDOME, OTTO FJORD FM
69F	770005	14	4475008	725000	GPSM	DUMBELLSDOME, OTTO FJORD FM
69F	770006	14	4488008	726200	GBBR	DUMBELLSDOME
69F	770007	14	4504008	725100	GBBR	DUMBELLSDOME
69F	770008	14	4507008	725400	GBBR	DUMBELLSDOME
69F	770009	14	4509008	724800	GBBR	DUMBELLSDOME
69F	770010	14	4516008	724200	GBBR	DUMBELLSDOME
69F	770011	14	4526008	723500	SNDS	ISACHSEN FM
69F	770012	14	4523008	723100	SNDS	ISACHSEN FM
69F	770013	14	4519008	722100	SNDS	ISACHSEN FM
69F	770014	14	4525008	720300	SNDS	ISACHSEN FM
69F	770015	14	4528008	719700	BCKS	ISACHSEN FM
69F	770016	14	4434008	727400	SNDS	HASSEL FM
69F	770017	14	4434008	727200	SNDS	HASSEL FM
69F	770018	14	4430008	727000	SNDS	HASSEL FM
69F	770019	14	4423008	727200	SNDS	HASSEL FM
69F	770020	14	4421008	727500	SNDS	HASSEL FM
69F	770022	14	4418008	727500	SNDS	HASSEL FM
69F	770023	14	4414008	726800	SNDS	HASSEL FM
69F	770024	14	4411008	727800	SNDS	HASSEL FM
69F	770025	14	4405008	727400	CLSD	HASSEL FM
69F	770026	14	4400008	727400	CLSD	HASSEL FM
69F	770027	14	4394008	727400	SNDS	HASSEL FM
69F	770028	14	4388008	727400	SNDS	HASSEL FM
69F	770029	14	4385008	725300	SNDS	HASSEL FM
69F	770030	14	4394008	725100	SNDS	HASSEL FM
69F	770031	14	4389008	724300	SNDS	HASSEL FM
69F	770032	14	4390008	724000	CLSD	HASSEL FM
69F	770033	14	4385008	723500	SNDS	HASSEL FM
69F	770034	14	4383008	723600	SNDS	HASSEL FM
69F	770035	14	4403008	724300	SNDS	HASSEL FM
69F	770036	14	4412008	724100	SNDS	HASSEL FM
69F	770037	14	4410008	723000	SNDS	HASSEL FM
69F	770038	14	4412008	721700	SNDS	HASSEL FM

b) Ellef Ringnes Island, District of Franklin

NTS	SAMPLE NUMBER	ZONE UTM	COORDINATES EAST	NORTH	BEDROCK TYPE	GEOLOGICAL FORMATION
69F	770039	14	4416008	722800	SNDS	HASSEL FM
69F	770040	14	4430008	724700	SNDS	HASSEL FM
69F	770042	14	4434008	724600	BCKS	CHRISTOPHER FM
69F	770043	14	4435008	725300	BCKS	CHRISTOPHER FM
69F	770044	14	4466008	934100	BCKS	CHRISTOPHER FM
69F	770045	14	4469008	734800	SNDS	ISACHSEN FM
69F	770046	14	4469008	735900	BCKS	CHRISTOPHER FM
69F	770047	14	4471008	735700	SNDS	ISACHSEN FM
69F	770048	14	4481008	736400	SNDS	HASSEL FM
69F	770049	14	4490008	738600	SNDS	HASSEL FM
69F	770050	14	4493008	737800	SNDS	ISACHSEN FM
69F	770051	14	4499008	735300	SNDS	ISACHSEN FM
69F	770052	14	4491008	735000	SNDS	ISACHSEN FM
69F	770053	14	4489008	733800	SNDS	ISACHSEN FM
69F	770054	14	4475008	732300	SNDS	ISACHSEN FM
69F	770055	14	4469008	731300	SNDS	ISACHSEN FM
69F	770056	14	4469008	731000	SNDS	ISACHSEN FM
69F	770057	14	4471008	730300	SNDS	ISACHSEN FM
69F	770058	14	4464008	729800	SNDS	ISACHSEN FM
69F	770059	14	4456008	729100	SNDS	ISACHSEN FM
69F	770060	14	4454508	728900	SNDS	ISACHSEN FM
69F	770062	14	4457008	728650	SNDS	ISACHSEN FM
69F	770063	14	4458008	728750	SNDS	ISACHSEN FM
69F	770064	14	4487008	727900	GPSM	DUMBELLSDOME, OTTO FJORD FM
69F	770065	14	4485508	728100	GPSM	DUMBELLSDOME, OTTO FJORD FM
69F	770066	14	4485008	727900	LMSN	DUMBELLSDOME, OTTO FJORD FM
69F	770067	14	4486508	728300	LMSN	DUMBELLSDOME, OTTO FJORD FM
69F	770068	14	4493008	728600	LMSN	DUMBELLSDOME, OTTO FJORD FM
69F	770069	14	4430008	729700	SNDS	HASSEL FM
69F	770070	14	4438008	730100	SNDS	HASSEL FM
69F	770071	14	4445508	730800	BCKS	CHRISTOPHER FM
69F	770072	14	4445008	731100	SNDS	HASSEL FM&BCKS
69F	770073	14	4442508	731500	SNDS	HASSEL FM
69F	770074	14	4447508	732000	BCKS	CHRISTOPHER FM
69F	770075	14	4952008	732800	BCKS	CHRISTOPHER FM
69F	770076	14	4450008	733350	SNDS	HASSEL FM
69F	770077	14	4456008	733850	BCKS	CHRISTOPHER FM
69F	770078	14	4462008	732100	BCKS	CHRISTOPHER FM
69F	770079	14	4463008	731800	SNDS	HASSEL FM&BCKS
69F	770082	14	4474008	729500	LMSN	DUMBELLSDOME, OTTO FJORD FM
69F	770083	14	4492008	728000	GPSM	DUMBELLSDOME, OTTO FJORD FM
69F	770084	14	4485508	728100	LMSN	DUMBELLSDOME, OTTO FJORD FM
69F	770085	14	4485508	728100	LMSN	DUMBELLSDOME, OTTO FJORD FM
69F	770086	14	4486508	728300	LMSN	DUMBELLSDOME, OTTO FJORD FM
69F	770087	14	4485008	728500	LMSN	DUMBELLSDOME, OTTO FJORD FM
69F	770088	14	4489508	729100	GPSM	DUMBELLSDOME, OTTO FJORD FM
69F	770089	14	4493008	728600	LMSN	DUMBELLSDOME, OTTO FJORD FM
69F	770090	14	4494008	728950	LMSN	DUMBELLSDOME, OTTO FJORD FM
69F	770091	14	4500008	728200	LMSN	DUMBELLSDOME, OTTO FJORD FM
69F	770092	14	4508008	728900	LMSN	DUMBELLSDOME, OTTO FJORD FM
69F	770093	14	4502008	729850	LMSN	DUMBELLSDOME, OTTO FJORD FM
69F	770094	14	4502508	729400	GPSM	DUMBELLSDOME, OTTO FJORD FM
69F	770095	14	4504008	730100	LMSN	DUMBELLSDOME, OTTO FJORD FM
69F	770096	14	4506508	730150	LMSN	DUMBELLSDOME, OTTO FJORD FM
69F	770097	14	4504508	730550	LMSN	DUMBELLSDOME, OTTO FJORD FM
69F	770098	14	4517008	731100	GBBR	DUMBELLSDOME
69F	770099	14	4514008	731450	GBBR	DUMBELLSDOME
69F	770100	14	4524008	733050	BCKS	DUMBELLSDOME, OTTO FJORD FM
69F	770102	14	4526508	732950	SNDS	DUMBELLSDOME, OTTO FJORD FM
69F	770103	14	4521008	734100	BCKS	CHRISTOPHER FM
69F	770104	14	4519008	734300	BCKS	CHRISTOPHER FM

Table 13.3

Analytical Data: Water Samples

a) Melville Island, District of Franklin

Sample number		pH	ppm Cl-	ppm Na	ppm K	ppm SO_4^{2}	ppm Ca	ppm Mg	ppb Zn	ppb Cu	ppb F-	ppb U
78H	770002	7.08	0.6	0.5	0.4	.10	1.6	0.6	2.2	1.0	59	0.05
78H	770003	6.73	0.6	0.3	0.2	.10	1.1	0.3	0.5	0.5	51	0.05
78H	770004	8.31	0.7	2.4	0.9	.23	32.9	2.9	0.5	0.5	62	0.05
78H	770006	8.25	0.8	3.3	1.1	.33	27.4	3.7	0.5	0.5	59	0.05
78H	770007	5.96	0.5	1.6	1.4	.38	5.6	3.6	1.7	0.5	38	0.05
78H	770008	8.06	0.5	1.5	0.5	.25	21.0	1.9	0.5	0.5	50	0.26
78H	770009	8.21	0.5	2.7	0.7	.21	29.0	3.0	0.5	0.5	59	0.05
78H	770010	8.14	0.5	1.8	0.7	.23	26.3	2.8	0.5	0.5	56	0.05
78H	770011	8.12	0.5	6.2	0.5	.10	14.1	1.6	0.5	0.5	59	0.05
78H	770013	7.69	0.8	0.2	0.6	.21	9.6	1.8	0.5	0.5	54	0.05
78H	770014	8.15	0.5	0.4	0.8	.24	22.0	2.8	0.5	0.5	65	0.05
78H	770015	8.28	1.4	0.9	0.8	.10	23.0	3.5	0.5	0.5	62	0.26
78H	770016	7.87	0.9	0.4	0.4	.36	16.7	3.8	0.5	0.5	59	0.05
78H	770017	8.27	4.2	3.1	1.3	. 8	24.4	4.4	0.5	0.5	56	0.05
78H	770018	7.67	1.6	0.8	0.7	.14	16.1	2.7	0.5	0.5	59	0.05
78H	770019	7.86	3.5	1.7	1.0	.10	12.7	2.1	0.5	0.5	51	0.05
78H	770020	7.74	6.3	3.7	4.5	.10	8.4	2.7	0.5	0.5	54	0.10
78G	770012	7.50	0.5	0.2	0.9	.10	4.7	2.0	0.5	0.5	51	0.05
79B	770014	8.01	0.5	0.6	0.6	.10	17.7	2.0	0.5	0.5	44	0.10
79B	770015	8.04	3.3	2.5	0.6	6.74	220.4	8.7	0.5	0.5	46	1.35
79B	770016	8.05	3.4	3.1	0.9	6.44	199.7	9.3	0.5	0.5	51	1.40

b) Ellef Ringnes Island, District of Franklin

Sample number		pH	ppm Cl-	ppm Na	ppm K	ppm SO_4^{2}	ppm Ca	ppm Mg	ppb Zn	ppb Cu	ppb F-	ppb U
69F	770002	7.90	5.3	4.0	1.4	736	166.9	26.0	0.5	0.5	100	1.13
69F	770003	7.89	2.0	1.5	1.2	1420	534.7	6.3	2.9	0.5	100	2.70
69F	770004	7.85	1.0	0.6	0.4	1204	453.5	7.6	24.2	0.5	130	2.70
69F	770005	8.12	2.9	2.6	0.7	1380	509.4	9.8	0.5	0.5	141	1.95
69F	770006	7.78	1.1	1.0	0.4	430	188.7	2.9	0.5	0.5	72	0.81
69F	770008	8.01	0.6	0.6	0.5	648	325.3	5.2	0.5	0.5	62	0.81
69F	770009	8.16	4.6	3.3	0.6	1162	448.7	10.4	0.5	0.5	100	1.80
69F	770010	7.89	1.9	1.0	0.2	57	31.9	1.6	0.5	0.5	54	0.05
69F	770011	8.18	6.4	4.9	0.8	840	393.2	12.2	0.5	0.5	108	1.40
69F	770012	8.04	7.7	6.1	0.8	1716	567.2	20.0	0.5	0.5	163	3.05
69F	770013	8.15	3.2	2.3	0.8	1380	528.5	10.9	0.5	0.5	130	2.30
69F	770014	7.92	5.6	3.5	0.4	1112	410.4	8.2	0.5	0.5	118	1.73
69F	770015	7.89	1.3	2.3	0.8	940	335.2	13.2	4.0	0.5	112	0.60
69F	770022	7.80	0.7	0.6	0.9	43	16.0	5.6	0.5	0.5	68	0.39
69F	770023	6.90	1.4	1.0	1.7	40	8.7	5.4	0.5	0.5	62	0.17
69F	770024	4.27	2.0	2.0	3.2	188	23.3	22.1	627.6	4.5	130	0.05
69F	770027	7.74	1.1	0.7	1.0	45	18.6	5.7	5.6	0.5	79	0.05
69F	770028	8.06	1.8	1.3	1.4	90	46.5	11.5	8.7	0.5	72	0.17
69F	770029	7.70	1.6	1.9	3.0	89	20.4	12.6	1.0	0.5	72	0.05
69F	770030	8.23	4.6	6.5	7.6	232	39.8	38.5	0.5	0.5	100	0.05
69F	770031	7.32	4.4	1.7	1.3	38	6.7	4.3	0.5	0.5	65	0.05

b) Ellef Ringnes Island, District of Franklin

Sample number		pH	ppm Cl-	ppm Na	ppm K	ppm SO_4^{2}	ppm Ca	ppm Mg	ppb Zn	ppb Cu	ppb F-	ppb U
69F	770033	7.65	2.7	1.6	2.6	60	12.5	9.0	0.5	0.5	69	0.05
69F	770034	7.44	7.4	3.5	1.8	50	12.1	6.3	1.1	1.8	54	0.20
69F	770036	7.41	3.9	1.9	1.8	48	9.1	5.3	1.1	1.3	56	0.05
69F	770037	7.10	7.3	3.4	2.8	59	10.0	7.7	1.0	0.5	51	0.05
69F	770038	6.92	7.7	5.8	4.2	129	24.4	16.9	41.8	1.0	56	0.24
69F	770044	8.11	5.8	19.7	2.1	161	50.7	20.1	0.5	0.5	108	0.10
69F	770045	7.79	4.1	5.8	2.0	114	28.4	14.9	3.3	0.5	130	0.05
69F	770046	7.94	12.5	103.9	5.6	380	50.0	78.5	0.5	0.5	172	1.20
69F	770047	7.85	2.7	4.6	1.5	48	20.9	12.0	0.5	0.5	141	0.05
69F	770048	8.21	2.5	4.9	1.2	28	13.8	10.3	0.5	0.5	79	0.05
69F	770049	7.23	1.5	1.4	0.5	65	23.1	5.5	0.5	0.5	56	0.05
69F	770050	7.32	1.0	1.1	0.5	40	13.5	4.6	0.5	0.5	54	0.28
69F	770051	7.48	2.3	1.7	0.6	62	24.5	8.0	0.5	0.5	59	0.05
69F	770052	7.74	1.8	1.9	0.6	60	21.5	5.5	0.5	0.5	59	0.05
69F	770053	7.90	40.8	26.9	5.0	164	58.3	29.1	0.5	0.5	100	0.80
69F	770054	8.07	4.4	5.2	1.2	942	275.0	23.4	0.5	0.5	141	0.96
69F	770055	7.82	6.0	13.5	3.2	188	57.8	30.3	0.5	0.5	123	0.60
69F	770056	7.86	6.7	6.3	1.0	1286	502.2	26.8	1.7	0.5	190	1.76
69F	770057	8.10	0.9	1.3	0.7	968	366.9	3.4	0.5	0.5	91	1.00
69F	770058	8.26	4.3	4.0	1.4	636	136.7	19.7	0.5	0.5	210	0.67
69F	770059	7.98	18.0	11.4	3.4	976	225.8	30.4	0.5	0.5	91	0.60
69F	770060	8.08	7.7	4.2	1.6	1210	379.5	35.8	0.5	0.5	118	0.64
69F	770062	8.20	4.0	3.9	1.0	1264	429.8	14.4	0.5	0.5	87	2.50
69F	770064	8.21	1.8	2.4	0.5	1060	338.1	14.0	1.6	0.5	83	1.30
69F	770065	8.04	0.6	0.7	0.3	934	301.8	5.9	0.5	0.5	108	1.06
69F	770068	8.11	0.5	1.4	0.4	1210	435.1	12.5	0.5	0.5	108	2.10
69F	770072	7.77	7.1	21.2	1.9	430	28.2	12.2	1.0	0.5	83	0.10
69F	770073	4.45	2.1	3.3	0.7	72	8.7	6.5	38.9	1.0	100	0.05
69F	770074	8.25	8.1	37.3	2.7	496	56.3	20.8	0.5	0.5	190	0.05
69F	770077	7.65	16.5	29.7	1.1	474	27.4	12.6	0.5	0.5	180	0.05
69F	770079	7.92	4.7	31.7	1.7	802	202.2	14.8	0.5	0.5	118	1.03
69F	770082	7.99	2.0	2.1	0.7	540	85.1	7.0	0.5	0.5	46	2.45
69F	770083	8.00	0.7	1.4	0.3	982	329.0	10.0	0.5	0.5	100	0.78
69F	770086	7.98	1.3	1.3	0.4	1062	375.2	12.2	0.5	1.0	108	1.45
69F	770087	7.69	0.5	0.3	0.5	766	221.8	2.8	0.5	0.5	69	0.60
69F	770088	7.88	1.2	0.8	0.5	1102	397.7	3.0	0.5	0.5	62	1.70
69F	770089	7.98	1.0	1.5	0.4	996	368.6	12.1	0.5	1.0	83	1.80
69F	770090	7.55	1.9	1.2	0.7	1406	520.1	10.3	2.9	1.2	141	1.48
69F	770091	8.06	2.8	2.1	0.6	1438	530.2	14.6	0.5	0.5	150	2.60
69F	770092	7.59	0.5	0.1	0.1	21	9.1	0.5	0.5	0.5	44	0.10
69F	770093	7.82	0.9	0.8	0.2	1276	490.7	5.6	0.5	0.5	100	0.53
69F	770095	8.08	1.6	1.0	0.5	1362	547.2	9.7	4.0	0.5	141	0.92
69F	770097	8.11	1.7	1.3	0.7	1398	532.3	10.0	0.5	0.5	118	1.10
69F	770098	7.84	1.6	1.1	0.7	1128	402.2	9.7	0.5	0.5	96	0.74
69F	770099	8.08	2.1	1.9	0.9	1280	476.4	6.4	1.7	0.5	91	1.80
69F	770102	8.18	1.0	0.8	0.5	520	124.0	5.2	0.5	2.5	79	0.55
DETECTION LIMITS			1.0	0.1	0.1	10	0.1	0.1	1.0	1.0	40	0.10

Table 13.4

Analytical Data: Stream sediment samples (values in ppm except where noted)

a) Melville Island, District of Franklin

NTS	SAMPLE NUMBER	U	Zn	Cu	Pb	Ni	Co	Ag	Mn	%Fe	Ba	Mo	W	ppb Hg
78H	770002	6.5	28	8	4	8	5	0.1	170	0.95	400	1	2	20
78H	770003	1.2	10	2	2	3	3	0.1	90	0.45	275	1	2	20
78H	770004	2.1	82	6	7	16	8	0.1	75	2.45	425	1	2	20
78H	770005	1.5	70	4	6	10	7	0.1	50	2.20	350	1	2	10
78H	770006	2.7	74	8	7	15	8	0.1	60	2.10	400	1	2	20
78H	770007	2.4	92	10	10	17	8	0.1	65	2.70	400	1	2	20
78H	770008	1.4	38	4	4	7	4	0.1	60	1.25	350	1	2	20
78H	770009	1.5	56	6	5	11	6	0.1	65	1.70	400	1	2	20
78H	770010	1.5	26	6	3	8	5	0.1	65	1.00	300	1	2	20
78H	770011	2.4	16	8	6	11	5	0.1	150	1.10	425	1	2	10
78G	770012	1.4	22	8	4	8	5	0.1	185	0.95	300	1	2	10
78H	770013	1.5	20	6	3	6	3	0.1	250	0.80	425	1	2	5
78H	770014	1.0	20	8	4	7	3	0.1	270	0.85	425	1	2	20
78H	770015	1.6	44	10	5	9	5	0.1	295	1.35	425	1	2	10
78H	770016	1.2	24	6	4	6	3	0.1	235	1.00	350	1	2	5
78H	770017	1.3	44	8	4	9	5	0.1	230	1.20	425	1	2	10
78H	770018	1.9	52	14	7	16	8	0.1	465	1.90	525	1	2	10
78H	770019	1.2	28	8	4	9	5	0.1	185	1.05	475	1	2	5
78H	770020	2.2	46	10	6	12	8	0.1	370	1.45	450	1	2	10
79B	770014	4.8	50	18	6	35	14	0.1	175	1.75	550	4	2	10
79B	770015	2.3	34	16	7	30	13	0.1	205	1.55	550	3	2	10
79B	770016	2.1	22	16	4	25	11	0.1	205	1.50	675	1	2	10

b) Ellef Ringnes Island, District Franklin

NTS	SAMPLE NUMBER	U	Zn	Cu	Pb	Ni	Co	Ag	Mn	%Fe	Ba	Mo	W	ppb Hg
69F	770002	2.3	34	16	4	9	8	0.1	190	1.40	700	1	2	40
69F	770003	3.4	70	18	11	18	12	0.1	265	1.60	525	5	2	370
69F	770004	2.5	164	14	15	15	7	0.1	515	1.35	700	4	2	40
69F	770005	3.2	110	44	18	25	15	0.1	475	1.95	850	4	2	860
69F	770006	2.2	52	18	7	14	17	0.1	370	2.05	675	3	2	30
69F	770007	2.5	36	14	5	14	10	0.1	365	1.50	600	2	2	40
69F	770008	2.3	36	18	5	15	13	0.1	315	1.85	950	3	2	40
69F	770009	2.5	80	34	10	19	18	0.1	320	2.25	1125	4	2	80
69F	770010	3.0	80	28	8	14	26	0.1	420	3.10	850	2	2	50
69F	770011	3.0	78	26	15	20	13	0.1	410	1.80	1500	2	2	350
69F	770013	2.3	54	20	9	18	18	0.1	385	2.15	675	2	2	100
69F	770014	2.5	78	30	15	21	16	0.1	330	1.80	700	2	2	1000
69F	770015	3.2	180	36	16	18	11	0.1	630	1.50	600	2	2	50
69F	770016	1.7	20	10	3	3	5	0.1	60	1.10	450	1	2	10
69F	770017	1.7	26	10	5	7	9	0.1	140	1.05	475	1	2	20
69F	770018	1.9	32	12	6	9	10	0.1	165	1.25	600	1	2	30
69F	770019	1.3	28	12	5	8	8	0.1	120	1.00	525	1	2	30
69F	770020	1.5	22	10	4	5	4	0.1	65	0.80	450	1	2	30
69F	770022	1.0	18	6	2	5	6	0.1	90	0.55	450	1	2	10
69F	770023	1.6	26	8	4	7	9	0.1	110	0.80	575	1	2	30
69F	770024	1.9	24	10	4	6	6	0.1	70	0.75	450	1	2	40
69F	770025	2.4	22	10	4	7	5	0.1	75	0.75	500	1	2	40
69F	770026	2.1	36	16	7	11	9	0.1	100	0.95	525	1	2	60
69F	770027	1.3	28	8	2	8	8	0.1	115	0.95	500	1	4	20
69F	770028	1.4	24	8	4	7	7	0.1	80	0.65	475	1	2	20
69F	770029	1.2	20	4	2	5	5	0.1	75	0.50	500	1	2	10
69F	770030	1.9	26	6	4	5	6	0.1	85	0.60	575	1	2	20
69F	770031	2.0	24	8	4	6	8	0.1	140	0.90	625	1	2	20
69F	770032	1.1	18	4	2	5	7	0.1	145	0.70	450	1	2	20
69F	770033	1.6	22	6	4	7	8	0.1	140	0.85	500	1	2	20
69F	770034	1.3	20	6	3	6	7	0.1	125	0.70	475	1	2	20
69F	770035	1.2	22	8	3	7	8	0.1	125	0.80	525	1	2	20
69F	770036	1.8	16	4	2	5	6	0.1	130	0.60	875	1	2	20
69F	770037	2.3	38	16	7	14	11	0.1	200	1.40	675	1	2	50
69F	770038	1.8	36	10	6	8	10	0.1	185	1.05	600	1	2	30

b) Ellef Ringnes Island, District of Franklin

NTS	SAMPLE NUMBER	U	Zn	Cu	Pb	Ni	Co	Ag	Mn	%Fe	Ba	Mo	W	ppb Hg
69F	770039	2.4	28	18	7	12	10	0.1	200	1.30	600	1	2	50
69F	770040	1.2	22	8	3	6	7	0.1	135	1.10	525	1	2	30
69F	770042	2.2	38	12	6	9	8	0.1	110	1.35	675	1	2	30
69F	770043	3.6	74	36	11	16	10	0.1	105	2.85	550	1	2	70
69F	770044	1.7	44	14	6	21	12	0.1	305	1.80	575	1	2	50
69F	770045	1.6	28	6	5	14	8	0.1	165	1.00	475	1	2	20
69F	770046	2.5	44	12	8	18	10	0.1	225	1.95	600	1	2	40
69F	770047	2.5	30	6	5	14	9	0.1	240	1.20	525	1	2	30
69F	770048	2.6	38	6	5	16	11	0.1	420	1.34	575	1	2	30
69F	770049	1.2	28	6	3	12	9	0.1	255	1.05	550	1	2	30
69F	770050	1.5	36	8	5	16	10	0.1	375	1.30	625	1	2	60
69F	770051	1.5	30	6	5	13	9	0.1	310	1.05	600	1	2	40
69F	770052	2.4	3.6	6	5	15	10	0.1	320	1.35	575	1	2	30
69F	770053	1.4	3.8	8	5	11	9	0.1	235	1.25	650	1	2	50
69F	770054	2.1	28	6	5	5	5	0.1	95	1.15	525	1	2	60
69F	770055	3.1	56	14	12	16	7	0.1	265	1.25	1075	2	2	60
69F	770056	3.0	34	10	5	12	6	0.1	195	1.10	600	1	2	40
69F	770057	2.8	38	12	6	13	8	0.1	265	1.35	600	3	2	400
69F	770058	1.5	24	6	3	10	7	0.1	215	0.90	550	1	2	40
69F	770059	2.6	24	6	3	11	7	0.1	160	0.85	650	1	2	50
69F	770060	1.6	26	6	3	12	7	0.1	180	0.80	750	1	2	40
69F	770062	3.4	34	12	6	14	12	0.1	240	1.55	800	2	2	60
69F	770063	4.9	192	24	9	51	37	0.1	315	4.55	975	2	2	90
69F	770064	3.0	44	16	9	19	14	0.1	350	2.00	700	3	2	30
69F	770065	3.1	50	14	12	20	11	0.1	305	1.80	950	4	2	40
69F	770066	4.3	16	16	25	34	8	0.1	105	1.60	950	1	2	5
69F	770067	36.9	148	8	8	510	120	0.1	390	16.20	2500	85	4	150
69F	770068	3.5	34	14	9	19	11	0.1	355	1.45	675	5	2	40
69F	770069	3.0	18	10	5	4	3	0.1	25	1.65	500	1	2	20
69F	770070	2.0	28	12	3	5	6	0.1	70	1.90	600	1	2	20
69F	770071	2.1	34	12	4	9	9	0.1	145	1.75	550	1	2	30
69F	770072	1.6	36	12	4	10	7	0.1	120	1.95	575	1	2	30
69F	770073	8.8	24	10	4	4	4	0.1	50	1.70	625	1	2	20
69F	770074	2.4	60	26	8	16	13	0.1	145	2.85	625	1	2	40
69F	770075	2.9	60	32	7	15	12	0.1	115	3.10	575	1	2	70
69F	770076	1.4	28	12	2	6	6	0.1	75	2.00	525	1	2	20
69F	770077	2.2	38	14	4	9	7	0.1	100	2.25	575	1	2	20
69F	770078	2.6	70	32	9	19	14	0.1	240	3.05	575	1	2	50
69F	770079	2.8	50	18	8	17	13	0.1	300	1.95	775	1	2	40
69F	770082	4.0	40	14	5	17	17	0.1	295	1.95	775	4	2	50
69F	770083	3.2	50	16	10	20	12	0.1	330	1.75	700	5	2	60
69F	770084	3.5	46	16	10	21	13	0.1	375	1.90	675	5	2	30
69F	770085	17.1	156	22	34	51	14	0.1	340	1.65	3450	21	2	120
69F	770086	4.8	36	14	12	17	9	0.1	360	1.25	700	7	2	30
69F	770087	2.7	32	12	8	19	10	0.1	255	1.35	550	5	2	30
69F	770088	3.0	30	14	6	15	10	0.1	260	1.40	500	5	2	30
69F	770089	3.5	36	16	10	18	10	0.1	350	1.25	700	5	2	30
69F	770090	4.2	76	18	25	23	23	0.1	335	1.60	950	7	2	30
69F	770091	2.3	22	12	6	22	15	0.1	270	1.45	750	5	2	30
69F	770092	2.9	62	20	14	21	12	0.1	445	1.85	1225	2	2	90
69F	770093	3.0	52	14	14	20	10	0.1	275	1.30	950	5	2	70
69F	770094	4.5	104	14	22	17	9	0.1	370	1.20	1500	7	2	40
69F	770095	3.4	86	12	20	18	9	0.1	260	1.25	650	5	2	40
69F	770096	4.2	130	14	28	15	9	0.1	310	1.50	775	6	2	40
69F	770097	3.9	48	14	11	21	12	0.1	285	1.65	725	6	2	50
69F	770098	2.8	44	20	7	17	12	0.1	340	1.75	725	4	2	40
69F	770099	5.3	114	30	21	17	9	0.1	315	1.35	725	7	2	230
69F	770100	4.3	72	14	15	15	10	0.1	300	1.45	825	3	2	200
69F	770102	3.6	40	12	5	12	10	0.1	260	1.80	700	1	2	70
69F	770103	2.3	78	14	12	12	7	0.1	220	1.10	875	2	2	250
69F	770104	2.7	46	10	10	11	7	0.1	210	1.10	850	1	2	500

Table 13.5

Analytical data: rock samples from Melville and Ellef Rignes islands

NTS	SAMPLE NUMBER	TYPE	SITE	U	Zn	Cu	Pb	Ni	Co	Ag	Mn	%Fe	Ba	Mo	As
69F	770399	SNDS	20	2.9	10	20	1	2	2	0.2	480	5.9	nd	nd	2
69F	770407	SNDS	07	1.8	10	10	14	77	24	0.2	197	5.2	nd	nd	3
	770411	LMSN	66	20.1	48	11	69	30	2	1.0	364	1.4	nd	nd	16
	770412	LMSN	67	22.5	64	15	31	23	2	0.6	466	0.6	nd	nd	10
	770413	LMSN	67	30.7	29	20	31	23	2	0.6	466	0.9	nd	nd	10
	770414	LMSN	67	5.7	13	8	22	14	2	0.2	466	0.4	nd	nd	2
	770415	LMSN	67	25.7	370	16	48	105	16	0.8	371	2.7	nd	nd	51
	770416	LMSN	67	26.9	294	15	45	82	8	0.2	378	32.6	nd	nd	41
	770417	LMSN	67	24.4	235	18	77	64	8	0.8	385	2.7	nd	nd	44
	770418	LMSN	67	23.9	166	21	56	91	29	0.6	350	1.7	nd	nd	26
	770419	LMSN	68	28.7	80	21	40	30	2	0.4	466	4.3	nd	nd	12
	770421	LMSN	82	10.6	24	27	22	36	6	0.4	262	1.7	nd	nd	6
	770423	LMSN	63	13.7	78	21	31	26	15	0.2	500	1.7	nd	nd	4
	770424	LMSN	67	17.4	82	18	12	54	10	0.2	362	0.8	nd	nd	12
	770425	LMSN	90	29.8	60	18	24	26	6	0.2	392	1.9	nd	nd	13
	770426	LMSN	90	21.0	1710	20	150	60	10	1.6	203	23.5	nd	nd	29
	770427	LMSN	90	32.8	42	13	22	23	2	0.2	288	1.0	nd	nd	10
	770428	LMSN	90	54.2	105	16	31	64	15	0.4	546	1.3	nd	nd	22
	770430	LMSN	94	3.9	38	16	18	17	6	0.2	343	1.1	nd	nd	3
	770440	LMSN	90	40.3	65	11	26	23	6	0.4	533	0.8	nd	nd	9
	770441	LMSN	90	34.3	37	16	26	26	2	0.2	546	0.8	nd	nd	9
69F	770442	LMSN	90	31.0	52	15	31	30	5	0.2	460	1.0	nd	nd	9
69F	770701	DIBS	07	1.6	60	41	2	7	29	nd	1720	11.1	218	1	nd
	770702	DIBS	07	1.3	50	29	2	6	27	nd	1750	11.7	211	2	nd
	770707	DIBS	07	1.6	115	7	6	1	14	nd	1200	8.1	268	1	nd
	770710	DLMT	07	1.5	9	4	3	53	16	nd	229	6.3	61	3	nd
	776403	DIBS	64	1.2	68	40	2	5	19	nd	1700	10.5	473	1	nd
	776404	DIBS	64	1.2	456	28	4	4	24	nd	1780	10.1	194	2	nd
	776601	MGDM	66	1.4	211	2	15	14	3	nd	338	0.6	181	7	nd
	776602	MGDM	66	3.1	9	5	2	4	2	nd	290	0.4	13	6	nd
	776605	DLMT	66	1.8	437	14	13	6	2	nd	166	0.5	191	5	nd
	776607	ANDR	66	0.7	99	2	14	0	0	nd	25	0.0	18	4	nd
	776701	LMSN	67	27.1	237	14	48	87	15	nd	448	2.4	3800	38	nd
	776702	LMSN	67	4.6	42	43	60	45	6	nd	173	1.0	52	13	nd
	776703	LMSN	67	16.3	80	21	24	21	4	nd	522	0.7	748	25	nd
	776704	LMSN	67	5.7	11	3	4	9	2	nd	341	0.4	34	5	nd
	778901	LMSN	89	14.9	64	9	13	23	7	nd	330	1.2	274	9	nd
	778902	LMSN	89	1.4	14	8	2	22	8	nd	203	2.4	87	17	nd
	779001	LMSN	90	33.3	123	25	31	82	14	nd	522	3.2	4110	38	nd
78H	770801	IRFM	08	0.9	170	3	2	51	78	nd	73600	7.8	102	1	nd
79B	771401	DIBS	14	2.4	10	8	2	0	6	nd	592	6.8	109	1	nd
	771404	IRFM	14	1.2	22	10	0	9	8	nd	3930	28.9	250	1	nd
	771701	IRFM	17	0.9	20	9	0	5	4	nd	2300	31.9	832	1	nd
79B	771703	IRFM	17	0.9	19	5	0	2	4	nd	642	19.2	245	2	nd

Values in ppm except where noted.

SNDS = sandstone
DIBS = diabase
n.d. = no datum
LMSN = limestone
DLMT = dolomite
ANDR = anhydrite
MGDM = magnesian dolomite
IRFM = iron formation (ironstone)

For U, the stream sediments yield a similar areal distribution to that found in the water samples. Within the Isachsen Formation, samples 54-63 contain U in the range 1.5 – 4.9 ppm, levels which we view as anomalous. These values correspond well with some subtle water anomalies noted above. Close inspection of the underlying Isachsen sandstone revealed patches of coaly fragments and grey sandstone, some of which were found to be slightly radioactive (McPhar TV-1A). Similar situations prevail in the same rock type on the east side of the Dome (samples 11-14), and to the north (samples 46-47). In the last case, no associated radioactivity was observed. With the one exception (sample 73) where U reaches 8.8 ppm, Hassel sandstone, coaly or not, contributes little U to the stream sediments. This particular sample was also accompanied by an acid water (pH 4.45) which contains about 40 ppb Zn. The sediment contains 24 ppm Zn, average for this area. We have already ascribed the unusual chemistry of this sample site to the presence of oxidizing coal.

Stream sediments collected within the Dumbbells Dome structure commonly carried larger quantities of U in the range 2.3 – 5.3 ppm and exceptionally, 17.1 ppm. The areas of most consistent highs corresponded well with water anomalies described previously; viz., samples 3-10, 64-68, and 83-102. All of these samples lie within drainage basins dominated by Pennsylvanian limestone breccias and masses of gypsum.

Inspection of these rocks for radioactivity revealed moderate levels of activity which ranged from 500 cpm to 23 000 cpm (McPhar TV-1A); the highest levels were estimated at the time to be equivalent to 150 ppm U. Subsequent analysis of hand specimens from these sample sites (Table 13.5) yielded lower values. These are discussed later. Gypsum masses gave very low readings as did nearby diabase dykes and sills. Subsequent analysis of typical samples produced values of 1-3 ppm U (Table 13.5).

The data of Table 13.4b show some anomalous levels for other metals. For example, a little Zn, Cu, and Ni were found in streams draining diabase; Zn, Cu, Pb, Ni, Ba, and Mo were found to be associated with streams draining limestone and gypsum within the Dome, whereas streams draining sandstone are characterized by low levels of all other metals except perhaps Zn.

Discussion

Waters from the Dumbbells Dome area (69F) would be expected to carry U if it is present in underlying bedrock. They contain moderate to high levels of $SO_4^=$ and Cl^- (Table 13.3) as well as some $CO_3^=$ (inferred from pH values). In fact $SO_4^=$ levels found are calculated to be about one half of what would be obtained for saturated calcium sulphate solutions at 0°C, viz., 2400 ppm.

All of these ions are well known to complex uranyl ions strongly, but the overwhelming excess of $SO_4^=$ would likely ensure that bis-sulphato-uranyl ions predominate in solution.

Under these conditions dispersion trains in waters are found to be relatively long and diffuse, probably about 5 km, with U levels diminishing as a result of dilution from barren stream waters rather than by adsorption into bed sediments. In fact, this is to be expected, as in the presence of large amounts of sulphate ion, U will be leached from rocks and sediments and retained in solution rather than be reprecipitated into sediments. The overall effect of these processes is to produce very short dispersion trains in sediments. It is quite likely that other metal ions such as Fe and Zn, would also manifest long residence times in solution in these streams. Some detailed "soil" and stream sampling in the centre of Dumbbells Dome demonstrated just how short were dispersion trains in sediments in comparison with waters. Uraniferous limestones (Table 13.5), shattered by frost action to mounds of felsenmeer near sample site 67, were seen to be further weathered and leached to form highly oxidized iron-rich limy muds on the upper banks of a nearby stream, where U reached 36.9 ppm (Table 13.4b). Approximately 25 m farther downslope and just above the stream highwater line, these limy mud flows were found to carry 17.1 ppm U (sample 85). Zn, Ba, and Mo are also present in anomalous levels as they were at site 67.

However, a true stream sediment taken 25 m downstream contained a mere 4.9 ppm U and a little Mo. Fe, present in the upper bank muds at 16.2 per cent was largely depleted (< 2 per cent) in the lower bank muds. Sulphate content of waters washing these muds and sediments was found to be near 1000 ppm (samples 65, 86).

Outside the Dome, dispersion of metals in waters is very restricted, perhaps to less than 1 km. We regard dilution effects from snow melt and permafrost-derived groundwaters as more important controls than adsorption or precipitation of dissolved metal loads in these streams.

Geochemical Studies – Ellef Ringnes Island

Rocks

Analyses of selected hand specimens from the Dumbbells Dome area (69F) are presented in Table 13.5. Data are listed according to the stream site which receives the drainage from these rocks.

The analyses confirm the presence of low grade uranium mineralization in certain limestone breccias of Dumbbells Dome. Values were found to be one third of those predicted from field radioactivity measurements. We conclude that there is some disequilibrium between U and daughter elements such as Ra. In view of the brecciated nature of the rocks, coupled with the action of frost and related severe surface leaching in the area, a disequilibrium situation is not surprising. The hand specimens collected show evidence of supergene alteration; many have limonitic rinds and fracture fill. Visible pyrite commonly was partly oxidized.

The chemistry of Ra dictates that it be retained preferentially to U by adsorption onto barium sulphate, calcium carbonate, or coprecipitation with secondary calcite. In support of this model, inspection of Table 13.5 reveals a close relationship between U levels measured by neutron activation analysis and Ba content of the rocks. On the other hand U as uranyl ion is mobilized efficiently by carbonate ions and by sulphate ions from gypsum and oxidizing pyrite. We intend to analyze some of these samples for Ra to determine the extent of U leaching. In future field operations it will be necessary to dig some shallow pits to check for increased radioactivity at depth and, if possible, to obtain relatively less weathered samples for analysis.

Table 13.5 also indicates that the diabase dykes carry very little U. The evaporites, particularly those carrying fluorite, do carry small quantities of U.

General Discussion and Recommendations for Further Work

It has been established that low grade U mineralization can be found in significant quantities in certain geological settings in the high arctic.

However, the setting in which U was found ultimately was at first surprising. Upon later consideration, it was soon appreciated that a pyritic (now mainly limonitic) brecciated limestone should provide an excellent chemical and physical trap for stray fluxes of uraniferous brines. If this limestone immediately overlies the Otto Fiord (Penn.) evaporites, then it is certainly in close proximity to a possible source of U and perhaps Zn, Ni, Mo, and Ba. Few signs of uraniferous sandstone were found although the coaly Isachsen sandstone, which are also in close proximity to the evaporites, were found to manifest low radioactivity in places.

This and other similar Mesozoic sandstone should not be disregarded at this stage as possible hosts for U mineralization. The setting remains an excellent one. Further studies should be directed towards other evaporite diapirs and related anticlinal domes. These can be found on Axel Heiberg Island, Ellef Ringnes Island, Amund Ringnes Island, Ellesmere Island, and Melville Island. A gypsum mass or diapir within an impact crater on Devon Island is also an interesting site.

At this point it is relevant to discuss the usefulness of the geochemical techniques used in this study.

It was found that both geological and geochemical studies are severely restricted by the nature of the terrain in the high arctic. Rocks which do outcrop are generally badly frost-shattered and are often rendered to nothing more than fine sand or mud. This is especially true of sandstone and shale, whereas carbonate rocks are considerably more resistant to physical weathering processes. Sedimentary rocks which do survive essentially intact are commonly leached to depths of 10 cm or more and are sometimes iron-stained. Often the weathered rind is impregnated with ice crystals which serve as a cement. Even carbonate rocks have thick weathering rinds and in some situations secondary calcium carbonate can be found reprecipitated on the underside of boulders and cobbles. The effects on trace metal content are obvious from inspection of the stream sediment data presented and the very low levels of surface radioactivity observed on traverse. U is one of the more easily leached elements and simply does not persist at surface in this environment. Nor do its radioactive daughter elements whose presence would permit radiometric detection, except possibly in the carbonate breccias where there is some evidence of disequilibrium between U and Ra.

Consequently, as we have already noted, geochemical and radiochemical anomalies are of low level and very subtle. They can be interpreted correctly only with the help of appropriate geological information.

Dispersion trains in waters and sediments are of limited use in the detection of U and trace elements associated genetically with it. This is primarily a problem of dilution imposed upon initially low levels leached from source rocks. Radiochemical detection of sources of U is further restricted by the generally wet terrain. Except for certain relatively more resistant limy rocks and the diabase sheets within the evaporite diapirs, most of the flat-lying terrain is water-saturated or cut by numerous wet drainage channels. It was observed that precipitation of a few millimetres of rain has the effect of turning the top few centimetres of "soil" into a wet, sticky mass. Streams, which seem to flow partly within bed sands and partly above them, would rise perceptibly. Radiochemical measurements probably would be more useful if small pits and trenches were dug to penetrate surface materials, especially in limestone terrane.

Similar experiences have been noted in parts of the Barn and British Mountains of northern Yukon (Goodfellow, pers. comm.). There, similar suppressed geochemical responses occur in streams draining known U showings, and low radiochemical response in flat-lying sandstone and shale terrane were observed. Goodfellow shares our opinion that careful detailed geochemical and geological studies are mandatory to permit valid interpretation of more regional data which may be obtained.

At the present time, sampling of waters appears to be more immediately useful than stream sediments in both northern Yukon and in Queen Elizabeth Islands. Nevertheless, U data derived from each technique do serve to substantiate anomalies detected by the other. Measurements of other trace metal levels, chosen to fit the appropriate genetic models under test, will augment information gathered from U analyses and improve chances of finding significant anomalous areas and perhaps, mineral occurrences.

More extensive, integrated orientation studies of this type are required to establish optimum sample intervals for U and base metal exploration in the high arctic. It is important to note that changes of terrain will probably require specific and detailed attention in order to achieve these objectives, and that no universal methodology is in sight for the high arctic.

Acknowledgments

We wish to acknowledge that logistical assistance provided for us by Polar Continental Shelf Project and the personal advice of its Director, G.D. Hobson. We are also grateful to D.M. Barnett, formerly of the Terrain Sciences Division, for the benefit of his field expertise in arctic conditions, and to L.D. Jones for his assistance in drafting figures.

References

Stott, D.F.
1967: Geology of Ellef Ringnes Island, District of Franklin; Geological Survey of Canada, Map 4-1968, Paper 68-16.

Tozer, E.T. and Thorsteinsson, R.
1964: Geology, western Queen Elizabeth Islands, District of Franklin; Geological Survey of Canada, Memoir 332.

14.

TECTONO-STRATIGRAPHIC PROBLEMS IN THE CARMANVILLE AREA, NORTHEASTERN NEWFOUNDLAND

Project 730044

K.L. Currie, G.E. Pajari, Jr.[1], and R.K. Pickerill[1]
Regional and Economic Geology Division

Currie, K.L., Pajari, G.E., Jr., and Pickerill, R.K., Tectono-stratigraphic problems in the Carmanville area, northeastern Newfoundland; in Current Research, Part A, Geol. Surv. Can., Paper 79-1A, p. 71-76, 1979.

Abstract

Sedimentary rocks of the Carmanville map area formed during a continuous period of sedimentation extending from pre-Ordovician into Upper Ordovician or Silurian time. Standard stratigraphic terminology inadequately describes this sequence since it contains within it obducted slabs of ocean floor, which exhibit thrust faults at their base and unconformities at their top. Where these slabs are absent, the sedimentary section is continuous. The upper part of the section contains numerous olistostromes. The slides commenced after obduction and continued until the end of the sedimentation cycle.

Tectonic modelling suggests that the region formed the continental slope and toe of slope to a continent which lay to the east in Ordovician time. Despite the obduction in Llandeilo-Llanvirn time, significant deformation did not commence until latest Ordovician or Silurian time, and was essentially complete in a short period, although the climax of thermal activity was not reached until the Devonian. Although the deformation and plutonic activity clearly record plate interactions, we see no evidence of subduction. The data seem best explained by assuming that a projection of the "Avalonian" continent encountered a major transcurrent fault somewhere in the Carmanville region. As a result of this collision, a heat source was over-ridden by the continent, leading to later magmatic and metamorphic activity.

Introduction

The Carmanville map area records in unusual detail the complexities associated with the building and evolution of the eastern continental margin of the lower Paleozoic Iapetus Ocean and its eventual closure with concomitant metamorphism and igneous activity (Pickerill et al., 1978a; Williams, 1978). Some of these details cannot be easily reconciled with standard stratigraphic and structural nomenclature and we discuss here the nature of these problems and their possible solutions.

Stratigraphic Considerations

In Table 14.1 the mappable units of the Carmanville area are listed. We consider units 4 to 11 to result from a single cycle of sedimentation. These units comprise the Gander Lake Group of Jenness (1963). However, due to tectonic complexity, all of these rocks cannot be conveniently placed into one group, and attempts to do so have led to serious difficulties in terminology (Pajari and Currie, 1978; Brückner, 1978; Pickerill et al., 1978b). These difficulties result from the emplacement of older rocks locally on top of younger ones, namely ultramafic and related rocks of unit 1 emplaced by thrusting, and volcanogenic rocks of unit 2 emplaced by olistostrome formation. The emplacement of the ultramafic slices leads to a particularly intractable conundrum since each slice deformed the rocks below it resulting in the gently west dipping structures emphasized by Kennedy and McGonigal (1972) in the "Gander Group" (in the sense of Kennedy (1975)). Subsequent erosion produced localized unconformable sequences above the ultramafic rocks (cf. Blackwood, 1978). However, in regions where ultramafic rocks are absent, for example south of Island Pond, the sedimentary section is continuous and unit 4 exhibits neither an unconformity at its top nor a more complex structural history than the overlying rocks. No simple stratigraphic terminology correctly describes such a situation. We therefore reserve the question of terminology for future consideration and abandon all previous, now inadequate, terminology (Gander Lake Group, Gander Group, Davidsville Group) in favour of numerical descriptors.

The oldest unit of the sedimentary sequence (unit 4), comprises a monotonously uniform silty greywacke, rich in quartz and consistently containing small amounts of plagioclase. The rocks commonly exhibit fine foliation spaced 1-5 mm apart. South of the map area (at Jonathons Pond, for example) primary sedimentary structures are preserved in a few places, but within the map area virtually all of the unit lies above chlorite grade metamorphism, and the observed foliation appears to be of tectonic origin. Near the top of unit 4 a zone some 200 m thick is rich in chlorite and contains numerous lenses and boudined dykes of amphibolitic rocks. The character of this material and its chemical composition (Table 14.2) suggest that it represents volcanic rocks of icelandite affinity. This zone appears to be correlative to the volcanic rocks noted by Jenness (1963) along Gander Lake, which he believed characteristic of the middle Gander Lake Group. This locality has yielded fossils characterized by McKerrow and Cocks (1977) as Arenig to Llanvirn in age. This zone everywhere lies below the (tectonically emplaced) ultramafic rocks.

Since unit 4 lacks primary sedimentary structures, its structure and thickness cannot be determined. The thickness appears to be considerable, and no basement to the sedimentary sequence can be detected, in part because metamorphic grade increases toward the east. The Flinns Tickle complex (unit 14) consists largely of rocks equivalent to unit 4 metamorphosed to sillimanite grade. The characteristic thin foliation can still be readily recognized even at this grade. The nearest unit of contrasting lithology in an eastward direction is the compositionally distinctive (Table 14.2) Deadman's Bay Pluton (unit 21) of megacrystic granite. The Deadman's Bay Pluton exhibits primary foliation concordant with its gneissic envelope, and dykes are extremely rare. It could conceivably represent the basement to unit 4, but if so it must have been totally remobilized and homogenized.

[1]Department of Geology, University of New Brunswick, Fredericton, New Brunswick. E3B 5A3.

Table 14.1

Table of Formations

Cretaceous-Jurassic(?)		22	Lamprophyre dykes
			- intrusive contact -
Carboniferous		21	DEADMANS BAY PLUTON — coarse grained biotite quartz monzonite with megacrysts of microcline perthite; rare aplitic dykes
			- intrusive contact -
		20	RAGGED HARBOUR COMPLEX (units 19-20) — white muscovite-garnet leucogranite, aplitic to pegmatitic with graphic patches
			- relations unknown -
		19	Trachytoid, porphyritic pale grey biotite granodiorite
			- gradational contact(?) -
		18	ISLAND POND, ASPEN COVE and WHITE POINT COMPLEXES (units 17-18), Massive to foliated coarse, pink biotite-muscovite quartz monzonite, locally garnetiferous in leucocratic parts
			- relations uncertain -
Devonian		17	Fine-grained, equigranular biotite granodiorite and quartz monzonite
			- gradational contact -
		16	Heterogeneous granitoid gneiss and pegmatite with schlieren of 14a, 15a
			- intrusive contact -
		15	Migmatite, lit-par-lit gneiss, sheeted complex; 15a complex of 16 and 14a, 15b complex of 18 and 14b
			- gradational contact -
Silurian or Devonian		14	FLINNS TICKLE COMPLEX — quartz-feldspar-biotite-muscovite gneiss and schist, commonly containing garnet and/or sillimanite. Minor quartzite and amphibolite. 14a metamorphosed equivalent of unit 4, 14b metamorphosed equivalent of units 4-9 (may be older than 13 in part)
			- relations unknown -
Silurian or Devonian		13	ROCKY BAY, FREDERICKTON and TIMS HARBOUR PLUTONS — Homogeneous coarse grey tonalite with poikilitic biotite, commonly amphibole bearing. 13a foliated granodiorite rich in dykes, 13b dacitic to rhyolitic dykes
			- intrusive contact -
Silurian Llandovery		12	Greenish-grey siltstone with light grey limestone lenses and beds. Local conglomerate.
			- unconformity -
		11	Greenish-grey, frequently thick bedded, siltstones with numerous slumped and brecciated horizons. 11b silicified hornfels
			- gradational contact -
		10	Thin bedded grey to black slate and siltstone, greenish grey slate and siltstone with grey limestone layers and lenses. Numerous slumps and olistostromes. 10b pillowed basalt olistoliths
			- gradational contact -
Middle and Upper Ordovician	Caradoc	9	Olistostrome with black pyritic shale matrix and olistoliths of units 1-8. Large scale soft rock deformation, hydroplastic and thixotropic disaggregation. 9a hornfels around Rocky Bay Pluton
			- cross-cutting contact -
		8	Turbidite sandstone and siltstone, with local full Bouma sequences. Numerous minor slumps and soft rock deformation
			- gradational contact -
		7	Fine banded grey black siltstone and shale, with shale lenses, shale flake conglomerates, graded beds. Minor slump structures
			- gradational contact -
		6	Granule and conglomerate lenses with volcanic and ultramafic clasts in grey black siltstone and shale. 6a green sandstone and siltstone facies equivalent to above
			- gradational contact -
	Llanvirn	5	Red shale with local grey-green bleached areas, and occasional limestone beds, caps sequence of thin bedded black and white siltstones
			- gradational contact -
	Arenig(?)	4	Uniform thin bedded grey green siltstone and quartz wacke with occasional semi-pelitic interbeds all in green schist facies metamorphism. 4a green volcanogenic schist with amphibolite lits and dykes
			- tectonic contact -
Ordovician and older		3	Shattered, chloritized plagiogranite porphyry, trondjhemite dykes, sills stocks
			- intrusive contact -
		2	Volcanogenic sediments, tuff, agglomerate, minor pillowed basalt. 2a volcanogenic sediments and limestone, 2b debris flows, 2c hyaloclastites, 2d rubble of volcanic and ultramafic rocks, probably gradational to 6
			- intrusive contact -
		1	Massive to schistose pyroxenite, peridotite, dunite. 1a serpentinite, 1b magnesite and ankerite, 1c gabbro and diorite

The top of unit 4 is marked by a gradational transition to thinly bedded siltstone to shale sequence producing a black and white striped rock everywhere capped by a distinctive unit of red shale (unit 5) which has been traced more than 30 km from Weirs Pond to Island Pond Brook. South of Island Pond Brook the black and white siltstone-shale sequence strongly resembles unit 7, but it can be observed to pass continuously downward to unit 4. The red shale is locally bleached to pale yellowish green, but the characteristic reddish colour is found throughout its length. The red shale has not been recognized east of Shoal Pond, presumably because increasing metamorphism has destroyed its distinctive features.

Ultramafic slabs of unit 1 occur mainly within or at the base of unit 5. At Shoal Pond the ultramafic unit rests on silty greywacke and greenstone of unit 4, but northeast of Barry's Fifth Pond a sliver of ultramafic appears near the top of unit 5. The top of the ultramafics is marked by an unconformity, which at Weirs Pond, just south of the map area, is of Llanvirn-Llandeilo age (Blackwood, 1978). We assume this age to apply approximately to unit 5 in the southwestern part of the map area. A newly discovered fossil locality has yielded Lower to Middle Ordovician inarticulate acrotretid brachiopods and a conodont assemblage which is currently being examined.

Conglomerates and breccias composed of ultramafic, mafic volcanic rock and plagiogranite debris extend southwestward from the end of the Shoal Pond ultramafic slab and its associated mafic volcanic rocks and plagiogranites (unit 2d). This rubble occupies a zone nearly as wide as the slab and about 2.5 km long. Pebble and cobble horizons up to 10 m thick which occur in a matrix of fissile black shale or siltstones (unit 6) overlie the ultramafic slab. These horizons contain some debris derived from the slab as well as sediment transported from elsewhere. Both of these coarse horizons fine to the southwest and are facies equivalents of the greenish, fine banded siltstones with numerous lenses of granule conglomerates and sandstone (unit 6).

The ultramafic-mafic slabs at Weirs Pond had also shed coarse debris toward the southwest. In contrast to the reduced character of the Shoal Pond debris, the debris at Weirs Pond is thoroughly oxidized. This belt of relatively coarse clastic rocks therefore appears to be either continuous or a series of en echelon lenses over some tens of kilometres, although there are some striking facies variations. Along the highway at Barry's Brook the apple green siltstones and sandstones appear to be interbedded with black pebble conglomerates on a scale of a few metres. The reason for the alternate appearance of these strikingly different colours is not presently understood.

The fine banded, greyish black siltstone and shale of unit 7 constitute the material originally designated "Davidsville Group" by Kennedy and McGonigal (1972). The unit consists mainly of beds 5-10 mm thick grading from fine siltstone at the base to discontinuous shaly tops. Thin seams of shale-flake conglomerate or granule beds occur rarely. We interpret these features to be due to distal deposition from

Table 14.2

Average chemical composition of some units from Carmanville map area

	1	2	3	4	5	6	7
SiO_2	62.90	71.41	61.62	64.82	66.83	53.13	57.70
TiO_2	1.06	0.19	0.49	1.05	0.71	2.46	1.07
Al_2O_3	14.66	14.83	15.69	15.26	15.44	13.28	19.42
Fe_2O_3	0.61	0.51	0.96	1.31	1.32	5.31	1.68
FeO	5.33	1.44	4.46	3.08	3.14	6.69	7.97
MnO	0.14	0.07	0.11	0.11	0.07	0.22	1.55
MgO	2.07	0.87	2.10	1.84	2.01	3.70	2.71
CaO	2.87	1.23	8.49	2.36	2.07	11.32	0.95
Na_2O	3.51	3.86	3.54	3.22	3.47	0.61	1.15
K_2O	4.36	3.71	1.30	3.75	2.71	0.56	3.28
H_2O	1.76	1.36	0.86	1.81	1.63	2.08	2.11
CO_2	0.24	0.08	0.27	0.92	0.24	0.27	0.23
F	0.14	0.04	0.03	0.02	nd	nd	nd

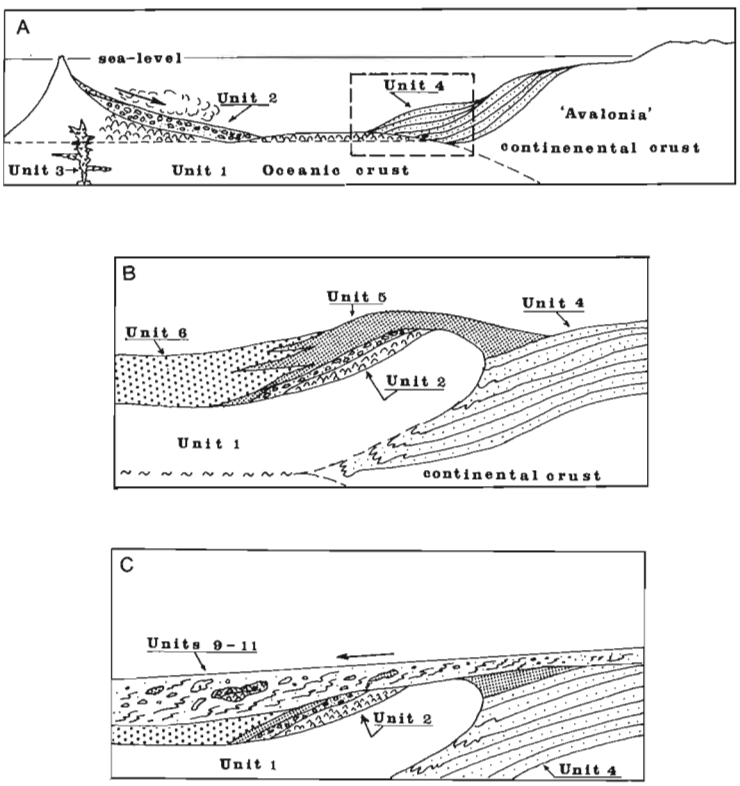
nd – not detected

1. Deadman's Bay Pluton (map unit 21, average of 6 analyses)
2. Ragged Harbour, White Point, Aspen Cove and Island Pond Plutons (map units 17-20, average of 19 analyses)
3. Frederickton and Rocky Bay Plutons (map unit 14, average of 9 analyses)
4. Flinns Tickle complex (map unit 13a, average of 6 analyses)
5. Quartz wackes of unit 4 (average of 4 analyses)
6. Volcanogenic rocks of unit 4 (average of 5 analyses)
7. Slates and siltstones of unit 7 (average of 9 analyses)

Chemical analyses by G.S.C. Rapid Methods Group

turbidity currents. The bedding commonly shows slump and soft sediment deformation on a small scale. Some of this deformation may be due to later formation of olistostromes.

More spectacular turbidity current deposits with partial and/or complete Bouma sequences occur in sandstone and siltstone of unit 8 along the shores of Gander Bay near the causeway. Much of this unit may be hidden by the waters of Gander Bay, but this unit also indicates a more proximal facies of turbidite deposition due to proximity to or confinement within a submarine channel. The large number of coarse conglomerate boulders found along the southern shores of Gander Bay, stemming from some part of the sedimentary succession not seen by us, reinforces this conclusion.



A. Pre Llanvirn time, the continental slope and toe of slope on the right is being built by accretion of continental sediment. Submarine volcanic rocks (left) are being built not only by eruption, but by debris and grain flows of volcanic material, forming the various parts of unit 2. The area enclosed by the broken rectangle is shown enlarged in Figures 14.1B and 14.1C.

B. Llandeilo-Llanvirn time. Slabs of the ocean floor have been emplaced by obduction, and the mafic and ultramafic rocks thus exposed give rise to chemical and muddy sediment which is deposited around the slabs (unit 5) and to coarse debris which is carried down slope (unit 6).

C. Caradoc time. The ultramafic slabs have been mostly buried by continuing sedimentation (units 7 and 8), but are now again exhumed by very large scale olistostroming which persists through the latter part of the sedimentary cycle.

Figure 14.1. *Cartoon of the sedimentological development of the Carmanville area. (Note: The diagrams are not to scale, and incorporate a large vertical exaggeration. The distance from the toe of the continental slope to the volcanoes offshore (Fig. 14.1A) is unknown).*

We have elsewhere described in detail the olistostrome of unit 9 (Pajari et al., in press). The olistoliths of this unit (which includes unit 2) have been described elsewhere (Pickerill et al., 1978; Pajari et al., in press). We here draw attention to the range of lithologies sampled, namely from units 1-8, as well as a very pure orthoquartzite which appears as well rounded cobbles. Comparison with other lithologies in eastern Newfoundland suggests that the only known source of such cobbles is the lowermost Cambrian(?) Random Formation (Jenness, 1963). If this deduction is correct, the slide event not only sampled lithologies on the continental slope, but also those on the continental shelf. The black, pyritic shale which commonly forms the matrix of the olistostrome has yielded Caradoc fossils (Bergström et al., 1974).

Along the west shore of Gander Bay, north of Rogers Cove, Williams (1964, 1972) mapped the sedimentary rocks as part of the Silurian Indian Islands Group and considered it to be separated from the older rocks to the south by faulting. We find no evidence of such faulting. The rocks north of Rogers Cove exhibit a style and intensity of deformation compatible with those of units 4-9, including soft rock slumping through to larger scale slides with pillow basalt olistoliths greater than 10 m in diameter. The olistostromes of units 10 and 11 differ from those in the lower units by the absence of intrusive and cross-cutting olistolith laden black shale, and are therefore compatible with a slide origin under conditions of lower hydrostatic pressure, i.e. toward the top of the sedimentary pile.

The stratigraphic relationships north of Rogers Cove are extremely complex largely because of the widespread soft rock slumps and slides which have destroyed most of the primary sedimentary features. Two localities, interpreted as unconformities, suggest that the sedimentary sequence was not continuous. Near Tims Harbour, a greyish black siltstone (similar to unit 6) is unconformably overlain by a less deformed greenish weathering grey siltstone with limestone lenses. Fossils collected near this locality by Williams (1972) have yielded **Favosites** cf. **favosus**, while presumably equivalent rocks from Goose Island are interpreted as Llandovery in age. The other locality in Shoal Bay exhibits an upward younging conglomerate overlying downward facing dark grey siltstones. The clasts have been derived from locally exposed rocks. A somewhat similar conglomerate at Main Point is assumed to be a correlative. The rocks have been tectonically deformed, and because the lithologic characteristics of the major units are not markedly different, the unconformity has not proved to be traceable. The younger rocks, on the basis of the paleontological implications above, may well be Silurian.

Our unit 10 consists of generally thinly bedded grey to black slate and siltstone, commonly rusty weathered and greenish grey slate which are frequently interbedded. Unit 11, of thicker bedded character, is composed of greenish grey to greenish black siltstones. Both units are extensively slumped with consequent loss of sedimentary features. Unit 10 contains pillowed basalt olistoliths indicative of larger scale transport which contrasts with widespread penecontemporaneous brecciation in unit 11.

The rocks above the unconformities along with other lithologically similar units are included in unit 12. Their geographic distribution may be somewhat greater than presently known.

Tectonic Considerations

We consider tectonic deformation in this region to have commenced with the emplacement of the ultramafic rocks. The evidence for superficial, tectonic emplacement of these bodies includes observation of an unconformity at the top of

the ultramafic rocks, the immediate shedding of ultramafic debris into overlying conglomeratic units, the observation of steep reverse faults at the base of the ultramafic bodies, the invariable association of small amounts of volcanic rocks with the ultramafics (showing that they cannot be simple intrusions) and finally the general occurrence of the ultramafic belt near a given stratigraphic horizon. The ultramafic rocks cannot have originated as hot diapirs, since they show no trace of contact metamorphism, nor as cold diapirs (cf. Strong and Malpas, 1975), since the structures associated with them dip gently to the west, imposing a series of tectonic fabrics on the rocks beneath the ultramafics (Pickerill et al., 1978a). All elements of an ophiolite suite, including abundant gabbroic dykes, are present, but the idealized ophiolite suite has not been seen at any single locality.

We interpret the ultramafic and volcanic rocks of units 1 and 2 to be slivers of the seafloor and superincumbent volcanic rocks thrust over the toe of the continental slope (as represented by unit 4). On the basis that the unconformity at the top of the ultramafics is of Llanvirn-Llandeilo age (Blackwood, 1978), we consider that emplacement of these slivers took place at this time, with a subsequent downslope (western) readjustment of the volcanic rocks by sliding in Caradoc time. If this interpretation is accepted, it can be further deduced that in lower Ordovician time there existed volcanic rocks offshore from the "Avalonian" continent. Presumably these rocks lay well offshore, since the sedimentary source prior to ultramafic emplacement was rich in quartz and evidently derived almost entirely from the continent, whereas after this time the sediments contain a substantial volcanogenic component.

The emplacement of the ultramafic slabs did not interrupt the process of sedimentation but led to the addition of a large volcanogenic component to the sediments. The process of sedimentation continued at least through Caradoc time, but had ceased before the deposition of unit 12. Since this unit rests with unconformity on older rocks, and since emplacement of the essentially posttectonic Frederickton Pluton took place about 405 Ma (Pajari and Currie, 1978), the major deformation of the sedimentary sequence took place during a short period of upper Ordovician and Silurian time, although deformation of unit 4 beneath the ultramafic slabs preceded this period, and late deformation, associated with faulting, may have extended into the Devonian. In our previous structural analysis (Pickerill et al., 1978a) we showed that at least four periods of deformation could be identified in units 4-11. However this deformation is extremely inhomogeneous. As pointed out by Kennedy and McGonigal (1972), large regions of the sedimentary rocks display only one cleavage and minor kinking. However, the same units when traced along strike can be found to exhibit all four periods of deformation, or even to exhibit "wild-folding" with folds striking and dipping in all directions. The reasons for this extraordinarily heterogeneous behaviour are not clear. We believe that it may be related to variations in lithifaction of the rocks before deformation, which may in turn be due to persistent emplacement of dacitic dykes prior to deformation. Another factor may have been the mechanically heterogeneous character of the sedimentary pile due to local inclusion of ultramafic slabs.

We here draw attention to the persistent association of magmatic activity with deformation. Dacitic dykes in units 5-6 have been deformed with their host rocks. According to the reasoning just advanced, they cannot be younger than early Silurian in age. The Frederickton Pluton, and by analogy the similar Rocky Bay and Tims Harbour plutons, are Silurian or earliest Devonian in age, whilst the Island Pond, White Point and Ragged Harbour plutons are mid-Devonian, and the Deadman's Bay possibly Carboniferous in age (Pajari and Currie, 1978). There appears to have been a steady progression in magmatic activity eastward, accompanied by a rise in metamorphic grade in the host rocks. Southeastward compression appears to have been more or less continuous throughout the whole process, since west-dipping reverse faults cut the Ragged Harbour Pluton.

A Tectonic Model for the Carmanville Area

We believe the sedimentary sequence (units 4-11) to represent the continental slope and base of slope of the eastern margin of the Iapetus Ocean. The Avalon Peninsula formed the stable craton east of this ocean. During deposition of the quartz wackes of unit 4, the Carmanville area received sediment from the east, that is from the continent, in the form of silts and fine sands containing substantial amounts of feldspars and rock chips. Primary structures are insufficiently preserved in this unit to determine the transport mechanism, but by analogy with younger units it seems likely that the rocks are turbidites. Toward the end of this unit 4 sedimentation minor magmatic activity (amphibolite dykes and greenstones) appeared whose chemistry suggests that rifting was involved. Indirect evidence suggests that the time of rifting was in the Arenig, and hence that most of the unit 4 sedimentation was older than this, possibly extending through the whole of the Cambrian, although there is no conclusive evidence.

We deduce the emplacement of the ultramafic slabs to have occurred in Llanvirn-Llandeilo time. The character of the slabs, containing abundant porphyry dykes and stocks, as well as gabbro and diorite bodies, suggests that they were not derived from normal ocean floor. Since small remnants of ultramafic rocks are also found with the volcanic rocks of unit 2, it seems reasonable to suppose that the volcanic and ultramafic rocks were emplaced as a package, presumably by obduction. We emphasize that this event cannot have resulted from a continental collision in the ordinary sense, since sedimentation continued after obduction, and compressive deformation did not begin for some millions of years. Further, prior to obduction the volcanic rocks must have been remote from the Carmanville area, since there was no volcanic component in the sediment. The mechanism of emplacement of the allochthonous rocks remains somewhat obscure. Brookfield (1977) pointed out that major obduction seems to be commonly associated with large scale transcurrent faulting, rather than ordinary subduction. The model of Christensen and Salisbury (1975), whereby an active magmatic zone is partially subducted and partially obducted due to buoyancy of the molten material, seems particularly applicable. Since the subsequent history indicates that emplacement was not primarily due to transport by or toward a subduction zone, we assume that transcurrent faults brought an active volcanic zone into juxtaposition with the toe of the continental slope, resulting in the overriding of a heat source. Both Brookfield (1977) and Christensen and Salisbury (1975) remark that the age of obducted volcanics is generally very close to the age of obduction. Unit 2 may be in large part younger than unit 4.

Following obduction of the ultramafic slabs, sedimentary deposition with a distinctly continental source again resumed and was apparently uninterrupted except for the influx of volcanogenic sediment. However, the emplacement of intermediate to acid dykes in the sedimentary rocks commenced almost immediately, presumably due to the presence of a major heat source below them. The eastward progression of this heat source may mark the trace of the overridden volcanic source. Compressive deformation, presumably associated with commencement of continental collision, began in latest Ordovician or Silurian time but did not reach termination until the Devonian, by which time the heat source had moved another 25 km eastward, gradually

heating more and more of the superincumbent rocks as its rate of advance slowed, so that the isotherms could rise upward.

The net effect of deformation in the Carmanville area was to stack the rocks in a generally west-facing sequence, with steepened dip. Only in local enclaves did complex deformation occur. This type of response to deformation presumably resulted from the mechanical properties of the sedimentary pile, which had been significantly altered by emplacement of igneous dykes.

The model here proposed is clearly incompatible with the geophysical model recently proposed by Haworth et al. (1978) who propose that a Paleozoic subduction zone dipped beneath the Carmanville region at a very shallow angle (less than 10°). No geological evidence for such a zone has ever been discovered and the total absence of volcanic rocks of Ordovician or later age east of the Carmanville seems very difficult to explain. Their model further would require a very thin crust for eastern Newfoundland (the thickness above the ultramafic layer) which is not observed. On our model the volcanic arcs of Notre Dame Bay (Strong, 1976) must all be associated with the western side of the Iapetus Ocean. If the "suture" line of McKerrow and Cocks (1977) is accepted the gross structural trends suggest that suture zone obliquely transected and presumably consumed these volcanic arcs, in accordance with the model previously stated.

References

Bergström, S.M., Riva, J., and Kay, M.
1974: Significance of conodonts, graptolites and shelly faunas from the Ordovician of western and north central Newfoundland; Canadian Journal of Earth Sciences, v. 11, p. 1625-1660.

Blackwood, R.F.
1978: Northeastern Gander zone, Newfoundland; Mineral Development Division, Newfoundland Department of Mines and Energy, Report of Activities for 1977, p. 72-79.

Brookfield, M.E.
1977: The emplacement of giant ophiolite nappes; 1. Mesozoic-Cenozoic examples; Tectonophysics, v. 37, p. 247-303.

Brückner, W.D.
1978: Carmanville map-area, Newfoundland; the north-eastern end of the Appalachians – Discussion; in Current Research, Part C, Geological Survey of Canada, Paper 78-1C, p. 127-129.

Christenson, N.I. and Salisbury, M.H.
1975: Structure and constitution of the lower oceanic crust; Reviews of Geophysics and Space Physics, v. 13, p. 57-86.

Haworth, R.T., Lefort, J.-P., and Miller, H.
1978: Geophysical evidence for an east-dipping subduction zone beneath Newfoundland; Geology, v. 6, p. 522-527.

Jenness, S.E.
1963: Terra Nova and Bonavista map-areas, Newfoundland; Geological Survey of Canada, Memoir 327.

Kennedy, M.J.
1975: Repetitive orogeny in the northwestern Appalachians – new plate models based on Newfoundland examples; Tectonophysics, v. 28, p. 39-87.

Kennedy, M.J. and McGonigal, M.H.
1972: The Gander Lake and Davidsville Groups of northeastern Newfoundland, new data and geotectonic implications; Canadian Journal of Earth Sciences, v. 9, p. 453-459.

McKerrow, W.S. and Cocks, L.R.M.
1977: The location of the Iapetus Ocean suture in Newfoundland; Canadian Journal of Earth Sciences, v. 14, p. 488-495.

Pajari, G.E., Jr. and Currie, K.L.
1978: The Gander Lake and Davidsville Groups of northeastern Newfoundland – a re-examination; Canadian Journal of Earth Sciences, v. 15, p. 708-715.

Pajari, G.E., Jr., Pickerill, R.K., and Currie, K.L.
The nature, origin and significance of the Carmanville ophiolitic mélange; Canadian Journal of Earth Sciences. (in press)

Pickerill, R.K., Pajari, G.E., Jr., Currie, K.L., and Berger, A.R.
1978a: Carmanville map-area, Newfoundland; the north-eastern end of the Appalachians; in Current Research, Part A, Geological Survey of Canada, Paper 78-1A, p. 209-216.

1978b: Carmanville map-area, Newfoundland; the northeastern end of the Appalachians – Reply; in Current Research, Part C, Geological Survey of Canada, Paper 78-1C, p. 129-132.

Williams, H.
1964: Botwood, Newfoundland; Geological Survey of Canada, Map 60-1963.

1972: Stratigraphy of Botwood map area, northeastern Newfoundland; Geological Survey of Canada, Open File 113.

1978: Tectonic lithofacies map of the Appalachian orogen; Memorial University of Newfoundland Map No. 1, St. John's, Newfoundland.

15.

PETROLOGIC STUDIES OF SAPPHIRINE-BEARING GRANULITES AROUND WILSON LAKE, LABRADOR

Project 680071

J. Gittins[1] and K.L. Currie
Regional and Economic Geology Division

Gittins, J., and Currie, K.L., Petrologic studies of sapphirine-bearing granulites around Wilson Lake, Labrador; in Current Research, Part A, Geol. Surv. Can., Paper 79-1A. p. 77-82, 1979.

Abstract

Sapphirine occurs sparsely disseminated in ancient gabbroic gneisses of granulite grade, but is more abundant in younger mafic gneisses and oxide-rich gneisses which have been altered and retrogressively metamorphosed. Sapphirine consistently coexists with hypersthene and sillimanite, and locally with quartz and cordierite. Kyanite developed after formation of sapphirine. The sapphirine-bearing rocks exhibit a complex polyphase metamorphic and structural history. Petrographic observations show that this history included significant alteration and/or metasomatism as well as several periods of deformation and metamorphism. Comparison with experimental data suggests that much of the sapphirine equilibrated at about 6 kb, 710°C, which was below the peak metamorphic conditions. Regional correlation suggests that ancient gneisses correlative to those at Wilson Lake underlie a large region of south central Labrador.

Introduction

A variety of sapphirine-bearing assemblages occur in gneisses near Wilson Lake (NTS 13E/7) (Morse and Talley, 1971; Leong and Moore, 1972; Bourne, 1978), together with assemblages typical of granulite facies metamorphism (orthopyroxene-alkali feldspar). Similar assemblages occur 50 km to the northeast (Emslie et al., 1978), suggesting that a very large area has been subjected to high grade metamorphism. The exact nature of the metamorphic conditions remains uncertain because the geological history, structure and composition of the relevent units are virtually unknown. We have therefore mapped in detail about 350 km^2 surrounding Wilson Lake in an attempt to unravel the complexity of the gneisses. These data bear on the structural development and metamorphic history of central Labrador.

General Geology

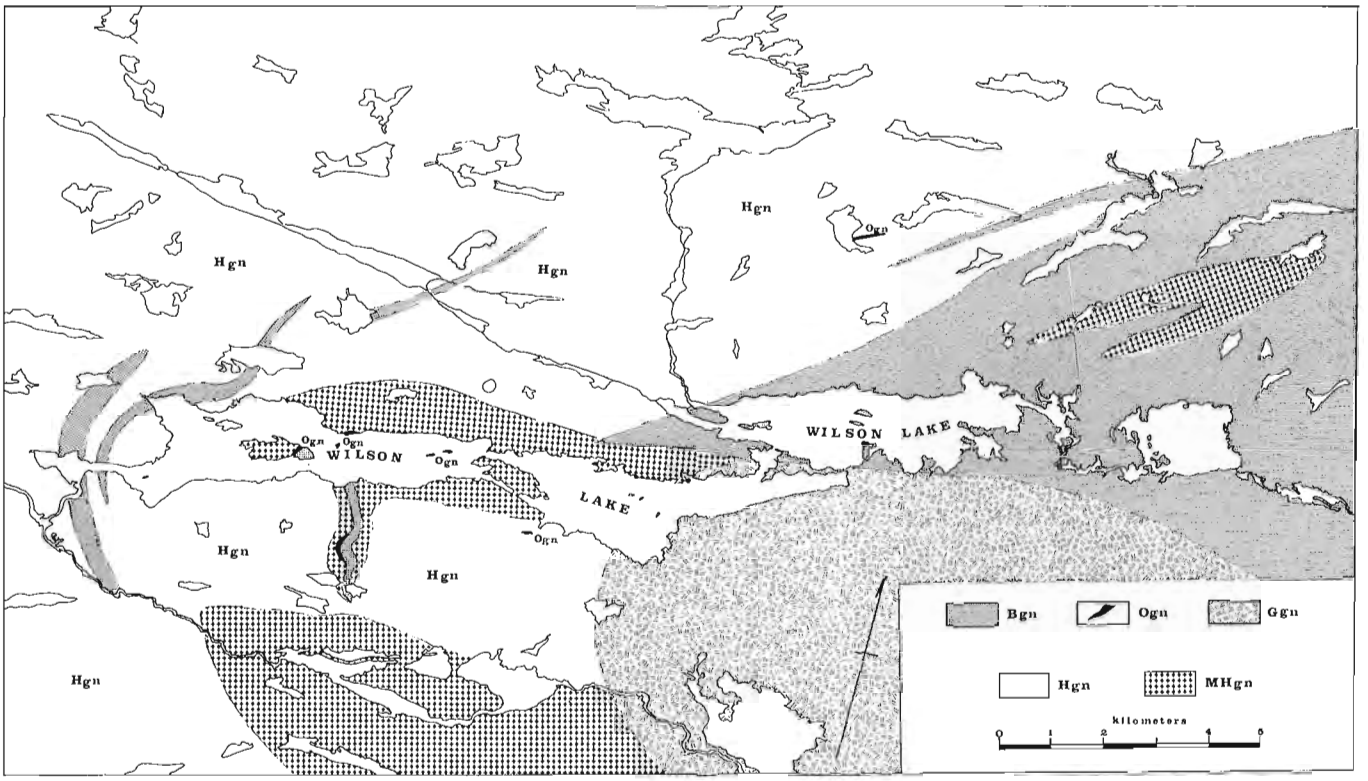
We find it convenient to divide the rocks of the Wilson Lake area into five lithologic units as shown in Figure 15.1. These grade into, and interdigitate with one another so that classification is in some cases arbitrary. The most widespread and oldest unit we term hypersthene gneiss (map unit Hgn). In hand specimen it appears identical to the Hope gneiss of Emslie et al. (1978), but contains much less quartz. High grade gneisses containing hypersthene + sillimanite and locally sapphirine, extend from the Ptarmigan complex (Emslie et al., 1978), at least 100 km to the southwest, and may extend a further 100 km to the vicinity of Churchill Falls. In outcrop the gneiss appears homogeneous and evenly banded on a scale of 2-10 mm. Outcrop colour varies from pale cream through various shades of buff or brown. The hypersthene gneiss characteristically displays fine grained layers of steely blue hue. These thin layers give a strong gneissosity to the rock, but felsic layers are also distinctly gneissic due to alignment and partial segregation of contained mafics. The composition of the felsic layers varies from essentially massive aplitic granitoid material (possibly derived from unit Ggn) through gneissic granodiorite to essentially quartz-free mafic granulite and anorthosite. These variations may occur within a few centimetres, and we were unable to consistently map compositional variation within the hypersthene gneiss. The overall composition of the complex approaches gabbroic, or anorthositic-gabbroic. In its most typical development the gneiss contains few veins, dykes or boudins, and even major composition changes are detected with difficulty on outcrop surface, particularly since the rock is hard and massive with few loose blocks or broken surfaces.

Preliminary petrographic examination suggests that the original mineral assemblage in the hypersthene gneiss was orthoclase perthite-antiperthitic andesine-orthopyroxene-quartz in the more felsic parts, and plagioclase-orthopyroxene-clinopyroxene in the more mafic parts. Accessory zircon, sphene, apatite and opaque are consistently present. Felsic minerals form a mosaic which locally shows strain and/or mortar texture. Plagioclase composition falls between An_{40}-An_{45} according to optical and electron probe determinations, regardless of bulk composition. The mafic layers consist mainly of orthopyroxene and opaque oxides (titaniferous hematite and magnetite) with lesser amounts of biotite, sillimanite, and rare sapphirine. All of these minerals except sapphirine occur disseminated in the salic bands. Petrographic evidence suggests that all except orthopyroxene developed subsequent to the original assemblage. Where later phases are abundant, we map the rock as modified hypersthene gneiss (MHgn).

In Table 15.1 are three chemical analyses of Hope gneiss. This sample shows the essentially gabbroic nature of the complex, although field observations suggest that a significant granitoid component was added prior to metamorphism. Despite the persistent presence of sillimanite, the bulk compositions are not aluminous, and none of the analyses suggests a sedimentary origin.

Various forms of alteration, retrogression and mobilization commonly occur within the hypersthene gneiss. Fine grained lustrous black biotite occurs along the edges of the mafic layers in many parts of the hypersthene gneiss. Honey brown prisms of sillimanite occur in radiating sprays within the mafic bands over a very large area. The style of development of these minerals leaves little doubt that they developed subsequent to the original assemblage, post-tectonically in the case of some sillimanite, but the character of the gneiss is not essentially modified by their appearance. Appearance of other minerals is accompanied by major changes in the character of the gneiss, which we map as modified hypersthene gneiss (map unit MHgn). This unit can readily be recognized by the development of a pale blue or greyish colour, presence of large numbers of granitic and basic dykes, and development of large amounts of hornblende, biotite and (locally) garnet. In many cases the development

[1] Department of Geology, University of Toronto, Toronto, Ontario. M5S 1A1
E.M.R. Research Agreement 2239-4-217/78.



Hgn - *hypersthene gneiss, strongly gneissic gabbro, diorite and anorthosite with lesser granitoid component, characterized by assemblage antiperthitic andesine-hypersthene-magnetite with rare sillimanite, biotite and sapphirine*

MHgn - *modified hypersthene gneiss; contorted with development of retrograde biotite and amphibole at the expense of pyroxene, abundant mafic and granitic dykes*

Bgn - *Basic gneiss, mainly hypersthene-diopside granulite of gabbroic composition with numerous zones retrogressed to biotite-hornblende gneiss and talc-actinolite schist*

Ogn - *oxide-rich gneiss, carrying zones of massive to dendritic and disseminated titaniferous hematite and magnetite, with interstitial sapphirine, cordierite, sillimanite and hypersthene*

Ggn - *Wilson Lake complex, gneissic biotite quartz monzonite, megacrystic quartz monzonite, lit-par-lit gneiss, migmatite*

Figure 15.1. *Geological map of the Wilson Lake area, Labrador*

of small folding is sufficiently intense that the overall trend of gneissosity is completely obscured. Massive or faintly foliated granitoid rocks commonly form thin shells about large mafic boudins in the rock, but may also occur as short dykes up to one metre in width, which cut all older units. In some cases these dykes may be referable to the Wilson Lake complex (map unit Ggn) but most appear to be of local derivation since they begin and end in transition zones. The amounts of biotite and hornblende increase with degree of anatexis, clearly replacing older ortho- and clinopyroxene. The most modified rocks approach quartz-feldspar-biotite-hornblende gneiss, commonly with garnet. In many cases relict mafic bands contain pyroxenes mantled by fine grained mixtures of biotite and hornblende. Many fine specimens of green sapphirine occur in such polymetamorphic zones.

Modified hypersthene gneisses occur along major fracture zones and near younger intrusions. The broad belt in the eastern part of Wilson Lake follows a major fracture system, and occurs near the younger intrusive rocks of the Wilson Lake complex. In the eastern part of this zone the rocks consist of lit-par-lit gneisses and migmatite, with biotite schist alternating with pegmatite on a scale of 2-5 cm. Field relations strongly imply that hypersthene gneiss must have undergone partial melting. The intensely folded character of the modified gneiss suggests a plastic condition for the whole unit. Late fracture surfaces cutting folded migmatite rarely exhibit rosettes of kyanite.

Chemical analyses of modified hypersthene gneiss (Table 15.1) suggest that its chemical composition is essentially identical to hypersthene gneiss except for water content. The differing mineralogies must therefore result from differing conditions of metamorphism. Field and petrographic relations clearly show that the onset of anatexis was accompanied by development of sapphirine, and followed by development of kyanite. Since these developments were clearly associated with introduction of water and structural dislocation, they can be termed retrogressive metamorphism of the earlier granulites.

Mafic gneiss (map unit Bgn) occurs around Wilson Lake in several different settings. Small mafic boudins up to several metres in length occur in the hypersthene gneiss. Such boudins are commonly rich in biotite and less gneissic than their host. Larger, mappable bodies of mafic rocks up to several kilometres in length occur in several places. Such bodies commonly exhibit haloes of more or less massive granite. Their map pattern and structural character clearly suggest that they are giant boudins. Rocks within a single boudin may vary irregularly from massive two-pyroxene mafic granulite through pyroxene amphibolite to hornblendite or mafic biotite schist. Mafic rocks consistently show less gneissosity than the surrounding gneiss, and in many cases are virtually massive.

Table 15.1

Chemical composition of some granulites from Wilson Lake

	1	2	3	4	5	6	7
SiO_2	50.11	50.55	55.60	48.50	56.00	47.35	66.90
TiO_2	0.73	1.31	3.37	0.69	3.02	1.02	0.63
Al_2O_3	17.09	12.25	13.10	17.53	14.73	13.45	16.20
Fe_2O_3	3.52	1.65	2.40	3.10	2.83	1.85	3.20
FeO	6.60	7.78	3.82	6.31	4.41	8.10	0.82
MnO	0.23	0.18	0.07	0.19	0.10	0.18	0.09
MgO	7.91	12.85	2.96	7.50	2.31	14.00	0.74
CaO	9.83	8.32	7.92	9.14	5.54	9.87	3.13
Na_2O	2.28	1.65	3.05	2.25	3.90	0.70	4.96
K_2O	0.73	1.60	2.98	0.86	3.17	1.12	1.16
H_2O	0.28	0.92	0.42	2.19	1.19	1.31	1.64
CO_2	0.51	0.48	0.07	1.22	0.00	0.38	0.06
P_2O_5	0.13	0.46	3.29	0.12	2.52	0.13	0.09
Ba	0.018	0.062	0.262	0.024	0.239	0.018	0.044
Co	0.003	0.003	0.001	0.003	0.002	0.005	0.000
Cr	0.011	0.092	0.012	0.010	0.004	0.107	0.000
Ni	0.011	0.038	0.009	0.009	0.006	0.051	0.000
Cu	0.013	0.001	0.027	0.005	0.014	0.031	0.001
Sr	0.020	0.045	0.198	0.000	0.155	0.014	0.061
V	0.018	0.024	0.018	0.016	0.017	0.024	0.053
Zr	0.005	0.011	0.157	0.005	0.129	0.005	0.038
Total	100.05	100.28	99.73	99.67	100.29	99.72	99.82

1-3. Hypersthene gneiss (orthopyroxene-plagioclase ± clinopyroxene ± sillimanite ± opaque) Hills north of east half of Wilson Lake.

4. Mafic two-pyroxene granulite, partly retrograded to biotite + hornblende. Narrows of Wilson Lake.

5. Intermediate sapphirine-hypersthene-sillimanite granulite. Large peninsula in west half of Wilson Lake.

6. Mafic sapphirine-hypersthene-sillimanite-cordierite granulite. Same locality as 5.

7. Gneissic biotite quartz monzonite. Wilson Lake complex, southeast corner of lake. Analyses by G.S.C. Rapid Methods.

Field relations of the mafic bodies suggest that they represent remnants of dykes intruded into the hypersthene gneiss, presumably at various times, since their structural relations vary considerably. The composition of the mafic rocks (Table 15.1) resembles mafic parts of the hypersthene gneiss. Preliminary petrographic examination suggests that the primary mineral assemblage in the mafic rocks was plagioclase-orthopyroxene-clinopyroxene with accessory sphene and apatite. This assemblage is commonly overprinted by amphibole+biotite which almost universally partly replaces both pyroxenes. Garnet is developed only in vein-like masses, or in narrow marginal zones around younger granite intrusions. Within the modified gneiss lower-grade assemblages are found in the mafic boudins, including talc-actinolite. The large mafic belt at the east end of Wilson Lake resembles the Beaver gneiss of Emslie et al. (1978), but in this case the mafic rocks clearly intrude the hypersthene gneiss, remnant screens of which are found within the mafic gneiss. This belt contains a variety of apparently primary mineral assemblages, including some containing garnet.

Perhaps the most distinctive unit in the Wilson Lake area is the oxide-rich gneiss (map unit Ogn) found in a linear belt down the centre of the lake, in a belt north of the east part of the lake, and as isolated patches in other localities. This unit contains a complex assemblage of iron oxides as disseminated grains, dendritic segregations, lenticles, and large dyke-like masses up to 10 m across. Preliminary petrographic and electron probe examination suggests a complex oxide assemblage dominated by titaniferous hematite and magnetite (Table 15.2). The country rocks may be either modified gneiss (MHgn) or mafic gneiss (Bgn), but the latter is more common. Oxide-rich zones cut the gneissosity and include boudins and ptygmatically folded fragments of the gneisses. The oxide veins are themselves complexly folded, and quartz veins which cross them have been doubly folded. Quartz veins occur commonly in the region of the oxide-rich gneisses, and in many cases exhibit a well developed tectonic foliation which causes them to superficially resemble quartzite. The oxide veins contain from 0-40 per cent of silicate minerals, including various combinations of orthopyroxene, sillimanite, biotite, sapphirine and cordierite. Sapphirine occurs disseminated in gneiss surrounding the oxide layers. Sapphirine in and around the oxide-rich rocks exhibits an unusual brownish green colour. The gneisses rich in oxides are cut by numerous reddened joints along which small amounts of dumortierite are developed.

The youngest rocks in the Wilson Lake area lie in a dome-like mass of granitic gneiss and migmatite at the east end of Wilson Lake (map unit Ggn). We propose the name Wilson Lake complex for this unit. In the central part of the dome fine grained, homogeneous, white quartz-feldspar-biotite gneiss outcrops. The periphery of the dome displays spectacular quartz monzonite with augen or megacrysts of microcline perthite up to 5 cm in length. Some of these crystals display rapakivi texture. This rock grades into medium grained pink leucogranite, and into biotite pegmatites which form a component of the marginal lit-par-lit gneisses and migmatites. These marginal rocks appear to have developed by reconstitution of the gneiss, and all stages of the transformation are displayed. A chemical analysis of porphyritic quartz monzonite from the Wilson Lake complex (Table 15.1) shows that it differs greatly from the hypersthene gneiss and related rocks.

Structural Geology

An extended and complex structural history can be deduced from mafic dykes and from transposition of fabrics in the Wilson Lake area. In its least modified exposures the gneiss exhibits a flinty, cataclastic appearance expressed in thin section as a fine mosaic (blastomylonitic) texture. Much of the foliation is believed to be cataclastic in origin. The characteristic mafic layers occasionally show isoclinal small

folds with attenuated limbs. In a few favourable outcrops the gneiss is very regularly and evenly small-folded on an amplitude of 10-20 cm. The noses of these folds are invariably obscured by a younger gneissosity developed parallel to axial plane cleavage. Comparison of regional trends of gneissosity with these axial plane cleavages strongly suggests that the regional trend has developed by transposition of an earlier gneissosity along axial plane cleavage. In order of decreasing age, these transposed fabrics trend 045, 110 and 070. These trends coincide with the trends of major fracture systems in the gneiss. Local transitions from jointing to close sheeting to gneissosity are common.

The mafic boudins within the gneiss rarely show strong gneissosity, except in relatively low-grade (retrograded) rocks. The gneissosity of the Hope gneiss around the boudins is commonly destroyed by development of near massive granite. We deduce that the mafic rocks were emplaced after gneissosity was well developed in the Hope gneiss.

The oxide zones exhibit a unique series of structures. The zones are commonly developed in or near a boudined mafic dyke, parts of which may be ptygmatically folded into the oxides. The oxides clearly cut all older gneissosities, but are themselves folded and cut by axial plane cleavage. The oxide layers and their enclosing rocks have been invaded by a swarm of quartz veins, many of which exhibit spectacular double folding about two nearly coaxial northwest-trending axes. The main oxide zone along Wilson Lake occupies the axial zone of a major fold in the gneissosity of the Hope gneiss which trends 290°, plunges 50° and has an axial plane dipping about 65° to the south. Many small folds of similar attitude can be observed along the lake, particularly on the south side.

The youngest structures observed in this region occur around the Wilson Lake complex where gneissosity concentric to the dome overprints and transposes gneissosity in the Hope gneiss. This gneissosity exhibits recumbent folds trending parallel to the dome, and verging away from it.

On the basis of these observations, we deduce that the Hope gneiss had been deformed at least three times and metamorphosed at least once prior to emplacement of the mafic rocks. Each period of deformation is now witnessed by a gneissosity which originally developed parallel to an axial plane cleavage. The metamorphic event transformed the rocks into pyroxene granulites. After emplacement of the mafic dykes, the rocks were again deformed, probably along pre-existing zones of weakness, to produce the boudinage and faint gneissosity of the mafic dykes. A further period of metamorphism converted the mafic rocks to amphibolite grade or to granulite grade metamorphic assemblages prior to formation of the oxide-rich rocks. The latter are doubly folded, and involved in deformation associated with emplacement of the Wilson Lake complex. Further, the oxide-rich zones exhibit metamorphism resulting in formation of sapphirine. The latter event could conceivably be associated with high-grade metamorphism and anatexis associated with formation of the Wilson Lake complex. However even making this assumption, the development of the rocks requires at least four distinct periods of deformation (deformation of the Wilson Lake complex, deformation of the oxide-rich rocks, deformation of the mafic dykes, and deformation of the Hope gneiss), and three periods of metamorphism. Such an extended and complex history suggests that the Hope gneiss must be very old.

Metamorphic Geology

The foregoing considerations suggest that the metamorphic history of the Wilson Lake area in general, and of the Hope gneiss in particular, must be complex. In this preliminary account we shall not attempt to unravel this history in detail, but concentrate on the genesis of sapphirine and accompanying assemblages, a topic which has led to controversy in the past (Morse and Talley, 1971; Leong and Moore, 1972). We emphasize several observations. Sapphirine occurs within generally gabbroic or anorthositic rocks, not pelitic rocks. The mineral occurs predominantly within certain zones which result from deformation and

Table 15.2

Electron microprobe analyses of minerals from Wilson Lake granulites

	1	2	3	4	5	6	7	8	9	10
SiO_2	57.64	52.60	44.67	37.73	0.72	14.45	57.65	50.16	51.46	0.59
TiO_2	nd	nd	0.80	5.02	nd	nd	nd	nd	nd	9.65
Al_2O_3	26.79	1.66	11.27	15.66	0.59	58.44	26.84	8.51	33.69	0.43
Cr_2O_3	nd	nd	0.23	0.21	3.23	0.20	nd	nd	nd	0.21
FeO*	0.27	23.35	13.73	13.66	88.43	9.10	nd	15.38	2.26	80.07
MnO	nd	1.49	0.24	nd	nd	0.45	nd	1.28	0.22	0.06
MgO	nd	20.98	12.42	15.01	nd	17.47	nd	25.19	11.89	0.30
CaO	8.64	0.41	11.54	nd	nd	0.03	8.88	0.03	nd	nd
Na_2O	6.37	nd	0.65	nd	nd	nd	6.18	nd	nd	nd
K_2O	0.18	nd	0.86	9.44	nd	nd	0.27	nd	nd	nd
Total	99.89	100.49	96.41	96.73	92.97	100.14	99.82	100.55	99.52	91.31

* Total Fe reported as FeO, nd - not detected. Analyst: J. Gittins

Analyses 1-5 on specimen P9-076 of modified hypersthene gneiss. All analyses quoted are the average of two or more spot analyses. The minerals analyzed are 1-plagioclase, 2–orthopyroxene, 3-amphibole, 4-mica, 5-magnetite.

Analyses 6-10 on specimen P9-083 of sapphirine granulite. Analyses quoted are the average of two or more spot analyses. The minerals analyzed are 6-sapphirine, 7-plagioclase, 8- orthopyroxene, 9-cordierite, 10-Ti-rich hematite.

hydration of two pyroxene granulites. Sapphirine coexists in textural equilibrium with sillimanite and hypersthene very commonly, and less commonly in equilibrium with cordierite, with feldspar and with quartz. Kyanite developed as a late metamorphic, post-sapphirine phase.

Consideration of the chemistry and mineralogy of the sapphirine-bearing assemblages suggests that the alumina incorporated into sapphirine and sillimanite must have derived originally from plagioclase. Since no other calcium-bearing phase coexists with plagioclase, the extraction of alumina must also have involved removal of calcium. The available evidence does not clearly distinguish between possible alteration and/or weathering along fractures at low temperatures, and metasomatic alteration at elevated temperatures. The occurrence of apparently post-kinematic sillimanite and kyanite crystals suggests that liberation of alumina continued throughout metamorphism and thus favours the second hypothesis. However the common occurrence of sillimanite and sapphirine in fracture zones is compatible with the first hypothesis. We believe that more detailed petrographic work and a better understanding of the metamorphic history of the rocks may resolve this ambiguity.

The pressure-temperature conditions of metamorphism for the assemblage cordierite-sapphirine-hypersthene-sillimanite-quartz can be deduced from the data of Newton et al. (1974) who calculated that the invariant point involving these phases lay at 840° C, 6.75 kb for the natural magnesian end members. The position of the invariant points is defined by the intersection of the reactions

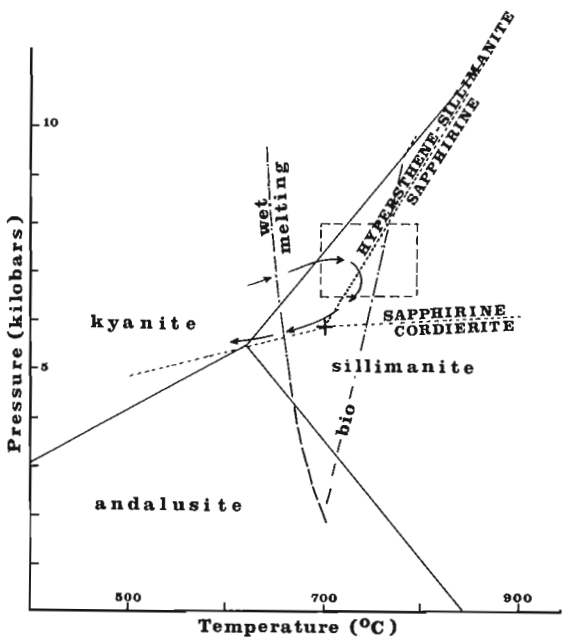


Figure 15.2. *Conditions of metamorphism for sapphirine granulites. Aluminosilicate phase boundaries after Richardson et al. (1968). Rectangle surrounded by broken line marks field of granulite facies metamorphism after Touret (1970). Dash-dot line shows beginning of melting for andesine-bearing rocks with excess water. Dash-dot line marked "bio" shows beginning of melting for dry granitoid rocks containing biotite. Calculated conditions of metamorphism for sapphirine-cordierite-absent assemblages lie along the dotted line extending upward to the right from the cross. The path marked by arrows would produce the observed mineral assemblages, subject to availability of water.*

$$9\ Mg_2Al_4Si_5O_{18} = 2\ Mg_7Al_{18}Si_3O_{40} + 4\ MgSiO_3 + 35\ SiO_2$$

and

$$7\ MgSiO_3 + 9\ Al_2SiO_5 = Mg_7Al_{18}Si_3O_{40} + 13\ SiO_2$$

where the formula for natural sapphirine is that of Newton et al. (1974). Assuming the volume change for these reactions to be invariant with pressure and temperature, and utilizing the data tabulated by Newton et al. (1974), the volume change for the first reaction is -9.261 cal/bar, and for the second -0.541 cal/bar. A thermodynamic condition for equilibrium can be written in the form

$$\Delta G = \Delta H° - \Delta T\, S° + (P-1)\Delta V + RT\sum \ln a_i^{m_i} = 0$$

where ΔG is the change in free energy on reaction, $\Delta H°$ the change in standard enthalpy on reaction, $\Delta S°$ the change in standard entropy on reaction a_i the activity of component i, and m_i the number of mols of i taking part in the reaction. ΔV is the volume change on reaction, here assumed known. For the pure phases considered by Newton et al. (1974) the a_i are all 1.0. Newton et al. (1974) show the equilibrium curves as straight lines, implying $\Delta H°$, $\Delta S°$ and ΔV are constants. Fitting the experimentally determined straight lines to the form $aT+bP+c=0$, and adjusting b to the value V therefore gives an estimate for $\Delta H°$ and $\Delta S°$. Assuming that sapphirine, enstatite and cordierite exhibit ideal ionic solutions among Fe and Mg therefore leads to the equations

$$43101+18.522T-9.261P+RT(4 \ln x_{en}^{mg} + 14 \ln x_{sa}^{mg} - 18 \ln x_{co}^{mg}) = 0$$

$$-15076+17.036T-0.541P+RT(7 \ln x_{en}^{mg} - 7 \ln x_{co}^{mg}) = 0$$

where x_j^i is the mol fraction of component i in phase j. Substituting the observed values (listed in Table 15.2) for sapphirine (sa) enstatite (en) and cordierite (co) gives the following equations

$$43101+12.301T-9.261P = 0$$

$$-15076+18.625T-0.541P = 0$$

These curves intersect at 710°C (983°A) and 6 kilobars[1] Subject to assumptions previously noted, this is the best estimate of the pressure and temperature of metamorphism of the cordierite-sapphirine bearing assemblages. Assemblages lacking cordierite, but containing sapphirine+enstatite+sillimanite presumably equilibrated at somewhat higher pressure and temperature along the second curve.

Although these estimates are subject to a number of assumptions, they seem plausible, and in accord with other experimental and observational data. The conditions of metamorphism for the cordierite-absent assemblages falls in, or very near, the granulite facies field as defined by Touret (1970), while the cordierite-bearing assemblages fall in the uppermost part of amphibolite facies. The conditions are generally compatible with those assumed by Seifert (1974) and Chatterjee and Schreyer (1972) for sapphirine-bearing assemblages.

The deduced temperatures are high enough that anatexis would have taken place if sufficient water were present. We have presented evidence for local anatexis and general plasticity in the sapphirine-rich zones. At present we do not know whether the water was introduced during metamorphism, or after one metamorphism and before another. This earlier history, together with the later episodes of retrogressive metamorphism, remains to be elucidated. If the late kyanite developed subsequent to the sapphirine, slow cooling at high pressure is indicated for the sapphirine-bearing rocks. Figure 15.2 shows a highly speculative P-T path of metamorphism which could account for all the known sapphirine-bearing assemblages.

[1] 1 kb = 10^5kPa

Regional Geological Correlation

Pioneering geological mapping (Stevenson, 1969) showed that central Labrador southeast of the "Grenville front" consists of gneisses of various kinds from which recognizable sedimentary rocks are virtually absent. Brummer and Mann (1961) suggested that a major fault separated the Neohelikian Seal Lake Group from these gneisses, and this tentative fault has been identified by several compilers with the "Grenville front" (Wynne-Edwards, 1972). However more recent work (A. Thomas, pers. comm., 1978) suggests that the Letitia Lake Group straddles the fault, or more accurately the series of faults, which separates the Seal Lake Group from the gneisses. None of these faults appears to have a large individual displacement, although the overall displacement, a thrust from south to north, may be substantial. Similar relations have been found by Emslie et al. (1978) in the Red Wine Mountains. The Letitia Lake Group occupies a key position in unravelling the geological history, since it is known to be unconformably overlain by the Seal Lake Group (Brummer and Mann, 1961) and appears to overlie unconformably part of the gneiss complex (Currie et al., 1975). These latter authors found an Archean lead component in eudialyte from the Red Wine alkaline complex (intrusive into the Letitia Lake Group) which almost certainly derives from the gneisses. On the basis of helicopter reconnaissance across the gneisses from Wilson Lake northward to the "Grenville front" we believe that all the gneisses belong to the same (Archean?) unit, defined on the following criteria; (a) presence of blue-black, fine grained mafic layers, (b) presence of two or more generations of boudined mafic dykes which are less gneissic than the host, and locally exhibit near-massive granitoid rims, (c) local presence of the unusual assemblage plagioclase-hypersthene-sillimanite, (d) presence of complex, polyphase metamorphism and deformation. The apparent age, composition and structural style of this vast gneiss massif invites comparison with the Hopedale gneiss north of the "Grenville front". Since mapping has shown that the "Grenville front" in this region does not mark either a major thrust fault or an abrupt increase in metamorphic grade, the tectonic significance and history of the "front" remain obscure.

References

Bourne, J.H.
1978: Metamorphism in the eastern and southwestern portions of the Grenville Province; in Metamorphism of the Canadian Shield, J.A. Fraser and W.W. Heywood, Geological Survey of Canada, Paper 78-10, p. 315-328.

Brummer, J.M. and Mann, E.L.
1961: Geology of the Seal Lake area, Labrador; Geological Survey of America Bulletin, v. 72, p. 1361-1382.

Chatterjee, N.D. and Schreyer, W.
1972: The reaction enstatite+sillimanite=sapphirine+quartz in the system MgO-Al_2O_3-SiO_2; Contributions to Mineralogy and Petrology, v. 36, p. 49-62.

Currie, K.L., Curtis, L.W., and Gittins, J.
1975: Petrology of the Red Wine alkaline complexes, Labrador, and a comparison with the Ilimaussaq complex, southwest Greenland; in Report of Activities, Part A, Geological Survey of Canada, Paper 75-1A, p. 271-280.

Emslie, R.F., Hulbert, L.J., Brett, C.P., and Garson, D.F.
1978: Geology of the Red Wine Mountains Labrador; The Ptarmigan Complex; in Current Research, Part A, Geological Survey of Canada, Paper 78-1A, p. 129–134.

Leong, K.M. and Moore, J.M.
1972: Sapphirine-bearing rocks from Wilson Lake, Labrador; Canadian Mineralogist, v. 11, p. 777-790

Morse, S.A. and Talley, J.H.
1971: Sapphirine reactions in deep-seated granulites near Wilson Lake, central Labrador, Canada; Earth and Planetary Science Letters, v. 10, p. 325-328.

Newton, R.C., Charlu, T.V., and Kleppa, O.J.
1974: A calorimetric investigation of the stability of anhydrous magnesium cordierite with application to granulite facies metamorphism; Contributions to Mineralogy and Petrology, v. 44, p. 295-311.

Richardson, S.W., Gilbert, M.C., and Bell, P.M.
1968: Experimental determination of kyanite-andalusite and kyanite-sillimanite equilibria; the aluminum silicate triple point; American Journal of Science, v. 267, p. 259-272.

Seifert, F.
1974: Stability of sapphirine: a study of the aluminous part of the system MgO-Al_2O_3-SiO_2-H_2O; Journal of Geology, v. 82, p. 173-203.

Stevenson, I.M.
1969: Lac Brulé and Winokapau Lake map areas; Geological Survey of Canada, Paper 67-69.

Touret, M.J.
1970: Le faciès granulitique métamorphisme en milieu carbonique; Académie des Sciences (Paris) Comptes Rendus 271, p. 2228-2231.

Wynne-Edwards, H.R.
1972: The Grenville Province; in Variations in Tectonic Styles in Canada, editors R.A. Price and R.J.W. Douglas; Geological Association of Canada Special Paper 11, p. 263-334.

16. # A REACTION GRID FOR BIOTITE-BEARING MAFIC GRANULITES

Project 780011

E. Froese and L.S. Jen[1]
Regional and Economic Geology Division

Froese, E. and Jen, L.S., A reaction grid for biotite-bearing mafic granulites; in Current Research, Part A, Geol. Surv. Can., Paper 79-1A, p. 83-85, 1979.

Abstract

Treating the activity of water as a function of pressure and temperature, a reaction grid based essentially on two invariant points accounts for many assemblages in biotite-bearing mafic granulites and for several proposed orthopyroxene-producing reactions. In the presence of quartz, plagioclase of constant composition, magnetite, and ilmenite, the two invariant points are: cummingtonite-hornblende-almandine-clinopyroxene-orthopyroxene and biotite-hornblende-almandine-clinopyroxene-orthopyroxene-K feldspar.

The appearance of orthopyroxene in plagioclase-bearing rocks is taken as the boundary of the granulite facies or regional hypersthene zone (Winkler, 1976). In this paper some possible reactions giving rise to orthopyroxene in mafic rocks are considered. It is assumed that the activity of water is a smooth function of pressure and temperature. Thus reactions, which plot as surfaces in P-T-a_{H_2O} space, project as lines on the P-T plane and are regarded as univariant.

Only mineral reactions in the presence of quartz, plagioclase of constant composition, magnetite, and ilmenite are considered. Phase relations among the remaining minerals may then be represented in the system

$A = Al_2O_3 - (Na_2O + CaO + K_2O)$

$K = K_2O \cdot Al_2O_3$

$F = FeO - (Fe_2O_3 + TiO_2)$

$M = MgO$

Furthermore, in biotite-bearing assemblages, phase relations among these minerals may be shown on the biotite composition surface (Froese, 1978). Changes in mineral compatibilities brought about by each univariant reaction are seen on the biotite composition surface by a change in topology. Each P-T field bounded by specified reactions is characterized by a unique topology of the subdivision of the biotite composition surface. In K_2O-rich granulites (charnockites), the invariant point almandine-hornblende-clinopyroxene-orthopyroxene-biotite-K feldspar has been suggested by Jen (1975) and Mueller and Saxena (1977). However, some disagreement concerning the relative composition of the coexisting minerals is reflected in different proposed reactions. The reactions deduced by Jen (1975) are based on chemical analyses of five minerals from the same specimen. These compositions are consistent with the topology of a phase diagram suggested by Reinhardt and Skippen (1970).

In order to extend the reaction

hornblende + almandine + plagioclase + quartz $\leftrightharpoons$ orthopyroxene + clinopyroxene + H_2O

not involving K feldspar to lower temperatures, we have used in Figure 16.1 the mirror image of the reaction sequence given by Jen (1975). The incompatibility of cummingtonite and K feldspar suggests that this reaction terminates at an invariant point where cummingtonite becomes stable together with the other four minerals.

Figure 16.1 shows a proposed reaction grid incorporating the two invariant points. In addition to the reactions around the invariant points, two reactions involving anthophyllite are shown to allow the coexistence of cordierite and orthopyroxene at higher grade.

In plagioclase-bearing rocks, orthopyroxene is first stabilized by the univariant reactions:

cummingtonite + clinopyroxene + almandine + quartz $\leftrightharpoons$ orthopyroxene + plagioclase + H_2O

cummingtonite + hornblende + almandine + quartz $\leftrightharpoons$ orthopyroxene + plagioclase + H_2O

In many rocks, orthopyroxene participates in bivariant reactions, represented in Figure 16.1 by a three-phase assemblage. The following reactions have been suggested by de Waard (1965):

hornblende + almandine + quartz $\leftrightharpoons$ orthopyroxene + plagioclase + H_2O

orthopyroxene + plagioclase $\leftrightharpoons$ clinopyroxene + almandine + quartz

hornblende + quartz $\leftrightharpoons$ orthopyroxene + clinopyroxene + plagioclase + H_2O

biotite + quartz $\leftrightharpoons$ orthopyroxene + almandine + K feldspar + H_2O

biotite + hornblende + quartz $\leftrightharpoons$ orthopyroxene + plagioclase + K feldspar + H_2O

Carmichael (1974) deduced an additional reaction

hornblende + plagioclase + quartz $\leftrightharpoons$ clinopyroxene + almandine + H_2O

not involving orthopyroxene from the first three reactions of de Waard (1965). These four bivariant reactions, as well as a reaction not involving quartz, proposed by Buddington (1966),

hornblende + orthopyroxene + plagioclase $\leftrightharpoons$ almandine + clinopyroxene + H_2O

intersect in the univariant reaction

hornblende + almandine + plagioclase + quartz $\leftrightharpoons$ orthopyroxene + clinopyroxene + H_2O

Therefore, as pointed out by Carmichael (1974), all five reactions are mutually consistent.

[1]Mineral Policy Sector, Department of Energy, Mines and Resources, 580 Booth Street, Ontario.

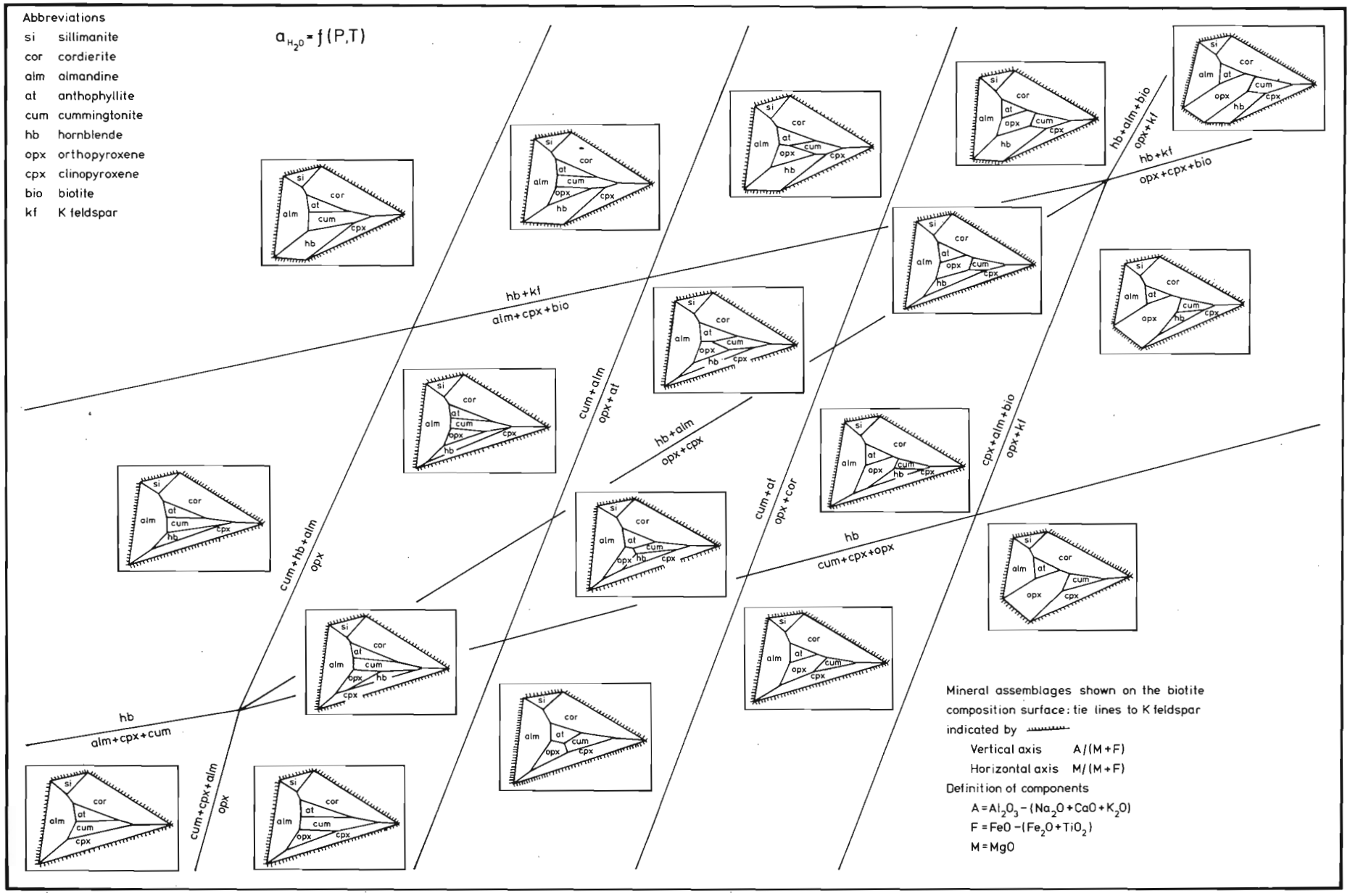


Figure 16.1. *Mineral reactions in biotite-bearing mafic granulites, in the presence of quartz, plagioclase of constant composition, magnetite, and ilmenite.*

References

Buddington, A.F.
1966: The occurrence of garnet in the granulite-facies terrane of the Adirondack Highlands, a discussion; Journal of Petrology, v. 7, p. 331-335.

Carmichael, D.M.
1974: Mineral equilibria in mafic granulites (abstract); Canadian Mineralogist, v. 12, p. 429-430.

de Waard, D.
1965: The occurrence of garnet in the granulite-facies terrane of the Adirondack Highlands; Journal of Petrology, v. 6, p. 165-191.

Froese, E.
1978: The graphical representation of mineral assemblages in biotite-bearing granulites; in Current Research, Part A, Geological Survey of Canada, Paper 78-1A, p. 323-325.

Jen, L.S.
1975: Spatial distribution of crystals and phase equilibria in charnockitic granulites from the Adirondack Mountains; Ph.D. thesis, University of Ottawa.

Mueller, R.F. and Saxena, S.K.
1977: Chemical petrology; Springer-Verlag, New York, 394 p.

Reinhardt, E.W. and Skippen, G.B.
1970: Petrochemical study of Grenville granulites; Geological Survey of Canada, Paper 70-1B, p. 48–54.

Winkler, H.G.F.
1976: Petrogenesis of metamorphic rocks, 4th ed.; Springer-Verlag, New York, 334 p.

17. REGIONAL GEOLOGICAL SYNTHESIS, CENTRAL SUPERIOR PROVINCE

Project 770070

K.D. Card
Regional and Economic Geology Division

Card, K.D., Regional geological synthesis, central Superior Province; in Current Research, Part A, Geol. Surv. Can., Paper 79-1A, p. 87-90, 1979.

Abstract

Reconnaissance field work, combined with existing geological data, permits preliminary subdivision of the rocks of the central Superior Province into several broad categories. Included are the greenstone belt metavolcanic-metasedimentary sequences and associated migmatite, gneiss of plutonic origin, paragneiss, and massive felsic plutons. Some tentative litho-tectonic subdivisions of the Wawa and Abitibi subprovinces and the Kapuskasing Structural Zone are presented.

Introduction

Reconnaissance field work was conducted during the past summer in parts of the Abitibi, Kapuskasing, Wawa, and Quetico subprovinces of the Superior Province (Stockwell, 1970) in the region bounded by 46°N to 49°30'N and 81°W to 86°W. Data were gathered along a number of sections or corridors, utilizing road and water access for the most part. Work was concentrated in areas shown on existing maps as predominantly granitic (Ayres et al., 1971) that have hitherto received little attention. One of the objectives of the present work is to subdivide these rocks, at least in a general way, into massive felsic plutons, gneiss, and migmatite, and, in addition, to establish the relationships between the various depositional, plutonic, metamorphic, and tectonic events that have affected this part of the Shield. The ultimate objectives of the project are to outline areas and problems requiring further study, to improve regional correlations of rock units and events, and to synthesize the geology of the central Superior Province.

Acknowledgments

The author was capably assisted by J.A. Percival, and also acknowledges assistance and information provided by S.B. Lumbers, Royal Ontario Museum; W.M. Schwerdtner, University of Toronto; D.G. Innes and R.P. Sage, Ontario Geological Survey; G.A. Pierce and R.M. Weeks, Geco Division, Noranda Mines Limited; and G. McVey and P.R. Coad, Texas Gulf Limited.

Major Rock Units

The distribution of major rock units, as determined from existing maps, with additional information from the summer's field work, is shown in Figure 17.1. The Archean rocks are subdivided into metavolcanic-metasedimentary supracrustal sequences of the greenstone belts, migmatitic rocks of metavolcanic and metasedimentary origin, gneissic rocks, mainly of plutonic derivation, but also including variable amounts of supracrustal rocks and massive felsic intrusive material, anorthositic and gabbroic intrusions, and massive felsic plutonic rocks. In general, the units are arranged in order of decreasing age, although this is not meant to imply that all of the rock units of a group are of a common age. Indeed, some of the gneissic units may be older than, and be basement to, some of the supracrustal sequences.

The metavolcanic-metasedimentary sequences of the greenstone belts comprise mainly mafic, intermediate and felsic flow and pyroclastic units interlayered with wacke, conglomerate, and chemical sediments, such as iron-formation. The rocks of the greenstone belts commonly show polyphase deformation and greenschist facies metamorphic mineral assemblages, although many of the smaller remnants are metamorphosed to amphibolite facies.

Migmatitic rocks derived by metamorphism, assimilation, migmatization, and granitization of the metavolcanic sequences typically occur at the margins or "terminations" of greenstone belts as contorted enclaves within the surrounding gneiss. Although lithologically and structurally complex, many of these migmatitic units can be traced long distances. Paragneiss and derived migmatite are present throughout the region, but are concentrated in the Quetico Subprovince and the Kapuskasing Structural Zone. They are typically monotonous sequences of immature clastic sediments metamorphosed to varieties of paragneiss and migmatite under amphibolite and granulite facies metamorphic conditions. The paragneiss units are isoclinally folded and pervasively invaded by granitic intrusions, many of which are anatectic in origin.

Granodiorite, tonalite, and trondhjemite gneissic rocks, mainly of plutonic origin, are present throughout the region. The structure of the gneissic terranes consists of elongate and oval domes, some of which represent diapirs (Schwerdtner et al., 1978). The gneissic terranes are probably the most lithologically heterogeneous and structurally complex parts of the region. They contain variable amounts of supracrustal rocks in the form of migmatites, xenoliths, and enclaves, as well as a variety of intrusions of several ages.

Massive to foliated felsic plutonic rocks occur within both the greenstone belts and gneissic terranes as batholithic complexes, plutons, dykes, and sills. They are mainly of granitic and granodioritic composition, although trondhjemite, quartz diorite, tonalite, and syenitic intrusions are also present. Many bodies have massive interiors and foliated margins. They cut the host rock foliation and commonly enclose trains of oriented country rock inclusions.

Litho-Tectonic Subdivisions

Some tentative subdivisions, herein termed domains, of the Wawa and Abitibi subprovinces and the Kapuskasing Structural Zone are shown in Figure 17.2. At the present state of knowledge, the geological significance, if any, and the location and nature of the boundaries of these subdivisions cannot be exactly stated. Rather, the subdivisions represent an attempt to group terranes of similar lithologic makeup and structural style for descriptive purposes. Each domain, although comprising a variety of rock types and structures of various ages, is characterized by a dominant rock type or association of rock types, and a dominant structural style. The metavolcanic domains include the greenstone belts and their migmatitic continuations with massive felsic plutons and subordinate gneiss. The

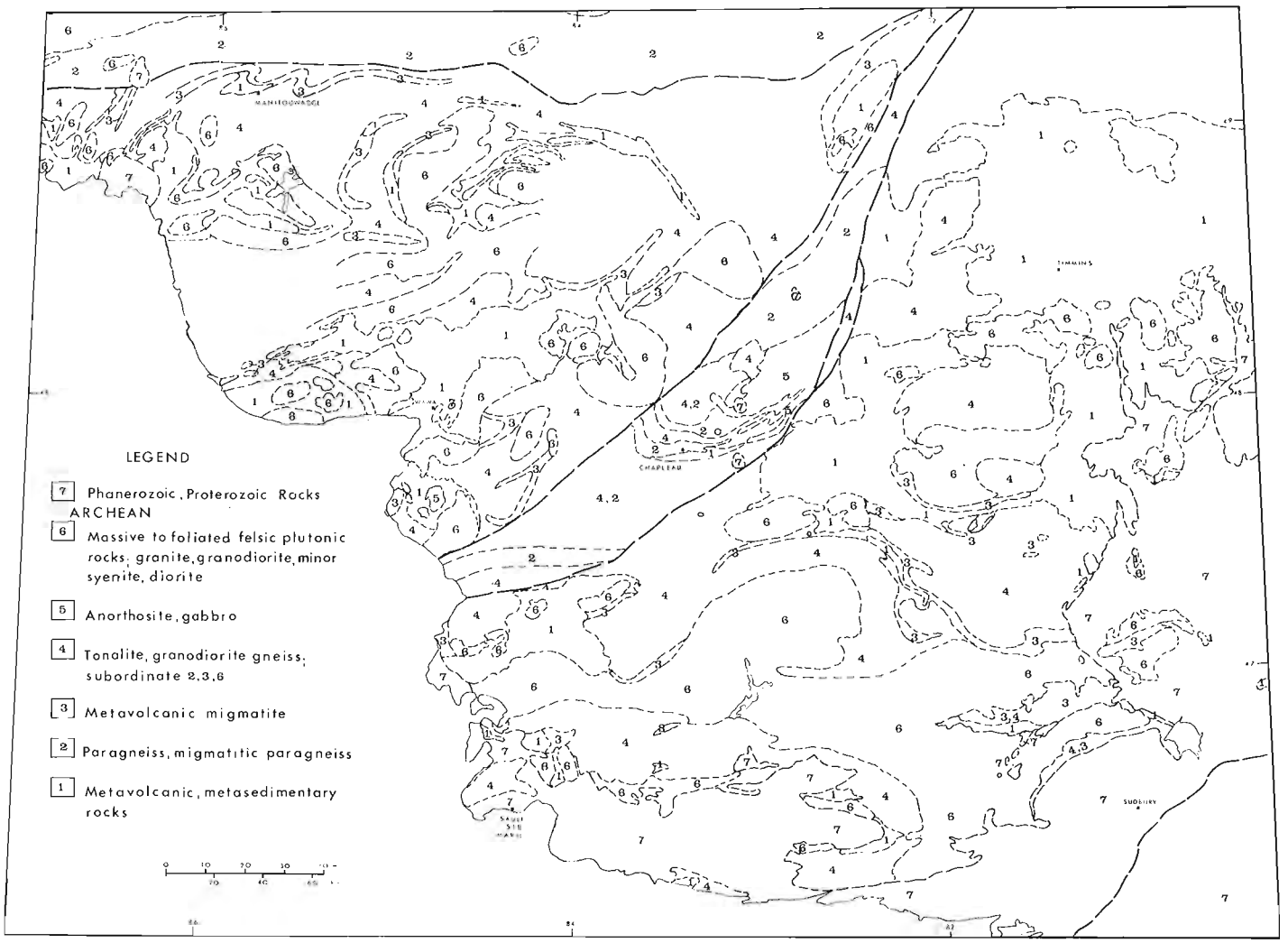
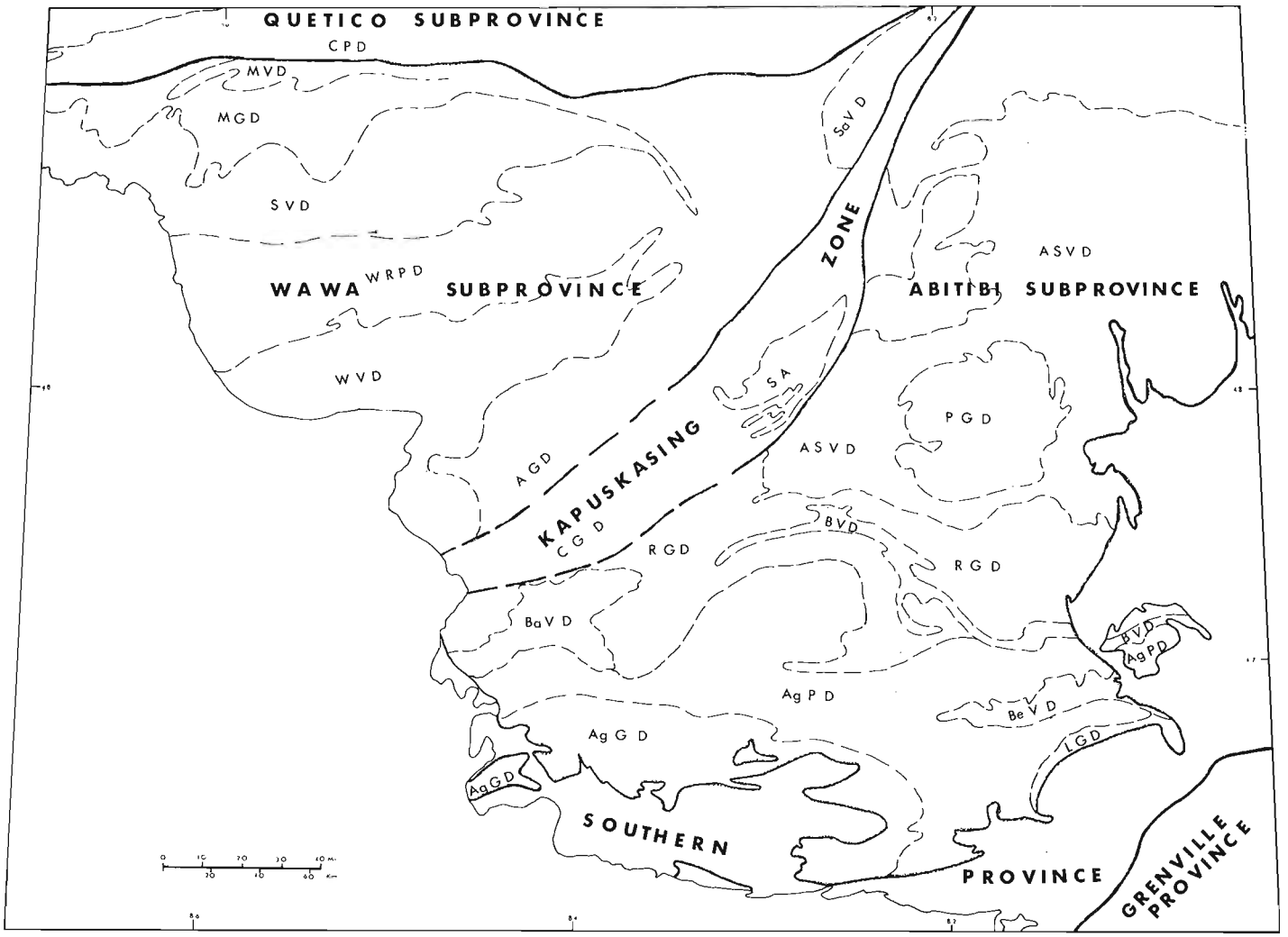


Figure 17.1. Distribution of major rock units.

supracrustal rocks of volcanic domains have been folded about subhorizontal and subvertical axes. The gneiss domains consist mainly of folded gneiss characterized by domal culminations, as well as massive felsic plutons and subordinate supracrustal rock remnants. The paragneiss domains include isoclinally-folded metasediments, their derived migmatites, and subordinate massive and gneissic felsic plutonic rocks. The plutonic domains consist of massive felsic plutonic rocks with minor gneiss and supracrustal remnants.

Subprovince Divisions

The Abitibi Subprovince is subdivided into the Abitibi-Swayze, Biscotasing, Batchewana, and Benny metavolcanic domains, the Peterlong, Ramsey, Algoma and Levack gneiss domains, and Algoma plutonic domain. The Peterlong gneiss domain comprises granodiorite-tonalite gneiss and foliated and massive granodioritic, dioritic, and granitic felsic plutonic rocks. The Ramsey gneiss domain, which links the Abitibi-Swayze and Batchewana volcanic domains, contains granodioritic and agmatitic granitic gneiss and foliated to massive granodiorite-granite plutons. Within the Ramsey gneiss domain there are abundant xenoliths and enclaves of supracrustal rocks, mainly of volcanic origin, and the largest of these has been distinguished as the Biscotasing metavolcanic domain. The Algoma gneiss domain, which surrounds and underlies the Proterozoic Huronian rocks of the Southern Province, consists of granitic, granodioritic and granitic gneiss with numerous greenstone enclaves and massive to foliated granite, granodiorite, and syenite intrusions. The Levack gneiss domain forms a narrow belt marginal to the North Range of the Sudbury Nickel Irruptive and consists of cataclastically foliated, high-rank metamorphic (amphibolite, granulite facies) granitic-dioritic gneiss with mafic xenoliths and enclaves of probable metavolcanic origin. The Levack gneiss domain represents the north limb of a major domal structure upon which the Sudbury Structure was superimposed (Card and Hutchinson, 1972). The Algoma plutonic domain constitutes one of the largest areas of massive felsic plutonic rocks in the southern Superior Province. This large batholithic complex consists mainly of coarse, porphyritic, leucocratic granite or quartz monzonite with subordinate granodiorite. The complex was emplaced as a series of magmatic intrusions at intermediate crustal levels following deformation and regional metamorphism of the gneiss and greenstone. Radiometric age determination by Rb/Sr whole rock isochron and U/Pb zircon methods indicates that these granitic rocks were emplaced at least 2500 Ma ago and possibly 2600 to 2700 Ma ago (Van Schmus, 1965; Hurst and Farhat, 1977). They have a low initial $^{87}Sr/^{86}Sr$ ratio, indicating little contamination by pre-existing radiogenic crustal materials.



ASVD — *Abitibi-Swayze Volcanic Domain*
PGD — *Peterlong Gneiss Domain*
RGD — *Ramsey Gneiss Domain*
BVD — *Biscotasing Volcanic Domain*
BaVD — *Batchewana Volcanic Domain*
AgPD — *Algoma Plutonic Domain*
BeVD — *Benny Volcanic Domain*
AgGD — *Algoma Gneiss Domain*
LGD — *Levack Gneiss Domain*
SA — *Shawmere Anorthosite Complex*
CGD — *Chapleau Gneiss Domain*
AGD — *Anjigami Gneiss Domain*
WVD — *Wawa Volcanic Domain*
WRPD — *White River Plutonic Domain*
SVD — *Schreiber Volcanic Domain*
MGD — *Manitouwadge Gneiss Domain*
MVD — *Manitouwadge Volcanic Domain*
SaVD — *Saganash Volcanic Domain*
CPD — *Caramat Paragneiss Domain*

Figure 17.2. *Litho-tectonic subdivisions of part of the Superior Province.*

The Wawa Subprovince is subdivided into the Saganash, Wawa, Schreiber and Manitouwadge volcanic domains, the Anjigami and Manitouwadge gneiss domains, and the White River plutonic domain. The Anjigami gneiss domain comprises granodiorite and tonalite gneisses with abundant xenoliths and enclaves of migmatitic rocks of metavolcanic and metasedimentary origin. Foliated to massive felsic plutonic rocks are prevalent. The rocks of the White River plutonic domain are similar, except that massive felsic plutonic rocks appear to be predominant, although information is lacking in several large areas. The Manitouwadge gneiss domain consists mainly of tonalite and granodiorite gneisses with abundant supracrustal remnants, especially near the Manitouwadge volcanic domain. The gneissic units display prominent domal structures and are cut by foliated to massive felsic intrusions of several ages. The granitic gneiss of the Manitouwadge area has an age of 2720 ± 50 Ma, based on isotopic lead data from zircons and sphene, and on Rb/Sr whole rock measurements (Tilton and Steiger, 1969). The Manitouwadge volcanic domain, located in the northern part of the Wawa Subprovince adjacent to the Quetico Subprovince boundary, includes the highly deformed, highly metamorphosed (amphibolite facies) metavolcanic-metasedimentary sequence of the Manitouwadge greenstone belt and the migmatitic equivalents of these rocks which continue eastward and westward for unknown distances. The contact between the Quetico and Wawa subprovinces, although relatively abrupt, does not appear to be faulted.

That part of the Quetico Subprovince within the map area, herein termed the Caramat paragneiss domain, consists of isoclinally folded, highly metamorphosed (amphibolite, granulite facies) metasediments and migmatitic paragneiss with abundant granitic intrusions. Many of the intrusions contain abundant paragneiss xenoliths. Pegmatite and granite from the Quetico Subprovince have yielded a Rb/Sr whole rock isochron age of 2612 ± 77 Ma (Wanless and Loveridge, 1972). The metasediments, originally fine grained wacke with minor quartz-feldspar sandstone, contain a variety of

metamorphic minerals, including garnet, cordierite, staurolite, sillimanite, and pyroxene. In the southern part of the Caramat paragneiss domain there are thin units of mafic gneiss, probably metavolcanics.

The Kapuskasing Structural Zone is a northeast-trending zone of structural discordance that transects the main east-west structural trends of the adjacent subprovinces (Thurston et al., 1977). The zone is characterized by high-rank metamorphic (amphibolite, granulite facies) gneiss with gently plunging rodding and mineral lineation, by a large Archean anorthosite intrusion, by Proterozoic alkalic rock-carbonatite intrusions, and by gravity and magnetic anomalies. The eastern boundary is marked by a fault zone with well-developed mylonite and pseudotachylite breccia. The western boundary has not been adequately defined, but is tentatively placed along a topographic lineament that probably represents a major fault zone. The southern termination of the structure is also problematical. The gravity and magnetic anomalies do not continue south of Chapleau, nor does the pyroxene-bearing gneiss. However, the boundary faults do continue, and in the south there is a prominent unit of paragneiss similar to some of the metasediments northeast of Chapleau. For these reasons, the Kapuskasing Structural Zone is tentatively shown as continuing southwestward to the coast of Lake Superior.

The rocks of the Kapuskasing Structural Zone include granodioritic-tonalitic gneiss of probable plutonic origin, mafic and felsic pyroxene-bearing gneiss, and pelitic and psammitic migmatitic paragneiss, also locally pyroxene-bearing. Foliated mafic rocks, probably metavolcanics, and clastic metasediments, including stretched-pebble conglomerate, wacke and arkose, are also present. The Shawmere Anorthosite Complex, a layered, deformed, metamorphosed body of anorthosite, gabbroic anorthosite, and gabbro, intrudes the supracrustal rocks. Associated with the anorthositic rocks are gneissic tonalite and monzonite. A K/Ar age of 2519 Ma on hornblende from gabbroic anorthosite (Watkinson et al., 1972) may represent the time of metamorphism or uplift.

The Kapuskasing Structural Zone was the site of sedimentation and volcanism, emplacement of the Shawmere Anorthosite Complex, and deformation and high-rank metamorphism during the Archean. During the late Archean or early Proterozoic, the area was faulted to form an upthrust horst-type transverse structure that controlled still later alkalic rock-carbonatite plutonic activity. Further work on this structure is planned to better define its boundaries, tectono-metamorphic history, and relationship to the adjacent subprovinces.

Mafic Dyke Swarms

Mafic dykes of Archean and Proterozoic age are abundant throughout the region where they form several prominent dyke swarms. Metamorphosed, foliated, east-trending dykes occur south of Manitouwadge. North to north-northwest-trending quartz diabase and porphyritic diabase dykes (Matachewan-type) of late Archean age are prevalent. Several large northeast-trending olivine diabase and quartz diabase dykes of probable early Proterozoic age are present in the east. North-northwest quartz diabase and porphyritic quartz diabase, and northwest-trending olivine diabase (Sudbury Swarm) dykes of middle Proterozoic age, are ubiquitous in the central part of the region. Lamprophyre and carbonatite dykes, probably associated with the Proterozoic alkalic rock-carbonatite complexes, occur northwest of Sudbury, near Chapleau, near Wawa, and north of Thessalon and Sault Ste. Marie.

Rock Alteration

Several large areas of brecciation, fracturing, and rock alteration were noted. The Archean and Proterozoic rocks immediately north of the Sudbury Nickel Irruptive are extensively brecciated, presumably as a result of the "Sudbury Event", either explosive volcanism or meteorite impact. Farther north along Highway 144 in Baynes and Edinburgh townships there are zones of brecciation, hematization, and feldspar alteration in the Archean granitic rocks. Zones of fracturing and hematization also occur east of Searchmont and north along Highway 17 to the Montreal River in the area north of Sault Ste. Marie. The fracturing and alteration of the Archean rocks along the coast of Lake Superior are probably connected with the formation of the Lake Superior structure.

References

Ayres, L.D., Lumbers, S.B., Milne, V.G., and Robeson, D.W.
1971: Ontario Geological Map, East Central Sheet; Ontario Department of Mines and Northern Affairs, Map 2198, scale 1 inch to 16 miles.

Card, K.D. and Hutchinson, R.W.
1972: The Sudbury Structure: Its regional geological setting; in New Developments in Sudbury Geology, J.V. Guy-Bray, ed., Geological Association of Canada, Special Paper 10, p. 67-78.

Hurst, R.W. and Farhat, J.
1977: Geochronologic investigations of the Sudbury Nickel Irruptive and the Superior Province granites north of Sudbury; Geochimica et Cosmochimica Acta, v. 41, p. 1803-1815.

Schwerdtner, W.M., Morgan, J., Osadetz, K., Stone, D., Stott, G., and Sutcliffe, R.H.
1978: Structure of Archean rocks in western Ontario; in Proceedings of the 1978 Archean Geochemical Conference, J.E.M. Smith and J.G. Williams, ed., p. 107-123.

Stockwell, C.H.
1970: Geology of the Canadian Shield – Introduction; in Geology and Economic Minerals of Canada, R.J.W. Douglas, ed., Geological Survey of Canada, Economic Geology Report 1, p. 44-54.

Thurston, P.C., Siragusa, G.M., and Sage, R.P.
1977: Geology of the Chapleau area, Districts of Algoma Sudbury and Cochrane; Ontario Division of Mines, Geological Report 157, 293 p.

Tilton, G.R. and Steiger, R.H.
1969: Mineral ages and isotopic composition of primary lead at Manitouwadge, Ontario; Journal of Geophysical Research, v. 74, p. 2118-2132.

Van Schmus, W.R.
1965: The geochronology of the Blind River-Bruce Mines area, Ontario, Canada; Journal of Geology, v. 73, p. 775-780.

Wanless, R.K. and Loveridge, W.D.
1972: Rubidium-Strontium age studies, Report 1; Geological Survey of Canada, Paper 72-73, p. 39-43.

Watkinson, D.H., Thurston, P.C., and Shafiqullah, M.
1972: The Shawmere anorthosite of Archean age in the Kapuskasing Belt, Ontario; Journal of Geology, v. 80, p. 736-739.

18.

THE NORTHEASTERN MARGIN OF THE APHEBIAN KILOHIGOK BASIN, MELVILLE SOUND, VICTORIA ISLAND, DISTRICT OF FRANKLIN

Project 740092

F.H.A. Campbell and M.P. Cecile[1]
Regional and Economic Geology Division

Campbell, F.H.A. and Cecile, M.P., The northeastern margin of the Aphebian Kilohigok Basin, Melville Sound, Victoria Island, District of Franklin; in Current Research, Part A, Geol. Surv. Can., Paper 79-1A, p. 91-94, 1979.

Abstract

In the northeastern part of the Kilohigok Basin, Aphebian sedimentation commenced with the deposition of interbedded shallow marine(?) dolomitic quartzites and planar-crossbedded quartzites equivalent to the lower part of the Burnside River Formation in the Bathurst Inlet area. With increased sediment supply, mega-crossbedded quartz grits and coarse grained quartzite spread across these earlier units. Fluvial avulsion and emergence locally stripped these rocks from the underlying Archean basement. Sedimentation in this part of the basin was renewed as northwesterly flowing braided rivers from tectonically active eastern source areas spread pebbly and conglomeratic quartzites across the remnant outliers and denuded Archean basement. Semicontinuous intraformational mega-boulder conglomerates within the Burnside River Formation in the Bathurst Inlet area may record the same tectonodepositional cycle.

Introduction

Examination of the Aphebian rocks of the Melville Sound, Victoria Island area was carried out in 1978 as part of the Helikian study of the same area. The work on the Aphebian is a continuation of the program initiated in 1974 as a study of the Goulburn Group in the Bathurst Inlet area (Campbell and Cecile, 1975, 1976a,b,c). Additional work on the Helikian was carried out in 1978 and is the subject of a separate report (Campbell, 1979).

The objective of this portion of the program was to delineate, if possible, the northeastern extent of the Kilohigok Basin, and define the formations, facies changes and distribution patterns along the margin of the basin (Fig. 18.1).

Previous geological studies (Fraser, 1964) had assigned some of these rocks to the Goulburn Group and others to the overlying Helikian Parry Bay Formation. On Victoria Island, Thorsteinsson and Tozer (1962) assigned the sediments of the Wellington High to the Hadrynian Shaler Group. Young (1974) followed their stratigraphic assignation, but suggested that the sediments may be equivalent to the Aphebian rocks of the Bathurst Inlet area. During the course of this field season, the Burnside River Formation was mapped along the southern and northern shores of Melville Sound and Elu Inlet, on Cape Alexander and an extensive section delineated on Victoria Island. It is lithologically, texturally, and structurally identical to the Burnside River Formation in the southern part of the Kilohigok Basin, in particular the section exposed in the northern part of the Bathurst Inlet in the Buchan Bay area (Campbell and Cecile, 1976a; also Table 18.1).

Burnside River Formation

The Burnside River outcrops in the Melville Sound area at few localities, mainly on the peninsula which terminates in Kongoyuar Point, and on the mainland to the south. The formation is exposed on both flanks of a northerly trending syncline which extends across Warrender Bay (Fig. 18.2). The formation is identical to that described by Campbell and Cecile (1976a) in the Buchan Bay area to the southwest (Fig. 18.2).

In Melville Sound, the Burnside River consists of deep red to pink, pebbly, trough crossbedded quartzite and quartz-pebble conglomerate. Over 90 per cent of the pebbles are quartz, and the remainder are Archean granitoid rocks and jasper. They range in size from coarse sand to 10 cm, but 2.5-4 cm pebbles are most common. Conglomerate beds are rare in the succession, and these are never more than 30 cm thick. They are composed almost exclusively of well rounded quartz pebbles set in a grit or coarse quartzite matrix.

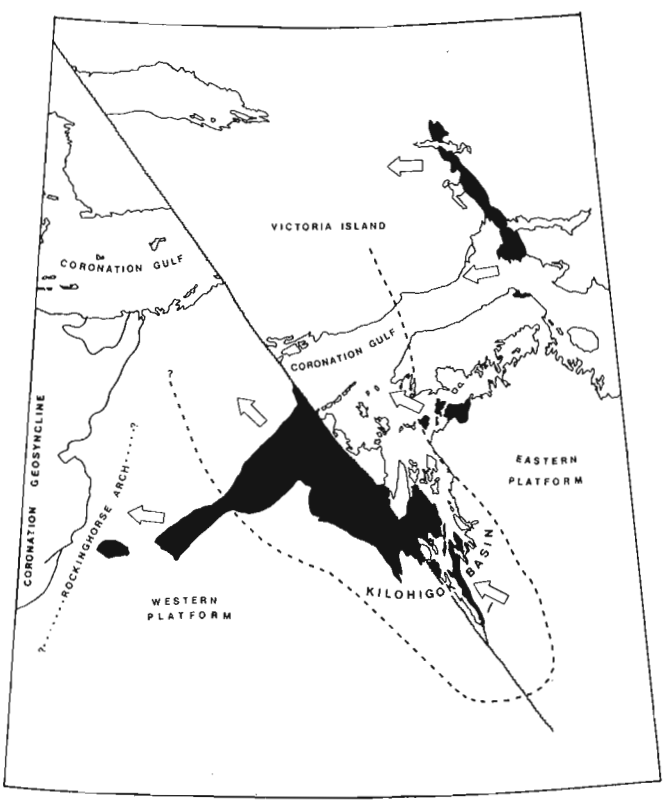


Figure 18.1. *Restored position of the segments of the Kilohigok Basin in the Coronation Gulf-Bathurst Inlet area. The total displacement on the major faults is approximately 140 km, with less than 1 km vertical movement, much of which is post-Helikian in age. The paleocurrent trends shown by the open arrows are from the lower part of the Goulburn Group (Western River to Quadyuk formations). The position of the Rockinghorse Arch, which separates the Kilohigok Basin from the correlative Coronation Geosyncline is extrapolated north and south from its known position.*

[1] Institute of Sedimentary and Petroleum Geology, Calgary, Alberta.

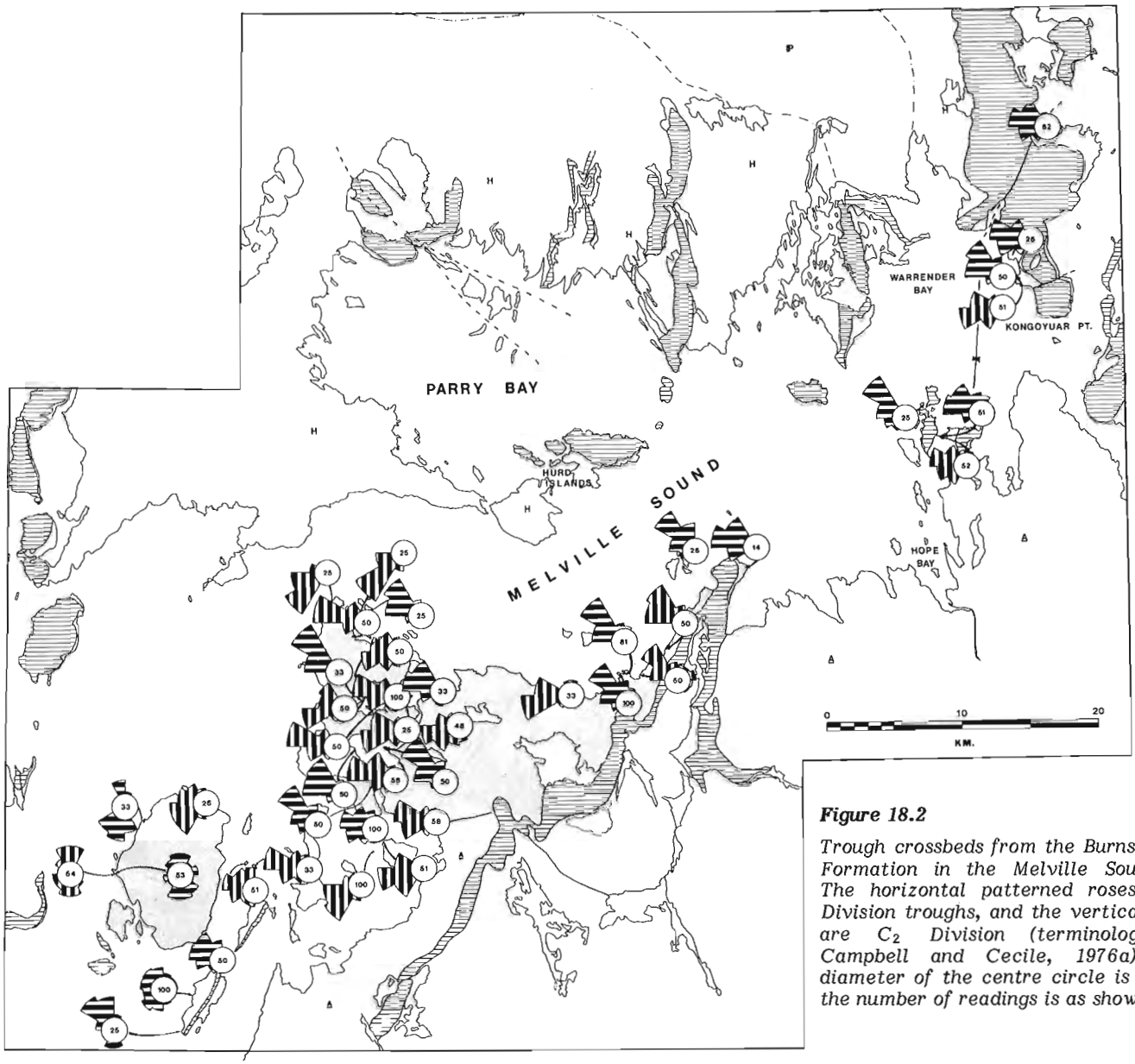


Figure 18.2

Trough crossbeds from the Burnside River Formation in the Melville Sound area. The horizontal patterned roses are C_1 Division troughs, and the vertical pattern are C_2 Division (terminology after Campbell and Cecile, 1976a). The diameter of the centre circle is 20%, and the number of readings is as shown.

Ubiquitous trough crossbeds occur in both the conglomeratic and nonconglomeratic parts of the formation. The fining-upward cycles distinguished previously in the formation (Campbell and Cecile, 1976a) are present in all outcrops. These consist of either an A division, with a scoured base, overlain by the C_1 Division, and passing upward into the C_2 Division. Most commonly, the base of the cycle commences with the C_1 Division and is topped by the C_2 Division; no D or E Divisions were noted in the area. One cycle observed contained the basal A, overlain by the massive, very rare, B Division, and topped by the C_1. As in the Buchan Bay area there is a slight variation in the paleocurrent pattern within the fining-upward cycles (Fig. 18.2). The A and C_1 Division crossbeds are more northerly directed than the smaller crossbeds in the C_2 Division. This same distinction is maintained in the areas to the west and also to the south in Bathurst Inlet. The reason for the discrepancy is unclear.

At Cape Alexander, on the northern tip of Kent Peninsula, a sequence of quartz-pebble conglomeratic quartzite and pink to mauve quartzite has been gently folded into a northerly trending syncline. Although highly fractured, the rocks appear identical to the remainder of the Burnside River Formation elsewhere in the Goulburn Group, particularly in the northern part of the Kilohigok Basin. The base of this succession is not exposed, and the top has been truncated by the basal conglomerates of the lowermost Ellice River Formation. Both formations are unconformably overlain by the Paleozoic rocks and the Paleozoic basal conglomerate is exposed at the western tip of Cape Alexander.

Trough crossbeds, while present in the Burnside at this location, are not well exposed. They average approximately 1.5 m in width and are rarely more than 0.5 m deep. Scattered quartz pebbles occur throughout the quartzite, and the largest observed was approximately 5 cm, with the average 3 cm. The maximum estimated thickness of the Burnside River Formation at this location is approximately 200 m.

Directly north of Cape Alexander at Starvation Cove on Victoria Island (Fig. 18.3), a similar quartz-pebble-bearing pink to red quartzite is overlain by a quartz- and quartzite- boulder conglomerate, with rare boulders of Archean gneiss. Well-exposed trough crossbeds in the quartzite are northerly directed, while similar, large-scale troughs in the conglomerate are westerly and southwesterly directed (Fig. 18.3). These results are similar to those reported by Young (1974) for the same area. The conglomerate here is identical to that in the Burnside River Formation to the south, where it also contains similar intraforma tional quartzite boulders derived from the underlying part of the formation. The conglomerate is exposed sporadically to the north, where it becomes more purplish and contains slightly smaller boulders.

Near Ferguson Lake the conglomerate conformably overlies a succession dominated by red to pink, medium- to coarse-grained planar-crossbedded quartzite, with minor quartzose doloarenite. This unit may be a part of the Burnside River Formation, particularly the upper quartzitic part; the lower, dolomitic, sequence may be equivalent to the Western River Formation. The base of the Aphebian succession is nowhere exposed on Victoria Island, as the contact relations are obscured by the Paleozoic cover rocks.

Southwest of Ferguson Lake the Burnside River conglomerates rest conformably on a sequence of pink and grey, very large-scale planar crossbedded quartzites, with planar crossbedded minor dolomitic units near the base. The sediments are well indurated and contain isolated, small quartz pebbles to 3 cm. The dolomitic part of the succession consists of quartzose doloarenites and dolomitic quartzite interbedded in units up to 50 cm thick. Large-scale planar crossbeds are common in this part of the formation, but decrease in both size and number upwards.

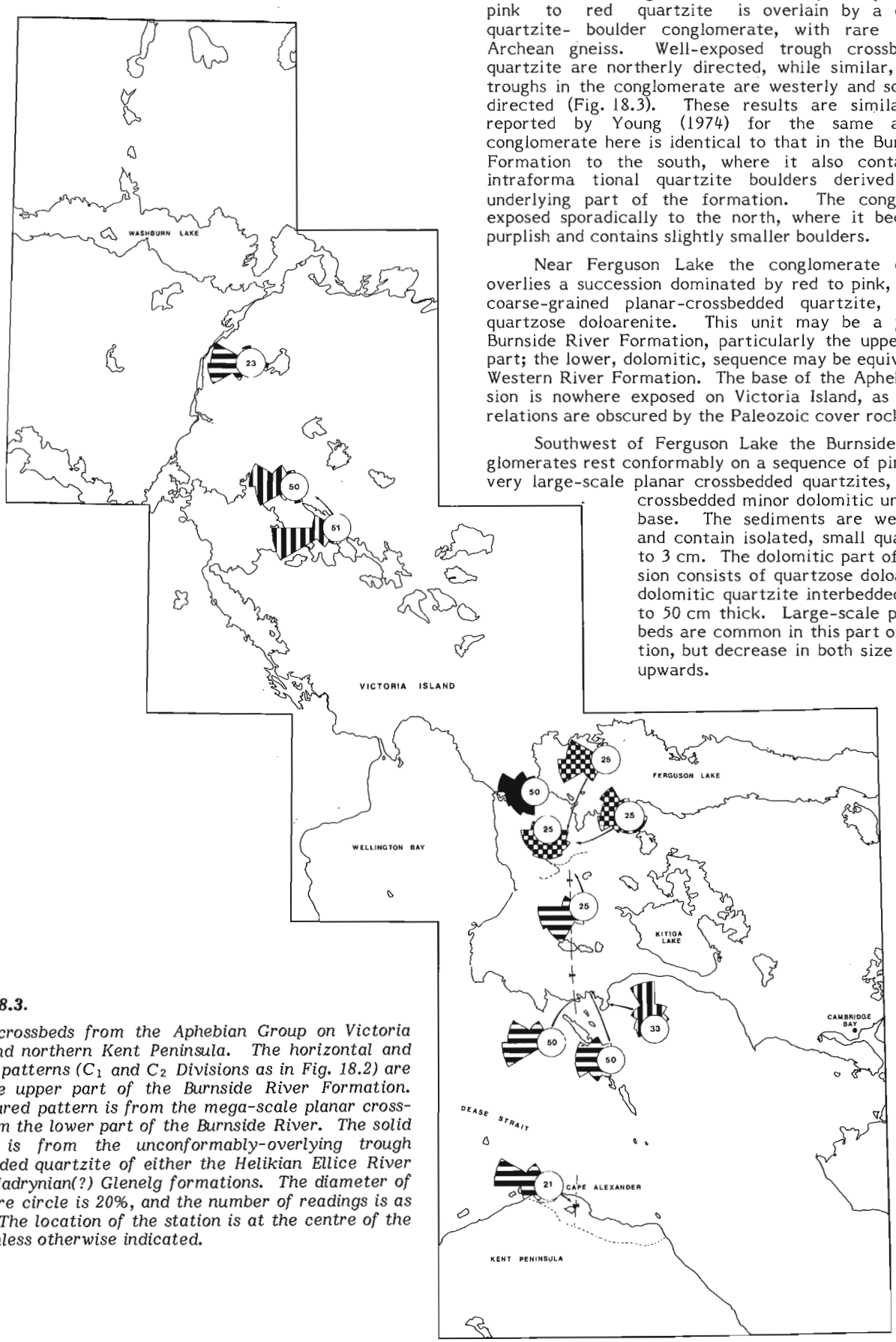


Figure 18.3.

Trough crossbeds from the Aphebian Group on Victoria Island and northern Kent Peninsula. The horizontal and vertical patterns (C_1 and C_2 Divisions as in Fig. 18.2) are from the upper part of the Burnside River Formation. The squared pattern is from the mega-scale planar crossbeds from the lower part of the Burnside River. The solid pattern is from the unconformably-overlying trough crossbedded quartzite of either the Helikian Ellice River or the Hadrynian(?) Glenelg formations. The diameter of the centre circle is 20%, and the number of readings is as shown. The location of the station is at the centre of the circle unless otherwise indicated.

Table 18.1

Burnside River Formation correlation parameters

	Bathurst Inlet and Melville Sound	Victoria Island
Quartz-cemented red, pink and purplish quartzite and conglomerates	Yes	Yes
Ubiquitous trough crossbeds	Yes	Yes
Westerly and northwesterly directed crossbeds	Yes	Yes
Trough crossbedded quartz-pebble conglomerates	Yes	Yes
Intraformational pink and red quartzite boulders	Yes	Yes
Archean boulders in the conglomerates	Yes	Yes
Fining-upward cycles in quartzite and conglomerate-based successions	Yes	Yes
Gently folded	Yes	Yes
Quartz veins	Yes	Yes
Unconformably on Archean rocks	Yes(M.S.)	Not exposed
Unconformably overlain by younger quartzite and conglomerate (Paleohelikian?)	Yes	Yes

The dolomitic part of the formation is conformably overlain by very large-scale planar-crossbedded reddish to pink quartzite, with rare ripple marks on the foreset surfaces and scattered pebbles. These crossbeds are up to 6 m thick and commonly extend for over 30 m. The initial size is unknown as the base of the succeeding unit truncates the underlying foreset beds. The largest of the crossbeds, however, measured approximately 7 m from the exposed, truncating base, to the erosion surface at the base of the overlying bed. The quartzite is poorly sorted and gritty units are common within the crossbedded sequences. There is no apparent difference in the grain size from the base of an individual crossbed to the top. The dip, however, consistently decreases upward within the individual crossbeds, from 18-30° near the base, to 5-10° near the top. The megacrossbedded and dolo itic units in this area are interpreted as a lower, protodeltaic facies of the Burnside River Formation, which was later the source of the intraformational red and pink quartzite boulders for the conglomerate.

North of Ferguson Lake (Fig. 18.3) outcrop is extremely sparse, but south of Washburn Lake, identical quartz-boulder conglomerates are interstratified with strongly trough crossbedded purplish to mauve quartzite. In this vicinity, as elsewhere in the same unit, quartz-filled tension gashes and thick quartz veins are common. The quartzite and quartz-boulder conglomerate outcrops nearly continuously from this area to north of Washburn Lake, with little apparent variation in lithology or grain size. Trough crossbeds from the quartzite and the quartz-pebble conglomerate show a westerly transport direction (Fig. 18.3), similar to those for the Burnside River Formation in the remainder of the Kilohigok Basin.

Intrusive rocks

North of Washburn Lake there is a pegmatitic granite which is basement to the overlying Paleozoic rocks, but its relationship to the Burnside River rocks is uncertain. No boulders which may have been derived from this granite were recognized in the conglomerate, but no metamorphic effects were noted either. W.A. Gibbins (Department of Indian and Northern Affairs, Yellowknife) has obtained a date of 1645 ± 20 Ma from muscovite on this intrusive.

References

Campbell, F.H.A.
1979: Stratigraphy and sedimentation of the Helikian Elu Basin and Hiukitak Platform, Bathurst Inlet – Melville Sound, Northwest Territories; Geological Survey of Canada, Paper 79-8.

Campbell, F.H.A. and Cecile, M.P.
1975: Report on the Geology of the Kilohigok Basin, Goulburn Group, Bathurst Inlet, N.W.T.; in Report of Activities, Part A, Geological Survey of Canada, Paper 74-1A, p. 297-306.

1976a: Geology of the Kilohigok Basin, Goulburn Group, Bathurst Inlet, District of Mackenzie, N.W.T.; in Report of Activities, Part A, Geological Survey of Canada, Paper 76-1A, p. 369-377.

1976b: Geology of the Kilohigok Basin; Geological Survey of Canada, Open File 342, map at 1:500 000 scale.

1976c: Tectono-depositional relationships between the Aphebian Kilohigok Basin and the Coronation Geosyncline, N.W.T.; Geological Association of Canada, Program and Abstracts, 1, p. 63.

Fraser, J.A.
1964: Geological notes on the northwestern District of Mackenzie; Geological Survey of Canada, Paper 63-40, 1 map, 20 p.

Thorsteinsson, R. and Tozer, E.T.
1962: Banks, Victoria, and Steffanson Islands, Arctic Archipelago; Geological Survey of Canada, Memoir 330.

Young, G.M.
1974: Stratigraphy, paleocurrents and stromatolites of Hadrynian (Upper Precambrian) rocks of Victoria Island, Arctic Archipelago, Canada; Precambrian Research, v. 1, p. 13-42.

19. GEOLOGY OF PART OF FOXE FOLD BELT, CENTRAL BAFFIN ISLAND, DISTRICT OF FRANKLIN

Project 740020

J.R. Henderson, David Shaw[1], Marcia Mazurski[2],
Mariette Henderson, Ron Green[3], and Dan Brisbin[2]
Regional and Economic Geology Division

Henderson, J.R., Shaw, D., Mazurski, M., Henderson, M., Green, R., and Brisbin, D., Geology of part of Foxe Fold Belt, central Baffin Island, District of Franklin; in Current Research, Part A, Geol. Surv. Can., Paper 79-1A, p. 95-99, 1979.

Abstract

Aphebian Piling Group supracrustal rocks overlying Archean basement gneiss comprise a lower, miogeoclinal quartzite-pelite assemblage with minor amphibolite and calcium-silicate gneiss, and an upper, thicker eugeoclinal metagreywacke assemblage. Both basement gneiss and supracrustal rocks were involved in at least two early deformations (D_1 and D_2) which produced isoclinal, recumbent folds, and a final major deformation (D_3) which produced the characteristic subhorizontal normal folds of the Foxe Fold Belt. Metamorphism culminated before D_3 and increased from northwest to southeast across the map area. The significant metamorphic changes produced in the rocks are a progressive increase in the volume of neosome in migmatitic metagreywacke, and an abrupt disappearance of muscovite from lower Piling quartzite. Ubiquitous graphite in Piling Group paragneiss causes characteristic rusty-weathering, but no mineral occurrences of economic interest were found.

Introduction

During the 1978 field season nine-sixteenths of the Ekalugad Fiord map area (27B) and about one-sixteenth of the Home Bay map area (27A) at a scale of 1:250 000 were mapped (Fig. 19.1). This was the third year of a continuing study of Foxe Fold Belt on Baffin Island; other work in relation to this study has been done by Morgan et al. (1975, 1976) and Tippett (1978).

Preliminary geological maps of the work done in 1978 are being prepared. Future field work is planned on map sheets 27A,B,C, and D.

General Geology

The Hudsonian Foxe Fold Belt (Jackson and Taylor, 1972) extends from southwest of Melville Peninsula to the east coast of Baffin Island (Fig. 19.2). On Baffin Island the belt contains metamorphosed and polydeformed Aphebian Piling Group (Jackson, 1971) supracrustal rocks overlying Archean granitoid basement gneiss. Metamorphic grade is lowest in the centre of the fold belt on Baffin Island where the Piling Group appears thickest; both grade of metamorphism and abundance of Hudsonian granitic material increase outward from the central Piling Basin (Jackson and Taylor, 1972; Morgan et al., 1975, 1976).

Piling Group comprises a lower, thinner miogeoclinal quartzite-pelite-carbonate assemblage, and an upper, thicker eugeoclinal mafic volcanic-distal turbidite succession. Along the north margin of the belt carbonate and quartzite make up the bulk of the miogeoclinal assemblage, whereas in the centre of the belt and farther south, calcareous rocks are rare or absent. Iron formation occurs near the base of the eugeoclinal sequence along the north and south margins of the belt, but is absent from the Piling Group in the centre and east end of the fold belt (Morgan et al., 1975, 1976; Tippett, 1978).

Posttectonic Helikian or Hadrynian diabase dykes intrude most rocks in the region. Near Foxe Basin and in Davis Strait Ordovician platform carbonate rocks occur. Most areas above 900 m elevation in eastern Baffin Island are covered by permanent ice or snow fields. In the area mapped bedrock exposure is excellent except in the northwest corner where ground moraine is extensive, and tundra polygons occur.

No mineral deposits of economic interest were found, but some malachite stain occurs in quartzite near the base of the Piling Group, and some pegmatites cutting basement rocks in Ekalugad Fiord exhibit higher-than-background uranium radioactivity.

Stratigraphy

Basement Gneiss

Rocks believed to be Archean underlie Piling Group. They are exposed in elliptical domes and concordant sheets along the east margin of the map area (Fig. 19.3). Basement gneiss also occurs near the centre of the area in several stratiform lenses on the limbs of a southeast-plunging normal synform. In the fiord country concordant sheets of basement gneiss appear in cores and limbs of early isoclines (F_1, F_2) as well as late normal folds (F_3).

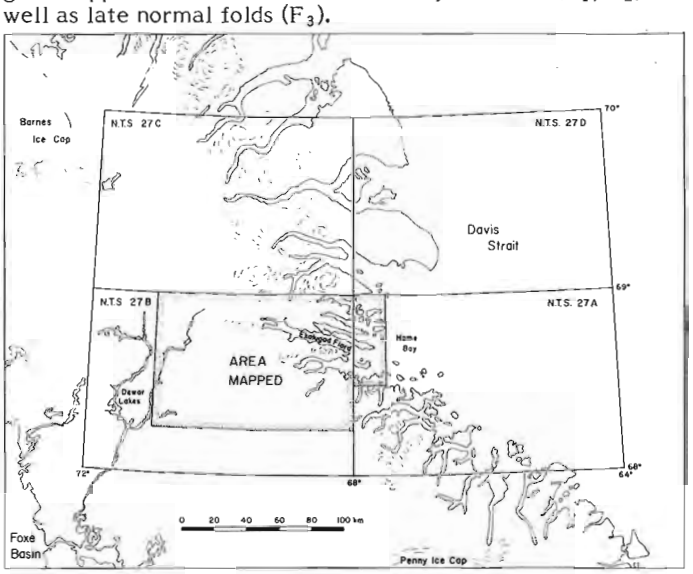


Figure 19.1. *Index map of areas referred to in central Baffin Island.*

[1] Department of Geology, Carleton University, Ottawa, Ontario K1S 5V6

[2] Department of Geology, Queen's University, Kingston, Ontario K7L 3N6

[3] Department of Geology and Geophysics, University of Utah, Salt Lake City, Utah 84112, U.S.A.

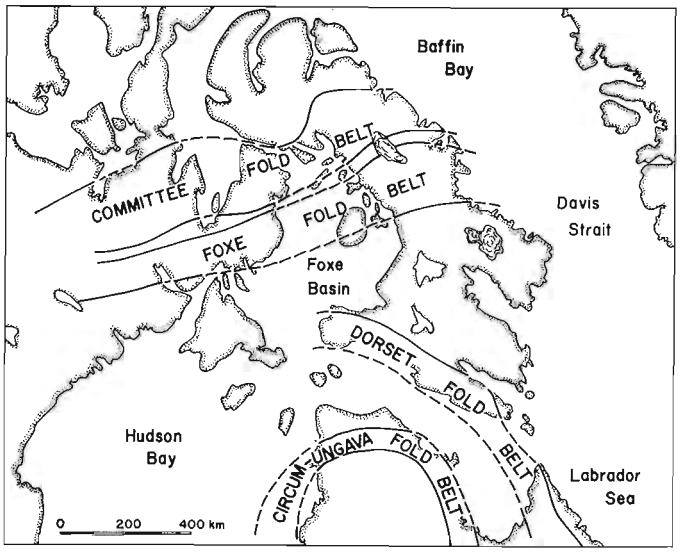


Figure 19.2. *Tectonic setting of Foxe Fold Belt in relation to other areas of Hudsonian folding in northeastern Canada (after Jackson and Taylor, 1972).*

Texture and composition of basement gneiss are variable; along the east margin of the area, mainly medium grained laminated orange or pink weathering biotite quartz monzonite occurs; in the centre of the region, coarse microcline-augen gneiss forms a large part of the exposed basement, and in the fiords, grey, granodiorite gneiss with abundant folded amphibolite boudins (Fig. 19.4) is common. In contrast to Piling Group rocks, basement gneiss does not weather rusty.

Wherever observed, the contact between basement rocks and Piling Group is sheared and foliations are concordant.

Lower Piling Group

A variety of lithologies appear in the lower Piling Group; quartzite is most common, but pelitic interbeds and concordant amphibolite layers are abundant locally. Marble and calcium-silicate gneiss outcrops in a few thin layers near the basement contact in Ekalugad and Kangok fiords (Fig. 19.3). Generally, quartzite occurs at the base of the group, but pelite or amphibolite are in contact with basement gneiss in many places.

In the northwest quarter of the map area (Fig. 19.3), where the metamorphic grade is lower, quartzite is medium grained, light grey, quartz-muscovite schist. To the east and

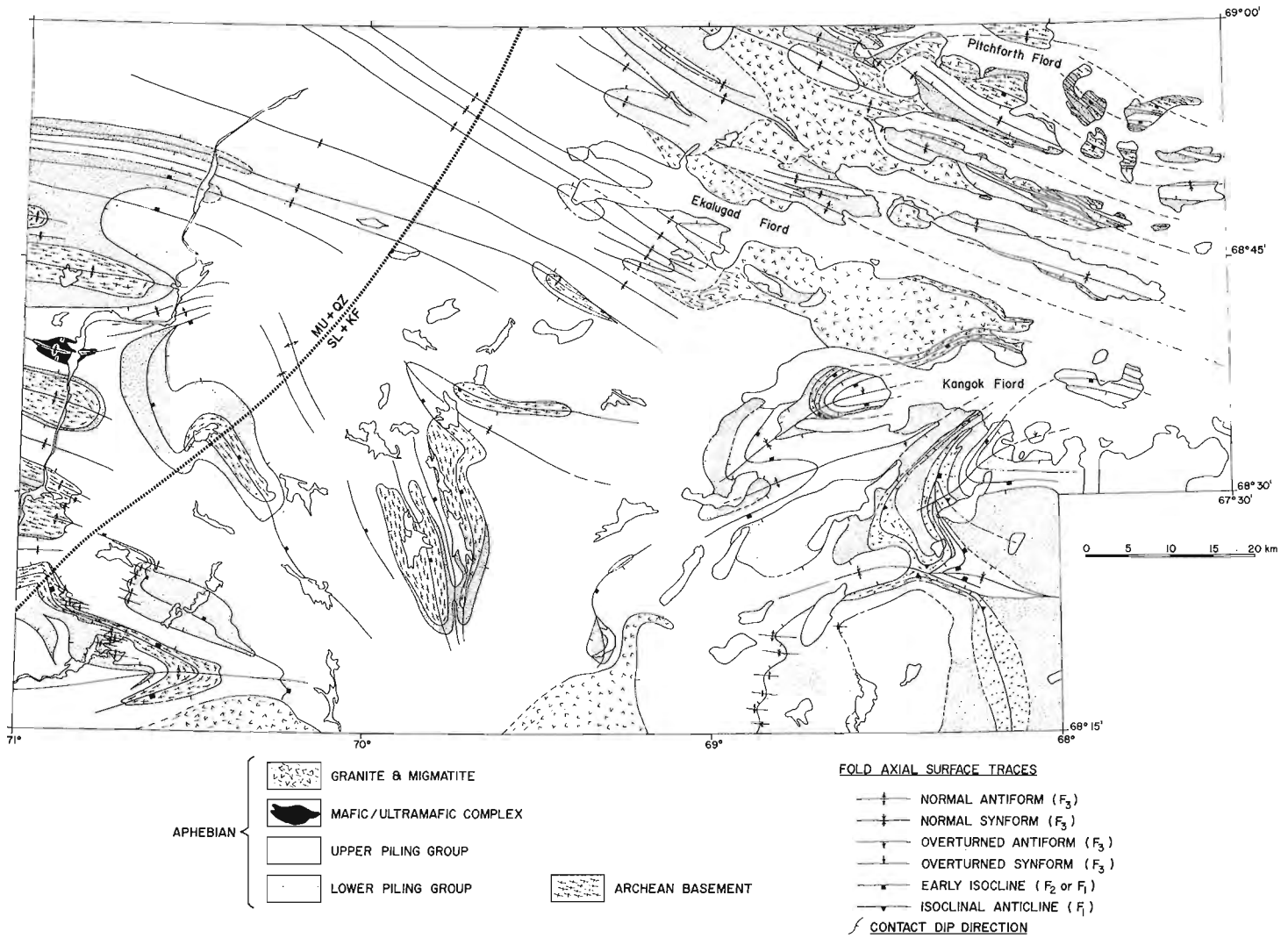


Figure 19.3. *Geological map of part of Foxe Fold Belt, central Baffin Island.*



Figure 19.4

Folded amphibolite boudins in granodiorite basement gneiss (north of Ekalugad Fiord).



Figure 19.5

Gently curving linear aggregates of quartz and feldspar (L_1) parallel to F_3 hinges in basement gneiss (north of Ekalugad Fiord).

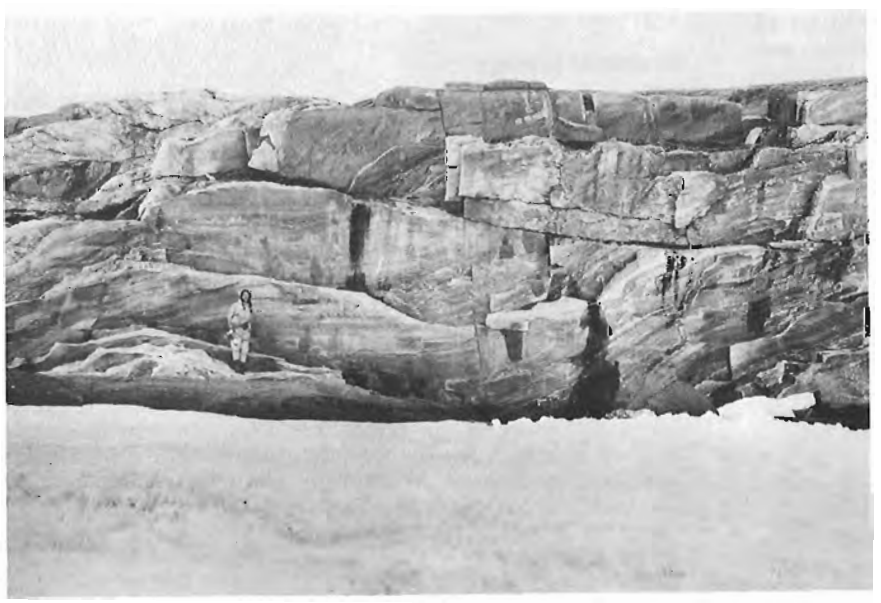


Figure 19.6

Linear aggregates of quartz, feldspar and sillimanite (L_1) transverse to mesoscopic F_3 fold hinges in lower Piling quartzite (island at mouth of Pitchforth Fiord).



Figure 19.7

Linear aggregates of quartz and feldspar (L_1) folded 180 on subvertical S_0 surfaces in basement gneiss (sea coast north side of Ekalugad Fiord).

south, quartzite is coarse grained, cream-coloured quartz-microcline-sillimanite-(garnet) gneiss. Low grade pelite is rusty weathering homogeneous fine grained mica-graphite-quartz schist, but in the higher grade terrain it is rusty weathering, coarse grained biotite-garnet-feldspar-quartz-graphite-sillimanite gneiss. Amphibolite varies from homogeneous fine grained hornblende-plagioclase biotite schist in the northwest of the map area to coarser grained garnet amphibolite gneiss in the fiord region.

No primary structures except parallel bedding are preserved in lower Piling Group rocks in the map area. Secondary mesoscopic structural elements are well-developed: mica foliation is ubiquitous and commonly is crenulated; quartz grains exhibit plate and rod habits; garnet and feldspar are flattened and elongated. Mesoscopic folds are developed locally in layered or foliated rocks; commonly they are boudined or have their limbs sheared-off. In some quartzitic paragneiss, intersecting sets of isoclinal folds produce anastomosing gneissosity bands on outcrop surfaces resembling pinch-and-swell structure.

Upper Piling Group

Characteristically, upper Piling Group rocks are a monotonous sequence of thin- to thick-layered (0.1 to 1.0 m), fine- to medium-grained, rusty weathering, dark grey metagreywacke. The principal minerals are quartz, feldspar, biotite, and graphite; in places, dark green calcium-silicate minerals are present and scattered small garnets appear in higher grade rocks. With increasing metamorphic grade, the proportion of white granite neosome progressively increases. The granite appears initially as discrete white laminae that pinch and swell parallel to foliation in the metagreywacke; with increasing volume of granitic component, the rock becomes a migmatite with scattered biotite-graphite schist schlieren. Garnets commonly occur in both paleosome and neosome.

Generally, upper Piling metagreywacke stratigraphically overlies lower Piling quartzite, but in places quartzite is absent and metagreywacke lies directly against basement gneiss.

Mafic-Ultramafic Complex

A mixed sequence of amphibolite, hornblendite, metagreywacke, and quartzite, occurs along the west margin of the map area (Fig. 19.3). The complex is synformal and structurally overlies upper Piling metagreywacke. However, the rocks previously were isoclinally folded (Chernis, 1976) and the true stratigraphic position of the complex is unknown. The succession of lithologies composing the complex resembles the transitional sequence of rocks separating Tippett's (1978) quartzite-schist unit (lower Piling of this paper) from his metagreywacke-siltstone unit (upper Piling of this paper).

Granite and Migmatite

In the south and east parts of the map area (Fig. 19.3) where the metamorphic grade is highest, extensive bodies of foliated granite, pegmatite, and granite-metagreywacke migmatite occur. The neosome in the migmatite varies from coarse grained or pegmatitic, light grey biotite-(garnet)-(cordierite) granite to pink biotite quartz monzonite with microcline augen. The proportion of rusty weathering biotite-graphite-(garnet)-(sillimanite) paleosome varies from about 5 to 50 per cent. Contacts with adjacent metagreywacke, quartzite, or basement gneiss, may be abrupt or gradational. The migmatization occurred before the late folding (F_3), and probably was coincident with the metamorphic culmination in the region.

Structural Geology

The structural features characterizing Foxe Fold Belt are normal antiforms and synforms (F_3) produced during the last penetrative deformation (D_3) of the region. The F_3 folds developed on a terrane of subhorizontal gneisses that had been deformed by at least two periods (D_1 and D_2) of isoclinal folding (F_1 and F_2). Macroscopic F_1 and F_2 isoclines are common in the region mapped; they can be differentiated only where F_2 overprints F_1, e.g. near the southeast corner of the map area (Fig. 19.3) where the limbs of a basement-cored F_1 isoclinal anticline are folded into an F_2 isocline and two F_3 synforms. In the southwest corner of the map area, the limbs of a basement-cored F_1 or F_2 isoclinal anticline are folded into and east-plunging F_3 normal antiform. F_3 folds in the region generally are readily distinguished as low-amplitude normal antiforms and synforms with subhorizontal hinges. In the map area the dominant trend of F_3 folds is east-southeast. South of Kangok Fiord (Fig. 19.3), however, a pair of northeast-trending F_3(?) normal folds become progressively overturned and isoclinal as they are followed northeast along their axial-surface traces.

Mineral foliation (S_1 schistosity) parallels differentiated layered (S_0 bedding or gneissosity) around the hinges of all mesoscopic folds observed in the map area, suggesting that a pre-D_1 penetrative deformation was obscured by later events.

Mineral lineation (L_1) is pronounced in some rocks of the map area; linear grains and grain aggregates commonly parallel axes of pre-D_3 boudined granitic laminae in metagreywacke and basement gneiss. Mineral lineations (L_1) commonly parallel hinges of F_3 folds (Fig. 19.5), but in some exposures L_1 is transverse to F_3 hinges (Fig. 19.6), and in one remarkable exposure L_1 is rotated 180° on planar S_0 surfaces striking parallel to local F_3 hinges (Fig. 19.7).

Metamorphic Geology

Metamorphism of the rocks in the map area apparently culminated when the gneisses were subhorizontal before D_3. The grade of metamorphism increases from northwest to southeast, as shown by the progressive increase in the volume of neosome in migmatitic metagreywacke, and the abrupt disappearance of muscovite from the rocks. The apparent trace of the surface of the reaction: muscovite + quartz $\leftrightharpoons$ sillimanite + K feldspar + vapour is drawn on the geologic map (Fig. 19.3). This reaction is strikingly apparent in lower Piling quartzite which is a quartz-muscovite-(sillimanite) schist northwest of the reaction boundary and a quartz-K feldspar-sillimanite gneiss to the southeast. Dark blue cordierite was observed in neosome of migmatite near the southeast corner of the area.

References

Chernis, P.J.
1976: Stratigraphy, structure and metamorphism of the Piling Group at Dewar Lakes, Baffin Island, N.W.T.; unpublished B.Sc. Thesis, Carleton University, Ottawa, 64 p.

Jackson, G.D.
1971: Operation Penny Highlands, south central Baffin Island; Geological Survey of Canada, Paper 71-1, Part A.

Jackson, G.D. and Taylor, F.C.
1972: Correlation of Major Aphebian rock units in the northeastern Canadian Shield; Canadian Journal of Earth Sciences, v. 9, p. 1650-1669.

Morgan, W.C., Bourne, J., Herd, R.K., Pickett, J.W., and Tippett, C.R.
1975: Geology of the Foxe Fold Belt, Baffin Island, District of Franklin; in Report of Activities, Part A, Geological Survey of Canada, Paper 75-1A, p. 343-347.

Morgan, W.C., Okulitch, A.V., and Thompson, P.H.
1976: Stratigraphy, structure and metamorphism of the west half of the Foxe Fold Belt, Baffin Island; in Report of Activities, Part A, Geological Survey of Canada, Paper 76-1A, p. 387-391.

Tippett, C.R.
1978: A detailed cross-section through the southern margin of the Foxe Fold Belt in the vicinity of Dewar Lakes, Baffin Island, District of Franklin; in Current Research, Part A, Geological Survey of Canada, Paper 78-1A, p. 169-173.

20. BASEMENT-SUPRACRUSTAL ROCK RELATIONSHIPS ON THE SOUTHERN MARGIN OF THE FOXE FOLD BELT, CENTRAL BAFFIN ISLAND, DISTRICT OF FRANKLIN

Contract 94753

Clinton R. Tippett[1]
Regional and Economic Geology Division

Tippett, Clinton R., Basement-supracrustal rock relationships on the southern margin of the Foxe Fold Belt, central Baffin Island, District of Franklin; in Current Research, Part A, Geol. Surv. Can., Paper 79-1A, p. 101-105, 1979.

Abstract

Along the southern margin of the Foxe Fold Belt on central Baffin Island, exposures of the supracrustal Aphebian Piling Group alternate with elongate west-northwest-trending domal culminations of remobilized Archean basement. This pattern is the result of a combination of compressional folding and active gneiss doming (D3). An earlier deformation involving recumbent isoclinal folding of the basement-cover interface produced interdigitation of thin tongues of basement and cover in a finite strain regime of strong horizontal flattening with the principal elongation oriented west-northwest (D2). High grade metamorphism preceded and accompanied the earlier deformation, reaching to progressively higher stratigraphic levels to the south, such that the postmetamorphic domes are encircled by apparent aureoles of high grade rocks which eventually merge into a uniform upper amphibolite facies terrane. Andalusite, sillimanite, and cordierite occur with increasing grade in this low pressure metamorphic belt which attained granulite facies conditions in the southernmost exposures of the study area. Within the Piling Group a single complex zone of amphibolite and ultramafic rocks of uncertain origin with associated calcsilicate gneiss, rusty schist and massive sulphide occurs near the base of a thick pile of metagreywacke and above an impure quartzite of variable thickness which generally blankets the basement complex.

Introduction

The 1978 field season was the second in a project initiated in 1977 (Tippett, 1978) to map a detailed 1:50 000 scale cross-section through the southern margin of the Foxe Fold Belt on central Baffin Island near DEW line site FOX 3 (Fig. 20.1). The project forms the basis of a doctoral study at Queen's University, sponsored by the Geological Survey of Canada under the supervision of W.C. Morgan. This year's work was conducted in conjunction with a helicopter-supported 1:250 000 scale mapping operation in the Ekalugad Fiord map area.

Regional Geology

The Aphebian Piling Group and the underlying Archean basement complex are folded together in a complex synclinorium which runs approximately east-west through central Baffin Island (Jackson, 1969, 1971) and forms part of the Foxe Fold Belt (Jackson and Taylor, 1972). Along the southern margin of the belt, basal Piling quartzite and schist generally blanket the basement complex and are overlain by a thick metagreywacke and metasiltstone sequence containing near its base a diverse assemblage of amphibolite, ultramafic rocks, calcsilicate gneiss, and rusty schist (Morgan et al., 1975, 1976; Tippett, 1978). Regional metamorphic grade gradually increases outward from the core of the synclinorium so that domal basement complex culminations are progressively surrounded southward by larger structurally produced high grade aureoles of recrystallization and migmitization which merge in the south to produce an overall upper amphibolite facies terrane (Fig. 20.1).

Stratigraphy

Minor additions and revisions to the stratigraphy given in Tippett (1978) are discussed below. Domes are numbered for convenience (Fig. 20.1) but their numbers do not correspond to those used previously (Tippett, 1978).

1. Basement Complex

Slabs of basement complex lithologies collected in 1977 were stained for K-feldspar. The results confirm that the composition of the granitoid gneiss ranges from granitic to trondhjemitic while clustering around a quartz monzonitic composition. Gneissic layers of highly different composition, however, commonly are interlayered on a 1 to 10 cm scale. Mafic-rich boudins and schlieren generally contain hornblende and plagioclase with accessory biotite, garnet, pyroxene, and sphene. Ultramafic rocks are rare in the basement complex of the study area and are unique to the core of Dome 6. Pegmatites, probably mobilizates from the gneiss, are generally quartz monzonitic and are characterized by their orange colour.

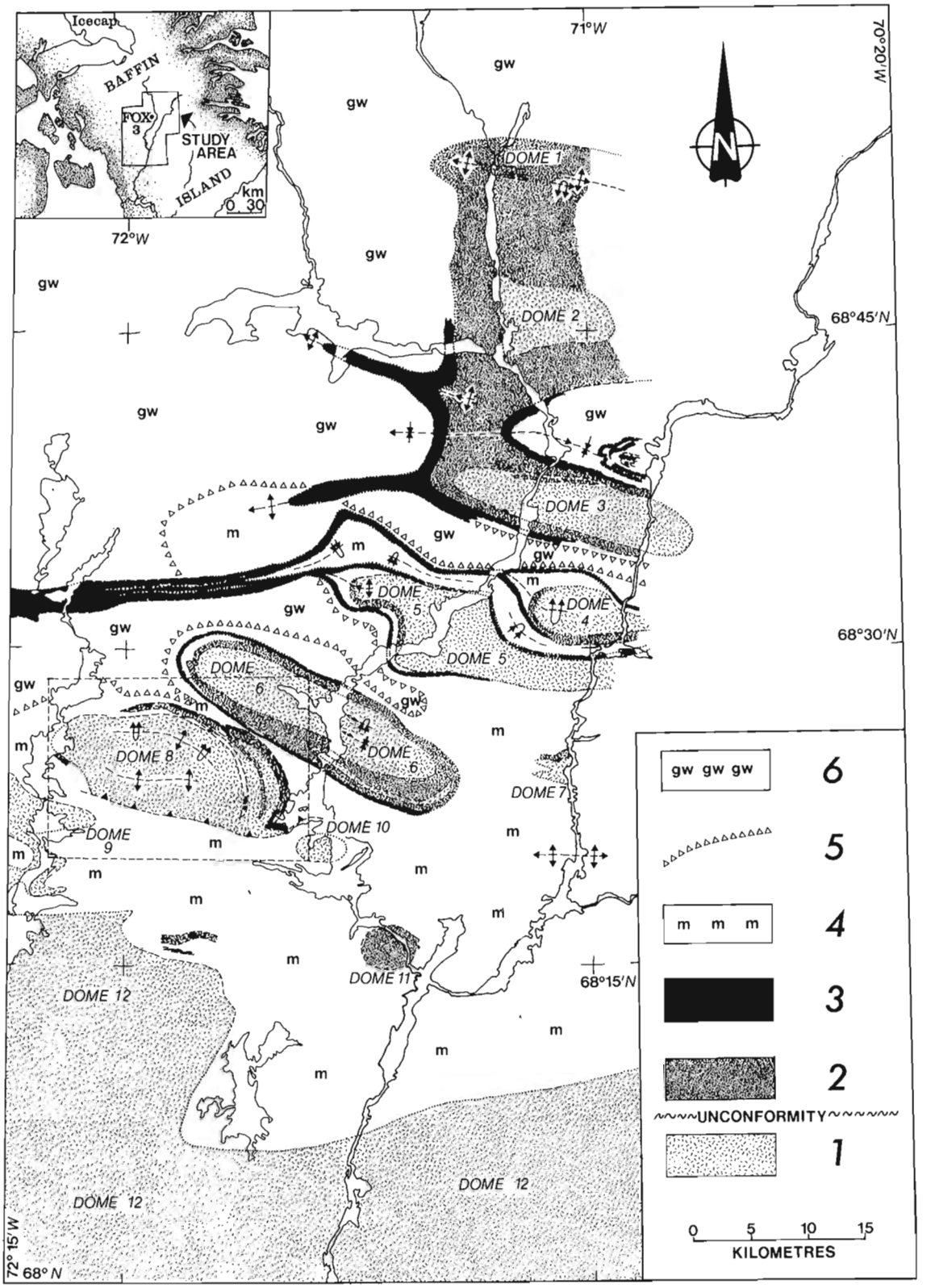
The southernmost granitoid basement complex (Dome 12, Fig. 20.1) is a mixture of megacrystic granitoids (K-feldspar up to 2 by 8 cm) and equigranular garnetiferous granitoids that form an anastomosing network of sills and dykes on all scales. Although they lack the layering of the gneiss present in domes farther north, the preferred orientation of biotite and K-feldspar augen define a schistosity dipping north under the paragneiss, suggesting an analogous structural position. Any interpretation of the complex must account for the following:

(i) Mafic-rich blocks, schlieren, and other possible restites do not contain pelitic index minerals (for example, sillimanite, which is ubiquitous in migmatitic paragneiss to the north). They are composed of hornblende, biotite, plagioclase, garnet, K-feldspar, and pyroxenes and consequently are unlikely to be high grade equivalents of the paragneiss.

(ii) The contact between the migmatitic paragneiss and the granitoid complex is sharp and therefore cannot simply represent a metamorphic transition.

(iii) North of the western section of the complex (Fig. 20.1), highly deformed quartzite and amphibolite within migmatitic paragneiss are part of the basal Piling Group.

[1] Department of Geological Sciences, Queen's University, Kingston, Ontario K7L 3N6



1. *basement complex*
2. *impure quartzite and schist unit*
3. *amphibolite and ultramafic rock unit*
4. *migmatitic paragneiss*
5. *metamorphic front separating greywacke (6) from its metamorphic equivalent – migmatitic paragneiss (4), teeth pointing towards the low grade side; and*
6. *greywacke and siltstone*

Figure 20.1. *Location and geology of the study area, excluding diabase dykes. Geology based on Tippett (1978), Morgan et al. (1976), Chernis (1976), reconnaissance data and David Shaw (pers. comm., 1978). Domes have been numbered 1 to 12 to facilitate reference to them. Axial surface traces of some D3 folds are illustrated. The area east of the coded study area was mapped during 1978 as part of the adjoining project. The block outlined in the west-central part of the figure is shown in detail in Figure 20.2.*

Megacrystic granitoids in this extensive southern terrane are interpreted as recrystallized basement gneiss which has been intruded by equigranular garnetiferous granitoids, although the latter are probably autochthonous on the scale of the whole complex.

Granitoids, which make up Dome 10, are also regarded as remobilized basement, although their marginal autoclastic zone and the absence of basal Piling Group lithologies suggest detachment from the basement complex and intrusion into the migmatitic paragneiss.

2. Impure Quartzite and Schist Unit

In the southern part of the study area, this basal unit is very thin or is absent (except for Dome 11) whereas to the north, a thick quartzite mantles Domes 1 and 2. Quartz-sillimanite faserkiesel characteristic of the quartzite south of Dome 6 are not developed to any extent elsewhere and appear to be typical only of medium grade metamorphism.

3. Amphibolite and Ultramafic Rock Unit

This unit is made up of hornblende- and tremolite/actinolite- rich ultramafic rocks and hornblende- plagioclase amphibolite with minor associated calcsilicate gneiss, rusty schist, and massive sulphide (Tippett, 1978). Internal stratigraphy and thickness change abruptly along strike so that the unit is often composed of a series of lenses rather than a continuous layer. Thick sections are restricted to the central and west-central portions of the area, with apparent stratigraphic pinching out to the north, east, and south. Interfolds of basal quartzite within the unit north and west of Domes 3 and 5 are interpreted to indicate that only one major stratigraphic unit of amphibolite and ultramafic rocks is present in the Piling Group, located at or close to the base of the metagreywacke-metasiltstone unit. Rusty quartzite associated with ultramafic rocks and calcsilicate gneiss northeast of Dome 3 (Chernis, 1976) may be recrystallized chert, as distinct from the basal quartzite.

4. Metagreywacke-Metasiltstone Unit

Petrographic examination of low grade rocks from this unit indicates a general deficiency of K-feldspar although scattered K-feldspar-rich layers are present. Clastic quartz, plagioclase, and K-feldspar suggest weathering of a granitoid terrane for a source area, an interpretation strengthened by the lack of clast compositions or textures which are

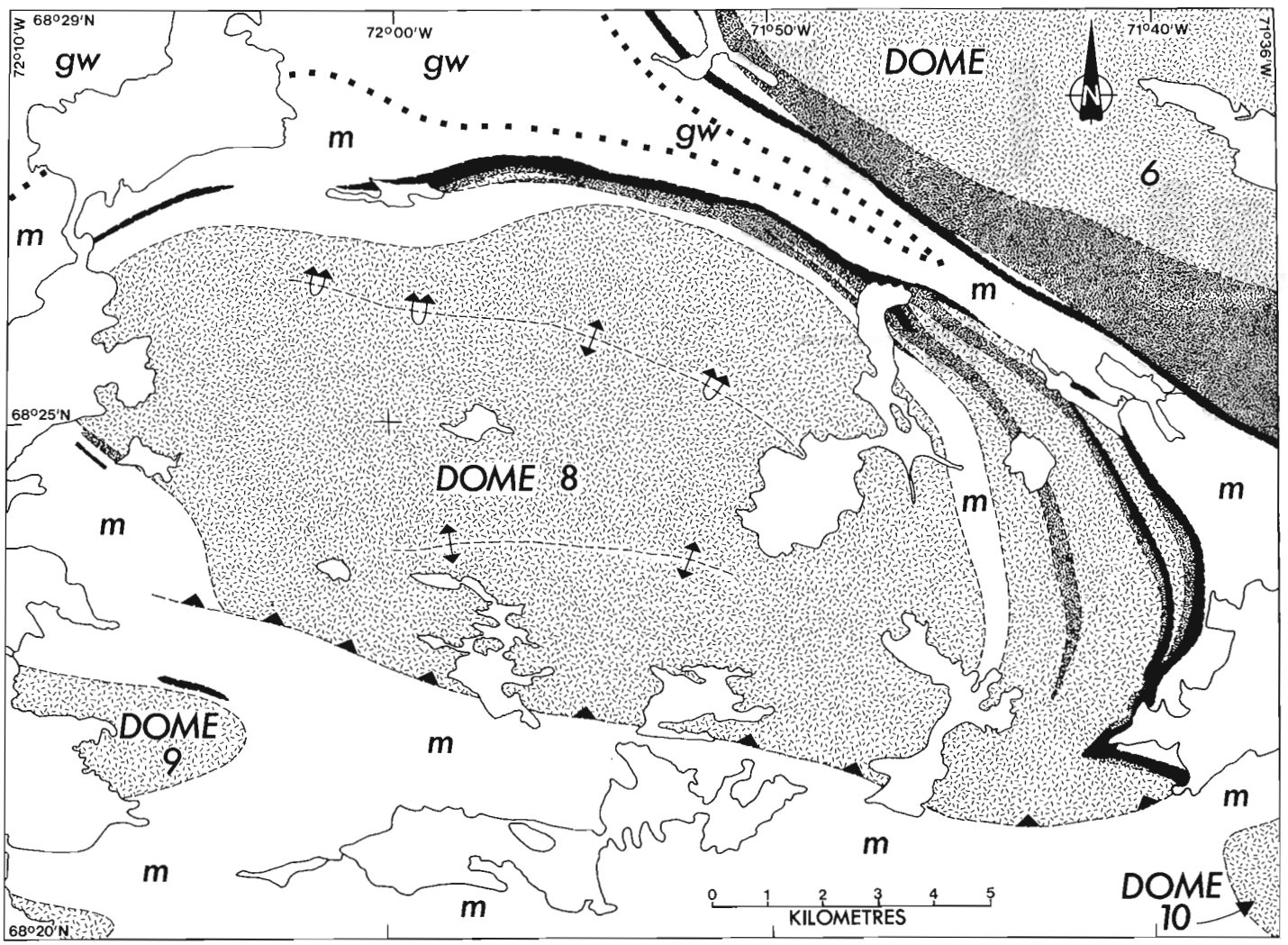


Figure 20.2. *Detailed geology of Dome 8 and vicinity, excluding diabase dykes, illustrating D2 interfolding of basement and cover along its northeastern margin. Axial surface traces of D3 folds within the core of this composite dome are depicted. Legend as for Figure 20.1 with the exception of the greywacke-migmatitic paragneiss front.*

recognizably volcanogenic or sedimentary. Concentrically zoned concordant calcsilicate nodules are probably metamorphosed carbonate concretions.

At higher grades of metamorphism the greywacke and siltstone are transformed into migmatitic paragneiss with the abruptness of the transition probably due to allochthonous mobilizate which has moved into the zone of incipient migmitization. Calcsilicate nodules containing garnet, diopside, and amphibole are locally preserved. Alternations of blocky biotite and biotite-garnet paragneiss with sillimanite paragneiss mimic compositional layering in the lower grade rocks. Mobilizate composition is predominantly quartz monzonitic with a range from granitic to trondhjemitic. Initial identification as predominantly trondhjemite was due to the identical white colour of K-feldspar and plagioclase plus poor twinning in the latter. Accessory muscovite, tourmaline, and garnet are typical of low grades while biotite, garnet, and rarely cordierite occur in higher grade mobilizate. Restites commonly contain the assemblage quartz-plagioclase-biotite and are deficient in K-feldspar due to a combination of low original content and depletion of K-feldspar into the mobilizate.

Isolated blocks of amphibolite and, more rarely, ultramafic rocks are present at various localities in the migmatitic paragneiss but, lacking markers to unravel structures in the unit, it is difficult to determine whether they were originally more continuous and/or limited to discrete horizons.

Metamorphism

Metamorphic assemblages specific to narrow P and T ranges are rare in the study area due to generally unfavourable bulk compositions. The breakdown of muscovite in the presence of quartz is the most important reaction in the supracrustal rocks given the widespread occurrence of that mineral at low grade.

North of Dome 3, the coexistence of andalusite and sillimanite in a quartz segregation close to several occurrences of quartz-muscovite-sillimanite-K-feldspar schist implies low metamorphic pressure as does andalusite-garnet-biotite-muscovite schist west of Dome 5. Faserkiesel in medium grade quartzite are made up of quartz and sillimanite and occur in a matrix of quartz-K-feldspar or quartz-K-feldspar-plagioclase. Similar nodules of muscovite-sillimanite-quartz in matrices of K-feldspar-quartz-biotite occur in slightly migmatitic medium grade paragneiss. Possibly an ionic equilibria similar to that suggested by Eugster (1970) involving the breakdown of K-feldspar would be an appropriate explanation.

The extent of partial melting in migmatitic paragneiss varies up to 90 per cent in the southernmost exposures, while averaging 40 to 60 per cent. Mobilizate and restite occur together both as thick sheets and as closely interfingering phases, implying a generally autochthonous origin with some mobilizate movement. The assemblage garnet-biotite-sillimanite is typical of schist layers in the migmatitic paragneiss. In the southernmost migmatitic paragneiss the development of cordierite gives rise to the assemblage sillimanite-biotite-cordierite-garnet-quartz-plagioclase-melt.

Whereas clinopyroxene is present locally in amphibolite of the basement complex and in supracrustal ultramafic rocks as far north as Dome 3, its occurrence with orthopyroxene in mafic-rich rocks of Dome 12 suggests the attainment of granulite facies conditions in that area.

The limited degree of partial melting in all domes, with the exception of Dome 12, must be due to the lack of a vapour phase given the highly migmatized paragneiss adjacent to them. This is confirmed in part by an increase in melting of the basement gneiss near the contact with the metasediments. Differentiation of nearly homogeneous gneiss in the central part of domes into well layered gneiss near their margins, especially in Domes 6 and 8, is problematic as it implies some sort of deformation-induced differentiation, possibly aided by a vapour phase.

Retrogression of most minerals to varying degrees is pervasive, limiting the use of mineral composition data. The peak of metamorphism and migmitization was either pre- or syn- D2 such that, given the intensity of D3 and the posttectonic polygonization of mineral grains indicated by their strain-free nature, it is probable that assemblages re-equilibrated under conditions different from those of their formation. Zones of highly altered red and orange coloured paragneiss with green biotite have widespread but non-systematic distribution.

Posttectonic pegmatites locally crosscut both the basement complex and the supracrustals. Small amounts of melt therefore were being redistributed, if not generated, until well after D3.

Structure

The evolutionary scheme described in Tippett (1978), involving early recumbent basement-cover interfolding with the development of a subhorizontal schistosity at lower levels, superceded by compressional folding and active gneiss doming, was supported by this year's work.

In the previously established nomenclature, D1 refers collectively to pre-Piling Group deformation of the basement complex. Second phase lineations (L2) defined by mineral elongations trend roughly west-northwest throughout most of the area. Although presumably related to the isoclinal interfolding of basement and cover, the lack of measurable D2 fold hinges makes it difficult to determine their true geometrical significance. Some boudins folded by D3 have axes perpendicular to L2 while S0-S2 intersections are west-northwest-trending. The most likely interpretation is that D2 isoclines have hinges which are curvilinear to an extreme and pass through 180°. Such a geometry is the logical result of an extremely intense deformation in which hinges with various original orientations rotate towards the principal extension direction as recorded by the mineral lineations. The geometry in three dimensions of the basement-cover interface is extremely complex and is probably dominated by thin mushroom-shaped tongues stretched out along west-northwest axes and very strongly flattened in the schistosity (S2).

Compressional D3 folding alone appears to have affected the low grade metagreywacke west of Domes 5 and 6 in addition to the previously documented areas, while being superimposed on the penetrative second phase schistosity in the wide belt of migmatitic paragneiss north of Dome 12. Minor D3 folds with "cascading" vergence diagnostic of active gneiss doming are developed marginally to most domes. Possible exceptions are Dome 1, whose narrowness and sharp closure suggest a compressional origin, and Dome 10 which seems to be intrusive.

The tectonic evolution of Dome 12 may be more complex in that, as part of an extensive granitoid terrane which dominates the geology far to the south (Garth Jackson, pers. comm., 1978), it may have been responsible for much of the D3 deformation not only immediately north of it but also well into the core of the fold belt. It is certainly a much larger feature than the other domes and since its dominant north-dipping fabric in the study area appears to be continuous with S2 in the migmatitic paragneiss, its evolution may be similar to that of the other domes, although on a larger scale.

Details of the geometry of Dome 8 are portrayed in Figure 20.2. D2 interfolding of basement and cover is well developed on the northeast margin of this dome, although the lack of symmetry of Piling Group lithologies around the outer basement tongues is suggestive of low angle thrust faulting. It is a composite dome as indicated by the D3 fold structures within it and by the re-entrant in its southeastern corner. Along the southern margin, a thrust fault displaces the gneiss over the migmatitic paragneiss. There is locally a discordance of 10 to 20° in fold trends across the break and the paragneiss is more strongly deformed in its vicinity. This structure may be the result of the predominantly southward sense of overturning of most of the domes in the study area.

The age of isoclinal interfolding of the amphibolite-ultramafic rock unit and the quartzite west of Dome 5 is uncertain. The geometry illustrated in Figure 20.1 provides the simplest explanation. The thick amphibolite north of Dome 5 is presumed to contain the fold hinge which plunges west off the nose of Dome 4. This implies that these folds are D3. However, if the interfolding is D2, there is no logical reason for the hinges of the folds to relate to the positions of the domes and a much more complex choice of patterns results.

Investigation of the amphibolite and ultramafic rock unit northeast of Dome 3 suggests that it is a simple syncline containing a folded S2 but without major D2 closures. The apparent difference in thickness of paragneiss between its south limb and Dome 3 and its north limb and Dome 2 may be partly caused by steeper dips to the south but is probably also due to more extreme flattening on that limb.

Economic Geology

Massive sulphides form an integral, although minor, component of the amphibolite and ultramafic rock unit. Two new pyritiferous zones have been noted. The first is in a continuation of the belt containing the showing previously reported (Tippett, 1978), being part of an extensive gossan near 68°32'30"N, 71°57'30"W. It is made up of a 1 m layer containing 50 per cent pyrite and 50 per cent black fine grained gangue. The second is a layer several tens of centimetres thick of massive pyrite with 1 to 2 per cent finely disseminated chalcopyrite located north of Dome 8 near 68°27'N, 71°52'W.

References

Chernis, P.J.
1976: Stratigraphy, structure and metamorphism of the Piling Group at Dewar Lakes, Baffin Island, N.W.T.; unpubl. B.Sc. thesis, Carleton University, Ottawa, Ontario, 64 p.

Eugster, H.P.
1970: Thermal and ionic equilibria among muscovite, K-feldspar and aluminosilicate assemblages; Fortschritte der Mineralogie, v. 47, p. 106-123.

Jackson, G.D.
1969: Reconnaissance of north-central Baffin Island; in Report of Activities, Part A, Geological Survey of Canada, Paper 69-1A, p. 171-176.

1971: Operation Penny Highlands, south-central Baffin Island; in Report of Activities, Part A, Geological Survey of Canada, Paper 71-1A, p. 138-140.

Jackson, G.D. and Taylor, F.C.
1972: Correlation of major Aphebian rock units in the northeastern Canadian Shield; Canadian Journal of Earth Sciences, v. 8, p. 1650-1669.

Morgan, W.C., Bourne, J., Herd, R.K., Pickett, J.W., and Tippett, C.R.
1975: Geology of the Foxe Fold Belt, Baffin Island, District of Franklin; in Report of Activities, Part A, Geological Survey of Canada, Paper 75-1A, p. 343-347.

Morgan, W.C., Okulitch, A.V., and Thompson, P.H.
1976: Stratigraphy, structure and metamorphism of the west half of the Foxe Fold Belt, Baffin Island; in Report of Activities, Part A, Geological Survey of Canada, Paper 76-1A, p. 387-391.

Tippett, C.R.
1978: A detailed cross-section through the southern margin of the Foxe Fold Belt in the vicinity of Dewar Lakes, Baffin Island, District of Franklin; in Current Research, Part A, Geological Survey of Canada, Paper 78-1A, p. 169-173.

21.

NEW EVIDENCE FOR THE EXISTENCE OF AN ICE FREE CORRIDOR IN THE ROCKY MOUNTAIN FOOTHILLS NEAR CALGARY, ALBERTA, DURING LATE WISCONSINAN TIME

Project 740095

L.E. Jackson, Jr.
Terrain Sciences Division, Calgary

Jackson, L.E., Jr., New evidence for the existence of an ice free corridor in the Rocky Mountain Foothills near Calgary, Alberta, during late Wisconsinan time; in Current Research, Part A, Geol. Surv. Can., Paper 79-1A, p. 107-111, 1979.

Abstract

A 12 m core from a bog near Turner Valley, Alberta, has yielded ^{14}C dates of 18 400 ± 380 years and 18 500 ± 1090 years B.P. from near its bottom. These dates provide minimum ages for the end of the last glaciation during which Rocky Mountain provenance ice advanced east of the mountain front and covered much of the Foothills. A buried soil horizon near southeast Calgary lies between the youngest glacial till and glaciolacustrine silts. The stratigraphic position of the soil horizon precludes an advance of the Laurentide Ice Sheet into the Foothills since at least the end of the early Wisconsinan stage.

Introduction

The limits of Rocky Mountain and Laurentide ice advances in the Rocky Mountain Foothills and adjacent prairies of southwestern Alberta during late Wisconsinan time has been a topic of continuing controversy. Stratigraphic and geomorphic evidence from the Prairies (Stalker, 1977; Stalker and Harrison, 1977) has indicated that the late Wisconsinan Laurentide advance stopped well short of the Foothills, leaving an ice free corridor to the west. Radiocarbon dates from areas of the southern Alberta prairies which were glaciated during the late Wisconsinan stage have indicated that much of the Prairies of southern and central Alberta was free of ice by at least 15 000 years ago (Reeves, 1973). This limits the time span available for the westward expansion of the Laurentide Ice Sheet during the late Wisconsinan and corroborates stratigraphic evidence for its most westerly position east of the Foothills.

The limit of the Rocky Mountain ice in the Foothills is even more problematic. Stratigraphic and geomorphic evidence suggests that at least three glacial advances from the mountains have occurred which were of sufficient size to extend well into the Foothills and the Prairies beyond (Rutter, 1972; Alley, 1973; Stalker and Harrison, 1977; Jackson, 1977). In addition, at least two subsequent advances, which were limited almost entirely to the Rockies, have been recognized. However, there is little radiocarbon evidence for the ages of these advances. A few radiocarbon dates from Bow and Highwood valleys have provided minimal ages in the range from 9000 to 12 000 years. The oldest of these dates was obtained from large vertebrate bones found in terrace gravels at Cochrane and Calgary (Stalker, 1968; Wilson and Churcher, 1978). The gravels appear to have been laid down as a valley train deposit during or at the close of a glacial advance (probably the Canmore Advance of Rutter, 1972), which reached the mountain front and probably advanced a number of kilometres beyond it (Stalker, 1968, 1973). Unfortunately these dates are close to the end of the late Wisconsinan stage (ca. 10 000 years B.P.). Consequently, they are not applicable to the problem of determining whether an ice free corridor existed during earlier parts of this stage (ca. 15 000 to 25 000 years B.P.).

Heretofore radiocarbon dates and stratigraphic evidence documenting ice free conditions within this zone have not been available. Field work during the winter of 1977-78 and spring of 1978, however, has resulted in the discovery of two sites which provide proof of the existence of an ice free corridor in the Foothills and westernmost Prairies of southwestern Alberta since the end of the early Wisconsinan stage.

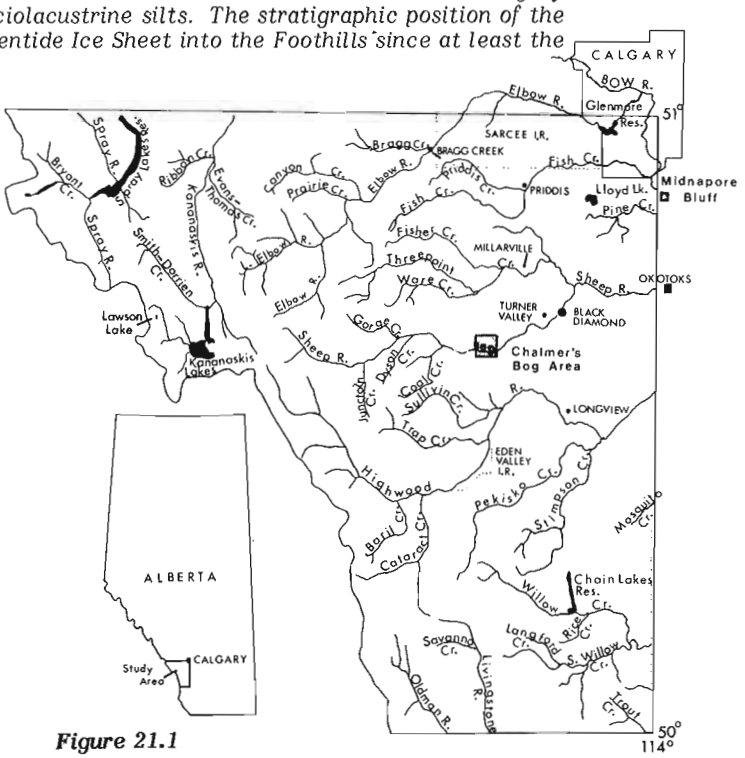


Figure 21.1

The area of southwestern Alberta in which Chalmers Bog and Midnapore Bluff are located. The area around Chalmer's Bog is detailed in Figure 21.2.

Chalmer's Bog

Chalmer's Bog is located in the Foothills approximately 15 km southwest of Turner Valley, Alberta (UTM grid location 680700, 5614500) at approximately 1370 m elevation (Fig. 21.1). The bog is situated in an east-trending meltwater channel directly north of Sheep River valley (Fig. 21.2).

Stratigraphic and geomorphic evidence indicates that the area around the meltwater channel (Jackson, 1977) was last covered by Rocky Mountain provenance ice during the glaciation, which brought the Foothills Erratics Train into the area (Stalker, 1956), as were most of the Foothills in the Calgary area. The channel last carried meltwater from retreating Rocky Mountain glaciers during the final stages of that glaciation. Since then, no advances of Rocky Mountain glaciers down Sheep River valley have reached closer than 10 km west of the channel. Consequently, Chalmer's Bog was chosen for exploratory coring in the hope that ^{14}C datable material might be found which could place a minimum age on the last extensive glaciation of adjacent areas of the Foothills.

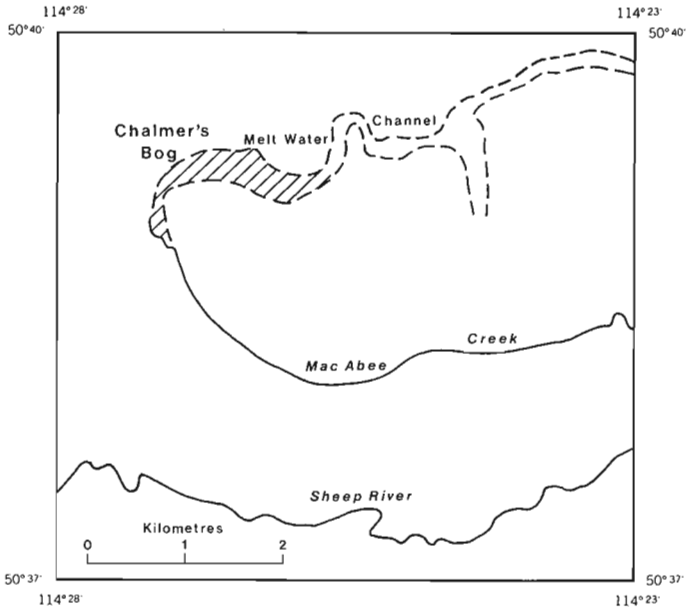


Figure 21.2. *The Chalmer's bog area.*

A 12 m x 38 mm core was obtained from the bog during March 1978 using a Livingstone-type piston corer. Sediments encountered in the core are depicted in Figure 21.3. Radiocarbon dates of 18 400±380 years (GSC-2668) and 18 500±1090 years (GSC-2670), from 9 m and 10.3 m depth, respectively, were obtained from bands of sphagnum moss. Palynological studies of the dated zone indicate it to be nearly devoid of pollen. Samples taken from the peat zone directly above the dated zone, however, indicate the presence of a plant community characteristic of arctic tundra conditions (R.J. Mott, GSC Paleoecology Lab., pers. comm., 1978).

The two dates demonstrate the absence of glacial ice at 1370 m in Sheep River valley during most of the late Wisconsinan stage. The closest ice terminus features that may mark the downvalley limits of the maximum advance during the late Wisconsinan stage are about 10 km west of Chalmer's Bog at the mountain front and are related to the Canmore Advance (Rutter, 1972; Jackson, 1977). Furthermore, since Sheep, Elbow, and Highwood river valleys all originate from the same general area of the Front Ranges and have comparable basin areas (Fig. 21.1), similar distances of glacial advances would be expected in each basin. This indeed appears to be the case because the Canmore Advance in each one of these valleys terminated at or near the mountain front (Jackson, 1977).

The bottom of Chalmer's Bog was not reached during 1978 coring operations. More coring is planned for the 1978-79 winter with the object of reaching the bottom of the bog.

Midnapore Bluff Buried Soil

Another indication for the existence of an ice free corridor in the Calgary area is a buried soil near Calgary. The soil is located near the top of 40 m high bluff on the east side of Bow River opposite the Calgary district of Midnapore (UTM 289700 5641100). This bluff is unnamed but for convenience will be referred to here as "Midnapore Bluff" (Fig. 21.1). The soil and enclosing sediments are exposed in the undisturbed scarp of a large slump near the top of the bluff. Figure 21.4 illustrates the stratigraphy of the scarp face, and Figure 21.5 details the soil sample.

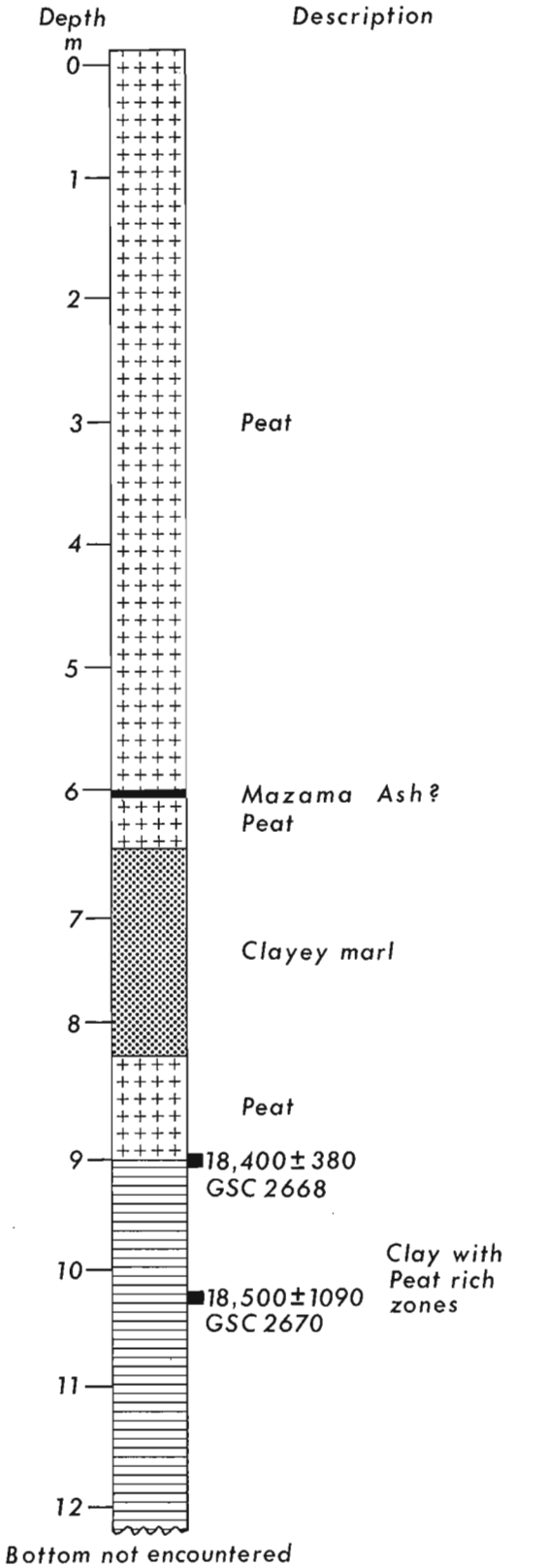


Figure 21.3. *Generalized stratigraphy of sediments encountered in the Chalmer's Bog core.*

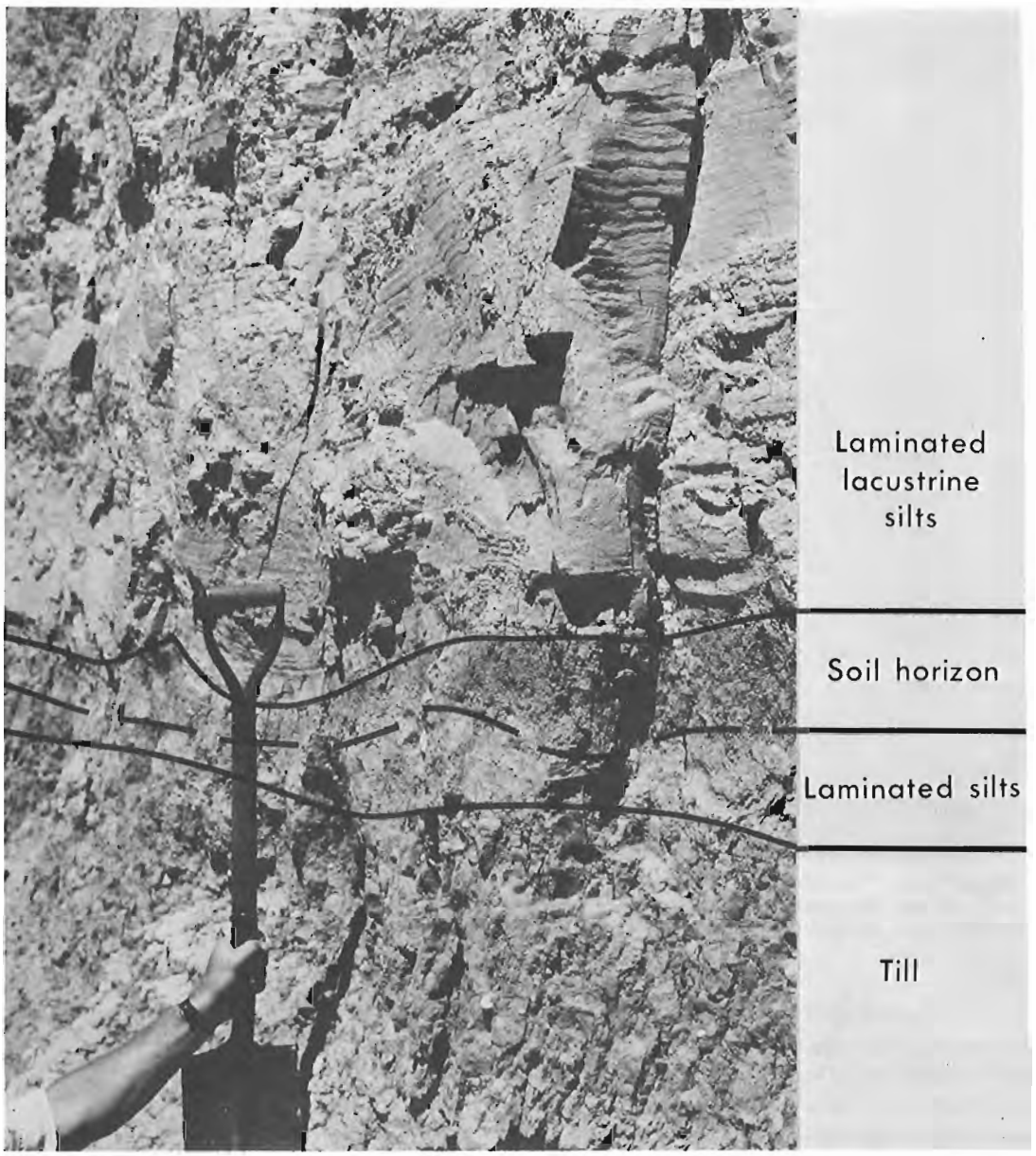


Figure 21.4. *Stratigraphy of Midnapore Bluff adjacent to the buried soil discussed in the text. Note the relief of the surface defined by the top of the soil. The dashed boundary denotes a gradational contact.*

The soil is approximately 3.5 m below the top of the cliff. It ranges from 8 to 16 cm thick, has a fine angular blocky structure, and is a mottled pale brown (10 YR 6/3). The soil is developed in about 10 cm of finely laminated pale brown (10 YR 7/4) silts which are overlain by very pale brown (10 YR 8/3) laminated lacustrine silt.

The mineralogy of the soil and enclosing silt was determined by X-ray diffraction. The mineralogy of the three samples appears to be essentially the same (Fig. 21.5, Table 21.1). The soil, however, contains a significant amount of gypsum whereas it is absent in the enclosing sediments. The presence of gypsum with no enrichment of carbonate would put it in a "Cs" soil horizon classification (Agriculture Canada, 1974).

A pedogenic origin for this gypsiferous band is favoured over other possible origins for the following reasons:

1. The band grades downward into nongypsiferous silt and is abruptly overlain by nongypsiferous silt even though the three sediments are similar in texture. These types of successional relationships could be associated with an eroded and buried soil but would not be a likely product of the zonation effects of groundwater fluctuations.
2. The surface of the soil is not planar but undulates. Maximum relative relief is about 15 m over the ~10 m length of the exposure (Fig. 21.3). Such undulations indicate that the surface of the horizon demarcates an erosional surface.
3. The lamellae of the overlying lacustrine silt thicken over troughs and thin over peaks defined by the surface of the soil. This corroborates the preceding point by indicating that an uneven surface was present at the time of the ponding of the lake that deposited the overlying lacustrine sediments.

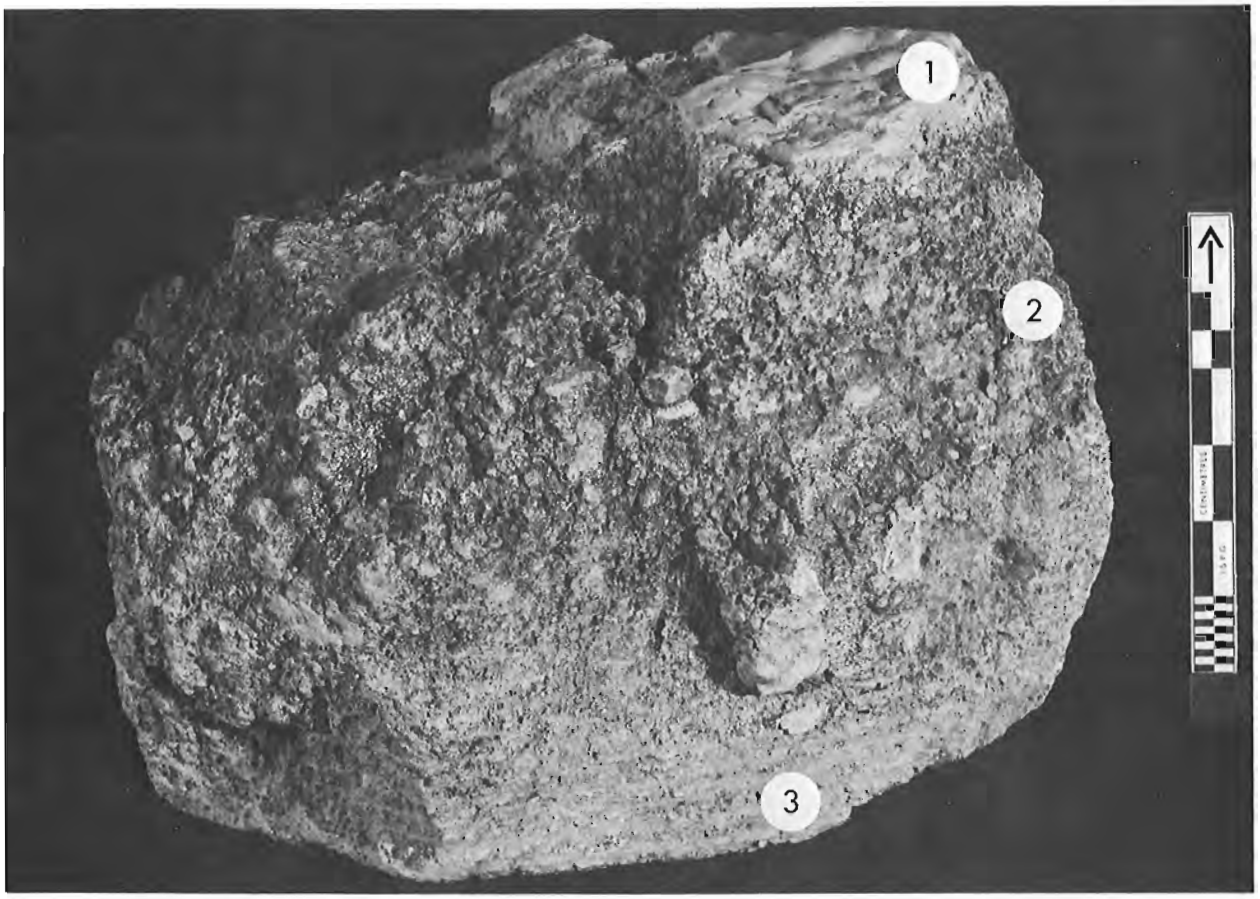


Figure 21.5. *A sample of the Midnapore Bluff soil showing the gradational nature of the contact between the soil and the underlying silt and the abrupt contact with the overlying silt. The numbers indicate the positions of samples analyzed for mineralogy (see Table 21.1)*

Table 21.1

Mineralogy of the Midnapore Bluff Soil and surrounding sediments determined by X-ray diffraction analysis[1]

Mineral (%)	Sample (cf. Fig. 21.5)		
	1	2	3
Montmorillonite	5	-	2
Illite	6	6	3
Gypsum	-	2	-
Kaolinite and chlorite	5	4	2
Quartz	70	75	70
Feldspars	4	5	10
Calcite	4	4	4
Dolomite	6	4	9

[1] Percentages are semi-quantitative results approximated from diffraction peak heights which may vary with type of mineral, its degree of crystallinity, crystal size, and with any amorphous material present.

The soil and silts are underlain by more than 2 m of till which is correlated with the till associated with the Foothills Erratics Train (Jackson, 1977, 1978a).

Significance of the Midnapore Bluff Soil

The till that directly underlies the Midnapore Bluff soil recently has yielded a small spruce log which produced a radiocarbon date of 49 400 ± 1000 years (GSC-2409; Jackson, 1978a,b). This log was exhumed during the excavation of a recreational lake several kilometres to the northwest in Midnapore (M. Wilson, pers. comm., 1977). The radiocarbon age is beyond the range of standard radiocarbon dating techniques. The till, therefore, probably is not late Wisconsinan in age. Furthermore, it would appear that the lacustrine sediments overlying the soil were laid down in a lake formed as a result of blockage of Bow Valley to the east by a late Wisconsinan advance of the Laurentide Ice Sheet. The maximum altitude of the surface of this lake, and presumably the margin of the ice sheet in Bow Valley, was approximately 1036 m. This figure is based on the highest elevation at which deposits of the lacustrine silt are found. This altitude agrees with Stalker's (1977) estimates as to the maximum elevations reached by the Laurentide Ice Sheet in the Calgary area.

The presence of the soil between till and lacustrine silt indicates a significant ice free hiatus between the two glacial episodes responsible for the deposition of these sediments.

The absence of any till unit above the soil, or evidence of ice overriding of the overlying lacustrine deposits, indicates that there have not been any advances of Laurentide ice into the Foothills in the Calgary area since at least the early Wisconsinan stage.

Conclusions

New evidence strongly supports the existence of an ice free corridor in the Foothills and westernmost prairies near Calgary since at least the early Wisconsinan stage. Two radiocarbon dates from a bog in Sheep River basin indicate that glaciers originating in the Rocky Mountains have not advanced beyond the mountain front for at least the last 18 500 years. Physiographic evidence and geomorphic considerations also indicate that glaciers from major drainage basins to the north and south of the Sheep River basin also terminated at the mountain front.

A buried soil of at least mid-Wisconsinan age is found near Calgary beneath lacustrine silts laid down in a proglacial lake dammed by the late Wisconsinan advance of the Laurentide Ice Sheet. The lack of any till units above the soil indicates that there was no advance of Laurentide ice beyond this point into the foothills since at least early Wisconsinan times.

Acknowledgments

The author expresses his appreciation to Angus Ferguson, Peter Putnam, Patrick Harte, and L.V. Hills who gave unselfishly of their time to aid in bog coring operations under difficult winter conditions.

References

Agriculture Canada
1974: The system of soil classification for Canada; Canada Department of Agriculture, pub. 1455, 255 p.

Alley, N.F.
1973: Glacial stratigraphy and the limits of Rocky Mountains and Laurentide ice sheets in southwestern Alberta, Canada; Canadian Society of Petroleum Geologists, Bulletin, v. 21, no. 22, p. 153-177.

Jackson, L.E., Jr.
1977: Quaternary stratigraphy and terrain inventory of the Alberta portion of the Kananaskis Lakes 1:250,000 sheet (82-J); unpublished Ph.D. dissertation, Department of Geology, University of Calgary, 478 p.

1978a: Quaternary stratigraphy and history of the Alberta portion of the Kananaskis Lakes 1:250,000 sheet (82-J) and its implications for the existence of an ice free corridor during Wisconsin time (Abst.); American Quaternary Association, 5th biennial meeting, p. 13-15.

1978b: Commentary on "Catastrophic termination of the last Wisconsin ice advance, observations in Alberta and Idaho" and "Inundation topography in the Columbia River system by C.W. Hunt in the June 1977 issue"; Bulletin of Canadian Petroleum Geology, v. 26, no. 1, p. 164-166.

Reeves, B.O.K.
1973: The nature and age of the contact between the Laurentide and Cordilleran ice sheets in the western interior of North America; Arctic and Alpine Research, v. 5, no. 1, p. 1-16.

Rutter, N.W.
1972: Geomorphology and multiple glaciation in the area of Banff, Alberta; Geological Survey of Canada, Bulletin 106, 54 p.

Stalker, A.M.
1956: The erratics train, Foothills of Alberta; Geological Survey of Canada, Bulletin 37, 31 p.

1968: Geology of the terraces at Cochrane; Canadian Journal of Earth Sciences, v. 5, p. 1455-1466.

1973: Surficial geology of the Kananaskis Research Forest and Marmot Creek basin region of Alberta; Geological Survey of Canada, Paper 72-51, 25 p.

1977: The probable extent of classical Wisconsin ice in southern and central Alberta; Canadian Journal of Earth Sciences, v. 14, no. 11, p. 2614-2619.

Stalker, A.M. and Harrison, J.E.
1977: Quaternary glaciation of the Waterton-Castle River region of Alberta; Bulletin of Canadian Petroleum Geology, v. 25, no. 4, p. 882-906.

Wilson, M. and Churcher, C.S.
1978: Late Pleistocene **Camelops** from the Gallelli Pit, Calgary, Alberta, morphology and geologic setting; Canadian Journal of Earth Sciences, v. 15, no. 5, p. 729-740.

22. RECONNAISSANCE STUDIES OF THE PRECAMBRIAN CRYSTALLINE BASEMENT ON DEVON ISLAND, DISTRICT OF FRANKLIN

Project 760023

Thomas Frisch
Regional and Economic Geology Division

Frisch, Thomas, Reconnaissance studies of the Precambrian crystalline basement on Devon Island, District of Franklin; in Current Research, Part A, Geol. Surv. Can., Paper 79-1A, p. 113-114, 1979.

Abstract

The metamorphic rocks on the south coast and part of the north coast of eastern Devon Island were mapped. Massive to gneissic biotite granulite is the predominant rock type. Retrogression of granulite to granitoid gneiss of amphibolite facies is common and in many places severe. Metasedimentary garnet ± sillimanite gneiss underlies large areas of the south coast and is commonly interlayered with granulite, suggesting that the latter is also of metasedimentary origin. Deformation has generally been intense and affected all units of the basement except the diabase dykes.

Introduction

Continuing the 1:250 000 scale reconnaissance mapping of the northernmost part of the Churchill Province, begun on Ellesmere Island in 1977, basement exposures on eastern Devon Island were studied during July 1978. Work was restricted to the southern, and parts of the northern coastal regions.

Basically, Devon Island consists of a west-dipping homocline of Paleozoic strata unconformably overlying Precambrian basement. The latter is exposed to an increasing degree eastward on the eastern half of the island (Fig. 22.1).

Crystalline Basement

By far the predominant rock in the basement areas mapped is massive to gneissic granulite, which has orthopyroxene and biotite as the chief mafic minerals and in which quartz is commonly blue. Typically, this rock is green on the fresh surface but weathers brownish or reddish. At numerous localities, the granulite has been downgraded to the amphibolite facies as a result of granitization. Attendant major changes in the field aspect of the rocks are a red or pink, rather than green, colour, an increase in potassium feldspar, and veining by pink granite. All gradations from green granulite to pink granitic gneiss are present. The retrogression in the Truelove Inlet area has been well documented by Krupička (1973).

Pink biotite-quartz-feldspar, i.e. granitic, gneiss, present locally along the south coast, may well be completely retrograded granulite.

Northeast of Dundas Harbour, at the edge of the ice cap, granulite gneiss contains concordant layers up to several metres thick of granitic gneiss. Primary features indicative of intrusion by the granite are preserved. Evidently, strong deformation occurred subsequently or at least concomitantly. This evidence and the fact that the granitized granulite is invariably highly deformed testify to the pre- or syntectonic nature of granitic intrusion in this part of the Churchill Province (Frisch et al., 1978).

Metasedimentary gneiss, rich in biotite and garnet and locally containing sillimanite, is common, particularly in Powell Inlet and the vicinity of Cape Sherard where extensive tracts occur. Interlayering of these rocks with typical biotite granulite on the scale of metres suggests that the latter is also of metasedimentary origin. In the Truelove Inlet area, Krupička (1973) has termed "garnet migmatites" what is here called metasedimentary gneiss. Marble was not seen, and amphibolite is sparse, on Devon Island, in contrast to Ellesmere Island where these rocks are relatively commonly associated with pelitic metasediments (Frisch et al., 1978).

Deformation has been intense throughout the crystalline basement, as shown by intricate small-scale folding, occasional major recumbent folds, and cataclasis. No preferred structural trends are apparent in the areas examined during the present work nor can structures in the overlying Paleozoic rocks be related to structures in the basement.

Unmetamorphosed diabase dykes of Precambrian age trend predominantly west-northwest and appear to be more abundant towards the east. Dykes in the basement seem to be more common on Devon Island than on Ellesmere Island.

Contacts with Younger Rocks

At the mouth of Powell Inlet, unmetamorphosed sedimentary rocks of the upper Proterozoic Strathcona Sound Formation (G.M. Narbonne, pers. comm., 1978) rest with angular unconformity on granulite gneiss. Elsewhere, the crystalline basement is overlain directly by Cambrian strata but the contact is rarely exposed. Wherever examined, the basement is notably free of weathering at contacts with younger rocks.

An early report of red sandstone overlying gneiss between Cape Warrender and Cape Sherard (Haughton, 1860) was found to be erroneous.

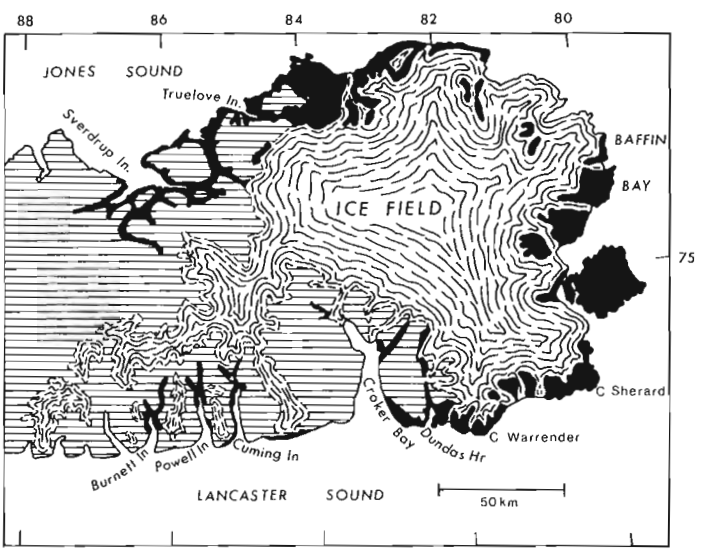


Figure 22.1. *Geological sketch-map of eastern Devon Island, showing the areas of Precambrian crystalline basement (black) and Paleozoic rocks (lined) and localities mentioned in the text.*

Acknowledgments

I am grateful to L. MacLaren for assistance in the field; to R. Thorsteinsson for providing base camp facilities and helicopter and Otter flying time; and to the Polar Continental Shelf Project for Twin Otter support.

References

Frisch, T., Morgan, W.C., and Dunning, G.R.
1978: Reconnaissance geology of the Precambrian Shield on Ellesmere and Coburg islands, Canadian Arctic Archipelago; in Current Research, Part A, Geological Survey of Canada, Paper 78-1A, p. 135-138.

Haughton, S.
1860: Geological account of the Arctic Archipelago; in A Narrative of the Discovery of the Fate of Sir John Franklin and his Companions, by F.L. M'Clintock; J. Murray, London, p. 371-396.

Krupička, J.
1973: Granulite facies rocks on northeastern Devon Island, Arctic Archipelago; Geological Survey of Canada, Paper 73-8.

MINERALS OF THE FRANCON QUARRY (MONTREAL ISLAND): A PROGRESS REPORT

Project 640048

Ann P. Sabina
Central Laboratories and Administrative Services Division

Sabina, Ann P., Minerals of the Francon Quarry (Montreal Island): A progress report; in Current Research, Part A, Geol. Surv. Can., Paper 79-1A, p. 115-120, 1979.

Abstract

Some sixty minerals are described from a dawsonite-rich silicocarbonatite sill which intrudes Ordovician limestone at the Francon quarry in Montreal, Quebec. Of these minerals, four are newly established species unique to this locality: weloganite, dresserite, hydrodresserite and strontiodresserite. In addition, there are four unidentified minerals, possibly new species, on which further investigation is in progress.

Since the original description of minerals occurring in the Francon quarry was published (Sabina, 1976), subsequent quarry operations exposed additional mineral assemblages, and the number of confirmed mineral species is now double that previously reported. Some of the minerals which were reported as "unknowns" have since been identified and two new species – hydrodresserite and strontiodresserite – established. This report describes briefly all minerals encountered to date in the sill rock. The quarry is operated by Francon Division de Canfarge Limitée to whom the author is indebted for granting frequent access to the quarry for collecting specimens.

The Francon quarry, located on Montreal Island, is a unique locality in which dawsonite-rich silicocarbonatite sills intruding Ordovician (Trenton) limestone contain an unusual suite of minerals including several new species – weloganite, dresserite, hydrodresserite, strontiodresserite – which are not known to occur elsewhere. The sills are composed principally of potassium feldspar and dawsonite with variable amounts of quartz, analcime, aegirine-augite, dolomite, siderite and albite (Jambor et al., 1976). An unusual feature is the significant zirconium and niobium content which is higher than the normal concentration of these elements in igneous rocks (Steacy and Jambor, 1969). The sills are characterized by numerous cavities ranging from a few millimetres to several centimetres in diameter; the cavities contain one or several of about sixty mineral species. Most of the minerals described in this report occupy cavities in the sill rock with notable different assemblages in the upper and lower level sills. In assemblage A, albite, quartz, dawsonite and calcite are the principal minerals lining vugs, with less abundant strontianite, barite, cryolite, fluorite, pyrite; the newly described species, and a few other minerals believed to be new species, are associated with assemblage A which is characteristic of the upper level sill. Assemblage B, which occurs in the lower sill, consists predominantly of calcite, dawsonite, fluorite, quartz, analcime and albite with abundant strontianite, celestine, barite, montmorillonite, marcasite and hematite. Of the new mineral species, this investigation found only weloganite to occur in assemblage B.

Acmite - Olive-green to brown blades averaging 1 mm long and generally associated with analcime.

Albite - Colourless, white plates generally in upright position lining vugs.

Analcime - Colourless, yellow, orange, green, brown trapezohedral crystals, white cubes; white powdery, sugary, porcelain-like. Globular aggregates commonly form an overgrowth on analcime-fluorite-ankerite assemblages. Shells of crystals are common in lower level.

Anatase - Tan compact finely granular aggregates in sill rock; powdery coating on brookite and ilmenorutile; grey submetallic flaky aggregates in vugs.

Ankerite - Cream-white, yellow, greenish yellow crystal aggregates, rosettes, commonly associated with dawsonite, analcime, fluorite, etc. in lower level.

Apatite - Smoky transparent euhedral grains in sill rock.

Baddeleyite - Tan-coloured, light yellow to amber scaly, finely granular, powdery sheets and coatings associated with assemblage B. Zircon (cyrtolite variety) is commonly intimately associated with it. Uncommon.

Barite - Colourless, white, grey, yellow, pink to orange-red tabular, acicular, blade-like crystals forming random and divergent groups; rosettes; stacked plates; granular massive; chalk white spheres, sheets, slivers, ellipsoids.

Brookite - Greenish black to black, submetallic or velvety plates forming rosettes (measuring up to 1 mm in diameter) on dawsonite-albite-quartz lining in vugs; granular aggregates in massive dawsonite along margin of vugs. Intimately associated with ilemnorutile. Uncommon.

Calcite - Colourless, white, yellow, lilac (rare), grey crystals and massive; varied habit including cones, barrel, spear and tulip shapes; globular. Shells of rhombohedrons with interior partly or completely leached out are relatively common. Crystal aggregates also occur in the limestone. Some of the calcite fluoresces pink under "short" ultraviolet light.

Celestine - Colourless, white, pink, yellow, grey, blue tabular prisms in random or divergent orientation; fibrous, acicular, blade-like; white porcelain-like crust on weloganite crystals. Commonly coated with botryoidal hematite. Very common in lower level.

Chalcedony - White, bluish, grey in vugs with calcite, quartz. Uncommon.

Cristobalite - White to bluish botryoidal associated with quartz-dolomite-celestine; chalk-white matted fibres forming compact and vesicular masses (up to 3 mm thick) associated with dolomite crystals, calcite cones, marcasite and pyrite.

Crocoite - Yellow waxy patches in microcrystalline intergrowths of dawsonite and K-feldspar which also contains pyrochlore, pseudorutile and siderite.

Cryolite - Colourless, yellow crystals and finely crystalline aggregates associated with weloganite. Yellow crystals (averaging 1 mm in diameter) are rare and were found in lower level; colourless crystals (measuring up to 4 mm in diameter) are relatively common in vugs containing weloganite, and are generally coated with: (a) a thin film consisting of fluorite admixed with unknown No. 3, or (b) with a crust of unknown No. 3 which, when the cryolite has been completely or partially leached out, forms shells that retain the original cryolite crystal form.

Cyrtolite - See zircon.

Dachiardite (sodium-rich) - White acicular crystals, fibres forming parallel and divergent groups associated with weloganite, analcime, ankerite, quartz in lower level. Pronounced silky lustre. Rare. Previously reported (Sabina, 1976) as unknown No. 9.

Dolomite - Colourless, white, light yellow, pink crystals; granular massive.

Dawsonite - Colourless prisms striated along length; acicular and fibrous forming tufts, spheres, rosettes and in random orientation; white waxy spheres; flaky, scaly, fibrous aggregates forming fluffy to compact masses with silky lustre.

Dresserite - Colourless transparent blades forming tufts, spheres (measuring up to 4 mm in diameter) associated with weloganite in upper level. Blades are bluntly terminated at surface of spheres and taper toward the centre. Dresserite – $BaAl_2(CO_3)_2(OH)_4.H_2O$ – is one of four newly described species from this locality (Jambor et al., 1969) and was named in honour of John A. Dresser in recognition of his contributions to the geology of the Monteregian Hills.

Elpidite - Colourless, white, fibrous, acicular aggregates in parallel, divergent or random arrangement; vitreous to silky lustre. Individual crystals measure up to 2 mm long. Associated with weloganite, yellow cryolite or synchysite in lower level. Rare.

Fluorite - Colourless, white, light to dark purple and almost black, pink, grey, brown, light green crystals (measuring up to 2 mm along the edge); lilac-coloured finely crystalline to sugary aggregates some of which form botryoidal crusts over finely fibrous masses of dawsonite; white spheres; black finely granular patches in massive dawsonite (particularly along edges of vugs) and in sill rock. Common, especially in lower level.

Galena - Crystals (averaging 2 mm along an edge) and massive associated with weloganite; also occurs in sill rock.



Figure 23.1. *Silicocarbonatite sill exposed at about midpoint along the east wall of the Francon quarry. This section of the sill contains weloganite and local concentrations of (1) unknown No. 10 and (2) unknown No. 5, both of which are believed to be new species. Lower part of the photograph shows southerly extent of quarry operations in the lower level in August, 1978. GSC 175385*

Garnet (almandine) - Pink massive associated with massive dawsonite in sill rock. Uncommon.

Goethite - Ochre yellow, brown, silky to velvety fibres and flakes forming rosettes, discs; earthy and scaly coatings. Relatively common in assemblage B.

Graphite - Flakes and aggregates in sill rock.

Gypsum (selenite) - Colourless platy sheets (commonly 5 cm thick) and tabular crystals associated with dolomite, quartz; acicular crystals and rosettes associated with natrojarsite. Uncommon.

Halite - Admixed with nahcolite forming friable white string-like and irregular patches on sill rock. Rare; in lower level.

Harmotome - Grey clay-like crust on weloganite, calcite, fluorite, etc. in lower level sill. Rare.

Hematite - Reddish brown to black pulverulent and finely botryoidal encrustations on celestine, calcite, quartz, barite, dawsonite, etc. in lower level.

Hydrocarbon - Amber, brown to black, transparent to opaque, celluloid-like film or crust on weloganite, calcite, dawsonite, quartz, albite. Smooth surface except on weloganite where it is ridged conforming to the transverse grooves on weloganite crystals. The hydrocarbon is brittle and can readily be peeled or washed off. Common in upper level.

Hydrocerussite - Grey to white powdery, silky coating on galena.

Hydrodresserite - White tuffs, hemispheres, spheres as in dresserite to which it dehydrates unless retained in a relatively humid atmosphere. Associated with weloganite in upper level. Hydrodresserite – $BaAl_2(CO_3)_2(OH)_4.3H_2O$ – is one of four newly described minerals from this locality and was named in allusion to its chemical composition and origin (Jambor et al., 1977). It was previously reported (Sabina, 1976) as unknown No. 2.

Ilmenorutile - Black velvety to greenish black submetallic plates (measuring up to 1 mm in diameter) in dawsonite-calcite masses in vugs and along margins of vugs; individual plates and rosettes on crystals of dawsonite, quartz, albite, calcite lining vugs. Uncommon; in upper and lower level sills.

Kaolinite - White silky to waxy flakes forming friable aggregates, microspheres; pulverulent, paint-like, compact. Previously referred to (Sabina, 1976) as unknown No. 7. Occurs in upper level, but more widespread in lower level.

K-feldspar - Pink, cream-white, platy in vugs with analcime, dawsonite, quartz.

Magnetite - Massive associated with smythite, pyrrhotite, pyrite, dawsonite. Rare.

Marcasite - Blades, prisms, plates, fibres forming rosettes, stars, crosses, spheres and randomly oriented aggregates. Very common in assemblage B; also occurs with crystal aggregates of calcite in limestone.

Molybdenite (2H) - Flakes associated with weloganite. Rare.

Montmorillonite - White, greyish green, waxy flakes, fibres forming felt-like, compact or friable masses and spherical aggregates. Expands with absorption of water and becomes viscose and gelatinous. Common in assemblage B. Previously referred to as unknown No. 8 (Sabina, 1976).

Mordenite - White matted, woolly or compact fibres forming sheets, hemispheres, irregular masses in association with (a) ankerite, analcime, dachiardite and weloganite, (b) with cristobalite, and (c) with dolomite, quartz, celestine and marcasite. Uncommon; in lower level.

Nahcolite - White friable silky to earthy fibrous or granular aggregates forming rosettes, string-like and irregular patches on sill rock. Intimately associated with halite. Rare; lower level.

Natrojarosite - Ochre yellow to rusty, earthy, scaly, powdery encrustations on crystals of marcasite and pyrite and on botryoidal pink sphalerite occurring in quartz-lined fractures in the sill rock. Uncommon; in lower level.

Pseudorutile - Black submetallic finely granular patches in microcrystalline intergrowth of potasium feldspar and dawsonite. Uncommon.

Pyrite - Crystals of various forms (measuring up to 1.5 mm along an edge); spheres (averaging 0.5 mm in diameter); acicular, fibrous, botryoidal. Common in upper and lower level sills. Also occurs with crystal aggregates of calcite in limestone.

Pyrochlore - Orange granular aggregates associated with (a) barite, pyrite, zircon in sill rock, and (b) with pseudorutile, siderite, crocoite in potassium feldspar-dawsonite intergrowths. Tan-coloured octahedra occur in sill rock (Jambor et al., 1976).

Pyrrhotite - Bronze flakes on crystals of colourless cryolite, weloganite, quartz and albite; also associated with smythite on bluish quartz lining vugs.

Quartz - Colourless, white, smoky prisms; colourless to white sheaf, artichoke, and leaf-like forms; rosettes, hemispheres and massive.

Rozenite - White powdery coating on pyrite, marcasite.

Siderite - Yellow, amber, greenish yellow crystal aggregates. Tan to dark brown, massive in sill rock.

Smythite - Dark brown to almost black metallic flakes, plates, rosettes (averaging 0.5 mm in diameter) commonly admixed with pyrrhotite. Associated with dawsonite, quartz, ankerite, calcite, albite in lower level. Rare.

Sphalerite - Yellow, amber, orange-red crystals or massive associated with dawsonite, weloganite, calcite; pink to reddish botryoidal aggregates associated with natrojarosite.

Strontianite - Colourless, white, yellow, yellowish green, amber, pink, tabular, prismatic, blade-like crystals; fibrous to acicular forming spheres, tufts, parallel bundles, sheaves; plates forming columns and roses; finely granular to porcelain-like masses; waxy globules. A very common mineral in upper and lower levels.

Strontiodresserite - White silky tapered blades forming ring-shaped and irregular coatings on frosty white quartz crystals in vugs containing strontianite, weloganite; radiating blades forming white spheres (measuring up to 1 mm in diameter) on weloganite and on quartz crystals. A new species originally described from this locality (Jambor et al., 1977), strontiodresserite – $(Sr,Ca)Al_2(CO_3)_2(OH)_4.H_2O$ – was previously referred to (Sabina, 1976) as unknown No. 6. It is a strontium analogue of dresserite and was so named in allusion to this chemical relationship. Occurs in upper level; uncommon.



Figure 23.2. *Scanning electron photomicrograph showing blade-like crystals forming sphere of dresserite. X70 GSC 203441*

Sulphur - Black sooty to earthy aggregates admixed with pyrite, and cream-coloured powdery masses admixed with sphalerite. Occurs in association with natrojarosite.

Synchysite - White silky spheres (measuring up to 1 mm in diameter); silky white, grey, tan-coloured fibrous, flaky or powdery aggregates. Associated with marcasite, celestine, barite in assemblage B. Also dark brown platy aggregates associated with dawsonite, weloganite in upper level. Uncommon.

Thenardite - Dull white powdery encrustations on sill rock and on limestone.

Thorbastnaesite - White silky to dull spheres (measuring up to 750 microns in diameter) composed of radiating fibres; aggregates of fine fibres forming coatings. Associated with baddeleyite, zircon (cyrtolite) in assemblage B. Rare.

Weloganite - Colourless, white, light yellow to greenish and orange-yellow grading to pink, light green to olive green, grey, reddish (due to iron oxide inclusions); transparent to opaque six-sided crystals with pedion or pyramidal terminations; tabular crystals; flaky and granular aggregates. Fluoresces (weak to moderately strong) when exposed to ultraviolet light: yellow, greenish and orange-yellow, pink to pinkish orange and dull red. Occurs in upper and lower levels, but more abundantly in upper level. Weloganite – $(Sr,Ca)_3ZrNa_2(CO_3)_6.3H_2O$ – was the first of four newly established species originally described from this locality (Sabina et al., 1968). It was named in honour of Sir William E. Logan, founder and first director of the Geological Survey of Canada, who laid the foundation of our knowledge of the geology of the Montreal area.

Zircon - Pink, yellow, amber, brown, grey euhedral grains embedded in sill rock. Grey, tan and cream-coloured granular aggregates forming plates and sheets in vugs containing minerals of assemblage B. Cyrtolite variety occurs as light yellow, tan, amber, grey, dull to waxy, sugary or smooth plates or sheets in assemblage B. Uncommon.

Unidentified Minerals - Of the six minerals previously reported (Sabina, 1976) as unknowns, two were since established as new species; hydrodresserite (unknown No. 2) and strontiodresserite (unknown No. 6), and the identification of three others was confirmed: kaolinite (No. 7), montmorillonite (No. 8) and sodium-rich dachiardite (No. 9). The current list of unknowns includes:

No.3: Chalk-white powdery coatings; also porcelain-like and waxy granular; white translucent globules and botryoidal crusts; white shells. Fluorescent and phosphorescent upon irradiotion with ultraviolet light: bluish white ("short" rays) and cream-white ("long" rays).

No. 5: White silky fine flakes forming compact, friable, or foamy aggregates associated with weloganite, dresserite, dawsonite, quartz, calcite, and unknown No. 3 from which it is distinguished by its silky lustre and nonfluorescent properties. A carbonate of Zr,Ti and Na. Occurs in upper level. Uncommon.

No. 10: White globules (measuring up to 250 microns in diameter) composed of radiating plates; porcelain-like surface and silky cross-section. Commonly occurs in clusters of globules. Generally occurs on weloganite crystals, but also on crystals of calcite and quartz. Associated minerals include: dawsonite, cryolite, unknown No. 3, albite, barite, dresserite, strontianite, pyrite, marcasite, fluorite and sphalerite. The weloganite, calcite and quartz crystals are commonly coated with a brown hydrocarbon and the white globules generally occur beneath and, less commonly, on top of this coating. Major elements as determined by qualitative microprobe analysis are Nb and Ca. Occurs in upper level; uncommon.

No 11: White finely globular crusts on crystals of quartz and calcite which line vugs. Believed to be an aluminum hydroxide with X-ray diffraction pattern similar to nordstrandite.



Figure 23.3. *Scanning electron photomicrograph of hydrodresserite showing coarse blades protruding from smooth surface of sphere. X60 GSC 203441-A*

Aids in Identifying and Collecting

Several of the minerals described in the preceding text occur as white spheres or hemi-spheres composed of radiating crystals. Minerals of the habit, which most closely resemble each other and commonly occur together, are difficult to recognize in the hand specimen; they include dresserite, hydrodresserite, dawsonite and strontianite. Dresserite and hydrodresserite are generally distinguishable only by X-ray diffraction. They may, however, be distinguished from dawsonite and strontianite when observed under magnification of 10x or higher. The distinguishing features are the individual crystals as they appear at the surface of the spheres: bluntly terminated blades in dresserite (Fig. 23.2) and hydrodresserite (Fig. 23.3); acutely pointed spears in strontianite (Fig. 23.4); and rhombic prisms in dawsonite (Fig. 23.5).

Synchysite and thorbastnaesite also occur as white spheres but do not exhibit characteristic crystal terminations at their surfaces which are relatively smooth and silky (synchysite) or waxy (thorbastnaesite). These two minerals are not known to occur in assemblage A with which dresserite and hydrodresserite are associated.

From the few specimens of strontiodresserite that were collected, it appears that its spheres are distinguishable from dresserite and hydrodresserite only by X-ray diffraction. Scanning electron photomicrographs indicate that the spheres are composed of obliquely terminated blades which taper toward the centre of the spheres as in dresserite and hydrodresserite.

Colourless crystals of cryolite and of calcite occur together and may pose difficulties in hand specimen identification. The features that distinguish these minerals are: calcite effervesces in HCl, whereas cryolite is unaffected; with a refractive index nearly that of water, cryolite disappears when immersed in water whereas calcite remains visible. Cavities containing cryolite crystals are commonly coated with a chalk-white crust composed of unknown No. 3 which may also form shells of crystals from which the cryolite is completely or partially leached out. As a guide to collecting, this chalk-white coating may be used as an indicator of the presence of cryolite in the cavities. It was also observed that cryolite is more common in the greenish grey or darker grey sill rock than in the greyish white portions of the sills.



Figure 23.4. *Scanning electron photomicrograph of strontianite sphere composed of radiating, acutely pointed spear-like crystals. X100 GSC 203441-B*

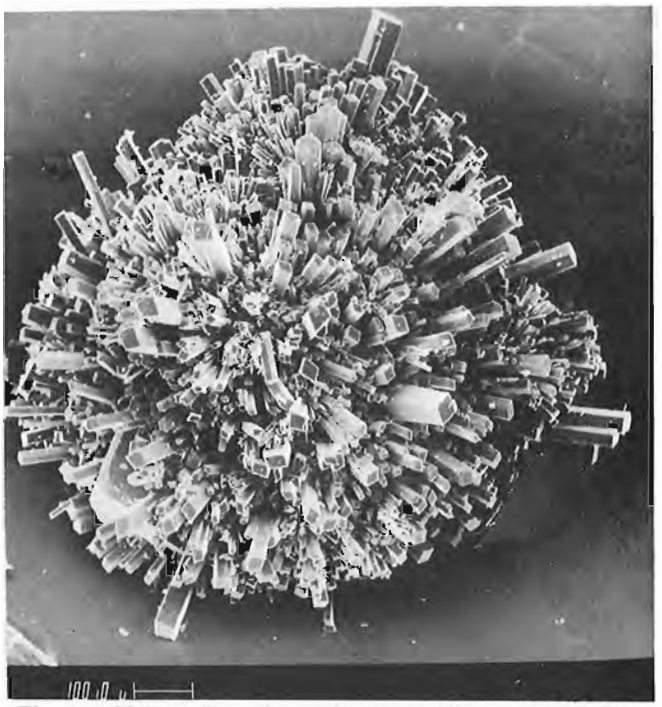


Figure 23.5. *Scanning electron photomicrograph showing rhombic prisms which form the dawsonite sphere. X80 GSC 203441-C*

Kaolinite and montmorillonite, both of which are common in the lower level, can readily be distinguished by the expansion of montmorillonite upon immersion in water; kaolinite is not affected.

Hematite may be used as in indicator of the presence of baddeleyite, thorbastnaesite and zircon in vugs; the hematite forms a prominent maroon-red to brownish red coating on crystals (calcite, celestine, dawsonite, quartz, etc.) lining cavities containing these minerals. Purple fluorite is a common accessory.

References

Jambor, J.L., Fong, D.C., and Sabina, Ann P.
1969: Dresserite, the new barium analogue of dundasite; Canadian Mineralogist, v. 10, p. 84-89.

Jambor, J.L., Plant, A.G., and Steacy, H.R.
1976: A dawsonite-bearing silicocarbonatite sill from Montreal Island, Quebec; in Report of Activities, Part B, Geological Survey of Canada, Paper 76-1B, p. 357-362.

Jambor, J.L., Sabina, A.P., Roberts, A.C., and Sturman, B.D.
1977: Strontiodresserite, a new Sr-Al carbonate from Montreal Island, Quebec; Canadian Mineralogist, v. 15, p. 405-407.

Jambor, J.L., Sabina, Ann P., and Sturman, B.D.
1977: Hydrodresserite, a new Ba-Al carbonate from a silicocarbonatite sill, Montreal Island, Quebec; Canadian Mineralogist, v. 15, p. 399-404.

Sabina, Ann P.
1976: The Francon quarry, a mineral locality; in Report of Activities, Part B, Geological Survey of Canada, Paper 76-1B, p. 15-19.

Sabina, Ann P., Jambor, J.L., and Plant, A.G.
1968: Weloganite, a new strontium-zirconium carbonate from Montreal Island, Canada; Canadian Mineralogist, v. 9, p. 468-477.

Steacy, H.R. and Jambor, J.L.
1969: Nature, distribution and content of zirconium and niobium in a silico-carbonatite sill at St-Michel, Montreal Island, Quebec; Geological Survey of Canada, Paper 69-20.

24.

A SCHEME FOR THE SEPARATION AND CHARACTERIZATION OF POSSIBLE METAL-ORGANIC SPECIES IN NATURAL WATERS: SOME PRELIMINARY DATA

Project 740081

Julian Lee
Resource Geophysics and Geochemistry Division

Lee, Julian, A scheme for the separation and characterization of possible metal-organic species in natural waters: Some preliminary data; in Current Research, Part A, Geol. Surv. Can., Paper 79-1A, p. 121-125, 1979.

Abstract

A trace metal speciation scheme is described which should aid attempts to elucidate the physiochemical nature of trace metals in natural waters. The technique involves a sequence of diafiltration and liquid chromatographic separations for the fractionation and characterization of water organics and associated metals. An ion-selective electrode is used to measure the copper binding capacity of natural waters before and after diafiltration. The distribution of Cu and Ni in various molecular weight fractions is determined. Preliminary measurements indicate that copper in stream waters is associated with organic matter of molecular weights near 5000.

Introduction

Over the last decade geochemical and environmental scientists have become increasingly aware of the significance of metal speciation in natural waters, and the need for reliable methods to determine the various chemical forms. Since the reactivity of any metal in natural waters is closely related to the chemical form in which it exists, a metals role is determined by the concentration of the different species present and not solely by the absolute metal concentration. Although the importance of metal speciation is now well appreciated, as attested to by the volume of recent literature, the present understanding remains incomplete and inadequate to explain a number of biological and geochemical phenomena.

Natural waters are not normally in a state of chemical equilibrium and many elements that form insoluble hydroxides are commonly present at concentrations greater than those predicted by computations based on solubility and acid-base equilibria alone. Naturally occurring organic materials such as humic and fulvic acids, carbohydrates and proteinaceous material play an important role in controlling the solubilities and activities of metals in natural waters, and in recent years the problem of the possible migration of chemical elements in the form of complex organic compounds, has attracted a great deal of attention (Singer, 1973; O'Shea and Mancy, 1976; Giesy and Briese, 1977; Florence and Batley, 1977; Takamatsu and Yoshida, 1978). The anomalous behaviour of Cu and Ni in sulphide rich environments may be explained in part by the exceptionally strong affinity these metals have for organic chelating agents which, perhaps, inhibits precipitation of metal sulphides (Gardner, 1974).

Methods for the measurement of trace metal speciation have been reviewed in papers by Florence and Batley (1976, 1977). Two basic approaches have been made; one making use of equilibrium and rate constants, together with total metal and ligand concentration data, to compute equilibrium concentrations of metal species; the other utilizing physical and chemical treatments, together with highly sensitive analytical methods, to provide direct measurements. Both methods possess inherent inadequacies in their approach. The lack of quantitative analytical data for natural waters and the failure to take into account "dissolved" metal present in a colloidal form, severely hinders the effectiveness of the computational treatment. Problems with the second approach arise in that many analytical and separation procedures used in chemical speciation studies may disrupt, at least to some extent, the solution equilibria between species. In the extreme, speciation artifacts may be produced.

This paper reports on preliminary studies involving methods for fractionating and characterizing natural water organics and measuring the relative importance of inorganic versus organic metal associations. Subsequent studies will be directed towards the goal of contributing to the understanding of the nature of metal-ion organic complexation and its role in hydrogeochemical and biological processes. The transition metals Cu and Ni were chosen for initial study because of their strong affinity to complex with carboxylic, hydroxyl and phenolic oxygen groups of natural water organic macromolecules. The analytical scheme outlined describes a combined diafiltration-chromatographical method for the fractionation of 'soluble' organic matter and associated metal. These procedures are coupled with analysis by anodic stripping voltammetry (ASV) and ion-selective electrodes (ISE). Routine analyses of selected fractions are performed by flameless atomic absorption spectrophotometry.

Methods and results

Diafiltration

Natural water samples are collected from just below the surface in 4-L polyethylene bottles which have been carefully cleaned with dilute solutions of nitric acid and doubly distilled water. Where precise dissolved organic carbon (DOC) analyses are to be performed, glass or pyrex containers precleaned with chromic acid and/or heating at 500°C are preferred. All samples are immediately filtered in the field through 0.2 µ macroporous filters; the necessary precautions having been taken to avoid contamination. Filters containing particulates are retained for future analysis and the filtrate stored at 4°C. A small aliquot is acidified for total element determinations by flameless atomic absorption methods (CRA).

Membrane ultrafiltration and dialysis has been used successfully to fractionate organic compounds from natural waters and separate them into nominal size fractions without losses and chemical extractions which may alter metal-organic associations (Gjessing, 1973; Schindler and Alberts, 1974; Giesy and Briese, 1977). The nature of Diaflo membrane filters theoretically minimizes membrane polarization. Simple salts are not retained by the membranes, and although they possess a net neutral charge there are some negatively charged membrane sites, and therefore the passage of negatively charged metal species may be restricted, even though they are small enough to pass (Hart and Davies, 1977). In this work diafiltration was selected as a convenient method for concentrating and manipulating natural water organics. The method has certain advantages over ultrafiltration or dialysis alone.

Table 24.1

Diafiltration of Cu, Ni and dissolved organics

Sample	% of total		Absorbance
	Cu	Ni	λ 254 nm
Trib. Indian River, Ont.[1]			
PM-10 retentate	< 1.0	0	0.080
PM-10 filtrate	99	100	0.305
DM-5 retentate	90	54	0.290
DM-5 filtrate	10	47	0.100
Clyde River, Ont.[2]			
PM-10 retentate	0	-	0.046
PM-10 filtrate	100	-	0.098
DM-5 retentate	-	-	0.103
DM-5 filtrate	-	-	0.038
UM-2 retentate	97.7	-	0.140

Properties of samples subjected to speciation studies:-

[1] XM-300A filtrate, 50 ppb Cu, Ni spike; pH 7.98; absorbance at 254 nm, 0.380; DOC, 14,000 $\mu g\ L^{-1}$

[2] 0.2 µm filtrate, 1.36 ppb Cu; pH 8.0; absorbance at 254 nm, 0.140; DOC, 6260 $\mu g\ L^{-1}$

Diafiltration offers a continuous or repeated exchange of process solution with fresh solvent washing out salts and micro-ions. The continuous process eliminates the requirement for constant operator attention and avoids the possibility of solute denaturation by over-concentration, which is of some importance in these studies. Diafiltration of natural water samples is effected using an Amicon TCF-10 ultrafiltration cell with Diaflo membranes offering a selection of macrosolute rejection levels from 500 to 300 000 molecular weight as calibrated with globular solutes. Each membrane is characterized by its nominal cut-off; i.e., its ability to reject molecules larger than a given size (Amicon Corporation, Lexington, Mass.). The best fractionation of natural water organics is obtained using UM-05 (mol. wt. cut-off 500) or UM-2 (mol. wt. 1000), DM-5 (mol. wt. cut-off 5000) and PM-10 (mol. wt. cut-off 10 000) membranes. All membranes have undergone the normal pretreatment procedures (i.e., removal of glycerine by washing with 10%-NaCl followed by flushing in the cell with large volumes of distilled water). The diafiltration equilibrium technique (wash-out) of Blatt et al. (1968) has been adapted to obtain binding profiles of copper and nickel to organic fractions from natural waters. Aliquots of natural stream or swamp water of known metal concentration (spiked or natural levels) are placed in the cell and diafiltered across a UM-2 or DM-5 membrane against doubly distilled water or 0.1M sodium bicarbonate buffer. Aliquots of the effluent are collected by an automated procedure and analyzed for the metal in question. Absorbance is routinely monitored at 254 nm to give a measure of organic carbon. The level of metal remaining in the cell, which represents bound species, is also obtained by appropriate analysis. The diafiltration process is discontinued when the metal concentration in the emerging dialysate has diminished close to background. A combination of pump speed and gas pressure is selected to provide a reasonable flow rate and moderate shear across the membrane. A very high shear rate, while attaining a faster flow, may be damaging to labile species.

The results from wash-out experiments of two natural river waters are reported in Table 24.1. In the first series Cu and Ni spikes of 50 $\mu g\ L^{-1}$ were added to 100 ml aliquots and diafiltration across selected membranes performed until the metal concentration and absorbance of the filtrate had fallen back to background. If it is assumed that retention is based on molecular weight only, and that absorbance at 254 nm is a measure of organic carbon, then the results indicate that the major part at the organic material has a nominal molecular weight of between 5000 and 10 000. Further fractionation of the DM-5 retentate by steric exclusion chromatography using Biol-Gel P-6 (Exclusion limit 6000 daltons) indicates the average molecular weight to be closer to 5000. For comparison, Alderdice et al. (1978) found average molecular weights of between 3600 and 6600, for fulvic acids from water samples. Copper is closely associated with this fraction, with 90 per cent being retained by the DM-5 filter. The somewhat lower binding capacity of nickel is reflected in the lower percentage retained by this membrane. The diafiltration profile for metal binding is sigmoidal in shape, with approximately five sample volumes of reservoir fluid through the membrane rendering exchange 99 per cent complete.

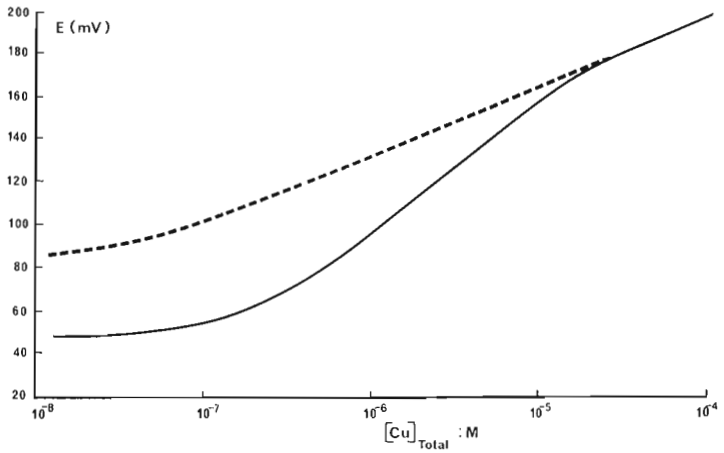
The second series of experiments was run with metal concentrations near natural levels. Taking into account the uncertainty of the method, close to 100 per cent recovery was achieved for copper using PM-10 and UM-2 filters.

Separation of fractions in this preliminary study was based on particle diameter only and although it is not possible using this technique to determine how metals are bound, the results indicate that copper, and to some degree nickel, is closely associated with organic carbon. For the water used in this experiment it appeared that maximum binding capacity for the higher molecular weight fraction was 45 $\mu g\ L^{-1}$ for copper and 27 $\mu g\ L^{-1}$ for nickel.

Fractionation on Macroreticular Resins

The methods of Junk et al. (1974), and Leenheer and Huffman (1976) are used to fractionate aliquots of the PM-10 filtrate on non-ionic macroporous resins (Amberlite XAD-2, XAD-8) into hydrophobic and hydrophilic components, the former being sorbed onto the column. The hydrophobic effect of the non-polar organic solutes in natural waters is due to their unfavourable entropy of solution caused by the ordering of water molecules around the organic macromolecule. This negative entropy promotes aggregation and removal of the non-polar solute with preferential adsorption onto the column (Thurman et al., 1978). Sequential elution with methanol and methanol-NH_4OH results in the collection of a neutral hydrophobic fraction and an acidic hydrophobic fraction. The distribution of Cu and Ni amongst the three fractions was determined.

Although the non-ionic, non-polar XAD-2 resin had a much greater adsorption capacity of natural water DOC than did the more polar XAD-8 (37 per cent versus 13 per cent) there was considerable irreversible adsorption on the XAD-2. Low recoveries of DOC by aqueous ammonia were also reported by Leenheer and Huffman (1976). From a Cu spike of 50 $\mu g\ L^{-1}$ into a natural water sample (DOC 6260 $\mu g\ L^{-1}$; pH 7.8), 16 per cent was contained in the hydrophilic fraction, approximately 6 per cent in the neutral hydrophobics with the remainder staying with the hydrophobic acids. Nickel tended to elute with the



——UM-05 retentate -----UM-05 filtrate

Figure 24.1. *Change in ion-selective electrode potential with increasing total copper concentration, pH 6.50, I.S.A. 0.1M $NaNO_3$, 25°C.*

hydrophilic fraction. Concentration and the time allowed for equilibration of the added metal with the natural water filtrates had a significant effect on the results. The concentration of Cu adsorbed on the resin doubled on going from 2 hours equilibrium time to 24 hours. The Cu associated with the hydrophobic fraction corresponds approximately to that retained with the DM-5 retentate from the diafiltration experiment.

Problems in reproducibility and increased adsorption with concentration of the samples indicate that there is probably no well defined break between the hydrophobic and hydrophilic organic solutes in the complex mixtures found in natural waters; hydrophobicity being closely related to increased molecular weight. It is also concluded that although XAD copolymers can be used for analytical separations and concentration of natural water organics, the strongly hydrolyzing acidic (pH <2) or basic (pH >8) solutions required for optimum elution, somewhat negate their usefulness in fractionating organic carbon molecules at the pH levels (pH 5-8) required to preserve existing metal-organic equilibria.

Measurement of complexation capacity

The use of ion-selective electrodes (Ramomoorthy and Kushner, 1975; Buffle et al., 1977; Takamatsu and Yoshida, 1978) and anodic stripping voltammetry (O'Shea and Mancy, 1976; Shuman and Woodward, 1977), can serve as convenient, precise and sensitive means of estimating the binding ability of natural water organics with a number of metal ions. Both methods are used to detect Cu present as cupric ion and data obtained from complexometric titrations are used to estimate conditional formation constants. The end-point of the titration of ligand with metal is an estimate of total free ligand concentration (or binding sites). It must be noted however that absolute estimations of so-called 'free' aquo-cupric ions by these methods are questionable, and instead, the data should be related to 'electrode detectable' copper, and may be compared to 'labile' forms. Simple inorganic and bidentate organic complexes are easily reduced and their contribution to the measured current, except for slight differences brought about by their diffusion rates, is the same as if all the metal existed as the simple aquated ion.

In this work a solid state cupric ISE (Model 94-29, Orion Research Inc., Cambridge, Mass.) is used to assess the degree of complexation of Cu with natural water organic molecules fractionated by diafiltration. The experimental conditions are similar to those reported by Buffle et al. (1977).

From the Nernst equation the response of the ISE is given by,

$$E = E_o + \frac{2.303\,RT}{nF} \log [Cu^{2+}]aq$$

at constant temperature and ionic strength. The degree of comlexation of Cu is defined as

$$\alpha = \frac{[Cu]_{Total}}{[Cu^{2+}]_{aq}}$$

From the Nernst equation log α may be computed:

$$\log \alpha = \log [Cu]_{Total} + \frac{E_o - E}{\rho}$$

E_0 and ρ (≃ 2.303RT/2F) are computed from a calibration curve. (e.g., titration curve of UV irradiated sample where organic matter has been destroyed). Plots of E versus $[Cu]_{Total}$ for the titration of a natural water sample (UM-05 retentate: MW>500) with cupric ions at pH 6.50 are shown in Figure 24.1. It can be seen that saturation of ligand(s) with copper occurs at about 2×10^{-5}M of metal ion concentration, further additions of Cu produce a typical Nernstran response. The computed curve for $\log\alpha = (\log [Cu]_{Total})$ is shown in Figure 24.2. The titration curve shown as the dashed line in Figure 24.1 is for the UM-05 filtrate of the same natural water sample at pH 6.50. Little or no cupric ion complexation is seen to occur and the curve approximates Nernstian behaviour. A similar result is obtained upon titration of a UV irradiated sample in which organic matter has been decomposed. This lends substantial weight to the argument that the ligand(s) titrated is organic in nature. Since the molecular weight range of the organic material was estimated to be from 500 to something a little in excess of 5000, three types of reactions for binding may be given: the formation of low molecular weight soluble com plexes with metal-ligand ratio 1:1 and probably labile; the complexation of metal by carboxylic and/or hydroxyl and phenolic sites of organic macromolecules; and the adsorption of hydrolyzed metal on colloidal organic matter or formation of mixed complexes with organic material and OH^-.

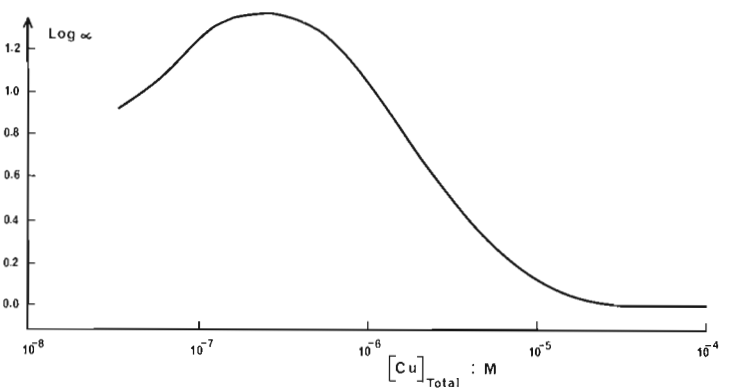


Figure 24.2. *Variation of α with total copper concentration (calculated from Figure 24.1).*

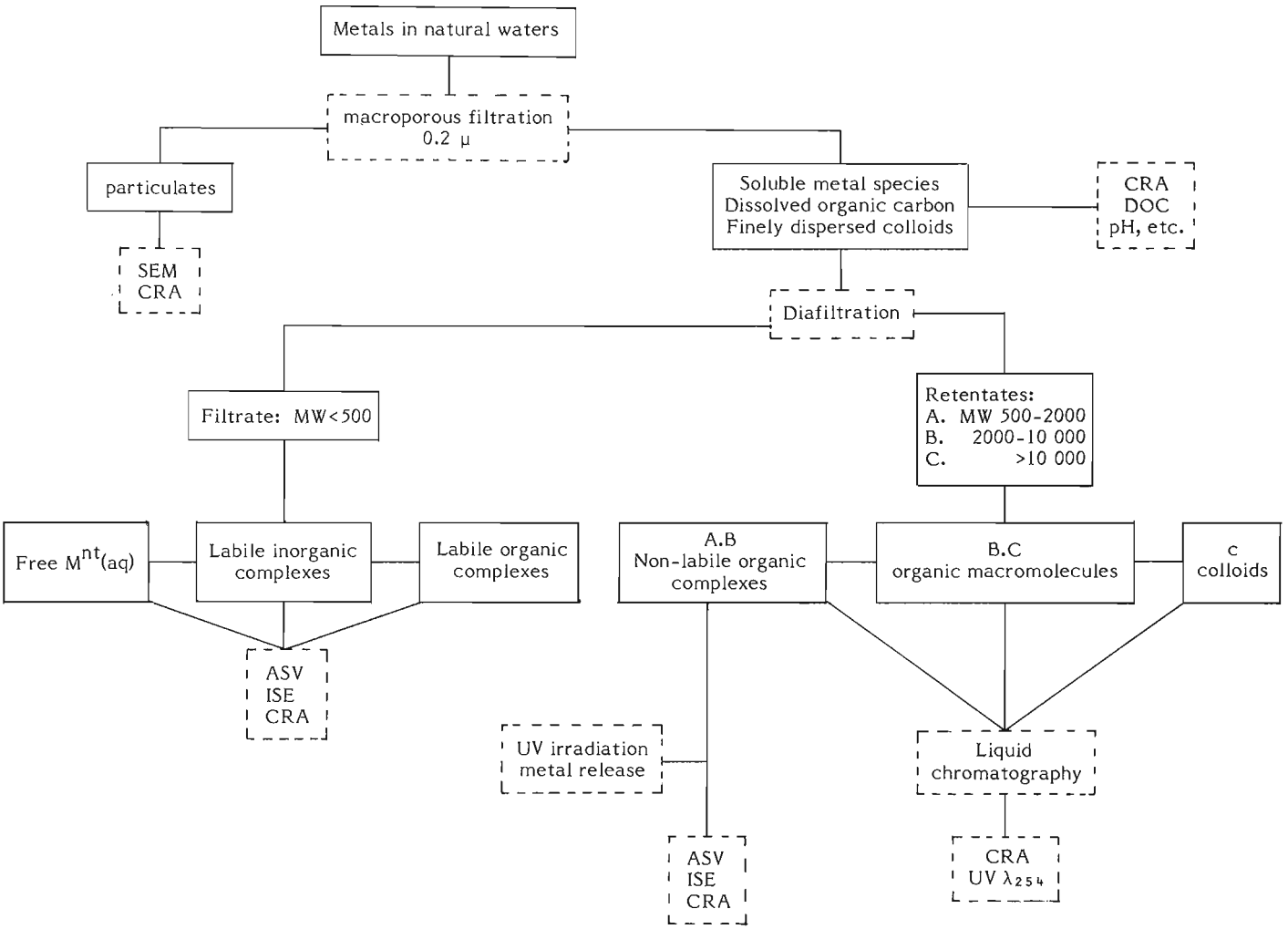


Figure 24.3. *Scheme for the study of chemical speciation in natural waters.*

It is hoped that further work utilizing the scheme shown in Figure 24.3 will be able to assess the relative importance of these mechanisms. No correlations were evident from this small sampling.

Discussion

A general scheme that will be implemented for the characterization of natural water samples is shown in Figure 24.3. Although it will not give absolutely complete analysis of the forms of various metals in natural water, it is hoped it will provide sufficient information to account for any effects the chemical characteristics of water may have on metal distribution. The analytical problems involved are complex and any scheme proposed for the study of metal speciation may induce some disturbances of solution equilibria. The procedures selected for this approach are designed to keep such effects at a bare minimum. Another serious limitation of the scheme is the time frame involved for analysis. Several hours and often days at the best are involved, therefore great care must be taken over the water storage.

The preliminary data using this system in natural waters show that significant differences exist between the size and composition of the organic macromolecules in unpolluted waters, and that there is substantial interaction of this material with inorganic cations. Further work is to be conducted to investigate various organic enriched natural waters containing varying levels of transition metals (Cu, Ni, Co). Diafiltration will be used to concentrate and manipulate water samples prior to further characterization and separation using liquid chromatographical techniques such as steric exclusion chromatography and reverse-phase high-pressure liquid chromatography. Conventional ASV and ISE is used for labile-total metal differentiation, where applicable, and includes an ultraviolet irradiation step to destroy complexing organic matter. It is noted that irradiation may also break down small inorganic colloidal particles, thus removing potential sorption sites for trace metals.

Ideally a complete dissolved metal speciation analysis of any water body for geochemical purposes should be accompanied by a study of suspended and bottom sediments, together with a limnological and geological interpretation of source material. However, these complications are reserved for future work.

References

Alderdice, D.S., Craven, B.R., Creswick, W., and Johnson, W.D.
1978: Humic substances in swamps of the Myall Lakes Region, N.S.W.; Australian Journal of Soil Research, v. 16, p. 41-52.

Blatt, W.F., Robinson, S.M., and Bixler, J.H.
1968: Membrane ultrafiltration: The diafiltration technique and its application to microsolute exchange and binding phenomena; Analytical Biochemistry, v. 26, p. 151-173.

Buffle, J., Greter, F., and Haerdi, W.
1977: Measurement of complexation properties of humic and fulvic acids in natural waters with lead and copper ion-selective electrodes; Analytical Chemistry, v. 49(2), p. 216-222.

Florence, T.M. and Batley, G.E.
1976: Proc. 47th ANZAAS Congress, Hobard, May, 1976.

1977: Determination of the chemical forms of trace metals in natural waters, with special reference to copper, lead, cadmium and zinc; Talanta, v. 24, p. 151-158.

Gardner, L.R.
1974: Organic versus inorganic trace metal complexes in sulfidic marine waters — some speculative calculations based on available stability constants; Geochimica et Cosmochimica Acta, v. 38, p. 1297-1302.

Giesy, J.P. and Briese, L.A.
1977: Metals associated with organic carbon extracted from Okefenokee swamp water; Chemical Geology, v. 20, p. 109-120.

Gjessing, E.T.
1973: Gel and ultramembrane filtration of aquatic humus: a comparison of two methods; Schweizerische Hydrol., v. 33, p. 592-600.

Hart, B.T. and Davies, S.H.R.
1977: A new dialysis — ion exchange technique for determining forms of trace metals in water; Australian Journal of Maritime and Freshwater Research, v. 28, p. 105-112.

Junk, G.A., Richard, J.J., Grieser, M.D., Witiak, D., Witiak, M.D., Arguello, R., Svec, H.J., Fritz, J.S., and Calber, S.V.
1974: Use of macroreticular resins in the analysis of water for trace organic contaminants; Journal of Chromatography, v. 99, p. 745-762.

Leenheer, J.A. and Huffman, E.W.D. Jr.
1976: Classification of organic solutes in water by using macroreticular resins; Journal of Research, U.S. Geological Survey, v. 4(6), p. 737-751.

O'Shea, T.A. and Mancy, K.A.
1976: Characterization of trace metal-organic interactions by anodic stripping voltammetry; Analytical Chemistry, v. 48(11), p. 1603-1607.

Ramomoorthy, S. and Kushner, D.J.
1975: Heavy metal binding sites in river water; Nature, v. 256, p. 399-401.

Schindler, J.E. and Alberts, J.J.
1974: Analysis of organic-inorganic associations of four Georgia reservoirs; Arch. Hydrobiol, v. 74(4), p. 429-440.

Shuman, M.S. and Woodward, J.G.P.
1977: Stability constants of copper-organic chelates in aquatic samples; Environmental Science Technology, v. 11(8), p. 809-813.

Singer, P.C.
1973: Trace Metals and Metal-Organic Interactions in Natural Waters; Ann Arbor Science Publishers, Ann Arbor, Michigan.

Takamatsu, T. and Yoshida, T.
1978: Determination of stability constants of metalhumic acid complexes by potentiometric titration and ion-selective electrodes; Soil Science, v. 125(6), p. 377-386.

Thurman, E.M., Malcolm, R.L., and Aiken, G.R.
1978: Prediction of capacity factors for aqueous organic solutes adsorbed on a porous acrylic resin; Analytical Chemistry, v. 50(6), p. 775-779.

25.

GEOLOGY OF THE PRECAMBRIAN ROCKS OF THE RIVIERE GRANDIN AND IN PART OF THE MARIAN RIVER MAP AREAS, DISTRICT OF MACKENZIE

Project 780010

J.C. McGlynn
Regional and Economic Geology Division

McGlynn, J.C., Geology of the Precambrian rocks of the Rivière Grandin and in part of the Marian River map areas, District of Mackenzie; in Current Research, Part A, Geol. Surv. Can., Paper 79-1A, p. 127-131, 1979.

Abstract

This is a preliminary report summarizing the geology of two areas mapped at a scale of 1:125 000 in the Great Bear Batholith. In the Mazenod-Faber lakes area of the Marian River map area a belt of dacite-trachydacite ash flow tuffs with intercalated dacite flows and mudstone was outlined, along with masses of subvolcanic dacite to rhyodacite porphyry intrusions that are the intrusive equivalents of the ash flows. Younger plutonic rocks are described and their mode of intrusion suggested. In the Rivière Grandin area the stratigraphy of two sequences of volcanic and sedimentary rocks is outlined. A major unconformity at the base of the Hottah Lake sequence was mapped and the extent of the basement beneath the unconformity was defined. A belt of quartzite that rests unconformably on rocks of the Great Bear Batholith complex is tentatively correlated with the Hornby Bay Group. Uranium mineralization is localized in this quartzite.

Introduction

Mapping of the two remaining areas of Precambrian rocks covered by Kidd's early reconnaissance work along the canoe route from Rae (on Great Slave Lake) to Great Bear Lake (Kidd, 1936) that were not subsequently remapped in the systematic 1 inch to 4 mile reconnaissance geological mapping in the region was completed at a scale of 1:125 000. The areas are in the Marian River map sheet (85N) west of longitude 116°53' and in the northwest corner of the Rivière Grandin (86D) map area (Fig. 25.1 and Fig. 25.2, respectively). The Aphebian supracrustal and plutonic rocks in both areas are part of the Great Bear Batholith (Fraser et al., 1972) which is a late orogenic volcanic-plutonic complex of the Coronation Geosyncline (Hoffman, 1973). This work was undertaken to continue the study of the Great Bear Batholith rocks, and in the Hottah Lake area (Fig. 25.2) to define the extent of older rocks beneath the major unconformity previously mapped in the Leith Peninsula map area (McGlynn, 1976).

Mazenod-Faber lakes Area, Marian River map sheet

The main elements of the geology in the Mazenod-Faber lakes area include a north-trending belt of volcanic rocks with intercalated volcaniclastic sedimentary rocks, syn- or sub-volcanic intrusive porphyries and younger masses of generally coarsely porphyritic granite and granodiorite (Fig. 25.1).

The oldest rocks (unit 1, Fig. 25.1) consist of a complex of dacite to rhyodacite and ash flow tuffs, with a few rather thin dacite flows and rhyolite ash flow tuffs. Many of the ash flows are massive, but horizons containing flattened, recrystallized pumice fragments and members that contain lithic fragments occur throughout the sequence. The few dacite lava flows occur near the base of the pile usually associated with sedimentary rocks. The tuffs are composed of phenoclasts of plagioclase highly altered to sericite quartz and variable amounts of alkali feldspar in a very fine grained matrix of feldspar quartz with grains of hornblende and biotite extensively altered to chlorite.

Sedimentary rocks (unit 2) occur within but near the base of the sequence around Mazenod Lake. A few thin horizons of sedimentary rocks also occur higher in the sequence east of Faber Lake. These rocks consist of greywacke turbidites and mudstones, and thin siliceous sandstones and siltstones interbedded with mudstones that commonly contain thin beds of volcanogenic clastics or lithic sandstones derived from nearby volcanic rocks. Thin beds of mottled chert-like rocks with very small clasts that may represent air fall tuffs occur within the sedimentary sequence. The sedimentary rocks, particularly the mudstones, are poorly exposed and in part are found on small islands in Mazenod Lake not shown on the map, and so are more extensive than shown on the map in Figure 25.1.

The volcanic and sedimentary rocks are only slightly metamorphosed to subgreenschist or very low greenschist facies. Near granitic masses a narrow aureole of epidote amphibolite or amphibolite facies is developed. The rocks strike northwest to west and generally have low dips. In the northern part of the belt the dips are gentle near the bordering granitic masses and away from the margin are almost flat. The supracrustal strata are more steeply dipping around Mazenod Lake. The sedimentary rocks are folded about north to northwest-striking axes and the volcanic rocks strike about northwest and appear to be broadly folded. The strata are steeply dipping near the margins of some intrusive porphyry masses.

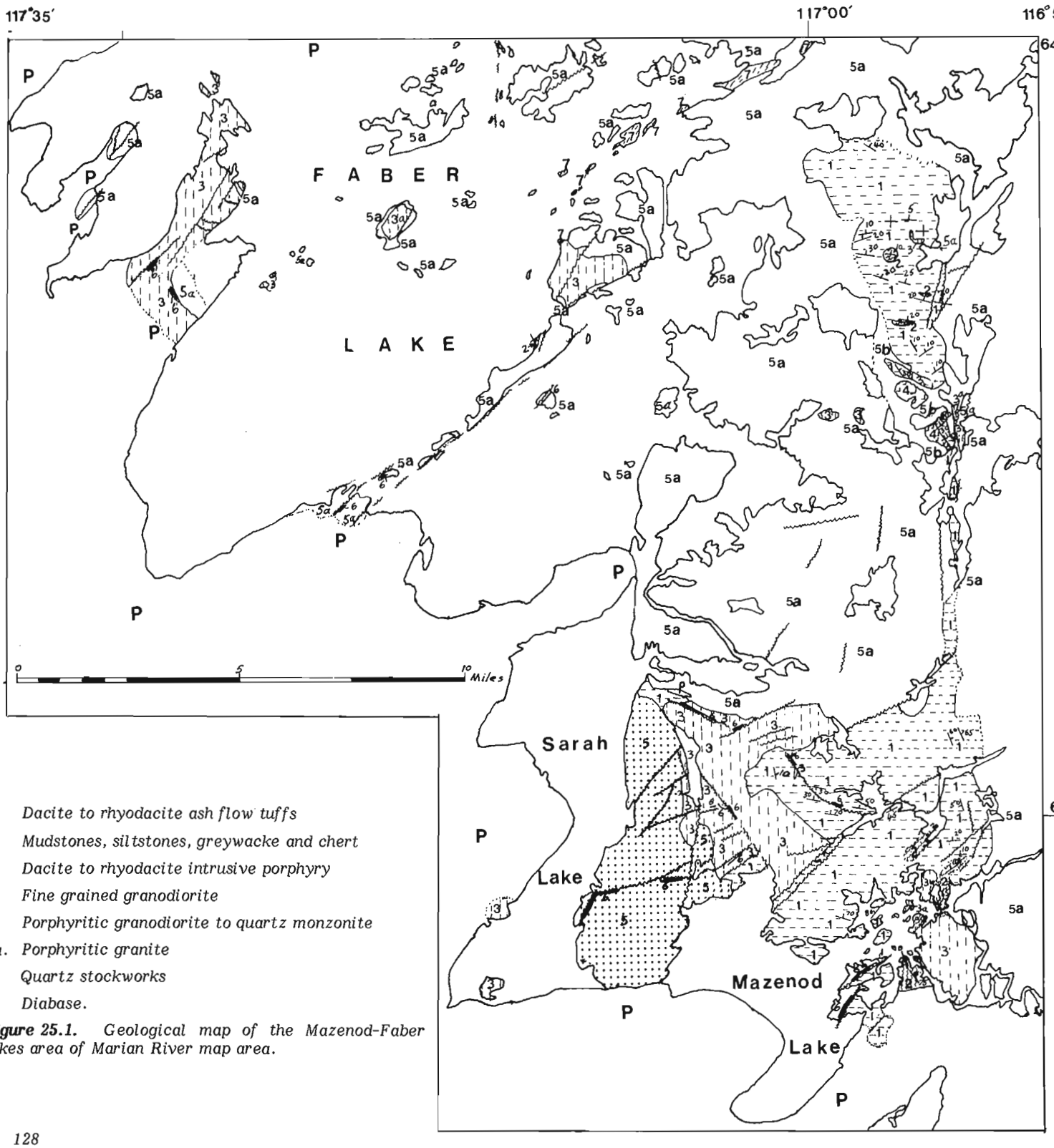
Dacite to rhyodacite intrusive porphyry (unit 3, Fig. 25.1) intrudes the volcanic and sedimentary rocks as dykes, sills and plutons. These rocks are composed of plagioclase, usually altered to sericite and often zoned, quartz, and variable amounts of alkaline feldspar as phenocrysts in a fine grained matrix of feldspar and quartz, with hornblende and biotite intensely altered to chlorite. In large masses the phenocrysts are larger and the groundmass perceptibly coarser grained than in smaller bodies. These rocks are about the same composition as most of the volcanic rocks, and commonly are intermixed with the ash flows. The porphyries are thought to be almost syn-volcanic and to represent intrusive equivalents of the volcanic rocks.

Several small masses of granodiorite or quartz-diorite (unit 4) occur in the volcanic rocks east of Faber Lake. The granodiorite is not porphyritic and is fine grained and massive.

The granitic rocks in the area intrude the volcanic and sedimentary rocks and intrusive porphyries. The body between Sarah and Mazenod Lake (unit 5) is medium-to coarse-grained porphyritic, massive, pink weathering rock consisting of phenocrysts of plagioclase up to 3.75 cm long in a medium- to coarse-grained matrix of quartz plagioclase and alkaline feldspar. Biotite forms less than 1 per cent of the rock and is extensively altered to chlorite.

The most extensive plutonic rock is a granite (unit 5a) which weathers a light pink-grey colour, is massive and always porphyritic. Perthitic alkaline feldspar occurs as phenocrysts that range from 1.8 to 5 cm in maximum dimension. These characteristically have a narrow rim of plagioclase. The groundmass comprises sericitized plagioclase, quartz and alkaline feldspar with less than 1 per cent of biotite extensively altered to chlorite, and rare grains of altered hornblende.

The granite is commonly cut by sheets of a fine grained granite (unit 5b) that is even grained or contains only small phenocrysts of alkaline feldspar. These sheets are flat lying or very shallow dipping and display sharp contacts with the granite. In places this rock cuts the volcanic rocks as sills or dykes. Near some contacts with the volcanic rocks or intrusive porphyries, the porphyritic granite grades to fine grained granite through a zone of granite with phenocrysts of decreasing size.



1. *Dacite to rhyodacite ash flow tuffs*
2. *Mudstones, siltstones, greywacke and chert*
3. *Dacite to rhyodacite intrusive porphyry*
4. *Fine grained granodiorite*
5. *Porphyritic granodiorite to quartz monzonite*

5a. *Porphyritic granite*

6. *Quartz stockworks*
7. *Diabase.*

Figure 25.1. *Geological map of the Mazenod-Faber lakes area of Marian River map area.*

Contacts between both the porphyritic granite and fine grained granite and older rocks, where observed, are almost invariably flat or very shallow dipping. The granite appears to intrude the older rocks as vast sheets or a complex of sheets of unknown thickness.

All of the rocks in the area are cut by northwesterly-striking right lateral strike faults. Where displacements can be measured in this map area, they are small – 1.5 km or less. Quartz stockworks or "giant" quartz veins (unit 6) occur along these faults or in faults subsidiary to them. The youngest Precambrian rock in the area is a northwest-striking diabase sheet (unit 7, Fig. 25.1).

Precambrian Rocks of the Rivière Grandin map sheet

The oldest rocks in the area (unit 1, Fig. 25.2) are found on Hottah Lake where they form a basement to a group of Bear Batholith volcanic and sedimentary rocks. The unit consists essentially of medium- to fine-grained equigranular granodiorite that contains remnants of basic volcanic rocks that are usually massive, but locally pillowed with interbeds of black mudstones that locally contain thin beds of siliceous siltstones and beds of chert. The volcanic rocks are metamorphosed to amphibolite or epidote amphibolite facies and cut by dykes of the granodiorite. The bands of volcanic and sedimentary rocks trend north or northwest and may be folded about north-northwest axes. The granodiorite contains inclusions of amphibolite. Small plutons and dykes of pink, medium grained quartz monzonite cut both the granodiorite and supracrustal rocks. All these rocks are commonly rather pervasively sheared. The strike of the shearing varies in the area but is commonly north to northwest.

These rocks are overlain unconformably by a group of sedimentary volcanic rocks that are part of the Bear Batholith sequence (units 2, 2a, Fig. 25.2). The angular unconformity is composed in many places along the east and south side of Bell Island. The basal unit of the sequence is a gritty conglomeratic lithic sandstone and arkose which fines upwards into a fine grained arkose. The thickness of this unit ranges from 3 to 90 m. The basal sandstone unit is overlain by mudstone, which in many places has a mudstone conglomerate or paraconglomerate at or near its base that is usually overlain by a boulder conglomerate with clasts of red acidic volcanic rocks. The conglomerate horizons are variable in thickness and in places missing from the sequence. At or near the top of the mudstones basalt flows, and locally dacite flows or ash flows, occur. Locally, the basalts are pillowed, usually along their lower contact. The flows may occur at several horizons near the top of the mudstone formation.

These units are conformably overlain by a complex of rhyodacite and rhyolite flows, and rhyodacite to rhyolite ash flows, usually with well developed eutexitic textures and irregularly shaped small rhyolite and rhyodacite intrusions (unit 2a, Fig. 25.2). Intercalated with these units are local areas of volcaniclastic sediments and mudstones. Both conglomerates and sandstones occur in the clastic units and the sediment is of local derivation. Towards the top of the sequence local horizons of basalt flows are found. Volcanism and sedimentation was in part synchronous as the acidic volcanic rocks occur as clasts in lower sedimentary units. This stratigraphy, with minor variations, is found on Bell Island and east of Bell Island on the east shore of Hottah Lake at the north end of the map area. The latter rocks and the faulted extension of the sequence on Bell Island occur also in the Leith Peninsula map area (McGlynn, 1976). It seems these two centres of acidic volcanism developed in a basin in which, except for basal clastics, the dominant fill was fine sediment. In the Leith Peninsula sheet mudstones are overlain by a thick sequence of pillowed and massive basalts (McGlynn, 1976). Basement occurs along the west side of the sequence to the north end of Hottah Lake and probably continues under the Phanerozoic cover. Along the eastern margin of the basement rocks (unit 1) the old rocks are cut by granites of the Great Bear Batholith. The sedimentary, volcanic sequence (units 2, 2a) is cut by Great Bear Batholith granites in the Leith Peninsula map area. The sedimentary sequence is part of the late Aphebian Great Bear Batholith complex. The age of basement rocks is unknown.

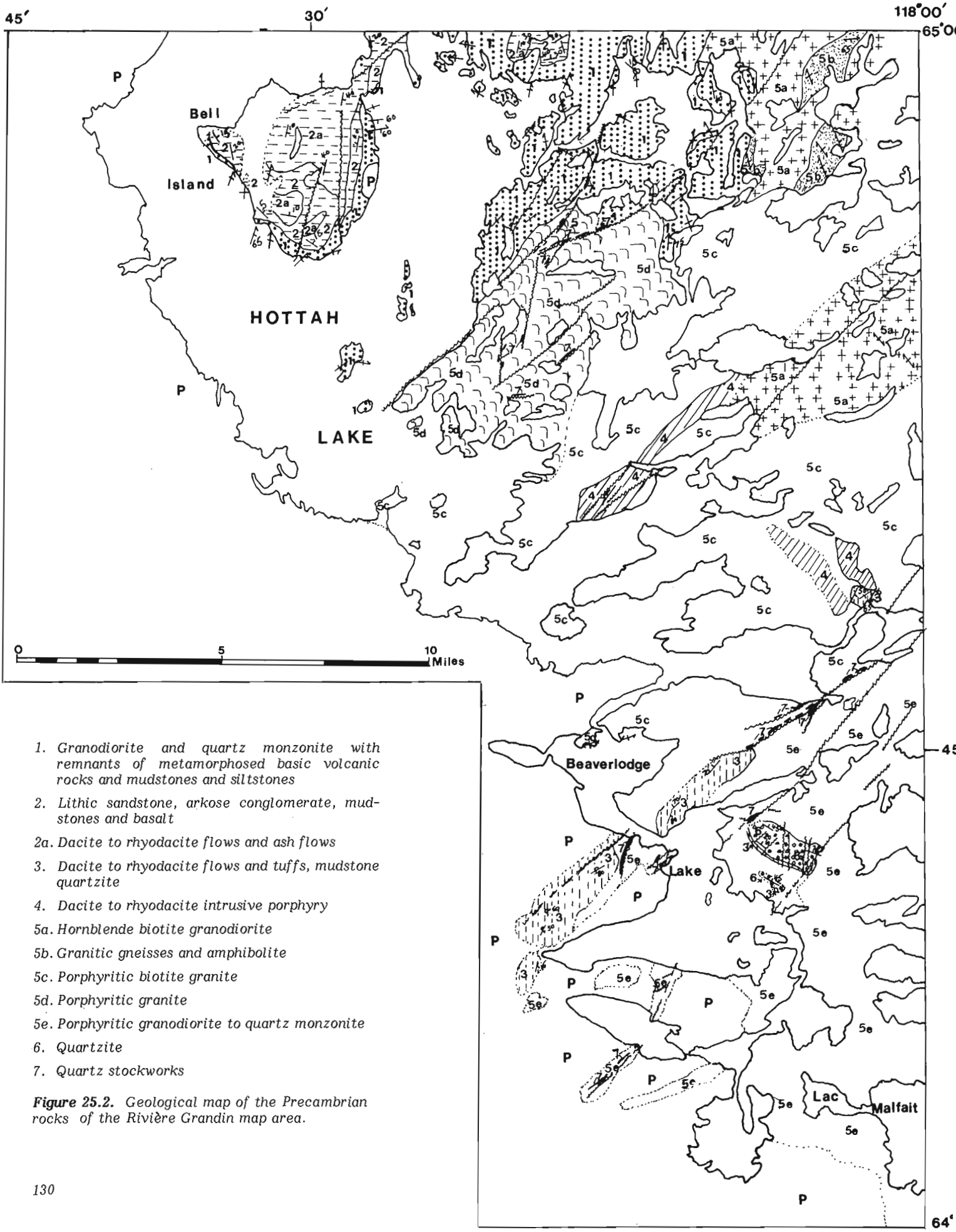
The supracrustal sequence is folded about upright axes that trend about north. On Bell Island the structure is a broad syncline with local small subsidiary folds on the limbs. The folded rocks are cut by north-trending faults of small displacement. The sequence on the mainland is also folded into a syncline of similar geometry.

A second group of volcanic and sedimentary rocks of the Great Bear Batholith occurs on the northeast-trending ridge at the narrows of Beaverlodge Lake (unit 3, Fig. 25.2). A large part of the ridge was previously mapped by Henderson (1949). The base of the sequence is not exposed as it is intruded by granitic rocks. The lowest units consist of dacite and rhyodacite flows and lithic ash flows. These volcanic rocks are cut by dacite or rhyodacite intrusive porphyry. The intrusive porphyry occurs as small crosscutting plutons, sills and dykes. Small masses of massive fine grained gabbro also occur in the volcanic sequence. The volcanic rocks are overlain conformably by mudstone that contains discontinuous bands of volcanic rocks, some of which are thin basalts that locally contain pillows near contacts with mudstones. Near volcanic rocks the mudstones contain wedges of para-conglomerates with clasts of nearby volcanic rocks and intrusive porphyries. The mudstones are overlain by white quartzite that is up to 400 feet thick. Gritty quartzites or feldspathic quartzites with mudstone interbeds in places occur between the mudstones and white quartzite. The quartzite near its top contains thin beds of mudstones and is overlain by black, green and pink weathering mudstones. The mudstones contain beds of cream or mottled cream and brown and white quartzite. The top of the sequence is not exposed. Northeast of the narrows on Beaverlodge Lake in places the mudstone unit beneath the quartzite is missing. The quartzite rests directly on volcanic rocks and pebbles or boulders of these rocks occur in the quartzite at its base. In one area southwest of the narrows quartzite with a thin lense of conglomerate at or near its base rests directly on dacite which protrudes up into mudstones that underlie the quartzite.

The succession is structurally conformable. In the lower part of the sequence there is interfingering between volcanic rocks and mudstones and paraconglomerates, suggesting that volcanism and sedimentation were in part synchronous. The quartzite, however, was deposited after erosion of parts of the sequence and on an irregular surface of some relief.

These rocks are folded into tight folds with vertical to steeply northwest-dipping axes. Southwest of the narrows the sequence occurs in a southwest-plunging syncline that is overturned slightly to the southeast. Northeast of the narrows the major fold is a northeast-plunging anticline. Younger granite separates the two parts of the sequence.

These structures are complicated by faults that strike northwesterly about parallel to fold axes. Some and possibly all of these faults have right lateral movement. They disrupt the sequence, locally causing repetition of and displacement of the stratigraphy. The faults extend beyond the supra-crustal sequence into the granitic rocks. Northeast of the granitic rocks south of the sequence the rocks are intensely sheared and faults may form the north boundary of this sequence. A few exposures of quartzite and mudstone on the river at the south end of Hottah Lake may be a faulted extension of part of the sedimentary sequence. It is possible that the whole sequence has moved to its present position along a strike-slip fault.



1. *Granodiorite and quartz monzonite with remnants of metamorphosed basic volcanic rocks and mudstones and siltstones*
2. *Lithic sandstone, arkose conglomerate, mudstones and basalt*

2a. *Dacite to rhyodacite flows and ash flows*

3. *Dacite to rhyodacite flows and tuffs, mudstone quartzite*
4. *Dacite to rhyodacite intrusive porphyry*

5a. *Hornblende biotite granodiorite*

5b. *Granitic gneisses and amphibolite*

5c. *Porphyritic biotite granite*

5d. *Porphyritic granite*

5e. *Porphyritic granodiorite to quartz monzonite*

6. *Quartzite*
7. *Quartz stockworks*

Figure 25.2. *Geological map of the Precambrian rocks of the Rivière Grandin map area.*

The sequence of unit 3 cannot be directly correlated with the sedimentary and volcanic rocks to the north on Hottah Lake. They are isolated from each other and separated by a number of strike-slip faults. The stratigraphy of each sequence is different. The orthoquartzite in the Beaverlodge Lake sequence has no equivalent in the sequence on Bell Island. The volcanic rocks in the Bell Island sequence appear to be somewhat more potash-rich. The orientation and intensity of folding is different. The volcanism in each sequence is typical of the Great Bear Batholith, but their relative ages remain a problem.

Unit 4 (Fig. 25.2) consists of dacite to rhyodacite intrusive porphyry which is locally associated with ash flow tuffs of similar composition. The rocks occur as isolated masses in granitic rocks and, as already described, are part of the sequence at Beaverlodge Lake. They are very similar to the dacite porphyries in the Mazenod-Faber lakes area in the Marian River map area (unit 3, 3a, Fig. 25.1).

The granitic rocks in the area are divided into five separate masses. Unit 5a (Fig. 25.2) is a hornblende biotite granodiorite or quartz monzonite. It is fine- to medium-grained, massive and is mostly even grained, but has porphyritic phases. The mafic content is about 10 per cent and the mafics are partly altered to chlorite.

Unit 5b is a peculiar complex of granitic gneisses with amphibolite bands and masses that are locally feldspathized. In places the foliation appears to be an imposed intense cleavage. These rocks are cut by the hornblende biotite granodiorite and by a small mass of dacite porphyry. The gneisses may be part of the oldest rocks in the area (unit 1) but they differ from any rocks found in that complex.

Unit 5c is a porphyritic biotite granite to quartz monzonite. It is a buff to light grey weathering, massive, medium grained rock that contains phenocrysts of alkaline feldspar up to 3.75 cm long. It is cut by thin sheets and dykes of fine, even grained granite that are thought to be a fine grained equivalent of the granite. Sheets of the fine grained granite also occur in the hornblende biotite granodiorite and thus the biotite granite is thought to be the younger of the two units.

A second biotite granite (unit 4d) may be a variety of unit 5c, but it is petrographically distinct. It is a light grey weathering porphyritic rock composed of coarse phenocrysts of alkaline feldspar from 2.5 to 7.5 cm long in a medium- to coarse-grained groundmass of plagioclase quartz alkaline feldspar, and minor amounts of chloritic biotite. The granite is coarser grained and contains more alkaline feldspar than the biotite granite of unit 5c. Sheets of this granite cut granodiorites of unit 1.

A mass of fine- to medium-grained, massive, porphyritic granodiorite (unit 5e) occurs in the southeast corner of the map area. Plagioclase and scattered alkaline feldspar phenocrysts range in size from .6 to 2.5 cm long. The mafics consist of hornblende and biotite and form as much as 10 per cent of the rock.

Unit 6 is a quartzite that rests unconformably on dacite porphyry and at the southeast end of the mass on the porphyritic granodiorite (unit 5e). The quartzite is fine grained, light grey or creamy coloured, commonly with browny red patches or zones. The rock is thinly to coarse bedded. Near the base of the sequence it contains scattered quartz pebbles and thin lenses of gritty quartzite or quartz-pebble conglomerates. The basal units also are somewhat feldspathic. Pyrite occurs in interstices between quartz grains in ill-defined zones. At the base of the quartzite small subangular pebbles of underlying dacite or granodiorite occur in the quartzite. Bedding in the quartzite strikes northwest and dips to the northeast at 30 to 45 degrees. It seems that the quartzite is tilted as a unit to the northeast. The quartzite is cut by numerous faults that become increasingly more closely spaced toward the southeast end of the belt. The northwest sides of the faults drops so that along the southeast side of many faults basement covered with quartzite is exposed. The rocks below the unconformity are intensely sheared and fractured.

This quartzite is lithologically unlike most of the quartzites in the sequence just to the northwest (unit 3). Although it rests on dacite porphyry, as does the quartzite in unit 3, it also lies on the granodiorite which is younger than the sequence to the north. The quartzite of unit 6 is deformed, but strikes northwest and has a persistent northeast dip as if simply tilted, in marked contrast to the northeast-trending tight folds found in the sequence of unit 3. It seems, therefore, that the quartzite of unit 6 is the younger of the two sequences and may be younger than all of the rocks of the Great Bear Batholith. It may therefore correlate with the quartzites of the Hornby Bay Group and represent an outlier of that sequence. This possibility is of economic interest. Uranium mineralization occurs in a number of places in this quartzite. The mineralizaiton is found in fractures in the quartzite commonly near its base. These fractures are related to the faults which cut the unit.

All of the rocks so far described are cut by northeast-striking vertical strike-slip faults. Quartz stockworks or "giant" quartz veins (unit 7) are localized along these fault zones.

References

Fraser, J.A., Hoffman, P.F., Irvine, T.N., and Mursky, G.
1972: The Bear Province; in Variations in tectonic styles in Canada, edited by R.A. Price and R.J.W. Douglas; Geological Association of Canada, Special Paper 11, p. 454-503.

Henderson, J.F.
1949: Pitchblende occurrences between Beaverlodge and Hottah Lakes, Northwest Territories; Geological Survey of Canada, Paper 49-16, p. 1-17.

Hoffman, P.F.
1973: Evolution of an early Proterozoic continental margin: the Coronation Geosyncline and associated aulacogens of the northwestern Canadian Shield; in A Discussion of the Evolution of the Precambrian Crust, edited by J. Sutton and B.F. Windley; Royal Society of London, Philosophical Transactions, v. 273, p. 547-581.

Kidd, D.F.
1936: Rae to Great Bear Lake, Mackenzie District, N.W.T.; Geological Survey of Canada, Memoir 187, p. 1-44.

McGlynn, J.C.
1976: Geology of the Calder River (86F) and Leith Peninsula (86E) map-areas, District of Mackenzie; in Report of Activities, Part A, Geological Survey of Canada, Paper 76-1A, p. 359-361.

26.

Fe-Mg CATION EXCHANGE THERMOBAROMETRY OF POLYMETAMORPHIC ROCKS FROM THE PRECAMBRIAN SHIELD OF NORTHEASTERN ALBERTA

Project 740017

Peter A. Nielsen
Regional and Economic Geology Division

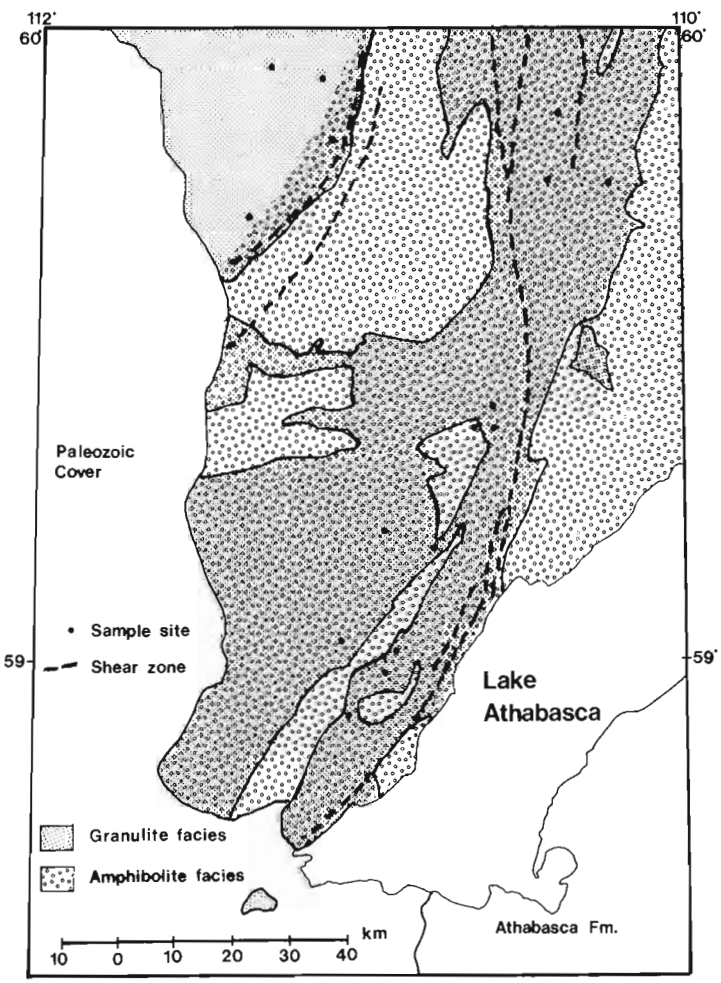
Nielsen, Peter A., Fe-Mg cation exchange thermobarometry of polymetamorphic rocks from the Precambrian Shield of northeastern Alberta; in Current Research, Part A, Geol. Surv. Can., Paper 79-1A, p. 133-137, 1979.

Abstract

A suite of polymetamorphic supracrustal gneisses from the Precambrian Shield of northeastern Alberta has been examined and microprobe analyses of coexisting garnet-biotite and garnet-cordierite pairs have been collected. P-T conditions were determined using Fe-Mg cation exchange thermometry and barometry. A moderate pressure granulite facies event and a low pressure amphibolite facies overprint have been identified and these events are tentatively correlated with the two radiometrically dated events in the study area.

Introduction

This project was initiated in order to place quantitative values on pressure and temperature of equilibration in polymetamorphic areas of the Precambrian Shield. Following the Symposium on Metamorphism in the Canadian Shield, in May, 1977, a suite of aluminous supracrustal gneisses from the western edge of the Churchill structural province was obtained from the Research Council of Alberta. This area was selected because of the availability of samples of the appropriate bulk composition and the relative abundance of supporting field and radiometric data (Fig. 26.1).



General Geology

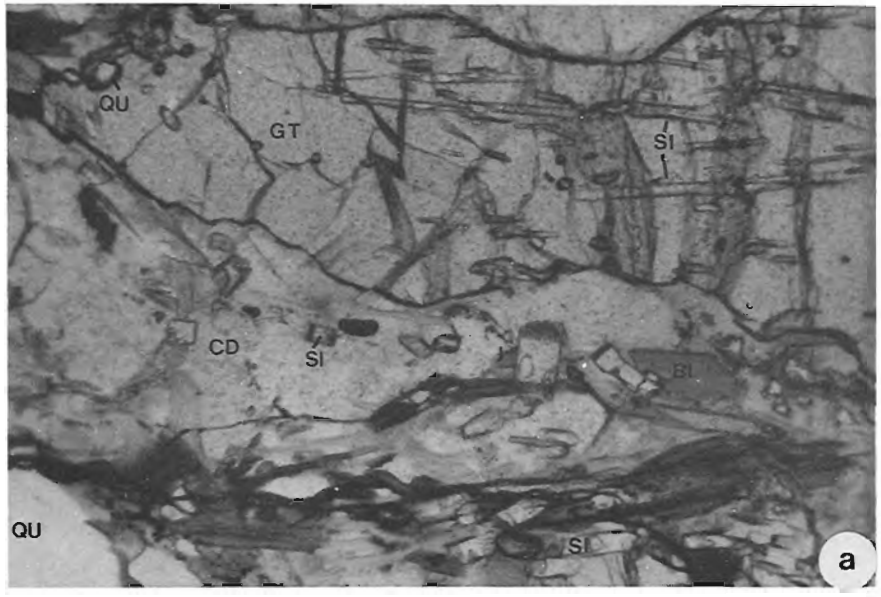
The Precambrian Shield of northeastern Alberta consists of massive to foliated granitoid rocks, granitic gneisses and metasediments (Godfrey and Langenberg, 1978). K-Ar data from biotites, and muscovites from the metasediments, granitic gneisses, and granitoid rocks display a narrow distribution of ages; the average age is 1790 ± 40 Ma (Baadsgaard and Godfrey, 1972). Rb-Sr whole rock isochrons for younger granites from the Andrew-Colin lakes district plot on an isochron with t=1893 ± 6 Ma and an initial $^{87}Sr/^{86}Sr$ ratio of 0.7083 (decay constant $\lambda=1.39\times10^{-11}$/yr). This high initial ratio may indicate contamination by older metasediments during emplacement or derivation by anatexis of pre-existing orthogneiss and paragneiss (Baadsgaard and Godfrey, 1972). In the Charles Lake district, pegmatites which cut orthogneiss and paragneiss yield an Rb/Sr isochron with t=2524 ± 24 Ma and an initial $^{87}Sr/^{86}Sr$ ratio of 0.7030. K-Ar data on micas from these pegmatites yield ages which range from 1690-1850 Ma (Baadsgaard and Godfrey, 1972). The lower age given by the K-Ar data is interpreted as a thermal overprint. Thus two distinct ages have been recognized in the Precambrian Shield of northeastern Alberta.

At present, two dated events are not distinguishable in terms of deformational style. A major deformation occurred during the Aphebian (Godfrey and Langenberg, 1978; Langenberg, pers. comm.). This deformation produced the foliation defined by biotite and oriented sillimanite prisms and flattened pre-existing garnet porphyroblasts.

Petrography

The samples investigated are all peraluminous paragneiss and contain variable proportions of sillimanite, cordierite, garnet, biotite, quartz, plagioclase, microcline-perthite, and microcline. Minor phases include ilmenite, magnetite, hercynite spinel, monazite, and apatite. Detailed petrographic examination has resulted in the identification of two metamorphic episodes, based on textural relations and equilibrium mineral assemblages.

Figure 26.1. *Metamorphic facies distribution in NE Alberta (after Godfrey and Langenberg, 1978).*

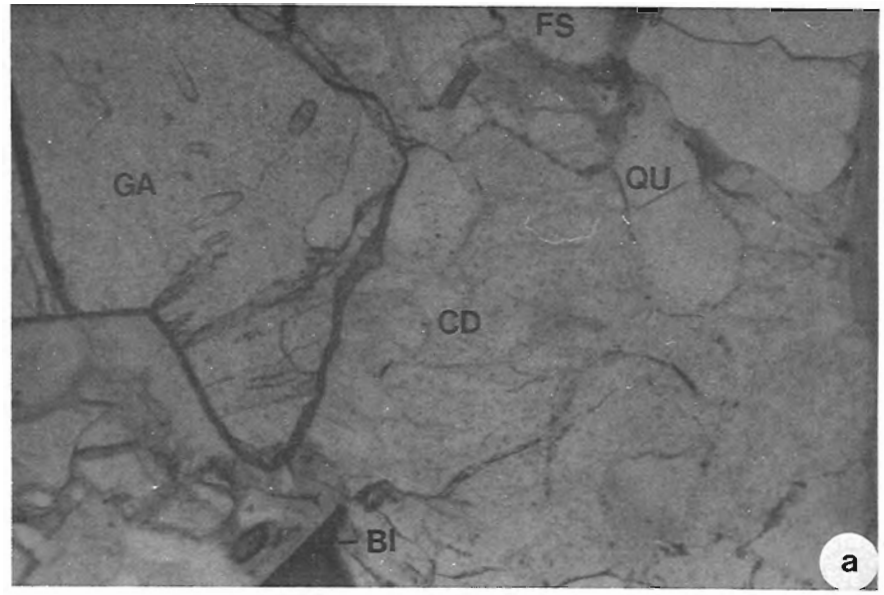




CD - cordierite *BI - biotite*
GA - garnet *QU - quartz*
SI - sillimanite *FS - plagioclase and alkali feldspar*

Figure 26.2. *a. Sample 125 - early granulite facies assemblage. Field of view 0.81 mm. Plane polarized light.*

b. Same view, crossed nicols.



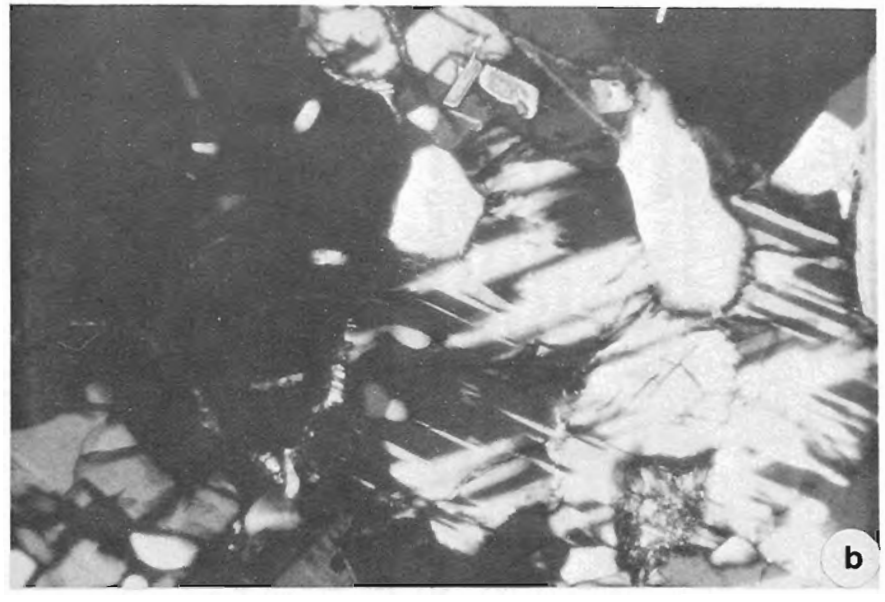


Figure 26.3. *a. Sample 125 - later amphibolite facies overprint assemblage. Field of view 0.81 mm. Abbreviations as in Figure 26.2. Plane polarized light.*

b. Same view, crossed nicols.

Table 26.1

Pressure (kbar) and Temperature (°C) conditions calculated from biotite-garnet and cordierite-garnet Fe-Mg partition coefficient data

Sample No.	Archean Assemblage					Aphebian Assemblage				
	Biotite-garnet		Cordierite-garnet			Biotite-garnet		Cordierite-garnet		
	T(N)[1]	T(F)[2]	T(N)[1]	P(Hu)[3]	P(Ho)[4]	T(N)	T(F)	T(N)	P(Hu)	P(Ho)
18	-	-	-	-	-	570	600	580	3.0	3.3
113A	640	690	640	4.3*	4.4	520	550	550	3.0	3.0
113B	-	-	650	3.8	4.5	530	570	550	3.0	3.0
124	640	695	760	5.1	4.5	550	580	560	3.0	3.1
125	680	710	700	4.5	4.7	615	620	600	3.4	3.4
136	700	760	740	4.6	4.8	610	660	580	3.4	3.2
137	-	-	-	-	-	565	565	-	-	-
140	680	740	710	4.3	4.7	550	580	550	3.0	3.0
147	690	760	750	4.6	4.5	560	600	580	3.4	3.3
148	-	-	780	5.5	5.2	-	-	-	-	-
153	675	750	730	4.9	5.1	520	550	550	3.2	3.0
154	-	-	715	4.5	4.9	590	600	600	3.5	3.5
155	-	-	-	-	-	600	610	-	-	-
157A	-	-	750	4.6	4.5	-	-	570	3.1	3.0
159	-	-	780	4.8	4.7	-	-	-	-	-
160A	-	-	780	4.8	4.7	-	-	-	-	-
163	-	-	780	5.3	5.3	570	615	-	-	-
166	-	-	720	4.3	4.2	-	-	-	-	-

[1] Nielsen (1977)
[2] Ferry and Spear (1977)
[3] Hutcheon et al. (1974)
[4] Holdaway and Lee (1977)
* 1 kbar = 10^5 kPa

Figures 26.2a,b illustrate the earlier metamorphic assemblage: cordierite-garnet-sillimanite-quartz. This critical assemblage is accompanied by biotite, plagioclase, perthitic alkali feldspar, and quartz in the surrounding matrix. Cordierite and garnet frequently contain inclusions of spinel and magnetite. Garnet also contains quartz and prismatic sillimanite. Cordierite is generally not twinned and shows variable amounts of pinite alteration. Reaction (1), coupled with reaction (2) produced this observed assemblage.

3 cordierite $\rightleftarrows$ 2 garnet + 4 sillimanite + 5 quartz (R.1)

3 Fe cordierite + 2 Mg garnet $\rightleftarrows$ 3 Mg cordierite + 2 Fe garnet (R.2)

Figure 26.3a,b illustrates the later metamorphic assemblage: cordierite$_2$-garnet$_2$-microcline-plagioclase-biotite. Sillimanite persists in the rock, but is not found in contact with biotite or garnet$_2$. It is confined to the quartzofeldspathic matrix or as inclusions in cordierite$_2$. Cordierite$_2$ generally shows well developed sector twinning and little or no pinite formation and has a higher Mg/Mg+Fe ratio than cordierite$_1$. Garnet$_2$ has a higher Fe/Fe+Mg ratio than garnet$_1$ and occurs as rims on garnet$_1$ as well as smaller subhedral porphyroblasts in the matrix. Reaction (3) produced the observed assemblage:

biotite + sillimanite + quartz $\rightleftarrows$ cordierite + garnet + K feldspar + v (R.3)

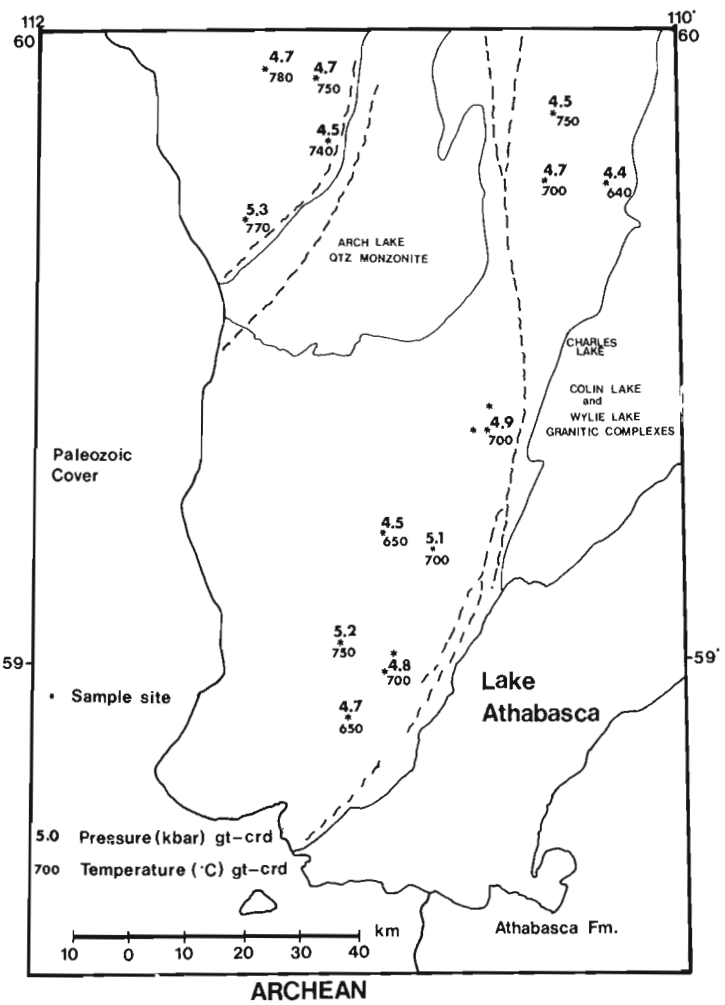


Figure 26.4.

Distribution of calculated P-T values for the early granulite facies event using garnet-cordierite thermometry (Nielsen, 1977) and barometry (Hutcheon et al., 1974; Holdaway and Lee, 1977).

Table 26.2

Chemical data for Specimen no. 125

	Early assemblage			Late assemblage				
	GRD	GAR	BIO	GAR	CRD	GAR	BIO	GAR
SiO_2	48.25	38.12	35.50	37.22	47.66	37.12	35.81	38.33
TiO_2	-	-	3.08	.12	-	.03	3.25	.03
Al_2O_3	33.00	22.03	17.42	21.63	32.85	21.50	17.57	21.90
FeO	9.84	35.67	18.57	34.65	8.08	35.98	18.42	35.85
MgO	7.98	4.94	9.62	4.73	8.73	4.15	10.12	4.19
MnO	.09	.58	-	.66	-	.67	-	.63
CaO	-	1.26	-	1.32	-	1.30	-	1.30
K_2O	-	-	9.48	-	-	-	9.57	-
Sum.	99.16	102.60	93.67	100.33	97.32	100.75	94.74	102.23
Si_{IV}	4.946	5.917	5.463	5.911	4.941	5.901	5.437	5.971
Al_{VI}	1.034	.083	2.537	.089	1.059	.099	2.563	.029
Al	2.934	3.942	.623	3.960	2.955	3.929	.581	3.992
Ti	-	-	.356	.014	-	.004	.371	.004
Fe^{+3}	.062	.042	2.390	.022	.043	.049	2.339	4.670
Fe^{+2}	.782	4.589		4.580	.658	4.734		
Mg	1.219	1.143	2.207	1.120	1.349	.983	2.290	.973
Mn	.008	.076	-	.089	-	.090	-	.083
Ca	-	.210	-	.225	-	.221	-	.217
K	-	-	1.861	-	.003	-	1.854	-
$Fe/_{Fe+Mg}$	.391	.801	.520	.804	.328	.828	.505	.828
$Fe/_{Fe+Mg+Mn+Ca}$	.389	.763	.520	.762	.328	.785	.505	.786
lnK(N)	1.833		1.329		2.289		1.548	
lnK(F)	-		-1.329		-		-1.548	
lnK1(H)	-4.035		-		-5.231		-	
lnK2(H)	6.969		-		8.508		-	
T(N)	730		680		580		615	
T(F)	-		710		-		620	
P(H)	4.45		-		3.40		-	

Methods of Thermometry and Barometry

Using the energy dispersive microprobe system at the Geological Survey of Canada under the guidance of Dr. A.G. Plant, 311 mineral analyses were collected. The analyses of cordierite, garnet, and biotite were then recast into mineral structure formulae (using 18, 24, and 22 oxygens respectively). Distribution coefficients of Fe, Mg and Mn between co-existing garnet-cordierite and garnet-biotite pairs were then calculated. Chemical data for sample 125 along with calculated K_Ds, pressures and temperatures of equilibration are shown in Table 26.1. Garnet-biotite data were used to calculate temperature of equilibration using the methods of Nielsen (1977) and Ferry and Spear (1977). Cordierite-garnet data were used to calculate equilibration temperature using the method of Nielsen (1977; in prep.) and pressure using the methods of Hutcheon et al. (1974) and Holdaway and Lee (1977). The results of these calculations are shown in Table 26.2.

Results

The P-T conditions calculated from Fe-Mg thermobarometry form two distinct populations which reflect the two metamorphic assemblages described above. The moderate pressure (P>4.5kbar) -high temperature (T>700°C) conditions are calculated from the early metamorphic assemblage. These data are plotted on Figure 26.4. The low pressure (P<3.5kbar) -low temperature (T≲600°C) are calculated from the later metamorphic assemblage and are plotted on Figure 26.5.

Both metamorphic assemblages formed under the condition of $P_{H_2O}<P_{total}$ ($X_{H_2O}<0.4$; see Holdaway and Lee, 1977 for discussion).

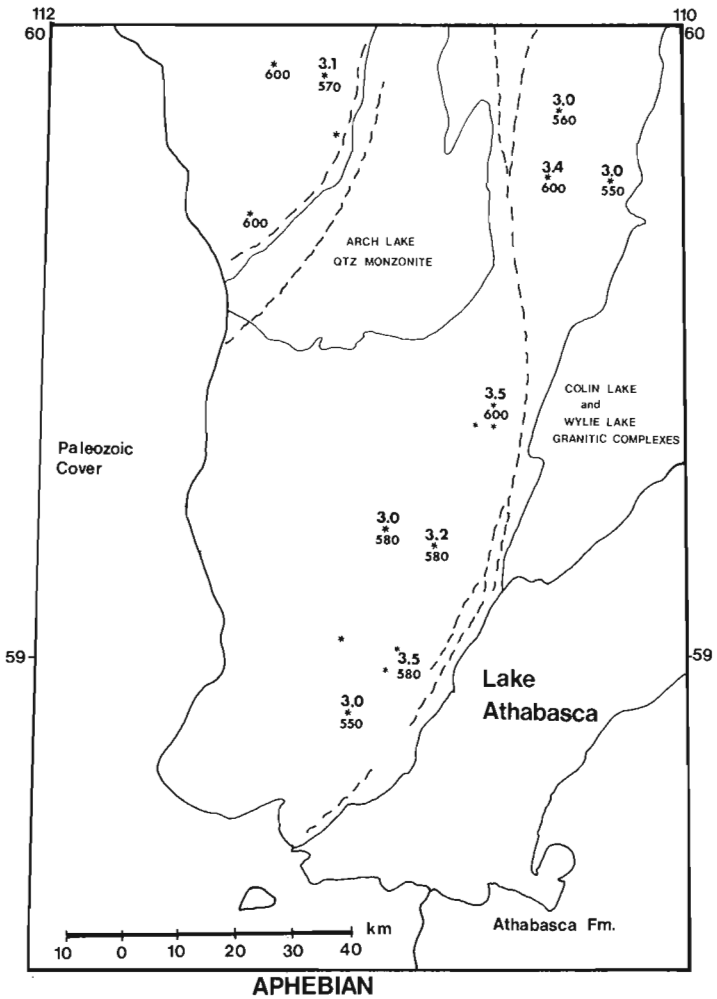


Figure 26.5. *Distribution of calculated P-T values for the later amphibolite facies overprint. Symbols and methods as in Figure 26.4.*

Conclusions

Fe-Mg cation exchange thermobarometry of high-grade supracrustal gneisses from the Precambrian Shield of northeastern Alberta indicate two stages of metamorphic equilibration. Petrographic data also suggest two metamorphic events. These events are correlated with the two radiometric events indicated by K-Ar and Rb-Sr geochronology (Baadsgaard and Godfrey, 1972).

1) Moderate pressure granulite facies event at t≈2500 Ma which produced co-existing cordierite$_1$-garnet$_1$- sillimanite-quartz by reactions R.1 and R.2.

2) Low pressure dry amphibolite facies metamorphic overprint at t≈1800 Ma which produced the assemblage cordierite$_2$-garnet$_2$-K feldspar by reaction R.3.

$^{40}Ar/^{39}Ar$ dating of feldspars from the supracrustal gneisses is being investigated in order to obtain better control on the ages of the two indicated metamorphic events.

Acknowledgments

The author acknowledges the co-operation of J. Godfrey and C.W. Langenberg of the Research Council of Alberta in providing the samples used in this study and for providing an unpublished map of the bedrock geology of the Precambrian Shield of northeastern Alberta. P.H. Thompson, M. Schau, and J.B. Henderson read earlier drafts of the manuscript.

References

Baadsgard, H. and Godfrey, J.D.
1967: Geochronology of the Canadian Shield in northeastern Alberta. I Andrew Lake area; Canadian Journal of Earth Sciences, v. 4, p. 541–563.

1972: Geochronology of the Canadian Shield in northeastern Alberta. II Charles-Andrew-Colin Lakes areas; Canadian Journal of Earth Sciences, v. 9, p. 863-881.

Ferry, J.M. and Spear, F.S.
1977: Experimental Calibration of the partitioning of Fe and Mg between biotite and garnet; Carnegie Institution of Washington Yearbook 76, p. 579-581.

Godfrey, J.D. and Langenberg, C.W.
1978: Metamorphism in the Precambrian Shield of Northeastern Alberta; in Metamorphism in the Canadian Shield; Geological Survey of Canada, Paper 78-10, p. 129-138.

Holdaway, M.J. and Lee, S.M.
1977: Fe-Mg cordierite stability in high grade pelitic rocks based on experimental, theoretical and natural observations; Contributions to Mineralogy and Petrology, v. 63, p. 175-198.

Hutcheon, I., Froese, E., and Gordon, T.M.
1974: The assemblage quartz-sillimanite-garnet-cordierite as an indicator of metamorphic conditions in the Daly Bay Complex, N.W.T.; Contributions to Mineralogy and Petrology, v. 44, p. 29-34.

Nielsen, P.A.
1977: Mineralogy and metamorphic petrology of the Arseno Lake area, N.W.T.; unpublished Ph.D. thesis, University of Alberta.

URANIUM AND THORIUM IN CANADA, 1978

Project 750010

V. Ruzicka
Regional and Economic Geology Division

Ruzicka, V., Uranium and thorium in Canada, 1978; in Current Research, Part A, Geol. Surv. Can., Paper 79-1A, p. 139-155, 1979.

Abstract

Results of field, laboratory and office investigations on uranium and thorium occurrences and resources are described briefly. Uranium and thorium resources in the Grenville Geological Province occur mainly in magmatic/anatectic deposits; in the Southern Geological Province they occur in Huronian quartz-pebble conglomerate; in the Superior Geological Province the pegmatitic occurrences prevail. The Churchill Geological Province contains high grade unconformity-type uranium deposits, and Precambrian sandstone-hosted deposits occur in the Bear Province. New uranium mineralization in polymetallic assemblages was identified in the Slave Geological Province. Appalachian Orogen contains environments favourable for deposits in peribatholithic pelite and in intragranitic structures. In the Cordilleran Orogen the main uranium deposits occur in volcanic environment, in clastic sediments, and in granitic-pegmatitic rocks. The Hudson Platform contains areas favourable for sandstone-type uranium mineralization.

Introduction

During 1978 the Uranium Resource Evaluation Section of the Geological Survey of Canada participated in the Uranium Resource Evaluation Program in areas studied in the previous years (E.M.R., 1978) and in new areas favourable for uranium mineralization (Fig. 27.1a, b). Several reports on these studies are included in this volume.

The author conducted field work and/or laboratory investigations during 1978 in the following geological provinces: Grenville, Southern, Superior, Churchill, Slave, Bear, Appalachian Orogen, Cordilleran Orogen, and Hudson Platform.

In addition to the field and laboratory work a radiometric survey on selected GSC sample collections was conducted which resulted in the discovery of several localities having uranium associated with other nonradioactive mineralization (Fig. 27.2).

Geological investigations were the basis for modification of previously established conceptual genetic models for various types of uranium deposits (Ruzicka, 1977b).

These data, along with computerized data collected in CANMINDEX (Ruzicka, 1977a), Atomic Energy Control Board files, Departmental Uranium Exploration Survey (E.M.R., 1978), Federal-Provincial Uranium Reconnaissance Program, Provincial Assessment files, and special subprojects, are being used for the 1978 assessment of Canada's uranium and thorium resources.

The investigations were conducted in close co-operation with exploration and mining companies, other provincial and federal organizations, and members of the Uranium Resource Evaluation Section, namely L.P. Tremblay (Saskatchewan and Quebec), S.S. Gandhi (Hornby Bay – Dismal Lakes area), and H.E. Dunsmore (Appalachian Orogen).

Studies on Canada's uranium and thorium resources are summarized in a Report on the International Uranium Resource Evaluation Project (IUREP) Phase I that is being prepared under the sponsorship of the Organization for Economic Co-operation and Development (OECD) and International Atomic Energy Agency (IAEA).

This paper outlines the results of field work in the geological provinces noted above and reports on current laboratory and office work in uranium and thorium investigations.

Grenville Geological Province

At present the only uranium-producing mine in the Grenville Geological Province is the Faraday mine at Bancroft, Ontario which is owned by Madawaska Mines Limited. The Bancroft segment is a part of the Pembroke-Renfrew area discussed below. The uranium mineralization occurs in a swarm of leucogranite, leucogranite pegmatite, and pyroxene granite and syenite pegmatite dykes that cut paragneiss and amphibolite country rocks (Ruzicka, 1971). The reported ore reserves (Worobec, 1978) in 1975 amounted to 928 127 tonnes with an average grade of 0.12 per cent uranium and resources additional to reserves of 1 451 494 tonnes with an average grade 0.08 per cent uranium.

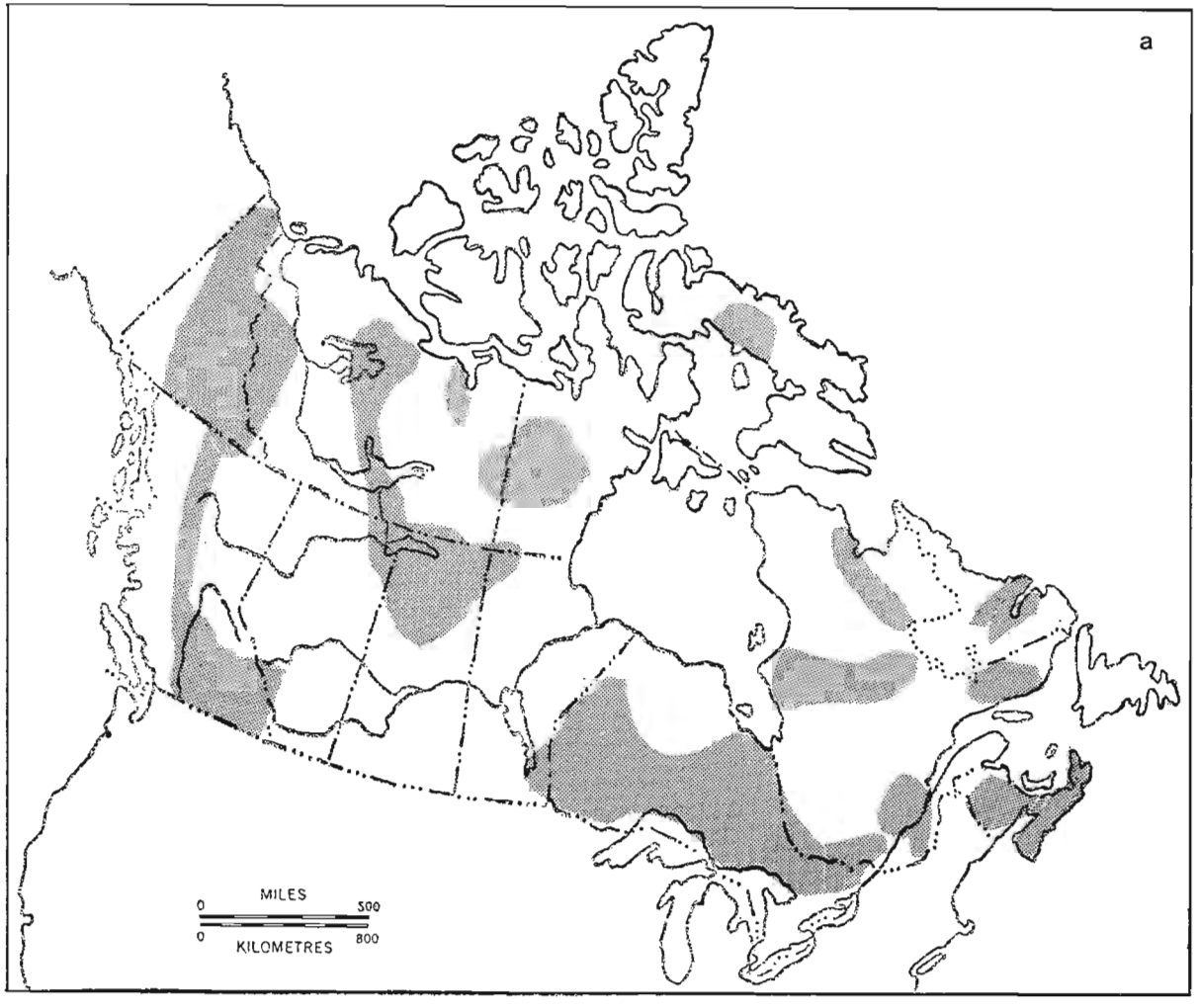
A similar type of mineralization prevails in several other areas of the Grenville Geological Province, such as (1)[1] Pembroke-Renfrew, (2) MacTier, and (3) Sharbot Lake in Ontario (Robertson, 1977) and (4) Fort Coulogne, (5) Mont Laurier, and (6) Johan Beetz in Quebec. In 1978 these areas were targets of industrial exploration and geological research.

The Ontario Geological Survey has conducted integrated geoscience surveys in the Pembroke-Renfrew area (1, Fig. 27.1) since 1977 (Gordon et al., 1977); detailed investigations of uranium occurrences in the Bancroft segment were carried out in 1978. The author visited this area along with J.A. Robertson and J.B. Gordon of the Ontario Geological Survey in 1978.

According to geological mapping conducted by the Ontario Geological Survey (Gordon et al., 1977) the uranium mineralization in the Bancroft segment is apparently stratigraphically and structurally controlled. If more evidence for this relationship is found this criterion will be used for delineation of areas favourable for uranium deposits elsewhere in the Grenville Geological Province. In some parts of the Bancroft area the uranium-bearing pegmatites are spatially related to garnetiferous gneiss. This observation led D. Hendrick of Kerr Addison Mines Limited (pers. comm.) to a similar conclusion that the uranium mineralization in the area is stratigraphically and structurally controlled.

Near Tooyi Lake (Brougham Township, Concession 18, Lot 31) in the Pembroke-Renfrew area the uranium and thorium occur in granite pegmatite dykes cutting calc-silicate gneiss. The mineral assemblage consists of magnetite, uraniferous thorite (Fig. 27.3), allanite, niobium sphene, and zircon.

[1]Numbers in brackets refer to locality numbers on Figure 27.1.



a. *Studies reported in this paper.*

b. *Patterned areas indicate field studies by URES members.*

Figure 27.1. *Areas studied by the Uranium Resources Evaluation Section (URES) in 1978.*

Legend for 27.1b

(A) Grenville Geological Province
1. Pembroke – Renfrew
2. Mac Tier
3. Sharbot Lake, Ontario
4. Fort Coulogne
5. Mont Laurier
6. Johan Beetz, Quebec

(B) Southern Geological Province
1. Elliot Lake
2. Agnew Lake
3. Cobalt Embayment, Ontario

(C) Superior Geological Province; areas
1. Prairie Lake
2. Kenora – Dryden
3. Favourable Lake
4. Timmins
5. Cobalt
6. Manitouwadge, Ontario
7. Pinawa
8. Bisset, Manitoba

(D) Churchill Geological Province; areas
1. Tazin Belt and cover
2. Wollaston Lake Belt and cover, Saskatchewan
3. Baker Lake
4. Amer Lake
5. Yathkyed Lake
6. Melville Peninsula, Northwest Territories

(E) Slave Geological Province

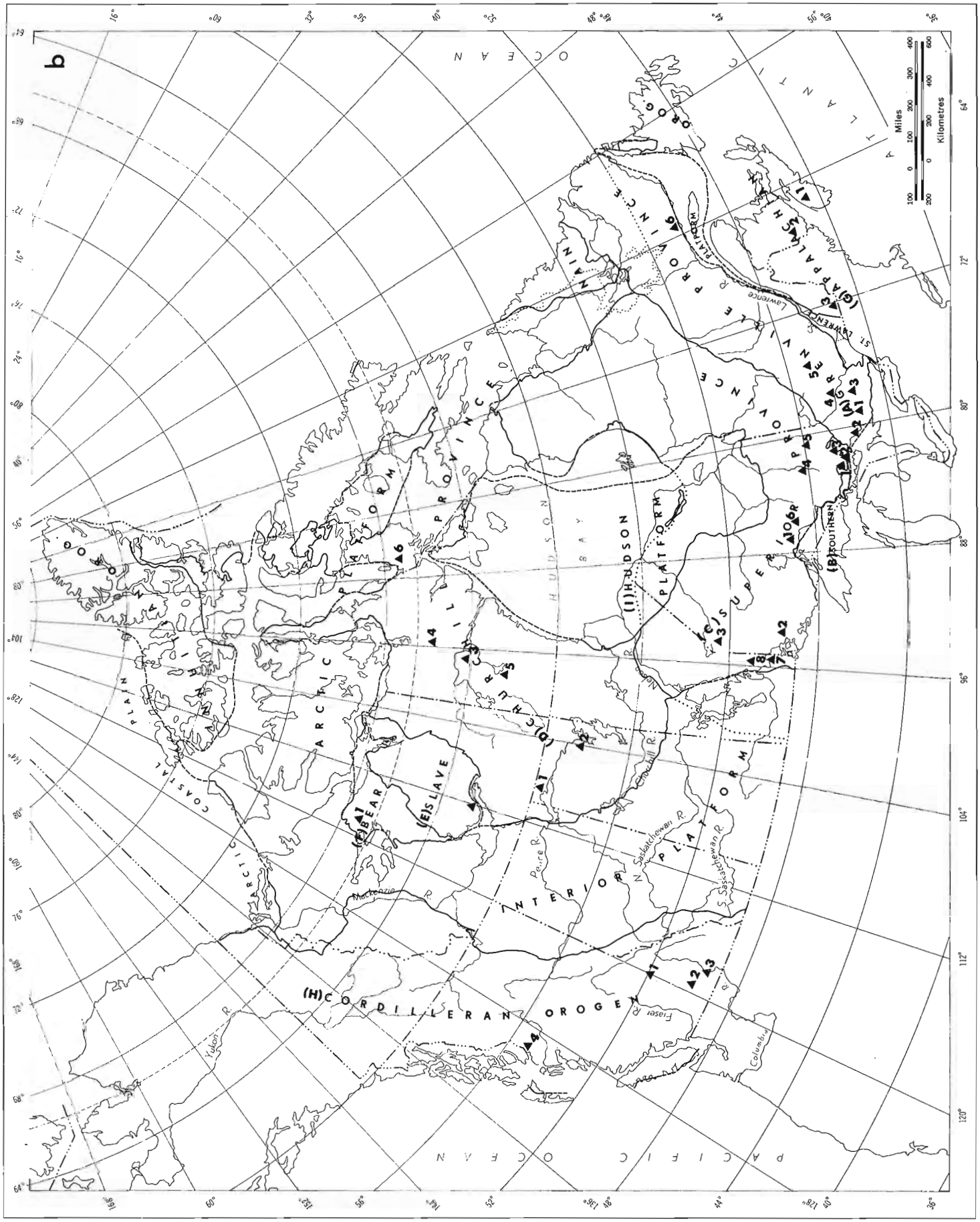
(F) Bear Geological Province; areas
1. Hornby Bay – Dismal Lakes

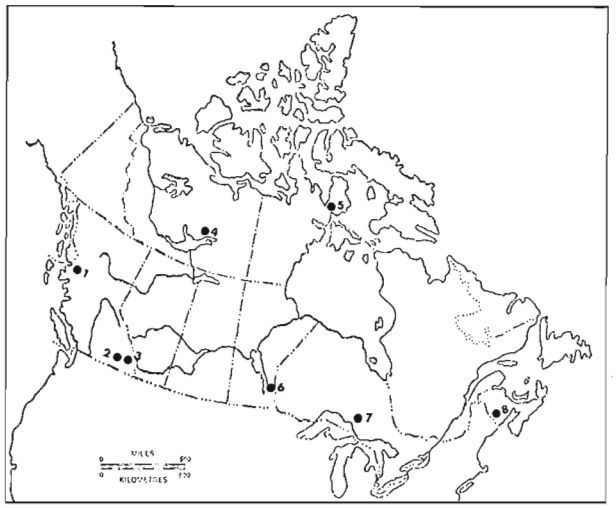
(G) Appalachian Orogen; areas
1. Annapolis Valley, Nova Scotia
2. Mactaquac, New Brunswick
3. St. Armand, Quebec

(H) Cordilleran Orogen; areas
1. Birch Island
2. Beaverdell
3. Grand Forks – Nelson
4. Coast Plutonic Complex, British Columbia

(I) Hudson Platform; area
1. Coral Rapids – Moosonee, Ontario

(The triangle symbols are in centres of the areas.)


b
Miles
Kilometres
(H) CORDILLERAN OROGEN
(I) HUDSON PLATFORM
(J) SUPERIOR PROVINCE
(K) CHURCHILL
(L) ALBERTA PLATEAU
(M) WILLISTON PLATFORM
(N) ARCTIC PLATFORM
(O) ARCTIC COASTAL PLAIN
(P) INTERIOR PLATFORM
(Q) GREAT BEAR
(R) SLAVE
(S) INTERIOR PLAINS
(T) ROCKY MOUNTAIN TROUGH
(U) ROCKY MOUNTAIN FOREDEEP
(V) GREAT PLAINS
(W) WESTERN CANADA BASIN
(X) ARCTIC PLATFORM
(Y) ARCTIC COASTAL PLAIN
(Z) ARCTIC PLATFORM
(A) ARCTIC COASTAL PLAIN
(B) FOUTHEN
(C) BEAR
(D) SLAVE
(E) SUPERIOR
(F) CHURCHILL
(G) ALBERTA PLATEAU



1. *Anyox mine near Prince Rupert, British Columbia; sulphide ore sample; collected by R.V. Kirkham.*
2. *Silver Hood mine, Ainsworth, British Columbia; fluorite and Ag-Pb-Zn mineralization; collected by R. Mulligan.*
3. *Purcell Mountains, British Columbia (50 12'37"N, 115 08'45"W); fault breccia with purple fluorite in Ordovician strata; collected by G.B. Leech.*
4. *Sachowia Lake, Northwest Territories (62 24'40"N, 111 51'30"W); Ni-Co-Bi arsenides; collected by R. Eckstrand.*
5. *Melville Peninsula, Northwest Territories; granite and augen gneiss; collected by J.E. Reesor.*
6. *Stratford Lake, Manitoba; pegmatite; collected by R. Mulligan.*
7. *Geco mine, Manitouwadge, Ontario; pegmatite in contact with a Cu-Zn-Ag-Pb ore; collected by R.V. Kirkham.*
8. *Mactaquac area, New Brunswick; mineralized shale; collected by D.F. Sangster.*

Figure 27.2. *Localities with uranium or thorium associated with nonradioactive mineralization; radioactivity of samples, collected from these localities, was detected during a radiometric testing of the GSC collections.*

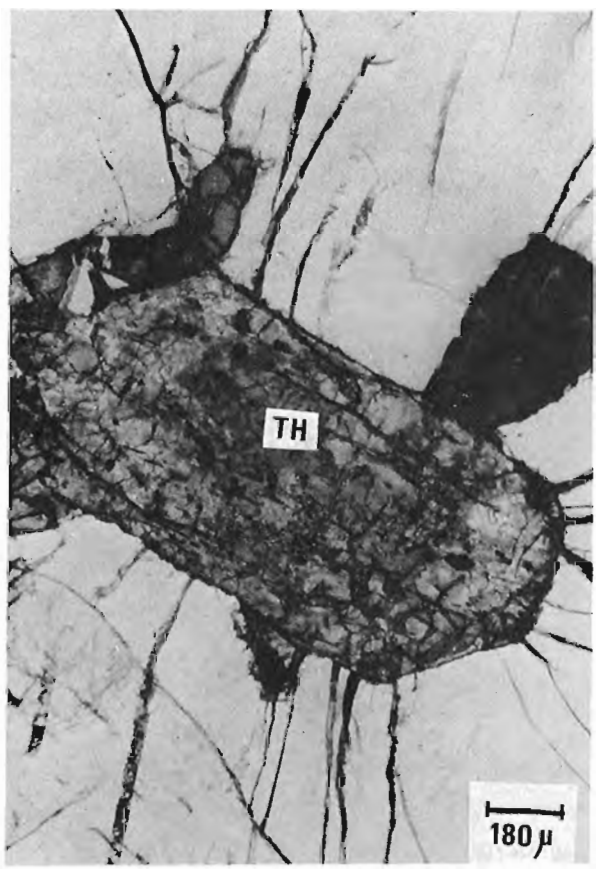


Figure 27.3. *Uraniferous thorite (TH) from a granite pegmatite dyke cutting calc-silicate gneiss near Tooyi Lake, Brougham Township, Ontario. (Reflected light.)*

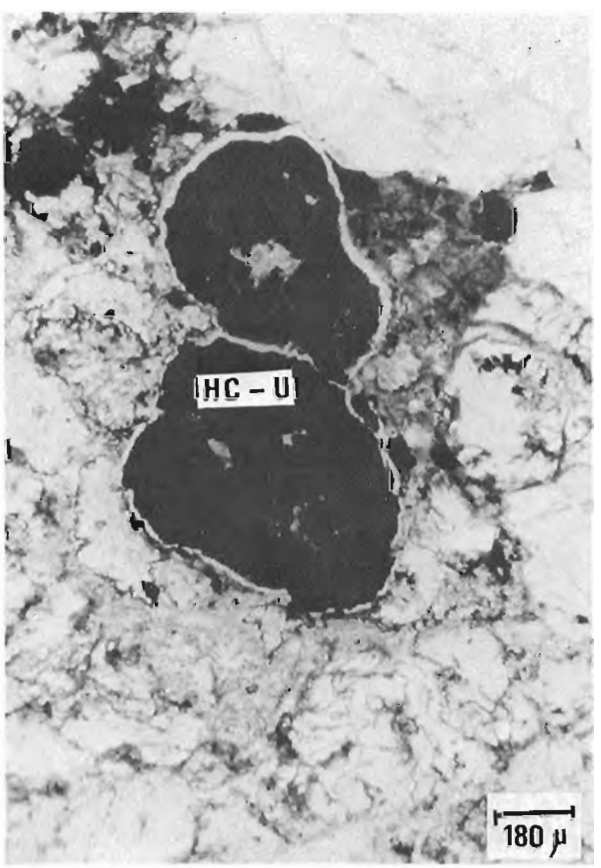


Figure 27.4. *Hydrocarbon containing uraninite (HC-U) ("thucholite") from Zenith mine near Renfrew, Ontario. (Reflected light, parallel nicols.)*

Table 27.1

Selected constituents of radioactive samples from some localities in Pembroke-Renfrew area, Ontario

Constituents in per cent[2]

Sample[1] Number	MnO	TiO_2	CaO	K_2O	SiO_2	Al_2O_3	MgO	FeO	Fe_2O_3	Na_2O	P_2O_5	Nb	Nd	S	Zn	Pb	U	Th
RAD77-405	0.04	1.69	2.51	3.72	49.4	15.1	10.9	5.4	1.7	2.2	0.24	0.01	N.F.	0.2	N.F.	N.F.	0.01	0.0
406	0.03	0.02	4.10	5.21	60.7	12.7	5.2	2.6	1.0	2.0	0.02	N.F.	N.F.	0.3	N.F.	N.F.	0.005	0.008
410	0.1	>16.0	21.0	0.6	>36.0	> 5.0	2.0	3.0	3.0	0.0	0.0	0.7	0.5	0.0	2.0	N.F.	0.05	0.07
415	0.02	2.02	1.52	0.35	80.5	4.8	0.43	2.4	4.5	1.7	0.17	0.015	0.05	0.0	N.F.	N.F.	0.01	0.28
416	0.1	0.8	5.0	1.0	71.0	8.0	0.50	0.5	5.0	2.0	0.0	0.03	0.1	0.0	N.F.	N.F.	0.08	0.32

	Occurrence (Area)	Latitude	Longitude
[1] RAD77-405	Zenith mine (Pembroke-Renfrew)	45°23'N	76°40'W
406	Zenith mine (Pembroke-Renfrew)	45°23'N	76°40'W
410	Opeongo mine (Pembroke-Renfrew)	45°29'N	77°12'W
415	Tooyi Lake (Pembroke-Renfrew)	45°17'N	76°58'W
416	Tooyi Lake (Pembroke-Renfrew)	45°17'N	76°58'W

[2] Analyses for: uranium: Atomic Energy Canada Limited by Neutron Activation
thorium: Geological Survey, G.R. Lachance by X-ray fluorescence
major constituents: Geological Survey, J.L. Bouvier by XFD-S30
Nb , Nd, S, Zn, Pb: Geological Survey, T. Lelites by QN-12b spectrometer.

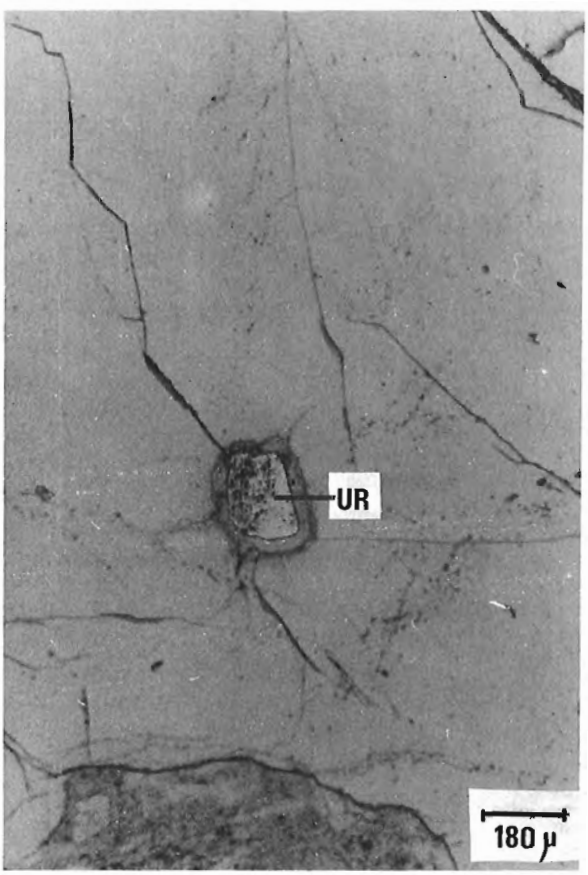


Figure 27.5. *Uraninite (UR) in a granite pegmatite from Midwest Development occurrence, Ogden Township, Ontario, approximately 5 km west of Clarendon Station. Note radiating fractures. (Reflected light, parallel nicols.)*

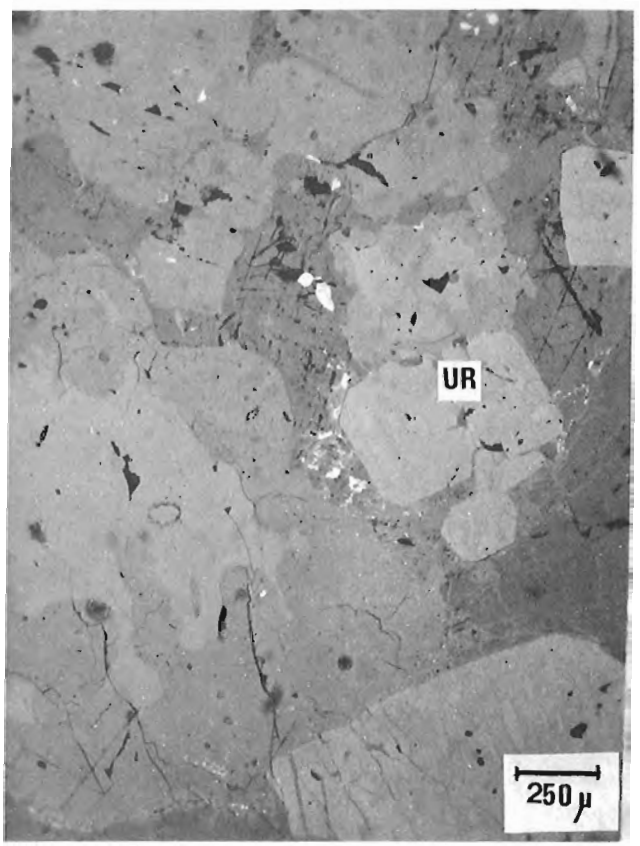


Figure 27.6. *Uraninite (UR) in a white pegmatite from Joliette Township, Mont Laurier area, Quebec. (Reflected light.)*

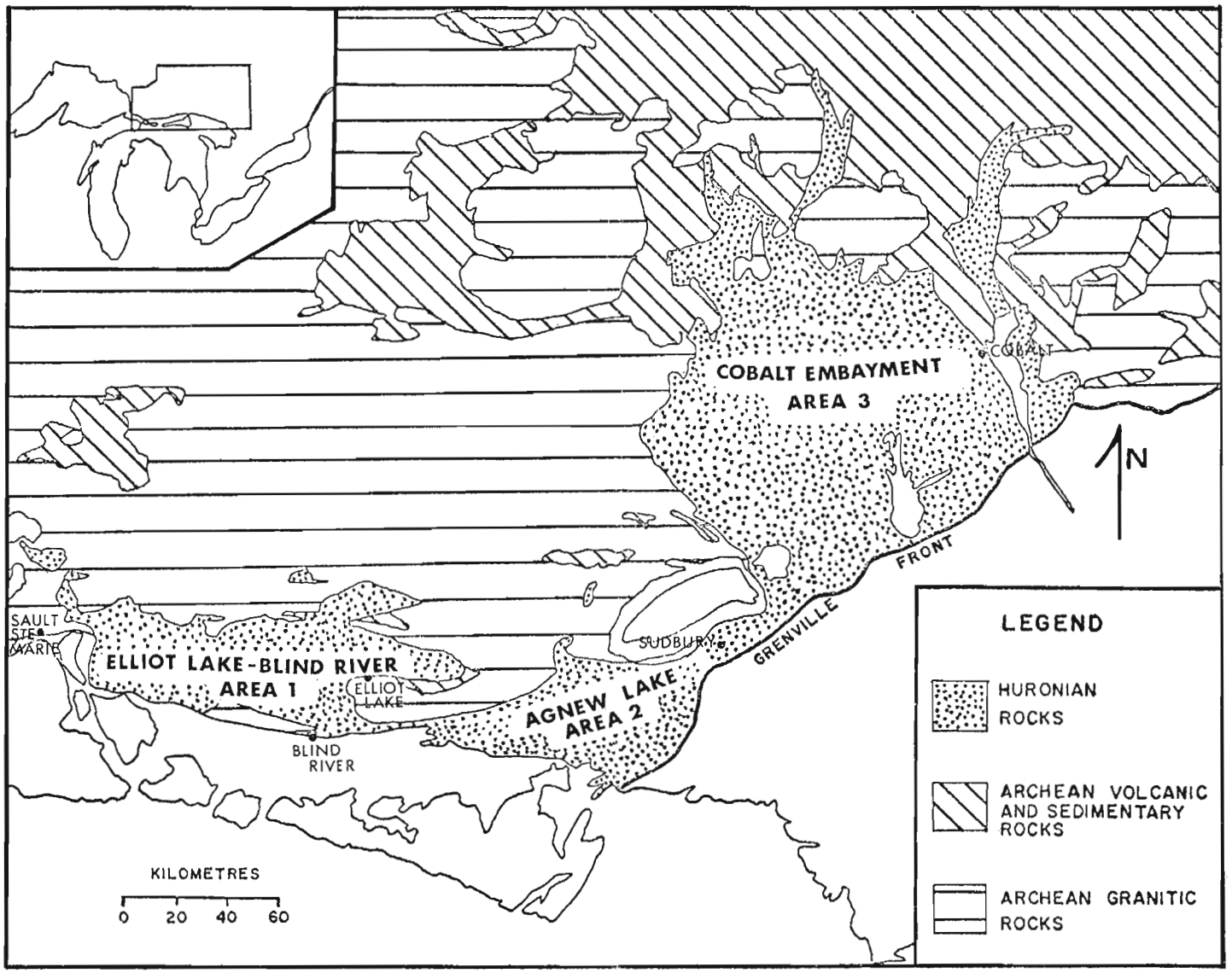


Figure 27.7. *Distribution of rocks of the Huronian Supergroup in the Southern Geological Province, Ontario.*

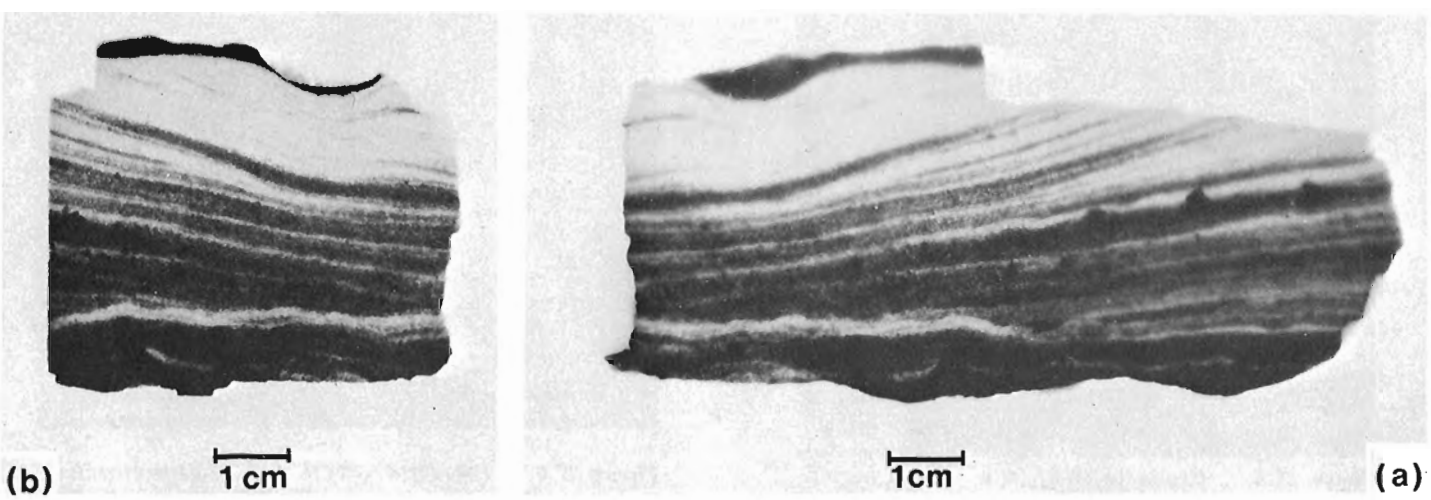


Figure 27.8. *Autoradiograph of a high grade ore sample from Quirke I mine, Rio Algom Limited, Elliot Lake, Ontario, Panel 507. Light bands indicate radioactive material. Side a of the sample is perpendicular to side b.*

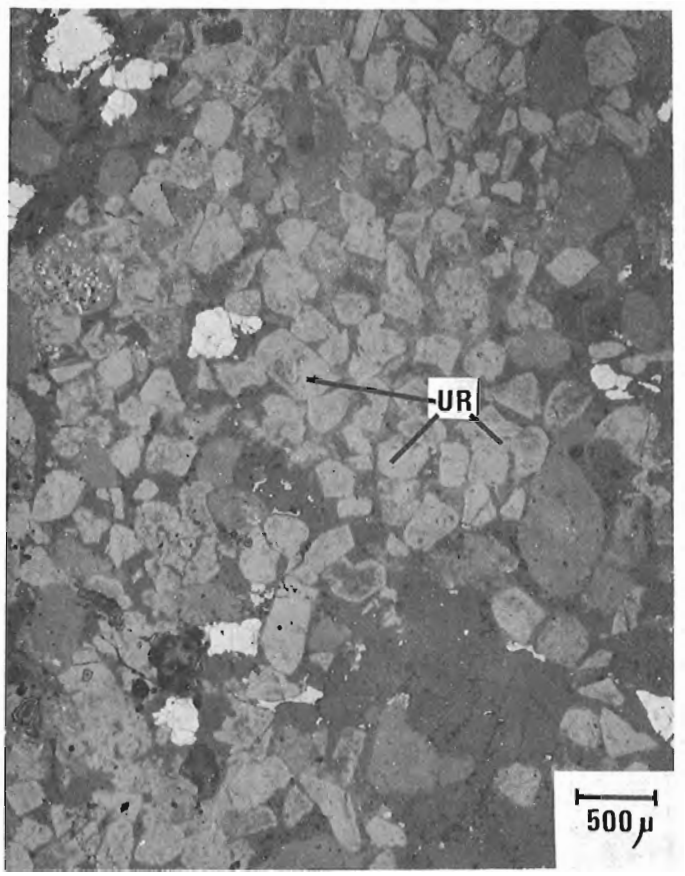


Figure 27.9. *Uraninite (UR) of a radioactive crossbed shown in Figure 27.8. (Reflected light.)*

Thorite is apparently the main radioactive mineral in the Opeongo mine (Sebastopol Township) where a syenite pegmatite dyke cuts a quartz-feldspar paragneiss. The thorite occurs in areas in the dyke rich in sphene.

The radioactive granite pegmatites of the Zenith Mine near Renfrew (Hewitt, 1967) contain microscopic inclusions of uraninite along with minor amounts of calcium, sulphur, and thorium in hydrocarbon (Fig. 27.4).

Selected chemical constituents of the radioactive samples from some localities in the Pembroke-Renfrew area are shown in Table 27.1.

In the MacTier area (2) the samples with uranium mineralization (investigated in the laboratory) were collected on claims owned by M. Phillips of Toronto. The main uranium mineral identified was uraninite locally associated with copper minerals in a granite pegmatite.

In the Sharbot Lake area (3) a uranium occurrence in Ogden Township, approximately 5 km west of Clarendon Station, was investigated in the field in 1977 (Ruzicka, 1978; Robertson, 1977) and through laboratory work in 1978. The radioactive mineralization is confined to red granite pegmatite dykes, 1 to 5 m wide, that occur in locally garnetiferous gneiss. In some places the gneiss contains quartz porphyroblasts and resembles strongly metamorphosed quartz-pebble conglomerate. The radioactive minerals are mainly uraninite (Fig. 27.5) and thorite. An approximately 0.5 kg sample (randomly collected) contained 0.02 per cent U and 0.007 per cent Th.

In the Fort Coulogne area (4) several exploration companies, including Copconda Mines Limited, Augmitto Explorations Limited, and Carling Copper Limited, conducted exploration of a large radiometric anomaly detected by a Geological Survey of Canada airborne survey near Hikey and Hart lakes. The host rocks of the uranium mineralization are granitized sediments (?) that are locally garnetiferous. Some of the mineralization occurs in limnonitized shear zones.

The main uranium mineral in samples collected in the Mont Laurier area (5), Joliette Township is uraninite (Fig. 27.6) in a white granite pegmatite.

Uranium mineralization in the Johan Beetz area (6) is being studied by J.Y.H. Rimsaite of the Uranium Resource Evaluation Section. This area contains, according to estimates made by the Section, several hundred million tonnes of mineralized granite rocks with an average content in the range between 100 to 200 ppm U.

Two important uranium metallogenic features of the Grenville Province that can be summarized from the field and laboratory studies and a review of the literature are:

(a) uranium mineralization commonly occurs in granitic or syenitic rocks that were apparently derived from original uraniferous sediments;

(b) certain crystalline radioactive minerals, such as uraninite and thorite, were formed under elevated thermodynamic conditions (Frondel, 1958).

Reasonably Assured and Estimated Additional uranium resources of the Grenville Geological Province, according to present estimates, amount to about two per cent of Canada's total uranium resources.

Southern Geological Province

At present most of Canada's uranium is produced in the Southern Geological Province at Elliot Lake and Agnew Lake. The uranium deposits occur in Lower Proterozoic (Aphebian) quartz-pebble conglomerate of the Huronian Supergroup (Roscoe, 1969; Robertson, 1977). This uranium-bearing region can be divided into three areas (Fig. 27.7):

(1) Elliot Lake extending from Sault Ste. Marie to Massey, Ontario, along the north shore of Lake Huron;

(2) Agnew Lake, Ontario between Massey and Sudbury; and

(3) the Cobalt Embayment, north of Sudbury.

Genesis of the uranium mineralization in the Huronian quartz-pebble conglomerate is still a subject of discussion. The author favours a syngenetic (detrital) origin of the uranium mineralization with some modifications during diagenesis of the conglomerate (Ruzicka and Steacy, 1976; Ruzicka, in press). These two genetic features can be demonstrated by some observations during recent studies on samples from Quirke 1 mine of Rio Algom Limited in the Elliot Lake area (1, Fig. 27.1b):

(a) an autoradiograph of a sample collected by D. Sprague of Rio Algom Limited shows crossbedding of the radioactive mineralization (Fig. 27.8). The radioactive crossbeds consist mainly of subrounded grains of uraninite (Fig. 27.9). This testifies to a detrital nature of the uraninite grains.

(b) Some of the uraninite grains of the same sample (Fig. 27.10a, b) have relatively fresh rims whereas their cores show effects of disintegration, apparently due to weathering. This is interpreted by the author as a feature developed during diagenesis when surfaces of some partly weathered uraninite grains were cemented (or 'healed') by uranium dissolved in the connate water.

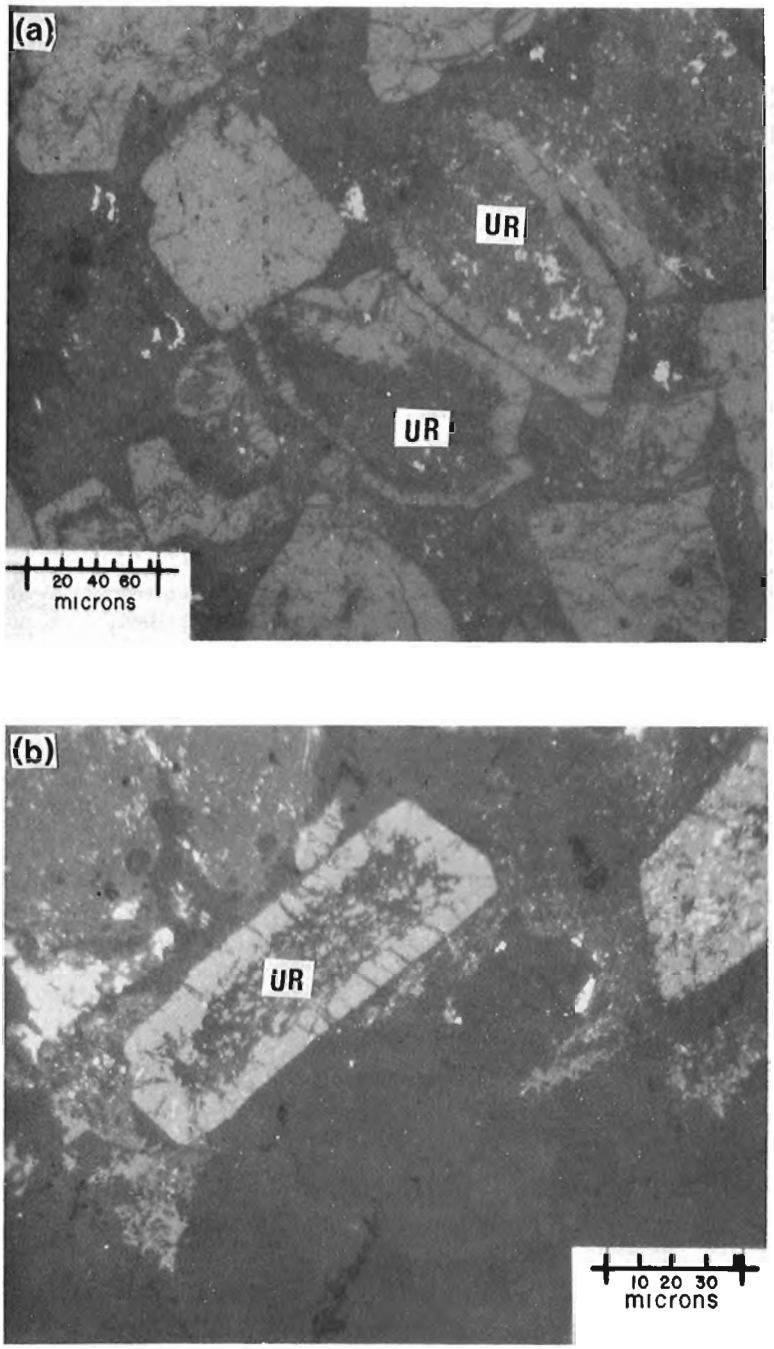


Figure 27.10. *Uraninite grains (UR) in a radioactive crossbed shown in Figure 27.8. The grains have weathered cores and "fresh" rims cemented ("healed") by uranium. (Reflected light.)*

Uranium-bearing hydrocarbon as a component of the Elliot Lake ores was described by Ruzicka and Steacy (1976), Roscoe (1969), and Ruzicka (in press). A new occurrence of the uraniferous hydrocarbon in Huronian conglomerate was identified in the Agnew Lake area (2) in May Township, near Wilson Lake on the Alexander occurrence (Robertson, 1968). The uraniferous hydrocarbon (also called 'thucholite' or 'carburan') occurs in a quartz-pebble conglomerate in association with pyrite (Fig. 27.11). Figure 27.12 shows an accumulation of the hydrocarbon (from the same locality) with inclusions of residual uraninite. The speck of the hydrocarbon may be interpreted as a remnant of an algal mat. This could be considered as additional evidence of the sedimentary syngenetic origin of uranium mineralization in the quartz-pebble conglomerate as postulated by the author's model (Ruzicka, 1977b).

Uranium associated with monazite and zircon was identified in a sample of a radioactive pebbly subarkose from a locality in Ermatinger Township (Thompson, 1960) in the Cobalt Embayment (3).

Reasonably Assured and Estimated Additional uranium resources of the Southern Geological Province occur mainly in Huronian quartz-pebble conglomerate. According to present estimates these resources constitute 59 per cent of Canada's Reasonably Assured and Estimated Additional uranium resources.

Superior Geological Province

No producing uranium mine exists in the Superior Geological Province. On the other hand several areas contain clusters of uranium occurrences.

The author conducted field and/or laboratory work in the following areas (Fig. 27.1b): (1) Prairie Lake, (2) Kenora-Dryden, (3) Favourable Lake, (4) Timmins, (5) Cobalt, and (6) Manitouwadge, all in Ontario. The field work in Ontario was conducted in close co-operation with the Ontario Geological Survey, particularly with J.A. Robertson, L. Tihor, H.L. Lovell, and L.S. Jensen.

During a spectrochemical examination of selected radioactive samples of ijolite from the Prairie Lake area (1) that is being explored by New Insco Mines Limited, levels of 10 to 20 per cent P_2Q_5, 0.5 to 1 per cent Nb, 0.15 to 0.20 per cent Nd, 0.3 per cent Sr, up to 0.1 per cent Zr, 0.2 to 0.3 per cent Ce, and up to 0.1 per cent La, were detected. Uranium contents, according to neutron activation, were in the range between 0.02 and 0.29 per cent U and thorium between 0.01 and 0.05 per cent Th. During a microscopic examination of the samples uranium was found in niobium titanates possibly euxenite type minerals (Fig. 27.13a, b). Laboratory examination of the samples continues.

In the Kenora-Dryden area (2) uraniferous granitic-pegmatitic rocks, a product of Kenoran Orogeny, contain several radioactive occurrences (Beard and Rivett, 1978; Robertson, 1977). However, uranium reserves were identified only in the New Campbell Island Mine near Dryden. The mine containing 590 000 tonnes of ore of an average grade 0.08 per cent U (Robertson, 1968) is dormant. The author visited most of the properties along with J.A. Robertson and R. Beard of Ontario Geological Survey in 1976 and 1977 and examined selected samples in 1978. Spectrochemical analyses of samples collected at the Petursson Lake occurrence (Beard and Rivett, 1978), explored by Sherritt Gordon Mines Limited, at the Coulee occurrence south of Game Lake in Bridges Township and from the Fairservice occurrence in the same township showed that a group of certain elements is commonly associated with uranium and thorium. These elements are: Mg, Ti, Mn, Cu, Mo, Pb, Sc, Sr, Y, and Yb (Table 27.2). Most of the uranium mineralization in the Kenora-Dryden area occurs in pegmatite dykes, commonly as minute inclusions of uraninite in magnetite (Fig. 27.14). Uraninite crystals in magnetite are frequently rimmed by hematite (Fig. 27.15). The magnetite exhibits fractures radiating around uraninite. The hematite rims may be

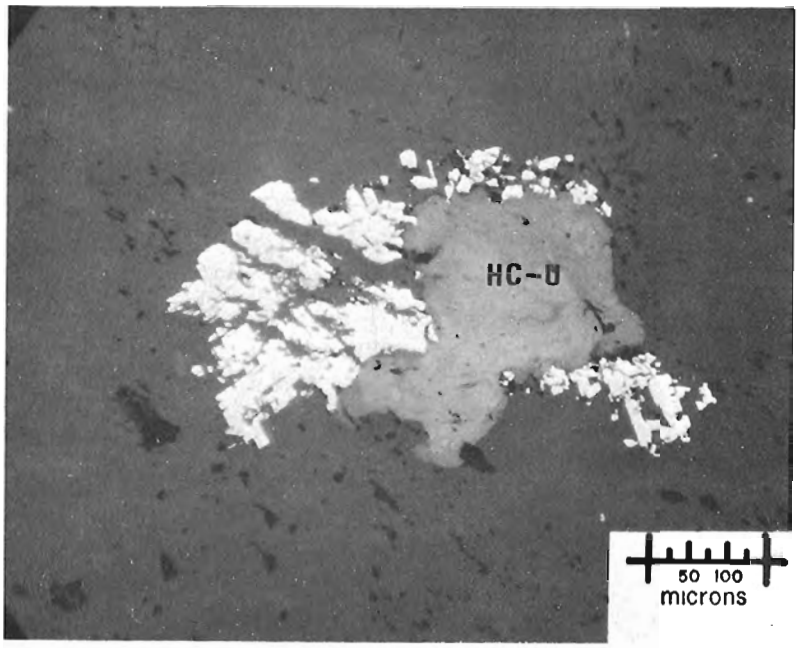


Figure 27.11. *Uraniferous hydrocarbon (HC-U) or "thucholite" associated with pyrite in radioactive quartz-pebble conglomerate from Alexander occurrence near Massey, Ontario. (Reflected light.)*

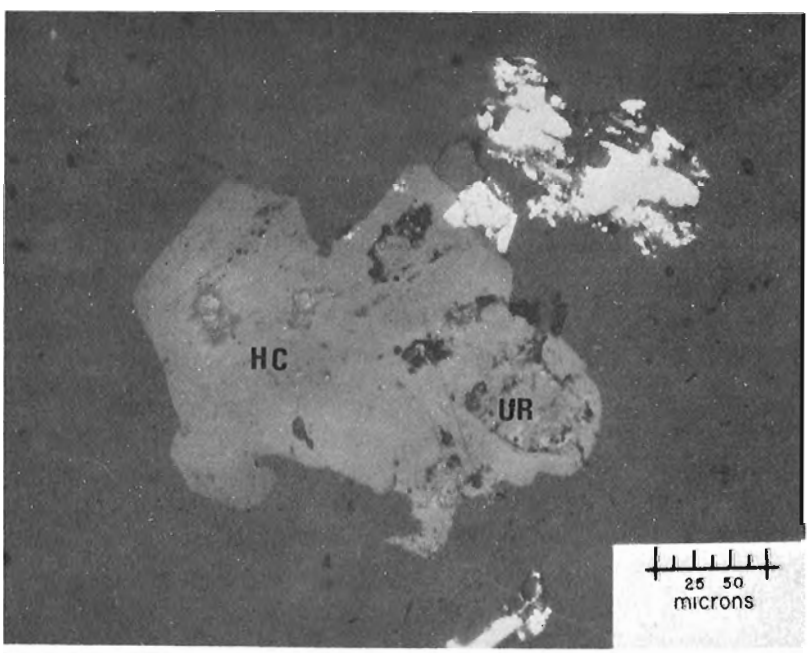


Figure 27.12. *Uraninite (UR) assimilated by hydrocarbon (HC) in Huronian quartz-pebble conglomerate from Alexander occurrence near Massey, Ontario.*

interpreted as effects of the uraninite on the surrounding magnetite, either due to ionization or due to release of oxygen during diagenetic processes. It is postulated that the uranium mineralization in the above occurrences was derived from uraniferous sediments and reworked by granitization.

The Kenoran granitic rocks host uranium mineralization in the Favourable Lake area (3). As in the Kenora-Dryden area the uranium and thorium is accompanied by a group of elements, such as Mg, Ti (up to 3 per cent), Mn, Cu, Mo, Pb (up to 0.3 per cent), Sc, Sr, Y, and Yb (Table 27.2).

The author visited the Beach Gold Mines Limited prospect near Gogama in Timmins area, Ontario (4) along with J.A. Robertson and L. Tihor of the Ontario Geological Survey. The uranium and thorium mineralization occurs in sheared granite pegmatite dykes that extend for several hundred metres.

Examination of the cobalt-silver deposits at Cobalt, Ontario (6) led to the discovery of two occurrences of uranium mineralization from this area. A sample of a cobalt-silver ore from the Kerr Lake mine (Kanadaka Mines Limited) on display at the Cobalt Mining Museum was tested and found to be radioactive. Radioactive mineralization was also found in argillitic rocks on a dump of the Silvermaque mine (number 139 on the Ontario Compilation map 2361). The radioactive mineral is pitchblende containing Pb, but no Th, accompanied by allanite, rich in rare earth elements (REE). The host rock is apparently argillite. This occurrence was discovered by application of a conceptual genetic model for vein type uranium deposits in peribatholithic shale (that commonly contains the so-called 'five element formation', i.e. Bi, Co, Ni, Ag, U association) to the geology of the Cobalt area (Ruzicka, 1971).

A radiometric testing of the Geological Survey sample collections led to discoveries of uranium mineralization in: (a) a sample from the Geco mine, Manitouwadge area (6), Ontario, collected by R.V. Kirkham and (b) a sample of monazite-bearing pegmatite from the Pinawa area (7), Manitoba, collected by R. Mulligan (see Fig. 27.2).

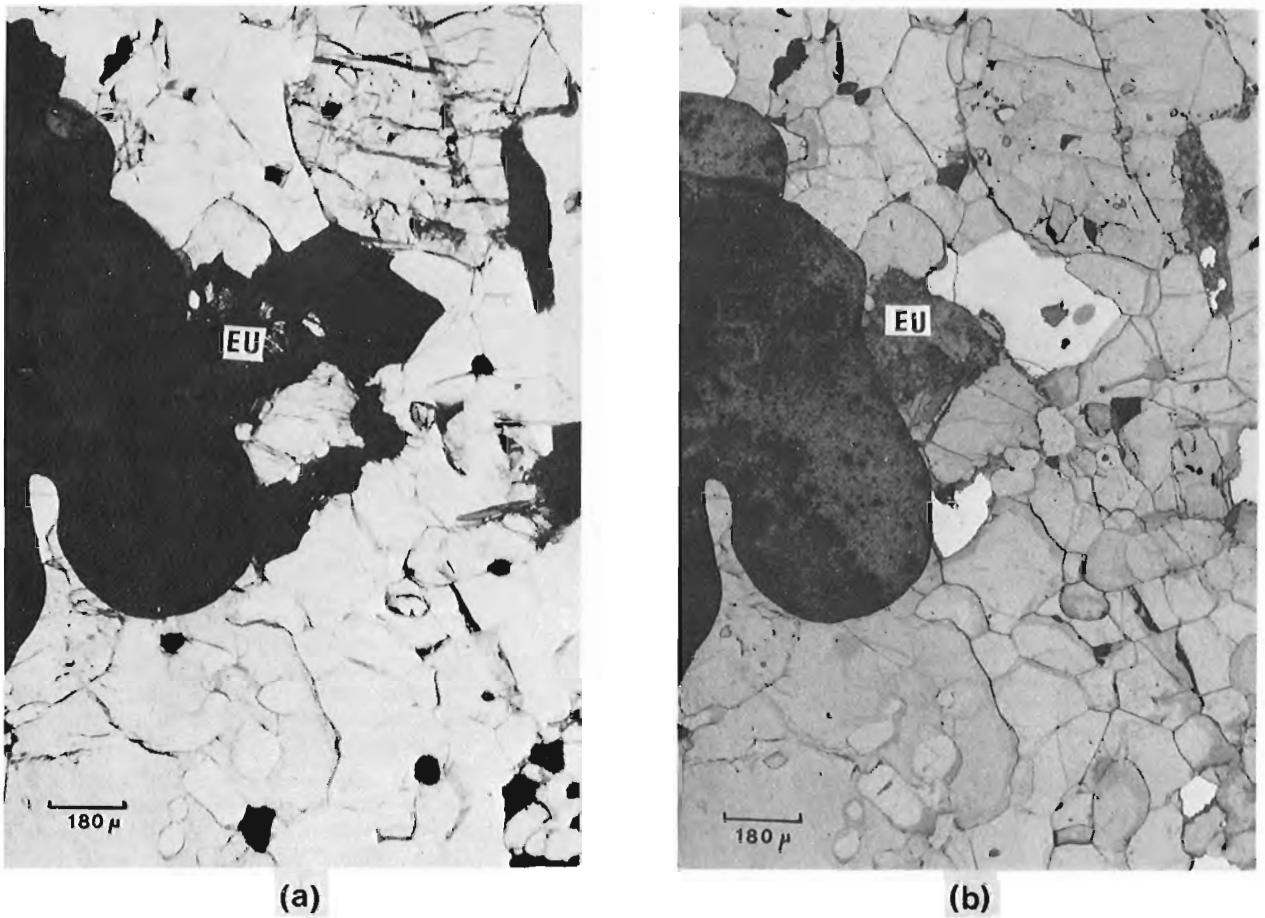
Lower Proterozoic pebbly arkose of the San Antonio Formation in the Bisset area, Manitoba (7), contain uranium mineralization commonly associated with fracture zones. The prospect is held by Dome Mines Limited.

The Superior Geological Province contains several occurrences in Quebec, such as that at Sakami Lake, owned by INCO and James Bay Corporation, or those being explored by Group Minier S.E.S. and Uranerz Exploration and Mining Canada Limited.

The known uranium occurrences in the Superior Geological Province belong to several types: (a) Precambrian quartz-pebble conglomerate (e.g. Sakami Lake, Quebec); (b) vein and/or unconformity related occurrences (e.g. Cobalt area, Ontario; Otish Mountains, Quebec); and (c) magmatic/anatectic and related deposits in granite and syenite pegmatites and associated rocks (e.g. Kenora-Dryden and Favourable Lake areas, Ontario). This geological province contributes approximately one per cent of Canada's Reasonably Assured and Estimated Additional uranium resources.

Churchill Geological Province

Two mines, the Beaverlodge operation of Eldorado Nuclear Limited, and the Rabbit Lake deposit of Gulf Minerals Limited, are producing uranium in the Churchill Geological Province and several deposits, such as Key Lake,



Transmitted light *Reflected light*

Figure 27.13. *Ijolite containing uraniferous niobium titanates (possibly euxenite type minerals) (EU). Sample from a New Insco Mines property at Prairie Lake, Ontario.*

Cluff Lake, Collins Bay, Maurice Bay and Midwest Lake are being thoroughly explored or developed for production in the 1980's. The amount of uranium in these deposits represents several hundred thousands of tonnes of uranium metal in ores commonly having average grades from 0.3 to 10 per cent U or even higher.

The author, along with L.P. Tremblay of the Uranium Resource Evaluation Section, examined deposits and occurrences spatially related to pre-Athabasca and pre-Martin unconformities in the (1) Tazin Belt and cover rocks, (2) Wollaston Lake Fold Belt and cover rocks in northern Saskatchewan (Fig. 27.16) and conducted studies on the (3) Baker Lake, (4) Amer Lake and (5) Yathkyed Lake areas in Northwest Territories (see Fig. 27.1b).

Uranium deposits in the Tazin Belt and cover rocks (1) can be classified into the following types: (a) vein and fracture controlled deposits (e.g. Fay-Verna in Beaverlodge); (b) unconformity deposits (e.g. Maurice Bay and Fond du Lac); (c) disseminations in pegmatites (e.g. Charlebois Lake and (d) intragranitic replacements (e.g. Gunnar, Beaverlodge). With the exception of the unconformity deposits, the geology and genesis

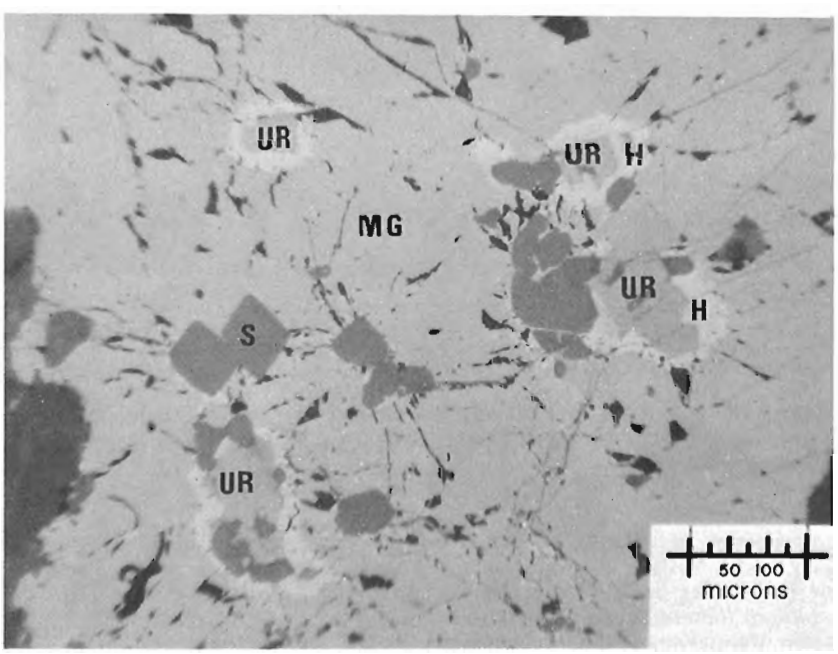


Figure 27.14. *Uraninite (UR) enclosed in magnetite (MG) and rimmed by hematite (H) in pegmatite from Kenora – Dryden area, Ontario. The sample contains sphene (S). (Reflected light.)*

Table 27.2

Elements associated with uranium and thorium in selected occurrences in Kenora-Dryden and Favourable Lake areas, Ontario

Sample[1] Number	Constituents in per cent[2] Mg	Ti	Mn	Ba	Cu	P	Mo	Pb	Sc	Sr	V	Y	Yb	Zn	U[3]	Th[4]
RAD77-1052	0.2	0.1	0.02	0.03	0.005	N.F.[5]	0.01	N.F.	N.F.	0.015	N.F.	N.F.	N.F.	N.F.	0.002	0.001
1060	0.7	0.5	0.1	0.01	0.0015	N.F.	0.7	0.15	0.001	0.015	0.002	0.01	0.0015	0.03	0.44	0.059
1061	0.5	0.2	0.07	0.007	0.002	0.5	0.07	0.2	0.0005	0.010	0.003	0.03	0.003	<0.005	0.65	0.073
1062	2.0	0.2	0.05	0.1	0.003	N.F.	<0.005	0.03	0.0003	0.01	0.007	0.005	0.002	0.010	0.045	0.059
1072	0.3	3.0	0.03	0.03	0.003	N.F.	0.15	0.30	0.001	0.01	0.007	0.03	0.003	0.1	1.76	0.33

	Occurrence (Area)	Latitude	Longitude
[1] Location of samples:	1052: Petursson L. (Kenora-Dryden)	49°50'N	93°50'W
	1060: Coulee (Kenora-Dryden)	49°50'23"N	93°37'12"W
1061 &	1062: Fairservice (Kenora-Dryden)	49°50'45"N	93°41'16"W
	1072: Bear Creek (Favourable Lake)	52°46'45"N	93°45'15"W

[2] Analytical method: QN-12b; analyst: K. Church of Geological Survey except for U and Th

[3] Neutron activation by AECL

[4] Scan/ratio by G.R. Lachance of Geological Survey

[5] N.F. = not found.

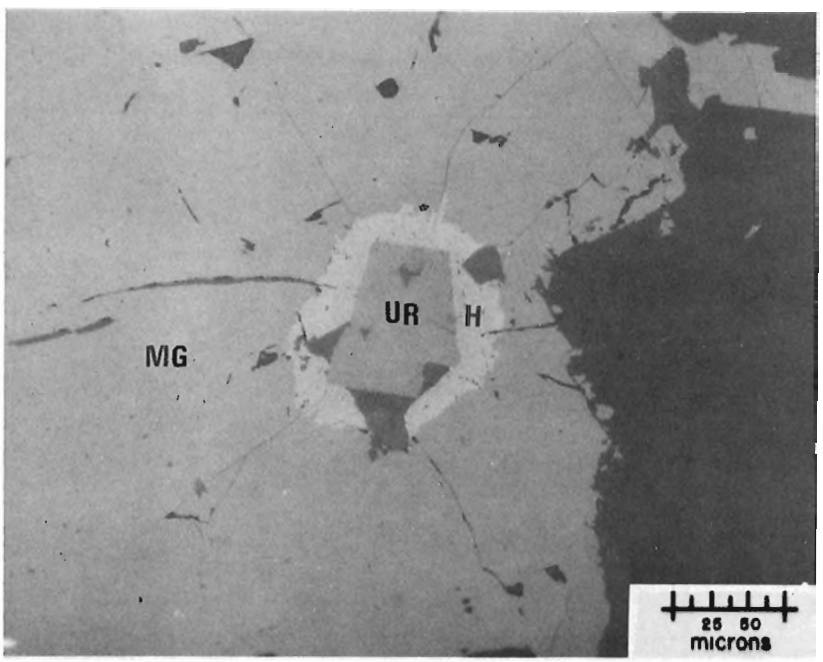


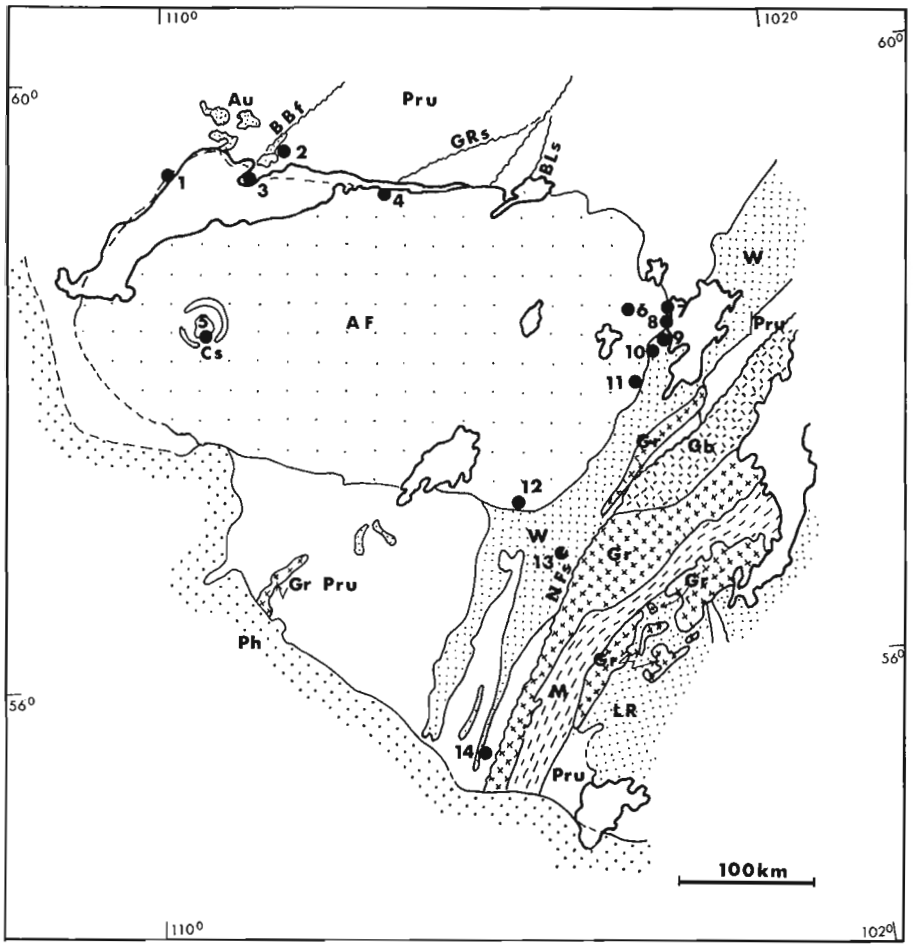
Figure 27.15. *Uraninite (UR) rimmed by hematite (H) in magnetite (MG). A detail from sample in Figure 27.14. (Reflected light.) Note radiating fractures in magnetite.*

of these types has been studied in detail and conceptual genetic models have been developed (e.g. Tremblay, 1972; Beck, 1969; Robinson, 1955). An outline of the geology and genesis of the unconformity deposit at Maurice Bay is presented below.

The Maurice Bay deposit (see Fig. 27.16) was discovered on the basis of: (a) the occurrence of a radioactive boulder field, and (b) analogy with the geological environment of the already known deposit at Key Lake. (C. Lehnert-Thiel of Uranerz Exploration and Mining Canada, Limited, pers. comm.). The mineralization occurs at the base of the Athabasca Formation in strongly altered (hematized, chloritized or kaolinized) sediments and chloritized regolithic or tectonic (?) clay containing chalcedony or vein quartz and graphite. Minor mineralization also occurs in the basement complex, as, for example with pyrite, feldspar and quartz in chloritized and hematitized biotite gneiss. The basement complex contains graphitic and/or pyritic pelite and is disturbed by regional faults. The uranium mineralization is monomineralic, represented only by sooty or massive pitchblende.

A schematic cross-section representing a generalized model of the unconformity-type deposit in the Tazin Belt and cover rocks is shown in Figure 27.17.

Uranium deposits in the Wollaston Lake Fold Belt and cover rocks (2) (Fig. 27.16) can be classified into two main types: (a) unconformity deposits (e.g. Rabbit Lake, Key Lake, Collins Bay and Midwest Lake); and (b) impregnation deposits (e.g. Duddridge Lake, Raven and Horseshoe).



Ph = *Phanerozoic rocks*
AF = *Athabasca Formation*
Au = *Aphebian rocks, undivided*
W = *Wollaston Domain*
LR = *La Ronge Domain*
Cs = *Carswell structure*
Pru = *Precambrian rocks, undivided (including Archean)*
M = *Migmatites of the Rottenstone Domain*
Gr = *Granitic rocks (Hudsonian)*
Gb = *Gabbro and associated gneiss*

Uranium Deposits

1 = *Maurice Bay*
2 = *Fay — Ace — Verna*
3 = *Gunnar*
4 = *Fond du Lac*
5 = *Cluff Lake ("D", "NR", "OP", Claude)*
6 = *Midwest Lake*
7 = *Collins Bay A*
8 = *Collins Bay B*
9 = *Rabbit Lake*
10 = *Raven and Horseshoe*
11 = *West Bear*
12 = *Key Lake*
13 = *Burbidge Lake*
14 = *Duddridge Lake*

Structures

BBf = *Black Bay fault*
GRs = *Grease River shear*
BLs = *Black Lake shear*
NFs = *Needle Falls shear*

(Geology partly after R.J. Mundy, with permission from an unpublished manuscript.)

Figure 27.16. *Uranium deposits in the Tazin Belt, Wollaston Lake Fold Belt and associated cover rocks.*

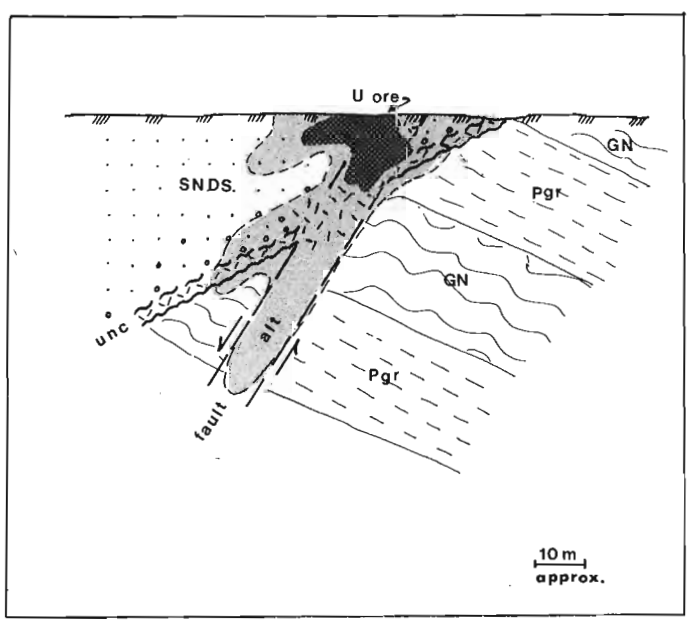


Figure 27.17. *A schematic cross-section representing a conceptual genetic model of an unconformity type uranium deposit in the Tazin Belt and associated cover rocks, Churchill Geological Province. SNDS = sandstone; GN = gneiss; Pgr = graphitic pelite; unc = unconformity; alt = zone of alteration.*

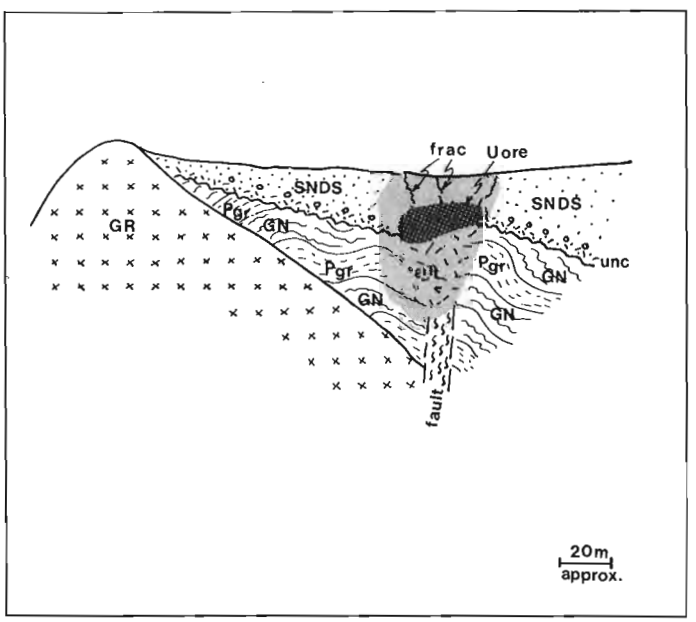


Figure 27.18. *A schematic cross-section representing a conceptual genetic model of an unconformity type of uranium deposit in the Wollaston Lake Fold Belt and associated cover rocks. GR = granite; GN = gneiss; Pgr = graphitic pelite; SNDS = sandstone; unc = unconformity; alt = alteration zone; frac = mineralized fractures.*

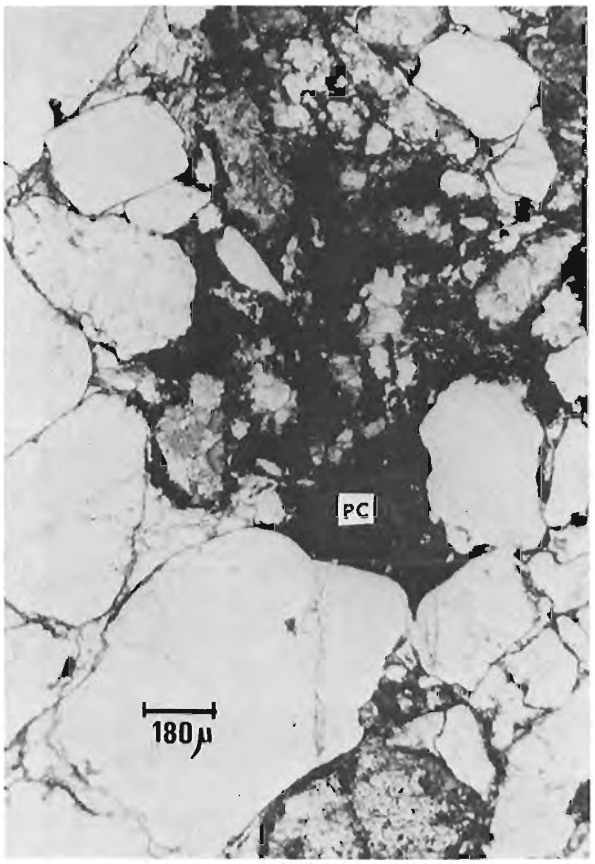


Figure 27.19. *Pitchblende (PC) as a cement in an arkose from Amer Lake area (about 2 km northwest of Amer Lake), Northwest Territories. (Reflected light.)*

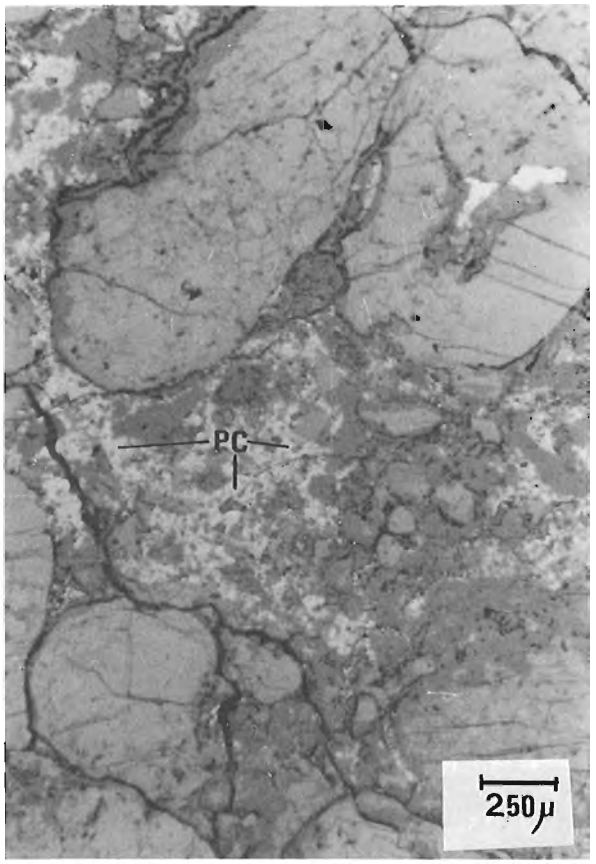


Figure 27.20. *Pitchblende (PC) as an original cement and as replacement of the cement in an arkose boulder collected about 5 km north of Amer Lake, Northwest Territories. (Reflected light.)*

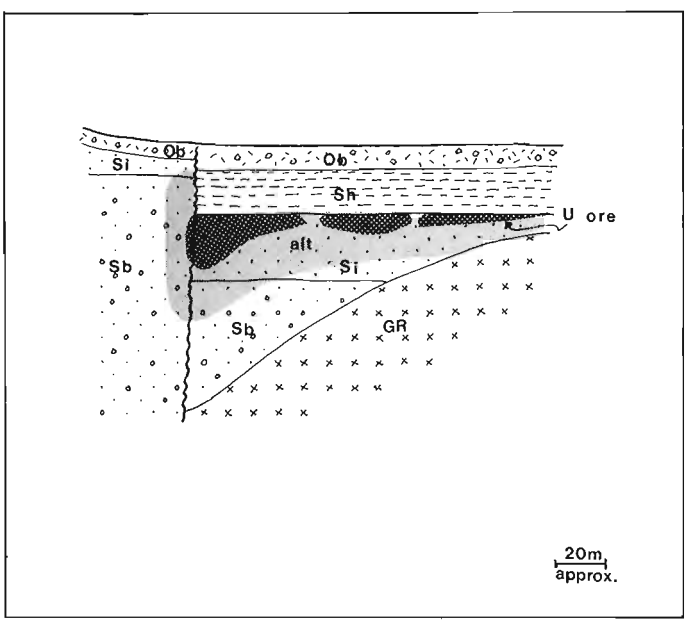


Figure 27.21. *A schematic cross-section representing a conceptual genetic model of a sandstone hosted deposit in the Hornby Bay — Dismal Lakes area, Bear Geological Province. Ob = overburden; Si = impure sandstone (arkosic and containing sulphides); Sb = basal sandstone containing coarse facies; Sh = pelitic rocks (mainly shale); alt = zone of alteration; GR = granitic rocks.*

A conceptual model of the unconformity type deposit postulates (see Fig. 27.18) (a) granitic domes as the original uranium source rocks; (b) peribatholithic metamorphosed shelf sediments including graphitic and/or pyritic pelite that may be either a source of uranium or a host for it; (c) an unconformity between the peribatholithic metasediments and permeable cover rocks with the unconformity containing regolithic clays; (d) structural and/or lithological traps for uranium; and (e) extensive zones of alterations, such as hematitization, kaolinization, chloritization, sericitization and graphitization. The uranium mineralization in this environment is commonly accompanied by nickel, silver, and cobalt. In general the genesis of the unconformity deposits in the Tazin Belt and cover rocks and in the Wollaston Lake Fold Belt and cover rocks is similar.

The impregnation deposits generally contain mineralization of a lower grade than the unconformity type. The mineralization is as a rule controlled by zones of weakness, zones of alteration, and by permeability of the host rocks.

The recent discovery of a substantial amount of uranium mineralization (in one of several holes with mineralized intersections approximately 0.85 per cent U across 33 m) in the Baker Lake area (3), Northwest Territories, by Urangesellschaft Canada Limited (The Northern Miner, 1978b) indicates a significant potential for this area that contains an extensive Aphebian/Helikian unconformity. The metallogenic characteristics here may be similar to those of northern Saskatchewan.

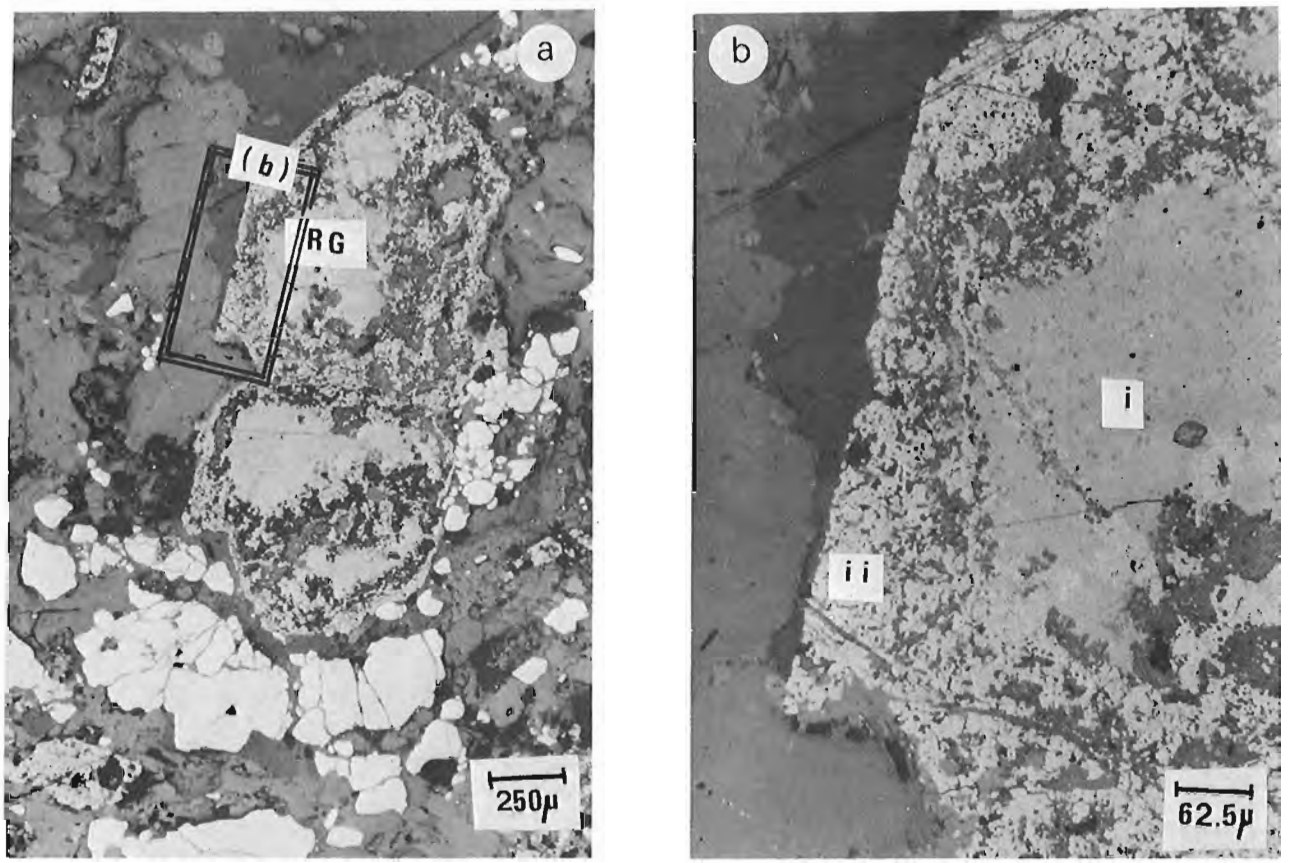


Figure 27.22. *Photomicrograph of a radioactive ore sample from the "BD" zone, Rexspar deposit, Birch Island area, British Columbia; (a) a radioactive grain (RG), (b) two phases within the grain: (i) inner core and (ii) outer rim. (Reflected light.)*

Uranium mineralization in the Amer Lake area (4) was described by Ruzicka (1978, p. 271). Laboratory studies on samples collected about 2 km northwest of Amer Lake and from a boulder found about 5 km north of Amer Lake show that pitchblende occurs as cement or replaces cement in arkose of the Amer Lake Group (Fig. 27.19, 27.20), indicating that the pitchblende crystallized during or after diagenesis of the arkose.

A radioactive sample collected in the Yathkyed Lake area (5), Northwest Territories (Ruzicka, 1978) contains very fine radioactive grains of a complex composition in which U is accompanied by Pb, Ti, and Si and probably represents a form of brannerite.

Two samples collected by J.E. Reesor in Melville Peninsula (6) (see Fig. 27.2) contain radioactive mineralization. The rocks are granite and augen gneiss.

In addition to the above mentioned areas the Churchill Geological Province contains uranium occurrences in the East Arm of Great Slave Lake and Nonacho Belt, Northwest Territories, in the Labrador Fold Belt in Quebec (e.g. Fort Chimo and Mistamisk Lake), and on Foxe Peninsula of Baffin Island.

The Churchill Geological Province presently accounts for about 34 per cent of Canada's Reasonably Assured and Estimated Additional uranium resources and additions to these resources seem likely in the future.

Slave Geological Province

Several uranium deposits occur in the Slave Geological Province. A new locality containing radioactive mineralization along with cobalt and bismuth was discovered by radiometric testing of samples collected by O.R. Eckstrand of the Geological Survey. The samples were collected from Sachowia Lake area, Northwest Territories (62°24'40"N, 111°51'30"W) (see Fig. 27.2) (Hornal et al., 1974).

At present only speculative resources are estimated for the Slave Geological Province.

Bear Geological Province

Since the closure of Eldorado's Port Radium mine no uranium has been produced from the Bear Geological Province. However many uranium occurrences are known near the western margin of the Province south of Port Radium (e.g. Terra mine, Contact Lake mine, and Rayrock mine).

New concepts in uranium exploration along with the discovery of uranium mineralization in the Hornby Bay – Dismal Lakes groups led to extensive exploration in a part of the Bear Geological Province underlain by rocks of these groups. Accompanied by S.S. Gandhi of the Uranium Resource Evaluation Section the author examined geological exploration targets of the following companies: Hudson Bay Oil and Gas Limited; Cominco Exploration Limited; Gulf Minerals, Canada, Limited; BP Minerals, Canada, Limited; Esso Minerals Limited and Uranerz Exploration and Mining, Canada, Limited.

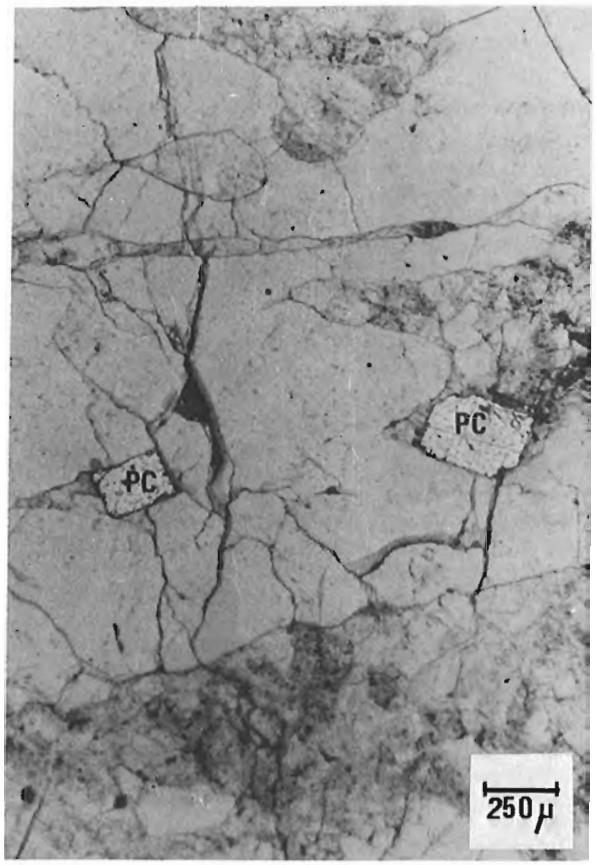


Figure 27.23. *Euhedral pitchblende from pegmatite; China Creek occurrence, Grand Forks – Nelson area, British Columbia. PC = pitchblende. (Reflected light.)*

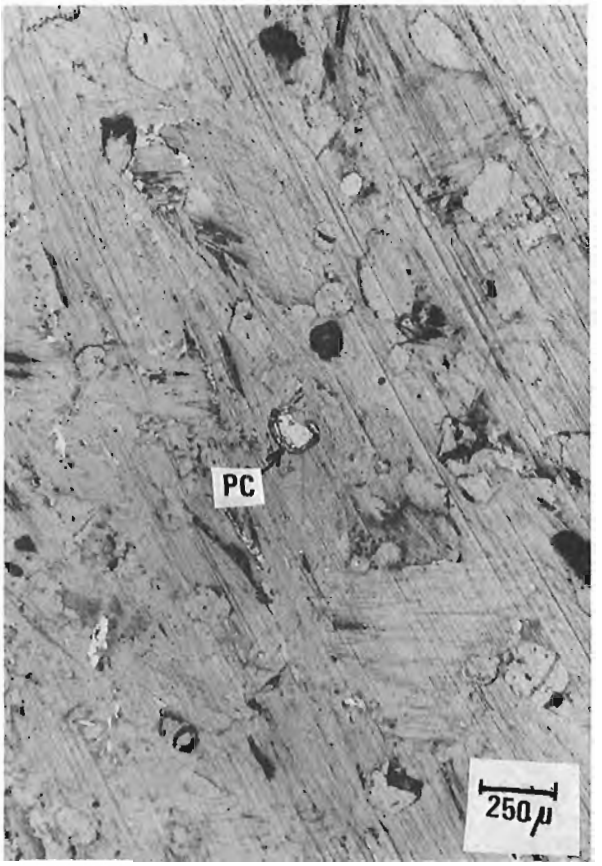


Figure 27.24. *Subhedral pitchblende (PC) from a pegmatite dyke, Consolidated Boundary occurrence near Grand Forks, Grand Forks – Nelson area, British Columbia. (Reflected light.)*

Results of the field investigations in the Hornby Bay – Dismal Lakes area (1) can be summarized as follows:

(a) At least four types of uranium deposits occur in the area: (i) sandstone hosted, (ii) intragranitic veins, (iii) mineralized shear zones, and (iv) quartz veins;

(b) uranium mineralization is commonly accompanied by copper and locally by nickel, cobalt or silver;

(c) structural control of mineralization was observed in connection with all the above mentioned types;

(d) an unconformity type of uranium mineralization, similar to northern Saskatchewan, has not yet been identified;

(e) the sandstone-hosted mineralization seems to be the most important type known to date.

The sandstone-hosted mineralization resembles to a certain degree that of the 'blanket' deposits of the United States (Ruzicka, 1975, p. 15). The host rock is mainly impure sandstone, commonly kaolinized, chloritized and containing iron sulphides. The alteration may be related to the dewatering of the overlying black shale. The uranium could be derived from the black shale during its compaction and introduced to the sandstone by the same connate waters that caused alteration of the sandstone matrix. The sulphides, chlorite and kaolin in the sandstone apparently participated in precipitation of the uranium and its deposition. The uranium mineralization is generally restricted to zones near and below the overlying shales. A proposed model is shown in Figure 27.21.

The Bear Geological Province contributes, according to present estimates, about 3 per cent of Canada's Reasonably Assured and Estimated additional uranium resources.

Appalachian Orogen

At present only speculative uranium resources are considered in the Appalachian Orogen by the author and H.E. Dunsmore of the Uranium Resource Evaluation Section.

During 1978 exploration for uranium in the Canadian Appalachian Orogen was oriented mainly toward environments favourable for: (i) sandstone-hosted mineralization; (ii) volcanogenic types of deposits; (iii) intragranitic mineralized zones, and (iv) fracture controlled mineralization in peribatholithic shale and slate.

The latter type of mineralization is widespread in the Hercynian Orogen in Europe particularly in the Iberian Peninsula (e.g. Fe deposit, Spain) and Bohemian Massif (e.g. Pribram deposit, Czechoslovakia) (Ruzicka, 1971). Several uranium occurrences of this type were discovered by Cuvier Mines Limited in the Annapolis Valley area (1), Nova Scotia, and by the author in the Mactaquac area (2), New Brunswick. A sample collected by D.F. Sangster from the latter area was found to be radioactive during routine testing of Geological Survey collections (Fig. 27.2).

Uranium-bearing dolomitic sandstone containing collophane was sampled by the author, L.P. Tremblay, and H.E. Dunsmore on Soquem Limited's property in the St. Armand Lake area (3) near Phillipsburg, Quebec to investigate genesis of the mineralization in the laboratory.

Cordilleran Orogen

Two areas in the Canadian part of the Cordilleran Orogen contain uranium deposits where Reasonably Assured and/or Estimated Additional resources are estimated: Birch Island (1) and Beaverdell (2), British Columbia. The remaining areas contain only occurrences. Uranium-bearing granite pegmatites occur in several localities in the Grand Forks-Nelson area (3) and in the Coast Plutonic Complex (4), British Columbia.

Laboratory examination of samples collected from the Rexspar deposit in the Birch Island area (1) showed high concentration of thorium, titanium associated with uranium, and niobium. The radioactive grains in an ore sample from the 'BD' zone consist of two phases. The inner cores and the outer rims of these grains have different compositions (Fig. 27.22a, b). The inner core (i) of a grain contains approximately equal amounts of titanium, uranium, and thorium and apparently represents a new thorium variety of brannerite. The outer rim of the grain (ii) consists of rutile with traces of niobium. This indicates elevated thermodynamic conditions during crystallization of the ore components.

The Beaverdell area (2) contains uranium mineralization (mainly autunite) in semiconsolidated clastic sediments in several localities. The largest deposit at present, the Blizzard, is estimated by the discoverer and owner, The Lacana Mining Corporation, as containing 2.2 million tonnes of open pit ore at 0.21 per cent U grade with an ultimate potential in the order of 5800 to 7700 tonnes of uranium metal (The Northern Miner, 1978a). Among the other occurrences are: Fuki, Donen, Venus, Kallis Creek, Hydraulic Lake, Tyee and Allandale Lake.

Radioactive granite pegmatites from the China Creek and Grand Forks segments of the Grand Forks – Nelson area (3) contain euhedral and subhedral grains of pitchblende (Fig. 27.23, 27.24). A similar crystalline form of pitchblende was reported from the Key Lake deposit, Saskatchewan (Ruzicka, 1977a).

A radiometric testing of samples in the Geological Survey collections collected by R. Mulligan from the Silver Hood mine, Ainsworth, by G.B. Leech from Purcell Mountains, Grand Forks – Nelson area, and by R.V. Kirkham from the Anyox mine near Terrace, Coast Plutonic Complex (4) identified radioactivity. These localities deserve field investigations.

The Cordilleran Orogen contains many other uranium occurrences in areas that are being studied by the British Columbia Department of Mines and Petroleum Resources and by the Geological Survey of Canada. Exploration of these occurrences is being conducted by industry in Yukon and northern British Columbia.

The Reasonably Assured and Estimated Additional uranium resources in the Canadian part of the Cordilleran Orogen represent approximately one per cent of Canada's totals.

Hudson Platform

Phanerozoic sediments of the Hudson Platform adjacent to the Kapuskasing Granulite Belt contain several uranium occurrences. Recently, Kerr Addison Mines Limited and Prospection Limited conducted exploration for uranium in the Coral Rapids – Moosonee area (1). The author examined several uranium occurrences in pegmatites in the basement rocks of the Kapuskasing Granulite Belt near Smoky Falls, Ontario. These rocks were apparently a source for the uranium mineralization in the fluviatile sediments of the Devonian Sextant Formation in the Coral Rapids – Moosonee area.

Assessment of the uranium potential of the Hudson Platform is at present being conducted by the Ontario Geological Survey and by the Geological Survey of Canada.

International Uranium Resource Evaluation Project (IUREP)

Canada participates in the International Uranium Resource Evaluation Project (IUREP) by reporting on present and past developments in research, exploration, exploitation, and evaluation of uranium resources in the country. The IUREP is jointly sponsored by the Organization for Economic Co-operation and Development (OECD) and International Atomic Energy Agency (IAEA). Participants in the IUREP also analyze the favourability of various geological environments in selected countries in the world and recommend appropriate steps for their assessment.

Acknowledgments

The author conducted his 1978 field work in close co-operation with the exploration and mining companies, particularly Eldorado Nuclear Limited; Gulf Minerals, Canada, Limited; Uranerz Exploration and Mining, Canada, Limited; Urangesellschaft, Canada, Limited; Hudson Bay Oil and Gas, Limited; Conwest Exploration Limited; BP Minerals, Canada, Limited; Cominco Limited; Esso Minerals Limited; Shell Resources Canada, Limited; Soquem Limitée; Copconda Limited; Augmitto Limited; Trigg, Woolet and Associates Limited and Consolidated Durham Mines Limited. Their co-operation is acknowledged. The author also acknowledges participation in the field of the Ontario Geological Survey, particularly J.A. Robertson, L. Tihor, G.B. Gordon, W. Karvinen, Ken Fenwick and R. Beard; Saskatchewan Geological Survey, particularly T.I.I. Sibbald; and A.A. Ruitenberg of the New Brunswick Department of Natural Resources. D.M. Watson of the Geological Survey of Canada and S. Kaiman of the Canada Centre for Mineral and Energy Technology provided identification of the radioactive minerals and discussed many aspects of the ore microscopy with the author. J.A. Kerswill of the Uranium Resource Evaluation Section assisted in the field in Ontario and provided preparation of the samples.

References

Beard, R.C. and Rivett, S.
1978: 1977 Report of Northwestern Regional Geologist and Kenora Resident Geologist; in 'Annual Report of the Regional and Resident Geologists, 1977', C.R. Kustra (ed.); Ontario Geological Survey Miscellaneous Paper 78, p. 1-27.

Beck, L.S.
1969: Uranium deposits of the Athabasca Region, Saskatchewan; Saskatchewan Department of Mineral Resources, Report 126.

Energy, Mines and Resources, Canada
1978: 1977 Assessment of Canada's Uranium Supply and Demand; Report EP78-3, June, 1978, 34 p.

Frondel, C.
1958: Systematic mineralogy of uranium and thorium; U.S. Geological Survey Bulletin 1064, 400 p.

Gordon, J.B. et al.
1977: Uranium and thorium deposits; in 'Summary of field work, 1977 by the Geological Branch', ed. by V.G. Milne et al.; Ontario Geological Survey Miscellaneous Paper 75, p. 192-194.

Hewitt, D.F.
1967: Uranium and thorium deposits of Southern Ontario; Ontario Division of Mines, Mineral Resources Circular 4, 76 p.

Hornal, R.W. et al.
1974: Mineral Industry Report 1969-70, Northwest Territories, West of 104° West Longitude; Department of Indian and Northern Affairs, v. 3, Open File.

Robertson, J.A.
1968: Uranium and thorium deposits of Northern Ontario; Ontario Department of Mines, Mineral Resources Circular 9, 106 p.

1976: The Blind River uranium deposits: the ores and their setting; Ontario Division of Mines, Miscellaneous Paper 65, 45 p.

1977: Uranium deposits of Ontario; in 'Summary of field work, 1977' ed. by V.G. Milne et al.; Ontario Geological Survey Miscellaneous Paper 75, p. 185-187.

Robinson, S.C.
1955: Mineralogy of uranium deposits, Goldfields, Saskatchewan; Geological Survey of Canada, Bulletin 31, p. 1-128.

Roscoe, S.M.
1969: Huronian Rocks and Uraniferous Conglomerates in the Canadian Shield; Geological Survey of Canada, Paper 68-40, 205 p.

Ruzicka, V.
1971: Geological comparison between East European and Canadian uranium deposits; Geological Survey of Canada, Paper 70-48, 195 p.

1975: New sources of uranium; Types of uranium deposits presently unknown in Canada; in Uranium Exploration '75', Geological Survey of Canada, Paper 75-26, p. 13-20.

1977a: Assessment of selected uranium occurrences and areas favourable for uranium mineralization in Canada; in Report of Activities, Part A, Geological Survey of Canada, Paper 77-1A, p. 27-29.

1977b: Conceptual models for uranium deposits and areas favourable for uranium mineralization; in Report of Activities, Part A, Geological Survey of Canada, Paper 77-1A, p. 17-25.

Ruzicka, V. (cont'd.)
1977c: Estimation of undiscovered uranium resources in Canada; in Uranium Resource Evaluation, Energy, Mines and Resources, Canada, Report ER77-1, p. 39-56.

1978: Evaluation of selected uranium-bearing areas in Canada; in Current Research, Part A, Geological Survey of Canada, Paper 78-1A, p. 269-274.

Some metallogenic features of the Huronian and post-Huronian uraniferous conglomerates; U.S. Geological Survey Professional Paper. (in press)

Ruzicka, V. and Steacy, H.R.
1976: Some sedimentary features of conglomeratic uranium ore from Elliot Lake, Ontario; in Report of Activities, Part A, Geological Survey of Canada, Paper 76-1A, p. 342-346.

The Northern Miner
1978a: Drills steadily enlarge Blizzard uranium deposit; The Northern Miner, September 28, 1978, p. 21.

1978b: Urangesellschaft 'U' find in Baker Lake area, N.W.T.; The Northern Miner, September 21, 1978, p. 1.

Thompson, J.E.
1960: Uranium and thorium deposits at the base of the Huronian system in the District of Sudbury; Ontario Department of Mines, Geological Report 1.

Tremblay, L.P.
1972: Geology of the Beaverlodge Mining area, Saskatchewan; Geological Survey of Canada, Memoir 367, p. 1-265.

Worobec, A., Editor
1978: Canadian Mines Handbook; Northern Miner Press Limited, Toronto, 404 p.

28. NEW DATA ON AN INTERGLACIAL PEAT DEPOSIT NEAR MAKINSON INLET, ELLESMERE ISLAND, DISTRICT OF FRANKLIN

Project 750063

W. Blake, Jr. and J.V. Matthews, Jr.
Terrain Sciences Division

Blake, W., Jr., and Matthews, J.V., Jr., New data on an interglacial peat deposit near Makinson Inlet, Ellesmere Island, District of Franklin; in Current Research, Part A, Geol. Surv. Can., Paper 79-1A, p. 157-164, 1979.

Abstract

Examination of peat samples collected in 1977 near Makinson Inlet has revealed the presence of fossils of ***Andromeda polifolia*** *and* ***Menyanthes trifoliata****, plants which do not live in the Arctic Islands today. Likewise, fragments of the ground beetle* ***Amara alpina*** *and the ladybird beetle* ***Nephus georgei****, neither of which occurs as far north today, are present. The occurrence of these fossils beyond their present limits, coupled with the fact that the uppermost layer of peat in the deposit is >52 000 years old (GSC-2677), suggests that the peat is an interglacial deposit.*

Introduction

One of the few pre-Holocene deposits of peat known from Ellesmere Island is situated 8.0 km due east of the head of Makinson Inlet's north arm (Fig. 28.1). This site, which is 2.5 km west of the edge of the ice cap covering much of east-central Ellesmere Island, was discovered in 1961 by J.G. Fyles during a reconnaissance survey of Quaternary deposits. A radiocarbon age determination on the sandy moss peat which he collected gave a value of >36 400 years (GSC-140; Dyck and Fyles, 1964). During a second run, carried out in 1973 on another portion of the original sample but in a larger counter (Table 28.1), a result of >44 000 years was achieved (GSC-140-2; Blake, 1974).

The peat deposit was revisited and resampled during the 1977 field season (Blake, 1978). The purpose of this paper is to give the result of a third radiocarbon age determination and to report details of a preliminary analysis of insect, arachnid, and plant macrofossils contained in the peat. Blake is responsible for the description of the site and the section on radiocarbon dating, Matthews is responsible for the section dealing with the fossil evidence. The final section, dealing with paleoclimatic interpretations, has been produced jointly.

Site Description

The peat deposit occurs as an isolated pocket high on the wall of a gully (Fig. 28.2) excavated in the soft rocks of the Late Cretaceous-Early Tertiary Eureka Sound Formation (cf. Christie, 1962). Fyles (in Dyck and Fyles, 1964) reported that the peat was underlain by bouldery gravel on sandstone and shale and was overlain by boulders. At the point where the 1977 collections were made the peat occurs above a banded silty bed. Thawing and slumping of this fine grained material have caused the more coherent moss peat to drape downward (Fig. 28.3, 28.4). Above the peat, estimated to be at least 1.5 m in thickness, is a unit several metres thick which is composed of large boulders, many of them more than 1 m in diameter. Granite and gneiss are the dominant lithologies in this unit. In places the ground surface above the peat resembles a boulder pavement, elsewhere it is more characteristic of a till. The possibility that some of this material is colluvium cannot be excluded. This deposit covers the floor of a major drainage channel at the point where it debouches into the main valley (Fig. 28.2). Present day deposits of peat were not noticed in the channel, although patches of vegetation are present, especially along a small stream which now flows out of the channel.

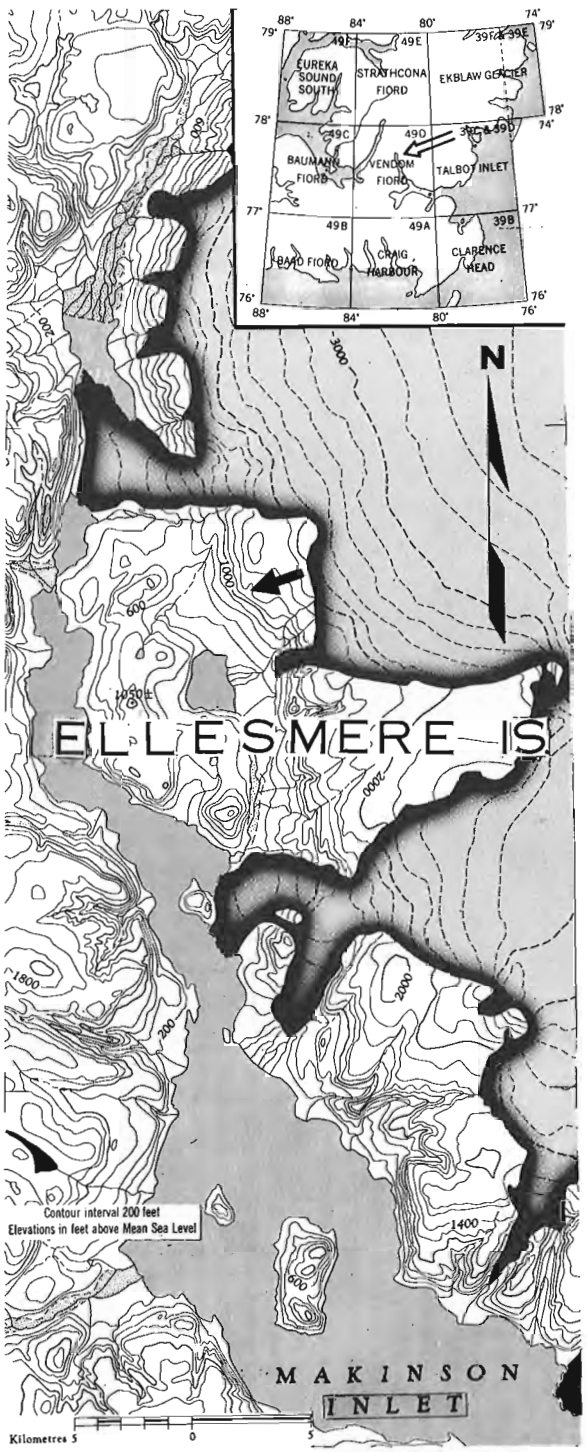


Figure 28.1. *Map showing the location of the peat site east of Makinson Inlet, Ellesmere Island.*

Table 28.1

Radiocarbon age determinations on organic deposits east of Makinson Inlet

Collector and year	Field sample no.	Sample weight (g)	Laboratory dating no.	^{14}C Age[1]	Counter (L)	Pressure (atm)	No. of days counted	References	Dominant Moss Species[2]	Site Information
J.G. Fyles, 1961	FG-61-162e	18.2	GSC-140	>36 400	2	2	2	Dyck and Fyles, 1964; Blake, 1974	**Calliergon giganteum**	Peat layer 1.2 m thick. Above boulders and sand, and below boulders (colluvial?) in channel.
		94.0	GSC-140-2	>44 000	5	1	4			
W. Blake, Jr., 1977	BS-77-242	115.0	GSC-2677	>52 000	5	4	5	This paper	**Calliergon giganteum**	Uppermost 2 cm of peat from top of unit.

[1] All age determinations from the Radiocarbon Dating Laboratory, Geological Survey of Canada, are based on a ^{14}C half-life of 5568 ± 30 years and 0.95 of the activity of the NBS oxalic acid standard. Ages are quoted in conventional radiocarbon years before present (B.P.), where "present" is taken to be 1950. All "greater than" age determinations from this laboratory are based on the 4σ criterion (99.9% probability that age is older than the value indicated). Pretreatment of sample FG-61-162e for both determinations included a hot (just below boiling) NaOH leach for 0.5 hour; for sample BS-77-242 this pretreatment lasted for 1 hour. The NaOH leach was followed, in each determination, by a hot HCl leach and distilled water rinses. For GSC-2677 the $\delta^{13}C$ value is -33.8 ‰, as determined at the Department of Earth Sciences, University of Waterloo, under the direction of Professor P. Fritz; DSS contract OST78-00037.

[2] For FG-61-162e the determination of moss species is by M. Kuc (unpublished GSC Bryological Report 258, 1973); for BS-77-242 the determination is by J.A.P. Janssens, Department of Botany, University of Alberta (unpublished Bryological Report JJ-163, 1978).



Figure 28.2. *Aerial view eastward towards the ice cap which covers most of the highland areas north and east of Makinson Inlet. The arrow indicates the site where the fossil peat is exposed, at the mouth of a major abandoned drainage channel. August 14, 1977 (GSC 174859).*

Radiocarbon Age Determinations

The two determinations carried out on the 1961 collection of peat have been mentioned in the introduction, and pertinent details with regard to both samples and counting procedures are summarized in Table 28.1 (cf. also Blake, 1974). When the first attempt at dating was made, the Geological Survey's Radiocarbon Dating Laboratory had available only one counter, of 2-L capacity. By 1964 a 5-L counter had been tested and installed (Dyck et al., 1965), hence a new determination was carried out to see if a finite age in the range of 37 000 to 43 000 years could be obtained. The result indicated that the peat was beyond the range of the 5-L counter when operated at normal pressure (1 atm), and insufficient material remained to do a determination at "high pressure" (4 atm).

Several large monoliths of peat from the top and middle parts of the deposit were collected in 1977 (Fig. 28.3). Because of uncertainty as to the exact level at which sampling had been carried out in 1961, it seemed important to date the uppermost peat in order to ascertain if the youngest part of the deposit was within the limits of our "high pressure" capability, i.e., roughly 45 000 to 50 000 years. The result, >52 000 years (GSC-2677), is based on a 5-day count, and the CO_2 utilized was obtained by treating a 2 cm-thick slice from the top of the uppermost peat horizon.

Fossil Evidence

Samples from various levels in the peat unit and fragments of the peat that had slumped have yielded well preserved macrofossils of plants, insects, and arachnids.



Figure 28.3.

General view of the peat collection site. Sample BS-77-242, dated at >52 000 years (GSC-2677) was collected from the uppermost peat, at the point indicated by the open arrow to the left of the shovel (each division on the shovel handle is 5 cm). The black arrow indicates where BS-77-240 was collected; cf. Figure 28.4. July 30, 1977 (GSC 174573).

Despite the fact that both the upper and lower parts of the unit are moss peat composed of essentially the same moss taxa (Table 28.2), the uppermost layer of the peat (Blake's field number BS-77-242), for which a radiocarbon age of >52 000 years was obtained (GSC-2677; Table 28.1), contained most of the arthropod fossils whereas the lower part of the peat yielded nearly all of the plant macrofossils. The autochthonous character of the peat is indicated by its fibrous nature and the excellent preservation of some of the plant and insect fossils. Many of the latter were found in a partially articulated state.

Fossils identified from the peat samples collected in 1977 are listed in Table 28.2. Distributions of six important species found in the samples and, with one exception, known presently only from more southerly areas, are shown in Figure 28.5. To aid in interpreting such information, a map showing tundra zones in North America also is included (Fig. 28.5A); the zonal boundaries are based on the relative depauperism of the floras at numerous arctic sites, but they also are thought to reflect differences in total summer warmth (Young, 1971), a climatic parameter that is just as likely to influence the distribution of insects as it does plants.

The more significant plant and arthropod taxa require further comment, as follows:

Andromeda polifolia L. (Fig. 28.6D): Fossils of this tundra plant and those of the emergent aquatic plant **Menyanthes trifoliata** (Fig. 28.6A) constitute the most climatically significant plant remains. Neither species occurs on Ellesmere Island today (Fig. 28.5B), and those that extend up the west coast of Greenland exist under a milder climate than is typical of sites at similar latitude on the east coast of Baffin Island (Fig. 28.5A; cf. Young, 1971). A fossil leaf of **Andromeda polifolia** L. (J.V. Matthews, Jr., unpublished GSC Plant Macrofossil Report 74-5)[1] has been recovered from sediments believed to be of interglacial age at Flitaway Lake, north-central Baffin Island (cf. Terasmae et al., 1966, for an early report of this site).



Figure 28.4. *Detail of the lower part of the peat exposure, showing how the layers drape downward because of thawing of the underlying silt-rich beds. Collection BS-77-240 was made where the shovel is standing. July 30, 1977 (GSC 174569).*

[1] Identified with the help of M. Kuc, Ottawa, Ontario.

Table 28.2

Fossils

Taxa	Sample No. [1]			
	BS-77-240	BS-77-242	BS-77-244	BS-77-238
PLANTS				
Bryophyta [2]				
Calliergon giganteum (Schimp.) Kindb.	++ [3]	++		
Drepanocladus revolvens (Sw.) Warmst.	+	+		
Meesia triquetra (Richt.) Ångstr.	++	+		
Scorpidium scorpioides (Hedw.) Limpr.		+		
Cinclidium arcticum (B.S.J.) Schimp.	+			
Tracheophyta				
Equisetaceae				
Equisetum sp.			+	
Cyperaceae				
Carex aquatilis Wahlenb. (= **C. stans** Drej.)		+	++	
C. maritima Gunn (Fig. 28.5C)	+			
Carex cf. **C. saxatilis** L. type	+			
Carex sect. Heleonastes Kunth	++	+	+	
Carex sp.	+			
Eriophorum spp.	++			
Juncaceae				
Juncus sp.	++	+		
Salicaceae				
Salix sp.	+			
Caryophyllaceae				
Stellaria spp.	++			
Melandrium apetalum (L.) Fenzl	+			
Ranunculaceae	+			
Ranunculus sp.	+			
Cruciferae, genus?	+			
Rosaceae				
Potentilla sp.	++			
Ericaceae				
Andromeda polifolia L. (Fig. 28.5D)			+	
Gentianaceae				
Menyanthes trifoliata L. (Fig. 28.5A)	+			
ARTHROPODS				
Insecta				
Coleoptera				
Carabidae				
Amara (Curtonotus) alpina Payk. (Fig. 28.5B)		+	+	+
Amara (Curtonotus) sp.		+		+
Dytiscidae				
Agabus moestus (Curtis)				+
Hydroporus cf. **H. morio** Aubé [4]		++	++	+
H. polaris Fall		+		
Staphylinidae				
Atheta? sp.		+	+	
Coccinellidae				
Nephus georgei (Weise) (Fig. 28.5F)		+	+	
Diptera				
Chironomidae			+	
Cyclorrhapha – muscoid			+	
Arachnida				
Acari				
Oribatidae				
Platynothrus sp. (Fig. 28.5E)	+	++	++	
Genus?		+		
Araneae				
Lynyphiidae				
Erigone sp.		+		

[1] BS-77-242 is from the uppermost exposed layer of peat; BS-77-244 is from a slumped block of peat; BS-77-238 represents fossils picked from a single slumped block in the field. Both -244 and -238 probably derived from the more compact peat in the upper part of the unit.

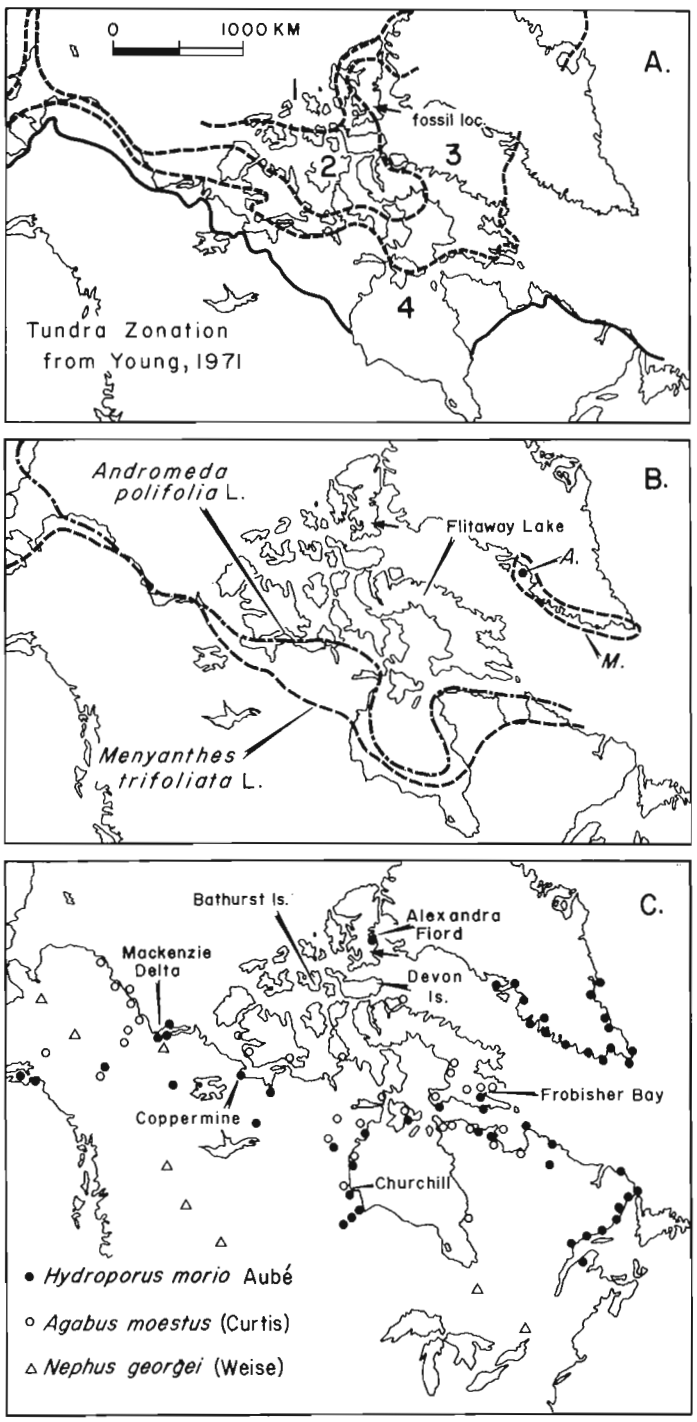
[2] Identified by J.A.P. Janssens, Department of Botany, University of Alberta, Edmonton (Bryological Reports JJ-163, -164 and -165, 1978). Preliminary examination of the collection made in 1961 by J.G. Fyles was carried out by M. Kuc (unpublished G.S.C. Bryological Report No. 258). No mosses from BS-77-244 and BS-77-238 have been examined.

[3] + presence of fossils of named taxon ++ fossils abundant.

[4] Identified by D.J. Larson, Department of Biology, Memorial University of Newfoundland, St. John's.

Dytiscidae: Fossils, a few of them articulated specimens of the predaceous diving beetle genus **Hydroporus,** were abundant in some of the peat samples. The majority of the fragments are referred, tentatively, to the species **H. morio,** a taxon which though northern in distribution previously was known only from sites south of Ellesmere Island (W.J. Brown[1], unpub. manuscript). In 1977, however, Blake collected two living specimens at Alexandra Fiord, north of Makinson Inlet (Fig. 28.5C), and this record is now the most northern for the species. **Hydroporus polaris** is more arctic in distribution than **H. morio,** having been found even at Lake Hazen, northern Ellesmere Island, whereas the apparent northern limit of the other dytiscid, **Agabus moestus,** is northern Baffin Island (W.J. Brown, unpub. manuscript) (Fig. 28.5C). Its fossils have been recovered by Matthews from sediments of the Stuart River Interglaciation on Bathurst Island (Blake, 1974). This locality is, like Ellesmere Island, north of the present range of the species.

Amara alpina Payk: (Fig. 28.6B) This ground beetle is the most northern member of the family Carabidae. It is almost always restricted to alpine and arctic areas, although it apparently does not inhabit Ellesmere Island at present (Fig. 28.5D). The identification of **A. alpina** from Makinson Inlet is based in part on articulated specimens which



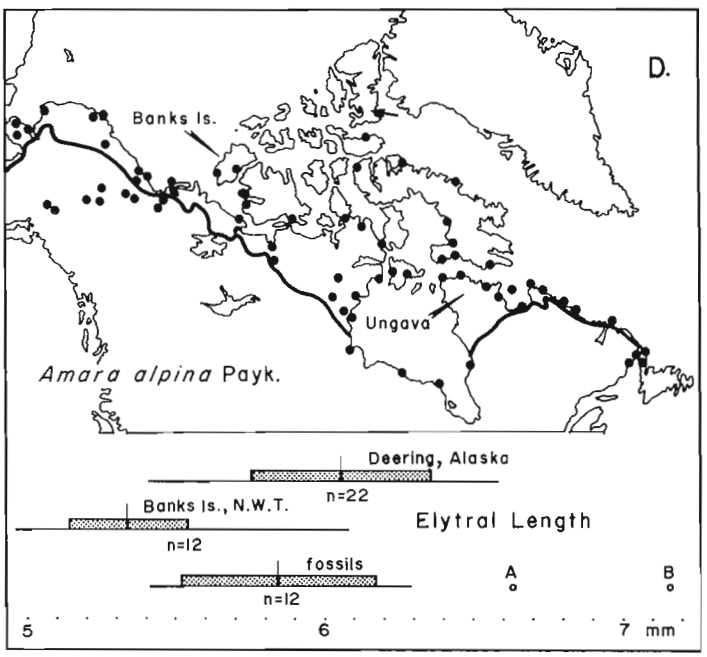


Figure 28.5

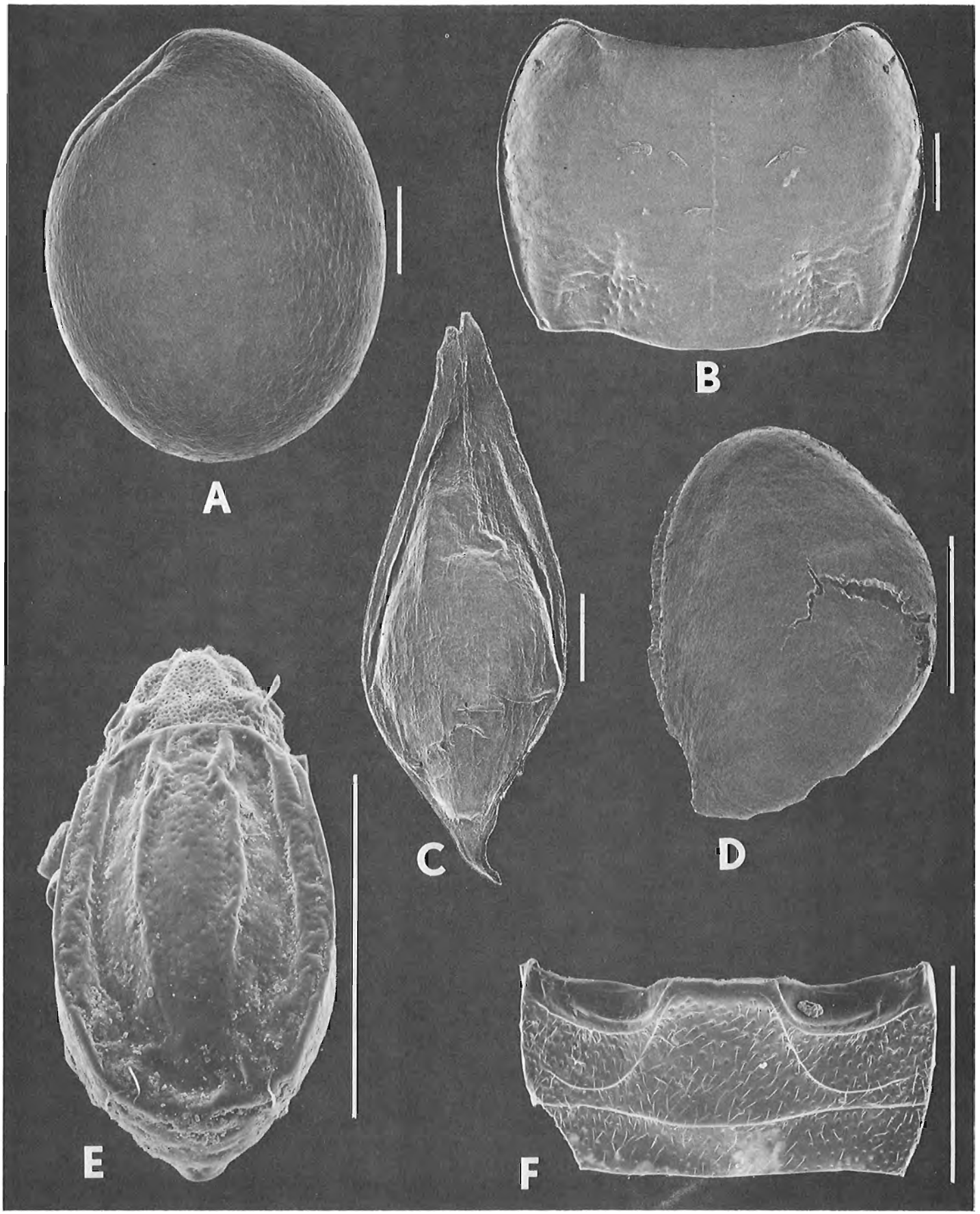
A Tundra zones (Young, 1971). Zone 1 has the most depauperate flora; zone 4 – low arctic or hypoarctic – the richest. These zones apparently reflect the degree of summer warmth as measured at arctic sites by the aggregate of mean temperatures of months with a mean temperature above 0 C (Young, 1971). The heavy line marks the forest-tundra boundary. Note that Makinson Inlet (marked on this and other maps by an arrow) falls within tundra zone 3. The scale bar is the same for all four maps in this figure.

B Present northern limits of two plant species found in the Makinson Inlet peat (see Table 28.2). Note in comparison with Figure 28.5A that both plants have their distributional limits essentially within zone 4. The northern extent of ***Menyanthes trifoliata*** *over much of North America coincides approximately with the forest-tundra boundary. Distributional information from Hultén (1970) and Porsild and Cody (in press).*

C Present known distribution of three beetle species found in the Makinson Inlet peat. Based on data from Belicek (1976), Gordon (1976), and an unpublished manuscript prepared by W.J. Brown.

D Present distribution of the ground beetle ***Amara alpina*** *and preliminary comparison of elytral lengths. The dark line on the map marks the forest-tundra limit. Mensural data: horizontal line = total range of elytral lengths in mm; vertical line = mean; and horizontal bar, one standard deviation on either side of the mean. A and B represent lengths of two elytra which, because of their large size, probably do not represent* ***A. alpina.*** *Elytral length measured from basal transverse line near scutellum to apex. Distributional data from Lindroth (1963) and recent collections by staff of the Geological Survey of Canada.*

[1] Deceased; formerly on the staff of the Biosystematics Research Institute, Agriculture Canada, Ottawa. Publication of this manuscript by Brown and Matthews is anticipated.


A
B
C
D
E
F

preserved the diagnostic genitalia. Among the **Amara** fossils are isolated elytra which, on the basis of meagre statistical data, appear to be outside the size range of **A. alpina** (Fig. 28.5D). These fossils obviously represent the subgenus **Curtinotus** to which **A. alpina** belongs but are probably from one of the other **Curtinotus** species. If so, it is significant that at present there are no other species of the subgenus living on the eastern islands of the Arctic Archipelago (Lindroth, 1968; W.J. Brown, unpub. manuscript). One species which has elytra most similar to the large fossils in size and other characteristics is **Amara hyperborea** Dejean, but confirmation of its presence in the Makinson Inlet peat must await discovery of fossils of pronota or heads. **A. hyperborea** occurs across most of northern Ungava, but is not a true tundra insect (Lindroth, 1968; Larochelle, 1975).

Nephus georgei (Weise): (Fig. 28.6F) Ladybird beetles (Coccinellidae) are not typical of arctic regions. Only 27 species extend onto the tundra of North America (Belicek, 1976), and the species **Nephus georgei** is not one of these. It is a rare beetle, as indicated by the paucity of collection records shown in Figure 28.5C. Because a few of its localities are near treeline, we assume that the species is at least a rare component of the fauna of the low arctic tundra zone (Fig. 28.5A, 28.5C). Note, however, that the fossil locality is not within the low arctic zone.

The identification of **N. georgei** is based on a comparsion of fossil elytra, some of which preserve hairs and maculae, and abdominal fragments (Fig. 28.6F), with modern specimens and descriptions in Belicek (1976) and Gordon (1976).

Platynothrus sp.: (Fig. 28.6E) Fossils of mites representing this genus are abundant in some of the peat samples, numbering in the hundreds of specimens in samples BS-77-242 and BS-77-244. The distribution of many northern mites is still poorly known, but **Platynothrus** is apparently not a high arctic animal. It occurs at sites beyond treeline in the Mackenzie Delta region; Coppermine, Northwest Territories; Churchill, Manitoba; and at Frobisher Bay, but as yet it has not been found on Ellesmere Island (Hammer, 1952; V. Behan, pers. comm., 1978), nor was it recorded during extensive IBP (International Biological Programme) research in northern Devon Island (Ryan, 1977).

Both North America species of **Platynothrus** occur at sites characterized by a thick moss cover, and individuals are usually abundant (V. Behan, pers. comm., 1978), so the large number of fossils from the Makinson Inlet peat is not unusual.

Figure 28.6. (opposite)

Scale bar = 0.5 mm

A ***Menyanthes trifoliata*** *L.: fruit; GSC-60878; sample BS-77-240.*

B ***Amara alpina*** *Payk.: pronotum; GSC-60879; sample BS-77-242.*

C ***Carex maritima*** *Gunn.: perigynium with achene enclosed; GSC-60880; sample BS-77-240.*

D ***Andromeda polifolia*** *L.: "seed"; GSC-60801; sample BS-77-244.*

E ***Platynothrus*** *sp.: Dorsum of entire individual, lacking legs; GSC-60882; sample BS-77-244.*

F ***Nephus georgei*** *(Weise): First and second abdominal sternites; GSC-60883; BS-77-242. First sternite has evenly arcuate postcoxal lines which characterize the species.*

Paleoclimatic Interpretations

During Pleistocene time the sequence of events which led to the present-day development of the landscape near Makinson Inlet must have included, in the first place, an episode of channel cutting. The configuration of the channels along the valley wall suggests that they were incised by streams flowing along, or close to, the margin of a glacier. This glacier presumably filled the broad valley now occupied, in part, by the northern arm of Makinson Inlet. Following the creation of the channel, small ponds and bogs developed in a tundra environment dominated by a luxurious growth of mosses. The period of peat formation terminated more than 52 000 years ago (GSC-2677). In a succeeding glacial episode, a layer characterized by boulders several metres thick was deposited by ice, or meltwater, or both, on top of the peat. However, part of the material present today may represent colluvium that has accumulated since deglaciation. The size of the boulders and the steepness of the slope made it hazardous to attempt excavations, but examination of the natural exposures along the gully gave no indication that more than one boulder rich unit overlay the peat unit, or that any other massive accumulation of peat was present higher in the section. The last event to have occurred is headward erosion by gullying. This process has resulted in the exposures we now see.

A radiocarbon age determination on marine pelecypods indicates that the sea had penetrated to the head of the northern arm of Makinson Inlet, and the valley leading to it, by approximately 7400 or 7300 years ago (Blake, 1978). Because well preserved glacial features more than 60 km to the southeast (down-glacier) occur at elevations of more than 300 m, i.e., less than 100 m below the elevation at which peat outcrops, it is clear that some 8000 years ago glacier ice still covered the peat site. Thus the surface till or till-like material overlying the peat relates to the late Wisconsinan Glaciation or to the late Foxe Glaciation in the terminology proposed by Miller et al. (1977) for Baffin Island.

We have shown that several of the fossils from the site east of Makinson Inlet represent taxa whose present northern limits can be assumed to lie far to the south. Taken singly, any of these facts would constitute inadequate evidence of paleoclimate. After all, the distributional limits of many northern species still are poorly known, a situation likely to lead to erroneous conclusions. For example, one can easily envision the conclusion that might have been drawn from the presence of the **Hydroporus** cf. **morio** fossils had not Blake collected living beetles of this species in some of the ponds near Alexandra Fiord. It is also true that a few of the species listed in Table 28.2, e.g. **Menyanthes trifoliata**, are aquatic plants and thus are not always sensitive indicators of climate (Young, 1971). **Andromeda polifolia** is not in this category, however, and the fact that not only plant fossils, but those of insects as well, portray extralimital records at Makinson Inlet supports the conclusion that the peat represents growth during a period of warmer climate. At the time when the peat-forming mosses were accumulating, the Makinson Inlet area was probably within a low arctic or hypoarctic zone with the treeline considerably farther north than it is today.

Realizing that certain deposits assigned to interstadials within the last glaciation contain fossils indicative of a warmer climate than that of the present (Dreimanis and Raukas, 1975)[1], we conclude, nevertheless, that the evidence for a warmer climate at Makinson Inlet, like similar information from Bathurst Island (Blake, 1974) and Worth Point on Banks Island (Kuc, 1974), implies that the peat formed during one of the Pleistocene interglacials, most probably the last one. If so, the actual age of the Makinson Inlet peat is in all likelihood well beyond the minimum age indicated by the radiocarbon age determination (Table 28.1).

[1] In this connection it should be noted that none of the sites referred to by those authors were from high latitudes.

Acknowledgments

Base camp facilities and helicopter support in the field were provided by T. Frisch, Regional and Economic Geology Division, and general logistical support was furnished by the Polar Continental Shelf Project (G.D. Hobson, Director). R.J. Richardson assisted in the field and with the help of J.P. Bridgland and P.B. Smith was responsible for picking out many of the insects and seeds reported here. D.J. Larson, Department of Biology, Memorial University of Newfoundland, examined the dytiscids; J.A.P. Janssens, Department of Botany, University of Alberta, determined the mosses. We are particularly grateful to both of them for the alacrity with which they examined our material. The "high pressure" age determination was carried out by the staff of the Radiocarbon Dating Laboratory, under the supervision of J.A. Lowdon. W.J. Cody, Biosystematics Research Institute, Agriculture Canada, provided us with up-to-date distribution maps of **Menyanthes** and **Andromeda** from his forthcoming monograph. M. Kuc, formerly of the Geological Survey, determined the mosses in the original collection of peat from Makinson Inlet and aided Matthews in the identification of **Andromeda** from Flitaway Lake, Baffin Island; J.T. Andrews, INSTAAR, University of Colorado kindly allowed us to cite this unpublished record. We have benefitted from comments on the manuscript provided by C.R. Harington, National Museum of Natural Sciences, and J.T. Andrews.

References

Belicek, J.
1976: Coccinellidae of western Canada and Alaska with analysis of the transmontane zoogeographic relationships between the fauna of British Columbia and Alberta (Insecta: Coleoptera: Coccinellidae); Quaestiones Entomologicae, v. 12, p. 283-409.

Blake, W., Jr.
1974: Studies of glacial history in Arctic Canada. II. Interglacial peat deposits on Bathurst Island; Canadian Journal of Earth Sciences, v. 11, p. 1025-1042.

1978: Aspects of glacial history, southeastern Ellesmere Island, District of Franklin; in Current Research, Part A, Geological Survey of Canada, Paper 78-1A, p. 175-182.

Christie, R.L.
1962: Geology, Alexandra Fiord, Ellesmere Island, District of Franklin; Geological Survey of Canada, Map 9-1962.

Dreimanis, A. and Raukas, A.
1975: Did Middle Wisconsin, Middle Weichselian and their equivalents represent an interglacial or an interstadial complex in the Northern Hemisphere?; in Quaternary Studies, ed. R.P. Suggate and M.M. Cresswell; Royal Society of New Zealand, Bulletin 13, p. 109-120.

Dyck, W. and Fyles, J.G.
1964: Geological Survey of Canada radiocarbon dates III; Radiocarbon, v. 6, p. 167-181.

Dyck, W., Fyles, J.G., and Blake, W., Jr.
1965: Geological Survey of Canada radiocarbon dates IV; Radiocarbon, v. 7, p. 24-46.

Gordon, R.D.
1976: The Scymnini (Coleoptera: Coccinellidae) of the United States and Canada; Key to genera and revision of **Scymnus, Nephus** and **Diomus;** Bulletin of the Buffalo Society of Natural Sciences, v. 28, 362 p.

Hammer, M.
1952: Investigations on the Microfauna of Northern Canada, pt. 1, Oribatidae, Acta Arctica, Fasc. IV, 108 p.

Hultén, E.
1970: The circumpolar plants, II. Dicotyledons; Kungliga Svenska Vetenskapsakademiens Handlingar, Fjärde Serien, Bd. 13, Nr. 1, 463 p.

Kuc, M.
1974: The interglacial flora of Worth Point, western Banks Island; in Report of Activities, Part B; Geological Survey of Canada, Paper 74-1B, p. 227-231.

Larochelle, A.
1975: Les Carabidae du Québec et du Labrador; Départment de Biologie du Collège Bourget, Rigaud, Québec, Bulletin 1, 255 p.

Lindroth, C.H.
1963: The fauna history of Newfoundland; Opuscula Entomologica, Supplement 23, 112 p.

1968: The ground-beetles of Canada and Alaska, Part 5; Opuscula Entomologica, Supplement 33, p. 649-944.

Miller, G.H., Andrews, J.T., and Short, S.K.
1977: The last interglacial-glacial cycle, Clyde foreland, Baffin Island, N.W.T.: stratigraphy, biostratigraphy, and chronology; Canadian Journal of Earth Sciences, v. 14, p. 2824-2857.

Porsild, A.E. and Cody, W.J.
Vascular plants of the continental Northwest Territories; National Museums of Canada, Publications in Botany, No. 8. (in press)

Ryan, J.
1977: Invertebrates of Truelove Lowland; Appendix 7 in Truelove Lowland, Devon Island, Canada: A High Arctic Ecosystem, ed. L.C. Bliss; Edmonton, University of Alberta Press, p. 699-703.

Terasmae, J., Webber, P.J., and Andrews, J.T.
1966: A study of late-Quaternary plant-bearing beds in north central Baffin Island, Canada; Arctic, v. 19, p. 296-318.

Young, S.B.
1971: The vascular flora of St. Lawrence Island, with special reference to floristic zonation in the Arctic regions; Contributions from the Gray Herbarium of Harvard University, No. 201, p. 11-115.

29.

AN EQUILIBRIUM MODEL FOR HUMMOCKS (NONSORTED CIRCLES), GARRY ISLAND, NORTHWEST TERRITORIES

Project 680047

J. Ross Mackay[1]
Terrain Sciences Division

Mackay, J. Ross, An equilibrium model for hummocks (nonsorted circles), Garry Island, Northwest Territories; in Current Research, Part A, Geol. Surv. Can., Paper 79-1A, p. 165-167, 1979.

Abstract

Hummocks (nonsorted circles) are a widely distributed type of patterned ground in the boreal forest of lower Mackenzie Valley and the tundra of the Western Arctic coast. An equilibrium model for hummocks in fine grained soils with high liquid limits is suggested, based upon summer and winter field studies during 1963 to 1978 at Garry Island, Northwest Territories. At the top of a hummock the surface of winter heave and summer subsidence is concave down, whereas at the bottom of the hummock it is concave up. In consequence, an upward cell circulation develops, because movement near the top of the hummock is down and radially outward and movement at the bottom is up and radially inward.

Hummocks are a widely distributed type of patterned ground in permafrost areas of the boreal forest of lower Mackenzie Valley and in the adjacent tundra of the Western Arctic coast (e.g. Crampton, 1977; Heginbottom, 1973; Kerfoot, 1969; Mackay, 1963; Mackay and MacKay, 1976; Zoltai and Tarnocai, 1974; Zoltai and Pettapiece, 1974; Zoltai et al., 1978). Hummocks belong to the category of nonsorted circles in Washburn's (1973) classification of patterned ground, but as the descriptive word "hummock" is firmly entrenched in the literature dealing with Mackenzie Valley, the term will be used here. If the hummock is covered with vegetation, it is commonly referred to as an earth hummock, but if the centre is bare, it is termed a mud hummock, there being a continuum between earth and mud hummocks. The typical Garry Island hummock is about 0.75 to 1.5 m in diameter with the domed centre rising 0.25 to 0.50 m above a vegetated interhummock depression. The fine grained hummock soils are subject to ice lensing. Field observations at Garry Island for the 1963 to 1978 period show that hummocks are remarkably stable features, and measurements within them reveal only minor internal movements. Thus the stable hummocks of Garry Island contrast with the active mud boils described by Shilts (1978) from the District of Keewatin in external form, stability, soil type, and liquid limits.

Most theories of hummock origin are based upon some variant of the cryostatic theory (e.g. Crampton, 1977; French, 1976; Jahn, 1975; Nicholson, 1976; Zoltai et al., 1978). According to the cryostatic theory, there is an upward injection of uniform material confined between the ground surface and a lower impermeable surface by progressive downward freezing that generates large hydrostatic pressures in pockets of such material (Gary et al., 1972, p. 169). The purpose of this paper is to suggest that: 1) cryostatic pressures play a subordinate role in hummock growth and that 2) hummocks are an equilibrium form produced by differential heave and subsidence, primarily at the top and bottom of the active layer where the processes occur at sites with opposite curvatures, the result being a slow upward movement of material from the bottom of the active layer to the top.

Objections to the Cryostatic Theory

In hummocks that are composed of frost-susceptible soils, ice lenses will form near the ground surface by downward freezing. In areas of cold permafrost, such as at Garry Island, ice lenses also will form at the bottom of the active layer by upward freezing. Because freezing is in a closed system, the growth of ice lenses at the top and bottom of the hummock can only take place at the expense of water withdrawal from and desiccation of the unfrozen portion of the hummock. Consequently, the unfrozen core progressively becomes consolidated and immobile and not the reverse as is so generally assumed in the cryostatic theory. There is abundant field evidence from winter excavations at Garry Island to verify the above conclusion, and it is common knowledge (e.g. Vtyurina, 1974) that a downward decrease in water content in the active layer generally is observed in the winter profile of the active layer in fine grained soils. On the other hand, if the active layer has relatively coarse grained soils that are not frost susceptible, downward freezing could lead to pore water expulsion and a saturated active layer at depth, particularly if there is some groundwater movement. Under such conditions, cryostatic pressures are more likely to develop, and winter artesian pressures have been measured in one such area of Tuktoyaktuk Peninsula, Northwest Territories.

An Equilibrium Model for Hummocks

The type of hummock found on Garry Island has a late summer frost table that is a mirror image of the ground surface, with the greatest depth beneath the hummocks and the least beneath the interhummock depressions (Fig. 29.1). This type of relief inversion, which is widespread in vegetated areas, is the result of a thermal effect and is most striking where bare and vegetated ground are associated with mounds and depressions. At Garry Island, in late summer, the frost table beneath a hummock is bowl shaped, concave upwards, and may have a closure ranging from a few centimetres to more than 30 cm, that is, water can accumulate to these depths when the hummock is excavated. The lower portion of the hummock below the closure, therefore, becomes saturated and mobile at the end of the summer. When freeze-back commences, ice lenses tend to form subparallel to the ground surface by downward freezing and also subparallel to the bowl-shaped frost table by upward freezing. Since ice lens growth causes heave at right angles to the freezing plane, the direction of upward heave associated with freezing at the top of the active layer will have a radially outward component and at the bottom will have a radially inward component (Fig. 29.1). During the thaw period, conditions reverse. In early summer when ice lenses melt at the top of the active layer, the ground will subside with a radially outward component; in late summer when ice lenses melt at the bottom of the active layer subsidence will have an inward component, because of the bowl-shaped frost table (Fig. 29.1). As the bottom of the active layer is then

[1]Department of Geography, University of British Columbia, Vancouver, British Columbia, V6T 1W5

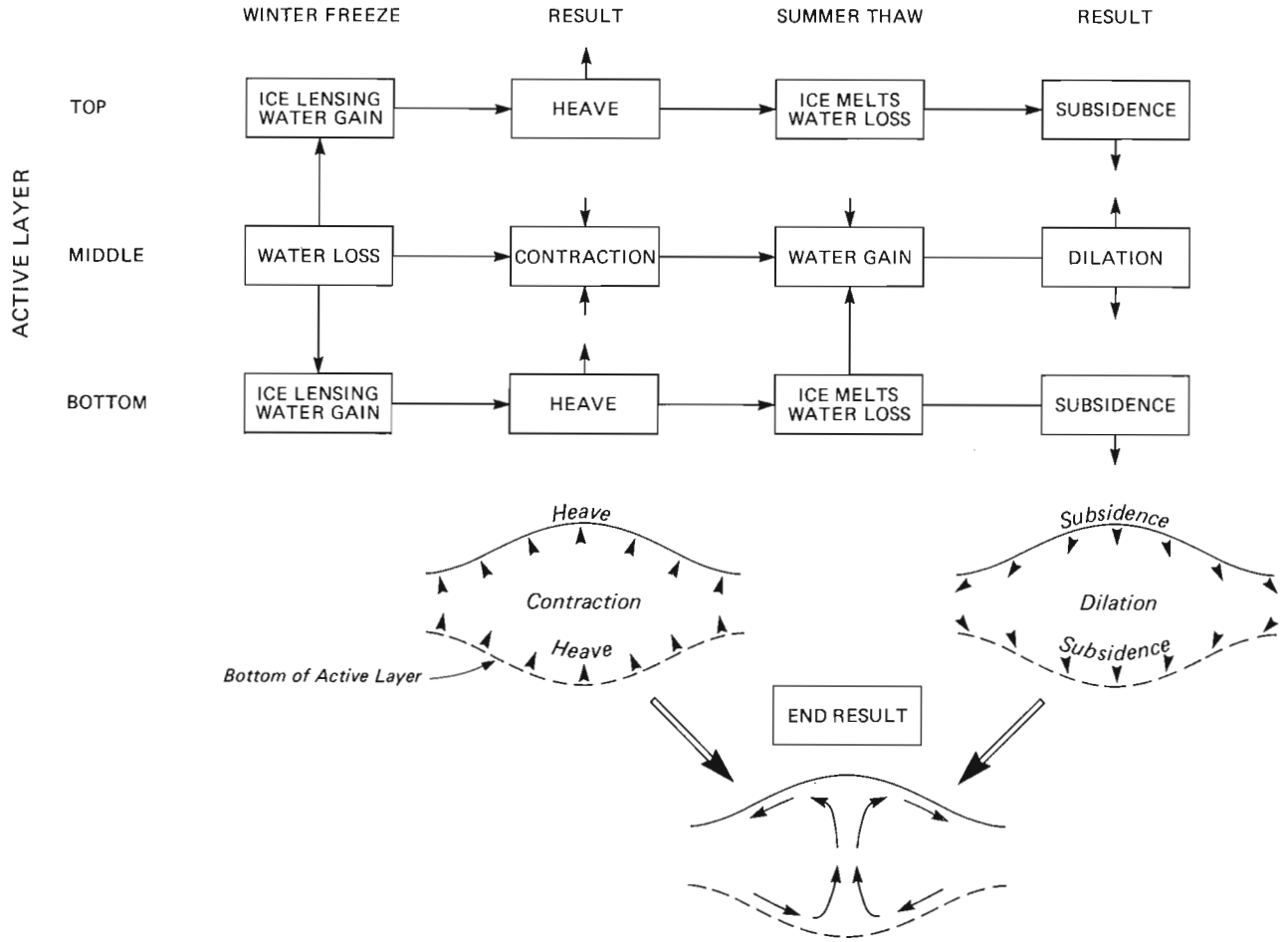


Figure 29.1. *Schematic diagram of the equilibrium model proposed for the growth and maintenance of hummocks, Garry Island, Northwest Territories.*

saturated, tongues of mud are squeezed upwards to produce the cell circulation so frequently observed by many researchers in hummock profiles. The basic cause, according to the model proposed here, is not cryostatic pressure generated during fall freeze-back, but the end result of heave-subsidence at the top and bottom of the active layer at sites with opposite curvatures, thus generating an upward cell circulation.

Conclusion

The hummocks of Garry Island and similar features elsewhere are characterized by a late summer frost table which is a subdued mirror image of the ground surface. Heave and subsidence at the top of the active layer then produce a net downward and outward movement of material, whereas those at the bottom produce a net upward and inward movement, the two processes combining to produce a slow upward cell-type circulation. The cell-type circulation results because the freeze/thaw surfaces at the top of the active layer are concave down, whereas those at the bottom of the active layer are concave up. This equilibrium model can be applied, with minor changes to take into account soil type and surface form, to some other types of patterned ground where the late summer frost table is concave upwards. The equilibrium model proposed here differs fundamentally from that of the cryostatic model not in the upward cell circulation, but in the causes of the circulation.

References

Crampton, C.B.
1977: A study of the dynamics of hummocky microrelief in the Canadian north; Canadian Journal of Earth Sciences, v. 14, p. 639-649.

French, H.M.
1976: The Periglacial Environment; Longman Group Limited, London, 309 p.

Gary, M., McAfee, R., Jr., and Wolf, C.L. (ed.)
1972: Glossary of Geology; American Geological Institute, Washington, D.C., 805 p.

Heginbottom,J.A.
1973: Some effects of surface disturbance on the permafrost active layer at Inuvik, N.W.T., Canada; in Permafrost, North American Contribution, Second International Conference (Washington); National Academy of Sciences, p. 649-657.

Jahn, A.
1975: Problems of the Periglacial Zone; Foreign Science Publications, TT72-54011, Washington, 223 p.

Kerfoot, D.E.
1969: The geomorphology and permafrost conditions of Garry Island, N.W.T.; unpublished Ph.D. thesis, University of British Columbia, Vancouver, 308 p.

Mackay, J.R.
1963: The Mackenzie Delta area, N.W.T.; Ottawa: Mines and Technical Surveys, Geograph. Br., Memoir 8, 202 p.

Mackay, J.R. and MacKay, D.K.
1976: Cryostatic pressures in nonsorted circles (mud hummocks), Inuvik, Northwest Territories; Canadian Journal of Earth Sciences, v. 13, p. 889-897.

Nicholson, F.H.
1976: Patterned ground formation and description as suggested by low arctic and subarctic examples; Arctic and Alpine Research, v. 8, p. 329-342.

Shilts, W.W.
1978: Nature and genesis of mudboils, central Keewatin, Canada; Canadian Journal of Earth Sciences, v. 15, p. 1053-1068.

Vtyurina, E.A.
1974: The Cryogenic Structure of Rocks in a Seasonally Thawing Layer; Nauka Publishing House, Moscow, 126 p.

Washburn, A.L.
1973: Periglacial Processes and Environments; Edward Arnold, London, 320 p.

Zoltai, S.C. and Pettapiece, W.W.
1974: Tree distribution on perennially frozen earth hummocks; Arctic and Alpine Research, v. 6, p. 403-411.

Zoltai, S.C. and Tarnocai, C.
1974: Soils and vegetation of hummocky terrain; Task Force on Northern Oil Development, Department of Indian Affairs and Northern Development, report 74-5, 86 p.

Zoltai, S.C., Tarnocai, C., and Pettapiece, W.W.
1978: Age of cryoturbated organic matter in earth hummocks from the Canadian Arctic; in Proceedings, Third International Conference on Permafrost; National Research Council of Canada, v. 1, p. 325-331.

30. THE DENALI FAULT SYSTEM IN SOUTHWEST YUKON TERRITORY – A GEOLOGIC HAZARD?

Project 780037

J.J. Clague
Terrain Sciences Division, Vancouver

Clague, J.J., The Denali Fault System in southwest Yukon Territory – A geologic hazard?; in Current Research, Part A, Geol. Surv. Can., Paper 79-1A, p. 169-178, 1979.

Abstract

The Denali Fault is a major intracontinental crustal break, with Cenozoic dextral displacements perhaps as large as 350 km. Although parts of the fault in south-central Alaska are presently active, there has been no significant strike-slip movement on the Denali Fault System in Yukon Territory in Holocene time. Comparatively minor dip-slip movements on the Shakwak segment of the Denali Fault System probably occurred at the close of Kluane Glaciation of late Wisconsinan age and during early and possibly middle Holocene time. The evidence for these movements consists of scarps and aligned sediment mounds on the southwest side of Shakwak Valley between the Alaska-Yukon boundary and the south end of Kluane Lake. No evidence, however, has been found for displacements of latest Holocene age. Neither the 300 to 500 year-old shorelines and beaches of Neoglacial Lake Alsek and Kluane Lake, nor the surfaces of modern floodplains and alluvial fans are displaced where crossed by the Denali Fault in Yukon Territory.

Despite the apparent absence of late Holocene displacements on the Denali Fault System in Yukon Territory, the region is characterized by high seismicity. Ground accelerations equal to those produced during the largest earthquake in the Shakwak Valley area (M = 6.5, in 1944) are capable of seriously damaging man-made structures.

Mountainside scarps and trenches produced by gravitational spreading and subsidence ("sackung") are common in the Kluane Ranges in the vicinity of the Denali Fault System and Duke River Fault. These features probably formed during major earthquakes as a result of ground shaking.

Introduction

In response to a proposal by a consortium of companies to build a natural gas pipeline from Prudhoe Bay in Alaska through Canada to the midwestern United States, the Geological Survey of Canada in 1978 initiated a program to determine the Quaternary displacement history of the Shakwak and Dalton segments of the Denali Fault System in southwest Yukon Territory (Fig. 30.1). Concern was voiced as to the possibility of severe earthquakes and fault displacements occurring along the 180 km length of the Shakwak Fault in the Yukon near the route of the proposed pipeline.

The investigative approach used in the present study is primarily geomorphic in nature and is based on detailed photogrammetric and field examination of terrain adjacent to the Shakwak and Dalton faults for features indicative of tectonic displacement (e.g., scarps, sag ponds, offset streams). Exposures of Quaternary sediments crossed by the faults were inspected for evidence of deformation. Raised beaches and shorelines of two late Holocene[1] lakes crossed by the Denali Fault were examined on aerial photographs for possible strike-slip displacements and were surveyed for possible vertical displacements.

The preliminary results of this investigation are presented below, following a brief review of the tectonic setting and displacement history of the Denali Fault System.

Regional Setting

The Denali Fault is a major crustal break extending for more than 2000 km across south-central and southeast Alaska, southwest Yukon Territory, and northern British Columbia (Fig. 30.1). The fault system, which in part probably formed in the vicinity of a late Paleozoic or early Mesozoic continental suture (Richter and Jones, 1973), consists of many individual faults and splays which have different displacement histories and tectonic styles (Lanphere, 1978).

The fault system as a whole is characterized by large Cenozoic displacements, primarily dextral strike slip, although vertical separation has been suggested for parts of the system (St. Amand, 1957; Lanphere, 1978). Lanphere (1978), in a review of the displacement history of the Denali Fault System, concluded that about 350 km of dextral displacement occurred on the McKinley, Shakwak, and Dalton segments between 55 and 38 Ma ago, with subsequent displacements of less than 40 km.

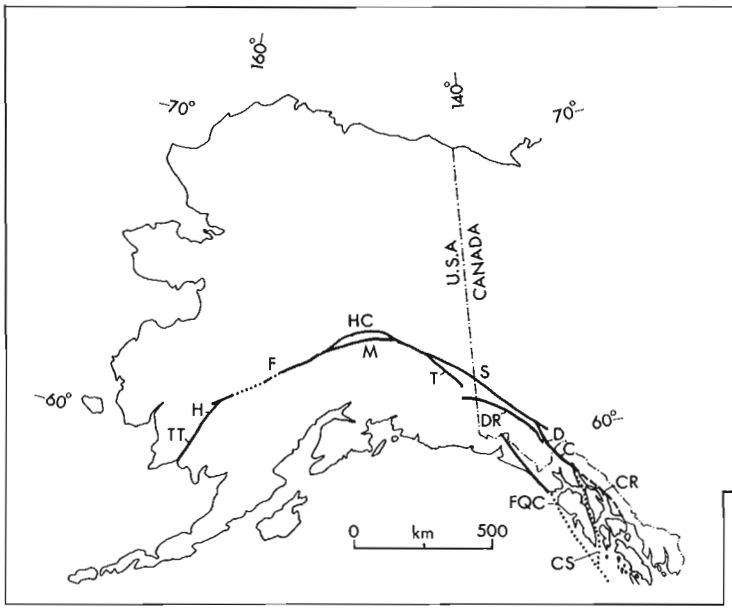
Some segments of the fault, notably the McKinley (Hickman and Craddock, 1973; Stout et al., 1973), Totschunda (Richter and Matson, 1971; Plafker et al., 1977), and western Shakwak (Richter and Matson, 1971), have been very active during the Holocene. For example, Wisconsinan glacial features along the Totschunda Fault and the Alaskan segment of the Shakwak Fault have been offset 110 to 350 m (Richter and Matson, 1971). Plafker et al. (1977) estimated a total late Cenozoic displacement on the Totschunda Fault of about 4 km.

The Denali and Duke River Faults in Yukon Territory

The Denali and Duke River faults in Yukon Territory are dextral strike-slip structures which intersect and dislocate other structures (St. Amand, 1957; Campbell and Eisbacher, 1974; Campbell and Dodds, 1975, 1978; Eisbacher, 1976). In this area the two faults are subparallel and trend northwest-southeast (Fig. 30.2). The Duke River Fault presumably branches off the Denali Fault System in northern British Columbia or southeast Alaska.

The Denali Fault System in Yukon Territory comprises the Dalton and Shakwak faults. From the Alaska-Yukon boundary (at about 62°10'N, 141°W) to the south end of Kluane Lake (61°N, 138°30'W), the Shakwak Fault follows the western edge of Shakwak Valley, a trench generally 3 to 8 km wide, with a maximum width of about 16 km, which is bounded on the northeast by the Kluane Plateau and on the southwest by the rugged Kluane Ranges (Bostock, 1948). The eastern flank of the Kluane Ranges, although breached in places by rivers draining the St. Elias Mountains to the southwest, rises from Shakwak Valley as a spectacular wall, with relief locally exceeding 1600 m.

[1] Holocene is defined as an epoch of the Quaternary Period extending from the end of the Pleistocene to the present. In this report this time interval is considered to be approximately equivalent to that of postglacial time.



TT	*Togiak-Tikchik Fault*
H	*Holitna Fault*
F	*Farewell segment*
HC	*Hines Creek segment*
M	*McKinley segment*
T	*Totschunda Fault*
S	*Shakwak Fault*
DR	*Duke River Fault*
D	*Dalton Fault*
C	*Chilkat River Fault*
CR	*Coast Range megalineament*
CS	*Chatham Strait Fault*
FQC	*Fairweather-Queen Charlotte Fault System*

Figure 30.1. *The Denali Fault System and other selected faults in northwest Canada and Alaska. Diagram modified from Lanphere (1978, Fig. 1).*

Southeast of Kluane Lake the Denali Fault System leaves Shakwak Valley and enters the Kluane Ranges. This segment of the fault system, referred to as the Dalton Fault (Campbell and Eisbacher, 1974), is defined topographically by a series of relatively narrow, high-gradient valleys within the Kluane Ranges. The Dalton Fault leaves the Kluane Ranges near the British Columbia-Yukon boundary (at about 60°N, 136°50'W) and extends southeast along the valley of Tatshenshini River, which separates the St. Elias Mountains and Coast Mountains physiographic provinces (Bostock, 1948).

The Duke River Fault, not well defined topographically, is subparallel to, and located about 1 to 15 km west of, the Denali Fault from the British Columbia-Yukon boundary to about 61°20'N. North of 61°20'N the Duke River Fault swings west-northwest away from the Denali and crosses into Alaska at about 61°27'N (Fig. 30.2).

The Dalton, Shakwak, and Duke River faults are the structural boundaries of distinct geologic terranes (Campbell and Dodds, 1978). Northeast of the Dalton and Shakwak faults are Jura-Cretaceous sedimentary and volcanic rocks which are cut by Cretaceous and Tertiary plutons. Between the Denali Fault System and the Duke River Fault is a belt of Pennsylvanian and Permo-Triassic sedimentary and volcanic rocks, with subordinate Jura-Cretaceous sedimentary and volcanic rocks. These rocks also are cut by Cretaceous and Tertiary plutons. Southwest of the Duke River Fault are Cambrian to (?) Permian sedimentary and volcanic rocks cut by plutons of Pennsylvanian to Tertiary age.

The Denali Fault System displaces Miocene volcanic rocks (Wrangell lava), showing that some fault movement is Pliocene or Quaternary in age. The age of the major displacement is Late Cretaceous or Tertiary (Campbell and Dodds, 1978). In contrast, the Duke River Fault locally cuts the base of the Wrangell lava, but not the youngest flows (Campbell and Dodds, 1975; Souther and Stanciu, 1975). The age of the major displacement is younger than Late Triassic, probably younger than late Early Cretaceous or early Late Cretaceous, but older than Miocene (Campbell and Dodds, 1978). However, related faults in the intensively deformed region between the Duke River and Shakwak faults cut the entire pile of Wrangell lava, hence movement on them is in part Pliocene or Quaternary in age.

Quaternary Faulting

Although the Denali and Fairweather fault systems in Alaska have been active during Pleistocene and Holocene time (e.g., Grantz, 1966; Page, 1969; Richter and Matson, 1971; Hickman and Craddock, 1973; Stout et al., 1973; Hickman et al., 1977; Plafker et al., 1977, 1978), major Quaternary dislocations have not been proven for the Denali Fault in Yukon Territory. Features attributed to Quaternary faulting along the Dalton and Shakwak faults are described and discussed below.

Sediment mounds and scarps in Shakwak Valley Bostock (1952, p. 9) noted a line of irregularly spaced, elongate mounds on the drift-covered floor of Shakwak Valley near Donjek River (Fig. 30.3). He attributed these mounds to fault movement in "recent centuries", although no supportive evidence was given. He further noted that the mounds occur discontinuously from near the Alaska-Yukon boundary to the south end of Kluane Lake along the west side of Shakwak Valley.

These features were investigated in more detail by the author during the 1978 field season. The mounds, which are a few ten to several hundred metres long and several metres high, occur on drift within Shakwak Valley along a nearly straight line approximately parallel to the valley wall (Fig. 30.2, 30.3). Although there are no exposures from which their internal structure can be deduced, the mounds apparently consist of sand and gravel. They are best developed near Donjek River, but occur elsewhere near or on the presumed trace of the Shakwak Fault.

The mounds are continuous with, and grade laterally into, linear ridges and scarps (Fig. 30.2). Slopes of scarps range from a few degrees to about 35°; heights locally exceed 20 m. In most areas scarp slopes have been reduced by slumping, soil creep, and erosion. All escarpments face east to northeast. The scarps pass laterally into landforms which are transitional to the sediment mounds described above. These include ridges and asymmetric, elongate mounds characterized by higher southwest than northeast bases.

The mounds and scarps, although commonly subdued and difficult to recognize on the ground, are clearly visible on aerial photographs, and, by their linear continuity, readily are distinguished from glacial landforms such as drumlins, flutings, and eskers.

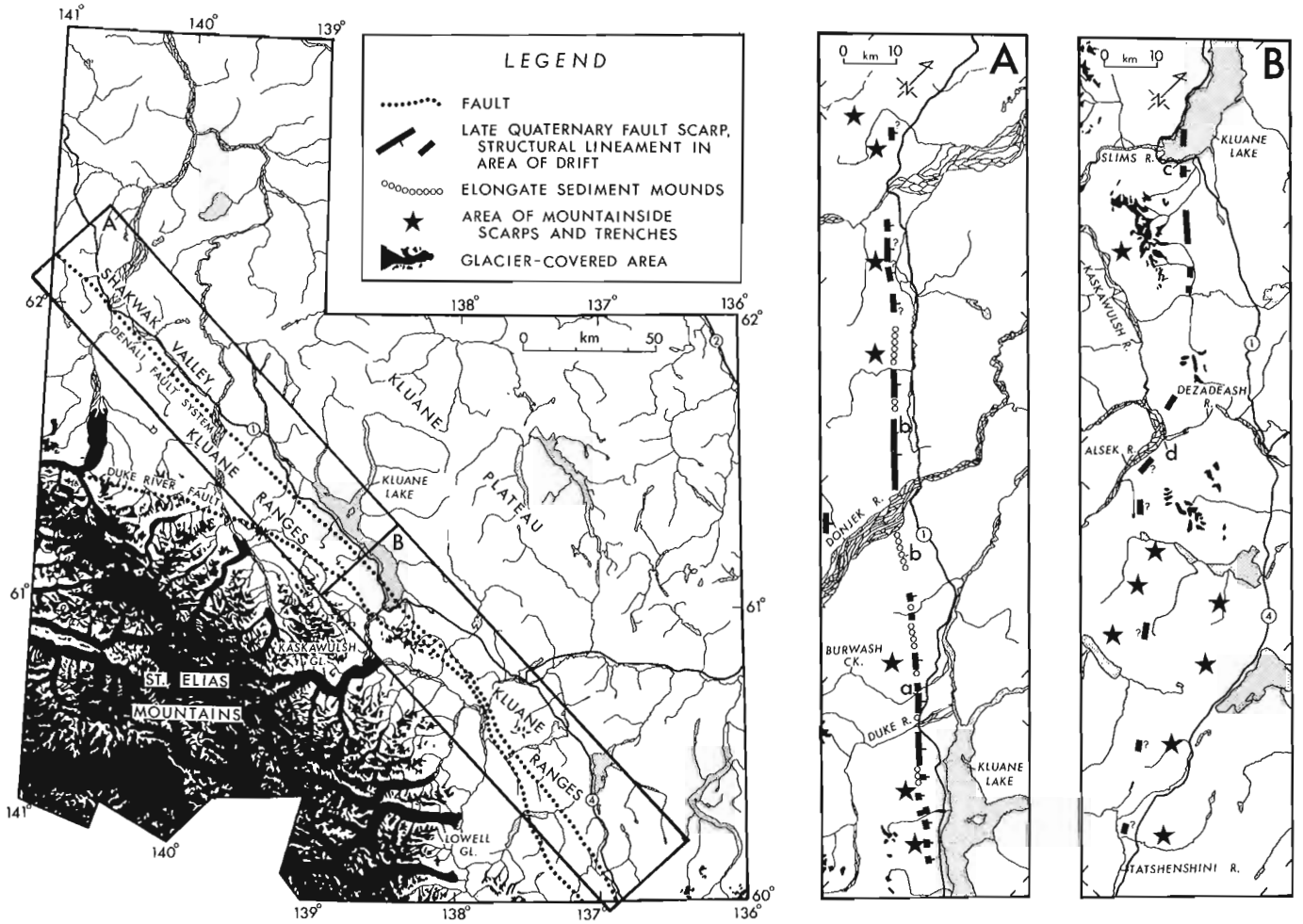


Figure 30.2. *The Denali and Duke River faults in Yukon Territory. Shown in A and B are late Quaternary fault scarps and elongate sediment mounds, minor lineaments of uncertain age, and centres of areas of common mountainside scarps and trenches. Lower-case letters in A and B indicate locations of features discussed in the text.*

In most areas the mounds and scarps are developed on Pleistocene sediments, the youngest of which were deposited during the late Wisconsinan Kluane Glaciation (Denton and Stuiver, 1967) and during the ensuing interval of deglaciation. Although scarps do not occur on modern floodplains or active alluvial fans, at a few localities they do cross Holocene river terraces and, possibly, the inactive portions of Holocene fans.

At Burwash Creek (Fig. 30.2, location a), for example, two terraces, 8 and 12 m above the modern floodplain, are cut by a scarp which trends northwest, faces northeast, is up to 5 m high, and slopes up to 30°. The trend of this scarp relative to present and past flow patterns of Burwash Creek, and its continuity with nearby mounds and scarps developed on glacial sediments indicate that the feature is structural rather than erosional in origin. The ages of the Burwash Creek terraces are not known precisely; however, they likely formed in a period of downcutting during or shortly after deglaciation of Burwash and Shakwak valleys. It is possible, however, that the terraces are of middle, or even late, Holocene age.

Northwest and southeast of Donjek River (Fig. 30.2, location b) discontinuous sediment mounds and scarps cross Holocene alluvial fans and terraces built by streams flowing northeast out of the Kluane Ranges into Shakwak Valley. Although locally in this area the Holocene alluvium banks up against and partially covers the mounds and scarps, elsewhere it appears to be truncated by the scarps.

Because of their linearity and coincidence with the trace of the Shakwak segment of the Denali Fault System, the scarps and ridges described above probably were generated by faulting. Their spatial association with constructional landforms (i.e., mounds of unconsolidated sediment), however, is unusual and requires explanation. One explanation, suggested by V.N. Rampton (pers. comm., 1978), that is consistent with the available information is that the sediment mounds formed in fault-controlled fractures in or at the base of the Shakwak Valley glacier at the close of Kluane Glaciation. According to this theory, faulting that localized deposition of the sand and gravel of the mounds also generated the displacements recorded in the scarps. If this explanation is correct, the faulting temporally is associated with deglaciation of southwest Yukon Territory about 10 000 to 13 000 years ago. Apparently, however, faulting continued into Holocene time, as evidenced by probable offsets on alluvial fans and terraces in Shakwak Valley near Donjek River.

Scarps similar to those described above also occur along the Shakwak Fault west of the International Boundary in Alaska (Richter and Matson, 1971, their Fig. 3). As in Shakwak Valley, these scarps face northeast. They exhibit no systematic change in height along the trend of the fault.

It has not been possible to assess adequately the sense of displacement associated with this late Pleistocene-Holocene faulting. The presence of scarps facing consistently

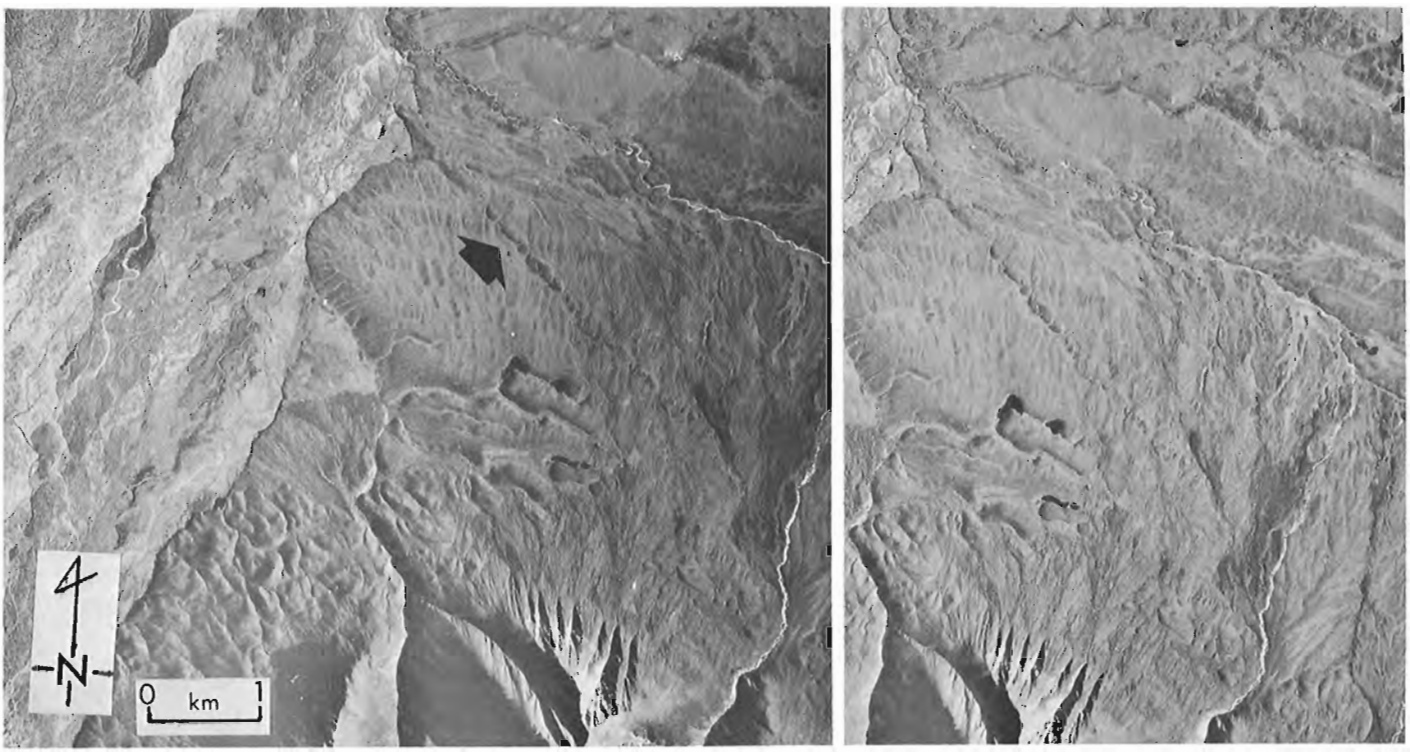


Figure 30.3. *Stereogram of area east and southeast of Donjek River. The mounds occur on drift of late Wisconsinan age, are partly covered by alluvial fan sediments on the right side of the photo, and are truncated at the edge of the Donjek River floodplain on the left. Photo numbers A15728-89 and -90 (National Air Photo Library, Canada Department of Energy, Mines and Resources).*

northeast and east suggests at least local dip-slip movement. Lateral offsets were not observed on glacial landforms, although most of these landforms are parallel or nearly parallel to the trace of the Shakwak Fault, thus lateral offsets might not be apparent. Nor are stream traces offset where they cross the fault. However, although large strike-slip displacements apparently did not occur during this episode of faulting, it is possible that small transcurrent displacements, for which geomorphic evidence is lacking, may have occurred.

Richter and Matson (1971) likewise found no evidence of strike-slip faulting along the Denali Fault between the Alaska-Yukon boundary and Nabesna River, a distance of approximately 90 km. At five localities northwest of Nabesna River, however, drainage courses and Wisconsinan glacial sediments are displaced in a right-lateral sense. The amount of separation increases from 110 m near Nabesna River to 350 m west of Mentasta Pass, 75 km distant, indicating a marked increase in late Quaternary fault activity to the northwest.

Considerable effort was made to find exposures of Pleistocene sediments intersected by the Shakwak Fault. Unfortunately, such exposures are uncommon, and, in general, colluvium covers the critical portions of those that are available. Even at the excellent section on the north side of Duke River just west of the Alaska Highway, colluvium covers that portion of the exposure intersected by the fault. Although the evidence here is somewhat equivocal, it appears that parallel-bedded gravels, forming much of the section, are faulted. The attitude of the gravels differs on opposite sides of the fault (Fig. 30.4). Although this difference in attitude is perhaps explainable as a primary depositional characteristic of the sediments, the uniform strike and dip of strata for several hundred metres southwest of the fault and the coincidence of the change in attitude of strata with the fault itself argue against this.

Shakwak Fault beneath the floor of Kluane Lake In 1977 a shallow seismic geophysical survey was conducted in the southern part of Kluane Lake by Terrain Analysis and Mapping Services Ltd. (Stittsville, Ontario). Good penetration of subbottom lacustrine sediments was achieved with two profiling systems, a Raytheon Model RTT 1000 (7 kHz) and an Atlas-Deso 10 (33 kHz and 200 kHz). Of interest here is the fact that the Shakwak Fault crosses Kluane Lake within the survey area, thus providing an opportunity to determine whether or not the Holocene lacustrine sediments in the vicinity of the fault have been offset.

The trace of the Shakwak Fault is shown on the seismic profiles by the inflection of subbottom reflectors (Fig. 30.5). These reflectors, however, are not broken, but rather appear to drape over an older scarp. The relief over the scarp decreases upward towards the uppermost reflectors. The records thus indicate that the last substantive movement on the Shakwak Fault occurred just prior to or early during the deposition of the lowest lacustrine sediments seen in the seismic profiles (Terrain Analysis and Mapping Services Ltd., 1978, p. 30). These lowest sediments are thought to have been deposited when Kluane Lake drained south through Slims River Valley from about 10 000 to 300-500 years ago. They are overlain by sediments which thicken towards the mouth of Slims River and which were deposited during the last 300 to 500 years when Slims River flowed into Kluane Lake.

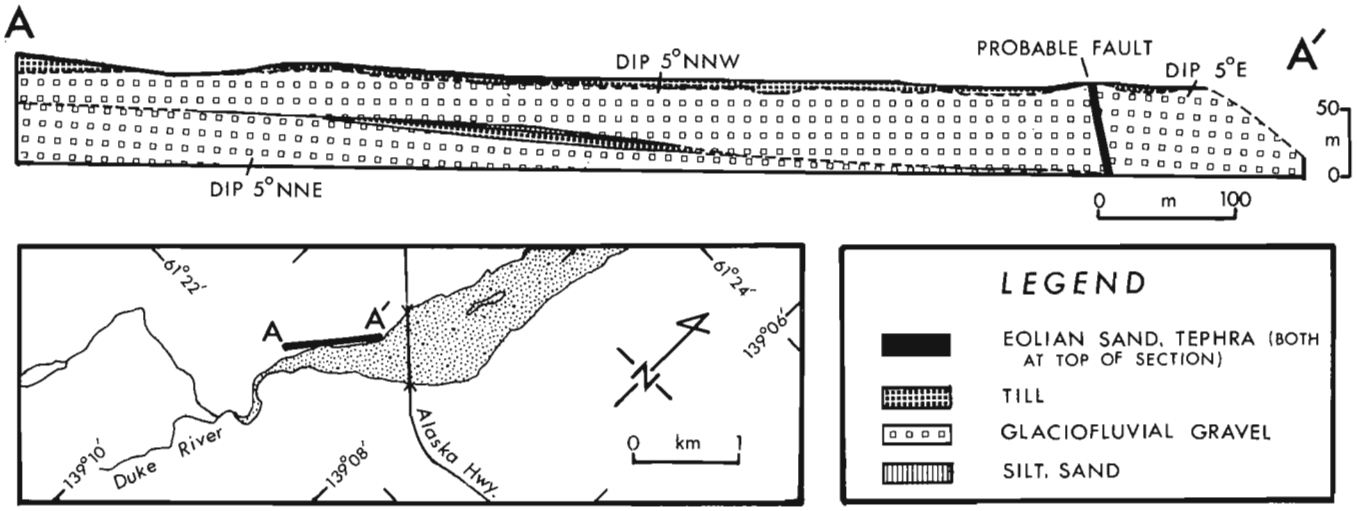


Figure 30.4. Generalized stratigraphy of Duke River valley wall southwest of the Alaska Highway bridge. The attitude of the upper gravel unit is different on opposite sides of the Shakwak Fault.

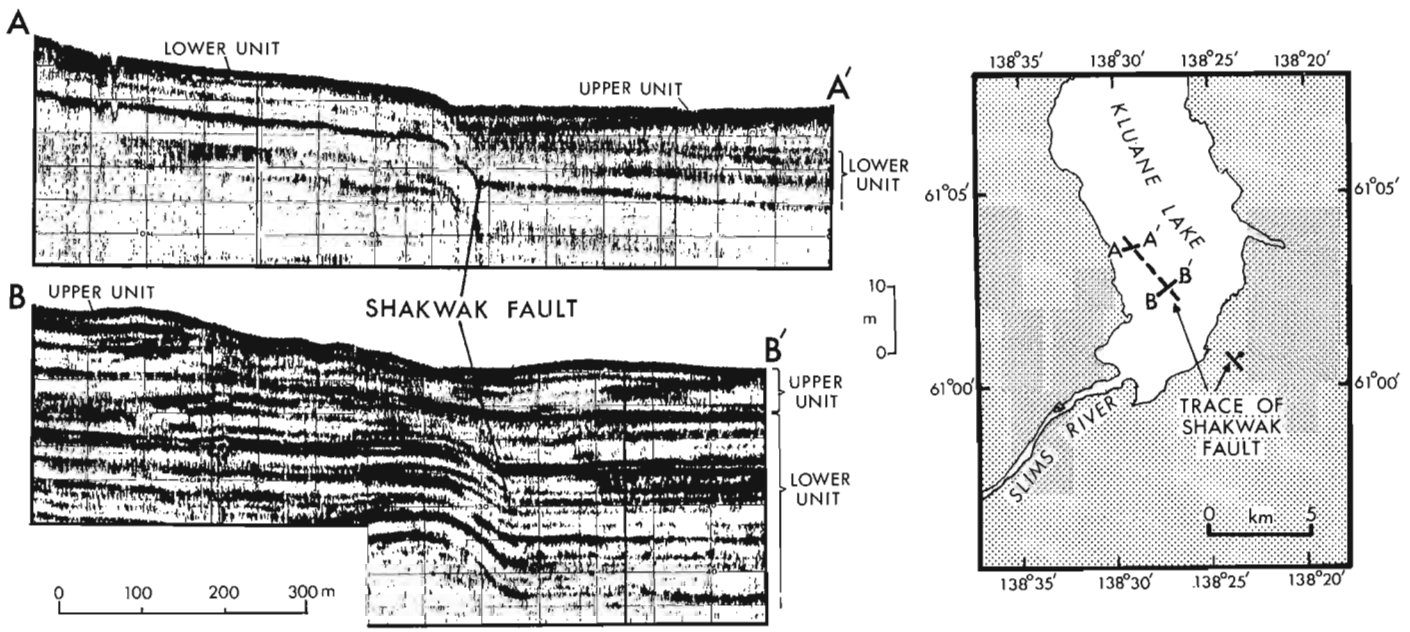


Figure 30.5. Seismic profiles across the Shakwak Fault at the south end of Kluane Lake. Lacustrine sediments drape over an escarpment but are not themselves offset by faulting. The significance of the upper and lower lacustrine units is discussed in the text. The seismic records were obtained with a Raytheon Model RTT 1000 subbottom profiling system by Terrain Analysis and Mapping Services Ltd. (1978).

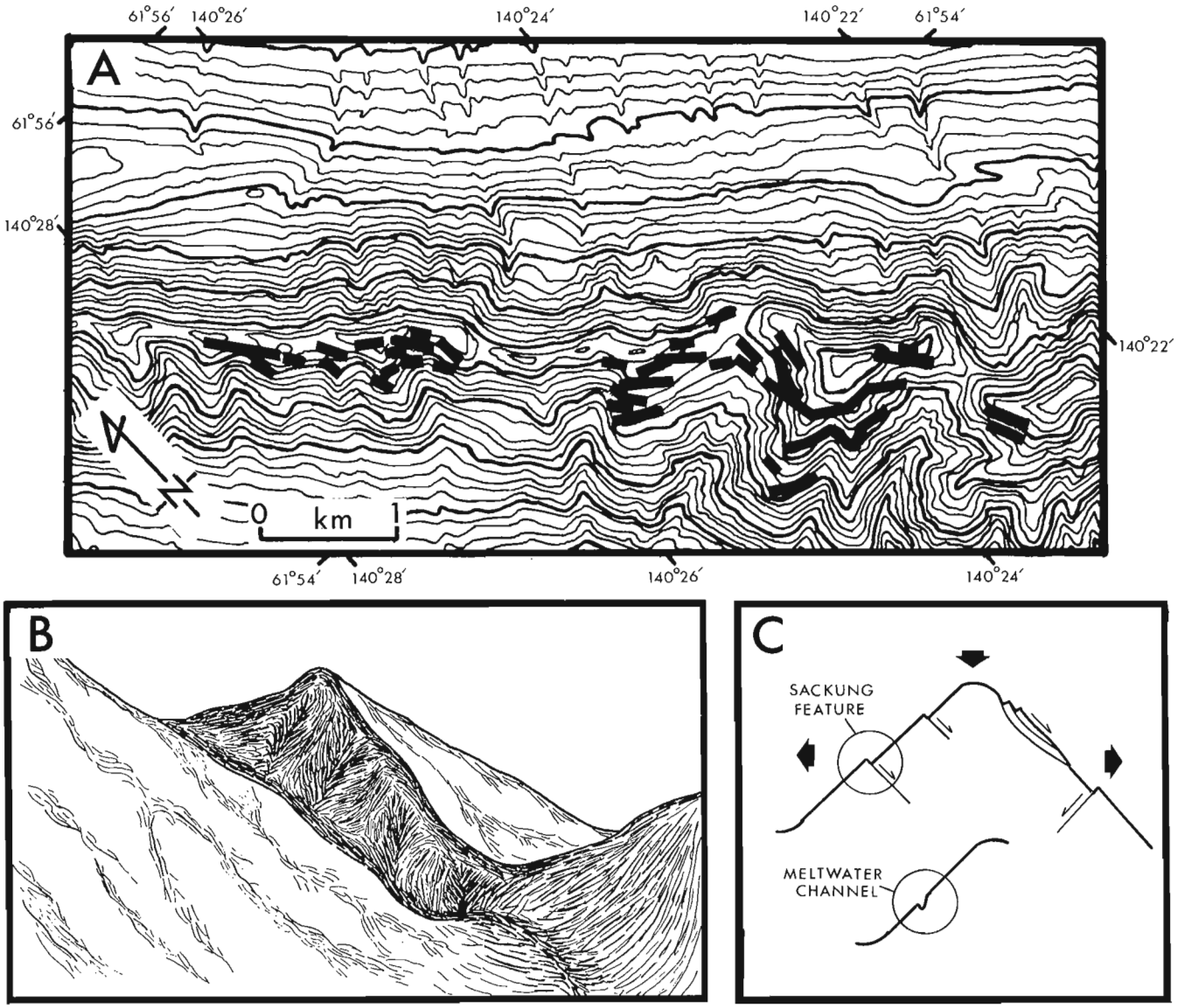
The reversal of the Slims River drainage 300 to 500 years ago resulted from the blockage of the Slims-Kaskawulsh valley by Kaskawulsh Glacier during the advance of the latter to its maximum Neoglacial position (Bostock, 1969; Hughes et al., 1972). As the glacier blocked the valley and reversed drainage, the level of Kluane Lake rose to about 13 m above present mean lake level, whereupon an outlet at the north end of the lake was occupied and downcutting was initiated. Raised beaches related to this high-level phase of Kluane Lake are older than 250, but younger than about 320, calendar years (Hughes et al., 1972, p. 13).

Raised beaches at the south end of Kluane Lake (Fig. 30.2, location c) were surveyed and examined on low-level aerial photographs (scale ca. 1:8000) for fault offsets. The beaches were found to be continuous across the projected trace of Shakwak Fault without displacement, thus indicating that there has been no major movement along the fault in this area during at least the last few hundred years.

Mountainside scarps and trenches formed by gravitational spreading and subsidence ("sackung") Locally within the Kluane Ranges in the vicinity of the Denali Fault System and Duke River Fault are irregular mountainside scarps and trenches, the former generally facing in an upslope direction (Fig. 30.2, 30.6). Although these features trend more or less parallel to the axes of the mountains on which they occur, they locally "climb" and "descend" mountain slopes. The scarps and trenches commonly occur in groups and are best developed on moderate to steep slopes within about 5 km of the Shakwak Fault and within about 15 km of the Dalton Fault. Relief and slope angle are variable, even for individual features; maximum measured scarp heights are 20 m, and trench walls and scarps slope up to 35°.

The scarps and trenches occur in bedrock, generally in Pennsylvanian (?) to Cretaceous sedimentary and volcanic rocks. The relationships between these features and local structure and stratigraphy, however, have not been determined. It is not known, for example, whether or not the scarps are associated with major bedrock discontinuities.

Trenches separating the scarps from the adjacent mountain slope superficially resemble meltwater channels. An origin by meltwater erosion, however, is precluded by the following: (1) Some of the trenches occur above the known limit of glaciation. (2) Mountain slopes exhibit separation on opposite sides of the trenches (Fig. 30.6C).



A. Surface dislocations, including trenches and uphill-facing scarps, on one ridge in the Kluane Ranges. Topographic contour interval = 30 m (100 feet).

B. Field sketch of an uphill-facing scarp. Maximum relief on scarp = 20 m.

C. Diagrammatic cross-section of a ridge showing nature of movements that produce sackung features. The trenches and scarps differ morphologically from mountainside meltwater channels.

Figure 30.6. *Gravitational ridge spreading ("sackung") in the Kluane Ranges.*

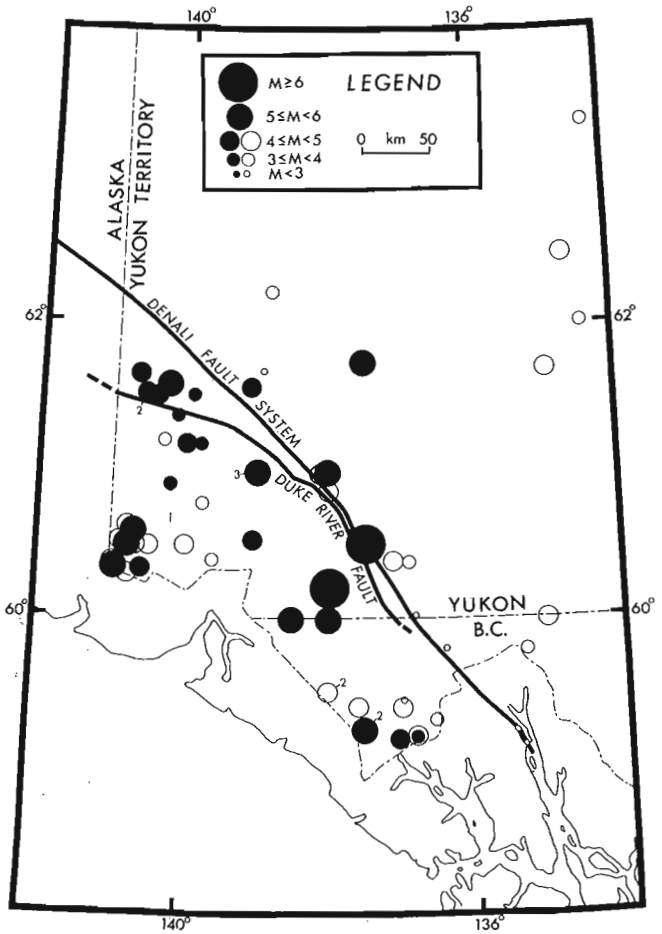


Figure 30.7. *Earthquake epicentres in southwest Yukon Territory, 1899-1975. Small numbers indicate number of coincident epicentres. The black circles represent more reliable epicentre locations. Data supplied by Division of Seismology and Geothermal Studies, Earth Physics Branch.*

These mountainside scarps and trenches are thought to originate by gravitational spreading and subsidence within the Kluane Ranges as a result of ground shaking during major earthquakes. Specifically, the following mechanisms are proposed (Fig. 30.6C): (1) The core of the mountain is displaced downward a short distance relative to at least one flank. (2) A slab of rock on the mountain flank is displaced downward without loss of coherency and without movement of the mountain core itself. The first mechanism appears to be the dominant one in the study area.

The term "sackung" (literally "sagging") has been applied to gravitational spreading of steep-sided ridges (Zischinsky, 1969; Radbruch-Hall et al., 1976). The mountainside scarps and trenches in the Kluane Ranges are morphologically similar to sackung features in the western United States described by Radbruch-Hall et al. (1976) and to "ridge-top trenches" (Gary et al., 1972, p. 609).

Although these features cannot be dated, some are fresh and little modified by erosion and therefore are almost certainly late Holocene in age. Some possibly have formed within the past few hundred years.

Dalton Fault Scarps similar to those in Shakwak Valley are uncommon on the Dalton Fault. Although there are lineaments on late Wisconsinan drift, these, in general, lack significant topographic expression and are recognizable only on the basis of breaks in vegetation and soil moisture patterns. In a few places aligned ponds occur along the lineaments. These are possibly, although not necessarily, sag ponds.

The significance of these features is uncertain. Because neither dip-slip nor strike-slip displacements can be proven, it is possible that at least some of these features have formed by differential glacial erosion of highly sheared rocks along the Dalton Fault, with subsequent deposition of drift and alluvium insufficient to mask completely the eroded lineaments. Alternatively, minor Holocene fracturing or faulting may have occurred along parts of the Dalton Fault, although displacements of more than a few metres appear to be ruled out.

Bearing on the problem of the age of last movement along the Dalton Fault are beaches and wave-cut benches of Lake Alsek, a Neoglacial lake formed by the damming of Alsek Valley by Lowell Glacier (Kindle, 1952). An altimeter survey showed that strandlines 320 to 500 calendar years old (Rampton, in press) are not offset vertically where crossed by the fault near the confluence of the Kaskawulsh and Dezadeash rivers (Fig. 2, location d).[1] Thus it is tentatively concluded that there has been no significant displacement (i.e., more than a few metres) on the Dalton Fault during the last 300 years, and perhaps for much of postglacial time.

Seismicity

The absence of geologic evidence for displacements on the Dalton and Shakwak faults during at least the last few hundred years is not to be construed to mean that this area is tectonically inactive. On the contrary, the eastern St. Elias Mountains and Shakwak Valley are located near the eastern edge of an area of high seismicity related to the interaction of the Pacific and North American crustal plates. The Fairweather Fault (Fig. 1), for example, which is parallel to the Dalton-Shakwak faults and only about 100 km to the southwest, is thought to be the present transform boundary between the two plates and is characterized by minimum average displacement rates during the last millenium of at least 4.8 cm/a and probably closer to 5.8 cm/a (Plafker et al., 1978). A 7.9-magnitude earthquake occurred on the Fairweather Fault in 1958, resulting in displacements along its entire 280 km onshore length, with maximum measured displacements of 6.5 m dextral slip and 1 m dip slip.

Although no such recent offsets have been recognized along the trace of the Denali Fault in Yukon Territory, this area is one of high earthquake activity. Figure 30.7 is a plot of epicentres for southwest Yukon Territory for the period 1899-1975. Clearly, substantial stress release is occurring in the eastern St. Elias Mountains and possibly in Shakwak Valley, although there is no obvious coincidence of epicentres with the Denali and Duke River faults.

It is important, however, to bear in mind the limitations of the data presented in Figure 30.7. With the existing seismograph network, epicentral locations are probably accurate to only about 20 km, and prior to the establishment of the Whitehorse seismograph station in 1971, they are less accurate (R.B. Horner, Earth Physics Branch, pers. comm., 1978). Thus, even if recent earthquakes are clustered along the Denali and Duke River faults, their true locations may not be revealed in the epicentral plot of Figure 30.7. Furthermore, the data set for southwest Yukon is incomplete for smaller earthquakes. Although all earthquakes greater than magnitude 4 have been detected since 1971, consistent detection of earthquakes with magnitudes less than 6 was not possible prior to 1964. Thus the data set of Figure 30.7 is biased towards larger earthquakes, with many smaller earthquakes in the area not recorded due to limitations in the seismograph network.

[1] The detection limit for vertical offsets is estimated to be 1 to 2 m. Thus smaller displacements of the strandlines might not be revealed by the survey.

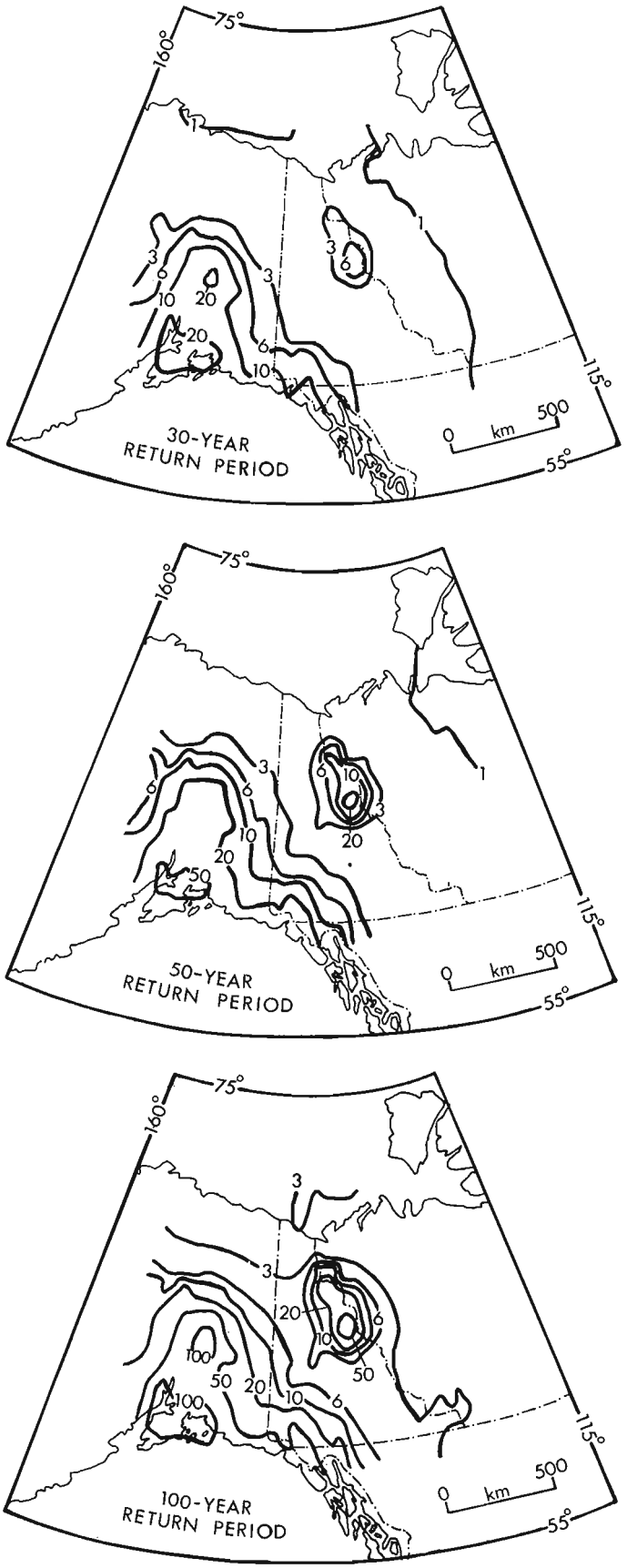


Figure 30.8. *Predicted acceleration amplitudes for the Yukon Territory and adjacent areas. Contours are in % g. Diagram modified from Stevens and Milne (1974, Figs. 8-10).*

The high seismicity of the area also is indicated by the results of a microearthquake survey of the Denali Fault System conducted in 1967. Using high-gain portable seismographs, Boucher and Fitch (1969) found that all segments of the fault system have significant microearthquake activity (average of 5 events per day of less than 2-second S-P interval, that is, with epicentral distances of less than about 17 km). On the basis of limited evidence from two crossings of the fault, they thought that these small earthquakes are preferentially generated on the Denali Fault. Microearthquake activity along that portion of the fault in Alaska thought to be presently active is comparable to that along the Dalton and Shakwak segments, thus Boucher and Fitch concluded that the latter are probably active as well.

This conclusion seemingly is in disagreement with the apparent lack of significant recent displacements along the Denali Fault System in Yukon Territory. The mechanism of stress release associated with these small earthquakes, however, is not understood. Microearthquakes may occur without surface dislocations, although if this seismicity is indeed localized along the Denali Fault and has occurred throughout late Quaternary time, some displacement might be expected. Another possible explanation is that the earthquakes are not generated preferentially on the Denali Fault System, but rather are widely dispersed along many small faults within the seismically active St. Elias Mountains. Alternatively, late Holocene ground-surface breaks may be too small to detect utilizing the geomorphic approach employed here.

Clearly, additional seismic investigations are required in southwest Yukon Territory to assess better the seismicity of the area. In response to this need, the Division of Seismology and Geothermal Studies of the Earth Physics Branch in 1978 installed three temporary seismograph stations in the vicinity of the Dalton and Shakwak faults and is attempting to determine first-motion solutions for the larger earthquake events in the southwest Yukon.

Earthquakes cause ground accelerations which are potentially damaging to structures such as pipelines and pumping stations. Risks posed by such accelerations may be evaluated for the southwest Yukon from the locations and magnitudes of recorded earthquakes.

Using data from 1899 to 1970, Stevens and Milne (1974) predicted ground accelerations in Yukon Territory and adjacent areas of western Northwest Territories and eastern Alaska for return periods of 30, 50, and 100 years (Fig. 30.8). These accelerations may vary by a factor of two or more from actual values due to the short earthquake history of the region, uncertainties in the locations and magnitudes of past earthquakes, lack of measured ground accelerations in the region, and the unknown modifying influence of crustal materials. Nevertheless, large ground accelerations with a short return period (30-100 years) are to be expected in the eastern St. Elias Mountains and Shakwak Valley. Engineers commonly consider 10% g as the threshold of accelerations that are damaging to ordinary structures on firm soil (Stevens and Milne, 1974, p. 160). Accelerations of this magnitude have a return interval of 30 to 100 years for the Shakwak Valley area. Past strain release in this area is equivalent to one or more magnitude-6 earthquakes or five or more magnitude-5 earthquakes per 10^4 km^2 per 100 years (Stevens and Milne, 1974, their Fig. 6).

Conclusions

Late Quaternary faulting is well displayed along parts of the Denali Fault System in Alaska in the form of laterally and vertically offset glacial features of Wisconsinan age. However, late Quaternary strike-slip displacements on the Denali Fault decrease southeast of the Totschunda Fault

junction and are not present in Yukon Territory. Richter and Matson (1971) have proposed that the fault system southeast of the Totschunda Fault has been nearly passive since early and middle Pleistocene time, and that, instead, stress has been released along the Totschunda Fault.

Although there has been no significant late Quaternary strike-slip movement on the Denali Fault System in Yukon Territory, there has been limited dip-slip movement. The evidence for this is northeast-facing scarps and aligned mounds of sand and gravel on the southwest side of Shakwak Valley between the Alaska-Yukon boundary and the south end of Kluane Lake. The scarps probably formed during late Wisconsinan time and during early and middle Holocene time. Faulting may have occurred, in part, during final deglaciation of southwest Yukon Territory 10 000 to 13 000 years ago.

Neither the Neoglacial beaches and wave-cut benches of Lake Alsek and Kluane Lake, nor surfaces of modern floodplains and alluvial fans are offset where crossed by the Shakwak and Dalton faults. It is thus concluded that there has been no significant faulting along this part of the Denali Fault System during the last several hundred years.

Lineaments on the Dalton Fault, in contrast to those on the Shakwak segment, lack significant topographic expression. Rather, they are recognized largely on the basis of vegetation and soil moisture patterns. No dip-slip or strike-slip displacements can be documented for these lineaments, and it is possible that they have formed by the differential glacial erosion of, and subsequent deposition of sediments over, sheared rocks of the Dalton Fault.

Irregular scarps and trenches occurring in the Kluane Ranges in the vicinity of the Dalton, Shakwak, and Duke River faults result from gravitational spreading and subsidence of mountain ridges during major earthquakes. Although these features cannot be dated, differing degrees of freshness suggest a range in age, the freshest probably having formed in the last few hundred years.

Although the Denali Fault System in Yukon Territory appears to have been active to only a minor extent during late Quaternary time, present-day seismicity in the region is high. At least two large earthquakes (M = 6.0 and 6.5) have occurred in the Shakwak Valley-Kluane Ranges area since 1899 when earthquake data collection began. Potentially high ground accelerations have been predicted from the past seismicity of the area. An improved seismograph network is required, however, in order to assess seismic risk more accurately and to decipher the relationship between the seismicity and the structural framework of the southwest Yukon.

Acknowledgments

This program is part of joint studies, partially funded by Foothills Pipe Lines South Yukon Ltd., concerning environmental aspects relating to pipeline concerns in Southern Yukon Territory. Logistical support for field operations generously was provided by R.B. Campbell of the Geological Survey of Canada. R.B. Campbell and C.J. Dodds (Geological Survey of Canada), R.B. Horner (Earth Physics Branch) and V.N. Rampton (Terrain Analysis and Mapping Services Ltd.) supplied information on the bedrock geology, seismicity, and surficial geology of the area, respectively. C.J. Dodds, R.J. Fulton, and V.N. Rampton reviewed the manuscript. Foothills Pipe Lines (Yukon) Ltd. permitted its consultant, V.N. Rampton, to accompany the author in the field to provide advice concerning the Quaternary geology of southwest Yukon Territory.

References

Bostock, H.S.
1948: Physiography of the Canadian Cordillera, with special reference to the area north of the fifty-fifth parallel; Geological Survey of Canada, Memoir 247, 106 p.

1952: Geology of northwest Shakwak Valley, Yukon Territory; Geological Survey of Canada, Memoir 267, 54 p.

1969: Kluane Lake, Yukon Territory, its drainage and allied problems (115G, and 115F E); Geological Survey of Canada, Paper 69-28, 19 p.

Boucher, G. and Fitch, T.J.
1969: Microearthquake seismicity of the Denali fault; Journal of Geophysical Research, v. 74, p. 6638-6648.

Campbell, R.B. and Dodds, C.J.
1975: Operation Saint Elias, Yukon Territory; in Report of Activities, Part A, Geological Survey of Canada, Paper 75-1A, p. 51-53.

1978: Operation Saint Elias, Yukon Territory; in Current Research, Part A, Geological Survey of Canada, Paper 78-1A, p. 35-41.

Campbell, R.B. and Eisbacher, G.H.
1974: Operation Saint Elias; in Report of Activities, Part A, Geological Survey of Canada, Paper 74-1A, p. 11-12.

Denton, G.H. and Stuiver, M.
1967: Late Pleistocene glacial stratigraphy and chronology, northeastern St. Elias Mountains, Yukon Territory, Canada; Geological Society of America Bulletin, v. 78, p. 485-510.

Eisbacher, G.H.
1976: Sedimentology of the Dezadeash flysch and its implications for strike-slip faulting along the Denali Fault, Yukon Territory and Alaska; Canadian Journal of Earth Sciences, v. 13, p. 1495-1513.

Gary, M., McAfee, R., Jr., and Wolf, C.L. (ed.)
1972: Glossary of Geology; American Geological Institute, Washington, D.C., 805 p.

Grantz, A.
1966: Strike-slip faults in Alaska; U.S. Geological Survey, Open-file, 82 p.

Hickman, R.G. and Craddock, C.
1973: Lateral offsets along the Denali fault, central Alaska Range, Alaska; in Abstracts with Programs, Geological Society of America, North-Central Section, 7th Annual Meeting, Columbia, Missouri, v. 5, p. 322.

Hickman, R.G., Craddock, C., and Sherwood, K.W.
1977: Structural geology of the Nenana River segment of the Denali fault system, central Alaska Range; Geological Society of Ameria Bulletin, v. 88, p. 1217-1230.

Hughes, O.L., Rampton, V.N., and Rutter, N.W.
1972: Quaternary geology and geomorphology, southern and central Yukon (northern Canada); 24th International Geological Congress (Montreal), Guidebook, Field Excursion A11, 59 p.

Kindle, E.D.
1952: Dezadeash map-area, Yukon Territory; Geological Survey of Canada, Memoir 268, 68 p.

Lanphere, M.A.
1978: Displacement history of the Denali fault system, Alaska and Canada; Canadian Journal of Earth Sciences, v. 15, p. 817-822.

Page, R.
1969: Late Cenozoic movement on the Fairweather fault in southeastern Alaska; Geological Society of America Bulletin, v. 80, p. 1873-1877.

Plafker, G., Hudson, T., Bruns, T., and Rubin, M.
1978: Late Quaternary offsets along the Fairweather fault and crustal plate interactions in southern Alaska; Canadian Journal of Earth Sciences, v. 15, p. 805-816.

Plafker, G., Hudson, T., and Richter, D.H.
1977: Preliminary observations on late Cenozoic displacements along the Totschunda and Denali fault systems; in The United States Geological Survey in Alaska: Accomplishments during 1976, ed. K.M. Blean, U.S. Geological Survey, Circular 751-B, p. B67-B69.

Radbruch-Hall, D.H., Varnes, D.J., and Savage, W.Z.
1976: Gravitational spreading of steep-sided ridges ("Sackung") in western United States; International Association of Engineering Geology Bulletin, no. 14, p. 23-35.

Rampton, V.N.
Surficial deposits and landforms of Kluane National Park; Geological Survey of Canada Paper. (in press)

Richter, D.H. and Jones, D.L.
1973: Structure and stratigraphy of eastern Alaska Range, Alaska; in Arctic Geology, ed. M.G. Pitcher, American Association of Petroleum Geologists, Memoir 19, p. 408-420.

Richter, D.H. and Matson, N.A., Jr.
1971: Quaternary faulting in the eastern Alaska Range; Geological Society of America Bulletin, v. 82, p. 1529-1539.

Souther, J.G. and Stanciu, C.
1975: Operation Saint Elias, Yukon Territory: Tertiary volcanic rocks; in Report of Activites, Part A, Geological Survey of Canada, Paper 75-1A, p. 63-70.

St. Amand, P.
1957: Geological and geophysical synthesis of the tectonics of portions of British Columbia, the Yukon Territory, and Alaska; Geological Society of America Bulletin, v. 68, p. 1343-1370.

Stevens, A.E. and Milne, W.G.
1974: A study of seismic risk near pipeline corridors in northwestern Canada and eastern Alaska; Canadian Journal of Earth Sciences, v. 11, p. 147-164.

Stout, J.H., Brady, J.B., Weber, F., and Page, R.A.
1973: Evidence for Quaternary movement on the McKinley strand of the Denali fault in the Delta River area, Alaska; Geological Society of America Bulletin, v. 84, p. 939-947.

Terrain Analysis and Mapping Services Ltd.
1978: Geology and limnology of Kluane Lake. I. Preliminary assessment; Geological Survey of Canada, Open File 527, 51 p.

Zischinsky, U.
1969: Über Sackungen; Rock Mechanics, v. 1, p. 30-52.

31. GEOLOGICAL STUDIES: TEBESJUAK LAKE MAP AREA, DISTRICT OF KEEWATIN

Project 780008

A.N. LeCheminant, M.B. Lambert, A.R. Miller, and G.W. Booth[1]
Regional and Economic Geology Division

LeCheminant, A.N., Lambert, M.B., Miller, A.R., and Booth, G.W., Geological studies: Tebesjuak Lake map area, District of Keewatin; in Current Research, Part A, Geol. Surv. Can., Paper 79-1A, p. 179-186, 1979.

Abstract

Continental sediments and volcanics of the Paleohelikian or Late Aphebian Dubawnt Group fill northeasterly trending basins in the Tebesjuak Lake (65 O) map area. Sedimentation commenced with the deposition of alluvial fan and fluvial deposits on an irregular basement of Archean and Aphebian granitoid gneisses. The overlying rocks of the Christopher Island Formation comprise about 65 per cent trachyte lavas and breccias, 15 per cent tuffs and 20 per cent volcaniclastic sediments. Five cycles of subaerial alkaline volcanism are represented within a fault bounded homoclinal succession 7300 m thick. Four of the five cycles began with explosive activity followed by effusions of mafic then felsic lavas. Intercalated volcaniclastic sediments are predominantly fluvial and shallow water turbidite deposits. Mass wasting or landslides formed local talus cones and sheets of laharic breccia. Small intrusions of biotite lamprophyre and syenite are probably cogenetic with the alkaline lavas.

Wedges of red alluvial fan sediments unconformably overlie lavas of the Christopher Island Formation and locally extend over basement gneisses. Volcanism resumed with eruptions of calc-alkaline lavas and welded ash flow tuffs of the Pitz Formation. Two plutons of micrographic granite and numerous quartz-feldspar porphyry dykes intrude basement gneisses and both the alkaline and calc-alkaline volcanics.

Introduction

The Tebesjuak Lake map area (65 O) contains basins of unmetamorphosed continental sediments and volcanics of the Paleohelikian or Late Aphebian Dubawnt Group. In the southeastern corner of the area thick successions of these rocks fill structural depressions separated by gneisses of Archean and Aphebian ages. Previous work in the region was limited to reconnaissance helicopter traverses during Operation Baker (Wright, 1955, 1967).

Two parts of the region were mapped in detail in July, 1978 to determine structural and stratigraphic relations prior to beginning 1:250 000 scale mapping in 1979. Figure 31.1 outlines the two areas studied and shows their geological setting. The Kunwak River area lies near the southwestern limit of a basin of Dubawnt Group rocks that extends northeastward to the eastern outlet of Baker Lake (Donaldson, 1965; Wright, 1967). The Nutarawit Lake area is at the northern end of a smaller basin, containing similar rocks, that extends to the southwest (Eade, 1976). This paper describes the stratigraphy of the volcanic and sedimentary rocks of the Dubawnt Group in these two areas and interprets the environments of deposition. High level intrusions of syenite and granite are genetically related to the Dubawnt Group volcanic successions.

Nutarawit Lake Area

The Nutarawit Lake area straddles the contact between basement gneisses and basal formations of the Dubawnt Group (Fig. 31.2). The basement consists of migmatitic granitoid gneisses intercalated with thinly layered, cataclastic leucocratic and mafic gneisses. Chlorite and epidote veining and alteration are widespread. Foliation trends are dominantly east to northeast. Northeast trending diabase dykes that intrude the gneiss complex commonly have sheared margins.

Rocks of the Dubawnt Group unconformably overlie, or are in fault contact with, the granitoid gneisses. The westerly dipping succession comprises basal units of conglomerate and arkose overlain conformably by mafic and felsic trachyte lavas, pyroclastics and intercalated volcaniclastic sediments.

Basal Sedimentary Sequence

The basal unit of the Dubawnt Group is a massive to poorly bedded polymictic conglomerate containing rounded to subrounded clasts (1-70 cm) of felsic gneiss and granodiorite set in a maroon to light maroon chloritic matrix. The conglomerate grades upwards into grey to light pink, medium grained arkose. The arkosic rocks contain both laminar and crossbedded fining-upwards cycles. A continuous succession of conglomerate and arkose (section A-A[1], Fig. 31.2) is made up in part of overlapping clastic wedges so that the true stratigraphic thickness may be less than the apparent 1500 m. The succession probably represents alluvial fan and fluvial deposits.

Rocks of the arkosic unit are intensely altered in the upper 80-100 m of the succession and also where they are in fault contact with basement gneisses. Silicification and sericitization has altered them to well indurated greenish white rocks resembling orthoquartzites. Quartz stockwork veins are spacially associated with the alteration.

The conglomerate-arkose sequence is correlated with the South Channel and Kazan formations in the Baker Lake area (Donaldson, 1965) on the basis of lithology and stratigraphic position.

Christopher Island Formation

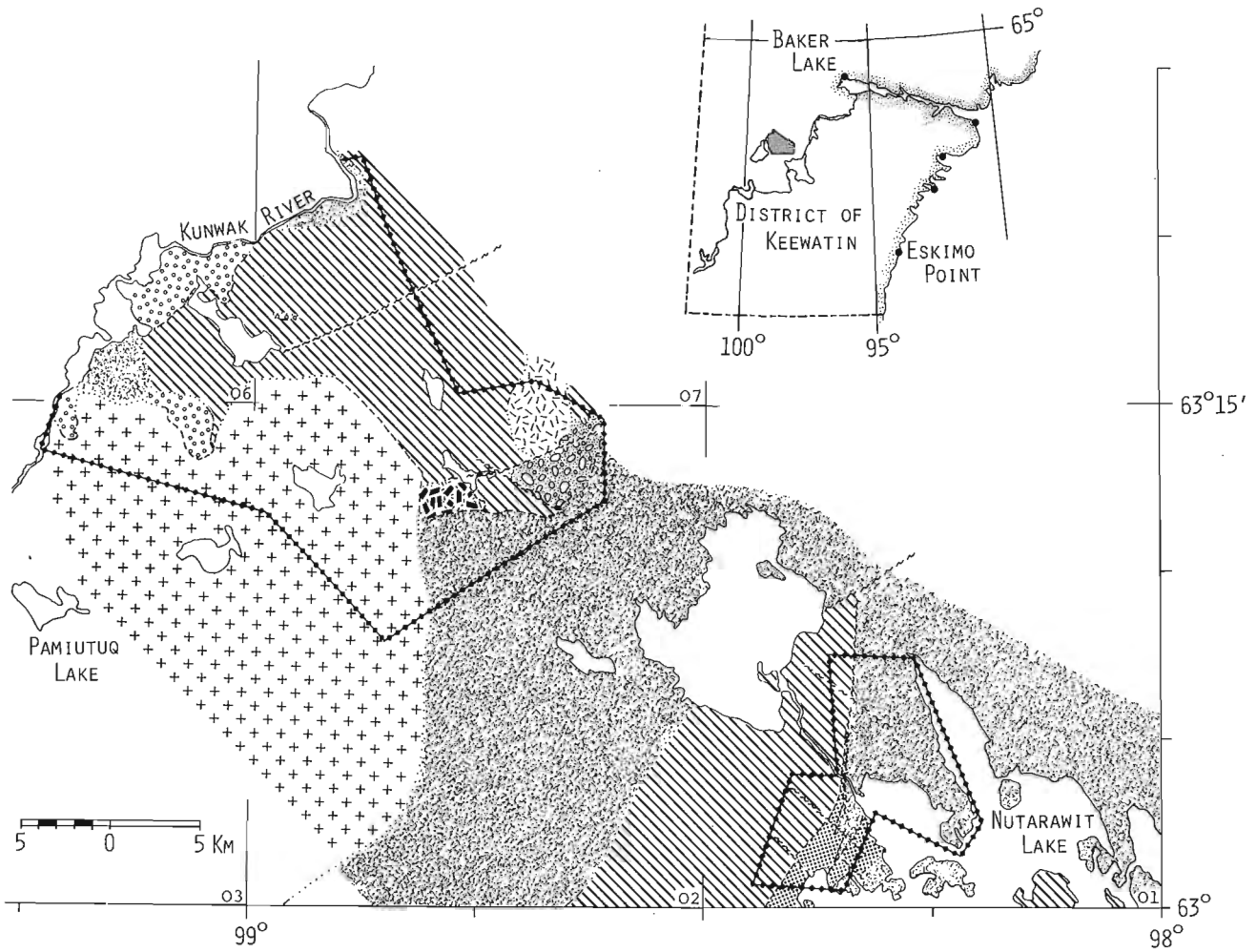
Lavas, pyroclastics and volcaniclastic sediments of the Christopher Island Formation conformably overlie the basal clastic succession. The volcanic rocks are similar to those described by Blake (in press) who concluded from petrographic and chemical studies that compositions lie mainly within the trachybasalt-trachyandesite-trachyte fields. Lavas were classified in the field as either mafic or felsic trachytes. The western limit of the Nutarawit Lake area does not extend to the top of the Christopher Island Formation but the total succession mapped exceeds 2300 m. The main lithologies are mafic trachyte lavas and breccias (45%), felsic trachyte lavas and lithic welded tuffs (15%), and volcaniclastic sediments (40%).

[1]University of Toronto, Toronto, Ontario

Mafic trachyte lavas are dark maroon to red brown and contain phenocrysts of phlogopite (biotite) with subordinate clinopyroxene and feldspar. Felsic trachyte lavas are maroon-grey to grey and contain abundant feldspar and scattered biotite phenocrysts. Felsic welded tuffs are interbedded with mafic trachyte lavas and volcaniclastic sediments in the north part of the area. The tuffs are polylithic and contain (1) angular to subrounded ash and lapilli of biotite mafic trachyte and felsic trachyte, (2) rounded clasts of granitoid gneiss, and (3) subhedral and broken crystals set in a microcrystalline felsic matrix.

Volcaniclastic sediments vary from conglomerates and wackes to fine grained red sandstones and siltstones. The coarser sediments are poorly sorted with crystal and lithic fragments derived mainly from trachyte lavas. Clasts of granitoid gneiss and quartz are present throughout the succession.

Propylitic alteration (epidote, chlorite and calcite) is ubiquitous throughout lavas and sediments of the Christopher Island Formation. Tremolite/actinolite needles are locally present. Rocks of the Christopher Island Formation adjacent to the eastern boundary fault are intensely chloritized and locally schistose. No significant alteration is associated with northwest trending faults that displace both the basal sedimentary sequence and the Christopher Island Formation.



PALEOHELIKIAN OR LATE APHEBIAN

DUBAWNT GROUP

PITZ FORMATION: RHYOLITE LAVAS AND WELDED TUFFS; MINOR RHYOLITE-COBBLE CONGLOMERATE

FANGLOMERATES, RED SANDSTONE AND CONGLOMERATE

CHRISTOPHER ISLAND FORMATION: LAVAS, PYROCLASTICS AND VOLCANICLASTIC SEDIMENTS

CONGLOMERATE, PEBBLY ARKOSE AND ARKOSE

APHEBIAN AND ARCHEAN

GRANITOID GNEISS; MINOR PARAGNEISS AND AMPHIBOLITE

PAMIUTUQ GRANITE: PORPHYRITIC, MICROGRAPHIC

GRANITE: MIAROLITIC, FLUORITE-BEARING

SYENITE AND PORPHYRITIC MICROSYENITE

Figure 31.1. *Simplified geological map of the southeast corner of the Tebesjuak Lake (65 O) map area. The Nutarawit and Kunwak River areas, shown in Figures 31.2 and 31.3, are outlined.*

Intrusive Rocks

Biotite lamprophyres and two types of syenite intrude the basement complex and the Dubawnt Group. Narrow lamprophyre dykes and sills, similar in mineralogy and composition to the mafic trachyte lavas, are most abundant in the conglomerate-arkose sequence.

Mafic fine- to medium-grained biotite and/or hornblende syenite, similar to the Martell Syenite south of Baker Lake (Donaldson, 1965; Blake, in press), occur throughout the Nutarawit Lake area. Leucocratic bostonitic syenite, characterized by a pink to cherry red colour and anomalous radiometric response, forms a northwesterly trending swarm of dykes and small irregular intrusions. This latter type of syenite is discussed further by Miller (1979).

Kunwak River Area

The Christopher Island Formation is the oldest unit of the Dubawnt Group in the Kunwak River area. Lavas, tuffs and sediments of this formation comprise thick homoclinal successions which lie unconformably on or are faulted against basement gneisses in the southeastern and northwestern parts of the area (Fig. 31.1 and 31.3). Wedges of red volcaniclastic sediments, and lavas and tuffs of the Pitz Formation overlie the Christopher Island Formation. All units are intruded by granitic plutons.

The basement complex consists of irregularly layered pink to white leucocratic orthogneiss and minor layered cummingtonite-biotite-plagioclase-quartz gneiss, hornblende-biotite gneiss and amphibolite. The basement rocks are

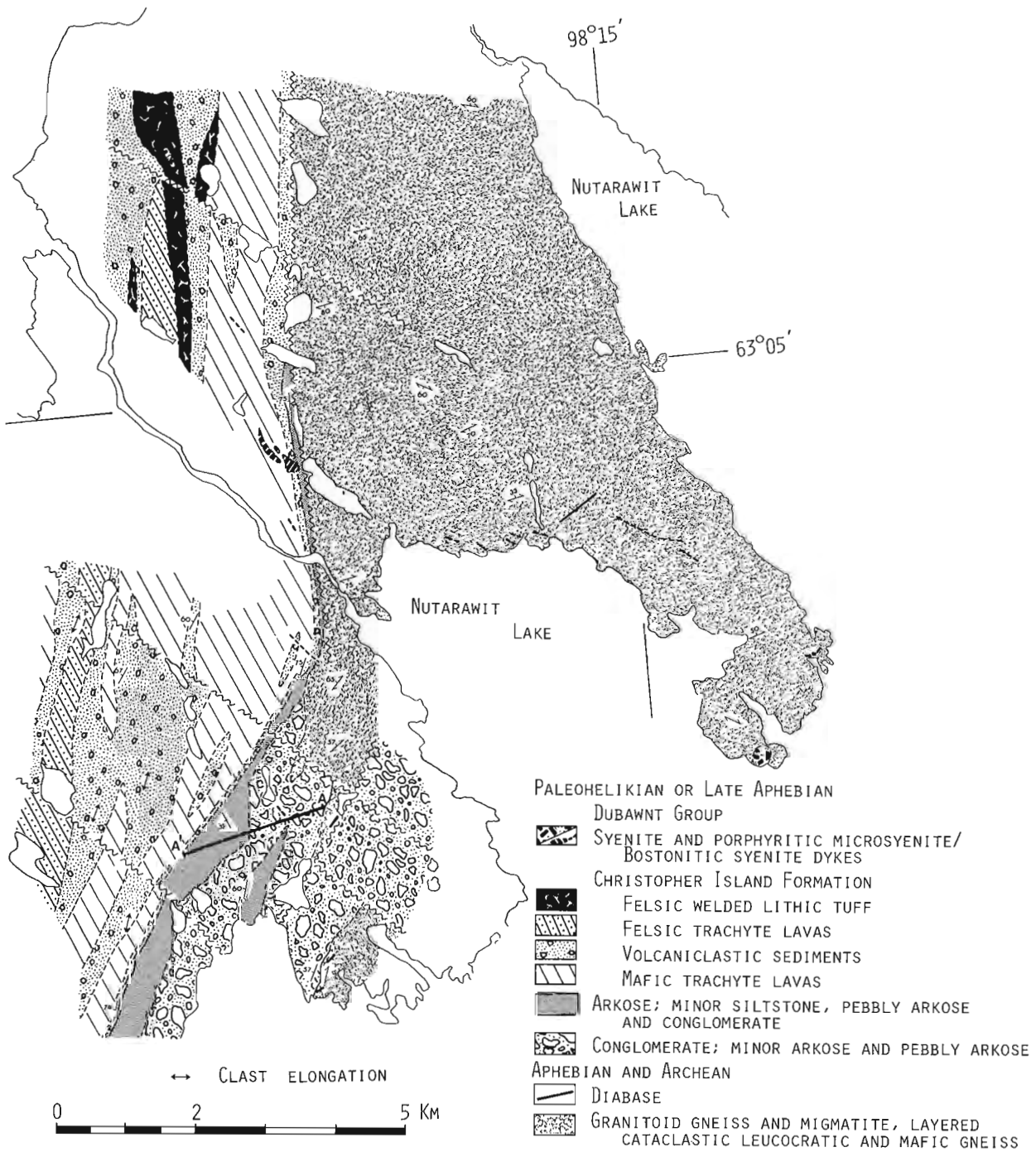


Figure 31.2. *Geology of the Nutarawit Lake area.*

(1) overlain unconformably by all formations of the Dubawnt Group mapped in the area; (2) faulted against Dubawnt Group rocks; or (3) intruded by granitic and syenitic plutons. Clasts of basement rocks are common within all sedimentary sequences and are locally present as accidental fragments in tuffs and lavas throughout the Dubawnt Group.

Christopher Island Formation

The Christopher Island Formation in the Kunwak River area comprises about 65 per cent trachyte lavas and breccias, 15 per cent tuffs and 20 per cent volcaniclastic wackes and epiclastic breccias. Major 060° and 120° trending faults divide the volcanic terrane into a central block, a western block and a small wedge in the southeastern corner of the area mapped (Fig. 31.3). The three fault blocks contain homoclinal successions, each with different attitudes. Although beds within the blocks have been rotated, the present dips over most of the area are shallow (20-40°) and no folds are present. The central block contains a southeasterly dipping succession 7300 m thick whereas the western block contains at least 4300 m dipping north-northeasterly and the eastern wedge contains about 4100 m dipping easterly. Although the stratigraphic position of the units in one fault block relative to the others is not known, the total thickness is probably greater than 10 000 m.

Stratigraphy within the central and western fault blocks is detailed in columnar sections B-B^1 and C-C^1 (Fig. 31.4). Within the central fault block, five volcanic cycles (numbered I to V in Fig. 31.4) are separated by pyroclastic and epiclastic deposits 250 to 500 m thick. In all cycles except I, the lower lavas are dominantly phlogopite- or pyroxene-phyric mafic trachyte, whereas the uppermost flows are either felsic trachytes, or mafic trachytes in which feldspar is a phenocryst phase.

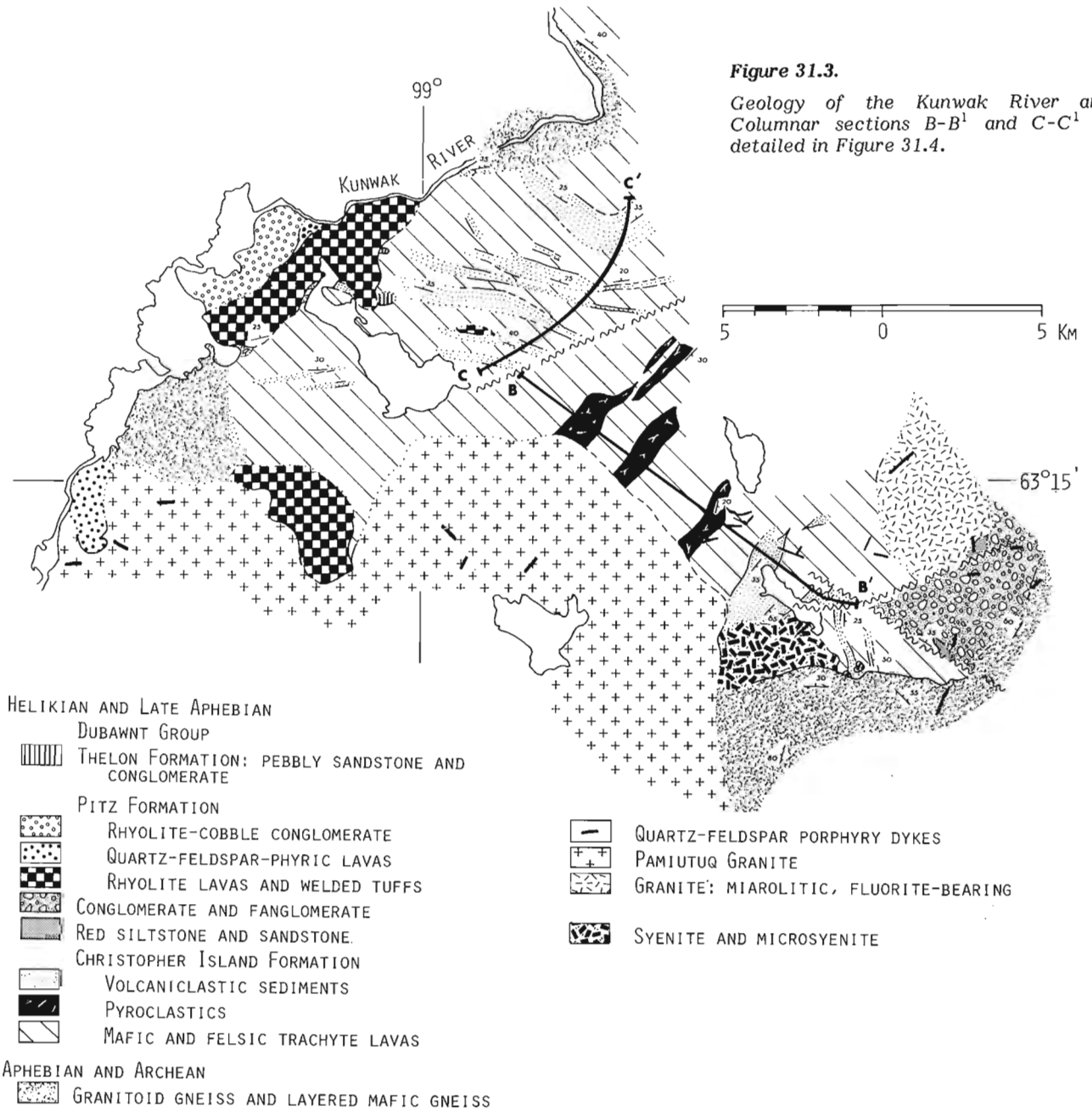


Figure 31.3.

Geology of the Kunwak River area. Columnar sections B-B^1 and C-C^1 are detailed in Figure 31.4.

Mafic and Felsic Trachyte Lavas Mafic trachyte lavas form 75 per cent of the volcanic succession. Individual flow units range from 10 m to possibly 250 m thick. Within a series of lavas, boundaries of flow units are indicated by (1) interflow units of volcaniclastic sediments or pyroclastics; (2) local wedges of coarse epiclastic breccias and sheets of laharic breccia; (3) brecciated and amygdaloidal flow tops; (4) upper and lower zones of flow breccia that grade inward into massive lava; and (5) abrupt changes in lithology, commonly shown by changes in phenocryst populations and weathering colour of the matrix. Although most flows are massive, autobrecciation is common at their margins, and in some places an entire flow unit is brecciated. No pillowed lavas or hyaloclastic breccias were recognized.

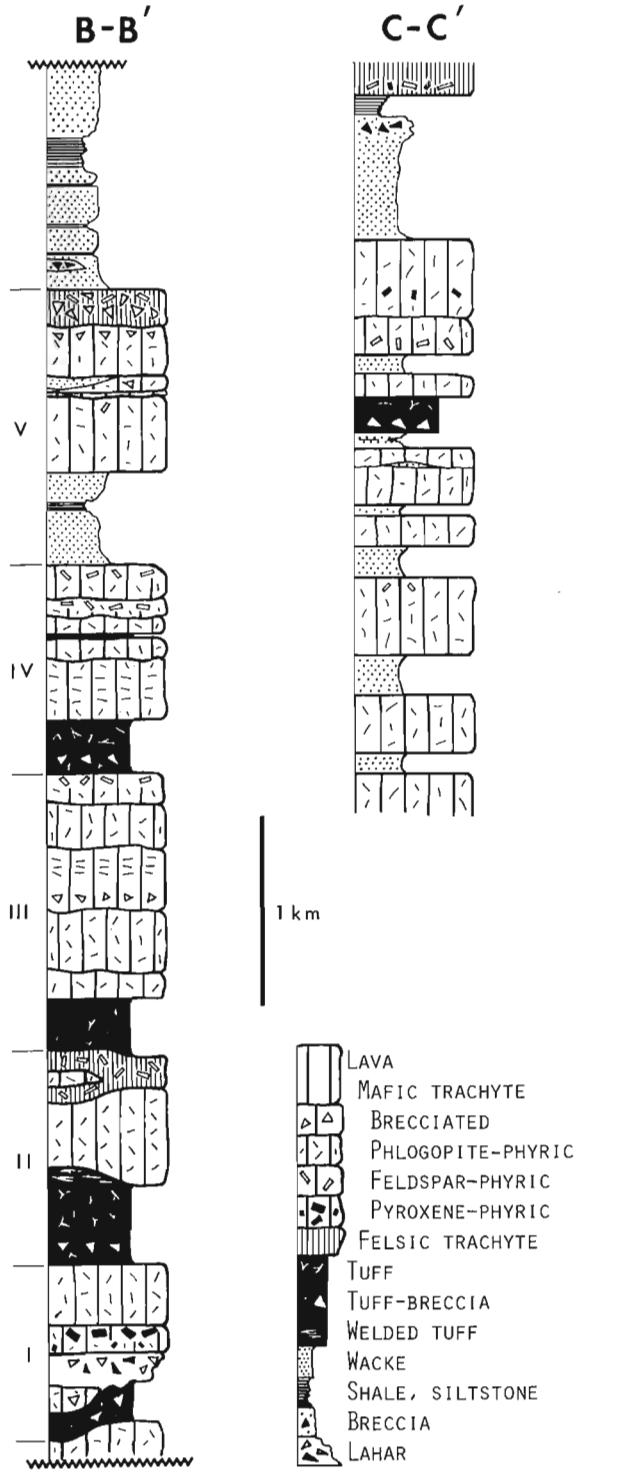


Figure 31.4. Composite columnar sections through parts of the Christopher Island Formation in the Kunwak River area.

The lithology of the mafic trachyte lavas is remarkably similar throughout the area. They weather maroon, maroon-grey, dark grey, greenish grey and, occasionally, buff. Virtually all lavas are porphyritic containing phenocrysts averaging 2-5 mm and ranging up to 10 mm across. Phlogopite is ubiquitous and generally is the most abundant phenocryst. It makes up 5-20 per cent of the rocks and has random orientation, except in several flows near the centre of section B-B^1 where it has a strong preferred orientation parallel to the margins of the flows. Phenocrysts of dull, dark grey to green clinopyroxene make up 1-10 per cent of many lavas. One flow, near the bottom of section B-B^1, however, contains 35 per cent cumulate clinopyroxene crystals in its lower part, whereas its upper part is sparsely porphyritic. Plagioclase and alkali feldspars form 1-10 per cent of the phenocrysts in some flows. In thin section, the aphanitic matrix of these flows is a mat of stubby potassic feldspar microlites, 0.05-0.15 mm, and microphenocrysts averaging 0.3 mm. In some flows thin tabular feldspar microlites display a strong trachytic orientation. Amygdules, having smooth rounded outlines, but also irregular, angular boundaries, are filled by calcite, chlorite, sericite and epidote.

Felsic trachytes comprise 15-25 per cent potassic feldspar and sodic plagioclase phenocrysts, 5 to 10 mm across and 1-2 per cent phlogopite. The phenocrysts have random orientation in a pink to pale maroon, aphanitic matrix. Felsic trachytes form two units in section B-B^1 that range from 150 to 200 m thick. The lower unit is massive, whereas the upper unit is a 200 m thick flow breccia. This monomictic breccia contains tightly packed, angular to subangular blocks of trachyte in a fine matrix of crushed trachyte fragments and aphanitic material that contains chlorite and epidote alteration.

Laharic Breccias At the eastern end of the central fault block, a cliff section exposes about 40 m of flows and volcanic breccias that underlie a 4 km^2 plateau. The lower half of this section comprises mafic and felsic flows and flow breccia, whereas the upper parts are polymictic breccias. The breccias contain a mixture of mafic and felsic trachyte fragments that weather various shades of dark green, maroon, maroon-grey, pink and buff. Fragments, ranging from 5-30 cm, are dominantly angular to subangular, but some are rounded. The matrix is a coarse grit of the same composition as the fragments. Fragments and matrix are mixed together in unsorted massive units with no hint of internal layering. The lithological and structural characteristics of these breccias and their distribution suggest that they are mass flow deposits, probably lahars, that "sloughed off" of the volcanic pile.

Pyroclastic Rocks Pyroclastic rocks, including lithic and crystal tuffs, welded tuffs, tuff-breccias and breccias, comprise about 20 per cent of the volcanic succession. Moreover, some of the sedimentary units contain significant amounts of pyroclastic material. Three major pyroclastic units, ranging from 270 to 500 m thick, mark the boundaries between eruptive cycles I to IV in section B-B^1. Individual units pinch and swell abruptly (Fig. 31.3). The main tuff successions are dominantly lithic tuffs or crystal-lithic tuffs, whereas thin pyroclastic units within the lava successions tend to be crystal tuffs.

Pyroclastic rocks at the base of cycle II form a 500 m thick unit that pinches out abruptly to the northeast; then, two thinner units appear to the east at almost the same stratigraphic horizon (Fig. 31.3). These units contain a variety

of lithic, lithic-crystal (phlogopite-phyric) tuffs, lapilli-tuffs and tuff-breccias that weather maroon, grey and greenish grey and welded crystal-vitric tuffs that alter orange-brown. Nonwelded tuffs and tuff breccias of the thick unit are massive, poorly sorted rocks in which maroon weathering angular lapilli of mafic trachyte, generally less than 3 cm (but some are up to 10 cm), are part of a completely unsorted crystal-vitric-lithic tuff matrix. Tuffs of the two thinner units are massive to crudely bedded and poorly sorted, except for the upper 28 m which are well bedded and contain an 8 m thick unit of moderately welded tuff. The welded unit is an altered crystal-vitric tuff that has a eutaxitic foliation parallel to bedding. Such welded tuffs are rare amongst pyroclastics of the Christopher Island Formation.

The tuff unit at the base of cycle III is a massive, maroon weathering lithic lapilli-tuff carrying angular volcanic rock fragments, from 4 to 20 mm, in a matrix of buff to grey, fine tuff. Rare clasts of cataclastic granitic material are present. Most of the massive, unsorted tuffs at the base of cycles II and III are believed to be nonwelded ash flow deposits.

The pyroclastic unit at the base of cycle IV constitutes about 150 m of massive, crystal-lithic tuff breccia overlain by 100 m of thin bedded tuffs. The tuff breccias carry dominantly angular, maroon weathering clasts of mafic trachyte to 4 cm, and crystals of phlogopite (biotite) in a dark grey clastic matrix. The matrix contains (1) angular to subrounded lithic fragments of mafic trachyte, microcrystalline matrix from trachyte lavas, microsyenite, and rarely, cataclastic granitic material from basement terrane; (2) crystal fragments of biotite, phlogopite, potassic feldspar, and pyroxene; and (3) altered relicts of shards. The overlying bedded units are dark grey, fine and coarse tuffs that typically have diffuse boundaries. Although the originally glassy shards in these tuffs are completely replaced by sericite, chlorite, calcite and pale brownish phyllosilicate, they are recognized by their irregular, ragged and cuspidate margins.

In one locality, in the eastern wedge of Christopher Island rocks, a massive, coarse tuff breccia is associated with a 3 m thick crystal tuff unit. The crystal tuff contains white potassic feldspar and phlogopite phenocrysts and brick-red weathering shards in an aphanitic matrix. The unit shows rhythmic normal and reverse graded bedding of feldspar crystals, which are crudely aligned parallel to bedding. This feldspar-rich tuff is probably a crystal accumulation of air-fall origin that is genetically related to the felsic trachytes.

Sedimentary Rocks Volcaniclastic sediments make up about 25 per cent of the volcanic-sedimentary succession. The thickest deposits, 500-1100 m thick, occur near the top of sections B-B^1 and C-C^1. The sediments are predominantly maroon to grey weathering, immature wackes that form medium to thick beds. Beds, that generally range from 5-20 cm, commonly up to 50 cm and, rarely, to 200 cm, have straight, parallel sides, show graded bedding and lack cross-bedding. Wackes commonly have boulders and blocks of trachyte, to 15 cm, suspended near the base of massive beds. The wackes at the bottom of cycle V contain volcanic conglomerate beds 30-40 cm thick. Wackes are immature, poorly sorted volcanic clastic arenites comprising angular to subangular crystal and lithic fragments derived mainly from trachyte lavas and tuffs. Lithic fragments include mafic and felsic trachyte and altered devitrified glass. Crystal fragments include phlogopite, biotite, clinopyroxene and feldspar that lie in planes parallel to bedding. Some wackes, or possibly tuffaceous wackes, are essentially concentrations of crystals and contain up to 35 per cent clinopyroxene and 15 per cent phlogopite. Such units may be derived from pyroxene-rich, mafic trachyte lavas or may be reworked mafic crystal tuffs.

Argillite and siltstone occur as local thick units near the top of section B-B^1. In general, however, red siltstone and shale occur as thin beds or rip-up clasts within coarse wacke successions. Thin shale beds are commonly fragmented and the chips are rotated and displaced within enclosing massive wacke units. Some shale beds contain mudcracks and concave upward mud chips. Siltstones are more common in sediments in the northwestern fault block than in the central block.

Sediments that form lenses and continuous layers within the volcanic succession are dominantly volcanic clastic wackes, but contain minor maroon siltstone and shale beds and local thick pods of very coarse breccia.

Near the top of section B-B^1 a very coarse sedimentary breccia forms a wedge within wackes. The unit, which is completely unsorted and unbedded, contains 75 per cent cobbles and boulders of mafic and felsic trachyte, and maroon wacke, to 80 cm, in a coarse grit matrix. This fragment supported breccia may represent a landslide or talus cone.

A very coarse breccia that occurs within the wacke sequence near the top of section C-C^1 comprises angular to subrounded blocks of maroon to grey mafic and felsic trachyte, as well as maroon siltstone ranging to 50 cm in a coarse grit or crystal-lithic wacke matrix. Layering in matrix grit and siltstone deforms around and moulds between blocks of the breccia to give the impression that this deposit was "dumped" in soft sandy and silty sediments. This unit is interpreted as a mass flow deposit possibly of landslide origin.

Environments of Deposition A subaerial environment for the Christopher Island Formation volcanism is suggested by the massive nature of the lavas with their autobrecciated margins and the absence of pillowed flows or hyaloclastic breccias. Although most of the pyroclastic rocks are welded and nonwelded ash flow tuffs and rare air fall tuffs, some of the bedded tuffs may be water-laid. Five cycles of volcanism are present in the central fault block. Cycles I to IV began with explosive activity which produced dominantly lithic tuffs, both of ash flow and air fall origin. Abundance of lithic fragments and the position of the thick tuff deposits at the base of each cycle suggests that they represent vent clearing explosions that were the precursor to each major effusion of lava.

No eruptive centres were recognized in the Kunwak River area. The successions may represent the flanks of a large stratovolcano complex. The tremendous stratigraphic thicknesses portrayed in Figure 31.4 probably never were vertically stacked sequences. The successions are interpreted as overlapping series of units, derived from several eruptive centres, which have since been tilted to give the impression of thick stratigraphic piles.

In view of the environmental constraints suggested by the volcanic rocks, the sediments, which are predominantly thick bedded, massive wackes, are interpreted as proximal facies of turbidites deposited in shallow water flanking the volcanic edifice. Desiccation cracks, lenses of conglomerate and wedges of volcanic landslide or talus breccia, within some of the wacke units, suggests fluvial or very shallow water deposition of material derived from the immediately adjacent volcanic pile.

Red Volcaniclastic Successions

Red, poorly sorted, immature volcaniclastic sediments unconformably overlie the Christopher Island Formation. A triangular area near the eastern limit of mapping contains a heterogeneous assortment of fanglomerates, sandstones and conglomerates (Fig. 31.3). A 100 m succession of laminated to thin bedded mudstone, siltstone and sandstone with rare pebble beds unconformably overlies altered (weathered?) biotite-feldspar trachyte lava of the Christopher Island

Formation. The sediments range from reddish brown to reddish grey with cream to white reduction spots. Minor structures include well developed lamination, load features, scour-and-fill structures and graded bedding. Mudcracks indicate intermittent subaerial exposure. Limited data from trough crossbeds suggest sediment transport from southwest to northeast.

The fine grained sediments are overlain by dark grey to reddish brown polymictic conglomerates containing subrounded clasts of mafic trachyte, syenite, granitoid gneiss and quartz. Mean clast size is 5-10 cm with rare boulders to 60 cm. Within the triangular area the proportion of basement clasts increases from less than 50 per cent near the southwestern boundary to more than 95 per cent near the eastern and northeastern limits. On the eastern side the conglomerate rests directly on a dark chlorite-epidote-rich regolith developed on granitoid gneiss.

At the western apex of the triangular area mudflow deposits and fanglomerates are exposed northeast of a fault trending 120°. Angular to subangular clasts of trachyte, volcaniclastic sediments, and rare quartz and granitoid gneiss are randomly oriented in a heterogeneous muddy matrix. The clasts become less angular and the proportion of matrix abruptly decreases with distance away from the fault trace.

Near the western limit of mapping a 15-20 m section of well indurated, poorly bedded red conglomerate and sandstone is exposed along the Kunwak River. Rounded to subrounded clasts of mafic trachyte with minor quartz and gneissic granite are set in a sandy matrix. The section is conformably overlain by welded tuffs of the Pitz Formation.

The red clastic successions are interpreted as wedges of alluvial fan sediments consisting of interbedded mudflow and stream-channel deposits. The successions have the same stratigraphic position as the Kunwak Formation (LeCheminant and Leatherbarrow, in prep.) and the stream channel deposits have similar lithologies.

Pitz Formation

The Pitz Formation in the Kunwak River area comprises flow-banded rhyolite, welded lithic-crystal tuff, quartz-feldspar-phyric rhyolite and rhyolite-cobble conglomerate. Greyish red to deep red-brown sparsely porphyritic flow-banded rhyolite lavas and welded crystal-lithic tuffs unconformably overlie the Christopher Island Formation. The flows are exposed in 10-40 m sections capping low hills east of the Kunwak River. Flow-banded rhyolites typically contain 1-5 per cent quartz phenocrysts (1-2 mm) and 5-10 per cent potassic feldspar phenocrysts (1-4 mm) set in a flow-banded aphanitic matrix. Deep purple fluorite is a common accessory mineral. The lavas are closely associated with moderately to densely welded crystal-lithic lapilli tuffs. The tuffs are weakly to strongly eutaxitic and some have columnar jointing. Collapsed pumice fragments, clasts of gneissic granite and rhyolite, and euhedral and broken crystals of alkali feldspar and quartz are set in a red-brown matrix of welded and devitrified shards. Mauve and purple rhyolites rich in quartz and feldspar phenocrysts, that are similar to lavas of the Pitz Formation in the type locality (Donaldson, 1965), are exposed in only a few outcrops in the Kunwak River area.

The lavas are overlain by poorly sorted, unbedded conglomerates containing abundant subangular to subround clasts of both quartz-feldspar-phyric and flow-banded rhyolite set in a quartz-rich sand or grit matrix. Fluorite is a common accessory in both clasts and matrix. The clast population changes drastically in the southwestern outcrops of the unit. Basement clasts of white gneissic granite appear as a constituent and become the predominant lithology over a distance of less than 100 m.

Thelon Formation

Poorly bedded quartz-rich grit and conglomerate overlie Christopher Island Formation trachytes and flank hills of Pitz Formation flow-banded rhyolite south of the Kunwak River. The sediments contain clasts of trachyte, rhyolite, quartz, red sandstone and grey recessive weathering carbonate. The source for the latter two lithologies is unknown. The beds are tentatively correlated with the Thelon Formation (Donaldson, 1965).

Intrusive Rocks

Stocks of fine- to coarse-grained leucocratic red syenite occur along the contact between the Christopher Island Formation and basement in the southern part of the area. Coarse grained syenite in the central parts of the intrusions comprise up to 80 per cent perthitic potassic feldspar laths to 3 cm, with plagioclase and minor quartz, chloritized biotite and epidote. The fine grained margins of the intrusions and associated 1-4 m wide microsyenite dykes are anomalously radioactive (Miller, 1979). The syenites and microsyenite intrude basement gneisses and mafic trachytes and volcaniclastic sediments of the Christopher Island Formation. Rare biotite-clinopyroxene lamprophyre dykes cut the microsyenites.

A pluton of miarolitic fluorite-bearing granite intrudes both the Christopher Island Formation and the overlying red clastic succession in the northeast part of the Kunwak River area. This massive, medium grained, red granite is porphyritic with feldspar phenocrysts set in a micrographic groundmass containing 1% evenly distributed biotite grains. Miarolitic cavities to 1 cm are filled or lined with fluorite, quartz, fluoromica(?), chlorite and sulphides. A zone of biotite hornfels less than 1 m wide is developed in laminated siltstone of the red clastic succession along the southeastern contact of the pluton.

The Pamiutuq Granite, named after a small lake within the intrusion, underlies almost 700 km^2 in 65 O/2 and 65 O/3 (Fig. 31.1) and extends south into 65 J (Eade, 1976). The northern and northeastern contacts of the body were mapped in 1978. The granite intrudes basement gneisses, Christopher Island Formation volcanics and sediments, and Pitz Formation flow-banded rhyolites. With the exception of a coarsely porphyritic chill margin ranging from tens to several hundreds of metres thick, the intrusion is remarkably homogeneous. The pink porphyritic granite contains phenocrysts of potassic feldspar, sodic plagioclase and quartz set in a fine grained micrographic groundmass. Round quartz phenocrysts have a characteristic thin black rim of intergrown chlorite and pale green amphibole. Green amphibole and chloritized biotite are the main mafic minerals. The colour index of the intrusion rarely exceeds 5. Scattered sodic plagioclase megacrysts, minor concentrations of gneissic xenoliths and a discontinuous red banding account for most of the limited internal variation in the body.

Quartz-feldspar porphyry dykes intrude all units except the Thelon Formation in the Kunwak River area. These 10-45 m wide dykes are irregular in shape and trend (Fig. 31.3). The dyke rocks are coarsely porphyritic containing up to 40 per cent spectacular ovoid alkali feldspar phenocrysts to 3 cm and round quartz eyes. The dark reddish grey matrix ranges from aphanitic in chill margins to fine grained in the centre of dykes.

Quartz-feldspar-phyric lavas of the Pitz Formation, the Pamiutuq Granite and the quartz-feldspar porphyry dykes are spatially related and are strikingly similar in both texture and mineralogy of phenocrysts. The rocks are probably comagmatic and represent successive extrusive and high-level intrusive events related to a single period of acid magmatism.

Summary and Comments

The Dubawnt Group sequences mapped in the Nutarawit Lake and Kunwak River areas record a complex history of Paleohelikian or Late Aphebian continental sedimentation and volcanism. In the Nutarawit Lake area alluvial fan and fluvial sediments were deposited on an irregular basement of Archean and Aphebian gneisses. The clastic succession is conformably overlain by alkaline volcanics and volcaniclastic sediments of the Christopher Island Formation. In the Kunwak River area the basal clastic succession is missing and the alkaline volcanics and volcaniclastic sediments unconformably overlie basement gneisses. Three fault blocks contain homoclinal successions of trachyte lavas, tuffs, laharic breccias and volcaniclastic sediments up to 7300 m thick. The lavas and tuffs were erupted for the most part in a subaerial environment. Cycles of volcanism began with vent clearing explosions followed by voluminous effusions of mafic then felsic alkaline lavas. The pattern possibly reflects differentiation in the magma chamber during eruptive cycles. Mass wasting or landslides within or from the volcanic edifice formed local talus cones and sheets of laharic breccia. Thick bedded wackes were deposited by turbidity currents in shallow water flanking the volcanic edifice. Small stocks, sills and dykes of syenite are probably cogenetic with the alkaline lavas.

Red clastic successions unconformably overlie weathered lavas of the Christopher Island Formation and locally extend over the basement outside the fault blocks. The successions are interpreted as wedges of alluvial fan sediments consisting of interbedded mudflow and stream channel deposits.

Rhyolite flows of the Pitz Formation indicate a major change from alkaline to calc-alkaline volcanism. The lavas of the Pitz Formation are probably comagmatic with the Pamiutuq Granite and late quartz-feldspar porphyry dykes. Plutons of fluorite-bearing porphyritic Nueltin Granite (Wright, 1967) possibly correlate with the calc-alkaline lavas and intrusions.

References

Blake, D.H.
Volcanic rocks of the Paleohelikian Dubawnt Group in the Baker Lake-Angikuni Lake areas, District of Keewatin, N.W.T.; Geological Survey of Canada, Bulletin 309. (in press)

Donaldson, J.A.
1965: The Dubawnt Group, Districts of Keewatin and Mackenzie; Geological Survey of Canada, Paper 64-20.

Eade, K.E.
1976: Geology of the Tulemalu Lake map-area (65J), District of Keewatin; in Report of Activities, Part A, Geological Survey of Canada, Paper 76-1A, p. 379-381.

Miller, A.R.
1979: Uranium Geology in the Central Baker Lake Basin; in Current Research, Part A, Geological Survey of Canada, Paper 79-1A, report 12.

Wright, G.M.
1955: Geological notes on central District of Keewatin; Geological Survey of Canada, Paper 55-17.

1967: Geology of the southeastern barren grounds, parts of the Districts of Mackenzie and Keewatin (Operation Keewatin, Baker, Thelon); Geological Survey of Canada, Memoir 350.

32. INVESTIGATION OF BASE METAL MINERALIZATION IN PROTEROZOIC METASEDIMENTS, MELVILLE PENINSULA, DISTRICT OF FRANKLIN

Project 750051

E.M. Cameron
Resource Geophysics and Geochemistry Division

Cameron, E.M., Investigation of base metal mineralization in Proterozoic metasediments, Melville Peninsula, District of Franklin; in Current Research, Part A, Geol. Surv. Can., Paper 79-1A, p. 187-196, 1979.

Abstract

In 1977 a National Geochemical Reconnaissance survey that consisted of sampling lake sediments and waters was carried out over the southern part of Melville Peninsula, District of Franklin. Among the more interesting features of the data were extensive, strong and coincident Zn and Ni anomalies. These are principally associated with paragneiss of the lower Proterozoic Penrhyn Group and occur throughout the outcrop area of this group.

A brief study of a number of the anomalous areas was made in August, 1978. This relied principally on sampling of surface waters, which were then analyzed in a field laboratory, to identify, more precisely, mineralized ground.

This work has shown that there is widespread Zn- and Ni-bearing mineralization in sulphidic, and often graphitic, paragneiss and schist. These metals are present as sphalerite and pentlandite. Lesser amounts of Cu also occur and Pb, Ag and Au were found locally. Recent oxidation of the base metal sulphides has been intense and has removed all but traces of these minerals from the surface. This makes evaluation of the mineralization difficult, but no bodies of obvious economic interest were seen in the limited area examined.

The extent of the anomalies suggests that there was a major influx of base metals into this Proterozoic basin, which forms part of the Foxe Fold Belt. The rocks of the belt on Melville Peninsula and Baffin Island appear to have been deposited in an intracratonic rift. Intracratonic rift basins were the locus for important sediment-hosted base metal mineralization during the Proterozoic. There is some evidence to suggest that Zn, where present in such basins, has the most extensive primary distribution of any of the base metals. The identification of Zn-rich strata may, therefore, provide the key for more detailed exploration for base metal targets within the Foxe Fold Belt.

Introduction

In 1977 a National Geochemical Reconnaissance lake sediment and water survey was carried out in 30 000 km^2 of Melville Peninsula (Geological Survey of Canada, 1978a, 1978b). This region (Fig. 32.1) is underlain by Archean rocks, mainly granites and granitic gneisses, and by lower Proterozoic (Aphebian) metasediments, the Penrhyn Group.

Collectively, the Melville Peninsula lake sediments contain high levels of a number of elements, compared to sample sets previously collected from other large regions of the Shield. This may be illustrated by comparing median and 95 percentile data for this region with similar data for the Nonacho Belt (Hornbrook et al., 1976a, 1976b, 1976c). The latter region, bounded by latitudes 60° and 63° and by longitudes 108° and 110°, has a broadly similar geological setting of an Aphebian metasedimentary belt enclosed within Archean granitic rocks. The comparison (Table 32.1) shows that, at the median level, Mn, Fe, Co, Ni, Cu, Zn, Pb and U are greater in the Melville samples by a factor ranging from 1.6 to 6.5. Of these, Mn, Fe and U are not notably enriched at the 95 percentile level in the Melville samples, but Co, Ni, Zn, Pb, plus Ag and As are. The 95 percentile provides a measure of element levels reached by the more anomalous samples in each area.

To examine more closely the distribution of selected elements in the Melville samples, the data have been grouped in terms of the dominant lithology of the lake catchment area (Table 32.2). The latter information was derived from detailed (1:50 000) geological maps. For all elements listed in this table the median concentrations are reasonably similar for all lithologies. For some of the elements, the 95 percentiles are also reasonably similar from rock type to rock type. In these cases the ratio of the 95 percentile to the median is mostly in the range 2 to 3. Other elements show exceptions to this, notably Zn and Ni in lake sediments associated with paragneiss and Ni with metaquartzites. These have 95 percentile/median ratios in the range of 5 to 8, indicating that strong anomalies exist, relative to regional background. These are the most obvious targets for detailed investigation.

Some qualification should be given of the above discussion. Firstly, the detailed geological mapping used to construct Table 32.2, mainly covers the Proterozoic fold belt. Elsewhere in the geochemical survey area interesting anomalies that are not reflected in this table occur in the Archean. Secondly, subtle geochemical anomalies may often disclose mineralized targets. For instance, lake sediment anomalies may be weaker in the alkaline surface environment of carbonate terrane.

On the basis of the data given in Table 32.2 it was decided to investigate the Zn and Ni anomalies associated with paragneiss of the Penrhyn Group. Zn and Ni anomalies are associated with this lithology throughout the Penrhyn Group, but field work was largely confined to map area 46N/1, reasonably close to the base at Repulse Bay, with lesser amounts of work carried out in areas 46O/2 and 46O/4. Field work was carried out over a period of two weeks during August, 1978.

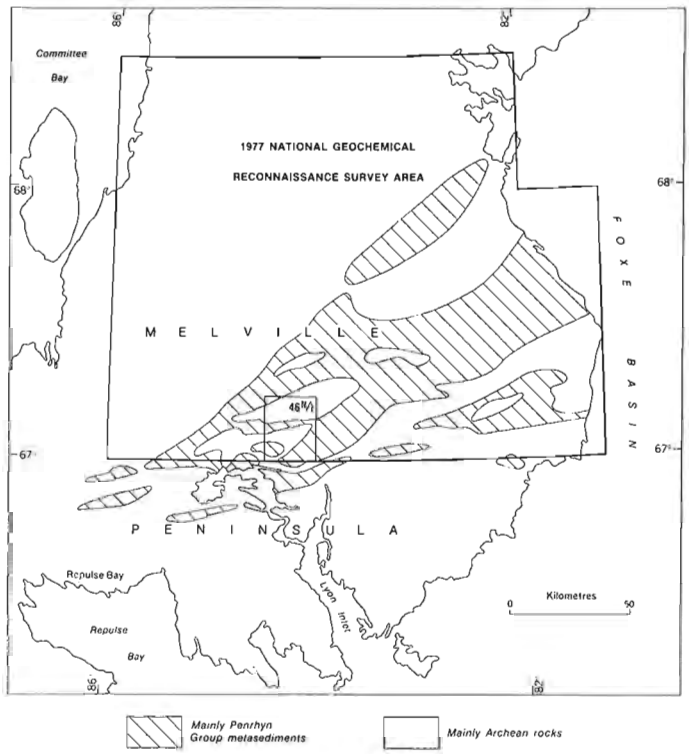


Figure 32.1. *Location map, Melville Peninsula.*

Geology

The first comprehensive account of the geology of the region was by Heywood (1967). Using this as a framework, much detailed mapping has since been carried out by the Geological Survey of Canada. The Proterozoic rocks, which form part of the Foxe Fold Belt (Jackson and Taylor, 1972), have been mapped by T. Gordon, J.R. Henderson, I. Hutcheon, A.N. LeCheminant, A.V. Okulitch and J.E. Reesor. This work has been described in a series of 1:50 000 maps and in reports by Reesor, 1972, 1974; Reesor et al., 1975; and Okulitch et al., 1977, 1978. The following summary of the geology is based on these maps and reports and refers principally to that part of the fold belt near longitude 84°.

The Penrhyn Group rests unconformably on an Archean basement composed mainly of granitoid gneiss and foliated granite. The basal Penrhyn consists of a thin orthoquartzite and a thin rusty schist. A possible metaregolith and an amphibolite have been recognized in places. These are succeeded by marble and biotite-quartz-feldspar paragneiss and schist. Above this is calc-silicate gneiss with marble, schist and paragneiss. At the highest observed levels are biotite-quartz-plagioclase schist and quartzite. Much of this sequence appears to be sulphidic, giving rise to rusty weathering rocks. In the lower part of the succession sulphidic, graphitic metasediments are common. Folding and metamorphism has made it difficult to determine stratigraphic thicknesses.

Two major episodes of folding of the Penrhyn rocks along east-northeast axes have produced broad, doubly plunging anticlinal zones of basement with narrow, tight synclinal in folds of Penrhyn Group rocks.

The Penrhyn Group has been metamorphosed to upper amphibolite grade. Foliated pretectonic or syntectonic granitic rocks, including abundant pegmatites, intrude the Penrhyn Group. Migmatites developed in the paragneiss suggest that the granites were, in part, derived from the metasediments. Metamorphism of the Penrhyn ended at about 1700 Ma and the metasediments were intruded by massive, posttectonic granites with an age of approximately 1600 Ma.

Exploration activity

The only major search for base metals in the area was by Aquitaine Company of Canada Ltd. during 1970-1972. The company carried out airborne electromagnetic and magnetic surveys, then ground follow-up comprising geological, V.L.F., magnetic and geochemical soil surveys. Shallow drilling was carried out at one location (the DUC claim group). A description of the work is given in assessment reports available from the Department of Indian and Northern Affairs, Ottawa.

Numerous targets were identified, principally within the graphitic and sulphidic Penrhyn metasediments, but disappointing results were obtained from surface outcrops and drilling on the DUC zone. This drilling showed that the graphitic biotite paragneiss had abundant pyrrhotite and pyrite, with inconspicuous sphalerite and minor chalcopyrite. Analysis indicated that the principal base metal is Zn with lesser Ni, Cu and Mo. For instance, the richest section of core analyzed, 44-48 feet from DUC Number 2, contained 8% Zn, 1850 ppm Ni, 700 ppm Cu, 295 ppm Mo and 75 ppm Pb.

Clearly, the Penrhyn Group is difficult terrane for base metal exploration. The widespread distribution of graphite and pyrrhotite causes a multitude of geophysical targets with Zn-sulphide mineralization being, in itself, a nonconductor. Soil geochemistry is not an appropriate exploration method for mineralization whose principal components are Zn and Ni. These elements are generally not retained in the permafrost soils overlying mineralization, unless buffered by carbonate minerals. Indeed it has been shown (Cameron, 1977a, 1977b) that mobile base metals may actually be at their lowest level in the soils overlying the higher grades of mineralization, because of the acidic conditions caused by sulphide oxidation.

Approach to follow-up of lake sediment anomalies

The approach taken to follow-up is determined by the mobility in the surface environment of the northern Shield of the elements found in base metal mineralization. The order, from most to least mobile, has been estimated as: Zn=Ni >Cu, >Fe,>As,>Ag,>Pb,>Hg,>Au (Cameron, 1977a, 1977b). The elements with the greatest mobilities, such as Zn, are removed from surface rocks, and soils. They are carried away in the drainage waters and eventually precipitate in the sediments of the lakes. For example, in following up a Zn anomaly in lake sediments, this element is measured in waters collected up-drainage from the anomaly. Once the source has been defined within a few hundred metres, soils may be collected and analyzed for the less mobile elements present in the mineralization. If immobile elements are absent in the mineralization, pinpointing the target is more difficult, but may be done by sampling seeps and pools of surface water.

The initial step in Melville Peninsula field investigations was to carry out detailed sampling of lake waters over Penrhyn Group rocks. This was done over all such terrane in map area 46N/1 (Fig. 32.1) and in parts of 46O/2 and 46O/4. The waters were obtained using a helicopter-borne sampling system (Cameron, 1978). This allows rapid rates of collection, in this case 30-40 lakes per hour, using a Bell 206-B helicopter. On the basis of analyses for "total" heavy metals in a field laboratory, more detailed water and soil sampling was then carried out.

Analysis

In the field laboratory the waters were analyzed for "total" heavy metals, pH and conductivity. The heavy metal test, which principally measures Zn, is the dithizone method using Bloom's buffer. The detection limit of 1 ppb was more than adequate for the relatively high threshold (compared to other northern waters) of 10 ppb Zn.

Table 32.1

Comparison of lake sediment data from National Geochemical Reconnaissance operations in Nonacho Area, N.W.T. (2688 samples) and Melville Peninsula, N.W.T. (2185 samples)

ELEMENT	MEDIAN (PPM)			95% PERCENTILE (PPM)		
	NONACHO	MELVILLE	RATIO MELVILLE/ NONACHO	NONACHO	MELVILLE	RATIO MELVILLE/ NONACHO
Mn	260	415.	1.6	1680.	1400.	0.8
Fe	1.35%	4.0%	3.0	6.8%	9.4%	1.4
Co	6.	17.	2.8	14.	38.	2.7
Ni	8.	52.	6.5	25.	126.	5.0
Cu	26.	82.	3.2	74.	196.	2.6
Zn	90.	148.	1.6	178.	325.	1.8
As	2.	1.5	0.7	5.	14.5	2.9
Mo	5.	4.	0.8	17.	13.	0.8
Ag	<0.2	<0.2	-	<0.2	0.5	>2.5
Hg	40.	40.	1.0	100.	80.	0.8
Pb	3.	17.	5.7	9.	46.	5.1
U	8.6	18.4	2.1	50.3	58.7	1.2
L.O.I.	36.9%	10.4%	0.3	67.2%	29.0%	0.4

Table 32.2

Lake sediment data for selected elements in terms of dominant lithology of lake drainage basins based on 1:50 000 geological maps of N.T.S. sheets 46N 1, 2, 3, 4, 7, 8, 9; 46O 1-16; 46P 3-6, 11-13; 47A 3

		ARCHEAN	APHEBIAN			
		GRANITE/ GNEISS	PARAGNEISS	QUARTZITE	MARBLE	GRANITE
NUMBER OF SAMPLES		510	197	48	206	82
Fe %	MEDIAN	4.70	3.60	3.90	3.75	3.90
	95 PERCENTILE	10.00	9.80	11.60	8.50	8.95
	RATIO 95/M	2.1	2.7	3.0	2.3	2.3
Ni ppm	MEDIAN	52.	58.	65.	58.	54.
	95 PERCENTILE	100.	290.	510.	200.	168.
	RATIO 95/M	1.9	5.0	7.8	3.4	3.1
Cu ppm	MEDIAN	92.	72.	84.	70.	66.
	95 PERCENTILE	190.	174.	295.	154.	166.
	RATIO 95/M	2.1	2.4	3.5	2.2	2.5
Zn ppm	MEDIAN	174.	158.	132.	168.	136.
	95 PERCENTILE	300.	1200.	345.	725.	615.
	RATIO 95/M	1.7	7.6	2.6	4.3	4.5
Pb ppm	MEDIAN	23.	14.	14.	16.	20.
	95 PERCENTILE	50.	43.	57.	56.	57.
	RATIO 95/M	2.2	3.1	4.1	3.5	2.85
U ppm	MEDIAN	20.3	19.1	21.1	21.3	27.4
	95 PERCENTILE	57.0	58.0	98.2	65.1	75.1
	RATIO 95/M	2.8	3.0	4.7	3.1	2.7

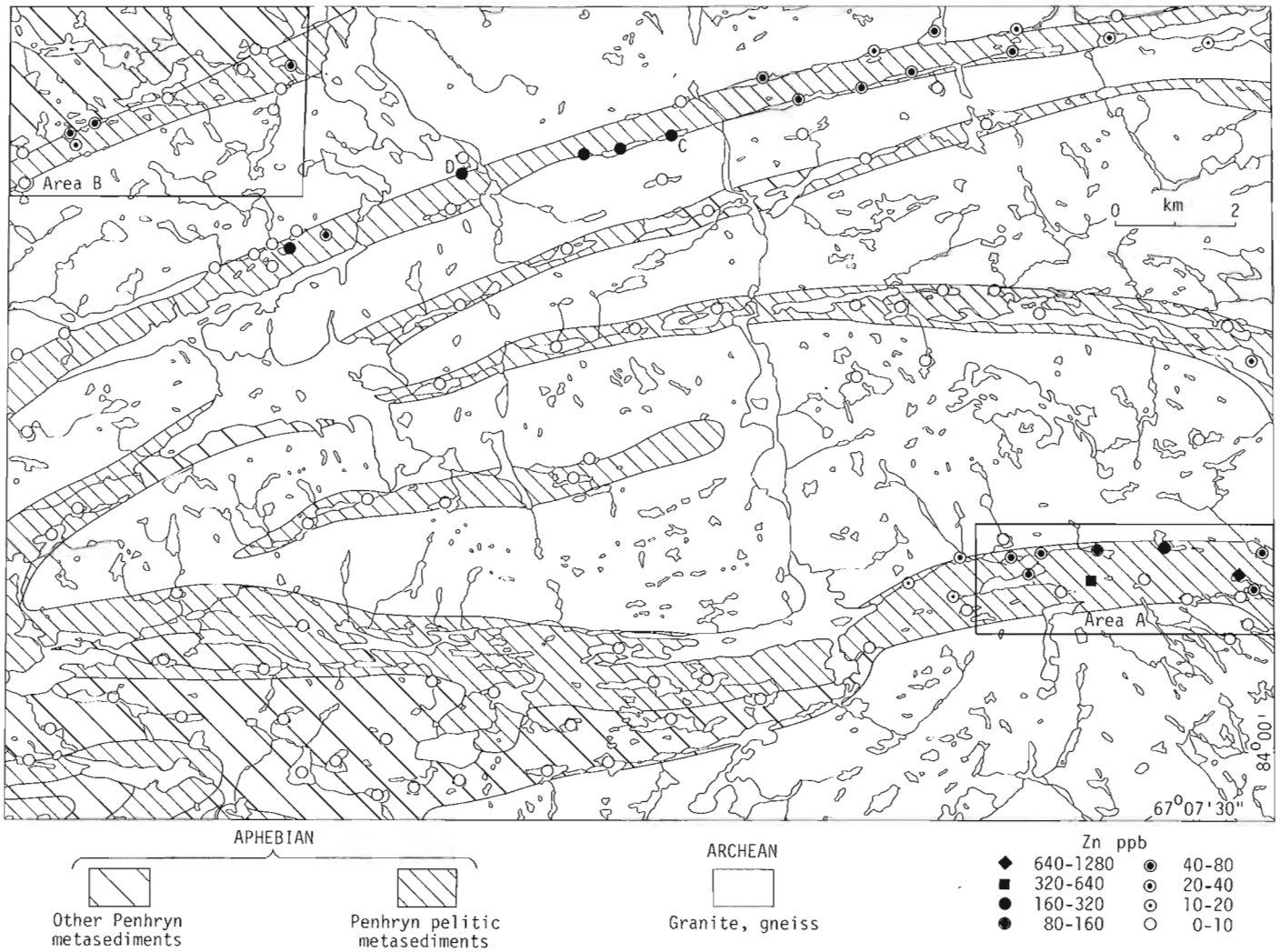


Figure 32.2. *Zinc in lake waters, north half, N.T.S. Sheet 46N/1. Geology after Reesor et al., 1976.*

The waters were reanalyzed in Ottawa for Zn, Cu and Ni. This was done by direct aspiration into an atomic absorption spectrometer for waters with >10 ppb of the element. Waters with less than this amount were treated with A.P.D.C.-M.I.B.K., to chelate and extract the heavy metals. This provided a detection limit of 1 ppb for each of the three elements. Following previous practice (Cameron, 1978), samples were not acidified or filtered, but analysis, in Ottawa, was completed within a month of sampling. Only the Ottawa analyses are reported in this paper.

Soil samples were sieved to minus 80- mesh, then extracted with a hot mixture of 1 part concentrated HCl to 3 parts concentrated HNO_3. Rocks were extracted by heating with HF, taken to dryness, then again heated with a mixture of 2 parts concentrated $HClO_4$ and 5 parts concentrated HNO_3. The soil and rock extracts were then analyzed by atomic absorption spectrometry for Zn, Cu, Fe, Mn, Ni, Pb and Ag using background correction for the latter three elements. Soil samples to be analyzed for Au were pre-concentrated by fire assay method, then extracted and measured by atomic absorption spectrometry.

Results

To illustrate the results, data for Zn in lake waters from the northern half of map area 46N/1 are shown in Figure 32.2 and the histograms of Zn, Cu, Ni, pH and specific conductivity for these waters are given in Figure 32.3. A correlation matrix for the same samples is listed in Table 32.3. These illustrations show that the most common type of lake water is weakly acidic, has a low content of total dissolved solids, and contains less than 2.5 ppb of each of the three base metals. These are typical northern Shield waters from unmineralized terrane, similar to those described from the northern part of the Slave Geological Province (Cameron, 1978).

As well as these "unmineralized" waters there are waters with anomalous levels of one or more base metals, and commonly with an acidic pH. These waters owe their distinctive composition to the present day oxidation of nearby base metal mineralization. They show a strong positive correlation between the elements Zn and Cu and Ni and between these variables and water acidity. Specific conductivity has a U-shaped distribution when plotted against pH. Higher conductivities occur in the acidic waters and also in the weakly alkaline waters. This results in weaker correlation between the base metals and specific conductivity than between these metals and pH.

The mineralized lake waters overlying the Penrhyn Group are much more anomalous in Zn than are similar waters from the northern part of the Slave Province (Cameron, 1978). In the latter region, lake waters with high contents of Zn (i.e. 40 ppb or more) are rare. These are

Table 32.3

Correlation matrix for 113 lake water samples, north half of N.T.S. Sheet 46N/1

	Log Zn	Log Cu	Log Ni	pH
Log Zn				
Log Cu	.79**			
Log Ni	.83**	.60**		
pH	-.69**	-.51**	-.80**	
Spec. Cond.	.25*	.41**	.15	.12

**Indicates significant correlation at 99.9% level
*at 99.5% level

usually found close (<2 km) to exposed massive sulphide bodies. The 95 percentile for Zn in a 1218 sample lake water survey from the northern Slave Province was only 2.8 ppb. By contrast, the data shown in Figures 32.2 and 32.3 have a 95 percentile of 193 ppb and waters with 40 ppb or more are relatively common. The markedly anomalous nature of Zn in many lake sediments collected over the Penrhyn Group discussed in the Introduction, may thus be related to a high flux of dissolved Zn passing into the lake systems.

For Ni, suitable comparative data are sparse, but this element is also believed to be strongly anomalous in many of the waters collected from above Penrhyn Group rocks. For Cu, the differences from previous data sets are less marked.

The 10 ppb level for Zn is a convenient threshold (Fig. 32.3) for distinguishing anomalous waters. In the northern half of map area 46N/1 such waters are confined to three principal areas (Fig. 32.2): the two most northerly infolds of Penrhyn rocks and the easternmost portion of the southern infold. The airborne surveys carried out by Aquitaine Company of Canada Ltd. found conductive zones throughout all areas of Penrhyn rocks exposed within map area 46N/1. Gossanous soils and outcrop are also ubiquitous in those parts of this area that are underlain by the Penrhyn Group. But there is no apparent correlation between the relative distinctiveness of gossanous zones and the geochemical results. For the area shown in Figure 32.2, the most extensive and colourful gossans are in the western half of the most southerly Penrhyn infold. This area has low contents of base metals in lake waters.

For two of the more anomalous areas shown in Figure 32.2 more detailed information is given below.

Area A (Fig. 32.4)

This area is underlain by a steeply dipping infold of Penrhyn metasediments, enclosed by Archean granitic rocks. There is a thin border of metaquartzites along the flanks of the infold. Within this is paragneiss with some marble beds. The Proterozoic succession appears to have been derived from a miogeoclinal-type succession containing shale, silt, quartzite and carbonate. Pegmatites are common and generally lie parallel to the strike of the metasediments.

The zone of base metal enrichment, as indicated by the water data, has a stratigraphic trend. Samples from lakes within the Archean or from the marginal zone of the infold, have background levels of base metals (Fig. 32.4). It is the central, more pelitic, metasediments that contain the highest content of base metals. Within this zone, the mineralization is widely distributed. This is apparent from the large number of lakes and ponds with anomalous waters, many of which have a local drainage basin.

The Penrhyn rocks within the mineralized area are well exposed. Most have a rusty weathering surface, the product of the oxidation of sulphides. In most cases, the amount of sulphide present in rock samples, or likely to have been present prior to oxidation, is small. But there are also zones where sulphide has been a major or a dominant component. When exposed, these zones appear as limonitic rock, with residual iron sulphides. Pyrite is most resistant to weathering and is commonly seen as prominent crystals standing out from the weathered surface. Pyrrhotite is less commonly found in surface exposures. Only trace amounts of sphalerite, chalcopyrite and pentlandite were observed.

It is inferred that sulphide zones underlie marshy depressions that contain mineralized seeps. The soils of the depressions are unusually soft, with a high water content and the principal vegetation is a black moss. The mineralized nature of the waters may be immediately determined in the field by their low pH and high conductivity. On analysis they show a strongly anomalous base metal content. Two such seeps are shown in Figure 32.4 and may be identified by their Zn contents of 2204 ppb and 2245 ppb. The waters also contain substantial levels of Ni and Cu. By comparison, the principal seep above the Agricola Lake massive sulphide body in the Slave Province (Cameron, 1978, Fig. 5) was measured as 1080 ppb Zn, 867 ppb Cu, 23 ppb Ni, pH 3.4.

Soil samples were also taken from these seep areas (Table 32.4). Sample 784041 is adjacent to the seep containing 2204 ppb Zn (Fig. 32.4). The low pH of this residual soil sample indicates that any anomalous levels of Zn, Ni or Cu

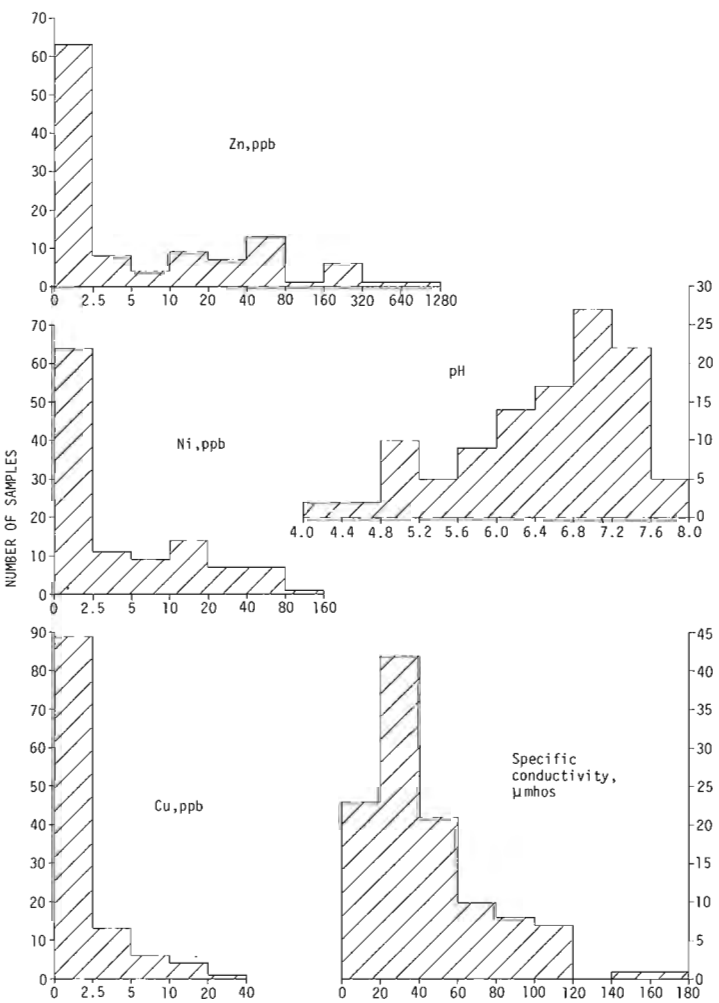


Figure 32.3. Histograms for Zn, Ni, Cu, pH and specific conductivity. Lake waters from north half, N.T.S. Sheet 46N/1.

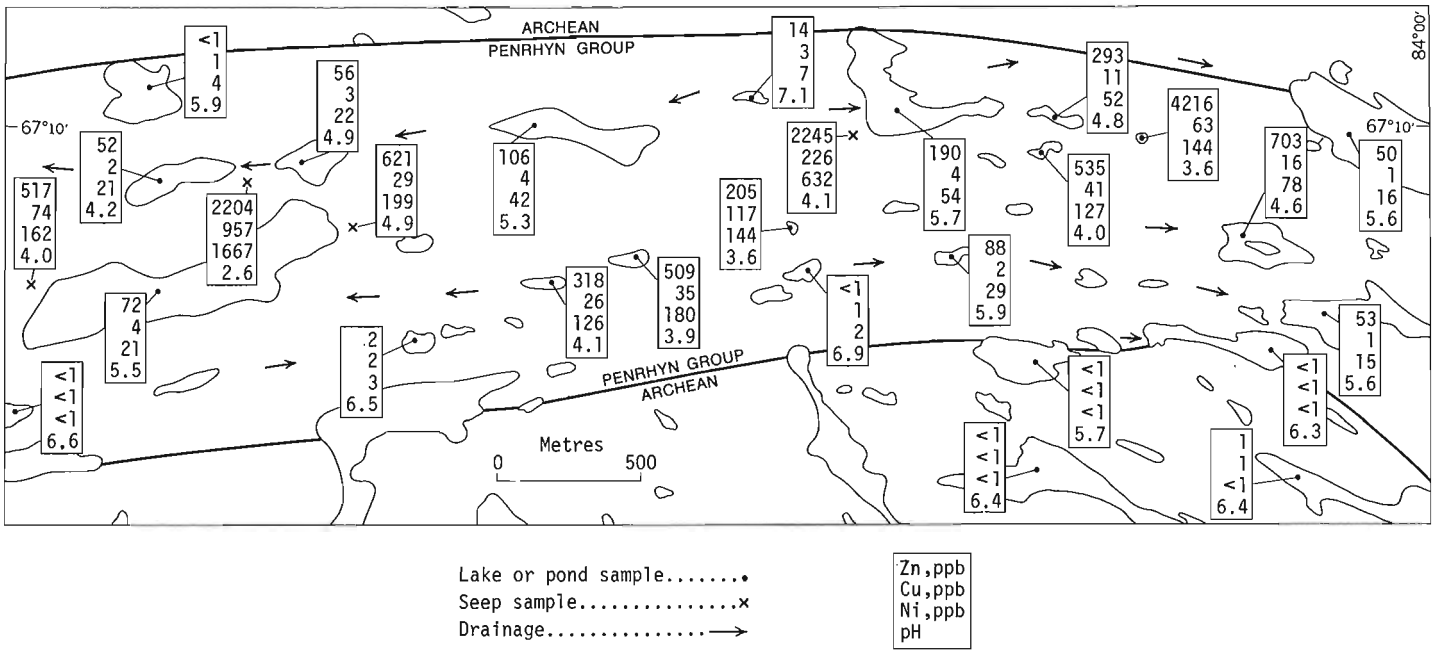


Figure 32.4. *Lake and pond water analyses, Area A (see Fig. 32.2). Geology after Reesor et al., 1976.*

present in the parent material would not have been retained in the soils. This is confirmed by the actual data for these elements. But also, the soil does not contain anomalous levels of the immobile elements Pb, Ag and Au. This implies that these are not present in the Zn-, Ni- and Cu-bearing mineralization from which the seep waters were derived.

Soil sample 784056 (Table 32.4) was taken near the pond measuring 4216 ppb Zn (Fig. 32.4). It is similar to the soil described above, but at this location the mineralization does appear to contain Ag and Au.

In summary, the area of Penrhyn metasediments shown in Figure 32.4 contains several zones in which sulphides, including base metal sulphides, are believed to have been a major or dominant component. At the surface they appear as limonitic rocks, with residual iron sulphides, or as topographic depressions containing base metal-rich seep waters. Water and soil analyses indicate that Zn is the dominant base metal in the mineralization and is accompanied by lesser amounts of Ni and Cu. The elements Ag and Au are present in one zone. Because of soil or blockfield cover no attempt was made to estimate the dimensions of the zones, but it is doubtful if any exceed a maximum length of 100 m and width of 10 m. For all zones observed, long dimensions are parallel to the strike of the metasedimentary rocks.

Area B (Fig. 32.5)

This area is principally underlain by steeply dipping Penrhyn Group metasediments. Relief is low and much of the area drains to the north through a chain of three larger lakes in the northwest quadrant of the area. The central lake of this chain was sampled during the 1977 geochemical reconnaissance and was the only lake sampled within the area shown in Figure 32.5. The sediment sample from this lake (773008, Table 32.4) is strongly anomalous in a number of elements.

The detailed lake water sampling shows that waters from Archean terrane and over much of the Penrhyn contain background concentrations of base metals. But the waters are strongly anomalous, particularly in Zn, along the part of the Penrhyn succession composed of paragneiss and schist. These mineralized waters flow into the chain of three lakes noted above and cause their waters to be moderately anomalous. The strongly anomalous nature of lake sediment sample 773008 undoubtedly derives from this source. It is a good example of a lake sediment anomaly displaced from source. The data listed in Figure 32.5 illustrate the complementary nature of lake sediment reconnaissance and lake water follow-up.

A soil sampling traverse was made across strike, near the apparent source of the base metals (Fig. 32.6). Much of this traverse is over ground that slopes gently to the north and is underlain by paragneiss and schist. In places these rocks are graphitic and sulphidic. The paragneiss appears to have been derived from a succession containing a good deal of quartzite. At the northern end of this traverse is a contact with marble. Along and to the south of this contact is low ground carpeted by black moss and the site of a seep.

The soils along the part of the traverse that overlies the paragneiss/schist are acidic, in the range pH 2.8-4.2. Any anomalous levels of Zn and Ni in the rocks would not have survived in these acid soils. But the single soil sample taken over the marble has a slightly alkaline pH and with this, strongly anomalous levels of Zn and Ni. Surface waters were taken from the north and the south sides of the seep area. Sample 783314 (Table 32.5) was taken at 5 m along traverse 77 (Fig. 32.6) and sample 783316 at 15 m. Sample 783316 is acidic and very strongly anomalous in Zn and Ni. Sample 783314 is faintly alkaline and, while still significantly anomalous in Zn and Ni, is less so than the other sample. In the pool of water from which sample 783314 was collected there is a light coloured, flocculent precipitate.

Table 32.4

Soil and lake sediment analyses (ppm)

SAMPLE		Zn	Ni	Cu	Pb	Ag	Au
Soil	784014	435	48	740	15600	12.1	0.16
Soil	784041	35	9	59	15	0.8	0.01
Soil	784056	170	4	275	45	11.8	0.23
Lake Sediment	773008	3400	530	295	39	0.1	-

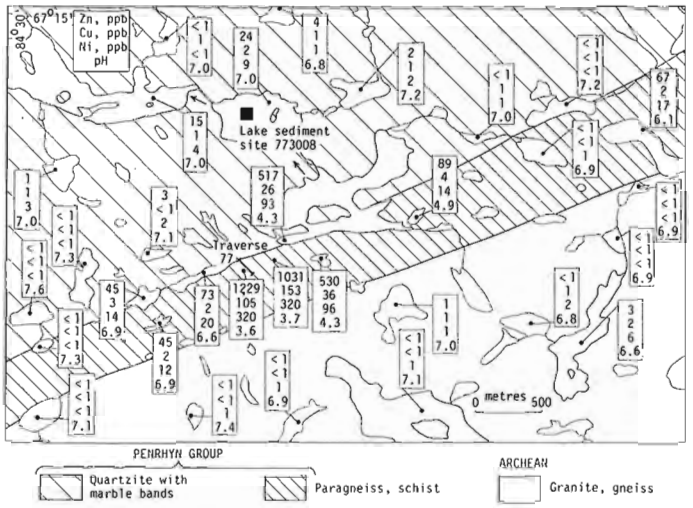


Figure 32.5. *Lake water analyses, Area B (see Fig. 32.2). Geology after Reesor et al., 1976.*

These water data complement the soil data. Over the paragneiss, the oxidation of sulphides has created an acidic environment in which Zn and Ni are released into surface waters. At the contact with the marbles, the slightly alkaline environment allowed these elements to remain in the soils and/or to precipitate from the surface waters.

The seep area near the paragneiss/marble contact is believed to overlie the maximum development of base metal mineralization at this locality. This is suggested by the extreme values of Zn and Ni in sample 783316. The maximum width of this seep zone is 15 m and the feature can be traced for several hundred metres.

From the water data it is clear that some Cu accompanies the Zn and Ni in the mineralization. The soils along this traverse show low values for other metals: <5-41 ppm Pb, 0.5-2.5 ppm Ag and <5-5 ppb Au. On a similar soil traverse 200 m to the west, one sample contains 20 ppm Ag, indicating that significant amounts of this metal may be present locally.

Other areas

Several other localities were examined in similar fashion to areas A and B. These are located in other parts of map area 46N/1 and in map areas 46O/2 and 46O/4. At all of these localities, the source of anomalous levels of base metals in lake sediments and waters is similar to that found in areas A and B: Zn-rich mineralized zones in sulphidic and frequently graphitic Penrhyn metasediments. The only additional feature found in these areas that supplements the information given above is a soil sample (784014, Table 32.4) rich in Pb, Ag and Au collected near a Zn, Ni, Cu-rich seep (sample 783123, Table 32.5). The U.T.M. co-ordinates of this sample are 376600 E, 7456650 N, Zone 17. This indicates that Pb may also be present locally in the mineralization.

Examination of sulphides

Preliminary mineralogical examination has been carried out of polished sections of sulphide-rich paragneiss. One is an outcrop sample from area A, close to soil sample 784056. The U.T.M. co-ordinates are: 629000E, 7429000N, Zone 16. The other samples are core from the DUC 7 and DUC 8 drillholes. The U.T.M. co-ordinates of both holes are: 407900E, 7487850N, Zone 17. Sulphide minerals occur in the samples as veins or coarse segregations.

The major sulphide present is pyrrhotite. All samples contain lesser and variable amounts of sphalerite, pentlandite, chalcopyrite and pyrite. The latter commonly occurs as veins in pyrrhotite, while pentlandite occurs as blebs exsolved within pyrrhotite. Some chalcopyrite is present as blebs exsolved within sphalerite. Grains that have been tentatively identified as silver pentlandite occur in many of the samples. They are often present within chalcopyrite. Microprobe analyses indicate that Ni is held as a solid solution impurity in pyrrhotite and pyrite. The most readily oxidized sulphide mineral is pyrrhotite. The alteration of pyrrhotite is illustrated in Figure 32.7, a polished section of the outcrop sample.

Interpretation of results

The results presented above show that sulphide lenses containing base metals are an important feature of paragneiss and schist of the Penrhyn Group. The units in which they occur have a generally sulphidic character and are variably graphitic. The apparent disposition of individual lenses and the trend of geochemical anomalies along strike suggest that the mineralization is stratiform. Surface water analysis indicates that Zn is the most abundant base metal with lesser amounts of Ni and minor Cu. This order of abundance is confirmed by examination of the limited amount of sulphide material available.

The Zn and Ni anomalies in lake sediments and waters are stronger and more extensive than have been measured over mineralized Archean greenstone belts in the northern Shield. This might suggest that the total amount of these metals, present as sulphides, is greater in the Penrhyn Group than in a similar volume of rock from a greenstone belt. But before this conclusion is reached some consideration must be given to whether the Penrhyn mineralization is more susceptible to weathering. Pyrrhotite is abundant and is readily oxidized, thus contributing to the acidity of the surface environment; the graphitic gneiss, being fissile, readily allows water infiltration; and the presence of the conductor, graphite, may facilitate electrochemical reactions. This question can only be answered by examining unweathered drill core of the mineralized zones and their host rocks.

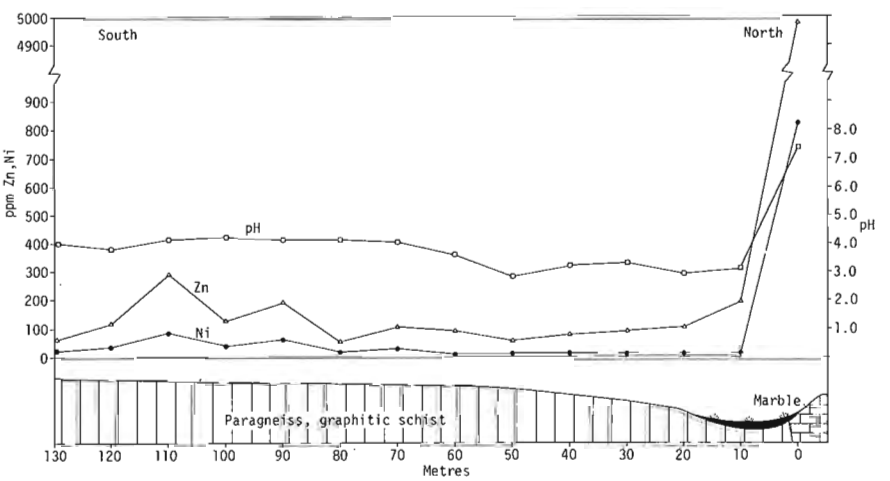
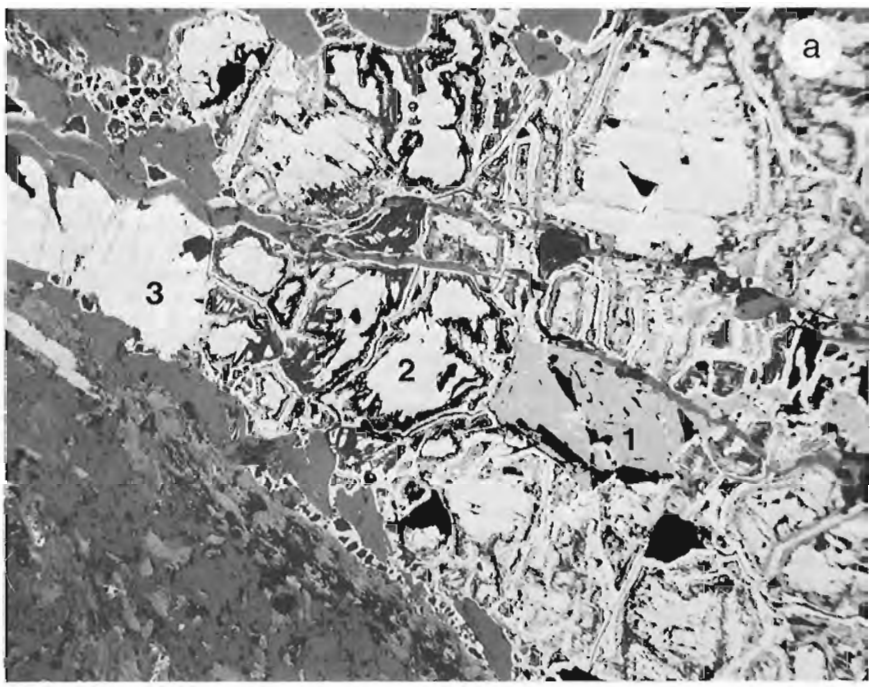


Figure 32.6. *Soil traverse 77. For location see Figure 32.5.*

Metallogenic Considerations

Many of the major sediment-hosted stratiform base metal deposits of the world are of Proterozoic age. The development of plate tectonic concepts has allowed the distribution of these deposits in time and space to be better understood. In particular, they are known to be associated with intracratonic and cratonic margin rifts (Burke and Dewey, 1973; Vokes, 1973; Dunnet, 1976; Sawkins, 1976a, 1976b; Raybould, 1978). The rifts may have allowed metal from a deep source to reach the surface or, alternatively, allowed the escape of heat to provide the driving force for near-surface redistribution of metals. The deposits occur in miogeoclinal sedimentary sequences and there is often some development of basaltic lavas, characteristic of a tensional environment.

One of the most striking examples of the clustering of stratiform deposits around a plume-generated triple rift junction is at Mount Isa, Australia (Dunnet, 1976). These deposits occur near the intersection of the Paradise aulocogen with the geosyncline that developed along the margin of the Proterozoic craton. Known Cu deposits are restricted to a zone at the craton boundary marked by a thick sequence of flood basalts and which is above the hypothetical position of the mantle plume. The Pb-Zn deposits have a wider geographic range. To the north, the McArthur Zn-Pb-Ag deposit occurs in the Batten Trough, a rift similar to the Paradise aulocogen, with a thickened platformal sequence of sediments, but removed from the craton boundary. Other important Proterozoic stratiform deposits in a broadly similar environment include Sullivan, British Columbia (Kanasewich et al., 1968; Burke and Dewey, 1973); the Copperbelt of Zambia and Zaire (Burke and Dewey, 1973; Raybould, 1978); and Whitepine, Michigan (Sawkins, 1976b).





a. General view, 2.2 x 1.7 mm

1. *Sphalerite with exsolved chalcopyrite*
2. *Pyrrhotite remnant and alteration products*
3. *Pyrite*
4. *Graphite in matrix*

b. Detail of pyrrhotite weathering 0.55 x 0.43 mm

1. *Pyrrhotite remnant*
2. *Marcasite*
3. *Intermediate phase (Einaudi, 1971; Fleet, 1978)*

Figure 32.7. *Textures in partially oxidized sample of sulphide-bearing paragneiss.*

Table 32.5

Surface water analyses
(metals in ppb; specific conductivity as μmhos)

SAMPLE	Zn	Ni	Cu	pH	Specific Conductivity
783123	3280	706	353	2.8	837
783314	461	217	8	7.7	440
783316	11030	2540	500	3.1	1170

The rocks of the Foxe Fold Belt on Melville Peninsula and Baffin Island appear to have been deposited within an intracratonic rift trough. The miogeoclinal-type succession rests on Archean basement and similar Archean rocks flank the belt on either side. There is an apparent thinning of the succession and a narrowing of the belt westwards. On Baffin Island, the succession – here comprising the Piling Group (Jackson and Taylor, 1972) – is essentially similar to that of the Penrhyn Group. Quartzite, at the base, is succeeded by marble and this by deeply weathered, rusty, graphitic and sulphidic gneiss, up to 300 m thick. This, in turn, is overlain by a thick sequence of metagreywacke and metasiltstone. Important differences from the Penrhyn are a 60 m thick zone of oxide-facies iron formation at the same stratigraphic level as the rusty gneiss and also metabasalt, up to 760 m thick, in the basal part of the metagreywacke unit. That portion of the fold belt on Baffin Island may have lain closer to the cratonic margin or mantle plume. Mapping on Baffin Island, presently being carried out by G.D. Jackson and W.C. Morgan, should provide important evidence on the tectonic setting of the belt.

The work of Lambert and Scott (1973) and Lambert (1976) on the Middle Proterozoic McArthur Zn-Pb-Ag deposit of Australia has given valuable insight into the extensive regional distribution of metals in a mineralized shale unit. The deposit occurs near the base of a 500 m section of pyritic, carbonaceous and tuffaceous shale. The 200 million ton deposit, grading 10% Zn, 4% Pb, 45 ppm Ag, extends over 1.5 km^2 with an average thickness of 55 m. At this horizon base metal mineralization is regionally widespread, but consists mainly of Zn. Thus the W-Fold prospect, 8 km distant, contains 2-3% Zn but only minor galena. Pyritic shales as far as 20 km from the deposit may contain 0.5% Zn and 0.1% Pb. Silver has a very limited dispersion halo around the deposit. Nickel is low in both ore and host shale. Pyrite is abundant throughout the shale member and reaches 20-30% Fe near the deposit.

Conclusions

The Zn and Ni lake sediment anomalies outlined during the 1977 geochemical reconnaissance of the Penrhyn Group have been related to base metal-bearing, stratiform mineralization in sulphidic paragneiss and schist. Zinc is the principal base metal and is accompanied by lesser amounts of Ni and minor Cu. These elements are present as sphalerite, pentlandite and chalcopyrite. Also occurring locally are Pb, Ag and Au. Because of intensive surface oxidation, all but traces of the base metal sulphides have been removed from the surface exposures examined.

The markedly anomalous nature of the Zn and Ni lake sediment anomalies is directly related to the high flux of these metals entering the lake basins in solution. This, in turn, may imply a particularly high total content of Zn and Ni in sulphide form in the paragneiss, compared to, say, an equivalent volume of rock in a mineralized Archean greenstone belt. However, an alternative explanation is that the Penrhyn mineralization is more susceptible to weathering. An answer to this question, providing perspective on the economic significance of the mineralization, can only be obtained by subsurface sampling.

There can be no doubt however, about the extensive nature of the base metal mineralization within the Penrhyn basin. Although the follow-up work was carried out over a limited area, the coincidence of strong Zn and Ni lake sediment anomalies over paragneiss throughout the Penrhyn basin implies that introduction of base metals was a regional phenomenon.

The Foxe Fold Belt appears to have been the site of an intracratonic rift. Such features were the focus of stratiform mineralization during the Proterozoic. Of particular interest in this respect are basaltic volcanic rocks, typical of tensional regimes, on Baffin Island. They occur in close stratigraphic proximity to sulphidic gneiss that is possibly correlative with the mineralized rocks on Melville Peninsula.

Study of Middle Proterozoic shale-hosted Zn-Pb-Ag mineralization in the Batten Trough of Australia, an intracratonic rift, has shown that Zn has the widest primary distribution. The Pb and Ag occur in significant concentrations only at the McArthur deposit. Therefore, by analogy, the presence of Zn-rich stratigraphic horizons within the Penrhyn Group, and the possible occurrence of similar rocks on Baffin Island, may provide a key for more detailed exploration for base metals in the Foxe Fold Belt.

While the surface oxidation of the base metal sulphides presents obvious difficulties in studying the mineralization, it has created extensive secondary dispersion halos in surface waters and lake sediments. The sampling of surface waters by helicopter and their analysis for Zn in a field laboratory is a rapid and effective means of outlining mineralized ground for more detailed investigation.

Acknowledgments

The writer was very ably assisted in the field and office by Paul MacKay. The analytical work was performed under the direction of Ms. Gwendy Hall. Larry Cotter was the helicopter pilot. The mineralogical studies were carried out by Gordon Pringle, A.G. Plant and D.M. Watson, while Greig Lund provided the statistical data. Dr. A.V. Okulitch kindly arranged for fuel to be supplied and provided the base map for Figure 1. The field work was carried out in the company of Dr. Yvon Maurice, who investigated uranium anomalies in the same general area. Dr. Maurice also kindly provided critical comment on this paper. I am most grateful to all these persons for their generous contribution to the work.

References

Burke, K. and Dewey, J.F.
1973: Plume-generated triple junctions: key indicators in applying plate tectonics to old rocks; Journal of Geology, v. 81, p. 406-433.

Cameron, E.M.
1977a: Geochemical dispersion in mineralized soils of a permafrost environment; Journal of Geochemical Exploration, v. 7, p. 301-326.

1977b: Geochemical dispersion in lake waters and sediments from massive sulphide mineralization, Agricola Lake area, N.W.T.; Journal of Geochemical Exploration, v. 7, p. 327-348.

1978: Hydrogeochemical methods for base metal exploration in the northern Canadian Shield; Journal of Geochemical Exploration, v. 10.

Dunnet, D.
1976: Some aspects of the Panantarctic cratonic margin in Australia; Philosophical Transactions of the Royal Society of London, A280, p. 641-654.

Einaude, M.T.
1971: The intermediate product of pyrrhotite alteration; American Mineralogist, v. 56, p. 1297-1302.

Fleet, M.E.
1978: Pyrrhotite-marcasite transformation; Canadian Mineralogist, v. 16, p. 31-35.

Geological Survey of Canada
1978a: National Geochemical Reconnaissance release, regional lake sediment and water geochemical reconnaissance data, Melville Peninsula, N.W.T. NGR 32A-1977 or 32B-1977, NTS 46N and part of 47B; Geological Survey of Canada, Open File 521A or 521B.

1978b: National Geochemical Reconnaissance release, regional lake sediment and water geochemical reconnaissance data, Melville Peninsula, N.W.T. NGR 33A-1977 or 33B-1977, NTS 46O, P and part of 47A; Geological Survey of Canada, Open File 522A or 522B.

Heywood, W.W.
1967: Geological notes, northeastern District of Keewatin and southern Melville Peninsula, District of Franklin, Northwest Territories (Parts of 46, 47, 56, 57); Geological Survey of Canada, Paper 66-40.

Hornbrook, E.H.W., Garrett, R.G., and Lynch, J.J.
1967a: Regional lake sediment geochemical reconnaissance data, Nonacho Belt, N.W.T. (NTS 75C); Geological Survey of Canada, Open File 324.

1976b: Regional lake sediment geochemical reconnaissance data, Nonacho Belt, N.W.T. (NTS 75F); Geological Survey of Canada, Open File 325.

1976c: Regional lake sediment geochemical reconnaissance data, Nonacho Belt, N.W.T. (NTS 75K); Geological Survey of Canada, Open File 326.

Jackson, G.D. and Taylor, F.C.
1972: Correlation of major Aphebian rock units in the northeastern Canadian Shield; Canadian Journal of Earth Sciences, v. 9, p. 1650-1669.

Kanasewich, E.R., Clowes, R.M., and McCloughan, C.M.
1968: A buried Precambrian rift in western Canada; Tectonophysics, v. 8, p. 513-527.

Lambert, I.B.
1976: The McArthur zinc-lead-silver deposit: features, metallogenesis and comparisons with some other stratiform ores; in Handbook of Strata-Bound and Stratiform Ore Deposits, Editor K.H. Wolf, v. 6, p. 535-585, Elsevier, Amsterdam.

Lambert, I.B. and Scott, K.M.
1973: Implications of geochemical investigations of sedimentary rocks within and around the McArthur zinc-lead-silver deposit, Northern Territory; Journal of Geochemical Exploration, v. 2, p. 307-330.

Okulitch, A.V., Gordon, T., Henderson, J.R., Reesor, J.E., and Hutcheon, I.E.
1977: Geology of the Barrow River map area, Melville Peninsula, District of Franklin; in Report of Activities, Part A, Geological Survey of Canada, Paper 77-1A, p. 213-215.

Okulitch, A.V., Gordon, T., Henderson, J.R., Hutcheon, I.E., and Turay, M.
1978: Geology of the Barrow River and Hall Lake map-areas, Melville Peninsula, District of Franklin; in Current Research, Part A, Geological Survey of Canada, Paper 78-1A, p. 159-161.

Raybould, J.G.
1978: Tectonic controls on Proterozoic stratiform copper mineralization; Transactions of the Institute of Mining and Metallurgy, Sect. B, v. 87, p. 79-86.

Reesor, J.E.
1972: Penrhyn Group metamorphic complex, Melville Peninsula, District of Franklin; in Report of Activities, Part A, Geological Survey of Canada, Paper 72-1A, p. 106-107.

1974: Penrhyn Group metamorphic complex, Melville Peninsula, District of Franklin; in Report of Activities, Part A, Geological Survey of Canada, Paper 74-1A, p. 153.

Reesor, J.E., LeCheminant, A.N., and Henderson, J.R.
1975: Geology of the Penrhyn Group metamorphic complex, Melville Peninsula, District of Franklin; in Report of Activities, Part A, Geological Survey of Canada, Paper 75-1A, p. 349-351.

Reesor, J.E., LeCheminant, A.N., Henderson, J.R., Hutcheon, I.E., and Miller, A.
1976: 1:50 000 geological map, NTS Sheet 46N/1; Geological Survey of Canada, Open File 307.

Sawkins, F.J.
1976a: Widespread continental rifting; some considerations of timing and mechanism; Geology, v. 4, p. 427-430.

1976b: Massive sulphide deposits in relation to geotectonics; in D.F. Strong (Ed.) Metallogeny and Plate Tectonics; Geological Association of Canada, Special Paper 14, p. 221-242.

Vokes, F.M.
1973: Metallogeny possibly related to continental break-up in southwest Scandinavia; in D.H. Tarling and S.K. Runcorn (Eds.), Implications of Continental Drift to the Earth Sciences, v. 1, Academic Press, London, p. 573-579.

33. SAMPLING CONSIDERATIONS FOR REGIONAL GEOCHEMICAL SURVEYS

Project 750039

Robert G. Garrett
Resource Geophysics and Geochemistry Division

Garrett, R.G., Sampling considerations for regional geochemical surveys; in Current Research, Part A, Geol. Surv. Can., Paper 79-1A, p. 197-205, 1979.

Abstract

A number of aspects of sample design are reviewed in the context of regional geochemical studies. Particular attention is paid to optimal sample spacing and collection so that surveys can be executed at minimum cost. Procedures for undertaking quality control monitoring of sampling and analytical variability as integral parts of geochemical surveys are discussed in the light of new methods for carrying out analysis of variance. Finally, an approach is proposed for the estimation of survey efficiency. This proposal draws on aspects of both previously discussed topics and should aid the objective appraisal of survey results in mineral resource studies.

Introduction

This report documents some of the more interesting topics encountered by the author in studying and designing sampling programs for regional and exploration geochemistry. None of the projects from which the following observations were made were specifically sampling studies, however, they have all included sampling design stages as an integral part.

Before commencing a sampling program it is imperative to know clearly what the objective program will be in terms of the ultimate data requirements, these may be needed to assist some decision making process or map the variability in the area of interest. In this context, it has been found useful to divide sampling programs into two broad categories. Firstly, 'exploration' mode, where the objective is to cover a geographic or geological unit in the search for targets and then classify the resulting data into 'hits' or 'misses'. The 'hits' will be the focus of further mineral exploration activity, hopefully leading to the discovery of significant mineral occurrences. Secondly, 'evaluation' mode, where the objective is to prepare reliable maps of the variability of some parameter across a geographic or geological unit. Such maps may well be for purposes other than mineral exploration.

One concept which is of importance in sampling design is that of 'target population' and 'sample population'. The objective of a survey is to make statements about a whole area. All the possible samples of the material of interest one could collect from that area form the 'target population', i.e. the 'target population' is the totality about which one finally wishes to make statements. In almost all cases in geology it is physically and economically impossible to collect the 'target population'. What occurs is that according to some rules the geologist has defined a suite of samples is collected which form the 'sample population'. This suite is one of an infinite number that could be collected and is that geologist's realization of an infinite problem. From this 'sample population' will be inferred properties of the 'target population'. This concept of different populations was first introduced to geology by Rosenfeld (1954) and later discussed at length by Krumbein (1960).

The report is divided into three sections on topics related to 'exploration' mode, 'evaluation' mode, and a combined approach which evolves from the previous two sections. In 'exploration' mode the concern in sampling design is to collect sufficient samples to enable decisions to be made with a desired confidence, but not to collect more, as this would be wasteful of resources. Three separate methods will be discussed, the first is purely geometric in concept and assumes a minimum of geological knowledge, the remaining two require more detailed geological knowledge and make genetic assumptions concerning the relationship of mineral occurrences to geological units. In 'evaluation' mode the concern is to so structure the sampling design that it is possible to determine if any regional trends revealed by the survey are real, or could be due to the accumulated effects of sampling and analytical variability. In this sense 'exploration' mode work is focused on pre-survey design, whereas 'evaluation' mode focuses on quality control of the executed survey. The combined approach attempts to mate the geometric 'exploration' mode work with the quality control aspects of 'evaluation' mode and derive some measure of survey effectiveness which will aid decision making in mineral resource studies.

Exploration Mode Considerations

In mineral exploration it is common to have some a priori knowledge of the size of the target one is searching for. In geochemical exploration the target is usually larger than the actual mineral occurrence due to secondary dispersion from the occurrence and the primary halo about it, or in the case of lithogeochemical studies, due to primary dispersion patterns alone. In regional geochemistry, systematic sampling on a square or rectangular grid, as used in soil and some overburden/till surveys, is uncommon. More often some modification is employed, as the 'target population' is not available at all locations due to its very nature, or cover of some sort. For example, in a lake sediment survey all lakes in the area would form the 'target population' and these do not conveniently fall at grid intersections. Similarly, except in the rare cases of total exposure, rock samples are not available at all grid intersections due to lakes or overburden. The common reaction to this problem is to grid the area and collect a single sample from within each grid cell, or close to the grid intersections. In effect the geologist is using a sampling plan similar to one known to statisticians as a stratified random sample design.

Tables have been published by Savinskii (1965) to aid in determining optimal grid sizes, either square or rectangular, given the target size and its orientation relative to the grid. These tables are unfortunately of little use with stratified random sample designs which are commonly employed. An alternative approach which has been employed involved simulation studies (Garrett, 1977), or more recently a direct method, which is described below. The probability that a sample collected on a square grid will fall within the target, P(h), is defined as:

$$P(h) = \frac{At}{Ac}$$

where At is the area of the target, often approximated by a circle or an ellipse, and Ac is the area of the square grid cell.

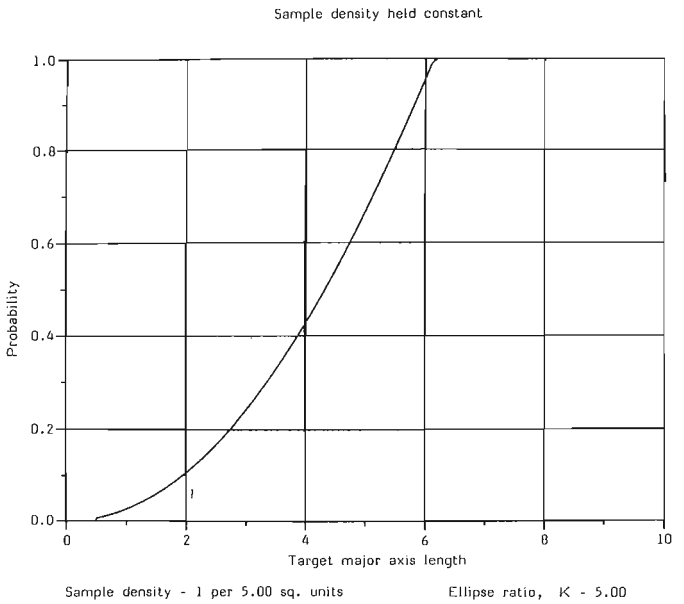


Figure 33.1. *Relationship of expectation of a 'hit' to target size.*

The probability varies from zero to one, greater values than one, which occur with fine grids and very large targets, being set to one. In the stratified random model the square grid is replaced by a quadrilateral formed by four randomly chosen points in four adjacent square cells. In sampling terms, these four points would represent four sample sites in four adjacent grid cells. An infinite number of quadrilaterals could be so formed. Works by Ghosh (1951), and later Matern (1960), show how the average distance between two randomly chosen points in adjacent squares can be computed. For the case of two adjacent unit size grid cells this average distance, d, is 1.08814 units. Using this distance, the quadrilaterals may be replaced by a single square grid whose sides are increased by the factor d. For instance, if sampling is at 1 sample per 13 km^2 (1 sample per 5 square miles) the grid squares will be $\sqrt{13}$, or 3.61 km, on a side and the effective square size for use in computing the expectation of a 'hit', i.e. that such a design will collect samples from within a target, is 3.92 km on a side (15.39 km^2). This expectation of a 'hit', E(h), can now be computed from a knowledge of the area of the basic sampling unit, Ac, and the factor d. At remains the area of the target.

$$E(h) = \frac{At}{Ac.d^2}$$

With this information in hand the expectation that an individual sample will be drawn from within a target of specified size can be determined. In all likelihood this expectation is an overestimate since it has been assumed that all samples from within targets will be correctly identified. The reality is that due to variability and errors in sampling and analysis there is some probability, less than one, that the 'hit' will be recognized as such. If we define E(h) as the expectation of a 'hit' on purely geometric grounds, and P(r) as the probability of recognition, then the actual expectation of success of the sampling design, E(s), will be

$$E(s) = E(h).P(r)$$

Current research by C.F. Chung of the Geological Survey of Canada is leading towards the definition of the true probability of a 'hit', P(h), for stratified random sample designs, which will in turn allow true probabilities of success to be estimated. In addition, currently there have been no numerical attempts to measure the probability of recognition, P(r), the problem of recognition has been recognized but not quantized objectively. At the present time an interactive graphics computer program, SEARCHSIM, has been developed so that the effects of varying search grid and target sizes can be displayed graphically. Figure 33.1 is a copy of the Cathode Ray Tube graphic output of SEARCHSIM, a sample density of 1 site per 5 square units is assumed and the target approximated by an ellipse five times longer than it is wide. It should be noted that the Y axis is labelled "probability"; this is premature in terms of program development and should more correctly be titled "expectation". The plot shows the relationship between the target major axis length and expectation of a 'hit'. For example, it is seen from the plot, that a target would have to be larger than 6 units long by 1.2 units wide to be hit with better than 0.95 expectation.

The preceding topic assumes very little geological information, only that orientation studies have defined the target sizes and geochemical thresholds in a geographic area. Two alternate approaches may be employed which use different assumptions than those for grid size selection. In the determination of optimal grid sizes it is assumed that the local environment is heterogenous, i.e. targets within an area. In both the next methods to be described it is assumed that the geological or geographic units to be sampled are relatively homogenous, the task being to discriminate the units associated with mineral occurrences from those that are not, i.e. to separate the "productive" from the "barren". The methods focus on aspects and properties of the frequency distributions of the data in two different manners. These approaches assume that there is some genetic link between the mineralization and geological unit in question that will be reflected in the local geochemistry. If such a link is missing the two methods to be described are inappropriate. Comparing these methods with that of optimal grid selection, in the grid case the "hit" is a single sample, or a group of adjoining samples. In the cases to be discussed below the "hit" is a whole suite of samples which represent some specific unit, where the whole unit forms the "hit". It is possible that a subsequent review of the data for the unit may reveal the most favourable areas to commence the next stage of field work, but that is not the prime objective of this type of sampling design.

It has been noted by many workers that geological units characterized by geochemically complex data are often hosts to mineral occurrences, and that where geochemical data lack contrast there are usually no mineral occurrences. This relates to the concept of relief in geochemical data. A numerical expression of relief is the coefficient of variation of the data set, cv; this is usually expressed in percentage terms as

$$cv\% = 100.s/\bar{x}$$

where s is the standard deviation and $\bar{x}$ the mean of the suite of 'sample population' individuals collected from a specific geological unit or area. Coefficient of variation has been used in several studies (e.g. Garrett, 1972; Hornbrook and Garrett, 1976) as a numerical measure of geochemical relief or contrast. General rules of thumb are, that coefficients of variation below 70% correspond to areas of low geochemical relief and low mineral potential; while coefficients above 100% correspond to complex situations, due to heterogeneity of geology or secondary environment, or the presence of mineral occurrences. The coefficient of variation is related to normal distribution theory, very high or very low values indicate that the data are possibly not drawn from a normal distribution (Koch and Link, 1971).

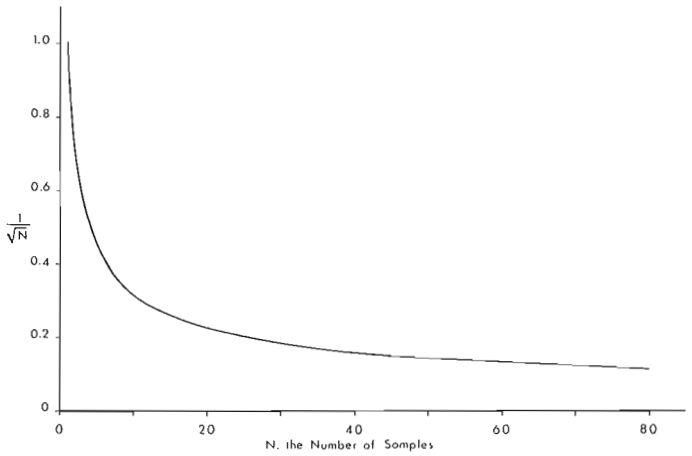


Figure 33.2. *Relationship of 1/N to N, the sample size.*

The question arises as to how many randomly selected samples should be collected from a geological unit, or area, to obtain precise estimates of the mean and standard deviation to be used to calculate the coefficient of variation. A measure of the reliability of the estimates of the mean and standard deviation are their standard errors. Respectively, $SE_{\bar{x}}$ for the mean, $\bar{x}$, and SE_s for the standard deviation, s, and where N is the number of individual samples collected and anlayzed.

$$SE_{\bar{x}} = \frac{s}{\sqrt{N}} \qquad \text{and} \qquad SE_s = \frac{s}{\sqrt{2N}}$$

From these two equations it is noted that the major control on standard error is the value of N and that the standard error of the standard deviation decreases twice as fast as that for the mean due to the 2N term in the denominator of the former. As the standard error of the standard deviation drops, and improves, twice as fast as the standard error of the mean, it need not concern us furthermore. Certainly if the standard error of the mean is acceptable that for the standard deviation will also be acceptable. Figure 33.2 shows the relationship between the controlling term, $1/\sqrt{N}$, and N. It can be seen that the controlling term drops very rapidly between 1 and 10, begins to level out around 30 and after 60 does not decrease significantly except with very large increases in N. Most statisticians agree that on empirical grounds to exceed 60 is probably passing the point of diminishing returns, i.e. the reductions in standard error do not justify the added costs. Often a figure of 30 is quoted as a more realistic value for N; the author has often used the value of 15 as a bare minimum in terms of the compromise between precise values for the mean and standard deviation and the costs of sample collection and analysis. The choice of the number of samples to be randomly collected to form the 'sample population' will depend upon the particular situation. However, Figure 33.2 puts the impact of the choice into easy graphical perspective, the improvement in precision can only be obtained by increased sampling and analysis, with their accompanying cost.

A technique for selecting optimal sample sizes, which makes no distributional assumptions, is used in the Soviet Union. The method is described by Beus and Grigorian (1977) and is based on tables published by Chernitskii (1957). It is unclear whether these tables are actually in the form reproduced in Beus and Grigorian, or, are simply tables of the cumulative binomial distribution. If the latter is the case, such cumulative tables are available in North America, e.g. from the Harvard Computation Laboratory. In practice a computer program, SMPSIZE, has been written to directly compute the tables necessary for geochemical use, these are presented and discussed below.

The method assumes that prior orientation work in areas, or geological units, that may be classified as 'barren' or 'productive' has been undertaken. The data distributions are plotted as cumulative frequency diagrams or histograms, as illustrated in Figure 33.3. The forms of the distributions are irrelevant, they may be normal, lognormal, mixtures or whatever. A threshold value T is chosen, such that the probability of a sample from the 'barren' population having a value above T is very small. The proportion of the 'productive' population falling above T is then noted. This proportion is the a priori probability of occurrence of a value > T. At this point Table 33.1 is entered at some desired probability of recognition, commonly the 0.95 level (as are the tables in Beus and Grigorian). The last item to be decided upon is how many samples, R, one wishes to have as a minimum to exceed the threshold T. If R, or more, of the N samples that Table 33.1 indicates should be collected exceed T in value then one can classify the unit as 'productive' at the appropriate probability of recognition. As an example, if the a priori probability of occurrence of a value greater than T, denoted, P, is chosen to be 0.10, the probability of recognition is chosen as, 0.95, and at least an R of three individual samples are to exceed T, then a total, N, of 61 randomly selected samples must be collected. If three or more of the 61 samples exceed T the unit is classified as 'productive' and further work planned; otherwise if less than three values exceed T the unit has to be classified 'barren'. In cases where there is a very clear distinction between the 'barren' and 'productive' data sets, such as with some pathfinder elements (e.g. Cd) or elements whose mineralogical form in the host rocks is the same as the ore minerals of interest, (e.g. W and Be), far fewer samples need be collected. An example would be that with an a priori probability of occurrence of 0.40, at a probability of recognition of 0.95, and wishing to obtain at least three samples again with values greater than the threshold, only 14 randomly collected samples are required. This latter example demonstrates the clear advantages of identifying appropriate pathfinder elements for deposit types whose major commodity is a ubitiquous element.

The technique would appear to have particular application to categorizing intrusive rocks or volcanic sequences such as found in Archean greenstone belts. Table 33.1 allows one to investigate the choice of increasing R (the minimum number of above threshold, T, individuals) or increasing the probability of recognition. If in the first example above R was

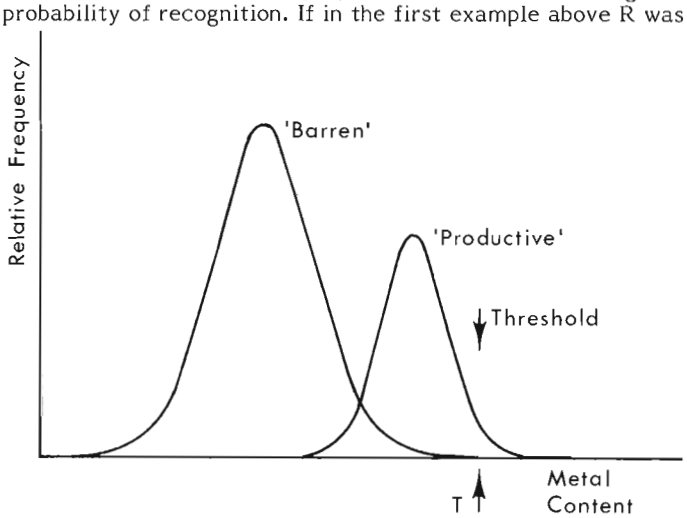


Figure 33.3. *Example of histograms for 'barren' and 'productive' units.*

increased to 4 a new total of 76 samples need to be collected and anlayzed for a decision at the 0.95 level. However, if R is held at 3 and the decision probability raised to 0.98, then 73 samples need to be acquired. In general, Table 33.1 reveals that it is less costly to increase the probability level associated with the decision than to increase the minimum number of above threshold samples. It should be noted that although the examples given above are for thresholds that are above the modes for the two distributions, the whole process can be reversed and the threshold be set to use very low values below the modes of the two distributions.

It is important to note that in both the latter two methods for sample size determination the samples from the unit should be selected randomly, i.e. giving all available parts of the unit an equal chance of being sampled. Collecting all the samples in one part of a unit and then using these to infer the properties of the whole is an invalid, and dangerous, procedure. A common approach is to grid the unit so that the appropriate number of samples may be collected, one from each grid cell or intersection. If this gridding technique is used and targets within the unit, rather than just associated with it, are expected, then the area of the target that would be intersected at some stated expectation can be estimated:

$$At = E(h).L^2.d$$

where At is the area of the target; E(h) is the expectation of a 'hit' (often set at 0.95); L is the side of the grid square; and d is the factor described previously (i.e. 1.08814). Once such an area has been estimated the linear form of the target can be approximated with a circle, ellipse or rectangle of equal area. However, this latter procedure is usually only of curiosity value as the targets may be buried within the unit or emplaced in other geological formations nearby.

Apart from the more general topic of coefficients of variation and their relationship to geochemical relief, the methods discussed in this section seem to be particularly applicable to lithogeochemical, soil/overburden and lake sediment surveys. Regional stream sediment surveys pose some different problems due to the formation of extensive

Table 33.1

Table of optimum sample sizes

OPTIMAL SAMPLE SIZES TO ENSURE THAT WITH STATED CONFIDENCE AT LEAST R ITEMS WILL EXCEED A VALUE T WITH PROBABILITY OF OCCURRENCE P

PROBABILITY OF RECOGNITION = .90
A PRIORI PROBABILITY OF OCCURRENCE, P

R	.01	.02	.03	.04	.05	.06	.07	.08	.09	.10	.12	.14	.16	.18	.20	.25	.30	.35	.40	.45	.50	.60	.70	.80	.90
1	230	114	76	57	45	38	32	28	25	22	19	16	14	12	11	9	7	6	5	4	4	3	2	2	2
2	388	194	129	96	77	64	55	48	42	38	31	27	23	21	18	15	12	10	9	8	7	5	4	4	3
3	531	265	176	132	105	88	75	65	58	52	43	37	32	28	25	20	16	14	12	10	9	7	6	5	4
4	667	333	221	166	132	110	94	82	73	65	54	46	40	36	32	25	21	18	15	13	12	9	8	6	5
5	798	398	265	198	158	132	113	98	87	78	65	56	48	43	38	30	25	21	18	16	14	11	9	8	7
6	926	462	308	230	184	153	131	114	101	91	76	65	56	50	45	35	29	25	21	19	17	13	11	9	8
7	1051	525	349	262	209	174	149	130	115	104	86	73	64	57	51	40	33	28	24	21	19	15	13	11	9
8	1175	587	390	292	234	194	166	145	129	116	96	82	72	63	57	45	37	32	27	24	21	17	14	12	10
9	1297	648	431	323	258	215	184	160	142	128	106	91	79	70	63	50	41	35	30	27	24	19	16	13	11
10	1418	708	471	353	282	235	201	175	156	140	116	99	87	77	69	55	45	38	33	29	26	21	18	15	13

PROBABILITY OF RECOGNITION = .95
A PRIORI PROBABILITY OF OCCURRENCE, P

R	.01	.02	.03	.04	.05	.06	.07	.08	.09	.10	.12	.14	.16	.18	.20	.25	.30	.35	.40	.45	.50	.60	.70	.80	.90
1	299	149	99	74	59	49	42	36	32	29	24	20	18	16	14	11	9	7	6	6	5	4	3	2	2
2	473	236	157	117	93	78	66	58	51	46	38	32	28	25	22	18	14	12	10	9	8	6	5	4	3
3	628	313	208	156	124	103	88	77	68	61	51	43	38	33	30	23	19	16	14	12	11	8	7	6	5
4	773	386	257	192	153	127	109	95	84	76	63	53	47	41	37	29	24	20	17	15	13	11	9	7	6
5	913	456	303	227	181	150	129	112	100	89	74	63	55	49	44	34	28	24	21	18	16	13	10	9	7
6	1049	523	348	261	208	173	148	129	115	103	85	73	63	56	50	40	33	28	24	21	18	15	12	10	8
7	1182	590	392	294	234	195	167	146	129	116	96	82	71	63	57	45	37	31	27	24	21	17	14	12	10
8	1312	655	436	326	260	217	185	162	143	129	107	91	79	70	63	50	41	35	30	26	23	19	16	13	11
9	1441	719	478	358	286	238	203	178	158	142	117	100	87	77	69	55	45	38	33	29	26	21	17	14	12
10	1568	782	521	390	311	259	221	193	172	154	128	109	95	84	76	60	49	42	36	32	28	23	19	16	13

PROBABILITY OF RECOGNITION = .98
A PRIORI PROBABILITY OF OCCURRENCE, P

R	.01	.02	.03	.04	.05	.06	.07	.08	.09	.10	.12	.14	.16	.18	.20	.25	.30	.35	.40	.45	.50	.60	.70	.80	.90
1	390	194	129	96	77	64	54	47	42	38	31	26	23	20	18	14	11	10	8	7	6	5	4	3	2
2	581	290	193	144	115	95	81	71	63	56	47	40	34	30	27	21	17	15	12	11	9	7	6	5	4
3	749	374	248	186	148	123	105	92	81	73	60	51	45	39	35	28	23	19	16	14	12	10	8	6	5
4	906	452	300	225	179	149	127	111	98	88	73	62	54	48	43	34	28	23	20	17	15	12	10	8	6
5	1055	526	350	262	209	174	148	129	115	103	85	73	63	56	50	39	32	27	23	20	18	14	12	9	8
6	1200	598	398	298	237	197	169	147	131	117	97	83	72	64	57	45	37	31	27	23	21	16	13	11	9
7	1340	669	445	333	265	221	189	165	146	131	109	93	81	71	64	50	41	35	30	26	23	19	15	12	10
8	1478	737	490	367	293	243	208	182	161	145	120	102	89	79	71	56	46	39	33	29	26	21	17	14	11
9	1614	805	535	401	320	266	227	199	176	158	131	112	97	86	77	61	50	42	36	32	28	23	19	15	13
10	1747	872	580	434	346	288	246	215	191	171	142	121	106	93	84	66	54	46	40	35	31	25	20	17	14

PROBABILITY OF RECOGNITION = .99
A PRIORI PROBABILITY OF OCCURRENCE, P

R	.01	.02	.03	.04	.05	.06	.07	.08	.09	.10	.12	.14	.16	.18	.20	.25	.30	.35	.40	.45	.50	.60	.70	.80	.90
1	459	228	152	113	90	75	64	56	49	44	37	31	27	24	21	17	13	11	10	8	7	6	4	3	2
2	662	330	219	164	130	108	92	81	71	64	53	45	39	34	31	24	20	16	14	12	11	8	7	5	4
3	838	418	277	207	165	137	117	102	91	81	67	57	50	44	39	31	25	21	18	16	14	11	9	7	5
4	1001	499	332	248	198	164	140	122	109	97	81	69	60	53	47	37	30	25	22	19	17	13	11	9	7
5	1157	577	383	287	229	190	162	142	126	113	93	79	69	61	55	43	35	30	25	22	19	15	12	10	8
6	1307	652	433	324	259	215	184	160	142	127	106	90	78	69	62	49	40	34	29	25	22	18	14	12	9
7	1453	725	482	360	288	239	204	178	158	142	118	100	87	77	69	54	44	37	32	28	25	20	16	13	11
8	1596	796	529	396	316	263	225	196	174	156	129	110	96	85	76	60	49	41	36	31	27	22	18	15	12
9	1736	866	576	431	344	286	244	213	189	170	141	120	104	92	83	65	53	45	39	34	30	24	20	16	13
10	1874	935	622	465	371	309	264	230	204	183	152	130	113	100	89	70	58	49	42	37	33	26	21	18	14

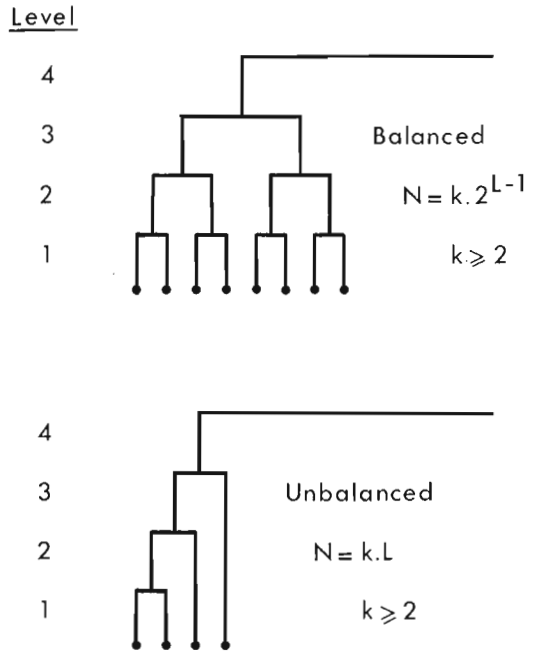


Figure 33.4. *Heirarchical sample designs.*

linear dispersion trains. Studies are currently underway using the techniques of autocovariance to investigate these dispersion trains and to determine the 'memory' of stream sediments in different physical environments and for different elements. A more formal determination of dispersion train geometry may eventually lead to numerical decision criteria for selecting sample spacings along stream drainages.

Evaluation Mode Considerations

In 'evaluation' mode surveys the ultimate objective is to produce a stable map which can be used to study systematic compositional changes. By stable is meant a map where local variability due to sampling and analytical sources is significantly smaller than variation across the area of interest. If the map is unstable, i.e. local variability is as large, or larger than, regional variability, systematic compositional changes will be unrecognizable. The classical method, or model, used to investigate such problems is analysis of variance (ANOVA), and the early applications in geology by Krumbein and Slack (1956) still stand as a landmark. Since that time Miesch and his coworkers in the Branch of Regional Geochemistry of the U.S. Geological Survey, Denver, have done much to develop the use of ANOVA methods in geochemical studies (e.g. Miesch, 1976). One of the major drawbacks of classical ANOVA studies has been the very large sampling and analytical load generated by multilevel studies of variability. In the past, except for some work at the U.S. Geological Survey, Denver, and at the Geological Survey in Ottawa, work has been largely restricted to the use of what are known as balanced designs (Fig. 33.4). In balanced sampling designs, samples are collected in equal replicates (usually pairs) at each level of the investigation. The notation used in Figure 33.4 is as follows: N is the total number of samples to be collected and analyzed, these consist of k replication groups each with L sampling levels of a nested, or hierarchical, layout. The number of replicated groups, k, has to be greater than two in order to assess the variability at the highest level. If the balanced design in Figure 33.4 described a bedrock study, then level 1 might represent analytical variation, level 2 variation in the outcrop, level 3 variation between outcrops a 100 m apart, and level 4 variation between groups of outcrops across the geological unit. Many package computer programs exist to handle such designs, but it can be seen that as the number of levels of variability increase, the number of samples required increases exponentially. In the four level design using pairs, multiples of 8 samples are required to study variability across a geological unit. Unbalanced designs are far more efficient in their use of survey resources, and in the four level example only multiples of 4 samples are required. The impact of using balanced (B) and unbalanced (UB) designs can be seen in Figure 33.5. The Y axis, N/K, of the figure is the number of samples needed for each replication of simple balanced (B) or unbalanced (UB) designs with the number of levels in the design increasing from 2 to 6. The relative efficiency of balanced versus unbalanced design can be obtained from the ratio UB/B and the right hand Y axis. For instance with a four level design the ratio is 0.5 and an unbalanced design requires only half as many samples as a balanced one. Unbalanced designs are particularly advantageous where greater than four levels are used and savings in sampling and analytical costs of 50 per cent and higher can be made. The problem in the past has been that the potential of unbalanced designs has not been publicized, and, perhaps more importantly, the more complex computer programs necessary to carry out unbalanced ANOVA studies have not been widely available. A computer program, UANOVA, to carry out the computations has been written in cooperation with Systems Approach Consultants Ltd. of Ottawa and will be published (Garrett and Goss, in prep.). It is hoped that the availability of this software to handle complex unbalanced data structures will encourage a greater use of ANOVA techniques in a variety of geological studies.

An application of unbalanced designs to regional reconnaissance surveys has been presented by Garrett and Goss (in press) and facets of the underlying statistical ANOVA model

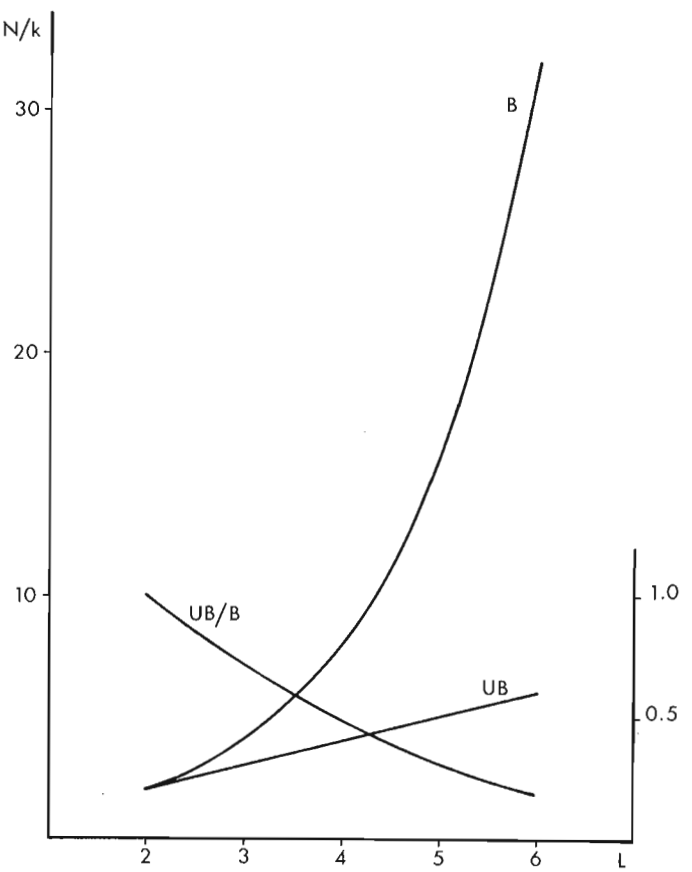


Figure 33.5. *Relationship of sample requirements to number of levels.*

Table 33.2

Analysis of variance to determine significance of variance components for uranium in the northwestern Ontario area

Variation Between	Sum of Squares	df	Mean Squares	Unit Size	Variance Component	V.C. %	Error Mean Squares	Error df	Approx F	Signif
Cells	320.73478	1679	0.19103	1680	0.101481	61.05	0.07054[1]	108.47[1]	2.71	>.999
Lakes in Cells	9.73124	105	0.09268	1785	0.059743	35.94	0.00525[1]	118.55[1]	17.67	>.999
Samples in Lakes	0.57682	105	0.00549	1890	0.001907	1.15	0.00309	105.00	1.78	.998
Analyses in Samples	0.32447	105	0.00309	1995	0.003090	1.86				
Total	331.36731	1994			0.166221	100.00				

[1]Error mean square synthesized and degrees of freedom computed by Satterthwaites (1946) formula

and assumptions by Goss and Garrett (in press). In 1977 the sampling design of the National Geochemical Reconnaissance lake sediment surveys carried out on the Canadian Shield was modified so that the proportion of the variation at regional, 13 km^2 grid cell, within lake and analytical levels could be determined. The design was essentially similar to that used as an example for the unbalanced case in Figure 33.4. The results of data for uranium in the 1977 Ontario survey are presented in Table 33.2. The distribution of the variability reveals some 61 per cent of the variation to be between the 13 km^2 cells, (i.e. regional), 36 per cent is due to lakes in cells, and the remaining 3 per cent is due to the effects of within lake sampling and analysis. These results are not too different in trend from those obtained for all 1977 lake sediment surveys where it was observed that some 65 per cent of the uranium variation was at the regional level, 30 per cent at the 13 km^2 level and the remaining 5 per cent at the within lake and analytical level. From the work so far carried out in exploration geochemistry it is clear that analytical variability is a very small contributor to the total variation in all but those trace elements, such as As, Hg and Ag, whose analysis at abundance levels is most difficult.

The old balanced designs lead to an abundance of anlayses at the lowest level where, in general, there is only a small portion of the total variability. This is wasteful of resources and it would be more useful to have larger numbers of samples analyzed from levels higher in the design so increasing the statistical degrees of freedom at those levels. The unbalanced design has just this effect and it can be seen in Table 33.2 that for the lowest three levels the degrees of freedom (df) are all equal, in fact corresponding to the number of blocks (replications) of data used in the example. The example in Table 33.2 also demonstrates a type of unbalanced layout, known as an inverted design (Bainbridge, 1963). In balanced ANOVA designs there are always more degrees of freedom at the bottom of the design, usually where they are not needed. In an inverted design there are more degrees of freedom at the top where they are most needed. In a regional survey the degrees of freedom at the top of the inverted design are mostly due to the samples collected singly from grid cells without any replication.

Apart from the establishment of the relative variability in the data, the variance components for each level can be tested to determine if they are significantly different from zero. If they are not significantly different from zero, then it is probable that the variation at that particular level can be explained by variation at lower levels. In the Table 33.2 example it can be seen that variation at the level of samples in lakes (level 2) is small and in part is due to the analytical variation. Following similar findings in the other areas where lake sediment surveys were carried out in 1977 for the National Geochemical Reconnaissance replication at this level (2) will probably be discontinued after 1978. At the level of variation between lakes within 13 km^2 grid cells (level 3) there is significant variability relative to the within lake and analytical components. From this it may be inferred that the sample density could be increased, if so desired, and the resolution of the geochemical map improved as there are mappable geochemical features at finer than 13 km^2 scale. Again this is not an unexpected situation in the relatively geologically heterogenous area of Shield rocks of the survey area. Finally, at the regional level, the variability is highly significant in terms of the lower local variability. This knowledge can only give one confidence in the geochemical map resulting from the survey and make one confident that the regional variations are real geochemical phenomena and not the result of random variation at local and analytical levels.

Traditionally, ANOVA techniques found their greatest application in orientation and sampling design studies, not in actual surveys, due to the very large overhead imposed by use of classical balanced designs. With the introduction of unbalanced designs, it has become feasible to use the ANOVA model as a quality control tool to continuously monitor relative variability and significance in large regional geochemical surveys. The main criteria for selection of sample densities in these surveys is a knowledge of the size of the dispersion targets being sought and the availability of funds. The information gained from using the ANOVA model as a quality control tool will allow modifications to be made to the basic sampling design evolved from orientation surveys. This can be particularly important if orientation survey data are expanded in application to cover geological and physiographic environments somewhat dissimilar to the original orientation area. Nothing can usually be done to put right a survey that has gone wrong, but the quality control monitoring should at least prevent making the same mistakes a second time.

The Combined OR-ANOVA Model

The techniques described for selecting grid size and the selection of minimum sample sizes via binomial probability may be considered Operations Research (OR) methods. They allow the planning of apparently optimal sample designs after orientation studies and before major surveys. In all likelihood the actual survey will not work out exactly as predicted and it would be beneficial to be able to assess the success of the survey after it has been carried out.

The combined OR-ANOVA model is an attempt to make use of the pre- and post-survey information and combine it to create an a posteriori probability of success for finding a particular target. The purely geometric aspect of estimating the probability of a sample falling within a dispersion halo is

combined with an empirical ratio derived from an unbalanced ANOVA model, which provides an a posteriori estimate of the probability of recognition. The product of these two probabilities will give an estimate of the a posteriori probability of success of a survey. Interest in this parameter is not purely academic. Areas for regional geochemical reconnaissance are commonly chosen because of geological indications that significant mineral occurrences are present. After a survey has been executed, and no promising results obtained, the question arises: is the area devoid of significant mineral occurrences detectable by the particular geochemical method, or was the survey technically insufficient? If the a posteriori probability of success was high and the survey well designed, then one would have to accept the hypothesis that it is unlikely, at some stated confidence level, that detectable significant mineral occurrences exist, and, it would be a poor decision to continue certain kinds of work in the area. Or alternatively, that the original assumptions as to the mineral potential of the area were wrong. Conversely, if the a posteriori probability was low, then it would have to be accepted that one way or another the survey was poor and should not be used alone, or at all, to write off an area as being unworthy of further work.

The combined OR-ANOVA model is put into the context of national regional geochemical surveys in Figure 33.6. These surveys are commonly multielement but 'tuned' for a particular element in a particular environment, and, as a result, they will be inadequate for some elements and overkill for others. It could be argued that the decision tree shown is idealistic in the sense that the maps or data will be published

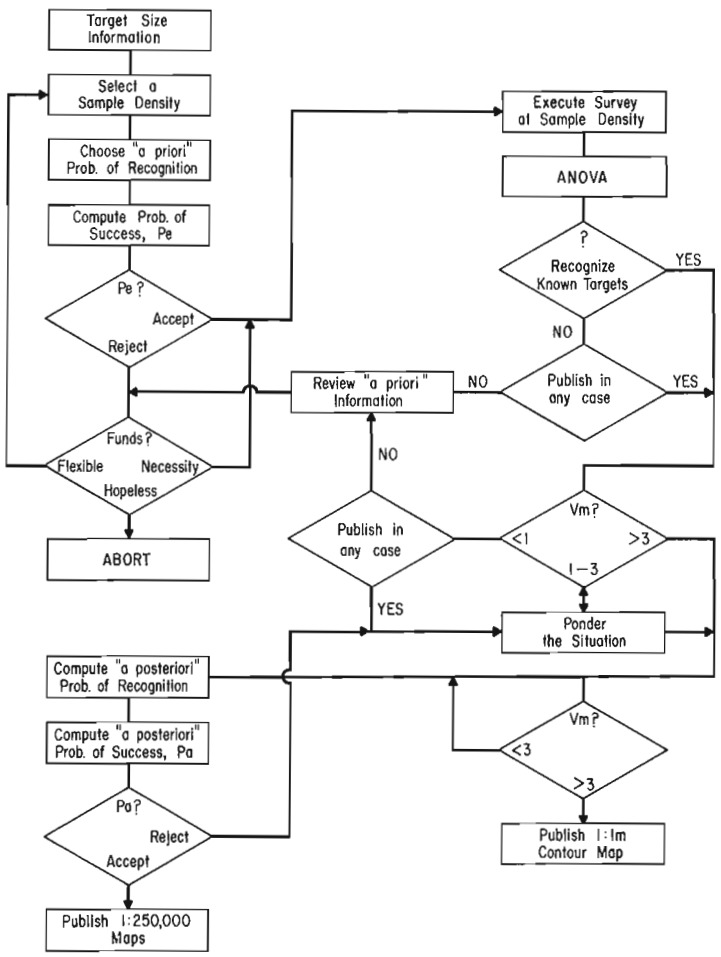


Figure 33.6. *The combined OR-ANOVA model.*

in any case. However, as unflattering as the tree is in places, it is probably close to reality. Even though a survey may have an associated probability of success that is low, this does not invalidate the map as a prospecting tool. Anomalous, above threshold, patterns should lead to mineral occurrences with correct follow-up procedures. In that sense, the survey can be deemed a success; however, in the absence of those successes, it would be extremely unwise to write the area off purely on the basis of such a geochemical survey.

Two numerical steps in Figure 33.6 need additional comment. A parameter V_m is introduced as being important, particularly in the decision as whether to publish 1:1 million scale contour maps. V_m is a measure of map stability proposed by Miesch (1976). This empirical variance ratio is derived from the ANOVA model and has proved to be a good practical guide to reliable (i.e. reproducible) contour map construction. Experience has shown that surveys yielding V_m ratios in excess of 3 lead to stable maps. Where lower values of V_m are found it is unsound policy to publish contour maps as replicate surveys for the area would very probably yield significantly different maps. Additionally, in such a case it would be unwise to continue with any sophisticated data analysis or production of derivative maps. In certain cases maps of greater stability, but lower resolution, can be prepared by using the means of blocks of adjacent data (Miesch, 1976). A low V_m would not invalidate some other kind of map at survey scale, say 1:250 000, using a symbolic or numerical presentation; however, one would be less confident in making geochemical or geological inferences as to the true patterns of regional variation from those maps.

The second numerical step needing additional comment is the flow from the ANOVA results to an a posteriori probability of recognition. This step is the subject of current research and the following method is only tentative. Empirical variance ratios are excellent guides to relative variability and are easily derived from the variance components computed in the ANOVA. Using the lake sediment survey case (Table 33.2) as an example, two ratios, V_1 and V_2, can be calculated that have some geochemical meaning. Let v_1, v_2, v_3, and v_4 respectively be the components of variance for the analytical, within lake, within cell and regional levels; and v_{123} be the sum of the of the components from the analytical up to the within cell level, and v_{12} be the sum of up to the within lake level, then

$$V_1 = v_4/v_{123}$$

and

$$V_2 = v_3/v_{12}$$

If V_1 is high, then most of the variation is regional, between cells, rather than local within cells, and a reliable map is derived from the data, in general values above 1 are at least adequate. Even if V_1 is low, the map is not worthless from a prospecting viewpoint. V_2 is a measure of the reliability within a cell, i.e. how good is the map at revealing local variation patterns. Again with V_2, as with V_1, one would hope to obtain high values, inferring that the variability due to sampling in a single lake, and analysis, is small. These two ratios, V_1 and V_2, intuitively seem to be useful as a guide to the probability of recognition, P(r), and could be used in an appropriate function, f,

$$P(r) = f(V_1, V_2)$$

However, the empirical variance ratios, V terms, are somewhat inconvenient as they range from zero to infinity. A convenient transform can be used, the inverse Fisher, to convert them to the range zero to one. Let x be the appropriate value of V_1 or V_2 and Z_1 or Z_2 be the corresponding transformed values, then

$$Z = (e^X-1)/(e^X+1)$$

Now the previous function can be rewritten

$$P(r) = f(Z_1, Z_2)$$

and two obvious candidates for explicit calculation of the function are

$$P(r) = Z_1.Z_2$$

and

$$P(r_2) = a_1Z_1+a_2Z_2$$

where a_1+a_2 are weights and sum to one. In both explicit functions P(r) will take on a value of between zero and one. In the case of the test data in Table 33.2, the corresponding values of P(r) are 0.65, and 0.83 if the weights a_1 and a_2 are equal, i.e. both 0.5 (Table 33.3). In terms of prospecting, local reliability may well be more important in leading to a mineral occurrence than broad scale regional reliability. If a_1 and a_2 reflect this by local reliability being thrice as important, i.e. $a_1 = 0.25$ and $a_2 = 0.75$, then a value for P(r) of 0.91 is obtained. If this result is applied to the demonstration case in Figure 33.1, i.e. the expectation of a 'hit' on a target, E(h), 6 units long by 1.2 units wide is 0.95, the actual expectation that the 'hit' will be recognized as such is the product of E(h) and $P(r_2)$, i.e. 0.86, which is approximately 9 times out of 10. Note that regardless of the target size, E(h) can never exceed 1.0; therefore, the expectation of recognition can never exceed P(r), which in this example is 0.91. This intuitively seems to be an underestimate, for if there were a cluster of sample sites within the target some at least would be recognized. This topic remains to be investigated in greater depth.

Practical experience with the combined OR-ANOVA model will have to reveal its true value. The most tenuous step at the moment is in the derivation of the a posteriori probability of recognition. The procedure outlined above is simplistic and direct. An alternative method, yet to be investigated, is one using Bayesian probability, which may prove to be the better method. It is planned to investigate the 1977 and 1978 National Geochemical Reconnaissance data using the OR-ANOVA model; this should shed light both on the reliability of the maps and data, and the model. The evaluation will have to be empirical as the truth as to the actual mineral resource endowments of the survey areas is not known.

Table 33.3

Generation of P(r)

$v_4 = 0.101481$

$v_3 = 0.059743$

$v_2 = 0.001907$

$v_1 = 0.003090$

$v_{123} = 0.064740$

$v_{12} = 0.004997$

$V_1 = v_4/v_{123} = 1.5675$ and $Z_1 = 0.6549$

$V_2 = v_3/v_{12} = 11.9558$ and $Z_2 = 1.0000$

$P(r_1) = Z_1.Z_2$

$R(r_2) = a_1Z_1+a_2Z_2$

Therefore $P(r_1) = 0.65$

and $P(r_2) = 0.83$ with $a_1 = a_2 = 0.5$

and $P(r_2) = 0.91$ with $a_1 = 0.25$ and $a_2 = 0.75$

Acknowledgments

The author would like to express his thanks to E.M. Cameron, T.I. Goss, E.H.W. Hornbrook and A.T. Miesch who have over several years discussed sampling problems with interest. Their criticisms and suggestions have helped in the formulation of the opinions written here, however, these remain the sole responsibility of the writer.

References

Bainbridge, T.R.
1963: Staggered nested designs for estimating variance components; American Society for Quality Control, Annual Conference Transactions, p. 93-103.

Beus, A.A. and Grigorian, S.V.
1977: Geochemical Exploration Methods for Mineral Deposits; Applied Publishing Ltd., 287 p.

Chernitskii, P.N.
1957: Probability Tables, Voenizdat, Moscow.

Garrett, R.G.
1972: Regional geochemical study of Cretaceous acidic rocks in the northern Canadian Cordillera as a tool for broad mineral exploration; Geochemical Exploration 1972; Institute of Mining and Metallurgy, London, p. 203-219.

1977: Sample density investigations in lake sediment geochemical surveys of Canada's uranium reconnaissance program. Hydrogeochemical and Stream Sediment Reconnaissance (HSSR) Symposium; U.S. Department of Energy, Grand Junction, p. 173-185.

Garrett, R.G. and Goss, T.I.
The evaluation of sampling and analytical variation in regional geochemical surveys; Geochemical Exploration, 1978. (in press)

Ghosh, B.
1951: Random distances with a rectangle and between two rectangles; Bulletin of the Calcutta Mathematical Society, v. 43(1), p. 17-24.

Goss, T.I. and Garrett, R.G.
A new unbalanced nested ANOVA model in geology – a down-to-earth design; Journal of the American Statistical Association. (in press)

Harvard Computation Laboratory
1955: Tables of the Cumulative Binomial Probability Distribution; Harvard University Press.

Hornbrook, E.H.W. and Garrett, R.G.
1976: Regional geochemical lake sediment survey, east-central Saskatchewan; Geological Survey of Canada, Paper 75-41, 20 p.

Koch, G.S., Jr. and Link, R.F.
1971: The coefficient of variation – a guide to the sampling of ore deposits; Economic Geology, v. 66(2), p. 293-301.

Krumbein, W.C.
1960: The "geological population" as a framework for analysing numerical data in geology; Liverpool and Manchester Geological Journal, v. 2(3), p. 341-368.

Krumbein, W.C. and Slack, H.A.
1956: Statistical analysis of low-level radioactivity of Pennsylvanian black fissile shale in Illinois; Geological Society of America Bulletin, v. 67(6), p. 739-762.

Matern, B.
1960: Spatial variation; Statens Skogsforskningsinstitut Band 49(5), 144 p.

Miesch, A.T.
1976: Geochemical survey of Missouri – methods of sampling, laboratory analysis and statistical reduction of data; U.S. Geological Survey Professional Paper 954-A, 39 p.

Rosenfeld, M.A.
1954: Petrographic variation in the Oriskany Sandstone; Geological Society of America, v. 65(10), p. 1298-1299.

Satterthwaite, F.E.
1946: An approximate distribution of estimates of variance components; Biometrics, v. 2(2), p. 110-114.

Savinskii, I.D.
1965: Probability tables for locating elliptical underground masses with a rectangular grid; Consultants Bureau, New York, 110 p.

FLOW MECHANISMS OF ARCHEAN SUBAQUEOUS BASALT AND RHYOLITE FLOWS

E.M.R. Research Agreement 2239-4-23/78

Erich Dimroth[1], Pierre Cousineau[1], Maxime Leduc[1],
Yves Sanschagrin[1], and Gilles Provost[2,3]

Dimroth, E., Cousineau, P., Leduc, M., Sanschagrin, Y., and Provost, G., Flow mechanisms of Archean subaqueous basalt and rhyolite flows; in Current Research, Part A, Geol. Surv. Can., Paper 79-1A, p. 207-211, 1979.

Abstract

Detailed mapping of Archean submarine basalt and rhyolite flows, and comparison, on the one hand, with Pleistocene pillow basalts and rhyolite hyaloclastite, on the other, with the formation of pillows and pillow breccias at the shoreline of Hawaii, has revealed surprising analogies, and has permitted detailed reconstruction of flow mechanisms. Flows surge from the feeding fissure to form a proximal domain of massive lava; in lava plains the massive facies occupies a pancake-shaped area centred on the feeding fissure, in rugged terrain the massive facies occupies leveed braided master channels. The levee facies contains strips of collapsed lava tubes oriented downslope from the levee. Large lava tubes (megapillows) branch from the massive domain; they subdivide downcurrent into curved second- and third-order distributaries. Lava sacs budded from the curving lava tubes. Under certain conditions (viscous lava, shallow water) flow-front pillow breccias advanced as delta-lobes showing foreset bedding on a very large scale.

Differences between rhyolite and basalt flows (thickness and extent, diameter of pillows and tubes) are the result of the higher viscosity of rhyolite. Differences between Archean and Recent pillows (few hollow tubes, large proportion of separated sacs, absence of distinct surface sculpture) are the effect of higher flow rates.

Pillows, Recent and Archean

Geometry

Most pillows observed during formation along the shoreline of Hawaii (Moore et al., 1973; Moore, 1975) and in the ocean flow (Ballard and Moore, 1977) are branching and curving tubes, and sac-like structures budding from such tubes and connected to them. The pillows form by spreading of cracks at the pillow surface. They have a characteristic surface sculpture, namely corrugations parallel to the spreading direction and small fault-scarps (1-5 cm) parallel to the open cracks from which pillows spread.

It is difficult to reconstruct the three-dimensional shape of Archean pillows. However, pillow mapping and observations at a few exceptional outcrops have permitted the following conclusions: (1) most of the very large pillows (megapillows, diameter larger than 3 m) are tubes, but tubes of smaller diameter are present. Most tubes are curved bodies, but some are straight; they bifurcate downcurrent. (2) Many pillows are interconnected; sacs connected to one another or to tubes are common. (3) Closed lava sacs are much more common in the Archean than in the flows observed during active advance. We know that these are indeed closed sacs, because we have removed a few entire pillows from favourable outcrops.

Flow Structures and Vesiculation

The flow structures and the distribution of vesicularity of Holocene pillows have not been described by Moore and his coworkers. The senior author, therefore, has observed them in Pleistocene and Oligocene pillows. Phenocrysts and microphenocrysts in Cenozoic and Archean pillows commonly show flow lamination in a zone several centimetres wide at the pillow margin. Recumbent flow folds have been observed in this flow-laminated zone.

Vesicles are concentrated at the pillow rim; not uncommonly several well vesiculated ribbons alternate with poorly vesiculated material. Vesicularity decreases toward the pillow centre whereas vesicle size decreases. Vesicles are concentrated (but are not restricted to) the upper part of pillows. Pipe vesicles, if present, dominate on the pillow base. These observations are valid for Archean and Cenozoic pillows.

Quench Crystals and Thermal Fractures

Pillows are covered by a glass crust. A few minute plagioclase quench crystals overgrown by spherulites are present at the base of the glass crust. Inward these coarsen and become more numerous until a spherulitic fabric is established. Farther inward a microlitic fabric of large plagioclase quench crystals showing a dendritic overgrowth develops and this gives way to a fully microlitic fabric in the core of the pillow.

The glass crust is intensely crackled; thermal fractures are conchoidal and, in general, are subconcentric. The concentric fracture pattern here and there persists to the pillow core. The pillow core fractured into irregular polygons or in a system of radiating columns. These fracture patterns are superposed on the concentric pattern.

Textures and structures defined by quench crystals and fracture patterns are identical in Archean and Cenozoic pillows. The feldspar spherulites grew across thermal contraction cracks; thus, they formed during very early devitrification.

Differences of Archean and Ballard-Moore (1977) Pillows

Hollow tubes and shelved tubes are much less common in the Archean than in the environments described by Moore and his coworkers. On the other hand, separated lava sacs appear to be much more common in the Archean. Furthermore, none of the distinct surface sculptures described by Moore was observed, although we have been able to examine hundreds of square metres of exposed pillow crust.

[1] Sciences de la Terre, Université du Québec à Chicoutimi, Chicoutimi, Québec.

[2] Département de Génie Minéral, École Polytechnique, Montréal, Québec.

[3] Present Address: Serem Ltée, 179 rue Perreault, Val d'Or, Québec.

We believe that these features indicate that Archean pillows formed at flow rates greater than flow rates of pillows observed in formation. Moore (1975) states that the small fault scarps on the pillow surface are characteristic of slowly forming pillows and at higher flow rates are replaced by corrugations parallel to the spreading direction. Low viscosity of the lava and high spreading rates should reduce the amplitude of corrugations; very small corrugations would not be preserved in the metamorphosed Archean pillows.

Moore (1975) also observed detachment of pillows, when a wide plastic zone formed at the spreading crack at high rates of lava flow. Thus, the large number of detached pillows in the Archean also may be interpreted as an effect of high flow rates. The absence of hollow tubes and of shelved tubes, except in well defined positions, also points toward high flow rates.

Structures, Analogous to Pillows in Subaqueous Rhyolites

The lava pods, lobes, and tongues of Pleistocene subaqueous rhyolite flows have been described by Saemundsson (1972) and Saemundsson and Noll (1974) and have been investigated in detail by Fridleifsson and his coworkers (Fridleifsson, pers. comm., 1977, 1978). Since Fridleifsson's data are unpublished I will not comment upon the Pleistocene acidic flows beyond the statement that personal examination of outcrops and thin sections by the senior author has confirmed that they are identical to the lava pods, lobes, and tongues in the Archean submarine rhyolite flows of Rouyn-Noranda area described by de Rosen-Spence (in Goodwin et al., 1972; de Rosen-Spence, 1976) and Dimroth et al. (1975). These structures were interpreted as analogs to pillows by Saemundsson (1972), Saemundsson and Noll (1974), and Fridleifsson (pers. comm., 1977, 1978). Andrée F. de Rosen-Spence (pers. comm., 1972) interpreted Archean breccias as hyaloclastites, an interpretation accepted by Dimroth et al. (1975). The analogies of these structures to basalt pillows in the following description are so obvious that they will not be pointed out specifically.

Geometry

In cross-section pods are elliptical, irregularly bounded masses of rhyolite lava with a diameter exceeding 10 m. Lobes are tabular sheets of lava, one to several metres thick and up to 100 m long, tongues are finger-shaped bodies of lava, 50 cm to 2 m thick and several metres long. The three-dimensional shapes of these structures are unknown, but are clear if compared with the structures of Holocene rhyolites in Iceland; pods and tongues largely are separated bodies, lobes are sheet-flows.

Flow Structures and Vesiculation

A very pronounced flow structure defined by the orientation of feldsapr microlites, by vesiculation, and by flow lamination is present in a zone 30-100 cm thick, at the margin of lava pods, lobes, and tongues. Most common is an alternation of bands, several centimetres thick of strongly vesiculated material (vesicularity > 50%; pumice) and dense, nonvesiculated or poorly vesiculated material. Flow lamination, shown by discontinuous streaks of globulite, can be demonstrated to have formed by the drawing out of vesicles during shear-flow. Vesicularity decreases rapidly toward to core of pods, lobes, and tongues.

Crystallization Textures and Thermal Fractures

The outer skin of Archean rhyolites is characterized by isolated albite spherulites. Inward, the spherulites coalesce, and then give way first to arborescent, then to felsitic, textures. Comparison with Pleistocene material from Iceland allows the origin of these textures to be determined: albite spherulites are formed by albite overgrowth during devitrification on multi-branched, star-shaped, hollow intergrown plagioclase needles; arborescent albite are formed by secondary albite overgrowth on hollow dendritic growth forms. Overgrowth occurred during devitrification.

The outermost skin of well preserved rhyolites shows intense thermal fracturing. Poorly vesiculated material show the conchoidal and perlitic fracture pattern characteristic of hyaloclastic granulation (Fig. 34.1). Breakage is between vesicles in well vesiculated material, whether mafic or acidic (Dimroth, 1977).

Basic Organization of Flows

Mafic Flows

Most flows have a proximal domain composed of massive lava, close to the feeding fissure. In many cases this proximal domain has a pancake-shaped geometry. It grades outward into a pillowed facies, first composed of very large pillows (megapillows), then of large pillows set in predominantly normal-sized pillows, finally into pillows of normal size. This facies gradation is consistent with the interpretation of the downcurrent flow changes outlined in the abstract.

Not uncommonly, the massive facies occupies linear channels of a braided geometry. These are bounded by a facies composed of pillows isolated by strips of a pillow breccia that has peculiar composition; it is composed exclusively of fragments derived from the outer zone of pillows, whereas fragments derived from the microlitic interior are absent. We interpret these strips as remnants of collapsed lava tubes. The strips are oriented so as to indicate flow laterally downward away from the master channels. This levee facies occupies a zone, several tens of metres wide, marginal to the massive channels. Pillowed basalt, most commonly megapillows set in predominantly normal-sized pillows, occupy the areas between the channels and their levees. The interpretation of the origin of this organization also follows from the abstract. The pillowed facies adjoining a channel-levee complex is thought to be fed by tubes branching from the channel farther up-current. The levee facies is fed laterally by flow sideways over the brink of the channel.

Mafic Flow Fronts

Most mafic flows have pillowed flow fronts. However, we have mapped flow front pillow breccia. Such breccia consists of lobes and tongues of massive lava (=megapillows) alternating with a breccia consisting of pillows and pillow fragments set in a hyaloclastite matrix. The flow front breccias show foreset bedding analogous to the foreset bedding of rhyolite flows (Fig. 34.2). Mapping has demonstrated that flow fronts advanced as lobes one or several 100 m across. Flow front breccias consist of complete pillows and fragments derived from complete pillows; evidence for collapse of hollow tubes was not common.

Rhyolite Flows

Rhyolite flows show, in a telescoped form, exactly the same facies distribution as mafic flows, except for the absence of a facies exclusively composed of structures analogous to pillows. Thus massive rhyolite grades laterally into a facies composed of isolated lava pods, lobes, and tongues set in a microbreccia or breccia. The breccia and microbreccia consists of a matrix of pumice shards and granules, analogous to the individual fragments in the crackled skin of pods, lobes, and tongues, into which are set fragments, 1 to 30 cm across, of lithic material showing all

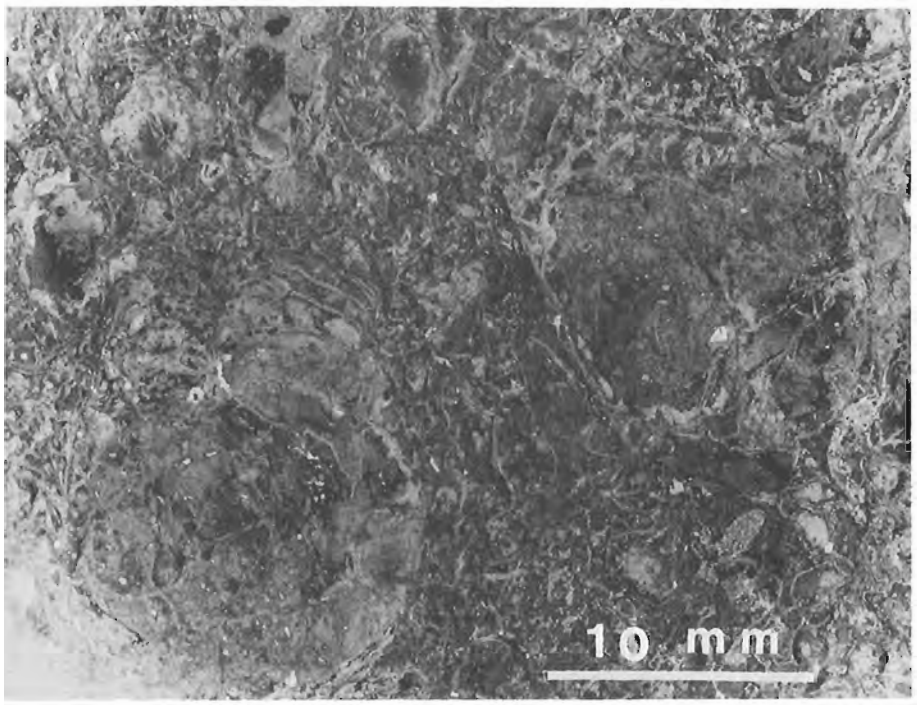


Figure 34.1.

Typical fracture pattern of in situ granulation in rhyolite hyaloclastite. Note large (15 mm) granulated globules bounded by perlitic fractures (lower left and upper right) and the conchoidal fracture patterns of thermally shocked glass. Section ARCHY-1, Destor township.

the crystallization textures (spherulitic, arborescent, felsitic) characteristic of the interior part of pods, lobes, and tongues. Lava, fragments, and hyaloclastite contain phenocrysts of the same size and morphology in equal proportion, thus are all derived from one homogeneous magma.

The pods, lobes, and tongues show flow folding that indicates flowage downward toward the flow front (Dimroth et al., 1975; Provost, 1978). Their arrangement and the layering of breccias suggest foreset bedding in advancing, overlapping lobes several 100 m wide, just as in the mafic flow front breccias. Figure 34.2 shows, in schematic form, a typical cross-section through a rhyolite flow.

Rhyolite flows differ from mafic flows in the following features: (1) they are thicker and less extensive; (2) lava pods, lobes, and tongues are larger than pillows; (3) the flow laminated skin on pods, lobes, and tongues is much thicker in rhyolite than basalt; (4) vesiculation in the strongly vesiculated bands is larger; (5) the hyaloclastite contains pumice fragments as well as nonvesiculated granules. These features are clearly functions of the greater viscosity and higher water content of acidic magmas. Structures and textures of the rhyolite flows are incompatible with their interpretation as pyroclastic rocks proposed by Gélinas et al. (1978).

Modification of Basic Organization

Composite flows, vertical structure sequence in simple flows and hyalotuffs are described below.

Composite Flows

Detailed mapping demonstrated that, in basalts and andesites, simple flows, well defined as separate flows at one locality, grade laterally into a single flow. The results of mapping indicate that flows advanced as overlapping lobes. A single flow formed where lava advance was continuous, an ensemble of several well defined simple flows (that is a composite flow) formed where advance was discontinuous. Tubes and pillows can be interpreted as individual, simple, flow units, as has been done by Ballard and Moore (1977).

Vertical Structure Sequence in Simple Flows

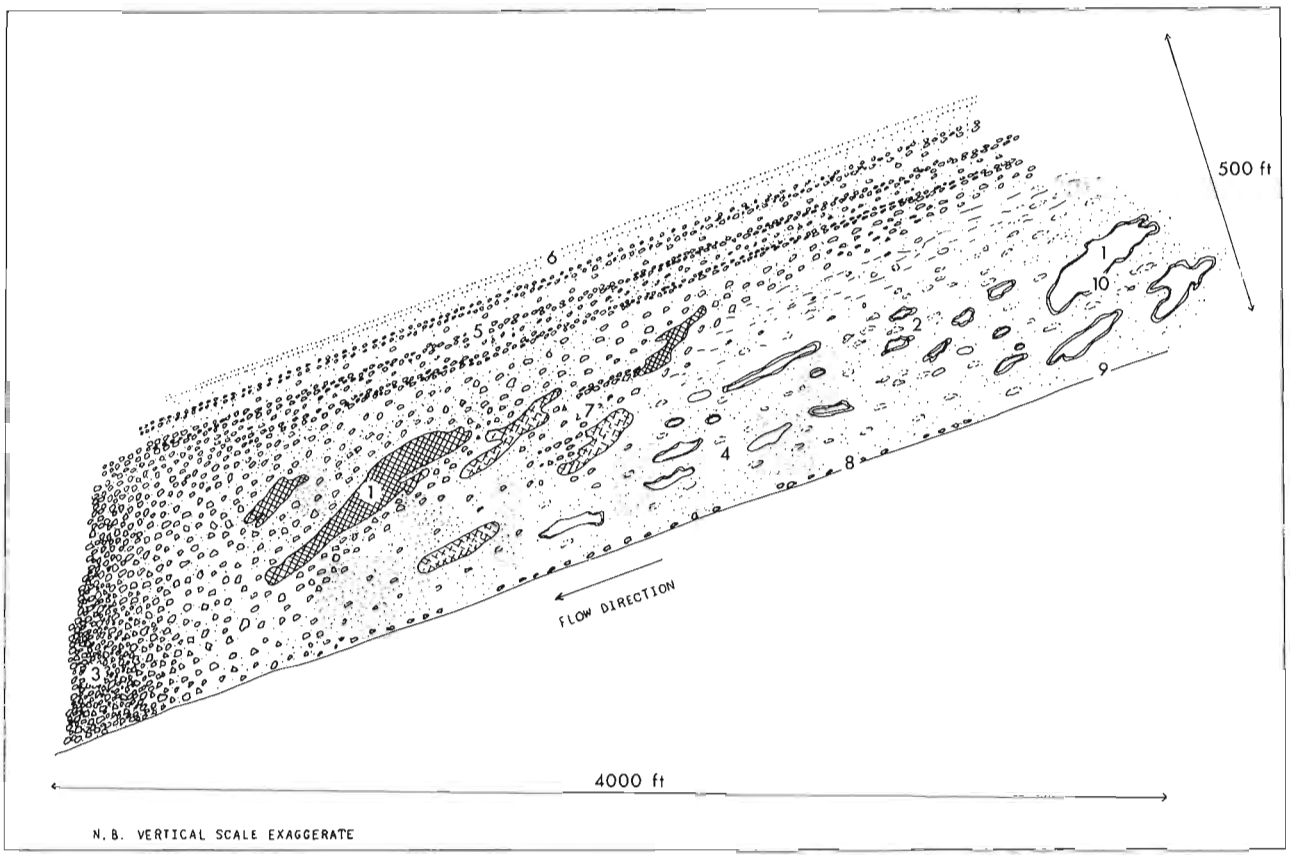
Dimroth et al. (1978) defined vertical structure sequences in simple flows: in particular flow-top pillow breccia commonly overlies a massive division; less commonly pillows may separate a massive flow-base from a flow-top pillow breccia. Commonly, pillow breccia also overlies mainly pillowed flows.

In the light of the model proposed above, these vertical sequences can be explained by changes in the rate of lava flow and by changes in lava viscosity. Vertical transition of massive into pillowed and finally brecciated rocks or analogous transitions (see Dimroth et al., 1978 for details) can be related to decreasing rates of flow of increasingly viscous lava during the terminal stage of the emplacement of each simple flow.

Hyalotuff

Hyalotuffs consist of whole pillows or, more commonly of pillow fragments set in a matrix of hyaloclastic granules or the equivalent vesiculated material (see Dimroth, 1977 for the petrography). In acidic rocks, hyalotuffs consist of the same materials as breccias or microbreccias. They show the typical structure sequences of subaqueous mass-flows (Walker, 1976; Rocheleau and Lajoie, 1974).

Dimroth et al. (1978) interpreted hyalotuffs as the product of submarine lava fountaining at a depth shallow enough to permit some explosive activity, but deep enough to prevent intense explosions of Surtsey-type. We propose an analogous interpretation for the rhyolitic hyalotuffs. Of course, some hyalotuffs may simply be the product of slumping of unstable piles of pillow breccia. However, considering that the relief of the Archean terrain demonstrably was relatively subdued (slopes generally less than 10°, Dimroth et al., 1975, 1978; Spence, 1976), slumping probably is only a minor source of hyalotuff. Furthermore, the common association of hyalotuff with evidence (like high vesicularity) of shallow water at the eruptive centre, points to an explosive origin for this rock.



White: *Lava, pods, lobes, and tongues (analogous to pillows) and their flow-ribboned and flow laminated margin.*

Cross-hatched: *pods, lobes, and tongues showing strong in situ brecciation.*

Stippled: *microbreccia.*

Block signature: *breccia; layered top: hyalotuff and hyalobreccia. Breccia and microbreccia are analogous to the pillow breccia of mafic flows.*

Figure 34.2. *Typical structure of the distal part of a rhyolite flow. Note the foreset-bedding of lobes and breccias. Based on the No. 5 flow of the Don rhyolite Complex (Provost, 1978).*

Hyalotuffs overlie only a minority of the mafic and rhyolite flows. Specifically, they occur rather consistently at the top of nearly all flows originating from a few well-defined centres. Flows originating from the majority of eruption centres in Rouyn-Noranda area are not overlain by hyalotuff. This is true of the rhyolites as well as of the mafic flows.

Some Speculations on Ocean Basalts

In this paper, we have pointed out that specific differences of Archean and Ballard-Moore pillows appear to be functions of higher flow rates of Archean basalts. Do these differences translate into consistent differences between Archean and Cenozoic basalts or are they accidental?

In this respect, five factors appear important to us:

(1) The pillows seen in active formation by Moore et al. (1973) and Moore (1975) formed at the extreme termination of a flow that advanced over 20 km before entering the sea.

(2) The pillows and pillow breccias observed by Ballard and Moore (1977) are from extremely small shield volcanoes.

(3) Moore et al. (1973), Moore (1975), and Ballard and Moore (1977) observed only flow fronts and flow tops; they have not observed cross-sections through flows; had they observed the fronts and tops of Archean flows, they would have seen only pillows and pillow breccias; they would not have observed a single part of the massive facies.

(4) Many recent oceanic basalt flows, like those of the eruption of Monna Ulu (Hawaii) or the Lakagigar eruption (Iceland, 1783) are commensurate to Archean flows.

(5) Massive flows may make up as much as 30 per cent of the ocean crust as shown by deep-sea drilling. This is commensurate with the proportion of massive basalt in Archean sections.

Extrapolating from our results and taking into account the five factors outlined above we predict the following: (1) Mapping of cross-sections of flows exposed in oceanic fault scarps will turn up basalt flows having a massive proximal facies and showing exactly the facies distribution described in this paper. (2) Pillows in large oceanic flows will predominantly lack the distinctive surface sculptures described by Moore (1975) and Ballard and Moore (1977) except for very small corrugations parallel to the spreading direction. (3) Flow rates of Archean and Recent basalts will turn up to be commensurate.

Acknowledgments

Most of the field work has been financed by the Quebec Department of Natural Resources. Work in the laboratory has been financed by C.N.R.C. operating grant A-9145 and Geological Survey of Canada research contract (No. 2239-4-10/77).

We gratefully acknowledge valuable contributions by P. Boivin, M. Larouche, R. Côté, and P. Trudel during early stages of this work. R.C. Bald contributed by mapping pillows; R.C. Bald and A.P. Lichtblau did much petrographic work. We are grateful to L. Gélinas for supervision of the M.Sc. thesis of Gilles Provost. Incisive criticism of our volcanological interpretation of the rhyolites by L. Gélinas and J. Lajoie has done much to sharpen our arguments.

Our greatest debt, however, is to Andrée F. de Rosen-Spence and to Ingvar B. Fridleifsson. Both guided us during field trips, Andrée to the rhyolites of Rouyn-Noranda, Ingvar to the classical rhyolite hyaloclastites of Landmannalaugar, Iceland, and they most generously shared with the senior author their experience and their unpublished conclusions. These field trips stimulated work that provided the vital clues for the interpretations presented here.

References

Ballard, R.D. and Moore, J.G.
1977: Photographic atlas of the mid-Atlantic rift valley; Springer-Verlag, New York, N.Y.

Dimroth, E.
1977: Archean autoclastic volcanic rocks, Rouyn-Noranda area, Quebec, Canada: Classification, diagnosis and interpretation; in Report of Activities, Part B, Geological Survey of Canada, Paper 76-1B, p. 107–111.

Dimroth, E., Cousineau, P., Leduc, M., and Sanschagrin, Y.
1978: Structures and organization of Archean subaqueous basalt flows, Rouyn-Noranda area, Quebec, Canada; Canadian Journal of Earth Sciences, v. 15, p. 902-918.

Dimroth, E., Gélinas, L., Provost, G., Rocheleau, M., and Tassé, N.
1975: Field trip and field conference on the volcanology and sedimentology of Rouyn-Noranda area; Published under the auspices of the Resident Geologist, Quebec Department of Natural Resources, Noranda, Quebec, p. 1-75.

Gélinas, L., Lajoie, J., Bouchard, M., Simard, A., Verpaelst, P., and Sansfaçon, R.
1978: Les complexes rhyolitiques de la région de Rouyn-Noranda. Rapport Préliminaire. Manuscript in files at the Resident Geologist's Office, Quebec Department of Natural Resources, Noranda, Quebec

Goodwin, A.M., Ridler, R.H., and Annells, R.N. with contributions by D.N. Briggs, A.J. Naldrett, A. Spence, and C.D. Spence
1972: Field Excursion A40-C40: Precambrian volcanism of the Noranda-Kirkland Lake-Timmins, Michipicoten, and Mamainse Point areas, Quebec and Ontario; 24th International Geological Congress, Montreal, 93 p.

Moore, J.G.
1975: Mechanism of formation of pillow lava; American Scientist, v. 63, p. 269-277.

Moore, J.G., Phillips, R.L., Grigg, R.W., Peterson, D.W. and Swanson, D.O.
1973: Flow of lava into the sea, 1969-1971, Kilanea Volcano, Hawaii; Geological Society of America Bulletin, v. 84, p. 537-546.

Provost, G.
1978: Les rhyolites du complexe "Don", région de Rouyn-Noranda, Abitibi-Ouest; Unpublished M.Sc. thesis, École Polytechnique, Montréal, 87 p.

Rocheleau, M. and Lajoie J.
1974: Sedimentary structures in resedimented conglomerate of the Cambrian Flysch, L'Islet, Quebec Appalachians; Journal of Sedimentary Petrology, v. 44, p. 826-836.

Saemundsson, K.
1972: Jardfraediglefsur un Torfajökulsvaedid; Natturu-fraedingurinn, v. 42, p. 81-99.

Saemundsson, K. and Noll, H.
1974: K/Ar ages of rocks from Husafell, Western Iceland, and the development of Husafell Central Volcano; Jökull, v. 24, p. 40-59.

Spence, A.F. de Rosen-.
1976: Stratigraphy, development and petrogenesis of the central Noranda volcanic pile, Noranda, Quebec; Unpublished Ms. doctoral dissertation, University of Toronto, Toronto, Ontario.

Walker, R.G.
1976: Facies models x^2. Turbidites and associated coarse clastic facies; Geoscience Canada, v. 3, p. 25-36.

35. FUSED CLUSTERS OF THE CONODONT GENUS *BELODINA* ETHINGTON FROM THE THUMB MOUNTAIN FORMATION (ORDOVICIAN), ELLESMERE ISLAND, DISTRICT OF FRANKLIN

Project 770077

Godfrey S. Nowlan
Regional and Economic Geology Division

Nowlan, Godfrey S., Fused clusters of the conodont genus **Belodina** *Ethington from the Thumb Mountain Formation (Ordovician), Ellesmere Island, District of Franklin; in Current Research, Part A, Geol. Surv. Can., Paper 79-1A, p. 213-218, 1979.*

Abstract

Two fused clusters of the Ordovician conodont species **Belodina compressa** *(Branson and Mehl) are described from the Thumb Mountain Formation on Ellesmere Island. The specimens each consist of two elements, but differ in elemental composition. A previous report of the species as a fused cluster shows profound differences in arrangement and size distribution of the fused elements. Comparison with this and other known fused clusters suggests that the examples from the Thumb Mountain Formation are not representative of the geometry of the species' apparatus, despite being composed of elements belonging to the species. It is suggested that the fusion may be of diagenetic origin.*

Introduction

Upon death of a conodont animal, the skeletal apparatus usually became disaggregated, and most collections of conodonts are of these disassociated, discrete elements. Hinde (1879) proposed the multielement concept of a conodont species. He suggested that an individual conodont animal contained one or more different element morphotypes, but it was not until the discovery of natural conodont assemblages from Carboniferous black shales in Germany and the United States (Schmidt, 1934; Scott, 1934) that the proposal gained widespread approval. In recent years, major advances have been made in the recognition of natural conodont species from disaggregated samples. These reconstructions are based on several lines of evidence including stratigraphic co-occurrence of elements, symmetry transitions between generally similar elements, and upon similarity of size, colour, denticulation, surface ornamentation, basal cavity and white matter distribution (for a review see Sweet and Bergström, 1972). Gradually, basic templates and concepts of genera and species have developed from both empirical and numerical studies of large collections (e.g. Bergström and Sweet, 1966; Kohut, 1969). Despite considerable success with apparatus reconstruction from discrete elements, perhaps the only unequivocal evidence is available through natural assemblages.

Assemblages of conodont elements occurring on shale surfaces may represent individual conodont animals; others may be coprolitic associations. In addition to the Carboniferous occurrences, assemblages are also known from the Cambrian (Miller and Rushton, 1973; Müller and Andres, 1976) and Devonian (Lange, 1968; Mashkova, 1972; Nicoll, 1977). Using the pattern of arrangement and numerical ratios of elements in the assemblages, it has been possible to reconstruct the apparatus of several conodont species. The number of taxa known from these assemblages is rather few, however, and none is recorded from the Ordovician.

The rarest type of natural association is the so-called fused cluster that may be found in residues of acidized samples. The preservation potential of this type of natural association is poor, considering the number of processes, both laboratory and taphonomic, to which the sample may have been subjected. Fused clusters have been reported from the Cambrian (Landing, 1977), Ordovician (Barnes, 1967), Silurian (Rexroad and Nicoll, 1964; Pollock, 1969), Carboniferous (Austin and Rhodes, 1969) and Triassic (Ramovs, 1978). With the exception of Landing (1977), Pollock (1969) and Ramovs (1978) these studies dealt with only one or two specimens. This report is concerned with two fused clusters of the species **Belodina compressa** (Branson and Mehl). The specimens are described and compared with the fused cluster of the same species described by Barnes (1967) from the Cobourg Formation, at Ottawa. The Cobourg is now considered Edenian (Sweet and Bergström, 1971) and so the locality is of Upper Ordovician age.

Locality and Age of Sample

The sample that yielded both specimens is from the Thumb Mountain Formation (Kerr, 1967a) in a section measured near the head of Svarte Fiord, Ellesmere Island (77°17'N; 84°24'W). The section is described by Kerr (1967b, p. 90) as section 45, and further description is available in Nowlan (1976) wherein the sample is described as #152. The Thumb Mountain Formation is characterized by massive, rusty weathering, locally grey-brown, calcisiltites and fine calcarenites. Sample 152 was taken of dark grey, massive, rubbly weathering calcisiltite, 55 m below the contact of the Thumb Mountain Formation with the overlying Irene Bay Formation.

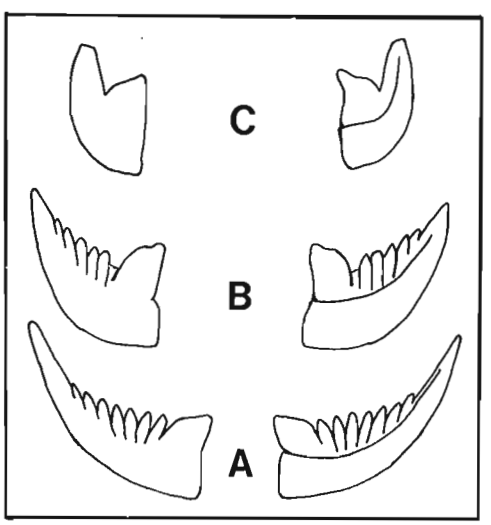


Figure 35.1. *Sketches of the component morphotypes of* **Belodina compressa** *(Branson and Mehl) as suggested by collections of disjunct elements. Outer and inner lateral views of: A., grandiform element (***B. grandis** *Stauffer s.f.); B., compressiform element (***B. compressa** *(Branson and Mehl) s.f.); C., eobelodiniform element (***Eobelodina fornicala** *(Stauffer) s.f.).*

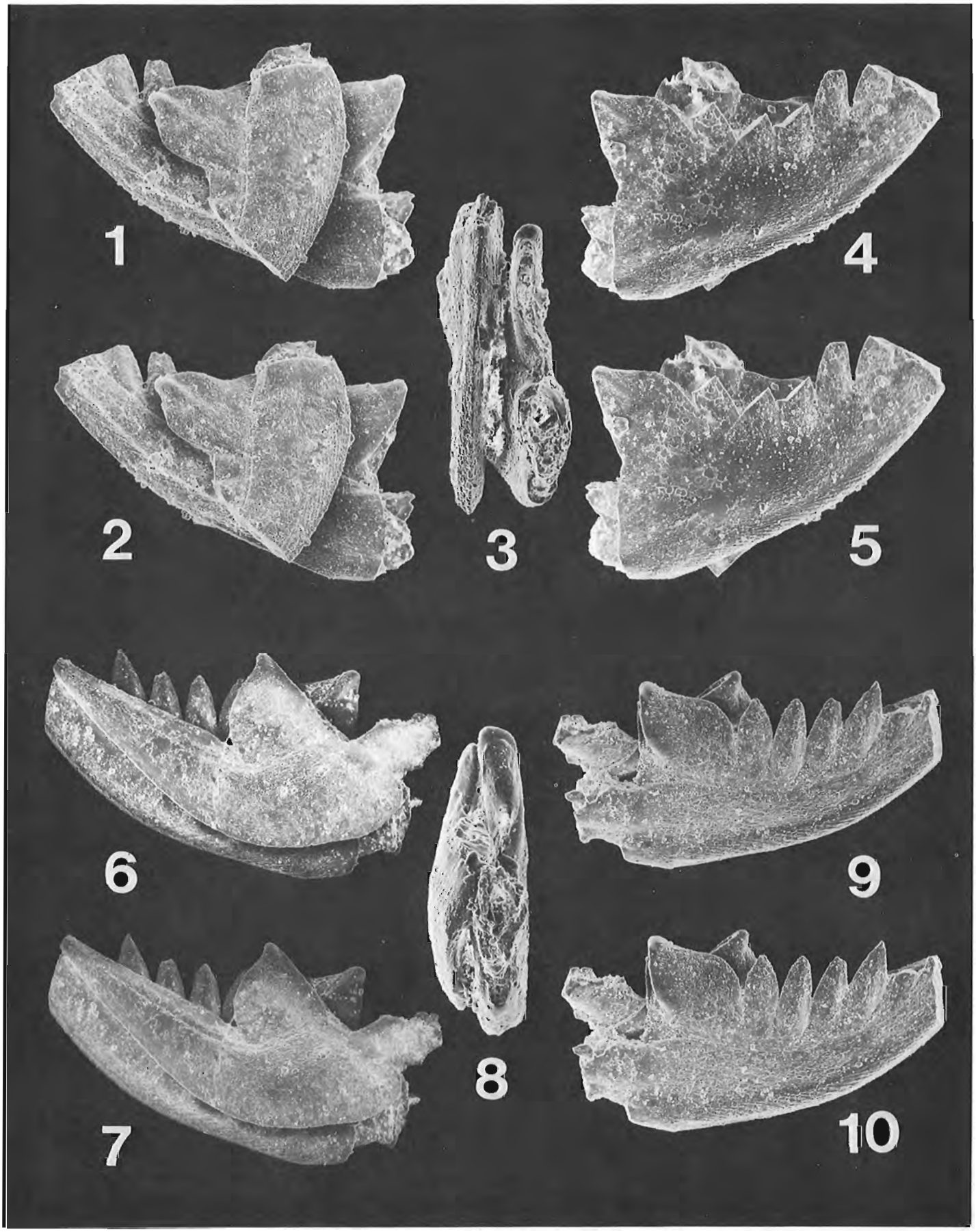

1
2
3
4
5
6
7
8
9
10

Plate 35.1. *(facing page)*

Fused clusters assignable to **Belodina compressa** *(Branson and Mehl). Stereopairs photographed at tilts of 10° and 20°.*

Figures 1-5. *1,2. Inner lateral view, stereopair, X120; probable compressiform element fused on a grandiform element. Note 90° rotation of compressiform relative to grandiform element.*
3, basal view, X200; shows basal opening of grandiform element and anterior margin of compressiform element.
4,5, outer lateral view, stereopair, X120; shows outer lateral side of grandiform element largely obscuring the underlying compressiform element. Specimen deposited as: GSC 59981; from the Thumb Mountain Formation, Ellesmere Island.

Figures 6-10. *6,7. Inner lateral view, stereopair, X120; eobelodiniform element fused on a grandiform element. Note that the cusps are subparallel.*
8, basal view, X200, shows basal opening of grandiform element; basal filling of eobelodiniform element obscures most of the basal opening of that element.
9,10, outer lateral view, stereopair, X120; shows grandiform element on eobelodiniform element. Specimen deposited as GSC 59982; from the Thumb Mountain Formation, Ellesmere Island.

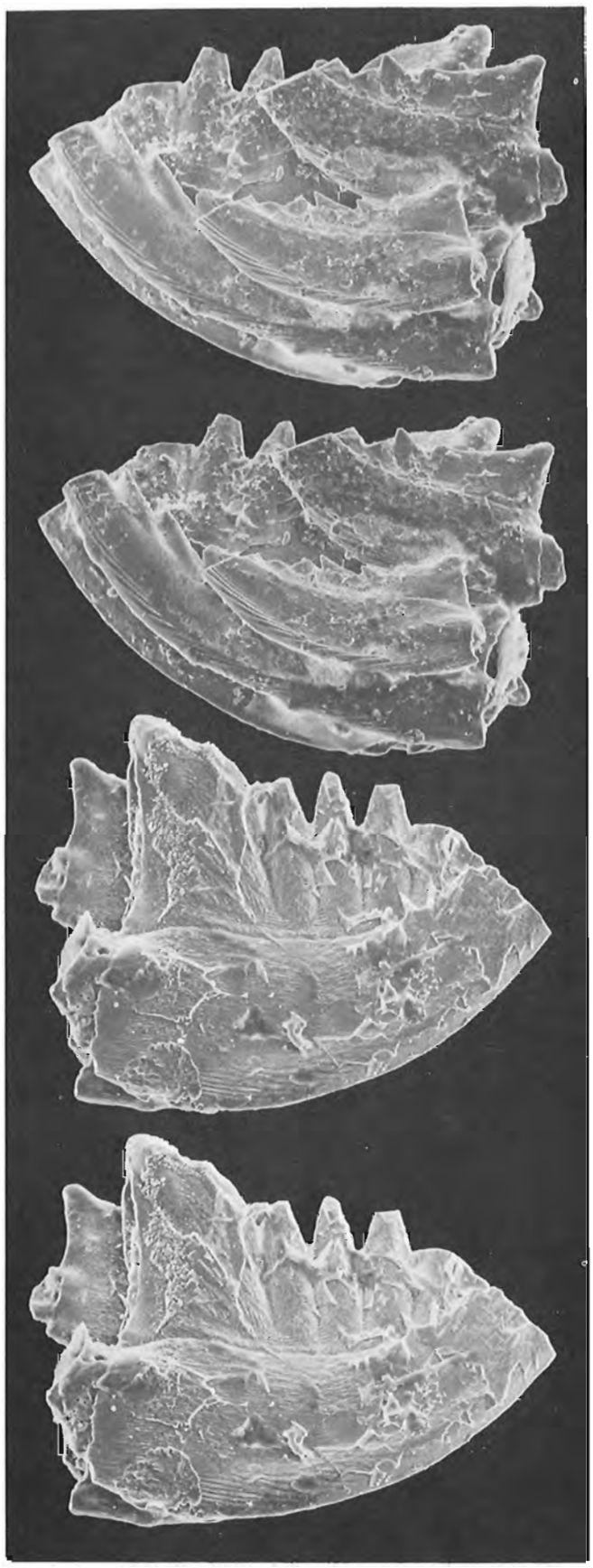


Figure 35.2.

Stereopair lateral views of the **Belodina** *assemblage reported by Barnes (1967, Text-fig. 2), from the Cobourg Formation (Upper Ordovician) at Ottawa; GSC 21396, X200; pairs photographed at tilts of 10° and 20°. Compare this specimen with the two illustrated on Plate 35.1.*

Regionally, the Thumb Mountain Formation ranges in age from Blackriveran at the base to late Edenian or early Maysvillian at the top, and is about 350-400 m thick. Species recovered from the sample, in addition to the fused cluster, include: **Belodina compressa** (Branson and Mehl), as disjunct elements, **Drepanoistodus suberectus** (Branson and Mehl), **Panderodus gracilis** (Branson and Mehl), **Paroistodus? mutatus** (Branson and Mehl) and **Plectodina tenuis** (Branson and Mehl). The fauna is largely undiagnostic although the presence of **P. tenuis** suggests an age younger than Kirkfieldian. Based on the high stratigraphic level of the sample, and on conodont data from elsewhere (Barnes, 1974; Nowlan, 1976), the upper Thumb Mountain Formation is probably late Shermanian to early Edenian in age. Fossils, other than conodonts, were absent from the sample locality and enclosing strata.

Nature of the genus *Belodina* Ethington

Ethington (1959) proposed the genus **Belodina** as a form genus to include elements with crowded, blade-like denticles on the posterior margin, a deep basal cavity and an expanded basal portion termed the heel. Bergström and Sweet (1966) revised the genus to multielement status and showed that the apparatus of the type species **(Belodina compressa)** consisted of belodiniform and eobelodiniform elements. This reconstruction has been followed by most authors (e.g. Sweet et al. 1975; Barnes, 1977). The apparatus of the type species consists of three types of elements: an elongate, broadly curved, slender, denticulate element (grandiform); a more tightly recurved, broad, denticulate element (compressiform), and a sharply recurved element, lacking denticles between cusp and heel (eobelodiniform) (Fig. 35.1). These elements can be viewed as a symmetry transition series with progressively increased recurvature. Other species of **Belodina** do not seem to follow this apparatus plan. Several lack an eobelodiniform element (e.g. **B. dispansa** Glenister), and others show a more complex group of morphotypes (e.g. **B. profunda** (Branson and Mehl)). A more detailed discussion of the variability within the genus **Belodina** is available in Nowlan and Barnes (in press).

Description and Interpretation of the Material

The fused assemblages reported here, show two different associations. The first (GSC 59981, Pl. 35.1, figs. 1-5) consists of a probable compressiform element fused to a grandiform element, and the second (GSC 59982, Pl. 35.1, figs. 6-10) consists of an eobelodiniform element fused to a grandiform element. The compressiform element of specimen 59981 is broken close to the heel and could possibly be a second grandiform element, but seems to possess a tight curvature of the anterior margin.

The two specimens differ not only in composition but also in the relative orientation of the elements. In the eobelodiniform-grandiform association, the elements lie with cusps virtually parallel; the difference in the angle of their basal openings being equivalent to the degree of recurvature of the specimens (Pl. 35.1, figs. 6, 7). In the compressiform-grandiform association, the compressiform element is rotated, so that its basal opening is at about 90° to that of the grandiform element (Pl. 35.1, figs. 4, 5).

Despite differences in composition and orientation of the two specimens, some similarities may be noted. Both specimens have elements of similar relative size; the eobelodiniform of one and compressiform of the other are slightly smaller than the grandiform elements to which they adhere. In addition, the inner lateral grooves of both elements in each specimen are similarly oriented, so that the inner lateral face of each grandiform element is fused to the outer lateral face of the associated element.

These clusters of **B. compressa** recovered from the Thumb Mountain Formation, differ radically from the fused cluster of the same species described by Barnes (1967) and reillustrated in this paper (Fig. 35.2) using SEM techniques. In Barnes' material, four specimens are stacked in an orderly fashion, with basal openings approximately parallel. The elements decrease in size from one side of the cluster to the other. Only grandiform and compressiform elements are fused together and no eobelodiniform elements are present either in the fused cluster, or among the discrete elements recovered in the same sample (Barnes, 1967, Table 1). Thus Barnes' (1967) specimen differs from the Thumb Mountain specimens in the following aspects: (a) composition: Barnes' (1967) specimen lacks any eobelodiniform elements; (b) size: the size differential from one side of the apparatus noted for Barnes' specimen is not exhibited by the Thumb Mountain specimens. These profound differences between the two reports of **B. compressa** clusters, bring into question the reliability of this type of association as a basis for apparatus reconstruction and interpretation. In both cases the elements fused together are elements that independent evidence has suggested belong together in the apparatus. However, the orientation, size and proportions are markedly different, which is surprising considering the two samples are of about the same age.

Examination of discrete elements of **B. compressa** in prolific samples, suggests a ratio of eobelodiniform elements to belodiniform elements of about 2:8 for the species (see Barnes, 1967, p. 1559 for discussion). As noted above, Barnes' (1967) specimen lacks an eobelodiniform element leading him to conclude (p. 1559) that "four pairs of **B. compressa** lie behind a single pair of **E. fornicala**", in the species. In the Thumb Mountain sample, additional discrete specimens of eobelodiniform and belodiniform elements of **B. compressa** are present in a 2:8 ratio (4 eobelodiniform, 16 belodiniform).

As there is little similarity between the two occurrences of fused clusters of **Belodina,** they do not clarify the nature and geometry of the apparatus. Examination of the discrete elements which belong to **B. compressa** indicates a symmetry transition from the grandiform element through the compressiform element to the eobelodiniform element. One might expect this transition series to be reflected in the geometry of the apparatus. The Cobourg specimen does show two grandiform elements stacked upon two compressiform elements which may be natural, but in one specimen from the Thumb Mountain Formation (GSC 59981), the two end members are juxtaposed; the latter situation suggests that the cluster may not be a natural one.

Comparison of the Thumb Mountain fused clusters with those of other ages, indicates some other dissimilarities. In the Cambrian examples of **Prooneotodus tenuis** (Müller), a definite size increase of elements suggests a progressive addition of new elements with growth (Landing, 1977). The **B. compressa** apparatus of Barnes (1967) also shows marked size gradation of elements, and the same is true for the Carboniferous cluster described by Austin and Rhodes (1969). Carls (1977) has recently advocated that conodont elements could be lost and replaced through life. This juxtaposition of elements of divergent sizes may be support for such a hypothesis.

It seems likely that the fused clusters recovered here do not represent the true geometry of the **B. compressa** apparatus. The question arises as to the mode and location of fusion. To have survived the sample preparation process (dissolution in 15% acetic acid, sieving, and separation with tetrabromoethane and a magnetic separator) the specimens must have been securely cemented together. Attempts to determine the nature of the cement by using an X-ray energy

spectrometer in conjunction with a scanning electron microscope were inconclusive. Emissions from the deep groove between the specimens were erratic, probably because they were effectively shielded by emissions from the specimens themselves. Certainly, no excess cementing material is visible and it may be that the fusion was effected through the soft tissue of the animal, or by diagenesis.

The preservation of the fused clusters and the discrete elements associated in the sample is the same. All specimens are reasonably well preserved, with only minor denticle breakage and a conodont colour alteration index of 1.5 (Epstein et al., 1977). This similarity of preservation eliminates the possibility of any special origin for the fusion as a result of heat or compression.

The question arises as to when and why fusion takes place. Rexroad and Nicoll (1964), Barnes (1967), Pollock (1969) and Austin and Rhodes (1969) have all suggested that fusion might be the result of a pathologic condition. It is to be expected that a disease would affect all individuals in a similar manner resulting in similar fused clusters. Although a pathologic origin is possible for some fused clusters, it is viewed as unlikely in the case of the Thumb Mountain specimens, for the following reasons. Firstly the composition of the two clusters is different, suggesting some element movement, and secondly they are different from the other report of the species suggesting a different origin. The fusion is more likely to be a result of some diagenetic process involving local phosphate mineralization, such as Landing (1977) has suggested for Cambrian examples. Even a diagenetic process favours fusion of elements related in the same apparatus, but the time lapse between death of an animal and fusion of elements will influence the natural appearance of the cluster. Those elements fused early in diagenesis, prior to disturbance, may resemble the original geometry of an apparatus in whole or in part, whereas those fused later may become rearranged in 'unnatural associations'. The diagenetic origin is not advocated for all fused clusters, but it is suggested that a pathologic condition resulting in some genetic defect would affect all individuals in the same manner and therefore produce similar clusters.

Conclusions

The fused clusters of **B. compressa** recovered from the Thumb Mountain Formation differ considerably from a fused cluster of the same species described by Barnes (1967). They are probably a result of diagenetic fusion, and as such, may not reflect the geometry of a **B. compressa** apparatus. The specimens contribute little to the understanding of Ordovician conodont apparatus geometry, but provide a caution to the interpretation of future occurrences of fused clusters as necessarily natural associations.

Acknowledgments

The specimens described in this report were recovered during the course of a doctoral dissertation at the University of Waterloo, Waterloo, Ontario, supervised by C.R. Barnes, who kindly read an earlier draft of this manuscript, and offered several helpful suggestions.

The figured specimens were photographed in stereoscopic pairs on an Etec Autoscan SEM, at 10° and 20°.

References

Austin, R.L. and Rhodes, F.H.T.
1969: A conodont assemblage from the Carboniferous of the Avon Gorge, Bristol; Palaeontology, v. 12, p. 400-405.

Barnes, C.R.
1967: A questionable natural conodont assemblage from Middle Ordovician limestone, Ottawa, Canada; Journal of Paleontology, v. 6, p. 1557-1560.

1974: Ordovician conodont biostratigraphy of the Canadian Arctic; in Proceedings of a Symposium on the Geology of the Canadian Arctic; Geological Association of Canada, Canadian Society of Petroleum Geology, Special Publication, eds. J.D. Aitken and D.J. Glass, p. 221-240. (Dated 1973.)

1977: Ordovician conodonts from the Ship Point and Bad Cache Rapids Formations, Melville Peninsula, southeastern District of Franklin; Geological Survey of Canada, Bulletin 269, p. 99-119.

Bergström, S.M. and Sweet, W.C.
1966: Conodonts from the Lexington Limestone (Middle Ordovician) of Kentucky and its lateral equivalents in Ohio and Indiana; Bulletins of American Paleontology, v. 50, no. 229, p. 271-424.

Carls, P.
1977: Could conodonts be lost and replaced?; Neues Jahrbuch für Geologie und Paläontologische, Abhandlungen, v. 155, p. 18-64.

Epstein, A.G., Epstein, J.B., and Harris, L.D.
1977: Conodont color alteration – an index to organic metamorphism; U.S. Geological Survey, Professional Paper 995.

Ethington, R.L.
1959: Conodonts of the Ordovician Galena Formation; Journal of Paleontology, v. 25, p. 1-17.

Hinde, G.J.
1879: On conodonts from the Chazy and Cincinnati Group of the Cambro-Silurian, and from the Hamilton and Genesee-shale divisions of the Devonian, in Canada and the United States; Quarterly Journal of the Geological Society of London, v. 35, p. 351-369.

Kerr, J.W.
1967a: New nomenclature for Ordovician rock units of the eastern and southern Queen Elizabeth Islands, Arctic Canada; Bulletin of Canadian Petroleum Geology, v. 15, p. 91-113.

1967b: Stratigraphy of central and eastern Ellesmere Island, Arctic Canada; Geological Survey of Canada, Paper 67-27, pt. II.

Kohut, J.J.
1969: Determination, statistical analysis, and interpretation of recurrent conodont groups in Middle and Upper Ordovician strata of the Cincinnati region (Ohio, Kentucky and Indiana); Journal of Paleontology, v. 43, p. 392-412.

Landing, E.
1977: **"Prooneotodus" tenuis** (Müller, 1959) apparatuses from the Taconic allochthon, eastern New York: construction, taphonomy and the protoconodont "supertooth" model; Journal of Paleontology, v. 51, p. 1072-1084.

Lange, F.G.
1968: Conodonten-Gruppenfunde aus Kalken des tieferen Oberdevon; Geologica et Palaeontologica, v. 2, p. 37-57.

Maskhova, T.V.
1972: **Ozarkodina steinhornensis** (Ziegler) apparatus, its conodonts and biozone; Geologica et Palaeontologica, SB 1, p., 81-90.

Miller, J.F. and Rushton, A.W.A.
1973: Natural conodont assemblages from the Upper Cambrian of Warwickshire, Great Britain; Geological Society of America Abstracts with Programs, v. 5, p. 338-339.

Müller, K.J. and Andres, D.
1976: Eine conodontengruppe von **Prooneotodus tenuis** (Müller, 1959) in naturlichem Zusammenhang aus dem oberen Kambrium von Schweden; Palaeontologische Zeitschrift, v. 50, p. 193-200.

Nicoll, R.S.
1977: Conodont apparatuses in an Upper Devonian palaeoniscoid fish from the Canning Basin, Western Australia; Bureau of Mineral Resources, Journal of Australian Geology and Geophysics, v. 2, p. 217-228.

Nowlan, G.S.
1976: Late Cambrian to Late Ordovician conodont evolution and biostratigraphy of the Franklinian Miogeosyncline, eastern Canadian Arctic Islands; unpublished Ph.D. dissertation, University of Waterloo, Ontario, December, 1976.

Nowlan, G.S. and Barnes, C.R.
Late Ordovician conodonts from the Vauréal Formation, Anticosti Island, Québec; Geological Survey of Canada Bulletin (in press).

Pollock, C.A.
1969: Fused Silurian conodont clusters from Indiana; Journal of Paleontology, v. 43, p. 929-935.

Ramovs, A.
1978: Mitteltriassische conodonten – clusters in Slowenien, NW Jugoslawien; Palaeontologische Zeitschrift, v. 52, p. 129-137.

Rexroad, C.B. and Nicoll, R.S.
1964: A Silurian conodont with tetanus?; Journal of Paleontology, v. 38, p. 771-773.

Schmidt, H.
1934: Conodonten-Funde in ursprünglichem Zusammenhang; Palaeontologische Zeitschrift, v. 16, p. 76-85.

Scott, H.W.
1934: The zoological relationships of the conodonts; Journal of Paleontology, v. 8, p. 448-455.

Sweet, W.C. and Bergström, S.M.
1971: The American Upper Ordovician Standard XIII: a revised time-stratigraphic classification of North American upper Middle and Upper Ordovician rocks; Geological Society of America Bulletin, v. 82, p. 613-628.

1972: Multielement taxonomy and Ordovician conodonts; Geologica et Palaeontologica, v. SB 1, p. 29-42.

Sweet, W.C., Thompson, T.L., and Satterfield, I.R.
1975: Conodont stratigraphy of the Cape Limestone (Maysvillian) of eastern Missouri; Missouri Geological Survey Report of Investigations 57, Pt. 1, p. 1-59.

36. BASIN TO PLATFORM TRANSITION, LOWER PALEOZOIC STRATA OF WARE AND TRUTCH MAP AREAS, NORTHEASTERN BRITISH COLUMBIA

Project 770044

M.P. Cecile and B.S. Norford
Institute of Sedimentary and Petroleum Geology, Calgary

Cecile, M.P. and Norford, B.S., Basin to platform transition, Lower Paleozoic strata of Ware and Trutch map areas, northeastern British Columbia; in Current Research, Part A, Geol. Surv. Can., Paper 79-1A, p. 219-226, 1979.

Abstract

Lower Paleozoic strata span a transition from platform to basin facies. These units are the Kechika, Skoki, Nonda, and Road River formations and Upper Ordovician dolomite and sandstone. Individual formations are divided into mappable units and, primarily on the basis of existing literature, are dated as latest Cambrian to Late? Silurian. The transition from Skoki to equivalent Road River rocks is narrow (20 km) and contains abundant slope breccias and dolomite debris-flow breccias. Basin unconformities correlative with eastern platform unconformities are found in the central Ware area and indicate reactivation of an older tectonic framework. Sedimentary barite is found in basin strata of latest Cambrian, Early Ordovician, Late Ordovician, and Middle to Late Silurian age. Phosphorite is found in Upper Cambrian strata and middle and upper Kechika and basal Road River formations. Uranium concentration of 196-220 ppm is noted in one phosphorite sample.

Introduction

Research into lower Paleozoic shelf to basin transitional facies in the Cordillera (Cecile, 1978) was continued in northeastern British Columbia. The purpose of the study is to increase knowledge of stratigraphic and sedimentological relationships of the carbonate-shelf and platform facies with shale-basin facies, to refine regional correlations, to locate and describe mineralized strata, and to contribute to the understanding of the fundamental tectonic-sedimentary framework of the transition zone.

Acknowledgments

G.C. Taylor ably introduced Cecile to the geology of northeastern British Columbia, and continually provided information and discussion on the stratigraphic units. Field assistance was given by Sharon Carr and Brenda Wright, both from the University of Calgary, and Denise Armstrong, Institute of Sedimentary and Petroleum Geology.

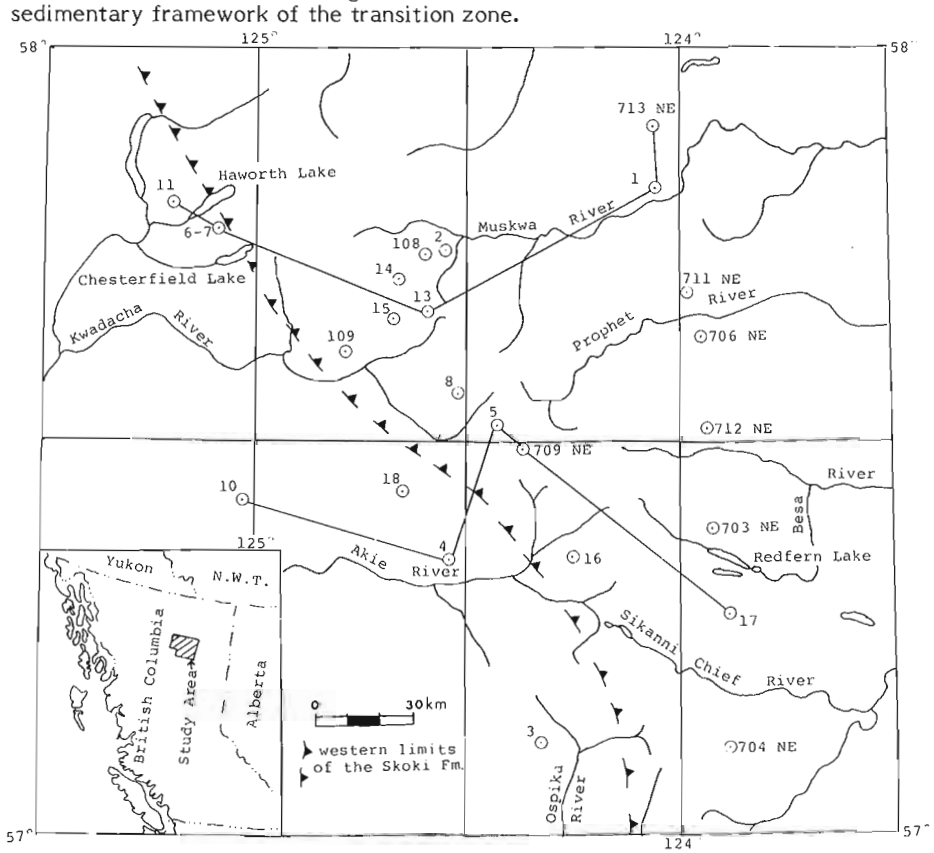


Figure 36.1. *Map showing the location of the Ware-Trutch area, section and traverse locations, line of cross-sections shown in Figure 36.3, geographic localities and the position of the Skoki shale-out.*

Previous Geological Work

Stratigraphic studies of Ordovician and Silurian rocks in the Ware-Trutch areas have been published by Jackson et al. (1965) and Norford et al. (1967). Important stratigraphic information is also given in an unpublished Ph.D. thesis by Davies (1966), and in publications by Taylor and Stott (1973), Gabrielse (1975) and Thompson (1976) that describe stratigraphic units in adjoining map areas. Paleozoic rocks in the Ware-Trutch areas have been mapped by Gabrielse (1977; Ware west half) and Taylor (in prep., Ware east half and Trutch west half).

Stratigraphic names used in this report originated in the following ways. The Kechika Group was first described in the McDame map area (Gabrielse, 1963, p. 32) and later the name was extended to the study area by Gabrielse (1977). The Skoki Formation was proposed by Walcott (1928, p. 217-218) in southwestern Alberta where its development has been fully described by Norford (1969, p. 18). Thompson (1976, 1978) recognized Skoki-equivalent strata in the Halfway River map area adjacent to the Ware-Trutch areas. The Road River Formation was proposed by Jackson and Lenz (1962) with a type area in the northern Yukon and the terminology was extended to northern British Columbia by Gabrielse (1975, p. 11; 1977). Silurian rocks, which are not formally named in the present report, have been described by Jackson et al. (1965) and Davies (1966) as the Sandpile Group but their usage is not

followed because the rocks differ substantially from the Sandpile Group as described by Gabrielse (1954, 1963) and by Norford (1962).

Other pertinent stratigraphic terms previously used in the Ware-Trutch area are Mount April and Cloudmaker formations proposed by Jackson et al. (1965) which are alternate names for parts of the Kechika and Road River formations, respectively.

Stratigraphy

Lower Paleozoic strata are preserved in regional scale, northwest-trending anticlinoria and synclinoria separated by west-dipping thrust faults. Lower Paleozoic strata studied in the Ware-Trutch area are, in ascending stratigraphic order: The Kechika Formation; the Skoki Formation and equivalent parts of the Road River Formation; Upper Ordovician dolomite and quartzite and equivalent parts of the Road River Formation; and two Silurian units within the Road River Formation (Fig. 36.2, 36.3). This succession ranges in age from latest Cambrian (Trempealeauan) to Middle and/or Late Silurian, is locally bounded by sub-latest Cambrian and Devonian unconformities, and in places shows evidence of early Late Ordovician and Early and Middle Silurian unconformities (Fig. 36.3). Platform and shelf facies rocks are mainly in the eastern study area, while equivalent basin strata occur in the western study area.

Overlying Devonian strata and underlying Cambrian rocks are described by Taylor et al. (1979) and Norford (1979).

The Kechika Formation is divisible into five subtle units. The Road River Formation and Skoki dolomite can be divided into seven and four, respectively, recognizable units (Fig. 36.2, 36.3).

The data presented here are based on 22 measured sections and traverse information (Fig. 36.1).

Kechika Formation

The Kechika is more appropriately considered as a formation within the study area but can be divided into five subtle units which, in ascending stratigraphic order, are as follows. A basal unit (OK_1), 60 to 120 m thick, consists of thin bedded grey 'platy limestones'. The basal part of the 'platy limestones' are typically arenaceous and slope-breccias are found in the upper part (slope breccia as used here conveys stratiform breccia of thinly bedded carbonate with large rectangular or angular clasts of one type of carbonate in a carbonate matrix).

T e OK_2 unit is a 30 to 500 m succession of recessive 'putty-grey' weathering, often nodular, argillaceous calcilutite. The 'putty-grey' limestone is typically thin bedded and monotonous and may have calcarenite and calcirudite beds in the upper part of the unit. Cleavage is common and rarely parallel to bedding.

T e OK_3 unit is a monotonous, 90 to 500 m thick, succession of 'banded limestones' consisting of thick intervals of calcilutite and calcisiltite alternately shale-rich or shale-poor; and minor coarser grained limestone. At Sections 1 and 713 NE, thick intervals predominated by calcarenite or calcirudite alternate with strata in which argillaceous calcilutite is predominant. At Sections 13 and 16, banding is due to the alternation of very thick intervals rich and poor in limestone nodules. At Section 11, banding is due to variations of shale content in a monotonous argillaceous calcilutite and calcisiltite succession.

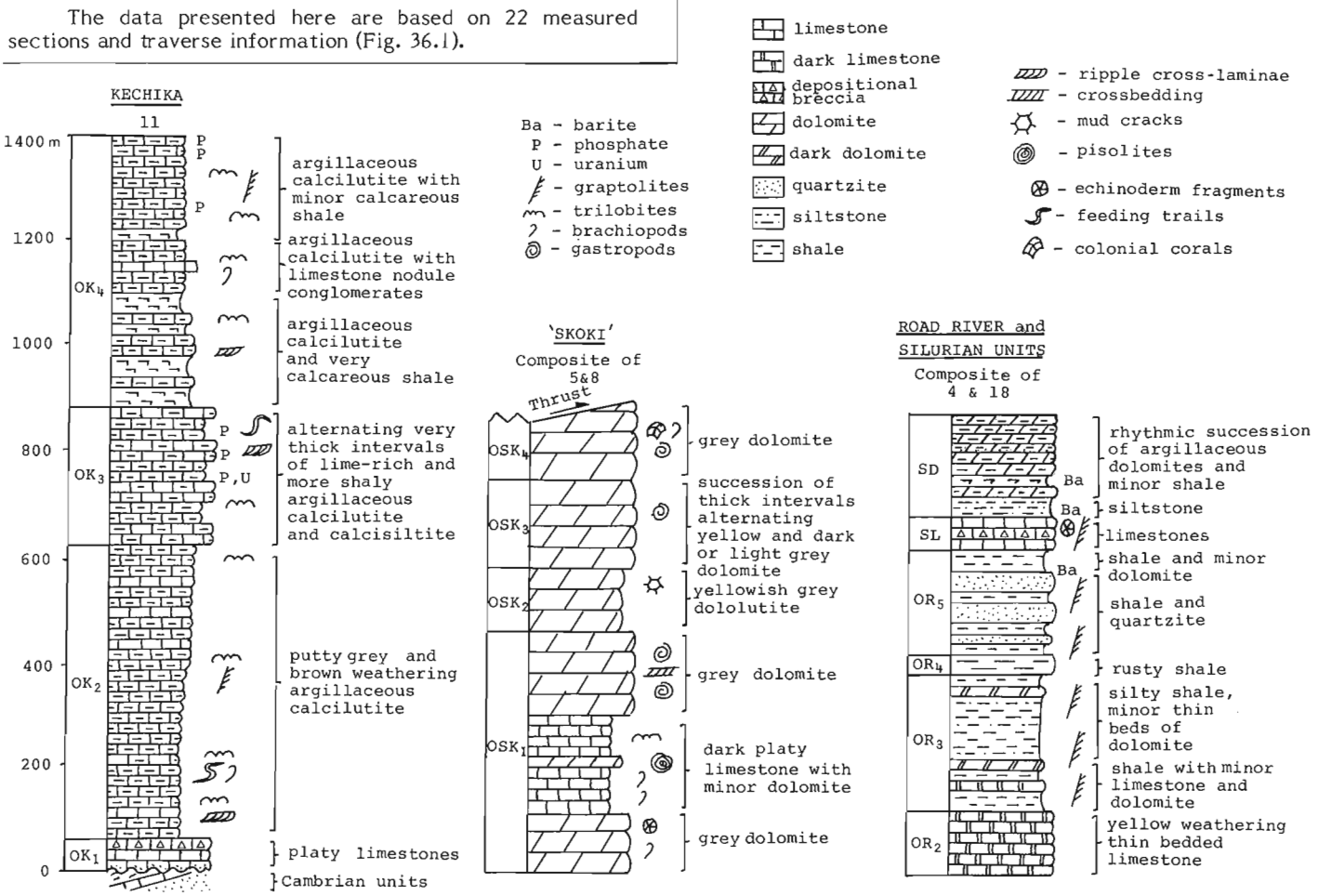


Figure 36.2. *Simplified stratigraphic sections showing most divisions of the Kechika, Skoki, Road River and basinal Silurian units. Section locations are shown in Figure 36.1.*

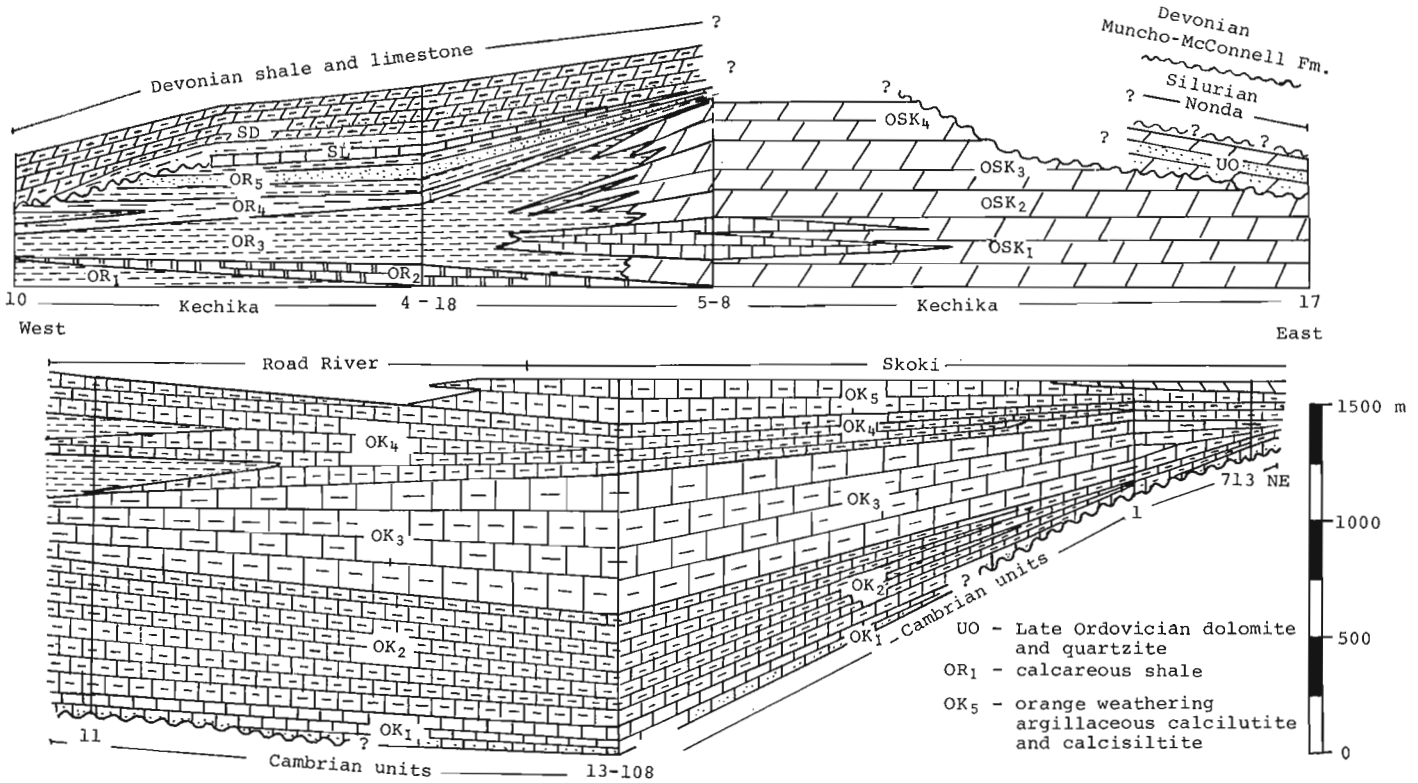


Figure 36.3. *Cross-sections through the transitional zones showing the relationships of laterally correlative facies, and the locations of unconformities. Skoki tongues west of Section 5-8 are either thinly bedded slope carbonates or stratiform carbonate breccias. Cross-sections are located on Figure 36.1 and additional legend in Figure 36.2.*

Unit OK_4 is an 'upper recessive' 70 to 500 m succession of argillaceous, often nodular, calcilutite. Unit OK_5 consists of 40 to 120 m of 'yellowish orange weathering limestones' that overlie the 'upper recessive' rocks in the central and eastern parts of the study area. The 'yellowish orange weathering limestones' consist primarily of slightly argillaceous calcilutite and calcisiltite but at Sections 1 and 713 NE some calcarenite and dolomite are present.

Argillaceous calcilutite is more susceptible to the development of cleavage than other Kechika lithologies and commonly is metamorphosed to a phyllitic rock. The soapy soft nature of the grey phyllitic material indicates talc is the predominant metamorphic mineral.

Contacts between Kechika units are broadly gradational, and some units cannot be recognized throughout the study area. Units can be mapped but the precise positions of the boundaries selected may vary considerably depending on individual mappers.

The sub-Kechika boundary at Sections 1 and 713 NE is an unconformity that cuts out Cambrian units (Taylor et al., 1979). At Section 11, the 'platy limestones' fill metre-scale depressions above a distinct pre-Kechika erosional surface, and clasts of Cambrian units occur in the lower part of the 'platy limestones'.

At location 108, Kechika rocks are gradational with a thick succession of Upper Cambrian sandstone, shale, and limestone. At the headwaters of the Prophet River (Fig. 36.1), Upper Cambrian strata, estimated to be as much as 2000 m thick, consist of similar argillaceous calcilutite and shale making definition of the sub-Kechika boundary difficult in this area.

Kechika rocks range in age from latest Cambrian to late Early Ordovician. A latest Cambrian age is assigned to the upper half of the 'platy limestones' by R.S. Tipnis (pers. comm.) based on the identification of conodonts at Section 11. Early Ordovician shelly faunal zones (A,B? D, and G?) have been identified from the Kechika Formation by Norford.

Preliminary interpretation of the Kechika Formation indicates that, from east to west, the successions are the result of deposition at the edge of a subtidal carbonate platform (Sections 1 and 713 NE) that rapidly passes to shelf facies (Section 13) and approaches the deeper part of the outer shelf at Section 11. Data supporting this interpretation are: increase in thickness of the Kechika from east to west; localization and abundance of calcarenite and calcirudite, and more abundant current-produced sedimentary features (scours and ripple cross-laminae) in eastern sections; a general reduction in carbonate grain size and increased shale content from east to west; and finally the occurrence of phosphorite pavements and shale tongues at Section 11 indicates proximity to the shelf edge (Fig. 36.3). Biostratigraphic correlation shows westward facies change of the upper part of the Kechika with coeval Road River Formation.

The implications of the vertical divisions of the Kechika Formation are less apparent. The only obvious conclusion is that the volume of lime sediment versus argillaceous sediment transported to the platform and shelf vary from one division to another and also rhythmically within the 'banded limestones'.



Figure 36.4. *This photograph illustrates the variety of transitional breccias in the Road River Formation, Section 11. Light coloured beds in the lower part of the photograph are beds of thinly bedded limestone or stratiform breccias. The upper cliff in the photograph has a lower unit with disrupted 1 m long limestone slabs, a middle unit of thinly bedded limestone, and an upper unit, cutting through the middle limestone, of platformal dolomite debris carrying gastropods and brachiopods. Scale: the upper cliff is about 40 m thick. (GSC 199405)*



Figure 36.5. *West of Cloudmaker Mountain Section 6-7; a succession of thinly bedded dolomite (↶50 m thick), right foreground, that gives way laterally to a complex succession of dolomite slope breccias, shallow water dolomite debris flows, all interstratified with shale (left background photograph). (GSC 199407)*

Skoki Formation

The Skoki dolomite is divided into four units on the basis of colour. The best and most complete exposures are at Sections 5 and 8, although the top of the Skoki is not preserved at either locality. The OSK_1 unit, the 'basal dark' division, is a 300 to 450 m succession of thickly bedded light and dark grey dolomite. At Section 5 the 'basal dark' rocks contain a middle subunit of grey thin bedded limestone. This subunit is a local feature associated with the transition to basinal facies (Fig. 36.3). At Section 17 the 'basal dark' unit contains some yellow to orange weathering dolomite in the lower 60 m. The OSK_2 unit is a 100 to 130 m succession of 'yellowish grey' and light olive-grey weathering dololutite with fine parallel to irregular laminae, rare small scale breccias, and very rare desiccation features. The contact between the OSK_1 and OSK_2 units is sharp. The OSK_3 unit is a 200 m succession of interstratified intervals of thickly bedded, dark grey, light grey and yellowish grey dolomite producing a 'banded Skoki' unit. The OSK_2 and OSK_3 are equivalent to a middle Skoki interval between the two dark units in the adjoining Halfway River area. The OSK_4, the 'upper dark', is a 100+ m, incomplete succession of thick bedded, dark and light grey dolomite. The same unit is 190 m thick in the northwestern corner of the Halfway River map area. Boundaries between the OSK_2, OSK_3, and OSK_4 units are gradational over a few metres, but all the units are mappable.

At location 109, near the edge of the shale-out of the formation, Skoki dolomite is entirely grey, undivided and estimated to be 380 m thick. Approximately 30 m of the central part of this unit is a mosaic dolomite breccia cemented by coarse white dolomite spar. The upper beds of the Skoki, at this location, are crinoid-rich bioclastic dolomite.

Immediately west of the Skoki transition to basin facies, and well exposed at Sections 11 and 6-7, there are spectacular examples of slope-breccias and massive debris flows composed of shallower water Skoki lithologies interstratified with Road River shale (Fig. 36.4). Slope-breccias are juxtaposed with intact successions of thinly bedded rhythmic or monotonous limestone and dolomite that are identical in composition, texture, and colour to the breccias (Fig. 36.5). The slope-breccias reveal a variety of degrees of movements. Some breccias consist of very large delicate disorganized slabs that have moved only centimetres or perhaps a few metres, others (see Fig. 36.6) are more disaggregated and mixed with carbonate matrix and have probably traveled long distances as debris flows or by a form of subaqueous solifluction. The zone of debris flow occurrences west of the 'Skoki' shale-out is about 20 km in width and testifies to an abrupt transition from carbonate-platform to basinal sediments. The nature and abundance of the breccias indicate a significant depositional slope to the transitional thin bedded dolomite and limestone deposited basinward of the Skoki shale-out.

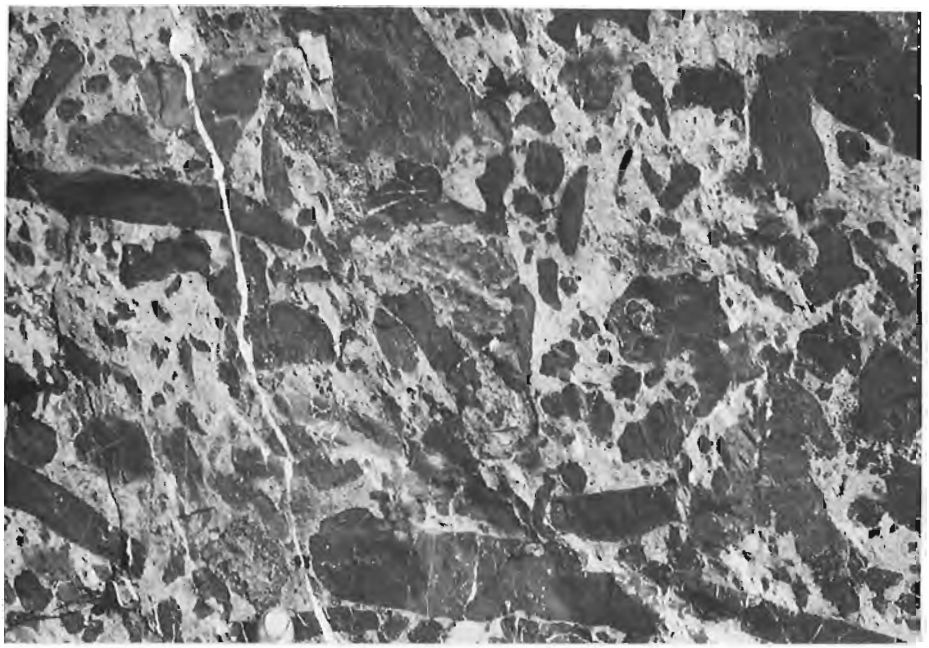


Figure 36.6. *Close up view of a disaggregated limestone slope breccia. On fresh surfaces both the matrix and clasts are fine grained dark grey to black limestone. The matrix weathers light yellow. Scale: the largest clast is 10 cm long. (GSC 199406)*



Figure 36.7. *Photograph of a nodule of large acicular calcite crystals developed syndepositional and oriented perpendicular to bedding. Note the flat base and rounded top. (GSC 199403)*

Skoki dolomite contains scattered brachiopods, abundant large gastropods (mostly **Maclurites**), and at Sections 5 and 706 NE a few corals. Large elongate stromatolite mounds, with north-trending axes, stromatolite biscuits, and laterally linked columns are also in the Skoki (OSK_2-OSK_3) at Section 712 NE, below an erosional base to the Upper Ordovician strata.

In the Halfway River map area the Skoki Formation ranges in age from late Arenig to early Caradoc.

Skoki dolomite represents a variety of tidal and shallow shelf facies. Dark grey weathering dolomite is commonly fine to medium crystalline, thickly bedded and fetid, and is often bioturbated. Macrofaunas are commonly only found in the dark grey beds. Some dark beds may be pisolitic or oncolitic, and, in one occurrence only, oolitic. Light grey weathering dolomite may have any of the features typical of the darker dolomite but is usually homogeneous, featureless, and medium crystalline. At the top of the 'basal dark' unit, Sections 5 and 17, light grey dolomite is crossbedded grainstone. The crossbeds are locally abundant, occur in tabular sets overlying a basal erosional surface, and mostly are less than 30 cm in height. Yellowish grey weathering dololutite represents the most restricted facies, probably lagoonal. The dololutite is fine grained, delicately laminated, free of organic staining, lacks shelly fauna, and contains rare features indicative of subaerial exposure, such as breccias and desiccation features.

Road River Formation – Ordovician Units

Five units can be recognized within the Ordovician part of the Road River Formation which is present only in the western and central study area. The basal unit OR_1 is a 120 to 200 m thick succession of calcareous shale, often with abundant limestone nodules, that was deposited conformably on the Kechika Formation. At Section 11 this unit contains Early Ordovician graptolites. The OR_1 unit is restricted to Sections 6-7, 10 and 11 and is not present at Section 5 where OR_2 rocks directly overlie the Kechika Formation.

The OR_2 unit is a distinctive succession of 'yellow weathering limestones' that is a useful marker within the basal Road River Formation. The limestone is black to dark grey on fresh surfaces, thin bedded, sometimes interstratified with shale, and the total unit is 20 to 130 m thick. This unit was not specifically identified by Jackson et al. (1965, Fig. 2) or Davies (1966, Fig. 7) at sections measured at or near locations 4 and 6-7. However from the lithological descriptions in both papers the 'yellow weathering limestone' underlies the **Paraglossograptus etheridgei** Zone (earliest Middle Ordovician) reported by those authors.

The OR_3 unit is a recessive 200 to 300 m thick succession of silty shale, shale, dolomitic shale, minor limestone, and minor dolomite. This unit contains the abundant slope breccias and debris flows associated with the Skoki shale-out (Fig. 36.4, 36.5, 36.6). Davies (1966, Fig. 7) identified the base of this unit as within the Zone of **Paraglossograptus etheridgei** and identified the Zone of **Climactograptus bicornis** about 50 m above the top of this unit. The age of the OR_3 unit therefore ranges from Llanvirn to early Caradoc,



Figure 36.8. *Bedding plane view of 1 cm thick black phosphorite pavement. The sample is from the Kechika Formation, Section 11, and contains approximately 25 per cent fluorapatite. (GSC 199409)*

and is a time correlative unit to the Skoki dolomite. Basic volcanic tuffs were found in the basal part of this unit at Section 3.

The OR_4 unit is a 30 to 40 m succession of very distinctive resistant 'rusty shales'. At Section 10 this unit is split into two 30 m 'rusty shale' successions separated by 70 m of calcareous shale. The upper 'rusty shale' at this location contains a unique set of syndepositional calcite nodules. The nodules have flat bases and irregular rounded tops and consist of large radiating acicular crystals of black calcite oriented perpendicular to bedding (Fig. 36.7). At Section 4, Davies (1966, Fig. 7) identified the Zone of **Climacograptus bicornis** immediately above the 'rusty shales' and Carodocian graptolites within the 'rusty shales'. At location 109, 'rusty shales' directly overlie Skoki dolomite near the carbonate-platform to basin transition.

Unit OR_5 is a 180 m thick succession of interstratified shale and quartzite with minor dolomite. Davies (1966, Fig. 7) dated this unit as lying within and between the probable Zone of **Orthograptus truncatus intermedius** in the basal part of the unit, and the Zone of **Dicellograptus complanatus ornatus** in the upper part. Thus the OR_5 unit ranges from late Middle to Late Ordovician and makes it, in part, a time correlative unit to Upper Ordovician dolomite and quartzite preserved in the eastern study area.

Road River units are distinctive with contacts both gradational and abrupt. The OR_5 unit is missing below an Early Silurian unconformity at Sections 10 and 6-7. This unconformity was first reported and dated by Jackson et al. (1965, Fig. 2).

Road River rocks are interpreted as basin facies because they are a monotonous thick succession of reduced black graptolitic shale. Road River quartzite, which generally have relatively little matrix and are homogeneous and blocky, are also interpreted as basinal because they are lensed or interstratified with the black graptolitic shale.

Upper Ordovician Strata

Laterally equivalent to, and east of, the OR_4 and OR_5 Road River units are an Upper Ordovician unconformity and a complex succession of dolomite, arenaceous dolomite and quartz sandstone (Sections 704 NE, 17, 703 NE, 712 NE, 706 NE, 711 NE, 713 NE). The sandstone is massive, cross-bedded and locally contains abundant fossil fish fragments. Dolomite is brown or grey and frequently contains colonial or solitary corals (including **Catenipora**, and **Bighornia**), articulate brachiopods, stromatoporoids and trilobite debris.

The postulated lateral transitions of these rocks to coeval Road River strata have been removed by erosion in the 60 to 100 km wide belt that separates the two areas of Upper Ordovician outcrop.

Road River Formation – Silurian Units

Several Silurian units can be recognized within the Road River Formation of the western part of the study area. The SL unit (20-100 m thick) is a succession of thinly bedded grey limestone with slope breccias, minor shale, and dolomite. Davies (1966, Fig. 7) reported the **Monograptus gregarius** Zone (Middle Llandovery) in these rocks and **Monograptus spiralis** (from felsenmeer) and cyrtograptids were collected at location 4 in 1978 and indicate the latest Llandovery **M. spiralis** Zone and perhaps younger (Wenlock) horizons. The SL unit apparently conformably overlies Ordovician Road River strata at Sections 4 and 18. A time equivalent unit is present at Section 6-7 where interstratified thinly bedded dolomite and shale were dated by Jackson et al. (1965, Fig. 2) as **Monograptus turriculatus** Zone (Late Llandovery but not latest) and rest with unconformity on Ordovician Road River beds. At Section 10 and location 109 the SL unit is absent and Ordovician Road River is directly overlain by the SD unit (see below) indicating a sub-Wenlock or younger unconformity during which the unit was removed by erosion. This unconformity is in addition to the sub-Middle Llandovery or older unconformity described earlier. The SL unit and the unit at Section 6-7 are approximately the time equivalents of the Nonda Formation of the eastern part of the study area that unconformably overlies Upper Ordovician rocks.

Above Ordovician Road River or the SL unit (where present) is the SD unit, a thick succession of greyish orange and yellowish orange weathering rhythmically bedded dolomite with variable proportions of siltstone, shale and quartz sandstone. Large fan-shaped feeding trails are present in the basal beds at some localities; at Section 15, dolomite breccias are prominent from 60 to 110 m above the base of the unit and at Section 6-7 the basal part consists of 100 m of interbedded quartzites and shales. The SD unit is 275 to more than 500 m thick and lies between successions dated as latest Early Silurian (latest Llandovery) and Early Devonian and therefore probably is Middle and/or Late Silurian.

Significance of Unconformities

One of the more interesting results of this study is the further recognition of basinal unconformities first reported by Jackson et al. (1965). Sub-Kechika, sub-Upper Ordovician and sub-Nonda (Norford et al., 1967) platform unconformities are recognized in the eastern study area, while sub-Kechika, sub-Middle Llandovery, and sub-Wenlock basin unconformities are recognized in the western study area. In the central

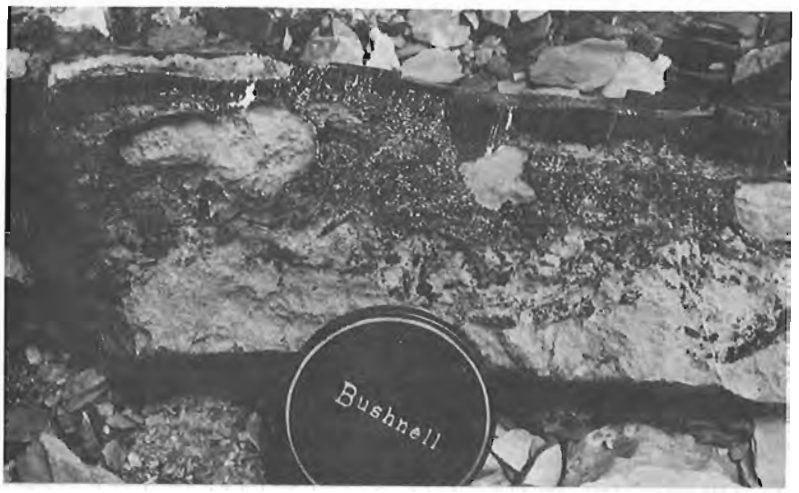


Figure 36.9. *View of a phosphorite pavement perpendicular to bedding. Debris at the base of the pavement is phosphatic trilobite debris. Trilobite debris is not typical of the pavement. (GSC 199404)*



Figure 36.10. *View of a nodule-lag conglomerate. These beds are medium to thick, planar bedded and occur scattered within deep water nodular Kechika calcilutite (top photo) at Section 11. Some conglomerate clasts are covered in a phosphatic coating. Scale: bed is 15 cm thick. (GSC 199408)*

study area sedimentation between units is continuous; Upper Cambrian units are transitional to Kechika rocks at Section 2 and at the headwaters of the Prophet River, and deposition is continuous from the Kechika through to the .SD strata at Section 4.

The paleogeographic implication of these data is that land masses were exposed in the eastern and western study areas, separated by a depositional trough, during latest Cambrian (sub-Kechika) and Early and Middle Silurian times. In the Late Ordovician, land masses could have existed only in the eastern area, although a Late Ordovician unconformity could be hidden by Early Silurian erosion in the basin area.

This paleogeographic pattern mimics, to a certain degree, that established in Cambrian times (G.C. Taylor, pers. comm.) suggesting that the tectonic framework that controlled sedimentation was a persistent repetitive feature of this area.

Economic Geology — Barite, Phosphorite and Uranium Occurrences

Five separate levels of stratiform barite mineralization are known. These occur in the Kechika (OK_1), Road River Formation (OR_1 and OR_5) and at two levels in the basal SD unit (Fig. 36.2). The Kechika barite occurs as scattered crystalline nodules in the middle of the 'platy limestones' at Section 2. The first Road River barite is found as abundant nodules in felsenmeer near the top of the OR_1 unit at Section 11. The second Road River barite occurs approximately 25 m below SL limestone at Section 4. Barite in a similar stratigraphic position to that at Section 4 has been recognized by C.W. Jefferson (pers. comm.) just northwest of Section 18. At Section 4, barite is 0.5 m thick, white, massive, medium crystalline, and occurs within graptolitic shale with minor quartzite. Davies (1966, Fig. 7) recognized the **Dicellograptus complanatus ornatus** Zone in a position which, by comparing sections, would be a few metres above this occurrence. This mineralization is particularly interesting because of the potential for laterally associated shale-hosted sphalerite-galena mineralization. Unfortunately the area of potential mineralization was severely reduced by Early and Middle Silurian erosion which removed the OR_5 unit at locations 10 and 6-7. The two barite occurrences in the SD unit are located at Section 18 and both can be traced laterally for at least 1 km. The lower comprises a zone of massive white barite, about 1 m thick, that is found at the base of the SD unit; the upper is a thin zone of crystalline barite nodules 80 m above the base of the SD unit.

In northeastern British Columbia as in the Bonnet Plume area (Cecile, 1978) sedimentary barite is found in several different ages of basinal sediments. The five occurrences reported here are latest Cambrian, Early Silurian, Late Ordovician, and Middle and/or Late Silurian. These occurrences are dwarfed by the numerous deposits found throughout Upper Devonian rocks in the same area.

Two areas of phosphorite mineralization (estimated 2-25 per cent fluorapatite) were discovered in 1978. At Section 2 phosphorite occurs as large (0.5-1 cm) black nodules scattered in Upper Cambrian shale in sporadic beds from 220 to 120 m below the Kechika Formation. At Section 11, measured at Grey Peak just west of Haworth Lake (Fig. 36.1, 36.2), phosphorite is scattered through 120 m of section in the upper 'banded limestones' (OK_3), at several positions near the top of the 'upper recessive' Kechika (OK_4), and scattered in the basal 60 m of the Road River Formation (OR_1). Phosphorite clearly occurs as thin (<1-5 cm) sea floor pavements (Fig. 36.8, 36.9) and, in at least one bed, includes significant associated uranium concentration. In the OK_4 unit the phosphorite is associated with 'nodule' conglomerate (Fig. 36.10) that appears to be a lag accumulation resulting from periodic washing of partly lithified Kechika sediments in deep water.

The position of Section 11 is interpreted to be close to the shelf edge (see previous discussion) and concentrated phosphorite probably accumulated during periods of slow sedimentation from phosphate-rich seawater (for discussion of marine phosphorites see Christie, 1978).

Uranium was found in significant concentration in one phosphorite sample (8 per cent fluorapatite) at Section 11 (see Fig. 36.2). This sample is analyzed as having 196 ppm uranium (neutron activation; Atomic Energy of Canada) to 220 ppm (spectrometer analysis; Geological Survey of Canada, Ottawa). Cathcart (1978) reports this level of uranium concentration as normal for marine phosphorites.

The Section 11 phosphorite occurrences are certainly noneconomic but they do indicate potential for phosphate exploration in northeastern British Columbia. Two possible exploration targets would be: more basinal Kechika facies where slow sedimentation rates may have persisted long enough for significant phosphate concentrations; and reworked and reconcentrated Kechika phosphorite below post-Kechika basinal unconformities including those in the Devonian (see Taylor et al., 1979). Reworked phosphates are also interesting uranium exploration targets. Cathcart (1978) reports significant enrichment of uranium in phosphates due to uranium scavenging by apatite.

Conclusions

Lower Paleozoic strata in the Ware-Trutch map areas span the transition from shelf to basin facies. The mainly Lower Ordovician Kechika Formation can be divided into five units shows rapid but continuous change from platform to deep shelf facies. Middle Ordovician Skoki dolomite, divisible into four units, passes laterally into equivalent parts of the Road River Formation, through a narrow zone containing spectacular stratiform carbonate breccias. The Road River Formation ranges in age from late Early Ordovician to Devonian and includes five Ordovician units that are western basin equivalents to the uppermost Kechika, Skoki, and Upper Ordovician quartzite and dolomite preserved in the eastern study area. In the central and western study area, Lower Silurian limestone and Middle to Upper Silurian argillaceous dolomite of the Road River Formation both conformably (central area) and unconformably (western area) overlie the Ordovician parts of the formation.

Latest Cambrian, possible Late Ordovician, Early and Middle Silurian unconformities are recognized in the western basin study area, and in the eastern platform area but not in the central area where deposition was continuous.

Sedimentary barite is reported from uppermost Cambrian, Lower Ordovician, Upper Ordovician, and Middle to Upper Silurian basin strata. Phosphorite with some uranium mineralization is found in noneconomic concentrations in Upper Cambrian and Lower Ordovician strata and indicate potential for exploration.

References

Cathcart, J.B.
1978: Uranium in phosphatic rock; U.S. Geological Survey, Professional Paper 988-A.

Cecile, M.P.
1978: Report on Road River stratigraphy and the Misty Creek Embayment, Bonnet Plume (106B), and surrounding map-areas, Northwest Territories; in Current Research, Part A, Geological Survey of Canada, Paper 78-1A, p. 371-377.

Christie, R.L.
1978: Sedimentary phosphate deposits – an interim review; Geological Survey of Canada, Paper 78-20.

Davies, E.J.L.
1966: Ordovician and Silurian of the northern Rocky Mountains between Peace and Muskwa Rivers, British Columbia; Unpublished Ph.D. Thesis, University of Alberta.

Gabrielse, H.
1954: McDame, British Columbia; Geological Survey of Canada, Paper 54-10.

1963: McDame map-area Cassiar District, British Columbia; Geological Survey of Canada, Memoir 319.

1975: Geology of Fort Grahame E1/2 map-area, British Columbia; Geological Survey of Canada, Paper 75-33.

1977: Geological map of Ware W1/2 and Toodoggone River map-areas; Geological Survey of Canada, Open File Report 483.

1977: Geological map of Ware W1/2 and Toodoggone River map-areas; Geological Survey of Canada, Open File Report 483.

Jackson, D.E. and Lenz, A.C.
1962: Zonation of Ordovician and Silurian graptolites of northern Yukon, Canada; American Association of Petroleum Geologists, Bulletin, v. 46, p. 30-45.

Jackson, D.E., Steen, G., and Sykes, D.
1965: Stratigraphy and graptolite zonation of the Kechika and Sandpile Groups in northeastern British Columbia; Bulletin of Canadian Petroleum Geology, v. 13, p. 139-154.

Norford, B.S.
1962: The Silurian fauna of the Sandpile Group of northern British Columbia; Geological Survey of Canada, Bulletin 78.

1969: Ordovician and Silurian stratigraphy of the southern Rocky Mountains; Geological Survey of Canada, Bulletin 176.

1979: Lower Devonian graptolites in the Road River Formation, northern British Columbia; in Current Research, Part A, Geological Survey of Canada, Paper 79-1A, Note.

Norford, B.S., Gabrielse, H., and Taylor, G.C.
1967: Stratigraphy of Silurian carbonate rocks of the Rocky Mountains, northern British Columbia; Bulletin of Canadian Petroleum Geology, v. 14, p. 504-519 (dated 1966).

Taylor, G.C. and Stott, D.F.
1973: Tuchodi Lakes map-area, British Columbia; Geological Survey of Canada, Memoir 373.

Taylor, G.C., Cecile, M.P., Jefferson, C.W., and Norford, B.S.
1979: Stratigraphy of the Ware E1/2 map area; in Current Research, Part A, Geological Survey of Canada, Paper 79-1A, Report 37.

Thompson, R.I.
1976: Some aspects of stratigraphy and structure in the Halfway River map-area (94B), British Columbia; in Current Research, Part A, Geological Survey of Canada, Paper 76-1A, p. 471-477.

1978: Geological maps and sections of the Halfway map-area, Alberta (94B); Geological Survey of Canada, Open File Report 536.

Walcott, C.D.
1928: Pre-Devonian Paleozoic formations of the Cordilleran provinces of Canada; Smithsonian Miscellaneous Collections, v. 75, no. 5.

37. STRATIGRAPHY OF WARE (EAST HALF) MAP AREA, NORTHEASTERN BRITISH COLUMBIA

Project 630017

G.C. Taylor, M.P. Cecile, C.W. Jefferson[1], and B.S. Norford
Institute of Sedimentary and Petroleum Geology, Calgary

Taylor, G.C., Cecile, M.P., Jefferson, C.W., and Norford, B.S., Stratigraphy of Ware (east half) map area, northeastern British Columbia; in Current Research, Part A, Geol. Surv. Can., Paper 79-1A, p. 227-231, 1979.

Abstract

Ware (east half, 94F, E1/2) map area in the Rocky Mountains of northeastern British Columbia is underlain by rocks ranging in age from Proterozoic to Cretaceous. Proterozoic rocks of Helikian age are exposed in the faulted core of the Muskwa Anticlinorium. Cambrian rocks occur in four separate facies assemlages, three associated with the Muskwa Anticlinorium and the fourth assemblage overlying upper Proterozoic rocks in the southwest corner of the map area. Ordovician rocks of the Kechika Formation are the most widespread unit exposed and record the onset of a differentiation in facies of Ordovician to Devonian rocks into a northeastern platformal assemblage and equivalent southwestern basinal assemblage. Upper Devonian clastics occurring unconformably on top of the basinal assemblages host significant barite and lead-zinc mineralization.

Introduction

The stratigraphic control established in the Ware (east half, 94F, E1/2) map area (see Fig. 37.1) during 1964 on Operation Liard (Taylor, 1965) was insufficient to warrant the compilation of a geological map. Field studies in adjacent map areas have established the regional stratigraphic framework which was applied and refined in the map area during the 1978 field season. Structural and mapping studies were carried out by G.C. Taylor; Cambrian stratigraphy by G.H. Eisbacher; Cambrian biostratigraphy by W.P. Fritz; Ordovician-Silurian stratigraphy by M.P. Cecile; Ordovician-Silurian biostratigraphy by B.S. Norford; and mapping and stratigraphic studies of the Road River through 'Black Clastic' successions by C.W. Jefferson.

Stratigraphy

The Ware (east half) map area is underlain by rocks ranging in age from Helikian to Early Cretaceous. Only in the extreme northeast corner are rocks of late Paleozoic and Mesozoic age exposed. Although well known from the adjacent Trutch map area (Pelletier and Stott, 1963; Gibson, 1971), these successions will not be discussed in this report. Figure 37.2 schematically illustrates the stratigraphic relationships of the Precambrian to Devonian successions. Figure 37.3 is a sketch map showing the distribution of gross lithological units.

Helikian

Three formations (Tuchodi, Aida, and Gataga) of the Tuchodi Lakes Helikian successions (Taylor and Stott, 1973) are represented in fault-cored anticlinoria of the northern part of the Ware map area. Progressively younger units of the formations are exposed beneath the sub-Cambrian unconformity westward in each structure. Basaltic dykes cut all three formations.

Hadrynian

In the extreme southwest corner of the map area, strongly metamorphosed (locally containing garnets) metasediments representative of the Missinchinka Group are exposed. Within this sequence is thin medium crystalline metadolomite that suggests a correlation with the Byng Formation of the Miette Group. The general succession exposed can be loosely correlated to the Upper Miette and upper Middle Miette successions of the Pine Pass and Monkman Pass map areas on the basis of lithological sequence. Nowhere, as yet, in northeastern British Columbia has a stratigraphic contact been observed between the presumed Helikian and Hadrynian successions.

?Hadrynian

North and east of Mount Lloyd George, an interesting sequence of diamictite approximately 900 m thick unconformably overlies the Aida and Gataga formations. This unit, first recognized by Fritz (1972), lies unconformably beneath well dated (**Nevadella** Zone) Lower Cambrian quartzite.

These diamictites occur in a tectonic setting that is similar to settings observed in both Lower and Middle Cambrian successions and are commonly found spatially related to the same sets of reactivated faults. They are unlike the diamictites observed in the Missinchinka Group and Miette Group of the Pine Pass (93O) and Monkman Pass (83I), respectively. These diamictites occur stratigraphically in the upper middle member of both groups. Although only the equivalent of the **Fallotaspis** Zone is available, the Lloyd George diamictites could be of Early Cambrian age.

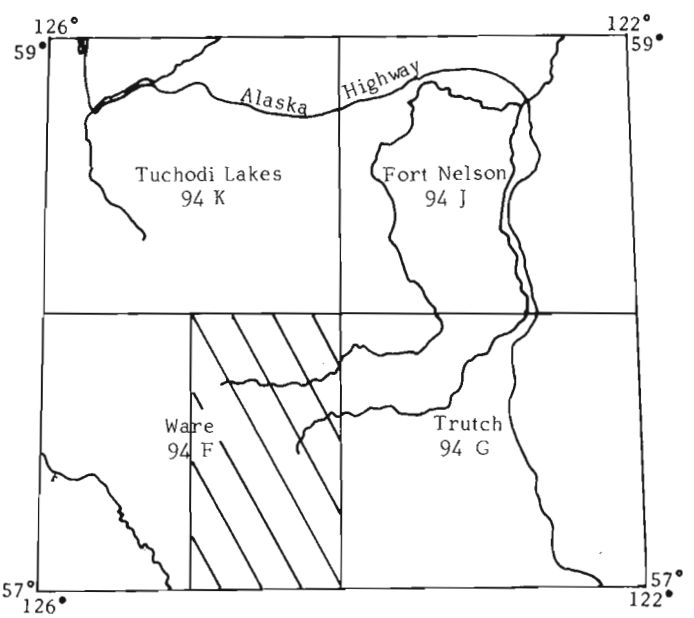
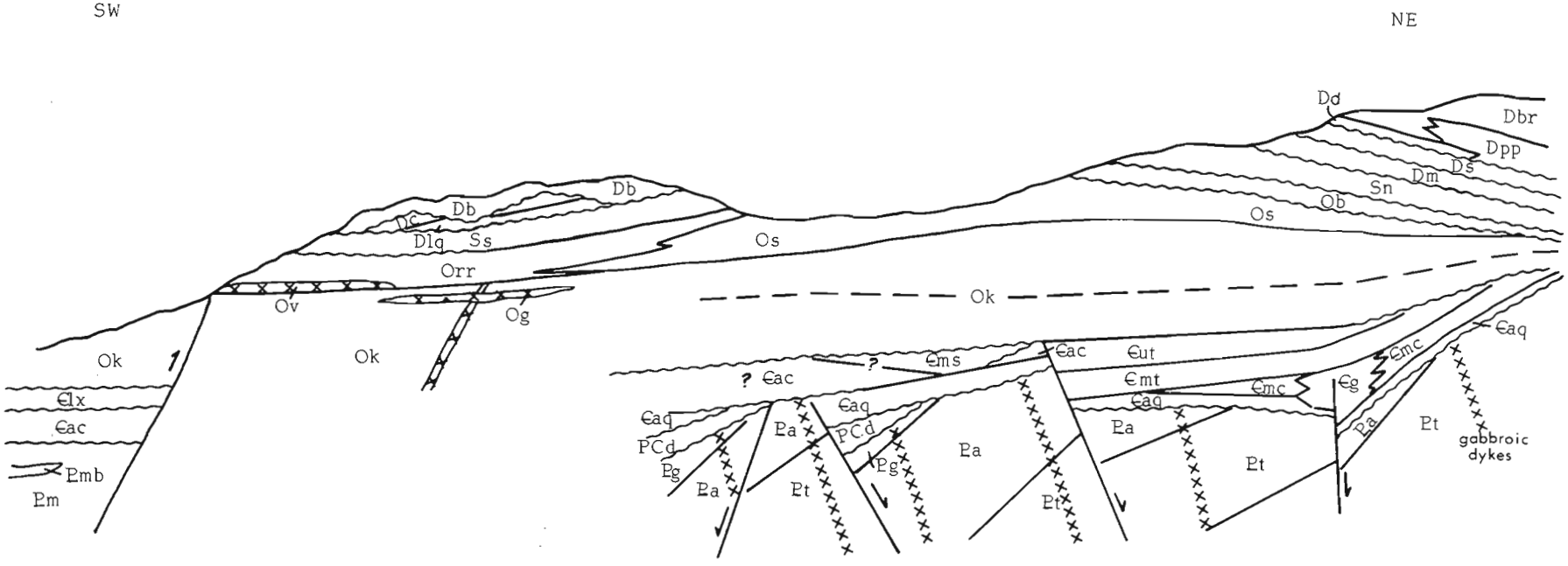


Figure 37.1. *Index map of northeast British Columbia.*

[1]University of Western Ontario, London



LEGEND

Dbr	Besa River Fm.	Ss/Sn	Silurian siltstones/Nonda Fm.	Eac	Atan Fm. – upper carbonate division
Db	"Black Clastics"	Orr	Road River Fm. (Ov–volcanics)	Eaq	Atan Fm. – lower quartzite division
Dpp	Pine Point Fm.	Ob	Late Ordovician quartzites and carbonates	PCd	Diamictite and carbonate olistostrome
Dd	Dunedin Fm.	Os	Skoki Fm.	Pm	Missinchinka Gp. (Pmb–Byng Fm.)
Dc	Devonian carbonates and shales (in part Early Devonian)	Ok	Kechika Gp. (Og–basic sill)	Pg	Gataga Fm.
Ds	Stone Fm.	Elx/Eut	Lynx Fm/late Cambrian calcareous turbidites	Pa	Aida Fm.
Dlq	Early Devonian orthoquartzites	Ems/Emt	Middle Cambrian basinal shales Middle Cambrian siliceous turbidites	Pt	Tuchodi Fm.
Dm	Muncho–McConnell Fm.	Emc	?middle Cambrian dolomites (includes – Eg – fanglomerates)		

Figure 37.2. *Schematic stratigraphic relationships, Ware (east half) map area.*

Elsewhere in the Cordillera, upper Precambrian diamictite has been interpreted as tillite. Close examination of the Lloyd George diamictite reveals it to be crudely bedded, with local channels filled by conglomerate, contain no demonstrable drop-stones, and most of the few faceted and striated clasts can be directly related to tectonic slip surfaces. Boulders up to 2 m in diameter occur locally and are derived from underlying rock types. Dolomite breccias and olistostromes are common at or near the top of the succession. An intense search did confirm the occurrence of exceedingly rare granite boulders previously reported by Fritz (pers. comm.). Although Fritz (1972) suggested that a glacial origin for these rocks was possible, no diagnostic evidence was observed and an alternative interpretation is one of mass flows originating from scarps and triggered by active faults. The occurrence of the dolomite olistostromes suggests deposition into a marine environment along an unstable coast. The source of the granite erratics is unknown.

Cambrian

The stratigraphic relationships of the various Cambrian units is extremely complex, and only partially resolved. Four distinct facies sequences occur and their correlations are not fully established. In the southwest portion of the map area there occurs, in a geologically complex faulted terrane, a succession of orthoquartzite, quartzose dolomite, dolomite, and shale which contain both trilobite and archaeocyathid faunas of Early Cambrian age. This succession weathers predominantly rusty brown to red-brown and near Pesika Creek is unconformably overlain by uniformly bedded medium grey weathering, nodular limestone of Late Cambrian age (Dresbachian-Trempealeauan). This unit has been assigned to the Lynx Group on the basis of both age and similar lithology. It is overlain, apparently conformably by the 'putty-grey' unit of the Kechika Formation.

The second major facies group is typified by the succession exposed in the Muskwa Anticlinorium. There Helikian formations are unconformably overlain by several hundred metres of fine grained orthoquartzite with prominent "**Skolithus**" tubes. Overlying the quartzite is a prominent red-weathering dolomite unit with a maximum thickness of 300 m. This dolomite unit thins to a feather edge along the west flank of the Muskwa Anticlinorium. It is overlain by more than 500 m of fine grained siliceous siltstone and shale with many aspects of turbidites. Among the sedimentary features exhibited are examples of graded beds, slump folds, convolute bedding, flame structures, and small scale cross-laminations. Fritz (pers. comm.) has recovered Middle Cambrian trilobites from these rocks near the feather edge of the underlying dolomite. The siliceous turbidites are overlain by calcareous turbidites containing carbonate debris flows near their top. Interbedded with the debris flows is a prominent sandstone member. Late Cambrian (late Franconian or early Trempealeauan) trilobites have been recovered from this succession. It is conformably overlain by the 'platy limestones' and the 'putty-grey' unit of the Kechika Formation(Cecile and Norford, 1979).

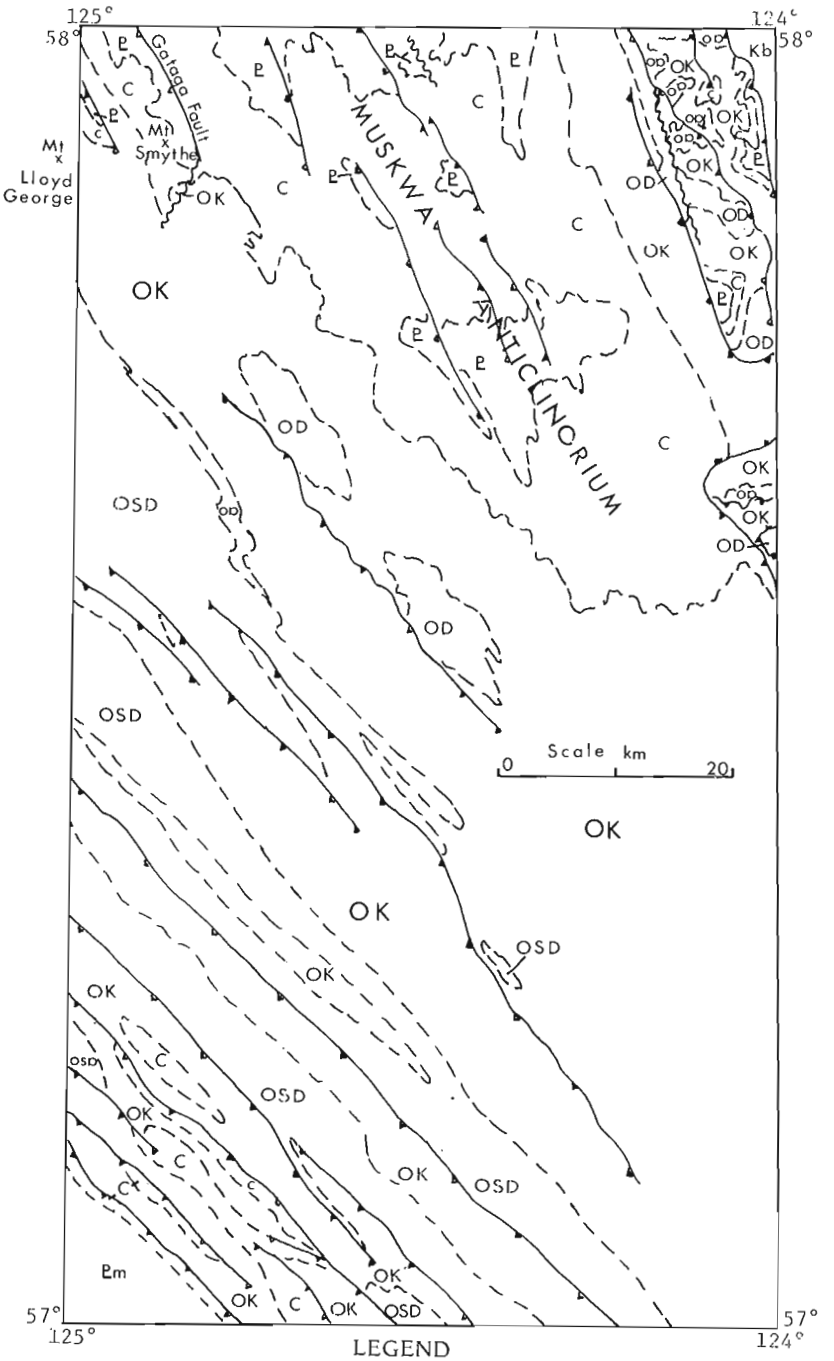


Figure 37.3. *Geological sketch, Ware map area (94F east half).*

The third major facies package of Cambrian sediments is exposed west of the Gataga Fault where 700 m of Lower Cambrian quartzite and siltstone unconformably overlie either the Aida Formation or locally the diamictite. Ten kilometres north of Mount Lloyd George, the quartzite is overlain by carbonate of the Atan Group that is unconformably overlain by a thin condensed section (40 m) of Middle Cambrian shale. Four kilometres east of Mount Lloyd George at Mount Smythe, the quartzite is overlain by 300 m of massive limestone lithologically similar to the Atan. In that section, the limestone oversteps a fault to lie directly on the Helikian Aida Formation or locally the diamictite. On the north face of Mount Smythe, this limestone either passes completely into a thick (more than 500 m) black shale or is overlapped by the shale. Fritz (pers. comm.) has recovered Middle Cambrian trilobites from the shale succession. Both the limestone and the thick black shale are unconformably overlain by Kechika carbonate. This third package with its many hiatuses abuts the second package across the Gataga Fault thus requiring an early pre-Ordovician phase of motion on that fault.

The fourth major facies package occurs mainly in the adjacent Tuchodi Lakes map area but the facies is present along the northern boundary of the Ware map area. There the succession includes a basal quartzite unit approximately 100 m thick commonly overlain by more than 800 m of tan weathering dolomitic sandstone, dolomite, and minor limestone. Coarse red-weathering conglomerate commonly occurs in channels and as sheets in the lower part of the sequence. Locally this conglomerate can be directly related to large normal faults active at the time of deposition. Vertical displacements in excess of 500 m have been established on three of these faults. In more westerly sections, dolomite predominates to an apparent shelf edge near longitude 125°. West of the facies change, thick basinal shale with extensive carbonate debris flows occupy the same stratigraphic position. Near this facies change large submarine channels, which cut into the dolomite, were observed by Eisbacher. Fritz (pers. comm.) has collected Middle Cambrian trilobites from relatively high in the quartzite-dolomite succession.

Ordovician

Four map-units of Ordovician age are recognized within the Ware map area. They are the Kechika Formation, 'Skoki' Formation, an unnamed Upper Ordovician quartzite-carbonate unit, and the Road River Formation.

The Kechika Formation is a westward thickening repetitious succession of fine grained argillaceous limestone. Kechika rocks exhibit the change in depositional environment from platform, westward into shelf and deep shelf facies recording the onset of differentiation of Paleozoic strata into platform and basin facies. The division into platform and basin facies becomes more abrupt in Skoki and Upper Ordovician rocks. Abrupt facies changes are a characteristic feature of Ordovician to Devonian rocks throughout the Selwyn Basin. The transition from platform facies on the northeast to basin facies on the southwest trends southeast through the Ware (east half) map area and intersects the Mountain Front in the Halfway River map area (Thompson, 1976, 1978) between Mount Kenny and Lady Laurier Lakes.

Silurian

Three map-units of Silurian age are recognized. In the northeast portion of the map area, approximately 210 m of carbonate and quartzite of the Nonda Formation (Norford et al., 1966) unconformably overlie the unnamed quartzite-carbonate unit of Late Ordovician age. In the west and southwest portion of the map area, two Silurian units are recognized. The older is a 20 to 100 m succession of Lower Silurian limestone, and the younger a 275 to 500 m succession of very argillaceous dolomite and siltstone with minor shale and quartzite (see Cecile and Norford, 1979, for detailed discussion).

Devonian

Seven units of Devonian age are recognized; four are mapped in the platformal succession and three units are recognized in the basinal facies. Complete sections of the platformal carbonate rocks of the Muncho-McConnell, Stone, and Dunedin formations are exposed along the Mountain Front north and south of the Muskwa River in the northeast corner of the map area. Highly deformed Besa River shale is also exposed there in the footwalls of the frontal thrusts. The carbonate formations are all thin relative to successions both north and south suggesting the presence of a local arch.

Two major successions separated by a major unconformity are present in the basinal facies in the west and southwest portion of the map area. The older succession, only locally preserved, includes calcareous quartzite along the northeast side of the basinal facies with interbedded calcareous shale, and cherty limestone debris flows. The interbedded shale has yielded Early Devonian graptolites (Norford, 1979) and the carbonate debris flows contain "two-holed" crinoid ossicles, also indicating an Early Devonian age. In western exposures of this basinal belt, rather resistant limestone occurs that may in part be the lateral equivalent of the clastics as well as including younger sediments. This limestone also represents carbonate debris flows and includes a transported fauna of middle Devonian age. Taylor (in Taylor and MacKenzie, 1970) referred these carbonate rocks to the Dunedin Formation, a somewhat cavalier usage that has persisted. The carbonate bears little resemblance to those typical of the Dunedin Formation of the platformal succession.

Unconformably overlying the Devonian carbonate, and locally the Silurian siltstone, is a thick monotonous unit of black siliceous shale with associated fine- to coarse-grained quartzite and pebble conglomerate. Informally referred to as the "Black Clastics", these rocks contain numerous showings of nodular and massive barite many of which have associated lead and zinc mineralization. North of Paul River (Ware west half), geologists of Cyprus Anvil Corporation have discovered Late Devonian ammonoids preserved in barite at their Cirque claims. Prominent gossans are associated with this distinctive stratigraphic unit. The "Black Clastics" are preserved in the faulted cores of three major synclinoria in the western and southern half of the map area.

References

Cecile, M.P. and Norford, B.S.
1979: Basin to platform transition, lower Paleozoic strata of Ware and Trutch map areas, northeastern British Columbia; in Current Research, Part A, Geological Survey of Canada, Paper 79-1A, Report 36.

Fritz, W.P.
1972: Cambrian biostratigraphy, western Rocky Mountains, British Columbia; in Report of Activities, Part A, Geological Survey of Canada, Paper 72-1A, p. 208-211.

Gibson, D.W.
1971: Triassic stratigraphy of the Sikanni Chief-Pine Pass region, Rocky Mountain Foothills, northeastern British Columbia; Geological Survey of Canada, Paper 70-31.

Norford, B.S.
1979: Lower Devonian graptolites in the Road River Formation, northern British Columbia, 94B, C, F; in Current Research, Part A, Geological Survey of Canada, Paper 79-1A, Note.

Norford, B.S., Gabrielse, H., and Taylor, G.C.
1966: Stratigraphy of Silurian carbonate rocks of the Rocky Mountains, northern British Columbia; Bulletin of Canadian Petroleum Geology, v. 14, no. 4, p. 504-519.

Pelletier, B.R. and Stott, D.F.
1963: Trutch map-area, British Columbia; Geological Survey of Canada, Paper 63-10.

Taylor, G.C.
1965: Operation Liard; in Report of Activities, Field 1964; Geological Survey of Canada, Paper 65-1, p. 66-67.

Taylor, G.C. and MacKenzie, W.S.
1970: Devonian stratigraphy of northeast British Columbia; Geological Survey of Canada, Bulletin 186.

Taylor, G.C. and Stott, D.F.
1973: Tuchodi Lakes map-areas; Geological Survey of Canada, Memoir 373.

Thompson, R.I.
1976: Some aspects of stratigraphy and structure in the Halfway River map-area (94B), British Columbia; in Report of Activities, Part A, Geological Survey of Canada, Paper 76-1A, p. 471-477.

1978: Geological maps of the Halfway River map-area (94B), 1:250 000 and 1:50 000; Geological Survey of Canada, Open File Report 536.

38. # LITHOFACIES INTERPRETATION AND CONODONT BIOSTRATIGRAPHY OF THE BLUE FIORD FORMATION IN THE SUBSURFACE OF CAMERON AND VANIER ISLANDS, CANADIAN ARCTIC ARCHIPELAGO

Projects 680101 and 750017

T.T. Uyeno and Ulrich Mayr
Institute of Sedimentary and Petroleum Geology, Calgary

Uyeno, T.T. and Mayr, Ulrich, Lithofacies interpretation and conodont biostratigraphy of the Blue Fiord Formation in the subsurface of Cameron and Vanier islands, Canadian Arctic Archipelago; in Current Research, Part A, Geol. Surv. Can., Paper 79-1A, p. 233-240, 1979.

Abstract

The carbonate rocks of the Blue Fiord Formation in the subsurface of Cameron and Vanier islands can be assigned to five lithofacies: open shelf, deep reef flank, upper reef flank, reefal margin, and bank interior. The lithofacies are distinguished mainly on the basis of the morphology of stromatoporoids and limestone texture. The carbonate rocks of the Blue Fiord Formation interfinger laterally with basinal shale of the Cape De Bray and Eids formations.

*The conodonts of the Blue Fiord Formation are well preserved to only moderately so, and range from the probable **gronbergi/inversus** Zones of late Early Devonian (Zlichovian-Dalejan) age, through the **serotinus** Zone to the **costatus costatus** Zone (Eifelian; early Middle Devonian). The intervening **patulus** Zone appears to be missing. The open shelf and upper reef flank lithofacies yielded the most prolific conodont faunas, both in terms of number and diversity. The bank interior and deep reef flank lithofacies yielded only small collections, and the reefal margin lithofacies was found to be barren of conodonts. The Blue Fiord conodonts have a coloration of about CAI 1.5 to 2 of Epstein et al. (1977). Paleoecological interpretations of the conodont faunas are ambiguous because of biased sampling.*

Introduction

During the spring of 1974 crude oil from the Lower and Middle Devonian Blue Fiord Formation was discovered in the Panarctic Tenneco et al. Bent Horn N-72 well on Cameron Island (Fig. 38.1). Subsequent to the discovery, about ten more wells were drilled on Cameron and Vanier islands, the most recent of which was completed in September 1978 and located about 10 km northeast of the Bent Horn N-72 wellsite. Several of these wells in the close vicinity of the discovery well encountered hydrocarbons in the structurally and diagenetically complex Blue Fiord carbonate. The present paper presents a preliminary interpretation of the carbonate lithofacies and conodont zonation of the Blue Fiord Formation in four of these wells, namely:

1) Panarctic Cape Fleetwood M-21 (Lat. 76°30'47.8"N, Long. 103°40'37.0"W);
2) Panarctic et al. West Bent Horn C-44 (Lat. 76°23'09.3"N, Long. 104°17'10"W);
3) Panarctic Tenneco et al. Bent Horn N-72 (Lat. 76°21'50"N, Long. 103°58'11.9"W);
4) B.P. et al. Panarctic Hotspur J-20 (Lat. 76°09'37"N, Long. 104°04'43"W).

The facies interpretations in this paper are based on examination of drill cuttings, cores, and geophysical wireline logs. Conodonts were obtained from cores and cuttings. Lithofacies descriptions are by Mayr; biostratigraphy and determination of colour alteration of conodonts are by Uyeno.

General Stratigraphy

In the Cameron, Vanier, and eastern Melville islands area, the Blue Fiord Formation forms one or several carbonate outliers, separated laterally by the fine grained clastics of the Eids and Cape De Bray formations (Kerr, 1974; Embry and Klovan, 1976) from the slightly younger occurrences of the formation along the east side of Bathurst Island. The Bent Horn N-72 well penetrated a complete section of the Blue Fiord Formation, together with an underlying shaly dolomitic interval and a thick carbonate sequence, assigned to the Eids and Disappointment Bay formations, respectively (Mayr, in press). The Blue Fiord Formation is overlain, probably disconformably, by the Cape De Bray Formation (Embry and Klovan, 1976).

Facies Interpretation

The carbonate penetrated by the four wells can be assigned to several depositional lithofacies (Fig. 38.1, Table 38.1) based on the models of Wilson (1975). The extent of the present information does not allow the development of an unequivocal facies model, but a basic facies pattern ranging from an open basin to bank interior is evident. Several assumptions are implicit in the model on Figure 38.1:

1) No structural duplication or omission of sequence is present in the four wells;
2) Paleotopographical relief at the disconformity at the top of the Blue Fiord Formation can be neglected;
3) The base of the Blue Fiord Formation in the Hotspur well is approximately contemporaneous with the base of the formation in the Bent Horn N-72 well.

The facies distinguished are basin, open shelf, deep reef flank, upper reef flank, reefal margin, and bank interior.

In Table 38.1 an attempt is made to express the level of confidence in the precision of the lithofacies interpretation. The grading is based on data quality and intuition. "Good" is used only for intervals where core is available and for the basinal intervals in the Hotspur well where shale and tentaculitids leave no other plausible choice than assignment to a basinal environment. Intervals which are represented by cuttings only are classed as "fair", and are further downgraded to "poor" in cases where other interpretations within the general frame of the model in Figure 38.1 are possible.

"Basin" refers to deeper areas surrounding the carbonate build-ups where little, if any, detrital carbonate deposition occurred. This facies is rich in pelagic fossils, in this particular case tentaculitids. It corresponds to Wilson's (1975) facies 1D. The facies is present in the Hotspur well

Table 38.1

Facies interpretation, Blue Fiord Formation, Cameron and Vanier islands

Facies		Panarctic Cape Fleetwood M-21			Panarctic *et al.* W. Bent Horn C-44			Panarctic Tenn. *et al.* Bent Horn N-72			BP *et al.* Hotspur J-20		
This paper	Wilson (1975)	Unit top (ft)	Main supportive evidence	Confidence	Unit top (ft)	Main supportive evidence	Confidence	Unit top (ft)	Main supportive evidence	Confidence	Unit top (ft)	Main supportive evidence	Confidence
Basin	1D										4 (lower part) 9000	shale, tentaculitids	G
											2 9436	shale, tentaculitids	G
Open shelf	3D				2 11320	crinoidal packstone and wackestone	F	2 (lower part) 11440	crinoidal wackestone, lime mudstone	G			
Deep reef flank	Toe of slope, foreslope										4 (upper part) 8634	graded bedding	G
											1 9583	stratigraphic position, crinoidal packstone	P
Upper reef flank	5D-7D	3 (upper part) 10886	tabular stromatoporoids, matrix with high micrite content	G	4 10408	corals, *Stachyodes* sp., coral baffle- and bindstone	G	3 (core 1) 10520	corals, matrix with high micrite content	G	3 9216	rich fauna with corals and stromatoporoids, skeletal grain and wackestone	F
Reefal margin	8D, sands on edge of platform	3 (lower part) 11080	coated grain grainstone, rare stromatoporoids	P				3 (lower part) 10720	massive stromatoporoids, skeletal grainstone	G			
		1 11460	massive stromatoporoids, coated grain grainstone	G				2 (upper part) 10992	coated grain and pelletoidal grainstone	P			
								1 (middle part) 11780	pelletoidal grainstone and packstone	P			
Bank interior	12D, 13D	2 11260	?cryptalgal limestone, coated grain grainstone, calcispheres (gradational to reefal margin)	P	1 11549	lack of fauna, pelletoidal packstone	P	1 (upper part) 11643	lime mudstone, impoverished fauna	P			
					3 10540	birdseye texture, impoverished fauna	F	1 (lower part) 11910	lime mudstone, impoverished fauna	F			

Level of confidence (see text for explanation) G = good, F = fair, P = poor

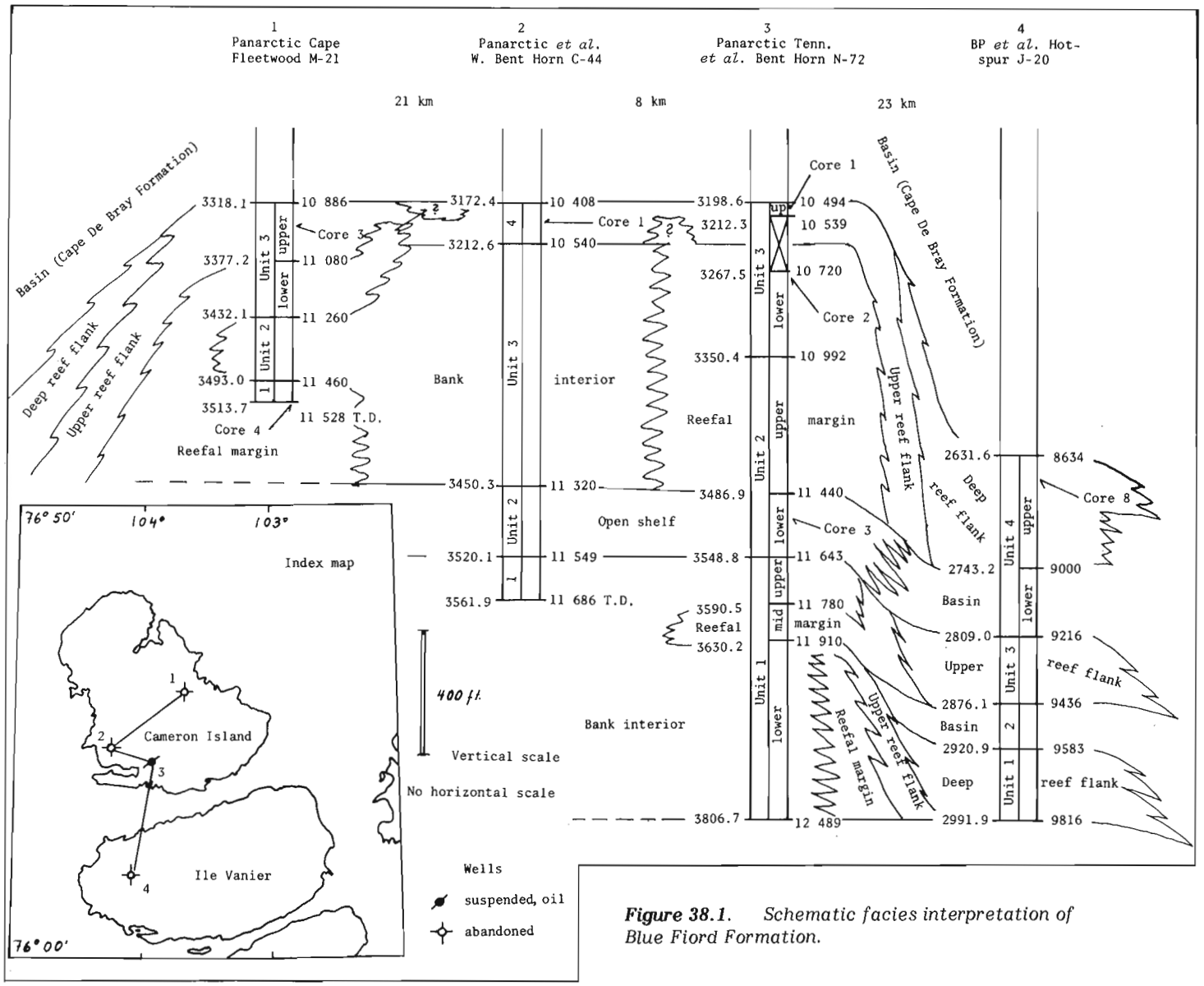


Figure 38.1. *Schematic facies interpretation of Blue Fiord Formation.*

and is formed by tongues of shale and siltstone, assigned to the Eids Formation, correlative with the lower part of the Blue Fiord Formation. The Cape De Bray Formation also contains rocks of basinal environment and, in the Hotspur well, is considered to be a lateral, argillaceous and silty equivalent of upper part of the Blue Fiord carbonate.

Carbonate rocks that are interpreted to be deposited below normal wave base and at some distance from shallow water carbonate build-ups are classed as "Open Shelf". They correspond to the sediments of Wilson's (1975) facies 3D. Two occurrences of this facies are present in the W. Bent Horn C-44 and Bent Horn N-72 wells. The two intervals presumably represent the same event when water depth increased over the initial Blue Fiord carbonate bank, and deposition of shallow water carbonate was suppressed.

"Deep Reef Flank" is the environment for carbonate of mostly detrital origin, derived from the topographically higher reef. Wilson's (1975) "toe of slope" and "foreslope" form this facies. The facies was observed only in the Hotspur well, where it is very well represented by the graded crinoidal deposits in core 8, in the upper part of unit 4. Unit 1 in the Hotspur well with its large amount of crinoidal limestone may indicate an open shelf facies, but has been placed in the deep reef flank facies because of its stratigraphical position. Deposition of this facies is visualized at the base of the carbonate build-ups. It is gradational with the basin facies.

"Upper Reef Flank" refers to the higher part of the fore-reef. It includes Wilson's facies 5D to 7D. It is characterized by coral and stromatoporoidal baffle- and bindstone. Stromatoporoids are dominated by tabular forms and **Stachyodes** sp. Rocks of this facies form unit 3 in the Hotspur well, the upper part of unit 3 in the Bent Horn N-72 well, unit 4 in the W. Bent Horn C-44 well and the upper part of unit 3 in the Cape Fleetwood well. Cores are present from the latter three intervals; for unit 3 in the Hotspur well the upper reef flank facies was determined on the basis of a rich fauna in the cuttings samples and the stratigraphic position of the unit. The presence of an apparently continuous upper reef flank facies in the upper part of the carbonate build-up indicates sea level fluctuations and incipient tectonic instability during the last stage of Blue Fiord deposition.

Plate 38.1

All figures x40. All specimens from the Blue Fiord Formation.

Figures 1-12. From the B.P. et al. Panarctic Hotspur J-20 well, GSC loc. C-11488. (1 and 2 from 8724.4-8725 ft (2659.2-2659.4 m), remainder from 9340-9440 ft (2846.8-2877.3 m)).

1,2. **Pandorinellina** sp. (either **P. expansa** Uyeno and Mason, or **P. exigua exigua** (Philip)). GSC 58320, inner and outer lateral views of Pb element.

3-5. **Pandorinellina** cf. **P. expansa** Uyeno and Mason. GSC 58321, outer lateral, and lower views of Pb element.

6,7. **Ozarkodina** sp. or **Pandorinellina** sp. GSC 58322, upper and inner lateral views of Pa element.

8-10. **Icriodus culicellus** (Bultynck). GSC 58323, upper, outer lateral, and lower views of I element.

11,12. **Pandorinellina exigua exigua** (Philip). GSC 58324, outer lateral and upper views of Pa element.

18,19. **Polygnathus** aff. **P. perbonus** (Philip). GSC 58325, lower and upper views of Pa element.

13-17. From the Panarctic Cape Fleetwood M-21 well, GSC loc. C-58250. (Both specimens from 10 912-10 972 ft (3326.0-3344.3 m.).

13-15. **Polygnathus costatus costatus** Klapper. GSC 58326, upper, inner lateral, and lower views of Pa element.

16,17. **Icriodus** n. sp. E of Weddige (1977). GSC 58327, upper and lower views of I element.

20. **Polygnathus costatus costatus** Klapper. GSC 58328, lateral view of a small (juvenile?) Pa element. From the Panarctic et al. West Bent Horn C-44 well, GSC loc. C-58247, from 10 444-10 504 feet (3183.3-3201.6 m).

21-48. From the Panarctic Tenneco et al. Bent Horn N-72 well, GSC loc. 58248 (intervals as indicated below).

21-23. **Icriodus** n. sp. E of Weddige (1977). GSC 58329, upper, inner lateral, and lower views of I element (10 524-10 528 ft, 3207.7-3208.9 m).

24-26, 34-36. **Icriodus culicellus** (Bultynck). 24-26: GSC 58330, upper, lateral, and lower views of I element (10 522.4 ft, 3207.2 m); 34-36: GSC 58331, upper, lateral, and lower views of I element (10 532-10 536.5 ft, 3210.2-3211.5 m).

27-33. **Polygnathus costatus costatus** Klapper. 27, 28: GSC 58332, lower and upper views of Pa element (10 528-10 532 ft, 3208.9-3210.2 m); 29, 30: GSC 58333, upper and lower views of small Pa element (10 534.8 ft, 3211.0 m); 31-33: GSC 58334, upper, inner lateral, and lower views of Pa element (10 528-10 532 ft, 3208.9-3210.2 m).

37,38. **Polygnathus** n. sp. A of Klapper and Johnson (1975). GSC 58335, upper and lower views of Pa element (11 500-11 530 ft, 3505.2-3514.3 m).

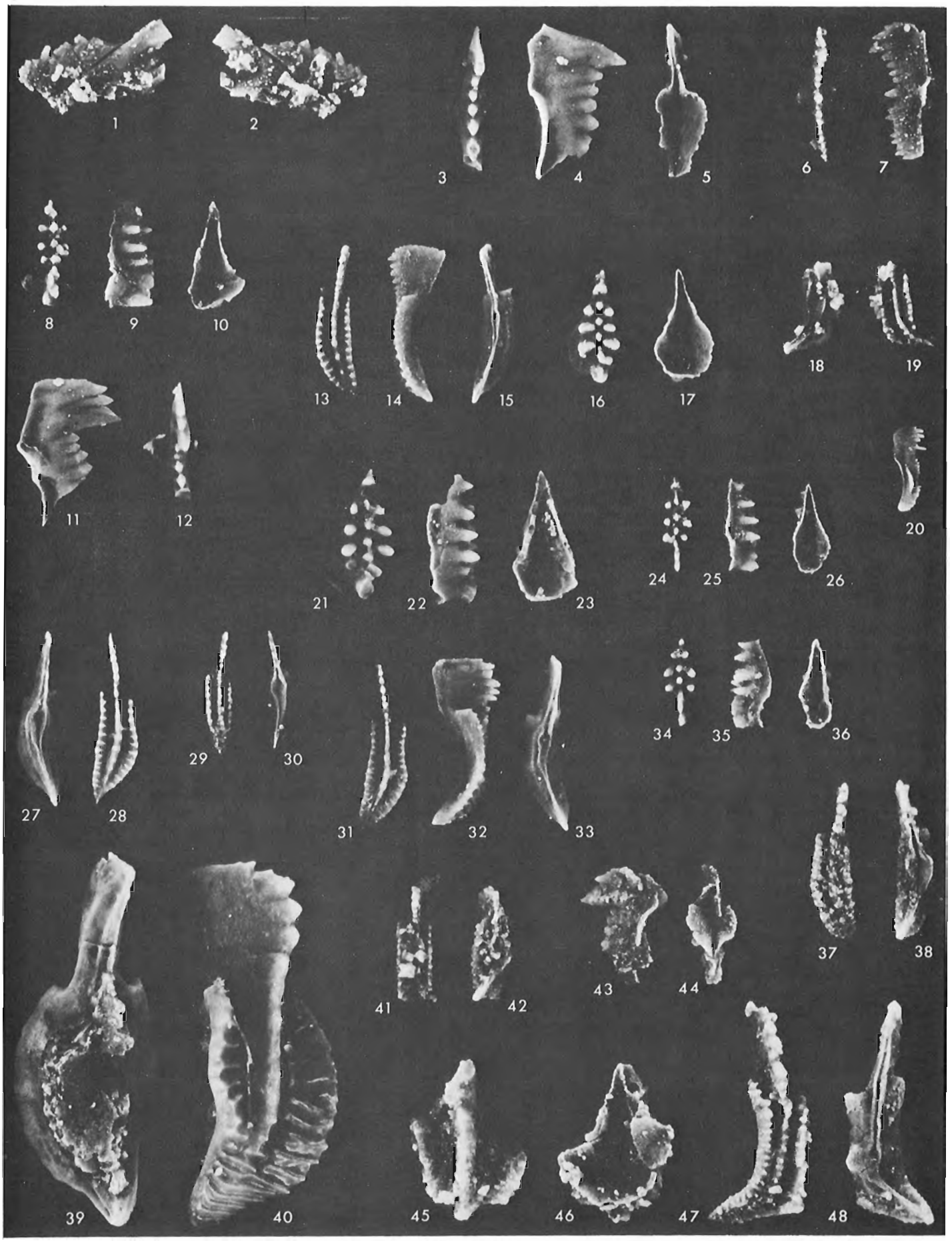
39,40. **Polygnathus linguiformis pinguis** Weddige. GSC 58336, lower and oblique upper views of Pa element (10 528-10 532 ft, 3208.9-3210.2 m).

41,42. **Polygnathus inversus** Klapper and Johnson. GSC 58337, upper and lower views of Pa element (11 520-11 525 ft, 3511.3-3512.8 m).

43,44. **Pandorinellina expansa** Uyeno and Mason. GSC 58338, lateral and lower views of Pa element (11 500-11 530 ft, 3505.2-3514.3 m).

45,46. **Sannemannia glenisteri** (Klapper). GSC 58339, upper and lower views of I element (11 500-11 530 ft, 3505.2-3514.3 m).

47,48. **Polygnathus serotinus** Telford. GSC 58340, oblique upper and lower views of Pa element (11 500-11 530 ft, 3505.2-3514.3 m).


1
2
3
4
5
6
7
8
9
10
11
12
13
14
15
16
17
18
19
20
21
22
23
24
25
26
27
28
29
30
31
32
33
34
35
36
37
38
39
40
41
42
43
44
45
46
47
48

Water depth increased by some tens of metres and deposition of reefal margin and bank interior carbonate rocks was generally inhibited. In shallower areas deposition of reefal margin carbonate may have persisted for some time, a possibility depicted in Figure 38.1. Contraction of the reefal margin into the central part of the Blue Fiord build-up is another possibility.

"Reefal margin" is the uppermost part of the seaward edge of the carbonate bank. It is above wave base and in an area of maximum turbulence. It is analogous to Wilson's (1975) facies 8D and includes also the sands of the bank margin. In the Blue Fiord carbonate, identification of this facies is based mostly on the presence of massive (hemispherical, irregular, non-tabular and non-branching) stromatoporoids in cores and of skeletal and other grainstone in cuttings samples. The best example of this facies is in core 4 (unit 1) of the Cape Fleetwood well which consists of a well winnowed stromatoporoidal floatstone. The lower part of unit 3 of the same well was assigned to the reefal margin facies because of the presence of coated grain grainstone in the cuttings samples. Similarly, pelletoidal (Milliman, 1974) and coated-grain grainstone is the main evidence for the uncored intervals in the Bent Horn N-72 well. The evidence is tenuous, as pelletoidal grainstone may also be found in the bank interior.

The last facies distinguished in the Blue Fiord carbonate is the "bank interior". It is back reef facies and comprises Wilson's (1975) facies 12D and 13D. It is characterized by lime mudstone, pelletoidal packstone, fenestral lamination, calcispheres and an impoverished fauna. In the lower part of the Blue Fiord Formation the facies forms a large part of unit 1 in the Bent Horn N-72 well and the basal part of the Blue Fiord Formation in the W. Bent Horn C-44 well. For the upper part it is represented by unit 3 in the W. Bent Horn C-44 well.

According to seismic information (Menely, 1976) both the Cape Fleetwood and the Bent Horn N-72 well are at the margin of the Blue Fiord carbonate build-up, while the W. Bent Horn C-44 well is farther inward. The schematic facies cross-section in Figure 38.1, based on interpretation of lithologies, corroborates those well positions. The Cape Fleetwood and the upper part of the Bent Horn N-72 wells are dominated by reef flank and reef margin carbonate, whereas the W. Bent Horn C-44 well contains mostly carbonate deposited farther away from the margin.

Previous Conodont Studies

The conodonts of the Blue Fiord Formation from other parts of the Canadian Arctic Islands have been studied previously by this author and others. These investigations include Klapper (1969) on northwestern Devon Island, Uyeno (in McGregor and Uyeno, 1972) on northeastern Bathurst Island and (in Miall, 1976, p. 26, 27) on Banks and Princess Royal islands, and Weyant (1975) and Klapper and Johnson (1975) on southwestern Ellesmere Island. A conodont biostratigraphic study of the Blue Fiord Formation at its type section in southwestern Ellesmere Island (McLaren in Fortier et al., 1963, p. 318, 319; loc. 5 of Uyeno and McGregor, 1970; Kerr and Thorsteinsson, 1972) is under preparation by the author.

The Blue Fiord Formation is a diachronous unit, ranging from late Early Devonian age (**gronbergi** to **serotinus** Zones) in southwestern Ellesmere Island (Klapper and D.B. Johnson, 1975, Fig. 4; see also J.G. Johnson in Harper et al., 1967, p. 430) to early Middle Devonian age on Bathurst Island (McGregor and Uyeno, 1972). An early Middle Devonian age for the formation has been suggested previously by McLaren (in Fortier et al., 1963, p. 612) and Ormiston (1967) based on the studies of brachiopods and trilobites.

Conodont Biostratigraphy

1. B.P. et al. Hotspur J-20 well

A single fragmentary polygnathan species from the relatively thick interval from 9340 to 9440 feet (2846.8-2877.3 m) in the Hotspur well is assigned to **Polygnathus** aff. **P. perbonus** (Philip) and is possibly a transitional form to **P. inversus** Klapper and Johnson (illustrated on Plate 38.1, fig. 18, 19). Also from the same interval are **Ozarkodina** sp. or **Pandorinellina** sp. (similar to the form identified as **Pandorinellina optima** (Moskalenko) Flood (1969, Pl. 2, fig. 10)), **Pandorinellina** cf. **P. expansa** Uyeno and Mason, **P. exigua exigua** (Philip), and **Icriodus** cf. **I. culicellus** (Bultynck). The zonal assignment of these conodonts cannot be stated precisely, but probably falls within the interval of **gronbergi** to **inversus** Zones (Klapper, 1977, Fig. 3) of late Early Devonian (Zlichovian to Dalejan) age (Klapper et al., 1978, Fig. 2). The fauna is possibly the oldest within the Blue Fiord Formation in the study area. **Polygnathus** aff. **P. perbonus** has been reported previously from the lower part of the Blue Fiord Formation in southwestern Ellesmere Island (Klapper and Johnson, 1975, Fig. 4).

In the interval from 8724.4 to 8725 feet (2659.2-2659.4 m; core 8), a single fragmentary Pb element of either **Pandorinellina expansa** or **P. exigua exigua** was recovered. Both species/subspecies range from late Early Devonian (Zlichovian) to the **costatus costatus** Zone of early Middle Devonian age (Klapper, 1977, Fig. 3, 6; Klapper et al., 1978, Fig. 2).

The only Cape De Bray conodonts from the Hotspur well were obtained from the 6468 foot (1971.4 m) level, consisting of four fragmentary specimens of **Icriodus** sp. This small fauna cannot be dated precisely, but the general icriodontan morphology suggests an early Middle Devonian age.

2. Panarctic Tenneco et al. Bent Horn N-72 well

The lowest interval in the Blue Fiord Formation with conodonts was at 12 000 to 12 100 feet (3657.6-3688.1 m). **Sannemannia glenisteri** (Klapper) was recovered, and this species continues on higher, as discussed below. It is indicative of late Early Devonian age.

The interval from 11 500 to 11 530 feet (3505.2-3514.3 m; core 3) was sampled at 5-foot (1.5 m) intervals; the uniform conodont fauna from this interval, however, suggests that it can be considered as a single unit. The fauna consists of **Polygnathus serotinus** Telford, **P.** n. sp. A of Klapper and Johnson (1975), **P. inversus** Klapper and Johnson, **Pandorinellina expansa**, and **Sannemannia glenisteri**, and can be assigned to the lower part of the **serotinus** Zone (Klapper, 1977, Fig. 3), of late Early Devonian (Dalejan) age (Klapper et al., 1978, Fig. 2).

No conodonts were recovered from the interval from 10 720 to 10 730 feet (3267.5-3270.5 m; core 2), nor from the Cape De Bray Formation in the interval 10 000 to 10 100 feet (3048.0-3078.5 m).

The interval from 10 520 to 10 536.5 feet (3206.5-3211.5 m; core 1) yielded a uniform fauna. The conodonts include **Polygnathus linguiformis pinguis** Weddige, **P. costatus costatus** Klapper, **Icriodus culicellus** (Bultynck), and **I.** n. sp. E of Weddige (1977), and can be assigned to the **costatus costatus** Zone (Klapper, 1977, Fig. 3; Weddige, 1977, Table 5) of early Middle Devonian (Eifelian) age (Klapper et al., 1978, Fig. 2).

3. Panarctic et al. West Bent Horn C-44 well

Conodont recovery from this well was poor. No conodonts were found in this interval from 11 460 to 11 580 feet (3493.0-3529.6 m).

A small (juvenile?) polygnathan element, assigned to **Polygnathus costatus costatus** on the basis of its similarity with small specimens of this species in the Bent Horn well, was recovered from the interval from 10 444 to 10 504 feet (3183.3-3201.6 m; core 1). The conodont is assignable to the **costatus costatus** Zone.

The Cape De Bray Formation at the interval from 10 000 to 10 100 feet (3048.0-3078.5 m) yielded three small fragmentary polygnathan elements. Although individually they are too fragmented for any specific identification, collectively they resemble a subspecies of **Polygnathus linguiformis** Hinde. No precise age determination can be made on the basis of this interval.

4. Panarctic Cape Fleetwood M-21 well

As was the case with the West Bent Horn well, conodont recovery from this well was poor. No conodonts were found in the intervals 11 500 to 11 528 feet (3505.2-3513.7 m; core 4), and 10 600 to 10 700 feet (3230.9-3261.4 m).

Polygnathus costatus costatus and **Icriodus** n. sp. E of Weddige (1977) were recovered from the interval 10 912 to 10 972 feet (3326.0-3344.3 m; core 3). These species indicate the **costatus costatus** Zone of Eifelian age.

A single indeterminate conodont fragment was recovered from the Cape De Bray Formation in the interval from 10 170 to 10 209 feet (3099.8-3111.7 m; core 2).

In summary, the conodonts from the Blue Fiord Formation in the four wells studied range from the probable **gronbergi/inversus** Zones (Zlichovian to Dalejan age; late Early Devonian), through the **serotinus** Zone to the **costatus costatus** Zone (Eifelian; early Middle Devonian). The intervening **patulus** Zone between the **serotinus** and **costatus costatus** Zones appears to be absent, and is presumably represented temporally, in the Bent Horn well, somewhere in the intervening 960 feet (292 m) of strata that belong to the "reefal margin" lithofacies. As previously noted by Klapper et al. (1978, p. 107) and Klapper (1977, p. 44, 45), the **patulus** Zone has not yet been found in western or Arctic North America.

The overlying Cape De Bray Formation has yielded only meagre collections, and its age can only be stated as probably Eifelian.

The placement of the Lower-Middle Devonian boundary is currently being discussed by the IUGS Subcommission on Devonian Stratigraphy. Consequently, the references above of certain conodont zones to Lower or Middle Devonian are pending on the final decision by the committee (see, e.g., discussion by Klapper et al., 1978, p. 107, 108).

Paleoecological Considerations

An attempt was made to match the different lithofacies of the Blue Fiord and Cape De Bray formations with the diversity and composition of the conodont faunas. But because there is no consistent congruence between lithofacies and conodont biofacies, as recently noted by Klapper and Barrick (1978), such correlations should be interpreted with caution. Another reason for caution is that there was bias in sampling procedure; i.e., some lithofacies that were considered more "suitable" for conodont occurrences were sampled more extensively than others. To a large extent, too, this bias was dictated by the availability of cored intervals. Given these cautions, one can generally state that the most prolific faunas, both in terms of number and diversity, occur in the "upper reef flank" and "open shelf" lithofacies. Both facies were deposited below wave base and both are characterized by relatively high argillaceous contents, with probable rich nutrient supply (see Johnson and Niebuhr, 1976, p. 1699). Thus it is not surprising that these lithofacies carry the abundant conodont faunas, which belong to Biofacies II of Druce (1973). A single sample from the "bank interior" facies yielded a very small fauna, and three samples from the "reefal margin" lithofacies were all barren. Only one of five samples from the "deep reef flank" facies yielded some conodonts. Of the five samples from the "basin" facies (Cape De Bray Formation), three yielded conodonts but in all cases were small and fragmentary.

In summary, owing to the small sampling, no specific conclusions can be made with regards to the paleoecology of the conodont habitat. The data generally support the finding presented by others earlier (e.g., Chatterton, 1976).

Conodont Preservation and Organic Metamorphism

The conodonts in the four wells studied range from well preserved to only moderately so, with fractures and matrix particles attached to the specimens. All the conodonts have coloration of about CAI 1.5 to 2 of Epstein et al. (1977). Based on the study of the Appalachian basin conodonts, these authors (ibid.) have found that a CAI value of 1.5 coincides with the level of organic metamorphism above which there is no known commercial oil and condensate production.

In terms of source rock potential, the transition between mature and overmature zones lies within or below the Blue Fiord Formation in the Bent Horn, West Bent Horn, and Cape Fleetwood wells (Powell, 1978, p. 59). In the Hotspur well, the Cape De Bray Formation has been regarded as probably overmature (Powell, ibid.).

References

Chatterton, B.D.E.
1976: Distribution and paleoecology of Eifelian and early Givetian conodonts from western and northwestern Canada; in Conodont Paleoecology, C.R. Barnes, ed.; Geological Association of Canada, Special Paper 15, p. 143-157.

Druce, E.C.
1973: Upper Paleozoic and Triassic conodont distribution and the recognition of biofacies; in Conodont Paleozoology, F.H.T. Rhodes, ed.; Geological Society of America, Special Paper 141, p. 191-237.

Embry, A. and Klovan, J.E.
1976: Middle-Upper Devonian clastic wedge of the Franklinian Geosyncline; Bulletin of Canadian Petroleum Geology, v. 24, p. 485-639.

Epstein, A.G., Epstein, J.B., and Harris, L.D.
1977: Conodont color alteration — an index to organic metamorphism; United States Geological Survey, Professional Paper 995.

Flood, P.G.
1969: Lower Devonian conodonts from the Lick Hole Limestone, southern New South Wales; Journal of the Proceedings of the Royal Society of New South Wales, v. 102, p. 5-9.

Fortier, Y.O. et al.
1963: Geology of the north-central part of the Arctic Archipelago, Northwest Territories (Operation Franklin); Geological Survey of Canada, Memoir 320.

Harper, C.W., Jr., Johnson, J.G., and Boucot, A.J.
1967: The Pholidostrophiinae (Brachiopods; Ordovician, Silurian, Devonian); Senckenbergiana Lethaea, v. 48, p. 403-461.

Johnson, J.G. and Niebuhr, W.W., II
1976: Anatomy of an assemblage zone; Geological Society of America, Bulletin 87, p. 1693-1703.

Kerr, J.Wm.
1974: Geology of Bathurst Island Group and Byam Martin Island, Arctic Canada (Operation Bathurst Island); Geological Survey of Canada, Memoir 378.

Kerr, J.Wm. and Thorsteinsson, R.
1972: Geology, Baumann Fiord, District of Franklin; Geological Survey of Canada, Map 1312A.

Klapper, G.
1969: Lower Devonian conodont sequence, Royal Creek, Yukon Territory, and Devon Island, Canada; Journal of Paleontology, v. 43, p. 1-27.

1977: Lower and Middle Devonian conodont sequence in central Nevada; in Western North America: Devonian, M.A. Murphy, W.B.N. Berry and C.A. Sandberg, eds.; University of California, Riverside, Campus Museum Contribution 4, p. 33-54.

Klapper, G. and Barrick, J.E.
1978: Conodont ecology: pelagic versus benthic; Lethaia, v. 11, p. 15-23.

Klapper, G. and Johnson, D.B.
1975: Sequence in conodont genus **Polygnathus** in Lower Devonian at Lone Mountain, Nevada; Geologica et Palaeontologica, v. 9, p. 65-83.

Klapper, G., Ziegler, W., and Mashkova, T.V.
1978: Conodonts and correlation of Lower-Middle Devonian boundary beds in the Barrandian area of Czechoslovakia; Geologica et Palaeontologica, v. 12, p. 103-116.

Mayr, U.
Stratigraphy and correlation of lower Paleozoic formations, subsurface of Bathurst Island and adjacent smaller islands, Canadian Arctic Archipelago; Geological Survey of Canada, Bulletin 306. (in press)

McGregor, D.C. and Uyeno, T.T.
1972: Devonian spores and conodonts of Melville and Bathurst Islands, District of Franklin; Geological Survey of Canada, Paper 71-13.

Meneley, R.A.
1976: Exploration prospects in the Canadian Arctic Islands; presentation to Canadian Society of Exploration Geophysicists, Panarctic Oils Ltd., Calgary.

Miall, A.D.
1976: Proterozoic and Paleozoic geology of Banks Island, Arctic Canada; Geological Survey of Canada, Bulletin 258.

Milliman, J.D.
1974: Marine carbonates; Springer-Verlag, New York.

Ormiston, A.R.
1967: Lower and Middle Devonian trilobites of the Canadian Arctic Islands; Geological Survey of Canada, Bulletin 153.

Powell, T.G.
1978: An assessment of the hydrocarbon source rock potential of the Canadian Arctic Islands; Geological Survey of Canada, Paper 78-12.

Uyeno, T.T. and McGregor, D.C.
1970: Silurian-Devonian biostratigraphy of the Arctic Islands, District of Franklin (49C, 49E, 58F, 59B, 89B); Geological Survey of Canada, Paper 70-1A, p. 110-110B.

Weddige, K.
1977: Die Conodonten der Eifel-Stufe im Typusgebiet und in benachbarten Faziesgebieten; Senckenbergiana Lethaea, v. 58, p. 271-419.

Weyant, M.
1975: Sur l'âge du membre inférieur de la formation Blue Fiord dans le sud-ouest de l'île Ellesmere (Archipel Arctique Canadien) d'après les conodontes; Newsletters on Stratigraphy, v. 4, p. 87-95.

Wilson, J.L.
1975: Carbonate facies in geologic history; Springer-Verlag, New York.

39. BEDROCK HEAVE IN THE CENTRAL CANADIAN ARCTIC

Project 770036

Larry Dyke
Terrain Sciences Division

Dyke, L., Bedrock heave in the central Canadian Arctic; in Current Research, Part A, Geol. Surv. Can., Paper 79-1A, p. 241-246, 1979.

Abstract

Sites for detailed study of bedrock heave motions and rates were established in gneisses of District of Keewatin and sedimentary rocks of the central Arctic Islands. Observations of heave suggest that freezing of standing water in otherwise vacant bedrock cracks may result in relatively large and rapid vertical displacements where the active layer is deep. The confinement of water by a downward-advancing freezing front through water-filled cracks may lead to the development of excess pore water pressure. Where free water is not present, water retained in soil infillings may be capable of causing smaller, more gradual displacements in bedrock masses by the development of segregated ice.

Introduction

The objective of this study is to examine the disruption of bedrock masses in the permafrost environment both as a process contributing to landform evolution and as a factor to be considered in engineering endeavours. To this end 25 sites in central District of Keewatin, on Boothia Peninsula and on Somerset, Bathurst, and Melville islands were established to study rock heave with respect to geologic, hydrologic, and permafrost conditions (Fig. 39.1).

The problem of rock heave really amounts to determining the cause and rate of bedrock movements so commonly seen in the arctic and subarctic. While it is assumed that climatic conditions that ensure freezing are essential, this is probably not sufficient. Other conditions must be important when it is considered that latitudes with a more temperate climate but still with freezing conditions commonly fail to exhibit rock heave features. It is suspected that the presence of permafrost is important because of the opportunity presented for the formation of closed hydrologic systems. Freezing from the surface allows a confined unfrozen layer to be formed, permitting excess pore water pressure to develop. In addition the process of ice segregation, whereby ice masses may grow by water migration to a freezing front, is a possible cause of heaving, especially where silty or clayey soils exist between bedrock blocks. Continuous freezing conditions allow prolonged development of segregated ice. Sites for detailed study were selected so as to incorporate a range of conditions assumed to have some influence on the amount of heaving.

Acknowledgments

Thanks are extended to A.N. Le Cheminant and A.S. Dyke for their scientific advice in the field and Polar Continental Shelf Project for logistical support from Resolute. P.A. Eggington suggested the use of the heave recorder discussed in the text.

Geomorphology of Rock Heave

Rock heave is the displacement of any discrete mass of rock in such a manner as to suggest that forces internal to the rock-soil-water system are responsible for the movements. Such forces presumably originate from the formation and growth of ice in fractures and pores. Of course, movements due to other processes are possible and caution must be used in assigning ice formation as the cause. Gravity-induced movements and movements caused by contact with flowing glacial ice are possibilities.

The correct identification of felsenmeer as a heaved and broken up bedrock surface can be difficult because of the possibility that the felsenmeer blocks first were transported by glacial ice. To be confident that frost heaving has been operative, it is desirable to find locations where the original positions of blocks in a bedrock mass can be traced back without doubt. One then can work from this reference and examine detached blocks for comparison with still intact bedrock. Blocks with sharp corners likely have not been subjected to glacial transport if glacial smoothing is otherwise evident nearby on intact bedrock.

At all localities visited it is evident that both lithology and bedrock structure exert some control on the surface expression of heave seen. While bedrock lithology may be associated with susceptibility to heave, the amount of heave actually taking place depends upon the availability of water and probably on the texture and abundance of soils in contact with the bedrock. The ability of segregated ice to form in certain soil types is well recognized, and an association of this process with rock heave seems likely. Thus, the ability

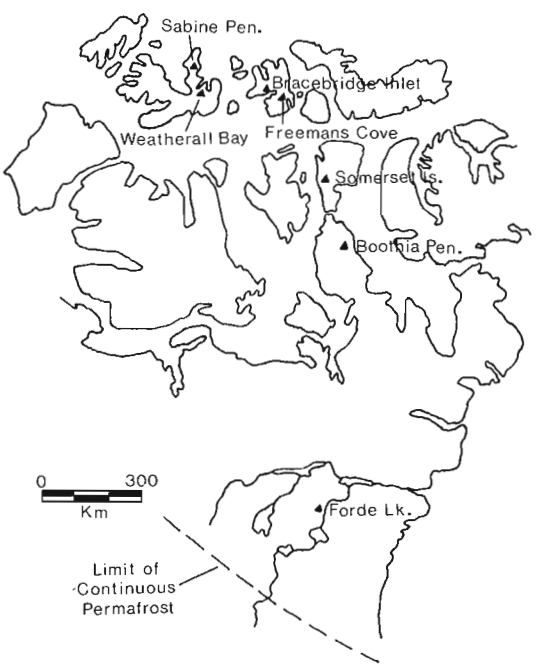


Figure 39.1. *Map of central Canadian Arctic showing location of rock heave study areas (triangles).*



Figure 39.2. *Displaced bedrock blocks on the flank of an outcrop, north end of Forde Lake. Till-covered plain in background has standing water at surface.*

of rock to weather to soil may influence its susceptibility to heave. Movements seem to be most obvious in resistant lithologies, but this only indicates the slow average rate of natural rock heave. Heaving in rocks that weather quickly may be just as fast, but the evidence is removed by physical and chemical breakdown on the granular scale.

Sites were chosen primarily to obtain a variety of bedrock types. Each site in turn offered a diversity of drainage conditions, topography, and soil occurrence. In the Churchill Province of the Canadian Shield a site at Forde Lake, about 100 km southwest of the settlement of Baker Lake, includes extensive areas of felsic and migmatitic gneisses in contact with coarse conglomerates of the Dubwant Group. The crystalline rocks are cut by abundant diabase, lamprophyre, and feldspar porphyry dykes (Le Cheminant, 1977). All of these rocks show heaving as the only major form of disintegration; otherwise glaciated surfaces commonly exhibit fine striae. This heaving takes several forms or at least degrees but seems to be confined to places where standing water is visible or close at hand, i.e., at a depth of less than 1 m. In the Forde Lake area the terrain is subdued, consisting of rounded bedrock ridges separated by valleys filled with silt-rich, bouldery tills. It is common to find open cracks and displaced blocks along the flanks of otherwise undisturbed outcrop ridges (Fig. 39.2). In early summer, water and ice often are visible in open cracks, but never soil. Where outcrops are most subdued, i.e. relief above surrounding unconsolidated deposits of less than about 3 m, outcrops up to a few tens of metres square commonly are "dilated". Horizontal movement has taken place so as to open vertical fractures in all directions. Crack widths are rarely greater than 1 m and usually are less than 10 cm. Of course an individual block may have moved considerably more than indicated by the spaces bounding it if a given exposure is "fitted" together.

Equally common are features that might aptly be termed "rock pingos" and "rock boils". These consist of bedrock slabs or blocks raised to form low mounds or simply isolated piles of blocks situated in till-covered areas (Fig. 39.3). The mound-like features appear in bedrock areas exhibiting horizontal fracturing and have been reported by DiLabio (1978) and A.R. Miller (pers. comm., 1978). If these features are assumed to have originated from the level of the immediately surrounding terrain, then vertical movements of up to a few metres are evident. Supporting evidence for such vertical movements is offered by occurrences of "ejected" blocks where a single fracture-bounded block rests by apparent frictional support above the level of the surrounding outcrop. Examples several square metres in cross-section and raised up to 3 m were encountered.

Shield terranes on northern Boothia Peninsula and Somerset Island show a considerably greater extent of bedrock disruption. The time since the last glaciation on Somerset Island is thought to be relatively long compared to mainland Canada. A high beach deposit has yielded marine shells that give a radiocarbon date of 32 000 years (Netterville et al., 1976), the time required for isostatic rebound since deglaciation. Indeed, the high degree of bedrock polish typical of central Keewatin is never seen in these regions. Except on steep slopes, outcrop is rare; rather a mantle of angular cobbles and boulders covers much of the level or gently sloping higher terrain. In low-lying areas extensive silty clay deposits are present, commonly exhibiting patterned ground features. Even amongst the coarsest boulders, circular accumulations of fines are seen which resemble mud boils (Fig. 39.4). These occur both on slopes and flat areas. There is some evidence for the existence of felsenmeer formed by frost heave in the case of gabbro dykes that cut the pure quartz to mafic-rich banded gneisses of west-central Somerset Island. The dykes are covered with boulders of the same distinctive rock type with no trace of exotic materials. On northern Boothia Peninsula the general aspect of the terrain seems to be intermediate between that of the District of Keewatin and Somerset Island with respect to progress of frost heave. Few solidly intact outcrops occur; on the other hand, there are many places where it is easy to identify displaced bedrock.

The sedimentary terranes of the Arctic Islands rarely display obvious evidence of rock heave in the form of large vertical displacements. It is probable that the rock types are

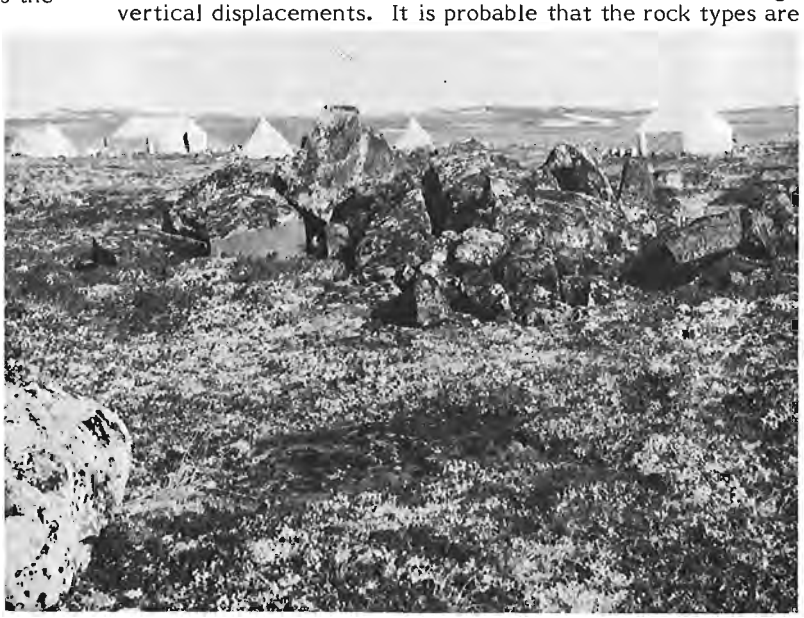


Figure 39.3. *Typical localized occurrence of vertical rock heave, north end of Forde Lake. Note lichen-free face of the block on the left.*



Figure 39.4. *Mud boil amongst boulders, central Somerset Island.*



Figure 39.5. *Furrow developed by possible ice wedging in carbonate outcrop, Freemans Cove, Bathurst Island.*

no less susceptible than rocks of the Canadian Shield, rather disintegration on the small scale is relatively rapid due to the close spacing of fracture and bedding planes and the overall lower degree of induration compared with Shield-type rocks (see Kerr, 1974 and Tozer and Thorsteinsson, 1964 for descriptions of lithologies on Bathurst and Melville islands, respectively).

On southeastern Bathurst Island, outcrops of the Disappointment Bay Formation, a thinly to massively bedded dolomite, generally are present only on the crest or sides of ridges. Rock heave in the sense of displaced large blocks rarely is seen. Outcrops seem to be under the influence of soil movement processes, however, as trails of rock debris lead away from the downhill side of many exposures. A relatively high density of fracturing, in places up to 20 vertical fractures per metre, contributes to this disintegration. A regolith of angular boulders covers the ground between outcrops on sloping areas and wherever excavated, was found to be cemented by ice at a depth of roughly 0.5 m. On level or near-level areas the regolith contains a high proportion of fines and rock fragments are accumulated on the surface. An active ice wedge was evident where one isolated outcrop on a broad ridge crest was cut by a furrow 2 m deep and several metres wide (Fig. 39.5). Blocks of the outcrop appeared to be caving into the furrow from the rims.

Thin bedded, calcareous siltstone of the Stuart Bay Formation behaves similarly to the Disappointment Bay Formation in that the chief result of frost action seems to be the production of a regolith rich in fines. Outcrop occurs on ridge crests, but even there it is greatly disturbed (Fig. 39.6). Excavation close by reveals ice sandwiched between beds at a depth of roughly 0.5 m, with ice comprising up to 50 per cent of the volume. Such a volumetric percentage probably does not persist with depth, but troughs a few metres long and a few centimetres deep appear in the regolith parallel to bedding strike, further suggesting the presence of near-surface ice growth.

At Weatherall Bay, Melville Island, thinly to massively bedded Griper Sandstone forms isolated outcrops on a plateau above the eastern arm of the bay. Vertical cracks up to 1 m wide are filled with sandy silt. In all cases outcrops are flanked by completely detached blocks which rapidly decrease in size with distance from the outcrop (Fig. 39.7). The massively bedded units are friable and appear to have yielded a sandy silt capable of promoting both horizontal and downslope movements. Solifluction in the sandy silt appears to be capable of transporting blocks of sandstone up to 3 m in size. Frost boils cover extensive areas. Ice wedges may be present where V-shaped troughs up to 1 m deep appear in flaggy, thinly bedded felsenmeer of the Griper Formation. Massive ice may be present in the thinly laminated shales of the Kanguk Formation on central Sabine Peninsula. Where outcrop of this formation is encountered, the shale commonly displays tight anticlines and synclines, yet on a regional scale the formation is essentially flat lying. The shales are interlaminated with ice at depths rarely exceeding a few tenths of a metre.



Figure 39.6. *Disturbed outcrop of near-vertically dipping calcareous siltstones, Bracebridge Inlet, Bathurst Island.*



Figure 39.7. *Laterally separated blocks of massively bedded sandstone, Weatherall Bay, Melville Island.*

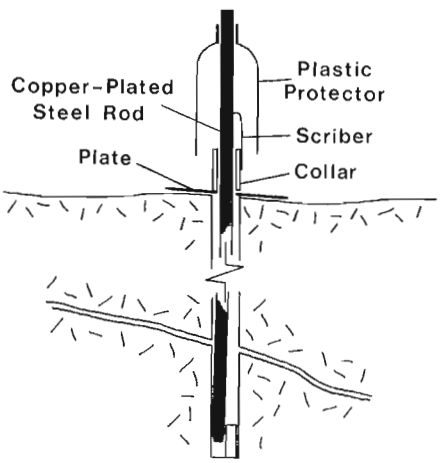


Figure 39.8. *Heave recorder. Upward movement of any block between jammed base and scriber will be recorded as scriber assembly is moved up the rod.*

Methods of Measuring Rates of Heave

Field observations indicate that both vertical and horizontal rock heave seldom exceed a few metres; however, rates of movement are much more difficult to ascertain. Assuming that a bedrock surface in a given area was intact after recession of continental ice, the time since the last deglaciation provides a maximum time interval within which heaving could take place. This results in a very slow average rate, even for the largest displacements observed, i.e., about 1 mm every few years.

At all sites visited, arrays of survey markers were installed in various bedrock features, and their positions relative to one another were determined with a theodolite and levelling rod. The markers are 10 cm lengths of 1 inch aluminum T-section bar driven into holes made with a Cobra carbide-bit rock drill. Most survey sites include several bedrock blocks in which at least one and commonly three markers (three allowing detection of rotations) are installed. For each array levelling and triangulation was carried out from at least three markers. While no marker can be considered absolutely fixed, those used for theodolite set-ups were chosen to be as stable as possible. The markers will be resurveyed in order to detect relative movement between blocks; each array spans an area large enough to reasonably ensure a diversity of motions, i.e., chances are slim that all markers will move an equal distance in the same direction. A Wild T16 theodolite, capable of measuring to 0.1 minute of arc, and a rod graduated in centimetres were used. For shots of 30 m or less this allows displacements of as little as 1 mm to be detected. While these sites constitute a relatively permanent set of rock heave monitoring locations, it will not be surprising if few or even no displacements are detected one year hence. In some cases a temporary equilibrium may have been established between heaving and those conditions bringing it about (e.g. depth of the saturated active layer, thickness of soil deposits between blocks). If this is the case, heaving could resume only if the equilibrium were disturbed by altering the controlling conditions.

Anticipating that rock heave in some cases may be cyclical rather than cumulative, devices capable of recording heave movements were installed at several of the marker array sites (see Fig. 39.8). A 1.5 cm diameter copper-plated rod was anchored in the bottom of a 3 cm diameter hole drilled at least 1 m into a bedrock block. The threaded end of the rod was jammed against another short length of steel in order to anchor it. A collar with a scribe point attached to it then was placed on the rod, resting on a plate which sits on the rock surface. The scriber records motions between the base of the rod and the scriber by making a scratch on the rod surface. Each recorder was placed so as to intersect at least one fracture or open crack.

Evidence of relatively recent movements is presented in places where lichen growth is absent from otherwise heavily covered block surfaces (Fig. 39.3, 39.9). Where seen, these barren patches are defined sharply, suggesting that the corresponding movement to expose the patch was abrupt. Movements of this sort are seen on individual blocks in heaved bedrock mounds and also on felsenmeer blocks where a matrix of fines is present. Movements of up to several tenths of a metre would have been necessary to expose surfaces presently free of lichen. By comparison with areas



Figure 39.9. *Lichen-free strip, 8 cm wide, on boulder, central Somerset Island.*

where rates of lichen growth have been measured (e.g. **Rhizocarpon geographicum** in Karlén, 1973), it is probable that these lichen-free surfaces have been exposed for less than 50 years. Therefore, much faster rates of movement than the average required to produce observed displacements since the time of deglaciation seem possible.

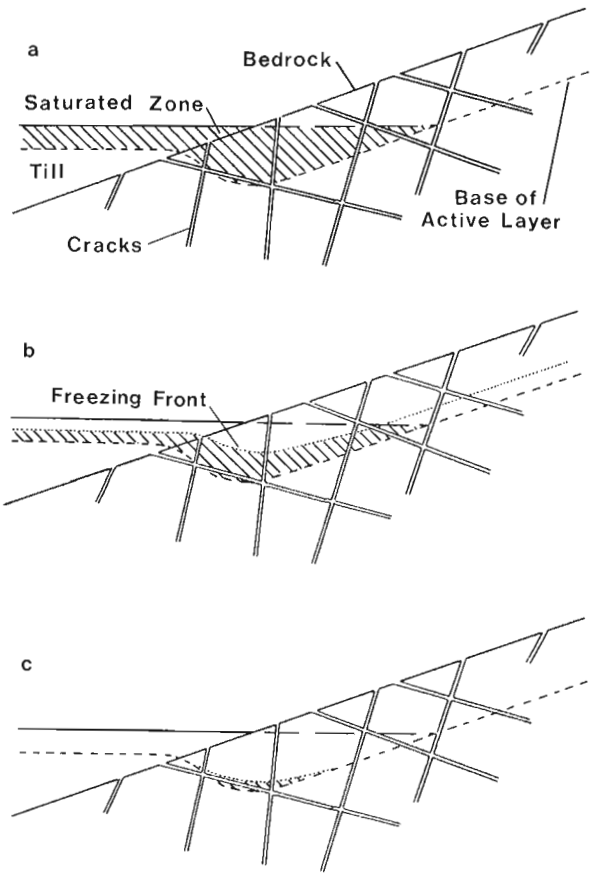
Speculations on Mechanisms of Rock Heave

Several associations between certain environmental conditions and rock heave suggest mechanisms for this process. It appears that the freezing of free water (i.e., water not under the influence of other than a gravitational potential) as well as water in soil pores with consequent ice segregation may be important in causing heave.

In the area of Keewatin visited displacements in bedrock apparently have resulted from the volume increase associated with the freezing of free water. The formation of segregated ice cannot be evoked as an explanation because it requires the presence of silts and clays, materials virtually absent from bedrock cracks and openings in this area. An enclosed layer with all cracks and openings filled with water may develop as the freezing front progresses downward. The water trapped between this freezing front and the permafrost may become overpressured if all the ice-rock contacts are capable of maintaining a seal. Thus, the potential volume increase available is proportional to the depth of the saturated active layer. The greater this depth, the greater will be the bedrock displacement. While this depth in till-covered areas is relatively shallow (usually 1 to 2 m), the presence of rock outcrop provides for a locally deeper active layer due to the generally greater thermal conductivity of rock. Such a difference is indicated by ground temperature measurements for several locations in the districts of Keewatin and Franklin (Brown, 1973, 1978).

A situation favouring the localization of rock heave exists along the flanks of outcrops where the rock disappears under the till cover. The sudden increase in thickness of the active layer under the outcrop flank, combined with a usually abundant water supply from the till-covered lowlands, will provide the opportunity for relatively large displacements when the active layer freezes (see Fig. 39.10). The pressure that actually causes movements may be in part the hydrostatic pressure generated in the unfrozen interval as a surface ice layer thickens downward. When melting occurs the tendency will be towards settling of the bedrock surface back to the original profile; however, uneven thaw and jamming of blocks to some extent will prevent this. It is conceivable that, during freezing of the active layer, water may break through to a point above the base of downward advancing ice and result in localized accumulations, much in the manner of a closed-system pingo. DiLabio (1978) has proposed this mechanism for crater-like features that may have originated as ice-cored domes. In most cases these features are small compared to pingos (i.e., a few metres in diameter), and enough water conceivably could accumulate in one season to form the necessary ice core.

Most of the other areas visited only show evidence of horizontal movement. Standing water close to outcrops, as is so common in the District of Keewatin, seldom is seen. Soils containing sand and finer fractions, on the other hand, commonly are found filling open cracks, and it is suspected that heaving may be accomplished by the freezing of water contained in these soils. The potential for heave in rock not having access to free water may be controlled by the ability of that rock to form a silt and clay fraction through weathering. Excavating to the permafrost table in thinly bedded calcareous siltstone and finely laminated shale reveals interbedded ice, silt, and clay. Similarly, greatest displacements in the friable sandstones seem to be associated with



a. Active layer thickens under bedrock because of increased thermal conductivity.

b. The freezing front advances more rapidly in the rock but is retarded in saturated rock zone because of latent heat produced by freezing of water.

c. Remaining saturated zone is sealed from communication with surface. Possible excess pore water pressure may be generated as the volume increase accompanying freezing takes place into the remaining volume left for water.

Figure 39.10. *Schematic diagram of bedrock outcrop flanked by a till deposit.*

cracks filled with sandy silt, probably a direct weathering product of the sandstone. Where fines are not present, lateral displacements are far less evident. In all these cases the only source of water would be from rainfall and snowmelt. Thus, ice is able to form only by permeation of water through the fine grained fractions from whatever is available beneath the freezing front. Compared to the rock displacements seen in Keewatin, displacements are relatively small and probably tend to occur as a gradual, incremental process due to the relatively small amounts of water available (see Fig. 39.11). The ultimate result of this process may be the complete disintegration of an outcrop to form a field of boulders (Fig. 39.7).

Where tills containing fine fractions have been deposited, a material ready made to promote heave may be available. On Boothia Peninsula fine grained tills commonly fill open cracks in bedrock. Of course this requires that the fine grained till be mobile enough to move into the openings.

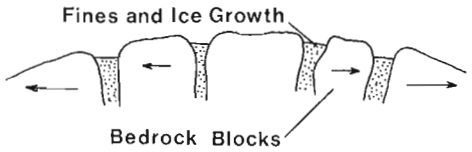


Figure 39.11. *Typical bedrock outcrop configuration in massively bedded sandstones. Growth of ice in soil-filled cracks results in lateral expansion of outcrop towards unconfined edges. Where fines are present between bedrock blocks, a similar mechanism may work at scales down to thinly laminated shales.*

The occurrence of mud boils in otherwise bouldery terrains on Somerset Island and Boothia Peninsula confirms that fines are mobile. Relatively recent displacements of boulders incorporated within mud boils are indicated by lichen-free surfaces. Also cyclical vertical heaving of up to 30 cm has been measured for mud boils in the Colorado Rockies (Fahey, 1973). These observations suggest that silt and clay fines, because of their ability to host the buildup of ice, may be capable of causing block displacements where, in the absence of fines, none would occur.

Determining the source of the silt-rock fragment regolith that mantles most of the level or gently sloping terrain underlain by carbonates on southeastern Bathurst Island must await further analysis. It is possible, however, that ice formation within the fines may assist in the disintegration of adjacent bedrock. Patterned ground and solifluction stripes suggest that the soil is mobile and capable of dislodging bedrock blocks. The ice content of the pure rock fragment regolith on the steeper slopes may promote downhill movement in a manner similar to a rock glacier. In places outcrops appear to have been undermined by removal of the regolith from the downhill side.

In all types of sedimentary terranes visited evidence for ice wedging in bedrock was seen. The mechanism is probably the same as that proposed for soils by Lachenbruch (1962); however, the orientation of the ice wedges is likely to be controlled by pre-existing fractures or bedding planes. In the case of the steeply dipping calcareous siltstones this is very evident where shallow linear furrows parallel the bedding strike.

Conclusions

From observations made of various rock types in various hydrologic regimes, hypotheses may be formed regarding the cause of heave in bedrock. Freezing of free water appears capable of producing relatively large vertical displacements where the active layer is both deep and fully saturated. Where outcrops are well drained, heave generally was not observed. On the other hand, in rocks that are well drained but that weather partly to silt and/or clay fractions, lesser displacements are possible where the fines collect between the bedrock blocks. The accumulation of fines permits water to be sorted in them. These displacements are primarily horizontal because the soils collect most readily in vertical cracks. Where free water is present displacements will be largest in the vertical direction because the motion required to react to the hydrostatic pressure increase is accomplished most easily in an upward direction.

It is difficult to substantiate these hypotheses in the field because of the probable temporary equilibrium to which most rock heave has come and because of the slow rates of heave involved. Laboratory experiments are planned, however, to examine the ability of freezing to cause displacements in both vacant and soil-filled cracks.

References

Brown, R.J.E.
1973: Influence of climatic and terrain factors on ground temperatures at three locations in the permafrost region of Canada; in North American Contribution, Second International Conference on Permafrost, National Academy of Sciences, p. 27-34.

1978: Influence of climate and terrain on ground temperatures in the continuous permafrost zone of northern Manitoba and Keewatin District, Canada; in Proceedings, Third International Conference on Permafrost, National Research Council of Canada, p. 15-21.

DiLabio, R.N.
1978: Occurrences of disrupted bedrock on the Goulburn Group, eastern District of Mackenzie; in Current Research, Part A, Geological Survey of Canada, Paper 78-1A, p. 499-500.

Fahey, B.D.
1973: Seasonal frost heave and frost penetration measurements in the Indian Peaks Region of the Colorado Front Range; Arctic and Alpine Research, v. 6, p. 63.

Karlén, W.
1973: Holocene glacier and climatic variations, Kebnekaise Mountains, Swedish Lapland; Geografiska Annaler, Series A, v. 55, p. 29-63.

Kerr, J.W.
1974: Geology of Bathurst Island Group and Byam Martin Island, Arctic Canada; Geological Survey of Canada, Memoir 378, 152 p.

Lachenbruch, A.H.
1962: Mechanics of thermal contraction cracks and ice-wedge polygons in permafrost; Geological Society of America, Spec. Paper no. 70, 69 p.

Le Cheminant, A.N.
1977: Geological studies: Thirty Mile Lake and Macquoid Lake map-areas, District of Keewatin; in Report of Activities, Part A, Geological Survey of Canada, Paper 77-1A, p. 205-208.

Netterville, J.A., Dyke, A.S., Thomas, R.D., and Drabinsky, K.A.
1976: Terrain inventory and Quaternary geology, Somerset, Prince of Wales, and adjacent islands; in Report of Activities, Part A, Geological Survey of Canada, Paper 76-1A, p. 145-154.

Tozer, E.T. and Thorsteinsson, R.
1964: Western Queen Elizabeth Islands, Arctic Archipelago; Geological Survey of Canada, Memoir 332, 242 p.

DETAILED GEOCHEMICAL STUDIES, SOUTHEASTERN ONTARIO

Project 760044

W.B. Coker and L.G. Closs[1]
Resource Geophysics and Geochemistry Divison

Coker, W.B. and Closs, L.G., Detailed geochemical studies, southeastern Ontario; in Current Research, Part A, Geol. Surv. Can., Paper 79-1A, p. 247-252, 1979.

Abstract

Detailed geochemical studies were carried out in 1977 in the Grenville Province of southeastern Ontario to follow up the reconnaissance lake sediment geochemical and airborne radiometric surveys of 1976. Preliminary interpretation of the U data from the detailed geochemical studies indicates that the levels of concentration of U in lake waters and sediments are controlled by a variety of natural processes which on occasion can adversely distort the geochemical distribution patterns of U.

Introduction

As part of the Federal-Provincial Uranium Reconnaissance Program (U.R.P.) (Darnley et al., 1975) regional geochemical and airborne radiometric surveys were carried out in southeastern Ontario during the summer of 1976.

The geochemical surveys covered map sheets 31F and 31C (N1/2) within Ontario (Fig. 40.1) and consisted of the collection of lake sediments at a density of one sample per 13 km^2. The lake sediment samples were anlayzed for Zn, Cu, Pb, Ni, Co, Ag, Mn, As, Mo, Fe, Hg, U and L.O.I. (loss on ignition) and these data were released in the spring of 1977 (Geological Survey of Canada, 1977a, b).

The airborne gamma-ray spectrometry, flown at five km line spacings, covered map sheets 31F and 31C. These data were presented as (1) contour maps of the integral count, the potassium, equivalent uranium and equivalent thorium concentrations, and the eU/eTh, eU/K and eTh/K ratios; and (2) stacked profiles of the seven radiometric parameters plotted for each flight line from each of the two map sheets. These data were also released in the spring of 1977 (Geological Survey of Canada, 1977c, d).

Detailed geochemical studies were carried out in the summer of 1977 over nine areas selected on the basis of the regional geochemical and geophysical data (Fig. 40.1) (Closs and Coker, 1977). Five of the areas are characterized by elevated concentrations of U in lake sediments and generally, complementary airborne radiometric highs (Fig. 40.1, areas 1, 4, 5, 7 and 8, (9); Table 40.1). Discussion will be limited to the detailed geochemical studies carried out in these areas.

Regional Geology

The survey area is typically underlain by a variety of plutonic rocks, including widespread anorthosite, mixed gneisses of igneous and metamorphic origin, and numerous remnants of rocks of superficial origin (i.e. metasediments, amphibolites of unknown origin, and metavolcanics)

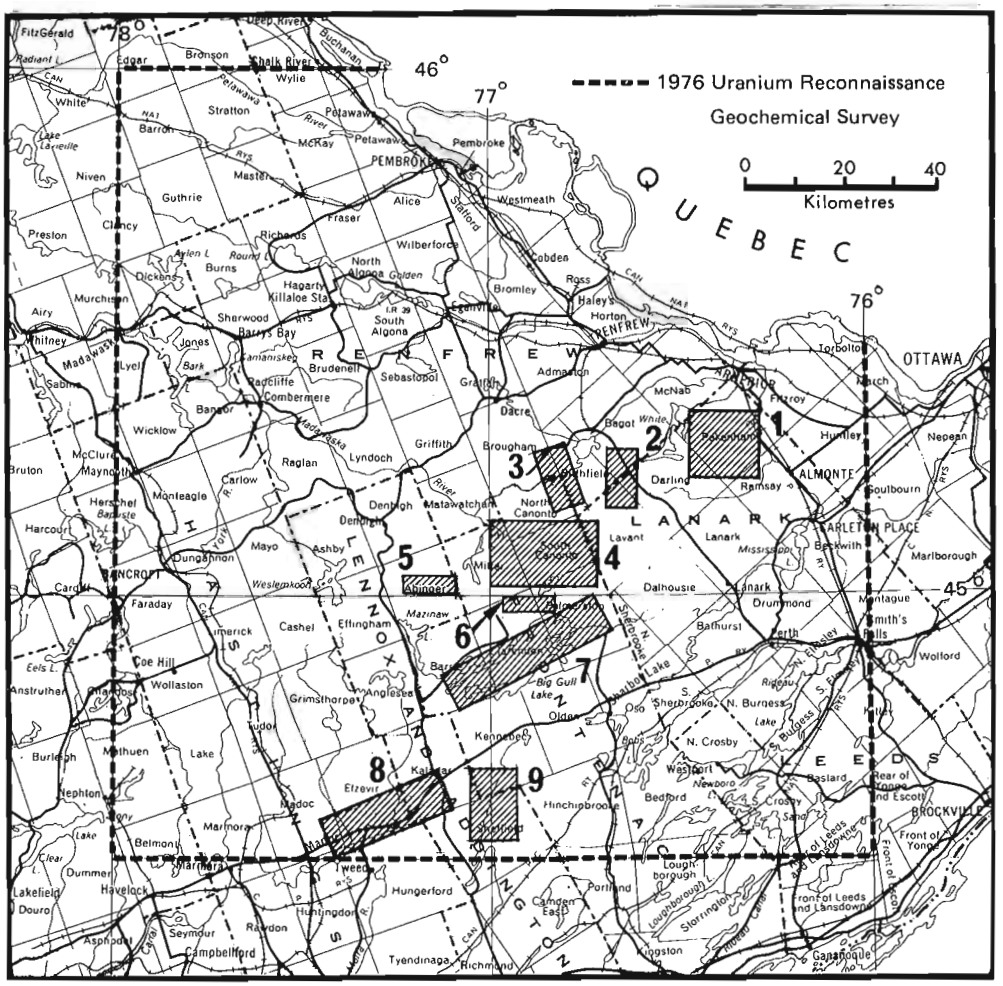


Figure 40.1. *Areas of detailed geochemical studies, southeastern Ontario (from Closs and Coker, 1977).*

[1]Geophysics/Geochemistry Section, Geological Branch, Ontario Ministry of Natural Resources

Table 40.1

Detailed geochemical studies – Uranium, southeastern Ontario

Area (Fig. 40.1)	Name	N.T.S.	Significant Metals	Type of Work performed
1	Pakenham Mts.	31 F 8	U, Hg	2 3 4
4	Mackie-Canonto L.	31 F 2	U	1 3 4
5	Browns-Wickware L.	31 F 3	U	1 3 4
7	Gull-Crotch L.	31 C 14/15	U	1 3 4
8	Kaladar	31 C 11	U	1 3 4
(9)	Puzzle L.	31 C 10/11	Zn(U)	1

1 Detailed lake water and sediment sampling
2 Stream water and sediment sampling
3 Bedrock sampling
4 Ground scintillometer measurements

(Lumbers, 1964). These remnant superficial rocks and mixed gneisses constitute the rocks of the Grenville Province. Although geological mapping has been carried out for many years in the Grenville Province by both the Ontario Department of Mines and the Geological Survey of Canada some regions remain essentially unmapped. Some of the geological mapping related to the areas in which detailed geochemical investigations were undertaken includes: Harding, 1944; Peach, 1958; Liberty, 1963; Hewitt, 1964; Lumbers, 1964; and Hill, 1974.

A large variety of metallic mineral occurrences, some of economic significance, are present. These include: gold, arsenic, iron, nickel, copper, lead, zinc, molybdenum, uranium and rare earth minerals, and some industrially useful rock and nonmetallic minerals described in summary by Lumbers, 1964.

Detailed Geochemical Studies

Sampling techniques and analytical procedures

Lake sediment samples were collected using a Geological Survey sampler from a float-equipped Hughes 500-C turbo-helicopter. Organic-rich sediments (generally brown-thixotropic gels) were collected from the profundal basins of permanent lakes, ponds and swamps. In some instances, intermittent swamps, flooded marshes and beaver-dammed ponds were sampled although the nature of the material obtained (i.e. containing coarse organics – wood, bark, leaves etc.) was not optimum.

Surface lake waters, which were generally clear or brown in colour, were collected directly into polyethylene bottles and acidified (250 µL of HNO_3 per 125 mL of water) on the day of collection. At each sample site measurements of surface water pH, dissolved oxygen content, temperature, and conductivity were made using the Martek Mark V Water Quality Analyser.

Stream waters, collected and acidified as were lake waters, and stream sediments were collected from active streams in the Pakenham Mountains area.

Bedrock samples were collected from the various lithologies present in the area. The average radioactivity over the exposed extent of the outcrop was measured using a McPhar TV-1A scintillometer.

The lake sediment, lake water, stream sediment, stream water and bedrock related field observations were recorded on field data cards, with some modifications, as described by Garrett (1974).

Lake sediment samples were prepared to pass a minus 80-mesh (180 µ) sieve by the staff of Golder Associates, Ottawa. Bedrock samples were ground to approximately 100-mesh (150 4 µ) at the Geological Survey.

The fluorometric method of analysis of the lake and stream water samples for acid-extractable U was based on the method described by Smith and Lynch (1969). These anlayses were performed by A.I. MacLaurin in the laboratories of the Geochemistry Subdivision, Geological Survey of Canada.

The delayed neutron activation method of analysis, by which the lake sediment, stream sediment, and bedrock samples were analyzed for total U, was developed by Atomic Energy of Canda Ltd., Commercial Products Division, and is described in some detail by Boulanger et al. (1975).

Results

Pakenham Mountains (area 1, Figure 40.1) Insufficient lake density for a detailed survey dictated that stream waters and sediments be utilized in this area. In most instances inorganic-clastic sediments and clear waters were obtained, although some sediments did contain minor organics and some waters were yellow-brown (humic rich) in colour. Neither the stream waters ($\bar{x}$ = 0.32 ppb, range = 0.05 to 0.66 ppb; n = 13) nor stream sediments ($\bar{x}$ = 2.3 ppm, range = 1.4 to 4.8 ppm; n = 11) contain significant levels of U. The higher concentrations are generally related to the presence of organics.

Bedrock in the area contains little U (Table 40.2) and although the area has been mapped as a plutonic complex (Hill, 1974) the possibility of being of remnant superficial origin should be considered. The area was primarily of interest geologically and of marginal interest on the basis of the reconnaissance geochemistry. The geochemical data obtained in the detailed study give little indication of any uranium potential.

Mackie – Canonto lakes (area 4, Fig. 40.1) Lake waters are somewhat enriched in U in the east part of this area, as depicted by 34 water samples having a mean U content of 0.45 ppb and range of 0.26 to 1.02 ppb. Lake sediments, however, are enriched in the west and central parts of the area, as indicated by 25 sediment samples with an overall mean U content of 38.4 ppm and range of 26.4 to 72.1 ppm. This variation reflects the measured chemical differences existing in the lake waters within this area. Lakes in the east, with U enriched waters, generally have more alkaline waters with pH > 7.0 and conductivities > 100 µmhos compared to the neutral to acid waters in lakes in the west, with U enriched sediments, and with pH < 7.0 and conductivities <50 µmhos.

Pegmatites in the area were found to be generally conformable with their host rock, frequently tourmaline bearing and somewhat enhanced radioactively, although only slightly enriched in U (see Table 40.2). The high degree of bedrock exposure and the trace amounts of U available in the pegmatites and gneisses in this area (Table 40.2) most probably account for the levels of U that occur in the waters and sediments of lakes in this area.

Browns – Wickware lakes (area 5, Fig. 40.1) Elevated concentrations of U exist in lake sediments in the south half of this area. There is no U response in lake waters. The main area of elevated U in lake sediments consists of three grouped samples in the west-central part of the area containing 30.2, 30.0 and 52.1 ppm U. Although exposed bedrock is plentiful, this area has not been geologically mapped to date. The bedrock lithologies encountered consisted of biotite and/or amphibole gneisses, quartzo-feldspathic rocks, and simple pegmatites (quartz, potassium feldspar, ± biotite). Only minor amounts of U were detected in the bedrock of this area (Table 40.2). The geochemical response in the lake sediments is likely due to a mass bedrock effect of little economic significance.

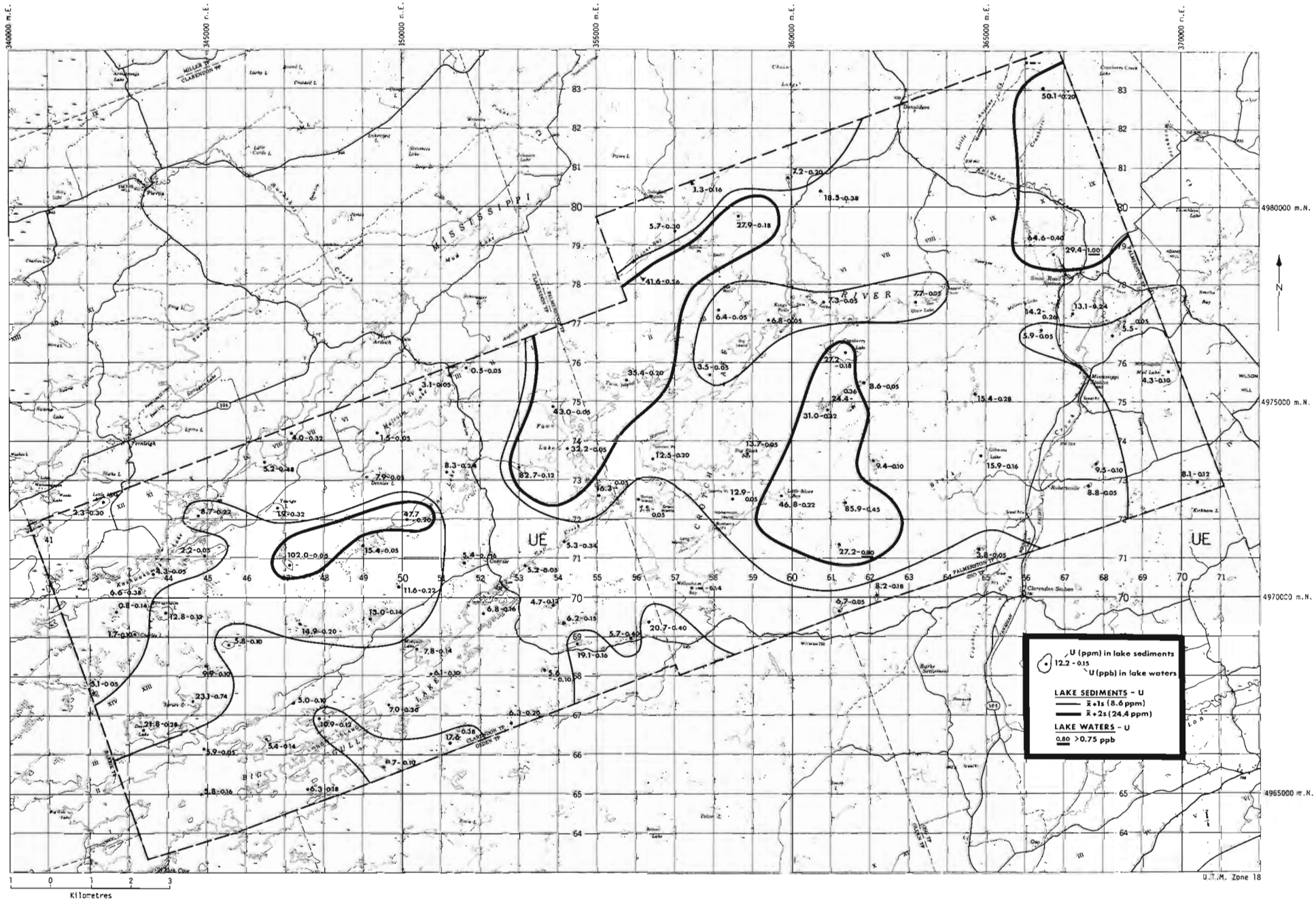


Figure 40.2. *Distribution of uranium in lake sediments and lake waters, Gull-Crotch lakes (31C/14, 15) area, southeastern Ontario.*

Gull – Crotch lakes (area 7, Fig. 40.1) Presentation of the distribution patterns of U in lake sediments from within this detailed study area, as well as within the Kaladar area, is based on the log-normalized distribution of U in the reconnaissance lake sediment samples (i.e. geometric $\bar{x}$ = 3.0 ppm, $\log_{10} \sigma$ = 0.482; therefore $\bar{x}+1\sigma$ = 8.6 and $\bar{x}+2\sigma$ = 24.4 (number of reconnaissance samples = 1254)). As no reconnaissance data were available for U in lake waters a threshold value of 0.75 ppb was chosen on the basis of previous work carried out in the Grenville province (Renfrew area, 31/F/7) by Coker and Jonasson (1977).

The distributions of U in the lake waters and sediments within this area are illustrated in Figure 40.2. There is general coincidence between the distribution patterns of U in both sample media. The large area of enhanced U in lake sediments, and to a lesser extent in lake waters, southeast of Crotch Lake is a reflection of U enriched mineralized pegmatites in that locality. Other areas of similar enrichment of U in lake sediments and/or waters occur coincident with the grey granite-granodioritic bedrock unit. Pegmatites sampled within this unit show enrichment in U (Table 40.2). There are at least two, and possibly three, types of pegmatites, all mineralogically simple (quartz, potassium feldspar, ± biotite, with traces of tourmaline), of either the conformable or unconformable type within this area. The most significant enhancement of U in lake waters and/or sediments generally occurs in conjunction with the grey granite – granodioritic unit in this area, and pegmatites (conformable?) within this unit show the highest enrichment in U.

Kaladar (area 8, Fig. 40.1) Uranium is enriched in the waters and sediments of lakes within a band trending from the northeast to the southwest of the Kaladar area (Fig. 40.3). This band of U enrichment roughly corresponds to the area mapped as grey granite – granodiorite containing some slightly U-enriched simple pegmatites (Table 40.2). Exposed bedrock constitutes approximately 70 to 75 per cent of this band. Intervening spaces between bedrock outcrops are occupied by intermittent swamps, marshes, streams, and ponds, as well as some true lakes, the drainage of which is largely controlled by the action of beavers. These waters are invariably acid (pH < 6.0) and organic-rich. The large volume of exposed bedrock, containing minor U (Table 40.2), subjected to these organic-rich acid waters, results in enhancement of the natural leaching processes and probably causes the extreme levels of enrichment of U in both the waters and sediments sampled within this band.

Puzzle Lake (area (9), Fig. 40.1) On the basis of the reconnaissance geochemical data this area was primarily of interest for Zn, and of only secondary interest for U.

Table 40.2

Distribution of uranium in bedrock samples, southeastern Ontario

Rock type \ Area	Pakenham Mt.	Mackie-Canonto Lakes	Browns-Wickware Lakes	Gull-Crotch Lakes	Kaladar
Amphibolite gneiss		0.9 (0.5-1.4)-(2)			1.9 (0.3-4.0)-(6)
Amphibolite				1.7 (0.5-3.7)-(4)	
Basic metavolcanic					0.8 (0.4-1.3)-(2)
Granodioritic rock	1.2			2.9 (1.3-5.5)-(8)	1.4 (1.0-1.9)-(5)
Granitic gneiss		1.8 (0.3-4.0)-(5)	3.1 (1.1-5.3)-(11)	2.4 (1.7-3.1)-(4)	3.5 (2.2-4.9)-(8)
Granitic rock	1.9 (0.8-3.1)-(8)				
Intermediate metavolcanics				1.0	
Marble		0.8 (0.1-2.1)-(6)			1.6 (0.3-4.2)-(5)
Pegmatite		6.0 (0.5-18.8)-(8)	2.1	26.7 (2.1-121.0)-(11)	15.5 (9.2-29.0)-(9)
Paragneiss		2.8 (0.6-4.9)-(2)			3.0 (2.6-3.4)-(2)
Syenitic rock				2.0	

Arithmetic mean

0.4
(0.2-0.8) - (10) – number of samples

Range (minimum - maximum)

However, the detailed geochemical studies indicate significant enrichment of U in lake waters (1.20 and 0.98 ppb) and sediments (26.3, 153.0, 85.5, and 32.7 ppm) associated with Mo occurrences in the southeastern part of the area. Perhaps these Mo occurrences should be examined for their U potential as has been suggested in other parts of the Grenville (Coker and Jonasson, 1977). In addition an isolated lake sediment sample containing 52.4 ppm U taken from a lake at the Precambrian-Paleozoic contact is perhaps indicative that this contact should be more closely examined for possible depositional environments for U.

Discussion and Conclusions

Interpretation of the distribution of U in lake waters and sediments within the detailed study areas, as presented, should be viewed as only preliminary in nature. Interelement relationships can significantly clarify certain limnologic, chemical and geological phenomena and add greatly to the final interpretation. The detailed geochemical studies of areas (2, 3, 6 and 9 – Fig. 40.1) characterized by elevated base metal concentrations will also be outlined later.

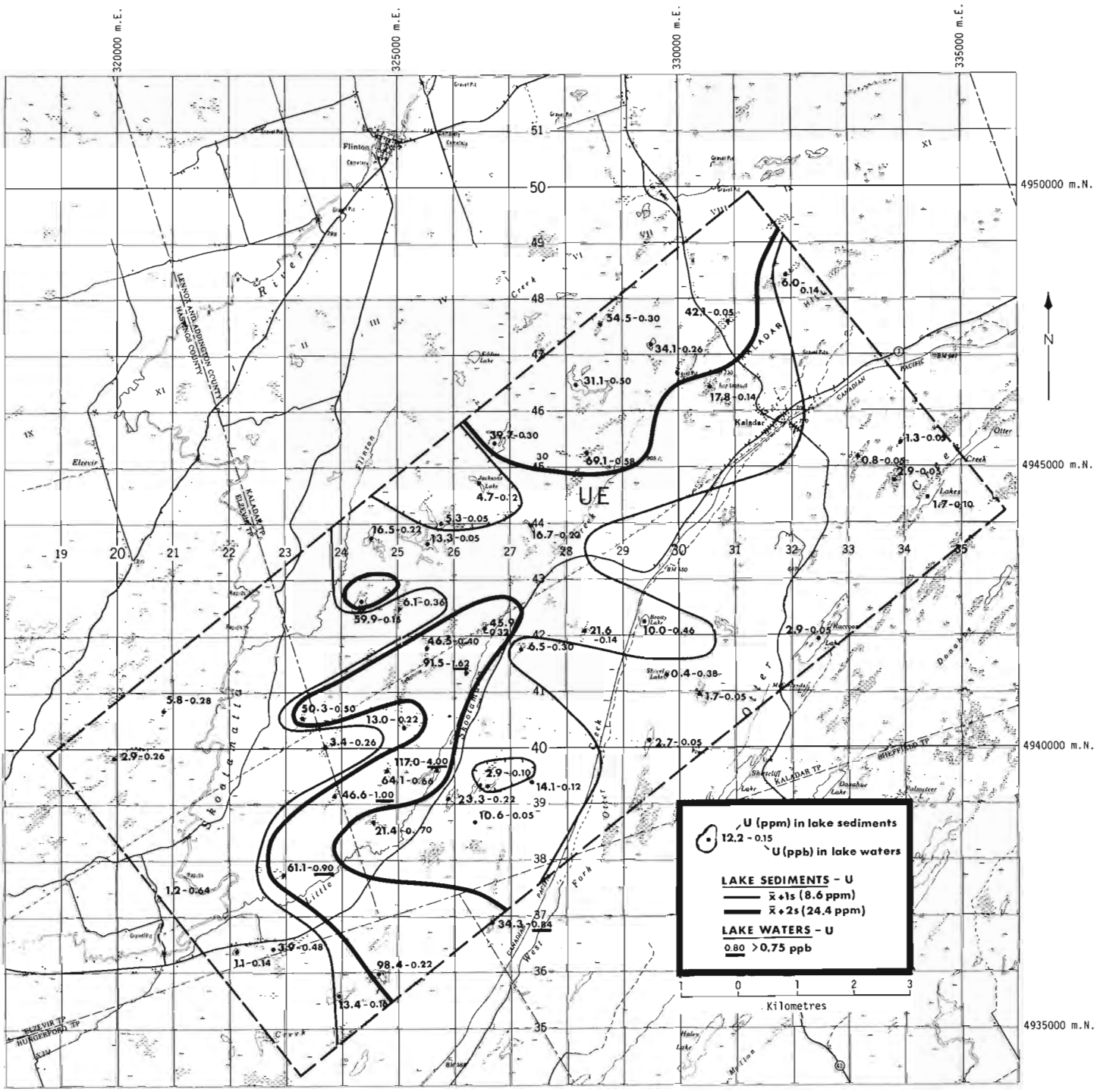


Figure 40.3. *Distribution of uranium in lake sediments and lake waters, Kaladar (31C/11) area, southeastern Ontario.*

In some cases, such as in the Mackie-Canonto lakes, Browns-Wickware lakes, and, possibly, the Pakenham Mountains areas the levels of U that occur in the waters and sediments are a reflection of a mass bedrock effect probably enhanced by organic activity. Lack of correspondence between the distribution patterns of U in lake waters and sediments can result from variations in the chemical conditions as indicated by variations in pH and alkalinity in the Mackie-Canonto lakes area.

In the Gull-Crotch lakes area elevated levels of U in lake waters and sediments are a reflection of mineralized pegmatites. Elevated levels of U in the lake waters and sediments of the Puzzle Lake area are associated with known Mo occurrences.

Unusual surficial chemical conditions, very acid and extremely organic-rich waters, have probably resulted in some enhancement of natural leaching processes causing relatively higher concentrations of U than would normally be expected to occur in both the waters and sediments within the drainage courses of the Kaladar area.

In general lake water and sediment geochemistry can be of value in the search for U mineralization within the Grenville Province. Caution, however, must be exercised in the interpretation of such geochemical data as the surficial chemistry within the Grenville Province is complex and can greatly distort the geochemical distribution patterns produced.

References

Boulanger, A., Evans, D.J.R., and Raby, B.F.
1975: Uranium anlaysis of neutron activation delayed neutron counting: Proceedings 17th Annual Symposium of the Canadian Mineral Analysts, Thunder Bay, Ontario, Sept. 22-23, 1975.

Closs, L.G. and Coker, W.B.
1977: Joint Federal-Provincial lake sediment geochemistry follow-up program; in Summary of Field Work, 1977, by the Geological Branch, edited by V.G. Milne, O.L. White, R.B. Barlow, and J.A. Robertson, Ontario Geological Survey, Miscellaneous Paper 75, p. 178-180.

Coker, W.B. and Jonasson, I.R.
1977: Geochemical Exploration for Uranium in the Grenville Province of Ontario; Canadian Mining and Metallurgical Bulletin, v. 70, no. 781, p. 67-75.

Darnley, A.G., Cameron, E.M., and Richardson, K.A.
1975: The Federal-Provincial uranium reconnaissance programs; in Uranium Exploration 1975; Geological Survey of Canada, Paper 75-26, p. 49-68.

Garrett, R.G.
1974: Field data acquisition methods for applied geochemical surveys at the Geological Survey of Canada; Geological Survey of Canada, Paper 74-52, 36 p.

Geological Survey of Canada
1977a: Regional lake sediment geochemical reconnaissance data, eastern Ontario, NTS 31C (N 1/2); Geological Survey of Canada, Open File 405.

1977b: Regional lake sediment geochemical reconnaissance data, eastern Ontario, NTS 31F; Geological Survey of Canada, Open File 406.

1977c: Airborne gamma-ray spectrometry data, Pembroke, Ontario, NTS 31F; Geological Survey of Canada, Open File 331.

1977d: Airborne gamma-ray spectrometry data, Kingston, Ontario, NTS 31C; Geological Survey of Canada, Open File 428.

Harding, W.D.
1944: Geology of Kaladar and Kennebec townships; Ontario Department of Mines, v. 51, 1942, pt. 4, p. 51-74, and map no. 51d.

Hewitt, D.F.
1964: Madoc-Gananoque area; Ontario Department of Mines Geological Circular no. 12, 33 p. with Maps 2053 and 2054.

Hill, P.,A.
1974: Geology, Arnprior, Ontario; Geological Survey of Canda, Map 1363A.

Liberty, B.A.
1963: Geology of Tweed, Kaladar and Bannockburn map-areas, Ontario, with special reference to Middle Ordovician stratigraphy; Geological Survey of Canada, Paper 63-14, 15 p., with Maps 24-1963 and 25-1963.

Lumbers, S.B.
1964: Preliminary Report on the Relationship of Mineral Deposits to Intrusive rocks and Metamorphism in the Grenville Province of Southeastern Ontario; Ontario Department of Mines, PR 1964-4, 37 p.

Peach, P.A.
1958: The geology of Darling township and part of Lavant township; Ontario Department of Mines, v. 65, 1956, pt. 7, p. 47-60.

Smith, A.Y. and Lynch, J.J.
1969: Field and laboratory methods used by the Geological Survey of Canda in geochemical surveys; No. 11, Uranium in soil, stream sediment and water; Geological Survey of Canada, Paper 69-40, 9 p.

41. COPPER-MOLYBDENUM OCCURRENCES OF THE MATACHEWAN AREA, ONTARIO

Project 770071

W.D. Sinclair
Regional and Economic Geology Division

Sinclair, W.D., Copper-molybdenum occurrences of the Matachewan area, Ontario; in Current Research, Part A, Geol. Surv. Can., Paper 79-1A, p. 253-258, 1979.

Abstract

Low-grade copper and molybdenum occurrences of Archean age in the Matachewan area exhibit similarities to porphyry deposits in younger rocks of the Canadian Cordillera. The Matachewan deposits are associated with high-level intrusions of porphyritic syenite. They consist of copper and molybdenum sulphides in quartz veins, fractures and disseminations in syenite porphyry and intruded metavolcanic and metasedimentary rocks. A multistage development of mineralization is indicated by crosscutting relationships between quartz veins. Associated alteration consists of chloritization, hematitization and silicification. Although none of the Matachewan deposits found to date are economic, they are poorly understood and their economic potential is yet uncertain.

Introduction

Mesozoic and younger porphyry deposits account for a major portion of world as well as Canadian reserves of copper and molybdenum. They have been studied extensively and many detailed descriptions of deposits and their geological settings exist in the literature. Typically, they are large, low-grade deposits of veinlet- and fracture-controlled hypogene mineralization associated with felsic to intermediate epizonal intrusions (Kirkham, 1972a). Despite increasing interest in porphyry deposits in Archean rocks of the Canadian Shield, few examples have been studied in detail and there is yet little appreciation of their general nature and economic potential. A possible indication of their potential is the copper zone in the Pearl Lake porphyry at the McIntyre mine, Timmins. This zone is expected to produce about 10 million tons averaging 0.8 per cent copper (Davies and Luhta, 1978). However, the entire zone contains more than 80 million tons of low-grade copper-gold-molybdenum mineralization and would undoubtedly yield much more than 10 million tons if it were available for open pit mining (Pyke and Middleton, 1970; Kirkham and Thorpe, 1973).

Current investigations of Precambrian porphyry deposits are part of a continuing study of copper and molybdenum deposits in Canada. Despite different degrees of regional metamorphism and deformation, similarities with economic porphyry deposits in younger rocks have been recognized (Kirkham,1972b; Ayres and Findlay, 1976; Findlay and Ayres, 1977). This paper presents initial impressions of some porphyry-type and related copper-molybdenum occurrences in the Matachewan area, Ontario.

The Matachewan area comprises Powell and Cairo townships and adjacent parts of Alma, Baden, Flavelle and Holmes townships, described in recent reports by Lovell (1967) and Moore (1966). The area is well-known for its gold deposits, two of which, the Young-Davidson and the Matachewan Consolidated, produced nearly a million ounces of gold from 1934 to 1956. However, there are also numerous copper and molybdenum occurrences. Approximately 5 million pounds of copper, with some gold and silver were produced from the Ryan Lake property from 1950 to 1964. A small amount of copper has also been produced from the Stancop property.

General Geological Setting

The geology of the Matachewan area (Fig. 41.1) is dominated by the Cairo stock, a large syenitic intrusion centred mainly in Cairo and Alma townships (Lovell, 1967). The Cairo stock and related dykes and plugs of syenite and syenite porphyry intrude an isoclinally-folded sequence of Timiskaming Group metavolcanic and metasedimentary rocks (Ridler, 1973). Granitic to dioritic rocks, locally gneissic, occur mainly in the southeastern part of the area. The syenite and granite to diorite bodies and the metavolcanic-metasedimentary sequence are cut by north-trending dyke swarms of Matachewan diabase. The southwestern and southeastern parts of the Matachewan area are overlain by Proterozoic sedimentary rocks of the Cobalt Group, mainly Gowganda conglomerate.

The age of the syenite has not been determined radiometrically, but it is at least older than the Matachewan diabase, dated at 2485 Ma (Fahrig and Wanless, 1963). The relationship between the syenitic and granitic rocks is uncertain (Lovell, 1967).

The syenite that forms the stock and related dykes displays a variety of textural and compositional types. The main part of the stock consists of medium to coarse grained hornblende syenite. Based on megascopic examination, orthoclase (60-80 per cent) is the main mineral present, with varying amounts of albite (5-10 per cent) and partly chloritized hornblende (15-35 per cent). Some quartz is also present locally. Wolfe (1972) described a zonation from quartz-bearing syenite in the central portion of the stock to more mafic syenite around the periphery of the stock. Although this zoning is probably gradational for the most part, xenoliths of mafic-rich syenite were observed in less mafic syenite near the eastern margin of the stock in the southeast corner of Alma Township. Along the western margin of the stock in Cairo Township there is a zone of coarse to very coarse grained, trachytic syenite in which individual crystals of orthoclase are 2 to 4 cm long. Both precious- and base-metal occurrences associated with this stock tend to be concentrated along its periphery.

Offshoots of the main stock mainly small plugs and irregular dykes, vary from syenite porphyry to equigranular trachytic syenite. Trachytic syenite is medium to coarse grained and consists mainly of orthoclase with minor amounts of albite. The syenite is typically brick red, apparently due to the presence of very fine grained hematite (alteration?) in the orthoclase. The trachytic texture is well developed and generally conformable with intrusive contacts. Trachytic syenite occurs mainly in a belt of east-trending dykes and irregular elongate bodies in the southern part of Powell Township. It was an important host for gold ore at the Matachewan Consolidated mine (Derry et al., 1948) (Fig. 41.1, loc. 1) and was the main host for gold at the Young-Davidson mine (North and Allen, 1948) (Fig. 41.1, loc. 2).

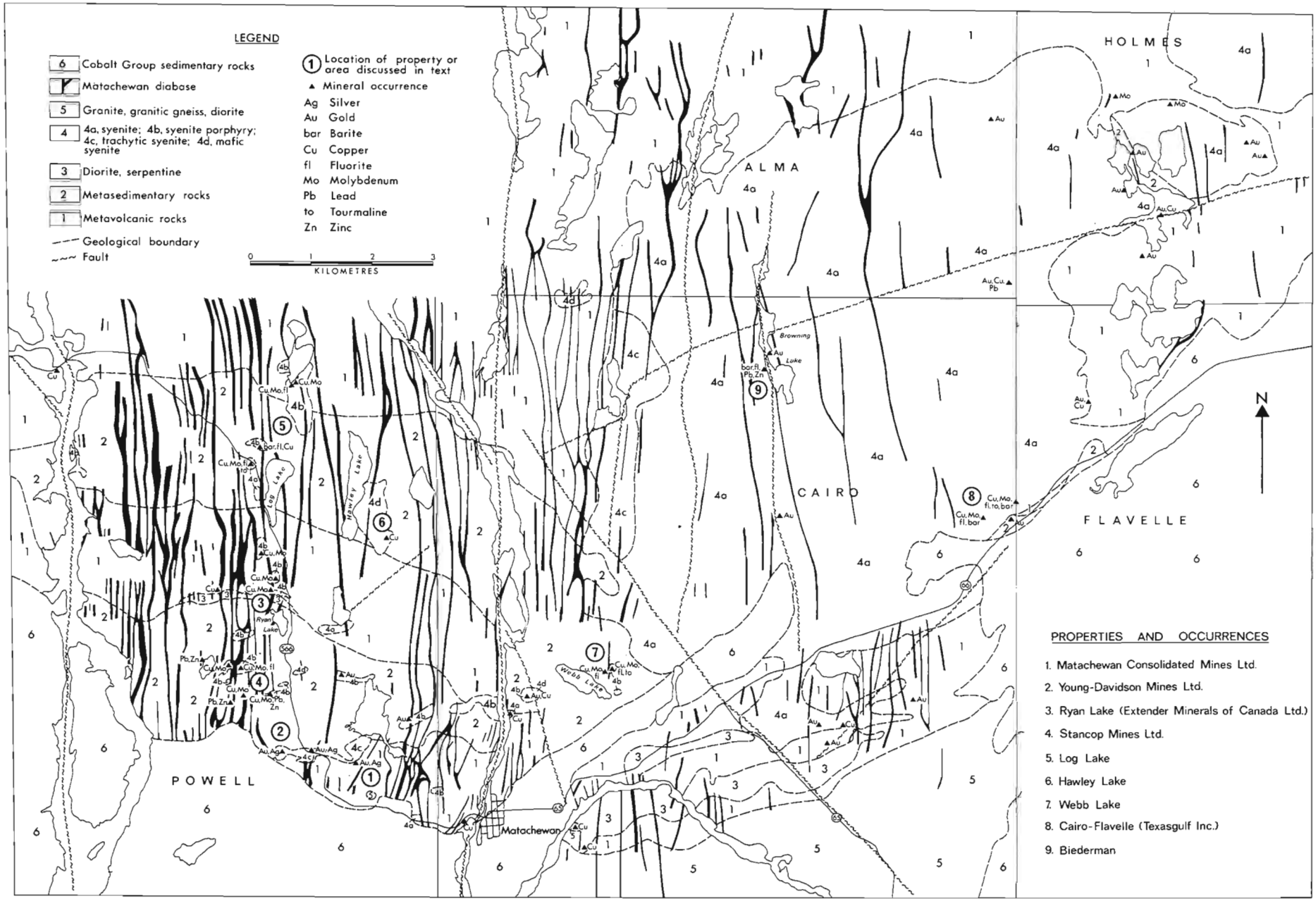


Figure 41.1. *General geology and mineral occurrences in the Matachewan area, Ontario (modified from Moore, 1966 and Lovell, 1967).*



Figure 41.2. *Syenite porphyry cut by quartz veins, Ryan Lake property. GSC 203425.*

Syenite porphyry is a massive, blocky phase characterized by up to 20 per cent orthoclase phenocrysts in a matrix of albite, hornblende and/or biotite that is mainly chloritized, and a little quartz. The orthoclase phenocrysts are pink to red, locally well zoned and average about 1 cm in size. The matrix is reddish grey and varies from aphanitic to porphyritic in texture. In the latter case, it consists of crowded white albite phenocrysts up to 3 mm in size in a fine grained, reddish grey groundmass. No distinct contact relationships have been observed between different textural varieties of the syenite porphyry. Numerous small plugs or stocks of syenite porphyry in Powell Township and the western part of Cairo Township are associated with copper-molybdenum occurrences, including those on the Stancop and Ryan Lake properties.

Small bodies of mafic syenite are also present in the Matachewan area. These generally consist of fine grained, roughly equigranular hornblende syenite in which most of the hornblende is chloritized. Magnetite is a common accessory. This phase of the syenite is probably a normal differentiate of the syenite magma although it may be due, in part, to assimilation of intruded volcanic rocks (Lovell, 1967). There are some copper-molybdenum occurrences spatially associated with mafic syenite (e.g. Hawley Lake).

Selected Copper-Molybdenum Occurrences

Some of the more significant copper-molybdenum occurrences are described below:

Ryan Lake Property

The Ryan Lake property (Fig. 41.1, loc. 3) currently owned by Extender Minerals of Canada Limited, was operated intermittently during the period 1950 to 1964. Most of the production came from high-grade copper zones related to easterly-trending fault zones between serpentinized peridotite and syenite porphyry (Vokes, 1963). Low-grade copper and molybdenum is associated with high-grade zones on the north side of the main fault zone. A block of this low-grade material was estimated by Pax International Mines Ltd. to contain 3.5 million tons of 0.4% Cu and 0.09% MoS_2 (R.A. Hill, pers. comm.).

Low-grade molybdenum-copper mineralization associated with syenite porphyry is also present in a pit 15 by 40 m situated 600 m north of the main fault zone. Exposed in the pit and surrounding outcrop is a reddish grey syenite porphyry cut by veins and stringers of white quartz that vary from 0.5 to 3 cm in width (Fig. 41.2). The distribution of these veins and stringers is variable. In places they form a stockwork in which individual veins are 4 to 5 cm apart; elsewhere, they are spaced 0.5 m apart or more. In general, the veins trend north to northeast and are vertical to steeply dipping.

Molybdenite and, to a lesser extent, chalcopyrite occur as coarse, disseminated grains and irregular patches in the quartz veins and as irregular, disseminated grains and stringers in the syenite porphyry. Molybdenite also occurs as coatings on fracture surfaces, commonly smeared out and very thin, but locally up to 1 mm thick. Pyrite is associated in places with molybdenite and chalcopyrite but is much less abundant. Powellite, identified by its yellow fluorescence, forms very thin coatings along hairline fractures in quartz veins, apparently from the alteration of molybdenite. Rare grains of scheelite are also present in the quartz veins. Many of the quartz veins have thin selvages of red, hematitic alteration.

The area of mineralized syenite porphyry exposed in the pit and surrounding outcrop is about roughly 30 by 60 m. To the west the syenite porphyry is bounded by barren diabase and metavolcanic rocks; in other directions the distribution of the porphyry is not known. During the early 1960's approximately 2000 tons averaging 0.32% MoS_2 and 0.25% Cu were mined from this pit (G.S. Welsh, pers. comm.).

Stancop Property

Occurrences of copper and molybdenum are widely distributed on the Stancop Mines Limited property immediately south of the Ryan Lake property (Fig. 41.1, loc. 4). Although most of the occurrences are very low grade, consisting of widely spaced and sparsely mineralized fractures in syenite porphyry and the intruded Timiskaming metasedimentary rocks, they include some higher grade zones. One such zone at the contact between porphyry and metaconglomerate is exposed 300 m west of Highway 566 in a pit 15 by 20 m and a trench 60 m long. In this area both the porphyry and the metaconglomerate are intensely silicified locally and cut by a stockwork of quartz veins that show at least two stages of development. The first stage consists of narrow (2-3 mm) veinlets of bluish grey, fine grained quartz in a randomly oriented, closely spaced network. The second consists of north-trending veins up to 3 cm wide and spaced 3 to 4 cm apart. Chalcopyrite, some bornite and minor pyrite, are present as very finely disseminated sulphides in the quartz veins and in the silicified host rocks. In the second stage veins the sulphides are typically concentrated in thin laminae paralleling vein contacts, giving the veins a banded appearance. The zone of intense silicification and quartz veining is up to 15 m wide and trends approximately north-south. Two thousands tons mined from this zone in 1965 averaged about 0.6% Cu (G.S. Welsh, pers. comm.). Outside this zone the stockwork of first stage veining extends for up to 30 m in both the porphyry and metaconglomerate.



Figure 41.3. *Early-stage quartz veinlets cut by late-stage quartz vein, Stancop property. GSC 203425-F.*

However, the second stage veins are less abundant and silicification is lacking. The first stage veins extend for about another 15 m in metaconglomerate but become more widely spaced and grade into narrow, sparsely mineralized fractures.

A third stage consists of widely spaced and randomly oriented veins of massive white quartz up to 10 m long and averaging 3 to 5 cm wide although locally up to 0.5 m wide (Fig. 41.3). These veins contain patches of coarse grained chalcopyrite and some pyrite, in many places accompanied by large clots of chlorite and pink calcite. Small amounts of galena and sphalerite are also present locally in these late-stage veins.

A second higher grade zone is exposed in a series of trenches 450 m northwest of the first zone. The principal rock type exposed is a grey to reddish grey syenite porphyry with approximately 10 per cent phenocrysts of white to pinkish orthoclase in a porphyritic matrix of 50 to 60 per cent albite phenocrysts. The porphyry is cut by hairline fractures and narrow, randomly oriented quartz veinlets that form stockworks locally but which are, in general, widely spaced. Chalcopyrite, molybdenite and minor pyrite occur in the quartz veinlets and fractures and molybdenite forms thin smears on fracture surfaces. Fine grained chlorite commonly accompanies the sulphides. Locally, there is intense reddish alteration of syenite porphyry along the borders of the quartz veins, apparently due to hematitization. In other places, specular hematite is associated with the sulphides.

The early veinlets are cut by later quartz-carbonate-chlorite veins that carry patchy chalcopyrite, molybdenite and pyrite. Specularite and coarse purple fluorite also occur locally in these veins.

The mineralized area covered by these trenches is about 150 by 250 m. Although the grade exceeds 0.2% Cu in a few places, work done by Majestic Construction Ltd. in 1974 indicated an overall grade of 0.05 to 0.1% Cu.

Approximately 400 m to the south of the second zone sulphides are exposed in several trenches cut in metaconglomerate. Sparse chalcopyrite, molybdenite and pyrite occur along fractures and in quartz veinlets. Some 250 m farther to the southwest, galena and sphalerite occur locally with pyrite as disseminated grains and in veinlets cutting the metaconglomerate.

The second higher grade zone is bounded on both the east and west sides by dykes of Matachewan diabase. On the west side, the diabase is up to 200 m wide. West of this diabase, sparsely mineralized syenite porphyry is exposed in small pits and trenches. To the north this porphyry intrudes argillite cut by numerous mineralized fractures and thin quartz veinlets that locally form a closely-spaced stockwork (Fig. 41.4). Alteration selvages associated with the fractures and quartz veinlets typically have a bleached appearance. To the south, the porphyry intrudes metaconglomerate containing traces of chalcopyrite in hairline fractures and quartz veinlets with some red alteration selvages locally.

Log Lake

Outcrops of mineralized syenite occur west of the north end of Log Lake, north of the Ryan Lake property (Fig. 41.1, loc. 5). The syenite, a brick-red, roughly equigranular variety, is cut in places by stockworks of quartz veins, exposed in small trenches and pits southwest of Highway 566. Two stages of veins are present, an early, relatively barren stage of quartz veinlets and a later stage of quartz-carbonate veins containing small amounts of chalcopyrite, molybdenite, pyrite, fluorite and some tourmaline. The sulphides appear to have a very limited distribution. They are exposed in two areas, the larger of which is no more than 5 by 10 m. The second area, 100 m to the north, is represented only by material excavated from a small pit.

A vein of barite in syenite porphyry is exposed in a small pit 250 m north and slightly to the west of Log Lake. The vein is 0.5 m wide and strikes 110°, dipping 80° south. The barite is coarse grained, white and contains some purple fluorite and a few specks of chalcopyrite. Fragments of syenite porphyry in the vein contain quartz veins terminated by the barite.



Figure 41.4. *Stockwork of mineralized fractures and quartz veinlets cutting argillite, Stancop property. GSC 203425-D.*

At the south end of a small lake 1.3 km north of Log Lake, several small pits have been blasted in syenite porphyry. Traces of chalcopyrite and molybdenite were observed along fractures and in quartz veins containing calcite and coarse grained, purple fluorite. On the southeast side of the lake there is an easterly trending quartz vein up to 12 m thick that contains local concentrations of molybdenite, chalcopyrite and pyrite.

Hawley Lake

Fine grained mafic syenite and hornfelsic metasedimentary rocks are exposed in trenches east of the south end of Hawley Lake (Fig. 41.1, loc. 6). Chalcopyrite and molybdenite occur as irregular streaks and patches in the syenite and hornfels and as disseminated grains and patches in quartz veins. Although some areas of good grade copper and molybdenum are present, the distribution of sulphides appears to be erratic. The extent of the mineralized area has not been determined.

Webb Lake

Copper-molybdenum sulphides spatially associated with a small plug of hornblende syenite are exposed in a number of small pits and trenches about 350 m northeast of Webb Lake in Cairo Township (Fig. 41.1, loc. 7). The syenite is pink to red, medium grained and contains 5 to 20 per cent chloritized hornblende. It is cut by narrow, bluish grey quartz veinlets that have a marked northerly trend. In places these veinlets are closely spaced and joined by similar veinlets trending about 75°, forming stockworks. Chalcopyrite occurs as disseminated grains in the veinlets and as thin coatings of very small grains along the centres of the veinlets or along the edges. Veins of massive, white quartz and pink calcite cut the bluish grey quartz veinlets. These later veins contain patches of chlorite, coarse grained purple fluorite, chalcopyrite, minor bornite and tourmaline. Tourmaline occurs as needles up to 1 cm long and as fine grained, granular masses that locally comprise up to 50 per cent of the vein. Diamond drilling by Midrim Mining Company Ltd. in 1966 intersected 0.1 to 0.15% Cu over an area approximately 60 by 120 m.

The west side of this area is bounded by a north-trending dyke of Matachewan diabase. West of this diabase, the syenite intrudes fine grained Timiskaming meta-arkose and metaconglomerate. The metasedimentary rocks are cut by stockworks of hairline fractures containing pyrite and sparse chalcopyrite accompanied by chlorite and traces of epidote. Late-stage quartz veins carry calcite and chlorite along with some purple fluorite and spots of coarse chalcopyrite.

Cairo-Flavelle Property

This property straddles the boundary between Cairo and Flavelle townships, immediately northwest of Highway 66 (Fig. 41.1, loc. 8). It is situated in the southern part of the main stock and covers both syenite and intruded metavolcanic rocks. The syenite varies from a red syenite with up to 15 per cent mafic minerals, mainly chloritized hornblende, to a grey or slightly pink syenite with less than 5 per cent mafic minerals and up to 5 per cent feldspar phenocrysts. The latter is distributed mainly in the outer periphery of the stock along the syenite-metavolcanic contact.

Traces of copper and molybdenum are widely distributed over the Cairo-Flavelle property. However, a zone of higher grade material exists near the boundary of the two townships and was drilled by Texasgulf Inc. in 1975. Within this zone chalcopyrite and molybdenite occur in narrow fractures, veinlets and, to a lesser extent, disseminations in the grey to pink syenite. At least two stages of veins are represented. The first consists of narrow (1-2 mm) veinlets of bluish grey quartz with very finely disseminated sulphides, mainly chalcopyrite, minor pyrite and, in places, molybdenite. The second consists of thicker (up to 4 mm) quartz veinlets and veins that contain some chalcopyrite and varying amounts of calcite, chlorite and purple fluorite. Tourmaline and white to orange barite were noted in a few places. Chlorite and hematite alteration occur in the syenite adjacent to some of the veinlets.

The metavolcanic rocks consist mainly of chlorite-epidote schist with locally abundant magnetite. Traces of chalcopyrite occur along hairline fractures and with quartz-calcite veinlets.

Discussion

The texture of the syenite forming the dykes, plugs and small stocks in the Matachewan area ranges from trachytic to porphyritic with a fine grained to aphanitic groundmass indicating a high-level, probably subvolcanic origin. The main part of the Cairo stock is generally medium to coarse grained and equigranular to trachytic in places. This suggests a deeper but probably still high level of emplacement although differences in texture may be due, at least in part, to the greater volume and, hence, longer cooling history of the Cairo stock. Gold-silver and copper-molybdenum occurrences are spatially associated with the smaller high-level syenite bodies and with the peripheral phases of the main stock.

Composition of the gold-silver and copper-molybdenum deposits reflects a regional zonation of metals. The gold-silver deposits, principally those of the Young-Davidson and Matachewan Consolidated mines, are associated with pyritic syenite that contains only small amounts of copper and molybdenum. North and Allen (1948) stated that mineralized syenite contains 2 per cent pyrite and examination of waste material and exposures around the mines indicates there is up to 10 per cent pyrite in places. The copper-molybdenum occurrences, in contrast, tend to be low in pyrite, with minor values in gold and silver. Scheelite occurs in small amounts in the gold-silver deposits (Little, 1959) but is a rare constituent of the copper-molybdenum occurrences. Lead and zinc, however, are present in minor amounts in both types of deposit and show no apparent regional variation. The association of gold and silver with pyritic syenite may be comparable to pyritic alteration zones of Cordilleran porphyry deposits that have associated veins of precious metals. More detailed work will be undertaken to investigate the relationship, if any, between the copper-molybdenum occurrences and the pyritic gold-silver deposits.

The copper-molybdenum occurrences show evidence of multiple stages of vein formation, an important characteristic of Canadian Cordillera porphyry deposits (Soregaroli, 1975). At least two stages of early veins consisting of bluish grey quartz with fine grained chalcopyrite, molybdenite and pyrite occur on the Stancop property and similar veins were recognized elsewhere in the Matachewan area. On the Ryan Lake property quartz veins that carry coarse grains and small patches of molybdenite and some chalcopyrite with pyrite may represent a third stage of early veining. The early veins at nearly all localities are cut by a later stage of veins of massive quartz with coarse calcite and patches of chlorite. Chalcopyrite and molybdenite occur in these veins as irregular masses commonly associated with coarse grained purple fluorite. Barite and tourmaline are minor and erratic constituents of these veins.

Barite also occurs in the Matachewan area in veins that trend consistently west to northwesterly. Examples of these veins include the Biederman deposit west of Browning Lake (Burrows, 1918) (Fig. 41.1, loc. 9) and the occurrence

northwest of Log Lake. They generally consist of massive barite with varying amounts of quartz gangue and minor fluorite, galena and sphalerite in places. A similar vein in Yarrow Township, south of the immediate Matachewan area, occurs in Proterozoic sedimentary rocks of the Cobalt Group (Burrows, 1918). Although the age of these veins is uncertain, they clearly postdate any mineralizing event associated with the emplacement or cooling of the syenite and represent a separate stage of barite and associated base metal mineralization.

Three main types of alteration associated with the copper-molybdenum sulphides have been recognized; silicification, chloritization and hematitization. Silicification occurs locally and pervades both syenite and metasedimentary rocks associated with intense quartz veining. Chloritization occurs as thin selvages along quartz veins. Widespread chloritization of mafic minerals in nonmineralized syenite is considered to be related to regional metamorphism and is unrelated, in general, to the copper-molybdenum mineralization. Hematitization is pervasive in the gold-bearing syenite but also occurs locally as envelopes around copper- and molybdenum-bearing quartz veins. The nature of these three and perhaps additional alteration types will be examined microscopically.

Conclusions

Copper-molybdenum occurrences in the Matachewan area exhibit many features comparable to Cordilleran porphyry deposits. These include relationship to epizonal, porphyritic intrusive rocks, distribution of copper and molybdenum sulphides in fractures and veins that show evidence of multistage development, and regional zonation of metals and alteration. However, no deposits of comparable size and grade have been found to date. Nevertheless, the number of occurrences and the widespread nature of the sulphides, particularly in the area of the Stancop and Ryan Lake properties, suggests that the hydrothermal-sulphide systems were quite large. It is hoped that the detailed studies to follow will lead to a better understanding of these systems and permit a more accurate assessment of their economic potential.

Acknowledgments

The author is grateful to R.V. Kirkham for an introduction to the Matachewan area and for discussions concerning porphyry deposits in general. Thanks are also extended to H.L. Lovel of the Ontario Geological Survey, prospectors G.S. Welsh and H. King of Matachewan and R.A. Hill of Extender Minerals of Canada Ltd. for information, services and other courtesies. Officials of Texasgulf, Inc. kindly permitted the author to study and sample diamond drill core from their property on the boundary of Cairo and Flavelle townships. R.V. Kirkham read the paper and offered helpful comments.

References

Ayres, L.D. and Findlay, D.J.
1976: Precambrian porphyry copper and molybdenum deposits in Ontario and Saskatchewan; in Report of Activities, Part B, Geological Survey of Canada, Paper 76-1B, p. 39-41.

Burrows, A.G.
1918: The Matachewan gold area; Ontario Department of Mines, v. 27, Part 1, p. 215-240.

Davies, J.F. and Luhta, L.E.
1978: An Archean "porphyry-type" disseminated copper deposit, Timmins, Ontario; Economic Geology, v. 73, p. 383-396.

Derry, D.R., Hopper, C.H., and McGowan, H.S.
1948: Matachewan Consolidated mine; in Structural Geology of Canadian Ore Deposits, Canadian Institute of Mining and Metallurgy, v. 1, (Jubilee volume), p. 638-643.

Fahrig, W.H. and Wanless, R.K.
1963: Age and significance of diabase dyke swarms of the Canadian Shield; Nature, v. 200, no. 4910, p. 934-937.

Findlay, D.J. and Ayres, L.D.
1977: Lang Lake – and early Precambrian porphyry copper-molybdenum in northwestern Ontario; in Report of Activities, Part B, Geological Survey of Canada, Paper 77-1B, p. 25-28.

Kirkham, R.V.
1972a: Porphyry deposits; in Report of Activities, Part B, Geological Survey of Canada, Paper 72-1B, p. 62–64.

1972b: Geology of copper and molybdenum deposits; in Report of Activities, Part A, Geological Survey of Canada, Paper 72-1A, p. 82-87.

Kirkham, R.V. and Thorpe, R.I.
1973: Studies of gold-copper deposits suggest red metal may be used as guide to gold; Northern Miner, 29 Nov. 1973, p. 55, 57.

Little, H.W.
1959: Tungsten deposits of Canada; Geological Survey of Canada Economic Geology Series no. 17, 251 p.

Lovell, H.L.
1967: Geology of the Matachewan area; Ontario Department of Mines, Geological Report 51, 61 p.

Moore, J.C.G.
1966: Geology of Holmes-Burt area; Ontario Department of Mines, Geological Report 44, 20 p.

North, H.H. and Allen, C.C.
1948: Young-Davidson mine; in Structural Geology of Canadian Ore Deposits, Canadian Institute of Mining and Metallurgy, v. 1, (Jubilee volume), p. 633-637.

Pyke, D.R. and Middleton, R.S.
1970: Distribution and characteristics of the sulphide ores of the Timmins area; Ontario Department of Mines, Miscellaceous Paper 41, p. 13.

Ridler, R.H.
1973: Regional metallogeny and volcanic stratigraphy of the Superior province; in Report of Activities, Part A, Geological Survey of Canada, Paper 75-1A, p. 353-358.

Soregaroli, A.E.
1975: Important characteristics of some Canadian Cordillera porphyry deposits; in Report of Activities, Part B, Geological Survey of Canada, Paper 75-1B, p. 59-62.

Vokes, F.M.
1963: Molybdenum deposits of Canada; Geological Survey of Canada, Economic Geology Report no. 20, 332 p.

Wolfe, W.J.
1972: Geochemical distribution of aqua regia soluble copper in felsic plutonic rocks, Cairo Township and parts of Alma, Holmes and Flavelle Townships, District of Timiskaming; Ontario Department of Mines, Preliminary map, p. 732.

TUNGSTEN AND BASE METAL SKARNS IN THE NORTHERN CORDILLERA

Project 740098

L.A. Dick[1]
Regional and Economic Geology Division

Dick, L.A., Tungsten and base metal skarns in the Northern Cordillera; in Current Research, Part A, Geol. Surv. Can., Paper 79-1A p. 259-266, 1979.

Abstract

Skarn deposits in southern Yukon, southwestern Mackenzie, and northern British Columbia host a variety of ore elements including tungsten, copper, zinc, lead, silver, molybdenum, and tin. A study of 33 such deposits and occurrences in 1977 and 1978 has shown that skarns in the study area may be divided into 4 main groups based on the major ore element assemblages which they contain. These are 1) W-Cu, 2) W-Mo, 3) Zn-Pb, and 4) W-Cu-Sn. Minor ore elements associated with these groups vary from deposit to deposit.

The only known economically significant skarn deposits are those of the W-Cu group. Group 2 skarns are not common and Mo is, with one exception, a minor component. Group 3 skarns are widely distributed in the region and, although they may attain significant ore grade, are usually very small in size. Little is known about the tin-bearing group 4 of skarns. These occur peripheral to tourmaline-bearing granite in southern Yukon and northern British Columbia. Most have been discovered only recently and their economic significance is yet to be ascertained.

Gangue mineral assemblages associated with the ore minerals are similar within individual skarn groups but are variable between the groups. These assemblages and the composition of minerals within the assemblages will be used to set limits on the conditions of formation of skarn deposits in the region.

Introduction

Skarn deposits in the northern Canadian Cordillera host a variety of ore elements: tungsten, copper, zinc, lead, silver, tin, and molybdenum. This study involving both field and laboratory investigations, compares some of the more important skarn-type deposits and occurrences in the region. The objective is to determine conditions of formation of the occurrences and the chemical and physical controls on ore and silicate mineralogy. To facilitate this, 33 ore-bearing skarn localities were visited in 1977 and 1978. Preliminary observations from 1977 field work have been reported previously (Dawson and Dick, 1978).

In 1978, selected occurrences were revisited for more detailed observation and geological mapping. Numerous other skarn occurrences, particularly those adjacent to Seagull and Cassiar batholiths, were visited for the first time. Figure 42.1 shows the location of deposits and occurrences studied in the field to date. Table 42.1 lists ore elements which are concentrated in these occurrences.

The deposits occur both in the Selwyn Fold Belt and in the northern Omineca Crystalline Belt. Most have been localized in relatively pure limestones, ranging in age from Upper Proterozoic to Devonian, near their contacts with Cretaceous intrusive stocks and batholiths. Compositions of the associated intrusive rocks range from alaskitic granite to granodiorite. The deposits and occurrences exhibit extreme variability in geological setting, form, and mineralogy.

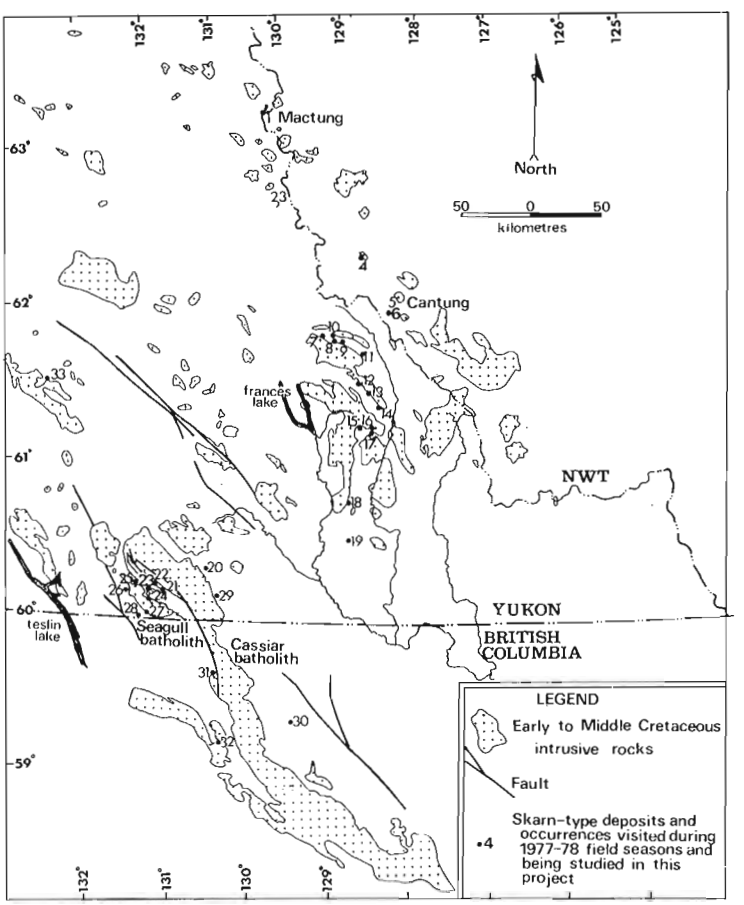


Figure 42.1. *Location of skarn deposits and occurrences being studied in this project.*

Categorization of Deposits

Skarn deposits in the study area may be categorized into groupings defined by the major ore element assemblages which they contain. However, minor elements associated with these groupings may be variable from deposit to deposit. A preliminary classification divided skarns in the study area into groupings within which the ore element assemblages W-Cu, W-Mo, and Zn-Pb predominate (Dawson and Dick, 1978). Another important group of skarns, those which contain tin-bearing minerals, were examined in 1978. These occurrences may be contrasted with those of the above

[1]Queen's University, Kingston, Ontario.

Table 42.1

Skarn deposits and occurrences visited in 1977 and 1978

Occurrence Number	Name	Ore-element assemblage
1	Mactung	W-Cu
2	Clea	W-Cu(Zn)
3	Omo	W-Cu(Zn)
4	Lened	W-Cu
5	Cantung	W-Cu(Zn)
6	Baker	W-Cu(Zn)
7	Woah	W(Mo);Zn(W)
8	Tai,Broten	W(Mo);Zn(W)
9	Tanya	W-Cu
10	Zeus	Zn(Pb,W,Cu)
11	Cali	W-Cu
12	Ron	Pb-Zn
13	Fir Tree	Zn-Pb(W,Ag)
14	Black Jack	Zn-Pb(W,Ag)
15	Max	W(Cu,Pb,Zn,Ag);Zn-Pb(W,Ag)
16	Glenna	Zn-Pb(Ag)
17	Miko	Zn-Pb(Ag);Zn(W)
18	Bailey	W-Cu
19	Hundere	Pb-Zn(Ag)
20	Mid,Nite	W(Mo);Zn(W)
21	Bar	Zn-Pb(Cu,Ag,Sn)
22	Atom	Zn(Pb,Cu,Ag,Bi)
23	Bom,Munson	Zn-Pb(Ag,Sn,Cu,W)
24	–	W-Sn(Zn)
25	–	W(Cu,Sn)
26	–	Sn-Cu;W-Sn(Zn)
27	–	Sn-Cu(Zn,W)
28	Logtung	W-Mo
29	Fiddler	W-Sn(vein)
30	Mt. Haskins	W-Mo;Pb-Zn
31	Blue Light	W(Sn)
32	Ash Mtn. area	Sn(in calc-silicates)
33	Stormy	W-Mo

groupings by virtue of their distinctive mineralogy and by the composition of the intrusive rocks with which they are associated. Exploration activity, particularly localized around the periphery of the Seagull batholith in 1977 and 1978, has shown that the area may have potential as an important tin district. Numerous tin-bearing skarns, a few of which have been visited by the writer, have been discovered in the area to date.

Two other occurrences visited in 1978, one of which is at present being actively explored, consist of scheelite and molybdenite-bearing vein stockworks which have been overprinted on calc-silicate skarn. These occurrences are briefly considered here, along with the W-Mo group of skarns.

Table 42.2 lists some of the gross characteristics of those metalliferous skarns currently being studied in the northern Cordillera. The classification is essentially that suggested in 1978 (Dawson and Dick, 1978) but includes some additional petrographic information and some preliminary observations on tin-bearing skarns.

Tungsten-copper skarns

The largest skarn deposits in the study area are those of the tungsten-copper group. The Canada Tungsten deposit (5) is the only skarn deposit in the region being actively exploited, although reserves have been proven at Mactung (1) and Bailey (18). Three other occurrences visited by the writer (2,4,6) were actively being explored in 1978.

Some of the characteristics of this group were reported by Dawson and Dick (1978). The deposits are associated with small stocks of quartz monzonite and granodiorite and are localized in limestone beds which may be interbedded with biotite and calc-silicate hornfels. The intrusions are locally intensely altered to greisen both peripheral to quartz veins which cut the intrusion as well as pervasively. Endoskarn is not observed at the contacts between intrusions and skarn. Minor tourmaline is common in quartz veins which cut the intrusion near skarn. At Clea (2) the quartz monzonite is locally heavily tourmalinized.

The extent of skarn development and ore mineralization in the limestones coincides with the limit of hornfelsic alteration of the interbedded or overlying pelitic sediments. As the plutons have generated extensive thermal aureoles, ore-bearing skarn can develop many hundreds of metres away from intrusive contacts, both in the lateral and vertical sense. The degree of skarn development and grade of mineralization are not necessarily proportional to the distance from the intrusive contact.

Blue-white fluorescing scheelite and chalcopyrite are the dominant ore minerals. Ferberite occurs at Mactung but is rare and occurs only in late quartz veins. Sphalerite is locally present in significant amounts in four deposits (2,3,5,6). Geological mapping and core logging at Cantung (5) defines a metal zoning in which garnet-pyroxene and biotite-amphibole skarn, containing scheelite, chalcopyrite and very minor sphalerite, gives way laterally to thinner skarn beds outside of the main underground workings which may contain sphalerite as a major component. The sphalerite is generally accompanied by coarse scheelite. In two samples studied petrographically, sphalerite is accompanied by pyrrhotite, abundant quartz, coarse subhedral scheelite and muscovite. Remnants of earlier formed amphibole, now largely replaced by quartz, are present locally. Other sphalerite-rich samples observed in hand specimen contain abundant epidote but this mineral is not common in the main tungsten-copper skarn.

Faint yellow-fluorescing scheelite, which indicates a minor powellite ($CaMoO_4$) component, occurs only locally in these deposits, and is restricted to sulphide deficient portions of skarn. Molybdenite has not been observed in skarn in this group of deposits although minor amounts can occur in fractures, often accompanied by scheelite, in the associated intrusion. At Clea (2) minor molybdenite can occur in diopsidic calc-hornfels which overlie the main skarn-bearing limestone unit, yet this mineral has not been deposited within the skarn itself. Conditions of formation of the major skarn deposits in the region, therefore, did not favour the deposition of both chalcopyrite and molybdenite.

Pyrrhotite is more abundant in this group of skarns than in all other groups. Pyrite is restricted to late quartz veins and faults which cut skarn. Magnetite is not observed. These are iron- and sulphur-rich deposits. In general, there is a positive correlation between increasing pyrrhotite content and increasing tungsten grade, although even in pyrrhotite-rich skarn, scheelite is extremely erratically distributed and may be absent altogether.

Petrographic evidence at Mactung (Dick, 1976) indicates that massive pyrrhotization of skarn occurred during retrograde metamorphism of early-formed calc-silicate minerals (i.e. garnet and pyroxene) and occurred late in the evolution of the skarn system. Heavily pyrrhotized skarn is generally accompanied by amphibole and/or biotite rather than garnet and pyroxene-rich silicate assemblages.

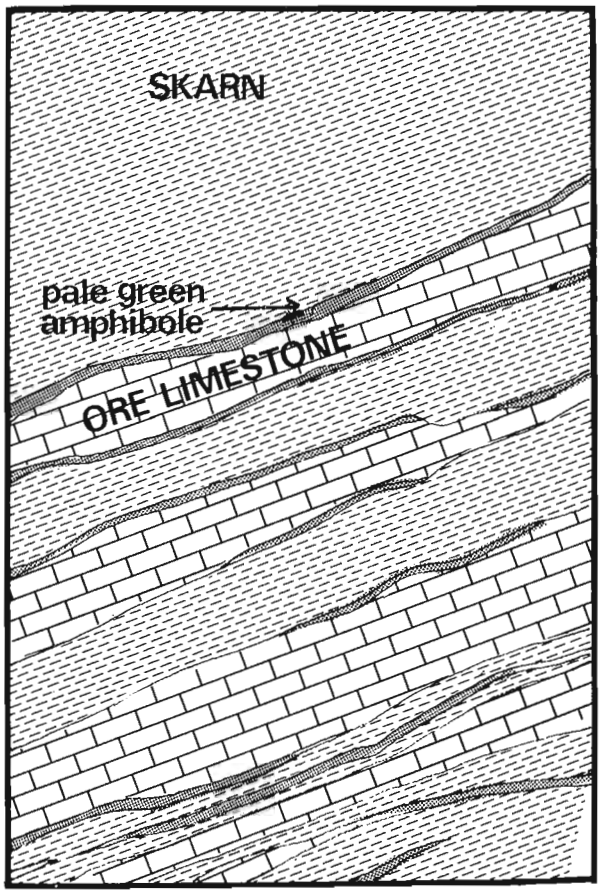


Figure 42.2. *Form of ore-bearing biotite (amphibole) skarn in the B-Zone orebody, Canada Tungsten deposit (traced from photograph).*

Calc-silicate assemblages are extremely variable in W-Cu skarns due mainly to retrograde metamorphism which has altered earlier formed assemblages. Garnet is not as abundant in this group of skarns as in the W-Mo group but garnet-rich portions can occur in all the W-Cu skarns observed. Skarn is most garnet-rich near contacts with unaltered marble. Garnet-rich skarn usually contains accessory vesuvianite, and occasionally at (1) and (5), massive pods of vesuvianite up to 20 cm in diameter are enclosed by garnet-rich skarn. Vesuvianite-rich skarn at both occurrences does not contain sulphide or scheelite. At Clea (2), vesuvianite is more widely disseminated throughout sulphide-poor portions of skarn and is associated with scheelite. Garnet-rich skarn contains negligible pyrrhotite, but at (1) and (5) contains chalcopyrite. Fluorite can occur as a minor accessory in garnet-rich portions. Pyroxene is the most abundant calc-silicate mineral present in W-Cu skarns and is always extremely hedenbergite-rich, although rare crystals at Mactung (1) exhibit extreme compositional zoning from end-member diopside cores to manganiferous, hedenbergite rims of crystals.

Garnet is often altered to clinozoisite and more rarely to anorthite, whereas pyroxene is commonly altered to ferrotremolite. Sphene is a minor but ubiquitous component of all W-Cu skarns. Quartz is erratic in distribution and skarn may vary from a quartz-free variety, to portions where pervasive late-stage silicification has occurred. Silicification is often accompanied by the introduction of coarse scheelite. Wollastonite is rare, due to the iron-rich nature of this group of skarns and has been observed only at (1), (2) and (5) as thin borders on sulphide-free garnetiferous skarn at the contact with unaltered marble.

Biotite-bearing skarn is restricted to this group (Dawson and Dick, 1978) and is an important ore host at (2), (4), and (5), less so at (1). At Cantung (5), two types of biotite skarn occur: that which is pyrrhotite-free and contains no scheelite and that which contains both pyrrhotite and scheelite. At Clea, biotite can occur interstitial to coarse garnet euhedra. This is the only deposit where garnet and biotite coexist.

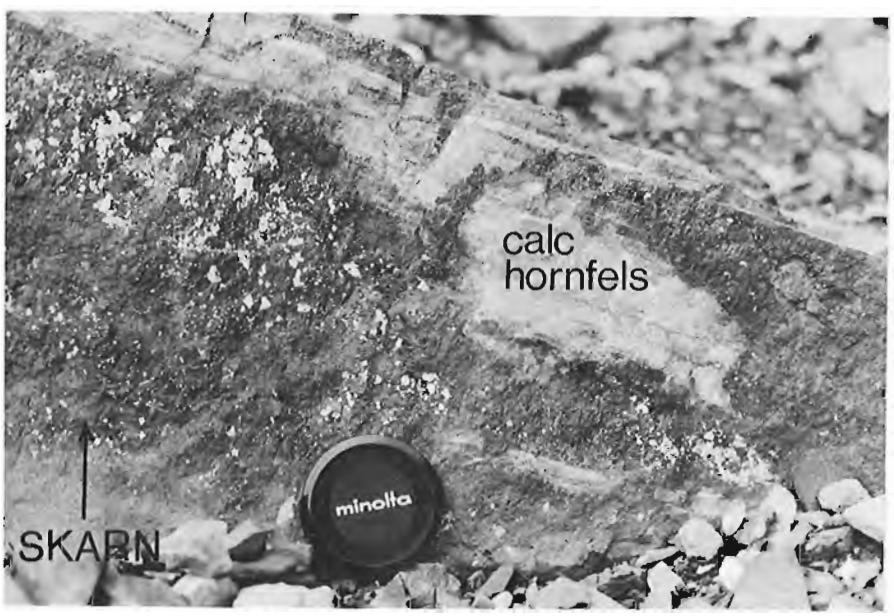


Figure 42.3. *Scheelite-bearing, black amphibole and tourmaline skarn replacing fine grained calc-silicate hornfels at the Clea deposit (2).*

Ore-bearing skarn can exhibit extreme conformability to bedding in the host limestones. The morphology of skarn is best illustrated in the underground 'E Zone' orebody at Cantung (5). Here, skarn 'beds' which vary in thickness from a few metres to less than one centimetre, have commonly generated coarse grained, light green amphibole 'selvages' at their contacts with marble (Fig. 42.2). This morphology suggests that mineralizing fluids travelled preferentially along bedding planes and were less efficient in replacing limestone across bedding. Commonly, scheelite exhibits anomalous concentrations along the borders of these beds.

Mineralization in this group of deposits is not restricted to skarn formed from limestone. At Cantung (5), biotite hornfels has been altered to diopside-bearing calc-hornfels near contacts with skarn and may host lower grade tungsten

Table 42.2

	Major Ore Assemblage	Minor Elements	Host Rocks	Host Rock Age	Intrusive Rock	Mineralization in Intrusive
1.	W-Cu	Zn	shallow dipping, relatively pure, coarsely crystalline limestone interbedded with biotite and calc-silicate hornfels	Lower Cambrian, Cambrian (1,4,5,6) Devonian (2,3,18)	variable; equigranular to highly porphyritic quartz monzonite and granodiorite stocks	minor molybdenite and scheelit in quartz veins (1,4,5)
	Comments: Large, pyrrhotite-rich skarn bodies, grossly stratiform in morphology. Exhibit extreme heterogeneity in mineral assemblages and ore grade within individual bodies. Biotite-bearing skarn important in this group.					
2.	W-Mo (a) skarn	none	massive, coarsely crystalline limestone (33,7,8) Interbedded limestone/biotite schist (20)	Upper Proterozoic (7,8,20) Lower Cambrian (33)	Even textured granodiorite (7,8,20) Porphyritic quartz monzonite (33)	Rosettes of coarse molybdenite minor scheelite (33) None observed at (7), (8), (20)
	Comments: Low sulphur skarn bodies which lack iron sulphides. Skarns are garnet and plagioclase rich. Silicate assemblage more homogeneous throughout skarn than W-Cu group. Molybdenite is a very minor component and is generally restricted to quartz veinlets (20), quartz-magnetite-actinolite veins (7,8) but can be heavily disseminated (33).					
	(b) vein stockwork overprint on skarn	peripheral Pb/Zn skarn (30) peripheral Zn skarn (28)	light/dark green skarn, calc-hornfels	Lower Cambrian (28)	diorite, porphyritic quartz monzonite, quartz porphyry (28) granite porphyry (30)	molybdenite and minor scheelit locally at both localities
	Comments: W-Mo mainly restricted to quartz-molybdenite-scheelite veinlets which overprint fine grained, iron and sulphur-poor skarn. Additional vein mineralogy at (30) include pyroxene-anorthite-fluorite-amphibole-calcite. Pyrite occurs in veinlets at (28). Veinlets at both localities may develop dark green amphibole selvages.					
3.	Zn-Pb; Zn	Pb,Cu,W,Ag	Usually thin limestone units interbedded with biotite schist. Generally in metamorphic terrane.	variable from Upper Proterozoic to Devonian	Extremely variable. Skarn localized adjacent to leucogranite boudins and sills adjacent to quartz monzonite and granodiorite batholiths at (12), (13), (14), (15), (7), (8), (10). Adjacent to granodiorite at (15), (16). None exposed at (19). Occurrences (21), (22), (23) near exposure of Seagull granite.	none observed
	Comments: Zn(Pb) skarns tend to be small yet may attain significant ore grade. In general, galena-bearing sphalerite skarns, or portions of skarns, do not contain scheelite. Amphibole, epidote, calcite, and chlorite more common than in other groups.					
4.	Sn-Cu-W	Zn,As	massive limestone to thinly laminated siliceous limestone, interbedded with biotite hornfels, calc-silicate hornfels, and quartzite	Devono-Miss.	leucocratic, tourmaline and fluorite-bearing alaskitic granite, occasional pegmatite dykes	not observed
	Comments: Boron, fluorine, chlorine, and beryllium-rich skarns. Mineralogy of skarns extremely heterogeneous. Tin not necessarily the most abundant ore element present.					

mineralization (the "chert ore" at Cantung). Similar calc-silicate hornfels at Mactung (1) is locally penetrated by hedenbergite-bearing veinlets which carry minor pyrrhotite and scheelite. At Clea, calc-silicate hornfels overlying the main skarn-bearing limestone unit is locally altered adjacent to fractures, or more pervasively to dark, tourmaline and amphibole-bearing skarn which is scheelite-bearing (Fig. 42.3).

W-Mo skarns

Molybdenite-bearing skarns are not an important type in the northern Cordillera, and with a few notable exceptions, molybdenite is not a common constituent of skarn deposits studied in the region. Molybdenite-bearing skarn does not contain chalcopyrite in the deposits studied and all are low in total sulphide content, in contrast to the W-Cu group. Scheelite coexisting with the molybdenite is generally faint yellow-fluorescent, indicating a minor powellite component. W-Mo skarns have been observed in three regions: (1) a series of skarn xenoliths (localities 7 and 8) nested in granodiorite in a broad region along the north flank of the Mount Billings batholith; (2) the Stormy Mountain deposit (33); (3) the Mid-Nite occurrence adjacent to granodiorite rocks of the Cassiar batholith. In southernmost Yukon and northern British Columbia, calc-silicate skarn adjacent to quartz-porphyritic intrusions have been overprinted by Mo-W-bearing vein stockworks.

In the first area, extremely garnet-rich xenoliths are nested in granodiorite near its contact with upper Proterozoic metapelites. A single limestone unit can be traced from the

Table 42.2 (cont'd.)

Alteration of Intrusive	Skarn Minerals major	minor	Ore Minerals	Form
greisen (sericite + quartz) is general	garnet (grossular-andradite-almandine) hedenbergite ferro-tremolite, biotite pyrrhotite, quartz	clinozoisite anorthite wollastonite vesuvianite sphene, fluorite, pyrite, calcite	scheelite, chalcopyrite sphalerite (2,3,5,6) ferberite (Mactung only)	Broadly stratiform. Skarn tends to follow bedding planes in host. Skarn may also replace interbedded or overlying calc-hornfels
Intense greisen at (33). Minor pyroxene + epidote endoskarn (7)	garnet (grossular-andradite) hedenbergite, anorthite quartz	actinolite (7,8, 33), magnetite (7,8), wollastonite (7,8,20)	scheelite, molybdenite	Xenoliths in granodiorite batholith (7,8). Broadly stratiform (20,33)
quartz porphyry locally greisen altered with minor pyrite at both localities	wollastonite (28) vesuvianite (28) garnet (28), pyroxene (28,30), quartz (28, 30), actinolite (28, 30)(vein), pyrite (28) (vein), fluorite (28, 30) (vein)		molybdenite, scheelite	vein stockwork overprinting skarn
none observed	pyroxenes (both diopside and hedenbergite can coexist) epidote, amphibole (actinolite, hastingsite), calcite	garnet magnetite pyrite chlorite pyrrhotite pyrite allanite smithsonite	sphalerite, galena, scheelite vein, chalcopyrite	semiconformable
Tourmalinization. Local greisen near skarn	axinite, beryl tourmaline, fluorite, vesuvianite, wollastonite, garnet (green, black, and red. May be tin-bearing) pyroxene (composition variable from diopside to hedenbergite), epidote, allanite, quartz, magnetite, pyrrhotite		malayaite, stannite chalcopyrite, sphalerite, scheelite, tetrahedrite? arsenopyrite	variable: from broadly stratiform replacement bodies to irregular pods, lenses, and veins

country rock into the batholith where the skarn xenoliths occur. Although pelitic rock has been largely assimilated by the intrusion, the limestone remained as a more or less refractory unit. The attitude of the resulting skarn xenoliths is, in most cases, the same as that of their protolith in the country rocks and indicates that the limestone has not been transported from its original attitude during intrusion of the batholith. Figure 42.4 shows the form of one of the many skarn xenoliths which occur in this belt (see also Fig. 55.2, Dawson and Dick, 1978). It is interesting to note that while approximately 10 km separate the two major concentrations of W-Mo skarn xenoliths in this belt, their mineralogy, late alteration, and form are identical. These were the most garnet-rich skarns. Extremely coarse euhedra of grossular-andradite-spessartine garnet coexist with anorthite, hedenbergite and quartz. Local accessories are wollastonite and epidote. Well-developed endoskarn, extending a metre or so into granodiorite from the skarn contact is locally well developed at locality (7). Late quartz veins cut the xenoliths and contain scheelite, molybdenite, two amphiboles (actinolite and ferrohastingsite) and magnetite. More pervasive alteration to black amphibole-bearing skarn also occurs.

At location (33), the Stormy Mountain deposit, rosettes of coarse grained molybdenite occur disseminated in skarn as well as in the roof of the immediately underlying, highly greisen-altered porphyritic quartz monzonite. Yellow-fluorescing scheelite is abundant, although it was noted that those portions of skarn richest in molybdenite contained the least scheelite and vice versa. Silicate minerals associated



Figure 42.4. *One of a series of garnet-rich scheelite (molybdenite)-bearing skarn xenoliths which occur in granodiorite at locality (7).*

with the mineralization here are garnet, plagioclase, calcite, quartz, compositionally-zoned pyroxene, and sphene. As at localities (7) and (8), plagioclase is an important component of skarn, and is an alteration product of garnet.

At location (20), very minor molybdenite occurs in garnet, pyroxene, plagioclase, and wollastonite-bearing skarn. Garnet can constitute up to 90 per cent of the skarn assemblage and iron sulphides are absent. Scheelite occurs as an interstitial filling between garnet euhedra.

Fine grained diopside-garnet-wollastonite-brown vesuvianite skarn at locality (28) has developed adjacent to stocks of diorite, porphyritic quartz monzonite, and mafic-free quartz porphyry. The iron-poor skarn assemblage has been shattered by myriads of quartz, yellow-fluorescent scheelite, and molybdenite-bearing veinlets, occasionally with well developed actinolite-bearing selvages. Similar stockwork-type W-Mo mineralization was observed by the writer adjacent to a small quartz-porphyry stock or sill on the south flank of Mount Haskins (30) where previous exploratory work has been centred on delimiting Zn-Pb skarns which occur peripheral to the tungsten-molybdenum mineralization, and also on molybdenum mineralization within the porphyry. As at locality (28), very fine grained, light green diopside, plagioclase, quartz calc-silicate rock has been shattered by veinlets which contain quartz, fluorite, pyroxene, anorthite, and scheelite. The veinlets occasionally contain minor molybdenite (Fig. 42.5). The veinlets have generated dark green, actinolite-rich selvages. Scheelite and molybdenite also occur in greisened zones within the quartz porphyry which has been dated by K/Ar means as 49.8 ± 0.7 Ma (Christopher et al., 1972).

Zn-Pb skarns

Skarns in which sphalerite is the dominant ore mineral are widely distributed in the northern Cordillera. They tend to be small in size, yet may attain significant grade. None are being exploited commercially. Sphalerite, in addition to being the major component in this group of skarns, may occur as a minor component in W-Cu and tin-bearing skarns, and extremely sphalerite-rich zones may be present within these skarn groups. Sphalerite has not been observed as disseminations in molybdenite-bearing skarns although a sphalerite-bearing vein cuts W-Mo skarn at locality (20), and sphalerite-bearing skarn occurs nearby. At localities (7) and (8), sphalerite-rich skarn is generated at the contact of intrusive granodiorite and country-rock limestone, whereas xenoliths of W-Mo skarn within the batholith are sphalerite-free (Fig. 55.2, Dawson and Dick, 1978).

Although blue-white fluorescing scheelite may be a minor accessory in sphalerite-rich skarns (8, 10, 13, 14, 15, 17, 20, 23) and sphalerite may be a minor component in scheelite-rich skarns (2, 3, 5, 6, 15, 24, 26), galena-bearing skarns, or portions of skarns, with one notable exception (15), do not contain scheelite.

Most skarns of the zinc-lead group contain primary epidote rather than garnet as the aluminum-bearing calc-silicate mineral. Where garnet does occur (16, 19, 20, 22), coarse grained epidote is also present. Actinolite is common, either as alteration rims on pyroxene, or as coarse grained euhedra. In four localities (15, 7, 8, 17) two pyroxenes coexist as intergrowths; diopside and manganiferous hedenbergite. Coexisting pyroxenes have yet to be observed in other skarn groups. Manganiferous calcite, smithsonite, and sphene are common accessory minerals. Sphalerite grains are generally extremely isotropic in thin section, indicating they are iron-rich, although it is common for them to exhibit compositional zoning, with iron content increasing from the core to the rim of the crystal (e.g. 16, 26).

At localities (7) and (8), sphalerite coexists with pyroxene, epidote, actinolite, calcite and quartz. This assemblage contrasts with the garnet, pyroxene, and plagioclase assemblage which coexists with the W-Mo mineralization at the same locality.

Thin, stratiform, calc-silicate-bearing beds interbedded with biotite schist contain sphalerite and minor galena over a broad region stretching from locality (12) to (14). Here, sphalerite and galena coexist with a foliated assemblage of calcite, chlorite, epidote, and occasionally plagioclase.

Zn-Pb skarns can occur: (a) at the intrusive contact; (b) where intrusive rocks are not exposed at surface (e.g. 19), or (c) may be localized adjacent to conformable granitic boudins, in regional metamorphic terrane, as at occurrence (15).

Tin-bearing skarns

This group of skarns is restricted geographically in southern Yukon to the periphery of the Seagull batholith. Host rocks are Devono-Mississippian limestone units which are interbedded with pelitic and quartzitic sediments. Skarns occur at or near the contact of the Seagull batholith, a tourmalinized, alaskitic granite. This batholith is distinguished from other intrusive rocks associated with skarn in Yukon by its leucocratic nature and by the abundance of tourmaline within it. Tourmaline can occur: (a) as miarolitic



Figure 42.5. *Stockwork of quartz-fluorite-pyroxene-anorthite and scheelite-bearing veinlets cutting calc-silicate hornfels at locality (30).*



Figure 42.6. *Pseudo-hexagonal concentration of tourmaline dissected by tourmalinized fracture in Seagull batholith near locality (24).*

cavity fillings; (b) more commonly as ovoid to hexagonal-shaped concentrations which appear to replace the original granitic groundmass or; (c) as fillings and selvages on closely spaced subparallel, vertical fracture sets which are common near the roof of the intrusion. Figure 42.6 shows a typical, pseudo-hexagonal shaped concentration of tourmaline disected by a tourmaline-filled fracture at occurrence (24). Seagull granites are highly jointed, and fluorite is an important accessory mineral. Lepidolite-bearing pegmatite dykes have been observed within the batholith.

Tin-bearing skarn also occurs in northern British Columbia near Ash Mountain (30) (Mulligan and Jambor, 1967). Similar tourmalinized granite and lepidolite dykes were observed in this area.

Tin as malayaite ($CaSnTiO_5$), a tin-bearing isomorph of sphene, occurs at (24, 26, and 27), and has been observed at other localities peripheral to the Seagull batholith. The malayaite is very fine grained, commonly forms radiating clusters, and where observed in thin section (loc. 24 and 26), appears to have been introduced into skarn after initial calc-silicate formation, generally in thin quartz veinlets which cut across andraditic garnet, wollastonite, vesuvianite, and pyroxene. The pyroxene, as in all other skarn groupings, can exhibit pronounced compositional zoning from diopsidic cores to hedenbergite rims. Intergrown chalcopyrite and stannite can coexist in the quartz veinlets with the malayaite. Cassiterite has not been observed to coexist with malayaite in the few samples studied petrographically.

At (26) malayaite occurs in skarn composed of green andradite, hedenbergite, epidote, wollastonite, calcite, and quartz. The malayaite-bearing skarn is in sharp, more or less conformable contact with skarn which contains scheelite, sphalerite, arsenopyrite, and chalcopyrite. Accompanying minerals in the latter include beryl, tourmaline, actinolite, fluorite, vesuvianite, axinite, garnet, pyroxene, calcite and quartz. Scheelite and sphalerite-bearing zones do not appear to contain malayaite.

Tin, as a component of silicate minerals (garnet, epidote, ferroactinolite) was first noted in the northern Cordillera, in the Ash Mountain area (32), by Mulligan and Jambor (1967), who report andradite garnet containing up to 0.9 per cent SnO_2. They noted that no normal tin minerals occur with the tin-bearing silicate minerals. Tin occurs as a constituent of bright green andradite garnet near locality (25) (this study). The characteristic emission peak for tin was observed on the visual spectra of the microprobe, although precise concentrations have yet to be determined. Individual crystals of the andradite contain sector zones of colourless, more grossular-rich garnet which are intergrown with the andradite, and which contain no tin. The garnet coexists with diopside and calcite.

At locality (23), stannite and a stanniferous ludwigite-type borate mineral were identified by Gower (1952).

Tin is not restricted to skarn deposits in the region. At locality (26), cassiterite occurs in sericitized selvages on quartz-wolframite-fluorite veins which cut limy phyllites, and

near locality (22) quartz-cassiterite-fluorite veins cut biotite hornfels near an outcrop of greisened-altered Seagull granite.

In addition to the presence of tin, some features which distinguish the skarns occurring peripheral to the Seagull batholith and in the Ash Mountain area, from the skarn deposits studied in other parts of the northern Cordillera are:

(a) they may contain abundant axinite, fluorite, beryl and tourmaline;

(b) garnet may vary in colour from red to green, black or yellow. Garnets from all other skarns which have been studied are red in colour;

(c) vesuvianite and wollastonite are more common in these skarns than in all other groups.

(d) arsenopyrite and magnetite are common accessory minerals.

(e) some calc-silicate minerals show an anomalous concentration of chlorine. For example, black amphibole (chlorian potassian hastingsite) from locality (22) can contain up to 3.1% chlorine (Dick and Robinson, in press). Vesuvianite from malayaite-bearing skarn at locality (25) can contain up to 0.6% chlorine.

The mineralogy of skarns associated with the Seagull batholith indicates that the hydrothermal fluids generated during the cooling of the batholith were enriched in boron, chlorine, fluorine and beryllium. Minerals containing these elements are rare to absent in skarns generated by quartz monzonite and granodiorite stocks and batholiths in the study area.

Acknowledgments

The author acknowledges the support of the Geological Survey and in particular that of K.M. Dawson. Field work has relied on the co-operation of many mining companies actively involved in the exploration of skarn deposits in the region. The author is grateful for this support.

References

Christopher, P.A., White, W.H., and Harakal, J.E.
1972: Age of molybdenum and tungsten mineralization in northern British Columbia; Canadian Journal of Earth Sciences, v. 9, p. 1727-1734.

Dawson, K.M. and Dick, L.A.
1978: Tungsten and base metal-bearing skarns in southeastern Yukon and southwestern Mackenzie; in Current Research, Part A, Geological Survey of Canada, Paper 78-1A, p. 287-292.

Dick, L.A.
1976: Metamorphism and metasomatism at the MacMillan Pass tungsten deposit, Yukon and District of Mackenzie, Canada; unpublished M.Sc. thesis, Queen's University.

Dick, L.A. and Robinson, G.W.
Chlorian potassian hastingsite from a sphalerite skarn in southern Yukon: Canadian Mineralogist. (in press)

Gower, J.A.
1952: The Seagull Creek batholith and its metamorphic aureole; unpublished M.Sc. thesis, University of British Columbia.

Mulligan, R. and Jambor, J.L.
1967: Tin-bearing silicates from skarn in the Cassiar district, northern British Columbia; Canadian Mineralogist, v. 9, p. 358-370.

Mulligan, R.
1975: Geology of Canadian tin occurrences; Geological Survey of Canada, Economic Geology Report 28, 155 p.

43.

THE METAMORPHIC AUREOLE OF THE POKIOK-SKIFF LAKE GRANITE, SOUTHERN NEW BRUNSWICK

E.M.R. Research Agreement 2239-4-97/78

N. Rast[1] and G.G. Lutes[1]
Regional and Economic Geology Division

Rast, N. and Lutes, G.G., The metamorphic aureole of the Pokiok-Skiff Lake Granite, southern New Brunswick; in Current Research, Part A, Geol. Surv. Can., Paper 79-1A, p. 267-271, 1979.

Abstract

The southwestern part of Pokiok batholith can be divided into the north-south trending Hawkshaw adamellite and the (probably older) east-west trending Skiff Lake pluton. The metamorphic aureole of the plutons, which involves polydeformed Cambrian(?) to Silurian metasedimentary rocks, narrows from north to south suggesting a shallower depth of emplacement to the south. On the basis of pelitic assemblages, the wide part of the aureole can be divided into biotite, andalusite-cordierite, and sillimanite zones. Consideration of the metamorphic assemblages suggests maximum P-T conditions of about 550 C and 2-3 kb. Detailed textural examination indicates that contact metamorphism commenced with dehydration and formation of biotite and muscovite, followed by widespread formation of andalusite and cordierite. Later hydration led to widespread crystallization of muscovite and biotite within the sillimanite zone, and retrogression elsewhere. Growth of sillimanite (fibrolite) appears to be penecontemporaneous with, or slightly later than, hydration.

Introduction

The work described in this report is the continuation of the preliminary report by Rast (1977). The emphasis is on petrological investigations, but we also indicate the present status of stratigraphy, utilizing additional information from two maps by Venugopal (1977, 1978) of adjacent areas. Detailed mapping by Lutes has defined the positions of major faults indicated in Figure 43.1. Both Venugopal and Lutes have drawn isograds on the thermal aureole of the granite bodies. The aureole exhibits varied mineral assemblages, conditioned both by lithological variations and pressure-temperature environment. In addition, there is evidence for multistage development of minerals, permitting the reconstruction of the evolution of the metamorphic rocks. On the basis of these data we suggest P-T conditions during the processes of plutonic intrusion.

Stratigraphy-Lithology

The distribution of lithologic types is indicated in Figure 43.1. The stratigraphic succession proposed by Rast (1977) has been largely confirmed by Venugopal (1977, 1978), who has proposed informal stratigraphic names for the units (Table 43.1). The succession involves two main stratigraphic groupings assigned to the Siluro-Devonian and to the Cambro-Ordovician. Rast (1977) proposed that dark, reddish manganiferous slate with rare calcareous conglomerate and layers of greywacke are Llandovery in age, by analogy with the nearby ground described by Hamilton-Smith (1972). Venugopal (1977, 1978) and Lutes include these rocks in the Cambro-Ordovician sequence. There is no absolutely clear-cut evidence for either suggestion at present.

The metaquartzite and pelite sequence at the bottom of the stratigraphic succession is lithologically very similar to the Grand Pitch Formation in Maine (Neuman, 1967) which is unconformably overlain by Arenig deposits of the Shin Pond Formation. The volcanics-dark slate sequence may correlate with the Shin Pond Formation, but no field evidence of an unconformity between these rocks and the underlying metaquartzite and pelite has been discovered, despite an intensive search.

Although there has been an advance in tracing the main folds and faults around the Pokiok granite (Fig. 43.1), the general scheme is the same as that proposed by Rast (1977).

Table 43.1

Correlation

AGE		RAST (1977)	VENUGOPAL (1977)
CARBONIFEROUS		RED SANDSTONES	
		unconformity	
SILURO-DEVONIAN		CALCAREOUS PHYLLITES META BASALT CONGLOMERATE	HARTIN Fm. DORRINGTON HILL Fm. SCOTT SIDING SLATE POCOWOGAMIS Ggl.
			unconformity
SILURIAN	Llandovery	DARK AND REDDISH MANGANESE SLATES	BELLE LAKE SLATE POCOMOONSHINE VOLCS. (incl. Mang. Slate)
		unconformity	
ORDOVICIAN		DARK SLATES VOLCANICS	UNNAMED SLATE
CAMBRO-ORDOVICIAN		METAQUARTZITES AND PELITES	META QUARTZITE-SLATE

Three main episodes of deformation have been recognized. The first produces widespread interpenetrative cleavage (S_1) and associated mineral lineation in Cambro-Ordovician rocks. In parts of the sequence the first cleavage is subparallel to sedimentary layering. Very tight refolded folds of variable axial direction can be seen at some localities. The second deformation produced steep kink-like folds on both minor and fairly major scales (Fig. 43.2). Structures of this type (F_2) are found only in the Cambro-Ordovician sequence, and are entirely pre-Silurian. The general steep orientation of the F_2 fold axes suggests that the effect of the first deformation (F_1) was to throw the succession into a generally steep sequence of broad isoclinal folds indicated by reversals of facing (Fig. 43.2). We suggest that the (F_1) and (F_2) folds reflect the Taconian orogeny.

A third episode of minor folding (F_3) is associated with pervasive cleavage (S_3) often of crenulation type. This cleavage in the Ordovician rocks is coaxial with the main S_1 cleavage in the Silurian rocks. This cleavage, which transects older (F_2) folds, is the most commonly observed structure in the ground and is attributed to Acadian orogeny. To distinguish this cleavage from the earlier Taconian structure

[1] Department of Geology, University of New Brunswick, Fredericton, New Brunswick.

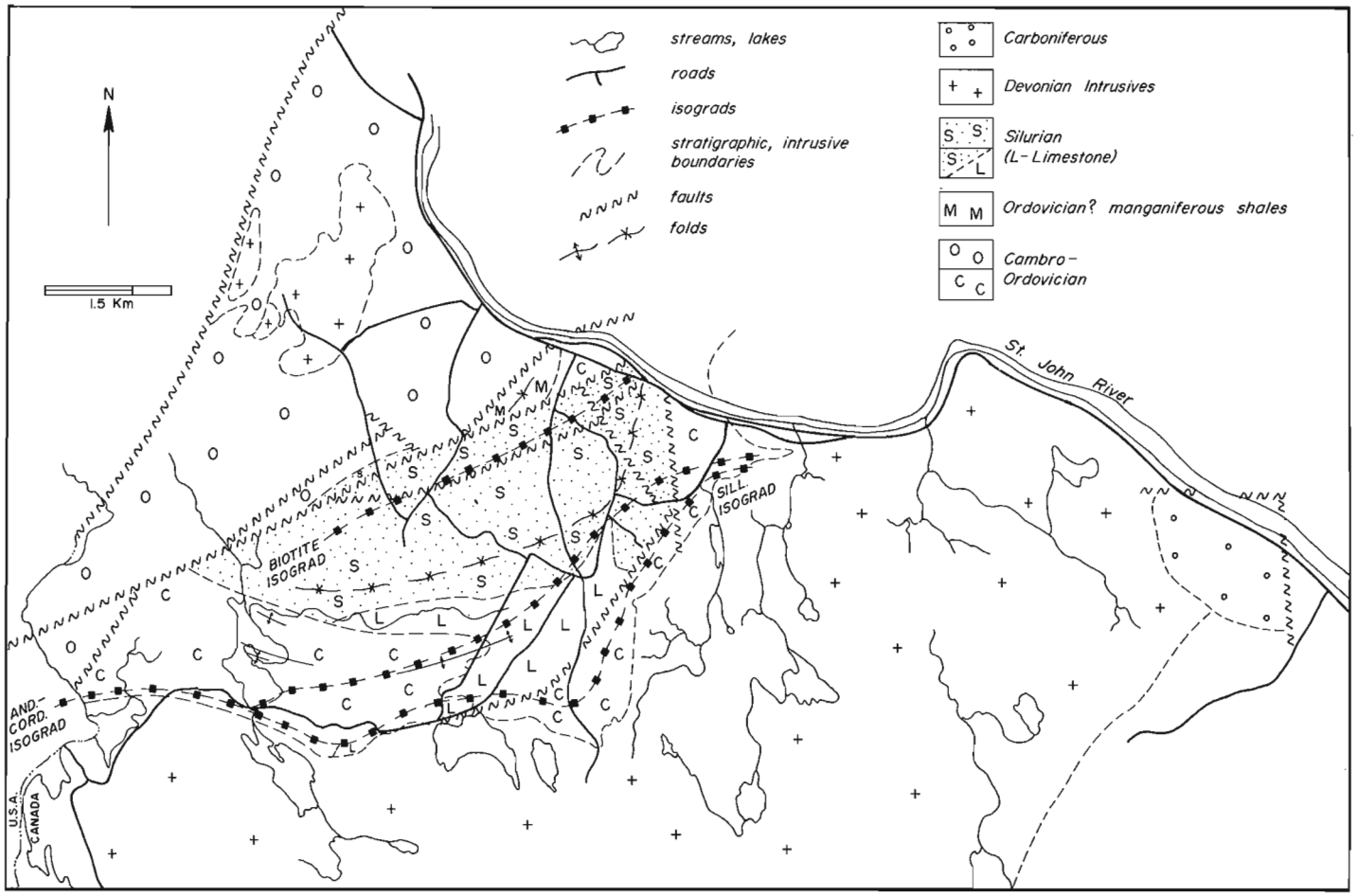


Figure 43.1. *Structural and metamorphic geology of the Skiff Lake aureole.*

we resymbolize them as S_1^1 for the Taconian and S_1^2 for the Acadian, where the superscripts 1 and 2 refer to the Taconian and Acadian respectively. The Taconian F_2 folding also generated a crenulation cleavage within the kinks, and this cleavage we refer to as S_2^1.

The plutonic body is posttectonic, but several phases of intrusion can be recognized. Magnetic intensity data and satellite photos demonstrate that the Skiff Lake intrusion is separate from the Hawkshaw intrusion (Fig. 43.3).

Metamorphism

To the west of the Pokiok batholith the biotite isograd of the thermal aureole can be located some 10 km west of the margin of the granite (Fig. 43.1). This broad thermal aureole is superimposed on a weak regional metamorphism. We have observed no regional assemblages of higher grade than lower greenschist facies.

Within the thermal aureole the following isograds have been approximately located: a) biotite, b) andalusite-cordierite, c) sillimanite. The tracing of these isograds through calcareous phyllite and carbonate (Hartin Formation of Venugopal, in part) presents considerable difficulties. Impure calcareous rocks of biotite grade commonly exhibit the assemblage actinolite-epidote (±quartz ±calcite ±phlogopite). Rocks belonging to the andalusite-cordierite zone contain grossularite-cummingtonite-hornblende-idocrase (±quartz ±biotite ±plagioclase ±calcite). All the calc-silicate rocks contain ore minerals, with pyrite and pyrrhotite predominating in lower grades, and hematite appearing in higher grades.

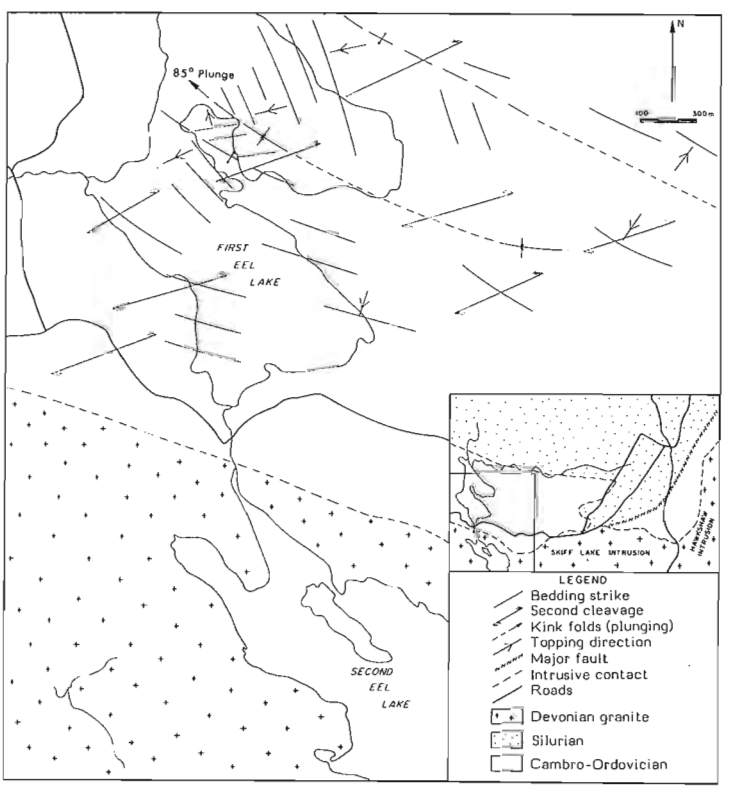


Figure 43.2. *Details of structure in Eel Lakes area.*

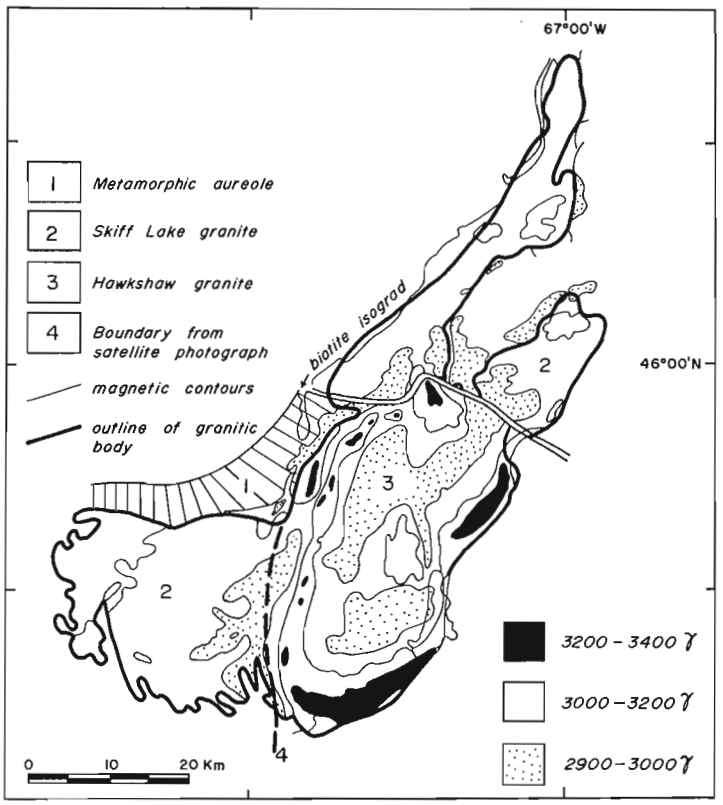


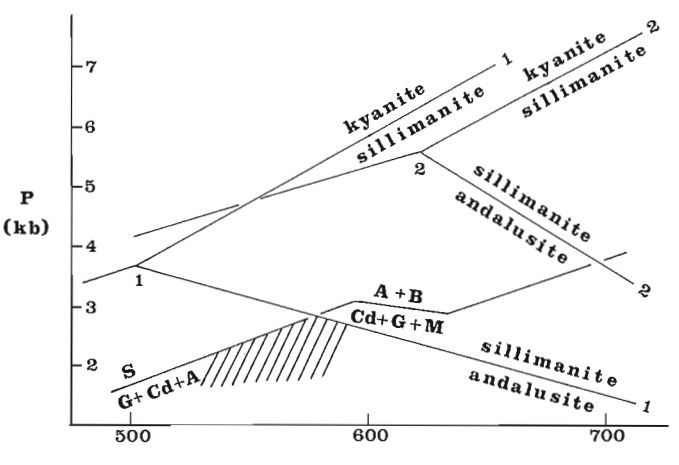
Figure 43.3. *The magnetic features of the Pokiok Multiple Pluton (after McGrath, 1970).*

The width of the metamorphic aureole, measured from granite to biotite isograd, narrows from northeast to southwest. Similar variation is observed around the northern margin of the batholith (Anderson and Poole, 1959). We interpret these variations to result from variations in the dip of the contact between the batholith and its surrounding country rocks. This interpretation is supported by geophysical data. The open file map of the gravity field of New Brunswick (Earth Physics Branch 1977) shows a steeper gravity gradient east of the batholith where the metamorphic aureole is narrower than west of the pluton. From gravity data K.B.S. Burke (pers. comm., 1977) calculated that the contact in the region of Canterbury dipped at an angle of 45°. Garland (1953) suggested 60° as an average for the western contact. The narrowing of the aureole west of Canterbury coincides with a steeper gravity gradient, and therefore with a steeper inclination of the contact.

Small crystals of euhedral garnet of almandine type occur rarely within pelite of the andalusite-cordierite zone, but too few localities have been found that reliably indicate the position of the garnet isograd. The appearance of this mineral may suggest relatively high pressure conditions, and therefore indicates that the pluton, in part at least, was intruded at considerable depth. The presence of andalusite and the absence of kyanite from the aureole indicate that the pressure never exceeded that of the aluminosilicate triple point, 3.5 kb according to Holdaway (1971) corresponding to a maximum depth of 11 km. Garland (1953) suggested from geophysical data that the present thickness of the cover was about 6 km west of the pluton. The depth of emplacement of the pluton is difficult to determine, particularly in the absence of analyses for the metamorphic minerals. Hess (1969) has suggested that garnet-cordierite-biotite assemblages are stable in the interval 1.5-4.5 kb. The garnet-cordierite geothermometer of Currie (1971, 1974) does not permit the coexistence of garnet, cordierite, and andalusite at pressures of lower than 3.5 kb except at temperatures lower than 500°C, and hence is incompatible with the aluminosilicate phase diagram of Holdaway (1971). If the aluminosilicate phase diagram of Richardson et al. (1969) is used together with the geothermometer of Currie (1971, 1974) and assumed compositions for the phases, pressures in the order of 3.5-5.5 kb are deduced for coexisting andalusite, garnet, and cordierite. This implies an original cover for the pluton of at least 15 km, which is considered to be unrealistically thick. However in thin sections containing coexisting garnet, cordierite, and andalusite, the last is not idiomorphic, and may be metastable. At present we consider the best estimate of P-T conditions to be given by the intersection of the curve of Hess (1969) for the assemblage cordierite-garnet-andalusite-biotite with the sillimanite-andalusite boundary of Holdaway (1971). This intersection lies at about 500-550°C and 2-3 kb (Fig. 43.4) that is depths of 5-7 km. Similar conclusions are reached by using the framework of Hutcheon et al. (1974, Fig. 2) but substituting Holdaway's for Richardson's data.

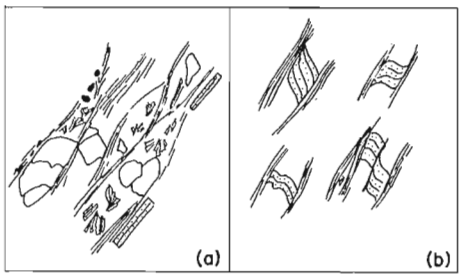
Metamorphic History

The metamorphic history of the aureole can be partially deciphered on the basis of interaction of tectonic movements and mineral growth. The regional metamorphic fabric can best be observed in greywacke outside the biotite isograd. Although two cleavages are commonly present in pelitic parts of the rock, the more psammitic parts do not show interpenetrative deformation. Cambro-Ordovician quartzose sediments contain angular fragments of quartz still showing original sedimentary outlines, although the grains commonly show no strain shadows, and therefore are completely recrystallized. In cleaved parts of the rock re-entrant angles between adjacent grains and planar outlines against cleavage planes (Fig. 43.5a) indicate pressure solution. The two cleavages are not entirely interpenetrative, and the planes exhibit concentrations of hydrated iron oxides. Crack-filling patches of recrystallized quartz grains, locally with serrated margins, indicate that complete equilibrium was never reached. Where detrital mica lies at a high angle to rock cleavage, the mineral cleavage is sigmoid.



A - andalusite *G - garnet*
B - biotite *M - muscovite*
Cd - cordierite *S - staurolite*

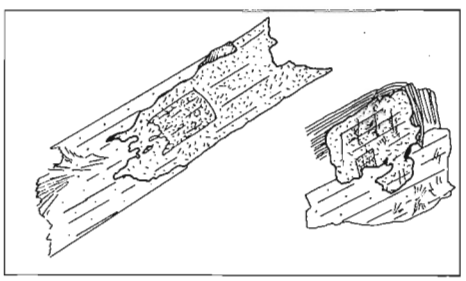
Figure 43.4. *Pt conditions of metamorphism. The alumina silicate triple point 1) after Holdaway (1971), 2) after Richardson et al. (1971). Equilibrium curves after Hess (1969). Shaded area is that in which metamorphism of the Pokiok Pluton has occurred.*



(a) two cleavages with concentrated biotite (closely lined) and one (black) with rosettes of thermal biotite in the matrix; grains of quartz unornamented, muscovite flakes with cleavage and dots. x250

(b) Sigmoids of clastic muscovite deformed between cleavage planes lined by biotite. x 250

Figure 43.5. *Details of regional fabric.*



Andalusite - closely stippled with minor pleochroic cores;
Biotite - closely lined; muscovite flakes with cleavage and open stipple; sheafs of fibrolite in muscovite.

Figure 43.6. *Replacement of andalusite by muscovite and (?) biotite.*

Biotite grade metamorphic rocks exhibit fine biotite lying along cleavage planes and forming decussate halos around quartz grains. Biotite crystals are not bent, and have clearly crystallized after formation of cleavage. Biotite commonly displays partial retrogression to chlorite. Some fairly large grains of muscovite appear to be detrital, but intergrown muscovite and biotite is clearly of metamorphic origin. Diaphthoresis of biotite to chlorite commonly occurs along quartz veins which are completely recrystallized, so that coarse grains only rarely show serrated grain boundaries.

In the andalusite-cordierite zone four stages of progressive mineral growth can be recognized, followed by a stage of retrogressive metamorphism. The oldest stage appears as thermal biotite in a decussate arrangment of stumpy prisms, now preserved in andalusite which grew subsequent to the thermal biotite. Cordierite almost invariably displays a poikiloblastic habit with the fabric inside and outside the crystal being of the same grain size. Fresh cordierite has occasional yellow halos. Andalusite also occurs in poikiloblastic crystals which are rarely idiomorphic and are often partially to completely converted to shimmer aggregate. Some specimens show post-andalusite crenulations which are overgrown by a second generation of decussate fine grained biotite and muscovite. The average grain size of inclusions of quartz, muscovite, and biotite in the andalusite crystals, representing the early stage of hornfelsing, is much smaller than that of the crenulated and recrystallized matrix around the crystals. Thus the rocks exhibit four stages of mineral growth, namely early biotite-muscovite, andalusite (followed by crenulation), late biotite-muscovite, cordierite. The rocks commonly exhibit retrogressive metamorphism with rosettes of penninitic chlorite in the matrix, and partial to complete conversion of cordierite to pinite. Late recrystallized patches of quartz are associated with retrogression and cut across the fabric. Some diaphthoresis took place in a tectonically active environment, as demonstrated by the subparallel orientation of chlorite grains replacing biotite.

In the sillimanite zone all pelitic rocks are strongly recrystallized so that the quartz-feldspar-mica matrix shows a granoblastic texture. Many biotite crystals appear to be in the process of replacement by fibrolite. Large crystals of andalusite lie corroded and surrounded by fine grained, twinned plagioclase. Andalusite porphyroblasts with inner pleochroic zones are in many cases replaced by muscovite and biotite containing semi-digested relicts of andalusite. The sequence of growth appears to be 1) biotite, 2) andalusite, 3) biotite+muscovite, 4) sillimanite+plagioclase(+muscovite?). Replacement of andalusite by large flakes of muscovite can be observed in many thin sections. The relations between late muscovite and sillimanite are difficult to determine precisely. Muscovite locally includes fibrolite and plagioclase, but in other places appears to be breaking down to fibrolite. These relations suggest a rise in water fugacity subsequent to crystallization of andalusite and penecontemporaneous to the formation of fibrolite. This episode of hydration may correlate with formation of retrogressive chlorite in lower grade rocks. This problem requires further investigation.

The sillimanite grade rocks just described border the Skiff Lake pluton. Rocks of similar grade bordering the Hawkshaw pluton contain a little andalusite, but are characterized by bluish tourmaline and fibrolite replacing biotite. These rocks contain smaller flakes of muscovite and display microcline in the matrix. The differences in mineralogy may be attributed to differing compositions, since the western part of the Hawkshaw pluton is entirely bordered by quartz wackes, whereas more pelitic rocks outcrop along the margin of the Skiff Lake pluton.

Summary and Conclusions

The southwestern part of the Pokiok batholith can be divided into the north-south trending Hawkshaw adamellite, and the probably older east-west trending Skiff Lake pluton. The metamorphic aureole of the plutons, which involves polydeformed Cambrian(?) to Silurian metasedimentary rocks, narrows from north to south, suggesting a shallower emplacement depth to the south. On the basis of pelitic assemblages, the wide part of the aureole can be divided into biotite, andalusite-cordierite, and sillimanite zones. Consideration of the metamorphic assemblages suggests maximum P-T conditions of about 550°C and 2-3 kb. Detailed textural examination indicates that contact metamorphism commenced with dehydration and formation of biotite and muscovite, followed by widespread formation of andalusite and cordierite. Later hydration led to widespread crystallization of muscovite and biotite within the sillimanite zone and retrogression elsewhere. The growth of sillimanite appears to be penecontemporaneous with, or slightly later than, hydration.

Acknowledgments

We wish to thank Sherri Townsend and Darlene Pajari for typing and drafting respectively, and K.L. Currie for useful comments.

References

Anderson, F.D. and Poole, W.H.
1959: Geology Woodstock-Fredericton, York, Carleton, Sunbury and Northumberland Counties, New Brunswick; Geological Survey of Canada, Map 37–1959.

Currie, K.L.
1971: The reaction 3 cordierite = 2 garnet + 4 sillimanite + quartz as a geological thermometer in the Opinicon Lake region, Ontario; Contributions to Mineralogy and Petrology, v. 33, p. 215-226.

1974: A note on the calibration of the garnet-cordierite geothermometer and geobarometer; Contributions to Mineralogy and Petrology, v. 44, p. 35-44.

Garland, G.D.
1953: Gravity measurements in the Maritime Provinces; Department of Mines and Technical Surveys, Publication of the Dominion Observatory, v. 16, no. 7.

Hamilton-Smith, T.
1972: Stratigraphy and structure of Silurian rocks of the McKenzie Corner area: New Brunswick Department of Natural Resources, Mineral Resources Branch; Rep. Invest. no. 15, 36 p.

Hess, P.C.
1969: The metamorphic paragenesis of cordierite in pelitic rocks; Contributions to Mineralogy and Petrology, v. 24, p. 191-207.

Holdaway, M.J.
1971: Stability of andalusite and the aluminum silicate phase diagram; American Journal of Science, v. 271, p. 91-131.

Hutcheon, I., Froese, E., and Gordon, T.M.
1974: The assemblage quartz-sillimanite-garnet-cordierite as an indicator of metamorphic conditions in the Daly Bay Complex, N.W.T.; Contributions to Mineralogy and Petrology, v. 44, p. 29-34.

McGrath, P.H.
1970: Magnetic investigations of the Charlotte and Pokiok Intrusions, southern New Brunswick; in The Geological Association of Canada, Proceedings, v. 21, p. 25-31.

Neuman, R.B.
1967: Bedrock geology of the Shin Pond and Stacyville quadrangles, Penobscot County, Maine; U.S. Geological Survey, Professional Paper 524-1.

Rast, N.
1977: Preliminary report on the geology of a part of the Pokiok Pluton and its surrounding metasediments, south-central New Brunswick; in Report of Activities, Part B, Geological Survey of Canada, Paper 77-1B.

Richardson, S.W., Gilbert, M.C., and Bell, P.M.
1969: Experimental determination of kyanite-andalusite and andalusite-sillimanite equilibria; the aluminum silicate triple point; American Journal of Science, v. 267, p. 259-272.

Venugopal, D.V.
1977: Geology of Meductic-Temple-Lower Parts Eel River H-22, Carleton and York Counties, New Brunswick; New Brunswick Department of Natural Resources, Mineral Resources Branch, Plate 78-27.

1978: Geology of Benton-Kirkland Upper Eel River Bend map area G-22 (21G/13E); New Brunswick Department of Natural Resources, Mineral Resources Branch, Map Report 78-3, 16 p.

44.

A STUDY OF THE REYKJANES RIDGE BY SURFACE WAVES USING AN EARTHQUAKE-PAIR TECHNIQUE

Project 770010

C.E. Keen, A. Fricker, M.J. Keen and L. Blinn[1]
Atlantic Geoscience Centre, Dartmouth

Keen, C.E., Fricker, A., Keen, M.J., and Blinn, L., A study of the Reykjanes Ridge by surface waves using an earthquake-pair technique; in Current Research, Part A, Geol. Surv. Can., Paper 79-1A, p. 273-279, 1979.

Abstract

Dispersion of surface waves generated by earthquakes beneath the Reykjanes Ridge is used to find a model for the shear wave velocity as a function of depth beneath a young crestal region. The Reykjanes Ridge and the WWSSN observatory AKU in Iceland lie close to a great circle, so it is possible to separate dispersion generated by paths on the Ridge itself from the total dispersion, which includes the effects of Iceland, using an adaptation of the station-to-station technique. As there are no pairs of stations, pairs of earthquakes are used; cross-correlation and filtering of the surface wave trains yields the travel times between earthquakes — and so the group velocities — at different periods. The observed dispersion of Love waves and Rayleigh waves seen over two paths along the Ridge are modelled using Backus-Gilbert inversion techniques, varying shear wave velocities with depth. The periods used are 6-18 s (Love) and 6-37 s (Rayleigh). Velocities in the crust (to 6.45 km) are fixed from seismic refraction observations. Model velocities below this increase to 4.3 km/s at 20 km, reflecting a high velocity lid, and decrease to 4.0 km/s by 40-50 km, reflecting the low-velocity zone. The base of this zone is not seen because the periods used are not sufficiently low, but it must lie below 100 km. This model can be interpreted in terms of a zone of partial melting only a few tens of kilometres wide below the high velocity lid; a density model based upon this feature can account for the observed gravity field.

Introduction

Studies of the crust and mantle of crestal regions of midocean ridges are important because new lithosphere forms beneath such regions, and an understanding of the processes of lithosphere formation requires a knowledge of the physical properties underneath the ridge crests. Some experiments, such as long-range refraction experiments, are difficult or expensive to do; observations of heat-flow near crestal regions may be difficult to obtain, or hard to interpret (Sclater et al., 1976). Deductions from dispersion of surface waves may be ambiguous because of the geometrical relationships between sources and receivers, the paths crossing oceanic provinces belonging to a great range of ages; consequently a path which is restricted to a region of uniform age with uniform properties along the path, would be valuable (Forsyth, 1975). Earthquakes along the Reykjanes Ridge, recorded at the WWSSN station AKU in northern Iceland provide such a path beneath the crestal region of a midocean ridge (Fig. 44.1). In this report we describe how surface waves generated along this path lead us to shear-wave velocities within young crust and mantle.

We need to determine group velocity as a function of period for Rayleigh or Love waves or both, but the two methods most commonly used cannot be applied. If there is a single source and a single station we must assume that the earth between is laterally homogeneous. This would clearly be an improper assumption to make, because most of Iceland lies between the Reykjanes Ridge and AKU. Paths of more restricted length — and so, hopefully, with more laterally uniform properties beneath — can often be obtained by using two stations with a single source beyond the line joining the two stations. Dispersion caused by the earth between the source and the closer station is, in essence, "subtracted" from the dispersion observed at the farther station, leaving only the dispersion caused by the earth between the stations (Landisman et al., 1969). However, there is only one station along the path Reykjanes Ridge — Iceland, and so instead of using pairs of stations we restrict the path lengths over which we measure dispersion to the Reykjanes Ridge itself by choosing pairs of earthquakes. The Ridge and AKU bear a convenient geometrical relationship one to another, so that pairs can be chosen which lie on a great circle from AKU. The effect of the earthquake closer to AKU is "subtracted" from the effect of the earthquake farther from AKU to leave the dispersion due only to the earth beneath the path between the earthquakes. In principle, this should yield results identical to the more usual "pure-path" techniques, but in this case we obtain group velocities between sources, instead of stations.

Figure 44.1 shows the locations of earthquake sources used in this study, in relation to the position of AKU. Each source location is the site of more than one event, usually a main shock followed by a sequence of aftershocks, so that a number of dispersion curves can be obtained for the same path. This allows mean dispersion curves to be calculated and errors to be estimated. The data have been divided between two paths, A and B, where the events at location 2 are common to both (Fig. 44.1). This division into two paths was made because (a) the paths are somewhat different, and (b) it yields some assessment of the effects of different source mechanisms. Since shear velocities have been estimated independently along each path this allows some estimate of the validity of the method to be made.

Analysis of Data

Our concern is to determine group velocities of surface waves generated by an earthquake as a function of period for a segment of a ridge crest. We can then compare these (experimental) velocities with the (theoretical) values generated from a model, and so obtain estimates of the model parameters which control the model group velocities — in this case, shear wave velocity as a function of depth. Consequently we need to find the travel time of phases over a range of periods between two points on the ridge crest, knowing the distance between them.

[1]Department of Oceanography, Dalhousie University, Halifax, N.S., Canada.

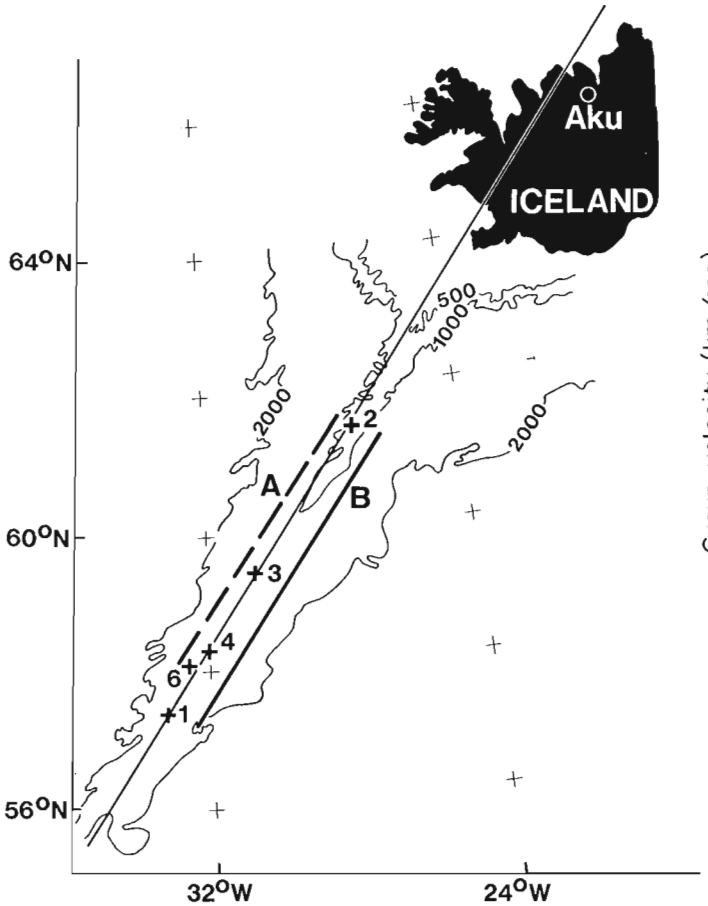


Figure 44.1. The Reykjanes Ridge and Iceland. Bathymetric contours are in metres. Path A lies between events 2 in the north and 4 and 6 in the south; path B lies between events 2 and 1. The long solid line shows the great circle path along the Ridge.

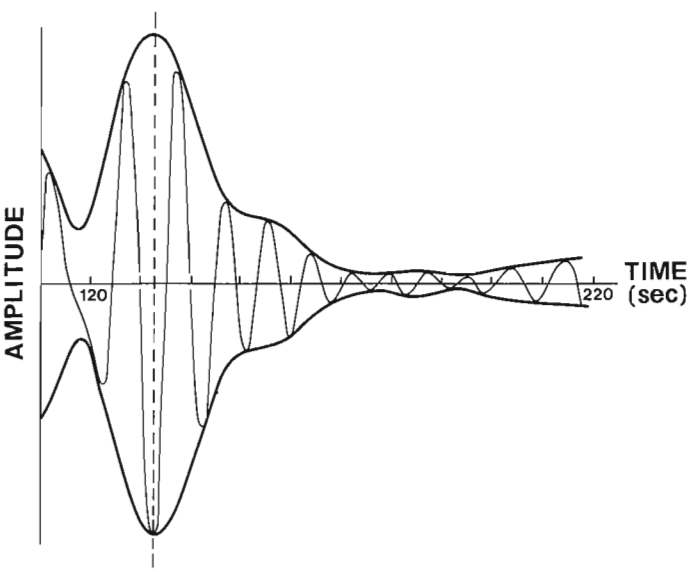


Figure 44.2. The filtered cross-correlogram for the pair 2A-4D, vertical component. Central filter period 9.9 s; event-to-event distance 436.6 km. The peak in the envelope at 132 s gives the group arrival time of signal energy at the central filter period.

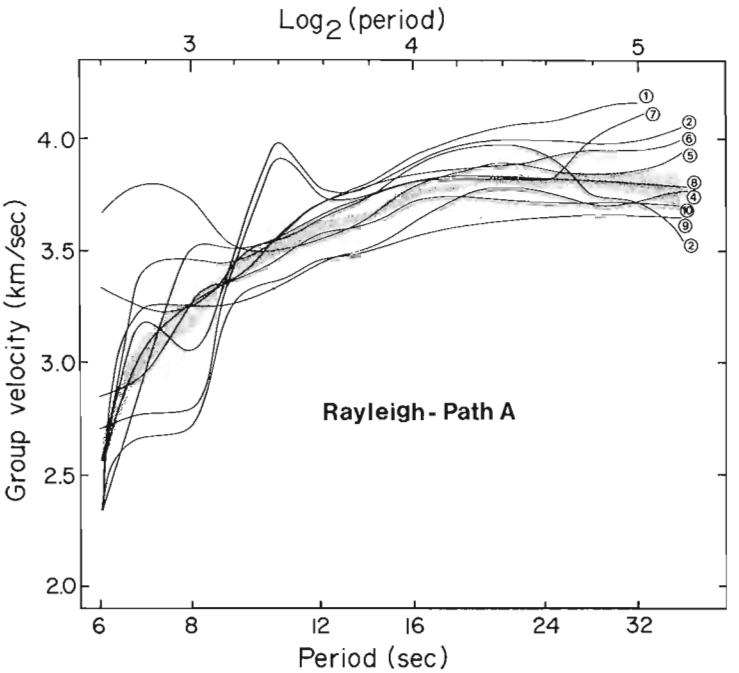


Figure 44.3. Group velocity-period for Path A, Raleigh. The solid curves show the observations for different pairs. Each number designates a particular pair, given in Table 44.2. The swathe encompasses one standard error on each side of the mean curve (see text). Observations made at increments of 0.2 on the log scale.

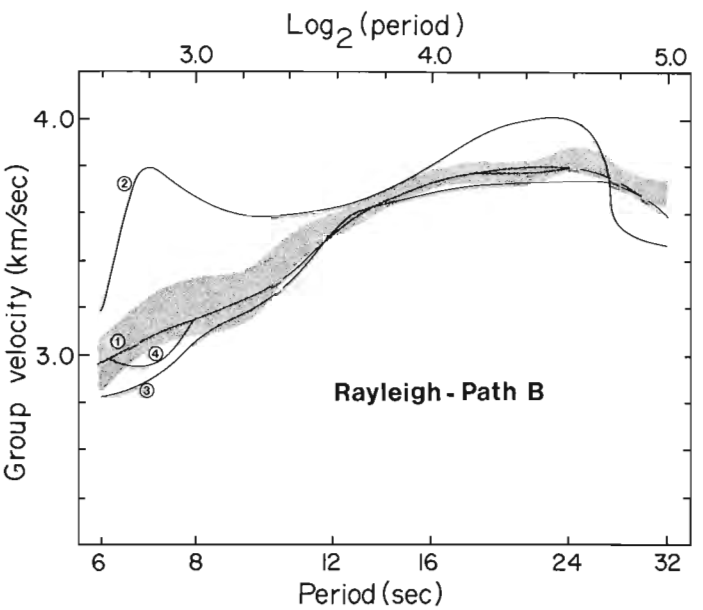


Figure 44.4. Group velocity-period for Path B, Rayleigh. The solid curves show the observations for different pairs. Each number designates a particular pair, given in Table 44.2. The swathe encompasses one standard error on each side of the mean curve (see text). Observations made at increments of 0.2 on the log scale.

Table 44.1

Earthquake sources

No.	Date	Time	Lat °N	Long °W	m_b	Azimuth°	Dist km
1A	1972 June 19	06:00:51.1 ± 0.99	57.37 ± 0.033	33.43 ± 0.036	5.0	228.3	1227.9
1B	1972 June 19	12:14:27.0 ± 0.96	57.39 ± 0.029	33.38 ± 0.031	4.8	228.2	1224.3
2A	1966 May 05	15:25:12.5 ± 0.21	61.49 ± 0.040	27.40 ± 0.048	4.7	228.8	655.9
2B	1966 May 05	15:52:40.9 ± 0.15	61.45 ± 0.031	27.49 ± 0.040	4.9	228.9	662.4
4A	1969 Sept 20	00:56:52 ± 1.3	58.27 ± 0.054	32.15 ± 0.054	4.9	228.1	1102.1
4B	1969 Sept 20	01:07:42 ± 1.1	58.29 ± 0.043	32.03 ± 0.046	5.0	227.8	1096.2
4C	1969 Sept 20	01:13:07 ± 1.2	58.19 ± 0.044	32.05 ± 0.046	5.1	227.6	1106.0
4D	1969 Sept 20	05:08:57.8 ± 0.12	58.35 ± 0.029	32.08 ± 0.030	5.6	228.2	1092.5
6A	1968 Sept 14	01:38:42.6 ± 0.28	58.08 ± 0.061	32.64 ± 0.060	5.1	228.6	1136.1

Notes:

These data have been taken from the Bulletin of the International Seismological Centre, Edinburgh, Scotland.
Distances to AKU were calculated using a spheroidal earth.
Azimuths are the great circle directions from the station towards the event.

Briefly, we obtain the Fourier Transform of a pair of seismograms, $f_1(t)$, $f_2(t)$, generated by two sources (in this case one at either end of Path A or B, Fig. 44.1) and received at one station. Cross-multiplication in the frequency domain, the equivalent of cross-correlation in the time domain, gives the phase difference as a function of frequency between the seismograms and removes the effect of the propagation paths lying between the station and the event closest to it. The cross-correlated spectrum is filtered using the Gaussian filter

$$G(\omega) = A\, e^{-a(\omega-\omega_o)^2}$$

centred at frequency ω_o for which we seek the group velocity. The advantage of this filter is that it gives the optimum resolution of both time (or group velocity) and frequency (Robinson, 1967). Here the parameter, a, was chosen to give equal fractional uncertainty in both group velocity and period (Fricker, 1971). Inverse Fourier transformation of the filtered signal allows the arrival time of the energy centred on ω_o to be obtained. Figure 44.2 shows an example of a typical filtered and inverse-transformed cross-correlogram. The envelope's peak defines the group arrival time centred on ω_o.

Nine earthquakes from the four locations, 1, 2, 4 and 6, were chosen from all occurring on the Reykjanes Ridge between March, 1962 and March, 1972 with body wave magnitudes $m_b > 4.7$ (Table 44.1). Their reported depths are the reference depth of 33 km, not the actual depths, likely to be in the range of 5 (or less) to 10 km (Weidner and Aki, 1973).

The records of all components were photo-enlarged three times, and digitized with a D-MAC pencil follower at intervals of approximately 1.5 s (and all maxima and minima); cubic spline interpolation was used to give evenly spaced data points at 0.75 s. The digitized seismograms were windowed, and the spectra found using a fast Fourier Transform algorithm; these spectra were corrected for the instrument response at AKU. The Rayleigh and Love modes were resolved using the horizontal and vertical components. In the case of Love waves the horizontal motion normal to the wave path (assumed to be the great circle path) was found from the east-west and north-south spectra; in the case of Rayleigh waves we usually used only the vertical spectra, because of higher noise levels associated with the horizontal spectra (so that the enhancement of signal: noise anticipated using horizontal components along the wave path together with the vertical component could not be realized).

The events were set in pairs, so that each event from one site could be cross-correlated with all events at a second site. This led to ten dispersion curves along path A, and four along path B, corresponding to events 2 and 4, 2 and 6 (path A) and 2 and 1 (path B) (Tables 44.1, 44.2). The spectral records, resolved for Rayleigh and Love modes, were then cross-multiplied and filtered as described already. Group velocities were found for periods of 6 to 37 s for the fundamental Rayleigh mode and 6 to 18 s for fundamental Love mode, the limits being selected on the basis of digitizing interval, signal energy, and the wavelengths at long periods – which become comparable to path length.

Because there are a number of pairs of earthquakes for each path, we can calculate mean values and standard errors of the group velocities at each period. The methods used are described only briefly here; details are given in Fricker (1971, 1976). The errors leading to differences in values of velocity are of two sorts. Errors common to all periods in one dispersion curve lead to general differences in "level" between curves of velocity-period for the different earthquake pairs, and are due to: mislocation of earthquakes; error in origin time; fault zones of finite length; and long term drift in instrument response not seen in calibration.

Table 44.2

Earthquake pairs for paths A and B

Pair	Path length (km)	Azimuth°
	Path A	
2A-4A (1)	446.2	228.5
2A-4B (2)	440.3	228.3
2A-4C (3)	450.1	228.2
2A-4D (4)	436.6	228.5
2B-4A (6)	439.7	228.5
2B-4B (7)	433.8	228.4
2B-4C (8)	443.6	228.2
2B-4D (9)	430.1	228.5
2A-6A (5)	480.2	228.7
2B-6A (10)	473.7	228.8
	Path B	
2A-1A (1)	572.0	228.6
2A-1B (2)	568.5	228.5
2B-1A (3)	565.5	228.6
2B-1B (4)	561.9	228.6

Note:

Numbers in brackets are those shown in Figures 44.3 and 44.4.

Table 44.3

Fixed parameters used in inversion

Depth to top of layer km	Density gm/cm^3	V_p km/sec	V_s km/sec
0.00	1.03	1.50	0.0000
1.62	2.84	4.20	2.1554
2.32	2.84	5.81	2.6096
3.31	2.84	6.53	3.0994
4.88	3.00	6.53	3.6752
6.45	3.20	7.20	
8.40	3.30	8.00	
9.55	3.30	8.00	
15.00	3.30	8.00	Inversion
25.00	3.30	8.00	
35.00	3.30	8.00	Parameters
40.00	3.30	8.00	
60.00	3.20	7.20	
80.00	3.20	7.20	
100.00	3.20	7.20	
125.00	3.20	7.20	
150.00	3.30	8.00	4.3300

These errors can be partly removed by "sliding" together the velocity-period curves using as criteria for adjustment the condition that the mean overall remains unchanged, and by seeing that the standard errors are minimized (in the least-squares sense). The errors which remain are random and due to: digitization; source mechanisms; and noise. In addition, "structural" effects between sources – sloping interfaces, for example – and interference by higher mode Love waves may make interpretation difficult. The second type of errors are random errors and lead to "wiggles" in the curves, not necessarily coherent from one curve to another. It is from these that the standard errors used here have been calculated.

The mean group velocity at any period is calculated after the errors common to all periods from each curve, as described above, are removed in the following way (Fricker, 1976). The arrival time at a particular period will be in error because of contamination by noise and the effects of the filter used to isolate the period. Consequently weights are assigned to each value on a group velocity-period curve which are functions of filter parameter, period, and the ratio of signal to noise. These weights give value to each point on a curve inversely proportional to the likely error in travel-time, which can be calculated (in terms of the factors mentioned). Means and standard errors are calculated from the weighted values of travel time (in essence, reciprocals of group velocity). The standard errors themselves should not fluctuate markedly from period to period, and are smoothed using a binomial smoothing scheme. These smoothed standard errors, due only to random errors, are used when modelling. The curves of mean group velocity-period should themselves vary smoothly from period to period, and so are smoothed (and interpolated) by cubic spline smoothing. The periods at which group velocities were determined are shown on Figures 44.3 and 44.4.

Figures 44.3 and 44.4 show the Rayleigh wave group velocity curves before any corrections for errors and smoothing have been applied as well as the band of values falling within one standard error unit of the mean, calculated as described above. Note that the fluctuation in the individual group velocity curves has been removed in the final curves and that the standard errors are appreciably less than those which might be estimated from any one curve alone. The differences between the standard errors shown and those which might seem intuitively reasonable, which are about five times greater, are due partly to the weighting of the individual curves. However, the standard errors shown are probably underestimates. The justification for the use of these smaller errors is that the linearized inversion scheme applied to the data to obtain a shear velocity model becomes unstable if larger errors are used, and hence the use of the smaller error estimates represents a compromise between

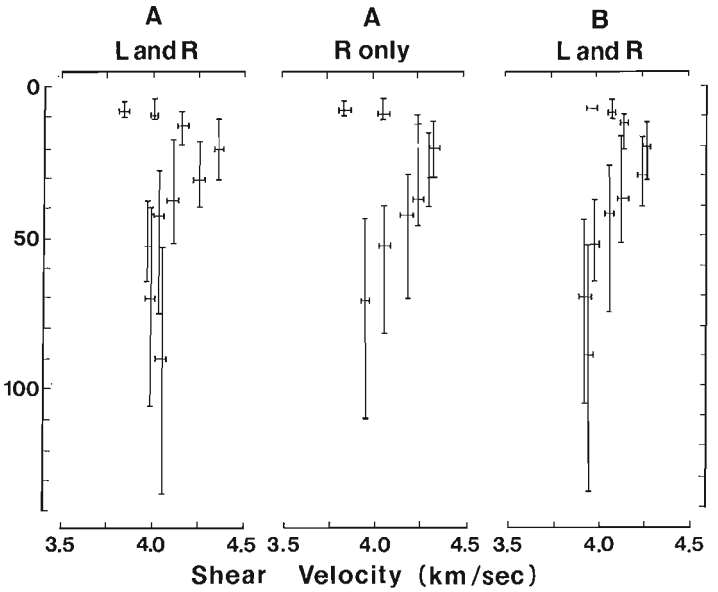


Figure 44.5. Shear-velocity against depth for Path A Love and Rayleigh (left), Rayleigh only (middle), and Path B Love and Rayleigh (right). Horizontal bars give standard errors in velocity, vertical bars give the spread in depth.

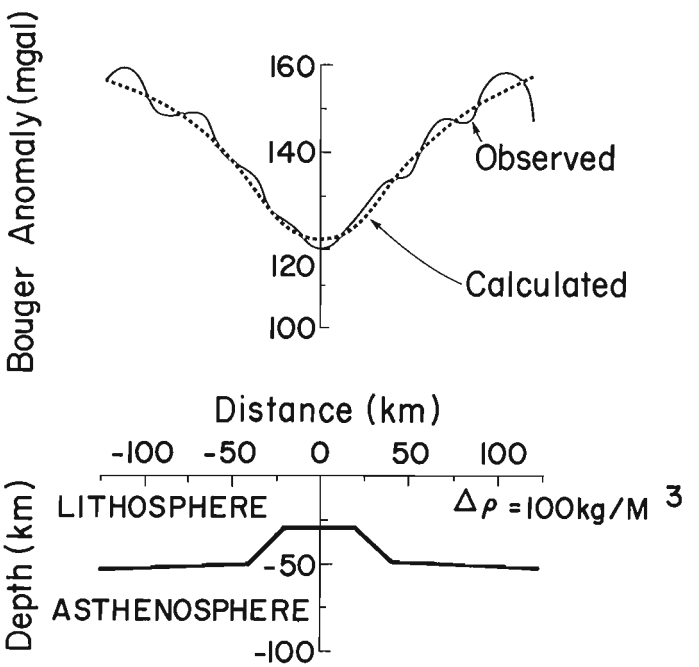


Figure 44.6. The observed Bouguer anomaly across the Reykjanes Ridge (from Talwani et al. (1971)) and the anomaly corresponding to the model beneath.

obtaining a model by means of the inversion technique and the need to rely on modelling techniques which give no estimates of the precision and resolution of the final models. The latter would be necessary if larger errors were used.

The weakest link in the method of analysis applied here is that the behaviour of all the source function is assumed to be the same and hence no corrections have been made for the effect of the source function and the phase as a function of frequency. While all the earthquakes are located on the Reykjanes Ridge crest, away from known fracture zones, and hence may have similar focal mechanisms representative of normal faulting, the effects of small differences in fault plane orientation and dip on the data has not been established, mainly because most of the earthquakes were not large enough to obtain reliable fault plane solutions. In addition, variations in velocity perpendicular to the ridge crest causing lateral refraction of the propagating waves have not been considered here. These effects, while important, would not in our opinion, change the basic results of the study but they should be considered in any further studies of this type.

Modelling

Models of shear velocity as a function of depth were obtained from the dispersion data, using linear inversion techniques (Backus and Gilbert, 1970). The use of these methods for surface wave studies has been described by Wiggins (1972) and specific details of the computations used in this study are given by Fricker (1976). The linear inversion method gives us both models which fit the data to within specified error limits and also estimates of the uncertainties of the models.

Theoretical data are calculated using Haskell's (1953) matrix formulation which approximates the elastic properties of the real earth by a stack of horizontal layers, each with uniform compressional and shear wave velocities and density. The values of these parameters are varied iteratively until all the theoretical data calculated from a particular model agree with the observations to within predetermined error limits, usually one standard deviation. For rapid digital computation, the Haskell matrices have been modified as described by Schwab and Knopoff (1970), among others.

If we start with an initial model which is close to the desired model, the required changes in the parameters necessary to bring the theoretical data, calculated from the model, into agreement with the observations may be estimated by the size of the partial derivatives of the theoretical data parameters with respect to the model parameters.

The derivatives with respect to shear wave velocities are much larger than those of compressional wave velocity or density. Variations of v_p and p affect the final model by an order of magnitude less than v_s. Thus v_p and p were not varied in producing the final models but were held at fixed values corresponding to the initial model. This starting model, as stated above, must be sufficiently close to the final result that the partial derivatives are valid indicators of the adjustments needed in the model to fit the data. Thus a certain amount of trial and error modelling is required before proceeding to the final inversion. In this study, we found that the calculated group velocities are very sensitive to water depth and the thickness of the first crustal layer. This problem was overcome by constraining the shear wave velocities of the upper crustal layers to be in reasonable accord with the compressional wave data for the Reykjanes Ridge described by Talwani et al. (1971), and by setting the water depth at 1.62 km — a reasonable mean value for paths used. Trygvasson (1962) has shown that the effects of sloping water interfaces on Rayleigh wave dispersion curves are small at periods greater than 8 s; Love waves are of course not affected at all. In addition, the group velocities at the periods considered here have no bearing on the model below 150 km. Therefore the shear velocity was held constant at 4.33 km/s below this depth. The parameters which have been fixed during inversion are shown in Table 44.3; we see here that shear velocity was allowed to vary during inversion in eleven layers between depths of 6.45 km and 150 km.

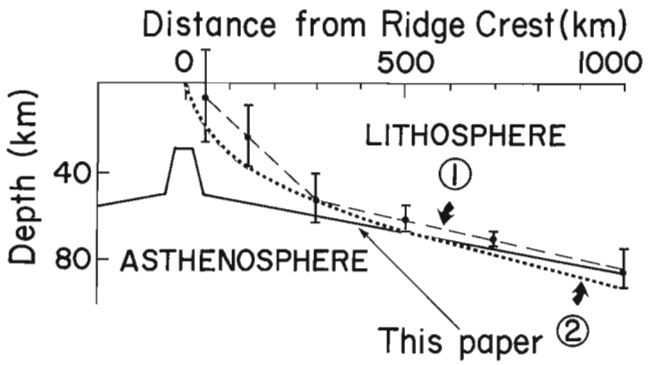


Figure 44.7. *Some models of the Reykjanes Ridge. The model corresponding to the density model of Figure 44.6 is shown solid. Model 1 is that derived from the surface wave study by Leeds et al. (1974) (who fixed the shear-wave velocities; see text) the vertical bars are their error limits; Model 2 is Parker and Oldenburg's (1973) (who assumed heat transfer by conduction only; see text).*

Wiggins (1972) showed that for real data a limited number of model parameters can be determined if a certain degree of precision of these parameters is desired. As in other linear inverse problems a compromise must be reached between a detailed model which is poorly defined, with large uncertainties in some of the parameters, and a model which includes less detail but which is accurate to a predetermined acceptable level. This is the trade-off between resolution and precision.

The surface wave inversion method involves the solution of a set of equations using least squares minimization of the difference between theoretical and observed data (Wiggins, 1972). Thus a desired level of accuracy, the standard error of the problem, σ, can be set. In this case a standard error of 0.01 was chosen which allows us to determine only three or four independent model parameters. This may be compared to the five independent parameters obtained by Forsyth (1975) for surface wave data in the Pacific. We attempted to fit both Love and Rayleigh wave data combined and Rayleigh wave data alone. Similar models were obtained in both cases, with the model data falling within about one standard error of the observations. In the case of Path A, it was not possible to obtain a really satisfactory fit to the combined Rayleigh and Love data, possibly because the fundamental Love mode was contaminated with higher mode interference. However, the model obtained, shown in Figure 44.5, is in agreement with the other models.

The shear velocity models are presented in Figure 44.5. The horizontal bars represent the standard errors in the shear wave velocities and the vertical bars, the depth resolution of these determinations. The resolution kernels (Backus and Gilbert, 1970) were generally compact, having a high value in only one layer. However, some degree of non-compactness was observed for the deeper layers.

A visual comparison of the shear velocity curve for paths A and B (Fig. 44.5) shows no significant differences between them. At shallow depths, the shear velocity increases with depth reaching 4.3 km/s at 20 km. The velocity then decreases to about 4.0 km/s between 40 and 50 km. Below this, the resolution is not sufficient to define the base of this low velocity zone.

Discussion

Our models showing shear-wave velocity as a function of depth are similar to those of others who have concerned themselves with young lithosphere and asthenosphere. Forsyth (1977) for example, points out that in the age range 0-5 Ma the high velocity lid will have a velocity of 4.3 km/s, and a thickness of 30 km (or less); we see the same velocity, and his depth to the base of the lid is compatible with the marked decrease in velocity below 30-40 km demanded by our models. The velocity below this, 4.0 km/s, also agrees with Forsyth's (1977) conclusions. These similarities are significant, because the two paths we have used lie wholly along the crest of a ridge, uncontaminated by dispersion caused by other structural elements, inevitable if dispersion is measured using an earthquake-station pair (because of the locations of the stations). This would not necessarily be true of a study such as the very interesting one of N. Girardin and W.R. Jacoby (unpublished manuscript).

The model of a low-velocity zone below 30-40 km is also in agreement with the conclusions of Solomon and Julian (1974), who, in a study of focal mechanisms of earthquakes on ridges (including one from the Reykjanes Ridge), suggested that a zone of anomalously low compressional wave velocity lay beneath the crests. They attributed this to the existence of a region of partial melting.

We have no information on the lateral extent of the low-velocity zone from our surface wave study; we can, however, model its equivalent roughly in terms of density variations, using gravity data, and compare the gravity field which would result with the observations of Talwani et al. (1971). This is done in Figure 44.6; we have not tried to model lateral changes in density in the lithosphere and asthenosphere (which would be predicted by the lateral changes in shear-wave velocity suggested by Forsyth, 1977), nor are the density contrasts shown obtained from the shear velocity models presented here, but were arbitrarily chosen. We show in Figure 44.7 how our suggestion of a relatively narrow asthenospheric wedge beneath the ridge crest compares with other models. The apparent lack of agreement near the crestal zone is hardly surprising. Parker and Oldenburg's (1973) model assumed heat to be transported by conduction, with no additional cooling by hydrothermal circulation; in their surface wave study Leeds et al. (1974) assumed that the shear-wave velocity in the high velocity lid was 4.6 km/s (rather than 4.3 km/s near the crests) so that they could model the change in thickness of the lid with age.

It is gratifying that the technique using earthquake-pairs is in such good agreement with the studies of Forsyth (1977), and Solomon and Julian (1974). The method could perhaps be extended with profit to seek variations in velocity-depth models along ridge crests, seeking regional variations along particular ridges, and variations with rates of spreading. We should perhaps point out that although sophistication in modelling has been achieved using Backus-Gilbert inversion techniques, nevertheless, as they are usually applied in studies with surface waves, no account is taken of anisotropy, or lateral inhomogeneities – which in crestal regions must be significant.

Acknowledgments

We thank the National Research Council of Canada for support, and Christopher Garrett and Lynn Smith for aid. Louis Blinn and Aubrey Fricker received scholarships from Dalhousie University. Comments on the paper from D. Forsyth, R. Falconer, C. Beaumont and S. Srivastava were most helpful.

References

Backus, G.E. and Gilbert, J.F.
1970: Uniqueness in the inversion of inaccurate gross earth data; Royal Society of London, Philosophical Transactions, Series A, v. 266, p. 123-192.

Forsyth, D.W.
1975: The early structural evolution and anisotropy of the oceanic upper mantle; Royal Astronomical Society, Geophysical Journal, v. 43, p. 103-162.

1977: The evolution of the upper mantle beneath mid-ocean ridges; Tectonophysics, v. 38, p. 89-118.

Fricker, A.
1971: A development of surface wave analysis and interpretation in the Canadian Shield; unpublished M.Sc. Thesis, Dalhousie University.

1976: Crustal models from seismic surface waves; unpublished Ph.D. Thesis, Dalhousie University.

Haskell, N.A.
1953: Dispersion of surface waves in multilayered media; Seismological Society of America Bulletin, v. 43, p. 17-29.

Landisman, M., Dziewonski, A., and Sato, Y.
1969: Recent improvements in the analysis of seismic surface wave observations; Royal Astronomical Society, Geophysical Journal, v. 17, p. 369-403.

Leeds, A., Knopoff, L., and Kansel, E.
1974: Variations of upper-mantle structure under the Pacific Ocean; Science, v. 186, p. 141-143.

Parker, R. and Oldenburg, D.
1973: Thermal model of ocean ridges; Nature, Physical Science, v. 242, p. 137-139.

Robinson, E.A.
1967: Statistical communication and detection; Griffin, London, 357 p.

Schwab, F.L. and Knopoff, L.
1970: Surface wave dispersion computations; Seismological Society of America Bulletin, v. 60, p. 321-344.

Sclater, J.G., Crowe, J., and Anderson, R.N.
1976: On the reliability of oceanic heat-flow averages; Journal of Geophysical Research, v. 81, p. 2997-3007.

Solomon, S.C. and Julian, B.
1974: Seismic constraints on ocean ridge mantle structure: anomalous fault plane solutions from first motions; Royal Astronomical Society, Geophysical Journal, v. 38, p. 265-285.

Talwani, M.C., Windisch, C.C., and Langseth, M.G.
1971: Reykjanes Ridge crest: a detailed geophysical study; Journal of Geophysical Research, v. 76, p. 473-517.

Trygvasson, E.
1962: Crustal structure of the Iceland region from dispersion of surface waves; Seismological Society of America Bulletin, v. 52, p. 359-388.

Weidner, D. and Aki, K.
1973: Focal depth and mechanism of mid-oceanic ridge earthquakes; Journal of Geophysical Research, v. 78, p. 1818-1831.

Wiggins, R.A.
1972: The general linear inverse problem; implication of surface waves and free oscillations for earth structure; Reviews of Geophysics, v. 10, p. 251-285.

45.

A PRELIMINARY ASSESSMENT OF THE URANIUM POTENTIAL OF SOUTHERN MELVILLE PENINSULA, DISTRICT OF FRANKLIN

Project 760047

Y.T. Maurice
Resource Geophysics and Geochemistry Division

Maurice, Y.T., A preliminary assessment of the uranium potential of southern Melville Peninsula, District of Franklin; in Current Research, Part A, Geol. Surv. Can., Paper 79-1A, p. 281-287, 1979.

Abstract

Widespread uranium enrichment in the lake sediments and waters of southern Melville Peninsula is traced to felsic igneous rocks that intrude the Penrhyn Group of metasediments. Some of these intrusives locally contain high concentrations of radioelements and they should be examined for associated vein-type uranium mineralization or uraniferous late magmatic differentiates. A rock suspected to be a radioactive skarn was discovered near a granitic pluton. Contact metasomatism could represent an important uranium ore forming process in southern Melville Peninsula.

Intense metamorphism of the Penrhyn sediments and relatively low uranium content of the nearby basement has drawn attention away from the Penrhyn unconformity as a possible host of uranium mineralization. A younger unconformity in the northwestern part of the survey area, however, may have greater potential as it overlies a uranium enriched basement and is marked by a thick regolith. The uranium content of basement rocks in that area appears to increase towards the unconformity and uranium enrichment seems to be partly fracture-controlled suggesting remobilization.

Introduction

In 1977, a 30 000 km^2 area, comprising most of southern Melville Peninsula (Fig. 45.1) was the object of reconnaissance lake sediment and water geochemical and airborne radiometric surveys carried out under the Uranium Reconnaissance Program (U.R.P.). The reader is referred to papers by Darnley et al. (1975) and Hornbrook and Garrett (1976) for details on the methodology employed in these surveys. The geochemical data were published in mid-1978 (Geological Survey of Canada, 1978a, 1978b) and the radiometric results are expected to be released in early 1979. Some preliminary radiometric data were available to the writer prior to the 1978 field season and these proved to be of great value at the planning stage of the follow-up program described in this paper.

Due to the shortness of the field season, it was only possible to examine a small fraction of the areas that were considered to warrant further investigation. This report is therefore preliminary; much additional field work as well as further analyses of the samples collected during the past field season will be required before final judgment can be passed on the uranium potential of this region.

General Geology

Southern Melville Peninsula includes part of the Foxe Fold Belt which comprises an Archean basement, composed essentially of granitoid gneissic rocks overlain unconformably by Early Proterozoic Penrhyn metasediments (Fig. 45.1). These consist of a mixture of paragneiss, schist, marble, calc-silicate gneiss, quartzite and minor amphibolite. A grey-green micaceous rock, possibly a meta-regolith, occurs at the base of the Penrhyn Group in certain areas (Okulitch et al., 1977).

The Penrhyn metasediments, as well as the basement complex, have been intruded by granitoid plutons before, during, and after the regional metamorphism that took place during the Hudsonian orogeny. Intrusive rocks are extremely widespread and their intermixing with the metasediments is very complex. In composition, they range from granitic to granodioritic and quartz-monzonitic. They generally exhibit a low colour index and their texture is highly variable ranging from aplitic to coarsely pegmatitic (Reesor et al., 1975).

Metasediments and metavolcanics of the Prince Albert Group occur in the northern part of the survey area (Fig. 45.1). These rocks have been described by Heywood (1967) and Schau (1975). They are Archean in age and comprise various units of greenstone, amphibolite, paragneiss, schist and quartzite; they also host economically interesting iron formations (Wilson and Underhill, 1971).

A gently dipping, slightly metamorphosed clastic sedimentary sequence (unit 16 of Heywood, 1967) rests unconformably on the Prince Albert Group and the granitic basement in the northwest corner of the survey area. Frisch (1974 and in prep.) reports a thick (up to 25 m) regolith at the base of this formation; it is overlain by granite- and quartz-pebble conglomerate, sericite schist, quartzite, marble and arkose. The sequence is at least 850 m thick. The age of these rocks is uncertain but indications are that they are younger than the Penrhyn, possibly post-Hudsonian.

Interpretation of the Reconnaissance Data

Uranium dispersion pattern

The reconnaissance lake sediment results show that the surficial environment of southern Melville Peninsula is, on average, considerably richer in uranium than most other areas of the Canadian Shield where similar surveys have been carried out (Table 45.1; see also Cameron and Hornbrook, 1976, Fig. 14).

A trend of U-enriched values follows the Penrhyn rocks as shown in Figure 45.2. There seems to be a certain amount of uranium dispersion away from the sedimentary belt towards the northwest, but this likely reflects the drainage pattern and/or glacial smearing. The strongest values along this trend (>50 ppm U) nearly all occur within the Penrhyn Group.

A second zone of U-enriched values occurs over Archean rocks in the northwestern part of the survey area (Fig. 45.2). This zone comes in contact with the Late Precambrian sedimentary formation in that area.

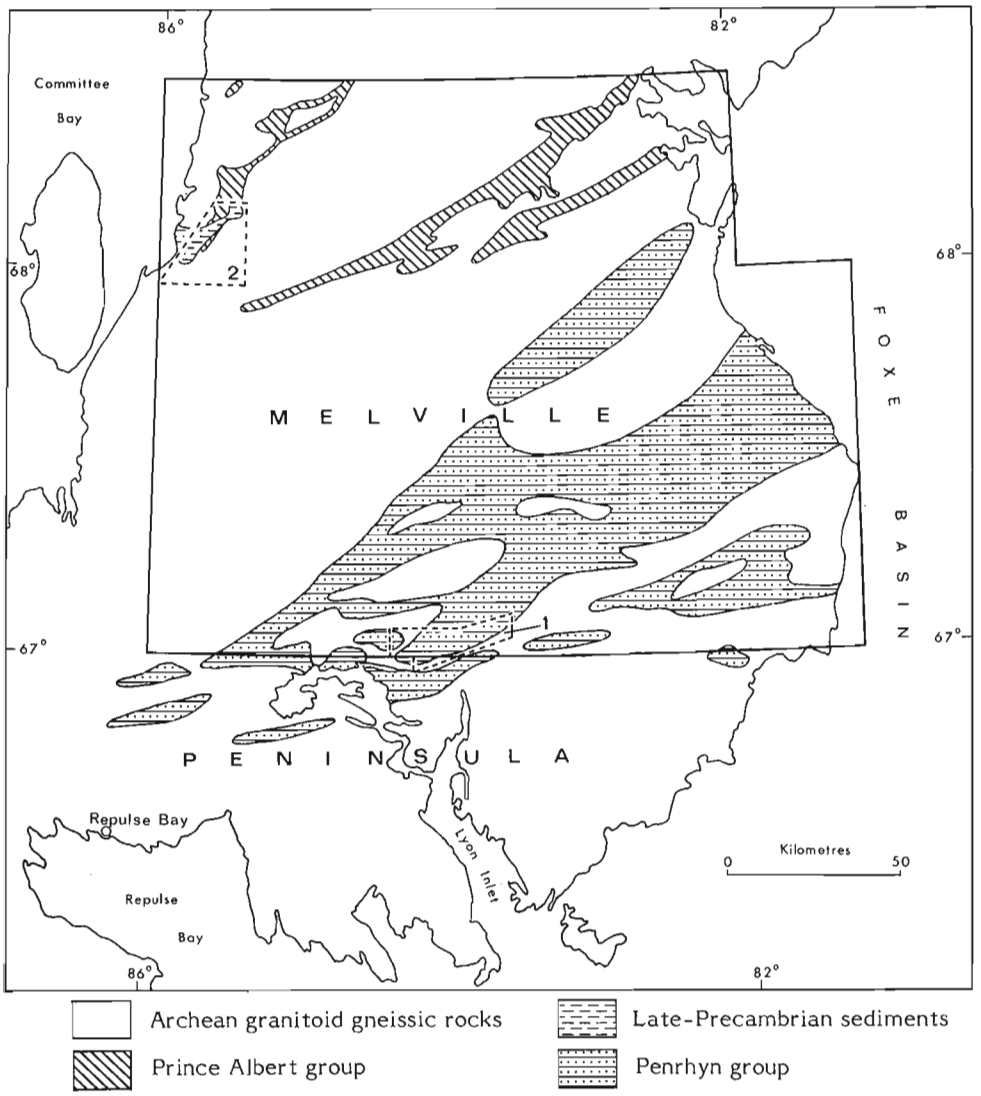


Figure 45.1. *Regional geology of southern Melville Peninsula.*

Interelement relationships

Factor analysis was used to examine interelement relationships in lake sediments and waters on a regional scale. The five factor model, which accounts for 79 per cent of the data variability, is presented in Table 45.2.

The first factor shows a strong relationship between the base metals and Fe and Mn. This reflects the presence of base metal sulphides in the Penrhyn metasediments. Cameron (1979) discusses the distribution of some of these elements.

Strong dependence of U-in-water on pH is shown in factor 2. The pH conditions are generally neutral to slightly acidic in southern Melville Peninsula except within the Penrhyn Group where they range from acid (pH 5-6) in proximity to oxidizing sulphidic zones, to weakly alkaline (pH 7-8) in areas of crystalline limestone bedrock. U-in-water anomalies (1.0 to 3.0 ppb), that coincide with anomalies in the lake sediments occur in the south and central parts of the Penrhyn where carbonate rocks are particularly abundant. Elsewhere the U concentration in lake waters seldom exceeds 0.5 ppb. Fluorine also varies with U-in-water and pH, but F levels in the lakes of southern Melville Peninsula are low; the significance of this association is not clear but is probably unimportant from a mineral exploration viewpoint.

The organic content of the lake sediments influences the distribution of Hg as indicated by factor 3.

The U-Pb association (factor 4) has been observed in other parts of the Canadian Shield (Maurice, in press). The sympathetic relationship of these two elements and their widespread enrichment in the lake sediments in southern Melville Peninsula probably reflects their enrichment in certain rock types, namely the felsic intrusives. The Pb distribution is further complicated by its association with the base metals (factor 1).

Factor 5, As-Mo, is probably related to the base metal sulphides. Although both components show relatively low geochemical relief in southern Melville Peninsula, Laporte (1974) reported high concentrations of Mo in drill intersections and soils near base metal occurrences within the Penrhyn Group.

Follow-up

Objectives

High concentrations of uranium in the lake sediments and waters in southern Melville Peninsula most likely reflect uranium enrichment in the bedrock. This is confirmed by the airborne radiometric data which generally show a high level of radiation in the areas of anomalous lakes. It is not known whether any of this uranium exists in economic concentrations.

The main objectives of the follow-up were (1) to determine which rock type(s) is responsible for the high uranium background and widespread lake sediment and water anomalies, and (2) to investigate whether favourable conditions for economic concentrations of uranium exist in southern Melville Peninsula.

Selection of study area and methodology

With respect to the first objective, traversing at random in areas of strong geochemical anomalies would have been sufficient. However, in order to focus on possible economic targets it was essential to apply discriminant parameters to select areas for follow-up. Geochemical indicators are often useful but since there were no known uranium occurrences that could be studied in southern Melville Peninsula, the nature of the element assemblages in the mineralization sought was unknown. Furthermore, the dispersion patterns for most potential pathfinders were complicated by numerous metalliferous concentrations in the rocks (i.e. base metal sulphides), most likely unrelated to uranium.

The most satisfactory procedure to identify potential areas in the Penrhyn Group was to use the airborne radiometric data in conjunction with the uranium geochemistry. Radiometric anomalies that occurred within or in proximity to geochemical anomalies were selected for detailed work. Priority was given to anomalies with high eU/eTh ratios and an attempt was made to select areas from different geological environments.

Table 45.1

Abundance of Uranium in lake sediments in various parts of the Canadian Shield

Area	Map number (NTS)	no. of samples	U in lake sediments geom. mean (ppm)
Baffin Island	36B-C	406	10.4
Baker Lake	55M	688	4.7
	65P	656	4.4
Ennadi Lake	65A	779	14.5
	65B	853	17.3
	65C	894	12.1
Labrador	13B	1026	0.8
	13F	825	1.7
	13G	832	0.8
	13H; 3E	758	1.5
	13J-O	865	5.9
Manitoba	54L	458	1.3
	54M	461	7.0
	64I	929	3.4
	64P	907	6.4
	64J-K-N-O	3661	8.0
Melville Peninsula	46N; 47B	1108	19.6
	46O-P; 47A	1098	16.9
Nonacho Lake	75C-F-K	2685	9.2
Ontario	31F	166	6.1
	42D-E	915	3.6
	52A-H	922	2.3
Saskatchewan	63M; 64D	3844	4.9
	64L-M	2019	6.3

In the northwestern part of the survey area, the existence of an unconformity adjacent to U-enriched basement rocks and the presence of a thick regolith at the paleosurface, was thought to constitute a favourable situation; detailed work was planned in that area.

The work performed consisted of ground traverses chosen to incorporate anomalous lake basins and/or radiometric anomalies; special care was taken to run traverses over such features as contact zones, structures, unconformities gossans, etc. In several cases, detailed lake waters were collected and analyzed prior to traversing in order to better define the anomalies. The water samples were analyzed in a field laboratory for U and pH. The uranium determinations were performed using a Scintrex UA-3 laser fluorimeter (Robbins, 1978).

Follow-up in the Penrhyn Group

Area 1 (Fig. 45.1) is one of several selected for detailed follow-up within the Penrhyn. About 250 lake water samples were collected and the results are shown in Figure 45.3. The area was chosen because (1) it contains a good selection of geochemical and airborne radiometric anomalies, (2) the radiometric anomalies are characterized by high eU/eTh ratios and (3) the reconnaissance data indicated that uranium was present in substantial amounts in the lake waters because of generally alkaline conditions.

Figure 45.3 indicates that there is generally good correspondence between the geochemical and radiometric data. Four ground traverses were carried out on the basis of these results and in all cases, radioactive felsic intrusives were encountered (localities 1 to 4, Fig. 45.3). These rocks intrude Penrhyn sediments, mostly crystalline limestone and paragneiss, but, in this area, the sediments in contact with the intrusives were not found to be radioactive or to have been affected in any way by the igneous activity.

The most interesting occurrence was found at locality 1 (Fig. 45.3). The radioactive rocks seem to underlie most of the area within the 5 ppb U contour line. Near the western edge of the intrusion, felsic sills intrude crystalline limestones. The sills are sometimes highly radioactive, and some show secondary uranium minerals. Chemical or mineralogical analyses of rock samples from that area are not available at the time of writing but radiometric analyses performed in Ottawa estimated the amount of uranium and thorium of one sample at 1200 ppm eU and 400 ppm eTh. In the field, readings of up to 2000 ur* were recorded on these sills. The main intrusive body gave field readings in the order of 500 to 900 ur. For comparison, nearby limestones produced less than 25 ur.

The granitic rocks at localities 2, 3 and 4 are not as radioactive: up to 175 ur at locality 2, 450 ur at locality 3, and 250 ur at locality 4. Nevertheless, they probably contain sufficient uranium to account for the anomalies detected in their vicinity. At all these localities, the uranium minerals appear to be disseminated rather than concentrated in fractures.

Several other radioactive occurrences have been found within the Penrhyn Group (Table 45.3). All are related to felsic intrusives penetrating Penrhyn sediments except at locality 5 where a radioactive skarn-type rock within metasediments was found in contact with a granitic intrusive. The skarn is soft, dark green and appears to be very local. The maximum radiometric response from this rock, measured in the field, was

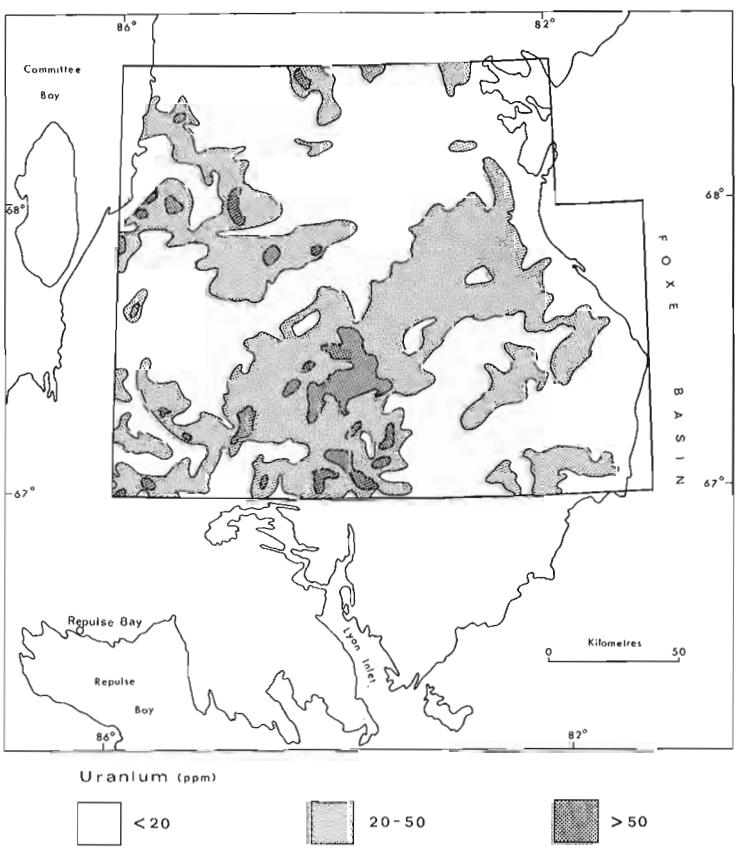


Figure 45.2. *Uranium distribution in lake sediments for 1977 U.R.P. survey in southern Melville Peninsula.*

* Unit of radioelement; a geological source with 1 ur concentration produces the same instrument response (e.g. count rate) as an identical source containing 1 ppm uranium in radioactive equilibrium (International Atomic Energy Agency, 1976).

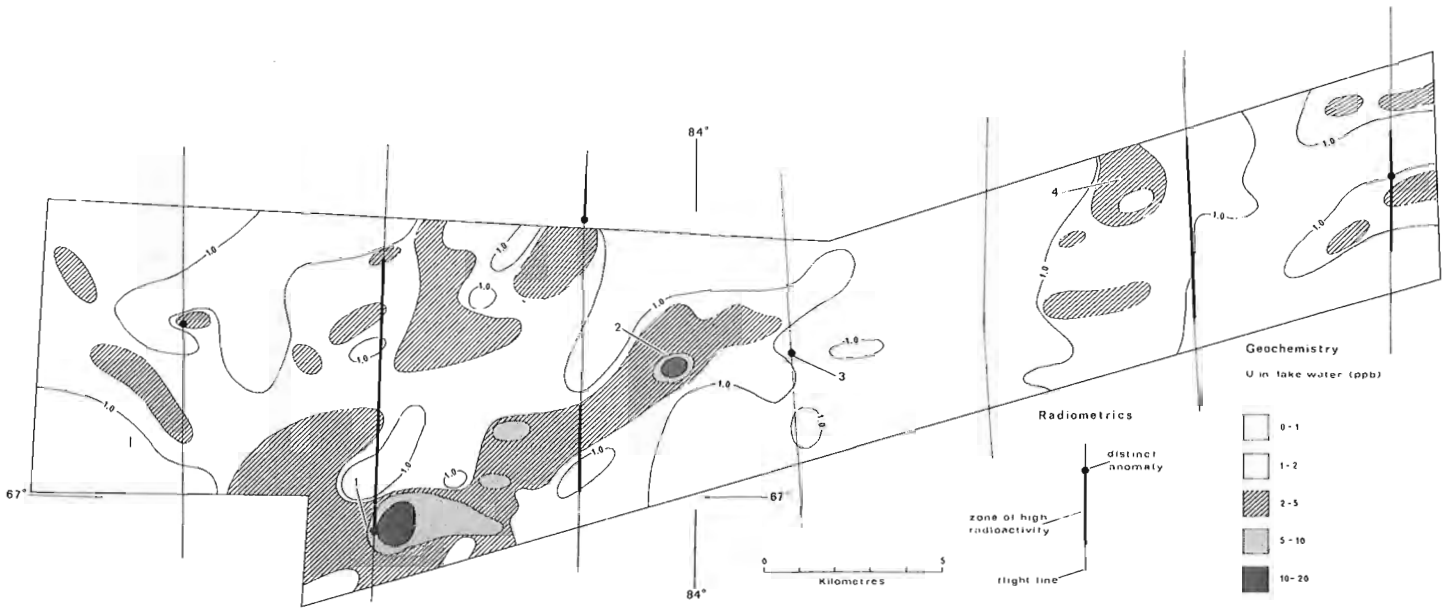


Figure 45.3. *Detailed uranium in lake water and radiometric data for area 1, Figure 45.1.*

450 ur. Laboratory measurements on a selected sample estimated the uranium and thorium contents at 400 ppm eU and 200 ppm eTh.

Petrological and minerological data for samples collected at locality 5 are not available at the time of writing so that one can only speculate on the nature and origin of the uranium in this rock. If, as suspected, contact metasomatism is involved, this occurrence could represent an important type of deposit to search for in southern Melville Peninsula. However, skarns and other contact metamorphic features do not appear to be common in the Penrhyn Group even though they have been reported (Hutcheon et al., 1977).

No common feature could be established among the various radioactive intrusives encountered. Their colour, mineralogy and texture are highly variable. They were probably emplaced over a long period of time as is suggested by the fact that some are foliated (preorogenic) while others are not (postorogenic).

Follow-up in the northwest corner

Figure 45.4 shows the results of a lake water survey carried out in an area that incorporates the Late Precambrian sediments (Frisch, 1974) and adjacent basement rocks (Area 2, Fig. 45.1). Because of the near absence of carbonate rocks resulting in slightly acidic lake waters, the uranium content of these waters was expected to be considerably lower than in the area underlain by the Penrhyn Group where high concentration of bicarbonate in the lake waters tends to keep the uranium in solution.

The results show a substantial increase in uranium in an area of granitoid basement rocks adjacent to the southern part of the Late Precambrian formation. It is of interest that the uranium concentrations increase towards the unconformity. Because the water samples were not analyzed in the field and airborne radiometric data were unavailable for that area, it was not possible to plan the ground work most efficiently. Nevertheless, the unconformity and adjacent rocks were examined at five different localities (A to E, Fig. 45.4).

At locality A, basement granites intruding a darker, gabbroic phase, were found to be slightly radioactive with maximum radioactivity concentrated along fractures (up to 120 ur). Radioactivity in the Late Precambrian sediments is low (<20 ur) except within a phyllite bed that occurs near the base within the conglomerates (up to 50 ur). T. Frisch (pers. comm.) found allanite in these phyllites which probably accounts for the increased radioactivity. Above background radioactivity was also found at locality C (Fig. 45.4) where the unconformity is very well exposed. The radiation (max. 45 ur) seem to be associated with a dark magnetite-bearing sandstone at the base of the Late Precambrian formation within inches of the unconformity.

Conclusions

Radioactive felsic igneous rocks that intrude the Penrhyn Group of metasediments constitute the bedrock source of widespread uranium enrichment in the lake sediments and waters of southern Melville Peninsula. Zones of high radioactivity were discovered in some of these intrusives and their economic potential should be examined in

Table 45.2

Varimax factor matrix of logarithmically transformed lake sediment and water data, southern Melville Peninsula, District of Franklin

Factor	Communality (%)	Components and Factor Loadings
1	39	Fe(.9), Co(.9), Ni(.8), Zn(.8), Cu(.8), Mn(.8), Pb(.7)
2	19	pH(.9), U_w(.8), F_w(.7)
3	10	LOI(.8), Hg(.5)
4	6	U_s(.8), Pb(.5)
5	5	As(.8), Mo(.7)

Note (1) pH, U_w, F_w = lake water data
(2) Only factor loadings $\geq$.5 are shown

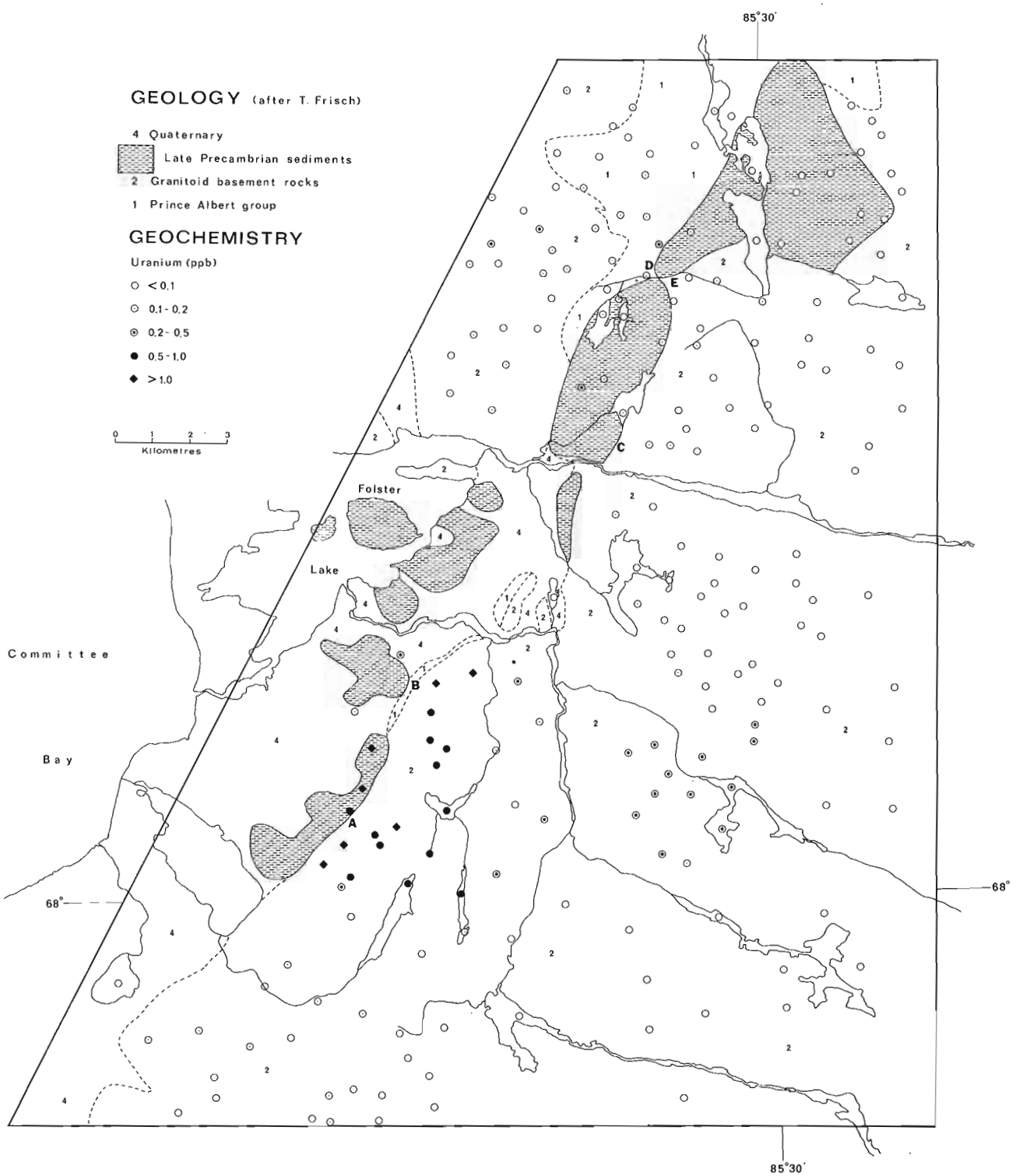


Figure 45.4. *Regional geology and detailed lake water data for uranium for area 2, Figure 45.2.*

the light of recent publications on the subject of uranium deposits in granites and similar rocks (Armstrong, 1974; Ruzicka, 1975; Derry, 1977). Future exploration in the area should search for uraniferous late magmatic differentiates or vein-type hydrothermal deposits more or less closely associated with the radioactive plutons. Certain types of intrusives, namely alaskite, leucocratic granite, two-mica granite, monzonite and granodiorite may be particularly favourable because similar rocks are known to host uranium concentrations in other parts of the world.

With respect to other types of deposits, two possibilities deserve further examination in southern Melville Peninsula:

1 - Skarn-type or contact metasomatic deposits

2 - Unconformity-type deposits.

The skarn-type deposits should be searched for at the contact of radioactive intrusives with highly reactive rocks such as carbonates. Preorogenic intrusives are perhaps more favourable than postorogenic intrusives as the

Table 45.3

Location of radioactive occurrences in southern Melville Peninsula

Localities	—(UTM co-ordinates)— Zone	Eastings	Northings	Max. radioactivity (ur)
1	16	622550	7433090	2000
2	16	629870	7437810	175
3	17	371860	7437730	450
4	17	380230	7441800	250
5	16	553340	7435630	450
6	17	374010	7483410	400
7	17	388630	7469990	450
8	16	627590	7444270	200
9	16	627670	7442230	200

Note: Localities 1, 2, 3 and 4 are shown in Figure 45.3

unmetamorphosed sediments are more likely to have undergone contact metamorphism and metasomatism than the regionally metamorphosed sediments. However, this need not be the case; the Mary Kathleen orebody, a metasomatic uranium deposit in Australia, was formed in proximity to a granodiorite which intruded regionally metamorphosed Proterozoic sediments composed essentially of calc-silicate rocks, schists and quartzites (Hughes and Munro, 1965).

Both the reconnaissance geochemical and radiometric data indicate the basement rocks in the vicinity of the Penrhyn Group to be relatively low in uranium. This situation and the high metamorphic grade of Penrhyn sediments has drawn the attention away from the Penrhyn unconformity as a possible host of uranium mineralization.

The Late Precambrian unconformity in the northwest of the study area, however, is more promising. A uranium-enriched basement adjacent to relatively unmetamorphosed and undeformed Late Precambrian sediments, and the presence of a thick regolith, is attractive. In addition, our investigations have shown an increase in the uranium content of the basement in the immediate vicinity of the unconformity with possible enrichment along fractures, suggesting remobilization.

Acknowledgments

Enthusiastic assistance in the field was provided by Michel Fortier (University of Ottawa) and Paul MacKay (Queen's University). G.E.M. Hall (G.S.C.) and Moire Wadleigh (Carleton University) skillfully performed the water analyses in the field. Larry Cotter (helicopter pilot) is also gratefully acknowledged. Special thanks are directed to T. Frisch for generously supplying unpublished geological data appearing in Figures 45.1 and 45.4. E.M. Cameron provided some useful comments on the manuscript.

References

Armstrong, F.C.
1974: Uranium resources of the future – "Porphyry" uranium deposits; in Formation of Uranium Ore Deposits, International Atomic Energy Agency, Ser. no. STI/PUB/374, p. 625-634.

Cameron, E.M.
1979: Investigation of base metal mineralization in Proterozoic metasediments, Melville Peninsula, District of Franklin; in Current Research, Part A, Geological Survey of Canada, Paper 79-1A, report 32.

Cameron, E.M. and Hornbrook, E.H.W.
1976: Current approaches to geochemical reconnaissance for uranium in the Canadian Shield; in Exploration for Uranium Ore Deposits, International Atomic Energy Agency, Ser. no. STI/PUB/434, p. 241-262.

Darnley, A.G., Cameron, E.M., and Richardson, K.A.
1975: The Federal-Provincial Uranium Reconnaissance programs; in Uranium Exploration 1975; Geological Survey of Canada, Paper 76-26, p. 49-68.

Derry, D.R.
1977: New types of deposits will provide future supplies of uranium; Canadian Mining Journal, March, p. 56–60.

Frisch, T.
1974: Geological studies in the Prince Albert Hills, western Melville Peninsula, District of Franklin; in Report of Activities, Part A, Geological Survey of Canada, Paper 74-1A, p. 163-164.

Geological Survey of Canada
1978a: National Geochemical Reconnaissance release, regional lake sediment and water geochemical reconnaissance data, Melville Peninsula, N.W.T. NGR 32A-1977 or 32B-1977, NTS 46N and part of 47B; Geological Survey of Canada, Open File 521A or 521B.

1978b: National Geochemical Reconnaissance release, regional lake sediment and water geochemical reconnaissance data, Melville Peninsula, N.W.T. NGR 33A-1977 or 33B-1977, NTS 46Ø, P and part of 47A; Geological Survey of Canada, Open File 522A or 522B.

Heywood, W.W.
1967: Geological notes, northeastern District of Keewatin and southern Melville Peninsula, District of Franklin, Northwest Territories (Parts of 46, 47, 56, 57); Geological Survey of Canada, Paper 66-40, 20 p.

Hornbrook, E.H.W. and Garrett, R.G.
1976: Regional geochemical lake sediment survey, east-central Saskatchewan; Geological Survey of Canada, Paper 75-41, 20 p.

Hughes, F.E. and Munro, D.L.
1965: Uranium ore deposit at Mary Kathleen; in Geology of Australian Ore deposits, Proceedings Eight Commonwealth Institute of Mining and Metallurgy (J. McAndrew, ed.), v. 1, p. 256-263.

Hutcheon, I., Gunter, A.E., and LeCheminant, A.N.
1977: Serendibite from Penrhyn group marble, Melville Peninsula, District of Franklin; Canadian Mineralogist, v. 15, p. 108-112.

International Atomic Energy Agency
1976: Radiometric reporting methods and calibration in uranium exploration; STI/DOC/10/174, 57 p.

Laporte, P.J.
1974: Melville Peninsula, Prospecting Permits 177 to 199; North of 60, Mineral Industry Report 1969 and 1970; Canada Department of Indian and Northern Affairs, Northwest Territories east of 104 west longitude, v. 2, p. 123-129.

Maurice, Y.T.
Methods of interpretation and follow-up of reconnaissance lake sediment data in the northern Canadian Shield; 7th International Geochemical Exploration Symposium, Denver, 1978. (in press)

Okulitch, A.V., Gordon, T., Henderson, J.R., Reesor, J.E., and Hutcheon, I.E.
1977: Geology of the Barrow River map-area, Melville Peninsula, District of Franklin; in Report of Activities, Part A, Geological Survey of Canada, Paper 77-1A, p. 213-215.

Reesor, J.E., LeCheminant, A.N. and Henderson, J.R.
1975: Geology of the Penrhyn Group metamorphic complex, Melville Peninsula, District of Franklin; in Report of Activities, Part A, Geological Survey of Canada, Paper 75-1A, p. 349-351.

Robbins, J.C.
1978: Field technique for the measurement of uranium in natural waters; Canadian Institute of Mining and Metallurgy Bulletin, v. 71, no. 793, p. 61-67.

Ruzicka, V.
1975: New sources of uranium? Types of uranium deposits presently unknown in Canada; in Uranium Exploration '75, Geological Survey of Canada, Paper 75-26, p. 13-20.

Schau, M.
1975: Volcanogenic rocks of the Prince Albert group, Melville Peninsula (47A-D), district of Franklin; in Report of Activities, Part A, Geological Survey of Canada, Paper 75-1A, p. 359-361.

Wilson, I.D.H. and Underhill, D.H.
1971: The discovery and geology of major new new iron deposits on Melville Peninsula eastern Arctic; Canadian Mining Journal, v. 92, p. 40-48.

46. COPPER METALLOGENY, NORTH SHORE REGION OF LAKE HURON, ONTARIO

Project 700059

William N. Pearson[1]
Regional and Economic Geology Division

Pearson, William N., Copper metallogeny, north shore region of Lake Huron, Ontario; in Current Research, Part A, Geol. Surv. Can., Paper 79-1A, p. 289-304, 1979.

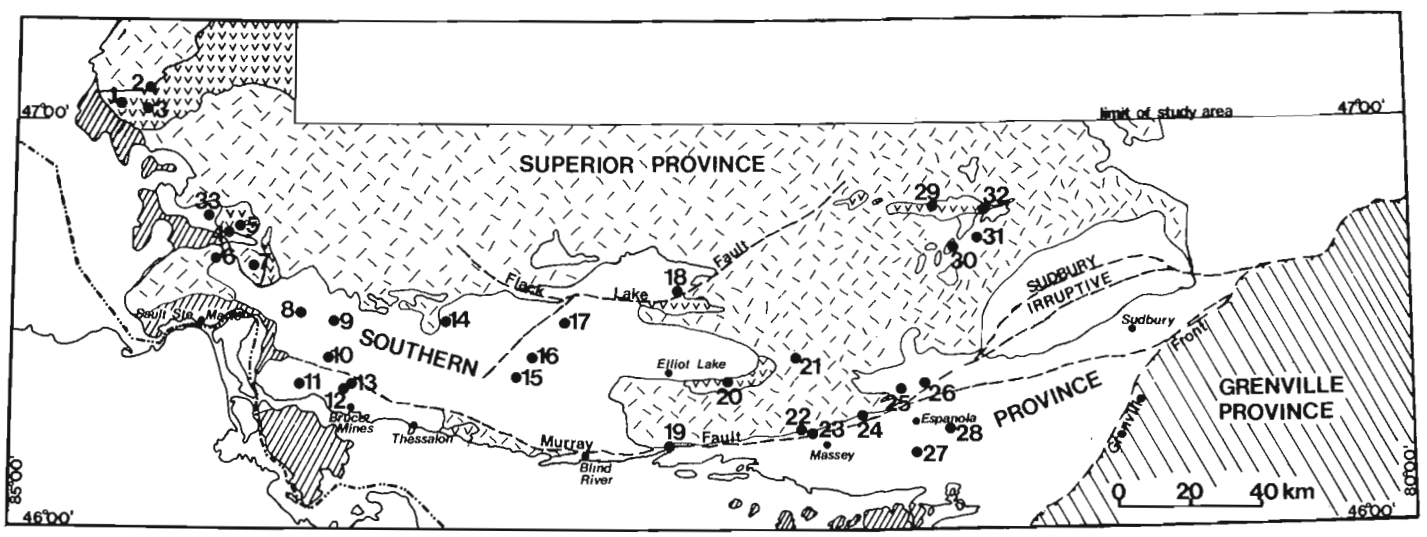
Abstract

Vein deposits, a W-Cu skarn deposit, a Cu-Ni deposit, "sedimentary" copper deposits, and possible volcanogenic exhalative deposits in the north shore region of Lake Huron are described in detail. New subdivisions within several copper deposit groups previously presented (Pearson, 1978) are proposed and a preliminary metallogenic scheme relating copper deposits to major lithologic units and tectonic events is discussed.

Introduction

A study of copper deposits in the north shore region of Lake Huron (N.T.S. 41I, J, K, and N/1, N/2; Fig. 46.1) was initiated in 1977 during which time 104 deposits and occurrences were examined. A tentative classification, brief descriptions of some occurrences and various deposit types, and preliminary thoughts on copper metallogeny were presented (Pearson, 1978). Work in the summer of 1978 focused on detailed mapping of representative deposits with the aim of clarifying genesis. Samples were collected for petrographic, isotopic, and chemical analyses.

The author is grateful to R.V. Kirkham of the Geological Survey of Canada for his continued help in this project and to D. Innes, Ontario Division of Mines, Mineral Deposits Section, in Sudbury, and P. Giblin, Regional Geologist, E.J. Leahy, and G. Bennett of the Ontario Division of Mines in Sault Ste. Marie for their invaluable support during the field work. Many local residents, prospectors, and industry and government geologists gave freely of information, services, and much enjoyed hospitality. R.V. Kirkham reviewed the manuscript and offered many helpful suggestions.



Late Precambrian and Paleozoic rocks
GRENVILLE PROVINCE
SOUTHERN PROVINCE
SUPERIOR PROVINCE
granitic rocks
metavolcanic rocks

1. *Jogran porphyry*
2. *Tribag Breccias (East, West, Breton, and South Breccias)*
3. *Palmer Township Breccia*
4. *Kirby-Legge*
5. *Kerr-Scott*
6. *Nystedt*
7. *Jardun Mines*
8. *Gimby*
9. *2-Horse Lake*
10. *minor copper occurrence in Gowganda Formation*
11. *Desbarats*
12. *Steinberg*
13. *Bald Dome*
14. *Gould Copper Mine*
15. *Montgomery Township occurrences*
16. *Crownbridge*
17. *White River Lead Prospect*
18. *Stag Lake*
19. *Pater Mine*
20. *East Pecors*
21. *East Bull Lake*
22. *Hermina Mine*
23. *Massey Mine*
24. *Alexander and Bishop occurrences*
25. *Falconbridge and Noranda Shakespeare prospects*
26. *Spanish River Mines*
27. *Mongowin Pluton*
28. *Foster Township W Prospect*
29. *Stralak*
30. *Hart Township skarn deposit*
31. *Hess Township magnetite occurrence*
32. *Lake Geneva Mine*
33. *Prace Mine*

Figure 46.1. *Locations of deposits and occurrences referred to in text and simplified geology of study area (after Card, 1978).*

[1]Department of Geological Sciences, Queen's University, Kingston, Ontario K7L 3N6

Regional Geological Setting

The project area is underlain predominantly by Proterozoic supracrustal rocks of the Southern Province, Archean granitic, metavolcanic, and metasedimentary rocks of the Superior Province, and highly deformed and metamorphosed rocks of the Grenville Province (Fig. 46.1; Pearson, 1978). Major lithologic units and tectonic events are summarized in Table 46.1. Detailed accounts of geology of the Southern Province and adjacent areas are given by Card et al. (1972) and Card (1978).

Geology of the Copper Deposits

As noted previously (Pearson, 1978) copper occurrences are highly varied in nature and are present within a wide spectrum of geological settings ranging from Archean granites to Paleozoic sediments. The tentative classification of copper deposit groups presented in 1978 and used here is as follows:

1. veins
2. contact metasomatic deposits
3. copper-nickel deposits in mafic and ultramafic intrusions
4. "sedimentary" copper deposits
5. volcanogenic massive sulphides and stringer zones
6. porphyry deposits

Work in 1978 has led to reassignment of several deposits into different categories and a revision and expansion of subtypes within the deposit groups. In this paper, subtypes within several deposit groups will be proposed, individual deposits within major groups described, and a preliminary copper metallogenic scheme presented.

Veins

On the basis of ore mineralogy and metal contents the veins were separated into four major types (Pearson, 1978):

1. chalcopyrite-pyrite ± specularite-bearing veins with minor precious metal contents
2. polymetallic veins of three main types – Zn-Pb-Ag-Cu, Pb-Ag-Cu, and Cu-Co ± Bi ± U ± Ni
3. bornite-chalcocite-native copper-bearing veins; and
4. Au-bearing arsenopyrite-pyrite-quartz veins with minor chalcopyrite

Based on 1978 field work, some general observations on vein deposits are as follows:

a. Vein deposits, although numerous throughout the Southern Province, are scarce within Superior Province rocks except in the Sault Ste. Marie area and north of Massey.

   The Zn-Pb-Ag-Cu veins in the Sault Ste. Marie (e.g. Jardun Mines, Kerr-Scott, Kirby-Legge, and Prace Mine) are hosted predominantly in Archean granitic and volcanic rocks, but are also present in argillite and paraconglomerate of the Gowganda Formation. These deposits typically consist of early galena-sphalerite-pyrite-chalcopyrite veins that are cut by later, commonly barren or weakly mineralized quartz-carbonate veins. Preliminary Pb isotope results from the Prace Mine suggest that these occurrences are probably related to the Keweenawan rift system.

   At the Hermina Mine, 13 km northwest of the town of Massey, a chalcopyrite-bearing quartz vein system is associated with a very dark coloured diabase dyke cutting Archean granite. The vein system is approximately 11 m wide, dips steeply northward and has been traced for a strike length of 970 m. In 1903 and 1904 a total of 454 701 kg of copper was produced from this system (Robertston, 1976). As noted by Robertson, the proximity of the deposit to the Huronian gabbro-anorthosite intrusions of the Massey area as well as the lithological similarity of the associated dyke to metadiabase within the mafic intrusions suggest that it and other similar but smaller copper-bearing quartz veins cutting Archean granite north of Massey may be genetically related to the mafic intrusive suite.

b. Many of the abundant quartz-carbonate-pyrite ± specularite vein swarms and vein breccia zones of the Elliot Lake region (e.g. Montgomery Township, Crownbridge, and Gould Copper Mine) are hosted in the Gowganda Formation. These breccia zones contain angular, commonly silicified and hematized fragments cemented by a quartz-carbonate-sulphide matrix. The matrices lack rock flour and the fragments are not generally sheared, suggesting that these zones are probably tensional in origin. The vuggy, crustiform nature of many of these deposits indicates an origin by open space filling; however, the source of metals is speculative.

c. At the Steinberg prospect, located 5 km north of Bruce Mines, an atypical quartz-carbonate-chalcopyrite-pyrite cemented vein breccia occurs in the Gowganda Formation (Fig. 46.2). The breccia fragments, consisting of silicified and hematized quartzite, are strongly aligned in a north-south trending zone that dips approximately 55° to the west. Published reserves are 112 700 tonnes grading 1.1% Cu (Shklanka, 1969, p. 56).

   The Bald Dome prospect, 2.6 km northeast of Steinberg, is a sheeted quartz-carbonate-chalcopyrite-pyrite vein system and vein breccia zone that occurs along a Nipissing diabase dyke and Gowganda siltstone contact. Many of the diabase and siltstone fragments are silicified and hematized and some, particularly those of altered diabase, contain finely disseminated chalcopyrite.

   The vein-like and breccia character of these two deposits and the similarity of their mineral assemblages to those of vein deposits in the Elliot Lake region, suggest that these deposits probably represent slight morphological variations of the quartz-carbonate-chalcopyrite-specularite vein group. The proximity of Nipissing Diabase intrusions to both occurrences suggests that there may be a genetic relationship between brecciation and copper mineralization and intrusive activity.

Contact Metasomatic Deposits

Contact metasomatic deposits developed in Huronian sedimentary rocks thermally metamorphosed by Nipissing Diabase intrusions are of two major types: (1) skarns that have formed within calcareous rocks of the Espanola Formation; and (2) deposits formed within noncalcareous sedimentary rocks that lack the calc-silicate assemblages typical of skarns. The discussion following will focus on skarn deposits; brief descriptions of contact metamorphic deposits lacking skarn mineralogy are given in Pearson (1978).

On the basis of their metal contents skarns are of three major types: (1) Fe-Cu; (2) Zn-Pb-Co-Cu; and (3) W-Cu-Mo-Zn.

Fe-Cu-bearing skarns are the most prevalent and typically are magnetite-rich with subordinate amounts of chalcopyrite and pyrite. The source of iron and copper is most probably the Nipissing Diabase intrusions and the presence of abundant magnetite indicates that oxygen fugacity was high relative to sulphur fugacity during deposit formation. This skarn type is present throughout the field area, notably at



Figure 46.2.

Quartz-carbonate-pyrite-chalcopyrite cemented breccia with orientated fragments of pink quartzite, Steinberg prospect. GSC 202516-Y.

Cobden River, 11 km north of Iron Bridge, Two-Horse Lake, located 16 km east of Echo Bay, and Hess Township, 1.5 km north of Cartier.

AZn-Pb-Co-Cu-bearing skarn in northern Hart Township has been described by Card and Innes (1976). At this locality contact metamorphosed rocks of the Espanola and Serpent formations contain veins, disseminations, and pods of magnetite, pyrite, sphalerite, galena, chalcopyrite, cobaltite, and smaltite. The deposit is erratically developed over approximately 300 m near the contact of a Nipissing Diabase intrusion. Calc-silicate minerals present include diopside, wollastonite, pectolite, and tremolite (Card and Innes, 1976).

The only known W-bearing skarn deposit is in Foster Township 19 km east of Espanola. This occurrence is unusual both because of the presence of tungsten and because of the extent of skarn development. Further, it is probably one of the oldest tungsten-bearing skarn deposits known, having been formed during Nipissing Diabase intrusion about 2150 Ma ago.

At the Foster Township locality tungsten occurs predominantly as fracture-controlled and disseminated scheelite associated with pyrrhotite, pyrite, chalcopyrite, molybdenite, and spahlerite in idocrase-diopside-garnet skarn developed in the Espanola Formation (Card, 1968a). The mineralization is erratic, but extensive, occurring over an area of approximately 450 by 1500 m. Samples assayed have yielded up to about 0.5% WO_3, 0.27% MoS_2, 0.29% Cu, and 0.36 oz/ton Ag (Card, 1978).

Figure 46.3 is a geological map of the Foster Township W area. The central portion of the figure encompassing the known mineral occurrences was mapped by the writer at a scale of 1 cm = 48 m. The geology of the surrounding area is taken from Card (1967) and stratigraphy is after Card (1978).

Sedimentary rocks in the map area comprise massive to poorly bedded feldspathic quartzite of the Serpent Formation and calcareous siltstone, siltstone, and limestone and their contact metamorphosed equivalents of the Espanola Formation. The contact between the Espanola and Serpent formations is conformable and gradational with small (about 0.5 to 1 m thick) calcareous siltstone beds near the base of the Serpent Formation. These rocks have been intruded by a northeast trending Nipissing diabase-gabbro intrusion and several small Keweenawan diabase dykes.

The degree of deformation and extent of skarn development is markedly different south of the Nipissing Diabase intrusion as compared to the north of it, despite the presence of Espanola Formation on both sides. To the south the Espanola and Serpent formations are folded into a tight overturned syncline and anticline couplet. The diabase-gabbro intrusion forms the core of the overturned anticline, however it is uncertain whether this intrusion is a sill conformable with folded Espanola Formation or a dyke occupying the axial region of the anticline. To the west of the deposit an extensive network of barren quartz veins and quartz-cemented breccia is developed in the hinge region of this fold. The breccia fragments are silicified in places but most are essentially unaltered. No significant movement occurred during brecciation and most fragments appear to have been merely pulled apart from their immediate neighbours by tensional forces that were probably generated during the latter stages of intense folding. Small scale, parasitic fold structures are well developed in the Espanola Formation on the south limb of the overturned syncline. Small fold axes plunge approximately 45° southwest and their axial planes strike northeast and dip 75° to 80° southeast.

Skarn development is pervasive throughout the Espanola Formation south of the intrusion as far as the major northeast trending fault that truncates the fold structure. North of the intrusion the Espanola Formation is much less deformed and contact metamorphic effects are limited to 1-2 m or less along the intrusive contact. The extensive quartz-cemented tension or "pull-apart" breccia-vein zone is cut by a sporadically developed spaced cleavage (H. Helmstaedt, pers. comm., 1978) which may be the last fabric to form during this Hudsonian deformation or be a later structure related to a Grenville overprint.

The Nipissing Diabase intrusion varies in width and lithology across the map area. In the central part of Figure 46.3 the intrusion is relatively thin and consists of pyritic diabase whereas its presumed northeast and southwest extensions are much more extensive and comprise gabbro containing only minor pyrite. The intrusion, therefore, is noticeably constricted and much finer grained in the area of skarn formation. In the most southwesterly pit adjacent to the synclinal fold hinge, a small (20 cm wide) highly pyritic diabase (?) dyke cuts the sedimentary rocks. The diamond-drill logs on file at the Resident Geologist's office, Ontario Division of Mines, Sudbury note many intersections of pyritic diabase. These diabase dykes were probably synchronous with, and altered at the time of skarn development.

Table 46.1

Major lithologic units and tectonic events, north shore region of Lake Huron, Ontario
(modified after Card, 1978 and Card et al., 1972)

	Approximate radiometric Age (Ma)
PHANEROZOIC	
CENOZOIC	
QUATERNARY	
Recent	
Swamp, lake and stream deposits	
Pleistocene	
Continental glaciation; erosion; deposition of sand, gravel and clay.	0.1-1
EROSION	
FAULTING	
PALEOZOIC	
ORDOVICIAN-SILURIAN	
Limestone, dolomite, and shale	
EROSION-LIPPALEAN INTERVAL	400-500
UNCONFORMITY	
PRECAMBRIAN	
HADRYNIAN(?)	
JACOBSVILLE FORMATION	
Sandstone, conglomerate, and shale	
GRENVILLE PROVINCE	
HADRYNIAN(?)	
FAULTING AND UPLIFT	
LATE PEGMATITE DYKES	
GRENVILLE OROGENY	1000 (Stockwell, 1972)
HELIKIAN	
FELSIC PLUTONIC ROCKS	
quartz monzonite, granodiorite, tonalite	1400
MAFIC INTRUSIVE ROCKS	
amphibolite, metagabbro	
INTRUSIVE CONTACT	
APHEBIAN-ARCHEAN	
METASEDIMENTARY ROCKS	
biotite and quartz feldspar gneiss, coarse clastic, siliceous, and calcareous metasedimentary rocks	

	Approximate radiometric Age (Ma)
INTRUSIVE CONTACT	
HURONIAN SUPERGROUP	
COBALT GROUP	
Bar River Formation – white orthoquartzite, ferruginous sandstone, and siltstone	
Gordon Lake Formation – finely bedded, varicoloured siltstone, argillite, and subordinate sandstone	
Lorrain Formation – arkose, hematitic and aluminous sandstone with quartz-jasper pebble conglomerate lenses, white orthoquartzite, minor purple siltstone, and green argillite	
Gowganda Formation – heterogeneous assemblage of paraconglomerate, orthoconglomerate, feldspathic sandstone, siltstone, and laminated argillite	
LOCAL DISCONFORMITY	
QUIRKE LAKE GROUP	
Serpent Formation – feldspathic sandstone, minor siltstone, limestone, and conglomerate	
Espanola Formation – calcareous siltstone and sandstone, limestone, and dolomite	
Bruce Formation – massive conglomerate with local sandstone and pelite interbeds	
LOCAL DISCONFORMITY	
HOUGH LAKE GROUP	
Mississagi Formation – quartz-feldspar sandstone with subordinate siltstone and argillite; minor conglomerate	
Pecors Formation – greywacke, siltstone, and mudstone with subordinate feldspathic sandstone	
Ramsay Lake Formation – conglomerate, siltstone, and sandstone	

FAULTING

SOUTHERN PROVINCE

HELIKIAN

LAKE SUPERIOR BASIN

Keweenawan flood basalts and continental red clastic sediments — 1000-1100

FELSIC INTRUSIVE ROCKS

felsite, quartz porphyry, quartz-feldspar porphyry; breccia pipes

MAFIC INTRUSIVE ROCKS

diabase dykes; amphibolite, metagabbro, trap, lamprophyre dykes; fenite breccia — 1200-1400?

CROKER ISLAND COMPLEX

monzonite-syenodiorite, diorite-gabbro, quartz monzonite — 1475

"HUDSONIAN-PENOKEAN" OROGENY

APHEBIAN

EDEN LAKE PLUTONS

trondhjemite, diorite, gabbro

GRENVILLE FRONT PLUTONS

quartz monzonite, quartz diorite, and granodiorite — 1600-1730

CUTLER GRANITE

granite, pegmatite — 1750

MONGOWIN PLUTON

peridotite, granophyric trondhjemite — 1770

INTRUSIVE CONTACT

WHITEWATER GROUP

Chelmsford Formation – greywacke
Onwatin Formation – carbonaceous and pyritic siltstone
Onaping Formation – tuff-breccia

SUDBURY NICKEL IRRUPTIVE

norite, gabbro, granophyre — 1956 ± 98 (Gibbons and McNutt, 1976)

INTRUSIVE CONTACT

NIPISSING DIABASE

gabbro, metagabbro, granophyre — 2150 (Van Schmus, 1965)

EARLY DEFORMATION

CREIGHTON PLUTON

quartz monzonite, granite — 2200

LOCAL DISCONFORMITY

MAFIC INTRUSIVE ROCKS –

Gabbro-anorthosite intrusions – gabbro metagabbro, anorthositic gabbro, gabbroic anorthosite, syenite
– amphibolite and metagabbro dykes

ELLIOT LAKE GROUP

McKim Formation – greywacke, laminated siltstone-argillite, and quartz-feldspar sandstone
Matinenda Formation – quartz-feldspar sandstone, siltstone, argillite, and uraniferous quartz pebble conglomerate
Thessalon Formation – metabasalt, minor metasedimentary rocks
Copper Cliff Formation – rhyolite, dacite, felsic intrusions, porphyry, crystal tuff and other pyroclastic rocks, minor metabasalt, and metasedimentary rocks
Stobie Formation – metabasalt, fragmental mafic metavolcanic rocks, mafic schist, metasedimentary rocks
Salmay Lake Formation – metabasalt, fragmental mafic metavolcanic rocks, metasedimentary rocks
Elsie Mountain Formation – metabasalt, minor metasedimentary rocks

INTRUSIVE CONTACT; FAULTING; EXTENSIVE EROSION

SUPERIOR PROVINCE

ARCHEAN

KENORAN OROGENY

FELSIC PLUTONIC AND MIGMATITIC ROCKS — 2550

Birch Lake Batholith, Gros Cap Batholith
Algoman Granite – granite, quartz monzonite, granodiorite, quartz diorite, and migmatitic granitic rocks

KEEWATIN GREENSTONE

– mafic and acid metavolcanic rocks; metasedimentary rocks

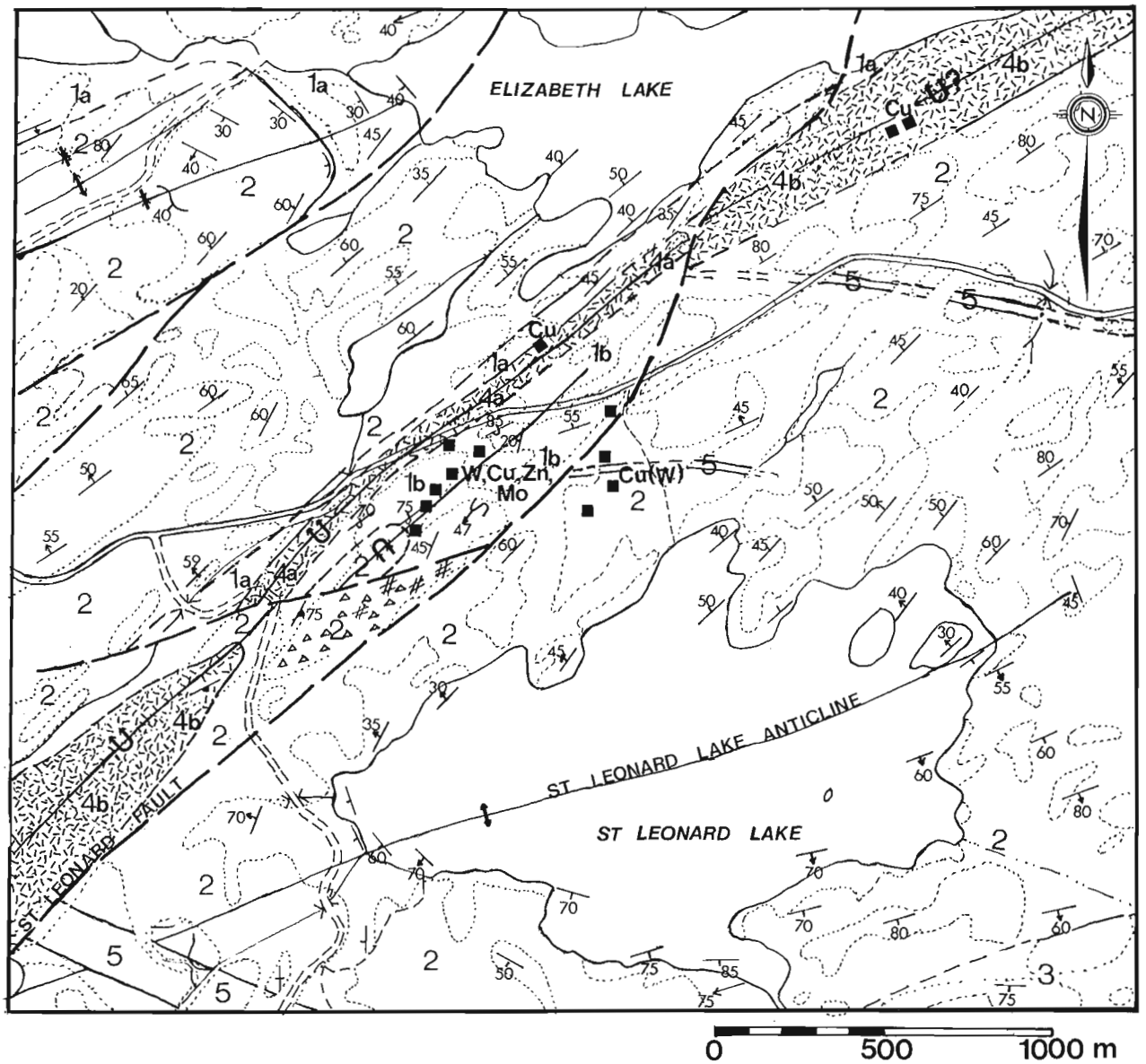


Figure 46.3. *Geological map of the Foster Township W area (modified after Card, 1967, with stratigraphy after Card, 1978).*

Table 46.2

A comparison of the Foster Township W-Cu-Mo-Zn skarn deposit to W-Cu (Zn, Mo) skarns of the Yukon (Dawson and Dick, 1978)

	Foster Township	W-Cu (Zn, Mo) skarns of the Yukon
Host rocks	Huronian Espanola Formation; calcareous siltstone, siltstone, and limestone	Cambrian to Devonian carbonates and interbedded shale
Associated Intrusion	Nipissing Diabase; pyritic diabase, gabbro	Lower-Mid Cretaceous plutons; characteristically quartz monzonite; border phases argillized; locally greisenized and tourmalinized
Ore Mineral Assemblage	Scheelite, chalcopyrite, sphalerite, molybdenite, some pyrrhotite-rich pods, subordinate pyrite; minor powellite and arsenopyrite (Card, 1968a)	Scheelite, chalcopyrite, sphalerite, molybdenite, abundant pyrrhotite, and subordinate pyrite
Silicate Assemblage	Idocrase-diopside-garnet; some mafic layers tentatively identified as biotite and actinolite; abundant quartz; wollastonite (Card, 1978)	Diopside-hedenbergite and garnet predominate; subordinate actinolite, biotite, quartz, chlorite, epidote, idocrase, and wollastonite
Form of orebody	Irregular, more or less concordant zones developed up to approximately 450 m from a steeply dipping intrusive contact	More or less concordant bodies, localized tens to hundreds of metres above shallowly dipping intrusive contacts

The formation of this unusual W-bearing skarn required a favourable stratigraphic and structural setting, a heat source, and a source of metals and sulphur. The Espanola Formation, by virtue of being the only significant limestone-bearing member of the Huronian Supergroup is the sole stratigraphic site for major skarn development. The heat source most probably was provided by the Nipissing Diabase and concentration of volatiles might have been enhanced by the constriction of this intrusion.

Deformation in the Southern Province began prior to the intrusion of Nipissing Diabase (Card et al., 1972; Card, 1978), thus the Huronian sediments probably were thoroughly lithified and dewatered before intrusion (Card, 1978). This probable lack of primary permeability in these sedimentary rocks combined with the dry nature of gabbroic magmas explains the characteristic limited development, or absence of, skarn formation in the region. However, at Foster Township the correlation between intense deformation and the presence of skarn suggests that structural permeability might have been an important factor in the extensive development of skarn. Fluids may have originated as structurally trapped connate water, or possibly from alteration of hydrous minerals. The extensive quartz-cemented pull-apart breccia is postmineral and is probably unrelated to the skarn.

Cu and Fe are common constituents of Nipissing gabbroic magmas, but rarely do deposits associated with these intrusions contain W, Mo, or Zn. Although published data on trace elements in the Espanola Formation are sparse, it is possible that all metals, and perhaps sulphur as well, came from the sedimentary rocks.

Dawson and Dick (1978) have defined four major groups of skarns in the Yukon and the Foster Township occurrence compares well with their group 1 – W, Cu (Zn, Mo) skarns. Table 46.2 lists the characteristics of this group and those of Foster Township. Despite the different geological settings of these deposits and the enormous age and compositional differences between associated intrusive bodies (Nipissing diabase-gabbro, 2.15 Ga old, versus Lower-Mid Cretaceous quartz monzonite-granodiorite), the similarities of mineralogy and metal contents are striking. The physical-chemical conditions required for skarn development are probably similar although the geological settings are vastly different.

The Espanola Formation might contain economic W-Cu skarn deposits. Exploration should focus on favourable structural settings, a closely associated intrusion, and evidence of hydrothermal activity. Additionally, the Foster Township occurrence warrants further exploration as the hinge region of the overturned syncline has not been adequately tested by geophysical surveys or drilling.

Copper-Nickel Deposits in Mafic Intrusions

Copper-nickel occurrences are hosted within Nipissing gabbroic intrusions in the East Bull Lake gabbro-anorthosite complex of probable Huronian age (D. Innes, pers. comm., 1977) and within the Mongowin Pluton, a small composite pluton dated at 1770 Ma (Card, 1968b). Deposits hosted within Nipissing Diabase intrusions are by far the most numerous, and are particularly abundant in the Sudbury area (Card, 1978; D. Innes, pers. comm., 1977). One of the largest known deposits in Nipissing Diabase, the Falconbridge Shakespeare prospect, located 1.2 km north of Agnew Lake, is estimated to contain 2.7 to 3.6 million tonnes grading 0.34% Ni and 0.40% Cu (Shklanka, 1969, p. 264), that is mineable by open pit methods. Figure 46.4 is a geological map of this occurrence.

At Falconbridge Shakespeare, pyrrhotite, chalcopyrite, and pentlandite occur as disseminations, irregular blebs, and small veinlets in Nipissing metagabbro. The sulphide zone trends northeast over an exposed strike length of approximately 520 m and reaches a maximum width of approximately 30 m. Sulphide content is highest in the southwestern portion of the zone whereas to the northeast the zone thins considerably and sulphide content is much less. White, probably albite-rich granophyre is abundant near the northeast limit of outcrop where it forms irregular bodies within the gabbro. Granophyre is also developed along the southern edge of the Mississagi quartzite outcrop to the northwest, suggesting that the granophyre may have formed as a result of assimilation of quartzite by the gabbroic magma. In contrast, Mississagi quartzite is present as unaltered xenoliths within metagrabbo in the southwest part of the area (Fig. 46.2). The sulphide zone has been strongly deformed and is offset by late faults.

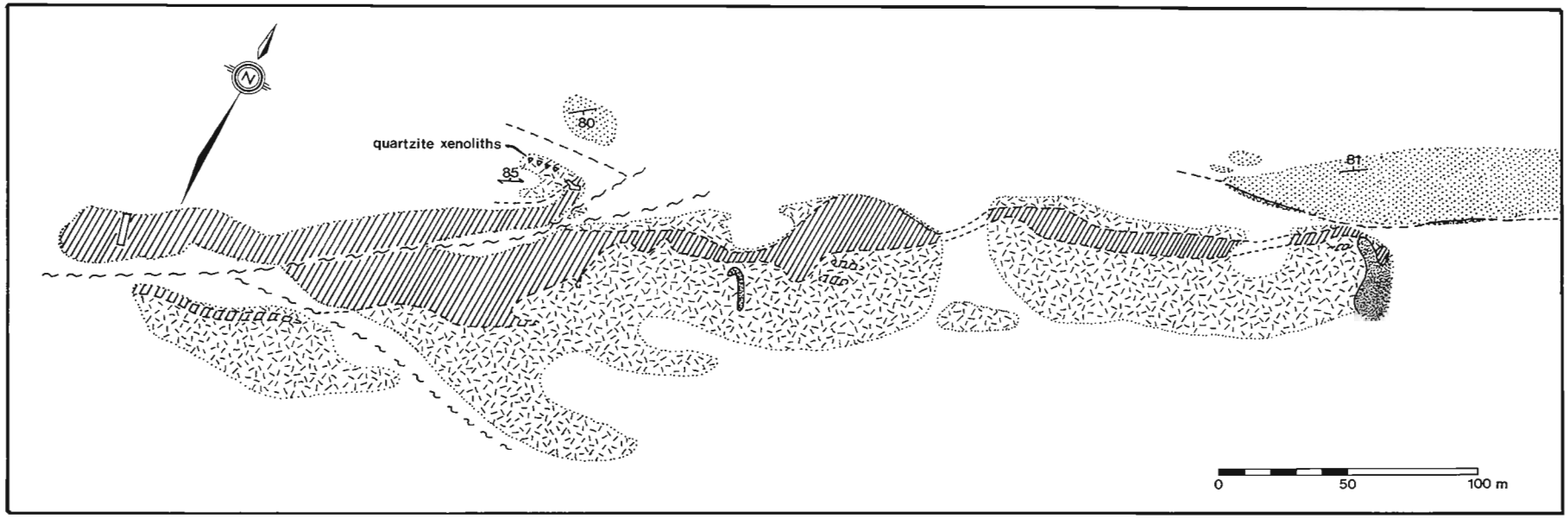


Figure 46.4. *Geological map of the Falconbridge Shakespeare deposit.*

This deposit appears to be of magmatic origin, however, the source of sulphur is uncertain. West of the occurrence, the Mississagi quartzite is underlain by phyllite of the Pecors Formation (Card, 1978) which could have been the source of sulphur. Alternatively the sulphur may have come from a deep magmatic source.

Gimby, 1.3 km south of Echo Lake, is an example of a sulpharsenide occurrence in Nipissing granophyre. Chalcopyrite is present as disseminations in small irregular bodies of pink granophyre that are scattered throughout Nipissing gabbro. The most extensive granophyre zone is up to 1 m wide and can be traced over a length of approximately 20 m. One hundred metres to the south, a cobaltite(?)-carbonate body, up to 50 cm wide and approximately 20 m long, is present within a segregation of pink granophyre, the latter containing some disseminated chalcopyrite. The cobalt-rich phase apparently represents the final product of fractional crystallization.

"Sedimentary" Copper Deposits

Significant sedimentary copper occurrences within the Huronian Supergroup appear to be restricted to the Lorrain Formation. Two significant but low grade deposits are known: the Desbarats prospect, 3.5 km northwest of the town of Desbarats and the Stag Lake occurrence, 22 km north of Elliot Lake. Figure 46.5 shows a stratigraphic column for each deposit as compiled from field mapping at Desbarats and logging of drill core from Stag Lake.

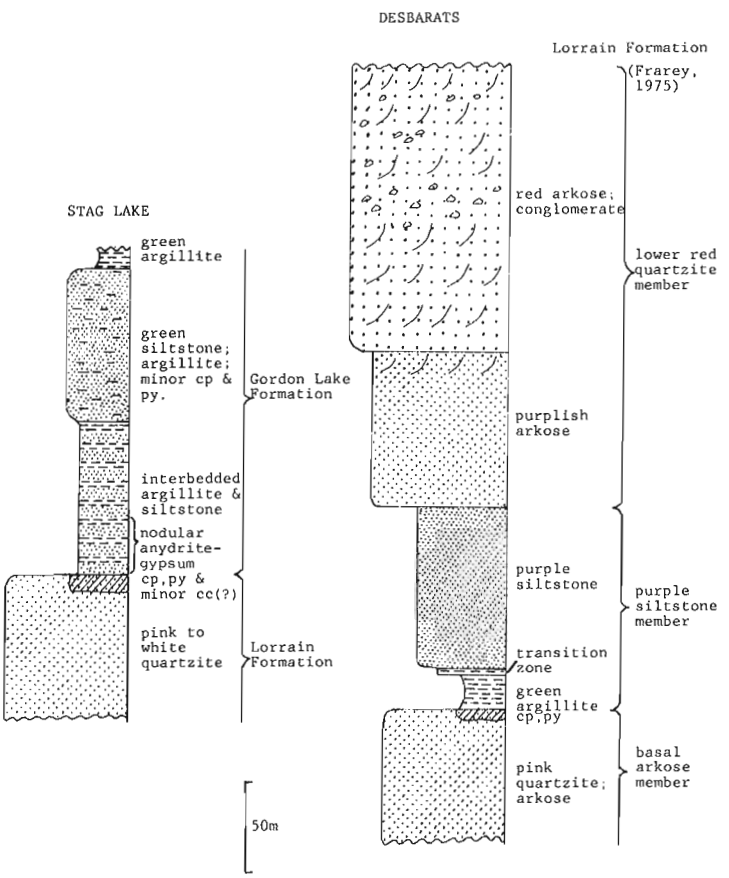


Figure 46.5. *Stratigraphy of the Desbarats and Stag Lake prospects.*

At Desbarats, chalcopyrite and pyrite occur as disseminations, blebs, and rare veins within slightly radioactive, hematitic, feldspathic quartzite that is overlain by green, recessive-weathering argillite and underlain by essentially barren pink quartzite. All units are in the Lorrain Formation (Frarey, 1975). The argillite unit is approximately 20 m thick and grades upward through a 3-4 m transitional zone of interbedded green argillite and fine grained purple siltstone into a 90 m-thick section of purple siltstone. Some disseminated pyrite is present near the base of this siltstone unit. The purple siltstone unit coarsens upwards and grades into a purplish arkose unit that is approximately 85 m thick. This in turn grades into a reddish, characteristically crossbedded arkose unit having a thickness of greater than 200 m. The upper part of this unit contains lenses of quartz-jasper pebble conglomerate. The beds are gently dipping and are folded into very open anticlines and synclines having fold axes that plunge gently to the west. An east-west trending vertical cleavage is best developed in the purple siltstone unit where it is micaceous.

The stratigrpahic sequence at Desbarats forms an upward coarsening sedimentary unit possibly representing a regression. A shallow water, slightly anoxic environment was probably succeeded by progressively higher energy littoral and fluvial environments. Ferric-ferrous ratios increase upsection as indicated by the change of colour from green to purple to red.

At Stag Lake, low grade disseminated chalcopyrite, pyrite, and minor chalcocite (?) occur within predominantly pink Lorrain quartzite over a strike length of 3.2 km (Sutherland, 1965). The quartzite is overlain by interbedded argillite and siltstone, siltstone, finely laminated argillite, and minor sandstone of the Gordon Lake Formation. Nodules and veins of gypsum and anhydrite are present near its base; these minerals are most abundant within approximately 2 m of the contact with Lorrain quartzite. Approximately 90-160 m above the contact, small amounts of chalcopyrite and pyrite are present within argillaceous siltstone as disseminations in coarse grained parts of thin, graded beds, in sandstone lenses, and in sandstone matrices of intra-formational breccias. A similar minor copper occurrence within the Gordon Lake Formation was noted by R.V. Kirkham and the writer in an outcrop located 0.8 km west of the intersection of Gordon Lake and Diamond Lake roads north of Bruce Mines. At this locality minor amounts of disseminated chalcopyrite, pyrite, and traces of bornite occur in scattered thin (of the order of centimetres) quartzite beds and lenses within a green interbedded argillite-siltstone sequence. The sulphides are confined to the coarser grained beds and lenses that were probably more permeable at the time of sedimentation and during early diagenesis.

The stratigraphic settings of both the Desbarats and Stag Lake occurrences are consistent with an origin related to sedimentary processes. At Desbarats, during the deposition of the green argillite unit, oxidized, copper-bearing solutions probably migrated through the permeable basal arkose member and were reduced, precipitating sulphides, upon contacting the less permeable, slightly anoxic, green argillite. The widespread but erratic and low grade nature of this deposit may reflect insufficient reductants in the green argillite unit to form a higher grade deposit, or alternatively, the sedimentary environment favourable for the accumulation of copper was ephemeral.

In contrast to the Desbarats prospect, the one at Stag Lake occurs adjacent to a major regional contact, between the Gordon Lake Formation that was probably deposited in shallow water with periodic influxes of fine terrigenous material (Card et al., 1972) and the Lorrain Formation, that

is interpreted to have been deposited in a fluvial (Frarey and Roscoe, 1970) or littoral regime (Card et al., 1977 and Card, 1978). The presence of nodular anhydrite near the base of Gordon Lake Formation could signify a sabkha environment of sedimentation. The Gordon Lake Formation is a minimum of 180 m thick in the Stag Lake area, indicating that an environment favourable for sedimentary copper accumulation could have been stable for a relatively long period of time. The extensive strike length of this occurrence suggests that sufficient copper probably was available in solution to form a sizable deposit, however a possible lack of sufficient reductants in the Gordon Lake Formation may have prevented the development of a higher grade deposit.

Exploration for sedimentary copper deposits in the Huronian Supergroup has received only limited attention. The recessive-weathering character of the green argillite unit at Desbarats and the argillaceous Gordon Lake Formation suggests that significant, unexposed deposits could exist, but would be difficult to detect by surface prospecting techniques. It is interesting to note that despite the long exploration and mining history in the Marquette area of Michigan, it was only recently (1960s) recognized that extensive sedimentary copper is present in the lower part of the Lower Proterozoic Kona Dolomite (Taylor, 1972). This is because the favourable unit is recessive weathering.

Volcanogenic Massive Sulphides and Stringer Zones

This broad category can be divided into two major groups:

1. polymetallic occurrences hosted in Archean metavolcanic and metasedimentary rocks; and
2. deposits within and close to Huronian volcanic rocks.

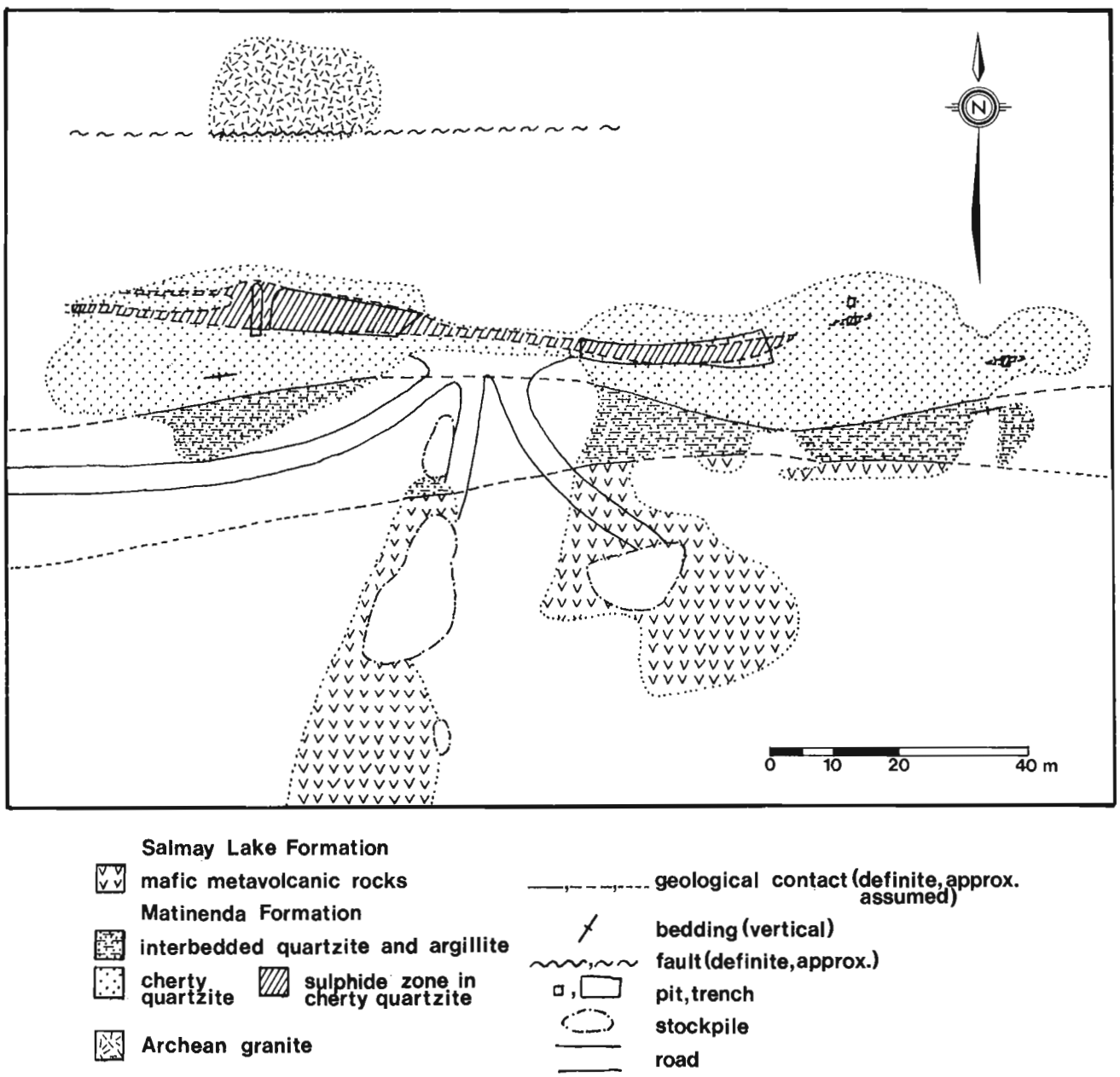


Figure 46.6. Geological map of the Alexander prospect.



Figure 46.7.

Typical "cherty quartzite", with stringers and disseminations of chalcopyrite and pyrite to the left of the lens cap, east trench, Alexander prospect. GSC 203438-B.

Archean-hosted deposits are of two main types:

1. polymetallic Zn-Pb-Cu-Ag stratabound volcanogenic massive sulphide deposits (e.g. Stralak, Lake Geneva Mine); and
2. copper-bearing sulphide-facies iron formation that is probably genetically related to volcanism (Goodwin, 1973) (e.g. East Pecors).

Brief descriptions of deposits in this group are given by Card and Innes (1976) and Pearson (1978).

Copper deposits that are associated with, and probably genetically related to, Huronian volcanic rocks, are of three major types:

1. Cu and Fe-bearing volcanogenic massive sulphide deposits (e.g. Pater Mine);
2. extensive sulphide-rich units within pelitic interflow metasedimentary rocks of the Stobie Formation (Card et al., 1977; Innes, 1972); and
3. copper deposits of the Massey Copper Belt (Robertson, 1976) that are typically hosted in highly siliceous "cherty quartzite" units that are overlain by, intercalated within, or are in close proximity to, mafic metavolcanic rocks of the Salmay Lake Formation.

Archean volcanogenic massive sulphide deposits have been well documented by many writers and the occurrences in this study area are small but typical examples of this deposit type with the exception that their lead contents are appreciable, in contrast to most Archean deposits (Sangster, 1972). The following discussion will centre on copper deposits associated with Huronian volcanic rocks, particularly those occurrences in the Massey Copper Belt.

The Pater Mine, located just east of Spragge, is hosted in mafic metavolcanic rocks of the lowermost part of the Spragge Group (Pater volcanics); these rocks are considered to be correlative to Huronian volcanic rocks of the Sudbury-Espanola area (Robertson, 1970). The ore zone trends east-west, dips 80° to 85° south, has an average width of 2.7 m, and was mined to a depth of 1250 m, with lateral workings extending up to 396 m (Robertson, 1970; Shklanka, 1969, p. 65). From 1960 to the end of 1968 total production was 32 027 392 kg of copper from 1 818 746 tonnes of ore milled (Shklanka, 1969, p. 65) giving a calculated grade of 1.76% Cu.

The host rocks at the Pater Mine are strongly deformed and metamorphosed mafic lavas, mafic pyroclastic rocks, and greywacke (Robertson, 1970). As a result of deformation the ore locally resembles a "conglomerate" consisting of scattered round quartz and amphibolite schist fragments surrounded by pyrrhotite and lesser chalcopyrite. Layers of finely comminuted, highly deformed pyrrhotite and chalcopyrite are characteristic. A "silicified zone" is associated with the ore horizon (Robertson, 1970), however, the cherty texture and banded nature of siliceous samples seen in the dumps and in outcrop near the old shaft suggests to the writer that this zone is recrystallized, interbedded, exhalative chert and mafic tuff. The ore zone trends obliquely to the strike of the metavolcanic rocks of the Spragge Group (Robertson, 1970), however, this probably reflects transposition of an originally conformable sulphide body during deformation. The features of this deposit are consistent with that of a strongly deformed and metamorphosed volcanogenic, exhalative massive sulphide deposit.

In the Huronian Stobie Formation, extensive sulphide-rich units occur within pelitic interflow metasediments. The zones are generally less than 3 m thick but have been traced along strike for some 25 km from Denison to Graham Township (Card et al., 1977; Innes, 1972). Pyrrhotite, pyrite, and chalcopyrite occur as disseminations, fracture-fillings, and stratiform layers with chalcopyrite most abundant in the "stirred" flow top portions of the metavolcanic-metasedimentary cycles (Card et al., 1977; Innes, 1972). These deposits are considered to be of volcanic exhalative origin (Innes, 1972).

Massey Copper Belt The Massey Copper Belt (Robertson, 1976) stretches from Victoria to May Township, a distance of approximately 30 km. This copper zone is roughly coincident with the area of Salmay Lake volcanic rocks and early Huronian gabbro-anorthosite intrusions. The latter are considered by Card (1978) to be intrusive equivalents of the former. Many of the copper-bearing quartz veins in the Massey area are probably genetically related to this intrusive suite (Robertson, 1976), however, the copper deposits hosted within "cherty quartzite" units appear to have volcanic affinities. Several deposits similar to this latter type are also present near the north shore of Agnew Lake approximately 13 km northeast of May Township.

During the summer of 1978, five of the larger and better exposed deposits within "cherty quartzite" (Massey Mine, Spanish River Mine, Alexander prospect, Bishop prospect, and Noranda Shakespeare) were mapped in detail. The following is a brief summary of this work. In assigning rocks to formations, the convention of Card (1978) has been followed, whereby mappable units of metasedimentary rocks within dominantly metavolcanic sequences are assigned to the Matinenda Formation.

The best exposed and least weathered example of this deposit group is the Alexander prospect, 7 km northeast of Massey (Fig. 46.6). At Alexander, chalcopyrite and pyrite occur as irregular, "net-textured", massive patches, blebs, and disseminations in "cherty quartzite" (Fig. 46.7) that is locally chloritic. The sulphide zone is up to 7 m wide, has an average width of about 3 m, and is exposed in outcrop over a length of approximately 95 m. To the east it appears to pinch out whereas to the west it disappears under overburden. Reserves are estimated at about 138 000 tonnes grading slightly better than 1.5% Cu (A. Alexander, pers. comm., 1978).

The "cherty-quartzite" typically has a flint-like cherty texture and lacks any recognizable clastic features. Except for local chlorite it is composed almost entirely of quartz. This unit is in fault contact with Archean granite to the north, however this fault predates at least the latest deformation because the fault zone is crenulated. To the south this unit becomes more argillaceous and is in sharp contact with the structurally overlying fragmental mafic metavolcanic rocks of the Salmay Lake Formation. This favourable cherty unit has been traced for about 1.2 km to the west and at least 1.5 km to the east where it is offset by several left lateral stike slip faults. Small copper showings occur sporadically in this unit, the most notable being about 300 m east of the Alexander prospect. The Alexander is however by far the most significant occurrence known.

The host rocks at Alexander have been strongly deformed, with quartz grains flattened in the foliation plane. The sulphide zone locally exhibits a "conglomerate-texture" similar to that at the Pater Mine.

The Bishop occurrence (Fig. 46.8), located approximately 1.4 km east-southeast of Alexander, is hosted in rocks that are very similar to that of Alexander, however, it is not certain whether they are stratigraphically equivalent. The rocks have been tightly folded into an overturned anticline having a fold axis that plunges 51° to the east and an axial plane that strikes approximately east-west and dips steeply to the north. Chalcopyrite and pyrite are the only visible sulphides and texturally, the sulphide zones resemble that at Alexander.

At the Noranda Shakespeare prospect, about 200 m north of the west end of Agnew Lake, a northeast trending sulphide zone occurs in "cherty quartzite" that is overlain by a phyllitic micaceous quartzite unit and underlain by cross-bedded feldspathic quartzite. All units are part of the Matinenda Formation (Card, 1978) (Fig. 46.10). Mafic metavolcanic rocks of the Salmay Lake Formation are not exposed in the immediate deposit area, however, they outcrop on the south shore of Agnew Lake directly opposite the showing (Card, 1978). Irregular pods and stringers of pyrrhotite, chalcopyrite, and subordinate pyrite are present within

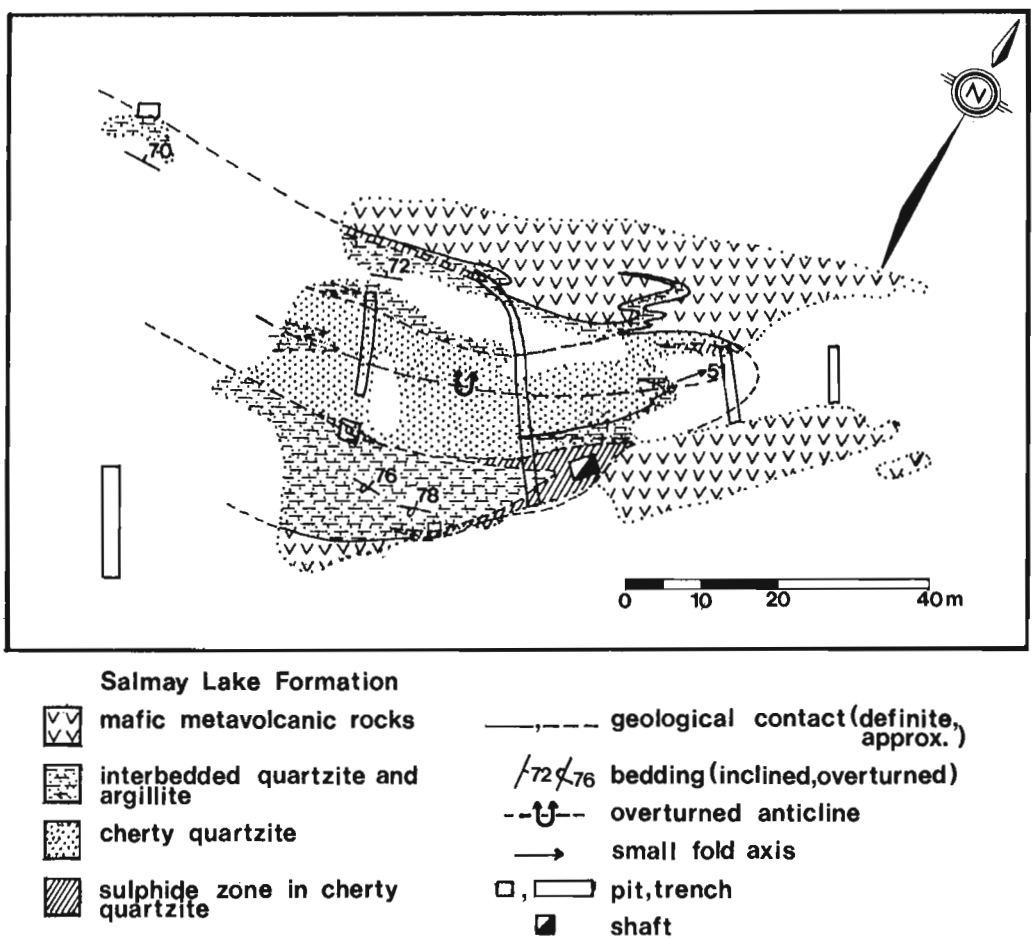


Figure 46.8. Geological map of the Bishop occurrence.

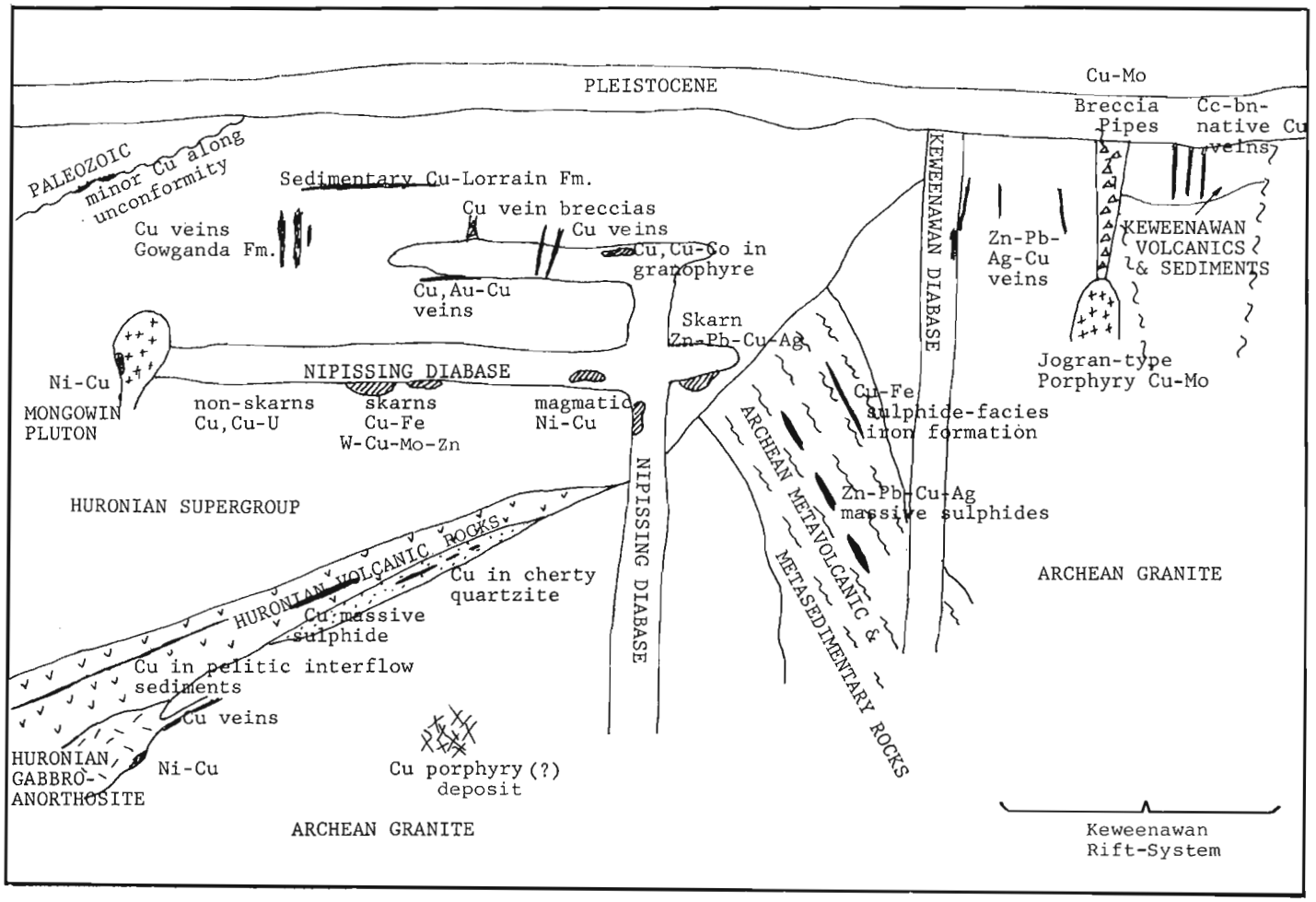


Figure 46.9. *Preliminary sketch illustrating relationships of copper deposits to major lithological units in the north shore region of Lake Huron (Sudbury Nickel Irruptive excluded).*

elongate zones hosted in "cherty quartzite". The main sulphide zone averages about 3 m in width, can be traced for approximately 340 m along strike and is reported to have an average grade of about 1% Cu (Shklanka, 1969, p. 265).

The origin of "cherty quartzite" hosting these three deposits is problematic. The cherty horizons are conformable, massive, quartz-rich units that have been highly deformed. Recognizable clastic detrital textures are lacking, although relict, ghost-like fragments that are possibly phyllitic quartzite clasts are present in the southwestern portion of the Noranda Shakespeare deposit. The close spatial relationship of these cherty rocks to mafic metavolcanic rocks of the Salmay Lake Formation suggests that they could be exhalative cherts, however, the characteristic chemical layering of such deposits is lacking. Alternatively, the rocks may have been formed by premetamorphic silicification of Matinenda sediments with primary features destroyed during later deformation.

The Massey Mine, 4 km northwest of Massey, and the Spanish Mine, near the north shore of the central part of Agnew Lake, have many similarities to the above deposits, however, there are some significant differences.

At Massey there are three main workings: the main shaft, the no. 4 shaft located 600 m west of the main shaft, and the west showing adit a farther 300 m to the west. The ore is hosted in "cherty quartzite" and argillaceous siltstone that is considered to be part of the Pecors Formation (Robertson, 1976). Chalcopyrite with subordinate pyrite occur as massive patches and irregular stringers in the cherty quartzite whereas porphyroblastic pyrite predominates in the adjacent argillaceous siltstones. The Massey Mine has had a sporadic production history dating from 1904 which is summarized in detail by Robertson (1976).

The Huronian rocks of the Massey Mine area are predominantly feldspathic quartzite (arkose) of the Matinenda Formation, Pecors argillite and quartzite, and Mississagi quartzite (Robertson, 1976). These rocks have been strongly deformed; however, the lack of sufficient outcrop and stratigraphic markers precluded delimiting large scale fold structures with certainty. Nevertheless, the presence of small folds (of the order of 1 m across) in several of the argillaceous units, suggests that tight folds similar to that of Bishop are probably present in the region. For this reason, the writer suggests that the sequence of rocks in the Massey Mine area may be tightly folded Matinenda and McKim formations rather than being largely formations higher in the section as considered by Robertson (1976).

At the main shaft and west showing adit, abundant breccia, considered by the writer to be of Sudbury-type because of its rock flour matrix and locally derived fragments, is present. Robertson (1976), however, interprets it as breccia developed along the Murray Fault. The matrix of this breccia is very sulphide-rich at the main shaft, however, much is barren at the west showing. Fragments within the

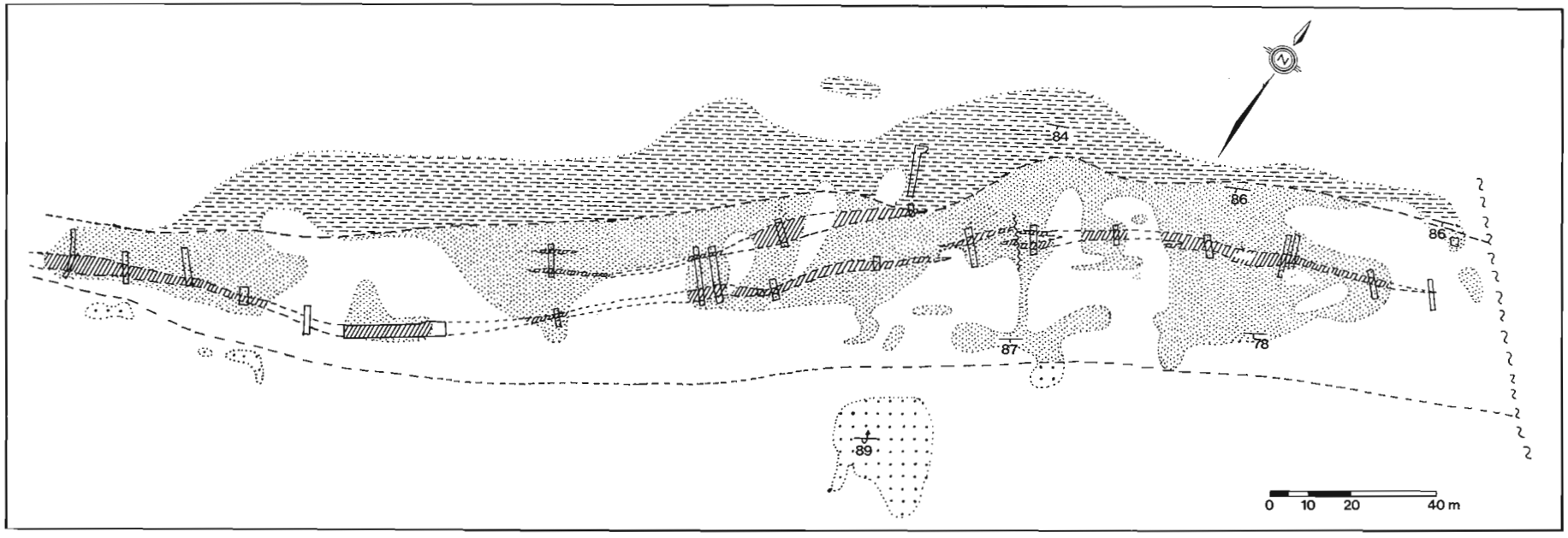


Figure 46.10. *Geological map of the Noranda Shakespeare prospect.*

breccia also contain small amounts of disseminated sulphides. At the no. 4 shaft, which is the probable extension of the main shaft zone, no breccia is evident, thus the breccia is probably postore. In the vicintiy of the west showing adit, a body of quartz-cemented breccia cuts the possible Sudbury-type breccia; fragments of the rock flour matrix of the earlier breccia are present along the margins of the quartz-cemented breccia body. The quartz-cemented breccia is similar to the tension or "pull-apart" breccia in Foster Township and may possibly have a similar origin.

Robertson (1976) notes that copper deposits of the Massey Mine, although hosted in sedimentary rocks, are close to the western limit of the Salmay Lake Formation and suggests that they are probably related to end stages of volcanic activity. The presence of "cherty quartzite" that is similar to that at Alexander, Bishop, and Noranda Shakespeare, suggests that these deposits have a similar, possibly exhalative, origin.

The Spanish River Mine is hosted in the lowermost part of the Mississagi Formation, that is underlain by Ramsay Lake conglomerate (Card et al., 1977). Chalcopyrite (commonly with exsolved laths of cubanite), pyrrhotite, and minor pyrite occur predominantly as stringers and disseminations in flint-textured "cherty-quartzite", however, in contrast to the previously described deposits, round, clastic quartz grains are evident in these cherty rocks. Quartz veins bearing a black vitrous mineral tentatively identified as a hydrocarbon (thucolite?) and sulphides are relatively common, but widely spaced. The sulphide body is vertically dipping, up to 23 m wide, has a strike length of 460 m and extends to a depth of 200 m. A second zone occurs approximately 460 m to the west and has been traced along strike for about 300 m (Shklanka, 1969, p. 230). Preproduction reserves were estimated at 994 844 tonnes grading 1.49% Cu (without dilution) over an average width of 5.6 m (Shklanka, 1969, p. 230).

The similarity of host rocks at Spanish River to those of the previously discussed deposits of the Massey Copper Zone, suggests a possible common genesis. Although Salmay Lake volcanism had ceased by the time of Mississagi Formation deposition (Card, 1978), it is possible that Spanish River may represent a last, isolated, spurt of this volcanic episode. The presence of clastic grains in the cherty quartzite unit, suggests that perhaps both chemical and clastic precipitation of silica were important. The quartz-sulphide-hydrocarbon (?) veins probably formed during deformation and represent remobilized material.

Porphyry Deposits

Kirkham (1972) defined a porphyry deposit as a "large, low- to medium-grade deposit in which the hypogene sulphides are primarily structurally controlled and which is spatially and genetically related to felsic or intermediate intrusions." As noted previously (Pearson, 1978), the Batchawana area breccia pipes (East, Breton, West, Palmer, and South Breccias), the Jogran Porphyry, and possibly the Nystedt prospect satisfy this definition. The Batchawana area pipes are of probable Keweenawan age and have been studied in detail by Blecha (1974) and Armbrust (1969). The Jogran Porphyry, also of probable Keweenawan age, is currently being studied in detail by G. Armbrust (pers. comm., 1978). At the Nystedt prospect, located 17 km north of Sault Ste. Marie, stockworks of quartz veins containing pyrite, chalcopyrite, and/or spectularite cut highly deformed syenitic to monzonitic phases within the Archean Gros Cap Batholith. This deposit have some porphyry affinities, however, its assignment to this class is tentative. Except for this one questionable occurrence, porphyry deposits are solely related to the Keweenawan rift system and plutonism, an unusual environment for this deposit type (Kirkham, 1973).

Copper Metallogeny

Figure 46.9 is a preliminary sketch illustrating relationships of copper deposits to major lithological units in the north shore region of Lake Huron.

Some preliminary conclusions and observations regarding copper metallogeny, in addition to those expressed in 1978 (Pearson, 1978) are:

1. Significant vein deposits within the Superior Province rocks appear to be related to Keweenawan and Huronian gabbro-anorthosite intrusions rather than to Nipissing Diabase. In contrast, vein deposits associated with, and probably genetically related to, Nipissing Diabase intrusions, are common throughout the Southern Province.
2. Copper occurrences throughout the Southern Province regardless of deposit-type are Pb-poor. The only significant exceptions are several deposits hosted in Huronian outliers in the Benny Belt area, and the White River lead prospects, located 32 km northwest of Elliot Lake. Archean massive sulphide deposits, however, contain appreciable Pb and veins that are probably associated with Keweenawan rifting are characteristically high in Pb and Zn. Pb contents of copper deposits, therefore, may be useful for discriminating the age and genetic association of the mineralization.

References

Armbrust, G.A.
1969: Hydrothermal alteration of a breccia pipe deposit, Tribag Mine, Batchawana Bay, Ontario; Economic Geology, v. 64, p. 551-563.

Blecha, M.
1974: Batchawana area – possible Precambrian porphyry copper district; Canadian Institute of Mining and Metallurgy Transactions, v. 77, p. 393-398.

Card, K.D.
1967: Foster Township District of Sudbury; Ontario Department of Mines, Preliminary Geological Map, P390.

1968a: Economic geology of the Espanola-Whitefish Falls area, District of Sudbury; Ontario Department of Mines, Open File Report 5017, 29p.

1968b: The Mongowin Pluton; Ontario Department of Mines, Miscellaneous Paper 14, 27p.

1978: Geology of the Sudbury-Manitoulin area, Districts of Sudbury and Manitoulin; Ontario Division of Mines, Report 166, 238p.

Card, K.D., Church, W.R., Franklin, J.M., Frarey, M.J., Robertson, J.A., West, G.F., and Young, G.M.
1972: The Southern Province; in Price, R.A. and Douglas, R.J.W. (eds.): Variations in Tectonic Styles in Canada; Geological Association of Canada, Special Paper 11, p. 335-379.

Card, K.D. and Innes, D.G.
1976: Benny area, Spanish-Johnson Lakes sheet, Sudbury; Ontario Division of Mines, Preliminary Map, P1110, Marginal Notes.

Card, K.D., Innes, D.G., and Debicki, R.L.
1977: Stratigraphy, sedimentology and petrology of the Huronian Supergroup in the Sudbury-Espanola area; Ontario Division of Mines Geoscience Study 16, 99p.

Dawson, K.M. and Dick, L.A.
1978: Regional metallogeny of the Northern Cordillera: tungsten and base metal-bearing skarns in southeastern Yukon and southwestern Mackenzie; in Current Research, Part A, Geological Survey of Canada, Paper 78-1A, p. 287-292.

Frarey, M.J.
1975: Bruce Mines – Lake George area, Ontario; Geological Survey of Canada, Map 1414A.

Frarey, M.J. and Roscoe, S.M.
1970: The Huronian Supergroup north of Lake Huron; in Baer, A.J. (ed.): Symposium on basins and geosynclines of the Canadian Shield; Geological Survey of Canada, Paper 70-40; p. 143-158.

Gibbons, W.A. and McNutt, R.H.
1976: The age of the Sudbury Nickel Irruptive and the Murray Granite; Canadian Journal of Earth Sciences, v. 12, p. 1970-1989.

Goodwin, A.M.
1973: Archean iron-formations and tectonic basins of the Canadian Shield; Economic Geology, v. 68, p. 915-933.

Innes, D.G.
1972: Proterozoic volcanism and associated sulphide-bearing metasediments in the Sudbury area, Ontario; unpublished B.Sc. thesis, Laurentian University, Sudbury.

Kirkham, R.V.
1972: Porphyry deposits; in Report of Activities, Part B, Geological Survey of Canada, Paper 72-1B, p. 62-64.

1973: Tectonism, volcanism, and copper deposits; in Volcanism and Volcanic rocks, Geological Survey of Canada, Open File 164, p. 129-159.

Pearson, W.N.
1978: Copper Metallogeny, Lake Huron area, Ontario; in Current Research, Part A, Geological Survey of Canada, Paper 78-1A, p. 263-268.

Robertson, J.A.
1970: Geology of the Spragge area; Ontario Department of Mines Geological Report, 76, 109p.

1976: Geology of the Massey area, Districts of Algoma, Manitoulin and Sudbury; Ontario Division of Mines, Geoscience Report, 136, 130p.

Sangster, D.F.
1972: Precambrian massive sulphide deposits in Canada: A review; Geological Survey of Canada, Paper 72-22, 44p.

Shklanka, R.
1969: Copper, nickel, lead and zinc deposits of Ontario; Ontario Division of Mines Mineral Resources Circular 12, 394p.

Stockwell, C.H.
1972: Revised Precambrian time scale for the Canadian Shield; Geological Survey of Canada, Paper 72-52, 4p.

Sutherland, W.D.
1965: Stag Lake copper prospect; Ontario Division of Mines, Resident Geologists Files, Sault Ste. Marie, SSM-708, 10p.

Taylor, G.
1972: Stratigraphy, sedimentology, and sulphide, mineralization in the Kona Dolomite; Ph.D. thesis, Michigan Technical University; University Microfilms, Ann Arbor, MI.

Van Schmus, W.R.
1965: The geochronology of the Blind River-Bruce Mines area, Ontario, Canada; Journal of Geology, v. 73, p. 775-780.

47. GEOLOGY OF PUDDLE POND MAP AREA, SOUTHWESTERN NEWFOUNDLAND

Project 770026

R.K. Herd and G.R. Dunning[1]
Regional and Economic Geology Division

Herd, R.K. and Dunning, G.R., Geology of Puddle Pond map area, southwestern Newfoundland; in Current Research, Part A, Geol. Surv. Can., Paper 79-1A, p. 305-310, 1979.

Abstract

The northwestern part of the Puddle Pond map area is underlain by a complex of igneous and metamorphic rocks of probable Grenvillian and younger ages. The oldest rocks are foliated hornblende-biotite and biotite granites and granitic gneisses, which locally preserve granulite facies mineralogy. These orthogneisses and inclusions of paragneiss, migmatite, and mafic plutonic rocks within them, are intruded by younger orthogneiss and granite. Structural trends vary from northwest to northeast. Interference fold patterns occur around Cormacks Lake.

The southeastern part of the map area exhibits an ophiolite complex, with pyroxenite, gabbro, sheeted diabase dykes, plagiogranite dykes, and pillow lava. The complex is conformable with the Ordovician volcanic rocks of the Victoria Lake area to the southeast, and is faulted against gneisses and granites to the northwest. Red beds of probable Carboniferous age occur southwest of the ophiolite.

Introduction

Mapping of Puddle Pond map area (12A/5) at a scale of 1:50 000 has continued (see Herd, 1978, for previous work); detailed mapping of 75 per cent of the area has been done. Ground and lakeshore traversing is now virtually complete in the area shown in Figure 47.1. For structural and stratigraphic continuity small portions of adjacent map areas to the north, west, and south have been mapped. Access to the map area was along Route 480, the Southwest Brook-Burgeo road, now complete through map sheet 12A/5, as well as by fixed-wing and helicopter support to remote fly-camps.

Puddle Pond and adjacent areas comprise an igneous-metamorphic terrane bounded on the northwest by the Long Range fault zone (Herd, 1978), on the north by the Ordovician Glover Formation volcanic sequence (Riley, 1957), on the northeast by the Topsails Batholith, and to the southeast by Ordovician volcanics of the Victoria Lake group (Kean, 1977). This terrane contains variably deformed and agmatized granodioritic and granitic gneisses, paragneisses, migmatites, amphibolites, metagabbros and associated rocks, anorthosites, and ultramafics, all cut by relatively undeformed younger granite and minor diabase dykes.

General Geology of Puddle Pond Area

Figure 47.1 is a sketch-map of the western and southeastern parts of Puddle Pond map area. Table 47.1 lists map units in more detail than the legend of the Figure 47.1.

A major structural discontinuity exists along the Lloyds River valley and subdivides the area. Northwest of this line, major structural trends vary from northeast to northwest, whereas southeast of it, trends are northeasterly and conformable with the strike of the Ordovician volcanic rocks of central Newfoundland. Further division of the western part of the area can be made along the valley of Little Barachois Brook. South of this line the geology is dominated by multiply-deformed rusty-weathering paragneisses, amphibolites and foliated biotite granites; north of this line foliated hornblende-biotite granites and granitic gneisses are host to large inclusions of metagabbro, norite, diorite, and complex migmatite containing both paragneisses and mafic rocks. The pattern of interference folds seen in the southwest area is lacking, and younger granite bodies are relatively abundant in the northern area.

Further division of the southeastern part of the map can be made along the south shore of Victoria Lake. Northwest of this line occur the gabbros, sheeted diabase dykes, and pillowed basalts of an ophiolite complex, with adjacent or contiguous lavas and pyroclastics of the Victoria Lake group (cf. Kean, 1976, 1977). Southeast of this line lies another gneiss terrane.

Geological relationships within major divisions of the map area are described separately.

Cormacks Lake Area

South and west of Little Barachois Brook lies topographically high country, characterized by abundant outcrop but with extensive glacial deposits as well. This entire southwest corner of the map area is underlain by foliated granite (unit 1c, d orthogneiss) with conformable layers of rusty-weathering paragneiss (unit 2c, d) and amphibolite (unit 5c, d). Locally quartzites and calc-silicate layers (unit 3) occur and the paragneiss is cut by granite veins and by aplites. The foliated granite (unit 1c) is relatively homogenous although hybrid gneiss (unit 1d) characteristically occurs along contacts with paragneiss. A distinctive northeast-trending quartz-augen foliated granite (unit 1e) occurs near Cormacks Lake, apparently in three domal regions. The granite, paragneiss and amphibolite are termed informally the Cormacks Lake complex. Quartz, feldspar, biotite, cordierite, sillimanite and magnesian amphibole (gedrite, probably also cummingtonite), hornblende, and actinolite occur in the paragneiss, and hornblende, feldspar, quartz, garnet and diopside in the amphibolites. Sulphides and magnetite both contribute to the rusty weathering of the paragneiss. The amphibolites locally preserve plagioclase augen textures suggestive of an origin from coarse grained igneous rocks (unit 5c) and elsewhere carry calc-silicate nodules and inclusions (unit 5d) suggestive of a supracrustal origin.

There is abundant evidence at all scales that the Cormacks Lake complex has been multiply deformed. At least three phases of folding have been recognized. Early isoclines are preserved in amphibolite, paragneiss, and foliated granite, and are recognized as intrafolial folds of variable amplitude and orientation. Directly south of Little Barachois Brook, near the west side of the map area, a major fold core in

[1]Department of Geology, Carleton University, Ottawa, Ontario K1S 5B6

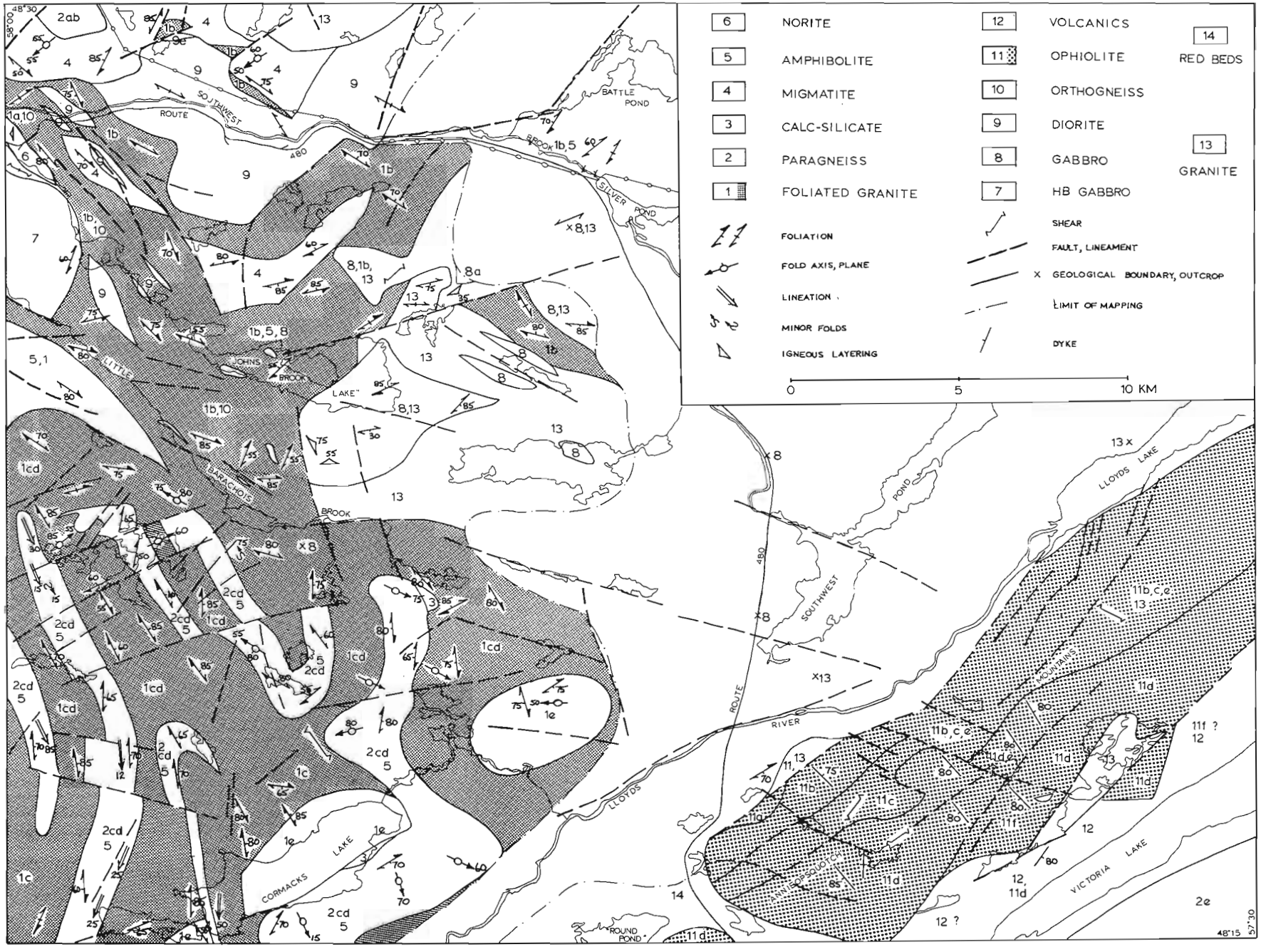


Figure 47.1. *Geological sketch-map of the Puddle Pond area; informal names are in quotation marks.*

Table 47.1

Detailed legend of units, Puddle Pond area

CARBONIFEROUS (?)	
14	Redbeds; sandstone, shale, limestone, conglomerate
DEVONIAN (?)	
13	Granite, pink, massive; 13a, massive granite; 13b, foliated pink granite; 13c, aplite, granite, pegmatite dykes
ORDOVICIAN (?)	
12	Volcanic and associated rocks; 12a, pillow lava; 12b, agglomerate; 12c, massive basalt
11	Annieopsquotch igneous complex; ophiolite and associated rocks; 11a, pyroxenite; 11b, gabbro; 11c, gabbro and diabase dykes; 11d,sheeted diabase dyke zone; 11e, leucogabbro/plagiogranite dykes; 11f, diabase dykes in mafic pillow lava; 11g, amphibolite, epidote-amphibolite zones
DEVONIAN AND/OR OLDER	
10	Orthogneiss; 10a, quartz diorite – granodiorite orthogneiss; 10b, mylonitic orthogneiss, pink, with epidote
9	Hornblende diorite and related rocks; 9a, diorite; 9b, quartz diorite; 9c, granodiorite; 9d, granite; 9e, hornblende-biotite ultramafic; 9f, diabase dykes in diorite
8	Gabbro, massive; 8a, pyroxenite; 8b, gabbro-metagabbro, coarse grained; 8c, anorthosite; 8d, hornblendite; 8e, serpentinite; 8f, diabase dykes in gabbro
7	Hornblende gabbro; 7a, noritic; 7b, ophitic; 7c, porphyritic (hornblende, plagioclase); 7d, leucocratic; 7e, troctolitic; 7f, diabase dykes in hornblende gabbro
6	Hornblende norite; 6a, medium grained, massive and coarsely jointed; 6b, layered; 6c, pegmatitic; 6d, porphyritic (hornblende); 6e, agmatite of norite in orthogneiss; 6f, diabase dykes in norite
5	Amphibolite; 5a, amphibolite in orthogneiss; 5b, amphibolite in migmatite; 5c, Cormacks Lake complex, metagabbro(?); 5d, Cormacks Lake complex, calc-silicate(?)
4	Migmatite composed of: paragneiss of unit 2, locally pelitic (4a) or calc-silicate – rich (4b), and granodioritic gneiss, with inclusions of amphibolite, gabbro, calc-silicate rock, sillimanite schist, rarely serpentinite, etc.
3	Marble, and calc-silicate rock with garnet, diopside, quartz, sphene, actinolite, tremolite, talc etc.
2	Paragneiss, biotite-rich; 2a, aluminous, pelitic; 2b, containing calc-silicates; 2c, Cormacks Lake complex, pelitic and magnesian paragneisses; 2d, Cormacks Lake complex, calc-silicate gneiss; 2e, paragneiss southeast of Victoria Lake
1	Foliated granite/orthogneiss; 1a, granulite facies; 1b, hornblende-biotite orthogneiss; 1c, Cormacks Lake complex, biotite orthogneiss; 1d, Cormacks Lake complex, hybrid biotite – magnesian amphibole orthogneiss; 1e, foliated quartz-eye granite.

amphibolite preserves isoclines which can be traced around the fold hinge; compositional layering in the rocks is therefore transposed bedding at best. A traverse across the layering southeast of this core reveals intersecting steeply-dipping foliations which define a synform; minor folds and lineations also define a synform plunging gently southeast. South of Cormacks Lake, fold interference is also noted; early isoclines in paragneiss are folded about relatively open folds which plunge consistently southeast. Another phase of folding is represented by open folds and crenulations in granite and paragneiss, which plunge variably southwest and northeast and consistently have a northeasterly axial trend. Left-lateral offset faults parallel this trend.

Gedrite garbenschiefer, confined to (? S_0/S_1) layering in paragneiss east of Cormacks Lake, indicate that metamorphism began early in the fold history. In thin section, cordierite mosaics are seen to mimic microfolds, indicating posttectonic recrystallization.

The foliated granites and folded horizons of the southwest part of the Puddle Pond area are continuous into the Main Gut area (12B/8) to the west and King George IV Lake area (12A/4) to the south (cf. DeGrace, 1974).

Southwest Brook Valley

The area north of Little Barachois Brook is part of the drainage system of Southwest Brook, and is marked by several large lakes in deep valleys and by higher plateau areas. The valleys are tree-lined and outcrops occur mainly in streams. The plateau areas are often boggy, but with relatively abundant outcrop.

The geology of this region contrasts with that of the region to the southwest. No extensive horizons of rusty-weathering paragneiss occur, although aluminous and calc-silicate rocks and amphibolite are components in migmatite (unit 4). At map scale no interference fold patterns can be seen, although examples have been observed in migmatite. The structure in Southwest Brook Valley is dominated by early north- to northeast-trending foliations and southwest-plunging synforms/antiforms, and by later northwesterly foliations. Indeed, northwest-trending foliations in orthogneiss (units 1, 10) with amphibolite and gabbroic inclusions are conformable across the valley of Little Barachois Brook, and provide an apparent link between the Cormacks Lake and Southwest Brook Valley regions. As well as the migmatites and foliated granites, there are large masses of hornblende-bearing plutonic rock (units 6, 7, 8, 9), bordered by orthogneiss (units 1, 10) and locally intruded by veins and networks of orthogneiss (unit 10); internal structures in the masses may be discordant to regional trends and primary structures such as igneous layering are often well-preserved. Magnetite-layered norites and hornblende-gabbros (mainly diabasic) occur in the west, and more norite occurs east of Battle Pond, whereas southeast of Silver Pond there are many gabbroic (unit 8) and amphibolitic (unit 5) inclusions in granite and orthogneiss. Along much of Route 480 in the northwest, hornblende diorite/granodiorite (unit 9) is exposed; this rock contains inclusions of gabbro and amphibolite, suggesting that it is relatively young, although its margins and some internal contacts have been affected by intrusion of quartz dioritic orthogneiss. Southwest of Silver Pond, inclusions of coarse grained hornblende metagabbro (unit 8b) locally grading to anorthosite (unit 8c) and to pyroxenite (unit 8a) occur in both foliated granite and in younger, more massive, pink, granite (unit 13). This gabbro is mineralogically and structurally similar to gabbros in the Annieopsquotch Mountains to the southwest; at one locality south of 'Johns Brook Lake' (informal name) the gabbro is cut by diabase and both diabase and gabbro are intruded by granite.

Relationships in the northwest portion of this area were described previously (Herd, 1978). Additional traverses along Southwest Brook have now shown that the orthogneiss (unit 10, Herd, 1978), formerly postulated as the youngest gneiss unit in the area, must contain components of both the youngest and oldest gneisses in the region. This is substantiated by the discovery of two-pyroxene-bearing (granulite facies) agmatitic quartz dioritic gneisses (unit 1a) with northeasterly foliation, intruded by biotite-bearing foliated quartz dioritic gneiss (unit 10) with northwesterly foliation. The granulite-grade gneisses occur adjacent to the norite body (unit 6) and are exposed on the banks of Southwest Brook; the northeast foliation is conformable to that postulated as the early trend, and the northwest foliation is similar to that postulated as the direction of later structures. It is probable that there are at least two ages of orthogneiss in Southwest Brook Valley: one of quartz diorite/granodiorite composition (unit 1a, 1b) which is a matrix and possibly a basement to the mafic plutonic rocks and to the paragneiss, amphibolite, etc., in the migmatite, and a second, less abundant quartz dioritic orthogneiss (unit 10) which is present as networks along the margins of the mafic bodies and often agmatizes them. The latter orthogneiss probably originated through local anatexis of the primary orthogneiss. These orthogneisses were not readily divided during mapping.

Annieopsquotch Mountains

Mapping southeast of Lloyds River has revealed a previously undescribed ophiolite (unit 11), termed informally the Annieopsquotch igneous complex, exposed on the high ground southwest of Lloyds Lake. To date, several zones typical of the upper portions of intact ophiolites have been recognized; this complex does not appear to be internally affected by thrust faults, and may be one of the largest and best-preserved ophiolites in Newfoundland. Its discovery means that geological features typical of Notre Dame Bay along the margins of the central volcanic belt of Newfoundland extend far inland (cf. the recent description of the Mings Bight Ophiolite Complex by Kidd et al., 1978).

The complex extends beyond the map area into the Victoria Lake area to the east and into the King George IV Lake area to the south, and therefore has a strike length of more than 20 km; previous maps (Kean, 1976, 1977; Williams, 1967, 1978a) show the Annieopsquotch Mountains as underlain by an intrusive gabbro or diorite complex, correlated with similar rocks occurring all along the northwestern margin of the central volcanic belt. The Annieopsquotch complex has an exposed thickness of at least 7 km and faces southeast where it grades into volcanic rocks of the Victoria Lake group (unit 12); whether a large or a small proportion of the latter is a constituent of the ophiolite sequence must be the subject of further detailed studies.

Stratigraphic and structural relationships within the Annieopsquotch Mountains are as follows:

Small exposures of cumulate pyroxenite (unit 11a; bronzitite) occur with gabbro (unit 11b) and minor diabase along the extreme northwestern margin of the complex. These ultramafic rocks may be more extensive, as inferred from the coincidence of a very high aeromagnetic anomaly with these exposures, although the anomaly may be enhanced by topographic contrast of the high mafic mountains with the drift-filled Lloyds River valley. Stratigraphically above the ultramafic rocks is a layer of coarse grained gabbro, locally with trough-layering and other cumulate features preserved, with an observed thickness of about 2 km. The gabbros contain clinopyroxene, plagioclase, orthopyroxene, and hornblende, and locally chlorite and fibrous amphibole alteration. The gabbro zone passes into a transitional zone of gabbro intruded by diabase dykes (unit 11c). The next unit stratigraphically upwards is a thick layer of sheeted diabase dykes, which individually strike north-south to northwest-southeast, and range in thickness from a centimetre to several tens of metres. The sheeted dyke zone (unit 11d) is at least 2.5 km thick and must contain thousands of dykes. The thin, finer grained, diabase dykes are the youngest and crosscut the larger, coarser grained, dykes along persistent fractures. Dykes of several different compositions occur, as shown by textures and weathered surfaces. Above the dyke zone and along the southeast margin of the mountains, above Victoria Lake, the sheeted dykes pass into pillow lavas cut by diabase dykes (unit 11f). A concentration of metre-scale white-weathering feldspar-rich dykes occurs in the complex near its geographic centre in the map area; these dykes (unit 11e) are late in the dyke sequence, brecciate both diabase and gabbro, and may be representative of the plagiogranite material commonly found in ophiolite complexes. Sulphides occur in these dykes and elsewhere. The zone of diabase dykes with pillow lavas may be up to 2 km thick and it passes into mafic volcanics along the northwest margin of Victoria Lake.

Major zones of the Annieopsquotch complex strike northeast and apparently dip steeply southeast, although the exact attitude of major contacts is not known. Along Victoria Lake, sheeted dykes with a northeast trend were observed, in contrast to the northwest trend of the majority of dykes. These northeast-trending dykes may be sills, or blocks of the complex that have been rotated by major northeast-trending faults which cut the complex and the Victoria Lake group. The complex is a preserved remnant in a much more severely deformed and migmatized terrane. Along its northwest margin, gabbro passes on outcrop scale into amphibolite intruded by granite, and, in addition to the northeast-trending faults, there are internal shear zones and northwest-trending faults which disrupt the stratigraphy. Locally in narrow shear zones gabbro and diabase are both recrystallized to folded amphibolite. Alteration of primary textures and mineralogy in the complex occurs to the northeast. A small granite body intrudes the sheeted dyke zone near Victoria Lake.

No sedimentary rocks have been recognized in the complex; however B. Kean (pers. comm.) reported chert within volcanic rocks on the northwest side of Victoria Lake.

Carboniferous(?) Sediments

DeGrace (1974) has described conglomerate, sandstone, and limestone occupying the trough-like area containing the northeast-southwest trending arms of King George IV Lake. Riley (1957) shows this rock unit as occurring at the southwestern base of the Annieopsquotch Mountains south of Lloyds River. The unit may be present in subcrop throughout the region marked by Riley (1957) around 'Round Pond' (informal name) and boulders of red sandstone, grit, and shale were found as erratics as far away as the northwest side of Cormacks Lake. New exposures of these relatively undisturbed rocks (unit 14), apparently a redbed sequence, occur on Route 480 south of the Lloyds River, and in drainage ditches along the road. Present in the new exposures are red sandstone, grit, and shale, and conglomerate with sandstone, granite, volcanic and carbonate fragments in a recrystallized carbonate matrix. The sandstone and conglomerate show graded layering and crossbeds. A single measurement suggests that the beds strike southeast and dip gently southwest. They are deposited unconformably on granite to the southwest (DeGrace, 1974), the latter perhaps correlatable with the granite that intrudes the Annieopsquotch complex. In Puddle Pond map area the beds clearly lap against the base of the Annieopsquotch Mountains and surround an outlier of diabase.

Correlations within Puddle Pond Area

Problems of stratigraphic and structural correlation exist because of discontinuities along Little Barachois Brook and Lloyds River. The simplest explanation allowing correlation from the Cormacks Lake to the Southwest Brook Valley area is that northwest trends in both regions belong to the same phase of deformation. Thus major northwest-trending fold axes in the Cormacks Lake area correlate with foliations in quartz dioritic orthogneiss in Southwest Brook Valley. Northeast trends in both regions represent an earlier phase of deformation, and in the Cormacks Lake area evidence of yet an earlier phase of deformation is preserved in isoclines.

Along the Lloyds River valley and in the region to the southeast, evidence of major faulting is seen in a mylonitized granite northeast of Southwest Pond, in the trends of mountain ridges in the Annieopsquotch, in deformation of gabbro along the northern margin of the Annieopsquotch complex, and in shearing of volcanic rocks along Victoria Lake. Correlation across this zone must be tentative. Evidence of northeast-trending faults with left-lateral offsets occurs in the Cormacks Lake area. Lithological similarities are noted between the mafic rocks occurring as pods in orthogneiss and granite in the Southwest Brook Valley area, and the rocks of the Annieopsquotch complex.

Metamorphism

In the Cormacks Lake area metamorphic conditions were of the middle to upper amphibolite facies, as is shown by assemblages with cordierite, garnet, sillimanite and gedrite in the paragneisses. Some very coarse grained crystal aggregates were noted of each of these phases, indicating that fluid pressures were probably high and that the peak of metamorphism was of some duration. Granulite facies assemblages with orthopyroxene and clinopyroxene, also orthopyroxene, cordierite and spinel, occur along Southwest Brook. Thin section evidence shows that these higher grade rocks have been affected by a later amphibolite facies event. In the metagabbros southwest of Silver Pond, amphibolitization of pyroxene occurs, as it does in the eastern portion of the Annieopsquotch complex. Shear zones with amphibolite grade assemblages transect the Annieopsquotch complex also. Metavolcanic rocks in the Victoria Lake area appear to be at greenschist grade or lower.

Economic Geology

The rusty paragneisses of the Cormacks Lake complex consistently carry minor sulphides, visible where fresh specimens can be obtained; occasionally large concentrations of pyrrhotite were noted. A gossan with calc-silicate skarn mineralogy (talc, carbonate, quartz, tremolite, garnet, diopside), magnetite and sulphides occurs northeast of Cormacks Lake.

The most economically interesting rocks in the map area are the mafic-ultramafic rocks, especially those of the Annieopsquotch complex. Sulphides have been noted in all of these rock types, and copper sulphide mineralization is known from volcanics in the Victoria Lake region. The ophiolitic rocks in Notre Dame Bay region of Newfoundland are host to small copper sulphide deposits, and the recognition of the Annieopsquotch complex means such mineralization should be sought in it.

The red-bed sequence at the base of the Annieopsquotch Mountains has undetermined economic potential; it must have formed in part from erosion of adjacent granites and gabbro-volcanic rocks.

Regional Correlations, Implications and Speculations

It is a working hypothesis that much of the western and northern portion of the Puddle Pond area contains rocks which originally belonged to the Grenville orogen, and have been subsequently remobilized and intruded by younger rocks. Similarly, stratigraphically younger rocks laid down upon, thrust upon, or intruded into, Grenville basement may also have been metamorphosed, and intruded by remobilized basement or by younger plutons. Thus it is impossible to be certain of the age of any rocks in the region. The fact that Devonian rocks in the La Poile River area to the south achieve a similar metamorphic grade to the paragneisses near Cormacks Lake (cf. Cooper, 1954) suggests caution should be exercised in equating grade with age. Structural evidence indicates that northwest trends in the Puddle Pond area developed relatively late, and are coincident with retrogression of earlier high-grade metamorphic or igneous mineral assemblages. Faulting associated with strong northeast trends in the Lloyds River – Victoria Lake region transects the northwest trends; major stratigraphic zones of the Annieopsquotch complex also strike northeast, but are also cut by the northeast-trending faults. If the Annieopsquotch complex is an Ordovician ophiolite sequence, then rocks to the northwest of the Lloyds River valley are pre-Ordovician in part, and the complexly-folded Cormacks Lake complex could be Grenvillian.

The Annieopsquotch complex is an ophiolite sequence which must now be considered in any attempt to trace the margin or the suture zone of a proto-Atlantic (Iapetus) ocean in the Appalachians. The complex clearly indicates oceanic crust, and it occurs faulted against high-grade gneisses and migmatites which suggest continental margin material, albeit of a deep crustal level. West of the Annieopsquotch complex large masses of igneous rocks occur in an agmatite terrane (Southwest Brook Valley area); some of these igneous rocks appear to have lithological similarities to the Annieopsquotch gabbros and to rocks of the Bay of Islands complex.

Indeed it can be speculated that the Lloyds River Valley marks the site of continent-ocean collision during closing of Iapetus, and that gabbros and norites northwest of the Annieopsquotch complex represent a train of obducted ophiolite material, which with the Annieopsquotch and Bay of Islands igneous rocks, was once part of the ocean crust. In such a model, the region around Cormacks Lake and the region north of Southwest Brook might be considered relict continental crust of Grenville age. The region of Southwest Brook Valley contains late northwest structural trends and is marked by the occurrence of quartz dioritic orthogneiss which agmatizes older gneisses and mafic igneous masses. The region may represent a rift or transform fault in the margin of the continental crust, into which plutonic rocks may have intruded or into which previously obducted ophiolitic rocks may have foundered as melting occurred. Such a model links the complex geology of the Puddle Pond area with some current models of Appalachian tectonics (e.g. Williams, 1978b).

Acknowledgments

Base-camp facilities were again provided at the Newfoundland Forest Research Centre, Pasadena (Environment Canada). Field assistance was provided by W.P. Carew, G.T. Noah, and P. Kavanagh. Assistance along Route 480 was given by the Department of Transport and Communications, Newfoundland, and by Chaulk's and Western construction companies. Viking Helicopters Newfoundland Ltd. and Labrador Airways provided aircraft support, and the Department of Mines and Energy, Newfoundland, assisted in

field logistics. Individuals to be thanked for work and/or discussions on this project include: P.L. Dean, J. Kinrade, B. Kean, P.A. Brown, J. Allan, W. Poole, N.A.C. Rey, K.L. Currie, J. MacManus, H. Williams, R. Smyth and H. Bostock. This project is proceeding in conjunction with mapping by the Mineral Development Division, Department of Mines and Energy, Newfoundland, under terms of the Canada – Newfoundland Mineral Development Subsidiary Agreement (1976-1981). Discussions on Newfoundland geology with all personnel of the Mineral Development Division are gratefully acknowledged. P.L. Dean first noted that the Annieopsquotch Mountains exposed an ophiolite complex (pers. comm., 1977, 1978).

References

Cooper, J.R.
1954: La Poile – Cinq Cerf map-area, Newfoundland; Geological Survey of Canada, Memoir 276.

DeGrace, J.R.
1974: Notes on the geology of the King George IV Lake area, southwest central Newfoundland; in Report of Activities, 1973, Mineral Development Division, Newfoundland Department of Mines and Energy, p. 43-49.

Herd, R.K.
1978: Geology of Puddle Pond area, Red Indian Lake map-sheet, Newfoundland; in Current Research, Part A, Geological Survey of Canada, Paper 78-1A, p. 195-197.

Kean, B.F.
1976: Geology of the Victoria Lake area; in Report of Activities, 1975, Mineral Development Division, Newfoundland Department of Mines and Energy, Report 76-1, p. 31-37.

1977: Geology of the Victoria Lake map area (12A/6), Newfoundland; Mineral Development Division, Newfoundland Department of Mines and Energy, Report 77-4.

Kidd, W.S.F., Dewey, J.F., and Bird, J.M.
1978: The Mings Bight Ophiolite Complex, Newfoundland: Appalachian oceanic crust and mantle; Canadian Journal of Earth Sciences, v. 15, p. 781-804.

Riley, G.C.
1957: Red Indian Lake (west half), Newfoundland; Geological Survey of Canada, Map 8-1957.

Williams, H.
1967: Geology, Island of Newfoundland, Newfoundland; Geological Survey of Canada, Map 1231A.

1978a: Tectonic lithofacies map of the Appalachian orogen; Memorial University of Newfoundland, Map No. 1.

1978b: Vestiges and margins of Iapetus in the Appalachian orogen; Geological Society of America, Abstracts with Programs, v. 10, p. 517.

48.

GRANULITES AND PLUTONIC COMPLEXES NORTHEAST OF BAKER LAKE, DISTRICT OF KEEWATIN

Project 760028

Mikkel Schau and K.E. Ashton[1]
Regional and Economic Geology Division

Schau, Mikkel and Ashton, K.E., Granulites and plutonic complexes northeast of Baker Lake, District of Keewatin; in Current Research, Part A, Geol. Surv. Can., Paper 79-1A, p. 311-316, 1979.

Abstract

An anorthositic layered suite was emplaced in country rock of unknown origin, but which may have been in part sedimentary. The complex was subsequently deformed and metamorphosed to granulite grade. The resulting complex was intruded on the east and possibly on the north by a granitic plutonic complex. Gabbro stocks were then emplaced. Near a north-south fault the gabbro stocks and plutonic complex were deformed and foliated. Later, movement along the east-west Chesterfield fault zone brought the granulite complex into juxtaposition, with amphibolite grade gneisses and schists to the south. After most movement ceased along the fault, a dyke swarm was emplaced along easterly trends in the Chesterfield fault zone.

The Dubawnt Group unconformably overlies the granulite complex and the Chesterfield fault zone. Dykes and diatremes associated with the volcanic rocks of the group cut all previous units. Tectonic activity ceased after northwest striking faults cut Dubawnt Group.

Introduction

During the 1978 field season, NTS areas 56 C/4 and the remainder of area 56 D/1 (except for those parts of 56 D/1 affected by land use closure) were mapped at a scale of 1:50 000. The geology of part of 56 D/1 has been previously described by Schau and Hulbert (1977).

The field work was delayed by unseasonably cold and snowy weather, along with problems associated with working in the unfamiliar tidal waters of Chesterfield Inlet and Quoich River (tidal range ~2 m). The authors thank L. Nadeau and B. Rigby for their field assistance. Aerotrades Limited provided helicopter support and Lambair and Calm Air fixed-wing service.

General Geology

The area consists largely of an anorthosite-granulite complex which has been variously faulted against, or intruded by, a plutonic complex near the Quoich River. The granulites are in fault contact with medium grade metamorphic gneisses of pelitic and quartzofeldspathic composition to the south. They are unconformably overlain by the Dubawnt Group to the west (Fig. 48.1).

Good exposures of anorthosites, granulites, and gabbro were found, whereas granitoid gneisses and other plutonic rocks are poorly exposed. Outcrops of granitoid plutonic units are free from pervasive lichen cover only in the intertidal zone.

Anorthosite and Granulite Complex east of Baker Lake

Granulites

The granulite suite comprises a large variety of rock types, the most common of which is a rock consisting of pyrobole-rich, brown, rusty weathering material interlayered with tan weathering pyrobole-bearing quartzofeldspathic rocks. The quartzofeldspathic units are well foliated. The layers are typically compositional rather than textural, with thicknesses ranging from centimetres to tens of metres. They are composed of various proportions of quartz, feldspars, pyroboles, and garnets. Orthopyroxene is the predominant mafic mineral, but clinopyroxene is present in various habits, and hornblende is sparsely present. The most common feldspar is calcic plagioclase, but antiperthite and perthite are present.

The pyrobole-rich layers include metre-thick garnet-pyrobolites that grade into garnetites (>70% garnet). Locally, metre-thick orthopyroxenite layers and boudins are present. In thin section they are seen to be composed of orthopyroxenes with thin diopside lamellae. Metre-thick bytownite-rich layers are infrequently layered by centimetre-thick pyrobole ± garnet layers. Rare quartz-rich units with less than 10 per cent feldspar and pyrobole are also present. Thin, well-layered, brilliant white to resinous yellow, rusty weathering, garnetiferous quartz feldspar (usually potassic) rocks with graphite, pyrite, and less commonly biotite, also occur and these locally contain sillimanite and in one layer both sillimanite and kyanite. Pyritic pyrobole-rich rocks are present in thin layers, as are graphite-rich garnetiferous quartzofeldspathic rocks.

The layering is the most obvious feature of the granulites and is planar and continuous along strike for tens of kilometres. In hand specimens quartz ribbons define the foliation. The rocks exhibit a shallow-plunging westwardly directed mineral lineation. The axes of relatively rare minor mesoscopic folds are parallel to this lineation. In such regions the foliation cuts across the layering. Sheared minor folds which resemble crossbeds are locally abundant. Plagioclase-rich and pyroxenite layers are most commonly boudinaged. A thin, distinctive, plagioclase unit was mapped in detail to demonstrate that, despite local minor structures, it is remarkably planar and continuous (Fig. 48.2).

It has been suggested that the granulites are in part sedimentary (Schau and Hulbert, 1977) and the observance this season of silicate-bearing rocks, sulphide iron-formation and graphitic units, strengthens this interpretation. On the other hand, Jak (1977) has concluded, on the basis of chemical analyses of some of the orthopyroxenite layers, that these are of igneous origin. A considerable portion of the complex may be of igneous origin, related either to the anorthosite discussed below or to earlier layered gneisses (charnockites of Schau and Hulbert, 1977). The age of the granulites is unknown, but they are known to predate the anorthositic part of the complex. A similar suite of granulite and anorthosite occurs to the east at Daly Bay (Gordon, pers. comm., 1978) but its correlation with that of the study area has not been established.

[1]Department of Geological Sciences, University of Saskatchewan, Saskatoon, Saskatchewan.

Anorthosites

The anorthosite suite is composed of relatively few rock types. The most abundant is a coarse grained, streaky, gabbroic-noritic meta-anorthosite. Blocks of meta-anorthosite are found within the streaky gabbroic meta-anorthosite unit to the west near Baker Lake. Metre-thick layers of meta-anorthosite and anorthositic metagabbro are interbedded farther east. Less abundant are conformable metagabbro layers and metaferrogabbro dykes.

The anorthositic suite locally exhibits primary igneous layering on a scale of 1 cm to 1 m and rarely, graded cumulate layering (Fig. 48.3). Coarse orthopyroxene crystals form zones which may also represent primary layering. Primary mineral features include schiller reflections in large relict plagioclases and lamellae of clinopyroxene in orthopyroxene. The thickness of the anorthositic suite varies and although tectonic thickening and thinning has undoubtedly played a role, the variations in thickness from hundreds of metres to the north to a few tens of metres to the south, is in part thought to be primary since adjacent marker horizons in the granulites do not show similar changes in thickness.

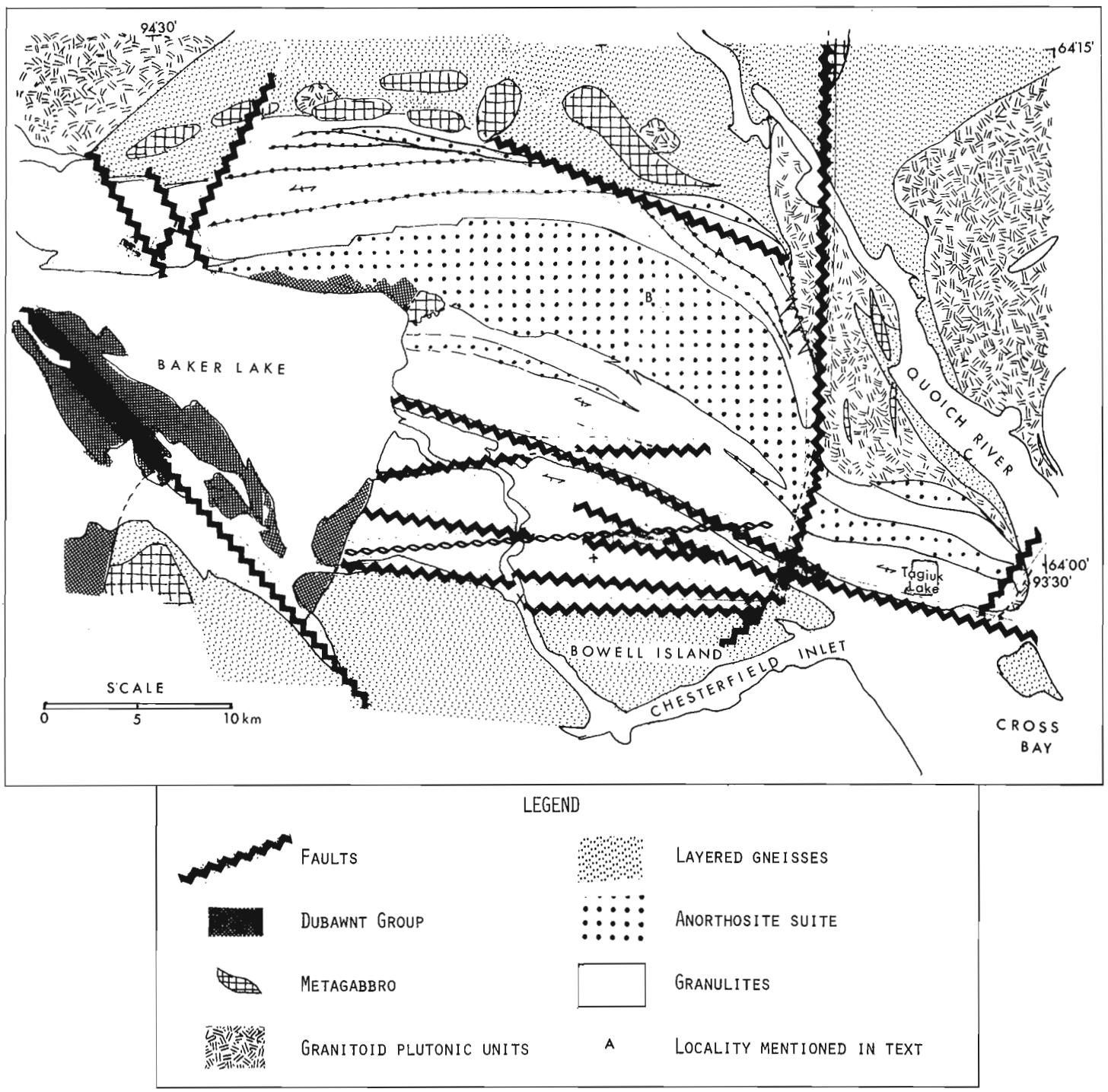


Figure 48.1. *Sketch map of region northeast of Baker Lake showing rock types and major fault zones.*

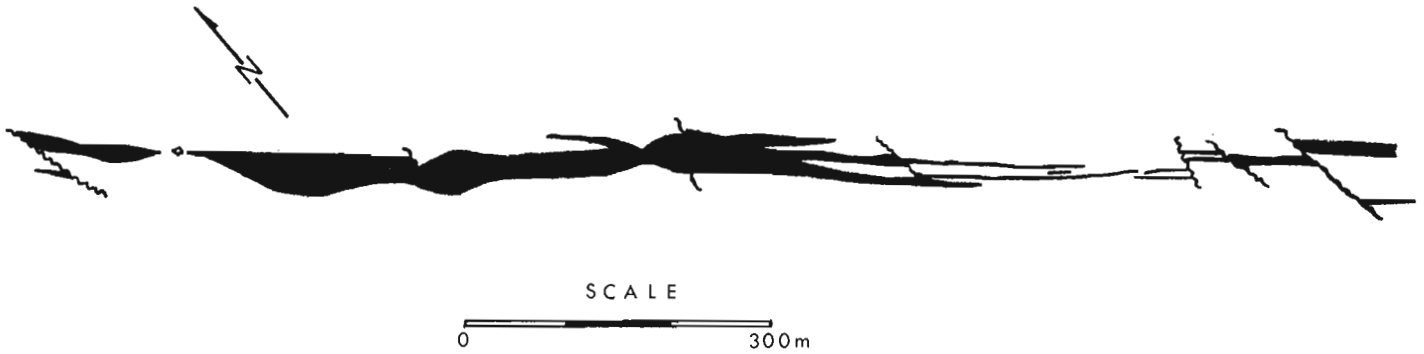


Figure 48.2. *Detailed plan of an anorthosite layer. Note structural complexity yet remarkable persistence along strike. Area is located on Figure 48.1 as A.*

Secondary structures include the flattening and granulation of plagioclase and pyroboles, resulting in the streaky foliation common in rocks of the western part of the central zone. Orthopyroxenes are kinked. Sheared zones consist either of granulated sugary-textured aggregates or of finely laminated alternating layers of pyrobole and plagioclase.

North of Tagiuk Lake the suite is well layered with brilliant white anorthosites alternating with lenticular dark brown orthopyroxene and garnet-rich layers. Along strike to the west the unit grades into streaky gabbroic-noritic anorthosite. Near Tagiuk Lake a dark layer forms a "Z" fold with shallow westerly plunge showing extremely small inter-limb angles, 50 cm across at its thickest and a middle limb 30 m long. In the west, folds in ferrogabbro have much greater inter-limb angles, are wider, and have much shorter middle limbs. Foliations are poorly developed in the west but are well developed in the east, suggesting that the eastern part of the complex has been more strained than the west. Both relict and metamorphic plagioclases are oriented to give the rock a fabric. Mafic rods are elongated at angles to compositional layering in the rock and individual coarse grained orthopyroxenes are surrounded by finer grained granoblastic pyroboles which define the foliation.

The granulite and anorthosite are usually conformable. In the north the contact is marked by a well-sheared and layered plagioclase-rich unit and pink weathering, garnet-bearing granulites. Along the south edge of the central zone inclusions of country rock, and dykes of anorthosite into country rock granulite are evidence for an intrusive relationship (Schau and Hulbert, 1977). It is concluded that the anorthosite suite was part of a large igneous complex which was intruded into country rock (in part sedimentary) that was later converted into granulite.

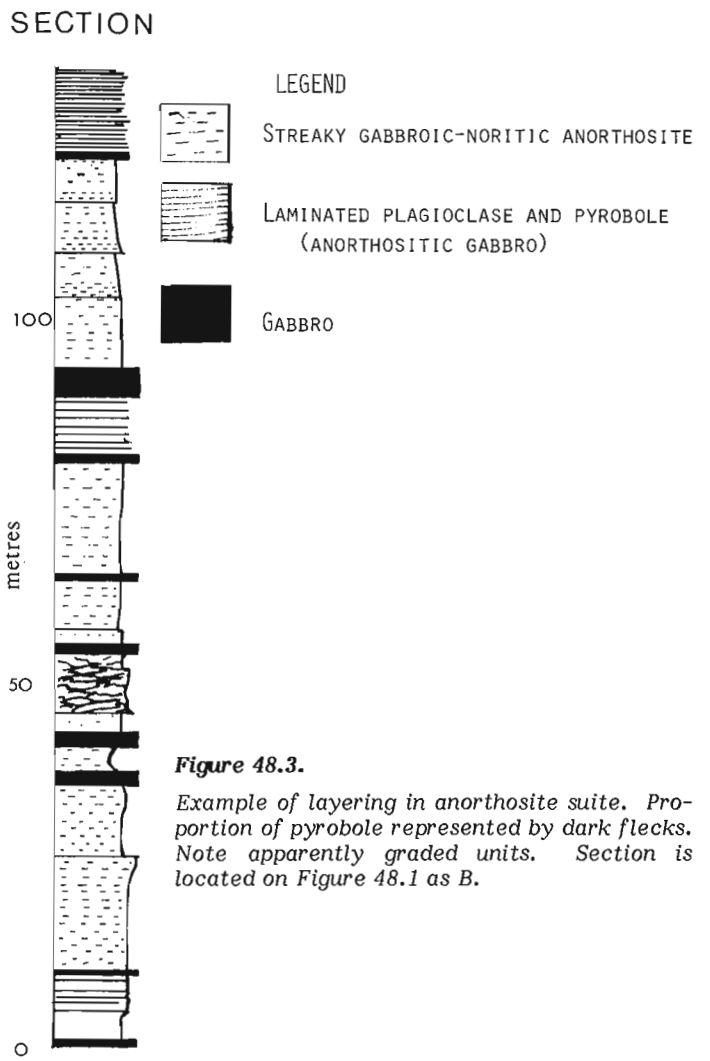


Figure 48.3.

Example of layering in anorthosite suite. Proportion of pyrobole represented by dark flecks. Note apparently graded units. Section is located on Figure 48.1 as B.

Plutonic Complex Exposed Along Quoich River

A large plutonic complex surrounds and intrudes the granulite complex to the north and east. It consists of several different, poorly exposed units, that include early layered gneisses and several types of quartzofeldspathic plutonic rocks, all of which contain hornblende and biotite. The complex is cut by gabbro stocks and dykes which have been variously affected by local deformation. An example of the type of deformation which affects these rocks is well exposed in the tidal range and a sketch map of this small region is shown in Figure 48.4.

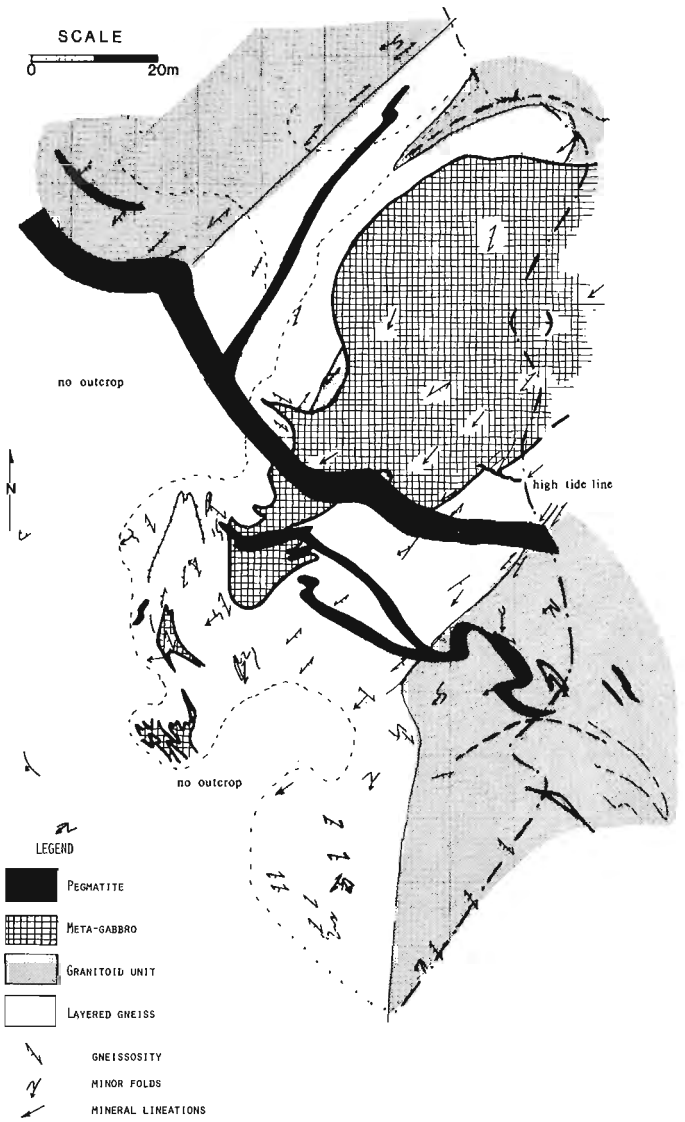


Figure 48.4. *Detailed map of relationships in plutonic complex. Area is located on Figure 48.1 as C.*

Layered gneisses

Layered gneiss occurs as septa and wedges in the eastern part of the area. It forms the host for the plutonic rocks. It is not well exposed, although one septa appears to occupy the valley of the Quoich River where a variety of rock types are present. The most common type is a thinly layered hornblende biotite diorite to quartz diorite gneiss with occasional accessory magnetite. Thin layers of epidote, garnet-rich layers and thin discontinuous actinolite chlorite schists are present. In the north, muscovite schists occur as enclaves in plutons. Near plutons the layered gneiss is the "paleosome" in migmatites and contains abundant porphyroblastic feldspars.

These gneisses are complexly folded. For instance a mesoscopic fold in whose limbs parasitic folds with axes oriented at angles up to 90° of the plunge of the main fold was seen.

The variety of rock types and possibly primary structures present in the gneiss suggests that its protolith was in part sedimentary. The gneiss predates the plutons, but its age relative to the granulites is unknown.

Abundantly porphyroblastic granodiorite

This rock type consists of abundant feldspar porphyroblasts set in a medium-grained biotite granodiorite matrix. Near the mouth of the Quoich River dykes of this unit cut isoclinally folded early layered gneiss. To the north the dykes are intruded by and folded around later plutonic units. Dykes of this unit cut the granulite suite to the east and blocks of the granulites are found as inclusions in the unit near the contact.

Sparsely porphyroblastic granodiorite

A white, pink, or red weathering fine- to medium-grained biotite granodiorite with sparse porphyroblasts of feldspar apparently underlies the central portion of the Quoich River plutonic area (Fig. 48.1). It contains small inclusions of early layered gneiss and locally, vaguely layered gneiss. Local accessory minerals in these rocks include magnetite, pyrite, and a glassy brown mineral. The unit is foliated parallel to the main north-south fault zone and the foliation swings easterly to follow contacts with the granulite complex. Near the fault the rocks exhibit retrograde effects, including chloritization. The sparsely porphyritic granodiorite cuts the more abundantly porphyroblastic rocks and may grade into or predate slightly the main plutonic unit described next.

Main granitoid plutonic unit

The main granitoid plutonic unit occurs east of the Quoich River and consists of white to pink weathering, medium grained, granodiorite to granite. Many variations occur within the pluton, including locally magnetite-rich granitic rocks. Most of the unit is massive, but foliated varieties occur, especially near septa and inclusions of earlier layered gneiss.

Gabbro stocks

Irregularly shaped gabbro stocks occur generally within but near the contact of the plutonic complex with the granulite complex. The rocks vary from metagabbro with well-preserved primary textures to well lineated amphibolites. One large stock near 94°W is relatively undeformed in the north but is sheared and deformed to the south. Other bodies in the south contain enclaves of relatively undeformed metagabbro with amphibolite rims. The metagabbros locally exhibit a vague foliation and folded layering. In some places the folds have been cut by subsequently folded quartz veins containing sulphides, and by pegmatites.

There appears to be only one generation of gabbro stocks and the variation in their deformation is an index to the intensity of local deformation.

Pegmatites

Biotite-bearing pegmatites are variably distributed. Many cut the gabbro stocks and early complex and are probably of several generations.

Gabbro dyke swarm on Bowell Island

A swarm of metre-thick brown weathering aphanitic to fine grained basic dykes cut a fault zone along Chesterfield Inlet. Although the dykes may have been mistaken locally for the gabbroic parts of the anorthosite which they resemble in the field, detailed mapping of the dykes indicates that there are many thin, easterly trending, steeply dipping postfolding dykes. The swarm is pre-Dubawnt Group, but apparently postdates movement on many east-west faults. On the other hand, near a north-south fault, they are chloritic and have been offset a metre or so.

Dubawnt Group

Diatremes and dykes of biotite-pyroxene lamprophyre, often with partially resorbed xenoliths of granite, are associated with the Dubawnt sedimentation (Schau and Hulbert, 1977; Blake et al., 1977). Similar diatremes with similar dykes were found this summer on Bowell Island. Dykes of biotite lamprophyre, some of which are quite magnetic, and irregular stocks are found along Chesterfield Inlet. There is a possibility that some dykes postdate the Dubawnt.

Structural geology

Large folds with planar limbs characterize the anorthosite and granulite complex (cf. Fig. 48.2) whereas small complex mesoscopic folds are noted in layered gneiss of plutonic complex (cf. Fig. 48.4). The plutonic units and gabbro stocks are foliated and flattened in an easterly direction.

The anorthosite suite and the adjacent country rock were metamorphosed to granulite grade while being deformed into a gently westward-plunging anticline-syncline pair. The fold is well outlined by the anorthosite suite and associated mafic oxide-rich layers. The quartz ribbons of the granulites indicate the axial plane of the fold, and minor folds and linear minerals indicate the plunge. The core of the fold is intruded by units of the plutonic complex.

The plutonic complex was emplaced in already deformed layered gneiss complex and the mesoscopic folds all show signs of several deformational events.

The plutonic complex, although generally younger than the granulites, contains very complex structures (Fig. 48.4), whereas the fabrics of the older granulite complex are essentially planar (Fig. 48.2).

A north-south fault forms a prominent feature which is subparallel with the contact between the plutonic complex and the granulite-anorthosite complex. In the south it cuts across the anorthosite suite and is terminated near the southern edge of the map area by a later east-west fault. The fault zone contains crush breccias, phyllonites, well foliated plutonic rocks, degraded, epidotized and chloritized plutonic rocks, deformed gabbro stocks and dykes. The fault trace coincides with a sharp discontinuity in the anomaly pattern of aeromagnetic maps of the region. The plutonic rocks near the fault zone are foliated parallel to it for many kilometres. The apparent movement of the fault is dextral.

The Chesterfield fault zone (Heywood and Schau, 1978) forms the southern boundary of the granulite complex. It is exposed from the eastern shore of Baker Lake (where it is unconformably overlain by the South Channel conglomerate) eastward along the 64°N latitude line beyond the map boundaries into Cross Bay on Chesterfield Inlet.

The fault zone is wide and consists of many easterly striking faults which cut the granulite complex. Usually faults are poorly exposed in valley bottoms, although crush zones, breccias and phyllonites have been seen. Trends of granulite layering do not coincide in crossing the fault valleys. Anorthositic rocks in the fault zone occur as breccia with football-sized fragments set in a white fine grained quartzofeldspathic matrix. The master fault, which forms the contact between the granulites and the layered gneisses, was seen in one locality (X on Fig. 48.1). Here, a tectonic breccia has been intruded by a muscovite granite that contains small red garnets, bright blue apatite, and abundant black tourmaline. In this distinctive rock are found crush zones and augen gneisses. Only a few metres to the south, phyllonites strike easterly and dip with moderately steep dips (60°) to the north. These features suggest that the fault zone broke, was intruded, and further movement took place to yield augen gneiss and then phyllonite. The aeromagnetic map indicates sharp changes in magnetic susceptibility in the rocks along the postulated trace of the fault. The fault zone separates the granulite complex to the north from amphibolite grade rocks to the south.

Faults other than those described above are present but are characterized by minor offsets. Such faults include east-west faults throughout the region along which Dubawnt Group lamprophyre dykes or hydrothermal veining has taken place. Northeast-trending faults bring granite in contact with anorthosite at the west end of the mouth of the Quoich River. These may be related to the Chesterfield fault zone. A much later set of northwest-striking faults are known to cut the Dubawnt Group, probably with oblique slip, especially on Christopher Island.

Economic potential

No mineral occurrences of economic interest were found in the area. The granulite complex is generally devoid of economically interesting minerals. South of Tagiuk Lake north and south of the inlet local iron-rich sulphide layers which give a considerable magnetic response have been staked and trenched. The exposures are mainly in layered pyrrhotite and pyrite-bearing garnet pyrobole rocks. Some nearby units are very thinly layered and may be examples of sulphide iron-formation. Electrical surveys in the area would probably indicate numerous graphite-rich zones. Along Chesterfield Inlet degraded serpentinized orthopyroxenites provide low grade soapstone localities.

The plutonic complex contains a sparsely distributed brown, glassy, slightly radioactive accessory mineral. Magnetic anomalies in this complex are due to accessory magnetite. Gabbro stocks contain veins of quartz and pyrite with minor chalcopyrite and rare molybdenite and other sulphides. Pegmatites are yellow-stained and somewhat more radioactive than country rock, but they are simple quartz, feldspar, rare biotite pegmatites rather than complex pegmatites. Hematite, carbonate, and epidote are present along the north-south fault where it cuts across the Quoich River in the north.

The Chesterfield fault zone contains a blue apatite-bearing granite that is uraniferous. The radioactive mineral has not yet been identified. Smaller east-west faults contain purple fluorite. Other fault zone minerals include quartz, calcite, dolomite.

The magnetic anomaly patterns are easily rationalized with various geologic map units. These include pyrrhotite layers in the granulite suite, magnetic ferrogabbros of the anorthosite suite in the granulite complex, magnetite-rich regions in the main plutonic suite of the plutonic complex, biotite lamprophyres and dykes, and a volcanic neck of the Dubawnt Group.

References

Blake, D.H., Miller, A.R., and Schau, Mikkel
1977: Potassic volcanic rocks of the Paleohelikian Dubawnt Group and associated Cu, U, and Se mineralization, Christopher Island region, District of Keewatin, N.W.T.; in Program of Abstracts, v. 2, Geological Association of Canada, p. 8.

Heywood, W.W. and Schau, Mikkel
1978: A subdivision of the northern Churchill Structural Province; in Current Research, Part A, Geological Survey of Canada, Paper 78-1A, p. 139-143.

Jak, A.G.
1977: A petrographic study of pyroxenites in granulite gneisses, Baker Lake, District of Keewatin, N.W.T.; unpublished B.Sc. thesis submitted to Carleton University.

Nadeau, L. and Schau, Mikkel
1979: Surficial geology near the mouth of the Quoich River, District of Keewatin; in Current Research, Part A,Geological Survey of Canada, Paper 79-1A, note.

Reinhardt, E.W. and Chandler, F.W.
1973: Gibson-MacQuoid Lakes map-area, District of Keewatin; in Report of Activities, Part A, Geological Survey of Canada, Paper 73-1A, p. 162-165.

Schau, Mikkel and Hulbert, L.
1977: Granulites, anorthosites and cover rocks northeast of Baker Lake, District of Keewatin; in Report of Activities, Part A, Geological Survey of Canada, Paper 77-1A, p. 399-407.

49.

STRATIGRAPHY, STRUCTURE, AND REGIONAL CORRELATION OF ROCKS AT GRAND LAKE, WESTERN NEWFOUNDLAND

E.M.R. Research Agreement 2239-4-124/78

D. Knapp[1], D. Kennedy[1], and Y. Martineau[1]
Regional and Economic Geology Division

Knapp, D., Kennedy, D., and Martineau, Y., Stratigraphy, structure, and regional correlation of rocks at Grand Lake, western Newfoundland; in Current Research, Part A, Geol. Surv. Can., Paper 79-1A, p. 317-325, 1979.

Abstract

Basement gneisses, anorthositic rocks and granites interpreted to be Grenvillian or older are overlain by amphibolite grade schists and paragneiss of presumed Hadrynian and Early Paleozoic age, and in turn by a Lower Paleozoic ophiolite sequence and a younger volcanic and volcaniclastic sequence bearing Early Ordovician graptolites. The ophiolites and other distinctive rocks indicate that the Baie Verte belt in the north extends southward through Glover Island. The basement, and schist and gneiss cover, have been multiply deformed and regionally metamorphosed during the Paleozoic and thrust westward upon multiply deformed Cambrian-Ordovician phyllites and carbonates of the platform sequence. These orogenic effects are probably Acadian. The Cabot Fault whose latest movement is post-Carboniferous contains an intruded granite, now brecciated, and may have a pre-Carboniferous history of fault movement and intrusion.

Introduction

The southwestern half of Grand Lake area (parts of 12A/12, 13, 12B/9, 16) was mapped during the 1978 field season, largely as part of the program to remap the Stephenville (12B) and Red Indian Lake (12A, west half) map areas. The area is divided roughly in half by the northeast-trending Cabot Fault. West of the Fault, rocks south of Grand Lake were mapped by Martineau and those north and northwest of Grand Lake by Kennedy. Knapp was responsible for the area east of the Fault. The results of this preliminary work are summarized below.

Area South of Grand Lake

The area described in this section is bounded by the Trans-Canada Highway (Route 1) to the west, the Cabot Fault to the east, Bottom Brook to the south, and Grand Lake to the north. It lies within the Long Range Mountains which form north-south trending ridges with relief of about 525 m. Grand Lake and Bottom Brook form major east-west depressions. Outcrops occur on the ridges, along stream gullies, and on the lake shore. Logging roads and Grand Lake provide good access.

The area may be divided into two domains: a carbonate sequence to the west, and crystalline rocks to the east. The carbonate sequence represents the most easterly exposures of the western Newfoundland Lower Paleozoic carbonate platform. The crystalline rocks consist of gneisses, granites and anorthositic rocks, alternating with zones of semipelitic to psammitic schists.

The gneisses are interpreted as basement and correlated with the Grenvillian Long Range and Indian Head complexes (Riley, 1962). The schists are interpreted as a Hadrynian-Lower Paleozoic cover sequence.

A major fault separates the carbonate and crystalline terranes. This fault is a southward continuation of the Corner Brook Lake Thrust (Kennedy, 1978) or the Grand Lake Thrust (Williams, 1978), and it juxtaposes Precambrian gneisses against the Paleozoic carbonate sequence.

Precambrian Rocks

The Precambrian terrane is composed of granitic and plagioclase-hornblende (amphibolitic) gneisses (unit 1a), granites (12a) and anorthositic rocks (12b). In the northern part of the area granitic gneisses predominate, while to the east, plagioclase-hornblende gneisses are more abundant. The anorthositic rocks are restricted to a fault-bounded area to the south near Bottom Brook.

The granitic gneisses (1a) are composed of pink feldspar, quartz, and some amphibole and/or biotite. The rocks vary from slightly foliated (oriented mafic minerals) to thinly banded to augened and to mylonitized, all irregularly distributed. An intrusive breccia contact between a fine grained foliated granitic gneiss and a banded granitic gneiss occurs northeast of a lake locally known as Tulk's Pond, indicating that some, if not most, of the granitic gneisses are of intrusive origin.

The plagioclase-hornblende gneiss (1a) consists of white plagioclase, hornblende, locally biotite, and minor quartz. The gneiss is structurally less variable than the granitic gneiss and exhibits banding and mineral foliations.

An isolated occurrence of calc-silicates and quartzites (1b) along the lakeshore has an outcrop width of about 30 m. These lie within the granitic gneisses but the contacts with the gneisses are not exposed.

The anorthositic rocks (12b) include norites, anorthosites and pyroxenites of variable grain size. They vary from massive to cataclastic to foliated. The unit is everywhere faulted against granitic gneisses.

The less tectonized granitic gneisses in the area, such as those found near the intrusive breccia mentioned above, resemble the gneisses of the Indian Head Range. The presence of anorthositic rocks in the Indian Head Range support this correlation. The Indian Head Range has yielded ages of 880 and 825 Ma on hornblende and biotite, respectively, by the $^{40}Ar/^{39}Ar$ method (Dallmeyer, 1978). It seems reasonable to assume a similar Precambrian age for the rocks in the map area. The fact that most anorthosite massifs are of Precambrian age provides further support. The age of the calc-silicates and quartzites found on the lakeshore is unknown. Similar rocks occur to the north of Grand Lake where they are interpreted as Precambrian.

Granites

Two large bodies of massive granitic rock occur in the central part of the area. Their composition varies from granite to syenite to mafic-rich syenite (up to 30 per cent mafic minerals). They are medium to coarse grained, pink,

[1]Department of Geology, Memorial University of Newfoundland, St. John's, Newfoundland, Canada A1B 3X5.

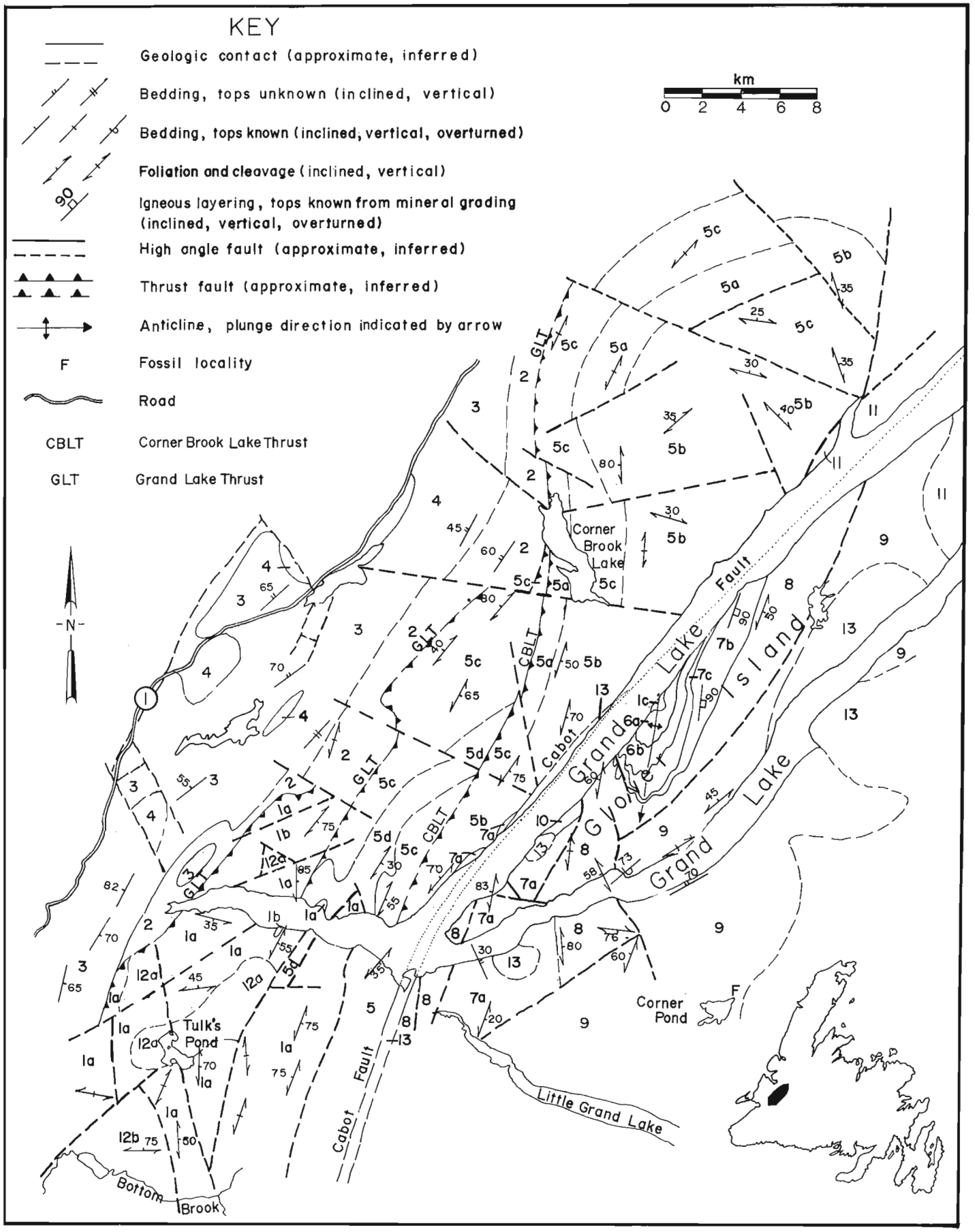

KEY
Geologic contact (approximate, inferred)
Bedding, tops unknown (inclined, vertical)
Bedding, tops known (inclined, vertical, overturned)
Foliation and cleavage (inclined, vertical)
Igneous layering, tops known from mineral grading (inclined, vertical, overturned)
High angle fault (approximate, inferred)
Thrust fault (approximate, inferred)
Anticline, plunge direction indicated by arrow
F Fossil locality
Road
CBLT Corner Brook Lake Thrust
GLT Grand Lake Thrust
km
0 2 4 6 8
-N-
Corner Brook Lake
Fault
Grand Lake
Island
Grand Lake
Cabot Fault
Tulk's Pond
Corner Pond
Little Grand Lake
Bottom Brook

Figure 49.1

Description for Figure 49.1

INTRUSIVE ROCKS

13 Carboniferous and older granites
12 Precambrian: 12a, granites; 12b, anorthositic rocks

STRATIFIED ROCKS

CARBONIFEROUS

11 Conglomerate, sandstone, siltstone and shale

DEVONIAN AND OLDER

10 Conglomerate, sandstone and purple shale in graded sequences up to 1 m in thickness

MIDDLE ORDOVICIAN TO LOWER CAMBRIAN

WEST OF GRAND LAKE THRUST

4 Table Head Formation: limestones and shales
3 St. George Group: marbles, dolostones and limestones
2 Grand Lake Brook Group: phyllitic schist, phyllite, sericitic marble and marble breccia

9 Pillow lavas, agglomerates, massive diabase and shales
8 Pillow lavas, tuffs and tuffaceous sediments overlying a conglomerate at base of unit composed of volcanic and minor, bright red, silicic clasts

GLOVER ISLAND COMPLEX

7 Mafic and ultramafic rocks of ophiolitic affinity; 7a, sheeted dykes and pillow lavas; 7b, cumulate and massive gabbro; 7c, variably serpentinized ultramafic rocks

HADRYNIAN TO LOWER PALEOZOIC

FLEUR DE LYS SUPERGROUP

5 Semipelitic schists and psammitic gneisses; 5a, banded feldspathic gneisses, metaconglomerate and amphibolite; 5b, feldspathic schists; 5c, garnet-quartz-mica schists and micaceous quartzites; 5d, calcareous schists and marbles

6 Semipelitic schists and psammitic gneisses; 6a, cyclically bedded schists and gneisses, micaceous quartzites and intraformational polymictic conglomerates; 6b, calcareous schist, marble and biotite schist, includes carbonaceous phyllite at top of unit

PRECAMBRIAN

1 1a, granitic gneiss and amphibolite; 1b, schists and gneisses with minor quartzite and calc-silicate gneiss; 1c, Grand Lake gneiss

and they are cut locally by shear zones. The age of these bodies is problematic, for although they are relatively undeformed, they are restricted to the Precambrian gneissic terrane. They may be Precambrian locally affected by Paleozoic deformation.

Hadrynian to Lower Paleozoic Metasediments

Semipelitic to psammitic metasediments east of Tulk's Pond are faulted against the gneisses. A crude stratigraphy is recognized in the largest of these fault-bounded blocks, although facing directions are unknown. The rocks at the contact with the gneisses are marbles, followed to the east by garnet-mica schists, quartzites and semipelitic schists (E. Stander, pers. comm., 1978). These rocks are thought to correlate with units 5d, 5c and 5b north of Grand Lake. A fault-bounded sliver of metasediments occurs west of the large metasediment block, and is composed of mica schists with large amphibole prisms on the foliation planes. This distinctive rock is correlated with unit 5d north of Grand Lake. Based upon lithological similarity of these metasediments with the Fleur de Lys Supergroup of the Burlington Peninsula (Church, 1969), the cover rocks of the Grand Lake area are correlated with the Fleur de Lys Supergroup, and interpreted as Hadrynian to Early Paleozoic in age.

Dykes

Mafic dykes, containing amphibole and lesser amounts of plagioclase, occur in the gneisses of unit 1. These trend northeast and dip steeply to the southeast. Many dykes occur along fault planes which are axial planar to, and truncate the hinges of, folds in the gneissic banding. Most dykes contain a northeast-trending foliation.

North-trending amphibolite layers locally rich in biotite occur in mylonitized to augened granitic gneisses, approximately 1 km southeast of Tulk's Pond, and are also interpreted as dykes.

The Tulk's Pond amphibolites are probably of Precambrian age, since they contain the same structural fabric as the gneisses. The northeast-trending set of dykes is difficult to date. They cut banding in the gneissic rocks (1), but do not cut the cover rocks (5). They are most likely of Early Paleozoic age.

Platformal Sequence

The platformal sequence (2, 3, 4), consisting of black phyllites and carbonates, lies to the west of the Grand Lake Thrust. To the north, black phyllites (2) are juxtaposed with

Precambrian gneisses along the Grand Lake Thrust. The phyllites contain thin (1 cm) sandy beds and, in places, carbonate beds. They are assigned to the Grand Lake Brook Group (Walthier, 1949) of Cambrian age.

To the southwest, the Grand Lake Thrust truncates the phyllites, and the carbonates (3) are juxtaposed with the gneisses. The carbonates consist of pink dolostones and grey limestones with thin greenish phyllite interlayers. These are correlated with the St. George Group of Early Ordovician age (Riley, 1962).

Structure

The structural fabric of the Precambrian gneisses is composite but trends are generally northeast and dips steeply to the southeast. The gneissic banding is truncated by mafic dykes. Locally a younger subparallel foliation is defined by the alignment of mafic minerals in the mafic-rich bands of the gneisses, and it may be equivalent to that developed in mafic dykes. Northeast-trending minor folds involve the gneissic bands of the plagioclase-hornblende gneiss and the younger foliation is axial planar to the minor folds. It seems probable that the gneissic banding is a Precambrian feature, which in most places was tightly folded by later Paleozoic deformation, such that it is now subparallel with the later foliation.

The anorthositic rock unit contains east-west mineral foliations in some places. These are interpreted as Precambrian structures which were unaffected by later deformations.

The metasedimentary cover sequence contains a predominantly northeast-striking schistosity that dips steeply southeast. This is possibly equivalent to the younger foliation of the gneisses and is of Paleozoic age.

Large folds in the platformal sequence west of the Grand Lake Thrust also trend northeast. Folding is tight, and a few bedding tops indicate some steeply dipping beds are overturned to the west.

Faults are common in the area but they generally occupy topographic lows and are poorly exposed. Sparse outcrop and the lack of good marker units make it difficult to determine the displacement along the faults, and important structural junctions are obscured.

The regularity of fault traces implies that they are steeply dipping. A set of northeast-trending faults is well exposed along Grand Lake. These dip approximately 70 degrees to the southeast. Mylonitic foliations in the gneisses along the Grand Lake Thrust dip steeply suggesting it is also a high angle fault. It is possible, however, that many of these fault planes have been rotated by later folding.

West of the map area, the Grenvillian Indian Head Range Complex is overlain unconformably by relatively undeformed Lower Paleozoic strata. Faulting and retrogression in the basement rocks is less apparent there. These features of the Indian Head Complex, compared to the gneisses at Grand Lake, suggest that the latter have been profoundly affected by Paleozoic deformation.

Comparison of the metasediments to the east of the Grand Lake Thrust and metasediments to the west, indicates a general westward decrease in metamorphic grade.

Summary

Recent mapping south of Grand Lake has resulted in delineation of a basement terrane bounded both east and west by younger cover rocks. Granitic gneisses, plagioclase-hornblende gneisses, anorthositic rocks and granites make up this terrane. Reactivation of this basement terrane during Paleozoic deformation has resulted in the development of a northeast-trending penetrative planar fabric. This was followed by extensive high angle faulting.

Area Northwest of Grand Lake

Reconnaissance mapping of the area northwest of Grand Lake was carried out as a preliminary step to more detailed work. The purpose of the study was to delineate the broad structural and stratigraphic features of the area. Emphasis was placed upon delineation of major thrust faults involving basement and cover rocks, and on the interpretation of stratigraphy in the eastern part of the area.

All the rocks in the area northwest of Grand Lake are deformed and metamorphosed. Three major stratigraphic divisions are recognized: 1) a sequence of well banded gneisses with amphibolite and granite (basement terrane); 2) a sequence of highly deformed gneisses and schists (eastern metamorphic terrane); and 3) a generally less deformed and metamorphosed clastic and carbonate sequence (carbonate terrane). Carboniferous plant-bearing clastic rocks (Riley, 1957) which outcrop in the northeast part of the area were not examined as part of this study.

The contacts between the major stratigraphic divisions are faulted. The rocks in the basement terrane are interpreted to form a structural slice which is thrust westward over the carbonate rocks, and the eastern metamorphic terrane rocks are apparently thrust westward over both basement and carbonate rocks.

The major lithic units within these stratigraphic divisions are disposed in a series of fairly continuous, slightly sinuous, northeast-trending belts that are generally continuous across Grand Lake to the southwest.

Basement Terrane

The rocks comprising the basement terrane outcrop in a fault-bounded block in the southwest part of the area. The main lithologies include: coarse grained, banded, pink, granitic gneiss; green, granodioritic gneisses; and schists, migmatites and amphibolite (1a). The amphibolite layers, generally about 1 m thick, are probably metamorphosed basic dykes. A fault-bounded sequence of buff coloured, feldspathic, psammitic and semipelitic schists and gneisses, minor calc-silicate schist and pure quartzite (1b), is also interpreted to be part of the basement complex. Medium grained, foliated, pink granite (unit 12a) outcrops within the basement terrane, but exhibits faulted contacts with the basement rocks and was not observed in contact with other rocks in the area. Its age is therefore uncertain, but it is tentatively considered to be Precambrian.

The distinctive lithologies and textures of these rocks, particularly the rocks of unit 1a, suggest they are correlatives of the Long Range Complex (Baird, 1960; Neale and Nash, 1963) and thus are part of the Grenvillian basement of western Newfoundland.

Eastern Metamorphic Terrane

Immediately west of the Cabot Fault is a wide belt of polydeformed schists and gneisses. Four distinct, mappable units are recognized, each of which is dominated by either feldspathic, quartzitic or calcareous rocks. Due to the extent of deformation and to the lack of critical outcrop exhibiting lithologic contacts or facing criteria, age relations amongst the four lithologic units are uncertain.

The first two lithologic units consist of dominantly feldspathic rocks and are distinguished from each other on the basis of texture and associated lithologies. The first (5a) outcrops in a narrow belt in the central part of the area and

comprises: finely banded, pink, quartzofeldspathic gneisses, locally micaceous and containing large (1 cm) biotite porphyroblasts; metaconglomerate with flattened quartz and feldspar clasts (some as large as 20 cm); minor green mica schist containing blue quartz grains; and discordant amphibolite, possibly metamorphosed basic dykes, with about 25 per cent porphyroblastic biotite.

The second feldspathic unit (5b) locally overlies unit 5a and consists of more micaceous, less well banded, quartz-feldspar schists and gneisses. The nature of the contact between the units is unknown, but it may be gradational. This unit is distinguished by its more schistose texture and lack of associated rocks such as metaconglomerate and amphibolite. Toward the northeast some feldspar and quartz form linear aggregates surrounded by coarse grained, anastomosing muscovite.

The third lithologic unit (5c) consists of dominantly quartzitic rocks and includes a continuum of lithologies from garnet-quartz-mica schists to micaceous quartzites. Its more micaceous variants are characterized by red, garnet porphyroblasts which seem to be larger (up to 3 cm) in the more westerly exposures. A 100-metre thick concordant layer of metavolcanic rock occurs within the southwestern-most exposure of this unit.

The fourth lithologic unit (5d) in the eastern metamorphic terrane is a very distinctive calcareous unit, of relatively limited areal extent, consisting of calcareous schists and marble. Quartz-mica and garnet-quartz-mica schists are characterized by radiating clusters of acicular amphibole with individual crystals up to 15 cm long. The amphibole locally forms 80 per cent of the rock, but averages about 20 per cent. These schists are commonly found interbedded with grey and white, coarsely crystalline marble. This calcareous unit structurally overlies the quartzitic unit, but the nature of the contact is not clear.

The four lithic units described above are interpreted as a metamorphosed sequence of dominantly sedimentary rocks. The lithologies, structural style, metamorphic grade and tectonic setting of these rocks all support their previous correlation with rocks of the Fleur de Lys Supergroup (Church, 1969; Williams et al., 1972, 1974; Williams and Stevens, 1974). The Fleur de Lys Supergroup has been interpreted as a continental margin clastic wedge (Church, 1969; Bird and Dewey, 1970; Williams and Stevens, 1974) consisting of coarse clastics and conglomerate in its basal portion and clastics and carbonate rocks in its upper portion (Bursnall and de Wit, 1975). By analogy with this model, the coarse feldspathic rocks of units 5a and 5b may be equivalent to basal parts of the Fleur de Lys Supergroup, with more quartzitic rocks of unit 5c and carbonate rocks of unit 5d equivalent to upper parts.

Carbonate Terrane

West of the eastern metamorphic and basement terranes is a wide, northeast-trending belt of dominantly carbonate rocks. The stratigraphy of the lower, more easterly, part of the carbonate succession was studied in more detail than that of the upper part of the succession, which has been described elsewhere (Walthier, 1949; Riley, 1962; Brückner, 1966).

The Grand Lake Brook Group (2) (Walthier, 1949) consists of phyllitic schist and phyllite at the base of the succession and grades upward into interbedded phyllite and marble, sericitic marble and marble breccia consisting of flattened clasts up to 15 cm long. The Grand Lake Brook marbles locally grade into thickly bedded, calcitic and dolomitic marbles of the overlying St. George Group (3). To the west the St. George Group is unmetamorphosed and much less deformed and is locally disconformably overlain by Table Head Formation (4) limestone, shaly limestone and shale (Riley, 1962).

West of the map area, the carbonates of the St. George Group and Table Head Formation together with the carbonates and clastics of the underlying Kippens, March Point and Petit Jardin formations have been interpreted as a Cambrian to early Middle Ordovician carbonate bank sequence (Williams et al., 1972, 1974; Williams and Stevens, 1974). The lithologies of the Grand Lake Brook Group and its stratigraphic position beneath the St. George Group suggest that it represents the eastern, metamorphosed and deformed, shaly facies equivalent of the Cambrian carbonates and clastics to the west. The presence of coarse marble breccia in the upper part of the Grand Lake Brook Group suggests it was deposited near the edge of a carbonate bank.

Structure

The dominant structural trend in the area northwest of Grand Lake is northeasterly and the overall intensity of deformation increases from west to east. Metamorphic grade also increases from west to east, being sub-biotite grade in the carbonate terrane and reaching garnet grade in the central and eastern parts of the eastern metamorphic terrane.

Two major deformations are clearly recorded in the area. The earlier, more intense event was a penetrative deformation which produced isoclinal folds with an axial plane foliation that is preserved as the dominant planar structure in the area. Only small scale, gently northeast-plunging isoclines have been recognized, and these only in the Grand Lake Brook Group and metamorphic rocks of the eastern metamorphic terrane. This is significant in that it suggests a continuity of deformation between the eastern metamorphic terrane and the Grand Lake Brook Group which forms the base of the conformable, Cambrian-Ordovician, carbonate bank sequence. Medium grade metamorphism accompanied this deformation event, as evidenced by syntectonic garnet porphyroblasts in rocks of the eastern metamorphic terrane. Parallelism of the schistosity associated with this early event in the cover rocks and the schistosity in some of the basement rocks suggests that the basement rocks may have been reactivated to some degree by this intense early deformation event.

The later deformation event was less intense and apparently coaxial with the earlier event. It is characterized by tight, upright folding of the earlier foliation and an associated crenulation cleavage developed only in the more micaceous rocks. Mesoscopic and macroscopic folds of this generation plunge gently to moderately northeast and are recognized in all but the basement rocks in the area. Evidence of retrogressive metamorphism in medium-grade rocks suggests that a lower grade of metamorphism accompanied this event.

The sequence and style of the early and late deformation events, and the ages of the rocks they affect, suggest they are correlatives of the regionally recognized Taconic and Acadian orogenic events, respectively (Williams et al., 1972, 1974). Subsequent deformation in the area is represented by minor kinking and warping and extensive block faulting.

Faults, particularly east-dipping thrust faults, are a prominent feature of the overall deformation in the area. This was first noted by Walthier (1949) who suggested that a major thrust, the Corner Brook Lake Thrust, carried "Precambrian gneisses and schists" westward over the carbonate rocks. He recognized this thrust contact between gneisses and carbonate rocks near Corner Brook Lake and

assumed it to be continuous with the thrust separating basement gneisses and carbonates in the southwest part of the area at Grand Lake. Present field work shows that the thrust identified by Walthier near Corner Brook Lake actually extends south-southwest through the eastern metamorphic terrane and is not continuous with the more westerly thrust at Grand Lake involving basement rocks. The Corner Brook Lake Thrust, as used here, refers to that thrust involving only rocks of the eastern metamorphic terrane and extending south-southwest from Corner Brook Lake.

The northern extension of the Corner Brook Lake Thrust is part of a more significant structural/stratigraphic contact which Williams (1978) has named the Grand Lake Thrust. This thrust extends from southwest of Grand Lake at least 25 km to the northeast. The Grand Lake Thrust is not one continuous fault, but rather is composed of a number of relatively short thrusts terminating in high-angle faults. Most of the thrust faults in the area are marked by zones of mylonitization and contrasts in metamorphic grade. The Grand Lake Thrust, for example, juxtaposes mainly garnet grade rocks of the eastern metamorphic terrane and biotite and sub-biotite grade rocks of the carbonate terrane. The Grand Lake Thrust is regionally and tectonically significant because it marks the contact between autochthonous carbonate bank rocks and allochthonous rift facies clastics and basement rocks (Williams, 1978).

The age of thrusting in the area is uncertain, but is thought to be late Paleozoic. The thrusts may have developed during the Acadian Orogeny, since thrusts involving basement and metamorphosed cover rocks are more likely to develop in the type of deep-seated, tectonic regime suggested for this orogeny (Williams et al., 1972, 1974; Brown, 1976).

Two sets of high-angle faults have dissected the area into blocks. They trend northwest and northeast, with the northwest direction being dominant. Some of the northwest-trending faults may actually be coeval with the thrusts which they terminate, and may have originated as genetically related tear faults. The northwest-trending faults do not offset, and thus must predate, the Cabot Fault, which is a regional-scale, northeast-trending, high-angle fault. The Cabot Fault is known to affect Carboniferous rocks and is therefore a Carboniferous or later feature (Williams et al., 1970).

Summary

Preliminary work northwest of Grand Lake has distinguished three major stratigraphic divisions: 1) a sequence of gneisses, migmatites and amphibolites comprising a Grenville-age basement; 2) a sequence of polydeformed metasediments, here interpreted as Fleur de Lys Supergroup equivalents; and 3) a Cambrian-Ordovician carbonate bank sequence. This initial work suggests a tentative stratigraphic succession in the polydeformed metasediments from basal feldspathic and conglomeratic rocks to dominantly quartzitic rocks and then dominantly calcareous rocks.

The basement and eastern metamorphic terranes are interpreted to be allochthonous and are separated from each other and from the carbonate terrane by major east-dipping thrust faults. The Grand Lake Thrust is the major tectonic feature in the area and separates carbonate bank rocks from rift facies clastics and basement rocks.

Area East of the Cabot Fault

Ultramafic rocks of ophiolitic affinity outcrop on Glover Island in Grand Lake where they separate schists and gneisses to the west from volcanic and volcaniclastic rocks to the east. Regional correlations in this area confirm the interpretation of Williams and St-Julien (1978) that the Glover Island ophiolites represent a southward continuation of the Baie Verte – Brompton line (St-Julien et al., 1976) defined farther north.

Ophiolitic Rocks

Ophiolitic rocks in the Grand Lake area (7) outcrop in the central part of Glover Island, at the south tip of Glover Island, and along Grand Lake west of the Cabot Fault.

The best exposure of ophiolitic rocks is in the central part of Glover Island. At this locality a 1 km thick, east-facing, steeply inclined ophiolitic pluton is well exposed along the east limb of a major south plunging anticline, the Glover Island Anticline. The ophiolite consists of a basal, 150 m of variably serpentinized peridotite (7c) overlain by 800 m of medium to coarse grained (1-2 mm) cumulate layered gabbro and massive gabbro (7b). Cumulate layered gabbro constitutes the lower part of unit 7b. Graded mineral layers 10-20 cm thick are locally present within the cumulate layered section, and indicate the pluton faces to the east, consistent with the occurrence of ultramafic rocks at the base of the pluton. Fine grained, black, porphyritic and aphyric dykes as thick as 1 m with chilled margins cut all units of the ophiolite subparallel to the mineral layering.

Ophiolitic rocks are also exposed near the south tip of Glover Island, presumably along the west limb of a south-plunging syncline that was originally continuous with the Glover Island Anticline but which has been truncated by the Cabot Fault. Ophiolitic rocks of this southern section consist of sheeted dykes, pillow lavas and pillow breccia with minor grey chert rimming pillows (7a). Dykes are aphyric with chilled margins, generally trend north-south, and dip vertically. Numerous small intrusions of a feldspar porphyry intrude this dyke complex. Outcrop width of the ophiolite in this area is nearly 5 km. True thickness is probably much less, but could not be determined due to numerous minor faults of unknown displacement and lack of bedding attitudes.

Ophiolitic rocks also occur west of the Cabot Fault opposite the southern tip of Glover Island. At this locality a shear zone containing mafic and ultramafic rock fragments separates feldspathic schists to the west from sheeted dykes to the east.

The ophiolitic rocks described above are all informally referred to as the Glover Island complex. It is correlated directly with the Advocate complex of the Burlington Peninsula (Williams et al., 1977).

Rocks West of the Glover Island Complex

Rocks immediately west of the Glover Island complex are exposed on Glover Island in the core of the Glover Island Anticline. These rocks are divided into two groups, a basal, quartzofeldspathic basement terrane (1c) and an overlying cover sequence composed of semipelitic and psammitic schists and gneisses (6).

Pink, medium grained, quartzofeldspathic biotite gneisses (1c) are well exposed along the northwest shore of Glover Island and for a short distance inland along a stream cut. Numerous northeast-trending metamorphosed foliated mafic dykes cut the gneisses. A zone 10 m thick of pseudoconglomerate is present at the contact of this gneiss with the cover rocks. The pseudoconglomerate consists of rounded clasts of quartz and gneiss identical to that of the nearby gneiss and may represent a high-strain facies. Heterogeneity of strain is attributed to the mechanical contrast between the gneiss and the less competent cover rocks. This distinctive quartzofeldspathic gneiss is informally termed the Grand Lake gneiss. It is interpreted to be Precambrian in age, and to comprise an inlier of Grenvillian

basement, because of its similarity to Precambrian rocks of the Long Range and Indian Head Complexes of western Newfoundland (Riley, 1962).

Rocks overlying the Grand Lake gneiss are divided into a lower conglomeratic unit (6a) and an upper calcareous unit (6b). The lower conglomeratic unit is composed of cyclically bedded, locally graded schists and gneisses and minor intraformational polymictic conglomerates lacking any noticeable internal size grading. Clasts are rounded and generally range up to 2 cm in diameter. Quartz and granitic rock fragments are the dominant clast types. Blue quartz grains are present locally. This unit grades upward through about 30 m of well bedded, micaceous tan quartzite into calcareous schist and marble of the overlying unit (6b).

The calcareous unit (6b) consists of calcareous schist interbedded with lenses and layers of pure marble up to 1 m thick. Marble decreases upward and is generally absent toward the top of the section although disseminated calcite is present throughout. The top of the calcareous unit consists of very graphitic phyllites and fine grained, tan-weathering quartzites overlain by peridotites of the Glover Island complex. A high strain zone separates underlying schists and overlying rocks of the Glover Island complex. A variety of sheared, strongly retrograded mafic and ultramafic rocks occur at this contact.

The conglomeratic unit (6a) is interpreted to be broadly correlative with all or part of units 5a, 5b and 5c that outcrop northwest of Grand Lake. The calcareous unit (6b) is interpreted to be correlative with unit 5d. Based upon lithologic similarity and comparable structural position, gneisses and schists of the conglomeratic and calcareous units (6) are interpreted to be correlative with rocks of the Fleur de Lys Supergroup on the Burlington Peninsula (Church, 1969).

Rocks East of the Glover Island Complex

The Glover Island complex is overlain by a sequence of dominantly mafic volcanic and volcaniclastic rocks which are conglomeratic at the base and grade upward into fine grained tuffs, clastic rocks and pillow lavas (8). Green and black shales containing clasts of gabbro up to 10 cm in diameter locally overlie gabbro along the east limb of the Glover Island Anticline 3 km south of where this contact intersects Grand Lake. Farther south a green shale matrix conglomerate 100 m thick overlies pillow lavas and sheeted dykes of the Glover Island complex at the southern tip of Glover Island. This conglomerate is composed chiefly of rounded volcanic clasts. Angular clasts of bright red jasper, purple shale and light brown weathering volcaniclastic rock are also present but subordinate. The bright red jasper clasts in particular give a distinct appearance to the rock. Clasts average about 5 cm in diameter, but locally outsize clasts greater than 1 m in diameter are present.

This jasper-bearing conglomerate is conformably overlain by a monotonous section of feldspar crystal tuffs, fine grained tuffaceous sediments and pillow lavas. At the base of this section, multicoloured cherts are locally present rimming pillows. Northward around the Glover Island Anticline, the abundance of volcanic clasts diminishes and quartz content increases. Locally psammitic beds are present.

Rocks of unit 8 at Glover Island are correlated with a sequence of rocks at Flatwater Pond on the Burlington Peninsula that have been described by Kidd (1974) and are referred to as the Flatwater Group by Williams et al. (1977). These consist of a basal, black shale matrix megaconglomerate containing a variety of clasts including gabbro, ultramafic rock, quartz pebbles and volcanic rock. This unit is overlain by a green shale matrix conglomerate composed chiefly of volcanic clasts although ultramafic, gabbro and trondjemitic blocks are present (Kidd, 1974). This conglomerate is overlain by tuffaceous sediments and pillow lavas. It is suggested that this sequence of units at Flatwater Pond closely resembles that overlying the Glover Island complex, and considering the comparable stratigraphic position of the two rock sequences, it seems reasonable to interpret them as correlative.

Unit 8 is fault-bounded to the east by an east-facing, steeply dipping section of relatively undeformed vesicular pillow lavas, agglomerates, diabase and purple, black and green shales (9). Black shales of this unit at Corner Pond contain graptolites of Arenig age (Williams and St-Julien, 1978). Rocks of unit 9 at Glover Island are correlated with the Snooks Arm Group (Snelgrove, 1931; Upadhyay et al., 1971) of western Notre Dame Bay on the Burlington Peninsula. The Snooks Arm Group consists of pillow lavas, agglomerates, diabase and argillite lithologically indistinguishable from rocks of unit 9 at Grand Lake. The Snooks Arm Group contains an Arenig graptolite fauna (Snelgrove, 1931; Williams, 1963). Based upon lithic similarity and comparable graptolite fauna, unit 9 is interpreted to be correlative with the Snooks Arm Group.

Summary

Rocks east of the Cabot Fault consist of five major groups. In the west, basement rocks of the Grand Lake gneiss of probable Precambrian age are overlain by clastic metasediments and marbles correlative with the western division of the Fleur de Lys Supergroup of the Burlington Peninsula. Ophiolitic rocks of the Glover Island complex structurally overlie these metasediments along a high strain zone. The Glover Island complex is overlain by pillow lavas and sediments, a correlative of the Flatwater Group of the Burlington Peninsula, which in turn are faulted on the east against Lower Ordovician rocks with more pillow lavas and sediments, a correlative of the Snooks Arm Group of the Burlington Peninsula. Correlation of the Glover Island complex with the Advocate complex of the Burlington Peninsula is supported by the direct correlation of overlying and underlying rock groups at Grand Lake and the Burlington Peninsula. This confirms the extension of the Baie Verte – Brompton line to Glover Island and supports the contention that the Baie Verte – Brompton line represents a major, regional structural interface in the northern Appalachians (St-Julien et al., 1976; Williams and St-Julien, 1978) rather than a local feature unique to the Burlington Peninsula (e.g. Kidd, 1977).

Tectonic History

The western margin of the Appalachian Orogen has been interpreted according to a model of rifting and opening of a Proto-Atlantic Ocean and later deformation during the eventual closure of this ocean (Rodgers, 1968, 1972; Bird and Dewey, 1970; Williams and Stevens, 1974). Rocks exposed in the Grand Lake area closely parallel relationships predicted by this model.

Gneisses at Grand Lake are interpreted to be Precambrian, probably Grenville, in age, based upon correlation with the Indian Head and Long Range complexes of western Newfoundland. This correlation is greatly strengthened by the recognition of anorthositic rocks, generally restricted to Precambrian terranes, at Bottom Brook and Indian Head.

Mafic dykes and flows of the Lighthouse Cove Formation (Strong and Williams, 1972) cut the Long Range gneiss in northwestern Newfoundland and are interpreted to be related to rifting of the North American continent at the close of the Precambrian to form the Proto-Atlantic Ocean.

Mafic dykes that cut the Grand Lake gneiss and northeast-trending dykes that cut unit 1a south of Grand Lake may have the same significance.

Basement gneisses west of the Cabot Fault and on Glover Island are overlain by psammites and semipelites (units 5a, 5b, 5c and 6a) that may be interpreted as rift facies clastics. These rocks are rich in quartz and feldspar and vary from impure quartzite to arkose in composition. Blue quartz, similar to that in the basement rocks, is present locally. Cyclically bedded and locally graded sequences are interpreted to be turbidites, and intraformational polymictic conglomerates lacking any noticeable size grading may represent debris flows. Amphibolites, present locally within these clastic rocks, may represent mafic volcanics associated with rifting.

Coarse clastic rocks on Glover Island grade upward into micaceous quartzites that are overlain abruptly by marble and calcareous schist. The quartzites may represent deposits at a continental margin and overlying marbles may represent a distant, eastern facies of the Middle Cambrian to Middle Ordovician carbonate sequence exposed to the west.

Marble and calcareous schist is also present west of the Cabot Fault (5d) and although its relative stratigraphic position is uncertain, it may correlate with calcareous rocks on Glover Island (6b).

Carbonate-bearing rocks on Glover Island (6b) are stratigraphically overlain by graphitic phyllites. The gradational change from marbles into highly graphitic phyllites may correspond to a similar change from carbonates of the lower and middle Table Head Formation upward into shales of the Caribou Brook formation (Schillereff and Williams, this volume). This change in sedimentation has been interpreted to represent an influx of easterly-derived flysch (Stevens, 1970), signaling a disturbance to the east and assembly of the Humber Arm Allochthon. This allochthon was emplaced structurally above carbonates at the ancient continental margin of eastern North America in western Newfoundland.

The Baie Verte – Brompton line is interpreted as the root zone for higher igneous slices of the Humber Arm Allochthon (St-Julien et al., 1976; Williams et al., 1977; Williams, 1975, 1977). The base of the Glover Island complex is a high strain zone and the numerous highly sheared ultramafic and mafic masses there suggest extensive dislocation consistent with this interpretation. Rapid deposition of unit 8 appears to have followed initial obduction.

Taconic deformation involved development of a regional, generally northeast-trending schistosity throughout the area associated with lower amphibolite grade metamorphism west of the Cabot Fault and greenschist facies metamorphism east of the Cabot Fault. This regional schistosity is recognized in rocks both above (unit 8) and below (unit 6) the Glover Island complex, indicating that deformation and associated metamorphism postdates emplacement of ophiolitic rocks on Glover Island. It is possible, however, that this regional schistosity consists of several superposed, coplanar schistosities that formed at different times, thus implying a more complex structural history. Deposition of sandstones and shales of unit 10 took place after this deformation, probably during the Silurian or Devonian.

The Glover Island Anticline and northeast-trending folds west of the Cabot Fault are probable effects of Acadian Orogeny. Westward thrusting along the Grand Lake and Corner Brook Lake thrusts resulted in the juxtaposition of continental margin clastic rocks with rocks of the carbonate bank. Numerous high-angle faults disrupted the stratigraphic section and offset thrust faults probably during the final stages of Acadian Orogeny.

The last recognized tectonic activity in the Grand Lake area was during the Carboniferous. Plant-bearing, Carboniferous clastic rocks, deposited in the Grand Lake basin are deformed by movement along the Cabot Fault, a highly brecciated zone of unknown displacement.

In the Grand Lake area, the Cabot Fault is commonly marked by the presence of a coarse grained, pink, feldspar-quartz granite. This granite is restricted in distribution to the Cabot Fault zone and minor faults relating to it. The granite is intensely brecciated and only locally preserves original intrusive relationships indicating fault movement after granite emplacement. Localization of granites along the Cabot Fault may indicate actual intrusion along an ancestral zone of weakness, or possible structural emplacement during initial movements in this zone.

Acknowledgments

The authors thank D. Coombs, M. Blanchard and J. Elkins for assistance in the field, and Peter and Pam Betts for their hospitality and assistance in many ways during the field season. We thank E. Stander for making available unpublished data in the Grand Lake area. H. Williams critically read this paper.

Financial support for this work was provided by E.M.R. Research Agreement 2239-4-124/78 to H. Williams. Additional financial support was provided by Memorial University of Newfoundland Fellowships to Martineau and Knapp and a N.S.E.R.C. Scholarship to Kennedy.

References

Baird, D.M.
1960: Sandy Lake (west half), Newfoundland; Geological Survey of Canada, Map 47-1959.

Bird, J.M. and Dewey, J.F.
1970: Lithosphere plate-continental margin tectonics and the evolution of the Appalachian Orogen; Geological Society of America Bulletin, v. 81, p. 1031-1060.

Brown, P.A.
1976: Ophiolites in southwestern Newfoundland; Nature, v. 264, p. 712-715.

Brückner, W.D.
1966: Stratigraphy and structure of west-central Newfoundland; in Guidebook – geology of parts of the Atlantic provinces, Geological Association of Canada, p. 137-151.

Bursnall, J.T. and de Wit, M.J.
1975: Timing and development of the orthotectonic zone in the Appalachian Orogen of northwest Newfoundland; Canadian Journal of Earth Sciences, v. 12, p. 1712-1722.

Church, W.R.
1969: Metamorphic rocks of Burlington Peninsula and adjoining areas of Newfoundland, and their bearing on continental drift in North Atlantic; in Kay, M., ed., North Atlantic – geology and continental drift, American Association of Petroleum Geologists, Memoir 12, p. 212-233.

Dallmeyer, R.D.
1978: $^{40}Ar/^{39}Ar$ incremental release ages of hornblende and biotite from Grenville rocks within the Indian Head Range Complex, southwest Newfoundland: their bearing on Late Proterozoic-Early Paleozoic thermal history; Canadian Journal of Earth Sciences, v. 15, p. 1374-1379.

Kennedy, D.P.
1978: The geology of a section of the Corner Brook Lake Thrust, western Newfoundland; unpublished B.Sc. thesis, Memorial University, Newfoundland, 81 p.

Kidd, W.S.F.
1974: The evolution of the Baie Verte Lineament, Burlington Peninsula, Newfoundland; unpublished Ph.D. thesis, Cambridge University, England, 294 p.

1977: The Baie Verte Lineament, Newfoundland: ophiolite complex floor and mafic volcanic fill of a small Ordovician marginal basin; in Talwani, M. and Pitman, W.C., III, (editors), Island arcs, deep sea trenches and back-arc basins, Maurice Ewing Volume, American Geophysical Union, p. 407-418.

Neale, E.R.W. and Nash, W.A.
1963: Sandy Lake (east half) map-area, Newfoundland; Geological Survey of Canada, Paper 62-28.

Riley, G.C.
1957: Red Indian Lake (west half); Geological Survey of Canada, Map 8-1957.

1962: Stephenville map-area, Newfoundland; Geological Survey of Canada, Memoir 323.

Rodgers, J.
1968: The eastern edge of the North American continent during the Cambrian and Early Ordovician; in Zen, E-an, White, W.S., Hadley, J.B., and Thompson, J.B., Jr. (editors), Studies in Appalachian geology: Northern and Maritime; Wiley-Interscience, New York, p. 141-149.

1972: Latest Precambrian (post-Grenville) rocks of the Appalachian region; American Journal of Science, v. 272, p. 507-520.

Schillereff, S. and Williams, H.
1979: Geology of Stephenville map area, Newfoundland; this volume.

Snelgrove, A.K.
1931: Geology and ore deposits of Betts Cove – Tilt Cove area, Notre Dame Bay, Newfoundland; Canadian Institute of Mining and Metallurgy Bulletin, 43 p.

Stevens, R.K.
1970: Cambro-Ordovician flysch sedimentation and tectonics in west Newfoundland and their possible bearing on a Proto-Atlantic Ocean; in Lajoie, J. (editor), Flysch sedimentology in North America, Geological Association of Canada Special Paper 7, p. 165-177.

St-Julien, P., Hubert, C., and Williams, H.
1976: The Baie Verte – Brompton Line and its possible tectonic significance in the northern Appalachians; Geological Society of America, Abstracts with Program, v. 8, no. 2, p. 259-260.

Strong, D.F. and Williams, H.
1972: Early Paleozoic flood basalts of northwestern Newfoundland: their petrology and tectonic significance; Geological Association of Canada Proceedings, v. 24, p. 43-54.

Upadhyay, H.D., Dewey, J.F., and Neale, E.R.W.
1971: The Betts Cove ophiolite complex, Newfoundland: Appalachian oceanic crust and mantle; Geological Association of Canada Proceedings, v. 24, p. 27-34.

Walthier, T.N.
1949: Geology and mineral deposits of the area between Corner Brook and Stephenville, western Newfoundland; Newfoundland Geological Survey Bulletin 35, Part 1.

Williams, H.
1963: Botwood, Newfoundland; Geological Survey of Canada, Map 60-1963.

1975: Structural succession, nomenclature, and interpretation of transported rocks in western Newfoundland; Canadian Journal of Earth Sciences, v. 12, p. 1874-1894.

1977: Ophiolitic mélange and its significance in the Fleur de Lys Supergroup, northern Appalachians; Canadian Journal of Earth Sciences, v. 14, p. 987-1003.

1978: Tectonic lithofacies map of the Appalachian Orogen; Memorial University of Newfoundland, Map No. 1.

Williams, H., Kennedy, M.J., and Neale, E.R.W.
1970: The Hermitage Flexure, the Cabot Fault and the disappearance of the Newfoundland central mobile belt; Geological Society of America Bulletin, v. 81, p. 1563-1568.

1972: The Appalachian structural province; in Price, R.A. and Douglas, R.J.W. (editors), Variations in tectonic styles in Canada, Geological Association of Canada Special Paper 11, p. 182-261.

1974: The northeastern termination of the Appalachian Orogen; in Nairn, A.E. and Stehli, F.G. (editors), The ocean basins and margins, v. 2, Plenum Publishing Corp., New York, p. 79-123.

Williams, H. and Stevens, R.K.
1974: The ancient continental margin of eastern North America; in Burk, C.A. and Drake, C.L. (editors), The geology of continental margins, Springer-Verlag, New York, p. 781-796.

Williams, H., Hibbard, J.P., and Bursnall, J.T.
1977: Geological setting of asbestos-bearing ultramafic rocks along the Baie Verte Lineament, Newfoundland; in Report of Activities, Part A, Geological Survey of Canada, Paper 77-1A, p. 351-360.

Williams, H. and St-Julien, P.
1978: The Baie Verte – Brompton Line in Newfoundland and regional correlations in the Canadian Appalachians; in Current Research, Part A, Geological Survey of Canada, Paper 78-1A, p. 225-229.

GEOLOGY OF STEPHENVILLE MAP AREA, NEWFOUNDLAND

E.M.R. Research Agreement 2239-4-124/78

S. Schillereff[1] and H. Williams[1]
Regional and Economic Geology Division

Schillereff, S. and Williams, H., Geology of Stephenville map area, Newfoundland; in Current Research, Part A, Geol. Surv. Can., Paper 79-1A, p. 327-332, 1979.

Abstract

Hadrynian to Middle Ordovician sedimentary and igneous rocks comprise an allochthon which has been emplaced from the east during Middle Ordovician Taconic Orogeny upon Cambrian to Middle Ordovician platformal carbonates and sandstones. The assemblage is overlain by neoautochthonous Middle Ordovician and Silurian-Devonian platformal strata and was open-folded and cut by west-directed thrusts during the Devonian Acadian Orogeny.

The top of the autochthonous carbonates consists of upward fining limestone breccias which grade into shale and sandstone. In the allochthon, mélange occurs at the base and between the lower sedimentary story and the upper igneous story.

Introduction

The Port au Port – Fox Island River areas (12B/6, 10, 11) were mapped in 1978 as part of the program to remap the entire Stephenville map area (12B). Emphasis was placed on the stratigraphy of the upper part of the autochthonous succession, the extent and subdivision of transported rock groups, and the relationships between autochthonous and allochthonous rocks. Port au Port Peninsula was the responsibility of Williams, while Schillereff remapped the area east of Port au Port Bay. The following remarks summarize some of the highlights of this work.

Port au Port Peninsula

The southern part of Port au Port Peninsula is underlain by an autochthonous sequence of Cambrian to Middle Ordovician, mainly carbonate rocks. These form prominent bare ridges that trend east-west with the beds dipping gently to moderately north (Besaw, 1974). The sequence is offset by a series of northeast trending high angle faults. The northern portion of the peninsula is underlain by transported, mainly clastic sedimentary rocks of the Humber Arm Supergroup (Stevens, 1970) in the vicinity of West Bay, and by an autochthonous sequence of mainly grey micaceous sandstone and shale in the vicinity of Mainland. The clastic sedimentary rocks form tree-covered lowlands. The number Arm Supergroup is structurally complex with local steeply dipping sequence interrupted by zones of chaotic mélange. The Mainland sequence dips gently toward the northwest, except locally at the shoreline where beds are steeply dipping to northerly overturned. The prominent morphologic feature of Port au Port Peninsula, Long Point, is underlain by carbonates and clastics of the Middle Ordovician Long Point Group (Bergström et al., 1974). It is succeeded by mainly red sandstones of the Silurian-Devonian Clam Bank Formation (Riley, 1962; Rodgers, 1965). Beds of the Long Point-Clam Bank sequence dip moderately northwest in the vicinity of Winterhouse and they are vertical to overturned northerly in the vicinity of Lourdes and southwestward. The Long Point Group is interpreted to unconformably overlie the allochthonous Humber Arm Supergroup at West Bay (Rodgers, 1965). Contacts are modified by faulting farther southwest.

Carboniferous rocks occur in small, widely separated areas. They consist of flat lying to gently dipping coarse conglomerates, plant-bearing sandstones and profusely fossiliferous limestones.

For purposes of description, the rocks of Port au Port Peninsula can be subdivided into an autochthonous sequence (units 2 to 7), an allochthonous sequence (unit 8), a neoautochthonous sequence (units 13 and 14) and younger cover rocks (unit 15) as depicted in Figure 50.1.

Autochthonous Sequence

The autochthonous sequence is made up of rocks of Middle Cambrian to Middle Ordovician age. No major breaks occur within the section, except for an erosional disconformity between the Lower Ordovician St. George Group and the overlying Middle Ordovician Table Head Formation. The lowest exposed strata on Port au Port Peninsula consist of grey to pink crossbedded quartz sandstones and arkosic sandstones that are overlain by shallow water limestones (March Point Formation, unit 2) (Lochman, 1938). The basal sandstones are possible correlatives of the Lower-Middle Cambrian Hawke Bay Formation of western Newfoundland (N.P. James, pers. comm. 1978). The March Point Formation is overlain by a dominantly carbonate sequence comprised of the Petit Jardin Formation (unit 3), St. George Group (unit 4) and Table Head Formation (unit 5). The St. George Group has been subdivided into five units (Besaw, 1974), one of which, the White Hills unit (4a), is shown on Figure 50.1. More complete descriptions of the carbonate sequence and discussions of age and stratigraphy are given by Besaw (1974), DeGrace (1974), Schuchert and Dunbar (1934), Riley (1962), Corkin (pers. comm. 1965), Levesque (1977) and Rodgers (1965).

A conspicuous unit of limestone breccia, limestone conglomerate and shale, formerly assigned to the Cow Head Breccia or Humber Arm Supergroup (Schuchert and Dunbar, 1934), or included locally in the Table Head Formation (Riley, 1962; Besaw, 1974, etc.) can be traced from Caribou Brook, across the Goodyear Anticline to Piccadilly Head. The same unit occurs north of The Gravels and can be traced northward to Fox Island River. Its limestone conglomerates and breccias locally contain carbonate clasts exceeding 2 m diameter. These are derived mainly from the St. George Group and Table Head Formation. The carbonate breccias and conglomerates are thinner and finer in upper parts of the unit, where they alternate with, and are overlain by, dark grey shale and sandstone. A continuous section is exposed at the mouth of Caribou Brook and other sections can be seen in the headwaters of Victors Brook and north of The Gravels. This easily mappable unit is referred to informally as the Caribou Brook formation.

[1] Department of Geology, Memorial Unviersity of Newfoundland, St. John's, Newfoundland, A1B 3X5

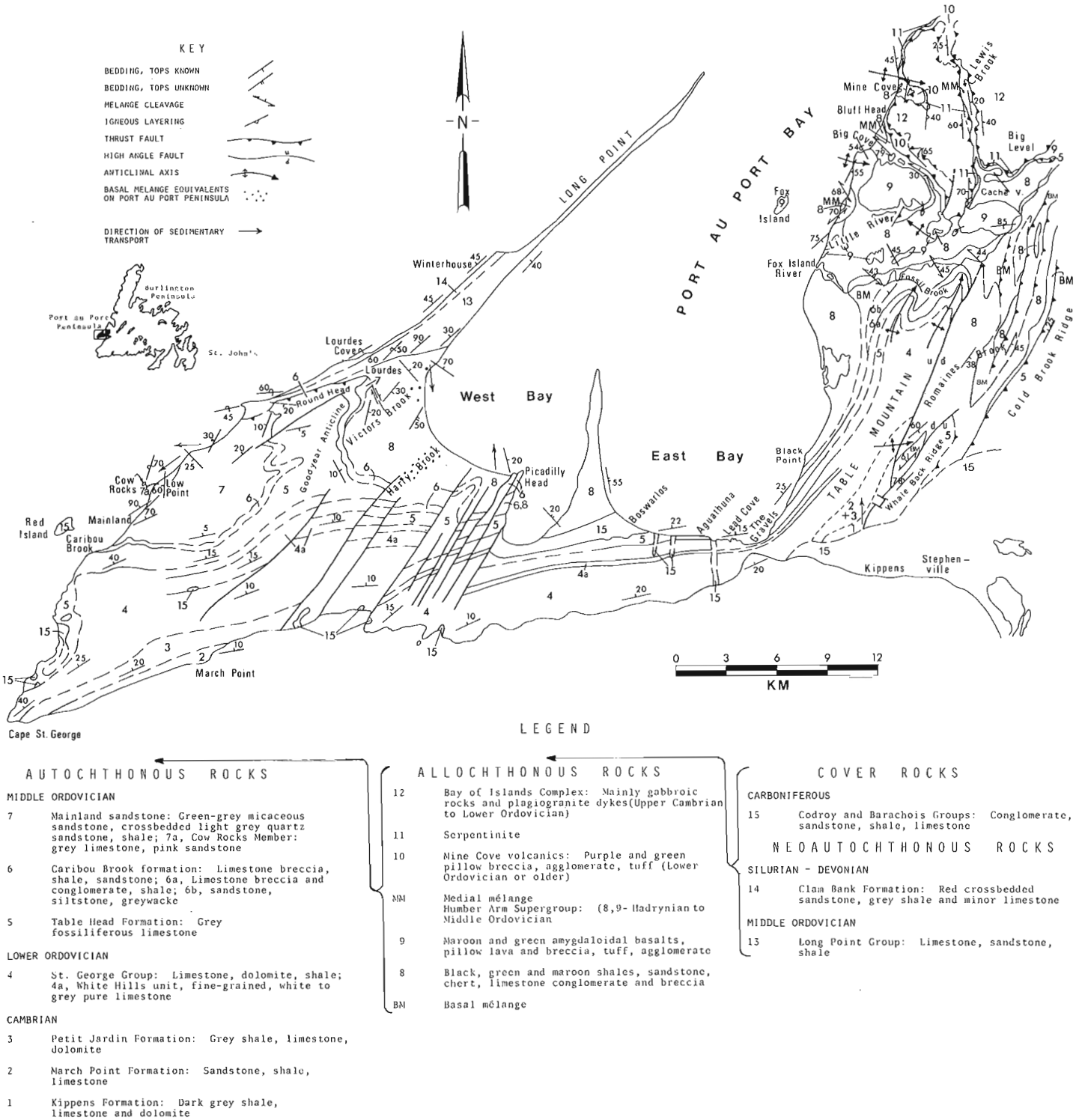


Figure 50.1. *Geology of Port au Port – Fox Island River areas (12B/6, 10, 11), southwest Newfoundland. Subdivisions of St. George Group after Besaw (1974).*

In the vicinity of Mainland, the Caribou Brook formation is overlain conformably and gradationally by a thick sequence of grey micaceous sandstone. This unit (7) that forms the top of the autochthonous sequence at Port au Port Peninsula is referred to informally as the Mainland sandstone. Toward its top at Low Point, cleaner grey crossbedded quartz sandstones are dominant (7a), and immediately offshore at Cow Rocks, grey limestone beds occur with minor interbeds of grey to pink crossbedded sandstone. Crossbeds within this unit (7a) at the top of the Mainland sandstone are inclined consistently to the west and southwest.

East of the Goodyear Anticline, the Mainland sandstone occurs only locally in conformable succession above the Caribou Brook formation. However, thick sections of sub-horizontal sandstone like that of the Mainland sandstone are a common and prominent constituent of the Humber Arm Allochthon.

Allochthonous Rocks

Allochthonous rocks of the Humber Arm Supergroup directly overlie the Caribou Brook formation. These are dominantly sandstones and shales with limy siltstones and limestone conglomerates. The Lower Ordovician Green Point Formation (Schuchert and Dunbar, 1934) is an integral part of the transported sequence. Near the base of the allochthon, intact subhorizontal sections of thin bedded limestone, limestone breccia, and graptolite-bearing shales are common. Other subhorizontal bedded sections of grey shale and limestone breccia can be matched with lithologies of the Caribou Brook formation, and sandstones with the Mainland sandstone. Farther from the base of the allochthon at West Bay, the transported rocks are moderately to steeply dipping with variable dip directions and sudden reversals in facing direction. Chaotic zones are widespread, especially along Harry Brook. These consist mainly of sandstone blocks in a shale matrix, but limestone breccia, green chert and pillow lava blocks are also present in some examples. Chaotic rocks or mélange are outlined in some places in Figure 50.1.

Neoautochthonous Rocks

The Long Point Group of Caradocian age (Bergström et al., 1974) is interpreted to lie unconformably on the transported Humber Arm Supergroup at West Bay (Rodgers, 1965). Although the contact is unexposed, the attitude of the Long Point Group and its gentle westerly dip and structural position with respect to the Humber Arm Supergroup make this interpretation the only reasonable explanation for the juxtaposition of the two units. Grey sandstones of the Long Point Group, containing carbonaceous plant-like remains (algae?), are overlain conformably and gradationally by red sandstones in a river section at the north end of Lourdes Cove. The contact between the Long Point Group and Clam Bank Formation is therefore tentatively placed at this easily recognizable lithic change. At the south end of Lourdes Cove, grey shales and sandstones of the Clam Bank Formation contain Silurian-Devonian brachiopods (Rodgers, 1965).

Carboniferous Cover Rocks

Carboniferous rocks vary considerably in lithology throughout the peninsula. Red Island consists of coarse red conglomerate and sandstone beds. The conglomerates contain mainly red rhyolite, tuff and porphyry cobbles and pebbles that are a common beach rock along the west coast of the peninsula, suggesting extensive red conglomerate like that of Red Island immediately offshore. Along the southern coast of the peninsula, isolated patches of Carboniferous rocks are mainly limestone boulder conglomerates and breccias. At Boswarlos, the Carboniferous rocks are grey plant-bearing sandstones; near The Gravels and at Aguathuna quarry they are limestones with abundant brachiopods, and at Kippens they include a thick gypsum bed. All of these Carboniferous rocks are undeformed and they overlie older formations with pronounced unconformity.

Structural Geology

Rocks of the Port au Port Peninsula were affected first by the Taconic Orogeny during the Middle Ordovician and again by Acadian Orogeny during the Devonian. Carboniferous deformation appears to be restricted to high angle faulting.

The effects of Taconic deformation are apparent only in the transported Humber Arm Supergroup. The random disposition of its rock units and the formation of chaotic mélange zones are attributed to the Middle Ordovician emplacement of the Humber Arm Allochthon. Where the allochthon includes rocks of the Caribou Brook formation and Mainland sandstone, the highest levels of the autochthonous succession are structurally incorporated and imbricated with more distant or farther-travelled correlatives and older rocks. West facing recumbent folds, developed in shales and sole marked sandstones of the Caribou Brook formation, are well displayed at the south shore of West Bay. Mélange zones along Harry Brook display the effects of subhorizontal shearing and contain isolated recumbent fold cores with detached and sheared-out limbs.

Overturning of the neoautochthonous Long Point-Clam Bank succession and local steepening and overturning of westerly parts of the Mainland sandstone are the result of Acadian deformation, for nearby Carboniferous rocks are undeformed. The portion of the Long Point-Clam Bank succession that is affected by westward overturning abuts the structurally elevated limestone breccias of the Caribou Brook formation at Round Head. The narrow gap between the Clam Bank Formation and Caribou Brook formation at the base of Round Head further implies either severe thinning of the Long Point Group, or structural superposition of the Caribou Brook breccias at Round Head upon the Long Point Group. Numerous subhorizontal slickensided surfaces with a northwest to north sense of transport are common in the Long Point Group and occur locally in the Clam Bank Formation where these rocks are overturned. All of these features suggest that the neoautochthonous Long Point-Clam Bank sequence is locally overthrust by the Caribou Brook formation at Round Head. The Goodyear Anticline is possibly a related structure of Acadian generation. Westward overturning of the Mainland sandstone in the vicinity of Low Point and southwestward suggests the southward continuation of a local overturned zone marked by the Round Head Thrust toward the north.

Stratigraphic continuity between the Mainland sandstone and Long Point Group cannot be demonstrated in the area, but this inferred relationship, which implies a western limit to the Ordovician Humber Arm Allochthon (Stevens, 1970), seems reasonable. It is suggested by the fact that rocks like the Mainland sandstone form an integral part of the allochthon at Victors Brook whereas farther west they conformably overlie the Caribou Brook formation and grade upward into more mature sandstones and limestone of platformal facies.

Many of the structural and sedimentological features of the Port au Port Peninsula are consistent with its position at the St. Lawrence Promontory in the more regional setting of the Northern Appalachians (Williams, 1978). Thus the arcuate outcrop pattern of the autochthonous carbonate terrane between Cape St. George and Fox Island River may reflect the ancestral form of the ancient continental margin of eastern North America. North-south directions of sedimentary transport in certain rocks of the Humber Arm Allochthon at West Bay support this suggestion, as does the northerly direction of thrusting at Round Head.

Economic Geology

Galena, chalcopyrite and pyrite occurrences are common in the limestones of the Table Head Formation. One occurrence discovered independently at the headwaters of Victors Brook has steeply dipping fractures filled with galena. Drilling and further assessment have already begun in this area. Base metal mineralization (galena, pyrite) is also present in Carboniferous limestones at Lead Cove.

The area has excellent potential for limestone quarrying (Besaw, 1974) and also for gypsum quarrying. A sinkhole topography between Boswarlos and Piccadilly suggests underlying gypsum. Celestite and barite are known locally in Carboniferous rocks (Johnson, 1954).

Fox Island River Area

The Fox Island River area, centred twelve miles north of Stephenville, presents a well exposed cross-section of rocks within and immediately beneath the Humber Arm Allochthon (Fig. 50.1). The structural succession there can be summarized as follows: (a) an autochthonous Lower to Middle Ordovician carbonate sequence (St. George Group, unit 4; Table Head Formation, unit 5) with a prominent carbonate breccia unit followed by grey shale and graptolite-bearing sandstone at its top (Caribou Brook formation, unit 6a, b); (b) a basal mélange zone (BM) consisting of greywacke, siltstone, chert and limestone breccia blocks in a black, green and maroon shale matrix; (c) sedimentary rocks of the Humber Arm Supergroup (unit 8) that may contain volcanic interlayers and contain circular areas of mafic volcanics (unit 9) up to 1 km in diameter that are probably structurally associated with surrounding sediments; (d) a medial mélange zone (MM), that is an integral part of the allochthon, containing sedimentary clasts and blocks of amygdaloidal basalt, pillow lava and gabbro; (e) a west-thickening wedge of purple-green amygdaloidal basalt and pillow breccia (Mine Cove volcanics, unit 10); and (f) an uppermost structural slice composed mainly of gabbro with a ramifying network of plagiogranite dykes (Bay of Islands Complex, units 11 and 12).

Folded autochthonous rocks form denuded northeast-trending ridges in the southern portion of the map area (Table Mountain, Whale Back Ridge). Northeast, in the valley of Romaines Brook, high angle faults bring the carbonate sequence into juxtaposition with transported Humber Arm Supergroup clastics and mélange. To the east at Cold Brook Ridge, limestones of the Table Head Formation are overthrust westward onto clastic rocks of the Humber Arm Allochthon.

Transported rock units north of Fox Island River are well exposed along the coast and in stream outcrops. Elsewhere they are shrouded by dense vegetation and muskeg. The basal mélange is well exposed along the meandering Fox Island River and in Romaines Brook. The geographically restricted medial mélange is well exposed in linear outcrop belts at Big Cove and in the valley of Lewis Brook. The prominent morphologic feature of the area, the flat-topped gabbroic massif east of Bluff Head, lies farthest north.

Autochthonous Rocks

The autochthonous sequence in the Fox Island River area is made up of rocks of Early Cambrian to Middle Ordovician age (Riley, 1962). The lowest exposed strata, of Early to Late Cambrian age (Kippens Formation, unit 1; unseparated March Point-Petit Jardin Formations, units 2 and 3), outcrop along the southwest flank of Table Mountain. In southern Romaines Brook grey shale, siltstone and dolomite beds (units 2 and 3) dip gently northwest beneath Table Mountain. Sole markings and streaming lineations in grey silty shale there indicate paleocurrent directions towards the north.

Conformable above units 2 and 3, limestones and dolomites of Early Ordovician age make up the St. George Group (unit 4). The best exposures occur in poorly drained barrens on top of Table Mountain. These rocks are folded into upright open anticlines that generally plunge 45 degrees north-northeast. Along an 11 km scarp flanking the eastern edge of Table Mountain, a west-side-up high angle fault zone juxtaposes the entire carbonate sequence, including the St. George Group, against transported clastics (unit 8) and basal mélange (BM).

Middle Ordovician rocks of the Table Head Formation (unit 5) overlie the St. George Group. Excellent exposures at the Aguathuna limestone quarry on Port au Port Peninsula indicate that the contact is a disconformity, reflecting an Early-Middle Ordovician depositional hiatus. The same stratigraphic relationship exists in the Fox Island River area. Excellent exposures of grey fossiliferous limestones capped by black shales, the dominant lithologies of the Table Head Formation, occur along the coast south of Black Point.

At Whale Back Ridge, a high angle fault juxtaposes gently east-dipping grey limestone (unit 5) with transported clastic rocks (unit 8). To the northeast, at Cold Brook Ridge, road-metal quarries expose a steep west-facing dip slope of Table Head limestone. Near the base of this dip slope, chaotically deformed grey and green shales containing clastic sedimentary blocks, dip gently southeast beneath the limestone. This strongly discordant contact is interpreted as a thrust fault, bringing parautochthonous folded Table Head carbonates (unit 5) westward over basal mélange (BM), rather than a simple stratigraphic contact within a synclinal core (Riley, 1962). A detached mass of grey limestone (Table Head Formation?) floored by mélange, which rests against the southeast flank of Big Level, may be a product of related thrusting.

The Middle Ordovician Caribou Brook formation conformably overlies the Table Head Formation and forms the stratigraphically highest autochthonous unit in the region. Two distinctly mappable subdivisions are recognized: a lower member (unit 6a) of platy limestone conglomerates, shales and limestone breccias; and an upper member (unit 6b) of olive green and grey siltstones, sandstones, and minor greywackes. Graptolites occur in laminated sandstones near the top of unit 6b in the vicinity of Fossil Brook.

The lower member (unit 6a) dips gently to moderately northwest along the western flank of Table Mountain, and forms a sinuous outcrop belt from Fox Island River to Round Head on Port au Port Peninsula. The upper member (unit 6b) is well exposed only in northeast-trending anticlines at the north end of Table Mountain. Its limited extent implies that it may have been structurally removed in some areas and incorporated with transported rocks of the Humber Arm Allochthon.

Allochthonous Rocks

Basal Mélange. The basal mélange (BM) lies directly above the Caribou Brook formation (unit 6) and forms the structural base of the Humber Arm Allochthon. The mélange occurs as broad outcrop belts well exposed in the meandering valleys of Fox Island River and Romaines Brook, and just south of Black Point along the coast. Where Fox Island River bends to flow west, outcrop widths of the basal mélange exceed 2 km. Blocks of greywackes, siltstones, platy limestone breccias and pods of alternating thin bedded limestones and siltstones are housed in a black, green and maroon shaly matrix. Many of these blocks are of deep water origin (N.P. James, pers. comm., 1978). Clast sizes range from fragmental chips to rafts of greywacke and bedded sediments 25 m long.

The mélange matrix is commonly sheared into a shiny, crumbly, fragmental hash. Where it is more cohesive, tight recumbent folds and rootless isoclinal fold hinges are common. The base of the mélange is defined at Black Point by a sharp structural contrast between well bedded grey siltstones below and sheared black shale above. At Fox Island River, the basal boundary is structurally transitional. There, the proximal upper member of the Caribou Brook formation (unit 6b) becomes increasingly boudinaged, folded, faulted, dismembered and rotated until true chaos is achieved within the mélange. In Romaines Brook, basal sediments of the lowest structural slice exhibit the same structural pattern, indicating that the upper boundary of the basal mélange is also transitional. This hazy interfacial character of the basal mélange is common in the Fox Island River area and provides a structural signature useful in distinguishing the basal from the medial mélange.

Humber Arm Supergroup Allochthonous rocks of the Lower Cambrian to Middle Ordovician Humber Arm Supergroup form the lowest intact structural slice of the Humber Arm Allochthon. Sediments (unit 8) and volcanics (unit 9) occur from Black Point to Bluff Head along the coast and underlie most of the Little River-Fox Island River-Romaines Brook inland areas.

The sedimentary rocks (unit 8) form the base of the lowest structural slice and lie directly above the basal mélange (BM). These rocks consist dominantly of multi-coloured shales, sandstones, a variety of disrupted limestones, and greywacke.

Extensive broken sequences of black and green shale and limy siltstone dip moderately southeast in the almost continuous outcrop within Romaines Brook. Lithologic similarities with the well known transported sedimentary sequence at Black Point and the intimate association with chaotic mélange suggest that the rocks in Romaines Brook are transported Humber Arm Supergroup sediments (unit 8). Farther north, underlying Cache Valley and most of the Little River area, allochthonous siltstones, sandstones and shales are moderately to steeply dipping with variable dip directions, having the same appearance as the transported clastics on Port au Port Peninsula. Along the coast south of Big Cove, beds of coarse, orthoclase-rich arkose dip moderately east. In the same section, beds of coarse conglomeratic greywacke, containing oblong boulders of recycled clastic sediments ("cannonballs"), also dip to the east, with abrupt reversals in facing direction.

Volcanic rocks of the Humber Arm Supergroup (unit 9) form separate morphologic ridges traceable from the eastern edge of the map area (at the southeastern flank of Big Level), westwards in a disconnected chain to the coast. Fox Island is also underlain by these volcanics (Riley, 1962). Interpretive airphoto mapping was used to delineate many of the rounded volcanic pods since outcrops are sparse in this area. Unit 9 consists of maroon amygdaloidal basalts, tuffs, purple-green pillow lavas and minor agglomerates. Within the unit, dips are moderate to steep, strikes are variable, and stratigraphic tops (best seen in the pillowed sequences) alternate sporadically.

North from the mouth of Little River, basalts and pillow lavas (unit 9) appear to be stratigraphically intercalated with clastic sediments (unit 8), without structural disruption across many of the contacts. However, in nearby coastal exposures, zones of sheared sediments 15-30 m wide border these volcanics. Farther inland, contacts are obscured and the overall scattered map pattern of rounded disaggregated blebs suggests some form of structural intermixing of the volcanics with nearby clastic sedimentary rocks.

Medial Mélange Situated above the Humber Arm Supergroup (units 8 and 9) and below the Mine Cove volcanics (unit 10), the medial mélange (MM) caps the lowest, sedimentary slice of the Humber Arm Allochthon. Where the Mine Cove volcanics are missing (Lewis Brook, Cache Valley), the mélange zone lies directly beneath the Bay of Islands Complex (units 11 and 12). This mélange is best exposed in Big Cove, Little River and Lewis Brook where it dips east to northeast and shows a restricted, linear map pattern. The heterogeneous components of the mélange include the entire range of basal mélange sedimentary ingredients plus clasts of pillow breccia, amygdaloidal basalt, pink crystalline dolomite, hydrocarbon-bearing limestone cataclastite and gabbro. Gabbro blocks are very scarce, and do not exceed 0.6 m in diameter. Only two localities show gabbro clasts clearly surrounded by sheared shale: in stream outcrops at Big Cove, and south of Big Cove along the coast. There are no ultramafic rocks in the medial mélange.

Mine Cove Volcanics A conspicuous unit of broken volcanics lies above the medial mélange (MM) and beneath the Bay of Islands Complex (units 11 and 12). This easily mappable unit is traceable from southeast of Bluff Head, north past Mine Cove to the mouth of Lewis Brook. It is informally referred to as the Mine Cove volcanics (unit 10). The dominant lithology is sheared pillow breccia with massive dark green and purple, finely crystalline basalts, and green chlorite- and epidote-rich tuffs. At Bluff Head and Mine Cove the section is roughly 150 m thick.

Along the coast north from Bluff Head, the volcanics dip moderately east and northeast, while near the mouth of Lewis Brook they dip moderately east and west. Gabbro at Bluff Head structurally overlies the Mine Cove volcanics and the contact is a subhorizontal thrust fault. Obscured contacts elsewhere (inner rim of the valley behind Mine Cove; north end of Lewis Brook) are also interpreted as thrust contacts. No mélange intervenes between the volcanics and the superjacent gabbros.

The Mine Cove volcanics have the overall geometry of a west-thickening prism structurally in front of, and overridden by, the highest plutonic slice of the Humber Arm Allochthon.

Bay of Islands Complex The Bay of Islands Complex (Smith, 1958) structurally overlies the Mine Cove volcanics (unit 10) to the west and directly overlies medial mélange (MM) to the east. These rocks form the highest slice of the Humber Arm Allochthon and, where exposed in the Fox Island River area, are structurally distinct from the underlying Mine Cove volcanics.

Gabbro, metagabbro and amphibolite with minor peridotite and pyroxenite (unit 12) comprise the bulk of the flat-topped massifs in the northern portion of the map area. At Bluff Head the gabbro is cut by a network of north-south trending subvertical plagiogranite dykes. A thin irregular zone of serpentinized ultramafic rocks (unit 11), which contains asbestos and chromite, forms a sole up to 60 m thick beneath the gabbro. The best exposures of this sole are at an abandoned asbestos mine in Lewis Brook and in exploration pits in the valley east of Mine Cove.

The contact between the serpentinite and the gabbro, exposed in northern Cache Valley, does not appear to be structural, but rather a relict igneous contact. Igneous layering in the gabbro massif east of Mine Cove dips moderately east. The structural base of the highest structural slice, as seen along the coast where ultramafic rocks overlie Mine Cove volcanics, is flat lying. In Lewis Brook the contact between the gabbro and the medial mélange is also flat.

Structural Geology

The rocks within and beneath the Humber Arm Allochthon in Fox Island River area are affected by several types and generations of structures. Chaotic mélange zones, occurring within the Allochthon, provide genetic constraints on slice assembly and emplacement. Later upright open folding, affecting the autochthonous and allochthonous rocks, is thought to be post-emplacement. Westward imbricate thrusting of the allochthon and the upper levels of the autochthon telescopes the sequence even more. Finally, high angle faulting modifies the relative geometry into its present state.

Analysis of the assembly and emplacement of the Humber Arm Allochthon in the Fox Island River area hinges on the interpretation of the mélange zones. The basal mélange (BM), containing deep water sedimentary clasts, is interpreted as a site of mass wastage (in accord with Brückner, 1975), during the later stages of transport when the overriding sedimentary slice moved across a shaly substrate in a deep water environment. Strong shearing and chaotic

folding of the matrix are not found outside the mélange, implying that these structures are genetic. Since there are no plutonic or volcanic clasts in the basal mélange, there is no direct evidence that higher igneous slices were proximal during the formation of the basal mélange (as proposed by Williams, 1975). The medial mélange is interpreted in a similar way, though its genesis requires a mixed volcanic/sedimentary source. The few gabbro clasts in the medial mélange are interpreted as debris from a distal igneous body, or as spurious clasts (certainly possible during the chaos accompanying obduction). If these interpretations are correct, then the basal mélange must have formed prior to the medial mélange (because there is no volcanic debris in the basal mélange), and the medial mélange must have formed prior to emplacement of the highest plutonic structural slice (since there are no ultramafic plutonic clasts in the medial mélange). In the Fox Island River area, the model of emplacement of a pre-assembled Allochthon (Williams and Stevens, 1974) is therefore suspect.

West-facing recumbent folds along the coast south of Big Cove (in unit 8) are refolded by east-west warps. These may have formed during emplacement of the allochthon, since they are not recognized in the allochthonous succession. Northeast trending upright folds affect the autochthonous rocks of Table Mountain and Cold Brook Ridge and the transported rocks of the lower structural slices. These are interpreted as postemplacement Acadian folds. Curiously, the uppermost structural slice of the Allochthon appears to have a flat bottom and to have remained unaffected by much of the deformation evident in underlying rocks. This implies either (1) the upper slice was emplaced after most of the underlying deformation was complete, or (2) the upper slice rode, unaffected, above the folded zone.

Following this, dominantly westward imbricate thrusting offset previous structures and is interpreted to have occurred during the Acadian Orogeny. The most salient effects of this are: (1) westward thrusting in Little River (MM and unit 8); (2) west- and south-directed thrusting in Romaines Brook (BM and unit 8); (3) thrusting of parautochthonous rocks at Cold Brook Ridge and the limestone klippe abutting Big Level; and (4) the removal of much of the upper member of the Caribou Brook formation (unit 6b).

The most recent structural event is high angle faulting, attributed to Carboniferous deformation. Examples are the west-side-up fault bordering Table Mountain, and the west-side-down fault at Whale Back Ridge which cut all older structures. High angle faults also offset rocks in Lewis Brook. However, since the upper structural slice shows little postemplacement structure, the relative timing of these faults is unknown.

Economic Geology

Asbestos occurs abundantly in serpentinite outcrops in Lewis Brook, Mine Cove and north along the coast. Chromite showings are reported atop the gabbro massif (Riley, 1962). Surface pits for chromite exploration are present at the head of the valley east of Mine Cove. Wiry native copper occurs within white carbonate veins cutting amygdaloidal volcanics (unit 9) along the coast opposite Fox Island.

Acknowledgments

The first author wishes to acknowledge financial support through a Memorial University of Newfoundland Fellowship. The second author acknowledges the support of field work through an E.M.R. Research Agreement, an N.S.E.R.C. Operating Grant and Canada Council Scholarship through the Killam Program.

The authors also wish to acknowledge the field assistance of Alex Pittman, Bill Hunt, and Bert Kendall; and the many hospitalities shown by our neighbours, the Betts family, and the St. George Community College of Stephenville.

References

Bergström, S.M., Riva, J., and Kay, M.
1974: Significance of conodonts, graptolites, and shelly faunas from the Ordovician of western and north-central Newfoundland; Canadian Journal of Earth Sciences, v. 11, p. 1625-1660.

Besaw, D.M.
1974: Limestone-Dolomite Evaluation, Project 4-1. Dolomite deposits of the Port au Port Peninsula; Newfoundland Department of Mines and Energy, Mineral Development Division Internal Report, 21 p.

Brückner, W.D.
1975: Origin of 'zones of chaotic structure' in certain orogenic belts; IXth International Congress on Sedimentology, Nice, 1975.

DeGrace, J.R.
1974: Port au Port Peninsula in Limestone resources of Newfoundland and Labrador; Newfoundland Department of Mines and Energy, Mineral Development Division, Report 74-2, p. 88-101.

Johnson, H.
1954: The strontium deposits of Port au Port Peninsula; Geological Survey of Canada Bulletin 27, p. 1-19.

Levesque, R.J.
1977: Stratigraphy and sedimentology of Middle Cambrian to Lower Ordovician shallow water carbonate rocks, Western Newfoundland; unpublished M.Sc. thesis, Memorial University of Newfoundland, 276 p.

Lochman, C.
1938: Middle and Upper Cambrian faunas from Western Newfoundland; Journal of Paleontology, v. 12, p. 461-477.

Riley, G.C.
1962: Stephenville map-area, Newfoundland; Geological Survey of Canada, Memoir 323, 72 p.

Rodgers, John
1965: Long Point and Clam Bank Formations, Western Newfoundland; Geological Association of Canada Proceedings, v. 16, p. 83-101.

Schuchert, C. and Dunbar, C.O.
1934: Stratigraphy of Western Newfoundland; Geological Society of America, Memoir 1, 123 p.

Smith, C.H.
1958: Bay of Islands Igneous Complex, Western Newfoundland; Geological Survey of Canada, Memoir 290, 132 p.

Stevens, R.K.
1970: Cambro-Ordovician flysch sedimentation and tectonics in West Newfoundland and their possible bearing on a Proto-Atlantic Ocean; in: Lajoie, J. (ed.), Flysch sedimentology in North America; Geological Association of Canada Special Paper No. 7, p. 165-177.

Williams, H.
1975: Structural succession, nomenclature and interpretation of transported rocks in Western Newfoundland; Canadian Journal of Earth Sciences, v. 12, p. 1874-1894.

1978: Tectonic-lithofacies map of the Appalachian Orogen; Memorial University of Newfoundland Map No. 1.

Williams, H. and Stevens, R.K.
1974: The ancient continental margin of eastern North America; in: The geology of continental margins, Burke, C.A. and Drake, C.L. (ed.), Springer-Verlag, New York, p. 781-796.

51.

GEOCHEMISTRY OF COPPER, LEAD, AND ZINC MINERALIZATION IN PROTEROZOIC ROCKS NEAR GILLESPIE LAKE, YUKON

Project 770025

W.D. Goodfellow
Resource Geophysics and Geochemistry Division

Goodfellow, W.D., Geochemistry of copper, lead, and zinc mineralization in Proterozoic rocks near Gillespie Lake, Yukon; in Current Research, Part A, Geol. Surv. Can., Paper 79-1A, p. 333-348, 1979.

Abstract

Interpretive studies of intensive and extensive coincident Pb, Zn and Cu sediment anomalies in streams intersecting Middle Proterozoic carbonate and clastic rocks located east of Gillespie Lake revealed the presence of previously unrecorded base metal mineralization. The mineralization occurs in a variety of geological settings including stratabound sphalerite finely dispersed throughout stromatolitic rocks, coarse grained sphalerite and galena occurring in fractures and fault-related breccias, and chalcopyrite disseminated in dolostone and intersecting fractures.

Although the stratigraphical and lateral dimensions of the mineralization are not known, the stream sediment and water geochemistry suggests that this area and other areas underlain by rocks of similar age and composition warrant further evaluation from an economic point of view.

Introduction

Regional stream sediment geochemical data released for the Nadaleen River (106C) and Nash Creek (106D) map areas (Geological Survey of Canada, 1978) showed extensive and intensive Pb, Zn and Ag anomalies in areas underlain primarily by Proterozoic carbonate and clastic rocks. In order to ascertain whether these geochemical anomalies reflected bedrock mineralization or were due to fortuitous environmental factors, one area located immediately east of Gillespie Lake was selected for detailed investigations. Rock exposures were examined and drainage systems were traversed to determine whether or not base metal mineralization was present and, if present, to characterize the type and style of mineralization. The physical and chemical factors affecting the availability of metals from the underlying rocks and the subsequent transport and deposition of metals in the drainage system were investigated by determining the chemistry of sediments and waters collected from streams intersecting the area.

Physiography and Geology

The area of study is located in the central-eastern Yukon Territory (Fig. 51.1) and forms part of the Rackla Ranges which are situated in the Wernecke Mountains. The geomorphology of the area has been affected strongly by several successive advances and retreats of glaciers during Pleistocene time. The Wernecke Mountains are characterized by jagged commonly fault-bounded ridges which are separated by deeply incised U-shaped stream valleys. Rock glaciers present in some of the cirques are a common feature on north-facing slopes.

Glacial deposits, that have been described by Ricker (1974) for the Nadaleen River map area, are composed of terminal moraines, ground moraines, drumlins and lateral and medial moraines. However, in the area of detailed study (Fig. 51.2), the surficial geology is represented by recent nonglacial deposits comprising alluvial sands and gravels and extensive talus.

The Nadaleen River map area has a continental climate characterized by low precipitation and broad temperature ranges. Most streams are fed by snow and ice melt and from groundwater. The Bonnet Plume River is the repository of thick alluvial fans comprising gravel and sand deposited during the heavy spring runoff. Silt-size stream sediment was difficult to obtain in torrential streams and where the underlying carbonates contributed very little fine sediment to the stream system.

The area of study is situated in the zone of discontinuous permafrost as outlined by Brown (1967). In general, the south-facing slopes are relatively free of permafrost. Solifluction of varying intensities has affected most slopes (Ricker, 1974).

The first extensive geological investigation of the area was carried out by Wheeler (1954). The area was subsequently remapped by Blusson and Tempelman-Kluit (1970) and Blusson (1974a, b). Recently, stratigraphic sections through Middle Proterozoic sedimentary rocks have been measured and described by Bell and Delaney (1977) and Delaney (1978).

The geology in the area of detailed investigation (Fig. 51.2) comprises a thick sequence of Middle and Upper Proterozoic carbonate and clastic rocks and minor mafic volcanic flows at the base of the "Pinguicula Group". The Middle Proterozoic rocks, referred to as the Wernecke Assemblage (Eisbacher, 1978) and alternatively as the Wernecke Supergroup (Delaney, 1978) have been subdividied into three major groups which are informally named from oldest to youngest the "Fairchild Lake Group", the "Quartet Group" and the "Gillespie Lake Group" (Fig. 51.3 and 51.4). The "Fairchild Lake Group" is composed of a thick sequence of light grey weathering, thinly bedded to laminated siltstone, slate, argillite with some interbedded carbonate. Rocks of this group have, in general, been regionally metamorphosed to the lower greenschist facies and locally metamorphosed to phyllites and chloritoid and garnet-chloritoid schist around breccia complexes. The "Quartet Group", which overlies the "Fairchild Lake Group" is composed of dark grey weathering interbedded siltstone, slate, argillite, sandstone and dolostone. The contact relation between the "Fairchild Lake Group" and "Quarter Group" is unclear because it is masked by structural complications (Young et al., in press). The "Gillespie Lake Group", which is in transitional contact with the underlying "Quartet Group", is composed of a thick (more than 4 km, Delaney, 1978) sequence of buff to orange to locally grey weathering dolostone with minor siltstone and sandstone. In the Gillespie Lake area, representative stratigraphic sections contain parallel laminated to wavy bedded dolosiltite which contain bioherms and biostromes of both bifurcating and isolated columnar stromatolites as well as algal debris (Delaney, 1978).

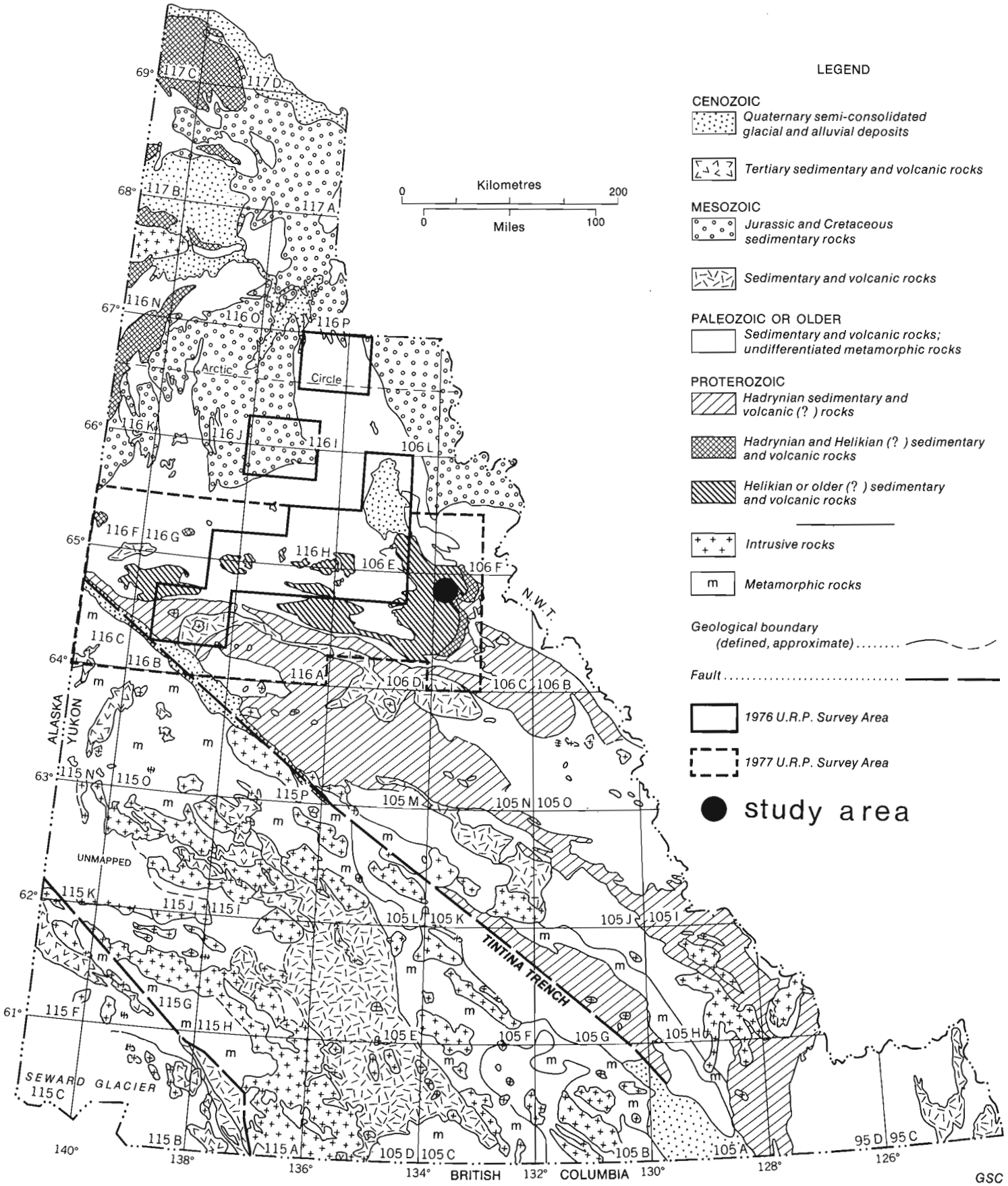
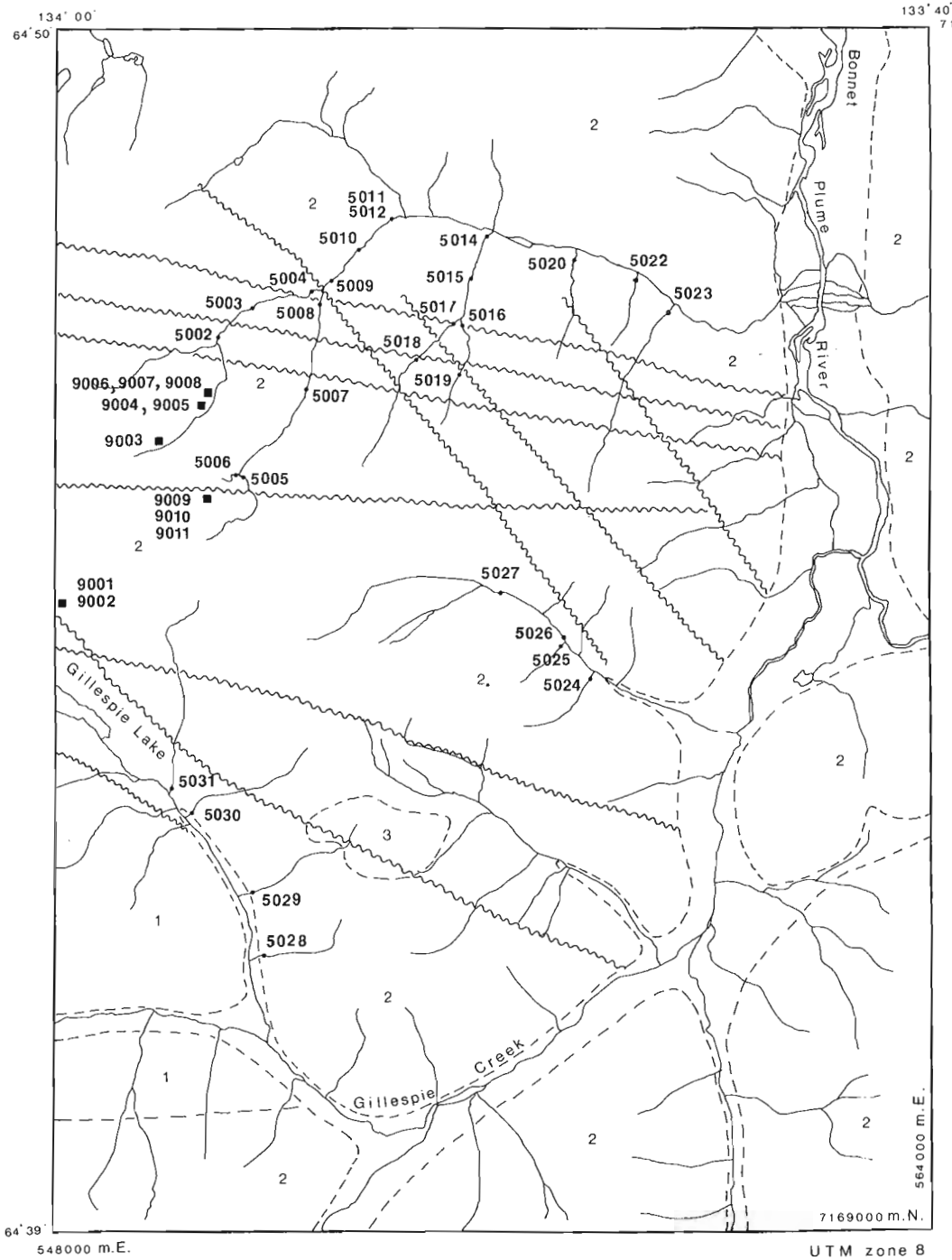


Figure 51.1. *General geology of the Yukon showing the location of the study area (after Findlay, 1975).*



LEGEND

UPPER PROTEROZOIC

3 Ekwi and Mackenzie Mountains Supergroups and Pinguicula Group

MIDDLE PROTEROZOIC

2 'Gillespie Lake Group' orange-, buff-, and grey-weathering dolostone; grey- and brown weathering slate and siltstone

1 'Quartet Group' dark grey-weathering slate, argillite, siltstone and sandstone

• stream sediment and water sample

■ rock sample

106C 78 - series

Figure 51.2

Geology, stream drainage and sample locations for the area of follow-up investigations located east of Gillespie Lake (geology by Delaney, 1978).

The structure of Proterozoic rocks in the Wernecke Mountains is characterized by open folds whose axes trend west-northwest. In the Gillespie Lake area (Fig. 51.2) high angle normal faults with two preferred directions (azimuth 095 and 140) and varying vertical displacements are common. Associated with these faults are extensive breccias, some of which host Pb and Zn mineralization.

Mineralization

Minor showings of Pb-Zn mineralization occurring mostly in fractures intersecting the "Gillespie Lake Group" of rocks have been previously observed by Green (1972) and Delaney (1978). From follow-up investigations in the area east of Gillespie Lake (Fig. 51.2), Cu, Pb and Zn mineralization was discovered to occur in a variety of geological settings.

Copper can occur as stratabound finely disseminated chalcopyrite in brown weathering light grey dolosiltstone (Fig. 51.5.1). In other samples, fracture surfaces intersecting laminated stromatolite are covered with a thick coating of malachite (Fig. 51.5.2). Chalcopyrite is also present as disseminations in fractures through grey dolostone (Fig. 51.5.3) associated with a small fault zone.

Zinc occurs as stratabound sphalerite disseminated throughout brown dolosiltstone that is rhythmically interbedded with pale green stromatolite and recrystallized coarser grained white curved dolomite (Fig. 51.5.4). In sample 789008, it is disseminated throughout laminated cream coloured stromatolite (Fig. 51.5.2). Zinc is also present as massive brown sphalerite associated with pyrite filling open space in brecciated stromatolite (Fig. 51.5.6). Some of the white recrystallized dolomite appears to post-date the sulphide mineralization.

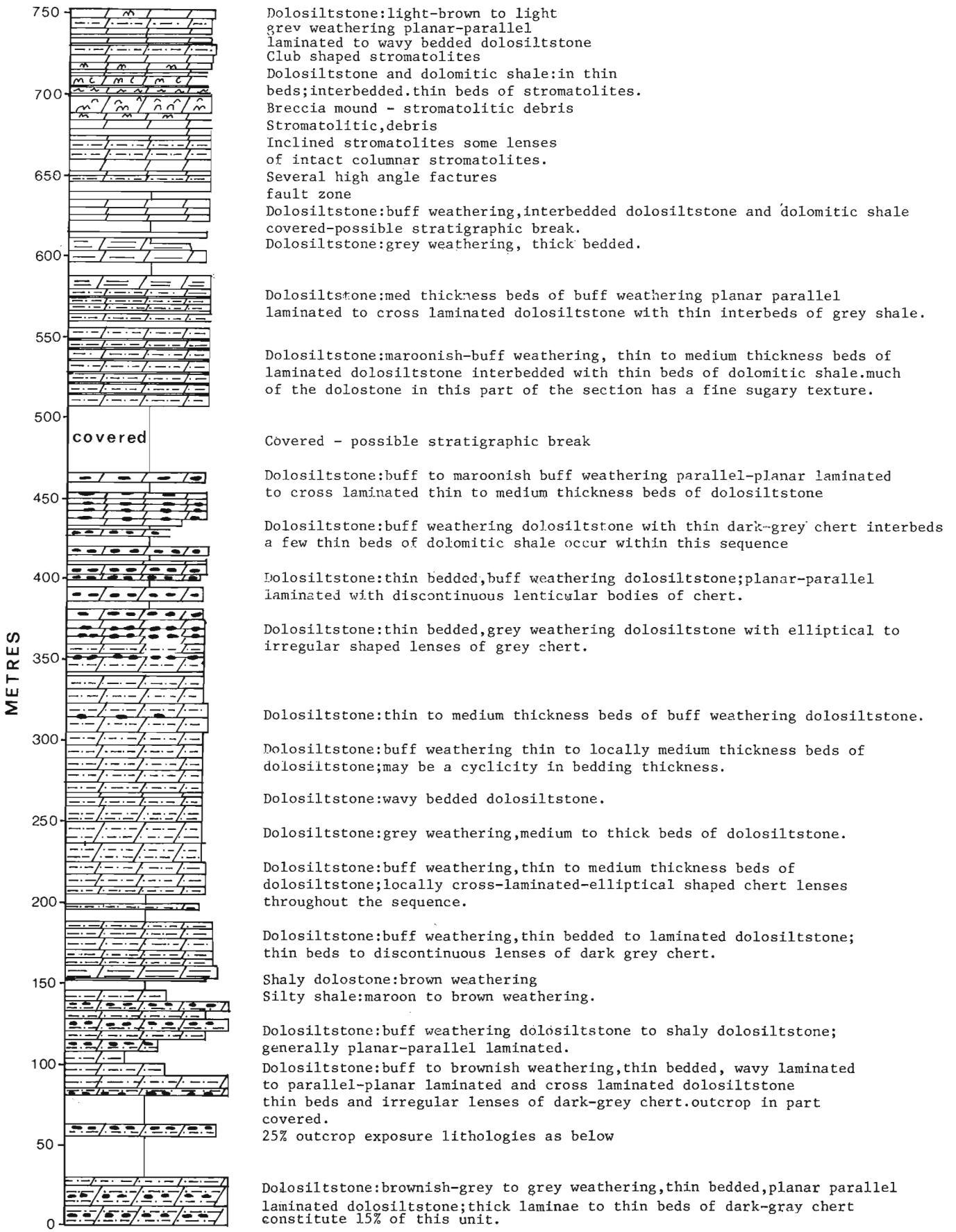


Figure 51.3. *Stratigraphic section through the "Gillespie Lake Group" located north of Gillespie Lake (after Delaney, 1978).*

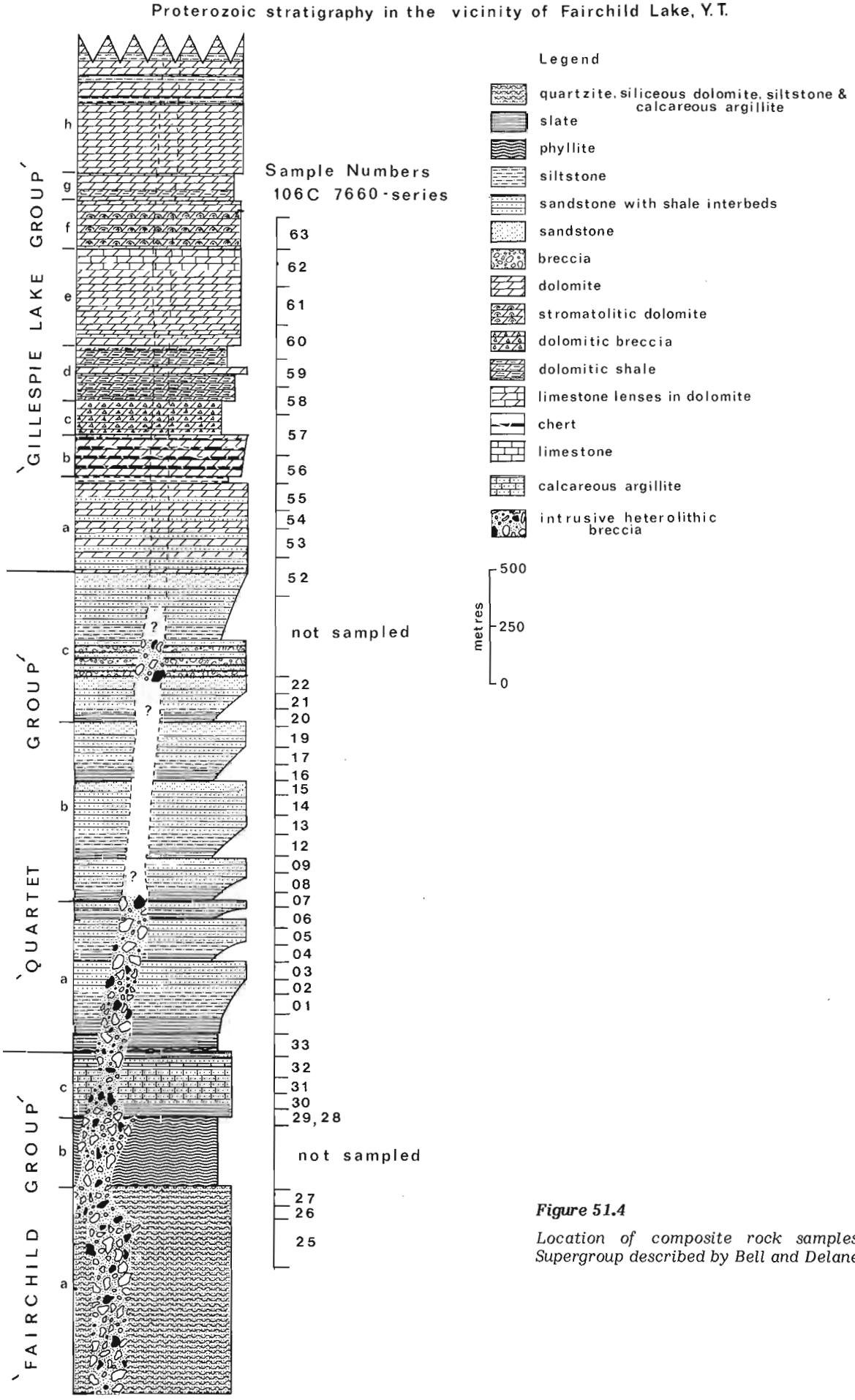
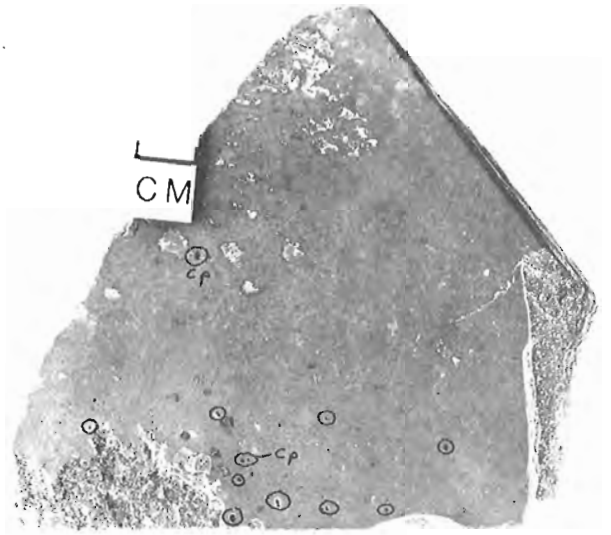
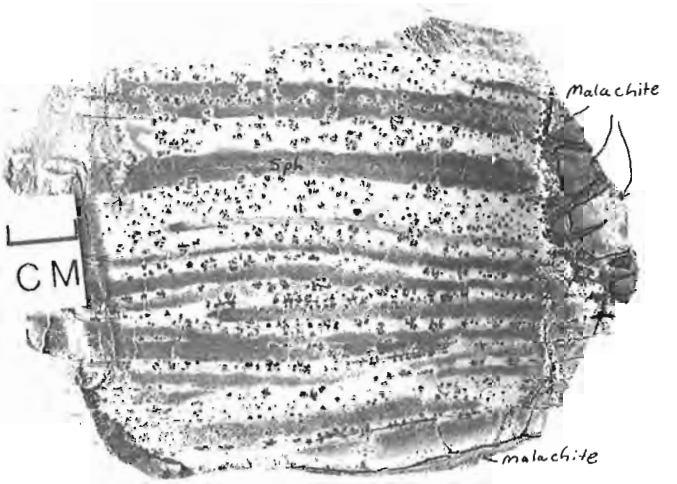


Figure 51.4

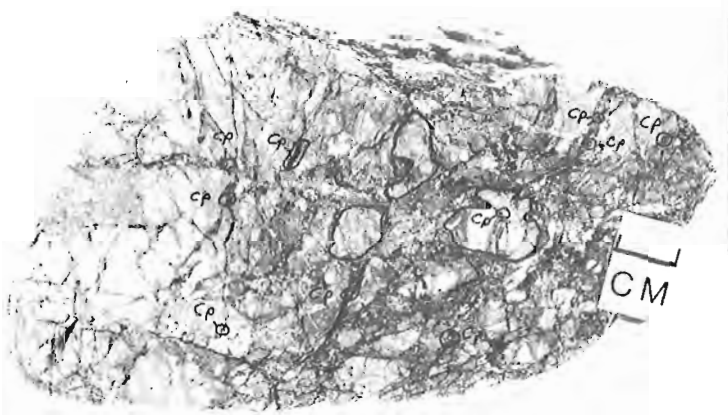
Location of composite rock samples from the Wernecke Supergroup described by Bell and Delaney (1977).


CM
cp
cp

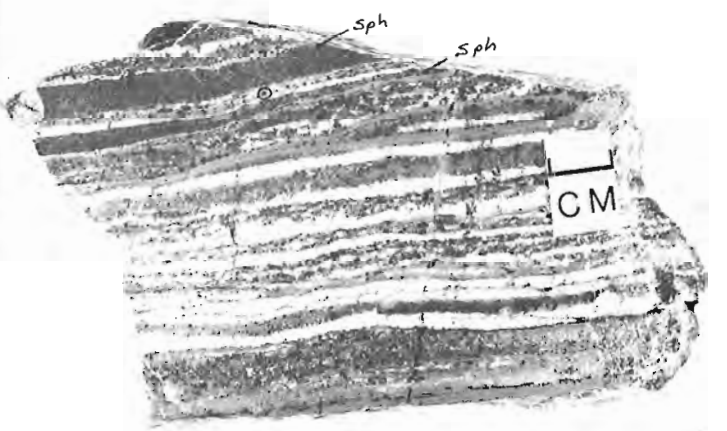
1


malachite
sph
CM
malachite

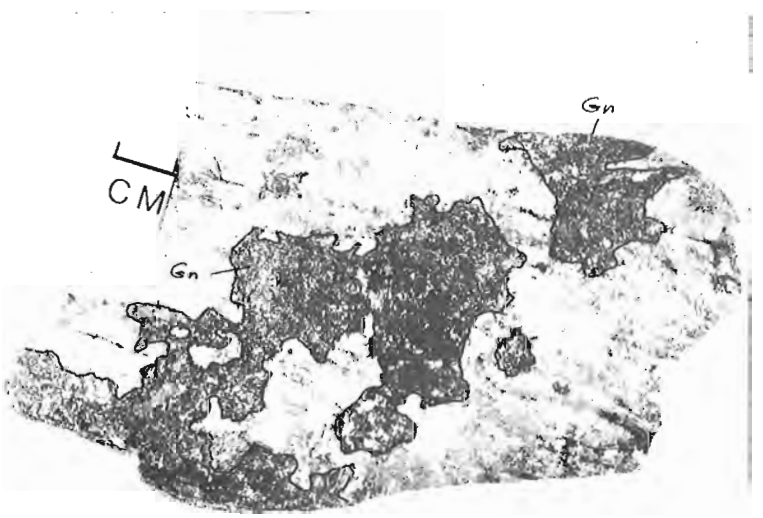
2


cp
cp
cp
cp
cp
cp
cp
cp
cp
cp
CM

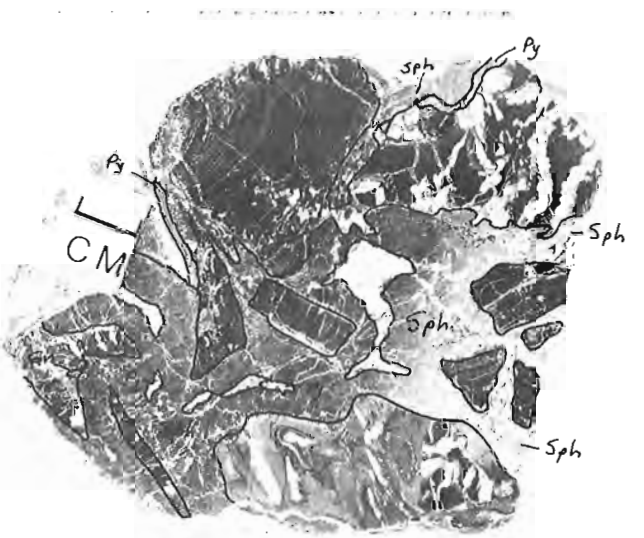
3


sph
sph
CM

4


Gn
CM
Gn

5


sph
Py
Py
CM
Sph
Sph
Sph

6

Table 51.1

Chemistry of rocks collected from the "Gillespie Lake Group"

SAMPLE NO.	Zn	Cu	Pb	Ni	Co	Ag	Mn	Fe**	Mo	V	Cd	ROCK TYPE
106C 789001	26	151	60	45	25	0.6	1084	12.92	2*	9	1*	Pyritic Quartzite
02	20	6	1	10	2	0.2*	541	1.54	2*	19	1*	Grey Dolostone
03	41	28	58	63	21	0.9	2139	5.99	2*	9	1*	Dolostone Breccia
04	898	12	18500	10	9	3.1	3276	1.74	2*	9	4	Dolosiltstone and Dolomicrite
05	1766	10	1359	6	9	0.7	3808	1.85	2*	9	10	Dolosiltstone and Dolomicrite
06	54	666	1	39	10	0.2*	1462	2.04	2*	24	1*	Light Grey Dolostone
07	55	23	14	33	6	0.2*	470	2.05	2*	57	1*	Light Grey Dolostone
08	38000	26500	118	19	21	0.2*	4441	1.21	2*	19	42	Stromatolite
09	98	1668	20	49	16	0.2*	1585	2.93	2*	30	1*	Dolosiltstone Breccia
10	7420	29	6	10	5	0.2	1789	1.68	2*	19	12	Dolostone Breccia
106C 789011	295000	41	335	72	6	36.9	213	4.12	4	5	1770	Stromatolite Breccia

* Lower detection limit
** Fe expressed in %; all other elements express in ppm

Lead most commonly occurs as coarse grained galena accompanying recrystallized white dolomite filling fractures intersecting in this case rhythmically interbedded dolosiltstone, stromatolite and white dolomite (Fig. 51.5.5). From chemical analysis, most of the galena is relatively low in Ag.

Most of the stratabound sphalerite is associated with bioherms and biostromes that have been described by Delaney (1978) to occur in the upper sections of the "Gillespie Lake Group" of rocks located just north of Gillespie Lake (Fig. 51.3). The chalcopyrite, however, occurs below the stromatolitic rocks in brown weathering grey dolostone. The structurally controlled mineralization appears more widely distributed occurring in faults and fault-related breccias intersecting lower dolostones as well as stromatolites. The lateral dimensions and stratigraphic thicknesses of zones of base metal mineralization is not known although the surficial geochemistry suggests they could be extensive.

Sample Preparation and Analysis

Rock samples weighing approximately 2 kg were crushed, pulverized and ground to minus -150 mesh (100 µ) and analyzed for Zn, Cu, Pb, Ni, Co, Ag, Mn, Fe, Mo, V, and Cd by atomic absorption spectrophotometry after decomposition with a strong HF-$HCLO_4$-HNO_3 acid mixture. Uranium was determined by both fluorometry (Smith and Lynch, 1969) and a delayed neutron activation procedure developed by Atomic Energy Canada Limited (Boulanger et al., 1975). Fluorine was determined by ion-selective electrode following sample fusion with sodium carbonate-zinc oxide flux. Major and minor element oxides were determined by X.R.F. on a glass pellet formed by fusing lg of sample with lithium metaborate. CO_2 and S were determined by the standard Leco furnace combustion method.

Stream sediments were air-dried, disaggregated, sieved to minus -80 mesh (177 µ) and analyzed for Zn, Cu, Pb, Ni, Co, Ag, Mn, Fe, Mo, V and Cd by atomic absorption spectrophotometry following a strong HF-$HCLO_4$-HNO_3 decomposition.

Stream waters were collected unfiltered and analyzed for Zn and Cu by atomic absorption spectrophotometry, F by ion-selective electrode and HCO_3^- by titration methods. Copper is not tabulated since it was below the detection limit of 1 ppb.

Rock Geochemistry

The trace and minor element chemistry of "grab" samples collected from both mineralized and unmineralized rocks from the "Gillespie Lake Group" is presented in Table 51.1. The sample locations are shown in Figure 51.2. In general, Cu contents range up to 2.65 per cent in one sample (sample no. 789006) of rhythmically interbedded stromatolite covered with a thick coating of malachite. The dolostone hosting what appears to be stratabound disseminated chalcopyrite, however, contains 0.067 per cent Cu. The zinc content of mineralized samples shows tremendous variation depending on the style of mineralization and ranges up to 3.80 per cent in laminated stromatolite and 29.5 per cent in brecciated stromatolite. Cadmium which substitutes readily for Zn in samples containing sphalerite grades up to 1770 ppm in sample 789011 containing 29.5 per cent Zn. The association of Ag with high Pb in sample 789004 in one case and high Zn in sample 789011 in the other case is less readily explained. The mineralized samples contain generally higher contents of Fe reflecting the presence of pyrite and siderite which are present in most of the rocks hosting sphalerite and galena.

In order to compare the chemistry of mineralized rocks from the "Gillespie Lake Group" with stratigraphically equivalent unmineralized rocks, whole rock and trace element data for an unmineralized stratigraphic section (Fig. 51.4) of the "Wernecke Supergroup" measured and described by Bell and Delaney (1977) are presented in Table 51.2 and 51.3. The carbonate rocks (mostly dolosiltstone) comprising the "Gillespie Lake Group" are low in all of the trace elements determined. The whole rock chemistry for the "Gillespie Lake Group" is controlled primarily by the relative proportion of carbonate (mostly dolomite) and silicate (mostly quartz)

***Figure 51.5** (opposite)*

1. *Light grey dolostone hosting stratabound disseminated chalcopyrite. Sample 789006.*
2. *Laminated stromatolite hosting malachite along fracture surfaces and stratabound sphalerite. Dark brown manganese with a dendritic habit disseminated throughout. Sample 789008.*
3. *Brecciated light grey-brown dolosiltstone hosting disseminated chalcopyrite along fractures. Sample 789009.*
4. *Rhythmically interbedded dolosiltstone, stromatolite lamina and white recrystallized dolomite hosting finely dispersed sphalerite associated with the dolosiltstone. Sample 789005.*
5. *Coarse grained galena associated with recrystallized dolomite in fracture intersecting sample 789005.*
6. *Dark grey brecciated stromatolite hosting coarse grained brown sphalerite and pyrite. White recrystallized dolomite also forms part of the matrix. Sample 789011.*

Table 51.2

Major element oxides in Proterozoic sedimentary rocks, Yukon

Map Sheet No.		SiO_2	Al_2O_3	TiO_2	FeO	Fe_2O_3	CaO	MgO	K_2O	Na_2O	P_2O_5	MnO	CO_2	H_2O	S	
106C	766001	59.1	18.1	0.58	1.7	2.1	2.93	1.8	6.18	0.0	0.14	0.16	5.0	2.9	0.16	
106C	766002	72.0	6.4	0.26	1.7	0.1	4.54	3.3	1.01	1.8	0.09	0.27	7.1	1.1	0.34	
106C	766003	75.3	12.7	0.60	3.1	0.3	0.06	1.1	2.49	1.8	0.09	0.05	0.0	2.5	0.25	
106C	766004	91.0	2.1	0.08	1.5	3.4	0.13	0.31	0.21	0.7	0.13	0.11	0.0	0.9	0.25	
106C	766005	80.8	9.6	0.33	3.2	0.0	0.07	0.81	1.26	1.7	0.07	0.03	0.0	1.8	0.12	
106C	766006	82.1	10.3	0.30	0.3	0.5	0.62	0.15	0.88	3.5	0.08	0.11	0.4	0.9	0.16	
106C	766007	82.7	8.5	0.10	0.1	2.0	0.42	0.43	2.37	0.9	0.09	0.19	0.5	1.3	0.27	
106C	766008	82.1	6.7	0.17	0.1	4.4	1.39	0.21	2.24	0.2	1.20	0.12	0.0	1.3	0.11	
106C	766009	87.1	5.1	0.08	0.8	2.4	0.17	1.0	1.17	0.0	0.10	0.22	0.1	1.8	0.07	
106C	766012	75.2	11.1	0.36	4.3	0.2	0.81	1.0	0.83	3.0	0.08	0.19	1.4	2.0	0.27	
106C	766013	72.0	15.7	0.49	2.1	0.1	0.05	0.68	3.53	2.7	0.08	0.01	0.0	2.4	0.25	
106C	766014	74.4	14.2	0.46	1.7	1.0	0.12	0.63	3.26	2.5	0.08	0.04	0.0	2.0	0.24	'QUARTET GROUP'
106C	766015	67.5	19.2	0.57	2.3	0.4	0.02	0.75	5.15	1.0	0.10	0.01	0.0	3.0	0.05	
106C	766016	70.7	15.5	0.55	2.6	1.2	0.21	0.90	3.76	2.4	0.08	0.05	0.1	2.3	0.21	
106C	766017	75.0	12.1	0.30	3.8	0.4	0.26	0.81	1.59	3.8	0.08	0.05	0.1	1.8	0.25	
106C	766019	73.1	15.1	0.44	1.9	0.6	0.03	0.79	4.06	1.7	0.09	0.03	0.0	1.9	0.09	
106C	766020	80.6	10.8	0.27	1.4	0.2	0.16	0.71	2.12	2.1	0.08	0.04	0.0	1.5	0.11	
106C	766021	72.2	14.2	0.53	3.3	0.5	0.08	1.33	3.82	1.3	0.11	0.03	0.0	2.6	0.22	
106C	766022	67.1	17.5	0.70	3.1	1.3	0.05	1.22	4.86	1.2	0.07	0.03	0.0	3.0	0.08	
106C	766025	39.2	8.9	0.33	2.3	0.4	21.7	0.79	2.39	0.0	0.20	1.40	21.6	1.3	0.24	
106C	766026	61.1	19.3	0.75	0.6	0.8	0.98	1.10	5.93	4.9	0.19	0.03	0.6	1.3	0.23	
106C	766027	48.1	14.0	0.32	0.2	0.1	7.20	0.36	9.24	1.6	0.50	0.12	6.6	0.5	0.21	
106C	766028	63.0	14.0	0.58	3.1	1.0	7.45	0.90	3.89	0.6	0.13	0.09	0.4	2.4	0.21	
106C	766029	70.6	10.1	0.38	4.0	0.5	2.70	2.31	2.19	0.2	0.27	0.15	4.4	2.1	0.11	
106C	766030	65.7	5.7	0.19	2.3	0.0	7.60	4.22	1.52	0.2	0.09	0.32	10.7	0.9	0.23	
106C	766031	69.4	6.3	0.10	0.8	0.0	7.90	2.70	2.90	0.2	0.10	0.60	9.4	0.7	0.31	
106C	766032	65.8	18.6	0.74	3.9	0.1	0.14	2.40	4.10	0.4	0.11	0.04	0.0	3.4	0.05	
106C	766033	64.3	18.6	0.73	0.0	4.1	0.19	2.40	3.66	1.4	0.17	0.06	0.0	3.7	0.21	
106C	766052	69.9	14.7	0.60	2.3	0.9	0.33	2.5	4.5	0.7	0.09	0.03	0.4	3.2	0.23	
106C	766053	73.1	13.5	0.52	2.1	0.3	0.06	2.2	4.8	0.6	0.10	0.01	0.0	2.6	0.19	
106C	766054	81.2	9.7	0.35	1.3	0.4	0.03	1.1	4.1	0.0	0.06	0.00	0.0	1.6	0.08	
106C	766055	73.1	13.4	0.53	2.2	0.1	0.52	2.4	4.7	0.1	0.09	0.03	0.7	2.3	0.09	
106C	766056	67.0	7.5	0.23	2.1	0.1	5.0	3.3	3.3	0.3	0.09	0.37	9.6	1.0	0.20	
106C	766057	56.0	5.0	0.15	2.5	0.0	9.2	6.0	2.4	0.0	0.04	0.35	17.5	0.8	0.09	
106C	766058	38.0	5.0	0.20	3.2	0.0	14.8	9.0	2.4	0.0	0.08	0.45	26.5	0.7	0.04	
106C	766059	60.0	7.0	0.28	2.0	0.1	6.5	5.2	3.0	0.4	0.09	0.18	13.4	1.7	0.19	
106C	766060	31.0	4.0	0.12	1.6	0.0	18.6	13.0	1.2	0.0	0.05	0.17	29.3	0.9	0.08	
106C	766061	15.0	0.6	0.00	1.7	0.0	24.7	17.0	0.1	0.3	0.4	0.26	39.5	0.3	0.23	
106C	766062	15.0	6.0	0.26	3.8	1.0	12.0	9.0	2.7	0.8	0.18	0.60	25.0	1.8	0.21	
106C	766063	33.0	5.8	0.11	4.4	0.0	16.0	10.6	3.1	0.5	0.07	0.56	24.0	1.7	0.32	

'FAIRCHILD GROUP'

'GILLESPIE LAKE GROUP'

Note: All element oxides expressed in %

Table 51.3

Minor and trace elements in Proterozoic sedimentary rocks, Yukon

Map Sample No.	Zn	Cu	Pb	Ni	Co	Ag	U(F)	U(NA)	F	
106C 766001	11	149	2	20	10	0.2	2.0	3.5	915	
106C 766002	12	1230	2	7	10	0.2	4.8	7.5	451	
106C 766003	47	17	15	24	15	0.2	2.6	3.8	405	
106C 766004	26	16	15	3	7	0.8	18.4	21.9	93	
106C 766005	42	12	2	20	11	0.7	1.6	2.1	150	
106C 766006	9	8	12	7	10	0.5	1.5	2.1	73	
106C 766007	39	17	27	10	13	0.4	1.2	1.3	183	
106C 766008	48	10	34	7	14	0.4	2.2	2.4	405	
106C 766009	25	6	14	5	8	0.2	1.3	1.6	170	
106C 766012	68	14	11	12	12	0.2	2.6	4.2	162	
106C 766013	42	5	2	7	10	0.2	3.6	3.7	328	'QUARTET GROUP'
106C 766014	43	14	15	8	11	0.2	2.8	3.3	279	
106C 766015	35	7	9	11	10	0.2	8.8	11.5	572	
106C 766016	44	7	8	13	13	0.2	2.4	3.4	370	
106C 766017	55	12	18	13	12	2.3	2.0	3.2	154	
106C 766019	18	17	2	16	12	0.2	2.6	3.5	314	
106C 766020	21	8	2	10	10	0.2	4.4	4.9	160	
106C 766021	30	22	2	16	13	0.2	2.0	3.6	470	
106C 766022	37	9	2	17	13	1.6	4.8	6.2	493	
106C 766025	11	45	15	22	18	0.2	0.7	3.2	230	
106C 766026	12	890	15	17	11	0.2	40.0	45.2	900	'FAIRCHILD GROUP'
106C 766027	10	38	2	4	5	0.2	1.2	1.5	154	
106C 766028	15	12	2	19	24	0.2	1.5	2.9	370	
106C 766029	19	16	2	10	10	0.5	14.0	1.6	450	
106C 766030	20	29	2	10	7	0.8	3.8	4.3	314	
106C 766031	8	7	2	5	1	0.2	2.6	2.0	341	
106C 766032	58	3	8	28	12	0.2	2.4	3.3	470	
106C 766033	58	3	2	7	8	0.2	8.8	11.6	470	
106C 766052	18	10	2	20	11	0.2	1.6	2.8	660	
106C 766053	13	10	2	11	7	0.2	3.2	5.0	425	
106C 766054	11	20	8	11	6	0.2	2.0	3.0	380	'GILLESPIE LAKE GROUP'
106C 766055	12	13	4	13	7	0.2	2.4	3.1	456	
106C 766056	10	22	2	6	8	0.2	10.4	2.1	271	
106C 766057	10	7	8	5	4	0.2	0.7	1.7	226	
106C 766058	12	5	7	6	4	0.2	0.7	1.7	261	
106C 766059	12	6	4	13	5	0.2	1.1	1.9	195	
106C 766060	11	5	2	5	3	0.2	1.3	1.1	271	
106C 766061	12	5	2	2	2	0.2	1.2	0.6	982	
106C 766062	26	6	7	8	4	0.2	1.1	2.0	665	
106C 766063	34	11	8	6	4	0.2	1.2	2.5	1065	

Note: All elements expressed in ppm.

minerals present. Although samples 766062 and 766063 represent composite samples of stromatolitic dolomite (Fig. 51.4), there is only a minor chemical indication of an organic component from the higher phosphorus content of sample 766062. Most of the iron, which is in the Fe^{+2} oxidation state, is present as siderite and pyrite.

The "Fairchild Lake Group" and the "Quartet Group" are generally enriched in Cu, Ag, U and occasionally Pb. These enrichments do not include mineralized breccias that contain high contents of U, Cu, Fe, Pb, Co, Mn and, in some breccia complexes, Ag, Mo, F, P, Y, Ce and As. The whole rock and trace element chemistry of the "Quartet Group" and "Fairchild Lake Group" are in most regards very similar with at least two notable differences; rocks of the "Fairchild Lake Group" are generally higher in Mg and lower in Na, possibly reflecting magnesium-alkali metasomatism commonly associated with intrusive breccia complexes.

Stream Sediment and Water Geochemistry

The regional distributions of Pb and Zn in sediments deposited from streams draining the western half of map area 106C and the eastern half of map area 106D are shown by contour plots in Figures 51.6 and 51.7. In general, there is a string of coincident Pb-Zn anomalies that have greater than 500 ppm Pb and greater than 1000 ppm Zn in areas underlain by mostly orange weathering grey, pink and buff fine grained dolomite mapped by Blusson (1974a). These rocks are equivalent to the "Gillespie Lake Group" named and described by Delaney (1978). An examination of the regional geochemical data reveals a close spatial association of high Pb-Zn anomalies with bioherms and biostromes described by Delaney (1978) as forming part of the "Gillespie Lake Group" in the area north and east of Gillespie Lake. This association of Pb and Zn with the presence of stromatolitic rocks in the "Gillespie Lake Group" was confirmed during follow-up investigations carried out east of Gillespie Lake.

Table 51.4

Chemistry of sediments and waters from streams intersecting the "Gillespie Lake Group" of rocks

	STREAM SEDIMENTS											STREAM WATERS				
SAMPLE NO.	Zn	Cu	Pb	Ni	Co	Ag	Mn	Fe	Mo	V	Cd	COND	pH	HCO_3	Zn	F
106C 785002	375	61	47	32	20	0.2	2000	3.75	2*	50	1*	158	7.9	103	0.5*	75
03	281	35	47	21	16	0.2	2237	2.81	2*	42	1*	153	8.1	110	0.5*	68
04	563	43	105	25	15	0.2	1895	2.81	2*	42	1*	164	8.1	115	0.5*	83
05	469	38	165	21	18	0.2	2000	2.96	2*	42	1*	105	7.6	72	0.5*	48
06	406	63	726	26	16	1.2	2895	5.13	2*	62	1*	208	8.2	87	0.5*	58
07	1897	40	300	24	11	0.5	1289	2.96	2*	38	2	181	8.3	100	3.3	58
08	1552	38	347	24	10	1.0	1053	3.90	2*	33	1*	195	8.3	113	7.9	83
09	1897	112	989	29	10	2.5	1474	7.79	2*	28	2	217	8.3	117	9.0	130
10	1983	106	705	27	9	2.5	1700	7.50	2*	24	2	223	8.1	121	9.3	200
11	2112	99	674	26	12	2.2	1605	7.79	2*	28	2	245	8.0	119	9.0	220
12	2069	99	642	26	11	2.0	1632	8.09	4	28	2	244	7.9	11	9.3	230
14	531	25	215	18	8	0.2	800	2.35	4	42	1*	205	8.0	129	5.0	97
15	594	29	165	25	10	0.2	775	2.65	4	66	1*	208	8.3	133	7.1	100
16	531	31	185	25	13	0.4	1053	3.12	4	47	1*	207	8.4	137	3.3	120
17	1336	33	275	26	12	0.8	900	2.81	4	52	1*	205	8.1	116	17.7	125
18	2328	33	453	24	13	0.8	1105	3.12	4	38	2	218	7.9	109	21.1	145
19	772	39	185	28	19	1.0	1316	3.51	4	47	1*	181	8.2	115	0.5*	61
106C 765020	469	48	79	28	6	0.2	1211	2.50	4	57	1*	184	8.3	134	5.0	55
106C 785022	238	26	53	20	8	0.2	875	2.50	2*	57	1*	231	8.3	151	0.5*	50
23	250	33	84	22	9	0.2	925	3.12	2*	66	1*					
24	200	33	47	21	14	0.2	925	3.12	2*	66	1*					
25	772	45	295	31	16	1.0	1895	5.39	2*	28	1*	260	8.3	138	1.7	97
26	619	40	195	29	15	0.5	1816	5.07	2*	47	1*	181	8.1	116	0.5*	100
27	563	57	235	35	18	0.2	1789	4.53	2*	64	1*					
28	219	29	63	24	12	0.2	1289	2.96	2*	74	1*	282	8.0	172	0.5*	65
29	219	31	84	27	12	0.2	1368	3.12	2*	57	1*	257	8.2	160	0.5*	65
30	281	115	115	26	12	1.0	1368	3.75	2*	57	1*	215	7.6	133	0.5*	60
106C 785031	438	33	205	21	9	0.2	1842	3.43	2*	42	1*	223	8.2	125	0.5*	60

* Lower than detection limit

NOTE: all elements determined in stream sediments expressed in ppm except Fe which is expressed in %; elements determined in stream waters expressed in ppb except HCO_3 which is express in ppm; specific conductivity is expressed in micro mhos.

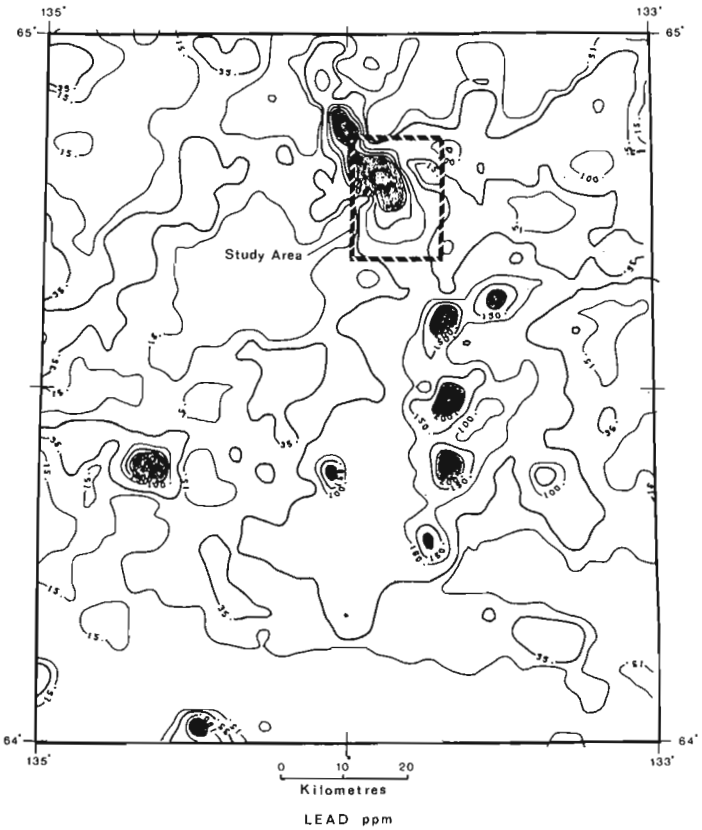


Figure 51.6. *Regional distribution of Pb in sediments from streams intersecting the west half of the Nadaleen River map area and the east half of the Nash Creek map area.*

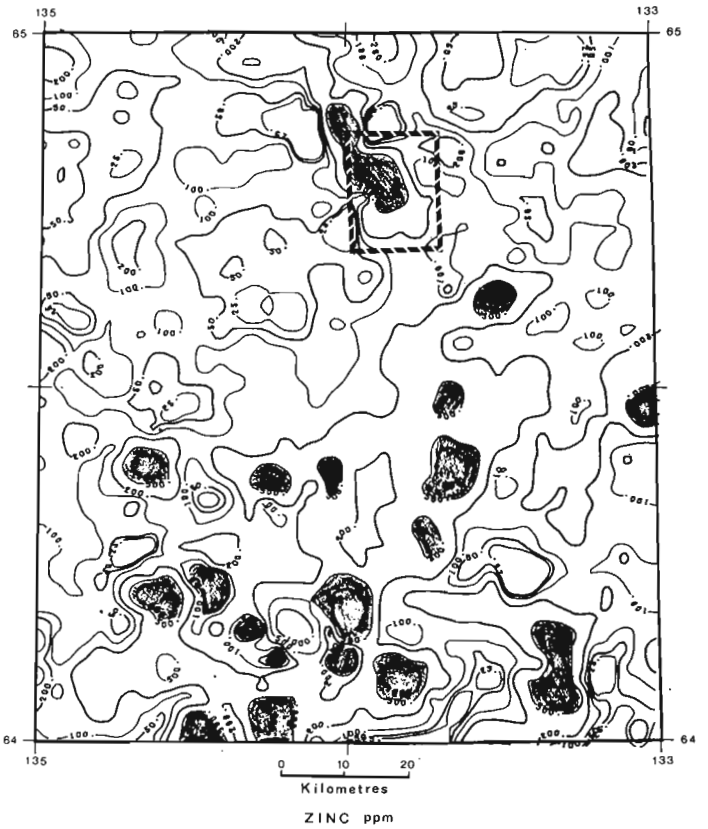


Figure 51.7. *Regional distribution of Zn in sediments from streams intersecting the west half of the Nadaleen River map area and the east half of the Nash Creek map area.*

Table 51.5

Chemistry of rocks from the Redstone Copper Belt, N.W.T.

Sample No.	Formation	Sub-Unit	Lithologies	Zn	Cu	Pb	Ni	Co	Ag	Mo	F	U
CJ-77-19	Coppercap	C-2	Shales and limestones	17	59	5	32	16	0.2*	2	970	1.5
CJ-77-423	Redstone River	RR-8	Redbeds,evaporites and carbonates	5200	190000	45	18	25	17.0	29	700	4.4
CJ-77-38D	Redstone River	RR-8	Redbeds,evaporites and carbonates	38	28000	84	7	3	7.8	74	195	1.2
CJ-76-698BF	Redstone River	RR-8	Redbeds,evaporites and carbonates	15	70000	1*	12	1*	8.8	8	310	2.0
CJ-76-36	Redstone River	RR-8	Redbeds,evaporites and carbonates	81	26	1*	41	11*	0.2*	1*	850	3.1
CJ-76-12	Redstone River	RR-4	Red mudstone	18	8	1*	20	10	0.2*	1*	750	0.8
CJ-76-559	Redstone River	RR-1	Evaporites and Redbed Breccias	7	75	1*	12	1*	0.2*	1*	825	1.4
CJ-76-234	Upper Little Dal	LD-16	Limestones and Stromatolites	7	49	10	8	1*	0.2*	1*	1350	1.2
CJ-76-157B	Upper Little Dal	LD-15	Sandstones	10	2600	1*	5	4	0.2*	1*	120	1.5
CJ-76-276	Upper Little Dal	LD-14	Vericoloured shales	8	15	5	18	1*	0.2*	1*	575	0.5
CJ-76-375	Unnamed	H5-5	Sandstones	5	18	1*	6	5	0.2*	1*	185	2.3

	SiO_2	Al_2O_3	TiO_2	Fe_2O_3**	CaO	MgO	K_2O	Na_2O	P_2O_5	MnO	CO_2	H_2O_T	S
CJ-77-19***	28	6	0.6	3.19	9	11	3	0.7	0.1	0.038	11.3	15.1	5.0
CJ-77-423***	9	4	0.3	2.10	8	16	1	0.1	0.1	0.227	30.4	2.5	4.6
CJ-77-38D***	21	2	0.2	1.39	22	14	0.2	0.7	0.0	0.219	32.8	1.2	0.62
CJ-77-698BF***	20	4	0.4	1.86	20	14	0.6	2.0	0.1	0.157	28.1	1.0	1.4
CJ-76-36	44.0	8.9	1.10	5.62	9.0	11.8	2.05	0.1	0.14	0.073	13.2	4.4	0.06
CJ-76-12	35.8	7.1	0.42	3.39	12.8	12.0	2.52	0.3	0.08	0.054	18.8	5.5	2.0
CJ-76-559***	13	2	0.1	0.54	9	32	0.3	0.0	0.0	0.007	26.8	2.1	5.2
CJ-76-234***	64	14	1.0	3.93	0	1	8	0.0	0.0	0.002	0.0	1.8	1.2
CJ-76-157B	90.6	4.3	0.19	1.03	0.0	0.13	1.06	0.0	0.01	0.002	0.0	0.8	0.33
CJ-76-276	53.4	25.1	1.20	5.01	0.0	0.78	7.67	0.0	0.01	0.002	0.0	4.8	0.22
CJ-76-375	88.2	5.1	0.23	2.99	0.0	0.10	1.08	0.1	0.02	0.004	0.0	1.6	0.77

* element concentration below the lower detection limit
** total Fe express as Fe_2O_3
*** major element oxide content approximate only
Note: Oxides expressed in %; trace elements express in ppm

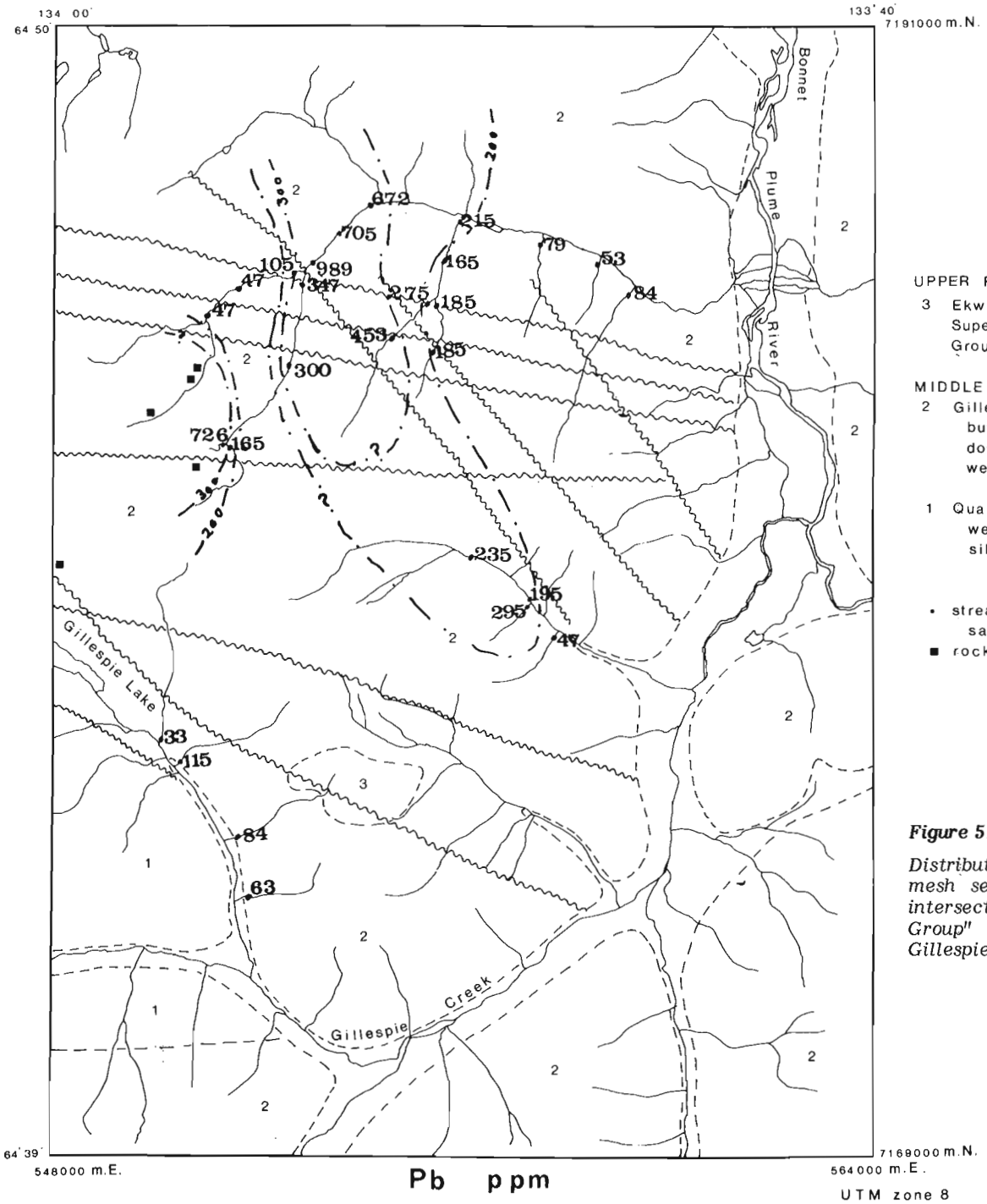


Figure 51.8

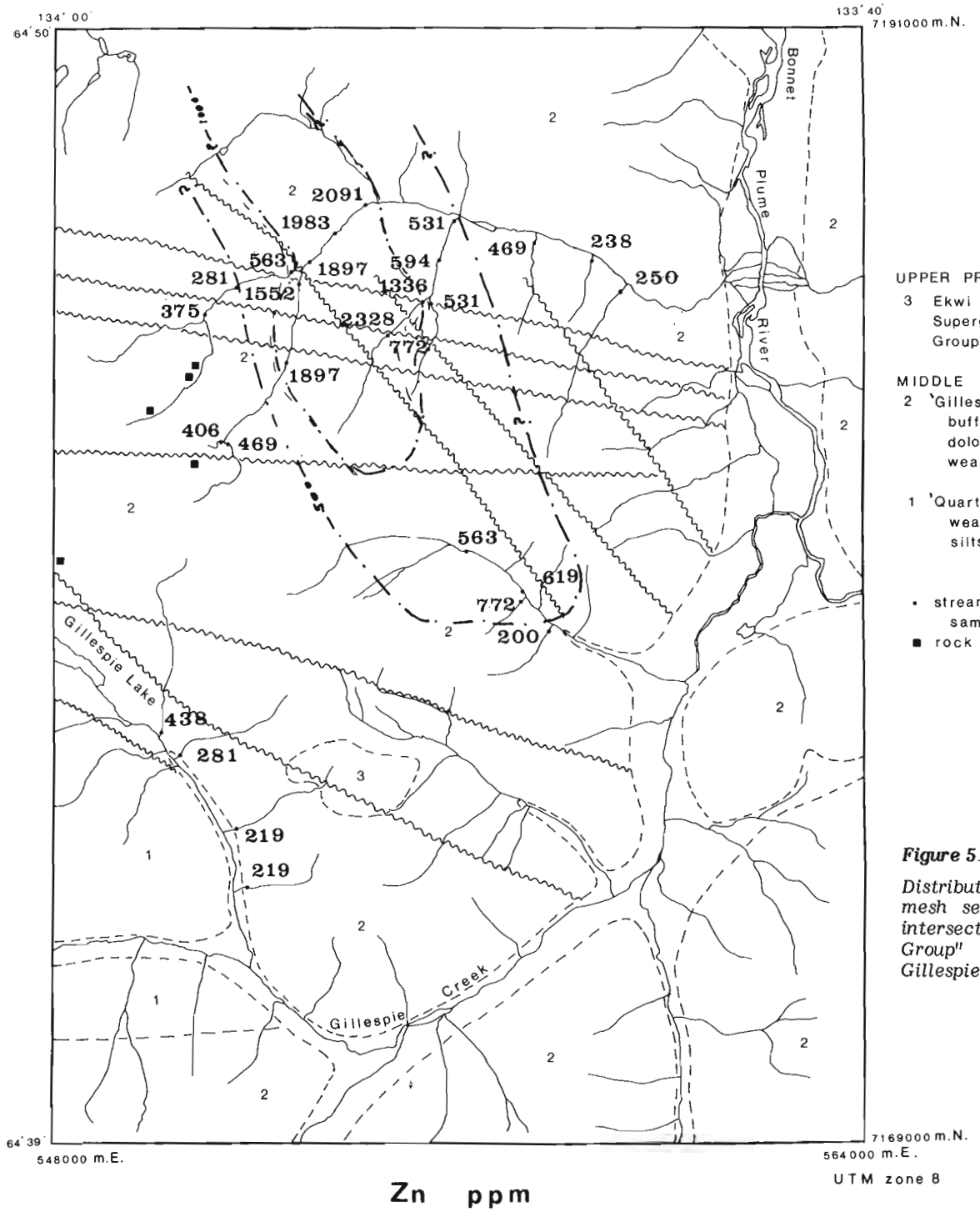
Distribution of Pb in minus -80 mesh sediments from streams intersecting the "Gillespie Lake Group" situated east of Gillespie Lake.

In order to determine the spatial significance of base metal mineralization and to assess the physical and chemical factors affecting dispersion of elements from this mineralization, one geochemically anomalous area located immediately east of Gillespie Lake was selected for more detailed study. Close-interval stream sediments and waters were collected and analyzed for most trace elements thought to be associated with this type of mineralization (Table 51.4).

The distribution of Pb and Zn, presented in Figures 51.8 and 51.9, outline an extensive and intensive northwest-southeast zone which parallels most of the bedding strikes recorded for the area as well as the surface projection of one of the major faults in the area. This relationship is not surprising considering that all the mineralization examined was either stratigraphically or structurally controlled.

Silver and Cd behave very similarly to Pb and Zn, no doubt reflecting their ability to substitute into the lattice of galena and sphalerite, respectively. The low contrast between mineralized and unmineralized areas for Ag and Cd is probably due to the high lower detection limit for analytical methods used for these elements (Table 51.4). Iron, which is present as pyrite or siderite in mineralized rocks, is distributed similarly to Pb and Zn.

Unlike Pb and Zn, the spatial distribution of Cu in stream sediments (Fig. 51.10) defines a relatively restricted and less intensive geochemically anomalous zone. Since most elements in this area are dispersed predominantly by the abrasive action of streams, the subtle Cu anomaly observed is most likely derived from low-grade Cu mineralization in the underlying rocks. The stream waters are characteristically



LEGEND

UPPER PROTEROZOIC

3 Ekwi and Mackenzie Mountains Supergroups and Pinguicula Group

MIDDLE PROTEROZOIC

2 'Gillespie Lake Group' orange-, buff-, and grey-weathering dolostone; grey- and brown weathering slate and siltstone

1 'Quartet Group' dark grey-weathering slate, argillite, siltstone and sandstone

• stream sediment and water sample

■ rock sample

Figure 51.9

Distribution of Zn in minus -80 mesh sediments from streams intersecting the "Gillespie Lake Group" situated east of Gillespie Lake.

alkaline (Table 51.4) due to the buffering action of carbonate dissolved from the underlying dolomitic rocks. Under these conditions, Cu and Pb form relatively insoluble carbonates as evidenced in the case of Cu by green malachite coating the fracture surface of mineralized rocks. Zinc, on the other hand, is more soluble under these conditions as shown by the relatively high Zn content of stream waters which coincides with anomalous Zn in stream sediments.

Fluorine in stream waters is dispersed similarly to Zn although the reason for this is not clear. It is possible that F may be associated with calcium phosphates that form an important constituent of algae. The association of high F with P in stromatolites of the "Gillespie Lake Group" (Tables 51.2, 51.3) would tend to support this conclusion. Also, F is a common constituent of carbonate hosted base metal deposits described elsewhere.

Discussion and Conclusions

The presence of Pb, Zn and Cu mineralization associated with stromatolitic rocks and faults and fault-related breccias of the "Gillespie Lake Group" opens up a large area with base metal potential in the central Yukon Territory. The size and magnitude of stream sediment geochemical anomalies indicate that this type of mineralization should be investigated further to assess its true economic potential.

The controls on the mineralization would at first glance appear to be the presence of bioherms and biostromes in the "Gillespie Lake Group" that have been intersected by faults. The presence of faults is reflected by the high Hg in stream sediments from the area east of Gillespie Lake (Geological Survey of Canada, 1978). The stromatolites in the upper

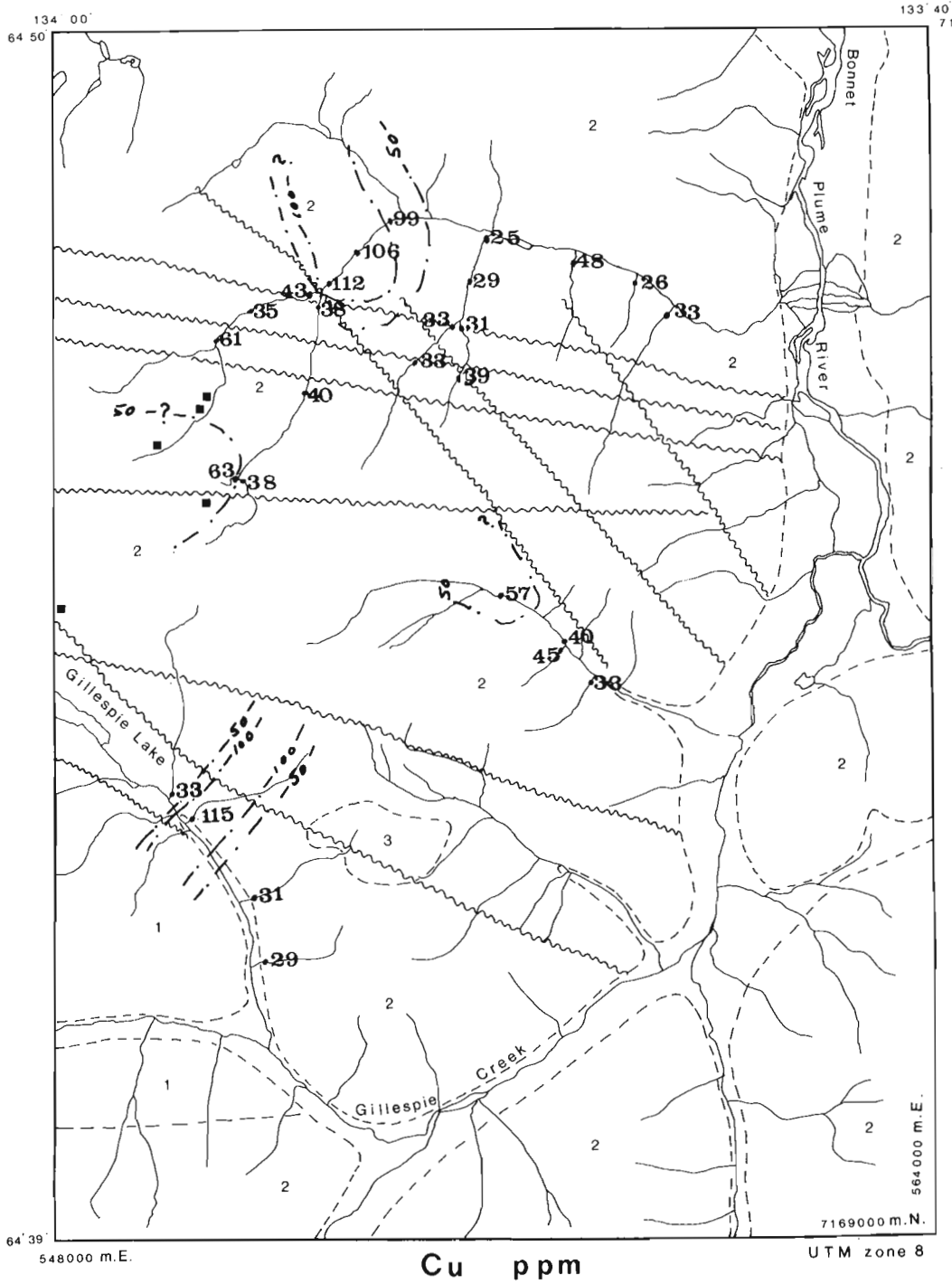


Figure 51.10

Distribution of Cu in minus -80 mesh sediments from streams intersecting the "Gillespie Lake Group" situated east of Gillespie Lake.

"Gillespie Lake Group" provide an excellent source for base metals that are available for mobilization and concentration after their initial deposition. Although algae are unlikely to accumulate large quantities of base metals by biochemical processes, organic matter derived from the bacterial degradation of algae on the seafloor is an efficient absorber of these metals from both sea and connate waters. An alternate source (not to mention a host) for base metals is provided by the underlying "Quartet Group" which is composed, in part, of what was originally organic-rich muds containing abundant organic matter and clays to act as efficient absorbers of base metals. This conclusion is supported by the generally higher contents of Cu, Pb, Zn and Ag present in rocks collected from the "Quartet Group" (Table 51.3).

During compaction and associated diagenesis of the underlying sedimentary sequence, these metals would become relatively labile due to the degradation of organic compounds and would therefore be available for transport, possibly complexed as chlorides, in connate saline fluids. This type of transporting mechanism has been demonstrated by Roedder (1967) from fluid inclusion studies of strataform Mississippi Valley Type ore deposits.

Fluid migration would follow pathways of least restriction such as the numerous fault zones intersecting the "Gillespie Lake Group". The precipitation of metal sulphides in open space may be achieved either by a biological process involving the reduction of SO_4^{-2} to S^{-2} by sulphate-reducing bacteria using in this case decomposing algal material as a nutrient source or by an inorganic process using methane in the following reaction proposed by Barton (1967):

$$CH_4 + ZnCl_2 + SO_4^{=} + Mg^{++} + 3\,CaCO_3 \rightarrow ZnS + CaMg(CO_3)_2 + 2Ca^{++} + 2Cl^{-} + 2HCO_3^{-} + H_2O$$

This reaction would not only account for the production of metal sulphide but would also explain the generally observed dolomitization of carbonate rocks. Evidence supporting this interpretation of the preliminary field and chemical data includes the close spatial association of Pb-Zn mineralization with rocks of organic derivation that are commonly intersected by faults, the presence of white recrystallized curve dolomite associated with stratabound and fault-controlled sphalerite mineralization, and the presence of accompanying elements (e.g. Cd, Ag, Fe) that characterize carbonate-hosted Mississippi Valley Type mineralization described elsewhere (Jackson and Beales, 1967). In regard to certain aspects, the Pb-Zn mineralization in the "Gillespie Lake Group" is similar to the Gayna River Pb-Zn mineralization that occurs in oolitic dolostones near bioherms (Hewton, 1977) that form part of the Little Dal Group of Upper Proterozoic age (Delaney et al., in press). The mineralization at Gayna River was described by Hewton (1977) to occur either as brightly coloured sphalerite within breccias or as pale to colourless sphalerite disseminated in fragments and in the matrix of sedimentary breccias.

The Cu mineralization in the "Gillespie Lake Group" occurs as fine grains disseminated throughout dolosiltstone and intersecting fault zones. In the former case, it appears to be stratabound although the regional geochemical data indicates that it is not laterally extensive. In general, Zn and Pb are associated with rocks that are mineralized with Cu (Table 51.1). This elemental association is not unlike that characterizing Cu-bearing rock specimens from the Redstone Copper Belt that contain, in addition to Zn and Pb, above normal contents of Ag and Mo (Table 51.5).

Sedimentary rocks hosting Cu mineralization in the Little Dal Group, Redstone River Formation and Coppercap Formation of the Redstone Copper Belt and in the "Gillespie Lake Group" of the Wernecke Mountains appear to represent different environments of deposition. Sabkha conditions during a marine transgression are indicated for sedimentary rocks from the Redstone Copper Belt that are transitional between gypsiferous red beds and fetid detrital limestone (Jefferson, 1975) while the "Gillespie Lake Group" is more characteristic of a shallowing intertidal to subtidal arid environment as evidenced by the presence of carbonates, stromatolite lamina, flat chip conglomerate and oolitic dolostone. Furthermore, red beds, evaporites and basalts have not been described for the "Gillespie Lake Group" which is considered by Yeo et al. (1978) to be older than the Little Dal Group.

Acknowledgments

The author wishes to thank C.W. Jefferson for providing rock samples from the Redstone copper occurrences and G. Delaney and R.T. Bell for providing rock samples from a composite section of the Wernecke Supergroup. H.E. Dunsmore and I.R. Jonasson are also thanked for stimulating discussions on the subject of Pb-Zn mineralization in carbonate rocks. P. Friske and C. Orssich provided able assistance during the field program. Trace elements were determined in the Geochemical Laboratories of the Geological Survey by A. MacLaurin and G. Gauthier. G. Lachance made arrangements for X.R.F. analyses.

References

Barton, P.B.
1967: Possible role of organic matter in the precipitation of the Mississippi Valley ores; in J.S. Brown (ed.), "Genesis of Strataform Lead-Zinc-Barite-Fluorite Deposits"; Economic Geology Monograph no. 3, p. 371-378.

Bell, R.T. and Delaney, G.D.
1977: Geology of some uranium occurrences in Yukon Territory; in Report of Activities, Part A, Geological Survey of Canada, Paper 77-1A, p. 33–37.

Blusson, S.L.
1974a: Nadaleen River map-area of Operation Stewart; Geological Survey of Canada Open File no. 205.

1974b: Nadaleen River map-area; Yukon Territory (106C-6, 7, 10, 11, 13, 14, 15); Geological Survey of Canada Open File no. 206.

Blusson, S.L. and Tempelman-Kluit, D.J.
1970: Operation Stewart, Yukon Territory, District of Mackenzie (105N, O; 106B, C); in Report of Activities, Part A, Geological Survey of Canada, Paper 70-1A, p. 29-32.

Boulanger, A., Evans, D.J.R., and Raby, B.F.
1975: Uranium analysis by neutron activation delayed neutron counting; Proceedings of the Seventh Annual Symposium of Canadian Mineralogical Analysts, Thunder Bay, Ontario, 10 p.

Brown, R.J.E.
1967: Permafrost in Canada; Geological Survey of Canada Map 1246A.

Delaney, G.D.
1978: A progress report on stratigraphic investigations of the lowermost succession of Proterozoic rocks, northern Wernecke Mountains; Dept. of Indian and Northern Affairs Open File Report EGS 1978-10, 12 p.

Delaney, G.D., Jefferson, G.W., Yoe, G.M., McLennan, S.M., Bell, R.T., and Aitken, J.D.
Some Proterozoic sediment-hosted metal occurrences of the northeastern Canadian Cordillera; Society of Economic Geologists, Couer d'Alene Field Conference, Wallace, Idaho, November 3-5, 1977. Idaho Bureau of Mines Special Publication. (in press)

Eisbacher, G.H.
1978: Two major Proterozoic unconformities, northern Cordillera; in Report of Activities, Part A, Geological Survey of Canada, Paper 78-1A, p. 53–58.

Findlay, D.C.
1975: Map showing the geology and mineral deposits of Yukon Territory and parts of the southwest District of Mackenzie, Northwest Territories; Geological Survey of Canada Open File 87.

Geological Survey of Canada
1978: Uranium Reconnaissance Program National stream sediment and water geochemical reconnaissance data, northern Yukon Territory; Geological Survey of Canada Open File no. 518.

Green, L.H.
1972: Geology of Nash Creek, Larsen Creek, and Dawson map-areas, Yukon; Geological Survey of Canada, Memoir 364, 157 p.

Hewton, R.S.
1977: Geology and mineralization at Gayna River, N.W.T. (abstract) Geological Association of Canada Annual Meeting, Vancouver, 1977. Program with Abstracts, v. 2, p. 24.

Jackson, S.A. and Beales, F.W.
1967: An aspect of sedimentary basin evolution: the concentration of Mississippi Valley-type ores during the late stages of diagenesis; Bulletin of Canadian Petroleum Geology, v. 15, p. 383-433.

Jefferson, C.J.W.
1975: Stratigraphy and sedimentology, Upper Proterozoic Redstone Copper Belt, Mackenzie Mountains, N.W.T. - a preliminary report; in Mineral Industry Report 1975, Northwest Territories; Indian and Northern Affairs Economic Geology Series 1979.

Ricker, K.E.
1974: Surficial geology of the Nadaleen River map-area, Yukon Territory - Northwest Territories; Geological Survey of Canada Open File no. 207, 34 p.

Roedder, E.
1967: Environment of deposition of stratiform (Mississippi Valley Type) ore deposits, from studies of fluid inclusions, in J.S. Brown (ed.), "Genesis of Stratiform Lead-Zinc-Barite-Fluoride Deposits", Economic Geology Monograph no. 3, p. 371-378.

Smith, A.Y. and Lynch, J.J.
1969: Field and laboratory methods used by the Geological Survey of Canada in geochemical surveys. No. 11, uranium in soil, stream sediment and water; Geological Survey of Canada, Paper 69–40, 9 p.

Wheeler, J.O.
1954: A geological reconnaissance of the northern Selwyn Mountains region, Yukon and Northwest Territories; Geological Survey of Canada, Paper 53-7, Map 53-7.

Yeo, G.M., Delaney, G.D., and Jefferson, C.W.
1978: Two major Proterozoic unconformities, northern Cordillera: discussion in Current Research, Part B, Geological Survey of Canada, Paper 78-1B, p.225–230.

Young, G.M., Jefferson, C.W., Long, D.G.F., Delaney, G.D., and Yeo, G.M.
Upper Proterozoic stratigraphy of northwestern Canada and Precambrian history of North American Cordillera; Society of Economic Geologists, Couer d'Alene Field Conference, Wallace, Idaho, November 3-5, 1977. Idaho Bureau of Mines Special Publication. (in press)

52.

THE DISPERSION OF URANIUM IN THE VICINITY OF MIOCENE 'BASAL TYPE' URANIUM OCCURRENCES IN LASSIE LAKE AREA, SOUTH-CENTRAL BRITISH COLUMBIA

Project 750051

D.R. Boyle
Resource Geophysics and Geochemistry Division

Boyle, D.R., The dispersion of uranium in the vicinity of Miocene 'basal type' uranium occurrences in the Lassie Lake area, south-central British Columbia; in Current Research, Part A, Geol. Surv. Can., Paper 79-1A, p. 349-356, 1979.

Abstract

Lassie Lake area in the Okanagan Highlands of British Columbia contains at least three occurrences of Miocene 'basal type' uranium mineralization in sediments underlying Plateau Basalt outliers. The results of a detailed geochemical drainage survey in this area are described. Stream and spring waters were analyzed for U, F, Na, K, Ca, Mg, Cl, $SO_4^=$, HCO_3^- pH and conductivity; associated sediments were analyzed for U, Cu, Pb, Zn, Fe, Mn, Ni, Ca, Mo, and loss on ignition (organic content).

Uranium in sediments shows no significant correlation with any of the base metals and the latter elements are, therefore, of little interpretative or pathfinder value when prospecting for this type of deposit. Water chemistry and sediment composition (organic content) have some effect on the dispersion and concentration of uranium, but lithology, structure and hydrology (e.g. fissure controlled waters) have been found to be more important in interpreting anomalies.

The observed dispersion patterns of uranium in the vicinity of mineralized and unmineralized sediments underlying the basaltic outliers are described and guidelines on sampling techniques which can be employed in the search for this type of mineralization are proposed.

Introduction

Subsequent to the joint Federal-Provincial geochemical reconnaissance program covering NTS sheets 82E, L and M (Geological Survey of Canada, 1976), and as part of a more extensive follow-up program, a detailed geochemical survey was carried out in the Lassie Lake area of the Okanagan Highlands, British Columbia (Fig. 52.1). The area contains economically interesting 'basal type' uranium mineralization and was studied for the following reasons:

a. to determine whether more specific exploration targets within regionally anomalous areas can be delineated geochemically;

b. to develop geochemical methods of assessing the uranium potential of fluvial sediments capped by Plateau Basalts;

c. to study the dispersion characteristics of uranium in the vicinity of known 'basal type' mineralization in the context of other types of anomalies that might occur in the Okanagan Valley and Highlands region of British Columbia.

The Lassie Lake area forms part of NTS map area 82E 10 and is about 50 km southeast of Kelowna and 50 km east of Penticton, British Columbia. The small settlement of Beaverdell is located 18 km to the southwest.

The area is within the Okanagan Highlands, a region of moderate relief consisting of plateau areas (e.g. Lassie Lake area) separated by incised river and creek valleys. The average elevation of the Lassie Lake plateau is approximately 1200 m with local topographic highs reaching 1400 m.

Drainage is generally restricted due mainly to the flat tableland aspect of the area. Kettle River to the east and Trapping and Copperkettle creeks to the north act as major drainage cutoffs.

Bedrock, although exposed in places on local topographic highs and along some stream beds, is generally mantled by a thick cover of glacial overburden (up to 20 m).

Geology

The Lassie Lake area is enclosed within a large intrusive body of quartz monzonite mapped by Little (1957, 1961) as part of the Valhalla Intrusions. Beginning in 1968,

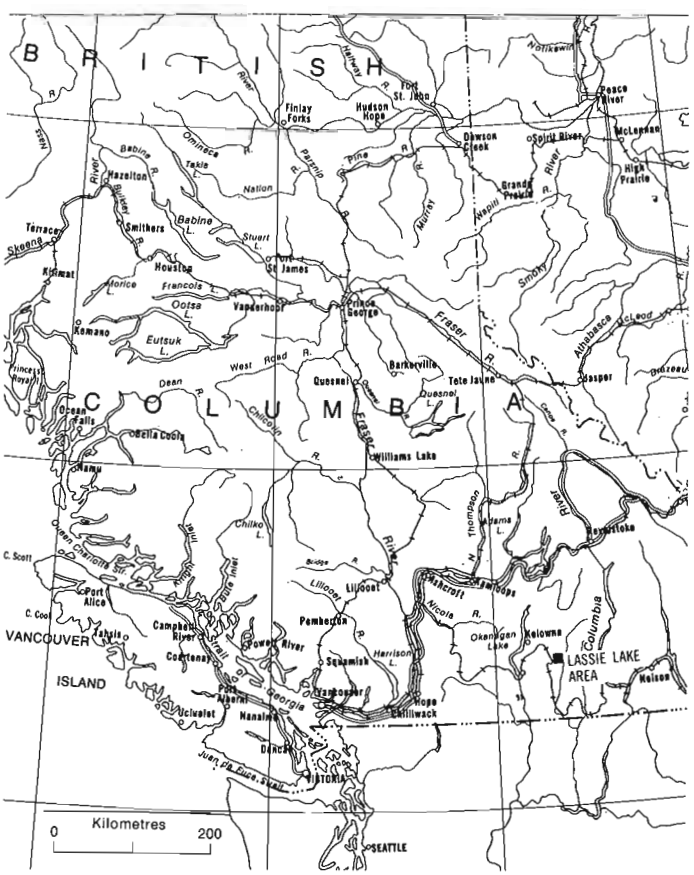


Figure 52.1. *Location of Lassie Lake area.*

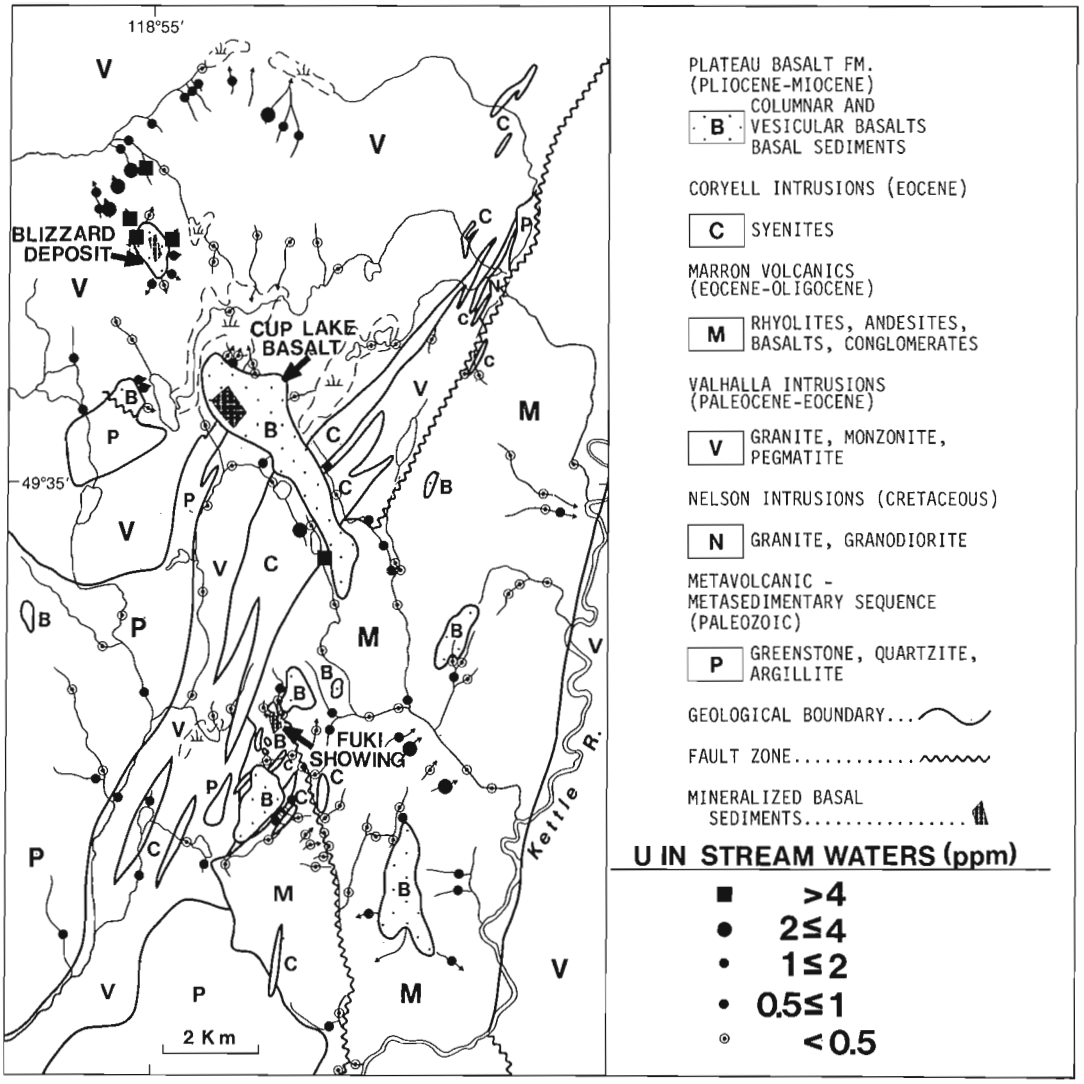


Figure 52.2. *Uranium in stream and spring waters.*

exploration and geological mapping by company geologists of the Power Reactor and Nuclear Fuel Development Corporation, Norcen Energy Resources Ltd. and Noranda Exploration Ltd. has resulted in a clearer understanding of the geology of the area. The generalized geology of the study area, summarized from company reports, is presented in Figures 52.2 and 52.3. Numerous ground checks by the author have confirmed the geology as presented to be reasonably accurate. A more comprehensive geological map of the area at a 1:50 000 scale is also available (Christopher, 1978).

The oldest rocks within the area are Paleozoic greenstones, quartzites and argillites forming three main roof pendants on the intrusive basement complex in the southwestern corner of the area. These pendant rocks have a very low radiometric total count (av = 10 ur, using McPhar TVIA instrumentation)[1] and are volumetrically small compared to the basement and Tertiary volcanic-sedimentary rocks.

The basement complex comprises rocks of the Nelson, Valhalla and Coryell intrusions.

The Nelson rocks consist of large blocks of granodiorite and diorite that have been rafted into the Valhalla complex. They have the lowest average radiometric total count of the intrusive rocks (13 ur).

The Valhalla rocks are volumetrically the most significant and consist of medium grained quartz monzonite and granite containing variable amounts of plagioclase, orthoclase, smoky quartz, muscovite, biotite and hornblende. Some phases are porphyritic containing large feldspar phenocrysts. In many places the main mass of the Valhalla complex contains segregations and dykes of very coarse grained leucocratic pegmatites basically having the same mineralogical composition as the Valhalla intrusive mass. These grade imperceptibly into the finer grained monzonite and granite phases. Distinct chill zones are observed only where the pegmatites intrude the Nelson granodiorite. Based on field relationships and age dating of the Valhalla elsewhere these rocks are most probably upper Cretaceous to Paleocene in age (pers. comm., P.A. Christopher, British Columbia Department of Mines and Petroleum Resources). The average total radiometric count for the monzonitic rocks is approximately 27 ur (35 readings); the pegmatites may range up to 40 or 45 ur.

In the eastern portion of the area the Valhalla basement rocks are mantled by Eocene-Oligocene volcanic-sedimentary rocks. These consist of rhyolites, rhyodacites, andesites, andesite tuff breccias, minor basalts and tuffaceous sediments. Radiometric total counts for this volcanic-sedimentary succession may vary from 13 to 27 ur.

[1] In accordance with the recommendations of IAEA Technical Report No. 174, measurements of total radioactivity are reported in terms of "units of radioelement concentration", abbreviated 'ur'.

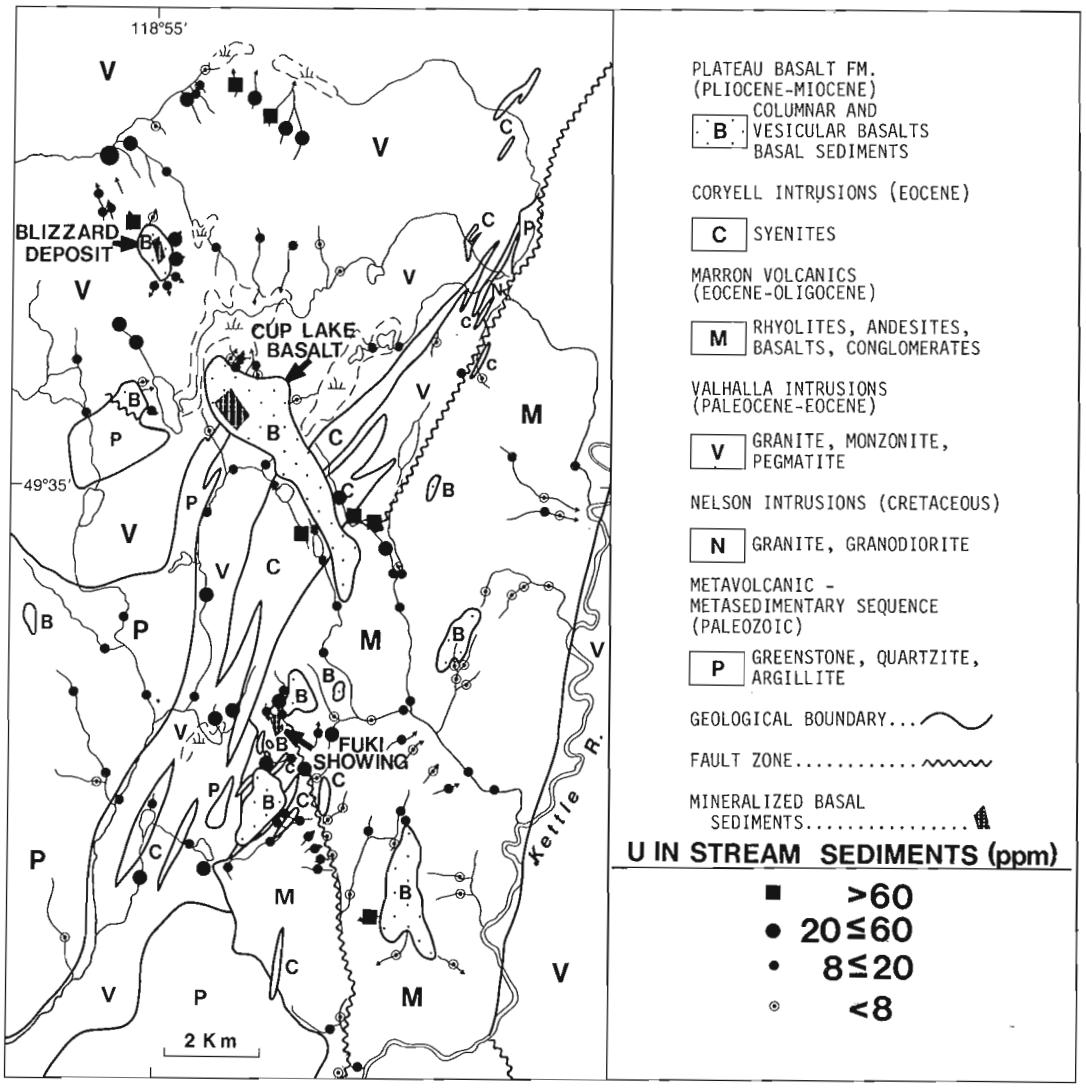


Figure 52.3. *Uranium in stream and spring sediments.*

The Eocene Coryell syenites, comprising both masses and dykes, are intrusive into all rock units except the Plateau Basalts and the Miocene sediments. The main mass centred around Cup Lake, consists of a slightly weathered pink to grey medium grained syenite. Elsewhere, numerous dyke equivalents of the Coryell are present in the intrusive and Tertiary volcanic rocks. These rocks, which may often have a trachytic composition and texture, consist mainly of aphanitic pink syenite porphyry and grey quartz feldspar porphyry. Their predominant trend is northeast, as is that of the main syenitic mass; dykes trending northwest and north are also present. With the exception of the mineralized Miocene sediments, the Coryell has the highest total radiometric count of all the rock units of the Lassie Lake area occasionally reaching 60 ur (av = 33 ur, 18 readings).

In this area the Miocene was a period of erosion during which Tertiary valleys were filled with clastic sediments. This was followed in the late Miocene or early Pliocene by eruption of alkali olivine-bearing basalts which filled the valleys and probably covered many of the upland areas. The 'capped' fluvial sediments afford excellent traps for uranium entering via groundwaters; because the Lassie Lake area contains a number of preserved 'basaltic caps', these have formed the foci of exploration activity throughout the Okanagan region.

The Plateau Basalt formation is flat lying and consists of vesicular and columnar olivine basalt flows with occasional interformational sediments. It has an average thickness of the order of 70 m and has been dated as Pliocene (4.7 ± 0.2 and 5.0 ± 0.5 Ma whole rock K-Ar ages; Christopher, 1978). The isolated basalt cappings in the Lassie Lake area generally form distinct topographic expressions as do most of the cappings in the Okanagan region. The basaltic outliers have either northwest or northeast orientations.

The Miocene sediments underlying the Plateau Basalts are composed of unconsolidated fluvial sandstones and conglomerates with intercalated mudstones. Cobbles within the conglomerates are predominantly granitic in composition and carbonaceous trash is abundant in all of the sedimentary beds. Channel structures (paleostream beds) occur at various horizons in the basal sediments.

Mineralization

Three occurrences of uranium mineralization in basal Miocene sediments have been found in the Lassie Lake area (see Fig. 52.2 and 52.3). A small showing (Fuki showing), which initially attracted mining companies to the area, is located in the south central portion of the area near the source of Dear Creek (Doi, 1969; Kikuchi and Kikuchi, 1970;

Table 52.1

General statistics (log_{10} transform) for elements in stream and spring waters, Lassie Lake area (all values in ppm except where noted)

	U (ppb)	F (ppb)	Cl	Na	K	Ca	Mg	HCO_3	SO_4	COND (μmhos)	pH
Minimum	0.07	96	0.5	0.3	0.2	1.9	0.5	7.5	2.0	20.8	6.0
Maximum	74.0	1000	57.0	50.0	60.1	38.0	29.4	539.0	71.9	781.0	8.5
Mean	0.49	236	0.6	2.8	0.9	7.7	2.5	44.8	3.3	83.2	7.4
Mean + One St. Dev.	1.24	359	1.0	5.9	1.7	15.8	5.7	99.1	7.7	167.5	7.9
No. Cases	149	149	149	149	149	149	149	149	149	149	149

Table 52.2

General statistics (log_{10} transform) for elements in stream and spring sediments, Lassie Lake area (all values in ppm except where noted)

	U	Zn	Cu	Pb	Ni	Co	Ag	Mn	Fe(%)	Mo	LOI(%)
Minimum	0.8	6	1	2	1	1	0.1	33	0.2	0.3	1.2
Maximum	178	296	77	36	212	105	1.4	17,313	44.1	21.0	78.4
Mean	12	39	15	10	11	6	0.2	582	2.0	1.6	11.4
Mean + One St. Dev.	27	71	35	18	31	12	0.4	1,580	3.6	4.1	24.9
No Cases	142	137	137	137	137	137	137	137	137	137	141

and Kikuchi, 1971). High total radioactivity is observed at this exposure (greater than 65 ur) but no recognizable uranium minerals are present; rather the uranium occurs as intergranular coatings on grains and cobbles in the conglomerate and in small carbonaceous silty lenses. A bulk channel sample of this showing assayed 527 and 1670 ppm U for minus 6 and minus 80 mesh material respectively.

Drilling on the northern part of the Cup Lake basalt by the Power Reactor and Nuclear Fuel Development Corporation (Japan) has outlined a paleochannel of high radioactivity. Estimated assays from down hole logging (7 holes) range from 0.02 to 0.3% U_3O_8 (Okuno, 1972). The radiometric anomalies, which occur over strata some 3 m thick, are present in the basal part of the fluvial sediments.

The discovery of concealed mineralization under the basalt capping north of Lassie Lake (Blizzard property) prompted an intensive drilling program which is presently being carried out by Norcen Energy Resources (optioned from Lacana Mining Corp.). Uranium mineralization in the form of autunite, saleeite and unidentified radioactive minerals associated with carbonaceous material occurs in a basal channel structure composed of unconsolidated sandstones with intercalated mudstones (pers. comm., T. Turner; Norcen Energy Resources). Intersections containing up to 140 lb/ton U_3O_8 have been reported (Northern Miner, 1978). The basalt covering this deposit is mantled with glacial till and does not outcrop.

Similar uranium mineralization in Miocene sediments also occurs in the Hydraulic Lake area, 30 km northwest of the present study area (B.C. Department of Mines and Petroleum Resources, Assessment Reports 4629, 5090, 5115, 5570, 5582, 6611, 6116, 6217 and 6243). The basic difference between the two mineralized areas is really one of mineralogy; uranium in the Hydraulic Lake area being associated mainly with authigenic iron sulphides in the form of marcasite whereas no sulphides of great significance have been recognized in the Lassie Lake occurrences.

Sampling Techniques

All major streams and their tributaries were sampled; the sampling distribution being outlined in Figures 52.2 and 52.3. Unacidified water samples were collected in 250 ml polypropylene bottles and stream sediments were dried and sieved to pass minus 80 mesh.

Pliocene uplift and glacial erosion have taken the basaltic outliers and their underlying Miocene sediments out of the hydrologic regime under which uranium mineralization would have formed and these deposits can therefore be classed as 'wasting deposits', although some are still well preserved under the basalts (e.g. Blizzard deposit, Fig. 52.2 and 52.3). An examination of the present hydrological regime showed that the basalt cappings, because of their topographic relief, store meteoric waters which eventually move downward and laterally outward, emerging at their base of slope. It was felt, therefore, that base of slope drainage sampling could be an effective way of differentiating productive from unproductive cappings. With this in mind detailed traverses, sampling all springs and seeps were carried out around known basalt formations.

Table 52.3

Pearson Correlation Coefficients (log_{10} transform) for Lassie Lake data (149 samples)

		SEDIMENTS											WATERS										
		U	Zn	Cu	Pb	Ni	Co	Ag	Mn	Fe	Mo	L.O.I.	U	F	pH	Na	K	Cl	COND	HCO_3	SO_4	Ca	Mg
SEDIMENTS	U	1.00																					
	Zn	.10	1.00																				
	Cu	.17	.59	1.00																			
	Pb	.28	.62	.63	1.00																		
	Ni	.02	.54	.79	.47	1.00																	
	Co	-.06	.62	.41	.48	.64	1.00																
	Ag	.21	.51	.70	.44	.44	.12	1.00															
	Mn	.17	.47	.15	.43	.21	.68	.07	1.00														
	Fe	-.02	.58	.39	.47	.45	.72	.24	.56	1.00													
	Mo	.27	.18	-.02	.30	-.11	.18	.02	.40	.26	1.00												
	L.O.I.	.37	.30	.54	.66	.32	.22	.37	.26	.22	.29	1.00											
WATERS	U	.44	-.12	.00	-.03	.04	-.12	-.05	-.13	-.07	-.04	.08	1.00										
	F	.06	.04	-.11	-.03	-.14	-.04	.02	.03	.13	.27	.04	-.03	1.00									
	pH	-.25	.22	.48	.01	.50	.11	.41	-.11	.20	-.34	-.02	.00	-.05	1.00								
	Na	-.14	-.06	.11	.08	.25	.17	-.06	-.03	.18	-.03	.16	.19	.02	.26	1.00							
	K	-.12	.03	.23	.10	.28	.13	.06	-.07	.11	-.10	.14	.09	-.03	.36	.47	1.00						
	Cl	.05	-.09	.02	.16	-.06	-.03	-.04	-.03	.07	.20	.25	.06	.17	-.04	.47	.61	1.00					
	COND	-.38	.20	.46	.07	.50	.19	.35	-.08	.25	-.26	.09	-.08	.07	.81	.42	.55	.25	1.00				
	HCO_3	-.35	.18	.47	.06	.51	.20	.33	-.07	.28	-.28	.11	-.11	.03	.84	.41	.51	.18	.95	1.00			
	SO_4	-.19	-.13	-.13	-.11	.10	-.03	-.08	.02	-.04	.03	.01	.11	-.12	.00	.25	-.02	.05	.05	.05	1.00		
	Ca	-.40	.27	.53	.09	.52	.20	.42	-.04	.24	-.29	.05	-.20	.05	.82	.21	.36	.06	.91	.91	.00	1.00	
	Mg	-.40	.07	.38	-.03	.51	.20	.23	-.10	.24	-.34	.05	-.02	-.04	.79	.48	.45	.11	.90	.93	.15	.82	1.00
		U	Zn	Cu	Pb	Ni	Co	Ag	Mn	Fe	Mo	L.O.I.	U	F	pH	Na	K	Cl	COND	HCO_3	SO_4	Ca	Mg
		SEDIMENTS											WATERS										

Table 52.4

Uranium and base metal content of matrix material (-80 mesh) from Miocene basal sediments, Okanagan region (all values are in ppm except Fe which is in wt %)

Location	U	Zn	Cu	Pb	Ni	Co	Ag	Mn	Fe	Mo	V	Remarks
Fuki Donen Showing, Lassie Lake	1670.0	72	21	17	21	24	0.2	122	1.30	6	97	mineralized channel deposit
Hydraulic Lake DDH-NT46												
40.27 - 41.27 m	252.0	64	11	7	3	4	0.2	48	2.09	17	13	mineralized channel
41.27 - 42.27 m	366.0	10	6	16	1	1	0.2	48	4.44	29	6	deposit, marcasite
42.27 - 43.27 m	531.0	24	6	15	1	1	0.4	40	17.82	239	2	present
43.27 - 44.27 m	412.0	16	5	11	1	1	0.2	31	9.51	249	3	
44.27 - 45.27 m	135.0	9	4	10	1	1	0.2	26	1.10	1	2	
45.27 - 46.27 m	159.0	5	4	7	1	1	0.2	26	0.64	1	5	
46.27 - 47.27 m	292.0	7	4	8	1	1	0.2	34	1.34	5	5	
47.27 - 48.27 m	1250.0	48	13	23	22	30	0.2	132	1.36	67	20	
48.27 - 49.27 m	1610.0	31	5	21	1	1	0.4	48	24.64	97	3	
West Kettle River (Venus Claims)												
oxidized layer	23.5	88	33	12	115	53	0.2	2040	11.63	2	152	slightly mineralized
unoxidized layer	56.5	140	48	18	85	40	0.2	856	5.13	1	196	sediments
silty layer	32.5	101	27	7	63	33	0.2	273	2.50	3	92	
Myra Station, Southwest of Kelowna	5.0	50	11	11	8	6	0.2	186	2.28	1	56	unmineralized
	4.9	61	11	7	9	4	0.2	371	2.34	1	77	channel deposits
	2.9	37	7	7	6	6	0.2	287	0.15	1	39	
Southwest of Lumby	7.2	310	86	7	131	37	0.2	6240	18.22	3	452	unmineralized
	7.8	101	58	6	34	20	0.4	1392	5.13	5	112	sediments
	11.0	180	105	15	115	50	0.7	2520	11.63	6	235	
	2.2	170	22	6	23	37	0.2	3950	8.50	1	116	
	1.0	75	22	1	20	48	0.2	5480	7.23	1	110	
West of Winfield												
unoxidized material	2.5	11	5	8	2	1	0.2	90	0.52	3	16	unmineralized
oxidized material	6.6	210	42	11	213	44	0.2	736	7.37	1	46	sediments

NOTE: Cd and Bi concentrations are less than 0.2 ppm for all samples

Analytical Techniques

Unacidified water samples were analyzed for U, F, Cl, Na, K, Ca, Mg, $SO_4^{=}$, HCO_3^{-}, pH and conductivity. The following analytical techniques were employed:-

U – Standard fluorometric method as described by Smith and Lynch (1969).

F – Orion specific ion electrode after buffering 1:1 with total ionic strength adjustment buffer (TISAB).

Cl – Standard colorimetric method using thiocyanate; read at 460 nm.

Na,K, Ca,Mg – direct aspiration into atomic absorption spectrometry system.

$SO_4^{=}$ – colorimetric method using 2-aminopyrimidine, read at 305 nm.

HCO_3^{-} – standard titrimetric method using weak H_2SO_4.

pH – pH meter and standard buffers.

Conductivity – Y.S.I. conductivity bridge (Yellow Springs Instruments).

Stream and spring sediments (-80 mesh) were analyzed for U, Cu, Pb, Zn, Fe, Mn, Ag, Co, Ni, Mo and loss-on-ignition (L.O.I.). Uranium was determined by delayed neutron activation analysis at Atomic Energy of Canada Laboratories using methods described by Boulanger et al. (1975). For the determination of the base metals a 1 gm sample was digested in 6 ml of a 4:1 mixture of HNO_3 and HCl. The samples were diluted to 20 ml and the elements determined using a standard atomic absorption technique with the required background corrections. Loss-on-ignition (L.O.I.), expressed as a percentage, is equal to the weight differential between a 1 gm sample dried for 2 hours at 120°C and the same sample ignited for 4 hours at 450°C. The organic content of the sample is considered to be directly proportional to the percentage loss on ignition (Coker and Nichol, 1975).

Results and Discussion

General statistics ($\log_{10}$ transformed data) for all of the elements in waters and sediments are presented in Tables 52.1 and 52.2. The mean uranium contents of waters and sediments in the study area are 0.49 ppb and 12 ppm respectively (149 samples). These results may be compared to the regional means of 0.29 ppb and 6.8 ppm respectively for NTS map area 82E (1546 samples). Based subjectively on the means and standard deviations, class intervals for uranium in waters and sediments (Fig. 52.2 and 52.3) have been chosen to best represent the anomalous groupings within the data. For waters and sediments the uranium content varies from 0.07 to 74 ppb and 0.8 to 178 ppm respectively. Distribution symbol plots for uranium are presented in Figures 52.2 and 52.3.

Pearson correlation coefficients for the data set are given in Table 52.3. Uranium in sediments shows no significant correlation with any of the base metals, Zn, Cu, Pb, Ni, Co, Ag, Mn, Fe and Mo. The uranium and base metal contents of some of the mineralized and unmineralized Miocene basal sediments in the Okanagan region are presented in Table 52.4. Base metals are often associated with certain U deposits (e.g. hydrothermal, skarn, sandstone types); for the Okanagan region, however, only Mo exhibits enrichment in the mineralized sediments, and this may only be indicative of the Hydraulic Lake occurrence. In fact the base metals, excepting Mo, would appear to be depleted in these deposits. It is evident both from the poor correlations in Table 52.3 and the analyses in Table 52.4 that, with the exception of perhaps Mo, base metals would be of very little value as pathfinders in drainage surveys directed at locating this type of deposit.

The correlation between U and F in waters is very poor and the distribution of F (not shown) bears little relation to the presence of uranium mineralization. These two elements, which are often associated in the primary environment, do

not appear to be concentrated together in the 'basal type' U deposits of the Okanagan. Fluorine is therefore not a good pathfinder for this type of mineralization.

Uranium in sediments shows a weak positive correlation with loss-on-ignition (r=0.37) and weak negative correlations with pH, conductivity and HCO_3^- in waters, suggesting that organic content and water chemistry have an effect on the concentration of uranium in sediments. The correlation between U in waters and their associated sediments is not strong (r=0.44) but when compared with the correlation coefficient for the regional data (r=0.03 for 82E, 1546 samples), the implication that secondary factors have less effect on the dispersion of U in the Lassie Lake area than the Okanagan area as a whole, seems valid. This is borne out by the poor correlation between U in waters and other water measured parameters (see Table 52.3) and by the much lower HCO_3^- and conductivity levels observed in this area compared with other areas in 82E. Lithology, structure and hydrology would seem to have more control on the dispersion of U and the patterns observed.

With few exceptions, the anomalous patterns for U in sediments and waters are reasonably coincident. The following anomalous areas merit further discussion:

a. the area around the basalt outlier north of Lassie Lake (Blizzard property, see Northern Miner, May 11, 1978).

b. the area northeast of the Blizzard property.

c. the anomaly around the southern part of the Cup Lake basalt.

d. the anomaly on the west side of the most southerly capping.

e. the area around the original Fuki showing at the top of Dear Creek.

The strongest anomalies in the area occur in springs and seeps emerging from the base of the Blizzard capping. Presently this property has the greatest potential for mineable reserves. The waters and sediments draining it range from 0.2 to 18.0 ppb and 4.5 to 178.0 ppm U respectively. Strong anomalies in waters and sediments are also observed just to the northwest of the capping. Drilling by Norcen Energy Resources indicates that the mineralized northwest trending channel structure is open in this direction and the anomalies may be related to the emergence at a steeper base of slope of more deep seated waters draining the basal sediments. They may also be associated with fissure controlled waters draining the Valhalla complex. This is almost certainly the case for the springs emerging at the base of the slope of the Valhalla, northeast of the Blizzard property. This type of false anomaly (fissure controlled) can sometimes be detected by more comprehensive water analysis (e.g. F, conductivity, $SO_4^=$), especially for larger fault zones, but geological reasoning encompassing structure, nature of bedrock and groundwater hydrology will also be key factors in their detection.

Strong anomalies occur on either side of the southern portion of the Cup Lake basalt. Waters and sediments range from 0.48 to 74.0 ppb and 16.3 to 118.0 ppm U respectively. One spring, located on the southeastern side, has a distinctly different water chemistry from other waters in the Lassie Lake area. It has much higher concentrations of Na and K and twenty times as much $SO_4^=$. It is not known whether this unique chemistry can be related to drainage of uraniferous basal sediments since no concentrations of sulphides similar to the Hydraulic Lake area, have as yet been reported for the Lassie Lake occurrences. The anomaly around the southern part of this capping may be attributed to one or a combination of two factors — 1) leaching of high background intrusive rocks (Coryell syenites) or 2) seepage from uraniferous basal sediments. The Coryell syenites have a higher uranium content than other rocks in this area, ranging from 3.7 to 14 ppm U and averaging about 6.7 ppm U (9 samples). This compares well with the regional mean for Coryell syenites of 6.2 (76 samples) for the Okanagan region. Streams and springs draining the Coryell in other parts of the Lassie Lake area and NTS map area 82E do not exhibit values as high as those at Cup Lake; the regional means and one standard deviation levels for waters and sediments draining the Coryell (147 sites) are 0.22 and 0.73 ppb and 11.2 and 25.4 ppm U respectively, well below the levels observed at Cup Lake. In addition, lake sediments from Cup Lake which may be considered to represent a composite of the drainage over the Coryell have uranium contents similar to other lakes in the area (Ballantyne, 1976). The fissure controlled waters and related sediments northeast of the Blizzard property, some of which appear to be related to Coryell syenites and pegmatite dyke swarms, exhibit anomalies similar to the aforementioned area and the possibility of this type of anomaly occurring cannot be ruled out. The stream sediments on the east side of the capping show a gradual increase in uranium content downstream, the element probably being added from seepage on the west side of the stream. The portion of the basalt south of Cup Lake, represented by this anomaly, has not been drilled as yet and the possibility of locating more mineralization, on the basis of the geochemistry, is therefore significant.

An area of high radioactivity in basal sediments under the northwest part of the Cup Lake basalt was outlined by drilling and down hole radiometric probing (Inazami and Yokoyama, 1973). Assays estimated from the logs range from 0.02% to 0.70% U_3O_8. Drainage around this part of the basalt is limited and the area was not delineated by geochemistry.

A single water-sediment anomaly occurs in a spring on the western flank of the most southerly basalt cap. Although loss-on-ignition is 60% for the sediment both the waters and the sediment are anomalous and drainage could therefore be coming from a small pocket of uranium-bearing sediments under the basalt. Elsewhere springs draining this basalt are not anomalous. Three drillholes on the northern half of this basalt displayed only background radioactivity (Kikuchi and Kikuchi, 1970).

Around the original Fuki showing there is a good grouping of sediment anomalies but the waters generally have low uranium concentrations indicating the need to sample the two compatible media.

Good seepage occurs at the base of the basalt situated on the west side of Lassie Lake. No anomalies were found here and down hole logging of two drillholes indicated no significant radioactivity in the basal sediments (Inazumi, 1976).

Conclusions

To date, a number of outliers of Plateau Basalt have been discovered in the Okanagan region of British Columbia. These have been found either as outcroppings or, in drift covered areas, by boulder tracing or speculative drilling of topographic expressions. Uranium mineralization in fluvial sediments underlying these basalts has been discovered in two principle areas of the Okanagan (Lassie Lake and Hydraulic Lake). Because of the channel like nature of the mineralization a final assessment of the uranium potential of basalt formations by low density drilling alone is tenuous. For this reason it is important to have some indication of the type and magnitude of geochemical dispersion around 'fertile' cappings. In the Lassie Lake area strong uranium anomalies occur around known mineralization underlying basalts (e.g. Blizzard property) whereas basalt formations known from drilling to

have no associated uranium mineralization display little or no anomalous expression. In some cases anomalies occur around untested portions of basalts capping radioactive sediments.

In the study area uranium in stream sediments displays no significant correlation with the base metals Cu, Pb, Zn, Fe, Mn, Ag, Co, Ni and Mo and its dispersion in waters and concentration in sediments is only weakly affected by water chemistry (e.g. pH, conductivity, HCO_3^-, $SO_4^=$) and sediment composition (L.O.I.). Interpretation of anomalies is, however, confused by such factors as high uranium values in waters and sediments associated with faults and small fracture zones or draining anomalous lithologies (e.g. alkaline intrusive and volcanic rocks). Although more detailed geochemical analysis can be helpful in these cases (e.g. F, conductivity, HCO_3^- content of waters and L.O.I. for sediments) sound geological interpretation will also be required to eliminate certain spurious anomalies.

The most effective means of geochemical exploration for this type of deposit should involve detailed sampling of drainage systems issuing at the base-of-slope of known or suspected basalt formations. For the Lassie Lake area both waters and sediments generate anomalies with high contrast. The length of the anomalous dispersion will naturally depend on the type of physiographic terrain being surveyed. For example in areas of moderate relief (e.g. Lassie Lake plateau) dispersion trains are short whereas in more openly drained areas they may be expected to be somewhat longer. Water chemistry and sediment composition also control the length of anomalous dispersion in certain cases. These factors tend to dictate the degree of detailed sampling required for successful discovery.

Acknowledgments

Technical assistance during the 1977 field season was provided by J. Greenough and B. Mepham. The author would like to thank D. Ellwood and B. Feader for supervision of the computor and statistical handling of the data. Analytical work was performed in the Geochemical Section Laboratories of the Geological Survey of Canada by A. MacLaurin and G. Gauthier under the supervision of G.E.M. Hall.

References

Ballantyne, S.B.
1976: Geochemical orientation surveys for uranium in southern British Columbia; Geological Survey of Canada, Open File 341.

Boulanger, A., Evans, D.J.R., and Raby, B.F.
1975: Uranium Analysis by Neutron Activation Delayed Neutron counting; Proceedings of the 7th Annual Symposium of the Canadian Mineral Analysts, Thunder Bay, Ont., Sept. 22-23, 1975.

Christopher, P.A.
1978: East Okanagan uranium area (Kelowna to Beaverdell) south-central British Columbia; British Columbia Department of Mines and Petroleum Resources Preliminary Map 29.

Coker, W.B. and Nichol, I.
1975: The relation of lake sediment geochemistry to mineralization in the northwest Ontario region of the Canadian Shield; Economic Geology, v. 70(1), p. 202-218.

Doi, K.
1969: Geological, geophysical and diamond drilling on the Fuki and Donen groups, Donen Reactor and Nuclear Fuel Development Corporation; British Columbia Department of Mines and Petroleum Resources, Assessment Report no. 2013.

Geological Survey of Canada
1976: Regional stream sediment and water geochemical reconnaissance data, southeastern British Columbia; Geological Survey of Canada Open Files 409, 410, 411.

Inazumi, S. and Yukoyama, A.
1973: Diamond drilling report on Donen mineral claims; British Columbia Department of Mines and Petroleum Resources Assessment Report no. 4630.

Inazumi, S.
1976: Diamond drilling report on PB and Donen mineral claims; British Columbia Department of Mines and Petroleum Resources Assessment Report no. 5982.

Kikuchi, K. and Kikuchi, T.
1970: Geological, Radiometric and Diamond Drilling Report on Fuki and Donen Mineral Claims; British Columbia Department of Mines Assessment Report no. 2484.

Kikuchi, K.
1971: Diamond Drilling and Bulldozer Trenching Report on Fuki and Donen Mineral Claims; British Columbia Department of Mines Assessment Report no. 3135.

Little, H.W.
1957: Geology of the Kettle River (East Half) Area, British Columbia; Geological Survey of Canada Map 6-1957.

1961: Geology of the Kettle River (West Half) area, British Columbia; Geological Survey of Canada, Map 15-1961.

Northern Miner
1978: Norcen Moving Extra Two Drill on Uranium Property, May 11, 1978.

Okuno, T.
1972: Diamond Drilling Report on Donen Mineral Claims; British Columbia Department of Mines Assessment Report no. 3775.

Smith, A.Y. and Lynch, J.J.
1969: Field and laboratory methods used by the Geological Survey of Canada in geochemical surveys: No. 11 Uranium in Soil, Stream Sediment and Water; Geological Survey of Canada, Paper 69-40, 9 p.

53. THE TRANQUILLE BEDS OF THE KAMLOOPS GROUP: A TERTIARY (MIDDLE EOCENE) COAL-BEARING SEQUENCE IN THE VICINITY OF KAMLOOPS LAKE, BRITISH COLUMBIA

Projects 760056 and 770047

Peter S.W. Graham and Darrel G.F. Long
Institute of Sedimentary and Petroleum Geology, Calgary

Graham, P.S.W. and Long, D.G.F., The Tranquille beds of the Kamloops Group: a Tertiary (middle Eocene) coal-bearing sequence in the vicinity of Kamloops Lake, British Columbia; in Current Research, Part A, Geol. Surv. Can., Paper 79-1A, p. 357-360, 1979.

Abstract

The probability that economic coal seams are present in the Tranquille beds of the Kamloops Group is considered remote. Deposition of most of the sequence in a protected lacustrine environment is indicated by the abundance of flat bedded mudrocks, presence of fresh water ferns, and absence of marine fossils. Massive sandstone and minor conglomerate in the sequence may have been deposited from mass sediment flows initiated on fan deltas at the margins of the lake. Coaly material in the sequence appears to be allochthonous. Thin seams might be expected in the subaerial parts of the fan deltas, but their locations cannot be accurately predicted using existing information.

Introduction

The Tranquille beds are one of several isolated Tertiary coal-bearing sequences in central British Columbia. The name was initially applied by Dawson (1896) to a sequence of conglomerate, sandstone, mudstone, and tuff within a predominantly volcanic sequence (Kamloops Group of Cockfield, 1948) which outcrops in structurally isolated blocks on the north and south shores of Kamloops Lake (Fig. 53.1) in map area 92I/9, 10, 15. The geological setting of the Tranquille beds has been described by Dawson (1896), Cockfield (1948), and Carr and Reed (1976). The initial purpose of this report is to discuss the coal resource potential of the Tranquille beds, based on observations of its stratigraphy, sedimentology, and structure. A supplementary study of the effects of contact metamorphism on low rank coaly material in the Tranquille beds was undertaken by Creaney (1979) who visited the area with the authors in May 1978.

Stratigraphic Age and Correlation

Sedimentary rocks assigned to the Tranquille beds are not limited to a single stratigraphic level within the Kamloops Group. North of Kamloops Lake, near Tranquille (Fig. 53.1), Dawson (1896) recorded the beds as a distinctive marker between the upper and lower volcanic sequences. Twenty kilometres west of Kamloops Lake, Hills (1965, p. 23) recorded similar tuffaceous sedimentary rocks which he interpreted, on the basis of palynology, to be at a lower level within the volcanic sequence. South of Kamloops Lake, in the vicinity of the Afton Mine, sedimentary rocks assigned to the Tranquille beds are unconformable with the orebody (Carr and Reed, 1976, p. 380). Radiometric (K-Ar) dating of volcanic rocks in the section north of Kamloops Lake (Rouse and Mathews, 1961; Hills, 1965; Hills and Baadsgaard, 1967) indicate a middle Eocene age for this section. This is supported by palynological observations by Rouse and Mathews (1961) and Hills (1965).

On a broader scale, some confusion exists in the correlation and relative ages of component units within the Kamloops Group. Rocks near Red Lake which Cockfield (1948) interpreted as Tranquille beds are now considered to postdate the Kamloops Group and have been referred to the (upper Miocene-Pliocene) Deadman River Formation (Mathews and Rouse, 1963; Campbell and Tipper, 1971). Traditionally, rocks of the economically important Coldwater beds (Group) have been interpreted as a basal part of the Kamloops Group (Dawson, 1896; Cockfield, 1948; Duffell and McTaggart, 1951) and hence older than the Tranquille beds. They occur in areas to the south (Cockfield, 1948) and west (Duffell and McTaggart, 1951; Church, 1975; Höy, 1975) of Kamloops Lake. As outcrops of the Coldwater Group are geographically separated from volcanic rocks of the Kamloops Group (except perhaps at Hat Creek; Church, 1975) the relationship of these beds to other units of Cockfield's (1948) Kamloops Group is not clear. Dawson (1896, p. 69b) suggested that an apparent absence of contemporaneous volcanic material, or derived volcaniclastic material (similar to volcanics of the Kamloops Group), along with a greater degree of deformation, supported his hypothesis that the Coldwater beds were older than volcanism in the Kamloops Group. Cockfield (1948) concurred with this interpretation, although he (p. 39) along with Duffell and McTaggart (1951) could find no positive evidence for this age assignment. In contrast Hills (1965) recorded volcanic rocks below the Coldwater Group near Princeton and Coalmont, and bentonites within the sequence at Quilchena and in coal seams at Coalmont. Church (1975) found tuff bands intercalated with coal in the Coldwater Group at Hat Greek and (p. 110) observed dacite lavas resting on top of the group in two localities, indicating that volcanic rocks of the Kamloops Group were partly coeval but mostly younger than the Coldwater Group. Hills (1965) suggested, on the basis of palynological observations, that rocks of the Coldwater Group, occurring south of Kamloops Lake, at Merritt, Nicola-Mamit and Quilchena, are younger than the Tranquille beds,

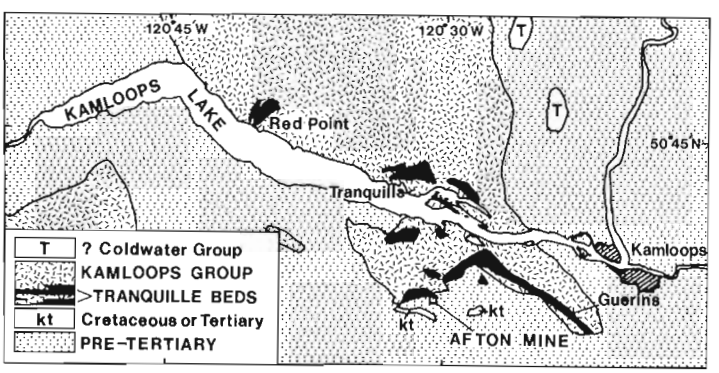
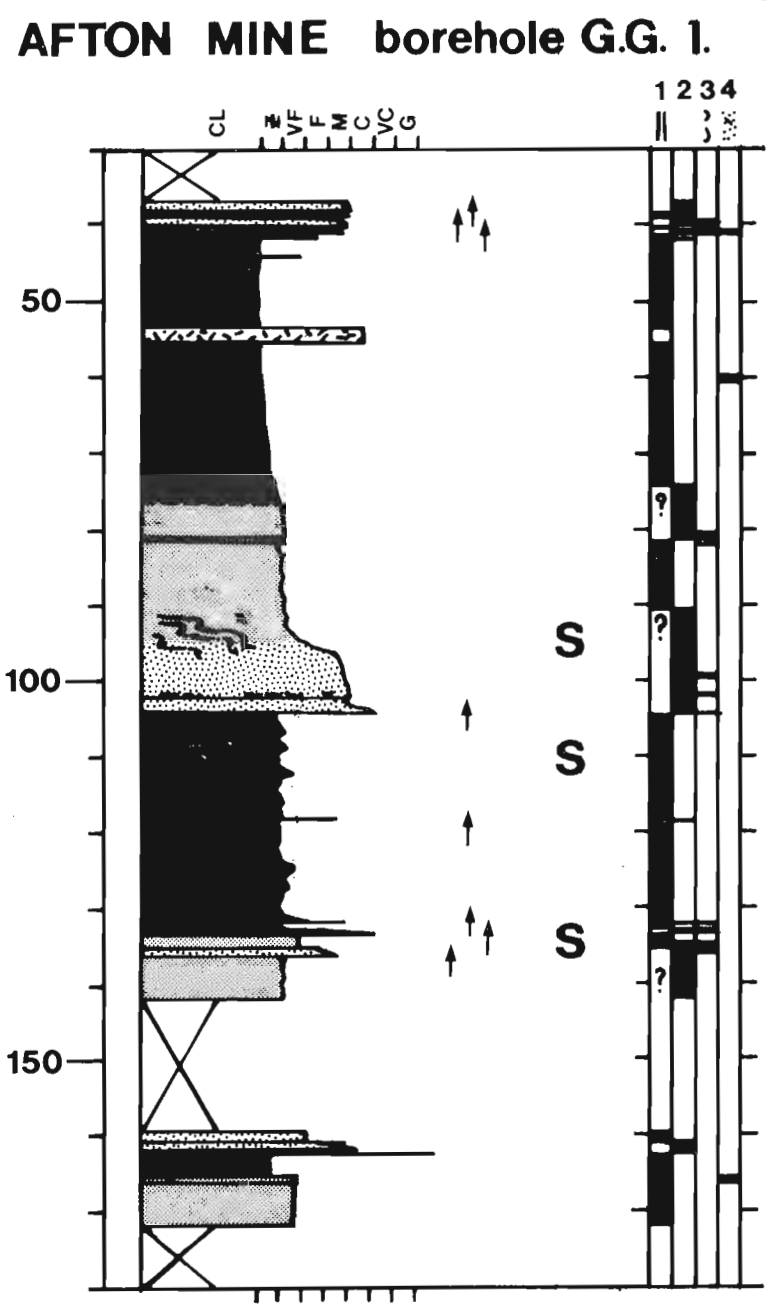


Figure 53.1. *Distribution of the Tranquille beds of the Kamloops Group, in the vicinity of Kamloops Lake and Afton Mine. Modified after Cockfield (1948) and Carr and Reed (1975).*

though are still assigned a middle Eocene age. Preliminary analysis of the palynology of Hat Creek may indicate a Late Eocene age for the coal-bearing sequence of the Coldwater Group in this area (W.S. Hopkins, pers. comm., 1978). This apparent conflict between earlier geological observations and palynological interpretations obviously necessitates further radiometric and palynological studies before the problem can be fully resolved.

Minor outcrops of conglomeratic rock near the Afton mine (unit KE and Carr and Reed, 1976, Fig. 3) may predate the Kamloops Group, and could be correlative with map unit 7 of Cockfield (1948) and map unit 21 of Duffell and McTaggart (1951). Rocks of the Chu Chua Formation, which underlie volcanic rocks in the Bonaparte Lake map area, were correlated with the Coldwater beds by Campbell and Tipper (1971). These beds may predate volcanism in the Kamloops Group, or may be equivalent to the Tranquille beds in the Kamloops area. Hills (1965) suggested that the Tranquille beds are correlative with middle Eocene rocks below the Princeton coal zone in the Allenby Formation at Princeton, and with the lower part of the succession in the Coalmont sediments near Tulameen.



Structure and Thickness of the Tranquille Beds

The Tranquille beds outcrop in structurally isolated blocks north and south of Kamloops Lake. The preserved thickness of the sequence increases rapidly to the north of the Afton Mine where drilling has indicated in excess of 500 m of section (Carr and Reed, 1976). Thickness of the sedimentary sequence north of Kamloops Lake is probably in excess of 300 m (Dawson, 1896, p. 174b). In the Kamloops Lake area, dips within the Tranquille beds have been recorded from nearly horizontal to 35°. Drilling in the proximity of the Afton Mine (Carr and Reed, 1976, Fig. 10) has revealed three principal fault sets. Two of these sets (orientation west-northwest and east-northeast) are high angle reverse faults, which have thrust the orebody onto the Eocene strata. The third set (north-northeast) has the effect of displacing Eocene strata to the south (or down) relative to the main body of Eocene rocks. The net result of this faulting has been to produce several isolated blocks which include essentially monoclinal strata. Other minor deformation can be related to early (or syndepositional) faults (resulting in slumped beds), and the diastrophic effects of volcanism both during emplacement of parts of the Kamloops Group and during emplacement of later volcanic sequences. Minor isoclinal folds are present close to faults in the Afton Mine exposures, although evidence of major folds is uncommon.

Lithology

In outcrops to the north of Kamloops Lake, the Tranquille beds consist of yellow to buff weathering tuffaceous sandstone, siltstone, and mudstone, with minor tuffs and conglomerate (Cockfield, 1948, p. 35). In outcrops within the Afton Mine (2070 ft level) and in core from boreholes located to the north of the mine, the Tranquille beds appear to be dominated by finely laminated tuffaceous siltstone and mudstone, with lesser amounts of sandstone and conglomerate (cf. Fig. 53.2). Organic material in the form of coalified plant detritus, including a few logs, is present in minor amounts throughout the sequence.

Sandstone contains abundant detritus of volcanic origin, presumably derived from underlying members of the Kamloops Group. Further volcanic material may have been derived from reworking of contemporaneous

---

Claystone (CL) and siltstone (Z) in black;
very fine sandstone (VF) in light stipple;
fine to very coarse sandstone (F, M, C, VC) heavy stipple;
G = granule cong;
S,L small and large pebble conglomerate;

Sedimentary structures:
1. *flat bedding;*
2. *no visible structures;*
3. *intraclasts, rip-up clasts;*
4. *detrital organic material*

S = slumped beds;
Arrows indicate conspicuous graded beds.

Figure 53.2. *Partial log of borehole GG1 illustrating style of sedimentary rocks in the Tranquille beds near Afton Mine. Depth below surface in metres.*



A = Rip-up clasts of mudstone (black) and volcaniclastic material (white) in very fine sandstone unit from the 81 m level of borehole GG1 (Fig. 53.2).

B = Finely laminated mudrock from the 165 m level of borehole GG1.

C = Graded laminated units of fine sandstone to claystone from the 214 m level of borehole GG6, located 750 m north of the Afton Mine.

Figure 53.3

volcanic rocks. Grain size range is from very fine to very coarse sand grade, with medium and coarse varieties most abundant. Although some very poorly sorted sandstone units were observed, most beds appeared to be moderately well to moderately poorly sorted. The bulk of the sandstone is devoid of any visible structure. Minor horizontal bedding, wavy bedding and ripple cross lamination were observed in outcrops within the mine, as was graded bedding which is more conspicuous in the core (Fig. 53.2). Rip-up clasts (Fig. 53.3A) are common in the graded beds. The lack of visible structure in many of the sandstone beds may in part be due to homogeneity of grain size, or in outcrop to local weathering conditions (cf. Hamblin, 1962) or may be a primary depositional feature. Structure may have been obliterated in some beds during slumping, perhaps associated with contemporaneous faulting.

Typically, mudstone strata are well laminated, with fine lamination (less than 1 mm) being most common (Fig. 53.3B) although some strata appear homogeneous. Colour (fresh) ranges from nearly black in the more organic rich beds to a light greenish brown in beds containing abundant volcaniclastic material (ash?). Small scale composite rhythms, resembling varves, were observed in parts of the section (Fig. 53.3C).

The general flat-bedded character of the finer grained sedimentary rocks and their lack of abundant bioturbation indicate that deposition of much of the sequence occurred in a relatively still water lacustrine environment. Massive and graded sandstone units may be the products of mass sediment flows (including grain flows and turbidity currents) which were initiated in shallower water, perhaps in response to development of fan deltas at the lake margins. A lacustrine origin is supported by the palynological observations of Hills (1965, p. 53) who considered the presence of both macro- and micro-fossils of **Azolla primeava** to indicate deposition in the quiet waters of a lake. Coaly material (including logs and detrital plant remains) appears to be allochthonous.

Igneous rocks occurring within the Tranquille beds (andesites and dacites) may include both intrusive and extrusive varieties. Due to poor exposure it is not always possible to determine the relationships of these rocks to the enclosing sedimentary rocks. However observations of vitrinite reflectance by Creaney (1979) indicate that at least some units encountered in boreholes north of the Afton Mine are of intrusive origin.

Coal Occurrences

Dawson (1896) reported "a small bed of lignite" near Red Point (Fig. 53.1) which was found during the progress of the Government Railway survey in 1878. McEvoy (in Dawson, 1896) recorded several thin coal seams from an exploration adit near Guerins (Fig. 53.1). The aggregate thickness of seven seams at this locality amounted to only 77 cm in 180 cm of section of interbedded mudstone and sandstone. Individual seams did not exceed 30 cm. Quality of coal appears to have been variable, and shale partings discontinuous. These occurrences could not be relocated during our investigations. Additional occurrences of coaly material were observed in the Afton Mine and in cores from the north of the mine. However, coal seams appear to be very rare in the sedimentary sequence. Individual seams are commonly clean, although in outcrop they appear to be thin (maximum 8 cm) and discontinuous. Coalified detritus is common in the associated sandstone and mudstone. Maceral analysis is as yet unavailable. Observations by Creaney (1979) indicate that away from intrusive bodies the coals are of sub-bituminous A rank.

Coal Potential

The probability of major coal seams occurring within the Tranquille beds both north of Afton Mine and in the vicinity of Kamloops Lake is extremely remote. A subaqueous (lacustrine) environment is postulated for much of the sequence in which coaly material is predominantly allochthonous. Coal seams may be developed in proximal (subaerial) parts of fan delta complexes at the margins of the lake in which the Tranquille beds were deposited, but the location of such potential sites cannot be predicted using existing information.

Acknowledgments

We thank L.V. Hills, S. Creaney, and J.D. Hughes for their comments on an earlier version of this paper. Afton Mines Ltd. and Canex Placer Ltd. granted permission to examine their property and drill core from the Afton property. A.J. Reed provided an illuminating discussion and tour of the Afton Mine site.

References

Campbell, R.B. and Tipper, H.W.
1971: Geology of the Bonaparte Lake map-area, British Columbia; Geological Survey of Canada, Memoir 363.

Carr, J.M. and Reed, A.J.
1976: Afton: A supergene copper deposit; Canadian Institute of Mining and Metallurgy, Special Volume 15, p. 376-387.

Church, B.N.
1975: Geology of the Hat Creek Coal Basin (92I/13E); British Columbia Minister of Mines and Petroleum Resources, Geology of British Columbia, 1975, p. G99-G118.

Cockfield, W.E.
1948: Geology and mineral deposits of Nicola map-area, British Columbia; Geological Survey of Canada, Memoir 249.

Creaney, S.
1979: Organic material in the Tranquille beds, of the (Tertiary) Kamloops Group, near Afton Mine, Kamloops, British Columbia; in Current Research, Part A, Geological Survey of Canada, Paper 79-1A, Note.

Dawson, G.M.
1896: Report on the area of the Kamloops map-sheet, British Columbia; Geological Survey of Canada, Annual Report 1894, v. VII, pt. B.

Duffell, S. and McTaggart, K.C.
1951: Ashcroft map-area, British Columbia; Geological Survey of Canada, Memoir 262.

Hamblin, Wm.K.
1962: X-ray radiography in the study of structures in homogeneous sediments; Journal of Sedimentary Petrology, v. 32, p. 201-210.

Hills, L.V.
1965: Palynology and age of early Tertiary basins, interior British Columbia; Ph.D. thesis, Department of Geology, University of Alberta, Edmonton, Alberta, Canada, 188 p.

Hills, L.V. and Baadsgaard, H.
1967: Potassium-argon dating of some Lower Tertiary strata in British Columbia; Bulletin of Canadian Petroleum Geology, v. 15, p. 138-149.

Höy, T.
1975: Geology of a Tertiary sedimentary basin northeast of Hat Creek (92I/NW); British Columbia Department of Mines and Petroleum Resources, Geological Fieldwork 1975, p. 109-115.

Mathews, W.H. and Rouse, G.E.
1963: Late Tertiary volcanic rocks and plant-bearing deposits in British Columbia; Geological Society of America Bulletin, v. 74, p. 55-60.

Rouse, G.E. and Mathews, W.H.
1961: Radioactive dating of Tertiary plant-bearing deposits; Science, v. 133, p. 1079-1080.

54.

A STUDY OF THE STABILITY OF URANIUM IN WATERS COLLECTED FROM VARIOUS GEOLOGICAL ENVIRONMENTS IN CANADA

Projects 580175 and 770076

G.E.M. Hall
Resource Geophysics and Geochemistry Division

Hall, G.E.M., A study of the stability of uranium in waters collected from various geological environments in Canada; in Current Research, Part A, Geol. Surv. Can., Paper 79-1A, p. 361-365, 1979.

Abstract

Since the inception of the Uranium Reconnaissance Program in 1975, measurement of uranium in water samples collected in support of this program has been used as an aid in the indication of possible occurrences. A thorough investigation of the stability of uranium in such waters was deemed necessary to ensure the validity of analytical data.

A project to study the stability of uranium in a variety of natural surface waters was initiated in May, 1978. Samples were collected in Ontario, northern British Columbia, the Yukon and on Melville Peninsula, District of Franklin. Twelve splits of each were made and the effect of filtration, addition of nitric acid, phosphate, carbonate and bicarbonate was examined. The methods of analysis used were conventional fluorometry and laser-induced fluorescence. A comparison of these two techniques was made. Various types of plastic bottles were also investigated.

The results show that uranium is stable in solution in all of the waters tested. Since these samples were taken from a variety of geological environments, it may be concluded that preservatives need not be added to surface waters (similar to those in this study) collected in Canada for uranium exploration purposes. The results show good correspondence between analyses for uranium by conventional fluorometry and by laser-induced fluorometry, although the latter technique is inconvenient to apply to the more organic-rich waters.

Introduction

A controversy exists amongst analytical chemists regarding the necessity of adding reagents to water samples to ensure maintenance of dissolved uranium levels. Some groups of samples, collected in surveys in support of the Uranium Reconnaissance Program, appeared to be unstable with respect to their solubilized uranium content (J.J. Lynch, pers. comm., 1977). As the analyses were not performed immediately and, indeed, were sometimes delayed several months, questions arose as to the validity of results.

The objective of this study was to examine the stability of uranium dissolved in waters collected from a variety of geological environments throughout Canada, to assess different preservation techniques and, to compare two methods of determining this element in such a medium. The various locations chosen had previously been sampled during surveys carried out in support of the Uranium Reconnaissance Program. The project commenced at the end of May, 1978 in the Thunder Bay area where seven sample sites were examined; it was continued at the end of June in northern British Columbia and the Yukon and finally extended to Melville Peninsula in August. A total of 27 lakes and streams were studied, each site producing 12 actual samples under various treatments and all 324 waters analyzed by two different techniques: conventional fluorometry and laser-induced fluorescence in the liquid state. Each untreated and filtered water was further analyzed for major, minor and trace cation components by inductively coupled plasma emission and for common anions (SO_4^{2-}, F^-, Cl^-, PO_4^{3-}, NO_3^-, HCO_3^-) by liquid ion chromatography (Smee et al., 1978). Conductivity and pH measurements were carried out in the field laboratory.

Sample collection and treatment

Samples were collected in 500 mL Nalgene linear polyethylene bottles similar to those used in the Uranium Reconnaissance Program – these bottles were not prewashed but rinsed twice with the particular sample prior to filling. At the field laboratory the waters were subjected to the predetermined set of treatments shown in Table 54.1 within the first two hours after collection. Nitric acid was chosen as a test preservative as it is commonly used for base metals and uranium standard synthetic solutions. Carbonate and bicarbonate were included as it is well known that uranium is very stable in solution as dicarbonate and tricarbonate complexes (Hostetler and Garrells, 1962).

Phosphate was also examined as the complex $UO_2(HPO_4)_2^{2-}$ is very stable and is the predominating solubilized uranyl species between about pH 4.5 and 7.5 at a phosphate concentration greater than 0.1 $\mu g\ mL^{-1}$ (Langmuir and Applin, 1977). The stabilities of uranyl chloride and sulphate are much less than the above mentioned complexes and, therefore, these anions were not included in this project.

A synthetic uranium solution, spiked at 0.4 $ng\ mL^{-1}$, was subjected to identical treatment and analyzed throughout this 4-month period. A water control solution, made in June 1977

Table 54.1

Description of various treatments carried out on the water samples

Sample Subscript	Treatment
0	None
1	1.0 mL conc. HNO_3 (Ultrex)
2	2.5 mL conc. HNO_3 (Ultrex)
3	300 mg Na_2CO_3
4	10.0 mL 0.75 M Na_2HPO_4 solution
5	300 mg $NaHCO_3$
6	filtered (0.45μ)
7	filtered (0.45μ), 1.0 mL conc. HNO_3
8	filtered (0.45μ), 2.5 mL conc. HNO_3
9	filtered (0.45μ), 300 mg Na_2CO_3
10	filtered (0.45μ), 10.0 mL 0.75 M Na_2HPO_4 solution
11	filtered (0.45μ), 300 mg $NaHCO_3$

Table 54.2

Mean uranium values obtained by conventional fluorometry over four-month period and brief sample description

	Sample	Notes		U/ng mL^{-1}	Number of Determinations	pH	Conductivity $\mu mhos\ cm^{-1}$	HCO_3^- $\mu g\ mL^{-1}$	Ca/ $\mu g\ mL^{-1}$
		Solution	Precipitate						
Thunder Bay	A_0	faint yellow	yellow	0.24 ± 0.08	12	7.5	34	17	4.74
"	B_0	faint yellow	yellow	0.14 ± 0.06	12	6.9	28	10	3.74
"	C_0	faint yellow	yellow	0.50 ± 0.08	12	8.3	189	141	31.5
"	D_0	colourless	slight	0.52 ± 0.08	12	8.1	168	139	30.9
"	E_0	faint yellow, 90 $\mu g\ mL^{-1}$ SO_4	brown	1.76 ± 0.16	12	8.0	459	94	67.0
"	F_0	faint yellow, 38 $\mu g\ mL^{-1}$ SO_4	little vis.	0.44 ± 0.10	12	8.1	275	119	45.7
"	G_0	faint yellow, 34 $\mu g\ mL^{-1}$ SO_4	brown	0.74 ± 0.12	12	8.3	306	306	62.4
B.C.	M_0	faint yellow	brown	2.20 ± 0.18	10	7.6	167	103	18.3
"	N_0	faint yellow	yellow	10.82 ± 1.32	10	7.8	220	154	29.4
"	$\emptyset_0$	colourless, 540 ng mL^{-1} F	little vis.	1.66 ± 0.18	10	7.3	33	23	5.5
"	P_0	colourless, 890 ng mL^{-1} F	little vis.	3.68 ± 0.24	10	6.8	18	11	2.5
"	R_0	colourless, 865 ng mL^{-1} F	little vis.	2.60 ± 0.15	10	6.4	16	7	2.3
Yukon	YA_0	faint yellow, 41 $\mu g\ mL^{-1}$ SO_4	dark grey	3.02 ± 0.32	10	8.3	236	92	45.2
"	YB_0	faint yellow, 31 $\mu g\ mL^{-1}$ SO_4	brown	1.24 ± 0.24	10	8.3	230	114	44.5
"	YC_0	yellow	little vis.	0.10 ± 0.05	10	8.0	119	54	21.0
"	YD_0	yellow, 100 ng mL^{-1} Fe	little vis.	0.22 ± 0.10	10	7.9	107	59	22.5
"	YE_0	yellow, 600 ng mL^{-1} Fe	thick brown	1.21 ± 0.30	10	8.0	232	59	39.9
"	YF_0	colourless	little vis.	0.82 ± 0.12	10	8.3	231	96	37.4
"	YG_0	faint yellow	light brown	1.64 ± 0.19	10	7.7	116	42	17.4
"	YH_0	colourless	little vis.	0.76 ± 0.14	10	8.0	111	45	16.6
"	YJ_0	colourless, 55 $\mu g\ mL^{-1}$ SO_4	little vis.	5.60 ± 0.41	10	8.6	395	219	52.5
"	YK_0	colourless, 98 $\mu g\ mL^{-1}$ SO_4	brown	4.64 ± 0.30	10	8.2	375	133	58.1
Melville	MPA_0	colourless	little vis.	1.72 ± 0.19	6	8.2	149	89	29.1
"	MPB_0	colourless	little vis.	0.84 ± 0.11	6	7.8	133	73	24.1
"	MPC_0	colourless	little vis.	0.70 ± 0.12	6	7.2	74	22	10.2
"	MPD_0	colourless	little vis.	0.76 ± 0.12	6	7.1	55	84	7.9
"	MPE_0	colourless	little vis.	1.46 ± 0.18	6	7.8	132	73	20.8

Table 54.3

Uranium and calcium values of samples treated with phosphate

	Sample	U/ng mL^{-1}	Ca/ug mL^{-1}
Thunder Bay	C_{10}	<0.10	17.2
"	D_{10}	<0.10	17.7
"	E_{10}	<0.10	17.3
"	F_{10}	<0.10	19.5
"	G_{10}	<0.10	12.7
B.C.	N_{10}	0.42	18.7
Yukon	YA_{10}	<0.10	25.5
"	YB_{10}	<0.10	21.4
"	YE_{10}	<0.10	23.4
"	YF_{10}	<0.10	22.5
"	YG_{10}	0.68	13.4
"	YH_{10}	0.14	13.2
"	YJ_{10}	<0.10	17.8
"	YK_{10}	<0.10	17.8
Melville	MPA_{10}	1.20	22.1

These values were obtained four weeks after collection.

and used to monitor the analysis of a variety of elements in the Geochemistry Laboratories, was included in each set of uranium determinations carried out. Blanks were also run to identify any uranium contamination introduced by the reagents added.

The stability of uranium was studied also with respect to different types of plastic bottles. One lake already included in the time study in the Thunder Bay region was used to study possible adsorption onto linear polyethylene, polypropylene and teflon bottles of various sizes.

Analytical methods

Conventional fluorometry

The method used is similar to that described by Smith and Lynch (1969), with the exception that the fusion was carried out using propane burners (3 minute melt) rather than a furnace as the latter requires too much power as a field technique. Of the two analytical methods employed, most reliance was placed on this one since its accuracy has been validated when applied to such a medium where possible interferences like iron and manganese lie well below quenching levels. The twelve splits of each sample were immediately analyzed after treatment and repeated for the following two consecutive days. Upon return to Ottawa uranium was determined in the samples weekly for three weeks and finally monthly.

Laser-induced fluorescence

This technique is also based on the fluorescent properties of UO_2^{2+} but, since a laser is used as the excitation source (at 337 nm) rather than UV lamps, the fluorescent signal can be measured in the water phase without the requirement of fusing with fluoride. Robbins (1978) designed this field-portable instrument and is currently engaged in refining the method. A 5 mL sample aliquot is placed in a quartz cell in the path of a pulsed nitrogen laser, the instrument zeroed, a complexing agent known as "Fluran" (sodium pyrophosphate/sodium monophosphate) added and the fluorescent signal of the uranyl pyrophosphate species measured on a photomultiplier. Initial "backing" is required to nullify organic fluorescence which, though short lived compared to uranyl emission, does tail off into the 500 nm region where measurement is made. Suppression can be caused by quenching of iron (80% signal at 8 µg mL^{-1}), manganese (80% signal at 1.5 µg mL^{-1}), silver and thallium but their concentration levels in most surface waters are much below interference levels (Moriyasu et al., 1977). This technique was carried out in the field at the same time as conventional fluorometry but proved to be somewhat slower in this particular study as the pH of samples treated with acid, carbonate and bicarbonate had to be adjusted to 7.0 where the uranyl pyrophosphate complex predominates.

Table 54.4

Water sample container study

LAKE G				
		2/6/78	22/9/78	4/8/78
Container	Treatment	U/ng mL^{-1}	U/ng mL^{-1}	Ca/ µg mL^{-1}
Linear Polyethylene				
1000 mL	UFUT	0.68	0.70	61.9
1000 mL	UFA	0.70	0.74	61.9
1000 mL	FUT	0.82	0.75	61.9
1000 mL	FA	0.78	0.70	62.0
Linear Polyethylene				
500 mL	UFUT	0.74	0.76	62.6
500 mL	UFA	0.74	0.78	61.9
500 mL	FUT	0.82	0.74	62.0
500 mL	FA	0.76	0.80	61.5
Linear Polyethylene				
250 mL	UFUT	0.78	0.76	40.0
250 mL	UFA	0.70	0.74	62.6
250 mL	FUT	0.72	0.69	61.1
250 mL	FA	0.76	0.75	60.8
Polypropylene				
250 mL	UFUT	0.70	0.72	37.6
250 mL	UFA	0.76	0.76	62.6
250 mL	FUT	0.72	0.74	35.5
250 mL	FA	0.69	0.79	61.1
Teflon				
250 mL	UFUT	0.79	0.80	31.4
250 mL	UFA	0.80	0.70	62.6
250 mL	FUT	0.75	0.73	28.6
250 mL	FA	0.68	0.69	60.8

UFUT – unfiltered, untreated
UFA – unfiltered, 1 mL conc. HNO_3/500 mL
FUT – filtered through 0.45µ
FA – filtered through 0.45µ, 1 mL conc. HNO_3/500 mL

Table 54.5

Comparison of uranium values obtained by the two methods employed in this study

		U/ng mL^{-1}	
	Sample	Conventional Fluorometry	Laser-induced Fluorescence
Thunder Bay	A_6	0.24	0.27
"	B_6	0.14	0.10
"	C_6	0.50	0.60
"	D_6	0.52	0.64
"	E_6	1.76	1.80
"	F_6	0.44	0.48
"	G_6	0.74	0.89
"	M_6	2.20	2.42
B.C.	N_6	10.82	11.30
"	O_6	1.66	1.74
"	P_6	3.68	3.99
"	R_6	2.60	2.42
Yukon	YA_6	3.02	3.01
"	YB_6	1.24	1.43
"	YC_6	0.10	0.10
"	YD_6	0.22	0.35
"	YE_6	1.21	1.40
"	YF_6	0.82	0.94
"	YG_6	1.64	1.70
"	YH_6	0.76	0.68
"	YJ_6	5.60	5.64
"	YK_6	4.64	4.78
Melville	MPA_6	1.72	1.60
"	MPB_6	0.84	0.98
"	MPC_6	0.70	0.61
"	MPD_6	0.76	0.71
"	MPE_6	1.46	1.54

Areas under examination

Thunder Bay region

Lakes A and B are situated in Archean felsic igneous and metamorphic rocks. Lakes C through to G are located in Proterozoic rocks (Keweenawan) of the Sibley Group consisting of various combinations of mudstone, siltstone, sandstone and shale. Samples were collected by boat and filtration through 0.45μ Millipore carried out on site.

Northern British Columbia

Samples M and N were taken from creeks draining into the east side of Atlin Lake. These have catchment basins which lie within the Fourth of July Creek Batholith, a zoned coast intrusion of Mesozoic age consisting of a core of medium to coarse grained quartz monzonite grading into an outer shell of granodiorite. Samples Ø, P and R were taken from creeks draining into Surprise Lake. These have catchment basins which lie within the Surprise Lake Batholith of Cretaceous age consisting of highly variable textured alaskitic rock.

The Yukon

Samples YA through to YE were collected in the Engineer Creek region off the Dempster Highway. This area intersects carbonaceous calcareous shales from the Canol Formation which is of Late Devonian age. Shales from this formation are characteristically pyritic, baritic and phosphatic and contain above normal contents of Zn, F, U, Mo, Ni, Cd and V.

Samples YF through to YK were taken from streams in the Hunker Creek area near Dawson. These waters intersect the Klondike 'schist' and Nasina 'series' which are composed primarily of quartz-muscovite-chlorite schist, schistose and chloritic schist and quartz-mica schist. In some areas, these metamorphic rocks are overlain by Tertiary andesite and basalt. As this region has not been glaciated during Pleistocene time, the rocks are fairly deeply weathered.

Melville Peninsula

Samples MPA through to MPE were collected within the Penrhyn Group which consists of a series of conglomerates, marbles, quartzites, paragneiss and calc-silicate gneiss intruded by felsic igneous rocks. These range in composition from granitic to quartz-monzonitic and granodioritic.

Results

The last set of fluorometric data was obtained on October 30, 1978 and, from the end of May to that date, it was found that none of the raw or filtered untreated water samples decreased in their dissolved uranium content. Thus, it is not possible to compare the properties of the various preservatives tested. The mean uranium value and standard deviation of each untreated sample is shown in Table 54.2 obtained by conventional fluorometry. With the exception of those waters to which phosphate solution was added, the mean and standard deviation data obtained for the analysis of each untreated water over the time period of this study was the same as that obtained within each set of determinations of the twelve splits on any given day. There was no detectable difference in the behaviour of the unfiltered waters (Table 54.1) as compared with those filtered through 0.45μ in any of the parameters measured or in the uranium detected by the three methods employed. It was observed that the relative standard deviation obtained by either conventional fluorometry or laser-induced fluorescence not only depended upon the level of uranium detected but also on the particular water sample. For example, stream N exhibited far more erratic behaviour than did R from a different area and of much lower conductivity. The synthetic control, CTP (in 0.5 M nitric acid), was analyzed 38 times and produced a mean of 1.08 ng mL^{-1} uranium with a coefficient of variation of 12.2%. The suite (0 to 11) of uranium standard solutions, spiked at 0.4 ng mL^{-1}, was analyzed a total of nine times to give a mean of 0.42 ng mL^{-1} and a coefficient of variation of 19.9% (n=108). Reagent blanks were below detection limit.

Almost all of the waters containing over 20 μg mL^{-1} calcium exhibited a drastic decrease in uranium content when sodium phosphate was added. This drop generally was detectable two days after treatment and continued over the following two weeks to plateau at the levels shown in Table 54.3. The critical initial concentration of calcium appears to be about 16-20 μg mL^{-1} but, in any case, as soon as there is a decrease in the calcium level, then the uranium also falls out of solution to varying extents. All samples to which carbonate had been added (subscripts 3 and 9) exhibited a large decline in calcium content to a final value in the range 1.0-6.0 μg mL^{-1}. However, uranium was not lost from solution in any of these treated waters.

Table 54.4 summarizes the results of the study of various plastic bottles, using Lake G as the test sample. It is evident that uranium is stable for this particular water in any of the three types of material. However, it is interesting to note the drop of calcium from solution in the unfiltered, unacidified samples in the three plastics. The 250 mL linear polyethylene bottle had a distinct yellow tinge, unlike the larger LPE bottles, which may explain the disparity in behaviour. Loss is due to the precipitation of calcium carbonate; this is not an uncommon occurrence with alkaline waters.

A comparison of results obtained by the two analytical techniques is shown in Table 54.5. In fact, all 12 splits of each sample have been analyzed by laser-induced fluorescence numerous times but since the results agreed, within experimental error, with conventional fluorometry it was decided to restrict the amount of data reported here. Standard addition was used to determine uranium by laser-induced fluorescence as the majority of samples exhibited suppressed curves and, in many cases, dilution was also necessary. For example, most of the Engineer and Hunker Creek waters (YA to YK) had to be diluted initially in order to reduce the noise of the readings which, in some cases, resulted in an error of ± 0.5 ng mL^{-1} on one particular aliquot. It is presumed that the organics in these samples created this fluctuation as very significant "backing-off" of initial fluorescence was required; in the case of YC this resulted in a negative uranium value until a fivefold dilution was made. In addition to the discrepancy caused by this noise factor, the error introduced by extrapolating an extremely suppressed standard addition calibration curve (up to 70% drop) can be unacceptably high. The Melville Peninsula waters, on the other hand, proved to be almost ideal by this technique and could be read directly, with the exception of MPA which exhibited slight suppression (10%). The mean uranium values obtained by this method matched well those arrived at by fluorometry but the variation of data was definitely greater in those waters requiring dilution. Sample YK had an overall standard deviation of ± 0.68 ng mL^{-1} (14.2%) whereas R was much superior at ± 0.18 ng mL^{-1} (7.4%). There was no difference whatsoever in the mean or standard deviation of the filtered versus the unfiltered splits.

Discussion

Uranium has remained in solution in all of the waters described. As these samples represent various geological environments and thus widely differing chemical composition, it is extremely doubtful that waters collected in surveys in support of the Uranium Reconnaissance Program lost any uranium from solution. The analyses will be continued throughout the year as it has been evidenced that some filtered samples are developing brown flocculant precipitates (especially F_6, YC_6, YD_6 and YE_6), indicating a change in equilibrium conditions. Uranyl ion, the exclusive entity of U^{6+} in aqueous solution, forms complexes with fluoride and sulphate at pH values below 4.5-5.5 whereas carbonate complexes ($UO_2(CO_3)_2^{2-}$ and $UO_2(CO_3)_3^{4-}$) generally predominate in the higher pH range. However, in the presence of phosphate (PO_4=0.1 µg mL^{-1}) in the pH range 4.5-7.0 the uranyl complex $UO_2(HPO_4)_2^{2-}$ dominates all others (Langmuir and Applin, 1977). Adsorption of this species onto precipitating calcium phosphate must explain the loss of uranium from solution of those samples indicated in Table 54.3. If the uranous ion, U^{4+}, exists in any of these waters it is probably complexed with the hydroxyl anion at these pH levels. Uranium will be lost from solution when a reducing environment is created whereby U^{4+} is formed and precipitated as UO_2. Uranium (U^{6+}) can also be adsorbed onto colloidal material (organics, ferric hydroxide, clays) and ultimately reduced. Standard solutions of uranyl nitrate in glass are well known for their lack of stability. The contrast in behaviour with these natural waters must be due in part to the lack of complexing anions in the synthetic solutions and the greater tendency of glass to adsorb compared to polyethylene.

Further investigation is being carried out into the determination of uranium by laser-induced fluorescence. This technique proved superior to conventional fluorometry in Melville Peninsula where the samples were relatively "clean" and extremely low in organic carbon content. However, the dilution and spiking necessary for most of the other waters indicates that the problem of quenching (by inner-filter effect, electron transfer or energy transfer) is more complex and common than originally thought. Organics probably create a negative interference by two mechanisms: quenching of fluorescence and formation of a stable uranium complex which is not dissociated by the phosphate buffer solution ("Fluran"). The latter possibility seems unlikely for these particular waters as none of the values obtained by this technique were significantly lower than conventional fluorometry. The author has encountered other samples, however, where this has been the case. Humic acids, which are condensed polyaromatic structures of high molecular weight with hydroxyl and carboxyl groups, are known to form complexes with uranium (Szalay, 1969). Low results occur above 5 µg mL^{-1} humic acid whereas fulvic acid does not appear to interfere with this method of analysis. This negative interference will be characterized by studying the lifetime of uranium fluorescence before and after destruction of organic matter with either ultraviolet irradiation or persulphate oxidation.

Acknowledgments

I wish to thank Alice I. MacLaurin for her invaluable assistance and input into this project. I also appreciate the help of the geochemists involved in the areas under examination: W.B. Coker, W. Goodfellow, S.B. Ballantyne and Y.T. Maurice. Thanks to Ms. Moire Wadleigh for much of the analytical support.

References

Hostetler, P.B. and Garrells, R.M.
1962: Transportation and precipitation of uranium and vanadium at low temperatures, with special reference to sandstone-type uranium deposits; Economic Geology, v. 57, p. 137-167.

Langmuir, D. and Applin, K.
1977: Refinement of the thermodynamic properties of uranium minerals and dissolved species, with application to the chemistry of ground waters in sandstone-type uranium deposits: U.S. Geological Survey Circular 753, p. 57-60.

Moriyasu, M., YuKoyama, Y., and Ikeda, S.
1977: Quenching mechanisms of uranyl luminescence by metal ions; Journal of Inorganic Nuclear Chemistry, v. 39, p. 2205-2209.

Robbins, J.C.
1978: Field technique for the measurement of uranium in natural waters; Canadian Mining and Metallurgical Bulletin, v. 71 (793), p. 61-67.

Smee, B.W., Hall, G.E.M., and Koop, D.
1978: Analysis of fluoride, chloride, nitrate and sulphate in natural waters using ion chromatography; Journal of Geochemical Exploration. (in press)

Smith, A.H. and Lynch, J.J.
1969: Uranium Determination in Soils, Stream Sediments and Water; Geological Survey of Canada, Paper 69-40.

Szalay, A.
1969: Accumulation of uranium and other micro-metals in coal and organic shales and the role of humic acid in those geochemical enrichments; Arkiv Mineralogi Geologi, 6, p. 23-36.

55.

A THEORETICAL ESTIMATION OF ION MOBILITIES THROUGH GLACIOLACUSTRINE SEDIMENTS: DIFFUSION DOWN A CONCENTRATION GRADIENT

Project 770023

Barry W. Smee
Resource Geophysics and Geochemistry Division

Smee, B.W., A theoretical estimation of ion mobilities through glaciolacustrine sediments: Diffusion down a concentration gradient; in Current Research, Part A, Geol. Surv. Can., Paper 79-1A, p. 367-374, 1979.

Abstract

The diffusion of ions down a concentration gradient is considered to be a possible mechanism for obtaining geochemical responses at surface which relate to base metal mineralization subcropping beneath glaciolacustrine sediments. A model for geochemical enrichment at surface is proposed which requires that the organic horizon of the soil bind diffused ions and that the fraction of diffused ions incorporated into growing vegetation be returned to the soil through the leaching of transpired salts by precipitation and through annual litter fall.

Estimations of the diffusive flux through five metres of glacial sediment for the ions H^+, K^+, Na^+, Ca^{+2}, Zn^{+2}, Cu^{+2}, SO_4^{-2}, Cl^- and F^- indicate that differences in concentration in the A soil horizon for H^+, K^+, Na^+, Ca^{+2}, SO_4^{-2} and Cl^- may be of a magnitude sufficient to be detected by routine geochemical methods. Samples taken within the B soil horizon will not reflect subcropping mineralization.

Introduction

The occurrence of anomalous surficial geochemical responses above base metal mineralization overlain by glaciolacustrine sediments was noted by Boyle and Dass (1967) in the A (organic rich) soil horizon in deciduous tree-covered areas of the Cobalt camp, Ontario. Govett and Chork (1977) noted an increase in organic carbon, hydrogen ion and total conductance in surface organic soils over covered base metal deposits, and Govett (1972, 1974, 1975, 1976) presented data which indicate an increase in soil conductivities and hydrogen ion concentration over buried deposits, one of which was overlain by glaciolacustrine sediments. These anomalies, occurring over clayey sediments, cannot be explained by either hydromorphic or mechanical migration models.

Exploration methods currently employed in the search for base metal mineralization within clay covered areas has been reviewed by Smee and Sinha (in press) and can be summarized as follows: (1) airborne geophysics; (2) ground geophysical follow-up of airborne anomalies; (3) drilling. At no point in any exploration program is an attempt made to evaluate geophysical anomalies according to their geochemical character on the surface, and rightly so, for at present no theory, either proven or unproven, has been advanced that can adequately explain the occurrence of anomalous concentrations of elements in surficial material overlying glaciolacustrine sediments.

The recently introduced theories of electrogeochemical transport of ions along naturally occurring electric current lines developed in the vicinity of sulphide mineralization (self potential phenomena) (Govett, 1972; Bolviken and Logn, 1974) may represent a possible transport mechanism for ions through clay cover. In clay-covered terrain, geochemical responses created by chemical transport of ions in water, or by abnormal residual concentrations of elements resulting from the physical and chemical degradation of sulphides are unlikely. Therefore, if a mechanism exists for developing detectable surficial responses through these clay-sized sediments, the mechanism must be closely related to diffusion of ions along grain boundaries and through pore water solutions in these sediments. As the hypothesis of electrogeochemical transport is essentially based on diffusional processes, the areas of the Canadian Shield which are overlain by glaciolacustrine sediments may provide an excellent environment in which to test these theories.

The purpose of this paper is to propose a model for these diffusional processes, and using currently accepted diffusion equations for ion movement through clay-rich sediments, to calculate parameters for various ions associated with base metal deposits. These parameters may be useful in determining whether a detectable response might be found at the surface. At the current stage of the study, the effect of an SP (self potential) gradient on diffusing ions is not considered in the calculations, but an effect due to this factor being present is incorporated into the model.

Model

The model developed for the series of calculations to follow is shown in Figure 55.1. A tabular, steeply dipping massive sulphide body, consisting largely of pyrite, pyrrhotite and chalcopyrite is assumed to occur within an acid volcanic sequence. This body is assumed to subcrop beneath a thin (approximately 1 m) lodgement till horizon which in turn is overlain by 5 m of layered (varved) glaciolacustrine sediments. The surface consists of a gleyed clay horizon within which root development is sparse or nonexistent. This is overlain by 1 m of an organic-rich horizon within which deciduous plants have rooted. The surface consists of plant litter. Vegetation includes deciduous plants such as alder, poplar, and birch; the lower vegetation comprises swamp grasses and mosses of the type prevalent throughout the clay belts of central and eastern Canada.

The existence of a thin lodgement till is considered essential to the model, since it provides access of relatively oxygen-rich groundwater to the subcropping sulphide body, which, in turn, promotes the breakdown of the base metal sulphide minerals and the release of ions, or ion complexes, to the overlying environment. This, in effect, forms an infinite reservoir of ions, necessary for the continuance of long-term diffusion processes. The specification that this till layer be thin, i.e. a metre or less, arises from the possibility that the hydraulic throughput of a thick till layer would quickly dilute ionic concentrations released from weathering mineralization to a point where an abnormally high concentration no longer exists. In addition, the electrical resistance of a coarse till is much greater than either the sulphide horizon or the overlying clay, a feature that could completely attenuate a self potential voltage originating at the subcrop surface of the mineralization before it could reach the clay layer.

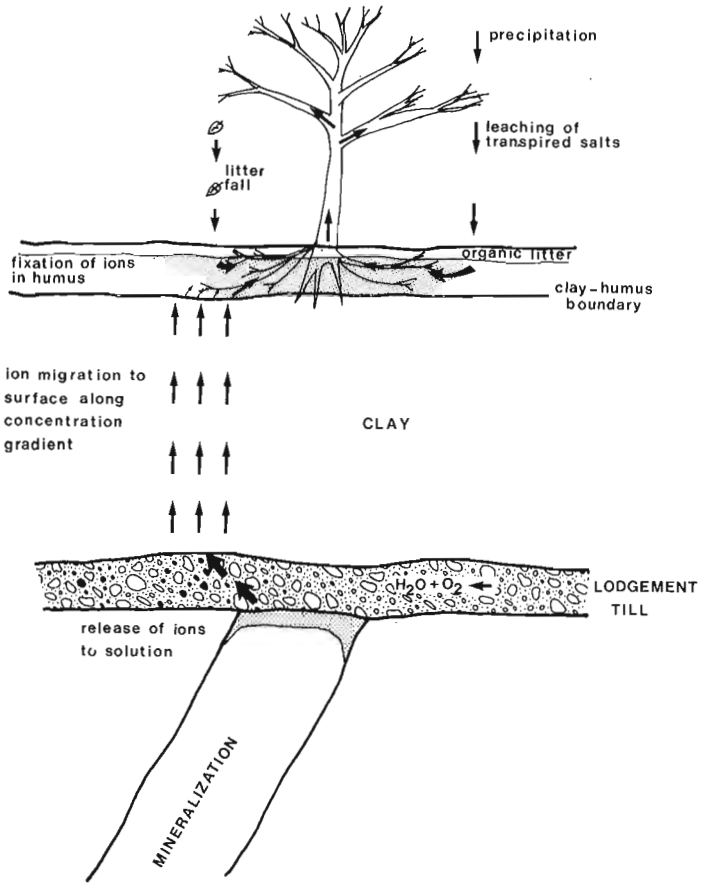


Figure 55.1. *Model showing diffusion of ions from mineralization to the clay-humus boundary and their subsequent enrichment in the humus horizon.*

It is also necessary to assume that the clay sequence is water saturated and has remained so since deposition. The electrical resistance of the clay must be less than the resistance of the country rock within which the mineralization occurs. The former factor allows the continued transport of ions through the clay column, either in pore water or along grain surfaces, and the latter will ensure that the electric current will travel preferentially in the clay horizon, the path of least resistance, before returning to the country rock.

The composition of a varved clay sequence does not include large amounts of true clay minerals, but mainly "rock flour" – small particles of rock forming minerals such as quartz, feldspars and amphiboles. The main phyllosilicates usually found in varved clay include illite, chlorite and vermiculite (Smee and Sinha, in press). Consequently, the cation-exchange-capacity (C.E.C.) of these sediments is relatively low, allowing the passage of both anions and cations through the pore spaces without appreciable losses of ions by adsorption. An estimation of a factor related to this phenomena, known as the distribution coefficient, is necessary before diffusion calculations can be attempted.

Another factor, related in part to grain size, must also be estimated prior to diffusion calculations. The increase in path length an ion must travel when diffusing through a sediment, essentially around grain boundaries, versus the straight line path taken by an ion in a solution, is known as the tortuosity of the sediment. It has been shown that this tortuosity factor can be calculated from the resistivities of the sediment and the pore waters (Turk, 1976); the ratio of the resistivity of the sediment to the resistivity of the solution is known as the formation factor. Estimates of the formation factors of various sediment systems are available from the literature.

What happens to diffused ions once they reach the upper boundary of the clay sequence? If they are adsorbed by materials near or at the surface boundary and allowed to interact with diffusing ions from below, a state will arise which will result in a high concentration of diffusing ions at or near the surface boundary, the destruction of the concentration gradient, and, therefore, a cessation of diffusion. In practice, the near surface materials are available to leaching by surface run-off, but more importantly, the diffusing ions are in a form readily incorporated by growing vegetation and may be chelated by the organic-rich soil horizons. If one assumes a removal of these ions by vegetation as they approach the interface between the clay and humus and their incorporation into plant parts, then the possibility of detecting anomalous amounts of the diffusing elements becomes more realistic. The enrichment process is envisioned as follows: a concentration gradient for various ions is established extending from the lodgement till – clay boundary upwards through the layered clay to the clay-humus boundary. A steady flux of ions arrives at this clay-humus boundary and are either incorporated by the humus or taken up directly by the higher vegetation. A significant fraction of the ions incorporated by the vegetation is returned to the soil either by annual litter fall or by the leaching of transpired nutrients from above-ground plant parts by precipitation. This cyclic system would tend to enrich the organic soil horizons in those ions which are diffusing in abnormal concentrations over time. Consequently, this model incorporates an estimation of the ionic flux at the clay-organic boundary for various ions assuming a steady-state diffusion rate, and the resultant total concentration increase of these ions in the organic layer because of this flux.

The length of time in which diffusion has been active is estimated to be 8000 years: the difference in time from the emplacement of the last varve and recession of the glacial lake and the present. For diffusion calculations the figure of 2.52×10^{11} s has been used. The mean temperature has been taken as 0°C.

Table 55.1

Diffusion coefficients in water at 0°C

Ion	λ, (0°C)	D_o, $cm^2/s \times 10^{-5}$
H^+	240	5.86
$\frac{1}{2}Ca^{2+}$	30	0.73
Na^+	26	0.63
K^+	40	0.99
$\frac{1}{2}Zn^{2+}$	20*	0.49
$\frac{1}{2}Cu^{2+}$	20*	0.49
$\frac{1}{2}SO_4^{2-}$	41	1.00
Cl^-	41	1.00
F^-	20*	0.49

*Estimates only.

Derivation of diffusion coefficients

An estimation of the coefficients of diffusion for any given ion at a particular activity can be derived from the Nernst relation:

$$D_o = \frac{RT}{n(F)^2\lambda} \quad (1)$$

where:

D_o is the coefficient of diffusion in cm^2/s

R is the Gas Constant in volt coulombs/deg. mole

T is the Absolute temperature in degrees K

n is the valence of the diffusing ion

F is Faraday's constant in coulombs/mole

λ is the equivalent conductance of the diffusing ion in ohm^{-1}. cm^2/mole

Although the diffusion coefficient is concentration dependent to some degree, molar concentrations of any ion studied under the model conditions outlined rarely exceed 1×10^{-4}. Therefore, it appears valid to substitute values of the limiting equivalent conductance in equation (1) for each ion, at 0°C. Values of λ are available from the literature.

Substituting 8.314 volt coulomb/degree mole for R, 273°K for T, and 9.65×10^4 coulombs/mole for F, equation 1 reduces to:

$$D_o = 2.44 \times 10^{-7} \frac{\lambda}{n} \ cm^2/s$$

Values calculated for various cations and anions are listed in Table 55.1.

The coefficients of diffusion for individual ions are considered to be conservative, since λ decreases by approximately 2 per cent per degree. If the mean temperature of the clay column was in fact 5°C, over 8000 years, then the coefficients of diffusion would be 10 per cent greater than those recorded in Table 55.1. On the other hand, it should be noted that these calculations of diffusion coefficients do not consider ion pair movement, that is, a cation must travel in conjunction with an anion in order to preserve the net charge at 0. In a multicomponent system such as the natural groundwater environment the faster cations will travel with the faster anions, leaving the slower cations to move with the slower anions. This effect will tend to slow the faster ions such as H^+ and greatly retard the slower ions, such as Zn^{2+}, Cu^{2+} and F^-. A more detailed explanation of this phenomena is given by Vinograd and McBain (1941) and is summarized by Garrels et al. (1949). The use of these diffusion coefficients in estimating ion mobilities and ion fluxes will result in a maximum value for each ion, and can be considered as a starting point for determining the usefulness of a particular element as an exploration tool in the suggested model.

Estimation of maximum distance travelled through a clay column

The distance travelled by an ion, diffusing down a concentration gradient in a solution can be derived from Fick's first law of diffusion:

$$J = -D_o \frac{dc}{dx} \quad (2)$$

where:

J is the flux of the diffusing ion in moles/cm^2. second passing through a unit area of surface normal to the direction of diffusion, per unit time

D_o is the diffusion coefficient of the ion in cm^2/second

c is the concentration of the diffusing ion in moles/cm^3

x is the distance travelled in cm

d is the differential operator

The solution of this equation depends upon the boundary conditions under consideration. For the case outlined in the model, a solution for aqueous diffusion is given in Garrels (1949) as follows:

$$\frac{C_o - C}{2C_o} = \text{erf} \frac{X}{\sqrt{2 D_o t}} \quad (3)$$

where:

C_o is the initial concentration of a diffusing ion in moles/cm^3

C is the concentration of a diffusing ion at the diffusion front in moles/cm^3

erf is the error integral function

X is the distance travelled by a given diffusion front in cm

D_o is the diffusion coefficient of the ion in cm^2/second

t is the time, in seconds required for the diffusion front C, to reach a distance X, from the initial diffusion boundary

In the assumed model, diffusion occurs through a sediment, a circumstance that requires adjustments to equation 3 to allow for an increase in X created by the tortuosity of the clay column, a conversion of ion concentration in solution to ion concentration per unit volume of sediment, and the effect of the distribution coefficient of the sediment on the concentration of the diffusion front in the sediment.

An estimation of the affinity of a sediment for a particular ion in a solution can be obtained simply by agitating a known concentration of the ion in solution with a known volume of sediment. The ratio of the concentration adsorbed by the sediment, Cads, in moles/cm^3 of sediment (calculated from the difference in concentration in the solution before and after agitation), to the concentration C (moles/cm^3), left in the solution after agitation gives the distribution coefficient, and can be written:

$$K = \frac{Cads}{C} \quad (4)$$

If a sediment has a large number of unfilled ionic binding sites on the surface of its constituent particles, the sediment will absorb ions from the surrounding solution until either the sites are filled or the ions in the solution are completely absorbed, thus causing K to become much greater than 1. At a time when a solution containing C_1 moles/cm^3 of diffusing ion comes in contact with a sediment having a fractional porosity of P and a distribution coefficient of K, the concentration of the ion in the sediment (C(o,o)) at the sediment-solution interface has been shown by Turk (1976) to be:

$$C_{(o,o)} = C_1(K(1-P)+P) \quad (5)$$

Combining the expressions in equations 4 and 5 with equation 3, the distance travelled by an ion within a fine-grained sediment which exhibits a concentration gradient of $C_{(o,o)}$ to $C_{(t,x)}$ moles/cm^3 of sediment, can be estimated from the relation:

$$\frac{C_{(o,o)} - C_{(t,x)}}{2C_{(o,o)}} = \text{erf} \left[\frac{X\sqrt{KF(1-P)+PF}}{\sqrt{2 D_o t}} \right] \quad (6)$$

where:

$C_{(o,o)}$ is the concentration in moles/cm^3 of an ion in the sediment at the sediment-reservoir interface at time 0.

$C_{(t,x)}$ is the concentration in moles/cm^3 of an ion in the sediment at some time t and distance x from the sediment-reservoir interface.

X is the distance in cm of the diffusion front from the sediment-reservoir interface

K is the distribution coefficient

F is the formation resistivity factor

P is the fractional porosity of the sediment

D_o is the diffusion coefficient in cm^2/s of the diffusing ion

t is the time in seconds diffusion has been proceeding

To calculate maximum distances of travel in the model outlined in 8000 years for various ions, an estimation of P, K, F, $C_{(o,o)}$ and $C_{(t,x)}$ is necessary. Measured values of P range from 0.20 to 0.35 with the mean of the nine samples of glaciolacustrine sediment studied being 0.30, that is, 30 per cent porosity. Values of K depend on the ion in question, and the concentration of that ion in solution. It would appear safe to assume that the K value will be greater than 1 even though this "rock flour" type of sediment has a relatively low cation exchange capacity (5-10 milliequivalents/100 g). This should occur because the sediments were deposited in glacial meltwater; the ionic strength of the resulting pore waters would be small compared to the number of ionic binding sites on the clay-sized particles. Therefore, for these calculations, a value of K=10 will be used throughout.

Formation resistivity factors for various clays and rocks have been published by Klinkenberg (1951) and Turk (1976). These factors vary inversely with the porosity of the substance being studied and are dependent on the ionic strength of the pore water solutions. Published values for kaolinite with pore water solutions of near 0.7M ionic strength and fractional porosities of near 0.4, lie near 2 (Turk, 1976). Klinkenberg (1951) calculated values of F between 2 and 3 for Cecil clay, and between 3 and 4 for various limestones with porosities between 0.11 and 0.34. Therefore, knowing the porosity of the model to be approximately 0.3, and the ionic strength of the pore water solution to be approximately 0.01M, a formation factor of 3 would appear reasonable.

Realistic values for the terms $C_{(o,o)}$ and $C_{(t,x)}$ in equation 6 of various ions have been estimated from the analysis of water in the lodgement till layer overlying a subcropping massive sulphide in northwestern Quebec. These values are listed in Table 55.2 as $C_{(resv)}$. The strength of the diffusion front was arbitrarily chosen, based on the $C_{(resv)}$ values.

The omission of Fe and Mn from the tables was necessitated because of a lack of conductance data in the literature, hence an estimation of diffusion coefficients. This paucity of data regarding these two key elements undoubtedly arises from their behaviour in the natural environment i.e. the precipitation of $Fe(OH)_3$ as the pH rises above 5, and the change in states of Mn^{+2} to various oxides as the pH and Eh change (Pourbaix, 1963).

Having estimated the various parameters necessary for the calculations of distance from equation 6, and changing $C_{(resv)}$ to $C_{(o,o)}$ using equation 5, a relative estimate of maximum travel distance in 8000 years can be obtained. These estimates are presented in Table 55.3.

It can be readily seen from Table 55.3 that the greatest movement, and therefore the greatest effect on surface concentrations occurs with H^+, K^+ and the anions SO_4^{2-} and Cl^-. The least amount of migration is shown by the base metals Cu^{+2} and Zn^{+2}. With the model in mind, it would be useful to estimate the total concentration contributed by these various ions to the surface, and to determine whether these concentrations could be located by routine geochemical analytical techniques.

Estimation of the total concentration of ions brought to surface

The diffusive flux of an ion in solution at any distance from the diffusion boundary and at a known concentration can be calculated using equation 2. For glaciolacustrine sediment systems, equation 2 must be modified to allow for the change in the effective diffusion coefficient of an ion created by the tortuosity, porosity and the distribution coefficient of the sediment. This modification was shown by Turk (1976) to be:

$$J_s = -\left[\frac{D_o}{F(K(1-P)+P)}\right] \frac{dC_s}{dx} \qquad (7)$$

where:

J_s is the flux in moles/cm^2.s of diffusing substances passing through a unit area of sediment surface normal to the direction of diffusion, per unit of time

D_o is the diffusion coefficient in cm^2/s

F is the formation factor of the sediment

K is the distribution coefficient

P is the fractional porosity

C_s is the concentration moles/cm^3 of the diffusing substance per unit volume of the bulk sediment system

x is the distance in cm

This estimation of ion flux, however, is only valid for steady state diffusion conditions, i.e. when the flux at the reservoir-sediment boundary equals the flux at the sediment-surface boundary. Therefore, in order to estimate the total concentration of an ion delivered to the upper boundary, one must first establish the time required for the ion to reach that boundary, the time required to establish a "steady-state" diffusion condition, and therefore the time that this equilibrium condition has been in effect.

Substituting the distance travelled (5 m) by a diffusion front from our model into equation 6, and using integral error functions from the Handbook of Mathematical Tables (1964) a solution can be obtained. The solutions are presented in Table 55.4.

The concentration conditions existent when "steady state" diffusion is in effect require that the concentration of a diffusing ion one half of the distance from x=0 to x=upper boundary, be equal to one half the concentration at the reservoir sediment interface.

For the proposed model, and from equation 6,

$$\frac{C_{(o,o)}-C_{(t,2.5m)}}{2\,C_{(o,o)}} \qquad \text{erf} = 0.68$$

for any ion studied.

Substituting this value into equation 6, the time required to reach equilibrium can be calculated from:

$$t = \frac{X^2(KF(1-P)+PF)}{.92\,D_o}$$

These values are presented in Table 55.5.

Table 55.2

Concentrations of various ions diffusing from a reservoir C(resv) to a diffusion front C(t,x)

Ion	C(resv), ppm in solution	C(resv), M/cm^3 in solution	C(t,x), ppm in sediment	C(t,x), M/cm^3 in sediment
H^+	pH = 4	1.0×10^{-4}	pH = 5	1.0×10^{-5}
Ca^{+2}	100.	2.5×10^{-3}	50.	1.2×10^{-3}
Na^+	100.	4.4×10^{-3}	50.	2.2×10^{-3}
K^+	5.	1.3×10^{-4}	2.	5.2×10^{-5}
Zn^{+2}	.050	7.6×10^{-7}	.025	3.8×10^{-7}
Cu^{+2}	.010	1.6×10^{-7}	.005	7.9×10^{-8}
SO_4^{-2}	25.	2.5×10^{-4}	10.	1.0×10^{-4}
Cl^-	20.	5.6×10^{-4}	10.	2.8×10^{-4}
F^-	.200	1.0×10^{-5}	.050	2.5×10^{-6}

Table 55.3

Estimation of distance travelled by given diffusion fronts in water saturated glaciolacustrine sediments in 8000 years

Ion	D_o cm^2/s $\times 10^{-5}$	C moles/cm^3	$C_s(o,o)$* moles/cm^3	$C_s(t.x)$ moles/cm^3	x** metres
H^+	5.86	1×10^{-4}	7.3×10^{-4}	1×10^{-5}	28.4
$\frac{1}{2}Ca^{+2}$	.73	2.5×10^{-3}	1.8×10^{-2}	1.2×10^{-3}	7.5
Na^+	.63	4.4×10^{-3}	3.2×10^{-2}	2.2×10^{-3}	6.9
K^+	.99	1.3×10^{-4}	9.5×10^{-4}	5.2×10^{-5}	9.2
$\frac{1}{2}Zn^{+2}$	.49	7.6×10^{-7}	5.5×10^{-6}	3.8×10^{-7}	6.4
$\frac{1}{2}Cu^{+2}$	.49	1.6×10^{-6}	7.9×10^{-6}	7.9×10^{-8}	5.8
$\frac{1}{2}SO_4^{-2}$	1.00	2.5×10^{-4}	1.8×10^{-3}	1.0×10^{-4}	9.1
Cl^-	1.00	5.6×10^{-4}	4.1×10^{-3}	2.8×10^{-4}	8.7
F^-	.49	1.0×10^{-5}	7.3×10^{-5}	2.5×10^{-6}	7.1

*$C_s(o,o)$ values calculated using K=10, P=.3

**x calculated using K=10, P=.3, F=3, t=2.52×10^{11}s.

Table 55.4

Time required for diffusion front to travel from subcrop to surface clay thickness = 5 m

Ion	D_o cm^2/s $\times 10^{-5}$	C(o,o) moles/cm^3	C(t,x) moles/cm^3	t s	t years
H^+	5.86	7.3×10^{-4}	1.0×10^{-5}	7.79×10^{9}	247
$\frac{1}{2}Ca^{+2}$	.73	1.8×10^{-2}	1.2×10^{-3}	1.10×10^{11}	3506
Na^+	.63	3.2×10^{-2}	2.2×10^{-3}	1.31×10^{11}	4153
K^+	.99	9.5×10^{-4}	5.2×10^{-5}	7.50×10^{10}	2381
$\frac{1}{2}Zn^{+2}$	.49	5.5×10^{-6}	3.8×10^{-7}	1.52×10^{11}	4808
$\frac{1}{2}Ca^{+2}$	.49	1.2×10^{-6}	1.2×10^{-6}	1.87×10^{11}	5924
$\frac{1}{2}SO_4^{-2}$	1.00	1.8×10^{-3}	1.0×10^{-4}	7.50×10^{10}	2379
Cl^-	1.00	4.1×10^{-3}	2.8×10^{-4}	8.27×10^{10}	2622
F^-	.49	2.3×10^{-5}	2.5×10^{-6}	1.24×10^{11}	3930

Table 55.5

Time required for diffusion to reach equilibrium

Ion	D_o (cm^2/s) x 10^{-5}	C(t,2.5m) moles/cm^3	t_e s	t_e years
H^+	5.86	3.65×10^{-4}	2.52×10^{10}	800
$\frac{1}{2}Ca^{+2}$	.73	$.9 \times 10^{-2}$	2.03×10^{11}	6436
Na^+	.63	1.6×10^{-2}	2.35×10^{11}	7451
K^+	.99	4.75×10^{-4}	1.50×10^{11}	4740
$\frac{1}{2}Zn^{+2}$	.49	2.75×10^{-6}	3.02×10^{11}	9577
$\frac{1}{2}Cu^{+2}$	.49	$.6 \times 10^{-6}$	3.02×10^{11}	9577
$\frac{1}{2}SO_4^{-2}$	1.00	$.9 \times 10^{-3}$	1.48×10^{11}	4693
Cl^-	1.00	2.05×10^{-3}	1.48×10^{11}	4693
F^-	.49	3.65×10^{-5}	3.02×10^{11}	9577

Table 55.6

Time from t_o that diffusion front has been in equilibrium

Ion	t_e (s)	$t_o - t_e$ (s)
H^+	2.52×10^{10}	2.27×10^{11}
$\frac{1}{2}Ca^{+2}$	2.03×10^{11}	4.93×10^{10}
Na^+	2.35×10^{11}	1.73×10^{10}
K^+	1.50×10^{11}	1.03×10^{11}
$\frac{1}{2}Zn^{+2}$	3.02×10^{11}	0
$\frac{1}{2}Cu^{+2}$	3.02×10^{11}	0
$\frac{1}{2}SO_4^{-2}$	1.48×10^{11}	1.04×10^{11}
Cl^-	1.48×10^{11}	1.04×10^{11}
F^-	3.02×10^{11}	0

Table 55.8

Concentration added to a 1 metre thickness of organic horizon; non-equilibrium conditions

Ion	$D_o \times 10^{-5}$ cm^2/s	C moles/cm^3 sediment	C in organic horizon*
$\frac{1}{2}Cu^{+2}$	.49	1.79×10^{-6}	1.14 ppm
$\frac{1}{2}Zn^{+2}$	.49	5.58×10^{-6}	3.65 ppm
F^-	.49	7.82×10^{-5}	1.49 ppm

*Assuming a density of the organic horizon of 1.0 gm/cm^2

Table 55.7

Concentration of diffusing ions added to a 1 m thickness of organic horizon during steady state diffusion

Ion	D_o cm^2/s x 10^{-5}	$t_o - t_e$ s	J_s moles/cm^2.s	J_T moles/cm^2	C* ppm
H^+	5.86	2.27×10^{11}	1.34×10^{-12}	.304	3040
$\frac{1}{2}Ca^{+2}$	.73	4.93×10^{10}	2.60×10^{-12}	.128	51 330
Na^+	.63	1.73×10^{10}	7.08×10^{-12}	.122	28 060
K^+	.99	1.03×10^{11}	7.69×10^{-13}	.079	30 890
$\frac{1}{2}Zn^{+2}$	.49	0	0	0	0
$\frac{1}{2}Cu^{+2}$	.49	0	0	0	0
$\frac{1}{2}SO_4^{-2}$	1.00	1.04×10^{11}	1.47×10^{-12}	.153	146 880
Cl^-	1.00	1.04×10^{11}	3.35×10^{-12}	.349	123 900
F^-	.49	0	0	0	0

*Assuming a density of the organic horizon of 1.0 gm/cm^3

It is readily seen that all ions except Zn^{+2}, Cu^{+2} and F^- have reached an equilibrium diffusion rate during the last 8000 years, and that equation 7 can be used to calculate the total flux of a particular ion during the time this "steady state" has been in effect. These times, representing the difference between t_o (8000 years) and t_e, the time to reach equilibrium, are shown in Table 55.6.

It is now possible to estimate the total concentration of ions delivered to the surface during steady state diffusion using dC_s as $C_{(o,o)}$-$C_{(t,5m)}$ from equation 6 and t values of t_e-t_o. The resulting flux is determined from equation 7. The results of this series of calculations are presented in Table 55.7.

To relate the figures in column 6 of Table 55.7 back to the model, assuming a 1 m thickness of organic matter, it quickly becomes evident that appreciable quantities of various ions may be moved to surface through the process of diffusion and the detection of a pH change and increased quantities of Ca^{+2}, SO_4^{-2} and Cl^- using routine geochemical methods should be possible.

To complete the data set, an estimation was calculated of the concentration of Cu^{+2}, Zn^{+2} and F^- moved to surface from the time the diffusion front arrived at the clay-organic boundary to the present. Because no steady-state diffusion yet exists for these ions, a graphical solution for the total concentration moved was implemented, rather than attempting to integrate the area beneath the concentration vs. time curve mathematically. These concentrations are presented in Table 55.8.

Discussion

The elements related to base metal mineralization which have been included in this exercise all exhibit the ability, at least in theory, to diffuse through five metres of glaciolacustrine sediment in the 8000 years since deposition. The assumption that all of the ions which have moved across the clay-organic boundary near surface have been fixed by organic matter either by chelation or by their incorporation into living organisms is undoubtedly optimistic. In reality, should this diffusional process occur, some percentage of the diffused ions would be dispersed by surface runoff, or diluted by inorganic debris, thus decreasing the detectable concentration in the organic horizon. Nevertheless, an intelligent application of analytical techniques may detect this diffusional process.

The most obvious technique would be the measurement of pH in A horizon soil slurrys. The pH values of organic soils are usually acid, and those in water saturated boggy soils may naturally lie in the region of pH 5 to 6. The detection of a systematic pH low in the A horizon, in conjunction with a ground geophysical response would increase the likelihood of that geophysical anomaly being related to sulphides.

The use of selective extractions on the A soil horizon, in an attempt to lower background and enhance the signal to noise ratio of various elements may prove useful. Techniques such as the use of high intensity ultraviolet light which can selectively break metal-chelate bonds, while ignoring adsorbed species have yet to be adequately explored. Weak extractions, including water, for the anions such as sulphate and chloride should be included in any geochemical survey.

Changes in Fe and Mn within the organic horizon may indirectly indicate the presence of abnormal pH or Eh conditions. Here again, weak extractions of these elements from the A horizon may prove useful.

The measurement of conductivity, when corrected for the overwhelming effect of the hydrogen and hydroxyl ions, may reveal the cumulative effect of an increase in a number of ions which, by themselves would be lost in the analytical variability between samples. This approach has previously been suggested by Govett (1976).

It is evident from the calculations that a number of techniques may not show anomalies over mineralization. The concentration of diffusing substances in the clay itself is too low to be detected by routine analytical methods. Sampling of B horizon soils will not discriminate diffusion related anomalies. It is equally unlikely that the sampling of live vegetation will prove a viable exploration tool, for the elements which move in the greatest quantities are also those which are naturally present in the largest amounts. However, data concerning the anions chloride and sulphate are lacking in the geochemical literature, and should be investigated.

Profiling through the clay, in search for an increase in metal concentration with depth, will not be successful for those elements which are in a "steady-state". The flux at the top of the column will be equal to the flux at the base. The data reveals that these concentrations are generally below most routine analytical techniques.

Conclusions

A theoretical treatment of diffusion through glaciolacustrine sediments reveals that the detection of subcropping base metal mineralization by use of A horizon soil sampling may be possible.

Of the elements considered, the cations H^+, Na^+, K^+, Ca^{2+} and the anions Cl^- and SO_4^{2-} may occur in detectable concentrations if the glaciolacustrine cover is 5 m or less in thickness. The use of pH and conductivity measurements on A horizon soils obtained over geophysical conductors may prove to be an inexpensive and rapid geochemical grading tool for differentiating graphitic conductors from sulphide conductors.

It should be stressed that the treatments included in this paper are theoretical and remain to be proven. The secondary effects of the self-potential fields in the vicinity of mineralization concerning the transport of ions through clayey sediments remain to be studied.

Acknowledgments

The author gratefully acknowledges the useful and stimulating discussions with R.W. Boyle, W. Dyck and P. Arp.

References

Bolviken, B. and Logn, O.
1975: An electrochemical model for element distribution around sulphide bodies; in Elliot, I.L. and Fletcher, W.K., Editors, Geochemical Exploration 1974; Association of Exploration Geochemists Special Publication No. 2, p. 631-648.

Boyle, R.W. and Dass, A.S.
1967: Geochemical prospecting – use of the A horizon in soil surveys; Economic Geology, v. 62, no. 2, p. 274-276.

Garrels, R.M., Dreyer, R.M., and Howland, A.L.
1949: Diffusion of ions through intergranular spaces in water saturated rocks; Geological Society of America Bulletin, v. 60, no. 12, p. 1809-1828.

Govett, G.J.S.
1974: Soil conductivity measurements: a technique for the detection of buried sulphide deposits; Institute of Mining and Metallurgy Transactions, v. 83, p. B29-B30.

1975: Soil conductivities:assessment of an electrogeochemical exploration technique; in Elliot, I.L. and Fletcher, W.K., Editors, Geochemical Exploration 1974, Association of Exploration Geochemists Special Publication No. 2, p. 101-118.

1976: Detection of deeply buried and blind sulphide deposits by measurement of H^+ and conductivity of closely spaced surface soil samples; Journal of Geochemical Exploration, v. 6, no. 3, p. 359-382.

Govett, G.J.S. and Chork, C.Y.
1977: Detection of deeply-buried sulphide deposits by measurement of organic carbon, hydrogen ion and conductance in surface soils; in Prospecting in Areas of Glaciated Terrain, 1977, Institute of Mining and Metallurgy, London, p. 49-55.

Klinkenberg, L.J.
1951: Analogy between diffusion and electrical conductivity in porous rocks; Geological Society of America Bulletin, v. 62, p. 559-564.

Pourbaix, M.
1963: Atlas D'Équilibres Electrochemiques à 25°C; Gauthier-Villars and Cie, Paris, 644 p.

Smee, B.W. and Sinha, A.K.
Geological, geophysical and geochemical considerations for exploration in clay covered areas: a review. (in press)

Turk, J.
1976: A study of diffusion in clay-water systems by chemical and electrical methods; unpublished Ph.D. thesis, University of California, San Diego, 111 p.

Vinograd, J.R. and McBain, J.W.
1941: Diffusion of electrolytes and their mixtures; American Chemical Society Journal, v. 63, p. 2008-2015.

Weast, R.C.
1964: Handbook of mathematical tables, 2nd ed. Supplement to the Handbook of Chemistry and Physics; C.R.C. publishers, Cleveland, Ohio.

56. REGIONAL METALLOGENY OF THE NORTHERN CORDILLERA: RECENT STRATIFORM BASE METAL DISCOVERIES IN YUKON TERRITORY AND DISTRICT OF MACKENZIE

Project 740098

K.M. Dawson
Regional and Economic Geology Division, Vancouver

Dawson, K.M., Regional metallogeny of the northern Cordillera: Recent stratiform base metal discoveries in Yukon Territory and District of Mackenzie; in Current Research, Part A, Geol. Surv. Can., Paper 79-1A, p. 375-376, 1979.

Abstract

Significant stratiform base metal mineralization has been discovered in Lower Paleozoic sedimentary rocks at three localities in Yukon Territory and District of Mackenzie. In the Pelly Mountains laminated and disseminated sulphides occur in Cambro-Ordovician, Ordovician-Silurian, and Devonian shale and carbonate. At Anderson Creek conformable Zn-Pb deposits occur in deformed basal Road River phyllite. In the Logan Mountains, volcanic flows and overlying black shale of Ordovician age host volcanogenic massive sulphides.

Introduction

In 1977 and 1978 three significant stratiform base metal discoveries were examined: the WOODSIDE in Pelly Mountains of central Yukon, the MAXI and a new occurrence in Logan Mountains of southeastern Yukon and southwestern District of Mackenzie, respectively. The latter two deposits are hosted by approximately equivalent beds of the Road River Formation, whereas the Pelly Mountains occurrences occupy several horizons in Lower Paleozoic strata.

'Woodside Project' Properties: MAY, MAG, SIR JOHN A, SUNSET, ROSS and ANGIE

Welcome North Mines Ltd. and Getty Mining Pacific Ltd., acting jointly in the 1977 Woodside Project, staked a belt of claims that includes the above groups and extends through the Pelly Mountains southwestward from Magundy River (105 K/4) about 100 km to the Ketza River area (105 F/16) as shown in Figure 56.1. Systematic prospecting, aided by the use of zinc solution, had revealed extensive base metal mineralization in the Lower Paleozoic sedimentary rocks in this relatively accessible and well-prospected terrane. A detailed description of geology and 1977 exploration work on some of these claims is given by Marchand (1978).

The MAY claims (62°03'N; 133°48'W) exemplify the oldest stratabound mineralization in the district, i.e. conformable skarns that contain varying proportions of sphalerite, galena, and scheelite in the assemblage pyroxene-amphibole-pyrrhotite-epidote. The laterally-continuous skarns are hosted by thin marble beds within an upper Proterozoic to lower Cambrian (Tempelman-Kluit, 1977) biotite schist unit that grades to migmatite and flanks the northwestern margin of the Fox Mountain stock. These skarns are essentially identical to the synmetamorphic (class 3) base metal skarns adjacent to the Mount Billings Batholith described by Dawson and Dick (1978).

On the SIR JOHN A (62°04'N; 133°09'W), SUNSET (62°03'N; 133°04'W), and adjacent occurrences, calcareous metasedimentary rocks of Cambro-Ordovician age (Tempelman-Kluit, 1977) host a 20 km belt of similar stratiform sphalerite-pyrrhotite-galena occurrences. Mapping of the project area under the direction of Frank Foster has shown the occurrences to be restricted essentially to one horizon. Sulphide laminae up to several centimetres thick occur within impure marble and calcareous phyllite that has been regionally metamorphosed to upper greenschist and locally, amphibolite facies. The regional development of biotite and garnet at this stratigraphic level is contrasted to development of an iron-rich skarn assemblage 60 m higher in the section at SUNSET. Calcareous beds within graphitic biotite schist host stratiform and discordant sphalerite-galena occurrences in a skarn assemblage of siderite-pyrrhotite-magnetite-garnet-actinolite.

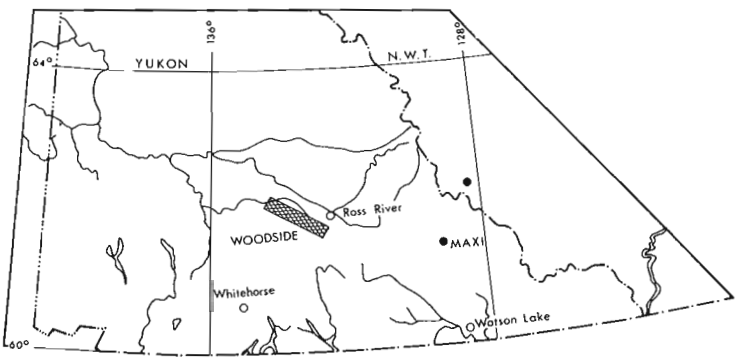


Figure 56.1. *Location of Woodside, Maxi and Logan Mountains base metal discoveries, Yukon Territory and District of Mackenzie.*

Siderite, commonly as quartz-siderite stockwork, is an ubiquitous component of base metal mineralization in the Pelly Mountains. On the MAG claims (62°09'N; 133°29'W) at the northwestern end of the Woodside trend lower Paleozoic argillite and limestone are veined and replaced by a quartz-siderite stockwork mineralized with sphalerite, galena, and chalcopyrite. Muscovite, green tourmaline, and tetrahedrite occur in quartz-siderite stockworks on ROSS, ANGIE and other claims at the southeastern end of the belt.

Calcareous metasediments in the SUNSET belt are conformably overlain by an interdigitated sequence of sooty limestone and calcareous argillite of Ordovician-Silurian age (Tempelman-Kluit, 1977). A zone of stratiform Zn-Pb occurrences in these rocks about 300 m above the siderite-rich skarn zone is detected at several localities along the SUNSET-SIR JOHN A belt. Equivalent but less metamorphosed beds 20 km southeast of SUNSET at Danger Creek and ROSS claims host disseminated sphalerite-pyrite with little or no lead but locally significant silver values.

A third horizon of stratiform Zn deposition occurs at the southeastern end of the Woodside belt in a Devono-Mississippian sequence of siltstone, limestone, shale, and acidic flows. On the ANGIE claims (61°55'N; 132°40'W) fine grained stratiform disseminations and fracture fillings of sphalerite and pyrite with some silver values occur in carbonaceous limestone and calcareous siltstone. Relationships of the stratiform mineralization to the overlying Mississippian flows and to bedded barite at about the same horizon elsewhere in the area, is not known.

MAXI claims: 61°38'N; 129°11'W

In late 1977 prospectors of Welcome North Mines Ltd. discovered conformable Zn-Pb occurrences in a tributary of Anderson Creek in southeastern Yukon. Beds and lenses of sphalerite-galena hosted by isoclinally folded graphitic to calcareous phyllites occur in six mineralized zones along 500 m of canyon exposure. S.L. Blusson, who visited the property with the writer in 1977, noted (Blusson, 1978, p. 80) that its stratigraphic position about 30 m above the Cambro-Ordovician 'wavy banded' limestone places the deposit in the same basal Road River Formation horizon as the significant Zn-Pb deposits at Howard's Pass, 90 km to the north. A second visit by the writer in 1978 confirmed the stratigraphic position of the deposit and adjacent rocks, and the regional significance of mineralization at this horizon.

The originally stratiform shale-hosted Zn-Pb deposits have been modified by both regional and thermal metamorphic events. Galena and sphalerite with little or no iron sulphides are concentrated with quartz and siderite as transposed lamellae in the axial and crestal regions of overturned isoclinal folds. Insufficient data were available to ascertain if the exposed mineralized zones are discreet horizons or fold repetitions of one or two main zones. The abundance of discordant remobilized sulphide-bearing veinlets increases southwards in canyon outcrops, as does the abundance of Fe, Pb, Ag, and Cu in the sulphide mineralization, although the two trends are not necessarily related. In addition, southernmost mineralized outcrops show thermal metamorphic mineral assemblages of pyrrhotite after pyrite and magnetite intergrown with coarse grained galena, sphalerite, chalcopyrite, quartz, and pyroxene. Similar skarn-type mineral assemblages were observed 6 km to the east at the AK and MITE occurrences but they occur within a higher grade regional metamorphic terrane. Phyllites in the canyon are intersected by several large granite dykes apparently related to adjacent Cretaceous stocks. Thus the originally stratiform mineral deposits may have been modified morphologically and chemically by both a regional metamorphic event of probable pre-Late Devonian age (Blusson, 1978) and a Cretaceous intrusive event. Drilling of the deposit by Utah Mines Ltd. was of too preliminary a nature to permit estimation of grade and extent of the deposit.

Logan Mountains

Several stratiform occurrences of massive sphalerite-galena-pyrite were found in southern Logan Mountains in 1978.

Massive sulphides are hosted by a cherty and carbonaceous black shale horizon 100 m or less thick that overlies a pyritic amygdaloidal basalt flow of similar thickness. The shale unit grades upward and the volcanic rocks pass downward to dark grey crinoidal limestone ascribed by Blusson et al. (1967) to the Middle Ordovician Sunblood Formation. The graptolitic shale and underlying flows correspond to Blusson's (1967) Unit 10 and are believed to be equivalent to Road River Formation host rocks at Howard's Pass, but they are located updip of the basinal shale within transitional carbonate of the outer shelf facies. The deposit is the first volcanogenic massive sulphide known to occur in rocks of this age in the northern Cordillera.

The black shales are localized, along with sulphides, in a small basin that overlies amygdaloidal flows and extends southeastward beyond the pinched out volcanic unit for at least 0.5 km. The volcanic unit extends for several kilometres beyond the limits of the massive sulphide mineralization, but sulphide deposits and host shales appear to diminish and disappear over a total strike length of about 4 km. At the main showing, massive laminated Zn-Pb-Fe sulphides are developed preferentially above intensely pyritized volcanic rocks, and grade laterally to pyritic massive sulphides with interstitial sphalerite, and stratigraphically upward to sphalerite-pyrite-cemented cherty shale conglomerate. About 500 m northwestward along strike from the massive sulphide zone pyritic ore grades to a laminated assemblage of pyrite-barite-fluorite with disseminated galena and sphalerite. Sulphide mineralization appears to diminish northwestward, giving way to a distal(?) bedded barite-fluorite-minor galena assemblage. Barite-purple fluorite-galena veinlets form a conspicuous stockwork in both the footwall and massive sulphide horizons. Chalcopyrite is a minor constituent of the massive sulphide ore.

Table 56.1

		DY883A	DY883B
Delayed neutron activation (AECL)	U	247 ppm	119 ppm
	Th	<20	60
Optical emission spectroscopy (GSC)	P_2O_5	15.3%	20.0%
	C total	7.8	5.5
	Ba	0.88	1.20
	Sr	0.32	0.64
	Zn	410 ppm	520 ppm
	Pb	<700	<700
	Cu	520	360
	V	650	810
	Mo	73	130
	Mn	<50	<50

A second massive sulphide occurrence, discovered after the writer's visit, reportedly has a similar stratigraphic setting in volcanics and shale within Ordovician limestone, but may be several hundreds of metres stratigraphically above the main showing.

An interesting aspect of the Logan Mountains occurrence is the high radioactivity in black shale overlying the volcanic flows. About 10 km along strike northwest of the main showing, carbonaceous graptolitic shale with fine grained pyrite laminae and encrustations of gypsum and hydrozincite registers 70 000 total counts per minute on the scintillometer (TV-1), and assays up to 247 ppm U. Table 56.1 gives assays of a specimen of black shale with pyrite laminae and quartz veinlets (DY883A), and a brecciated shale cemented by quartz, gypsum, and unidentified secondary minerals (DY883B).

Noteworthy in the assays are the very high P_2O_5 contents in conjunction with high U, Zn, and V that indicate that an organic metal concentrating component exists in the shale. Both the high Ba content and the high Sr/Ba ratio may relate to a volcanic source. The extent of the phosphatic uranium-bearing shale has not been determined.

References

Blusson, S.L.
1978: Regional geologic setting of lead-zinc deposits in Selwyn Basin, Yukon; in Current Research, Part A, Geological Survey of Canada, Paper 78-1A, p. 77–80.

Blusson, S.L., Green, L.H., and Roddick, J.A.
1967: Nahanni, geology; Geological Survey of Canada, Map 8-1967.

Dawson, K.M. and Dick, L.A.
1978: Regional metallogeny of the northern Cordillera: Tungsten and base metal-bearing skarns in southeastern Yukon and southwestern Mackenzie; in Current Research, Part A, Geological Survey of Canada, Paper 78-1A, p. 287-292.

Marchand, M.
1978: 1977 Yukon mineral industry report; Open File Edition, June 1978.

Tempelman-Kluit, D.J.
1977: Quiet Lake (105F) and Finlayson Lake (105G) map-areas; Geological Survey of Canada, Open File 486.

57.

PETROLOGICAL AND GEOCHRONOLOGICAL STUDIES ON THE RAINY LAKE GRANITOID COMPLEX, NORTHWESTERN ONTARIO: A PROGRESS REPORT

EMR Research Agreement 203-4-78

R.H. Sutcliffe[1] and J.J. Fawcett[1]
Regional and Economic Geology Division

Sutcliffe, R.H. and Fawcett, J.J., Petrological and geochronological studies on the Rainy Lake Granitoid Complex, northwestern Ontario: A progress report; in Current Research, Part A, Geol. Surv. Can., Paper 79-1A, p. 377-380, 1979.

Abstract

The Rainy Lake Granitoid Complex consists of a number of elements. The earliest intrusive phase is tonalite-granodiorite gneiss which forms diapiric domes. These early gneisses contain septa of amphibolite facies xenoliths, ranging in composition from mafic to ultramafic, which are thought to be correlative with the supracrustals of the Wabigoon greenstone belt. The later Jackfish-Weller Lakes Pluton, whose composition ranges from diorite to monzonite, forms a conformable sheet between the tonalite granodiorite gneiss and the main body of Wabigoon supracrustals to the north. The last phase of igneous activity was the intrusion of discordant biotite granite on the southern border of the complex. Cataclasis along the Quetico fault zone has affected all of the granitoid rocks of the complex.

The three groups of granitoid rocks are chemically distinct and it is expected that trace and rare-element modelling of the granitoids and xenoliths will throw some light on the source rocks of the younger phases.

Introduction

The Archean Rainy Lake Granitoid Complex is situated in the southwestern portion of the Wabigoon volcanic-plutonic belt of the Superior Province and occupies an area of approximately 1500 km^2. On its northern, eastern, and western boundaries it is in contact with metavolcanic rocks of the Wabigoon belt and the southern boundary has been placed at the Quetico Fault zone. The town of Fort Frances is approximately 15 km south of the complex.

The initial regional mapping of the Rainy Lake area was done by Lawson (1888). More recently the Ontario Geological Survey has mapped marginal portions of the Rainy Lake Granitoid Complex on detailed and semidetailed scales (Blackburn, 1973, 1976; Edwards and Lorsong, 1976; Edwards and Sutcliffe, 1977). This work has been combined with reconnaissance mapping by the first author in the interior of the complex at a scale of 1:63 360. The reconnaissance mapping was initiated in 1977 with the support of the Ontario Geological Survey and completed in 1978 with support from the Department of Energy, Mines and Resources. In addition to this field work, Longstaffe et al. (1977) have reported the results of geochemical investigations in an area including the southwestern portion of the Rainy Lake Complex. The major aim of the current project is to determine the sequence of structural, metamorphic and intrusive events in the evolution of the complex and to determine the magma sources for the massive to foliated granitoid rocks.

Mapping has shown that the granitoid complex is composed of four lithologically and structurally distinct elements (Fig. 57.1): 1) an early suite of foliated to gneissic tonalite-granodiorite; 2) amphibolite facies supracrustal rocks which locally define discontinuous septa within the tonalite-granodiorite; 3) foliated and lineated to massive diorite-monzodiorite-monzonite of the Jackfish-Weller Lakes Pluton; and 4) a late granite suite of foliated to massive biotite granite and pegmatite. Studies of other large granitoid complexes in northwestern Ontario (Sage et al., 1974; Schwerdtner and Sutcliffe, 1978) have revealed that these four elements are repeatedly observed. In this respect the Rainy Lake Complex is typical of the Archean granitoid complexes in the region and due to its accessibility from Rainy Lake the complex is particularly well suited to petrological and geochronological studies.

This report briefly summarizes the field relations, structure and chemistry of the rocks which form the complex and outlines the scope of the investigations currently in progress.

Lithology and Structure

Highly foliated to gneissic, leucocratic biotite tonalite-granodiorite forms the earliest intrusive phase of the complex. Structural mapping of portions of the gneiss indicates that it was emplaced as several gneiss domes, the largest of which is the centrally located Ash Bay Dome. The strain pattern of the Ash Bay Dome is consistent with the emplacement of a diapir inclined to the southeast and indicates that a relatively high level of the diapir is presently exposed (Schwerdtner et al., 1978). The tonalite-granodiorite is fine grained, equigranular and recrystallized. The essential mineralogy is quartz (20-30%), microcline (5-15%), oligoclase (50-60%), and biotite (5-15%). Where present the gneissic banding is defined by leucotonalite-granodiorite bands 1-2 cm wide, smaller discontinuous metamorphic segregations with microcline metablasts and locally pegmatoidal granite mobilizates.

Amphibolite facies xenoliths ranging in composition from mafic to ultramafic, and exhibiting varying degrees of reaction with the tonalite granodiorite host form discontinuous septa around the perimeter of the Ash Bay Dome and the northern margin of the gneiss. The xenoliths are highly strained and migmatized and relict porphyritic textures are the only primary features preserved. The distribution of the xenoliths, however, suggests that they were derived from Wabigoon supracrustal rocks prior to the emplacement of younger granitoids along the gneiss-metavolcanic contact.

The Jackfish-Weller Lakes Pluton represents the second major episode of intrusion within the complex. The pluton has a foliated to lineated fabric and the stain pattern of the body indicates that it has risen as a conformable sheet along the gneiss-supracrustal interface. The pluton has a variable composition but most rocks are in the range diorite-monzodiorite-monzonite. Most rock types however are characterized by the presence of clotty aggregates of mafic minerals which range in length from less than 1 cm up to 10 cm. Larger hornblendite and amphibolite enclaves up to

[1] Department of Geology, University of Toronto, Toronto, Ontario.

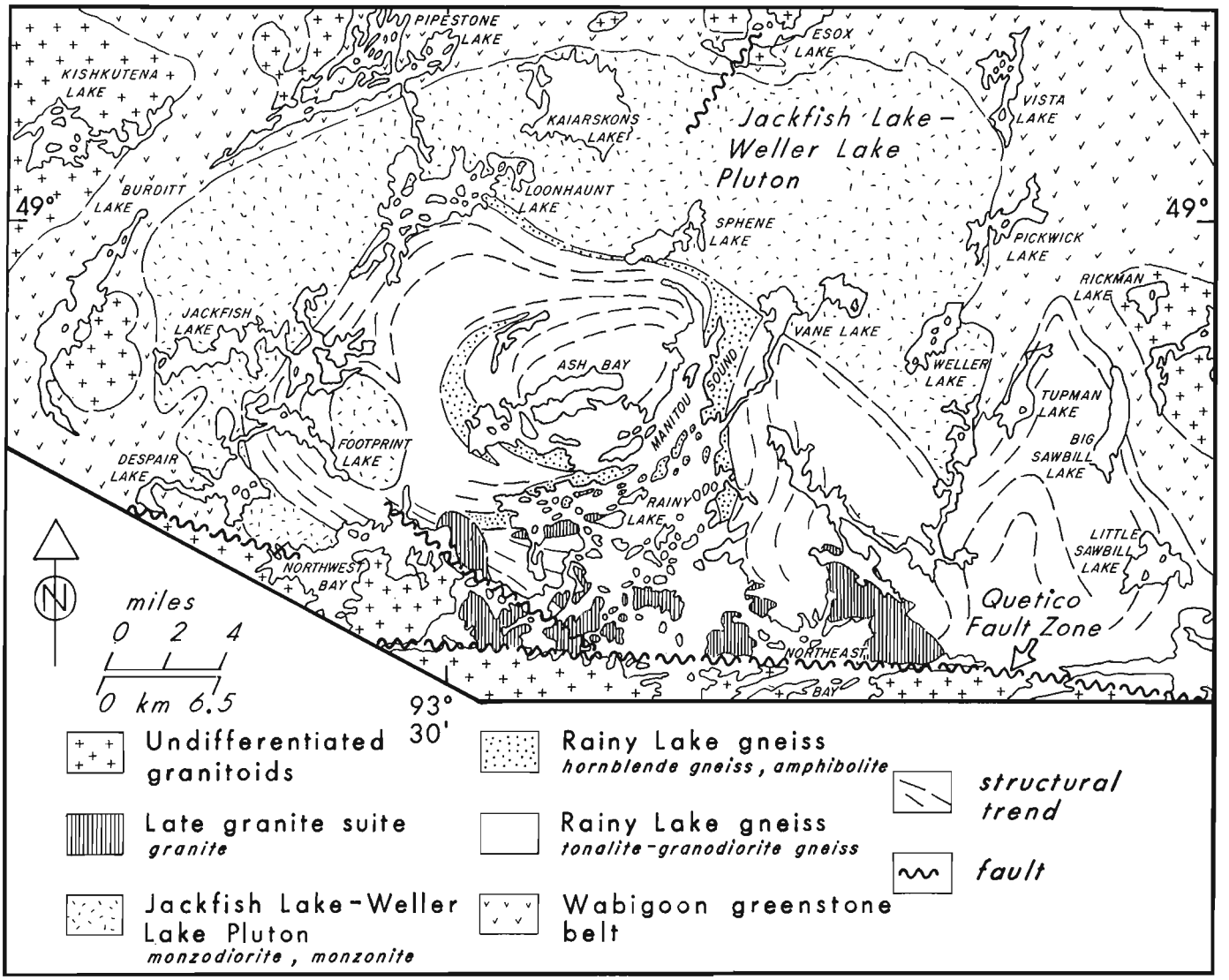


Figure 57.1. *Generalized geology of the Rainy Lake Granitoid Complex. In part based on mapping by the Ontario Geological Survey (Blackburn, 1973, 1976; Edwards and Lorsong, 1976; Edwards and Sutcliffe, 1977).*

1 km long are abundant throughout. In the granitoids, quartz is usually minor (0-10%) and interstitial, microcline (0-25%) varies from interstitial to 1-2 cm megacrysts but always shows features of late stage crystallization, and plagioclase (45-60%) varies from oligoclase to andesine. The mafic minerals, predominantly hornblende, account for 20-40% of the rock. Biotite and clinopyroxene are also present in variable amounts and locally clinopyroxene is the predominant mafic. Clinopyroxene also frequently occurs as relict cores in the hornblende. The characteristic accessory phases are apatite, sphene and zircon, all of which are usually associated with the mafic clots. Minor occurrences of bismuthinite mineralization in the western portion of the Jackfish-Weller Lakes Pluton have been described by Blackburn (1976).

Late, discordant biotite granites intrude the gneiss on the southern margin of the complex and represent the last phase of intrusive activity. In contrast to the Jackfish-Weller Lakes Pluton the granites are largely massive and appear to have induced brittle fracturing in the gneissic host rocks. Numerous fine grained dykes of granite invade the gneiss over a wide area and locally intrude the Jackfish-Weller Lakes Pluton. Fragments of gneiss are commonly present in granite near the contacts of the intrusion, and in the vicinity of the Northeast Bay of Rainy Lake metasedimentary schlieren are abundant. The late granites are undeformed and clearly postdate the diapirism of the tonalite-granodiorite.

The granites have a fine- to medium-grained, equilibrium texture and are characterized by widespread micrographic intergrowth of quartz in microcline and oligoclase. Quartz, microcline and oligoclase are present in subequal amounts. Biotite is the predominant mafic and accessory garnet is sometimes present. Abundant pegmatites which occur as gradational pods within the granite and as discordant dykes are the source of minor uranium mineralization in the Rainy Lake area (Blackburn, 1973).

The Quetico Fault zone, a 1 to 2 km wide zone of cataclasis has affected all the granitoid rocks of the Rainy Lake Complex. Augen gneiss and mylonite are the predominant cataclastic rocks. Pseudotachylite is locally developed, particularly along fracture sets oblique to the cataclastic foliation. A predominance of minor z drag folds and the asymmetry of slickensides on joint surfaces within the zone indicate a subhorizontal dextral movement along the fault zone. Granitoid rocks persist south of the fault but in the absence of correlation across the zone, the fault is used here as the southern boundary of the Rainy Lake Granitoid Complex.

Table 57.1

Preliminary chemical analyses of typical lithologies, Rainy Lake Granitoid Complex

	S76-31	S77-101	S77-25	S77-109	S76-35	S76-25	S77-77	S77-28	S77-36	S77-41
SiO_2	69.78	71.96	43.65	50.47	53.73	62.67	64.08	75.74	74.22	71.42
TiO_2	0.34	0.20	1.57	0.74	0.70	0.53	0.47	0.08	0.09	0.29
Al_2O_3	15.32	15.39	9.86	14.43	16.66	15.36	16.10	13.12	13.91	14.56
Fe_2O_3	1.11	0.14	5.05	3.48	2.31	1.12	1.57	0.42	0.51	0.66
FeO	1.38	0.86	8.17	7.90	4.82	3.29	2.02	0.31	0.55	1.16
MnO	0.04	0.03	0.25	0.23	0.14	0.09	0.08	0.05	0.04	0.04
MgO	0.76	0.70	10.56	7.62	5.84	3.50	2.21	0.08	0.22	0.60
CaO	3.09	1.99	14.78	10.52	8.08	4.48	3.16	0.59	1.00	1.46
Na_2O	4.82	5.01	1.23	2.88	5.02	4.44	4.82	3.64	3.88	4.20
K_2O	1.65	2.45	0.97	0.88	0.88	2.92	4.42	5.10	5.06	4.47
P_2O_5	0.15	0.11	1.90	0.25	0.42	0.26	0.30	0.01	0.02	0.08
Loss	0.65	0.30	2.35	1.62	1.18	1.03	0.75	0.40	0.43	0.60
Total	99.09	99.14	100.34	101.02	99.78	99.69	99.98	99.54	99.93	99.54
Ba	491.	891.	-	-	-	-	-	201.	795.	1407.
Rb	47.	60.	-	-	-	-	-	275.	218.	183.
Sr	546.	853.	-	-	-	-	-	116.	207.	374.
K/Rb	291.	337.	-	-	-	-	-	154.	192.	203.
Rb/Sr	0.09	0.07	-	-	-	-	-	2.37	1.05	0.49

S76-31 Tonalite, Ash Bay Dome
S77-101 Granodiorite, Ash Bay Dome
S77-25 Ultramafic amphibolite, perimeter of Ash Bay Dome
S77-109 Amphibolite, perimeter of Ash Bay Dome
S76-35 Biotite-Hornblende Diorite, Jackfish-Weller Lakes Pluton
S76-25 Biotite-Hornblende Monzodiorite, Jackfish-Weller Lakes Pluton
S77-77 Biotite-Hornblende Monzonite, Jackfish-Weller Lakes Pluton
S77-28 Pegmatitic Biotite Granite, Late Granite Suite
S77-36 Biotite Granite, Late Granite Suite
S77-41 Biotite Granite, Late Granite Suite

All elements by XRF (except FeO and loss). Above results are preliminary; final results from duplicate analyses with Na_2O by flame photometry are in preparation. Analysts: major elements by M.P. Gorton and R.H. Sutcliffe; trace elements by D.R. Mason at Memorial University.

Chemistry

Representative preliminary chemical analyses of major lithologies within the Rainy Lake Complex are given in Table 57.1. The three groups of granitoids are very distinct chemically and the general characteristics of each suite are discussed below.

The tonalite-granodiorite gneiss shows a restricted range in composition for most elements and is characterized by generally higher Na_2O than the other granitoids. Local variability of alkali elements appears to be due to mobility of these elements during metamorphic conditions, possibly during diapirism. Major elements and K/Rb and Rb/Sr ratios of the tonalite-granodiorite are comparable to the Northern Light gneiss in northeastern Minnesota (Arth and Hanson, 1975).

The Jackfish-Weller Lakes Pluton displays the widest compositional variation of the granitoid suites present. The pluton is calc-alkalic (Peacock alkali-lime index) and metaluminous with Mol $Al_2O_3/(CaO+Na_2O+K_2O)$ ranging 0.7 to 0.9. Na_2O is generally high with Mol Na_2O/K_2O greater than 1.5. As a group the rocks are also consistently higher in CaO, FeO*, MgO, TiO_2 and P_2O_5 than other granitoids of the complex.

In contrast to the Jackfish-Weller Lakes Pluton, the late granites are peraluminous with Mol $Al_2O_3/(CaO+Na_2O+K_2O)$ generally 1.0 to 1.1 and corundum normative (<1% Corundum). The granites are relatively restricted in composition and have the highest K_2O and lowest CaO, MgO, and TiO_2.

Research Currently in Progress

The primary aim of the petrological research is to determine the magma sources of the two younger suites of granitoids within the complex. Emphasis is being placed on the distinct petrographic and chemical nature of these granitoids and their association with distinct suites of xenoliths. Some of the xenoliths are clearly country rock inclusions; however, others are believed to be cognate residual material from the anatexis of crustal sources (cf. White and Campbell, 1977). Models for the genesis of the late granitoids developed from such petrological constraints will be tested by trace element and rare earth element modelling on the granitoids, xenoliths and potential source rocks. At present crustal origins for both suites are favoured.

U-Pb zircon dates for the three major granitoid lithologies are currently under way with T.E. Krogh at the

Royal Ontario Museum. Determining the age of the gneissic suite is particularly important in understanding the history of the complex. At present the age relations between the gneiss domes and the main portion of the Wabigoon belt remains uncertain. The structural style of the domes however suggests that they may be remobilized plutons with an initially more massive fabric and therefore a date considerably older than the younger granitoids is possible. Additional dates on the younger granitoids will establish the timing of late granitoid plutonism in the Rainy Lake Complex with respect to felsic volcanism in the adjacent Wabigoon belt and other granitoids in the region.

References

Arth, J.G. and Hanson, G.N.
1975: Geochemistry and origin of the early Precambrian crust of northeastern Minnesota; Geochimica et Cosmochimica Acta, v. 39, p. 325-362.

Blackburn, C.E.
1973: Geology of the Otukamamoan Lake area, Districts of Rainy River and Kenora; Ontario Division of Mines, G.R. 109, 42 p.

1976: Geology of the Off. Lake-Burditt Lake area, District of Rainy River; Ontario Division of Mines, G.R. 140, 62 p.

Edwards, G.R. and Lorsong, J.
1976: Pipestone Lake area (Southern Half), Districts of Rainy River and Kenora; Ontario Division of Mines, Preliminary Map, P. 1103, Geological Series, Scale 1:15 840 or 1 inch to 1/4 mile. Geology 1975.

Edwards, G.R. and Sutcliffe, R.H.
1977: Straw Lake area, Districts of Rainy River and Kenora; Ontario Division of Mines, Preliminary Map, P. 1243, Geological Series, scale 1:15 840 or 1 inch to 1/4 mile. Geology 1976.

Lawson, A.C.
1888: Report on the geology of the Rainy Lake region; Geological Survey of Canada, Annual Report, v. 3, pt. 1, p. 1F-182F.

Longstaffe, F.J., McNutt, R.H., and Schwarcz, H.P.
1977: Geochemistry of Archean rocks from the Lake Despair area, Ontario: A preliminary report; in Report of Activities, Part A, Geological Survey of Canada, Paper 77-1A, p. 169-178.

Sage, R.P., Breaks, F.W., Stott, G.M., and McWilliams, G.M.
1973: Operation Ignace-Armstrong; in Summary of Field Work, Milne, V.G. Hewitt, D.F., and Wolfe, W.J., editors, Ontario Division of Mines, Miscellaneous Paper 56, p. 38-70.

Schwerdtner, W.M. and Sutcliffe, R.H.
1978: Structure and lithology of two Archean granitoid complexes, Ontario (Abst.), Geological Society of America, Abstracts with Programs, 1978.

Schwerdtner, W.M., Sutcliffe, R.H., and Tröent, Björn
1978: Patterns of total strain in the crestal region of immature diapirs; Canadian Journal of Earth Sciences, v. 15, no. 9, p. 1437-1447.

White, A.J.R. and Chappell, B.W.
1977: Ultrametamorphism and granitoid genesis; Tectonophysics, v. 43, p. 7-22.

ORGANIC MATERIAL IN THE TRANQUILLE BEDS OF THE (TERTIARY) KAMLOOPS VOLCANIC GROUP NEAR AFTON MINE, KAMLOOPS, BRITISH COLUMBIA

Project 750088

S. Creaney
Institute of Sedimentary and Petroleum Geology, Calgary

Vitrinite reflectance determinations and microscopic observations were made on 26 samples collected as part of a study of the Tranquille beds (Graham and Long, 1979) from the Afton Pit, and associated boreholes, GG 1 and GG 6, near Afton Mine, Kamloops, British Columbia (NTS 92I/9, 10). Much of the material collected contained visible vitrain stringers but some samples of shale showing no visible organic material were also taken. All samples were crushed, mounted in cold setting epoxy resin and relief polished through two grinding and two polishing stages. Microscopic observations and vitrinite reflectance determinations were carried out on a Leitz MPV2 microscope equipped with a photometer and digital display. The technique of measurement was as prescribed by the International Committee for Coal Petrology (ICCP, 1971), mean maximum reflectance ($R_{\bar{o}}$ max) being determined in all cases.

Vitrinite reflectance results

Vitrinite reflectances cover a broad rank range (Table 1), samples from the Afton pit showing a range in reflectance values of 0.61% (subbituminous) to 3.40% (anthracite). However, no correlation between reflectance and possible heat sources, to explain this' large localized variation, could be established in the pit due to the poor exposure of the Tertiary rocks and the degree of faulting although igneous material is recorded in associated boreholes (Graham and Long, 1979).

Table 1

Vitrinite reflectance results from the Afton Tertiary succession

Sample Number	Locality	Depth (if applicable)	Mean Maximum Vitrinite Reflectance % ($R_{\bar{o}}$ max)
364/78	Afton Pit	-	0.85
362/78	Afton Pit	-	0.61
363/78	Afton Pit	-	0.61
368/78	Afton Pit	-	1.76
360/78	Afton Pit	-	3.40
359/78	Afton Pit	-	0.92
354/78	Afton Pit	-	1.69
365/78	Afton Pit	-	2.31
361/78	Afton Pit	-	3.16
366/78	Afton Pit	-	0.77
367/78	Afton Pit	-	0.73
369/78	Borehole G.G. 6	78.3 m	N.D.P.
358/78	Borehole G.G. 6	422.5 m	3.95
356/78	Borehole G.G. 6	423.1 m	N.D.P.
357/78	Borehole G.G. 6	593.8 m	0.62
355/78	Borehole G.G. 6	596.5 m	0.62
391/78	Borehole G.G. 1	41.2 m	2.11
387/78	Borehole G.G. 1	43.3 m	2.04
393/78	Borehole G.G. 1	53.6 m	6.05
390/78	Borehole G.G. 1	57.0 m	N.D.P.
386/78	Borehole G.G. 1	61.0 m	1.43
394/78	Borehole G.G. 1	70.4 m	0.62
388/78	Borehole G.G. 1	72.9 m	0.55
395/78	Borehole G.G. 1	162.8 m	0.46
383/78	Borehole G.G. 1	166.0 m	0.54
384/78	Borehole G.G. 1	166.4 m	0.55

N.D.P. = No Determinations Possible

From: Scientific and Technical Notes in Current Research, Part A; Geol. Surv. Can., Paper 79-1A.

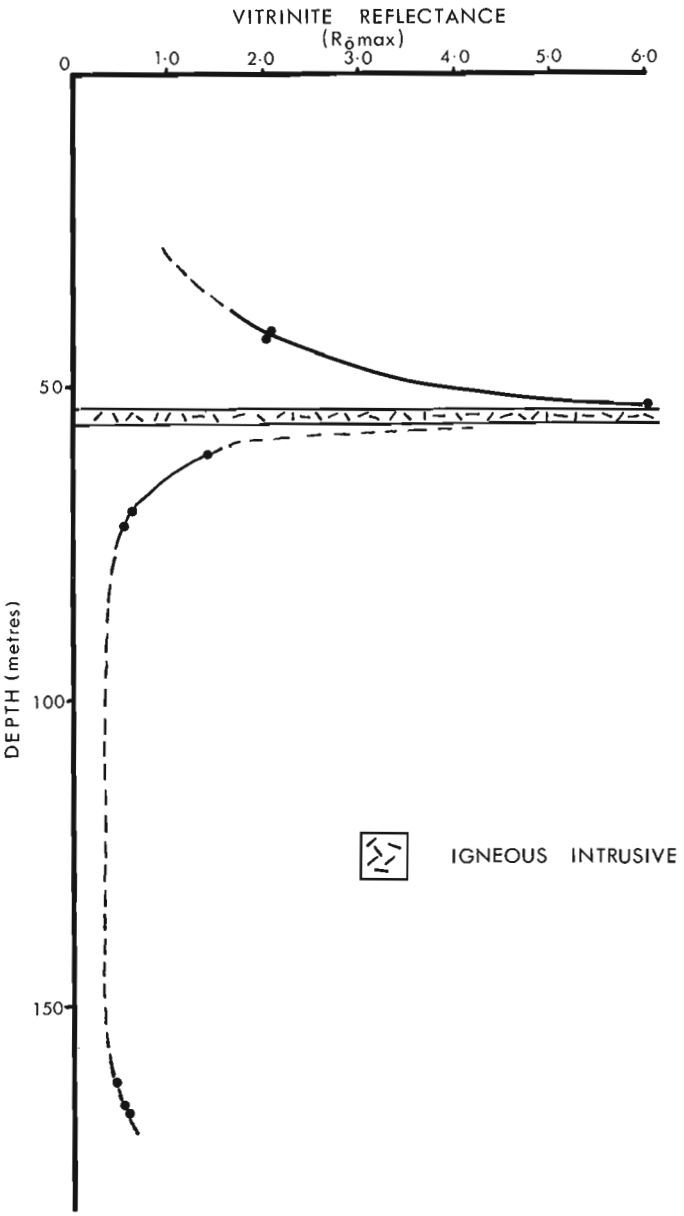


Figure 1. *Plot of vitrinite reflectance versus depth, borehole GG 1, Afton mine.*

The results of reflectance determinations on material from borehole GG 1 are shown in Figure 1. The most obvious feature is the exponential increase of reflectance towards both contacts of the igneous body, confirming it to be a sill. The background reflectance level is approximately 0.50% (subbituminous A) increasing to a measured maximum of 6.05% directly adjacent to the sill. The small increase of reflectance at the base of this hole is possibly indicative of a second, lower intrusive.

The scant data available for borehole GG 6 are presented in Figure 2. Reflectance is again very high adjacent to the upper contact of the igneous body (3.95%) indicating that this is also a sill. The two values farther from and below this body are both 0.62% (subbituminous A).

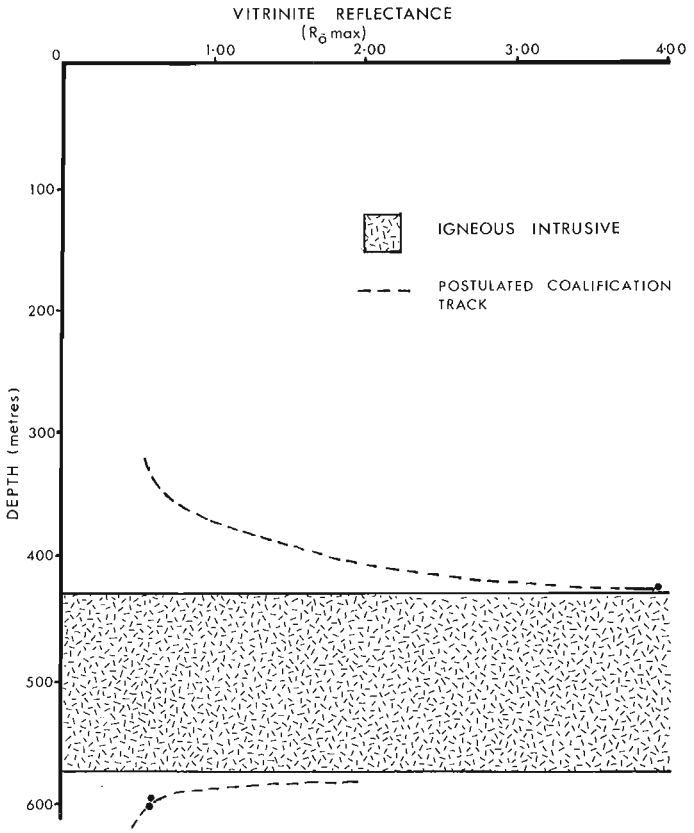


Figure 2. *Plot of vitrinite reflectance versus depth, borehole GG 6, Afton mine.*

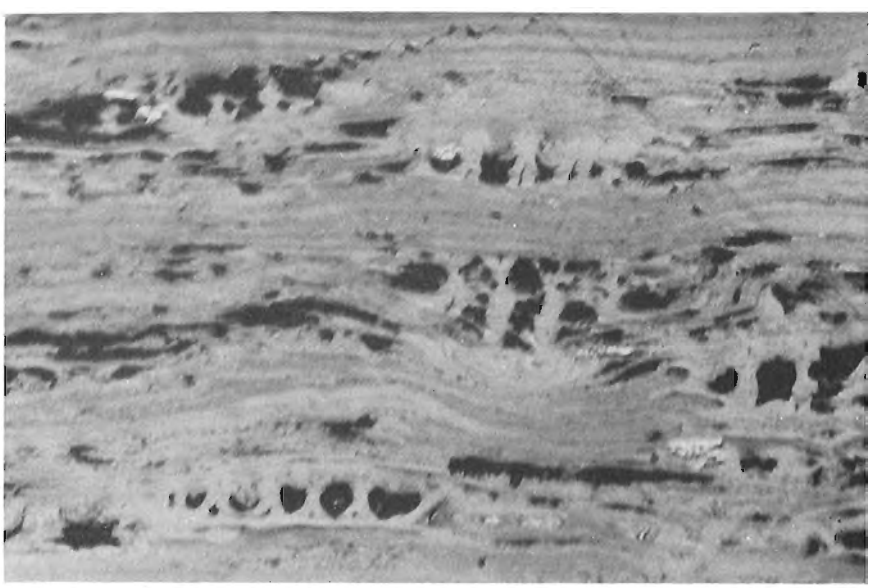


Figure 3. *Texto-ulminitic texture preserved in vitrinite ($R_{\bar{o}}$ max - 2.11), sample 391/78, x575. (ISPG 1158-36)*

It seems likely from the vitrinite reflectance data that this Tertiary sequence includes two intrusive bodies, a thick basal sill and a thinner upper sill. In this basin, background rank levels approximate the subbituminous/high volatile bituminous boundary, which is consistent with other basins of similar age in central British Columbia.

Organic Petrography

No detailed petrography has been carried out on the available organic samples but some general observations have been made. In all the low rank samples studied vitrinite is the major component, liptinites are not common and inertinites are rare. This is also true for the higher rank material with the exception that the liptinites are no longer visible due to their response to increased coalification

A peculiar feature of the thermally metamorphosed organic particles is the absence of any of the accepted features of metamorphism, such as vesiculation and loss of internal structure as described by Jones and Creaney (1977). Internal structure is, in fact, preserved to very high levels of maturity as shown by Figure 3 where a texto-ulminitic structure (common in subbituminous coal) has been retained to a rank level of semianthracite (2.11%). The only metamorphic feature observed in these samples has been the occasional development of "slits" in the vitrinite which are similar to those described by Jones and Creaney (1977, Fig. 3) from a subbituminous A coal.

It is possible that igneous metamorphism of a very low rank coal (<subbituminous) can increase the rank without destroying the original low rank textural characteristics. This possibility necessitates further investigation.

References

Graham, P.S.W. and Long, D.G.F.
1979: The Tranquille beds of the Kamloops Group: a Tertiary (middle Eocene) coal bearing sequence in the vicinity of Kamloops Lake, British Columbia; in Current Research, Part A, Geological Survey of Canada, Paper 79-1A, report 53,.

International Committee for Coal Petrology
1971: International Handbook of Coal Petrography; Supplement to the 2nd Edition, Publications du Centre National de la Recherche Scientifique, Paris, France.

Jones, J.M. and Creaney, S.
1977: Optical character of thermally metamorphosed coals of northern England; Journal of Microscopy, v. 109, pt. 1, p. 105.

LOWER DEVONIAN GRAPTOLITES IN THE ROAD RIVER FORMATION, NORTHERN BRITISH COLUMBIA

Project 610019

B.S. Norford
Institute of Sedimentary and Petroleum Geology, Calgary

Lower Paleozoic rocks of graptolitic facies extend southward from the Selwyn Basin into British Columbia as a belt between the carbonate rocks of the Cassiar Platform and those of the Rocky Mountains. The belt extends beyond the southward extremity of the Cassiar Platform to the southern part of the Rocky Mountain Trench and the Nelson map-area and continues into northeastern Washington and Idaho (Fig. 1). Various stratigraphic names have been used for these rocks (upper division of the Kechika, Cloudmaker, Sandpile siltstones, Glenogle Shales, Active Formation) and several rock units can be discriminated (Gabrielse, 1964, 1976; Jackson et al., 1965; Thompson, 1976) all of which can be regarded as members within the Road River Formation or formations within the Road River Group.

In the Ware, Mesilinka River (Fort Grahame) and Halfway River map areas of British Columbia, the predominantly shaly sequence of the Road River Formation includes volcanic rocks, sediments derived from the adjacent carbonate shelf and quartz sands eroded from the craton. These incursions into the mud regime occurred at various times and permit local lithostratigraphic subdivision of the sequence. Graptolites allow effective biostratigraphic zonation of the Ordovician rocks (Jackson et al., 1965; Davies, 1966) but only scanty dating of the Silurian rocks where graptolites not only are very rare but generally are very poorly preserved in quartz-siltstones.

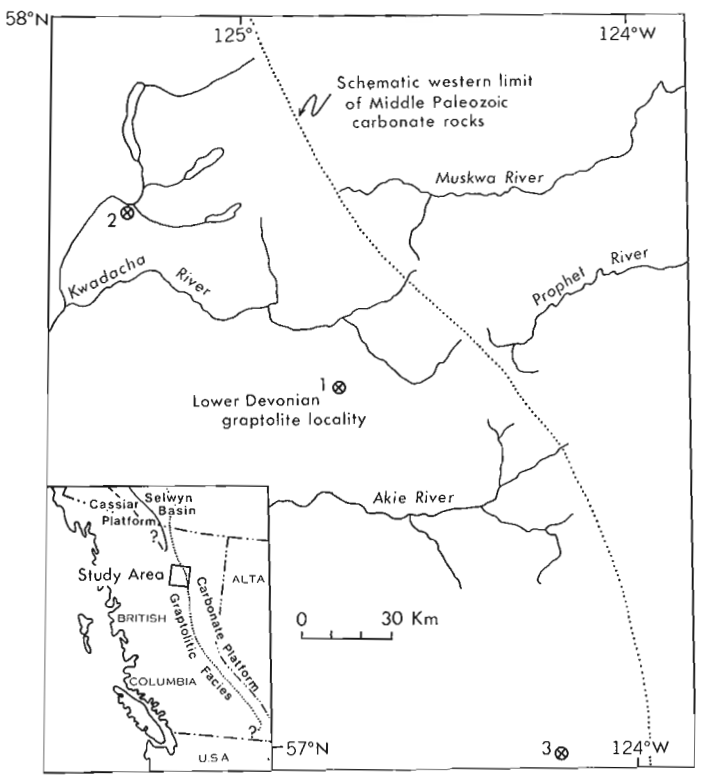


Figure 1. *Locality map showing graptolite localities.*

From: Scientific and Technical Notes in Current Research, Part A; Geol. Surv. Can., Paper 79-1A.

Lower Devonian graptolite faunas are widespread in the upper Road River Formation in the Yukon and adjacent District of Mackenzie (Jackson and Lenz, 1962, 1963, 1969; Norford, 1964; Lenz and Jackson, 1971; Jackson et al., 1978) and the following sequence of zones has been recognized:

	M. yukonensis	Zone	PRAGIAN
LOWER DEVONIAN	**M. thomasi**	Zone	
	M. hercynicus	Zone	LOCHKOVIAN
	M. uniformis uniformis	Zone	
UPPER SILURIAN	**M. angustidens**	Zone	PRIDOLIAN

In northern British Columbia, recent field studies by H. Gabrielse, G.C. Taylor and B.S. Norford have provided a number of collections that indicate the presence of Lower Devonian graptolite faunas similar to those described from the territories:

GSC locality		
	1, measured section at 57°30'N, 124°44'W.	
C-77735	dendroid graptolite **Monograptus** cf. **M. hercynicus** Perner	671-672 m
C-77734	**Monograptus** sp.	650.5-652.5 m
C-77733	**Monograptus** aff. **M. hercynicus** Perner	about 632-634 m
C-79142	**Climacograptus** sp.	402-402.25 m
(Ordovician)	**Dicellograptus** cf. **D. complanatus** Lapworth **Orthograptus** sp.	
	2, isolated outcrop at 57°43.6'N, 125°18.8'W	
C-27712	**Monograptus** sp. possibly ex gr. **M. yukonensis** Jackson and Lenz	
	3, isolated outcrop at 56°58'N, 124°12'W.	
C-27705	**Monograptus hercynicus** Perner **M. thomasi** Jaeger **M. ?telleri** Lenz and Jackson **M.** ex gr. **M. yukonensis** Jackson and Lenz	

The best preserved and most varied material is from C-27705, which was identified by D.E. Jackson (in Gabrielse, 1976, p. 26); his comments show that more than one age is represented in that **M. hercynicus** indicates the **hercynicus** Zone and **M. telleri** and **M.** ex gr. **M. yukonensis** indicate the younger **yukonensis** Zone. Berry (in Gabrielse, 1976, p. 26) reported **M. yukonensis** and **M. aequabilis? notoaequabilis** Jaeger and Stein from the same general locality as C-27705 and correlated their occurrence with the **yukonensis** Zone.

The collections indicate the presence of both the **hercynicus** Zone (C-27705, C-77733, C-77735) and the **yukonensis** Zone (C-27705, ?C-27712) in the uppermost Road River Formation of northern British Columbia. The **yukonensis** and the **thomasi** zones have not been observed in the measured section. In northwestern Canada, the **yukonensis** Zone is probably more than 200 m thick and the **thomasi** Zone is about 3 m thick (Jackson et al., 1978). The incomplete **hercynicus** Zone at the measured section is at least 40 m thick and the total thickness of the Lower Devonian part of the Road River Formation in the Ware and Mesilinka River map areas may be 200 to 300 m.

The stratigraphic section provides some data on the thickness and lithologies of the Lower Devonian rocks. The highest Ordovician collection (C-79142) probably represents the Ashgillian **Dicellograptus complanatus ornatus** Zone but possibly belongs to the older **Orthograptus quadrimucronatus** Zone. This horizon is separated from Devonian rocks by more than 60 m of faulted quartzites that probably are Upper Ordovician, followed by about 125 m of a putatively Silurian unit that weathers yellowish brown and pale reddish brown and consists of silty and platy mudstones, argillaceous siltstones, shales and argillaceous dolomites together with a quartzite member. The Devonian rocks are at least 67 m thick (631.5-699 m in the measured section) and form the top of the stratigraphic section that ends in the core of a syncline. Quartzites and dolomitic quartz-sandstones dominate; some are turbidites showing graded bedding and load casts into underlying shale interbeds. Shale-pebbles are present in some beds as are a few fragments of the coral **Favosites.** The interbedded shales amount to perhaps 25 per cent (totalling about 18 m) of the stratigraphic thickness; also present are argillaceous dolomites and dolomites rich in quartz-sand.

The graptolites are poorly preserved but those in both C-77733 and C-77735 are closely related to **Monograptus hercynicus.** The shape of the apertural part of the sicula is a criterion vital to the discrimination of **hercynicus,** this feature is not well shown in either collection and the possibility exists that the specimens may be more closely related to **M. praehercynicus** Jaeger, a slightly older Devonian species but still within the **hercynicus** Zone as recognized in Canada.

Acknowledgments

D.E. Jackson of the Open University kindly identified the graptolites from GSC locality C-27705. C.W. Jefferson participated in the study of the stratigraphic section.

References

Davies, E.J.L.
1966: Ordovician and Silurian of the northern Rocky Mountains between Peace and Muskwa Rivers, British Columbia; unpublished Ph.D. thesis, University of Alberta.

Gabrielse, H.
1964: McDame map-area, Cassiar District, British Columbia; Geological Survey of Canada Memoir 319 (dated 1963).

1976: Geology of Fort Graham E1/2 map-area, British Columbia; Geological Survey of Canada Paper 75-33 (dated 1975).

Jackson, D.E. and Lenz, A.C.
1962: Zonation of Ordovician and Silurian graptolites of northern Yukon, Canada; American Association of Petroleum Geologists Bulletin, v. 46, p. 30-45.

1963: A new species of **Monograptus** from the Road River Formation, Yukon; Palaeontology, v. 6, p. 751-753.

1969: Latest Silurian graptolites from Porcupine River, Yukon Territory; Geological Survey of Canada Bulletin 182, p. 17-29.

Jackson, D.E., Lenz, A.C., and Pedder, A.E.H.
1978: Late Silurian and Early Devonian graptolite, brachiopod and coral faunas from northwestern and arctic Canada; Geological Association of Canada Special Paper 17.

Jackson, D.E., Steen, G., and Sykes, D.
1965: Stratigraphy and graptolite zonation of the Kechika and Sandpile Groups in northeastern British Columbia; Bulletin of Canadian Petroleum Geology, v. 13, p. 139-154.

Lenz, A.C. and Jackson, D.E.
1971: Latest Silurian (Přidolian) and Early Devonian **Monograptus** of northwestern Canada; Geological Survey of Canada Bulletin 192, p. 1-25.

Norford, B.S.
1964: Reconnaissance of the Ordovician and Silurian rocks of the northern Yukon Territory; Geological Survey of Canada Paper 63-39.

Thompson, R.I.
1976: Some aspects of stratigraphy and structure in the Halfway River map-area (94B), British Columbia; in Report of Activities, Part A, Geological Survey of Canada Paper 76-1A, p. 471-477.

THERMOKARST TERRAIN NEAR WHITEHORSE, YUKON TERRITORY

Project 770031

R.W. Klassen
Terrain Sciences Division, Calgary

Introduction

Thermokarst lakes occur in some of the glaciolacustrine deposits in valley bottoms in the Whitehorse map area (National Topographic System 105 D). They are shown on surficial geology maps on a scale of 1:100 000 (Klassen, 1978) prepared as part of a surficial geology reconnaissance mapping project in the southern Yukon (Klassen et al., 1978).

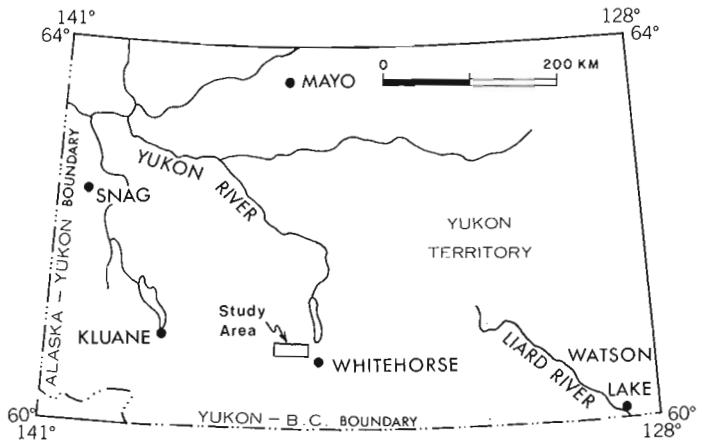


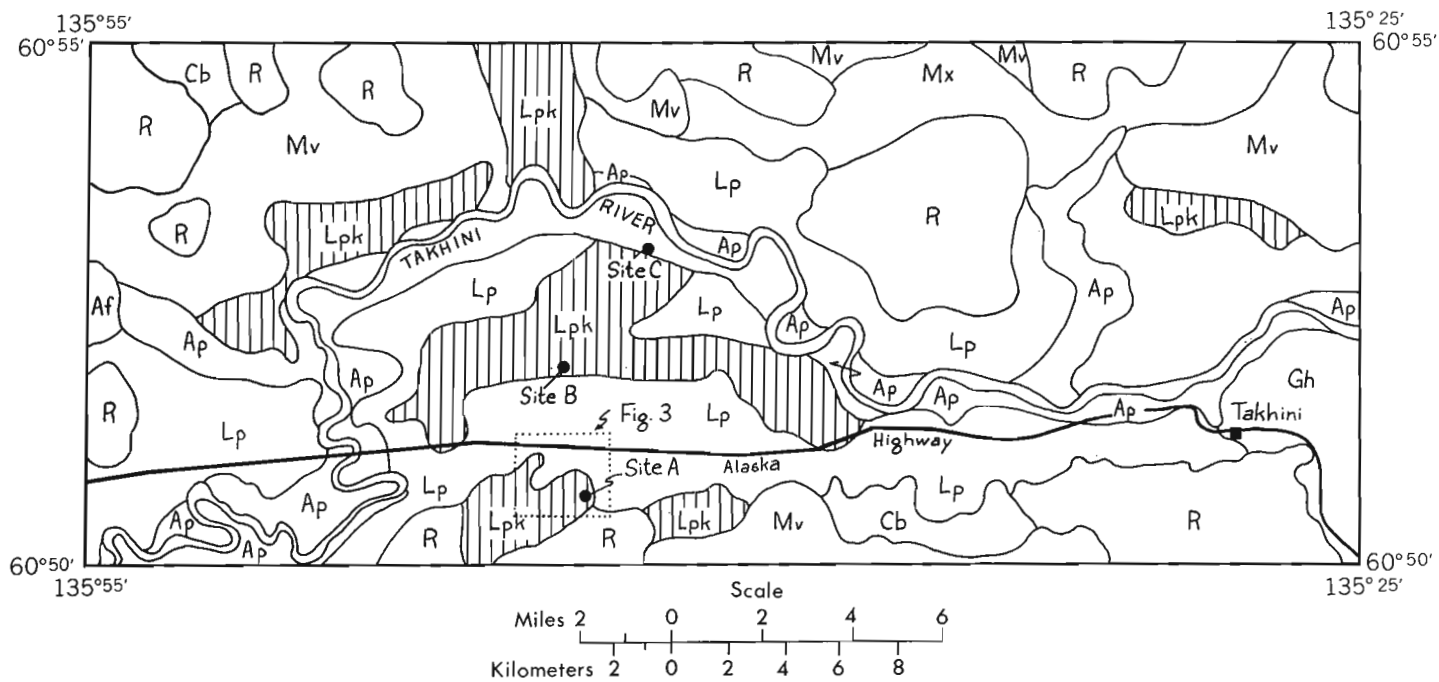
Figure 1. *Index map showing the study area.*

The most extensive occurrences are clusters of thermokarst lakes in Takhini Valley some 50 km northwest of Whitehorse (Fig. 1); the discussion of these features is based on field observations made during the summers of 1977 and 1978 and on borehole data obtained in the spring of 1978. The latter are from three sites where seven shallow boreholes were completed by EBA Engineering Consultants Ltd. of Edmonton on contract tendered by the Geological Survey of Canada and jointly financed by Foothills Pipe Lines South Yukon Ltd. and the Geological Survey of Canada.

Thermokarst is a general term applied to "karst-like topographic features produced in a permafrost region by the local melting of ground ice and the subsequent settling of the ground" (Gary et al., 1972, p. 736). The thermokarst terrain described in this report is similar to a type of thermokarst that has been referred to as "cave-in lakes" (Wallace, 1948; Gary et al., 1972, p. 112), "thaw-lakes" (Hopkins, 1949; Washburn, 1973, p. 235), or "thermokarst lakes" (Gary et al., 1972, p. 736). Although Wallace's (1948) conclusions drawn from his study of "cave-in lakes" in southeast Alaska have direct application to the features described in this report, I prefer to use the term "thermokarst lakes" because of the connotation with the term thermokarst terrain.

Thermokarst Lakes

Thermokarst lakes occur mainly in glaciolacustrine clay and silt that cover the lower Takhini valley bottom within the Whitehorse map area (Fig. 2). On aerial photographs they appear as distinct clusters of ponds nearly circular to irregularly shaped in plan. Vegetation in this area consists of scattered stands of alder, poplar, pine, and spruce, much of which appears to be second growth after a fire some 20 years ago. Sparse grasses and sedges occur over much of



cb — colluvial cover on valleysides;
Lp — glaciolacustrine plain;
Af — alluvial fan;
Gh — glaciolacustrine hummocky terrain;
Mx — valley complex;
Lpk (vertical lines) — thermokarst lake clusters;
Ap — alluvial plain and terraces;
Mv — morainic cover on valleysides;
R — bedrock hills and mountain slopes.

Figure 2. *Surficial geology of Takhini Valley in the Whitehorse area (NTS 105 D). Area enclosed by dotted line is shown in Figure 3.*

From: Scientific and Technical Notes in Current Research, Part A; Geol. Surv. Can., Paper 79-1A.

the valley floor. Two localities along the Alaska Highway just east of the Takhini River bridge were studied on the ground. One was along the southern margin of the largest cluster of thermokarst lakes, and the other was within a smaller but more distinctive cluster south of the Alaska Highway about 6 km east of the Takhini River bridge. The largest cluster is roughly Y-shaped in outline, about 8 km long and 2 km wide (Fig. 2), whereas the smaller one is about 4 by 2 km (Fig. 2,3). The surface within these areas has a local relief from 1 to 10 m and in places is some 20 m below the level of the adjacent nearly flat or gently irregular glaciolacustrine plain which is underlain by clay and silt. The depressions range from nearly circular or oval and 15 to 150 m across, to irregular outlines up to 1.5 km long (Fig. 3). Although the bottoms of most depressions are covered in part or entirely with water, some are grassy flats. One irregular bottom about 400 m long is an alkali flat.

The edges of the depressions are marked by abrupt banks 1 to 5 m high or gentle slopes covered with scattered trees, shrubs, and grasses (Fig. 3,4,5,6). Recent collapse is evident along segments of the banks and is reflected by fresh cracks along the upper parts of banks and by separated blocks and dead vegetation along the bank faces (Fig. 5). Comparison of aerial photographs taken in 1964 and 1978 indicates that some depressions have changed in size and shape, apparently as a result of collapsed banks, although most features show no obvious evidence of such changes. Actual rates of enlargement were not determined; Wallace (1948, p. 179), however, calculated rates of 6 to 19 cm per year for similar features in southeast Alaska which he based on tilting of trees along the depression margins.

Borehole Data

Seven boreholes were completed to depths of 6 to 9.5 m at three sites. Two sites are in thermokarst lake terrain (Fig. 2, sites A and B), and one site is in the adjacent alluvial plain (site C) of Takhini River. Core and grab samples were taken to provide adequate lithological control (EBA Engineering Consultants, 1978).

Three boreholes were completed at site A around a shallow, nearly circular pond about 75 m in diameter bordered by gently sloping banks 1 to 2 m high (Fig. 6). Boreholes 1 and 3 were located 10 m and 30 m, respectively, from the north shore of the pond, and borehole 2 was drilled through ice near the centre of the pond (Fig. 3,6). Ground ice up to 25 cm thick in clay (Fig. 7) was penetrated in boreholes 1 and 3, beneath 3 m of massive and varved clay; these holes were terminated in ice at depths of 9.5 m and 6.5 m

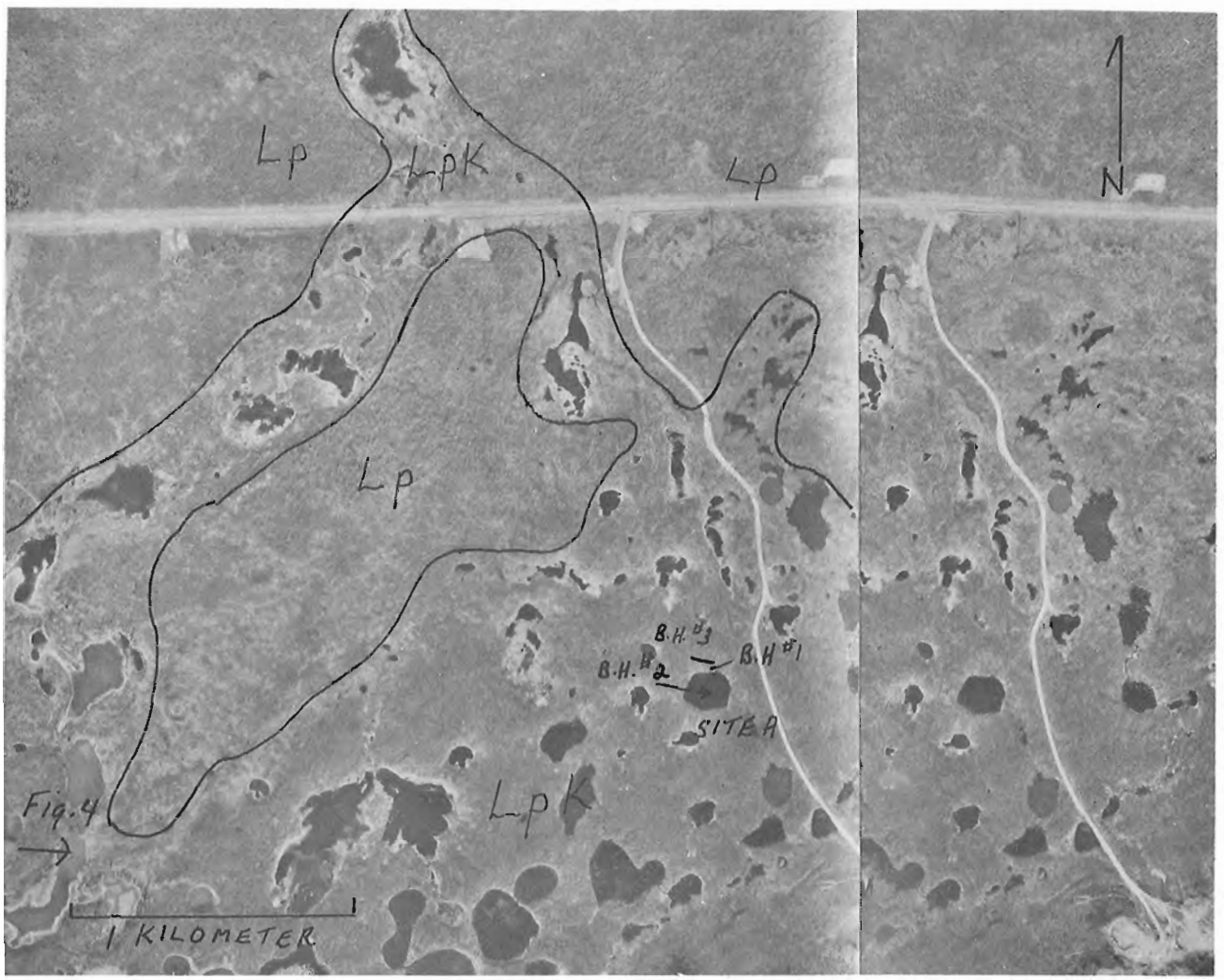


Figure 3. *Airphoto stereopair of thermokarst lake cluster (LpK) and glaciolacustrine plain (Lp). Area covered by photograph is shown in Figure 2. Three boreholes were drilled at Site A (cf. Fig. 2). (A18400-79, 80).*

respectively. Fossiliferous material (macrospores, ostracods, and mollusc fragments) occurs in the upper 0.5 m of surface material in borehole 1, but the clay below is barren. Ground ice was absent in the clay penetrated to 5 m depth in the pond covered by 0.5 m of ice over 2.5 m of water. The upper 2.5 m of clay is a pond deposit as it contains organic detritus, macrospores, and ostracods, but the lower 2.5 m is of glaciolacustrine origin as it is weakly varved and barren.

Site B (Fig. 2) is a grass bottomed depression along the southern margin of the largest cluster of thermokarst lakes. Banks up to 4 m high, marked by freshly detached blocks, rim the depression. Borehole 1, located at the edge of the bank, penetrated a 9.5 m succession of clay and ground ice similar to that found in boreholes 1 and 3 at site A. An unfrozen succession of clay and silt, beneath 2 m of seasonally frozen clay, was penetrated in borehole 2, drilled to 6.4 m depth in the depression bottom.

Site C (Fig. 2) was located in the Takhini River alluvial plain about 150 m beyond the northern edge of the largest cluster of thermokarst lakes. It is a flat-bottomed depression, oval shaped in plan, about 200 m long, with banks up to 2 m high. Parts of the banks are freshly collapsed. Borehole 1, located on the southern bank, penetrated 2.5 m of perennially frozen silt with minor ground ice stringers beneath 2 m of unfrozen silt and 2 m of seasonally frozen surface clay. Borehole 2 reached 4.5 m depth and penetrated unfrozen sandy silt beneath 1.75 m of seasonally frozen silt.

Evidence of ground ice in areas outside the clusters of thermokarst lakes is limited to the occurrence of earth flows (retrogressive-thaw flow slides?), which are evident on aerial photographs, at two localities where the Takhini River banks are cut in the glaciolacustrine plain. Ground ice was exposed in the river bank near Takhini in the summer of 1978 (V.N. Rampton, Terrain Analysis and Mapping Services Ltd., pers. comm., 1978). Boreholes drilled for Foothills Pipe Line South Yukon Ltd. in the glaciolacustrine plain outside the thermokarst lake cluster penetrated permafrost, but ground ice was absent (W.A. Slusarchuk, R.M. Hardy and Associates Ltd., pers. comm., 1978).

Conclusions

Thermokarst lakes, mostly in glaciolacustrine clay, in the Takhini valley bottom in southwest Yukon resulted from collapse due to the melting of ground ice. These features are similar in form and origin to ones named "cave-in lakes" in southeast Alaska (Wallace, 1948) and "thaw lakes" in northeast Alaska (Hopkins, 1949).

Ground ice in clay occurs from about 3 m depth to at least 9.5 m depth between depressions and is absent to a depth of at least 4.5 m below the bottoms of water-covered or grassy depressions. The thickness of the



Figure 4. *Oblique view to the east across part of the thermokarst lake cluster shown in Figure 3. Note collapsed bank in foreground. (ISPG 1143-3).*



Figure 5. *Collapsed bank along the margin of a typical thermokarst lake. Note scale in feet to right of centre. (ISPG 1151-1).*



Figure 6. *Oblique view to the southeast across the thermokarst lake where site A boreholes were located (cf. Fig. 3). (ISPG 1143-1).*



Figure 7. *Core taken at 5.3 to 5.8 m depth in borehole 1 at Site A. The light part of the core is ground ice, about 25 cm thick, between dark clay with ice stringers near contact. (ISPG 1134-19).*

permafrost layer, and its occurrence at depths greater than 4.5 m in depression bottoms, is not known. The total thickness of permafrost most likely is less than 12 m as suggested by data from boreholes to 15 m depth through permafrost in similar terrain in southeast Alaska.

Thermokarst lakes are actively enlarging in places, as indicated by freshly collapsed segments of banks and minor enlargements and changes in outlines of certain lakes. The latter is evident from comparisons of aerial photographs taken in 1964 and 1978. Rates of bank recession were not determined, although in southeast Alaska, Wallace (1948, p. 181) calculated a rate of 6 to 19 cm per year and resulting ages of thermokarst activity from 500 to 1600 years. Melting of ground ice probably was caused by the removal of an insulating ground cover of vegetation and the thermal effects of water as suggested by Wallace (1948, p. 181) for southeast Alaska. If this is so, it follows that because the vegetation cover, and probably also the vegetation history, is similar for most of the valley bottom, extensive ground ice probably only underlies the areas marked by thermokarst features.

References

EBA Engineering Consultants Ltd.
1978: Geotechnical investigation southern Yukon; report submitted to Geological Survey of Canada.

Hopkins, David M.
1949: Thaw lakes and thaw sinks in the Imuruk Lake area, Seward Peninsula, Alaska; Journal of Geology, v. 57, p. 119-131.

Klassen, R.W.
1978: Surficial geology, southern Yukon; Geological Survey of Canada, Open File 539.

Klassen, R.W., Thorsteinsson, E., and Hughes, O.L.
1978: Surficial geology and terrain evaluation, southern Yukon; in Current Research, Part A, Geological Survey of Canada, Paper 78-1A, p. 465.

Wallace, R.E.
1948: Cave-in lakes in the Nabesna, Chisana and Tanana River Valleys, eastern Alaska; Journal of Geology, v. 56, p. 171-181.

Washburn, A.L.
1973: Periglacial Processes and Environments; Edward Arnold (Publishers) Ltd., London.

Gary, M., McAfee, R., Jr., and Wolf, C.L. (ed.)
1972: Glossary of Geology; American Geological Institute, Washington, D.C.

SURFICIAL GEOLOGY NEAR THE MOUTH OF THE QUOICH RIVER, DISTRICT OF KEEWATIN

Project 760028

L. Nadeau[1] and Mikkel Schau
Regional and Economic Geology Division

Introduction

In 1978 Quaternary mapping was conducted as an adjunct to bedrock mapping in 56C/4 and east sixth of 56D/1 (see Schau and Ashton, 1979). The area is accessible by boat from Baker Lake.

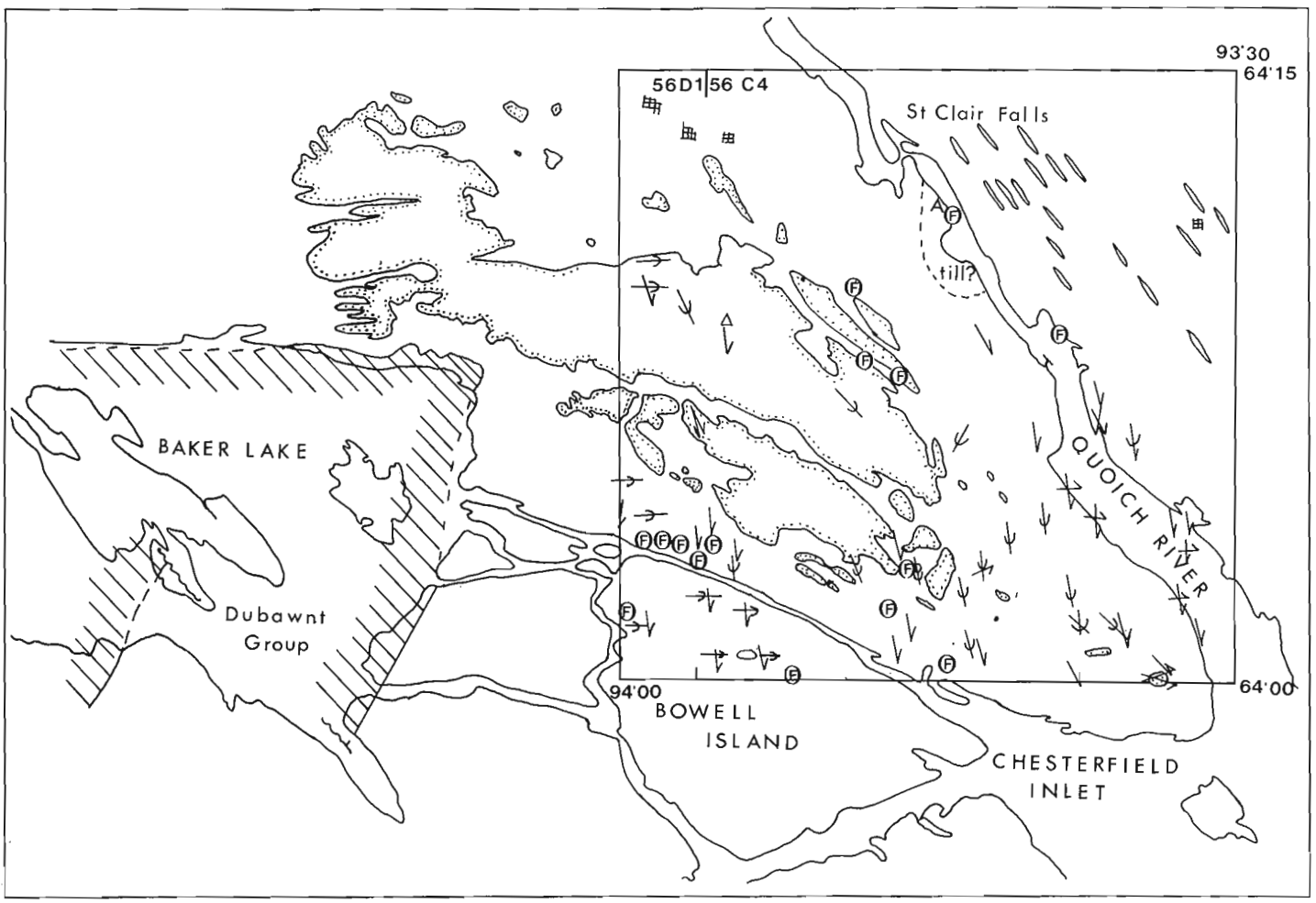
Surficial deposits

The area can be divided into two physiographic regions: a southwestern region, which is hilly and characterized by elongate lakes and oriented drainage following the well exposed bedrock structures, and a northeastern region, which is characterized by sparse outcrops and flat topography.

In the southern area the highest hills are smooth and rounded and expose anorthosites and related rocks, whereas the somewhat lower but deeply incised and more rugged topography is mainly developed in granulitic rocks. The relatively low, flat areas in the northern physiographic region are underlain by medium grade granitoid gneisses and plutonic complexes; the few hills there usually consist of amphibolite or metagabbro.

In the outcrop region the surficial geology reflects mainly glacial erosional events, although beach deposits formed during a subsequent marine inundation are locally prominent. In the northeastern region units are mainly of glacial depositional origin and have been more or less reworked by the marine inundation. In the region near 64°09'N and 93°59'W a diamicton, probably periglacially modified till, occurs near the top of ~160 m high hills. On their lower slopes are gravel beaches. Perhaps the hilltops in this region were not immersed in the Tyrrell Sea.

Glacial erosional features such as roches moutonnées, glacial grooves, glacial striae and glacial polish are well developed in the region. The distribution of some of these features is shown on Figure 1.



Legend

- Drumlinoid Feature
- Glacial Striation
- Roches Moutonnées
- Patterned Ground
- Shell Beach
- Highest Point
- 300' Contour Line
- A — Locality mentioned in text

Figure 1. *Selected glacial features in map area.*

[1] Département de Géologie, Laval Université, Québec, P.Q.

From: Scientific and Technical Notes in Current Research, Part A; Geol. Surv. Can., Paper 79-1A.



Figure 2

Roches moutonnées are well developed in the granulites and in the anorthositic complex. These larger structures are generally oriented eastward (Fig. 2a) being rounded on their west-facing sides. Finer structures such as striae are generally oriented southward across the larger easterly-directed structures (Fig. 2b). This is especially the case on Bowell Islands. In a few localities coarser, easterly-directed grooves are cut by finer (narrowed, less deeply gouged) southerly-directed ones.

Fragments of Dubawnt Group sandstones, conglomerates and volcanic rocks are common on beaches in the centre of the region mapped. They also occur on top of all hills in the western part of the area. The size of boulders and cobbles generally increases to the southwest towards the area of outcrop of the group (see Schau and Ashton, 1979), but metre-long boulders of Dubawnt Group have been seen near the centre of 56C/4. Dubawnt fragments were not seen above high-tide level east of the Quoich River. Boulders of granulite and anorthosite have been found east of their outcrop area, but only west of the Quoich River. We therefore conclude that eastward movement of considerable amounts of detritus took place. The lack of unique rock types in the north precludes any estimates about a southward flux of material.

Glacial constructional features such as drumlins are well developed in the northeast area. They trend southeasterly (Fig. 1). The glacial landforms have been modified by marine processes operating in the Tyrrell Sea. Beaches are well developed and step down towards the Quoich River. Grading is seen, with coarse boulder beaches near the top of hills and cobble to granule beaches lower down. Sandy beaches ring outcrops and drumlins in the northeast region. Large shell banks have developed throughout the area (Fig. 1). These now vary in altitude from 130 m a.s.l. to -3 m a.s.l. Their fauna, which includes **Hiatella arctica, Chlamys islandicus, Mytilus edulis, Balanus** sp., **Hemithiris psittacea,** and other genera, and its mode of preservation in well-sorted banks, indicate that they were generally nearshore assemblages. Marine clays, silts and other reworked glacial deposits apparently underlie the swampy and grassy areas in the northeastern area, as well as appearing in valley bottoms throughout the area. Mudboils have formed in regions of massive clay and shells are often arranged symmetrically on top.

Sandy fluvial or deltaic deposits are found in the upper parts of cliffs below St. Clair Falls. A massive red clay (locally a diamicton) (A, Fig. 1) is exposed in these cliffs separating the upper sandy beds from laminated to finely bedded graded grey silts. Whether the red unit is a thin till and the underlying sediments interglacial or interstadial, or whether the diamicton has an unspecified postglacial prefluvial origin must be decided by further work. W.W. Shilts (pers. comm., 1978) suggests that it has the appearance of till. The lateral extent of the red unit is not great (Fig. 1). The red clay may be derived from the only red bedrock in the region (i.e. Dubawnt Group) but the boulders in the clay are generally granitoid gneisses. A 5 cm thick shell hash with many well-preserved marine fossils rests immediately upon the red clay and a thin oxidized sand horizon overlies the shell hash.

The results presented here further constrain models of the history of the Keewatin ice divide. The earlier easterly-directed motion, followed by southerly-directed ice motion reported here, suggests that the ice divide lay to the west and later to north of the area mapped. Cunningham and Shilts (1977) and Lee (1959) have presented preliminary data on probable location and migration of the ice divide.

R.N.W. Dilabio and W.W. Shilts read earlier versions of the manuscript and their comments are acknowledged with thanks.

References

Cunningham, C.M. and Shilts, W.W.
1977: Surficial Geology of the Baker Lake Area, District of Keewatin; in Report of Activities, Part B, Geological Survey of Canada, Paper 77-1B, p. 311-314.

Lee, H.A.
1959: Surficial Geology of Southern District of Keewatin and the Keewatin Ice Divide, Northwest Territories; Geological Survey of Canada Bulletin 51, 42 p.

Schau, Mikkel and Ashton, K.E.
1979: Granulites and plutonic complexes northeast of Baker Lake, District of Keewatin; in Current Research, Part A, Geological Survey of Canada, Paper 79-1A, report 48.

NEW DATA ON UNNAMED $CaZrSi_2O_7$ FROM KIPAWA, QUEBEC

Projects 620308 and 680023

A.G. Plant and A.C. Roberts
Central Laboratories and Administrative Services Division

In their description of the occurrence of vlasovite, $Na_2ZrSi_4O_{11}$, in the alkaline rock complex at Kipawa River, Villedieu Township, Temiskaming County, Quebec, Gittins et al. (1973) reported the identification of an unnamed mineral of composition $CaZrSi_2O_7$. The material occurs as an alteration product along cleavages of vlasovite, where it forms radiating sheaves of prismatic crystals 0.1-0.3 mm long. Their small size did not permit the determination of any optical or physical properties, except that a very low birefringence was noted. Microprobe analysis showed that the material has the ideal composition $CaZrSi_2O_7$. Gittins et al. (op. cit.) suggested that it formed when calcium-rich solutions penetrated along the cleavages of vlasovite either during the late igneous history of the complex or during its subsequent regional metamorphism.

We are currently studying a suite of specimens collected from the Kipawa complex for the National Mineral Collection by H.G. Ansell, who first noted the occurrence of some small, egg-shaped pods in pegmatitic portions of the complex. These pods, (NMC specimen no. 19558) which have a maximum dimension of 2 cm, are pearly grey in colour and generally have a smooth exterior surface, sometimes stained with fluorite, against enclosing eudialyte (Fig. 1a). Thin sections of the pods show that they consist of a fine grained mixture of two phases in a texture indicative of eutectic crystallization. The texture is most clearly seen in reflected light (Fig. 1b) where the difference in reflectivity between the phases is apparent. Lenses of coarser grained material are present within the pods and consist of the same two phases as occur in the matrix (Fig. 1c and 1d). Graphite, fluorite and eudialyte were noted in the thin sections.

Qualitative microprobe analysis using an energy dispersive spectrometer showed that the phase with higher reflectivity contains only Ca, Zr, and Si, and the lower reflectivity phase only Ca, K, Si, and minor Al and Na, with no other elements detected in the spectra. Subsequent quantitative analysis (CaO 18.4, ZrO_2 40.3, SiO_2 40.8, total 99.5) showed that the higher reflectivity phase is stoichiometric $CaZrSi_2O_7$ and is chemically similar to the mineral reported by Gittins et al. (1973). The composition of the second phase (CaO 23.5, K_2O 4.5, Na_2O 0.4, SiO_2 51.0, Al_2O_3 0.4, total 79.8) is consistent with reported compositions of apophyllite.

Subsequent to the analyses, very small fragments, both of the coarser lenses (Fig. 1c) and of the fine grained matrix (Fig. 1b), were removed from the polished thin section for X-ray diffraction study. This showed that the lower reflectivity phase is indeed apophyllite. For the unnamed $CaZrSi_2O_7$, a Guinier pattern was obtained through the assistance of J. Stewart, CANMET, and the measured X-ray data are given in Table 1. These data have been indexed on a monoclinic cell by analogy with thortveitite, $Sc_2Si_2O_7$ (PDF 19-1125). The approximate unit cell parameters derived by this method were refined on the basis of 14 lines between 5.31Å and 1.668Å for which unambiguous indexing was possible. The refined unit cell parameters are: a = 6.869(4)Å, b = 8.667(8)Å, c = 4.681(2)Å, β = 101.82(3)°, V = 272.77Å^3. If $CaZrSi_2O_7$ is, in fact, isostructural with thortveitite then the space group of this new mineral is C2/m (12) and the number of formula weights per unit cell is 2.

Table 1

X-ray powder data for unnamed $CaZrSi_2O_7$**

	I_{est}	$dÅ_{meas}$	$dÅ_{calc}$	hkl
*	6	5.31	5.31	110
*	4	4.59	4.58	001
*	1	4.34	4.33	020
*	2	3.79	3.79	111
*	8	3.225	3.221	111
*	10	3.151	3.148	021
*	7	3.023	3.021	201
	7	2.655	2.656	220
			2.654	130
	1	2.478	2.479	201
			2.479	221
	<½b	2.387	2.382	131
	½	2.296	2.291	002
*	5	2.221	2.220	131
	<½	2.169	2.170	310
			2.167	040
*	2	2.153	2.152	221
*	1	2.130	2.131	311
*	1	2.105	2.104	202
	½	2.027	2.025	022
	½	2.001	1.990	112
	½	1.958	1.959	041
*	3	1.892	1.893	222
	<½	1.823	1.826	311
			1.821	240
	½	1.808	1.808	132
	½	1.767	1.771	330
	½	1.757	1.759	312
	½	1.746	1.749	331
*	1	1.735	1.735	202
	<½	1.692	1.694	401
	1b	1.677	1.681	400
			1.679	150
*	3	1.668	1.669	132
	<½	1.630	1.631	241
	<½	1.610	1.611	222
	<½	1.599	1.603	151
	<½	1.581	1.579	421
	½b	1.573	1.574	042
	½b	1.564	1.567	420
	½	1.546	1.551	151

** Guinier camera, Co $K\alpha_1$ radiation (λ = 1.7889Å). Intensities estimated visually. Diffraction lines belonging to apophyllite have been deleted.

b = broad line
* = lines used in unit cell refinement.
Indexed with a = 6.869Å, b = 8.667Å, c = 4.681Å, β = 101.82°

An electron diffraction study to test this hypothesis is planned for the near future. The probability that C2/m is correct is greatly enhanced by the fact that all Miller indices of the powder diffraction pattern conform to the space group extinction rules required for C2/m. Assuming a theoretical formula of $CaZrSi_2O_7$, the calculated density of the mineral is 3.645 g/cc.

Reference

Gittins, J., Gasparrini, E.L., and Fleet, S.G.
1973: The occurrence of vlasovite in Canada; Canadian Mineralogist, v. 12, p. 211-214.

Figure 1 overleaf.

From: Scientific and Technical Notes in Current Research, Part A; Geol. Surv. Can., Paper 79-1A.

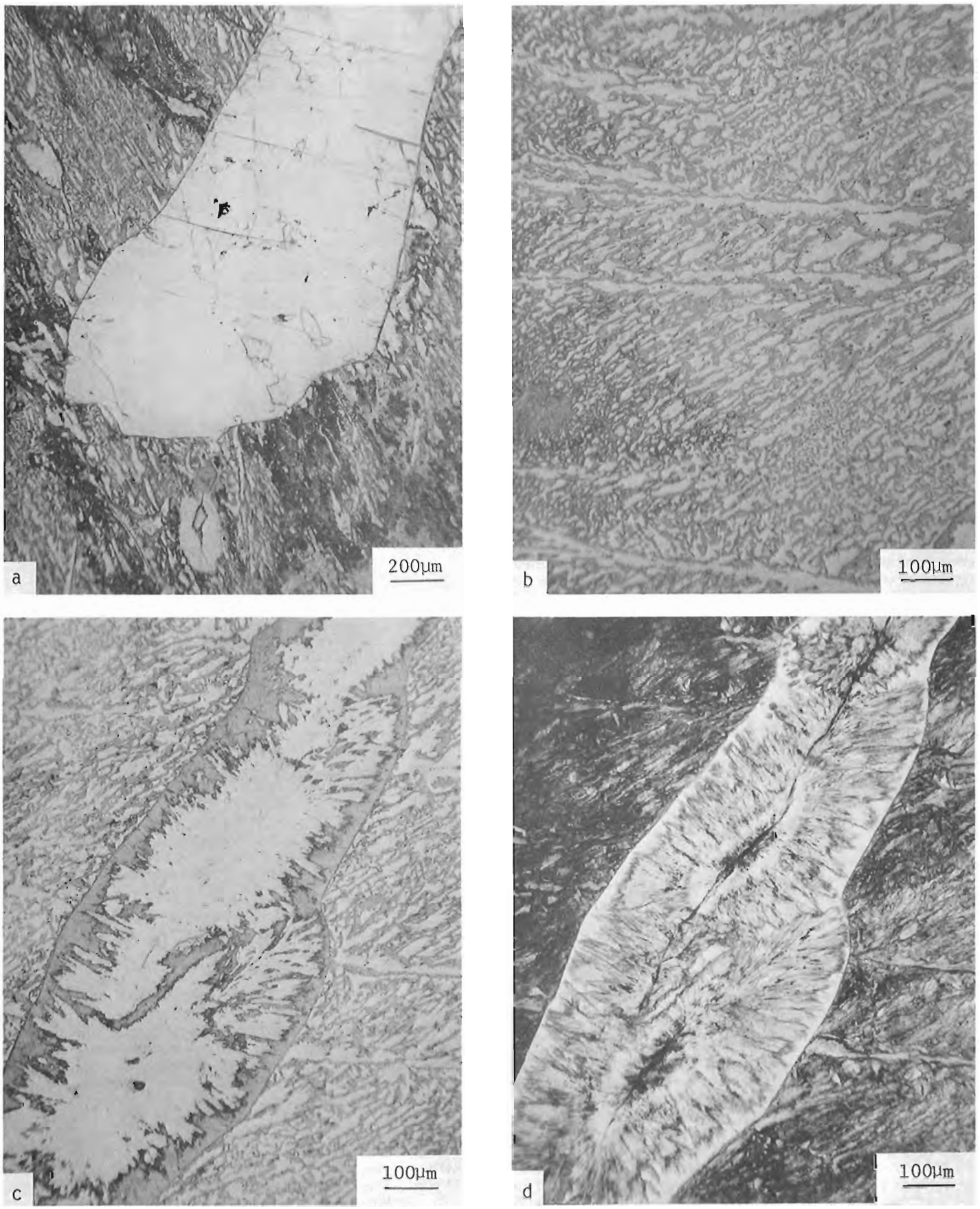


Figure 1. *(a) Sharp contact between fine-grained matrix of pod and an embayment of enclosing eudialyte. Reflected light.(b) Detail of pod matrix in reflected light showing the eutectic texture of unnamed $CaZrSi_2O_7$ (higher reflectivity) and apophyllite (lower reflectivity).(c) and (d) Reflected and transmitted light views respectivity of coarser grained lens of unnamed $CaZrSi_2O_7$ and enclosing apophyllite within the matrix of the pod.*

DISTRIBUTION AND EMPLACEMENT HISTORY OF PLUTONS WITHIN THE HOTAILUH BATHOLITH IN THE CRY LAKE AND SPATSIZI MAP AREAS, NORTH-CENTRAL BRITISH COLUMBIA

Project 770016

R.G. Anderson
Regional and Economic Geology Division, Vancouver

Introduction

Geological mapping of the Hotailuh Batholith in Cry Lake (104 I) and Spatsizi (104 H) map areas continued during the 1978 field season with the purpose of establishing the relationships between bordering volcanic rocks and the batholith, and the sequence of intrusion of plutons within the batholith. Field work was carried out with casual helicopter support provided by Operation Dease based at Dease Lake.

Field work was concentrated in the Cake Hill Pluton, the Gnat Lakes Ultramafite, and the Three Sisters Plutons and along the contact between the Cake Hill Pluton and the Beggerlay Creek Pluton (Fig. 2). Preliminary descriptions of the plutons in the Hotailuh Batholith, except for the Gnat Lakes Ultramafite, were given previously (Anderson, 1978) and additional data on the above four plutons relevant to their composition and sequence of intrusion is given below. The sequence of intrusion amongst these various plutons and also between them and the adjacent volcanic rocks is given in Figures 1 and 3.

Cake Hill Pluton

The Cake Hill Pluton consists of a homogeneous, moderately to well foliated, equigranular medium grained to coarse grained hornblende syenodiorite to granodiorite. Uncommon accessory minerals, magnetite and sphene, are widespread and elongate fine grained diorite and rounded hornblendite to hornblende gabbro inclusions were seen although they comprise much less than 1 per cent of the outcrops. Foliations in the Cake Hill Pluton east of the Cassiar-Stewart Highway are somewhat variable both on a regional (Fig. 2) and on an outcrop scale, but generally strike northwesterly and dip steeply northeast or southwest. West of the Cassiar Highway, a strong east-west trending steep to moderate northerly or southerly dipping foliation is developed in garnet amphibolite and fine- to medium-grained hornblende diorite included in the Cake Hill Pluton. Rare mineral lineations appear to have no consistent trend or plunge.

Cobbles of foliated and lineated granodiorite and syenodiorite are found in the basal basalt flow of a nonconformable sequence of volcanics and sediments of probable late Triassic age (H.W. Tipper, pers. comm., 1977). The Beggerlay Creek Pluton cuts the Cake Hill Pluton and includes blocks of cataclastized and well foliated diorite of the latter pluton at their mutual contact. Pyroxenite dykes of the Gnat Lakes Ultramafite intrude the Cake Hill Pluton and locally form an agmatite. Augite porphyry dykes are also intrusive into the Cake Hill Pluton. Apophyses of fine- to medium-grained biotite-hornblende syenodiorite of the syenodiorite-diorite

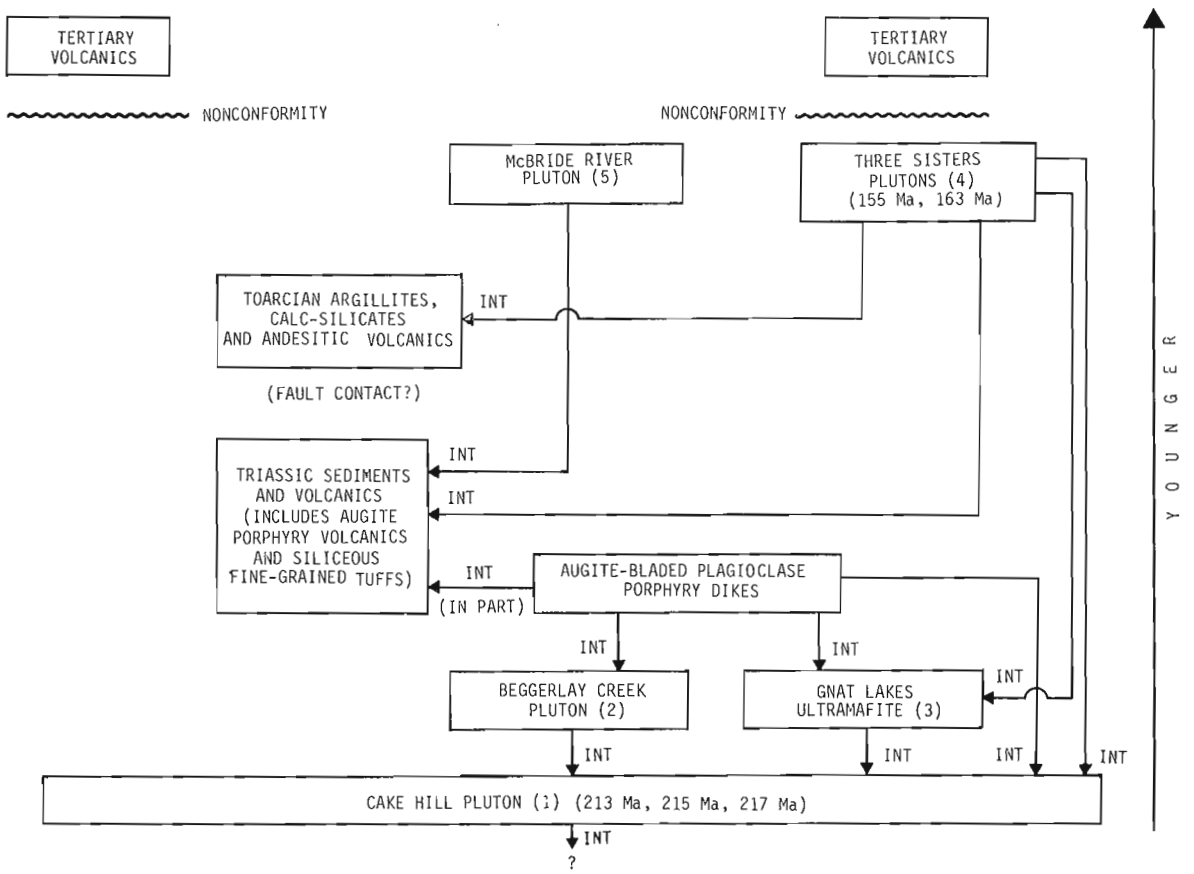
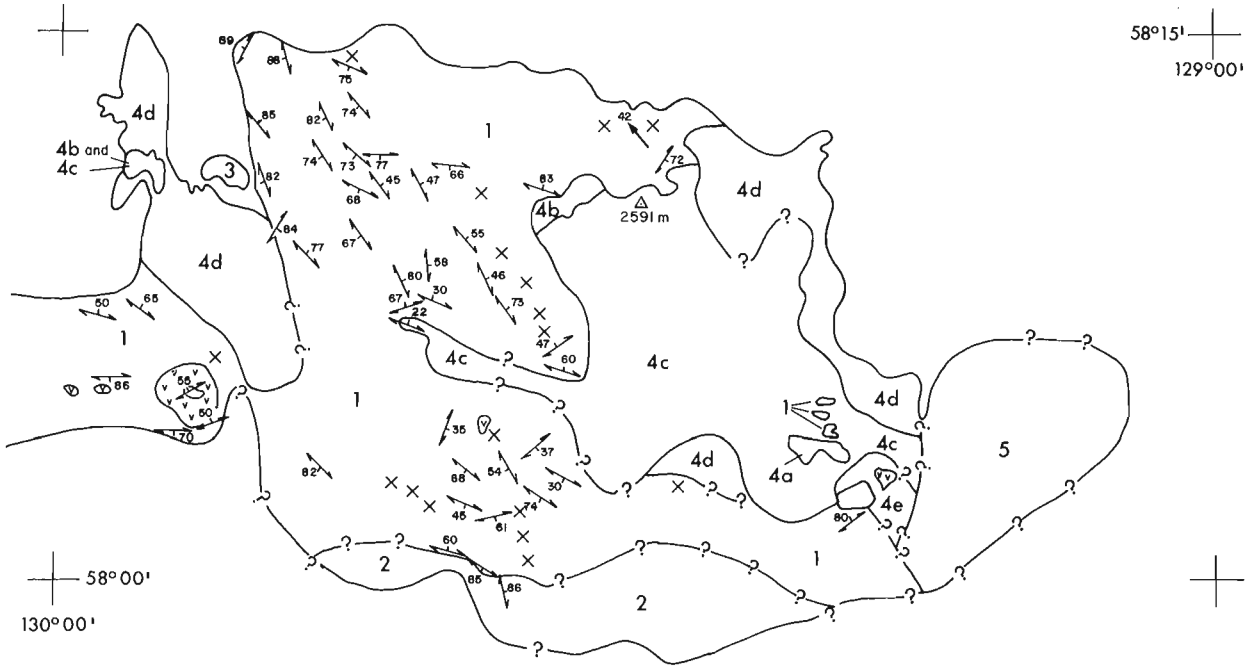


Figure 1. *Intrusive relationships amongst plutons in the Hotailuh Batholith and amongst plutons and country rock. The symbol "INT" indicates an intrusive relationship. Numbers refer to map units in Figure 2.*

From: Scientific and Technical Notes in Current Research, Part A; Geol. Surv. Can., Paper 79-1A.



LEGEND

TERITARY

Olivine Basalt

JURASSIC AND TRIASSIC

Bladed and medium-grained plagioclase porphyry, augite porphyry, andesite and andesitic volcanic breccia, siltstone, greywacke, maroon tuffs and tuffaceous mudstones, acidic tuffs and rhyolite, minor quartz arenite and limestone

TRIASSIC AND YOUNGER

THREE SISTERS PLUTONS

- 4e — LEUCOCRATIC PHASE: leucocratic hornblende quartz diorite and diorite
- 4d — POTASSIC MARGINAL PHASE: hornblende-biotite syenite, hornblende-biotite granite, hornblende-biotite monzonite
- 4c — SYENODIORITE-DIORITE PHASE: biotite-hornblende syenodiorite and diorite (155 Ma, 163 Ma)
- 4b — MAFIC PHASE: acicular hornblende diorite, equant hornblende porphyry diorite, equigranular hornblende gabbro
- 4a — FINE-GRAINED PHASE: hornblende diorite and syenodiorite

McBRIDE RIVER PLUTON

- 5 — granodiorite

TRIASSIC OR OLDER

- 3 — GNAT LAKES ULTRAMAFITE: hornblende pyroxenite, hornblende gabbro, hornblende diorite
- 2 — BEGGERLAY CREEK PLUTON: biotite-hornblende gabbro, biotite-hornblende diorite, biotite-hornblende syenodiorite, hornblende pyroxenite
- 1 — CAKE HILL PLUTON: hornblende syenodiorite, hornblende granodiorite, hornblende monzonite (213 Ma, 215 Ma, 217 Ma)

5 0 5 10 15
Km.

50 Mineral Foliation

42 Mineral Lineation

× Massive Outcrops: used only for Cake Hill Pluton. All other plutons are massive unless otherwise shown.

Figure 2. *Distribution of plutons in the Hotailuh Batholith (contacts are approximate).*

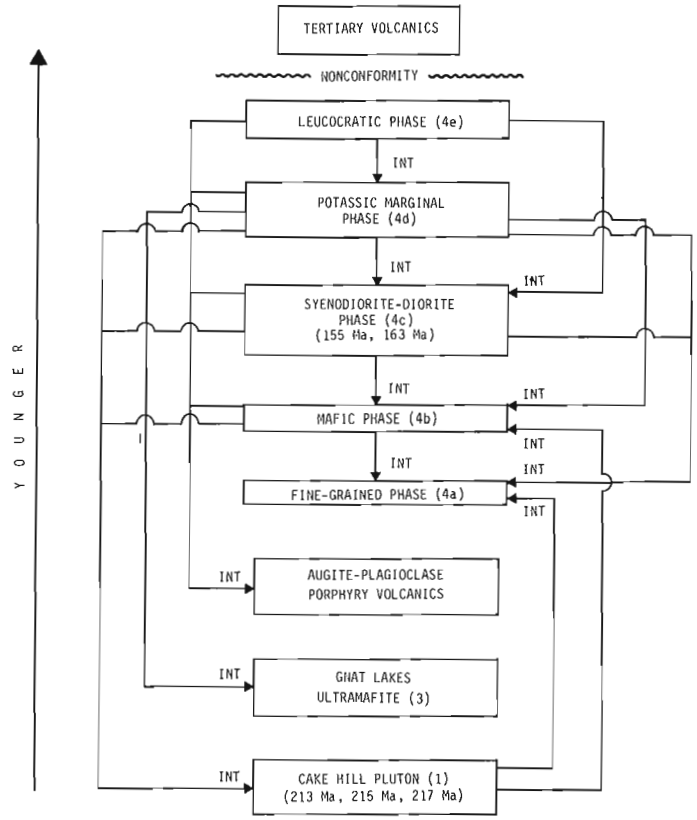


Figure 3. *Sequence of intrusion within the Three Sisters Plutons and between the pluton and country rock. The symbol "INT" indicates an intrusive relationship. Numbers refer to map units in Figure 2.*

and potassic marginal phases intrude the Cake Hill Pluton near the contacts between these bodies. Locally at the contact, inclusions of the Cake Hill Pluton are present in these younger rocks. At one locality the Cake Hill Pluton is intrusive into medium- to coarse-grained equigranular hornblende gabbro of the mafic phase of the Three Sisters Plutons. In the Cake Hill Pluton inliers in the southeastern corner of the batholith, however, chilled acicular hornblende diorite dykes are clearly intrusive. Also near the contact between the Three Sisters Plutons and Cake Hill Pluton on the northwestern flanks of peak 2591 m, the Cake Hill Pluton contains common (up to 5 per cent) large, rounded, fine grained syenodiorite inclusions which are lithologically similar to inclusions in the syenodiorite-diorite phase and to the fine grained phase of the Three Sisters Plutons. Biotite is also developed as the subordinate mafic mineral in the Cake Hill Pluton at these localities. The contact relations between the Cake Hill Pluton and the McBride River Pluton were not resolved. Fresh olivine basalt of probable Tertiary age nonconformably overlies the Cake Hill Pluton.

Gnat Lakes Ultramafite

The Gnat Lakes Ultramafite consists of a heterogeneous, medium- to coarse-grained hornblende pyroxenite with minor massive equigranular hornblende gabbro. The hornblende pyroxenite is locally layered. At one locality, coarse grained randomly oriented skeletal to acicular hornblende diorite to hornblendite alternates with medium grained pyroxenite. At another location, coarse grained hornblende pyroxenite alternates with augite porphyry. Locally, medium grained magnetite is a common accessory mineral. The intrusive relations of the Gnat Lakes Ultramafite in the Hotailuh Batholith are given in Figure 1.

Three Sisters Plutons

Five phases may be mapped within the Three Sisters Plutons: a fine grained phase, a mafic phase, a syenodiorite-diorite phase, a potassic marginal phase, and a leucocratic phase. These phases are included within the Three Sisters Plutons because they have a common spatial association and a similarity of intrusive relations with nongranitoid and other granitic rocks. The sequence of intrusion is given in Figure 3 but not everywhere is the intrusive sequence consistent or unequivocal amongst the phases especially between the syenodiorite-diorite and potassic marginal phases. The intrusive relations are deduced by observations of apophyses of dykes of one phase clearly intruding the other and/or inclusions of one phase in another. The syenodiorite-diorite and potassic marginal phases have been described by Anderson (1978) and the remaining phases comprising the Three Sisters Plutons are described below.

The fine grained phase is a homogeneous, massive, equigranular, fine grained hornblende syenodiorite. It is lithologically and petrographically similar to the fine grained dioritic to syenodioritic inclusions which comprise 2 to 4 per cent of the syenodiorite-diorite phase. The mafic phase is a moderately to very heterogeneous, massive, medium- to coarse-grained acicular hornblende diorite, equant hornlende porphyry diorite, and equigranular hornblende gabbro. All lithologies appear gradational with respect to one another. It locally contains 2 to 5 per cent small to large rounded to angular inclusions of fine grained diorite, fine- to medium-grained acicular hornblende diorite and rarely, fine- to medium-grained hornblendite with distinctive graded cumulate layering. Also, uncommon, green, metamorphosed volcanic (augite porphyry?) inclusions in a medium grained hornblende gabbro of the mafic phase were seen locally. The leucocratic phase consists of a homogeneous, massive, medium grained, equigranular, leucocratic quartz diorite to diorite with uncommon distinctive lime green, chloritized(?) hornblende. The fine grained phase and leucocratic phase lack the characteristic fine grained inclusions comprising 1 to 5 per cent of the other phases of the Three Sisters Plutons.

Reference

Anderson, R.G.
1978: Preliminary report on the Hotailuh Batholith: its distribution, age and contact relationships in the Cry Lake, Spatsizi, and Dease Lake map areas, north-central British Columbia; in Current Research, Part A, Geological Survey of Canada, Paper 78-1A, p. 29-31.

JURASSIC BIOSTRATIGRAPHY OF SKIDEGATE INLET, QUEEN CHARLOTTE ISLANDS

Project 750035

H.W. Tipper and B.E.B. Cameron
Regional and Economic Geology Division, Vancouver

The biostratigraphic studies of the Jurassic formations of Queen Charlotte Islands begun in 1974 (Tipper, 1975, 1976, 1977) were continued with particular emphasis on the Maude Formation. Extensive collections of macrofossils were made from the type section on Maude Island and from the south shore of Skidegate Inlet. Sections previously unrecognized were found and several gaps within the Maude Formation succession were filled in. These new collections, together with previously collected material (McLearn, 1949; Sutherland Brown, 1968), indicate that the Maude Formation spans all of Pliensbachian time and probably all of Toarcian time.

The Yakoun Formation was briefly examined. Collections were made from the lower volcanic part and indicate that much of Middle Bajocian time is represented. From the upper sedimentary part of the formation several collections of ammonites indicate Bathonian and Early Callovian ages and possibly Late Bajocian and Middle Callovian ages.

From collections made in 1978 and in previous years by many workers it is apparent that in the Queen Charlotte Islands a nearly complete section of Jurassic strata of Sinemurian to Middle Callovian age is present. The material available for study is abundant and among the best preserved Jurassic fauna found anywhere in the Canadian Cordillera.

The area is structurally complex. Many normal faults juxtaposed strata of different ages in an intricate mosaic. As a result, a section can only be reconstructed from many short sections on the basis of contained macrofauna and lithologic similarities. Fossil preservation is excellent but outcrop exposure is limited to intertidal areas, a few creeks, and some road-cuts.

Samples of limestone and shale from measured sections and dated by the macrofaunas were obtained for disintegration and study of the microfauna. Several samples obtained in previous years yielded abundant well-preserved radiolaria, foraminifera, ostracoda, fish teeth, and skeletal debris. Samples collected in 1978 were systematically obtained from the measured sections and if preliminary results are an indication, a well-preserved and varied microfaunal succession will eventually be obtained in this area.

References

McLearn, F.H.
1949: Jurassic Formations of Maude Island and Alliford Bay, Skidegate Inlet, Queen Charlotte Islands, British Columbia; Geological Survey of Canada, Bulletin 12.

Sutherland Brown, A.
1968: Geology of the Queen Charlotte Islands, British Columbia; British Columbia Department of Mines and Petroleum Resources, Bulletin 54.

Tipper, H.W.
1975: Taseko Lakes (92C) and Smithers (93L) map-areas, British Columbia; in Report of Activities, Part A, Geological Survey of Canada, Paper 75-1A, p. 49-50.

1976: Biostratigraphic study of Mesozoic rocks in Intermontane and Insular Belts of the Canadian Cordillera, British Columbia; in Report of Activities, Part A, Geological Survey of Canada, Paper 76-1A, p. 57-61.

1977: Jurassic Studies in Queen Charlotte Islands, Harbledown Island, and Taseko Lakes area, British Columbia; in Report of Activities, Part A, Geological Survey of Canada, Paper 77-1A, p. 251-254.

From: Scientific and Technical Notes in Current Research, Part A; Geol. Surv. Can., Paper 79-1A.

GEOLOGY OF SOME URANIUM OCCURRENCES IN WESTERN CANADA

Project 750069

R.T. Bell and L.D. Jones
Regional and Economic Geology Division

This note concerns preliminary data on some uranium (and thorium) occurrences and mineralization anomalies (Fig. 1, Table 1) investigated during the summer of 1978 in Western Canada by means of a carborne scintillometer survey (Fig. 2). Whereas conditions were not fully satisfactory to evaluate quantitatively these radiometric results, qualitative evaluation of local response was followed by immediate geological investigations. Visits to several other regions by helicopter in the Yukon established a more comprehensive regional overview. More comprehensive reports will follow.

Specimens 22 and 23 (Table 1) were found to be significantly radioactive during a routine, preliminary investigation of rock specimens stored at the Geological Survey's Institute of Sedimentary and Petroleum Geology in Calgary. K.M. Dawson sent the authors specimens 18 to 21 (ibid.). Some pertinent reports concerning these specimens are referenced here.

(A) Stewart, British Columbia

A small pluton on the Stewart road contains coarse quartz-feldspar muscovite-biotite pegmatitic phases which gave a significant radiometric response. Small dark spots contain pyrite, biotite, uraninite and cyrtolite. A selected specimen (Table 1, no. 1) contains 988 ppm U and 200 ppm Th. Elsewhere in the same pluton disseminated chalcopyrite is found associated with fractures, small shear zones and thin pegmatite dykes.

(B) Granites in southern Yukon

Granites, particularly near the Seagull Creek batholith in the Cassiar Mountains (Mulligan, 1975) and near Rose River in the Pelly Mountains (Table 1, no. 2) show a high radiometric response (up to 5 times background).

A sample (ibid. no. 3) collected in greisens containing cassiterite and arsenopyrite on the STQ claims contained 31 ppm U and 2000 ppm Th. The radioactive mineral(s) have not yet been identified.

(C) Granites in northern Yukon

A strong radiometric response is associated with mid-Paleozoic granitic rocks and their contact zones in the British and Barn mountains. The Sedgwick pluton shows up to 5 times background radiometric response in creek-bed outcrops. This response is associated with fractures and thin shear zones in the pluton. Sericite and disseminated chalcopyrite and molybdenite are also present.

Small granite stocks in the Barn Mountains have strong radiometric anomalies (up to 10 times background) associated with scheelite, arsenopyrite and molybdenite-bearing skarn zones. Some fluorescent radioactive secondary minerals are present but have not yet been identified.

(D) Sedimentary Rocks - Northern Yukon

(i) Strong radiometric anomalies are associated with basal Carboniferous(?) rudites (ibid. no. 4 and 5) immediately south of the Barn Mountains (BON claims). A similar occurrence which may be in basal Cretaceous strata (LIN claims) is found about 10 km southeast of Bonnet Lake (ibid. no. 6). These rocks occur as deeply weathered, rusty rubble or scree. No uranium minerals other than radioactive chert on fractures have been identified. The rudaceous rocks are made up of very angular to subrounded cherty fragments in a siliceous and rusty matrix. Mineralization may be directly related to intensive faulting in the area.

(ii) Radiometric Lower Paleozoic cherts and intraformational chert-breccias south of Bonnet Lake also show anomalous radioactivity (ibid. no. 7 to 10). Preliminary chemical analyses show that two specimens, no. 9 and 10 (Table 1) contain 640 and 2700 ppm Ba respectively, 359 and 20 000 ppm Sr respectively, and 12.4% and 7.8% P_2O_5 respectively. Malachite stain and pyrite are locally present. These cherts are associated with dark siliceous pelites and overlain unconformably by Carboniferous and/or Mesozoic terrigenous sedimentary rocks.

(E) Wernecke Mountains - Yukon

Three more styles of uranium mineralization in addition to those previously described (Bell, 1978; Morin, 1978) are present in the Wernecke Mountains: brannerite in quartz veins; brannerite and uraninite on the margins of pinch-and-swell quartz veins parallel with the bedding; and, masuyite-cored nodules.

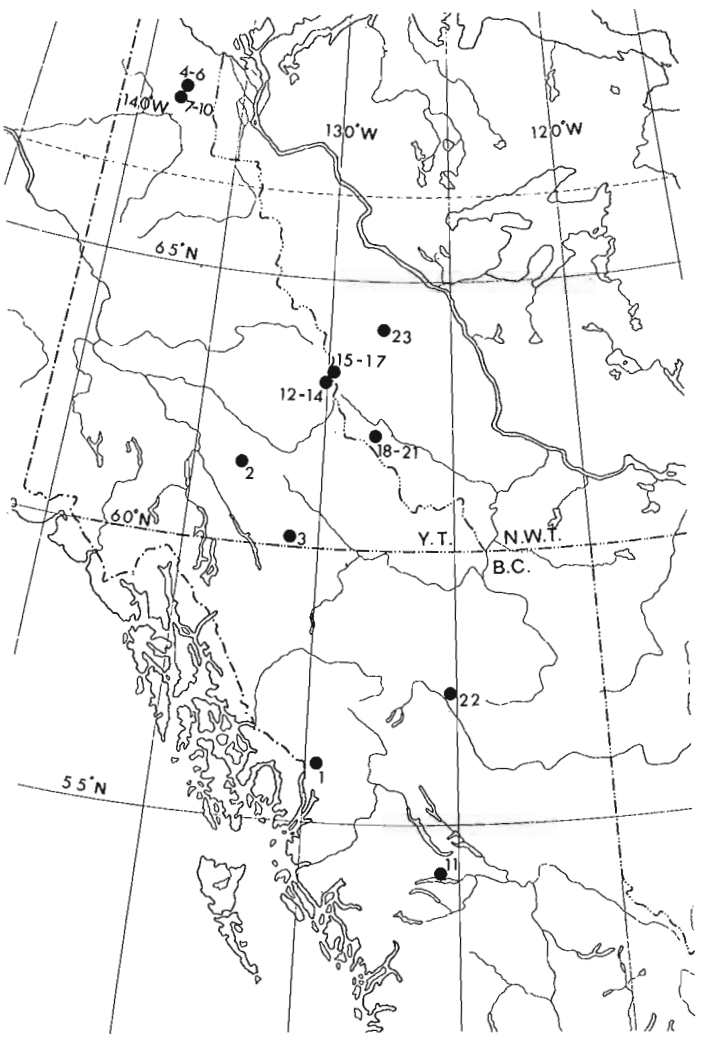


Figure 1. *Sample locations.*

From: Scientific and Technical Notes in Current Research, Part A; Geol. Surv. Can., Paper 79-1A.

Table 1

No.	Name	NTS	Latitude	Longitude	Lithology	Assoc. Elements	U ppm	Th ppm
1.	Stewart	104A	56°06'N	129°31'W	pegmatite	Cu,Mo?	988.0	200
2.	Rose R.	105F	61°32'N	133°04'W	granite	-	16.5	70
3.	STQ	105B	60°10'N	131°13'W	greisen	Sn,W,As	31.7	1226*
4.	BON	117A	68°16'N	137°47'W	cgl.	-	18.1	
5.	BON	117A	68°16'N	137°47'W	cgl.	-	405.0	
6.	LIN	117A	68°10'N	137°39'W	cgl.	-	272.0	
7.	TAB	116O	67°12'N	138°16'W	bl. shale	Cu,P,Sr	68.9	
8.	TAB	116O	67°12'N	138°16'W	breccia	Cu,P.Sr	156.0	<40
9.	TAB	116O	67°12'N	138°16'W	chert	Cu,P,Sr	52.1	<40
10.	TAB	116O	67°12'N	138°16'W	breccia	Cu,P,Sr	22.5	
11.	François L.	93K	54°05'N	125°45'W	rhy. breccia	-	14.6	<40
12.	OJV	105O	63°08'N	130°14'W	bl. shale	Pb,Zn,P,C,Ba	230.0	4.0*
13.	OJV	105O	63°08'N	130°14'W	bl. shale	Pb,Zn,P,C,Ba	50.5	
14.	OJV	105O	63°08'N	130°14'W	bl. shale	Pb,Zn,P,C,Ba	4.2	
15.	MacPass	105O	63°16N	130°06'W	breccia	Pb,Zn,P,C,Ba	33.7	
16.	MacPass	105O	63°16'N	130°06'W	breccia	Pb,Zn,P,C,Ba	31.1	
17.	MacPass	105O	63°16'N	130°06'W	breccia	Pb,Zn,P,C,Ba	39.8	<40
18.	DY883A	105I			bl. shale	Pb,Zn,P,C,Ba	247.0	<40
19.	DY883B	105I			breccia	Pb,Zn,P,C,Ba	119.0	40
20.	DY883C	105I			bl. shale	Pb,Zn,P,C,Ba	30.5	<40
21.	DY883D	105I			bl. shale	Pb,Zn,P,C,Ba	62.4	<40
22.	Kechika	94F	57°47'N	125°11'W	phos. limestone	P	196.0	8.7*
23.	Katherine	96D	64°07'N	127°51'W	sandstone	-	42.0	114*

U by neutron activation; Th by X-ray fluorescence, Th* by gamma ray spectroscopy.

(i) In the LOON claim group (NTS 106E/1; Morin, 1978), in addition to disseminated brannerite in breccias, there is coarse disseminated brannerite in thick quartz veins. The latter occurs as long striated crystals resembling coarse rutile. This, and evidence elsewhere, suggests that some of the brannerite is pseudomorphous after rutile.

(ii) West of Kiwi Lake in the DEER claim group (NTS 106E/2), in scree and frost-heaved talus, brannerite and uraninite occur at the border of concordant pinch-and-swell quartz veins in chloritic metasedimentary rocks. Minor breccia is present. In some cases very radioactive thin layers parallel with the bedding are present, but it is uncertain whether these represent a true syngenetic phenomenon or not. In some cases the pinch-and-swell quartz veins are demonstrably later than the uranium minerals.

A feature not stressed in earlier notes on the Wernecke breccias is the role of intense silicification, which along with hematization is a characteristic of almost all these breccia bodies. Quartz veining is particularly impressive in most breccias, and in the adjacent rocks, notably those containing brannerite.

(iii) At about 2 m depth in trenches on the DEER claims below the previously mentioned site there is a thin layer of irregular nodules (0.5 cm to 15 cm in diameter) containing uranophane, betauranophane, curite, kasolite and masuyite. The last mineral generally forms the cores of the nodules. Minor amounts of torbernite and autunite have also been identified. This area was originally found on the basis of a very spectacular anomaly in the regional Uranium Resources Program geochemical survey (Jonasson and Goodfellow, 1976).

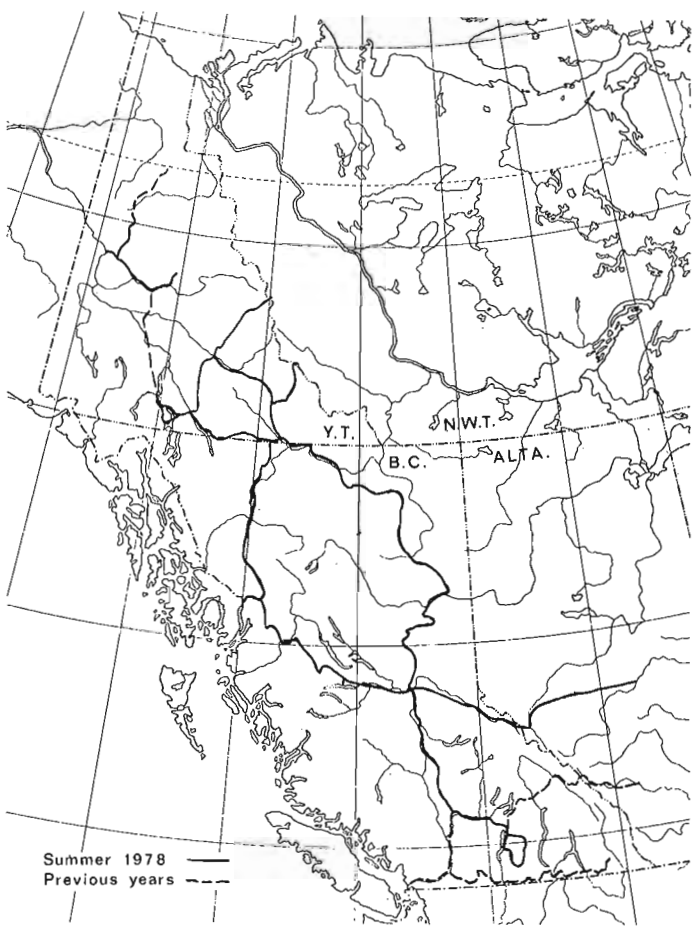


Figure 2. *Carborne radiometric survey.*

(F) François Lake, B.C.

Radiometric response over sedimentary and acid volcanic rocks of units 13 and 14 (Armstrong, 1965) is about 3 times regional response. While no significant uranium mineralization was observed, this environment warrants closer investigation (Table 1, no. 11).

(G) Uranium Associated with Shales

Anomalous radioactivity was detected in black pelites and associated rocks. Some preliminary analyses are tabulated here and include some material obtained during routine examination of specimens in Calgary (iv, below) and specimens collected by K.M. Dawson (iii, below):

(i) Lower Paleozoic cherts, shales and breccias in Northern Yukon (ibid., no. 7 to 10);

(ii) Lower and mid-Paleozoic intraformational black shales and cherty breccias in the Macmillan Pass in drill core from the JASON property (ibid., no. 12 to 14) and cherty phosphatic breccias near the Macmillan Tungsten property (ibid., no. 15 to 17);

(iii) Upper Proterozoic to mid-Paleozoic shales and phyllites which are distinctly anomalous along the Cantung Road at the Yukon-NWT border, with analyses (ibid., no. 18 to 21, see Dawson, 1979) of some black shales collected by K.M. Dawson north of this road; and

(iv) Lower Paleozoic phosphatic units in the Kechika Group collected by M. Cecile (Table 1, no. 22; see also Cecile and Norford, 1979).

(H) Proterozoic Sandstones

A grey and red mottled, fine grained quartzite specimen from routine stratigraphic sampling of the lower part of the Katherine Group collected by D. Long (Aitken et al., 1978) is modestly radioactive and contains 40 ppm U and 120 ppm Th (Table 1, no. 23).

Acknowledgments

The authors are grateful for co-operation and courtesies extended by personnel from DINA in the Yukon, and from companies working in the Cordillera, particularly Aquitaine, Archer, Cathro and Associates, Cordilleran Engineering, Dupont, Pamicon, Urangeschellschaft Canada Ltd., and Utah International.

References

Aitken, J.D., Long, D.G.F., and Semikhatou, M.A.
1978: Progress in Helikian stratigraphy, Mackenzie Mountains; in Current Research, Part A, Geological Survey of Canada, Paper 78-1A, p. 481-484.

Armstrong, J.E.
1965: Fort St. James map-area, Cassiar and Coast Districts, B.C.; Geological Survey of Canada, Memoir 252, 210 p.

Bell, R.T.
1978: Breccias and uranium mineralization in the Wernecke Mountains, Yukon Territory - A Progress Report; in Current Research, Part A, Geological Survey of Canada, Paper 78-1A, p. 317-322.

Cecile, M. and Norford, B.S.
1979: Basin to platform transition, Lower Paleozoic strata of Ware and Trutch (94C) map areas, northeastern British Columbia; in Current Research, Part A, Geological Survey of Canada, Paper 79-1A, report 36.

Dawson, K.M.
1979: Regional metallogeny of the northern Cordillera: recent stratiform base metal discoveries in Yukon and Mackenzie District; in Current Research, Part A, Geological Survey of Canada, Paper 79-1A, report 56.

Goodfellow, W.D., Jonasson, I.R., and Lund, N.G.
1976: Geochemical orientation and reconnaissance surveys for uranium in central Yukon; in Report of Activities, Part C, Geological Survey of Canada, Paper 76-1C, p. 237.

Jonasson, I.R. and Goodfellow, W.D.
1976: Uranium Reconnaissance Program: Orientation studies in uranium exploration in the Yukon; Geological Survey of Canada, Open File 388, 97 p.

Lund, N.G. and Goodfellow, W.D.
1976: Stream sediment and water geochemical reconnaissance data, northern Yukon Territory; Geological Survey of Canada Open File 419.

Morin, J.A.
1978: Uranium-copper mineralization and associated breccia bodies in the Wind-Bonnet Plume River Area, Yukon Territory; in Morin, J.A., Sinclair, W.D., Craig, D.B., and Marchand, M., Mineral Industry Report, 1976, EGS 1977-1, p. 101-107.

Mulligan, R.
1976: Geology of Canadian tin occurrences; Geological Survey of Canada, Economic Geology Report 28, 155 p.

HEALEY LAKE MAP AREA, DISTRICT OF MACKENZIE

Project 780009

John B. Henderson
Regional and Economic Geology Division

The Healey Lake map area (NTS 76B) is situated in both the Slave Structural Province and the Queen Maud Block of the Churchill Structural Province and includes part of the Thelon Front, the boundary between the two provinces. The nature of the boundary is not understood. Although there is general agreement that Archean rocks occur on both sides (Fraser, 1978), the significance of subsequent events is not clear. Thus the rocks in the Churchill Province east of the front may represent:

(1) a high grade "Hudsonian" metamorphic overprint on lower grade Archean rocks,

(2) the more deeply eroded high grade equivalent of Archean supracrustal and granitic rocks intrusive into them that are presently exposed at higher levels in the Slave Province,

(3) older crustal material that is basement to the Archean supracrustal rocks,

(4) a combination of the above.

The area is of considerable interest from a geophysical point of view as distinct gravity and magnetic anomalies, each defining a separate "front", occur adjacent to and are presumably related to the structural front. The northwest corner of the map area is underlain by the lowest grade, least deformed Archean supracrustal rocks in the Slave Province (Lambert, 1976, 1978; Henderson, 1975). Thus, within the map area, supracrustal and intrusive rocks can be traced up to and possibly across the Thelon Front through zones of increasingly intense deformation and metamorphic grade that rises into granulite facies (Fraser, 1978).

Geological mapping of the Healey Lake area at a scale of 1:250 000 was started in 1978, with two weeks being spent in the field along the Back River in the northwest part of the area. The area mapped this year is underlain mainly by greywacke-mudstone turbidites of the Yellowknife Supergroup, and is contained between the major felsic volcanic complex to the west and north (Lambert, 1976, 1978) and an intrusive quartz diorite to granodiorite batholith of probable Archean age to the east and south.

The sediments are similar to the greywacke mudstone turbidites found elsewhere in the province, although in some cases the greywackes appear to have a greater volcanogenic component. Silicate iron formation occurs locally in the succession as massive to finely laminated, slightly brownish to rusty units on the order of a metre thick. In the vicinity of the felsic volcanic complex there is an increasing proportion of siderite layers interbedded with the silicate iron formation. At the east side of the volcanic complex near the north boundary of the map area there is an extensive iron formation consisting mainly of siderite and chert (Henderson, 1975). The silicate iron formation is of interest as in the Point Lake-Contwoyto Lake region of the Slave Province gold is associated with sulphides in similar silicate iron formation. In the Back River region, however, no sulphides were seen associated with the silicate iron formation mapped thus far.

A few felsic volcanic units are intercalated in the sedimentary sequence east and south of the Back River. These vary from a massive unsorted breccia on the order of tens of metres thick with clasts up to 8 cm composed dominantly of felsic volcanics with minor mudstone clasts, to units several hundred metres thick of centimetre to metre thick layered tuff, cherty tuff and fine grained breccia. Small intrusions of felsic quartz feldspar porphyry in the sediments may have been feeders to these volcanic fragmental deposits.

The Yellowknife rocks are less deformed and metamorphosed in this area than is usual in the Slave Province. The sediments are deformed into relatively open folds, in contrast to the generally upright isoclinal folds that are so common in other parts of the province. Limbs dipping at 45° are common. The trend of axial planes is generally easterly to northeasterly. The sediments are metamorphosed. Near the felsic volcanic complex in the northern part of the area mapped this year, argillaceous sediments contain white mica, chlorite, but no biotite. The grade increases to the east and south towards the intrusive quartz diorite to granodiorite batholith. No coarse metacrysts of cordierite, andalusite or staurolite, which makes the transition from greenschist to amphibolite grade metamorphism so easy to map elsewhere in the province, were seen. However, an assemblage consisting of quartz-plagioclase-biotite-muscovite-cordierite was identified in thin section from a locality near the contact with the batholith.

The field work, under rather trying circumstances, was facilitated by the enthusiastic assistance of Edgar Froese, Allan Baxter, Paul Kavanagh and Alain Leclair. The support of the Resident Geologist's Office, Department of Indian and Northern Affairs and Helen Mary Oliver, expeditor, is greatly appreciated.

References

Fraser, J.A.
1978: Metamorphism in the Churchill Province, District of Mackenzie; in Metamorphism in the Canadian Shield; Geological Survey of Canada, Paper 78-10, p. 195-202.

Henderson, J.B.
1975: Sedimentological Studies of the Yellowknife Supergroup in the Slave Structural Province; in Report of Activities, Part A, Geological Survey of Canada, Paper 75-1A, p. 325-330.

Lambert, M.B.
1976: The Back River Volcanic Complex, District of Mackenzie; in Report of Activities, Part A, Geological Survey of Canada, Paper 76-1A, p. 363-367.

1978: The Back River Complex – A Cauldron Subsidence Structure of Archean Age; in Current Research, Part A, Geological Survey of Canada, Paper 78-1A, p. 153-158.

From: Scientific and Technical Notes in Current Research, Part A; Geol. Surv. Can., Paper 79-1A.

EVALUATION OF THE MORPHO-SEDIMENTOLOGIC CHARACTER OF THE NANAIMO RIVER DELTA TIDAL FLATS USING SELECTED REMOTE SENSING AND PHOTOGRAMMETRIC TECHNIQUES – PRELIMINARY REPORT

Project 780027

Jane Leroux[1] and J.L. Luternauer
Regional and Economic Geology Division, Vancouver

Introduction

The Nanaimo River Delta, the largest delta on Vancouver Island, is situated southeast of the City of Nanaimo on the east coast of Vancouver Island (Fig. 1). The tidal flats are primarily the subaqueous top-set beds being produced by the Nanaimo River. Sediment types on this surface range from mud to gravel although sand is most widespread.

The intertidal area is used extensively for log booming and storage by local sawmills. A general assessment of the impact of this industrial activity on local biology is included in a report prepared by Bell and Kallman (1976). It is believed that eelgrass communities and fish habitats have been adversely affected. The degradation of the estuarine environment has been related in part to increases in erosion of the intertidal surface linked to log tow-boat activity. Propeller wash and boat keels create depressions and trough-like scars which are not readily irradicated.

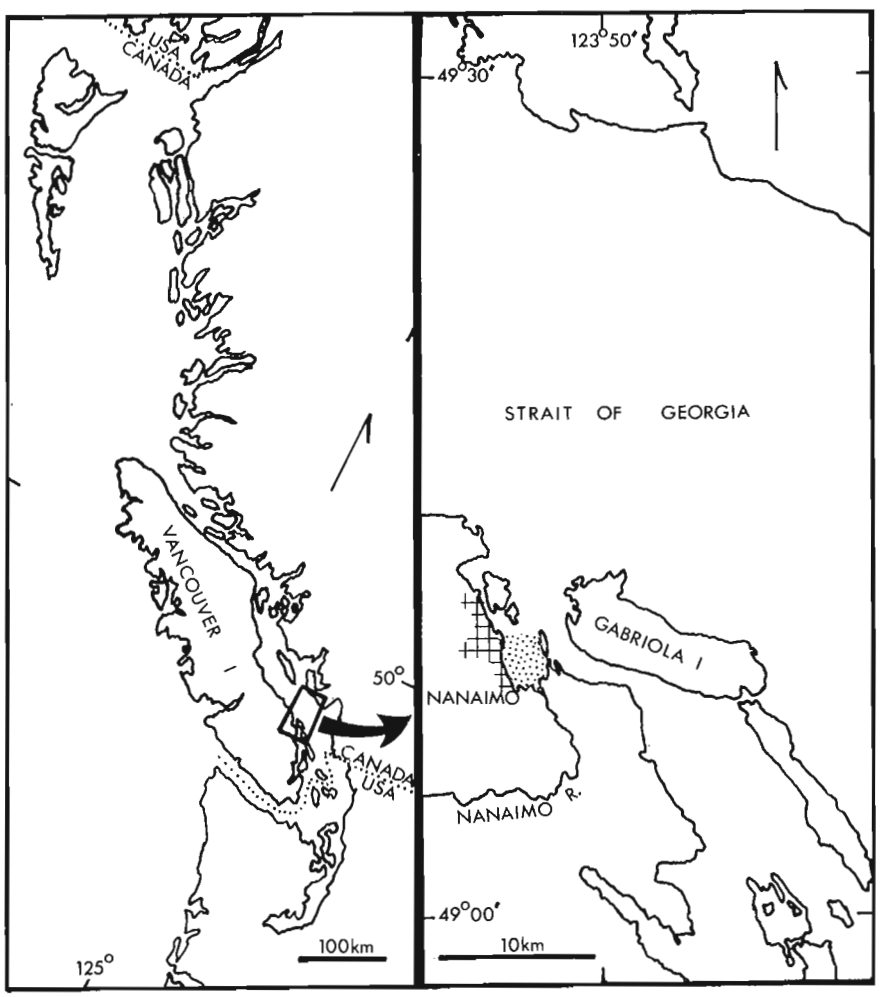


Figure 1. *Index map.*

Recent Geological and Biological Surveys

Generalized mapping of the intertidal sediment distribution was performed in 1976 by the Pacific Biological Station and Department of Geological Sciences at the University of British Columbia (J. Sibert, pers. comm.). During the summer of 1978 a survey was initiated (by Pacific Biological Station) to map precisely the areal distribution of eelgrass beds.

Focus of this Study and Techniques to be Employed

Adequate environmental management and land use planning in the Nanaimo Estuary can be more effectively accomplished if natural and man-imposed alterations to sediment distribution and morphology are more precisely distinguished. As a first step in this effort a thesis study has been initiated (involving the co-operation of the Geological Survey of Canada, Department of Geological Sciences at the University of British Columbia and photogrammetric facilities at the British Columbia Institute of Technology). The investigation will consist primarily of mapping sediment distribution from low level colour and colour infrared aerial photography and photogrammetric mapping of morphology from a set of historical aerial photographs.

Colour and colour infrared aerial photographs were simultaneously exposed over the Nanaimo River Delta at scales of 1:4000 (Fig. 2) and 1:9000, respectively, on June 20, 1978 at low tide. On June 23, 1978, colour and colour infrared photographs were exposed simultaneously with a radiometer at low tide. From this photography and sensitometry, a large scale detailed sediment distribution map will be produced. On July 18, 1978, twenty-nine surface samples were collected from the Nanaimo River Delta tidal flats during low water with the aid of a helicopter. This ground truth will serve as control data during the preparation of the sediment map from the air photos.

Photogrammetric analysis of intertidal morphology will consist of the aerial triangulation of and subsequent precise mapping of features evident on aerial photographs exposed on May 17, 1958 at a scale of 1:16 000 acquired from the Government of British Columbia. The morphologic stability of the tidal flat surface will be assessed by comparing the compiled map to a detailed topographic map of the present intertidal surface prepared by the Pacific Biological Station.

Acknowledgments

The assistance of Dr. C. Godwin, Department of Geological Sciences, University of British Columbia in the preparation of the photographic plate of the airphoto mosaic is greatly appreciated.

Reference

Bell, L.M. and Kallman, R.J.
1976: The Nanaimo River Estuary – Status of Environmental Knowledge to 1976; Special Estuary Series No. 5, Report of the Estuary Working Group, Department of the Environment, Regional Board, Pacific Region, 298 p.

Figure 2 overleaf.

[1] Department of Geological Sciences, University of British Columbia, Vancouver, B.C.

From: Scientific and Technical Notes in Current Research, Part A; Geol. Surv. Can., Paper 79-1A.



Figure 2. *Mosaic of colour aerial photographs exposed over the Nanaimo River Delta on June 20, 1978 at 600 m a.s.l. At the southern end of the tidal flats, the Nanaimo River bifurcates and major distributaries follow the western and eastern margins of the tidal flats. The vegetated marsh extends approximately 1 km seaward from the bifurcation. Beyond it the surface of the flats is covered with a patchwork of muds, sands, gravels and log booms. The bar scale represents 1.5 km.*

FROST HEAVE AT GROUND TEMPERATURES BELOW 0°C, INUVIK, NORTHWEST TERRITORIES

Project 680047

J. Ross Mackay[1] J. Ostrick[2], C.P. Lewis[2], and D.K. MacKay[3]
Terrain Sciences Division

Introduction

It is well known from numerous laboratory studies that volume changes can occur in many fine grained soils when temperatures are lowered below 0°C. In 1975 a field program was started at Inuvik, Northwest Territories to determine if volume changes could be measured in the active layer after the entire active layer had cooled to below 0°C and had frozen through to permafrost. The purpose of this report is to show that ground surface heave of at least 2 cm had been measured at Inuvik in the January to May period after the active layer had frozen through to permafrost. The Inuvik results are of potential importance to the assessment of long-term heave in frozen ground at temperatures below 0° such as might occur when permafrost aggrades around a cold buried gas pipeline over a period measured in years.

Field Site

The field site selected for the study is 3 km north of Inuvik where clayey mud hummocks, 1 to 2.5 m diameter, are numerous. The hummocks are composed of colluvium with about 50% of the particles finer than 0.002 mm; the liquid limit is about 40% or higher; and the unfrozen water content, based upon the specific surface area of the hummock clays, is estimated at about 9% at -5°C and 7% at -10°C (Mackay and MacKay, 1976). Part of the experimental site had been bulldozed in 1968 at the time of the Inuvik fire.



Figure 1. *A telescoping heavemeter ready for insertion at Inuvik, Northwest Territories.*

[1] Department of Geography, University of British Columbia, Vancouver, B.C. V6T 1W5
[2] Inuvik Research Laboratory, Inuvik, Northwest Territories
[3] Environment Canada, Ottawa

From: Scientific and Technical Notes in Current Research, Part A; Geol. Surv. Can., Paper 79-1A.

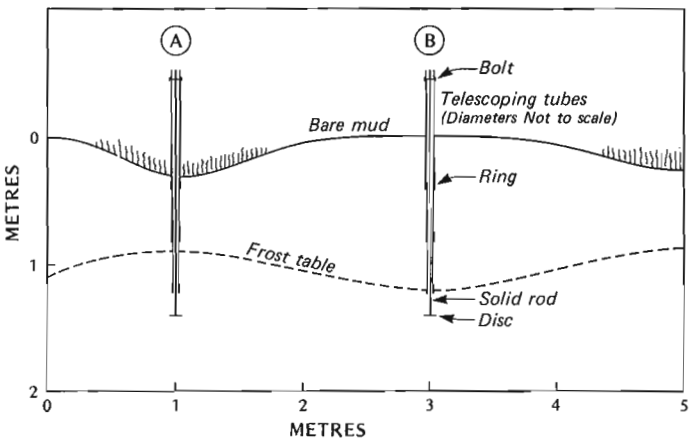


Figure 2. *Schematic diagram of telescoping tubes with one set being installed in an interhummock depression, the other in the hummock centre. The bolts serve to keep the tubes in position during insertion.*

Field Instrumentation

Ground temperatures were measured with thermistors installed in two hummocks. Three different methods were used to measure frost heave:

First, three vertical invar rods were anchored in permafrost to serve as datum bench marks, and the height changes of six invar spindles, resting on the bare centre of one hummock, were referenced to the datum rods by a conventional "bedstead" arrangement (cf. James, 1971, p. 10-12). Height changes were measured with a micrometer to an accuracy of better than 1 mm.

Second, five heavemeters were used to monitor differential heave at the site (cf. Baracos and Marantz, 1953). The heavemeter assemblage used at Inuvik consisted of four telescoping aluminum tubes with a solid rod in the centre (Fig. 1). The centre rod had a disc strongly attached to the bottom, and the tubes and rod were held in position by a bolt at the top (Fig. 2). The telescoping units first were inserted into augered holes with the discs of the central rods anchored in permafrost; the bolts then were removed to permit up and down movement of the telescoping tubes (Fig. 3). Changes in height were measured with a micrometer depth gauge to an accuracy of better than 1 mm.

Third, wooden stakes 2 cm in diameter and 40 cm long were driven to a depth of 20 cm, and then the tops of the rods were levelled with reference to the three datum invar rods mentioned above. A total of 47 stakes was used, 38 being located so as to monitor heave of a bare mud hummock and the surrounding interhummock depression; 9 stakes were placed in the centres of 9 different mud hummocks in an area that had been bulldozed in 1968 at the time of the Inuvik fire and where the active layer was unusually deep. The accuracy of the survey was to 1 mm or better.

Frost Heave Components

Although a great deal is known about frost heave in temperate regions, it is difficult to identify the specific cause(s) of ground surface frost heave in a cold permafrost environment, because the observed heave may result from the interplay of more than one factor, viz.:

1) Sublimation of ice from the top of the active layer to the overlying snow to produce a loose, friable surface layer. The contribution to frost heave is unknown.

2) Frost heave from ice lensing near the top of the active layer from downward freezing. This produces a positive heave.

3) Frost heave from ice lensing near the bottom of the active layer from upward freezing. This produces a positive heave.

4) Consolidation of the mid-portion of the active layer by water loss to the upper and lower freezing fronts (Tsytovich, 1975, p. 60-61). This produces a desiccated zone, usually in the lower half of the hummock, and presumably a ground contraction or negative heave.

5) Progressive freezing of unfrozen pore water as the active layer is cooled below 0°C. This normally would produce a positive heave, but laboratory experiments have shown that under certain conditions there may be contraction and negative heave. The effect would depend upon the source of the water and the site of freezing.

6) Formation of cavities within the active layer by differential heaving. This produces a positive heave. A cavity 5 cm high was observed in a hummock excavated in April 1978 near Inuvik.

Discussion

The field measurements show that ground surface heave averaging 1 to 2 cm has occurred at the Inuvik experimental site following the freeze-back of the active layer to the top of permafrost. Although thermistors were not located at each hummock whose surface changes were being measured, nearby temperature measurements suggest that freeze-back was complete by early December and certainly was complete by December 31 in 1976 and 1977. Ground surface heave was registered by each of the three different methods used in the study:

First, heave was measured from all six invar spindles; the results for spindle number 2 are plotted in Figure 4. As shown in the graph, there was a heave of 1 cm in the period January to May 1978, this heave being equal to the volume expansion in the freezing of 10 cm of water.

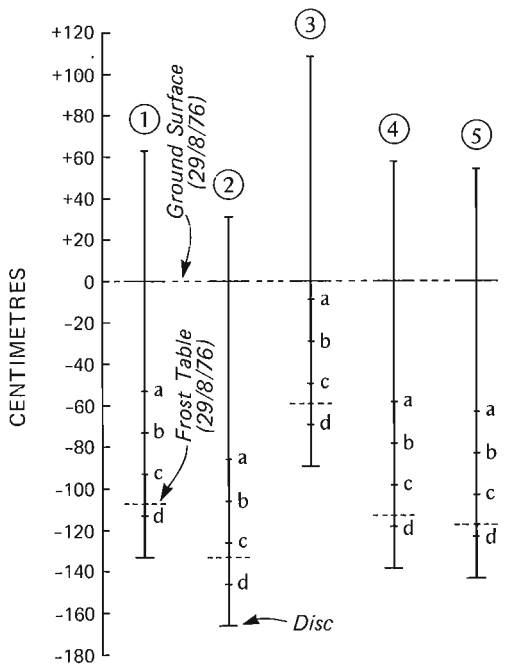


Figure 3. *The depth of the active layer and positions of the telescoping tubes are shown for the installation date, August 28, 1976.*

Second, the differential movements of the five telescoping heavemeters are plotted in Figure 5. Since the heaves of the shortest tubes (a in Fig. 3) accompanied the onset of freezing, heave was doubtless due to ice lensing near the ground surface. Ice lensing decreased with depth as shown by the smaller uplifts of the longer tubes (b, c, and d) which extended to greater depths and then were not affected by near surface ice lensing. In January and February 1978, tubes b and c in heavemeter number 2 and tubes a, b, c, d in heavemeter number 3 all decreased in height relative to the centre datum rod. Such a decrease suggests consolidation of the mid-portion of the hummocks from upward and downward

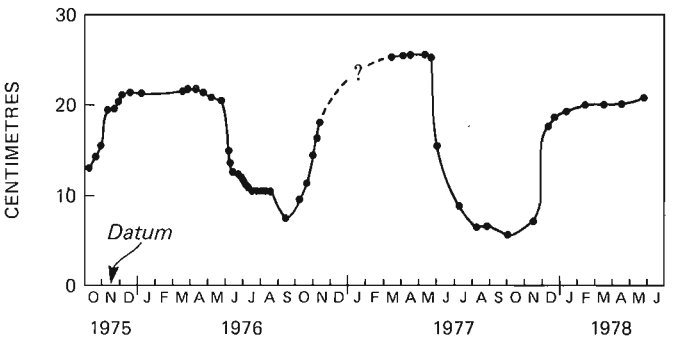


Figure 4. *Graph showing the amount of heave of one of the six invar spindles (number 2) which rested on the surface of a mud hummock.*

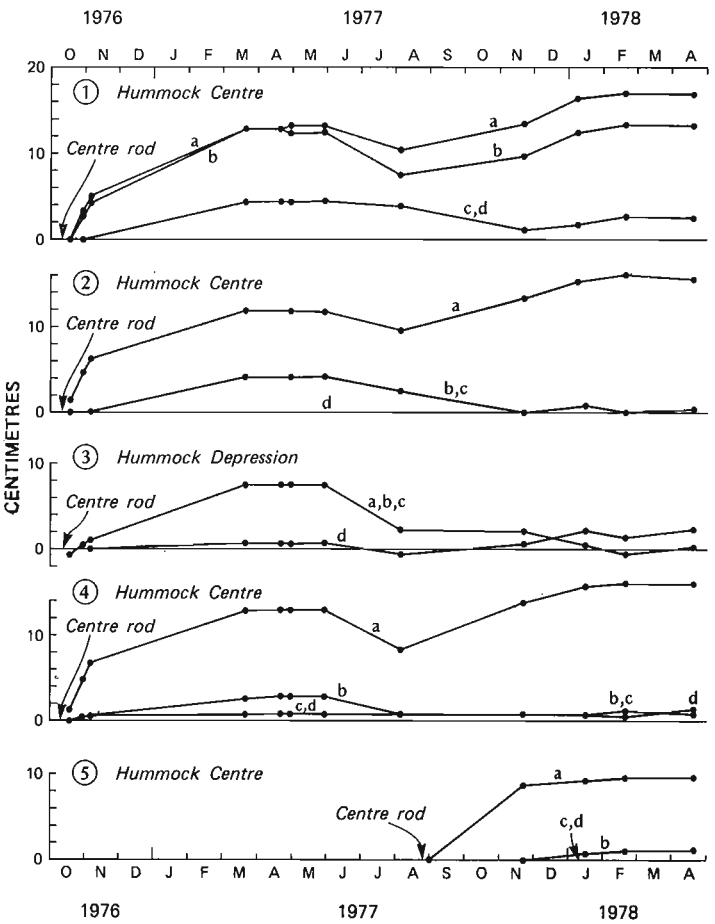


Figure 5. *Graph showing the amount of heave of the five sets of telescoping (tubes a, b, c, d) heavemeters referenced to their datum centre rods.*

Table 1

Mean ground surface heave (in cm) for hummock areas, Inuvik, Northwest Territories, 1977-1978

	Number of Observations	1977		1978						
		Oct. 4	Nov. 16	Dec. 15	Jan. 7	Feb. 1	Mar. 14	Apr. 18	May 15	May 31
Undisturbed Site	38	0.00 (datum)	4.70	8.84	9.87	10.08	10.25	10.21	10.29	10.39
Disturbed Site	9	0.00 (datum)	6.52	9.83	12.03	13.16	13.91	13.88	13.98	14.09

water loss to the freezing planes, i.e. a negative heave. The ground surface heave for the period 1976-77 ranged from 8 cm in an interhummock depression of heavemeter number 3 to 13 cm for the hummock centre for number 1 (Fig. 5). If heave arose solely from the volume expansion of the freezing of pore water at each site, about 80 cm of water would have been required to produce a surface heave of 8 cm in the interhummock depression and 130 cm for a heave of 13 cm in the hummock centre. But as the active layer for heavemeter number 3 was only 60 cm on August 29, 1976 and from 110 to 135 cm thick for heavemeters 1, 2, and 4, substantial amounts of pore water therefore must have migrated from adjacent areas and then frozen in order to account for the observed heaves.

Third, the ground surface heave averaged for 38 wooden stakes placed across one hummock and in the surrounding depression and for the 9 stakes placed in the centres of 9 individual hummocks in a bulldozed area are shown in Table 1. The datum used for each stake was the height of the stake on October 4, 1977 at the commencement of the freeze-back period. The mean heave of the 38 stakes from January 7 to May 31, 1978 was 0.5 cm or equivalent to the heave expected from the freezing of 5 cm of water. The mean heave of the 9 stakes in the bulldozed site, where the active layer was thicker, for the same January to May period was 2 cm, or equivalent to the heave from the freezing of 20 cm of water.

Conclusion

Frost heave of the ground surface at Inuvik in an area of fine grained soils has been shown to occur from January to late spring after the entire active layer was at a temperature below 0°C. The frost heave, following complete freeze-back of the active layer, has been measured by the heave of six invar spindles referencd to a datum; by differential heave of 5 sets of telescoping tubes, each set referenced to its own datum; and by levelling 47 stakes, each referenced to a datum. The cumulative results show that ground surface heave of 1 to 2 cm has occurred after January, with some heave continuing until May. The amount of heave seems directly related to the thickness of the active layer. At present, data are insufficient to permit a detailed analysis of the components which produced the measured heave. The telescoping tubes performed satisfactorily, and they can be used in remote areas to monitor total and, to some extent, differential heave at a site.

References

Baracos, A. and Marantz, O.
1953: Vertical ground movements; Proceedings, Sixth Canadian Soil Mechanics Conference (Winnipeg); National Research Council of Canada, Tech. Mem. 17, p. 29-36.

James, P.A.
1971: The measurement of soil frost-heave in the field; British Geomorphological Research Group, Tech. Bull. 8, 43 p.

Mackay, J.R. and MacKay, D.K.
1976: Cryostatic pressures in nonsorted circles (mud hummocks), Inuvik, Northwest Territories; Canadian Journal of Earth Sciences, v. 13, p. 889-897.

Tsytovich, N.A.
1975: The Mechanics of Frozen Ground; McGraw Hill, 426 p.

NOTE TO CONTRIBUTORS

Submissions to the *Discussion* section of *Current Research* are welcome from both the staff of the Geological Survey and from the public. Discussions are limited to 6 double-spaced typewritten pages (about 1500 words) and are subject to review by the Chief Scientific Editor. Discussions are restricted to the scientific content of Geological Survey reports. General discussions concerning branch or government policy will not be accepted. Illustrations will be accepted only if, in the opinion of the editor, they are considered essential. In any case no redrafting will be undertaken and reproducible copy must accompany the original submissions. Discussion is limited to recent reports (not more than 2 years old) and may be in either English or French. Every effort is made to include both *Discussion* and *Reply* in the same issue. *Current Research* is published in January, June and November. Submissions for these issues should be received not later than November 1, April 1, and September 1 respectively. Submissions should be sent to the Chief Scientific Editor, Geological Survey of Canada, 601 Booth Street, Ottawa, Canada, K1A 0E8.

AUTHOR INDEX

	Page
Anderson, R.G.	393
Ashton, K.E.	311
Bell, R.T.	397
Blake, W., Jr.	157
Blinn, L.	273
Booth, G.W.	179
Boyle, D.R.	349
Brisbin, D.	95
Brown, R.L.	33, 35
Cameron, B.E.B.	396
Cameron, E.M.	187
Campbell, F.H.A.	91
Campbell, R.B.	17
Card, K.D.	87
Cecile, M.P.	91, 219, 227
Clague, J.J.	169
Closs, L.G.	247
Coker, W.B.	247
Conaway, J.G.	41
Cousineau, P.	207
Creaney, S.	381
Currie, K.L.	71, 77
Dawson, K.M.	375
Dick, L.A.	259
Dimroth, E.	207
Dodds, C.J.	17
Dunning, G.R.	305
Dunsmore, H.E.	61
Dyke, L.	241
Fawcett, J.J.	377
Fricker, A.	273
Frisch, T.	113
Froese, E.	83
Garrett, R.G.	197
Gittins, J.	77
Goodfellow, W.D.	333
Gordey, S.P.	13
Graham, P.S.W.	357
Green, R.	95
Hall, G.E.M.	361
Henderson, J.B.	400
Henderson, J.R.	95
Henderson, M.	95
Herd, R.K.	305
Iannelli, T.R.	45
Jackson, L.E., Jr.	107
Jefferson, C.W.	227
Jen, L.S.	83
Jonasson, I.R.	61
Jones, L.D.	397
Keen, C.E.	273
Keen, M.J.	273
Kennedy, D.	317
Klassen, R.W.	385
Knapp, D.	317
Lambert, M.B.	179
LeCheminant, A.N.	179
Leduc, M.	207
Lee, J.	121
Leroux, J.	401
Lewis, C.P.	403
Long, D.G.F.	357
Luternauer, J.L.	401
Lutes, G.G.	267
MacKay, D.K.	403
Mackay, J.R.	165, 403
Martineau, Y.	317
Matthews, J.V., Jr.	157
Maurice, Y.T.	281
Mayr, U.	233
Mazurski, M.	95
McGlynn, J.C.	127
Miller, A.R.	57, 179
Nadeau, L.	389
Nielsen, P.A.	133
Norford, B.S.	219, 227, 383
Nowlan, G.S.	213
Ostrick, J.	403
Pajari, G.E., Jr.	71
Pearson, W.N.	289
Pickerill, R.K.	71
Plant, A.G.	391
Provost, G.	207
Psutka, J.F.	35
Rast, N.	267
Read, P.B.	33, 37
Roberts, A.C.	391
Ruzicka, V.	139
Sabina, A.P.	115
Sanschagrin, Y.	207
Schau, M.	311, 389
Schillereff, S.	327
Shaw, D.	95
Sinclair, W.D.	253
Smee, B.W.	367
Sutcliffe, R.H.	377
Taylor, G.C.	227
Tempelman-Kluit, D.J.	1
Thorstad, L.	21
Tipper, H.W.	31, 396
Tippett, C.R.	101
Uyeno, T.T.	233
Williams, H.	327
Woodsworth, G.J.	25